STELLAR ATMOSPHERES

STELLAR ATMOSPHERES

Edited by JESSE L. GREENSTEIN

Edited by JESSE L. GREENSTEIN

STARS AND STELLAR SYSTEMS
VOLUME
VI

CONTRIBUTORS

Lawrence H. Aller, H. W. Babcock, L. Biermann, Karl-Heinz Böhm, A. D. Code, Armin J. Deutsch, Jesse L. Greenstein, S. Huang, Alfred H. Joy, Philip C. Keenan, Robert P. Kraft, R. Lüst, Andrew McKellar, Dean B. McLaughlin, Paul W. Merrill, Guido Münch, Jorge Sahade, O. Struve, Anne B. Underhill, O. C. Wilson

Volume VI of STARS AND STELLAR SYSTEMS
...a nine-volume compendium of astronomy and astrophysics

GERARD P. KUIPER, General Editor
BARBARA M. MIDDLEHURST, Associate General Editor



CHICAGO

STELLAR ATMOSPHERES

EDITED BY JESSE L. GREENSTEIN

STARS AND STELLAR SYSTEMS

VOLUME VI



CHICAGO

3rd printing

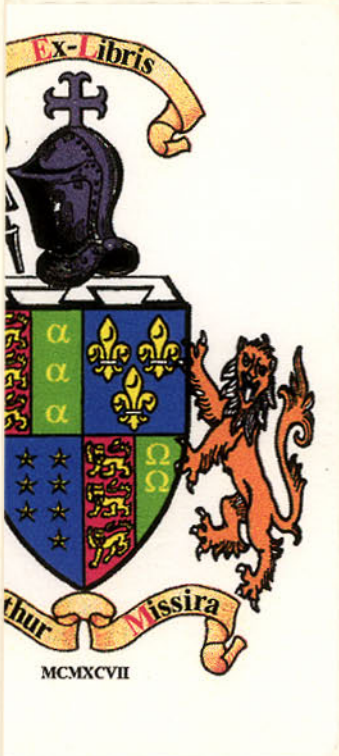
STARS AND STELLAR SYSTEMS

Volume VI: STELLAR ATMOSPHERES

***Edited by* JESSE L. GREENSTEIN**

Leading scientists in the field of stellar atmospheres and stellar spectroscopy contribute in this volume to a detailed account of the methods of interpretation and the results of observation of stellar spectra. The chapters, complete in themselves, provide an introduction to the mathematical and physical theories concerning the transfer of radiation through stellar atmospheres into space, a review of the present state of knowledge of stellar spectra, and an interpretation of the physical conditions—composition, temperature, pressure, state of motion, magnetic fields, turbulence, corpuscular radiation, and streams of gas —in the atmospheres of the stars.

JESSE L. GREENSTEIN is professor of astrophysics, California Institute of Technology, and a member of the staff of the Mount Wilson and Palomar Observatories.



STARS AND STELLAR SYSTEMS

Compendium of Astronomy and Astrophysics

(IN NINE VOLUMES)

GERARD P. KUIPER, *General Editor*

BARBARA M. MIDDLEHURST, *Associate General Editor*

I
TELESCOPES

II
ASTRONOMICAL TECHNIQUES

III
BASIC ASTRONOMICAL DATA

IV
CLUSTERS AND BINARIES

V
GALACTIC STRUCTURE

VI
STELLAR ATMOSPHERES

VII
NEBULAE AND INTERSTELLAR MATTER

VIII
STELLAR STRUCTURE

IX
GALAXIES AND THE UNIVERSE

CONTRIBUTORS

LAWRENCE H. ALLER
H. W. BABCOCK
L. BIERMANN
KARL-HEINZ BÖHM
A. D. CODE
ARMIN J. DEUTSCH
JESSE L. GREENSTEIN
S.-S. HUANG
ALFRED H. JOY
PHILIP C. KEENAN
ROBERT P. KRAFT
R. LÜST
ANDREW McKELLAR
DEAN B. McLAUGHLIN
PAUL W. MERRILL
GUIDO MÜNCH
JORGE SAHADE
O. STRUVE
ANNE B. UNDERHILL
O. C. WILSON

STELLAR ATMOSPHERES

Edited by

JESSE L. GREENSTEIN



THE UNIVERSITY OF CHICAGO PRESS
CHICAGO AND LONDON

This publication has been supported in part by the
NATIONAL SCIENCE FOUNDATION

Library of Congress Catalog Card Number: 61-9045

THE UNIVERSITY OF CHICAGO PRESS, CHICAGO 60637
The University of Chicago Press, Ltd., London W. C. 1

© *1960 by The University of Chicago. All rights reserved. Published 1960. Third Impression 1968. Printed in the United States of America*

Preface to the Series

THE SERIES "Stars and Stellar Systems, Compendium of Astronomy," comprising nine volumes, was organized in consultation with senior astronomers in the United States and abroad early in 1955. It was intended as an extension of the four-volume "Solar System" series to cover astrophysics and stellar astronomy. In contrast to the "Solar System" series, separate editors have been appointed for each volume. The volume editors, together with the general editors, form the editorial board that is responsible for the over-all planning of the series.

The aim of the series is to present stellar astronomy and astrophysics as basically empirical sciences, co-ordinated and illuminated by the application of theory. To this end the series opens with a description of representative telescopes, both optical and radio (Vol. **1**), and of accessories, techniques, and methods of reduction (Vol. **2**). The chief classes of observational data are described in Volume **3**, with additional material being referred to in succeeding volumes, as the topics may require. The systematic treatment of astronomical problems starts with Volume **4**, as is apparent from the volume titles. Theoretical chapters are added where needed, on dynamical problems in Volumes **4**, **5**, and **9**, and on astrophysical problems in Volumes **6**, **7**, and **8**. In order that the chapters may retain a greater degree of permanence, the more speculative parts of astronomy have been de-emphasized. The level of the chapters will make them suitable for graduate students as well as for professional astronomers and also for the increasing number of scientists in other fields requiring astronomical information.

The undersigned wish to thank both the authors and the volume editors for their readiness to collaborate on this series, which it is hoped will stimulate the further growth of astronomy.

The editors wish to acknowledge the support by the National Science Foundation both in defraying part of the costs of the editorial offices and in providing a publication subsidy.

GERARD P. KUIPER
BARBARA M. MIDDLEHURST

Preface

A LARGE fraction of the observational effort in astronomy and of theoretical work in astrophysics is devoted to the study of stellar spectra and their interpretation in terms of the nature and composition of the stars. From one point of view the sophisticated methods developed for the study of stellar atmospheres have outrun their applications to the normal stars. Conversely, our observational knowledge of complex phenomena in actual stellar spectra offers problems far beyond the present development of theory. The sun, studied in greater detail than any other star, shows peculiarities of surface and envelope activity, unobservable in the stars, sufficient to provide both observers and theoreticians with fundamental problems for many years. Why, then, should we study stellar spectra? Why try to read the fragile clues which we can capture on a spectrogram, usually with insufficient scale, the spectrum of the whole body of the star averaging out all its variations in time and space? For very few cases of spectroscopic interest do we know the mass, temperature, composition, surface activity—in fact, any of the parameters needed for a physical theory.

The answer lies in one aspect of the nature of astronomy, which is still a science of discovery. A purely logical, deductive approach, based on what facts we know and on our present stage of theory, would never have predicted the unexpected, strange experimental laboratories which nature has provided. Some of the "high-energy" phenomena displayed by the sun are detectable in stellar spectra. The border line between the well-established and well-understood features of the normal or slightly disturbed star and the violent phenomena of close binary systems is clearly visible in the organization of this volume. The normal star can be treated by the elaborate apparatus of modern theoretical astrophysics, insofar as its continuous and absorption-line spectra are concerned. The early chapters of this volume show some of the successful aspects of modern theory; but it is interesting to note the rarity of equations in the later chapters dealing with observational problems in stellar spectra. It is clear that an empirical approach is still required for many types of objects. For the spectroscopist, the pathological case is often the most revealing. We should remember the difference between the X-ray and rocket ultraviolet spectrum of the sun, which shows emission lines of high excitation, and the photospheric and reversing-layer absorption spectrum which dominates the normal spectral regions. The non-thermal phenomena in the sun produce the chromosphere and the corona; other stars have more extended atmospheres; binary systems have enormously complex extended envelopes, but coronal phenomena have not

yet been detected. A large fraction of this book is devoted to stars with such disturbed outer envelopes, with the implication of significant instability, exchange, or loss of mass as a common feature in late-type stars, rotating or binary systems, and stars of high luminosity. Stellar evolution must take into account the exchange of matter between stars and between the stars and the interstellar medium.

This volume was organized and most of the material received in late 1958; a few authors have modified their chapters to include new data through 1959. Because so much of astrophysical research has appeared only in technical journals, the bibliographies are long and refer, in general, to specialized treatments.

Chapters 1–5 outline fairly completely the basis for the standard methods of theoretical analysis of stellar atmospheres. That part of solar astrophysics concerned with the chromosphere, the corona, and deviations from local thermodynamic equilibrium is not discussed. The major sources of energy for these high-level, high-temperature phenomena are probably convection and magnetic fields. Some of the effects of these are discussed in chapters 6–8, in the context of stellar, rather than solar, astrophysics. The discussion of stars with high luminosity or extended atmospheres, including binaries, is contained in chapters 8–12. Certain individual types of stars are covered in chapters 13–19, including the normal and variable stars of late type, the dwarf variables, novae, and the various strange types of subluminous stars. Chapter 15, on the mass loss by stars, is significant in questions of stellar evolution, and chapter 16, on isotopes, touches close to problems of nucleogenesis, topics to be discussed elsewhere in this series.

The future of stellar spectroscopy must be in a middle ground between the elaborately developed theory of the static stellar atmosphere and the accumulation of data on real systems of stars. We are now at a stage in which, after much pioneer effort, we can hope for real progress. More elaborate stellar models can be constructed and more precise determinations of temperature made. Better spectroscopic data will be needed not only on the stars but also on such properties of atoms as transition probabilities and collisional cross-sections. The complex streams of matter around close binaries deserve further study, and it is probable that current space-satellite–oriented, computational programs in the restricted three-body problem will be of assistance. Spectroscopic abundance determinations in the various types of cooler stars have not yet been attempted; the peculiar stars (with high abundance of normally rare elements) have been studied only by approximate methods. The general problem of the abundance of the elements and their connection with nuclear processes and stellar evolution is another one of the many unfinished chapters of stellar spectroscopy.

I am grateful to Naomi K. Greenstein and Barbara Middlehurst for invaluable editorial assistance.

JESSE L. GREENSTEIN

Table of Contents

1. THE THEORY OF MODEL STELLAR ATMOSPHERES 1
Guido Münch

1. Introduction 1
1.1. Definitions 1
1.2. Formulation of the Problem 3

2. Radiative Transfer 4
2.1. The State of Radiative Equilibrium 4
2.2. The Exact Temperature Distribution in a "Gray" Atmosphere 8
2.3. The Milne Problem Solved by Method of Discrete Ordinates 9
2.4. Variational Solutions of the Milne Problem 11
2.5. Non-gray Atmospheres 11
2.6. Chandrasekhar's Solution of the Non-gray Problem . . . 12
2.7. Mean Absorption Coefficients for Non-gray Atmospheres . 16
2.8. Variational Solutions of the Non-gray Problem 18

3. Thermodynamic Principles 20
3.1. The State of Local Thermodynamic Equilibrium 20
3.2. Departures from the State of Radiative Equilibrium . . . 22
3.3. Radiation Pressure in High-Temperature Stars 24

4. The Process of Continuous Absorption 26
4.1. The Probability Coefficients for Photoionization and Recombination 26
4.2. The Sources of Continuous Absorption 29
4.3. Continuous Absorption by Neutral Hydrogen 30
4.4. The Absorption of H^- 31
4.5. The Continuous Absorption of He I 31
4.6. The Continuous Absorption of He II 32
4.7. The Continuous Absorption of the Metals 32
4.8. The Continuous Absorption of the H_2^+ Molecule 33
4.9. Scattering by Free Electrons 34

5. Interaction of Continuous and Line Spectra 34
5.1. Effect of Absorption Lines on Temperature Distribution of a Stellar Atmosphere 34
5.2. Chandrasekhar's "Picket-Fence" Model 35
5.3. Discontinuities in the Continuous Absorption Coefficient . . 37
5.4. Numerical Methods 38

6. Model Stellar Atmospheres 38
6.1. "Empirical" Models for the Sun 38
6.2. The Theoretical Model Solar Atmosphere 40
6.3. Approximate Model Stellar Atmospheres 42
6.4. High-Temperature Models 43

References 47

2. Stellar Energy Distribution 50
A. D. Code

1. Introduction 50

2. Integral Effective Intensity 52

3. Relative Spectrophotometry 55

4. Absolute Calibration 61

5. Absolute Spectrophotometry 66

6. Line Blanketing 75

7. Monochromatic Magnitudes 82

References 85

3. Basic Theory of Line Formation 88
Karl-Heinz Böhm

1. Introduction 88

2. Formulation of the Problem 89

3. The Thermodynamic State of a Stellar Atmosphere 93
3.1. Atmospheres in Radiative Equilibrium 93
3.11. The Assumption of Local Thermodynamic Equilibrium . 93
3.12. The Hypothesis of Local Thermodynamic Equilibrium and Its Limitations 96
3.13. General Approximations for the Source Function . . 106
3.2. Atmospheres Which Are Not in Radiative Equilibrium . . 114

4. The Line Absorption Coefficient 114
4.1. The Harmonic Oscillator and the Theory of Radiation Damping 114
4.2. Doppler Broadening and the Voigt Profile 117
4.3. Pressure Broadening of Spectral Lines 120
4.31. Derivation of Different Approximations from the General Theory 120
4.32. The Phase-Shift Theory 126
4.33. The Static Theory of Line Broadening 128
4.34. Non-adiabatic Effects in Phase-Shift Theories . . . 132
4.35. Hydrogen Lines Broadened Simultaneously by Ions and Electrons 133

5. Coherent and Non-coherent Re-emission 134
5.1. General Remarks 134
5.2. Radiation Damping 136
5.3. Pressure Broadening 137
5.4. Doppler Effect 138
5.5. Coherent Scattering and Polarization 138

6. Theoretical and Experimental Determination of Oscillator Strength and Transition Probabilities 139
6.1. Wave Functions and Atomic Structure 139
6.2. Transitions 142
6.3. The Theoretical Determination of Oscillator Strengths . . 143
6.4. The Experimental Determination of Oscillator Strengths . . 146

References 149

4. Quantitative Analysis of Normal Stellar Spectra 156
Lawrence H. Aller

1. Brief Historical Summary 156

2. Method of Fine Analysis 160
2.1. The Mechanism of Line Formation 160
2.2. Selection of Model Atmospheres 164
2.3. Calculation of Theoretical Line Intensities 166
2.4. Application of the Model-Atmosphere Procedure 176
2.5. Results Obtained for the Cooler Stars and the Sun . . . 187

3. The Curve of Growth 193
3.1. The Schuster-Schwarzschild Approximation 194
3.2. Curves of Growth for the Milne-Eddington Model . . . 197
3.3. Comparison of Curves of Growth 200
3.4. Construction of the Curve of Growth 201
3.5. Applications of the Curve of Growth to Specific Stars . . 204
3.6. Effects of Turbulence on the Curve of Growth and on Line Profiles 206
3.7. Specific Advantages and Disadvantages of Curve of Growth . 208
3.8. Comparison of Curve-of-Growth and Model-Atmosphere Results 209

4. Absolute-Magnitude Effects 210

5. Hydrogen Lines as Criteria for Determination of Surface Gravity . 212

6. Abundances of Elements in Normal Stars 218

References 224

5. Interpretation of Normal Stellar Spectra 232
Lawrence H. Aller

1. The Isothermal Approximation 232

2. The Relation between Gas and Electron Pressure 234

3. The Coefficient of Continuous Absorption 237

4. Mean Electron Pressure and Mass above Photosphere 240

5. Variation in Number of Absorbing Atoms with Temperature for Dwarfs, Giants, and Supergiants 244

6. Comparisons between Theory and Observation, Absolute-Magnitude Effects 250

7. The Role of Molecules in Stellar Spectra 252

References 258

6. NON-THERMAL PHENOMENA IN STELLAR ATMOSPHERES 260
L. Biermann and R. Lüst

1. Introduction 260

2. Observations 262
2.1. Turbulence in the Solar Photosphere 263
2.2. Motions in the Solar Chromosphere and Corona 263
2.3. Non-thermal Emissions of the Sun 264
2.4. Turbulence in Stellar Atmospheres 265
2.5. Motions in Double Stars and Eclipsing Binaries 267
2.6. Active Magnetic Stars 268
2.7. Flare Stars 269

3. Theoretical Interpretations 269
3.1. The Hydrogen Convection Zone 269
3.2. Acoustic Waves 271
3.3. Hydromagnetic Waves 273
3.4. Ambipolar Diffusion 274
3.5. Emission of Corpuscular Radiation 275
3.6. Emission of Radio-Frequency Radiation 276
3.7. Emission of Cosmic Radiation 277
3.8. Chromosphere and Corona in Other Stars 277

References 278

7. STELLAR MAGNETIC FIELDS 282
H. W. Babcock

1. Introduction 282

2. Observations 284

3. Magnetic Classification 289

4. Anomalous Line Intensity 297

5. Spectrum Variables 299

6. Spectroscopic Binaries 303
7. Comments on Certain Magnetic Stars 304
8. Line Width and Obliquity of Rotating A-Type Stars 307
9. The Periodic (α) Magnetic Variables 313
9.1. The Magnetic Oscillator or Solar-Cycle Model 314
9.2. The Oblique Rotator 317
References 319

8. Stellar Rotation and Atmospheric Turbulence 321
S.-S. Huang and O. Struve
1. Introduction 321
2. Rotation of Stars 322
2.1. Evidence of Stellar Rotation 322
2.2. Methods of Measuring the Rotation of a Star 323
2.3. Stellar Rotation along the Spectral Sequence 326
2.4. Other Statistical Results concerning Stellar Rotation . . . 329
2.5. Effects of Rotation on the Stars 330
3. Significance of Rotation in the Study of Stellar Evolution and Star Formation 335
3.1. Braking Mechanisms of Stellar Rotation 335
3.2. Rotation of Stars along the Evolutionary Sequences . . . 338
3.3. Origin of the Rotational Angular Momentum 341
4. Turbulence as Understood in Aerodynamics 343
4.1. The Reynolds Number 343
4.2. Theories of Turbulence 344
4.3. Thermal Instability and Convection 346
4.4. Near-sonic and Supersonic Turbulence 347
4.5. Turbulent Motion in a Conducting Medium under the Action of a Magnetic Field 349
5. Turbulence as Understood in Stellar Spectroscopy 350
5.1. The Two Kinds of Doppler Broadening of Stellar Spectral Lines 350
5.2. Physical Doppler Broadening 352
5.3. Geometrical Doppler Broadening 356
5.4. General Conclusions concerning the Doppler Motion in Stellar Atmospheres 359
References 361

9. The Spectra of Supergiants and Cepheids of Population I . . 370
Robert P. Kraft
1. Introduction 370
2. The Cepheid Spectrum as a Galactic Research Tool; Critique of the Analysis of Cepheid Spectra at Low Dispersion 372

3. High-Dispersion Studies: Rotation and Turbulence in Supergiants and Cepheids 378

4. Variation of Atmospheric Parameters of Cepheids through Cycle; Tests of Running-Wave Hypothesis; Derivation of Mean Radius . 388

5. The Ca II Emission 397

6. Cepheids and Stellar Evolution: Concluding Remarks 403

Appendix I, The Colors of Cepheids at Maximum Light 406

Appendix II, The Applicability of Wesselink's Method to Classical Cepheids 406

Appendix III, The Wilson-Bappu Effect 407

References 407

10. EARLY-TYPE STARS WITH EXTENDED ATMOSPHERES 411
Anne B. Underhill

1. Introduction 411

2. The Be Stars 413

3. Shell Spectra 418

4. The B-Type Supergiants and P Cygni Stars 422

5. The Of Stars 425

6. The Wolf-Rayet Stars 428

References 433

11. ECLIPSES BY EXTENDED ATMOSPHERES 436
O. C. Wilson

1. Introduction 436

2. Available Binary Systems 437

3. Comparison of ζ Aurigae, 31 Cygni, 32 Cygni, and VV Cephei . . 437

4. Detailed Studies of Eclipse Phenomena 438
4.1. ζ Aurigae 438
4.11. Spectroscopic Orbit 439
4.12. Mass Ratio 439
4.13. Dimensions, Temperatures, Luminosities, Masses . . 439
4.14. Light-Curves 441
4.15. Observations of Chromospheric Absorption Lines . . 442
4.16. Interpretation 450
4.2. 31 Cygni 454
4.21. Spectroscopic Orbit 454

4.22. Mass Ratio 455
4.23. Dimensions, Temperatures, Luminosities, Masses . . 455
4.24. Light-Curves 456
4.25. Observations of Chromospheric Lines 456
4.3. 32 Cygni 459
4.4. VV Cephei 461

5. Concluding Remarks 463

References 464

12. Composite and Combination Spectra 466
Jorge Sahade

1. Introduction 466

2. Close Binary Systems 467
2.1. Superposition of Normal Spectra 467
2.2. Peculiarities in the Spectrum 468
2.3. Gaseous Rings 469
2.4. Concentration of Matter at Lagrangian Points 471
2.5. Absorption Effects of Gaseous Streams 473
2.6. Absorption Effects of Rings 475
2.7. Mechanism of Mass Loss 476
2.8. Expanding Shells 480
2.9. Escape of Matter through External Lagrangian Points . . 481
2.10. Emission of Ca II 483
2.11. Emissions of Another Kind 485
2.12. Variable Line Intensities 485
2.13. Peculiar Line Structure 488
2.14. Discussion 488

3. Symbiotic Stars 494
3.1. Observational Results 494
3.2. Interpretations 498
3.3. Discussion 501

4. Concluding Remarks 503

References 503

13. Spectra of Long-Period Variables 509
Paul W. Merrill

1. Introduction 509

2. Temperature 510

3. Density 511

4. Veiling 512

5. Absorption Lines 513
5.1. General 513
5.2. Comparison of M-, S-, and N-Type Variables 514
5.3. Changes with Phase 515
5.4. Displaced Components 516
5.5. High-Velocity Variables 518

6. Emission Lines 518
6.1. General 518
6.2. Special Notes 519
6.3. Hydrogen Lines 519
6.4. Ca II Lines 520
6.5. Emission Lines of AlH 522
6.6. Unidentified Lines 523
6.7. Absolute Intensities 524

7. Period and Amplitude of Light-Variation 524

8. Brighter Variables of Various Types 526

References 528

14. PHYSICAL PROPERTIES OF THE RED GIANTS 530
Philip C. Keenan

1. Properties Derived from Classification of Late-Type Spectra . . 530
1.1. Effective Temperatures 531
1.2. Absolute Magnitudes 532

2. Atmospheric Composition 534

3. Opacities of the Atmospheres 537

References 541

15. THE LOSS OF MASS FROM RED GIANT STARS 543
Armin J. Deutsch

1. Introduction 543

2. Observational Evidence for Mass Loss from Late-Type Giants . . 546
2.1. Circumstellar Absorption Lines 546
2.2. The Normal Giants 547
2.3. Two Simple Models 548
2.4. The Supergiants 550
2.5. Line Profiles 552
2.6. The H and K Lines 553
2.7. Turbulent Velocities 555
2.8. The Mass-Loss Process 556
2.9. Binary Stars and Variable Stars 557

3. The Rate of Mass Ejection 560

References 566

16. Isotopes in Stellar Atmospheres 569
Andrew McKellar

1. Applications in Atomic Spectra 571
1.1. Hydrogen and Deuterium 572
1.2. Helium 573
1.3. Lithium 574
1.4. Technetium 574

2. Applications in Molecular Spectra 574
2.1. Hydrogen 575
2.2. Nitrogen 576
2.3. Oxygen 576
2.4. Magnesium 576
2.5. Silicon 576
2.6. Scandium 577
2.7. Titanium 577
2.8. Vanadium 577
2.9. Yttrium 577
2.10. Zirconium 578
2.11. Lanthanum 578
2.12. Carbon 578

3. Future Work and Prospects 582

References 583

17. The Spectra of Novae 585
Dean B. McLaughlin

1. Introduction 585
1.1. Historical 585
1.2. Nomenclature 586

2. Distribution and Luminosities 587
2.1. Galactic Distribution 587
2.2. Distances and Luminosities 587

3. Light-Variations 591
3.1. Nova Light-Curves in General 591
3.2. Light-Curve Data 592
3.3. Light-Curves of Typical Fast Novae 595
3.4. Novae of Moderate Rate 596
3.5. Light-Curves of Slow Novae 597
3.6. Light-Curves of RT Serpentis Stars 597
3.7. Continuing Variations 598

3.8. Recurrent Novae 599
3.9. Nova-like Variables 601
3.10. Relation of Luminosity to Rate of Fading 601
3.11. Comparison of Galactic Novae with Those of M31 . . . 602

4. Spectroscopic Characteristics and Variations 602
4.1. Outline of Spectral Development 602
4.2. The Spectrum before Outburst 604
4.3. The Premaximum Spectrum 605
4.4. The Principal Spectrum 606
4.5. The Diffuse Enhanced Spectrum 608
4.6. The Orion Spectrum 608
4.7. The Nebular Stage 610
4.8. The Postnova Spectrum 610
4.9. Comparison of Fast and Slow Novae 611
4.10. Spectra of Recurrent Novae 612
4.11. Oscillatory Variations in Magnitude and Spectrum . . . 614
4.12. Spectra of Supernovae 616

5. Velocities of Absorption Systems; Emission Structures 618
5.1. Velocities of Premaximum Absorption 619
5.2. Velocities of Principal Spectra 620
5.3. Velocities of Diffuse Enhanced Spectra 621
5.4. Velocities of Orion Spectra 622
5.5. Undisplaced Absorption Lines 622
5.6. Structure of Emission Bands 625
5.7. The Expanding Nebulae 626
5.8. Structure of the Nebula about v603 Aquilae 628
5.9. Typical Development of Nova Spectra 629

6. Physical Measurements 631
6.1. Intensities of Emission Bands 631
6.2. Color Temperatures 632
6.3. Photoionization Temperatures 634
6.4. Excitation Temperatures 636
6.5. Electron Temperatures and Densities; Mass of Material Ejected 636
6.6. Photospheric Dimensions 638
6.7. Masses of Novae 640

7. Interpretation of Nova Phenomena 640
7.1. The Rise to Maximum 641
7.2. Maximum Light; the Postmaximum Transformation . . . 642
7.3. Evolution of the Principal Spectrum 642
7.4. Diffuse Enhanced and Orion Spectra 643
7.5. The Transition Stage 644
7.6. The Nebular Stage 645
7.7. Origin of Nova Outbursts 646

References 647

18. SPECTRA OF DWARF VARIABLE STARS 653
Alfred H. Joy

1. Classification 654
2. Classes of Dwarf Variable Stars 654
   2.1. Group I: Rapid Irregular Variables 654
   2.2. Group II: UV Ceti Flare Stars 655
   2.3. Group III: SS Cygni Variables 655
3. Group I: Rapid Irregular Dwarf Variables 655
4. General Considerations of Variables in Nebulosity 662
5. Spectral Peculiarities of Stars in Nebulosity 664
6. Group II: The Spectra of UV Ceti Flare Stars 666
7. Group III: The Spectra of SS Cygni Stars 670

References 673

19. SPECTRA OF STARS BELOW THE MAIN SEQUENCE 676
Jesse L. Greenstein

1. Introduction 676
2. Spectra of Old Novae 677
3. The SS Cygni Stars 684
4. The White Dwarfs 687
5. The Hot Subdwarfs 703
6. Faint Blue Stars 705
7. The Nuclei of Planetary Nebulae 706
8. The F and G Subdwarfs 707

References 710

SUBJECT INDEX 713

STAR INDEX 718

CHAPTER 1

The Theory of Model Stellar Atmospheres

GUIDO MÜNCH
Mount Wilson and Palomar Observatories
California Institute of Technology, Carnegie Institution of Washington

§ 1. INTRODUCTION

1.1. Definitions

By a "stellar atmosphere" we shall mean the layers of a star directly accessible to observation, in the sense that a detectable amount of the radiation characteristic of those layers reaches the observer without being absorbed or scattered. From the observational point of view, a stellar atmosphere has been divided into three superincumbent strata, named the "photosphere," the "reversing layers," and the "chromosphere." The boundaries between these regions are not accurately defined, but in a general way they represent the layers where the continuous spectrum, the absorption-line spectrum, and the emission-line spectrum originate, respectively. Often when speaking about the chromosphere, implicit reference is meant to the layers producing the flash spectrum at solar eclipses. But recently the same term has been used also in context with stars, to denote those layers which do not seem to be supported by hydrostatic forces alone. In this chapter we shall be restricted to the study of the physical state of the photosphere and reversing layers, which is determined by the amount of radiant energy flowing out from the deep stellar interior and by the acceleration of gravity, g. For simplicity, we shall refer to the most often encountered case of an atmosphere in the steady state and with linear extent small compared with the radius of the star. The net flux of radiation, πF, through the atmosphere is then a constant. A model atmosphere for a star of given πF, g, and relative number abundances $\{A_i\}$ of the various atomic species, expresses the physical variables, total pressure, p, and temperature, T, as functions of a suitably defined variable measuring depth in the atmosphere.

In order to make this definition meaningful, it will be necessary to prove that thermodynamic variables can be specified locally through the stellar atmosphere that we may be dealing with.

The characterization of a model atmosphere by the two parameters πF and g, for a fixed set $\{A_i\}$ of abundances, corresponds in a one-to-one fashion with position in the HR diagram, through a co-ordinate transformation involving the mass-luminosity relation. The theory of stellar atmospheres in the large is concerned with the problem of inferring the parameters of a model from observed spectral features of a star. In principle, then, a complete theory of model atmospheres would enable us to reconstruct the HR diagram without making reference to astrometric data (parallaxes). At present, however, our knowledge of the underlying physical processes is not so complete as would be needed for studying the problem in its full generality. And as a preliminary stage in the complete analysis of a stellar atmosphere, we consider the determination of its model as characterized by πF, g, and only a few numbers A_i. This approximation to the general problem can be made because the thermodynamic state of the atmosphere depends on the abundances of those elements producing appreciable continuous absorption. The role played by discrete atomic transitions (line absorption) in the heat-transfer problem is of secondary importance, except for the coolest stars, and can be taken into account in higher approximations (blanketing effect). Because of the large cosmic abundance of hydrogen and helium, the radiation field interacts with matter effectively only through the continuous absorption of these elements, and the model depends only on their abundances, A_1 and A_2. The abundance of the heavy elements may enter into the problem only if they contribute enough free electrons to affect sensibly the state of ionization of the effective source of absorption, which is the negative ion of hydrogen (H^-) in stars with spectral types later than about A5.

The development of the theory of stellar atmospheres may be followed largely through the successive analyses of the continuous and/or line spectra of the sun carried out between 1906, when the fundamental memoir of K. Schwarzschild appeared, and 1940, when the work of B. Strömgren was published. The latter investigation showed clearly the advantage of the use of model atmospheres in a purely deductive analysis of the solar spectrum. It was on account of incompleteness in our knowledge of the nature of the process of continuous absorption (the existence of H^-) that such an approach had not been carried out before, although essentially it had been outlined by E. A. Milne (1929) in his Bakerian Lecture. At present it can be stated with some degree of certainty that every major physical process playing a role in determining the thermal state of a stellar atmosphere has been taken into consideration. It is only in regard to some quantitative aspects of theories related to the formation of spectral lines that some questions remain unsolved, as is discussed in chapter 3 of this volume.

1.2. Formulation of the Problem

In a general way it is not difficult to sketch the procedure involved in the calculation of a model atmosphere. Let it be supposed that we deal with an atmosphere stratified in parallel planes normal to the direction of gravity (z-direction). If the atmosphere is in a state of macroscopic mechanical equilibrium, we have, as one of the fundamental equations of the problem,

$$\frac{dp}{dz} = -g\rho , \tag{1}$$

where ρ is the density and p is the resultant of the kinetic gas pressure, p_G, and the radiation pressure, p_R:

$$p = p_G + p_R . \tag{2}$$

The second fundamental equation relates the temperature and the depth. In most atmospheres the mechanism transporting heat energy outward from the star interior may be shown to be predominantly radiative. The theory of radiative transfer through an atmosphere in local thermodynamic equilibrium, then, provides a well-defined finite procedure to compute the temperature, T, in the form

$$T = T_e f(\tau) , \tag{3}$$

where the effective temperature, T_e, is related to the net flux, πF, by

$$\pi F = \sigma_R T_e^4 , \tag{4}$$

σ_R being Stefan's constant. In equation (3) the independent variable τ is called "mean optical depth" and is related to the geometric depth, z, by

$$d\tau = -\bar{\kappa}\rho dz , \tag{5}$$

where $\bar{\kappa} = \bar{\kappa}(T, p_G, A_i)$ is some mean value over the frequency, ν, of the monochromatic absorption coefficient per gram, κ_ν. It is through $\kappa_\nu = \kappa_\nu(T, p_G, A_i)$ that the abundance parameters enter into the problem. Using equation (5), we may express equation (1) in terms of the independent variable τ in the form

$$\frac{d}{d\tau}(p_G + p_R) = \frac{g}{\bar{\kappa}(p_G, T, A_i)} . \tag{6}$$

As we shall show later, $p_R = p_R(\bar{\kappa}, T)$, and then, through equation (3), we may express the right-hand side of equation (6) as a function of p_G and T alone. The relation $p = p(\tau)$ follows by integration under the boundary condition

$$p = 0 \qquad \text{at} \qquad \tau = 0 . \tag{7}$$

The density $\rho = \rho(\tau)$ can be found from the equation of state, which always may be taken as the perfect-gas law:

$$p_G = \frac{k}{\mu H}\rho T , \tag{8}$$

where k is the Boltzmann constant, H is the mass of the hydrogen atom, and $\mu = \mu(A_i)$ is the mean particle weight. The integration of equation (5) establishes the correspondence between optical depth and geometrical heights $z - z_0$ above an arbitrary level z_0.

A model is considered representative of an actual star when a satisfactory agreement between the computed and observed spectra is reached. As a general rule, the number of parameters characteristic of a model is far less than the number of available features in the continuous or line spectrum. Consequently, a consistent model may be required to satisfy quite stringent conditions. The case of the solar atmosphere, in particular, offers an extremely accurate test of the theory, since πF and g are known with high precision and the model depends only on the relative abundance H:M of the elements with high ionization potential, $IP \geq 10$ ev, and of the metals, $IP \simeq 6$ ev. The number of observable features in the continuous and line spectrum to be explained on the basis of a model in this case is very large.

In this chapter the procedures and basic assumptions involved in the construction of atmospheric models will be considered. Our discussion will presuppose some knowledge of the more elementary aspects of the theory of stellar atmospheres. The availability of several recent monographs and textbooks on the subject (Chandrasekhar 1950; Kourganoff 1952; Aller 1953; Woolley and Stibbs 1953; Unsöld 1955) would make superfluous a self-contained presentation.

§ 2. RADIATIVE TRANSFER

2.1. The State of Radiative Equilibrium

Of fundamental importance in the theory of model atmospheres is the determination of the function $f(\tau)$ defined in equation (3). We shall begin our discussion, thus, by formulating the problem of determining the temperature distribution in an atmosphere in the steady state, with negligible curvature and with given chemical composition. The axially symmetric radiation field will be characterized by the specific intensity of ν-radiation, $I_\nu \equiv I_\nu(z, \mu)$, as a function of z, the height in the atmosphere, and the angle $\cos^{-1}\mu$ between the direction considered and the outward normal. Polarization effects in the radiation field will be neglected, even when scattering by free electrons plays a role in the process of energy interchange. We define the mean intensity over all solid angles by

$$J_\nu(z) = \frac{1}{2}\int_{-1}^{+1} I_\nu(z, \mu)\, d\mu. \tag{9}$$

The net flux of ν-radiation is

$$\pi F_\nu(z) = 2\pi \int_{-1}^{+1} I_\nu(z, \mu)\, \mu d\mu; \tag{10}$$

furthermore, let

$$K_\nu(z) = \frac{1}{2}\int_{-1}^{+1} I_\nu(z, \mu)\, \mu^2 d\mu. \tag{11}$$

The interaction of the matter with the radiation field will be described by the coefficient of continuous absorption, $\kappa_\nu = \kappa_\nu(z)$, per unit mass ($cm^2\ gm^{-1}$) and its coefficient of spontaneous continuous emission, $\epsilon_\nu = \epsilon_\nu(z)$ (erg gm^{-1} steradian^{-1}). In a later paragraph we shall consider the problem of expressing κ_ν in terms of the radiative cross-sections of the constituent atoms and ions. For the time being, κ_ν will be considered as an a priori given function of frequency ν, depending implicity on z through the variables temperature and pressure which determine the excitation and ionization conditions and the properties of the free-electron assembly.

The balance of radiant energy in an elementary cylinder of height $ds = dz/\mu$ along a ray of intensity $I_\nu(z, \mu)$ is expressed in the equation of transfer,

$$\mu \frac{\partial I_\nu}{\partial z} = -\kappa_\nu \rho I_\nu(z, \mu) + \rho\epsilon_\nu . \tag{12}$$

Let us introduce, as an independent variable, a mean optical depth,

$$\tau = \int_z^\infty \bar{\kappa}\rho dz , \tag{13}$$

where $\bar{\kappa}$ is a mean value of κ_ν over frequency to be specified later. Further, let the source function, $\mathfrak{S}_\nu(z)$ be defined by

$$\mathfrak{S}_\nu(z) = \frac{\epsilon_\nu(z)}{\kappa_\nu(z)} . \tag{14}$$

We may then rewrite the equation of transfer in the form

$$\mu \frac{\partial}{\partial \tau} I_\nu(\tau, \mu) = \eta_\nu' [I_\nu(\tau, \mu) - \mathfrak{S}_\nu(\tau)] , \tag{15}$$

where

$$\eta_\nu'(\tau) = \frac{d}{d\tau}\eta_\nu(\tau) = \frac{\kappa_\nu}{\bar{\kappa}} \tag{16}$$

represents the derivative of the monochromatic optical depth with respect to the total optical depth.

If energy is transported only by radiative processes, the atmosphere is said to be in a *state of radiative equilibrium*. The integrated net flux should then be independent of depth. Integrating equation (15) over all μ, we obtain

$$\frac{1}{4}\frac{dF_\nu}{d\tau} = \eta_\nu' [J_\nu(\tau) - \mathfrak{S}_\nu(\tau)] , \tag{17}$$

and the state of radiative equilibrium thus implies

$$\int_0^\infty [J_\nu(\tau) - \mathfrak{S}_\nu(\tau)]\, \eta_\nu' d\nu = 0 . \tag{18}$$

It is of importance to notice that multiplying equation (15) by $\mu d\mu$ and integrating over all μ, we obtain

$$\frac{dK_\nu}{d\tau} = \tfrac{1}{4}\eta_\nu' F_\nu , \tag{19}$$

independently of $\mathfrak{J}_\nu(\tau)$.

Now, in an inclosure in thermodynamic equilibrium at a temperature T, it is proved (Hilbert 1912, 1913) that Kirchhoff's law of emission holds; i.e.,

$$\mathfrak{J}_\nu \equiv B_\nu(T) = \frac{2h\nu^3}{c^2}\left(e^{h\nu/kT} - 1\right)^{-1}, \tag{20}$$

where $B_\nu(T)$ is the specific intensity of black-body radiation. Although in the strict sense of the term a stellar atmosphere is not an inclosure in thermodynamic equilibrium, as will be shown in a later paragraph, Kirchhoff's law holds to a reasonable degree of approximation. Equation (20) may then be used to define the temperature at every point in a stellar atmosphere. This definition constitutes what Milne called the "hypothesis of local thermodynamic equilibrium."

It will now be shown how the equation of transfer in local thermodynamic equilibrium,

$$\mu \frac{\partial}{\partial \tau} I_\nu(\tau, \mu) = \left[I_\nu(\tau, \mu) - B_\nu(\tau)\right] \eta_\nu'(\tau), \tag{21}$$

together with the condition of a constant net flux,

$$\int_0^\infty \left[J_\nu(\tau) - B_\nu(\tau)\right] \eta_\nu' d\nu = 0, \tag{22}$$

provides an equation for the determination of $T = T(\tau)$. Let it be assumed that the atmosphere is not exposed to incoming radiation at its outer boundary:

$$I_\nu(\tau = 0, -\mu) = 0 \qquad \text{for} \qquad 0 < \mu \leq 1 . \tag{23}$$

Equation (21) may be then formally integrated in the form ($\mu > 0$)

$$I_\nu(\tau, \mu) = \int_\tau^\infty B_\nu(t) \exp\left[-\frac{\eta_\nu(t) - \eta_\nu(\tau)}{\mu}\right] \eta_\nu'(t)\, dt \tag{24}$$

and

$$I_\nu(\tau, -\mu) = \int_0^\tau B_\nu(t) \exp\left[-\frac{\eta_\nu(\tau) - \eta_\nu(t)}{\mu}\right] \eta_\nu'(t)\, dt . \tag{25}$$

Substituting these formal integrals in definition (9), we obtain

$$J_\nu(\tau) = \frac{1}{2}\int_0^\infty B_\nu(t) E_1\left[\,|\,\eta_\nu(t) - \eta_\nu(\tau)\,|\,\right] \eta_\nu'(t)\, dt, \tag{26}$$

where $E_n(x)$ stands for the exponential integral of order n. Let the result of applying the integral operator, $\Lambda_\tau^{(n)}$, to the function $B_\nu(\tau)$ be defined by

$$\begin{aligned}\Lambda_\tau^{(n)}(\eta_\nu, B_\nu) = &\int_\tau^\infty B_\nu(t) E_n\left[\eta_\nu(t) - \eta_\nu(\tau)\right] \eta_\nu' dt \\ &- (-1)^n \int_0^\tau B_\nu(t) E_n\left[\eta_\nu(\tau) - \eta_\nu(t)\right] \eta_\nu' dt .\end{aligned} \tag{27}$$

Equation (26) is then rewritten as follows:

$$J_\nu(\tau) = \tfrac{1}{2}\Lambda_\tau^{(1)}(\eta_\nu, B_\nu). \tag{28}$$

In a similar fashion, the formal integrals (24) and (25), when substituted in equations (10) and (11), give

$$F_\nu(\tau) = 2\Lambda_\tau^{(2)}(\eta_\nu, B_\nu) \tag{29}$$

and

$$K_\nu(\tau) = \tfrac{1}{2}\Lambda_\tau^{(3)}(\eta_\nu, B_\nu). \tag{30}$$

Substituting equation (28) in equation (22), we obtain

$$\int_0^\infty B_\nu(\tau)\,\eta_\nu'(\tau)\,d\nu = \frac{1}{2}\int_0^\infty \Lambda_\tau^{(1)}(\eta_\nu, B_\nu)\,\eta_\nu'(\tau)\,d\nu, \tag{31}$$

an integral equation for the determination of $T = T(\tau)$, through definition (20). From equation (29) and the condition of constant net flux we also obtain

$$F = 2\int_0^\infty \Lambda_\tau^{(2)}(\eta_\nu, B_\nu)\,d\nu, \tag{32}$$

an alternative form of the same integral equation.

It should be noticed that η_ν' is explicitly known as a function of p and T, variables whose dependence on τ is to be determined. Equations (31) and (32) thus have to be considered simultaneously with the equation of mechanical equilibrium (6). For the case when κ_ν can be expressed as

$$\kappa_\nu(z) = \alpha(z)\,\beta(\nu), \tag{33}$$

$\alpha(z)$ being independent of ν and $\beta(\nu)$ independent of z, equations (31) and (32) can, in principle, be solved independently of the equation of mechanical equilibrium; for $\alpha(z)$ may be then absorbed in the definition of $\bar{\kappa}$, in such a way that η_ν' is independent of τ. This case has been considered by Hopf (1934), who proved the existence of the solution. The complexity of the fundamental nonlinear integral equation is still so great, however, that no result of practical importance can be obtained. Assumption (33) in any case is not always realistic. In stars in which the photoelectric ionization of hydrogen or helium produces the continuous absorption, the height of the absorption edges at the various series limits depends on T, and the separation of variables indicated in equation (33) cannot be carried out. When the photoionization of H^- is the main source of absorption, on the other hand, κ_ν depends on T and p mainly through the ionization equation, and the separation of variables is possible, provided that the contribution of the free-free transitions is not too great. In view of the analytical intractability of the fundamental equations (31) and (32), it has been found necessary to follow numerical procedures, which we shall consider later.

2.2. The Exact Temperature Distribution in a "Gray" Atmosphere

When $\kappa_\nu = \bar{\kappa}$ is independent of ν, the atmosphere is said to be "gray," and equation (31) may be integrated over frequency in the form

$$B(\tau) = \tfrac{1}{2}\Lambda_\tau^{(1)}(B), \tag{34}$$

where (cf. eq. [20])

$$B(\tau) = \frac{\sigma_R}{\pi} T^4(\tau). \tag{35}$$

Equation (34) is generally known as the "Milne integral equation." It is linear for $B(\tau)$ and has a singular nucleus. The Wiener-Hopf method of solving such classes of equations provides a solution of the form (Hopf 1934)

$$B(\tau) = c\,[\tau + q(\tau)], \tag{36}$$

where c is an arbitrary constant and $q(\tau)$ is a monotonic increasing function of τ, such that

$$q_0 \leq q(\tau) < q_\infty, \tag{37}$$

where

$$q_0 = \frac{1}{\sqrt{3}} \tag{38}$$

and

$$q_\infty = \frac{6}{\pi^2} + \frac{1}{\pi}\int_0^{\pi/2} \left(\frac{3}{\theta^2} - \frac{1}{1-\theta\cot\theta}\right) d\theta = 0.710446\ldots. \tag{39}$$

The function $q(\tau)$ has not been expressed in terms of known transcendentals, but it has been numerically computed by Mark (1947).

The value of the constant c may be obtained from the K-integral (cf. eq. [19]), which for the case may be written

$$K(\tau) = \tfrac{1}{4}F\tau + \text{constant}. \tag{40}$$

If K is substituted from equation (30), letting $\tau \to \infty$, we have

$$\tfrac{1}{4}F = \frac{c}{2}\lim_{\tau\to\infty}\frac{1}{\tau}\int_0^\infty [t + q(t)]\,E_3(|t-\tau|)\,dt; \tag{41}$$

and, since $q(t)$ is bounded by an elementary integration, it follows that

$$c = \tfrac{3}{4}F. \tag{42}$$

Equation (36) is thus finally written

$$B(\tau) = \tfrac{3}{4}F[\tau + q(\tau)], \tag{43}$$

and the local temperature, $T(\tau)$, is given in terms of the effective temperature, T_e by (cf. eqs. [4] and [35])

$$T^4(\tau) = \tfrac{3}{4}T_e^4[\tau + q(\tau)]. \tag{44}$$

The emergent integrated intensity,

$$I(0, \mu) = \int_0^\infty B(t)\, e^{-t/\mu} \frac{dt}{\mu}, \tag{45}$$

has the explicit value (Hopf 1934)

$$I(0, \mu) = \frac{\sqrt{3}}{4} F(1 + \mu) \exp\left\{\frac{\mu}{\pi}\int_0^{\pi/2} \frac{\ln[\sin^2\theta/(1 - \theta\cot\theta)]}{\cos^2\theta + \mu^2 \sin^2\theta}\, d\theta\right\}, \tag{46}$$

from which it can be shown that, for small μ,

$$I(0, \mu) = \frac{\sqrt{3}}{4} F(1 - \tfrac{1}{2}\mu \ln \mu) \qquad (\mu \ll 1). \tag{47}$$

The function $I(0, \mu)$, as given by equation (46), has been numerically evaluated by Chandrasekhar (1944) and by Placzek (1947). In terms of $I(0, \mu)$, the relatively simple expression

$$q(\tau) = q_\infty - \tfrac{1}{8}F\int_0^1 \frac{e^{-\tau/\mu} d\mu}{I(0, \mu)[(1 - \mu \tan h^{-1}\mu)^2 + \pi^2\mu^2/4]} \tag{48}$$

has been given by Mark (1947).

While the Wiener-Hopf method has provided an exact solution for the Milne problem, it cannot be applied to the case of non-gray atmospheres. It is of importance, therefore, to consider alternative procedures by means of which the non-gray problem may be approached.

2.3. The Milne Problem Solved by Method of Discrete Ordinates

Consider the equation of transfer for a gray atmosphere in radiative equilibrium,

$$\mu \frac{\partial}{\partial \tau} I(\tau, \mu) = I(\tau, \mu) - \frac{1}{2}\int_{-1}^{+1} I(\tau, \mu')\, d\mu', \tag{49}$$

and evaluate the integral over μ' by means of a Gauss-Jacobi quadrature formula (Szegö 1939) in terms of the zeros μ_i of the $2n$th Legendre polynomial and associated Christoffel numbers, a_i, in the form

$$\mu_i \frac{dI_i}{d\tau} = I_i(\tau) - \frac{1}{2}\sum_{j=-n}^{n} a_j I_j(\tau) \quad (i = \pm 1, \ldots, \pm n). \tag{50}$$

The solutions of this system of linear equations which do not increase exponentially as $\tau \to \infty$ and which satisfy the net flux condition are (Chandrasekhar 1950, § 25.1)

$$I_i(\tau) = \tfrac{3}{4}F\left(\tau + \mu_i + Q + \sum_{a=1}^{n-1} \frac{L_a}{1 + \mu_i k_a} e^{-k_a\tau}\right), \tag{51}$$

where the k_a's are the non-vanishing positive roots of the characteristic equation

$$\sum_{j=1}^{n} \frac{a_j}{1-\mu_j^2 k^2} = 1\,, \tag{52}$$

and the L_a's and Q are n integration constants which are fixed by requiring that no radiation is incident at $\tau = 0$:

$$I_{-i}(\tau) = I(\tau, -\mu_i) = 0 \qquad \text{at} \qquad \tau = 0\,. \tag{53}$$

The value of the source function, then, is

$$J(\tau) = \tfrac{3}{4}F\left(\tau + Q + \sum_{a=1}^{n-1} L_a e^{-k_a \tau}\right), \tag{54}$$

which provides for the emergent intensity the general expression

$$I(0, \mu) = \tfrac{3}{4}F\left(\mu + Q + \sum_{a=1}^{n-1} \frac{L_a}{1+\mu k_a}\right). \tag{55}$$

Alternatively, $I(0, \mu)$ may be expressed in a form analogous to equation (46) by eliminating the explicit dependence of the integration constants. It is found (Chandrasekhar 1950, § 25.5) that

$$I(0, \mu) = \frac{\sqrt{3}}{4} H(\mu)\,, \tag{56}$$

where, for any finite n,

$$H(\mu) = \left[\prod_{i=1}^{n}\left(1 + \frac{\mu}{\mu_i}\right)\right]\left[\prod_{a=1}^{n-1}(1 + k_a \mu)\right]^{-1}. \tag{57}$$

In the limit as $n \to \infty$, $H(\mu)$ satisfies

$$H(\mu) = 1 + \tfrac{1}{2}\mu H(\mu) \int_0^1 \frac{H(\mu')}{\mu + \mu'}\, d\mu'\,. \tag{58}$$

The relation between the Wiener-Hopf solution of the Milne integral equation and the function $H(\mu)$ defined by equation (58) has been studied by Chandrasekhar (1950, § 89) and also by Case (1957).

The integral equation (58) satisfied by $H(\mu)$ may be obtained directly from physical considerations, independently of the equation satisfied by $J(\tau)$. The basic idea of this derivation, originally due to Ambarzumian (1943), is the invariance of the radiation emergent from a semi-infinite plane-parallel atmosphere to the addition (or subtraction) of layers of arbitrary optical thickness to (or from) the atmosphere. The principles of invariance, developed mainly by Chandrasekhar (1950, chaps. iv and vii) have provided powerful tools to deal with complicated scattering problems, which cannot be attacked by Milne's methods. Since our main interest here is the source function, however, we shall not enter into details.

2.4. Variational Solutions of the Milne Problem

It can be established by elementary considerations that the solution of Milne's integral equation is monotonic and asymptotically linear (cf. eq. [36]). On this basis alone, then, one may postulate for $B(\tau)$ an expression of the form

$$B(\tau) = \tfrac{3}{4}F\Big[\tau + A_0 + \sum_{i=1}^{n} A_i\phi_i(\tau)\Big], \tag{59}$$

where the functions $\phi_i(\tau)$ are a priori selected to have the required behavior. The constants A_i may then be fixed in such a way that $B(\tau)$ satisfies the condition of constant net flux in some optimum sense. Since equation (59) is not the exact solution of Milne's problem, the quantity (cf. eq. [29])

$$\mathfrak{F}(\tau) = 2\Lambda_\tau^{(2)}[B(A_0, A_1, \ldots, A_n)] \tag{60}$$

cannot be exactly equal to the given flux F for any choice of the A_i's. However, we may select n depths, τ_j, and require that

$$\mathfrak{F}(\tau_j) = F \tag{61}$$

in such a way as to obtain a system of linear equations for the determination of the A_i's. Alternatively, we may require $\mathfrak{F}(\tau)$ to be equal to F in some least-squares sense. Setting

$$\xi(A_0, \ldots, A_n) = \int_0^\infty w(\tau)\left[\frac{\mathfrak{F}(\tau)}{F} - 1\right]^2 d\tau, \tag{62}$$

where $w(\tau)$ is an arbitrary weight function, we can minimize ξ with respect to the A_i's, to obtain

$$\frac{\partial \xi}{\partial A_i} = 0 \qquad (i = 1, 2, \ldots, n), \tag{63}$$

a system of the equations for the unknown constants.

The success of these methods depends on the choice of the functions $\phi_i(\tau)$. Among the functions which have been used are the exponential integrals, $E_i(\tau)$, with which highly accurate solutions of Milne's problem have been reached. These functions make $B'(\tau)$ non-analytic at $\tau = 0$, as required by equation (47). These approximate methods and their arithmetic properties have been discussed in detail by Kourganoff (1952, chap. v).

2.5. Non-gray Atmospheres

The difficulties involved in finding a direct solution for the source function in a non-gray atmosphere have led to the development of approximate methods, generally based on the assumption that the temperature distribution in a suitably defined gray atmosphere provides a "first approximation" in one sense or another. So far, we have left the mean absorption coefficient, $\bar{\kappa}$, undefined. We may now ask the question as to how to define $\bar{\kappa}$ if the gray-body solution is to approximate the solution of the problem for the given κ_ν. We have seen that for

κ_ν = constant the equations of the problem admit the K-integral (cf. eq. [40]). From equation (19) we see that the non-gray problem will also admit a K-integral, if we make

$$\int_0^\infty \eta'_\nu F_\nu d\nu = F \tag{64}$$

or, equivalently,

$$\int_0^\infty \frac{1}{\eta'_\nu}\frac{dK_\nu}{d\tau}\,d\nu = \frac{dK}{d\tau}, \tag{65}$$

equations which may be taken as definitions of $\bar{\kappa}$, in the form

$$\bar{\kappa}F = \int_0^\infty \kappa_\nu F_\nu d\nu \tag{66}$$

or

$$\frac{1}{\bar{\kappa}}\frac{dK}{d\tau} = \int_0^\infty \frac{1}{\kappa_\nu}\frac{dK_\nu}{d\tau}\,d\nu. \tag{67}$$

If we managed to evaluate $\bar{\kappa}$ in this fashion, it could be said that a gray atmosphere with τ measured in terms of such $\bar{\kappa}$ is an approximation of the non-gray atmosphere in the sense that both admit the same K-integral. But such a statement does not imply that the source function in the gray atmosphere also approximates that for the non-gray case. Writing the condition of radiative equilibrium (22) in the form

$$B(\tau) = J(\tau) + \frac{1}{4}\int_0^\infty (\eta'_\nu - 1)(J_\nu - B_\nu)\,d\nu, \tag{68}$$

it is readily seen that the gray-body relation between the integrated Planck function and the mean intensity does not hold for non-gray atmospheres, independently of the choice of $\bar{\kappa}$. In any case, it is apparent that the definitions of $\bar{\kappa}$ by means of equation (66) or (67) have only formal interest, since both functions $F_\nu(\tau)$ and $K_\nu(\tau)$ are unknown. In practice, these functions often have been approximated on the basis of the solution for a gray atmosphere in a sense not always made precise. The analytical approach developed by Chandrasekhar considered in the next paragraph is of importance because it provides a definite scheme of successive approximations.

2.6. Chandrasekhar's Solution of the Non-gray Problem

Let the general equation of transfer (21) be formally integrated over frequency in the form

$$\mu\frac{\partial}{\partial\tau}I(\tau,\mu) = I(\tau,\mu) - B(\tau) + \int_0^\infty (\eta'_\nu - 1)(I_\nu - B_\nu)\,d\nu, \tag{69}$$

and suppose that a mean value $\bar{\kappa}$ of κ_ν can be found such as to make small the integral over ν appearing in the right-hand side of the equation. We may then

attempt to solve the problem by a perturbation method, consisting in solving, first, the equation

$$\mu \frac{\partial}{\partial \tau} I^{(1)}(\tau, \mu) = I^{(1)}(\tau, \mu) - B^{(1)}(\tau) \tag{70}$$

and then using the solution $I^{(1)}(\tau, \mu)$ to evaluate the integral over appearing in equation (69). In the second approximation we would solve

$$\mu \frac{\partial}{\partial \tau} I^{(2)}(\tau, \mu) = I^{(2)} - B^{(2)} + \int_0^\infty (\eta'_\nu - 1)(I_\nu^{(1)} - B_\nu^{(1)})\, d\nu . \tag{71}$$

The extension of the method to the nth approximation is, in principle, possible, and its convergence does not depend on $|\eta'_\nu - 1|$ being small but rather on the possibility of making the integral term of equation (69) small.

The general solution of equation (70) under the condition of constant net flux,

$$J^{(1)} = B^{(1)} , \tag{72}$$

by the method of discrete ordinates has been given above in equation (54). In the second approximation we have to solve

$$\mu \frac{\partial I^{(2)}}{\partial \tau} = I^{(2)} - B^{(2)} + \mu \int_0^\infty (\eta'_\nu - 1) \frac{\partial I_\nu^{(1)}}{\partial \tau}\, d\nu , \tag{73}$$

under the condition of constant net flux, which is now

$$B^{(2)} = J^{(2)} + \frac{1}{4} \int_0^\infty (\eta'_\nu - 1) \frac{dF_\nu^{(1)}}{d\tau}\, d\nu . \tag{74}$$

It should be noticed here that in the second approximation the integrated Planck function differs from the mean intensity by an amount which depends on the non-constancy with depth of the monochromatic fluxes. Combining equations (73) and (74), we obtain

$$\mu \frac{\partial I^{(2)}}{\sigma \tau} = I^{(2)} - J^{(2)} + \int_0^\infty d\nu\, (\eta'_\nu - 1) \frac{\partial}{\partial \tau} \Big[\mu I_\nu^{(1)} - \frac{1}{2} \int_{-1}^{+1} \mu' I_\nu^{(1)}(\tau, \mu')\, d\mu \Big] . \tag{75}$$

Following the discrete ordinate method of § 2.3, we replace this equation by the system of $2n$ linear equations,

$$\mu \frac{dI_i^{(2)}}{d\tau} = I_i^{(2)} - \frac{1}{2} \sum_j a_j I_j^{(2)} + \int_0^\infty d\nu\, (\eta'_\nu - 1) \frac{d}{d\tau} \Big[\mu_i I_{\nu i}^{(1)} - \frac{1}{2} \sum_j a_j \mu_j I_{\nu j}^{(1)} \Big] \qquad (i = \pm 1, \pm 2, \ldots, \pm n) , \tag{76}$$

where the various symbols have the same meaning as in equation (50). The system (76) is solved by the method of variation of parameters. Since its homo-

geneous part is the same as that of equation (50), we seek a solution of the form

$$I_i^{(2)} = \tfrac{3}{4}F\Big[\tau + \mu_i + Q^{(2)} + \sum_{a=-n+1}^{n-1} \frac{L_a^{(2)}(\tau)}{1+\mu_i k_a} e^{-k_a\tau}\Big], \tag{77}$$

where one of the constants of integration has been fixed so as to obtain constant net flux F. Substituting in equation (76), we find the variational equation

$$\begin{aligned}\tfrac{3}{4}F\mu_i\Big[\sum_{a=-n+1}^{n-1} \frac{e^{-k_a\tau}}{1+\mu_i k_a}\frac{dL_a^{(2)}}{d\tau} + \frac{dQ^{(2)}}{d\tau}\Big] \\ = \int_0^\infty d\nu\,(\eta_\nu' - 1)\frac{d}{d\tau}\Big[\mu_i I_{\nu i}^{(1)} - \frac{1}{2}\sum_j a_j\mu_j I_{\nu j}^{(1)}\Big].\end{aligned} \tag{78}$$

Of these $2n$ equations, only $2n-1$ are linearly independent, since equation (77) gives a constant flux. The order of the system may be further reduced to $2n-2$ by a proper selection of $\bar{\kappa}$. Multiplying equation (78) by $a_i\mu_i$ and adding over all i's, we find

$$\tfrac{1}{2}F\frac{dQ^{(2)}}{d\tau} = \int_0^\infty d\nu\,(\eta_\nu' - 1)\frac{d}{d\tau}\sum_i a_i\mu_i^2 I_{\nu i}^{(1)}, \tag{79}$$

in virtue of the identities

$$\sum_i \frac{a_i\mu_i^2}{1+\mu_i k_a} = 0 \qquad \text{and} \qquad \sum_i a_i\mu_i^2 = \tfrac{2}{3}. \tag{80}$$

According to equation (79), if we arrange that

$$\int_0^\infty d\nu\,(\eta_\nu' - 1)\frac{d}{d\tau}\sum_i a_i\mu_i^2 I_{\nu i}^{(1)} = 2\int_0^\infty (\eta_\nu' - 1)\frac{dK_\nu^{(1)}}{d\tau}\,d\nu = 0, \tag{81}$$

we shall have the integral

$$Q^{(2)} = Q^{(1)} + \Delta Q, \tag{82}$$

where ΔQ is a constant. Equation (81) implies that $\bar{\kappa}$ should be identified with the mean $\bar{\kappa}_c$ defined by

$$\bar{\kappa}_c\frac{dK^{(1)}}{d\tau} = \int_0^\infty \kappa_\nu'\frac{dK_\nu^{(1)}}{d\tau}\,d\nu, \tag{83}$$

or, equivalently,

$$\bar{\kappa}_c = \frac{1}{F}\int_0^\infty \kappa_\nu F_\nu^{(1)}(\tau)\,d\nu. \tag{84}$$

With $\bar{\kappa}$ chosen in this fashion, $Q^{(2)}$ is a constant, and the variational equations become

$$\begin{aligned}\tfrac{3}{4}F\mu_i\sum_{a=-n+1}^{n-1}\frac{e^{-k_a\tau}}{1+\mu_i k_a}\frac{dL_a^{(2)}}{d\tau} = \int_0^\infty d\nu\,(\eta_\nu' - 1)\frac{d}{d\tau}\Big[\mu_i I_{\nu i}^{(1)} \\ - \frac{1}{2}\sum_j a_j\mu_j I_{\nu j}^{(1)}\Big] \qquad (i = \pm 1, \ldots, \pm n).\end{aligned} \tag{85}$$

Because the rank of this system is only $2n - 2$, it may be solved most conveniently by multiplying by $a_i\mu_i^{m-1}$ $(m = 1, 2, \ldots, 2n)$ and then adding over all i's, to obtain

$$\tfrac{3}{4}F \sum_{a=-n+1}^{n-1} D_m(k_a)\, e^{-k_a\tau} \frac{dL_a^{(2)}}{d\tau} = \delta_m - \frac{\epsilon_m}{m}\delta_1 \qquad (m = 1, 2, \ldots, 2n), \quad (86)$$

where

$$D_m(k) = \sum_i \frac{a_i\mu_i^m}{1+\mu_i k} = \frac{1}{k}\left[\frac{2}{m}\epsilon_m - D_{m-1}(k)\right], \quad (87)$$

$$\epsilon_m = \begin{cases} 1 & \text{if } m \text{ is odd} \\ 0 & \text{if } m \text{ is even}, \end{cases} \quad (88)$$

and

$$\delta_m = \int_0^\infty d\nu\,(\eta_\nu' - 1)\frac{d}{d\tau}\sum_i a_i\mu_i^m I_{\nu i}^{(1)}. \quad (89)$$

Since $D_1(k_a)$, $D_2(k_a)$, and δ_2 are identically zero, equation (86) is identically satisfied for $m = 1$ and 2, and it suffices to determine the $2n - 2$ $L_a^{(2)}$'s apart from the integration constants. The boundary condition as $\tau \to \infty$ requires

$$L_{-a}^{(2)}(\tau) \to 0 \quad \text{as} \quad \tau \to \infty \quad \text{for} \quad a = 1, \ldots, n-1. \quad (90)$$

Also, if we write

$$L_a^{(2)}(\tau) = L_a^{(1)} + \Delta L_a(\tau), \quad (91)$$

the condition of vanishing incoming radiation at $\tau = 0$ requires that

$$\sum_{a=1}^{n-1} \frac{\Delta L_a(0)}{1-\mu_i k_a} + \Delta Q = -\sum_{a=1}^{n-1} \frac{L_{-a}^{(2)}(0)}{1+\mu_i k_a} \qquad (i = \pm 1, \ldots, \pm - n). \quad (92)$$

These equations make the solution determinate. With the $L_a^{(2)}$'s expressed in the form (91), the source function may be finally written as

$$B^{(2)}(\tau) = B^{(1)}(\tau) + \tfrac{1}{2}\delta_1 + \tfrac{3}{4}F\left[\Delta Q + \sum_{a=1}^{n-1}\Delta L_a(\tau)\, e^{-k_a\tau} + \sum_{a=1}^{n-1} L_{-a}^{(2)}(\tau)\, e^{+k_a\tau}\right]. \quad (93)$$

When $n = 1$, the term in brackets appearing in equation (93) vanishes. For $n = 2$, $k_1 = \sqrt{35}/3 = 1.97203$, and the solution of equations (86) and (91) under the boundary conditions (92) leads to

$$\begin{aligned} B^{(2)}(\tau) = B^{(1)}(\tau) &+ \tfrac{1}{2}\delta_1 \\ &- 0.3328\,(1 + 0.1156\, e^{-k_1\tau}) \int_0^\infty e^{-k_1\tau}\,(\delta_3 - \tfrac{1}{3}\delta_4 + k_1\delta_4)\, d(k_1\tau) \\ &+ \tfrac{3}{4}\, e^{-k_1\tau} \int_0^\tau e^{k_1\tau}\,(\delta_3 - \tfrac{1}{3}\delta_1 - k_1\delta_4)\, d(k_1\tau) \\ &+ \tfrac{3}{4}\, e^{+k_1\tau} \int_\tau^\infty e^{-k_1\tau}\,(\delta_3 - \tfrac{1}{3}\delta_1 + k_1\delta_4)\, d(k_1\tau). \end{aligned} \quad (94)$$

It should be noticed that, strictly speaking, the function $B^{(1)}(\tau)$ appearing in equation (93) does not take the same values for every value of n. The averages, δ_m, also depend through their weight functions on the approximation n of the gray-body source function. The optical depth τ, thus, is not measured in terms of the same $\bar{\kappa}$ for every n. While this scheme of approximation has not been worked explicitly beyond $n = 2$, it would be expected that the use of the exact gray-body source function for $B^{(1)}(\tau)$ in equation (93) would lead to better results than those obtained with $B^{(1)}(\tau)$ for the particular n considered. The numerical values of the weight functions,

$$W_m(\tau) = \sum_j a_j \mu_j^m \frac{dI_{\nu j}^{(2)}}{d\tau} \simeq \int_{-1}^{+1} \frac{dI_\nu^{(1)}}{d\tau} \mu_j^m d\mu, \tag{95}$$

have been computed by Chandrasekhar (1950, § 79) for $m = 3$ and 4 by using the gray-body temperature distribution in the fourth approximation of the discrete ordinate method. A concrete application of these developments to the case of the solar atmosphere has been carried out by Münch (1947).

2.7. Mean Absorption Coefficients for Non-gray Atmospheres

Considering that Chandrasekhar's procedure for solving the non-gray problem has been the subject of some discussion, a few additional remarks regarding the use of mean absorption coefficients in non-gray problems seem in order. In the first place, it should be emphasized that $|\eta'_\nu - 1|$ in practice is never found to be a small number for every ν. Indeed, it may take quite large values, say, at the ionization frequencies of hydrogen and helium. However, as was remarked at the beginning of § 2.6, the validity of Chandrasekhar's method does not depend on the requirement that $|\eta'_\nu - 1| \ll 1$ everywhere. Rather, it assumes that some $\bar{\kappa}$ may be found such that, for all μ,

$$\left| \int_0^\infty (\eta'_\nu - 1)[I_\nu(\tau, \mu) - B_\nu(\tau)]\, d\nu \right| \ll |I(\tau, \mu) - B(\tau)|. \tag{96}$$

In this context, then, some of the remarks made by Kourganoff (1952, § 35.4) are irrelevant. Because of the appearance of μ in the inequality (96), it is clear that no $\bar{\kappa}$ can exist such as to make its left-hand member vanish. We may attempt instead to satisfy relation (96) in the mean,

$$\left| \int_0^\infty (\eta'_\nu - 1)[J_\nu(\tau) - B_\nu(\tau)]\, d\nu \right| \ll |J(\tau) - B(\tau)|. \tag{97}$$

The departures of the temperature distribution from that in a gray atmosphere would then be small. But the requirement that inequality (97) be satisfied is in no way related to the question of the existence of a K-integral of the type (40).

A procedure to evaluate $\bar{\kappa}$ in such a way that a K-integral of the form (40)

is approximately satisfied has been proposed by Unsöld (1948, 1955, § 33). It is based on the approximate value of $F_\nu(\tau)$,

$$\tfrac{1}{2}F_\nu(\tau) = B_\nu(\tau)E_3(\eta_\nu) + [\tfrac{2}{3} - E_4(\eta_\nu) - \eta_\nu E_3(\eta_\nu)]\frac{1}{\eta_\nu'}\frac{dB_\nu}{d\tau}, \quad (98)$$

which results from expanding the function $B_\nu(t)$ being operated on by $\Lambda_\tau^{(2)}$ in equation (29), as a first-order Taylor series around $t = \tau$. Introducing equation (98) into (64), it follows that

$$\frac{1}{\bar{\kappa}}\int_0^\infty \left(\Gamma_1 + \frac{\kappa_\nu}{\bar{\kappa}}\Gamma_2\right)d\nu = \int_0^\infty \frac{1}{\kappa_\nu}\left(\Gamma_1 + \frac{\kappa_\nu}{\bar{\kappa}}\Gamma_2\right)d\nu, \quad (99)$$

where

$$\Gamma_1 \equiv \Gamma_1(\nu, \tau, \eta_\nu) = 2[\tfrac{2}{3} - E_4(\eta_\nu) - \eta_\nu E_3(\eta_\nu)]\frac{dB_\nu}{d\tau} \quad (100)$$

and

$$\Gamma_2 \equiv \Gamma_2(\nu, \tau, \eta_\nu) = 2B_\nu(\tau)E_3(\eta_\nu). \quad (101)$$

Since $0 < E_3(x) < \frac{1}{2}$ and $0 < E_4(x) + xE_3(x) < \frac{1}{3}$, the ratio Γ_1/Γ_2 is nearly equal to $d \ln B_\nu/d\tau$. Unsöld finds that this quantity has approximately the value $\Gamma_1/\Gamma_2 = 1.75$ at $\tau = 0$ and increases rapidly with τ to $\Gamma_1/\Gamma_2 = 20$ at $\tau = 3$. From equation (99) it would follow, then, that when $\eta_\nu' \simeq 1$, the definition of $\bar{\kappa}$ is effectively

$$\frac{1}{\bar{\kappa}}\int_0^\infty \Gamma_1 d\nu = \int_0^\infty \frac{1}{\kappa_\nu}\Gamma_1\, d\nu, \quad (102)$$

which is a harmonic mean rather than the straight mean suggested by the Chandrasekhar method of § 2.6. Letting $\tau \to \infty$ in equation (102), the definition of the Rosseland mean, $\bar{\kappa}_R$, is recovered:

$$\frac{1}{\bar{\kappa}_R}\int_0^\infty \frac{dB_\nu}{dT}\, d\nu = \int_0^\infty \frac{1}{\kappa_\nu}\frac{dB_\nu}{dT}\, d\nu, \quad (103)$$

the use of which in the theory of the stellar interior is justified by quite different consideration.

In regard to this argument given by Unsöld as a criticism of the Chandrasekhar mean, it should be recalled that first-order Taylor expansions of the type (98) may be quite inaccurate, as Kourganoff (1952, § 34.5) has remarked. For $\tau < 1$ the gray-body temperature distribution gives non-negligible values for the first and higher τ-derivatives of T. In fact, the expansion is meaningless near $\tau = 0$, since here $dT/d\tau$ diverges logarithmically. But, besides the slow convergence of the series expansion, a more important point is that in determining $\bar{\kappa}$ by equation (99), there is no reason to expect that the inequality (97) will be satisfied, and this is precisely the condition insuring that the temperature distribution will approach that in a gray atmosphere.

If we wish to satisfy inequality (97) within the framework of Unsöld's

scheme, we may derive from equation (28) the first-order Taylor expansion,

$$J_\nu(\tau) - B_\nu(\tau) = \Gamma_4 + \frac{\bar{\kappa}}{\kappa_\nu}\Gamma_3, \tag{104}$$

where

$$\Gamma_4 = -\tfrac{1}{2}B_\nu(\tau)E_2(\eta_\nu) \tag{105}$$

and

$$\Gamma_3 = \tfrac{1}{2}[E_3(\eta_\nu) + \eta_\nu E_2(\eta_\nu)]\frac{dB_\nu}{d\tau}. \tag{106}$$

Following the same approximations as those used by Unsöld for his estimate of Γ_1 and Γ_2, we find that $\Gamma_3 < -\Gamma_4$. The ratio $-\Gamma_4/\Gamma_3$ has the value 2.7 at $\tau = 0$ and increases monotonically to 8.74 at $\tau = 3$. The inequality (97) will thus be approximately satisfied if

$$\int_0^\infty (\eta'_\nu - 1)\Gamma_4 d\nu = 0 \quad \text{or} \quad \bar{\kappa}\int_0^\infty \Gamma_4 d\nu = \int_0^\infty \kappa_\nu \Gamma_4 d\nu, \tag{107}$$

which is a straight mean, like κ_c defined in equation (84), rather than a harmonic mean, like κ_R defined in equation (103). If the dependence on η_ν of Γ_3 could be disregarded, equation (107) would lead to the "Planck mean,"

$$\bar{\kappa}_P B(T) = \int_0^\infty \kappa_\nu B_\nu(T)\, d\nu, \tag{108}$$

used by Michard (1949).

The generality of the arguments leading to definitions (102) and (107) is only superficial. They are subject to the same objections that may be raised against Chandrasekhar's method of § 2.6. That is to say, for some type of frequency variations of κ_ν the series expansions on which they are based break down. In such cases purely numerical methods must be followed. The practicability of numerical iteration procedures is based essentially on the fact, shown clearly by equations (104), (105), and (106), that as η_ν increases, $J_\nu \to B_\nu$ rapidly. Consequently, the gray-body temperature distribution always provides some sort of approximation, except for small τ. Since the meaning of such an approximation is well defined only in Chandrasekhar's method of § 2.6, it should be considered as the logical starting point for the numerical solutions which we consider next.

2.8. Variational Solutions of the Non-gray Problem

Suppose that for a stellar atmosphere of given parameters πF, g, and $\{A_i\}$, a model were constructed in the manner explained in § 1.1, using an a priori adopted temperature distribution $T^{(1)}(\tau)$. The mean absorption coefficient, $\bar{\kappa}$, measuring τ may be arbitrarily defined. If the monochromatic fluxes $F_\nu^{(1)}(\tau)$ are computed from equation (29), we may find out to what extent the atmosphere approaches a state of radiative equilibrium by evaluating

$$F_\nu^{(1)}(\tau) = 2\int_0^\infty \Lambda_\tau^{(2)}\{\eta_\nu, B_\nu[T^{(1)}(\tau)]\}\, d\nu. \tag{109}$$

The choice of $T^{(1)}(\tau)$ and $\bar{\kappa}$ being arbitrary, in general it will be found that

$$\Delta F^{(1)}(\tau) = F^{(1)}(\tau) - F \neq 0 . \tag{110}$$

The problem of introducing variations in $T^{(1)}(\tau)$ such as to make the corresponding flux equal to the given constant F then arises.

The highly complex dependence on τ of the functions being operated on by $\Lambda_\tau^{(2)}$ in equation (109) makes impractical any attempt to introduce variations in $T^{(1)}(\tau)$ directly in this equation. Instead, we may evaluate the source function $B^{(2)}(\tau)$ in a gray atmosphere with flux $F_g^{(2)}(\tau)$ equal to $F - \Delta F^{(1)}(\tau)$. The non-gray flux $F^{(2)}(\tau)$, evaluated from an equation similar to (109) but involving $T^{(2)} = T^{(2)}[B^{(2)}(\tau)]$, would then be expected to be more nearly equal to the constant F than $F^{(1)}(\tau)$ was. Because η_ν and $\bar{\kappa}$ also vary when $T(\tau)$ is changed, there is no assurance that $F^{(2)}(\tau)$ will be constant. But in an obvious manner a series of successive iterations could be carried out which would be expected to converge to the desired solution, on account of the monotonic nature of the operator $\Lambda_\tau^{(2)}$ (Hopf 1934, § 31). This method of solution is referred to as the "$\Lambda^{(2)}$ or flux iteration process."

i) Strömgren has developed a convenient method to carry out the flux iteration process (cf. Swihart 1956*a*). It is based on a starting approximation of the form

$$B^{(1)}(\tau) = \tfrac{3}{4}F[a_0 + a_1\tau + a_2E_2(\tau) + a_3E_3(\tau)] . \tag{111}$$

A functional dependence on τ of the form (111) represents the source function in a gray atmosphere very closely with the constants a_i given by Kourganoff (1952, § 25.3). The integrations required to obtain $F_\nu^{(1)}(\tau)$ are approximated by Gauss-Jacobi weighted sums over the appropriate representative levels (Chandrasekhar 1950, § 23; Reisz 1950, 1954), and the integration over ν leading to $F^{(1)}(\tau)$ is performed numerically. Now let the source function $B^{(2)}(\tau)$ be represented by an equation of the form

$$B^{(2)}(\tau) = B^{(1)}(\tau) + \tfrac{3}{4}F[\Delta a_0 + \Delta a_1\tau + \Delta a_2E_2(\tau) + \Delta a_3E_3(\tau)] . \tag{112}$$

The equation for the variations Δa_i of the parameters, then, are

$$\sum_{i=0}^{3} \Delta a_i\phi_i(\tau) = -\frac{4}{3}\frac{\Delta F^{(1)}}{F}, \tag{113}$$

where

$$\begin{aligned} \phi_0(\tau) &= 2\Lambda_\tau^{(2)}(1), & \phi_2(\tau) &= 2\Lambda_\tau^{(2)}[E_2(\tau)], \\ \phi_1(\tau) &= 2\Lambda_\tau^{(2)}(\tau), & \phi_3(\tau) &= 2\Lambda_\tau^{(2)}[E_3(\tau)], \end{aligned} \tag{114}$$

either are elementary functions or may be found tabulated (Kourganoff 1952, Appendix II). Writing down equation (113) for four particular values of τ, the variations Δa_i are readily found.

ii) Unsöld (1955, § 43.B) follows a somewhat different procedure to evalu-

ate $B^{(2)}(\tau)$ in terms of $\Delta F^{(1)}(\tau)$. The conservation of energy in a gray atmosphere with flux F (not necessarily constant) requires that

$$B(\tau) = J(\tau) - \frac{1}{4}\frac{dF}{d\tau}. \tag{115}$$

The K-integral, on the other hand, under the approximation $J = 3K$ (Eddington approximation), gives

$$\frac{dJ}{d\tau} = \tfrac{3}{4}F, \tag{116}$$

an equation which may be integrated in the form

$$J(\tau) = \tfrac{1}{2}F(0) + \frac{3}{4}\int_0^\tau F\,d\tau, \tag{117}$$

when the approximate boundary condition $2J(0) = F(0)$ is imposed. The variation $\Delta B^{(1)}(\tau)$ of the source function may then be obtained from equations (115) and (117) in the form

$$\begin{aligned}\Delta B^{(1)}(\tau) &= B^{(2)}(\tau) - B^{(1)}(\tau)\\ &= -\tfrac{1}{2}\Delta F^{(1)}(0) - \frac{3}{4}\int_0^\tau \Delta F^{(1)}(\tau)\,d\tau + \frac{1}{4}\frac{d}{d\tau}[\Delta F^{(1)}(\tau)]\,.\end{aligned} \tag{118}$$

The approximations involved in the procedure discussed above restrict its applicability to the deeper layers ($\tau < 0.3$), and on this account Strömgren's method of § 2.8i has definite advantage.

iii) An alternative method (Unsöld 1947; Pecker 1950) to correct an initial temperature distribution $T^{(1)}(\tau)$ is based on the numerical determination of the mean intensity,

$$J_\nu^{(1)}(\tau) = \tfrac{1}{2}\Lambda_\tau^{(1)}\{B_\nu[T^{(1)}], \eta_\nu\}. \tag{119}$$

From the equation of radiative equilibrium (22), written in the form

$$\int_0^\infty \kappa_\nu J_\nu^{(1)}(\tau)\,d\nu = \int_0^\infty \kappa_\nu B_\nu[T^{(2)}(\tau)]\,d\nu, \tag{120}$$

it is then attempted to determine $T^{(2)}(\tau)$ by a purely numerical process of trial and error. In a straightforward manner, this $\Lambda^{(1)}$ iteration process is generalized to arbitrarily high orders. An actual proof of the convergence of the process has been constructed by V. Weidemann (1952), disregarding variations of κ_ν at successive iterations.

§ 3. THERMODYNAMIC PRINCIPLES

3.1. The State of Local Thermodynamic Equilibrium

The determination of the thermal properties of a stellar atmosphere, considered in the preceding paragraphs, depends critically on the degree of ap-

proximation to which the Kirchhoff-Planck relation (20) may be locally satisfied. A rigorous evaluation of the emission and absorption coefficients in a medium not in strict thermodynamic equilibrium would depend on the detailed description of events following "collisions" of photons and material particles. The complexity of the mathematics involved and our lack of quantitative information regarding collision cross-sections prevent us from considering any physically significant problem in such general terms. Attempts to "justify" Kirchhoff's law thus have to be restricted to an evaluation of the relative importance of processes which tend to establish equilibrium and those that disrupt it. Let us consider an element of volume $\Delta V = R^3$ in a stellar atmosphere and the course of events following the photoionization of one constituent atom or ion. Were the density of matter so low that the photoelectron was recaptured before exchanging energy with other particles of the medium, the quantum emitted during recombination would only have been scattered without change in its energy. If, on the contrary, many elastic particle collisions take place between ionization and recombination, the energy of the re-emitted quantum will not keep a direct relation to that of the ionizing quantum and, instead, will reflect statistically the kinematic properties of the particle assembly. A temperature (kinetic) characteristic of ΔV may then be defined, when R is large compared with the kinetic mean-free path of the material particles, but small with the mean-free path of a quantum of radiation. Such a condition is amply satisfied even under conditions as extreme as those found in the interstellar medium (Böhm and Aller 1947). Now the emission and absorption properties of the gas depend on the distribution of the atoms among their various energy states and on the probabilities of transition between such states. Consider again the element of volume ΔV, where the kinetic temperature T prevails, and an identical volume $\mu V'$ in strict thermodynamic equilibrium at temperature T'. The transition probabilities are universal constants, but the distribution of atoms among the energy states may be different in ΔV and $\Delta V'$. If, however, collision processes are predominant over radiative processes for populating the energy states, the emission and absorption in ΔV and $\Delta V'$ will be the same, and hence Kirchhoff's law, valid in $\Delta V'$, will also hold in ΔV.

The application of this criterion is particularly simple in the case of solar-type atmospheres, where the continuous absorption is predominantly produced by the negative ion of hydrogen (H^-). We then have to compute the population of only one level—the ground state—of energy $-h\nu_0$. Let a_ν be the cross-section for photoionization of an H^- ion. The number of ionizations taking place per unit time and expressed per H^- ion in the volume ΔV, where the mean intensity of radiation is J_ν, is then given by

$$\int_{\nu_0}^{\infty} a_\nu J_\nu \frac{d\nu}{h\nu}, \tag{121}$$

and this quantity in the steady state is also equal to the number of recombinations taking place. The difference from unity of the ratio between (121) and the corresponding number in thermodynamic equilibrium,

$$C = \frac{\int_{\nu_0}^{\infty} a_\nu J_\nu d\nu / h\nu}{\int_{\nu_0}^{\infty} a_\nu B_\nu d\nu / h\nu}, \tag{122}$$

then measures the departure of the relation between the emission and the absorption coefficients from the value given by Kirchhoff's law. The calculations of Rudkjöbing (1941) and Swihart (1956*b*) have shown that the departures from unity of the quantity C are negligible in the solar atmosphere. Pagel (1956) has shown that this conclusion holds true even in the lower chromosphere.

When photoionization from an excited state is an effective absorption agent, as in the case of neutral hydrogen, the calculations become quite difficult, as the population of the excited state is determined by the strength of an absorption line. An approximate evaluation of the degree of ionization of hydrogen at an optical depth $\tau = 0.01$ in the model atmosphere of 10 Lacertae has been carried out by Traving (1957), who found $C = 0.87$.

3.2. Departures from the State of Radiative Equilibrium

The mechanism of energy transport by radiative processes may, under certain conditions, become unstable against a small perturbation. Consider an element of gas Δm in a medium in radiative equilibrium. When Δm undergoes a sudden increase in temperature, it will expand and move upward. If Δm rises sufficiently slowly, it will do so in pressure equilibrium with its surroundings, and its temperature will change adiabatically. Inertia and friction forces then do not come into play. Now, if the adiabatic temperature gradient is not steeper than the radiative one prevailing in the surrounding medium, Δm will remain during its motion at a higher temperature than its surroundings, and hence it will continue to be lifted upward. If, on the contrary, Δm changes its temperature at a faster rate than that of the neighborhood, it will eventually reach a point where the temperature, pressure, and density are the same in Δm and in the surrounding medium. The disturbance will then die out. An entirely similar argument may be constructed when Δm suffers a sudden decrease in temperature, leading to the same relation between the temperature gradients. In this fashion Schwarzschild (1906) established the criterion stating that the radiative temperature gradient is unstable whenever its absolute value exceeds that of the adiabatic gradient,

$$\left|\frac{dT}{dz}\right|_{\text{ad}} < \left|\frac{dT}{dz}\right|_{\text{rad}}. \tag{123}$$

A more convenient form of (123) may be derived from the equation of hydrostatic equilibrium (1) and the equation of state (8). When radiation pressure is negligible, we have

$$\frac{k}{\mu H}\frac{dT}{dz} = -g\frac{d\ln T}{d\ln P}, \tag{124}$$

and (123) may be rewritten in the form

$$\left|\frac{d\ln T}{d\ln P}\right|_{\text{ad}} < \left|\frac{d\ln T}{d\ln P}\right|_{\text{rad}}. \tag{125}$$

For the radiative gradient we can write

$$\left|\frac{d\ln T}{d\ln P}\right|_{\text{rad}} = \frac{P\bar{\kappa}}{4g}\frac{1+q'(\tau)}{\tau+q(\tau)}, \tag{126}$$

where $q(\tau)$ specifies the source function for the particular atmosphere considered through equation (43).

Suppose, now, that the matter were a gas with ratio of specific heats γ. Then

$$\left|\frac{d\ln T}{d\ln P}\right|_{\text{ad}} = \frac{\gamma-1}{\gamma}, \tag{127}$$

and for a monatomic gas this ratio would be $\frac{2}{5}$. We thus see that if the radiative temperature gradient, as given by equation (126), became larger than 0.40, it would be unstable, and a small perturbation would lead to a system of up-and-down convective currents. However, the material in a stellar atmosphere does not behave, in this respect, like a monatomic gas, for a temperature rise in an element of mass Δm not only increases the kinetic energy of the particles but also may perform ionization work. A gas undergoing ionization in its behavior approaches a polyatomic gas, and its effective $(\gamma - 1)/\gamma$ becomes less than 0.40. Because of the large cosmic abundance of hydrogen, as Unsöld (1931) first pointed out, at those layers where the ionization of hydrogen becomes appreciable, the effective γ diminishes and $\bar{\kappa}$ increases, with the consequence that inequality (125) is generally satisfied. It is for this reason that the regions of the cooler stellar atmospheres where equation (127) is satisfied are referred to as the "hydrogen convection layers."

From general thermodynamic principles (Unsöld 1955, § 56) it is an easy matter to calculate the ratio of specific heats for a gas mixture of any composition and state of ionization. Once a model atmosphere has been computed on the assumption of strict radiative equilibrium, the application of the Schwarzschild criterion to test its stability against convection is a quite straightforward procedure. However, the hydrodynamic problem of finding out the exact nature of the eventual state of equilibrium in those cases when the radiative temperature gradient is unstable offers great difficulties, essentially unsolved today. Whenever the internal energy of an element, Δm, is large compared with the net

amount of energy flowing through it, the actual temperature gradient must have very nearly the adiabatic value. For, under such circumstances, even very slight mass motions are sufficient to reduce a superadiabatic gradient to a stable one which differs from the adiabatic gradient by a negligible amount (Biermann 1932, 1935; Cowling 1934). In a stellar atmosphere, however, this condition is not always satisfied, and an appreciable superadiabatic gradient may be maintained. Convection may diminish the temperature gradient from its radiative value, but it never becomes the predominant process of energy transfer. Attempts have been made to calculate the energy transport by convection, using the results of phenomenological theories of fully developed turbulence which may not be applicable to a convective regime. Besides, they involve "unspecified constants of order unity" and dimensional parameters such as the "mean-free path of turbulent elements" which cannot be computed on first principles. With some success these theories have been applied to the solar atmosphere (Biermann 1938; Böhm-Vitense 1953), where we have observational information regarding some parameters of the convective regime (granulation), but they are far from being applicable to the case of stars. It is on this account that the calculation of certain types of model stellar atmospheres may be subject to uncertainty. In the case of A-type atmospheres, where the upper limit of the hydrogen convection zone is at an optical depth as small as $\tau = 0.2$, the uncertainties in the temperature gradient may have observable effects on their line spectrum. In the solar atmosphere, convection sets in at around $\tau = 1.4$, so deep that it does not affect the temperature in those regions where the line spectrum originates and also hardly influences the observable continuum. In the coolest stars (M dwarfs) the hydrogen convection zone is sufficiently deep not to affect directly the observable spectrum. However, it is so extensive that it determines the structure of the stars as a whole (Osterbrock 1953; Limber 1958).

3.3. Radiation Pressure in High-Temperature Stars

Consider a pencil of radiation with axially symmetric intensity $I_\nu(z, \mu)$ traversing an element of surface dS in a direction $\cos^{-1}\mu$ with its normal. Since the amount of energy flowing through dS in time dt within a solid angle $d\omega$ and in the frequency range $(\nu, \nu + d\nu)$ is

$$dE_\nu = I_\nu(z, \mu)\, \mu d\omega d\nu dS dt\,, \tag{128}$$

it carries a momentum dE_ν/c. The normal component of the momentum transferred across dS is $\mu dE_\nu/c$, and the net rate of transfer of momentum across dS, expressed per unit area and unit frequency range, by definition equal to the radiation pressure $p_R(\nu)$, will be

$$p_R(\nu) = \frac{2\pi}{c}\int_{-1}^{+1} I_\nu(z, \mu)\, \mu^2 d\mu = \frac{4\pi}{c} K_\nu(z)\,. \tag{129}$$

The τ-gradient of the total radiation pressure, entering in the equation of hydrostatic equilibrium (6), in view of equation (19) may be written thus:

$$\frac{dp_R}{d\tau} = \frac{\pi}{c}\int_0^\infty \eta'_\nu F_\nu d\nu . \tag{130}$$

For a gray atmosphere ($\eta'_\nu = 1$) or for a non-gray atmosphere with a mean $\bar{\kappa}$ defined exactly by equation (64), we would have

$$\frac{dp_R}{d\tau} = \frac{\pi}{c}F = \frac{\sigma_R}{c}T_e^4, \tag{131}$$

a constant independent of depth. The practical definitions of $\bar{\kappa}$ as the Chandrasekhar mean or the Rosseland mean, however, will not, in general, lead to a constant radiation-pressure gradient.

For atmospheres in which radiation pressure is not negligible, scattering by free electrons is an important source of opacity. We then have to modify the definition of η'_ν, as it appears in equation (130), in order to include the coefficient of electron scattering per gram, σ_e, in the form

$$\eta'_\nu = \frac{\kappa_\nu + \sigma_e}{\bar{\kappa} + \sigma_e}. \tag{132}$$

The condition of constant net flux, however, remains the same, as in the pure absorption case, being given by equation (22). It is for this reason that we do not simply add σ_e to $\bar{\kappa}$ and then form a suitable mean. The total optical depth, of course, is measured in terms of $\bar{\kappa} + \sigma_e$, and the equation of hydrostatic equilibrium is

$$\frac{dp}{d\tau} = \frac{g}{\bar{\kappa} + \sigma_e} - \frac{\pi}{c}\int_0^\infty \eta'_\nu F_\nu d\nu . \tag{133}$$

In order to have a mechanically stable atmosphere, the τ-gradient of the gas pressure should be positive, and we should thus have

$$g \geq \frac{\pi}{c}(\bar{\kappa} + \sigma_e)\int_0^\infty \eta'_\nu F_\nu d\nu . \tag{134}$$

In the outermost layers of high-temperature stars, $\bar{\kappa} < \sigma_e$. Approximating the integral appearing in inequality (134) by its gray-body value, we may then take

$$g_0 = \frac{\sigma_R}{c}\sigma_e T_e^4 \tag{135}$$

as the minimum value that the surface gravity of an atmosphere with effective temperature T_e may take and still be mechanically stable. For ionized material, composed of 85 per cent hydrogen, by number, and the rest helium, $\sigma_e = 0.315$, and g_0, according to Miss Underhill (1949), takes the values given in Table 1. When radiation pressure is not negligible in a stellar atmosphere, the margin of stability against convection is also reduced. From Schwarzschild's criterion in

the form (123) it may be shown readily that the condition of instability when $p_R \neq 0$, instead of equation (125), is

$$\left|\frac{d \ln T}{d \ln p_G}\right|_{ad} < \left|\frac{d \ln T}{d \ln p_G}\right|_{rad}. \tag{136}$$

Writing

$$\frac{d \ln T}{d \ln p_G} = \frac{p_G}{T}\left(\frac{dp_G}{d\tau}\right)^{-1}\frac{dT}{d\tau}, \tag{137}$$

we see that, since radiation pressure diminishes the gas-pressure gradient, the right-hand side of the inequality will increase. On the other hand, for an inclosure containing a monatomic gas and radiation, which in this respect behaves like a gas with ratio of specific heats $\gamma = \frac{4}{3}$ (Chandrasekhar 1939), we have

$$\left|\frac{d \ln T}{d \ln P}\right|_{ad} = \frac{4p_R/p_G + 1}{16p_R/p_G + 5/2}, \tag{138}$$

and, therefore, the left-hand side of inequality (136) diminishes as p_R/p_G increases. The consideration of partial ionization in equation (138) (Underhill

TABLE 1

MINIMUM VALUES FOR SURFACE GRAVITIES OF MECHANICALLY STABLE ATMOSPHERES

T_e (°K)	g_0 (cm sec^{-2})	T_e (°K)	g_0 (cm sec^{-2})
10,000	6.0	30,000	0.48×10^3
15,000	30	40,000	1.52×10^3
20,000	95	50,000	3.72×10^3
25,000	230	60,000	7.41×10^3

1949) may further reduce the value of the adiabatic gradient, with the over-all consequence that the condition for instability (136) is more easily satisfied than when radiation pressure is not disregarded.

§ 4. THE PROCESS OF CONTINUOUS ABSORPTION

4.1. THE PROBABILITY COEFFICIENTS FOR PHOTOIONIZATION AND RECOMBINATION

The calculation of the absorption coefficient per gram of stellar material depends on the specification of single radiative transitions of the constituent particles. The interaction of an atom with radiation was first described by Einstein for transitions between two discrete states of energies, E_n and E_m ($E_n > E_m$), in terms of the well-known probability coefficients A_{nm}, B_{nm}, and B_{mn} of spontaneous emission, induced emission, and absorption, respectively. Since our main interest is the process of continuous absorption, we shall define here the corresponding probability coefficients for electron transitions between discrete and free-energy states. Consider an atom of ionization energy $h\nu_0$, in its

ground state, exposed to radiation of intensity I_ν. We postulate that the probability for the atom to become ionized in a time dt by the absorption of radiation in the frequency interval $(\nu, \nu + d\nu)$ is

$$\text{Prob. absorption:} \qquad p_\nu I_\nu d\nu dt \,. \tag{139}$$

The probability that in time dt the corresponding ion will capture in the ground state a free electron with velocity in the range $(v, v + dv)$ and distance in the interval $(r, r + dr)$ is postulated to be of the form

$$[f(v,r) + g(v,r)\, I_\nu]\, dt \,. \tag{140}$$

Consider an inclosure of unit volume in thermal equilibrium at temperature T, containing n_0 neutral atoms and n_1 ions, both in their ground states, and n_e free electrons. The number of electrons, dn_e, in the interval $(v, v + dv)$ is

$$dn_e = n_e \left(\frac{m}{2\pi kT}\right)^{3/2} e^{-mv^2/2kT} v^2 dv \,, \tag{141}$$

and the fraction of these electrons, which, moving in directions confined to a solid angle $d\omega$, will pass at a minimum distance in the range $(r, r + dr)$ from a given ion is

$$2\pi r dr\, v dt dn_e d\omega \,. \tag{142}$$

The number of electrons that travel in all directions with velocities $(v, v + dv)$ and at distances $(r, r + dr)$ follows, by integrating over all solid angles:

$$8\pi^2 r dr\, v dt dn_e = 8\pi^2 n_e \left(\frac{m}{2\pi kT}\right)^{3/2} e^{-mv^2/2kT} v^3 dv\, r dr\, dt. \tag{143}$$

The total number of such encounters in the inclosure per unit time, then, is

$$dN(v,r) = n_1 n_e 8\pi^2 \left(\frac{m}{2\pi kT}\right)^{3/2} e^{-mv^2/2kT} v^3 dv\, r dr \,. \tag{144}$$

Integrating between the minimum distance r_1, at which a non-quantal description of electron collisions is still allowed, and the distance r_2, at which the consideration of two-body encounters ceases to be valid (Debye radius), we obtain the total number of electron captures,

$$dN(v) = n_1 n_e 8\pi^2 \left(\frac{m}{2\pi kT}\right)^{3/2} e^{-mv^2/2kT} [F(v) + I_\nu G(v)]\, v^3 dv \,, \tag{145}$$

where

$$2\pi F(v) = 2\pi \int_{r_1}^{r_2} f(v,r)\, r dr \tag{146}$$

and

$$2\pi G(v) = 2\pi \int^{r_2} g(v,r)\, r dr \tag{147}$$

are the spontaneous and induced recombination cross-sections, respectively. In equilibrium the total number of ionizations, given by equation (139), multiplied by n_0 should balance that of the recombinations (145):

$$n_0 p_\nu I_\nu d\nu = n_1 n_e 8\pi^2 \left(\frac{m}{2\pi kT}\right)^{3/2} e^{-mv^2/2kT} [F(v) + I_\nu G(v)] v^3 dv. \quad (148)$$

Relating $d\nu$ to dv through the equation of the photoelectric effect,

$$h\nu = h\nu_0 + \tfrac{1}{2} m v^2, \quad (149)$$

we derive

$$p_\nu I_\nu = \frac{n_1 n_e}{n_0} \frac{8\pi^2 h}{m} \left(\frac{m}{2\pi kT}\right)^{3/2} e^{-mv^2/2kT} [F(v) + I_\nu G(v)] v^2. \quad (150)$$

Requiring that

$$\frac{n_1 n_e}{n_0} = 2 \frac{\varpi_1}{\varpi_0} \frac{(2\pi mkT)^{3/2}}{h^3} e^{-h\nu_0/kT} \quad (151)$$

and

$$I_\nu = \frac{2h\nu^3}{c^2} (e^{h\nu/kT} - 1)^{-1}, \quad (152)$$

we obtain

$$\frac{F(v)}{G(v)} = \frac{2h\nu^3}{c^2} \quad (153)$$

and

$$p_\nu = 2 \frac{\varpi_1}{\varpi_0} \frac{4\pi^2 m^2 c^2}{h^3} \frac{1}{\nu^3} v^2 F(v). \quad (154)$$

The probabilities of ionization and recombination are internal properties of the atom considered, and relations (153) and (154) hold in the absence of thermal equilibrium. Their values can be derived from quantum theory alone, independently of thermodynamic arguments, in terms of the matrix element of the position vector of the transition electron with respect to the initial and final states. It is of interest to notice that p_ν, being an atomic function, cannot depend on v. Since the probability for absorption at the ionization frequency is non-vanishing and finite, we see from equation (154) that, for small velocities, the spontaneous recombination cross-section is of the form

$$F(v) = \frac{\text{constant}}{v^2}. \quad (155)$$

The relation between the macroscopic absorption coefficient and the probability for absorption p_ν, defined above, may be established by considering the energy balance at the frequency ν in an elementary cylinder of height ds. The difference between the energy emitted and the energy absorbed equals the intensity gradient:

$$\frac{1}{h\nu} \frac{dI_\nu}{ds} = -n_0 p_\nu I_\nu + n_1 n_e \frac{8\pi^2 h}{m} \left(\frac{m}{2\pi kT}\right)^{3/2} e^{-mv^2/2kT} v^2 [F(v) + I_\nu G(v)]. \quad (156)$$

Rewriting this equation in the form of the equation of transfer (12), it is seen that

$$\kappa_\nu = \frac{h\nu}{\rho} n_0 p_\nu \left[1 - \frac{n_1 n_e}{n_0} \frac{8\pi^2 h}{m} \left(\frac{m}{2\pi kT} \right)^{3/2} e^{-mv^2/2kT} \frac{v^2 G(v)}{p_\nu} \right]. \quad (157)$$

From equations (149), (151), (152), (153), and (154) this expression may be reduced to the form

$$\kappa_\nu = \frac{h\nu_0}{\rho} n_0 p_\nu (1 - e^{-h\nu/kT}) . \quad (158)$$

The preceding considerations may be generalized without difficulty so as to include ionizations and recombinations from and to excited states, by suitably describing the relative population of excited states in terms of the combined Boltzmann and Saha equations. In the same manner the generalization to transitions between two positive energy states is carried out.

The macroscopic absorption coefficient, κ_ν, is thus evaluated as the aggregate of the atomic absorption coefficients

$$a_\nu = h\nu p_\nu , \quad (159)$$

weighted according to the population of the lower states of the transitions involved and multiplied by the factor $1 - e^{-h\nu/kT}$, which corrects for the effect of stimulated emissions.

4.2. The Sources of Continuous Absorption

We have outlined in the introduction the process of interpretation of a stellar spectrum in two successive steps. The first one consists in determining a model, and, on this basis, the properties of the spectrum to be compared with observation are then calculated. Such a dichotomy of the problem is possible only when an approximate estimate of the relative abundance of the elements producing continuous absorption is available. But, as Milne first pointed out, the intensity of a particular absorption line depends on the abundance ratio between the corresponding element and the elements producing the continuous absorption. Since the sum of the relative abundances of all elements is unity, it follows that, in a general way, the average strength of the line spectrum is fixed. In other words, the strength of the line spectrum determines the continuous absorption coefficient which must be accounted for by physical theory. It is on this account that serious difficulties were encountered in the early studies of stellar spectra. On the one hand, the classical analysis of the solar spectrum by Russell (1929) had indicated a hydrogen-to-metals abundance ratio (H:M) of the order of 10^3 by number. On the other hand, Unsöld (1938, § 36) found that, to account for the discontinuity observed in the continuous spectrum of stars along the spectral sequence, at the head of the Balmer series, an abundance ratio H:M $\simeq$ 50:1 was required. This low value of H:M followed from the assumption that the increasing continuous absorption of the metals is responsible for the de-

creasing Balmer jump between stars of type A and those of solar type. But, if such were the case, the predicted discontinuities in the continuous spectrum of the ionization limits of the abundant metals would be much larger than the observed ones. In fact, metal absorption edges were never observed, and, by extrapolating the line intensities of the corresponding series, it could be estimated that they would be essentially unobservable. A possible solution to this fundamental problem was suggested by Wildt (1939*a*, *b*), in terms of the absorption which could be attributed to the negative ion of hydrogen (H^-). The stability of this ion had been predicted theoretically by the same quantum-mechanical methods as those followed to study the ground state of the neutral helium atom. However, it was not until Chandrasekhar (1946) carried out his extensive study of H^- that the main features observed in the continuous spectrum of the stars were satisfactorily accounted for (Chandrasekhar and Münch 1947). With the recognition of H^- as a major source of continuous absorption, a full understanding of the relationship between the line and continuous spectrum of the stars has been achieved.

4.3. Continuous Absorption by Neutral Hydrogen

The quantum-mechanical calculations of the absorption coefficient of one hydrogen-like atom of nuclear charge Z in the state n provide a value

$$a_{\nu n}(\mathrm{H}) = \frac{64\pi^4}{3\sqrt{3}} \frac{m e^{10}}{c h^6} \frac{Z^4}{n^5 \nu^3} g_\nu(n) \qquad \text{for} \qquad \nu > \nu_n , \tag{160}$$

where $h\nu_n$ is the ionization energy of an atom in the state n and $g_\nu(n)$, the Gaunt factor, is a number which, for the region of the spectrum we are interested in, has a value close to unity. By summing over the states $n \leq 4$, approximating the sum over the remaining discrete states by an integral, and adding the contributions of the free-free transitions, Unsöld (1955, § 45) writes the continuous absorption coefficient per atom in the form

$$a_\nu(\mathrm{H}) = F \frac{D}{\alpha^3} , \tag{161}$$

where

$$\alpha = \frac{h\nu}{kT} , \tag{162}$$

$$F = \frac{64\pi^4}{3\sqrt{3}} \frac{m_e e^{10}}{c h^3} \frac{Z^4}{k^3 T^3} e^{-\alpha_1} , \tag{163}$$

and

$$D = \sum_{\alpha_n < \alpha}^{\alpha_4} \frac{e^{\alpha_n}}{n^3} + \frac{1}{2\alpha_1} e^{\alpha_5} . \tag{164}$$

Values of F and D for hydrogen ($Z = 1$) and various temperatures have been tabulated by Unsöld (1955, § 45) and Strömgren (1944).

4.4. The Absorption of H^-

The existence of H^- is due to incomplete shielding of the proton charge and to the high polarizability of the electron in the neutral hydrogen atom. Thus, although neutral helium and H^- are isoelectronic, their structure is not entirely alike, and the description of the more loosely bound ion required special consideration. The early efforts directed toward the evaluation of the radiative cross-sections of H^- (Massey and Bates 1940; Wheeler and Wildt 1942), not fully realizing this fact, were only partially successful. And it was through the theoretical work and numerical calculations of Chandrasekhar (1946) and his associates that reliable values for the absorption coefficient of H^- due to bound-free and free-free transitions became available. They are based on a wave function for the ground state involving eleven parameters determined by Henrich (1944*a*, *b*) so as to minimize the energy. Such a function predicts a binding energy of 0.747 ev for the outer electron, and the ionization limit is thus at λ 16500 A. The wave function used by Chandrasekhar for the positive energy state was that of an electron moving in the Hartree field of the hydrogen atom in the ground state, disregarding exchange and polarization effects. Recently Chandrasekhar (1958) has shown that the use of the twenty-parameter wave function computed by Hart and Herzberg (1957) improves his earlier calculations of the photoionization cross-sections by only a few per cent. The inaccuracies introduced into the absorption coefficients by the exchange and polarization forces is probably also quite small. Staver (1951) has shown that exchange and polarization forces contribute to the absorption coefficient in opposite senses, with the result that the values of the continuous absorption produced by free-free transitions, as evaluated by Chandrasekhar, probably are accurate within 20 per cent, while those for the bound-free transitions are accurate to 5 per cent.[1]

4.5. The Continuous Absorption of He I

The absorption coefficient of one neutral He atom, as in the case of hydrogen, is obtained by adding the contributions from each of the continua extending beyond the various series limits. Cross-sections for photoionization from the ground state, 1^1S, and from the metastable states, 2^3S and 2^1S, have recently been re-evaluated by Huang (1948). Those corresponding to the P–D and P–S continua from $n = 2$ have been calculated by Goldberg (1939). Since no calculations have been made for the photoionization cross-sections from levels with $n = 3$ or for free-free transitions, their contribution can be estimated only on the assumption that it is hydrogen-like (Underhill 1950; Vitense 1951). The

[1] *Note added in proof.*—The continuous absorption coefficients due to free-free transitions of H^-, recently evaluated by T. Ohmura and H. Ohmura (*Ap. J.*, **131**, 8, 1960), taking into consideration exchange and polarization, are about 60 per cent of those given by Chandrasekhar and Breen.

addition of the contribution of all discrete states with $n \geq 3$ and of the free-energy states leads to

$$a_\nu(\text{He I}, n \geq 3) = \frac{64\pi^4}{3\sqrt{3}} \frac{m e^{10}}{c h^6} \frac{e^{-a_1}}{\nu^3} \left[Z_{\text{eff}}^4 \left(\sum_{n>3}^{5} \frac{e^{a_n}}{n^3} + \frac{e^{a_5} - 1}{2 a_1} \right) + \frac{2}{a_1} \right], \quad (165)$$

a formula differing from equation (161) only by the appearance of the effective charge, Z_{eff}, which may be estimated from the position of the series limits and is found to be quite close to unity. The different statistical weights of He I and H account for other differences between equations (161) and (165). Tables of a_ν (He I) for the range $0.10 < 5040°/T < 0.50$ and at 35 wave lengths between 228 and 2279 A have been published by Ueno, Saito, and Jugaku (1954).

4.6. The Continuous Absorption of He II

The cross-sections for photoionization of He II differ from those of H only through the charge Z and the Gaunt factors. They are computed on the assumption that the Gaunt factors are unity and setting $Z = 2$ in equation (164), with corresponding changes in the a_n's. A table of a_ν (He II) for $0.10 < 5040°/T < 0.20$ and at 28 wave lengths between 228 and 2279 A has been published by Ueno, Saito, and Jugaku (1954).

4.7. The Continuous Absorption of the Metals

Quantum-mechanical calculations of the photoionization cross-sections for the ground state of a few of the heavier atoms and ions have been carried out. A review of the methods followed and the numerical results available has been given by Bates (1946*a*, *b*). These calculations, however, are not directly applicable to the stellar problem, since photoionization from excited states is quite important. Lacking any other approach, it has been found necessary to use hydrogen-like approximations for these excited states (Vitense 1951). By introducing in equation (164) the appropriate a's and effective charges Z_{eff}, an estimate of the contribution of the heavier atoms and ions to the continuous absorption coefficient may be obtained when their abundances are known. To give an idea of the contribution of the metals to the continuous absorption coefficient in solar-type atmospheres, we summarize Swihart's (1956*b*) results. Adopting $\text{H:M} = 10^{3.8}$ and substituting for the metal mixture an average element with ionization potential 7.75 ev and effective charge 2.5, this author obtains the continuous absorption coefficients per gram given in Table 2. The values refer to $T = 5850°$ K and $\log p_e = 1.50$. It may thus be seen that at the Balmer limit the continuous absorption of the metals amounts to about 20 per cent of that produced by H and H^-, increasing rapidly toward the ultraviolet. Their contribution to the mean absorption coefficient is, nevertheless, relatively small, because of the small values of the weight function in the ultraviolet. The increase in $\bar{\kappa}$ due to metal absorption, according to Swihart (1956*c*) increases the monochromatic fluxes of a model solar atmosphere to the

red of the Balmer limit by about 14 per cent. The contribution of the metals to the continuous absorption coefficient for other temperatures has been evaluated by Miss Vitense (1951) on a hydrogen-like approximation and was included in her extensive graphical representation of $\kappa_\nu\ (p_e, T)$.

The hydrogen-like approximation is not expected to give good results even for non-penetrating orbits of a single electron outside a closed core (Bates 1939, 1946*a*, *b*). By using self-consistent field approximations for the wave functions of the initial and final states, the main effect of the core on the valence electron may be taken into account. The calculations for lithium thus made by Trumpy (1931) are in fair agreement (Dichtburn 1956) with the observations of Tunstead (1953). The observed variation with wave length of the photoionization cross-sections is predicted satisfactorily, although the calculated absolute values are about 40 per cent higher than the experimental values. The calculations by Seaton (1951) using Hartree-Fock exchange-wave functions for sodium are in better agreement with observations (Dichtburn, Jutsum, and

TABLE 2

MASS ABSORPTION COEFFICIENT OF METALS
($T = 5850\,°\mathrm{K}$; $\log p_e = 1.50$)

λ (A)	κ_ν (M)	κ_ν (H+H⁻)	λ (A)	κ_ν (M)	κ_ν (H+H⁻)
3647.....	0.08	0.45	2084.....	2.4	0.21
2652.....	0.39	0.28	1459.....	130	0.18

Marr 1953). For other atoms than the alkali metals the agreement between theoretical and experimental cross-sections is much worse. For example, Bates and Massey (1941) calculate for calcium at the ionization limit a cross-section equal to 25×10^{-18} cm², a value which is fifty times larger than the observed one (Jutsum 1954). These and other open disagreements between theory and experiment raise the serious problem as to whether the estimates made in the past of the absorption coefficients of such astrophysically important elements as carbon, nitrogen, and oxygen, are reliable.

4.8. THE CONTINUOUS ABSORPTION OF THE H_2^+ MOLECULE

Some time ago Wildt (1947) suggested that a significant contribution to the continuous absorption might arise from bound-free absorption by H_2^+ ions,

$$H_2^+ (1s\sigma) + h\nu \rightarrow (H + H^+)(2p\sigma),$$

and from free-free absorption by colliding H atoms and H^+ ions,

$$(H + H^+)(1s\sigma + h\nu) \rightarrow (H + H^+)(2p\sigma).$$

Wildt estimated approximately the absorption coefficient due to these processes and found that, for the case of the solar atmosphere, it becomes of the same

order of magnitude as that of H^-, at around λ 2000 A, and increases toward shorter wave lengths. It thus appears that H_2^+ produces appreciable continuous absorption only in the far ultraviolet, but even in this region it is of less importance than the metals.

A more accurate evaluation of the absorption cross-section of H_2^+ has been recently made by Bates (1952). No calculation of the resulting contribution to the mass absorption coefficient has been published in detail. However, according to Osawa (1956), Strömgren (unpublished) has revised his earlier tabulation of $\bar{\kappa}$ and η_ν' (Strömgren 1944), incorporating the best values now available for the absorption coefficients of the various sources. In an atmosphere with T_e = 7560° K and log g = 4.0 computed by Osawa (1956), the absorption produced by H_2^+ amounts to about 10 per cent of that resulting from H and H^- in the violet and visual regions of the spectrum. The consideration of H_2^+ as an absorption source would thus appear to be of importance in F-type stars.

4.9 Scattering by Free Electrons

The cross-section of an electron for scattering of natural (unpolarized) light is given by Thomson's classical formula,

$$\sigma_e = \frac{8\pi}{3}\frac{e^4}{m^2c^4} = 6.65 \times 10^{-25}\ \mathrm{cm}^2, \tag{166}$$

which holds independently of frequency in the non-relativistic region of the spectrum. The scattered light is plane-polarized at right angles to the plane of scattering and the intensities of the scattered light in directions parallel and perpendicular to the plane of scattering are in the ratio $\cos^2\Theta$:1, where Θ is the angle of scattering. In stellar atmospheres of high effective temperature and low surface gravity, electron scattering may become as effective an agent to transport energy as photoionization is. It is always true, however, that only absorption processes are relevant for establishing the thermal equilibrium of the particles. For an atmosphere composed only of ionized hydrogen, the coefficient of electron scattering per gram would be

$$\sigma = \frac{\sigma_e}{\mathrm{H}} = 0.40\ \mathrm{cm}^2\ \mathrm{gm}^{-1}, \tag{167}$$

a quantity which clearly represents an upper limit to the value of the mass-scattering coefficient. In combining electron scattering with other sources of absorption, to compute either the mean absorption coefficient or the monochromatic fluxes, it should be recalled that σ_e is not multiplied by the stimulated emission factor $1 - e^{-h\nu/kT}$.

§ 5. INTERACTION OF CONTINUOUS AND LINE SPECTRA

5.1. Effect of Absorption Lines on Temperature Distribution of a Stellar Atmosphere

While discussing the thermal state of a stellar atmosphere, we have so far disregarded the possibility that discrete atomic transitions might be an effective

process of energy interchange. Observations of the cooler stars indeed suggest that the fraction δF of the total energy removed by the lines from the continuous spectrum is not entirely negligible. In the case of the solar spectrum, δF is only about 10 per cent (Mulders 1934; Wempe 1947; Michard 1950). But in cooler stars—say supergiants of type M—the crowding of the absorption lines becomes so great that the very concept of continuous spectrum loses its meaning (Spitzer 1939). The problem of the formation of the continuous spectrum cannot then be even approximately separated from that of the line spectrum. Restricting ourselves to the case of small δF, we shall study the manner in which the line spectrum may modify the structure of a stellar atmosphere.

The theory of line formation is considered in detail in chapter 3 of this volume. For our present purposes we may recall that most absorption lines, being subordinate ones, are formed nearly in a pure absorption process. The probability that a quantum of radiation absorbed in certain line transition is re-emitted with the same frequency is vanishingly small. Rather, the balancing downward transition very probably involves a different quantum related to the temperature via the continuum. Resonance lines are so few that we may disregard them in this context, especially since the mechanism of non-coherent scattering, which gives them origin, also has the characteristics of an absorption process. We may consider the line spectrum, then, as producing sharp variations in the wave-length dependence of the continuous absorption coefficient. The problem of calculating the effect of the line spectrum on the temperature distribution or, as Milne called it, the "blanketing effect of the reversing layer" would thus seem to depend on the complete specification of the line absorption coefficient as a function of wave length and depth. The dependence of the line absorption coefficient on temperature and pressure is, however, so complicated that it is hardly feasible to include such a dependence as part of the problem we wish to solve. Instead, we suppose that the model atmosphere obtained, disregarding the lines, is a good first approximation, on the basis of which the line absorption coefficient may be explicitly calculated. Such a perturbation procedure necessarily has to be carried out numerically. It is of interest, thus, to consider, first, a highly idealized model for the distribution of lines in a stellar spectrum to illustrate the general effects to be expected.

5.2. Chandrasekhar's "Picket-Fence" Model

Imagine an atmosphere with continuous absorption coefficient κ_1 independent of frequency and with absorption lines distributed throughout the spectrum with uniform probability w_2. The probability that the interval $(\nu, \nu + d\nu)$ s free of absorption lines, then, is $w_1 d\nu = (1 - w_2)d\nu$. Suppose, further, that the line absorption coefficient has the value κ_2 independent of frequency in the interval covered by lines. The equations of transfer for radiation in the continuum and in the lines, then, are

$$\mu \frac{\partial}{\partial \tau} I_\nu^{(\alpha)} = \eta_\alpha' [I_\nu^{(\alpha)} - w_\alpha B_\nu] \qquad (\alpha = 1, 2), \quad (168)$$

where the subscript α denotes that radiation refers to the continuous ($\alpha = 1$) or to the lines ($\alpha = 2$). As in § 2.1, the optical depth τ is measured in terms of a mean absorption coefficient $\bar{\kappa}$, to be specified later, and

$$\eta'_\alpha = \frac{\kappa_\alpha}{\bar{\kappa}}. \tag{169}$$

We wish to solve the system of equations under the condition of a constant net flux,

$$\int_0^\infty [F_\nu^{(1)} + F_\nu^{(2)}]\, d\nu = F \qquad \text{(constant)}. \tag{170}$$

Integrating equation (168) over frequency and over angle, we find that equation (170) is equivalent to

$$\sum_\alpha \eta'_\alpha J^{(\alpha)} = B(\tau) \sum_\alpha w_\alpha \eta'_\alpha, \tag{171}$$

and the equations to be solved are thus

$$\frac{\mu}{\eta'_\alpha}\frac{d}{d\tau} I^{(\alpha)} = I^{(\alpha)} - \frac{w_\alpha}{\left(\sum_\beta \eta'_\beta w_\beta\right)} \sum_\beta \eta'_\beta J^{(\beta)} \quad (\alpha = 1, 2). \tag{172}$$

By the method of discrete ordinates, this system of simultaneous equations may be easily solved (Münch 1946). It is found that, in the nth approximation,

$$B(\tau) = \frac{3}{4}\frac{F}{\sum_\alpha w_\alpha/\eta'_\alpha}\left(\tau + Q + \sum_{\beta=1}^{2n-1} L_\beta e^{-k_\beta \tau}\right), \tag{173}$$

where the k_α's are the positive roots of the characteristic equation

$$\sum_\alpha w_\alpha \eta'_\alpha \left(1 - \frac{1}{2}\sum_{j=-n}^{n} \frac{a_j}{1 + k\mu_j/\eta'_\alpha}\right) = 0 \tag{174}$$

and the L_β's are fixed by the boundary conditions

$$\sum_{\beta=1}^{2n-1} \frac{L_\beta}{1 - k_\beta \mu_i/\eta'_\alpha} + Q = \frac{\mu_i}{\eta'_\alpha} \qquad \begin{pmatrix} i = 1, 2, \ldots, n \\ \alpha = 1, 2 \end{pmatrix}. \tag{175}$$

Quite generally, independently of n, it has been proved that

$$B(\tau = 0) = \frac{\sqrt{3}}{4} F\left[\left(\sum_\alpha w_\alpha \eta'_\alpha\right)\left(\sum_\alpha \frac{w_\alpha}{\eta'_\alpha}\right)\right]^{-1/2}; \tag{176}$$

and, since

$$\begin{aligned}\left(\sum_\alpha w_\alpha \eta'_\alpha\right)\left(\sum_\alpha \frac{w_\alpha}{\eta'_\alpha}\right) &= \left(w_1 + w_2 \frac{\kappa_2}{\kappa_1}\right)\left(w_1 + w_2 \frac{\kappa_1}{\kappa_2}\right) \\ &= 1 + w_1 w_2 \frac{\kappa_1}{\kappa_2}\left(\frac{\kappa_2}{\kappa_1} - 1\right)^2,\end{aligned} \tag{177}$$

it follows from equation (176) that

$$B(\tau = 0) < \frac{\sqrt{3}}{4} F \tag{178}$$

if $w_2 \neq 0$ and $\kappa_2 \neq \kappa_1$. Recalling that $F\sqrt{(3)}/4$ is the value of the source function at the boundary of a gray atmosphere (cf. eqs. [38] and [43]), from relation (178) we may infer that the presence of the absorption lines is to lower the temperature near $\tau = 0$ with respect to its value in a gray atmosphere.

On the other hand, as $\tau \to \infty$, we may have

$$B(\tau) = \tfrac{3}{4} F(\tau + Q) \tag{179}$$

if we set

$$\sum_a \frac{w_a}{\eta'_a} = 1 \quad \text{or} \quad \frac{1}{\bar{\kappa}} = \sum_a \frac{w_a}{\eta_a}. \tag{180}$$

At large depths, then, the temperature in an atmosphere with lines is the same as in the gray case, provided that the optical depth is measured in terms of the mean defined by equations (180).

The "picket-fence" model was generalized by Münch (1946) to account for a slow dependence of the line probability density w_2 on wave length. The method of solution closely followed Chandrasekhar's procedure for the non-gray atmosphere (§ 2.6), and it was applied specifically to the case of the solar atmosphere. Because of the drastic simplifications still introduced into these calculations, however, their interest is somewhat restricted, especially now that more realistic models have been calculated (see below § 5.4).

5.3. Discontinuities in the Continuous Absorption Coefficient

The model considered in the preceding paragraph for the distribution of lines in the spectrum may be used also to study the effect of the discontinuities of the continuous absorption coefficient in high-temperature stars, as Unsöld (1942) first pointed out. Consider the idealized case of an atmosphere with absorption coefficient having the constant values $\kappa_1 = \bar{\kappa}\eta'_1$ for $\nu > \nu_1$ and $\kappa_2 = \bar{\kappa}\eta'_2$ for $\nu < \nu_1$, the frequency ν_1 representing the Lyman limit. We may then integrate separately the equation of transfer (21) over frequencies higher than the Lyman limit—superscript (1)—and over lower frequencies—superscript (2)—in the form

$$\mu \frac{\partial}{\partial \tau} I^{(a)} = \eta'_a [I^{(a)} - B^{(a)}] \qquad (a = 1, 2). \tag{181}$$

This equation is formally equivalent to that considered in the preceding paragraph if we let

$$w_a = \frac{B^{(a)}}{B}. \tag{182}$$

But it should be noticed that the functions w_a now depend strongly on depth. And an essential characteristic of the non-gray problem is the energy interchange, taking place across the discontinuities, to an extent depending on

depth. As an example, we may evaluate the w_1 and w_2, as defined by relation (182), for various levels in the model atmosphere of τ Scorpii computed by Traving (1955). We find the values given in the accompanying table. In view of

	τ			
	0	0.2	1.0	3.0
w_1 . . .	0.059	0.230	0.378	0.424
w_2 . . .	0.941	0.770	0.622	0.576

the rapid variations in w_1 and w_2, it would seem that the arbitrary adoption of constant representative values, as Unsöld (1942) did, is not justified without further analysis. Because of the monotonic properties of the functions w_1 and w_2, however, one would expect the boundary temperature in a non-gray atmosphere to be always lower than the gray value, as indicated by inequality (178). Most numerical integrations of non-gray atmospheres so far published have shown that such is the case. And on this basis it is conjectured that the proposition "Of all atmospheres with the same effective temperature, the gray one has the highest boundary temperature" holds in general. The validity of this strong statement probably is related to the monotonic nature of the nucleus of the integral equation (32).

5.4. Numerical Methods

Suppose that, for an atmosphere with given parameters πF, g, and $\{A_i\}$, a model were constructed on the basis of a starting approximation $T_0(\tau)$ for the temperature distribution. The line absorption coefficient can then be computed as a function of wave length and depth. By grouping the Fraunhofer lines according to ionization and excitation potentials and wave length, a schematized calculation has been carried out for the solar spectrum by Labs (1951) and Böhm (1954). The modifications in the initial temperature produced by the lines can then be numerically calculated by the methods discussed in § 2.5. The computations involved are, of course, quite laborious and intrinsically difficult, because the line absorption coefficient may take very large values near strong Fraunhofer lines. The lack of success which Labs (1951) encountered in applying the $\Lambda^{(1)}$ iteration process to the solar atmosphere, led Böhm (1954) to reexamine the problem. This last author followed a method making use of the $\Lambda^{(1)}$-process in the top layers and of the $\Lambda^{(2)}$-process in the deeper layers, which proved to be quickly convergent.

§ 6. MODEL STELLAR ATMOSPHERES

6.1. "Empirical" Models for the Sun

In contradistinction to the methods described in the preceding sections of a purely inductive nature, it is possible to derive the temperature distribution in

the solar atmosphere from the analysis of limb-darkening observations. The emergent radiation, $I_\nu(0, \mu)$, at an angle $\cos^{-1}\mu$ with the normal is given by (cf. eq. [24])

$$I_\nu(0, \mu) = \int_0^\infty B_\nu(T_\tau) \exp\left[-\frac{1}{\mu}\eta_\nu(\tau)\right] \eta'_\nu(\tau) \frac{d\tau}{\mu}. \qquad (183)$$

If the left-hand side is determined from the observations and the dependence of η'_ν on τ is known, through a numerical solution of the integral equation (183) the values of $B_\nu(T_\tau)$ may be obtained. There are several ways in which this calculation may be carried out in practice (Barbier 1946; de Jager 1948), but we shall not enter into details here. Let it suffice to say that generally the observational values $I_\nu(0, \mu)$ are fitted by interpolation formulae involving a number of parameters (functions of ν) and with structure simple enough that $B_\nu(T_\tau)$ may be explicitly obtained in an elementary form. We may remark, however, that, according to equation (183),

$$B_\nu\{T[\eta_\nu(\tau) = \mu]\} \simeq I_\nu(0, \mu), \qquad (184)$$

the equality sign holding in the strict sense when B_ν is a linear function of $\eta_\nu(\tau)$. Since $\eta_\nu(\tau)$ is of order τ, we see from relation (184) that the temperature distribution at $\tau < 0.10$ is determined by darkening observations at points distant from the limb only by one two-hundredths of the solar radius, or about 5 seconds of arc. It is very questionable whether the limb-darkening measures used in the past for the purpose of determining a model are reliable out to points distant from the solar limb only a few seconds of arc. The bewildering variety of results obtained by various authors, mainly in the upper layers, $\tau < 0.2$, undoubtedly originate in the systematic errors of darkening observations at distances less than one-fiftieth of the solar radius from the limb. The value of $\lim I_\nu(0, \mu)$ as $\mu \to 0$ is then necessarily extrapolated from values of $\mu \simeq 0.15$ and will depend entirely on the assumed behavior of $I_\nu(0, \mu)$ at $\mu = 0$. On quite general grounds it would be expected (cf. eq. [47]) that $I_\nu(0, \mu)$ has a derivative diverging as $-\ln \mu$ as $\mu \to 0$; but this non-analytic nature of $I_\nu(0, \mu)$ has not always been incorporated into the interpolation formula adopted.

In view of the difficulties encountered in determining an empirical model for $\tau < 0.10$ from limb-darkening observations, the intensities observed in the cores of Fraunhofer lines have also been used to determine the source function. When the line arises from a highly excited level, it is formed effectively in a pure absorption process, and equation (183) applies, with $\eta'_\nu(\tau)$ representing the ratio of the line absorption coefficient, at a particular wave length within the line, to the continuous absorption coefficient. De Jager (1952) has used the observable lines of hydrogen to derive the temperature distribution in such a fashion. When comparing it with the one derived by inductive methods, we should keep in mind that it depends in a critical manner on the theory of line formation, which is far from being complete. It does not take into consideration

the variety of processes occurring in the lower chromosphere, which lead to the non-uniform appearance of spectroheliograms. The intensity in the cores of the Balmer lines varies appreciably from point to point as a result of inhomogeneities in the thermal or kinematic structure of the upper reversing layer.

As another example of an empirical determination of the solar source function up to $\tau < 0.02$, the work of Pagel (1955) may be mentioned. This author used limb-darkening observations of nine lines of Fe I near λ 15500 A, with excitation potentials high enough (around 5.6 ev) that they may be considered as arising in a pure absorption mechanism.

In order to compare with the results given by the inductive method, we shall adopt the model derived by Böhm-Vitense (1954) as typical of the empirical models. It is based on the analysis of observations of darkening in the continuum and also of residual intensities of Fraunhofer lines. Perhaps this hybrid feature of the model qualifies it as representative of the whole group.

6.2. The Theoretical Model Solar Atmosphere

Since Strömgren (1940) computed the first theoretical models for the solar atmosphere, a large number of additional calculations have been published, corresponding to slightly different assumptions or methods followed. So many solar models are now available that to describe them separately or even to compare them would be of little use. Instead, we shall describe and discuss briefly the results of Böhm's (1954) integrations, as they represent the most complete model published up to now, in the sense that he took into consideration the non-grayness arising from the continuous and line absorption coefficients. As a starting approximation, he adopted an empirical model (Model I) derived by Böhm-Vitense (1954) for $\tau < 2$, fitted to a radiative theoretical model for $\tau > 2$. On this basis he computes the continuous and line absorption coefficients as function of wave length and depth. The departures from constancy of the resulting net flux are then estimated, and the corrections to the source function are computed by the combined Λ-processes, as described in §§ 2.8, ii and iii. The derived model is found to be in good agreement with the empirical one (Model II) determined by Böhm-Vitense (1954), as can be seen in Figure 1. For $\tau > 0.1$ the difference between the theoretical and empirical models does not exceed 50° K. For $\tau < 0.1$ the discrepancies are larger, becoming 400° K at $\tau = 0.01$. At these small optical depths, however, deviations from thermodynamic equilibrium probably are taking place, and the whole theory is open to question (Pagel 1956; de Jager 1955). An illustration of this point has been given by Pagel (1956), who compares Böhm's final temperature distribution with the electron temperatures derived by analysis of continuum observations in the flash spectrum (Athay, Menzel, Pecker, and Thomas 1955), as is shown in Figure 2. The temperatures in Böhm's radiative model for the range $\tau < 0.02$ are too low to explain the observed continuum in the lower chromosphere.

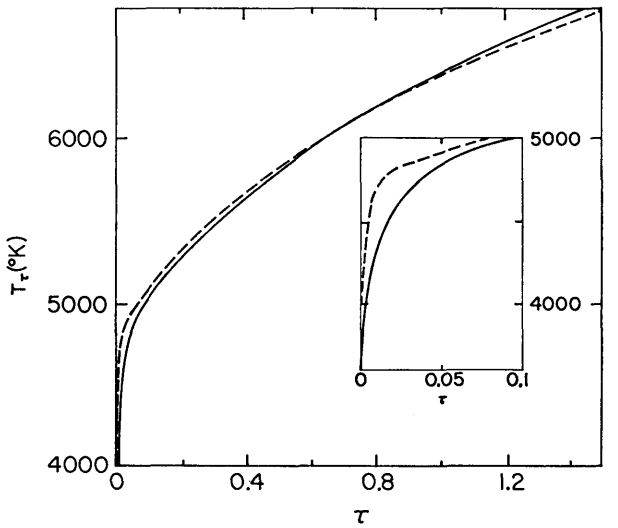


FIG. 1.—Comparison between the temperature distributions in the theoretical model of Böhm (1954) of the solar atmosphere (*full line*) and in the empirical model of Böhm-Vitense (1954) (*dashed line*).

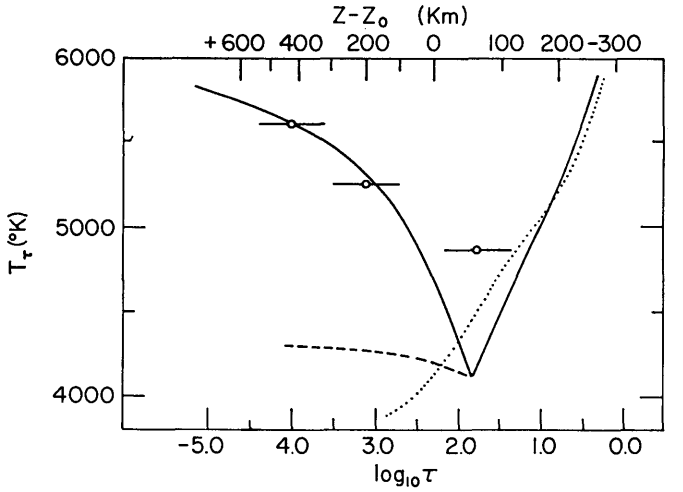


FIG. 2.—The temperature distribution in the outer layers of the solar atmosphere. The dotted line represents the radiative equilibrium model of Böhm (1954). The dashed line is the temperature derived by Pagel (1955) from the intensities of weak Fe I lines. The circles are values of the electron temperature derived from continuum observations of the chromosphere at an eclipse (Athay *et al.* 1955). The full line is the model adopted by Pagel (1956).

It is of importance to emphasize that Böhm used as a starting approximation an empirical model rather than a theoretical one. It might be thought that on this account the agreement of this final model with another empirical one cannot be much of a confirmation of the whole theory. But this is not the case. The starting model was selected because it would give more rapidly convergent results. The gray-body temperature distribution departs so much from the actual one for $\tau < 0.2$ that adopting it as a starting approximation would have led to the problem of convergence of the $\Lambda^{(1)}$-iterations which Labs (1951) encountered.

6.3. Approximate Model Stellar Atmospheres

In order to make a general interpretation of the main features observed in stellar spectra, it is convenient to have available a whole set of approximate models corresponding to different values of the parameters g and T_e not too widely spaced. This enables one to select, for a particular spectrum, approxi-

TABLE 3

Approximate Model Stellar Atmospheres

Author	No. of Models	log g	T (° K)	Sp.	log (H:M)
B. Strömgren (1944)..	45	3.0–4.5	5040–7200	G0–A5	3.0–4.2
C. de Jager and L. Nevén (1957).....	50	1.0–5.0	4500–25,000	K0–B0	3.7
A. Przybylski (1953)..	8	3.5–4.5	5040–8400	G0–A1	3.8

mate values of g, T_e, and the abundance parameters, on the basis of which a more refined analysis may be carried out. In Table 3 we have collected the descriptive information related to models of this kind that have been published up to June, 1958. The three sets of models are based on a temperature distribution of the form

$$T^4 = T_0^4 (1 + \tfrac{3}{2}\tau) . \qquad (185)$$

The value of T_0 is the parameter of the model used instead of T_e. The models by Strömgren and de Jager and Nevén are based on the use of the Rosseland mean, while Przybylski employed the Chandrasekhar mean. The value used by Strömgren for the radiative cross-section of H^- was only an estimate based on work previous to that by Chandrasekhar (1946), about equal to half its exact maximum value for bound-free transitions (λ 8200 A). For models later than A0, the abundance ratio which matters is H:M, i.e., that of the light elements H, He, C, N, O, and Ne to those of low ionization potential, Mg, Si, Fe, Ca, Al, Na. The relative abundance by number in the latter group is taken in the proportions 0.30:0.33:0.30:0.02:0.03:0.02, while the H/He ratio adopted in the high-temperature models is 85/15 by number. In the cooler models the

H/He ratio does not enter directly but only through the mean molecular weight, changes in which may be incorporated by varying g.

6.4. High-Temperature Models

The departures from grayness of atmospheres with spectral types earlier than about A5 are more pronounced than those of later types. Because of the position of the discontinuities in the continuous spectrum relative to the frequency with maximum flux, special problems arise in the calculation of their models. The published integrations of high-temperature models are briefly described in Table 4, which are identified by their parameters T_0 and g. The corresponding spectral types are only approximate and do not represent a calibration of the stellar temperature scale, except in those cases identified by the name of a particular star. The nature of the starting approximation is indicated in the column with heading "$q(\tau)$." In obvious notation, $q(\tau) = \frac{2}{3}$ refers to the Milne approximation, while $q(\tau)$ "gray" refers to the exact solution of the Milne problem. When $q(\tau)$ is qualified as "non-gray," it is implied that a starting approximation of the kind described in § 5.3 was employed. The effective temperatures, T_e, given are those corresponding to the "mean" non-gray flux found by the various authors on the basis of their starting approximation. In general, this flux is not constant with depth, and the meaning of its "mean" value is not the same in every case. Nevertheless, the range of fractional variation $\Delta F/F$ of the non-gray flux from that corresponding to the nominal effective temperature is included in Table 4 to indicate the extent to which the models approach a state of radiative equilibrium.

From the comparison of the general properties of the various models it is possible to draw some interesting conclusions. First, let us consider the ratios T_0/T_e in relation to the gray-body value $[\sqrt{(3)}/4]^{1/4} = 0.812$. It is seen that, with the exception of the models by Saito and Hunger, all models have $T_0 < T_e < 0.812$, as was anticipated at the end of § 5.3. The results of Saito should be taken with some caution, as they show the largest departures from radiative equilibrium. The high value of T_0/T_e derived by Hunger, on the other hand, is not in agreement with the result obtained by Osawa for an atmosphere quite similar to Hunger's. A more detailed comparison of Osawa's and Hunger's models is much needed. Without entering into the details of the numerical integrations (which are not published in any case), it is difficult to understand the reasons why two authors (as McDonald and Underhill, for example), following essentially the same methods, for atmospheres of nearly the same parameters ($T_e = 15{,}800°$ K) derive values of $\Delta F/F$ quite different. Considering the wide range over which $\Delta F/F$ varies for the various models, one can only wonder whether the numerical integrations (more so, if they are graphical) of the fluxes have been carried out in a too perfunctory fashion. It seems that little thought has been given to the question of the numerical accuracy of the fluxes, although probably it is the source of all the discrepancies apparent in Table 4. The specific

TABLE 4

HIGH-TEMPERATURE MODEL ATMOSPHERES

Author	Sp.	T_0 (° K)	log g	$q(\tau)$	$\bar{\kappa}$	T_e (° K)	$\Delta F/F$ (Per Cent)	T_0/T_e
Underhill.... (1951)	O5	35,000	4.2	2/3	Ch	44,600	−4.4, +7.0	0.785
Traving..... (1957)	10 Lac	27,700	4.45	Non-gray	R	37,450	.....	.739
Underhill.... (1950)	O9.5	25,200	4.2	2/3	Ch	36,800	−1.7, +3.6	.685
Rudkjöbing.. (1947)	O9.5	25,200	4.54	Non-gray	R	35,200	.....	.716
Traving..... (1955)	τ Sco	21,200	4.8	Non-gray	R	32,800	.....	.646
Underhill.... (1956)	B0.5	18,800	4.2	2/3	P	29,500	−0.5, +0.6	.638
		18,800	3.8	2/3	P	28,470	−0.1, +0.7	.660
Pecker..... (1950)	B1	17,700	4.48	Gray	R	27,300	.....	.649
	B1.5	17,300	4.48	Gray	R	26,360	.....	.656
Underhill.... (1956)	B2	16,800	4.2	2/3	P	27,870	−1.0, +0.9	.601
		16,800	3.8	2/3	P	27,000	−1.2, +1.5	.621
McDonald... (1953)	B2	16,800	3.8	Gray	Ch	22,700	±4	.740
Cayrel..... (1957)	ζ Per	15,800	3.6	Non-gray	R	27,000	+6.0, −7.7	.585
Saito..... (1954, 1956)	B2.5	16,550	3.8	Gray	R	20,530	+12.2, −4.7	.808
	B5	12,570	3.8	Gray	R	15,390	+10.0, −4.0	.815
	A0	8680	4.2	Gray	R	10,630	+ 6.0, −3.9	.816
Nevén and de Jager... (1954)	τ Sco	17,100	3.97	2/3	R			
	δ Cet	14,700	3.74	2/3	R			
	γ Peg	13,800	3.63	2/3	R			
	ι Her	12,200	2.90	2/3	R			
Hunger..... (1955)	α Lyr	7810	4.3	Non-gray	R	9500	±1.0	.822
		7481	4.3	Non-gray	R	9000	±1.0	.830
		7140	4.3	Non-gray	R	8660	±1.0	.823
		6730	4.3	Non-gray	R	8160	±2.0	.824
Osawa..... (1956)	A3	6760	4.0	Gray	R	8900	+5, ±1	.761
	A9	6000	4.0	Gray	R	7560		.794
Edmonds.... (unpub.)	α CMi	5260	3.4	Gray	R	6570	+1	0.801

case of Pecker's models should be mentioned in this context, for this author iterated the flux six times, using a graphical integrator. Certainly it is not a trivial matter to find the effects of rounding-off and smoothing errors in the end result of a process involving six iterations. There is, however, another effect playing a role in a determination of $\Delta F/F$. Notice that the Pecker models, where a Rosseland mean was used except in the last iteration, are bracketed in temperature by Miss Underhill's models with $T_0 = 16{,}800°$ K and $T_0 = 18{,}800°$ K and where a Planck mean was used. At face value, the small values of $\Delta F/F$ obtained by Miss Underhill would imply that the use of κ_P leads to values of the non-gray flux more nearly constant in depth. And it might be argued that such a result is understandable in the light of the remarks made in § 2.7, namely, that in the outermost layers, where the effects of non-grayness on T_τ are greatest, it is more proper to use a straight mean than a harmonic mean. Pecker's results themselves show the point clearly, for his final model was derived by using in the outer layers a Planck mean κ_P. Nevertheless, it should also be kept in mind that, for high temperatures, κ_P is two or three times larger than κ_P. The range $0 < \tau < 2$ generally taken to evaluate $\Delta F/F$, accordingly, represents quite a different range in monochromatic optical depth, depending on whether τ is measured in $\bar{\kappa}_P$ or $\bar{\kappa}_R$, being larger in the latter case. It would thus seem that the proper manner of comparing two models computed with different means would be to use some fixed η_ν as independent variable.

The models computed by Nevén and de Jager (1954) deserve a special comment, because they have been obtained by "correcting" the initial temperature distribution in such a manner as to account for the fluxes in the Balmer lines. The extent to which they may approach a state of radiative equilibrium was not computed by their authors. They should then be considered with the reservations discussed in § 6.1, especially since the boundary temperatures seem too low for the stars they are supposed to represent, in comparison with other results.

In evaluating how good or how bad a model may be, it should be kept in mind that it all depends on the use for which it is intended. Probably all models listed in Table 4 are accurate enough for the interpretation of the observed features in the continuous spectrum of the stars, which are relatively coarse and insensitive to temperature or gravity changes. The situation is quite different if the problem is the study of the line spectrum, say with the view of deriving the abundance of the elements or fixing the stellar temperature scale. The line spectrum originates, as a general rule, in the top layers of the atmosphere, where the effects of non-grayness are most serious. Since line intensities depend sensitively on temperature through ionization and excitation conditions, a model inaccurate in the outer layers will lead to parameters of the atmosphere not corresponding to those determined by continuum measures, i.e., to an error in the calibration of the stellar temperature scale. For the purpose of analyzing

the line spectrum, then, it is not sufficient to verify that the flux computed on the basis of the starting approximation is constant within a few per cent, but the iterated temperature distribution should be derived.

The results of Traving (1957) for the model atmosphere of 10 Lacertae will be considered, finally, in order to illustrate some characteristics of high-temperature atmospheres. Starting from an initial temperature $T_0(\tau)$, adopted from earlier work on τ Scorpii (Traving 1955), this author carried out two iterations of the flux, following the procedure of § 2.8, ii. The dependence on depth of the fluxes implied by the initial T_0 and iterated temperature distributions T_1 and T_2 is shown in Figure 3. It may be seen here that the departures

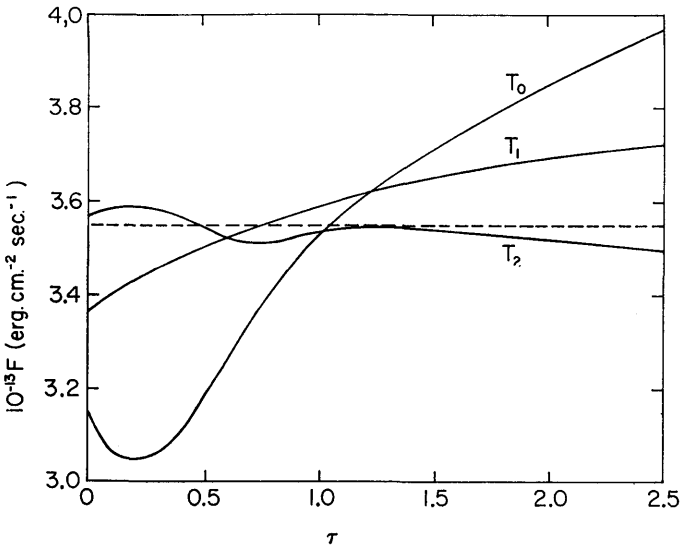


FIG. 3.—The net flux as a function of optical depth in the three approximations calculated by Traving (1957) for the temperature distribution in the atmosphere of 10 Lacertae.

of $F[T_2(\tau)]$ from a constant value do not exceed 1 per cent. The corresponding effective temperature $T_e = 37{,}450°$ K is thus well determined. On the basis of the model obtained from $T_2(\tau)$, however, it is found that the predicted intensities at the centers of the Balmer lines are too high compared with the observed ones. By taking into consideration the effect of the absorption produced by the Lyman lines, Traving shows how this discrepancy is removed. He finds that the radiative equilibrium of layers with $\tau < 0.01$ is altered by Lyman-line absorption, the boundary temperature being reduced to a value of 18,000° K, from $T_2(\tau = 0) = 27{,}700°$ K. These results have established the importance of taking into account the effect of the strong absorption lines on the temperature distribution in the outer layers of stars with early spectral type.

REFERENCES

ALLER, L. H. 1953 *Astrophysics*, Vol. 1: *The Atmospheres of the Sun and Stars* (New York: Ronald Press).

AMBARZUMIAN, V. A. 1943 *C.R. (Doklady) Acad. Sci. U.S.S.R.*, **38**, 229.

ATHAY, R. G., MENZEL, D. H., PECKER, C. J., and THOMAS, R. N. 1955 *Ap. J. Suppl.*, **1**, 505.

BARBIER, D. 1946 *Ann. d'ap.*, **9**, 173.

BATES, D. R. 1939 *M.N.*, **100**, 25.

1946*a* *Ibid.*, **106**, 423.

1946*b* *Ibid.*, p. 431.

1952 *Ibid.*, **112**, 40.

BATES, D. R., and MASSEY, H. S. W. 1941 *Proc. R. Soc., London, A*, **177**, 329.

BIERMANN, L. 1932 *Zs. f. Ap.*, **5**, 117.

1935 *A.N.*, **257**, 270.

1938 *Ibid.*, **264**, 395.

BÖHM, D., and ALLER, L. H. 1947 *Ap. J.*, **105**, 131.

BÖHM, K. H. 1954 *Zs. f. Ap.*, **34**, 182.

BÖHM-VITENSE, E. 1953 *Zs. f. Ap.*, **32**, 135.

1954 *Ibid.*, **34**, 209.

CASE, K. M. 1957 *Ann. Phys.*, **2**, 384.

CAYREL, R. 1957 Thesis, Paris.

CHANDRASEKHAR, S. 1936 *M.N.*, **96**, 21.

1939 *An Introduction to the Study of Stellar Structure* (Chicago: University of Chicago Press), § 2.12.

1944 *Ap. J.*, **99**, 180.

1946 *Ibid.*, **104**, 430.

1950 *Radiative Transfer* (Oxford: Clarendon Press).

1958 *Ap. J.*, **128**, 114.

CHANDRASEKHAR, S., and MÜNCH, G. 1946 *Ap. J.*, **104**, 446.

COWLING, T. G. 1934 *M.N.*, **94**, 768.

DICHTBURN, R. W. 1956 *Rocket Exploration of the Upper Atmosphere* (London: Pergamon Press), pp. 313–326.

DICHTBURN, R. W., JUTSUM, P. J., and MARR, G. V. 1953 *Proc. Phys. Soc. London, A*, **66**, 665.

EDMONDS, F. Unpublished.

GOLDBERG, L. 1939 *Ap. J.*, **90**, 414.

HART, J. F., and HERZBERG, G. 1957 *Phys. Rev.*, **106**, 79.

HENRICH, L. F. 1944*a* *Ap. J.*, **99**, 59.

1944*b* *Ibid.*, p. 318.

HILBERT, D.	1912	*Phys. Zs.*, **13**, 1056.
	1913	*Ibid.*, **14**, 592.
HOPF, E.	1934	*Mathematical Problems of Radiative Transfer* (Cambridge: Cambridge University Press).
HUANG, S. S.	1948	*Ap. J.*, **108**, 354.
HUNGER, K.	1955	*Zs. f. Ap.*, **36**, 42.
JAGER, C. DE.	1948	*Proc. Akad. Wetensch. Amsterdam*, **51**, 1159.
	1952	*Rech. Astr. Obs. Utrecht*, Vol. **13**, Part 1.
	1955	*Ann. géophys.*, **11**, 330.
JAGER, C. DE, and NEVÉN, L.	1957	*Rech. Astr. Obs. Utrecht*, Vol. **13**, Part 4.
JUTSUM, P. J.	1954	*Proc. Phys. Soc. London, A*, **67**, 190.
KOURGANOFF, V.	1952	*Basic Methods in Transfer Problems* (Oxford: Clarendon Press).
LABS, D.	1951	*Zs. f. Ap.*, **29**, 199.
LIMBER, N.	1958	*Ap. J.*, **127**, 363.
MCDONALD, J.	1953	*Pub. Dom. Ap. Obs. Victoria*, **9**, 269.
MARK, C.	1947	*Phys. Rev.*, **72**, 558.
MASSEY, H. S. W., and BATES, D. R.	1940	*Ap. J.*, **91**, 202.
MICHARD, R.	1949	*Ann. d'ap.*, **12**, 291.
	1950	*B.A.N.*, **11**, 227.
MILNE, E. A.	1922	*Phil. Trans. R. Soc. London, A*, **223**, 201.
	1929	*Ibid.*, **228**, 421.
MÜNCH, G.	1946	*Ap. J.*, **104**, 87.
	1947	*Ibid.*, **107**, 265.
	1948	*Ibid.*, p. 265.
MULDERS, G. F. W.	1936	*Zs. f. Ap.*, **11**, 143.
NEVÉN, L., and JAGER, C. DE	1954	*B.A.N.*, **12**, 103.
OSAWA, K.	1956	*Ap. J.*, **123**, 513.
OSTERBROCK, D.	1953	*Ap. J.*, **118**, 529.
PAGEL, B. E. J.	1955	*M.N.*, **115**, 493.
	1956	*Ibid.*, **116**, 608.
PECKER, J.-C.	1950	*Ann. d'ap.*, **13**, 433.
PLACZEK, G.	1947	*Phys. Rev.*, **72**, 556.
PRZYBYLSKI, A.	1953	*M.N.*, **113**, 683.
REISZ, A.	1950	*Ark. f. astr.*, **1**, 147.
	1954	*Ibid.*, p. 475.
RUDKJÖBING, M.	1941	*Zs. f. Ap.*, **20**, 228.
	1947	*Pub. mind. med. Kobenhavns Obs.*, No. 145.
RUSSELL, H. N.	1929	*Ap. J.*, **70**, 11.
SAITO, S.	1954	*Contr. Inst. Ap. U. Kyoto*, No. 48.
	1956	*Ibid.*, No. 69.
SCHWARZSCHILD, K.	1906	*Göttinger Nachr.*, No. 41.
SEATON, M. J.	1951	*Proc. R. Soc. London, A*, **208**, 418.
SPITZER, L.	1939	*Ap. J.*, **90**, 494.

STAVER, T. B.	1951	*Ark. math. og naturvidensk., Oslo*, **51**, 29.
STRÖMGREN, B.	1940	*Pub. mind. med. Kobenhavns Obs.*, No. 127.
	1944	*Ibid.*, No. 138.
SWIHART, T.	1956*a*	*Ap. J.*, **123**, 139.
	1956*b*	*Ibid.*, p. 143.
SZEGÖ, G.	1939	*Orthogonal Polynomials* (New York: American Mathematical Society).
TRAVING, G.	1955	*Zs. f. Ap.*, **36**, 1.
	1957	*Ibid.*, **41**, 215.
TRUMPY, B.	1931	*Zs. f. Phys.*, **71**, 720.
TUNSTEAD, J.	1953	*Proc. Phys. Soc. London, A*, **66**, 304.
UENO, S., SAITO, S., and JUGAKU, J.	1954	*Contr. Inst. Ap. U. Kyoto*, No. 43.
UNDERHILL, A. B.	1949	*M.N.*, **109**, 563.
	1950	*Pub. mind. med. Kobenhavns Obs.*, No. 151.
	1951	*Pub. Dom. Ap. Obs. Victoria*, **8**, 357.
	1956	*Ibid.*, **10**, 357.
UNSÖLD, A.	1931	*Zs. f. Ap.*, **1**, 138.
	1938	*Physik der Sternatmosphären* (1st ed.; Berlin: Springer-Verlag).
	1942	*Zs. f. Ap.*, **21**, 229.
	1948	*Ibid.*, **25**, 340.
	1955	*Physik der Sternatmosphären* (2d ed.; Berlin: Springer-Verlag).
VITENSE, E.	1951	*Zs. f. Ap.*, **28**, 81.
WEIDEMANN, V.	1952	Diplomarbeit, Kiel.
WEMPE, J.	1947	*A.N.*, **275**, 97.
WHEELER, J. A., and WILDT, R.	1942	*Ap. J.*, **95**, 281.
WILDT, R.	1939*a*	*Ap. J.*, **89**, 295.
	1939*b*	*Ibid.*, **90**, 611.
	1947	*Relations entre les phênomènes solaires et géophysiques* (Paris: Centre Nationale de la Recherche Scientifique), p. 7.
WOOLLEY, R. v.d. R., and STIBBS, D. W. N.	1953	*The Outer Layers of a Star* (Oxford: Clarendon Press).

CHAPTER 2

Stellar Energy Distribution

A. D. CODE[1]
Mount Wilson and Palomar Observatories
California Institute of Technology, Carnegie Institution of Washington

§ 1. INTRODUCTION

EDDINGTON once asked his readers to imagine a physicist on a cloud-bound planet, who, unaware of the stars above, has set himself the task of computing the physical properties of massive gaseous spheres. The present-day astrophysicist who sets about determining the structure and chemical composition of a stellar atmosphere is not so far removed from Eddington's hypothetical scientist as he should like. Vast portions of the electromagnetic spectrum are completely obscured by the terrestrial atmosphere, while the accuracy of the flux measurements in the observable region are substantially reduced by the variable atmospheric extinction. Until such time as it is practicable to make precise photometric observations from outside the earth's atmosphere, this opacity will represent the greatest single limitation on our knowledge of the spectral energy distribution of stars.

The observational basis upon which our knowledge of the stellar universe rests consists almost wholly of the measurement of the radiant flux from stars. We may determine the direction of propagation, the spectral distribution, and the state of polarization of this radiation, all as a function of time. Ideally, we should like such measurements for a large sample of stellar types, extending over the entire electromagnetic spectrum with a resolution sufficient to delineate the finest features present. We must naturally compromise these ideals because of the limitations imposed by the terrestrial atmosphere, the instruments, and the available time. It is reasonable to expect, however, that these compromises will be made consciously with a view to preserving the physical significance of the measurements. A filter band pass or spectral region isolated by a monochromator should not be chosen arbitrarily but rather with due cognizance of the

[1] Now at Washburn Observatory, University of Wisconsin.

physical problem under consideration and other factors, such as the blending of spectral lines and the presence of atmospheric bands, etc. The information to be derived from a set of photometric measurements which are directly translatable into a physical measurement of energy is necessarily greater than that obtained from a set of arbitrary colors or magnitudes.

Any stellar spectrophotometric measurement should be interpretable in terms of measured monochromatic fluxes, and these fluxes in turn must ultimately be understood in terms of physical theory. The first is basically an observational problem: Can we relate wide-band colors of stars, for example, to the spectral energy distribution? The second problem is this: Given the observed energy distribution, what do these results imply for the structure and chemical composition of the stellar atmosphere, within the framework of current theory?

Specifically, we may compare the observed flux with that predicted for a model stellar atmosphere specified by a given effective temperature, gravity, and chemical composition. For the few comparisons that have been made, the agreement is highly satisfactory. In the past, measurements of the energy distribution of stars have often been directed toward the determination of a single color temperature over a wide wave-length base line. The stellar energy distribution is thus compared to that of a black body. Here we shall adopt the more sophisticated view that stellar radiation may be well represented by the flux from a model stellar atmosphere. We may feel that we know more about the star if we have succeeded in representing it by a model. Current evolutionary ideas make use of the mapping of stars on the HR diagram; although the internal structure determines the bolometric magnitude, the star's position in the HR plane is more properly a problem for stellar atmospheres. A self-consistent theory of stellar evolution would require, as a part of the stellar model, the fitting of an appropriate atmosphere from which the bolometric correction and the color index of the model could be determined. If the effect of absorption lines were included, we should be in a position to assess the relative importance of the chemical composition and of the age on the stellar configuration.

The theory of the continuous spectrum is described in detail elsewhere in this volume. The general problem in which both the continuum and the line formation are treated simultaneously is extremely complex. Thus the usual procedure is to include only the continuous opacity at first, and, if additional effort is warranted, an attempt to correct the temperature distribution for the "blanketing effect" of the lines follows. This theoretical procedure of treating the problem of line formation and continuum separately has its direct analogue in the usual observational approach. The measurement of the stellar flux with sufficient resolution to construct the true line profiles, and at the some time extending the measurement over a sufficient wave-length range to describe the run of the continuum, is also extremely difficult. For this reason, it is customary to treat these observational problems separately. However, as it was with theory, the schism is not complete; we can no more construct the line profile with-

out knowledge of the position of the "true continuum" than we can determine the "true continuum" without measuring the equivalent widths of the absorption lines in the pertinent spectral interval. It might be added that the foregoing procedure may be taken to define the concept "true continuum" and should be consistent with the continuum measured in line-free regions or windows. We shall return to the problem of line blanketing after discussing some of the existing spectrophotometric data.

§ 2. INTEGRAL EFFECTIVE INTENSITY

The complete optical train involved in a spectrophotometric measurement includes the interstellar absorption, the atmospheric extinction, and the transmission of the telescope and photometer optics, as well as the spectral response function determined by filters or spectrometer and the characteristic sensitivity of the detector. The pointer reading or deflection produced by an astronomical radiation source observed through this optical train is called the "integral effective intensity" and is given by

$$I = \text{Constant} \int_0^\infty F_\nu a_\nu p_\nu S_\nu d\nu \,, \tag{1}$$

where F_ν is the monochromatic flux per unit frequency interval from the source; a_ν is the fraction transmitted by the interstellar medium; p_ν is the transmission of the terrestrial atmosphere; and S_ν is the instrumental sensitivity function and includes the transmission of the optics, as well as the spectral response of the detector and monochromator. The constant involves the angular diameter of the source and the relation between the arbitrary pointer reading and energy in some conventional units, such as watts or ergs per second. The only adjustable parameter in the integrand is S_ν. By the proper choice of detector and means of spectral isolation, any spectral region within the atmospheric windows may be observed. The interstellar absorption is as intrinsically interesting as the monochromatic flux in many contexts, but we shall, for the present, interpret it as a characteristic of the observed flux, only being careful to append the word "reddened" to a star so affected. The atmospheric extinction introduces a substantial problem in deriving information about the monochromatic flux from the integral effective intensity. In principle, it is an arbitrary function depending on atmospheric purity, moisture content, barometric pressure, etc. Practically, on nights when photometry is done, it may be represented by the following expression:

$$p_\nu = e^{-(A+B\nu^4)\sec Z - C(\nu)} \,, \tag{2}$$

where the non-selective term A is the extinction by haze per unit air mass and varies with the quality of the night and from site to site. The second term represents the molecular extinction, which follows this λ^{-4} law of Rayleigh scattering very closely. The coefficient B shows little change from night to night, being principally a function of barometric pressure. Except for very large zenith distances, Z, the air mass is equal to sec Z. The final term represents the absorption

in atmospheric bands and is zero elsewhere. Since the atmospheric bands show a curve-of-growth effect, the extinction does not necessarily vary linearly with air mass. For this reason, corrections for atmospheric extinction in the infrared and from the onset of the ozone absorption beyond 3300 A require somewhat greater effort.

In general, observations are made at varying zenith distances, and the integral effective intensity is reduced to outside the atmosphere. It is clear that, for sufficiently narrow band passes, equation (1) may be easily transformed to the corresponding quantity for zero air mass. It may be demonstrated that even for wide-band filter photometry this may be done, within the accuracy of the

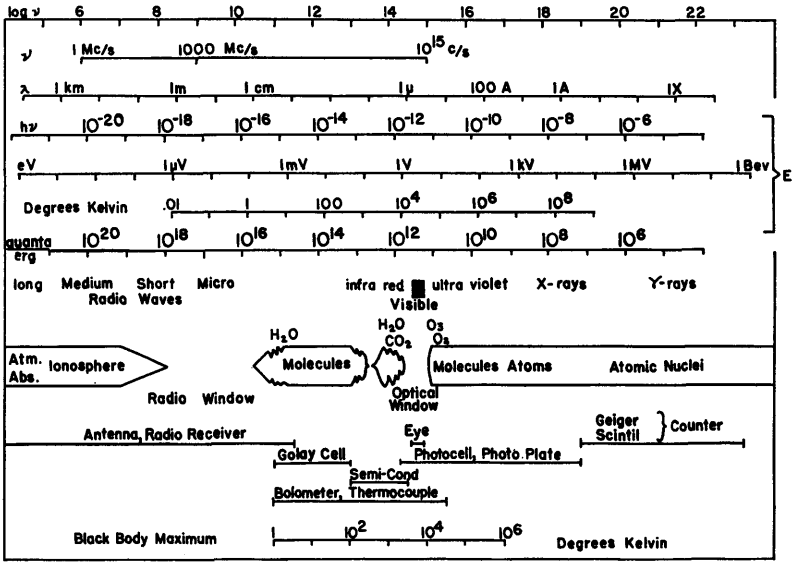


FIG. 1.—Energy relations throughout the electromagnetic spectrum

observations, if a dependence of extinction on color is allowed for. The problem of atmospheric extinction is dealt with in detail elsewhere in this series.

The integral effective intensity reduced to outside the atmosphere and incorporating the interstellar absorption in the flux is

$$I_0 = \text{Constant} \int_0^\infty F_\nu S_\nu d\nu . \tag{3}$$

In terms of equation (3) we may distinguish three classes of photometric investigation. *Relative* spectrophotometry focuses attention upon the variation of the integral effective intensity from star to star and does not attempt to make any inference about the nature of the integrand or the value of the constant. The results are usually given as colors and magnitudes, with a zero point defined

by a set of standard stars. What we shall refer to below as *absolute* spectrophotometry might logically be called "relative absolute spectrophotometry." Here the integral effective intensity plus knowledge of the instrumental sensitivity function is used to evaluate the monochromatic flux apart from a constant independent of frequency. A set of such measurements for one star with different functions S_ν describes a stellar energy-curve relative to some arbitrary frequency. The third class of spectrophotometric observations would attempt to assign a numerical value to the constant and is in essence the problem of determining the effective temperature; for the case of the sun it involves the solar constant and solar parallax.

In Figure 1, which has been adapted from van de Hulst (1945), various energy relations for electromagnetic energy are shown schematically, along with the atmospheric absorption and useful range of different detectors. While it is no

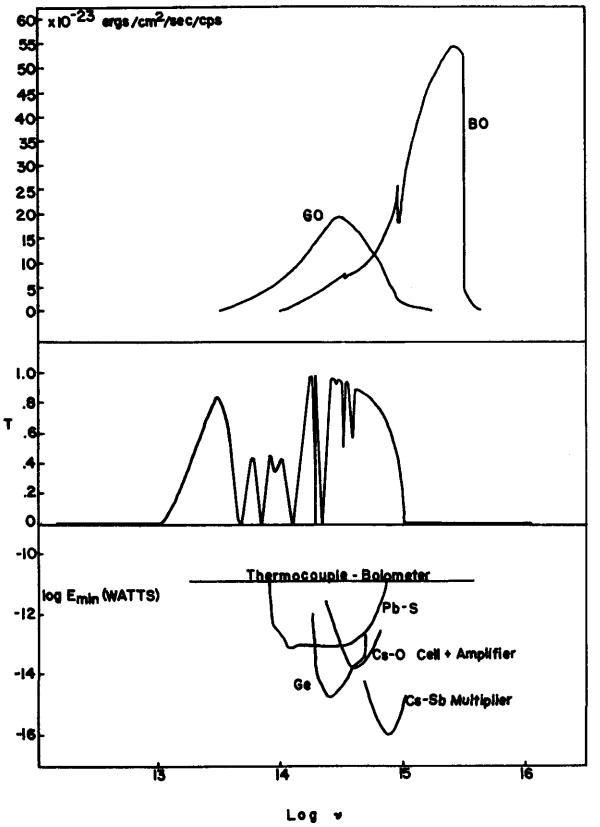


FIG. 2.—The upper curves show the approximate energy distribution of a B0 and a G0 star of visual magnitude 6.0 in ergs per second per square centimeter per unit frequency interval. Directly beneath is a plot of the average terrestrial atmospheric transmission per unit air mass, and at the bottom the response curves for several detectors.

coincidence that the sensitivity of the eye is centered in the optical atmospheric window or that this is the region of maximum radiation from the sun, it is interesting to note that this is also the region corresponding to an energy of a few electron volts and thus the region where the bulk of the atomic lines are to be found. We shall be concerned primarily with observations in this optical window and therefore with photographic plates and photoelectric devices in general. The linearity and high quantum efficiency of photoemissive detectors, plus the relative ease with which they may be calibrated, make these the most useful and flexible receivers. On the basis of sensitivity, one would choose the antimony-cesium (S4) photomultipliers or the new multialkali tubes for the region from about 6000 A to the atmospheric limit near 3000 A. From about 10,000 to 6000 A the cesium oxide on silver (S1) photomultipliers appear to be the best choice, while the germanium phototransistors provide the highest sensitivity in the 1.6 μ window and a lead sulphide cell would be recommended for the 2.2 μ window. Black receivers, such as the thermocouple, bolometer, or Golay pneumatic cell, are useful over the entire region; however, the much greater inherent noise level of any non-selective detector drastically reduces the sensitivity. Moreover, the non-selective nature of these heat-sensitive detectors does not greatly simplify the problem of absolute calibration directly, since the optical system and monochromator still introduce a frequency-dependent instrumental sensitivity function. Nevertheless, the black receivers can play an important role in calibrating a particular photometric system in the laboratory.

In Figure 2 the approximate form of the energy distribution for a B0 and a G0 star of visual magnitude 6.0 is illustrated. The energy scale corresponds to ergs per second per square centimeter per unit frequency interval incident outside the earth's atmosphere. Directly beneath the energy-curves is a plot of the average atmospheric transmisson per unit air mass. Finally, the response-curves for several detectors are shown. The approximate minimum detectable power corresponding to a signal-noise ratio of unity for a 15-second exposure is indicated. These data are adapted from the discussions by Whitford (1948) and Jones (1949).

§ 3. RELATIVE SPECTROPHOTOMETRY

The minimum information on stellar energy distribution is that provided by a single color index. The color index may be used to determine a color temperature over the pertinent spectral range. It is not possible, however, to separate out that part of the color that is due to the continuous spectrum and that due to the interstellar reddening and the effect of absorption lines. The addition of only one more color in the ultraviolet provides a powerful tool for determining reddening, as was first shown by Wilhelm Becker (1938).

The present U, B, V system of Johnson and Morgan (1953) has been adopted as a standard system by many of the investigators currently active in the field.

As such, there is a wealth of observational material on this well-defined three-color system. While the system is, in practice, defined by a set of standard stars and a prescribed set of filters, it may, in principle, be described in terms of physical systems. The U, B, V system has proved most valuable in problems of stellar astronomy. The systematics on the HR plane and the $U - B$, $B - V$ plane make it possible to derive interstellar absorptions and corrected distance moduli for clusters. In conjunction with accurate spectral types on the MK system, the discussion may be extended to field stars and stellar associations.

In the present discussion, however, it is proper to ask how much information about stellar energy distributions may be derived from wide-band multicolor photometric systems, such as the U, B, V system. To relate the integral effective intensity to the monochromatic flux, we attempt to choose a representative frequency or wave length, to which the integral effective intensity is said to correspond. The concept of an effective wave length for a given filter system is perhaps the most familiar. Actually, however, the stellar energy distribution and the interstellar absorption are smoother functions of frequency or wave number than of wave length, and the integral in equation (3) converges faster than does the corresponding integral in wave-length units. Whether for this reason or others, a number of investigators have chosen to use wave numbers measured in the inverse wave-length unit, μ^{-1}. If we let x be a simple function of wave length, say $1/\lambda$ or λ, we may choose the appropriate representative function x in two ways. The effective value of x, as usually defined, then, is

$$x_{\text{eff}} = \frac{\int_0^\infty x F_x S_x dx}{\int_0^\infty F_x S_x dx}, \tag{4}$$

and the integral effective intensity is then given by

$$I_0 = \text{Constant} \cdot F_{x_{\text{eff}}}, \tag{5}$$

where the constant allows for the different equivalent band width as well as the relation between pointer reading and stellar flux. Strömgren (1937) introduced the concept of the constant-energy wave length. In analogy we have the constant-energy value of x given by the equation

$$x_0 = \frac{\int_0^\infty x S_x dx}{\int_0^\infty S_x dx}, \tag{6}$$

in which case the integral effective intensity is to be regarded as given by

$$I_0 = \text{Constant}\,(F_{x_0} + \Delta F_{x_0}). \tag{7}$$

The quantity ΔF_{x_0} is a small correction term, depending on the width and shape of the band pass and the second and higher derivatives of the flux taken

about x_0. Thus, in both approaches, a priori knowledge of the energy distribution is assumed. The effective wave number or wave length is different for different energy distributions. On the other hand, the constant-energy wave number or wave length may be defined once and for all by the instrumental system, but the correction term, ΔF_{x_0}, depends upon the energy distribution. There can be no clear-cut choice between the two. If the flux is known exactly, equations (5) and (7) will both yield the same answer, but the computation would appear futile, as we already know the energy distribution. If a black-body distribution is assumed, it may equally well be applied to the determination of x effective or of ΔF_{x_0}. It would seem, however, that a constant-energy wave-length concept is a more concise description of the photometric system and that ultimately it must be resorted to in comparing one star with another. We do not wish to compare the flux at one wave length to the flux at a slightly different wave length in another star. We shall here, in general, make use of the constant-energy function and take x to be $1/\lambda$ measured in inverse micron units. If, following Strömgren (1937), we expand F_x about x_0, the integral effective intensity assumes the form

$$I_0 = \text{Constant} \int_0^\infty S_x dx \left[F_{x_0} + \frac{1}{2} \left(\frac{d^2F}{dx^2} \right)_{x_0} \mu_2 (x_0) + \dots \right], \tag{8}$$

where

$$\mu_n (x_0) = \frac{\int_0^\infty (x - x_0)^n S_x dx}{\int_0^\infty S_x dx}, \tag{9}$$

and the second term in the brackets is to be identified with the previously defined ΔF_{x_0}. Thus, if the band pass is narrow enough for the second and higher derivatives of the energy distribution to be sufficiently small, the integral effective intensity is a measure of the monochromatic flux at $x_0 = 1/\lambda_0$. These higher-order terms are not necessarily small, particularly in the ultraviolet, where the Balmer discontinuity or the crowding of absorption lines occurs. Not only is the relation between monochromatic flux and the integral effective intensity then obscure, but the transformations of one photometric system to another become non-linear. In fact, the assumption that a linear transformation exists between two photometric systems implies that some function x exists, such that F_x is linear, and the slope of the relation between the two systems is given by the ratio of the Δx_0's.

The values of $1/\lambda$ for the U, B, and V band passes are given in Table 1. These computations are based on the published sensitivity-curves by Johnson and Morgan (1953) and the reflectivity of two aluminum reflections. If, indeed, we can describe the U, B, V system as a physical system, it should be possible to derive the $U - B$ and $B - V$ colors of certain standard stars by numerical integration of equation (3). Using the absolute energy distributions described

below for several stars and performing the integration, we obtain the computed colors, Cy and Cu, for the natural system of the U, B, V photometry (Johnson and Morgan 1953). These colors are related to the $B - V$ and $U - B$ colors by the equations

$$B - V = Cy + 1.040\,, \qquad U - B = Cu - 1.120\,. \tag{10}$$

The results are tabulated in Table 2, where the successive columns are the name of the star, the $B - V$ observed, $U - B$ observed, $B - V$ computed, $U - B$ computed, the differences $B - V$ observed minus $B - V$ computed, and $U - B$ observed minus $U - B$ computed. Within the accuracy of the

TABLE 1

WAVE NUMBERS FOR U, B, V SYSTEM

	U	B	V
$1/\lambda_0$.....	2.89	2.29	1.83

TABLE 2

OBSERVED AND COMPUTED U, B, V COLORS

Star	$(B-V)_0$	$(U-B)_0$	$(B-V)_c$	$(U-B)_c$	$\Delta(B-V)$	$\Delta(U-B)$
10 Lac.....	−0.20	−1.04	−0.08	−1.26	−0.12	+0.22
α Lyr.....	.00	−0.01	+ .14	−0.10	− .14	+ .09
σ Boo.....	+ .37	−0.09	+ .54	−0.21	− .17	+ .12
π^3 Ori.....	+ .46	+0.00	+ .56	−0.18	− .10	+ .18
16 Cyg A.....	+ .64	+0.19	+ .78	−0.05	− .14	+ .24
51 Peg.....	+0.68	+0.20	+0.78	+0.02	−0.10	+0.18
Mean.....	.....	.....	.....	.....	−0m13	+0m17

computations, the differences $\Delta(B - V)$ and $\Delta(U - B)$ are nearly constant. Since the computed values of $B - V$ and $U - B$ were made for different air masses and reduced to outside the atmosphere in precisely the same manner as the reduction of the observations to outside the atmosphere, the difference may be attributed either to the monochromatic flux used in the integration or to the function S_x. It is difficult to attribute a difference as large as this to the monochromatic fluxes, particularly for a star as early as 10 Lacertae. In fact, if we attempt to reverse the procedure and determine from observations the absolute energy relative to V for early-type stars at the effective wave numbers of the U and B filters, we find a large ultraviolet deficiency quite in contradiction to the small measured Balmer discontinuity and near black-body energy distribution for these stars. While a discrepancy of the same nature is found for the six-color photometry of Stebbins and Whitford (1945), it has been possible to

predict the observed colors by this procedure for the multicolor systems used by Bahng (1957) and by Tifft (1958). The fact that the U, V band passes, in particular, for both the U, B, V system and the six-color system appear to be overestimated may be related to the fact that these two systems were both calibrated with the same monochromator and thermocouple and that, as one moves toward the ultraviolet, the calibration becomes more difficult and vulnerable to scattered light. It is likely, then, that the published sensitivity-curves for the U, B, V system are in error. It is probable that the values of $1/\lambda_0$ are nearly correct but that the areas of sensitivity-curves are affected by scattered light. We shall adopt the mean values of $\Delta(B - V)$ and $\Delta(U - B)$ shown in the last row of Table 2 as the appropriate corrections to convert theoretically derived $B - V$ or $U - B$ colors to the observed system. The six-color filter photometry of Stebbins and Whitford (1945) provides substantially more data on stellar energy distribution than does the U, B, V system, by virtue of the wider base line as well as the greater number of colors. The measurements in the red and infrared are essentially freed from the effects of line blanketing, while the

TABLE 3

WAVE NUMBERS, SIX-COLOR PHOTOMETRY

	U	V	B	G	R	I
$1/\lambda_0$.....	2.84	2.45	2.08	1.74	1.48	1.09

[U], [B], and [G] colors provide the same information as the U, B, V system. This work has been extended by Stebbins and Kron (1956), and the system has been calibrated by them against the sun and a standard lamp (Stebbins and Kron 1957). Table 3 gives the constant-energy wave number for the six-color photometer as given by Stebbins and Kron (1957).

In Whitford's critical discussion of the law of interstellar reddening he applied equations (8) and (9) to the six-color measurements of B stars to allow for the effect of the finite band passes of the system (Whitford 1958). It is, in fact, from the six-color data that a large part of our knowledge of the interstellar reddening-curve stems.

The Greenwich relative gradients (Greaves, Davidson, and Martin 1952) utilized a spectrograph for isolation of the spectral band passes, and the spectrophotometry was accomplished photographically. Measurements over the spectral region from $1/\lambda = 2.34$ to $1/\lambda = 1.58$ were used to specify a single relative gradient, G, defined as

$$G = \frac{d}{d\,(1/\lambda)} \log_e \frac{I_\lambda}{I_\lambda^0}, \tag{11}$$

where I_λ and I_λ^0 are the specific intensities at wave length λ for the star in question and a star adopted as a standard, respectively. The standard is se-

lected such that the mean value of G for nine stars of *Henry Draper* type A0 is zero. These relative gradients are therefore referred to the mean gradient of an A0 star. Extensive work, to be described later, has been expended to determine the absolute gradient of the mean A0 star and thus place the Greenwich work on an absolute basis. The relative gradient G may be regarded as an arbitrary color and as such has been carefully compared with many of the contemporary color equivalents by the Greenwich observers (Greaves, Davidson, and Martin 1952).

Kienle, Strassl, and Wempe (1938) published the results of an extensive program of relative spectrophotometry for thirty-six stars, using the photographic method. These results were tabulated for many wave lengths from 4014 to 6564 A and give a graphical representation of the relative energy distribution of

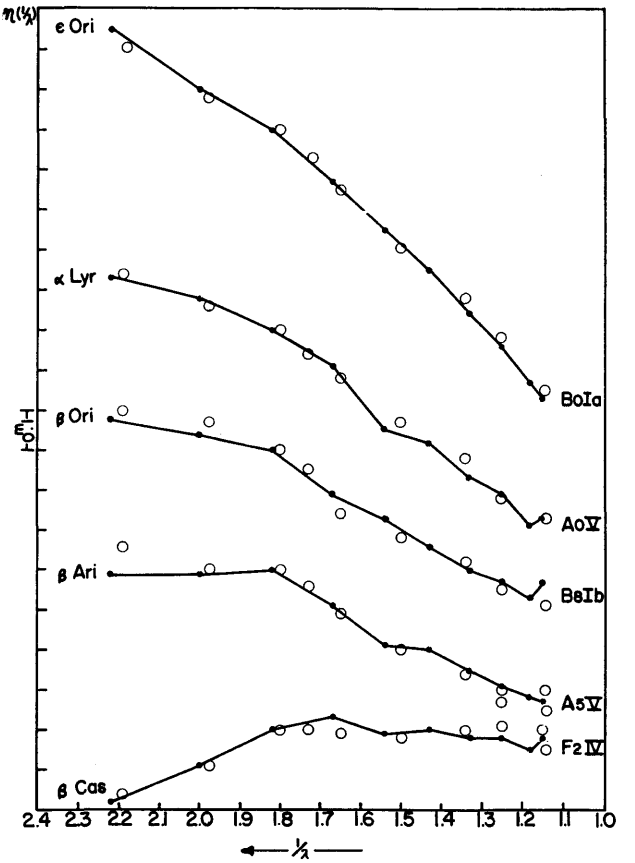


FIG. 3.—Comparison of the relative spectrophotometry of Hall with that of Whitford and Code. The small filled circles are the measurements of Hall. The systems are placed on absolute energy basis.

these stars. Absolute comparisons with a black body have been published and are still being undertaken for these observations and will be discussed in § 5.

A dispersing system to isolate spectral regions for relative photoelectric spectrophotometry was first used by Hall (1941). By means of an objective grating and a pair of slits at the focus of the Sproul and later the Amherst refractor, he could isolate well-defined spectral regions about 485 A wide. Observations on sixty-seven bright stars were made over the spectral region from 4560 to 10,300 A. By limiting his observations to wave lengths greater than 4500 A, Hall avoided the ambiguities introduced by the strong blending of absorption lines in the ultraviolet. The effect of the Paschen discontinuity was clearly shown in Hall's observations.

More recently, Whitford and Code at Mount Wilson have made spectral scans of sixty-seven stars of different spectral types and luminosity classes with a photoelectric scanning spectrograph (Code 1952; Whitford 1958). The spectrograph employs all-mirror optics, and the scanning is accomplished by rotating the grating with a precision drive. The slit in the focal plane of the spectrograph was usually set to isolate a spectral region of 10 A in the blue and 20 A in the infrared. Two separate photomultipliers were used to measure the region from 3000 to 6000 A and 5000 to 10,000 A, respectively. The observations were reduced at the following sixteen wave lengths: λ = 0.340, 0.365, 0.386, 0.404, 0.419, 0.459, 0.506, 0.556, 0.581, 0.605, 0.667, 0.746, 0.800, 0.875, 0.909, and 1.000 μ. These regions were selected to avoid as far as possible all spectral lines of equivalent width greater than 0.1 A for all spectral types. Figure 3 shows a comparison of these results for several stars with measurements by Hall.

Relative photoelectric spectrophotometry of the spectra of stars earlier than F0 have been published by Bonsack and Stock (1957) for sixty-five stars in the wave-length range from 3500 to 5000 A. This material was obtained with an objective prism on the Case Schmidt and a 1P21 photomultiplier mounted behind a slit at the focus. The scan is accomplished by trailing the telescope.

The relative spectrophotometry data described briefly above form the basis of our information on stellar energy distribution. The absolute calibration of a few of these stars will make it possible to place all this material on an absolute basis. In the following section we shall consider the problems encountered in absolute spectrophotometry.

§4 ABSOLUTE CALIBRATION

The measurement of the radiant energy for various wave-length intervals presents two problems: that associated with isolating the different wave-length intervals and that relating to the measurement of the energy within these intervals. In this respect it is a considerably more complex problem than the measurement of the total radiant flux. In the latter case a single measurement with a calibrated energy-measuring device such as a blackened thermocouple or bolometer suffices, while in the former it is necessary to determine the trans-

mission of the analyzer as well as the response of the detector. While the properties of a black receiver may be utilized for such measurements, it would appear that the black-body radiator is more suited to the problems encountered in stellar energy measurements.

Our basic problem, then, is to specify the function S_x or its integral for each wave-length interval; the interval is so chosen that all but the first term of equation (8) may be neglected. We may attempt to specify the optical properties of each component of our system—namely, the transmission of the telescope, the transmission of the filters or monochromator, and the response of the receiver—or, alternatively, we may observe the light from a standard radiation scource and thus determine the over-all response of the optical system. The first procedure has already been employed in the discussion of the filter photometry in the preceding section. The failure to predict the observed colors is perhaps an indication of the weakness of this technique. The majority of energy measurements to date have relied upon the use of a standard source. We shall, nevertheless, review both techniques, in order to illustrate the essential difficulties of the problem.

Unless one is prepared to invest considerable effort in the development of an optimum heat-sensitive detector, there appears to be little choice between the thermocouple and the bolometer. In either case the minimum detectable signal at the normal ambient temperature is of the order of 10^{-10} watt. This means that, in general, the spectral band pass for a bright star must be larger than 100 A, even with a 100-inch telescope, if reliable measurements are to be obtained. For this reason, the thermocouple has usually been employed at some intermediate step in the absolute calibration. In the case of the filter photometry cited above, the thermocouple was used for the determination of the spectral response of the Cs-Sb photomultiplier. The usual procedure is to isolate narrow spectral regions from the radiation of an incandescent lamp with a suitable monochromator and alternately expose the thermocouple and photocell to these nearly monochromatic fluxes. The thermocouple is assumed to be non-selective, and thus the ratio of photocell response to thermocouple response gives the relative spectral sensitivity of the photocell. A thermocouple coating of zinc black or platinum black will absorb essentially all the radiation normally incident from the ultraviolet to beyond 14 μ. This very non-selectivity, however, puts considerable demand upon the performance of the monochromator. Scattered light must be kept to a minimum, and the use of a double-pass monochromator is all but mandatory. The use of a line source rather than an incandescent lamp will greatly reduce the scattered light. By far the most important aspect of the problem, however, is the optical imagery. We must insure that the same radiation is measured by both receivers and also keep in mind that the sensitivity of the photocathode shows large variations across its surface. Thus we want to image the monochromator output on the photocathode in the same way as the star is imaged. This is accomplished by keeping the photomultiplier in its origi-

nal housing containing the Fabry lens and operating the monochromator at the same *F*-ratio as the telescope, with the light as nearly normal to the Fabry lens as possible. Since the photocathode shows definite variations in color sensitivity with temperature, the use of refrigerated photomultipliers, even when the reduction of dark noise is not necessary, is good practice. An effective cooling system establishes a definite operating temperature at all times, both during observing and for the calibration procedure. Since the photomultiplier is several million times more sensitive than the thermocouple, it is usually necessary to operate the photomultiplier as a simple photocell with all dynodes shorted to the anode, in order to cope with the bright source required for thermocouple response. This procedure is not expected to affect the spectral response, however.

The filter calibration is relatively simple and, if carried out carefully, will introduce no significant error. The light-output from the monochromator is observed directly with and without the filter by any suitable linear detector at appropriately spaced wave-length intervals. The transmission of some filters is temperature-dependent, while others exhibit fluorescence. These effects must not be ignored. The evaluation of the transmission of the telescope optics offers greater difficulty. For a small instrument, laboratory measurements may be made in a manner analogous to the technique used for determining filter transmissions. This has been done in a few cases. The reflectivity of the aluminum coating of larger instruments has occasionally been measured over small areas of the mirror, but the results do not adequately describe the over-all transmission of the telescope. In addition, the reflectivity depends on the age and condition of the mirror surfaces at the time of observation.

The calibration of a spectrograph or monochromator is more difficult than that of filters. One may employ the same technique of measuring a monochromatic source with and without the spectrograph in the optical train, but the procedure must be more elaborate. The transmission of a spectrograph depends on the extent to which the collimator is filled, what parts of the optics are used, and the adjustment of the slits and other aperture stops in the system. A double-pass monochromator may be calibrated by using each section separately and in combination. There are variants on the procedures described, but in any event it is clear that each step increases the possibility that sizable errors will enter into the final over-all sensitivity function.

The inherent simplicity of a direct comparison of stellar radiation with that from a black body is illusory. It is not an undertaking to be approached casually. The operation of a true black-body radiator, at a well-defined temperature, is an exacting enough procedure in a laboratory, to say nothing of its use at a site convenient for telescopic observation. In addition, many telescopes are not constructed so that it is convenient to focus on a nearby source or to point toward the horizon. Thus most measurements have made use of an auxiliary standard, such as a tungsten ribbon-filament lamp. The lamp's calibration, of course, ultimately depends on the properties of a black-body radiator. It has

sometimes been necessary to take rather elaborate steps, frequently with the intervention of other optics, to bring the light to focus in the focal plane of the telescope.

The primary photometric and radiometric standard is the black-body radiation from a source operated at the temperature of molten platinum. In the form that has been widely used (Wensel *et al.* 1931), the radiator itself consists of a small cylinder of pure fused thoria about 45 mm long, with an internal diameter of 2.5 mm. The cylinder is immersed in a larger crucible containing molten platinum maintained at the temperature of solidification, which is 2047° K. A lid on the crucible with a small hole in the center, about 1.5 mm in diameter, forms the exit aperture for the radiation. This crucible is imbedded in powdered thoria in a large refractory container and is heated by a high-frequency induction furnace. The power supply must be capable of providing about 7 kw at a frequency of the order of 1 megacycle in order to melt the platinum. On reducing the power and letting the temperature drop, it will stop near the solidification point for periods in excess of 20 minutes. This temperature regulation is much better than can be achieved by other techniques. The difference between the radiation of an ideal Planck radiator and the cavity radiation of a cylinder at the same temperature has been calculated (Gouffe 1945), and, in the case of the furnace described above, the emittance is within a few tenths of a per cent of unity. The spectral energy distribution of this source is therefore that of a black body at 2047° K. This source is also the primary photometric standard, and the luminance is, by definition, 60 candles/sq cm. Many black-cavity radiators have been constructed, and both the experimental work and the theoretical discussions have been summarized extensively (Forsythe 1937; de Vos 1954). Sources similar to the one described above, which operate at one of the primary standards of temperature such as the melting point of gold, palladium, or platinum, however, constitute the primary standards. The temperature of other black-body furnaces is usually measured with an optical pyrometer which has been calibrated against a primary standard. Similarly, the calibration of other secondary standards is referred to a primary standard. A tungsten ribbon-filament lamp provides a convenient secondary standard. Such lamps may be calibrated against Bureau of Standards sources; recently an Astronomical Standards Laboratory has come into existence at Heidelberg through the initiative of Kienle.

A tungsten ribbon-filament lamp may be operated at true temperatures between 2800° and 2900° K without exceeding their ratings or shortening the lifetime appreciably. At a temperature of 2850° K the energy per unit frequency interval decreases from 10,000 to 3000 A by nearly 9 mag., while the change in color over this base line is −0.0045 mag. per degree Kelvin. This large range in intensity may be accommodated with photoemissive detectors without difficulty. We should like to know the temperature to within a few degrees, however. A precision optical pyrometer will yield a temperature determi-

nation with a probable error of the order of $\pm 3^\circ$ K, although the systematic errors may be greater. It is interesting to note that the change in brightness for a temperature of 2850° K at the effective wave length of the optical pyrometer, approximately 0.65 μ, is only 0.003 mag. per degree Kelvin. The optical pyrometer measures brightness temperatures, S, which are related to the true temperature through the following relation:

$$I(\lambda, S) = \tau_\lambda \cdot \epsilon(\lambda, T) \cdot I(\lambda, T), \tag{12}$$

where $I(\lambda, S)$ is the radiant intensity of a black body with a temperature S; $I(\lambda, T)$ is the radiant intensity of a black body at the true temperature, T, of the tungsten ribbon; $\epsilon(\lambda, T)$ is the emissivity of tungsten at wave length, λ, and temperature T and τ_λ is the transmission of the lamp window at the wave length λ. For the values of λT that concern us here, no error as large as 0.01 mag. is introduced by the use of Wien's law. Equation (12) may therefore be written as

$$\frac{1}{S} - \frac{1}{T} = -\frac{\lambda}{C_2} \ln [\tau \times \epsilon(\lambda, T)]. \tag{13}$$

If we put $C_2 = 1.438$ cm degrees, $\lambda = 0.650\,\mu$, and $\tau = 0.92$, then equation (13) becomes

$$\frac{1}{S} - \frac{1}{T} = -1.041 \times 10^{-4} \log [0.92 \times \epsilon(\lambda, T)]. \tag{14}$$

The emissivity of tungsten may be expressed to an accuracy of the order of three-tenths of a per cent by the expression

$$\epsilon(0.65, T) = 0.4420 - 0.000018\,(T - 2000^\circ \text{K}). \tag{15}$$

In the range of temperatures considered, the brightness temperature of a tungsten lamp is less than the true temperature by about 305° K. De Vos (1954) has made a very careful study of the emissivity of tungsten ribbon filaments. Among his samples he found no variation in emissivity greater than about 0.3 per cent. It would appear, then, that, by the use of an accurately calibrated optical pyrometer and the emissivity-curves of de Vos, the spectral energy distribution of a tungsten ribbon-filament lamp could be specified to the precision presently required for astronomical radiation measurements. The brightness temperature determined from the optical pyrometer measurements would be converted to true temperatures by the application of equation (13) and the energy distribution then determined by equation (12) and the emissivity-curves.

One of the natural precautions indicated would be the use of several lamps. The period of operation should be limited, so as not to contaminate and coat the glass envelope. Lamps might be periodically broken and the transmission of the glass measured, although it must be admitted that this is a sad fate for a standard lamp. The voltage and current should be accurately measured and regulated. For lamps of this type a variation of 1° K corresponds to a variation in current of the order of 0.01 amp. One should therefore be prepared to measure

the current to a few hundredths of an ampere. If at any time the current should be significantly different for a given voltage than in the past, it is a sign that the lamp has changed its properties.

Other secondary light-sources in use are the positive crater of a carbon arc, the xenon high-pressure arc, the hydrogen-discharge lamp, and the "poudre fluorescent" light-source. Kienle (1955) has summarized the properties of these sources in a communication to the I.A.U.

In the preceding discussion we have indicated how a standard light-source may be established. It is implied that this source will be observed with precisely the same optical system as the stellar radiation. It is also desirable that the path length to the lamp be short, in order to avoid substantial horizontal extinction. If it is possible to vary the length of the light-path, the horizontal atmospheric extinction can then be determined. The methods of analysis of the radiation previously discussed for relative spectrophotometry are all applicable here. The spectral isolation provided by wide-band filters is not sufficient to specify accurately the spectral distribution. The wide bands are vulnerable to the ambiguities introduced by strong line blanketing. Interference filters have been employed, but the long tails of low transmission introduce complications. The use of a monochromator to isolate narrow spectral regions may avoid the difficulties introduced by line absorption only by careful selection of the spectral regions or by scanning across the spectrum. The choice of spectral regions was discussed in the section on relative spectrophotometry above, while a fuller discussion of the problems introduced by line blanketing will be considered later.

The basic problems encountered in absolute energy measurements are the calibration of the spectral response of the instrument and the determination of well-defined and unambiguous spectral band passes. It would appear that the most satisfactory procedure would be the direct comparison of stars with a primary standard through precisely the same optical system. The use of early-type stars for the fundamental reference stars would reduce the problems associated with line blanketing, and the employment of a photoelectric scanning spectrograph would insure linearity and well-defined, narrow band passes. In the following section we shall review the more important investigations that have been made to date.

§ 5. ABSOLUTE SPECTROPHOTOMETRY

The early investigations in this field were directed primarily toward the determination of a single color temperature to represent the average distribution of energy throughout a large part of the visual range. The color temperature is the temperature of a black body having the same relative intensity distribution, or color, as that of the source under observation. The color temperature of a star is usually defined in terms of the absolute gradient, given by

$$\phi = 5\lambda \; - \frac{d\,(\ln F_\lambda)}{d\,(1/\lambda)}. \tag{16}$$

On inserting the Planck formula for F_λ, we have

$$\phi = \frac{c_2}{T_c}(1 - e^{-c_2/\lambda T_c})^{-1}, \tag{17}$$

where T_c is the color temperature.

Tables of T_c and ϕ have been published by Kienle (1941), along with a useful graph of the various related functions. The relative gradient G discussed earlier is simply the difference $\phi - \phi_0$ between the star in question and a standard star. It is useful to rewrite the gradient in terms of the dimensionless variable $a = h\nu/kT = c_2/\lambda T$. Expressing F_a in units of the total flux $F = \sigma T^4$, equation (16) assumes the form

$$\phi = \frac{c_2}{T}\left[\frac{3}{a} - \frac{F}{F_a}\frac{d\,(F_a/F)}{da}\right]. \tag{18}$$

In the Wien approximation,

$$\frac{F_a}{F} = \frac{15}{\pi^4}\, a^3 e^{-a}, \tag{19}$$

and

$$\phi_{\text{Wien}} = \frac{c_2}{T}. \tag{20}$$

Thus, if the radiation may be characterized by the Wien approximation, the absolute gradient is independent of the wave length. The corresponding relations for a Planck radiator are

$$\frac{F_a}{F} = \frac{B_a}{F} = \frac{15}{\pi^4}\, a^3 e^{-a}(1 - e^{-a})^{-1}, \tag{21}$$

and

$$\phi_{\text{Planck}} = \frac{c_2}{T}(1 - e^{-a})^{-1}, \tag{22}$$

which was given above.

Quite generally we may express the radiant intensity of a source in terms of the Planck function B_a and a spectral emissivity, $\epsilon(a)$; thus

$$F_a = \epsilon(a) B_a . \tag{23}$$

In order uniquely to specify the spectral distribution of a source by a single color temperature, it is necessary that $\epsilon(a)$ be of the form

$$\epsilon(a) = K e^{ka}, \tag{24}$$

where K and k are independent of wave length. The special case $k = 0$ is the familiar gray body, which results in an equation identical with (17). Equation (24) holds only approximately for a tungsten lamp, and for this reason de Vos (1954) has proposed that a physical color temperature for such sources be defined in terms of the ratio of intensities at two wave lengths, namely, $\lambda_1 = 0.470\ \mu$ and $\lambda_2 = 0.660\ \mu$. A definition of this type has generally been implicit in the measurement of the color temperatures of stars.

In a stellar atmosphere in radiative equilibrium the observed energy distribution is the sum of the contributions from all layers from which radiation may escape and is a function of temperature gradient with depth in the atmosphere and the corresponding optical depth. If the atmosphere is in local thermodynamic equilibrium, the emergent flux is given by

$$F_\nu(0) = 2\int_0^\infty B_\nu(T_{\tau_\nu}) E_2(\tau_\nu)\, d\tau_\nu , \tag{25}$$

where the optical depth, τ_ν, is defined in terms of the mass absorption coefficient, κ_ν, as

$$d\tau_\nu = -\kappa_\nu \rho dx . \tag{26}$$

E_2 is the second exponential-integral function. In general, this integral cannot be expressed in terms of equations (23) and (24). Thus we should not expect to be able to characterize the stellar radiation by a single color temperature. The

TABLE 4

CORRECTIONS FOR EVALUATING THE GRADIENT ϕ

a	δ_a		a	δ_a	
	Planck Correction	Gray Atmosphere		Planck Correction	Gray Atmosphere
1.....	+0.582	+0.772	4.....	+0.019	−0.041
2.....	+ .157	+ .168	6.....	+0.003	−0.016
3.....	+0.053	+0.070			

simplest case to which equation (25) applies is that of a gray atmosphere in which κ_ν is a constant. The emergent flux from a gray atmosphere is not, however, that of a gray body, and it is of interest to compare the gradients obtained from equation (25) with that of a black body or a gray body. If we write the gradient as

$$\phi_a = \frac{c_2}{T}(1 + \delta_a) , \tag{27}$$

then $\delta_a \equiv 0$ for the Wien approximation and takes on the values given in Table 4 for the black-body and gray atmosphere, respectively. In the case of the gray atmosphere the temperature appearing in equation (27) is the effective temperature of the star, T_e, defined as the temperature of a black body having the same total emission as the star:

$$\int_0^\infty F_\nu d\nu = \int_0^\infty B_\nu(T_e)\, d\nu = \sigma T_e^4 . \tag{28}$$

Physical theory makes certain predictions as to the variation in the mass absorption coefficient with wave length and with depth in the stellar atmos-

phere. It is indeed the variation in color temperature with wave length that provides the observational basis to support any such theory.

The older visual measurements by Wilsing, Scheiner, and Münch (1919) and the early photographic work of Rosenberg (1914) and Plaskett (1923) are now chiefly of historic interest. This material has been thoroughly discussed by Brill (1932). Among these early efforts, however, the spectrophotometric observations made by Yü (1926) deserve special comment. Yü obtained stellar energy-curves for ninety-one stars in the spectral region extending from 3300 to 5100 A. The absolute calibration was based on the assumption that the B0 star ζ Ophiuchi radiated as a black body at a temperature of 22,000° K, an assumption that is not too far from the truth. His study was principally concerned with measurements of the Balmer discontinuity, although he published detailed energy-curves and "effective temperatures"—in reality, color temperatures—based on the fitting of black-body curves to the energy distribution longward of the discontinuity. These observations were utilized by McCrea (1931) to compare the observed fluxes with those calculated by his method of model stellar atmospheres. The work of Yü and the theoretical interpretation made by McCrea fully embody the spirit of present research on the energy distribution of stars.

Until the publication of the revised Greenwich absolute gradients (Greaves, Davidson, and Martin 1934), there was general agreement in the assignment of a color temperature between 10,000° and 13,000° K for the average A0 star. Their resultant color temperature was slightly over 21,000° K, a difference that was incompatible with assigned probable errors. The corresponding gradient of $\phi_0 = 0.91 \pm 0.05$ at λ 5000 was averaged with the value $\phi_0 = 1.07 \pm 0.05$ obtained by the Greenwich observers in 1932 (Greaves, Davidson, and Martin 1932), yielding a value of $\phi_0 = 0.99$, corresponding to a color temperature of 18,000° K. This value was adopted as the zero point of the Greenwich temperature scale. The principal difference between the early measures and the methods employed in the 1934 determination was the substitution of a tungsten filament lamp for the earlier, unsatisfactory acetylene burner used as a standard source up until 1932. Both these sources were calibrated for color temperature at the National Physical Laboratory, but this determination was not actually spectrophotometric. The method was to match visually the color of the unresolved light of the source against a black body, at a known temperature. If the emissivity is not of the form given by equation (24), the meaning of the color temperature so derived is not obvious. The spectrum of the lamp was modified by the use of a W78 filter, in order to match the stellar energy distribution more closely. The filter transmission was determined photographically and corresponded to a difference of absorption of $3^m.42$ between the violet and red ends of the spectral range used. To measure photographically this intensity ratio of 23 with great absolute accuracy is very difficult. The stellar spectra were measured at two groups of wave lengths in the red and the blue, and the mean behavior of the continuum in the visual range was specified by a single ϕ obtained

from these measures on the assumption of a linear run in $1/\lambda$. The mean value of $1/\lambda$ in the red was 1.582 μ^{-1} (corresponding to a wave length of 6321 A), and the mean blue measures at 2.131 μ^{-1} (4693 A) for late types 2.342 μ^{-1} (4270 A) for type A and 2.333 μ^{-1} (4285 A) for types O and B. The gradients are thus visual color indices on an absolute scale. The relations between the Greenwich gradients and a number of color systems were discussed in the second volume of *Observations of Colour Temperatures of Stars* in 1952 (Greaves *et al.* 1952).

At Ann Arbor, Williams (1939) instituted a program for the determination of the energy distribution in the spectra of seven early-type stars, motivated by the discouraging uncertainty in the so-called "zero point" indicated by the Greenwich work. The stars were compared directly with a tungsten ribbon-filament lamp by photographic techniques. The lamp was calibrated on four occasions at the Lamp Development Laboratory, Nela Park, where an instrument of known response was maintained and consisted of a quartz double monochromator which was used with both a thermopile and a photocell. The intensity distribution of the lamp as a function of wave length was determined and not simply a color temperature. In order to use the same optical train for both lamp and star without introducing significant horizontal extinction, the radiation from the lamp was collimated with a lens, which was also included in the lamp calibration measures. This collimated source was mounted at the upper end of the telescope and rotated to sweep out an annulus on the primary mirror about three times per minute. It was possible to observe α Lyrae by using only this same annular portion of the mirror. A Corning "daylight" filter made the radiation from the standard lamp very similar in color to that of an A0 star. Eleven wave lengths from 4040 to 6370 A were measured on the plates with a Moll-type microphotometer. The plates were calibrated by means of a wedge slit. The energy distribution for α Lyrae indicated that, throughout this spectral region, the energy distribution did not deviate from that of a black body by more than 5 per cent. The gradient of α Lyrae was found to be $\phi_0 = 1.16 \pm 0.04$, corresponding to a color temperature of 14,300° K. The average absolute spectrophotometric gradient of the seven standard stars of spectral class near A0 was $\phi_0 = 1.19 \pm 0.02$.

At Göttingen, Kienle and collaborators (Kienle, Wempe, and Beileke 1941) carried out an extensive and careful absolute calibration of their previous relative energy-distribution measures. The standard source was a tungsten ribbon-filament lamp with a quartz window. The radiation passed through a blue filter, to a plane mirror, and then to a spherical mirror of 50-cm focal length focused onto a thin gold-platinum–foil diaphragm. This "artificial star" was collimated by a 20-cm paraboloid of 300-cm focal length and directed into the prism camera, which was then completely filled. Thus precisely the same optical system was used on stars and on an "artificial star." Several tungsten lamps were calibrated in a number of different ways both photographically and photo-

electrically and compared against a black body. The filter transmission and collimator reflectivity were accurately measured. The actual comparison between star and source was made photographically, and complete energy-curves from $1/\lambda = 1.584$ to 2.66 μ^{-1} were published for eight A0 stars. This work then placed the relative energy distribution given for thirty-nine stars of types B to M on an absolute basis (Kienle, Strassl, and Wempe 1938). The Göttingen observations were extended to the infrared region from $1/\lambda = 1.172$ to 1.658 by von Hoff (1939). This list contains only two main-sequence stars, however.

The extension of the energy-curve of α Lyrae to the infrared was undertaken by Hall and Williams (1942) with the photoelectric spectrophotometer developed by Hall and the tungsten ribbon-filament lamp that Williams had employed in his earlier work. The use of photoelectric techniques considerably simplified the reduction procedure. While the photographic methods have the distinct advantage of measuring all wave lengths simultaneously, the greater inherent accuracy of the photocell, along with its ability to measure over a large intensity range, makes it the more dependable technique. In the spectral region extending from the visual to the Paschen limit at 8205 A, Hall and Williams found a color temperature near 15,000° K for Vega. The Paschen discontinuity was about 0.23 mag., and beyond the discontinuity the energy was greater than that of a black body at 15,000° K.

In the investigations described above, the violet limit was set by the last spectral region that appeared to be free from the confluence of the Balmer lines. The extension to the continuum on the shortward side of the Balmer discontinuity, studied by Yü, was complicated by the faintness of the standard sources in the ultraviolet. This important spectral region has been studied extensively by Barbier and Chalonge (1941) from observations made at the Jungfraujoch. High altitude is particularly important for studies in the ultraviolet. A hydrogen-discharge lamp was successfully used as the standard source for these ultraviolet measures. The gradients were determined for 240 stars, chiefly earlier than F8, for the spectral region 4600–3700 A (ϕ_1) and 3700–3150 A (ϕ_2). The Balmer discontinuity was defined in terms of the intensity longward and shortward of 3700 A as

$$D = \log \frac{I_c}{I_D}, \tag{29}$$

where I_c is the intensity extrapolated to 3700 A from the longward side and I_D is the intensity at 3700 A. In addition, Barbier and Chalonge have determined the wave length λ_1, defined as the wave length where the intensity has dropped by $\frac{1}{2}$ D. The four parameters ϕ_1, ϕ_2, D, and λ_1 characterize the violet and ultraviolet energy distribution. The most recent tabulation of these parameters is given by Chalonge and Divan (1952). Chalonge has also proposed an accurate system of spectral classification based on the two parameters λ_1 and D or on the three parameters λ_1, D, and ϕ 4250.

The present system of stellar color temperatures is based on the spectro-

photometric observations discussed above, namely, Greenwich, Ann Arbor, Göttingen, and Paris-Jungfraujoch observations. The standard sources used in Göttingen and Paris and the Jungfraujoch were compared with each other and calibrated against a black body (Kienle, Chalonge, and Barbier 1938). In 1939 Williams visited the national standards laboratories in the United States, Holland, Germany, France, and England, where he ran calibrations of his standard lamp and filter transmissions (Williams 1940). While some of the comparisons were divergent and difficult to explain, the three standards laboratories that entered into the determination of stellar color temperatures were in substantial agreement. The results of these investigations showed that a single color temperature could not represent the smoothed-out stellar continuum. In the infrared, the Paschen series limit affected the continuum. In the ultraviolet, coalescence of the Balmer lines and the Balmer discontinuity is important for

TABLE 5

GRADIENTS AND COLOR TEMPERATURES FOR MAIN-SEQUENCE STARS

MK Type Luminosity Class V	ϕ_{5000}	ϕ_{4250}	ϕ_{3500}	T_{5000} (° K)	T_{4250} (° K)	T_{3500} (° K)	D
B0	0.75	0.63	0.75	33,000	39,800	23,000	0.08
B5	0.88	0.80	1.07	22,500	23,400	14,200	.29
A0	1.10	0.99	1.45	15,300	16,700	10,000	.51
A5	1.40	1.19	1.63	11,000	13,000	8900	.46
F0	1.67	1.50	1.90	8950	9900	7600	.33
F5	1.90	1.91	1.98	7700	7600	7300	.18
F8	2.11	2.23	2.04	6900	6500	7000	0.13

stars of early spectral types. In the later types, the crowding of absorption lines shortward of the G band depressed the continuum. In the neighborhood of 5000 A a small discontinuity appears that has been discussed by Chalonge. This feature is not yet clearly understood, though it has been noted even in photoelectric filter photometry (Tifft 1958).

The results of these attempts to assign color temperatures for main-sequence stars are best summarized by Table 5. It is based upon the summaries by Kienle (1937), Gascoigne (1950), Greenwich, Greaves, *et al.* (1952), Chalonge and Divan (1952) (as revised by Cayrel de Strobel 1957), and Greaves (1956). The columns give the spectral type, the gradients at λ 5000, λ 4250, and λ 3500, along with the corresponding color temperatures and the magnitude of the Balmer discontinuity. The differences in color temperatures are reasonable in terms of the known sources of opacity and effects of absorption lines. The extension of these observations into the infrared is particularly important for two reasons. In those stars in which H^- provides the main source of opacity, the continuous absorption coefficient due to bound-free transitions reaches a maximum between 8000 and 9000 A and then decreases to a pronounced minimum at 16,000 A. Also, the

effect of line absorption in the F and G stars is extremely small longward of 6000 A. We have already described the measurements of α Lyrae by Hall and Williams in the infrared and the relative spectrophotometry of sixty-seven stars by Hall in the range 4570–10,320 A and the infrared observations of eighteen stars by von Hoff at Göttingen. The photoelectric spectral scans by Whitford and Code have been described above. An attempt to place these observations on an absolute basis was made in the summer of 1954 at Mount Wilson by Whitford and Code. A tungsten ribbon-filament lamp was observed through the

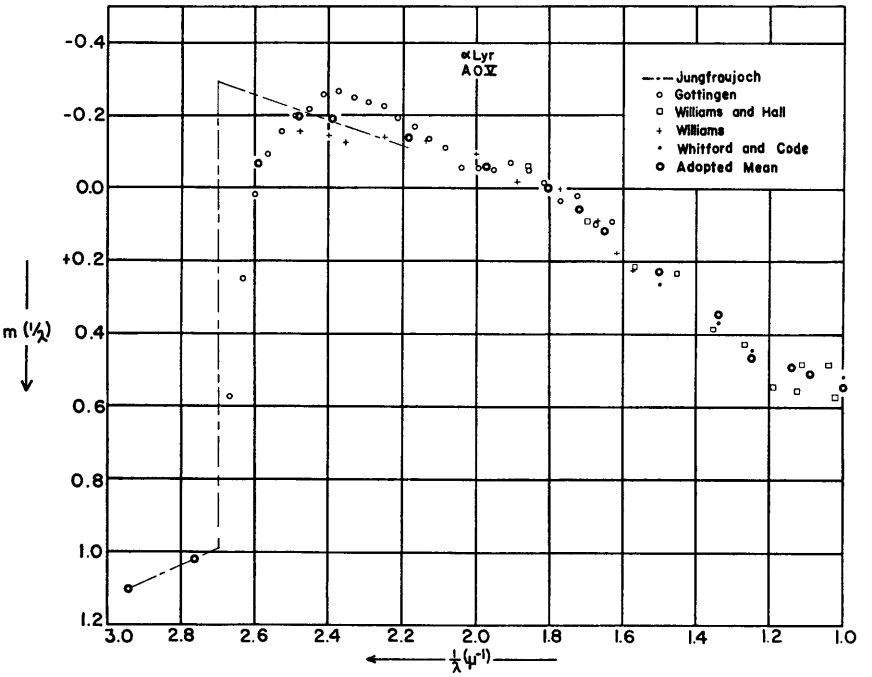


FIG. 4.—Comparison of the energy distribution for α Lyrae (A0 V) obtained by various investigators.

same optical system as that used for the stars. The spectral regions were isolated through the use of narrow-band interference filters. The lamp was calibrated at the National Bureau of Standards and with an optical pyrometer on several occasions. The steep intensity gradient of the lamp introduced large systematic errors in the measurements in the violet due to substantial transmission of the red wings of the interference filters. The observations in the red, however, were not seriously affected. The lamp was also observed directly with a thermocouple, and the transmission of the filters was accurately determined. The results in the red were in agreement with those found from the lamp calibration.

Stebbins and Kron (1957) have calibrated the six-color photometry against

the sun. An optical system designed to reduce the sunlight by 18.5 mag. was used to compare the sun with a tungsten ribbon-filament lamp. The lamp was then used to produce an artificial star that was compared with stars of solar type. The sun was found to match the color of a G2 V star exactly in the six colors and to have a $B - V$ color of $+0.63$ mag. These observations also yield an apparent magnitude for the sun on the international photovisual scale of -26.73 ± 0.03. It is then possible to calibrate the six-color system from the known energy distribution of the sun. It is probably correct, however, that the solar energy distribution is not known any better than that of α Lyrae based on the observations described above. In fact, the observations of the solar flux are poorly determined, and the influence of lines on these observations is not

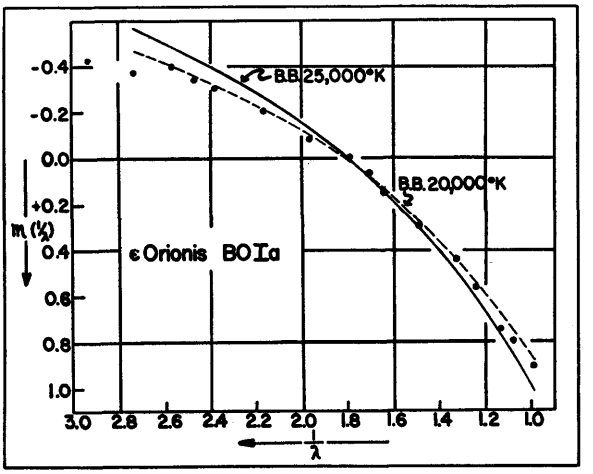


FIG. 5.—Energy-curve derived for ϵ Orionis (B0 Ia) compared with black-body curves

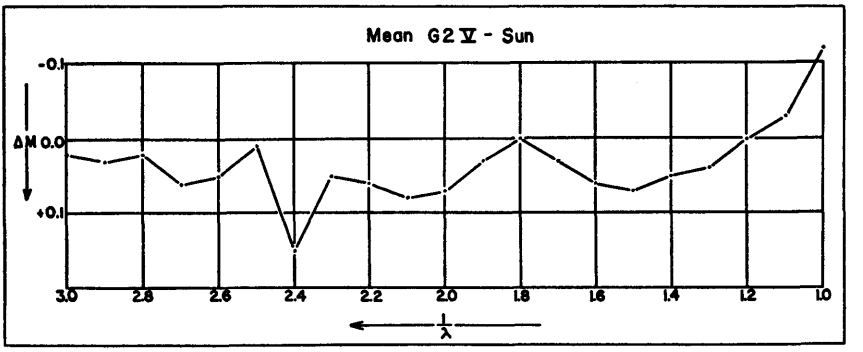


FIG. 6.—Comparison of a mean G2 V star based on the absolute energy calibration versus energy-curve from the sun.

well known. The best data for deriving a solar energy-curve come from the measurements of the intensity at the center of the disk and the measured limb darkening and may be derived from the data summarized by Minnaert (1956). Stebbins and Kron, however, have recently calibrated their lamps against a furnace and compared them with those of several other investigators. The absolute calibration of stellar energy distribution is currently being continued by Kienle at Heidelberg and by Code and Bless at Madison. Whitford has recently extended the measurements to the 1.6-μ region with a germanium phototransistor, and the effect of line absorption is now receiving the attention it deserves by several investigators.

In § 7 of this discussion the energy distribution for a representative sample, of spectral types is given in the spectral range from 3400 to 10,000 A. The data are based on the investigations described above. The spectral region from 4200 to 10,000 A depends primarily upon the star α Lyrae. The ultraviolet has been fitted to these observations from the Jungfraujoch measurements of 10 Lacertae (O9 V) and ϵ Orionis (B0 Ia). In Figure 4 the results for α Lyrae obtained by the various investigators are shown. The large circles represent the adopted means. The energy-curve of ϵ Orionis is shown in Figure 5, and, finally, the comparison of a mean G2 V star on this system with the solar flux is shown in Figure 6.

§ 6. LINE BLANKETING

The term "line blanketing" was introduced by Milne (1928) to describe the effect of the line absorption coefficient on the temperature distribution of the stellar atmosphere. The term has been used here more loosely to designate the total effect that the line absorption may have on the observed continuum. The presence of line absorption may produce a difference between the observed fluxes and those calculated for a model atmosphere, in which the only source of opacity is the continuous absorption coefficient, by three distinct mechanisms. An instrumental effect due to the limited resolving power of the spectrograph produces a spurious depression of the continuum and becomes increasingly important for later-type stars. The actual overlapping of spectral lines produces a real depression of the continuum and is displayed in early-type stars near the series limit of the Balmer lines, as well as in stars of the later types. The third effect of the lines is that to which Milne referred—the change in the emergent flux due to the modification of the temperature distribution resulting from the energy absorbed in lines. The first two effects refer to the observable region of the spectrum; that is, they are basically observational problems. The third effect depends on the total energy absorbed in the lines throughout the entire spectrum. It is believed, for example, that the Lyman-line absorption significantly modifies the temperature distribution of an A star. The problem comes about, of course, from the practical necessity of distinguishing between the line absorption coefficient and the continuous absorption coefficient. Should it be feasible to compute the mass absorption coefficient and mass-scattering coeffi-

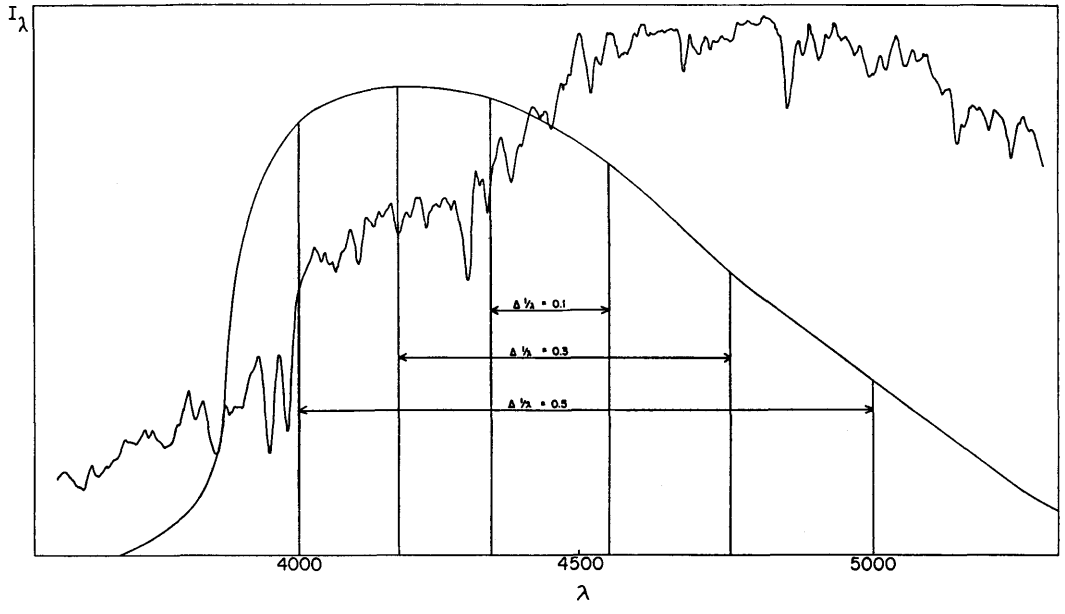


FIG. 7.—The energy-curve of β Comae (G0 V) in the neighborhood of the B filter band pass. Different band widths centered about $1/\lambda = 2.25\ \mu^{-1}$ yield different normalized integral effective intensities due to line blanketing.

cient, including the contribution by lines, for each wave length and optical depth, and adequately to solve the resulting transfer problem for the emergent flux, the line-blanketing problem would be non-existent.

The manner in which the presence of lines affects the spectrophotometry of the stellar continuum is illustrated in Figure 7. The energy-curve of β Com in the blue is shown, along with several band passes centered about $1/\lambda = 2.25$. The normalized relative flux per unit frequency interval measured for successively narrower band passes in terms of the flux transmitted by the B band pass of the *U*, *B*, *V* system is given in Table 6. The derived flux is quite sensitive to the choice of band width. The ambiguity can be removed only by measuring the total equivalent widths of the lines included and correcting the flux for the presence of the lines. The basic difficulty here is the determination of the continuum from which the equivalent widths are to be measured.

It is a fact that has not been wholly appreciated that the color indices of stars in the blue and ultraviolet are as profoundly influenced by the line spectrum as

TABLE 6

EFFECT OF LINES IN β COMAE

	B	1/λ		
		2.00–2.50	2.10–2.40	2.20–2.30
F.....	1.000	1.039	1.208	1.282

by the continuum. This is illustrated most vividly by comparing the colors derived for a set of main-sequence model stellar atmospheres with the colors obtained from observations. In Figure 8 the familiar relation between the $U - B$ and $B - V$ colors is compared with the theoretical colors for models. The plot has been constructed in the following manner. The integral effective intensity was computed from the emergent fluxes given by a set of model atmospheres representing main-sequence stars. The model atmospheres used include several computed by the author and by W. Melbourne, the model atmospheres of Swihart (1956*a*, *b*) and of de Jager and Nevén (1957). While these atmospheres differ in some respects as to the run of parameters with optical depth, the emergent fluxes are consistent. These computations then represent the colors to be expected in the absence of lines. A second set of integrations was carried out to determine the integral effective intensity for the observed spectrum based on the detailed energy-curves determined from spectral scans by Whitford and Code. These two sets of colors were then corrected for the zero-point error discussed in § 3 and tabulated in Table 2. The corrected colors computed from the spectral scans are found to agree with the observed colors of the same stars; in fact, this is the basis of the correction terms in Table 2. A plot

of the resulting colors for model stars and the observed relation for main-sequence stars is shown in Figure 8. The difference between these plots is to be accounted for in terms of the effect of the lines on the color. The rapid drop in the ultraviolet common to both curves is due to the continuous absorption of hydrogen. The dip in the observed curve is produced by the absorption in the hydrogen lines and their convergence toward the Balmer limit. The observed curve remains depressed below the theoretical curve as other lines begin to manifest themselves, and the steep decline in the ultraviolet for G and K stars is due to the strong ultraviolet-line blanketing. The influence of the lines is greater than the corresponding effect on the colors due to variations in surface gravity. These assumptions may be tested quantitatively by measuring the equivalent widths of the lines included in the band pass. The open circle shows the observed position of the star β Com on the $U-B$, $B-V$ plane; the filled circle indicates the colors of this star corrected for the effect of lines as determined from microphotometry of high-dispersion spectra.

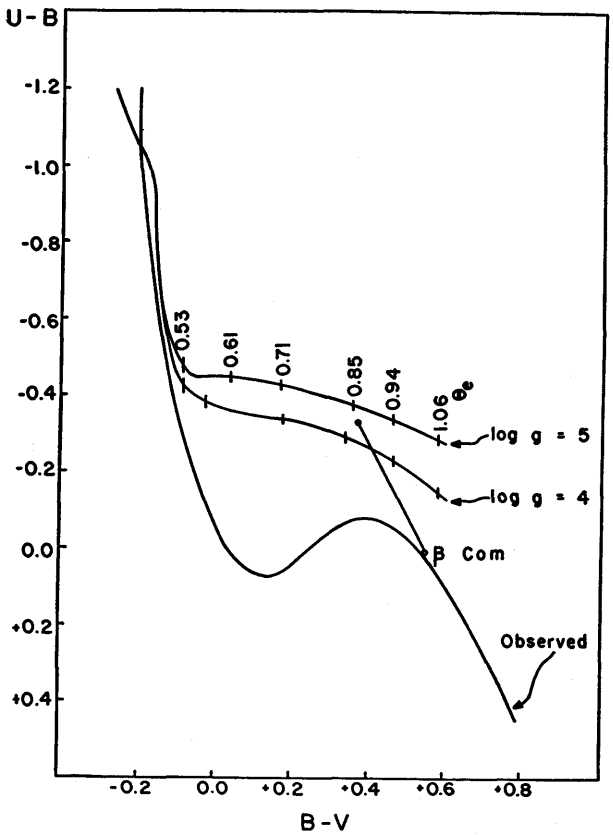


FIG. 8.—$U-B$ versus $B-V$ plot for model stellar atmospheres compared with the observed relation. The difference between these curves is attributed to the effect of line blanketing.

The import of these results is clear. A change in chemical composition may manifest itself in three ways. It will change the interior structure of the star and hence the effective temperature. It may modify the flux in the continuum through its effect on the continuous absorption coefficient, although this effect is known to be small. Finally, the change in chemical composition will alter the line strengths, an effect that, as we have seen, can be quite large (Wallerstein [1960]). A striking example of the variation in color and in spectral energy distribution by a variation in line strengths is provided by the subdwarfs (Schwarzschild, Searle, and Howard 1955; Code 1957, 1959) and is doubtless of no less importance for the red giants (Helfer, Wallerstein, and Greenstein [1959]).

If the total energy absorbed in the lines is small as compared with the total integrated flux, the effect of line absorption on the temperature distribution will be negligible, although the observed continuum may be distorted in the vicinity of the lines. In this case the comparison of observations with theory is relatively simple. The observed flux in line-free regions may be directly compared with the computed fluxes of a model, and elsewhere the observed fluxes may be corrected for the influence of lines from measurements of equivalent widths. An agreement between the computed and observed fluxes may be taken as a determination of the effective temperature and, to a lesser degree, the surface gravity and chemical composition of the star. This procedure is probably applicable only to the F stars and subdwarfs. For normal main-sequence stars later than G0, the flux absorbed in the lines exceeds 10 per cent of the integrated flux, while for early-type stars the absorption in the Lyman lines is likely to be appreciable. Definite answers on this question, however, await the results of extra-terrestrial observations.

It is an empirical fact that models may be constructed that will represent the observed flux, corrected for line absorption, within the uncertainties of observation. The relation between these models and the real stellar atmosphere is, however, not so obvious if the line absorption is large. Usually a model stellar atmosphere is constructed under the assumption of hydrostatic equilibrium and radiative equilibrium, and departures from grayness are allowed for by readjusting an initial temperature distribution in such a manner that the net flux remains constant throughout the atmosphere. This procedure has been discussed in detail, along with the modifications introduced by convection and by the presence of line blanketing. The problem of line blanketing has been discussed by Chandrasekhar (1936) and by Münch (1946) under certain simplifying assumptions regarding the nature and distribution of the line absorption. The line absorption is generally of importance in the outer layers of the atmosphere and acts to reduce the boundary temperature. The flux that is thrown back into the atmosphere at first increases the gradient, while at optical depths of the order of unity in the continuum the gradient approaches that of a gray atmosphere. The temperature, however, is somewhat higher than that at the corre-

sponding depth in an unblanketed atmosphere. We may view the problem in the following terms. Consider the radiation field to consist of two components, one the flux in the continuum and the other the flux in the lines. Thus at each depth the true net flux, F, could be represented by the flux computed according to the theory of the continuous spectrum, F_c, minus the total flux, ΔF, that is subtracted through all the absorption lines. If ΔF were known as a function of optical depth, a model atmosphere could be constructed in which the net flux was allowed to vary. Several attempts have been made to specify the variation in ΔF with depth for the sun (Labs 1951; Pecker 1951), but the uncertainties are quite large. In the absence of any detailed theory for the variation of ΔF with depth, it is customary to assume that ΔF is constant and equal to the ob-

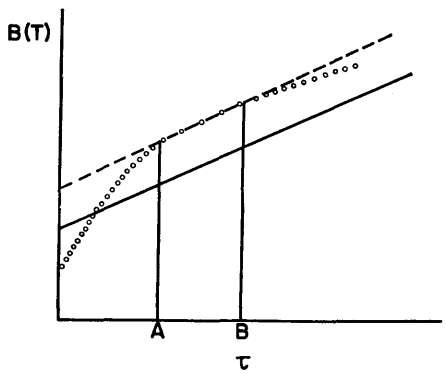


FIG. 9.—Schematic representation of the variation of the Planck function with optical depth. The solid line represents a model with no line absorption. The dotted curve illustrates the effect of line blanketing on this model, and the dashed curve shows the line-free model that would best fit the observed flux.

served value for the emergent flux. While this is certainly not true, there is reason to believe that the error introduced by such an assumption is small. This is because the modification to the temperature gradient is most important for optical depths smaller than those that make the principal contribution to the continuum. It should be added, however, that a discussion of the line formation itself is very dependent on the nature of the temperature gradient at small optical depths.

We may summarize the view outlined here by reference to Figure 9. The variation in the Planck function with a mean optical depth in the continuum for a model atmosphere of a given effective temperature T_e, computed from the theory of the continuum, is represented here by the solid line. The presence of line absorption in the outer layers would modify the temperature distribution in the manner indicated by the dotted curve. Now if the main contribution to the continuum between the lines occurs between optical depths A and B, then the observed continuum will be similar to that predicted by a model with the

temperature distribution indicated by the dashed line. This corresponds to a continuum model with a higher temperature, T_e^*. The assumption is that

$$\sigma T_e^4 = \sigma T_e^{*4} - \Delta F \,, \tag{30}$$

namely, that the energy removed by the lines ΔF appears between the lines and that it is distributed in wave length in the same manner as for a continuum model of higher effective temperature corresponding to a net flux, F_c. To correct the observed fluxes, we require measurements of the line absorption in the observed region. Only a few such measurements have been made. The most complete data are those for the sun (Mulders 1936; Wempe 1947; Michard 1950; Bell 1951). Shajn (1934) published line absorption corrections to visual and photographic magnitudes in 1934, and the problem appears to have received little additional attention until 1950, when Milford (1950) compiled line-

TABLE 7

BLANKETING COEFFICIENTS (γ)

λ	β Ari A5 V	σ Boo F2 V	π^3 Ori F6 V	110 Her F6 V	β Com G0 V	51 Peg G4 V	HD 140283 sd F5	HD 19445 sd F6
3400.....	0.92	.....	0.74*	0.79*	0.74*	0.66*	0.98	0.89
3650.....	.95	0.81	.77*	.74*	.65*	.69*	.98	.92
3860.....	.91	.88	.85	.81	.53*	.59*	.96	.94
4040.....	.97	.90	.87	.85	.77	.75	> .99	.96
4190.....	.96	.93	.87	.86	.75	.75	> .99	.98
4590.....	.96	.94	.91	0.92	.87	.85	>0.99	> .99
5060.....	> .99	.99	.98	.....	.95	.93	.....	> .99
5560.....	> .99	> .99	.98	.....	.96	.93	.....	> .99
5810.....	> .99	> .99	.99	.....	.97	.96	.....	> .99
6050.....	>0.99	>0.99	>0.99	.....	0.99	0.99	.....	>0.99

* Continuum undoubtedly suppressed, making these upper values.

blanketing data based on planimetry of the tracings in the Hiltner-Williams *Atlas* (1941). Other tabulations have been made by Iwanowska (1937) and Schwarzschild, Searle, and Howard (1955). None of these investigations has extended into the accessible ultraviolet, however. Recently W. Melbourne has carried through a program utilizing high-dispersion plates obtained with the coudé spectrograph on the Mount Wilson 100-inch reflector. Table 7 reproduces the data kindly supplied by Melbourne in advance of publication. The quantity γ is the ratio of observed flux in a rectangular band pass 15 A wide to the flux referred to the estimated continuum given by

$$\gamma = \frac{\int_{\lambda-7.5A}^{\lambda+7.5A} F_\lambda d\lambda}{\int_{\lambda-7.5A}^{\lambda+7.5A} F_c d\lambda} \,. \tag{31}$$

The quantity $1 - \gamma$ is equal to the blanketing factor, η, usually employed.

Until recently the application of the procedure outlined above for comparing

the predicted and observed stellar flux has not been practical because of the relatively incomplete data on energy-curves and line blanketing. The author (Code 1954) discussed the energy distribution of the F2 V star σ Boo, and Bless (1958) has carried out a program on A stars. Bless used a scanning spectrometer on the Heber D. Curtis Schmidt of the University of Michigan for obtaining energy-curves, which he then compared with the model atmospheres of Osawa (1956).

The solid line of Figure 10 shows the energy-curve of π^3 Orionis (F6 V) as

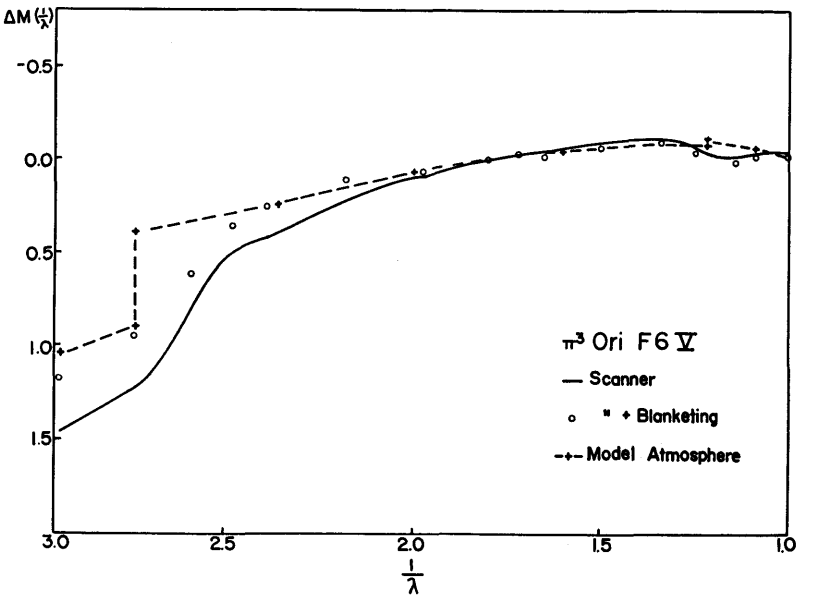


FIG. 10.—A comparison of the observed monochromatic flux from π^3 Ori (F6 V), before and after correction for lines, with a model atmosphere.

observed; a model atmosphere constructed by Swihart (1956) is shown by the dashed line; and, finally, the open circles indicate the observed flux corrected for line blanketing from Table 7.

§ 7. MONOCHROMATIC MAGNITUDES

In this section the monochromatic magnitudes for a representative sample of spectral types are tabulated. The data are based on the absolute calibration discussed in § 4 and the spectral scans of Whitford and Code. The wave lengths are those found to be relatively free of strong lines and correspond to the regions measured by Melbourne for blanketing. The magnitude per unit frequency interval relative to $1/\lambda = 1.80$ for a band pass of 10 A is given in Table 8:

$$m\left(\frac{1}{\lambda}\right) = -2.5 \log \frac{F(1/\lambda)}{F(1.80)}. \qquad (32)$$

TABLE 8

MONOCHROMATIC MAGNITUDES

$m\,(1/\lambda)$

	λ	0.340	0.365	0.386	0.404	0.419	0.459	0.506	0.556	0.581	0.605	0.667	0.746	0.800	0.875	0.919	1.000
	$1/\lambda$	2.94	2.74	2.59	2.48	2.39	2.18	1.975	1.80	1.72	1.65	1.50	1.34	1.25	1.14	1.09	1.00
10 Lac	O9 V	−0.48	−0.45	−0.44	−0.40	−0.32	−0.28	−0.12	0.00	+0.08	+0.21	+0.35	+0.53	+0.65	+0.81	+0.82	+0.86
ϵ Ori	B0 I*a*	−0.44	−0.42	−0.40	−0.36	−0.30	−0.17	− .10	.00	+ .07	+ .14	+ .27	+0.42	+0.56	+0.72	+0.80	+0.98
υ Ori	B0 V	−0.58	−0.51	−0.52	−0.45	−0.43	−0.30	− .11	.00	+ .03	+ .22	+ .42	+0.67	+0.79	+1.00	+1.01	+1.18
55 Cyg	B3 I*a*	+1.02	+0.76	+0.56	+0.63	+0.49	+0.32	+ .19	.00	− .01	− .06	− .07	−0.09	−0.13	−0.11	−0.12	−0.18
η U Maj	B3 V	0.00	+0.05	−0.29	−0.37	−0.33	−0.28	− .12	.00	+ .08	+ .21	+ .29	+0.47	+0.61	+0.70	+0.65	+0.78
β Ori	B8 I*a*	+0.16	−0.09	−0.23	−0.17	−0.16	−0.10	− .07	.00	+ .05	+ .18	+ .20	+0.30	+0.42	+0.51	+0.49	+0.59
δ Cyg	B9 5 III	+1.08	+0.86	−0.14	−0.19	−0.16	−0.12	− .06	.00	+ .06	+ .14	+ .24	+0.36	+0.47	+0.48	+0.48	+0.52
α Lyr	A0 V	+1.14	+1.04	−0.07	−0.19	−0.18	−0.14	− .06	.00	+ .06	+ .12	+ .22	+0.35	+0.46	+0.48	+0.51	+0.56
α Cyg	A2 I*a*	+1.10	+0.96	+0.05	+0.04	+0.05	+0.10	+ .01	.00	+ .06	+ .18	+ .13	+0.24	+0.32	+0.28	+0.31	+0.30
β Tri	A5 III	+1.60	+1.37	+0.31	+0.06	+0.03	−0.02	− .02	.00	+ .04	+ .09	+ .15	+0.23	+0.33	+0.34	+0.31	+0.40
β Ari	A5 V	+1.38	+1.22	+0.25	+0.02	−0.02	−0.06	.00	.00	+ .04	+ .11	+ .19	+0.30	+0.37	+0.41	+0.38	+0.40
ρ Gem	F0 V	+1.48	+1.26	+0.56	+0.36	+0.28	+0.14	+ .09	.00	+ .03	+ .03	+ .04	+0.07	+0.11	+0.02	+0.08	+0.12
σ Boo	F2 V	+1.40	+1.19	+0.66	+0.48	+0.41	+0.20	+ .11	.00	− .03	− .02	− .06	−0.07	−0.07	0.00	−0.08	−0.16
π^3 Ori	F6 V	+1.46	+1.22	+0.79	+0.50	+0.42	+0.22	+ .11	.00	− .03	− .02	− .08	−0.11	−0.06	−0.01	−0.03	−0.04
λ Ser	G0 V	+1.70	+1.41	+1.20	+0.81	+0.72	+0.36	+ .17	.00	− .06	− .10	− .13	−0.21	−0.20	−0.12	−0.16	−0.22
16 Cyg A	G2.5 V	+1.81	+1.52	+1.40	+0.88	+0.76	+0.39	+ .19	.00	− .05	− .07	− .15	−0.20	−0.22	−0.16	−0.22	−0.38
51 Peg	G4 V	+1.71	+1.47	+1.28	+0.81	+0.81	+0.36	+ .19	.00	− .04	− .14	− .19	−0.21	−0.19	−0.08	−0.24	−0.34
16 Cyg B	G4 V	+1.91	+1.56	+1.47	+0.88	+0.78	+0.37	+ .19	.00	− .05	− .07	− .16	−0.20	−0.21	−0.23	−0.25	−0.39
α Tau	K5 III	+4.70	+4.02	+3.74	+2.73	+2.48	+1.04	+ .60	.00	− .24	− .36	− .66	−1.11	−1.17	−1.22	−1.39	−1.38
61 Cyg A	K5 V	+3.62	+3.13	+2.90	+2.03	+1.73	+0.73	+ .53	.00	− .20	− .25	− .44	−0.65	−0.74	−0.78	−0.90	−1.00
α Ori	M2 I*a*	+5.20	+4.71	+4.26	+3.29	+2.90	+1.41	+0.58	0.00	−0.30	−0.44	−0.78	−1.50	−1.62	−1.76	−1.88	−2.22

Table 9 tabulates the corrections to be added algebraically to the magnitudes given by Hall (1942) to place this system of relative spectrophotometry on the absolute basis of Table 8. While the probable error of the mean of these energy-curve determinations is of the order of a few hundredths of a magnitude, systematic errors of the order of a tenth of a magnitude may well be present as a result of the present uncertainties in the absolute calibration. The ambiguities introduced by our lack of detailed information on the line absorption may be even more serious in many cases.

It is frequently necessary in certain theoretical applications to determine the flux of radiation received from a star in energy units, such as ergs cm^{-2} sec^{-1} per unit frequency interval, say. While such determinations are more difficult, they

TABLE 9

CORRECTIONS TO HALL (*Ap J.*, VOL. 94)

AMHERST			SPROUL		
λ	1/λ	Δm	λ	1/λ	Δm
0.450	2.22	−0.12	0.456	2.19	−0.11
.500	2.00	− .06	0.505	1.98	− .06
.550	1.82	− .01	0.553	1.81	.00
.600	1.67	+ .03	0.601	1.66	+ .14
.650	1.54	+ .22	0.649	1.54	+ .22
.701	1.43	+ .29	0.696	1.44	+ .29
.751	1.33	+ .38	0.745	1.34	+ .36
.801	1.25	+ .50	0.794	1.26	+ .48
.851	1.18	+ .52	0.840	1.19	+ .51
0.881	1.14	+0.53	0.889	1.12	+ .53
			0.935	1.07	+ .56
			0.983	1.02	+0.60
			1.032	0.97	

are a by-product of a careful determination of the energy distribution of a star. The results, however, are somewhat less accurate. In principle, the surface brightness of the standard lamp is known from equation (12) or more directly from a comparison with the black-body radiator. If, then, the area of the filament observed and the distance of the lamp are known, the flux at the telescope may be computed. The surface brightness is, however, sensitive to temperature variations and hence varies toward the edge of the filament more rapidly than the spectral distribution.

In the case of the sun it is possible to employ a black receiver, and, by the use of the techniques described earlier, monochromatic fluxes for the sun are available. If we use the fluxes derived by Minnaert (1956) and the apparent magnitude of the sun of $V = -27.8$ (Stebbins and Kron 1956), we find that the flux incident outside the earth's atmasphere from a G2 V star of apparent visual magnitude $V = 0.00$ is 3.79×10^{-9} erg/cm²/sec/A at $\lambda = 5465$ A, the effective

wave length of the V magnitude. This value is subject to uncertainties in the apparent visual magnitude of the sun and to a lesser extent by the manner in which the blending of spectral lines is taken into account. The value quoted above is probably uncertain by about 5 per cent.

The monochromatic flux at $\lambda = 5560$ A was measured by Code and Bless in the course of the investigations leading to Table 8. A preliminary value of 3.9×10^{-9} erg/cm^2/sec/A was found. Willstrop (1958) has carried out similar measurements at the Cape Observatory, using interference filters to isolate selected spectral regions. He finds a value for the monochromatic flux from a star of visual magnitude $V = 0.00$ and color index $B - V = 0.0$ of 3.8×10^{-9} erg/cm^2/sec/A at 5400 A.

We shall adopt a value of 3.8×10^{-9} erg/cm^2/sec/A at 5560 A to provide a calibration for the monochromatic magnitudes tabulated in Table 8. This corresponds to 10^3 quanta/sec/cm^2/A. The monochromatic fluxes may therefore be derived from these data and the visual magnitudes of the stars. Programs to introduce higher precision in the absolute energy calibration of stars are presently under way, and the data described here must be regarded as preliminary.

We can look to the future for more precise absolute energy calibrations, more extensive data on line blanketing, and, most exciting of all, the extension of the observations to the far ultraviolet by measurements from space vehicles.

REFERENCES

Bahng, J. D. R.	1957	Thesis, University of Wisconsin.
Barbier, D., and Chalonge, D.	1941	*Ann. d'ap.*, **4**, 30.
Becker, W.	1938	*Zs. f. Ap.*, **15**, 225.
Bell, B.	1951	*Harvard Special Rept.*, No. 35.
Bless, R. C.	1958	Thesis, University of Michigan.
Bonsack, W. K., and Stock, J.	1957	*Ap. J.*, **126**, 99.
Brill, A.	1932	*Hdb. d. Ap.* (Berlin: Springer), **5**, 128.
Cayrel de Strobel, G.	1957	*Ann. d'ap.*, **20**, 55.
Chalonge, D., and Divan, L.	1952	*Ann. d'ap.*, **15**, 201.
Chandrasekhar, S.	1936	*M.N.*, **96**, 21.
Code, A. D.	1952	*Observatory*, **72**, 201.
	1954	*Proc. N.S.F. Conf. on Stellar Atmospheres*, p. 14.
	1957	*Ann. Rept. Mount Wilson and Palomar Observatories*, p. 45.
	1959	*Ap. J.*, **130**, 473.
Forsythe, W. E.	1937	*Measurement of Radiant Energy* (New York McGraw-Hill Book Co., Inc.).
Gascoigne, S. C. B.	1950	*M.N.*, **110**, 15.
Gouffe, A.	1945	*Rev. Opt.*, **24**, 1.

GREAVES, W. M. H.	1956	*Vistas in Astronomy*, ed. A. BEER (London and New York: Pergamon Press), **2**, 1309.
GREAVES, W. M. H., DAVIDSON, C. R., and MARTIN, E. G.	1932	*Observations of Colour Temperatures of Stars* (London: H.M. Stationery Office, Royal Observatory, Greenwich).
	1934	*M.N.*, **94**, 488.
	1952	*Observations of Colour Temperatures of Stars*, Vol. 2 (London: H.M. Stationery Office, Royal Observatory, Greenwich).
HALL, J. S.	1941	*Ap. J.*, **94**, 71.
	1942	*Ibid.*, **95**, 231.
HALL, J. S., and WILLIAMS, R. C.	1942	*Ap. J.*, **95**, 225.
HELFER, H. L., WALLERSTEIN, G., and GREENSTEIN, J. L.	1959	*Ap. J.*, **129**, 700.
HILTNER, W. A., and WILLIAMS, R. C.	1941	*Photometric Atlas of Stellar Spectra* (Ann Arbor: University of Michigan Press).
HOFF, H. VON	1939	*Zs. f. Ap.*, **18**, 157.
HULST, H. C. VAN DE	1945	*Nederl. Tij. Natuurkunde*, **11**, 210.
IWANOWSKA, W.	1937	*Bull. Obs. Astr. Wilno*, No. 18.
JAGER, C. DE, and NEVÉN, L.	1957	*Rech. astr. Obs. Utrecht*, Vol. **13**, No. 4.
JOHNSON, H. L.	1957	*Ap. J.*, **126**, 121.
JOHNSON, H. L., and MORGAN, W. W.	1951	*Ap. J.*, **114**, 522.
	1953	*Ibid.*, **117**, 313.
JONES, C.	1949	*J. Opt. Soc. America*, **39**, 344.
KIENLE, H.	1937	*Ergebnisse d. exakten Naturwiss.* (Berlin: Springer), **16**, 437.
	1941	*Zs. f. Ap.*, **20**, 239.
	1955	*Trans. I.A.U.*, **9**, 536
KIENLE, H., CHALONGE, D., and BARBIER, D.	1938	*Ann. d'ap.*, **1**, 396.
KIENLE, H., STRASSL, H., and WEMPE, J.	1938	*Zs. f. Ap.*, **16**, 201.
KIENLE, H., WEMPE, J., and BEILEKE, F.	1941	*Zs. f. Ap.*, **20**, 91.
LABS, D.	1951	*Zs. f. Ap.*, **29**, 199.
MCCREA, W. H.	1931	*M.N.*, **91**, 836.
MELBOURNE, W.	1958	Thesis, California Institute of Technology.
	1960	*Ap. J.*, **132**, 101.
MICHARD, R.	1950	*B.A.N.*, **11**, 227.
MILFORD, N.	1950	*Ann. d'ap.*, **13**, 243.

MILNE, E. A.	1928	*Observatory*, **51**, 88.
MINNAERT, M.	1956	*The Sun*, ed. G. KUIPER (Chicago: University of Chicago Press), p. 88.
MÜNCH, G.	1946	*Ap. J.*, **104**, 87.
MULDERS, G. F. W.	1936	*Zs. f. Ap.*, **11**, 132.
OSAWA, K.	1956	*Ap. J.*, **123**, 513.
PECKER, J.-C.	1951	*Ann. d'ap.*, **14**, 383.
PLASKETT, H. H.	1923	*Pub. Dom. Ap. Obs. Victoria*, **2**, 213.
ROSENBERG, H.	1914	*Abh. d. Kais. Leop.-Carol Deutsch. Akad. d. Naturforsch. Nova Acta*, Vol. **101**, No. 2.
SCHWARZSCHILD, M., SEARLE, L., and HOWARD, R.	1955	*Ap. J.*, **122**, 353.
SHAJN, G.	1934	*M.N.*, **94**, 642.
STEBBINS, J., and KRON, G. E.	1956	*Ap. J.*, **123**, 440.
	1957	*Ibid.*, **126**, 266.
STEBBINS, J., and WHITFORD, A. E.	1945	*Ap. J.*, **102**, 318.
STRÖMGREN, B.	1937	*Handbuch der Experimentalphysik*, ed. W. WIEN and F. HARMS (Leipzig: Akademische Verlags-Gesellschaft M.B.H.), **26**, 321.
SWIHART, T. L.	1956*a*	*Ap. J.*, **123**, 143.
	1956*b*	*Ibid.*, p. 151.
TIFFT, W. G.	1958	*A.J.*, **63**, 127; Thesis, California Institute of Technology.
VOS, J. C. DE	1954	*Physica*, **20**, 669.
	1954	*Ibid.*, p. 690.
WALLERSTEIN, G.	1960	*Ap. J.*, **132**, 37.
WEMPE, J.	1947	*A.N.*, **275**, 97.
WENSEL, H. T., ROESER, W. F., BARBROW, L. E., and CALDWELL, F. R.	1931	*Bureau of Standards J. Res.*, **6**, 1103.
WHITFORD, A. E.	1948	*Centennial Symposium* ("Harvard College Observatory Monographs," No. 7), p. 155.
	1958	*A.J.*, **63**, 201.
WILLIAMS, R. C.	1939	*Pub. Obs. Michigan*, Vol. **7**, No. 7.
	1940	*Ibid.*, **8**, 37.
WILLSTROP, R. V.	1958	*M.N. Astr. Soc. South Africa*, **17**, 40.
WILSING, J., SCHEINER, J., and MÜNCH, W.	1919	*Pub. Astr. Obs. Potsdam*, No. 74.
YÜ, C. S.	1926	*Lick Obs. Bull.*, **12**, 104.

CHAPTER 3

Basic Theory of Line Formation

KARL-HEINZ BÖHM
University of Kiel, Germany

§ 1. INTRODUCTION

A CONSIDERABLE part of our information on astronomical objects—especially on stellar atmospheres—is derived from a study of their absorption- and emission-line spectra. Therefore, it is necessary to improve the accuracy of the theory of line formation as far as possible.

Since many of the foundations of this theory were laid before 1930, there has been a tendency to believe that the theory is almost complete and that standard methods for the calculation of line profiles are available that satisfy practically every need of the observing astrophysicist. Only recently has it become evident that numerous difficulties are involved in the present form of the theory, which are not only of "academic" but also of practical interest if we wish to derive the structure of a stellar atmosphere accurately from the observation of line profiles. Part of the difficulty arises from the fact that it is very hard to get a real self-consistent picture of the thermodynamic and hydrodynamic state of a stellar atmosphere (and the determination of the thermodynamic structure of the atmosphere cannot be separated from the theory of line formation!), and another part comes from the present difficulties in the theory of line broadening.

With these facts in mind, it seems justified to put more emphasis on the present aspects and difficulties of the field than is customary in a review of this kind. We think that such a procedure is justified, as there exist a number of excellent reviews of the foundations of the theory. Especially we wish to refer to the books of Unsöld (1955), Aller (1953), and Woolley and Stibbs (1953). Nevertheless, we shall try to include enough of the early investigations that this article may in general be understood without too many references to the reviews quoted above.

§ 2. FORMULATION OF THE PROBLEM

We are concerned mainly with the following problem: Given the outer layers of a star, through which a certain energy flux is transported by radiation or convection or a combination of both, how can we derive the profile of an absorption (or emission) line in the stellar spectrum?

Often the thickness z_0 of the layers, from which the radiation leaves the star (without further absorption and re-emission processes taking place), is very small compared to the radius, R, of the star. In this case we call the outer layers a "stellar atmosphere." On the other hand, if z_0 is comparable to, or larger than, R, these layers are called a "stellar envelope." There are two main differences between the theory of atmospheres and envelopes: (1) stellar atmospheres can usually be considered as plane-parallel, which simplifies the mathematics of the

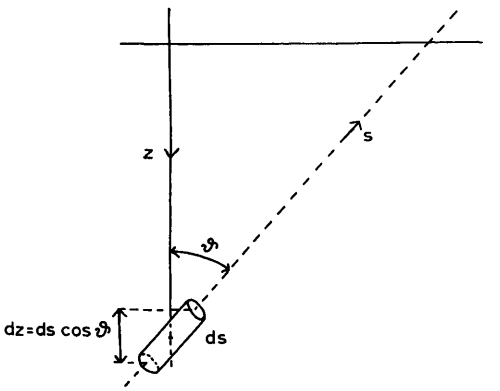


FIG. 1.—Definitions used in the equation of transfer

transfer equation, since for stellar envelopes the spherical symmetry of the problem has to be taken into account (see, e.g., Chandrasekhar 1950); (2) in stellar envelopes effects of the geometrical dilution of radiation play an important role; therefore, deviations from local thermodynamic equilibrium are usually greater than in stellar atmospheres (see below). We shall restrict ourselves mainly to the consideration of atmospheres. Usually we can assume that these are in a stationary state.

Let us consider what happens to a narrow beam of radiation with the intensity $I_\nu(\theta)$ when passing through a volume element of thickness ds (ν = frequency; θ = angle between the normal of the atmosphere and the beam of radiation; see Fig. 1). A certain fraction of the energy will be absorbed or scattered and therefore be lost from the beam. On the other hand, the volume element will emit radiation itself, and this radiation—as far as it goes in the direction θ—has to be added to the original intensity. The loss of intensity is proportional to the intensity itself, where the constant of proportionality is the sum of the continuous and line absorption coefficient, as well as the scattering coeffi-

cient, per centimeter. Let us call the absorption and scattering coefficient *per unit mass*, κ_ν and σ (continuum), l_ν and σ_ν (line). The emission per cm³ in the frequency range $d\nu$ and the solid angle $d\omega$ per unit of time will be written as

$$(\kappa_\nu + l_\nu + \sigma + \sigma_\nu)\, \rho S_\nu(\theta)\, d\nu d\omega\,. \tag{2.1}$$

The source function, S_ν, defined by (2.1) has to be determined by additional considerations. Consequently, we get the relation

$$\frac{dI_\nu}{ds} = -(\kappa_\nu + l_\nu + \sigma + \sigma_\nu)\, \rho I_\nu + (\kappa_\nu + l_\nu + \sigma + \sigma_\nu)\, \rho S_\nu\,. \tag{2.2}$$

We introduce the geometrical depth of the atmosphere, z (counted downward from the top),

$$dz = -ds\cos\theta\,, \tag{2.3}$$

and the optical depth x_ν,

$$dx_\nu = (\kappa_\nu + l_\nu + \sigma + \sigma_\nu)\, \rho dz\,. \tag{2.4}$$

Equation (2.2) may be written as follows:

$$\cos\theta \frac{dI_\nu(z,\theta)}{az} = (\kappa_\nu + l_\nu + \sigma + \sigma_\nu)\, \rho I_\nu(z,\theta) - (\kappa_\nu + l_\nu + \sigma + \sigma_\nu)\, S_\nu(z,\theta)\,, \tag{2.5a}$$

or

$$\cos\theta \frac{dI_\nu(x_\nu,\theta)}{dx_\nu} = I_\nu(x_\nu,\theta) - S_\nu(x_\nu,\theta)\,. \tag{2.5b}$$

We are interested in determining the "profile" of an absorption or emission line, i.e., $I_\nu(0, \theta)$ in the small frequency range in which l_ν and σ_ν for one line are essentially different from zero. This has to be done by solving simultaneously equations of the form (2.5*a*) or (2.5*b*) for different frequency ranges of the line profile. We can immediately write down the formal solution of (2.5*b*). If we restrict ourselves to the most important case of a semi-infinite atmosphere, we get

$$I_\nu(0,\theta) = \int_0^\infty S_\nu(x_\nu,\theta)\, e^{-x_\nu \sec\theta} dx_\nu \sec\theta\,. \tag{2.6}$$

In all stars except the sun and some eclipsing binaries, only the surface flux, πF_ν, where

$$F_\nu(0) = \frac{1}{\pi}\int_0^{\pi/2}\int_0^{2\pi} I_\nu(0)\cos\theta\sin\theta d\theta d\varphi\,, \tag{2.7}$$

can be observed. If the angular dependence of S_ν can be neglected (see below), we get, from equations (2.6) and (2.7),

$$F_\nu(0) = 2\int_0^\infty S_\nu(x_\nu) E_2(x_\nu)\, dx_\nu\,, \tag{2.8}$$

where

$$E_2(x) = \int_0^\infty \frac{e^{-xw}}{w^2}\, dw \tag{2.9}$$

is the well-known second exponential integral.

Obviously, our problem will be solved if we have determined S_ν and κ_ν, l_ν, σ, and σ_ν as functions of z or some arbitrarily chosen optical depth. How can this be accomplished? If there is local thermodynamic equilibrium everywhere in the atmosphere, S_ν can be replaced by the Planck function, B_ν, for the local temperature T:

$$B_\nu = \frac{2h\nu^3}{c^2} \frac{1}{\exp(h\nu/kT) - 1}, \tag{2.10}$$

where h = Planck's constant and c = velocity of light. Actually, I_ν is highly anisotropic near the surface of the star, and consequently we cannot base our arguments on considerations of thermodynamic equilibrium. In principle, relations like Kirchhoff's and Planck's law cannot even be applied separately to every volume element of the atmosphere. We have to solve these problems: (1) Under what condition may $S_\nu = B_\nu$ be considered a reasonable approximation? (2) How can we derive the source function and the absorption coefficient if this is not the case? These questions refer only to the thermodynamic state of a volume element if the radiation field is given.

Another problem is the question of the variation of S_ν within the atmosphere. If the atmosphere is in pure radiative equilibrium, and if, moreover, $S_\nu = B_\nu$ we can derive $S_\nu(x_\nu)$ by known methods (see Münch's chapter in this volume). If the radiative equilibrium is disturbed by hydrodynamic phenomena (like thermal convection), S_ν is no longer a unique function of x_ν, but fluctuations of S_ν occur for a given optical depth (the best example of such fluctuations is the solar granulation, see, e.g., Böhm 1954*b*).

The simultaneous occurrence of actual deviations from local thermodynamic equilibrium, i.e., from $S_\nu = B_\nu$, and of fluctuations in S_ν in many stars makes the problem rather complex. We shall put the main emphasis on the first problem, i.e., the determination of S_ν in a volume element where $I_\nu(\theta)$ is given. The problem of the fluctuations in S_ν (loosely referred to as the "temperature fluctuations") will be treated only briefly, as it leads immediately into hydrodynamic questions that lie outside the scope of this chapter.

For the determination of S_ν and $(\kappa_\nu + l_\nu + \sigma + \sigma_\nu)$, the only satisfactory method is one of microscopic analysis, which means that we have to consider the elementary radiative and collisional processes taking place in the different layers of a stellar atmosphere. In order to proceed, we first have to write equations (2.5*a*) and (2.5*b*) in their microscopic form. In order to get relatively simple formulae, we shall first restrict ourselves to the wave-length regions in which the line absorption coefficient is much greater than the continuous absorption coefficient and therefore the latter can be neglected. Later we shall see that taking into account the continuous absorption does not bring new difficulties.

We consider a frequency interval $\Delta\nu$ of a line, which corresponds to a transition between a higher level j and a lower level i. Let B_{ij}, B_{ji}, and A_{ji} be the well-known Einstein coefficients of absorption, induced and spontaneous emission, and N_i the occupation numbers. We introduce the probabilities $\psi_\nu\Delta\nu$ and

$\phi_\nu \Delta\nu$, that, if a transition takes place between j and i, the photon is emitted or absorbed in the frequency range $\Delta\nu$. Here ψ_ν refers to spontaneous emission, ϕ_ν to absorption and stimulated emission. The intensity emitted within $\Delta\nu = 1$ of the line $j \rightarrow i$ is

$$N_j \left(A_{ji}\psi_\nu + B_{ji} I_\nu \phi_\nu\right) \frac{h\nu}{4\pi}. \tag{2.11}$$

The transition probabilities are defined as in Milne's investigation (1930), i.e., B_{ij} and B_{ji} refer to the specific intensity I_ν. These B_{ij}'s and B_{ji}'s have to be multiplied by $c/4\pi$ in order to get the transition probabilities as originally defined by Einstein.

The absorbed energy is

$$N_i B_{ij} I_\nu \phi_\nu \frac{h\nu}{4\pi}. \tag{2.12}$$

Consequently, we get the equation of transfer,

$$4\pi \frac{\cos\theta}{h\nu} \frac{dI_\nu}{dz} = -N_j \left(A_{ji}\psi_\nu + B_{ji} I_\nu \phi_\nu\right) + N_i B_{ij} I_\nu \phi_\nu. \tag{2.13}$$

Making use of the well-known relations between the Einstein coefficients,

$$B_{ji} = \frac{g_i}{g_j} B_{ij}; \qquad A_{ji} = \frac{2h\nu^3}{c^2} \frac{g_i}{g_j} B_{ij}, \tag{2.14}$$

we get

$$4\pi \frac{\cos\theta}{h\nu} \frac{dI_\nu}{dz} = \left(N_i - \frac{g_i}{g_j} N_j\right) \phi_\nu B_{ij} I_\nu - \frac{2h\nu^3}{c^2} \frac{g_i}{g_j} B_{ij} N_j \psi_\nu. \tag{2.15}$$

By comparison with equation (2.5a), we find

$$l_\nu + \sigma_\nu = \left(N_i - \frac{g_i}{g_j} N_j\right) a_\nu, \tag{2.16}$$

where

$$a_\nu = \frac{B_{ij}}{4\pi} \phi_\nu h\nu \tag{2.16a}$$

is the absorption coefficient per atom in the ith level. For the source function, S_ν, we have

$$S_\nu = \frac{2h\nu^3}{c^2} \left(\frac{g_j}{g_i} \frac{N_i}{N_j} - 1\right)^{-1} \frac{\psi_\nu}{\phi_\nu}. \tag{2.17}$$

Obviously, equation (2.17) reduces to $S_\nu = B_\nu$ if $\psi_\nu = \phi_\nu$ and if N_i/N_j follows a Boltzmann distribution,

$$\frac{N_j}{N_i} = \frac{g_j}{g_i} \exp\left(-\frac{h\nu_{ij}}{kT}\right). \tag{2.18}$$

If equation (2.18) is fulfilled and, moreover, if the ionization follows the Saha equation,

$$\frac{N_{r+1}}{N_r} P_e = \frac{(2\pi m)^{3/2} (kT)^{5/2}}{h^3} \frac{u_{r+1}}{u_r} \exp\left(-\frac{\chi_r}{kT}\right) \tag{2.19}$$

(P_e = electron pressure, u_r = partition function, χ_r = ionization potential, the index r refers to r-times ionized atoms[1]), $(l_\nu + \sigma_\nu)$ reduces to the absorption coefficient in local thermodynamic equilibrium. The condition $\psi_\nu = \phi_\nu$ is fulfilled if we have either local thermodynamic equilibrium or completely noncoherent scattering (Warwick 1955; Thomas 1957; § 4 of this chapter). Under a relatively wide range of conditions, ψ_ν/ϕ_ν may not be too far from unity.

In equations (2.11)–(2.17) we have neglected the angular dependence of S_ν. This plays a role only if coherent scattering becomes important. In such a case (which does not occur very often in practice) equation (2.15) has to be generalized, as suggested by Warwick (1955).

As we see from equations (2.16) and (2.17), the problem is now to determine (1) the occupation numbers N_i (for the discrete states as well as for the continuum)[2] and (2) the absorption coefficient per atom a_ν and its frequency dependence. The first problem will be considered in the next section. To solve the second task, we have to know the oscillator strengths of the spectral lines, their broadening mechanisms, and the appropriate atomic constants (Stark effect constants, polarizabilities, etc.) These problems can be solved only in collaboration with experimental and theoretical physicists and will be considered in the later sections of this chapter.

§ 3. THE THERMODYNAMIC STATE OF A STELLAR ATMOSPHERE[3]

3.1. Atmospheres in Radiative Equilibrium

3.11. *The assumption of local thermodynamic equilibrium.*—If $S_\nu = B_\nu$, equations (2.6) and (2.8) reduce to

$$I_\nu(0,\theta) = \int_0^\infty B_\nu(x_\nu)\, e^{-x_\nu \sec\theta} dx_\nu \sec\theta \tag{3.1}$$

and

$$F_\nu(0) = 2\int_0^\infty B_\nu(x_\nu) E_2(x_\nu)\, dx_\nu, \tag{3.2}$$

with $dx_\nu = (x_\nu + l_\nu)\rho dz$. In this case the whole problem is reduced to a number of simple quadratures if we know the local temperature T and the pressure as a function of x_ν. Often it is convenient to consider, instead of I_ν or F_ν, the profile of the relative line depth, r_ν, defined by

$$r_\nu = \frac{I_0(0,\theta) - I_\nu(0,\theta)}{I_0(0,\theta)}, \tag{3.3}$$

where I_0 is the intensity of the neighboring continuum. The corresponding profile for the flux is usually designated as R_ν. The advantage of definition (3.3)

[1] For a simple derivation of eqs. (2.18) and (2.19), which are strictly valid only in thermodynamic equilibrium, see, e.g., Unsöld's book (1955).

[2] For simplicity, we shall call this problem the "determination of the thermodynamic state of the atmosphere."

[3] The logical relationship of the different sections of this chapter is illustrated in Fig. 2.

is that the integral of r_ν or R_ν, taken over the whole line, gives the equivalent width, W_ν.

If we wish to apply equation (3.1) or (3.2), we have to be aware of the following difficulty. In many cases the line absorption coefficient, l_ν, is very sensitive to small changes in the temperature stratification due to the temperature sensitivity of the Boltzmann and Saha equations (see Priester 1953; Böhm 1954*b*). Therefore, the temperature distribution has to be known with high accuracy, if we wish to calculate line profiles that can be compared with good

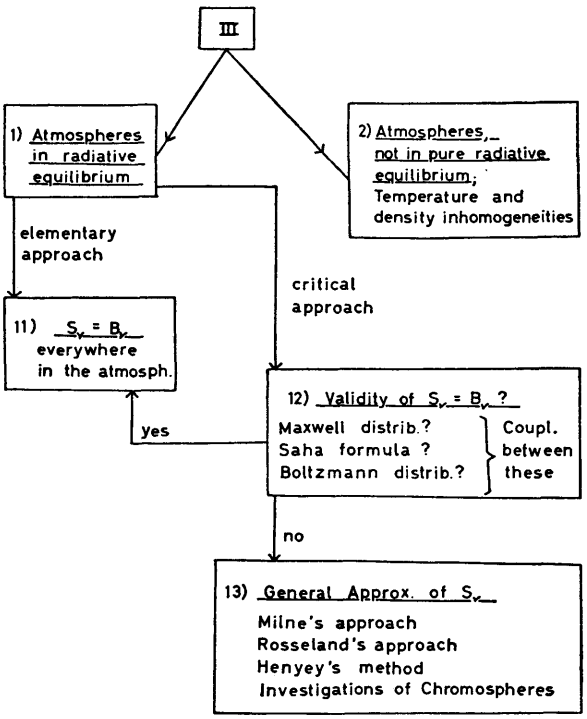


FIG. 2.—The structure of § 3

observations. It is very seldom that the gray approximation of the temperature distribution is accurate enough for this purpose.

The numerical quadrature according to equation (3.1) or (3.2) does not offer any difficulties if $T(x_\nu)$ is known. However, it is rather laborious to calculate a great number of line profiles in this way. For faint lines and the wings of strong lines, Unsöld (1932) has developed a much simpler method to calculate r_ν.

We introduce separate optical depths due to the line and the continuous absorption coefficient,

$$d\tau_\nu = \rho l_\nu dz \cdot \qquad d\tau = \rho \kappa_\nu dz\,, \tag{3.4}$$

and get

$$I_\nu(0,\theta) = \int_0^\infty B(\tau)\, e^{-\tau \sec\theta}\, e^{-\tau_\nu \sec\theta}\, d\tau_\nu \sec\theta + \int_0^\infty B(\tau)\, e^{-\tau \sec\theta} e^{-\tau_\nu \sec\theta} d\tau \sec\theta . \tag{3.5}$$

After reducing the second term on the right-hand side by a partial integration and using equation (3.3), we get

$$r_\nu(0,\theta) = \int_0^\infty \frac{l_\nu}{\kappa_\nu}\, g_1(\tau,\theta)\, e^{-\tau_\nu \sec\theta} d\tau , \tag{3.6}$$

where g_1 is the so-called weighting function:

$$g_1(\tau,\theta) = \frac{\int_\tau^\infty B(\tau)\, e^{-\tau \sec\theta} d\tau \sec\theta - B(\tau)\, e^{-\tau \sec\theta}}{\int_0^\infty B(\tau)\, e^{-\tau \sec\theta} d\tau \sec\theta} \sec\theta , \tag{3.7}$$

which depends only on the continuous absorption coefficient and not on l_ν. So far, no approximations have been introduced. Now, if $l_\nu \ll \kappa_\nu$, it follows from equation (3.6) that

$$r_\nu(0,\theta) = \int_0^\infty \frac{l_\nu}{\kappa_\nu}\, g_1(\tau,\theta)\, d\tau . \tag{3.8}$$

As κ_ν usually changes only slowly with wave length, one can often use one weighting function for a great number of lines. If we consider R_ν (the line depth in the flux spectrum), we get the weighting function,

$$G_1(\tau) = \frac{\int_\tau^\infty B(\tau) E_1(\tau)\, d\tau - B(\tau) E_2(\tau)}{\int^\infty B(\tau) E_2(\tau)\, d\tau} . \tag{3.9}$$

If we use the identity

$$B(\tau)\, e^{-\tau \sec\theta} = -\int_\tau^\infty \frac{dB}{d\tau}\, e^{-\tau \sec\theta} d\tau + \int_\tau^\infty B e^{-\tau \sec\theta} d\tau \sec\theta , \tag{3.10}$$

equation (3.7) can be brought into the form

$$g_1(\tau,\theta) = \frac{\int_\tau^\infty \frac{dB}{d\tau \sec\theta}\, e^{-\tau \sec\theta} d\tau \sec\theta}{\int_0^\infty B(\tau)\, e^{-\tau \sec\theta} d\tau \sec\theta} \sec\theta , \tag{3.11}$$

which shows in an instructive way that g_1 depends essentially on the gradient of B (ten Bruggencate, Lüst-Kulka, and Voigt 1955). In a similar way we derive, from equation (3.9),

$$G_1(\tau) = \frac{\int_\tau^\infty \frac{dB}{d\tau} E_2(\tau)\, d\tau}{\int_0^\infty B(\tau) E_2(\tau)\, d\tau} . \tag{3.12}$$

We shall not discuss here the integration of equation (3.6) or (3.8) over all frequencies ν to give the equivalent width W_ν and permit a derivation of the so-called curve of growth. These problems are discussed in L. H. Aller's chapters in this volume.

If we wish to get only a very rough estimate of I_ν or I_λ, we may use the method of Eddington-Barbier (see Barbier 1944) as extended by Unsöld (1948). Expanding B in a Taylor series at $x_\nu = \cos\theta$ and neglecting terms of second and higher order, we find

$$I_\nu(0,\theta) = B_\nu(x_\nu = \cos\theta) \tag{3.13}$$

and, for $l_\nu \ll \kappa_\nu$,

$$r_\nu(0,\theta) = \left(\frac{d \ln B}{d\tau}\right)_{\cos\theta} \int_0^{\cos\theta} \frac{l_\nu}{\kappa_\nu} d\tau . \tag{3.14}$$

Recently there has been a tendency to calculate line profiles by direct numerical integration of equation (3.1) or (3.2). As soon as an electronic computer

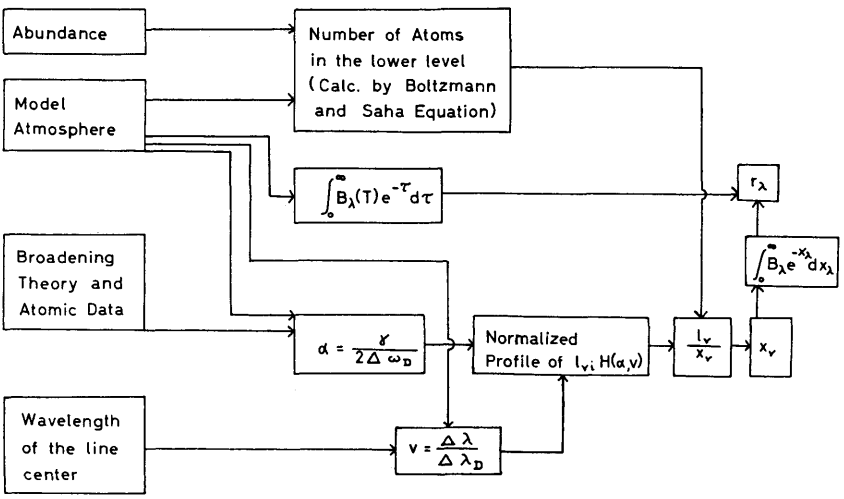


FIG. 3.—Schematic flow diagram for the calculation of line profiles formed in local thermodynamic equilibrium according to Heiser (1957) with minor changes.

is available, this straightforward method is certainly the best procedure (Cayrel 1957; Heiser 1957).

In Figure 3 we reproduce Heiser's schematic flow diagram (with minor changes), as it shows in a very instructive way the logical structure of such a calculation of line profiles in the case of local thermodynamic equilibrium. For the sake of simplicity, the computation is restricted to $\cos\theta = 1$. The symbols used have the following meaning: $\Delta\lambda_D$, $\Delta\omega_D$ = Doppler width of the lines in wave-length or angular frequency units; $H(a, v)$ = Voigt function (see § 4).

3.12. *The hypothesis of local thermodynamic equilibrium and its limitations.*—We have seen that the assumption of local thermodynamic equilibrium facili-

tates our problem considerably. Under what conditions can we apply this assumption? The derivation of a general criterion would be about as complex as a computation of the deviations from equilibrium themselves. Therefore, we have to be satisfied with a more heuristic point of view.

Even for a gray atmosphere (in which no lines are formed), the assumption $S_\nu = B_\nu$ cannot be fulfilled because of the non-isotropy of the radiation field I_ν. (The hypothesis $S_\nu = B_\nu$ contradicts the second law of thermodynamics; see Wildt 1956). In a non-gray atmosphere the deviation of I_ν from the Planck function is even greater than for the gray case, and consequently we should expect even greater deviation from local thermodynamic equilibrium. Hence it is not necessary to ask whether there are deviations from local thermodynamic equilibrium but only how great they are.

As we have seen in § 2, we have to know the deviations of the occupation numbers of the continuum and the discrete levels from their equilibrium values; in other words, we have to determine the deviations from (1) the Maxwell distribution, (2) the Boltzmann formula, and (3) the Saha equation. Strictly speaking, conditions 1, 2, and 3 are always coupled. Nevertheless, it is useful to consider them first separately:

Maxwell distribution: As we shall see below, in stellar atmospheres most of the free electrons are produced by photoionization from low levels or by collisional ionizations from high levels. After a certain lifetime the free electrons usually are captured in radiative recombinations (or by three-body recombinations into high levels). During its lifetime the free electron suffers elastic collisions with other electrons, ions, and atoms and inelastic collisions with atoms and ions. The elastic collisions tend to establish thermal equilibrium, which will be partly disturbed by the inelastic collisions, as these collisions influence only electrons with a kinetic energy beyond a certain critical value. The lifetime of a free electron will be of the order of

$$t_0 = \frac{m^{1/2}}{\sigma N (3kT)^{1/2}}, \tag{3.15}$$

where σ is the symbol for the cross-section for radiative recombination; N is the number of ions and atoms per cubic centimeter mainly responsible for electron capture. In atmospheres in which radiative capture occurs mainly by neutral hydrogen atoms (formation of H^-), σ will be 2.6×10^{-22} cm^2 at 6000° (Massey and Burhop 1952). In this case the rate of three-body recombinations is very small (cf. Geltman as quoted by Pagel 1959). In hotter atmospheres the recombination is due mainly to radiative capture by protons. By logarithmic extrapolation of the cross-sections calculated by Bates, Buckingham, Massey, and Unwin (1939) we get, for this process, $\sigma = 6 \times 10^{-21}$ cm^2 for $T = 10{,}000°$.

The most important elastic collisions are those between electrons. The relaxation time for an electron-ion collision is greater than that for electrons by a factor $(m/m_e)^{1/2}$ (= 43 for protons). The frequency of elastic electron-atom col-

lisions becomes greater than that of electron-electron collisions only if N_e/N_{total} is considerably smaller than 10^{-4}. In this case we underestimate the number of elastic collisions.[4] But this is of no importance in the present context, as we shall show that even if we neglect elastic electron-atom collisions, the number of elastic collisions is always much greater than the number of inelastic collisions.

The relaxation time for elastic collisions between electrons is, according to Spitzer (1956),

$$t_1 = \frac{m^{1/2}\,(3\,kT)^{3/2}}{17.9\,N_e e^4 \ln\,(r_0/p_0)}, \tag{3.16}$$

with N_e = number of electrons per cubic centimeter; r_0 = Debye shielding distance; p_0 = impact parameter for a 90° deflection. From equations (3.15) and (3.16) we get

$$\frac{t_0}{t_1} = \frac{17.9\,e^4 \ln\,(r_0/p_0)\,N_e}{(3\,kT)^2 \sigma N}. \tag{3.17}$$

Inserting numerical values for the constants (including the cross-section σ), we obtain

$$\frac{t_0}{t_1} = 2.12 \times 10^{16}\,\frac{\ln\,(r_0/p_0)}{T^2}\,\frac{N_e}{N} \tag{3.18}$$

for the case that the electrons are captured by neutral hydrogen atoms. In this case, σ does not depend strongly on T in the temperature interval that is of astrophysical interest. For solar conditions, $T = 6000°$, $N_e/N = 10^{-4}$, we get $t_0/t_1 \sim 4.5 \times 10^5$; in other words, an electron will make nearly 5×10^5 elastic collisions before it is recaptured. For hotter stars, t_0/t_1 will usually be even larger; for the fact that we now have to insert the larger capture cross-section for protons (see above) and larger T-values in formula (3.9) is more than compensated for by the assumption $N_e/N \sim 1$, which we also have to make. Therefore, we are sure that under conditions in normal stellar atmospheres the electrons will always make a very large number of elastic collisions before they are recaptured.

The next question is how many inelastic collisions take place during this time interval. At temperatures of about 10,000° K and below, collisions which excite hydrogen or helium from the ground level are certainly much less frequent than elastic collisions. The mean kinetic energy of the electrons lies below 1 ev for these temperatures, whereas even the second-quantum level of the hydrogen atom lies more than 10 ev above the ground level. For 10,000°, only 3×10^{-5} of the electrons have sufficient energy to excite the level $n = 2$ of hydrogen. We now have to consider inelastic collisions with ions and atoms other than hydrogen and helium. Obviously, atoms with low-lying levels will be of importance.

[4] The cross-section for elastic collisions of electrons with H atoms is of the order of 3×10^{-15} cm² for $T = 6000°$ (see Massey and Moiseiwitsch 1951; Massey 1956*a*, *b*).

There are three groups of such atoms and ions: (1) the alkali atoms with large excitation cross-sections (up to $100\,\pi\,a_0^2 = 8.8 \times 10^{-15}\,\mathrm{cm}^2$) (see Massey and Burhop 1952), but with low cosmic abundance ($\sim 3 \times 10^{-4}$ per cent); (2) the iron atoms, having a great number of low-lying levels but (probably) moderate cross-sections and an abundance of about 10^{-2} per cent; and (3) atoms like oxygen and nitrogen with smaller cross-sections ($\sim 10^{-16}$ cm^2 at 6000°) (Seaton 1953) but an abundance of about 0.1 per cent. Most of the relevant levels in the atoms of types 2 and 3 are metastable. Consequently, the exciting collisions are almost completely compensated for by collisions of the second kind and hence do not seriously disturb the Maxwellian distribution, except if there are extreme deviations from equilibrium. If we include them, we even overestimate the tendency toward deviations from the Maxwellian distribution. A numerical estimate shows that the numbers of inelastic collisions with atoms of types 1 and 3 are of the same order of magnitude at low temperatures ($T \sim 4000°$). The contribution of type 2 is probably not larger by an order of magnitude, so we may neglect it in an order-of-magnitude estimate. Assuming solar conditions, we find, for the ratio of the relaxation times for inelastic and elastic collisions, $t_2/t \sim 10^3$. (Under solar conditions most of the alkali atoms are already ionized. Consequently, the inelastic collisions with them are unimportant.)

For atmospheres which are essentially hotter than 10,000°, we can no longer neglect the inelastic collisions with hydrogen atoms in the ground level as well as in excited states. But for the conditions which occur in atmospheres of main-sequence stars we always find $t_2 \gg t_1$. The reason is that (1) the cross-section for electron-electron collisions is very large and (2) most of the hydrogen atoms are already ionized before the mean kinetic energy of the electrons is large enough to excite the atoms from the ground state or before the excitation is so great that inelastic collisions with excited atoms become important.

Our results $t_0/t_1 \gg 1$ and $t_2/t_1 \gg 1$ show that it is always a good approximation to assume that the electron velocities in a stationary stellar atmosphere follow a Maxwellian distribution for a certain electron temperature T_e.[5]

The next question is whether T_e is always identical with the kinetic temperature of the atoms and ions. This problem has been investigated by Bhatnagar, Krook, Menzel, and Thomas (1955). These authors restrict themselves to a hydrogen atmosphere and consider the balance between (1) energy transfer from atoms to electrons and (2) energy dissipation by the electrons. (In their paper they assume that the atoms gain energy from hydrodynamic motions.) The processes determining condition 1 are elastic collisions between atoms and electrons and between ions and electrons; condition 2 is determined by (i) in-

[5] Strictly speaking, it would be necessary to solve Boltzmann's equation in order to decide whether a Maxwellian distribution is always established. But in stellar atmospheres the number of elastic collisions is always larger by several orders of magnitude than the number of inelastic collisions, and such a complicated procedure can be avoided.

elastic collisions with atoms and ions, (ii) the excess of emission over absorption in free-free, and (iii) in free-bound or bound-free transitions. For conditions ii and iii the expressions derived earlier by Menzel (1937) are used. For condition i the cross-sections given by Matsushima (1952) have been applied. Though these are based on a relatively rough estimate, they are probably correct within a factor of 2 or 3 (compare Massey 1956*a*, *b*). Using the conditions for a stationary state, Menzel and his co-workers find

$$T_k - T_e < 10^{-3} T_e \quad \text{for} \quad 5 \times 10^3 < T_e < 10^5 \quad \text{and} \quad 10^{10} < N_e\,, \tag{3.19}$$

with T_k = kinetic temperature of atoms and ions.

The physical reason for this result is that, under the conditions that occur in stellar atmospheres, the energy transfer between electrons and heavy particles proceeds much faster than does the energy loss by all inelastic processes. The assumption that the atmosphere consists only of hydrogen does not affect the result seriously if $T_e \gtrsim 10{,}000°$, for in such a case the number of inelastic collisons with hydrogen atoms would be of the same order of magnitude as the number of all other inelastic collisions, if we assume the usual cosmic abundance ratios.

We have seen that in stellar atmospheres the free electrons must follow practically a Maxwellian distribution and that $T_k \sim T_e$ if the atmosphere is in a stationary state. Many of our following conclusions will be based on the first of these results.

Deviations from the Saha equation: Let us first consider this problem: What is the ratio of the number of radiative to that of collisional ionizations? As we are interested only in the order of magnitude of this ratio and as we do not expect very great deviations from local thermal equilibrium, we may use B_ν instead of the mean intensity J_ν, where

$$J_\nu = \int I_\nu \frac{d\omega}{4\pi}. \tag{3.20}$$

We shall assume that the absorption coefficient κ_ν for free-bound transitions follows Kramer's law. The number of radiative ionizations per r-times ionized atom in the level s is

$$Q^{(s)}_{r,r+1} = \int_{\nu_0}^{\infty} \frac{4\pi J_\nu}{h\nu}\,\kappa_\nu d\nu \sim \int_{\nu_0}^{\infty} \frac{4\pi B_\nu}{h\nu}\,\kappa_\nu d\nu \sim \frac{16\pi^2 e^2}{m c^3}\,\nu_0^2 f E_1\left(\frac{h\nu_0}{kT}\right), \tag{3.21}$$

with ν_0 = frequency of the series limit; f the oscillator strength for the transition $s \rightarrow$ continuum; and E_1 = the first exponential integral. If $h\nu_0/kT$ is not larger than 1, E_1 has to be replaced by

$$\int_{x_0}^{\infty} \frac{dx}{x\,(e^x - 1)} \qquad \text{with} \qquad x = \frac{h\nu}{kT}. \tag{3.22}$$

The corresponding number of collisional ionizations is

$$N_e S^{(s)}_{r,r+1} = N_e \int_0^{\infty} v f(v)\,\sigma(v)\,dv\,, \tag{3.23}$$

where $f(v)$ is the Maxwellian distribution and σ is the cross-section. As we are concerned with the orders of magnitude only, we may use for σ a semiclassical formula in analogy with Thomson's (1912) classical formula:

$$\sigma = 3f\frac{\pi e^4}{\epsilon}\left(\frac{1}{\chi_r - \chi_{r,s}} - \frac{1}{\epsilon}\right), \tag{3.24}$$

with χ_r and $\chi_{r,s}$ the ionization and the excitation energy, ϵ = mean kinetic energy of the electrons. For low energies the results of this formula agree with the quantum-mechanical calculations of Swan (1955) for ionizations from the second-quantum level of hydrogen within a factor of 3, i.e., the accuracy is sufficient for our purpose. From equations (3.21), (3.23), and (3.24) one gets, for the ratio of radiative to collisional ionizations,

$$\frac{Q}{N_e S} = \frac{4\sqrt{2}\pi^{3/2}\nu_0^2}{3m^{1/2}e^2c^3}\frac{(kT)^{3/2}}{N_e}\left(\frac{h\nu_0}{kT}\right)\frac{E_1(h\nu_0/kT)}{E_2(h\nu_0/kT)}. \tag{3.25}$$

After inserting numerical constants (cgs units),

$$\frac{Q}{N_e S} = 8.88\times 10^{-23}\frac{T^{3/2}\nu_0^2}{N_e}\left(\frac{h\nu_0}{kT}\right)\frac{E_1(h\nu_0/kT)}{E_2(h\nu_0/kT)}, \tag{3.26}$$

and E_1/E_2 changes from about 1.5 for $h\nu_0/kT = 1$ to 1 for $h\nu_0/kT \to \infty$. Figure 4 shows the numerical results, which have been obtained from equation (3.25) for different T and N_e values (when necessary, E_1 has been replaced by the integral [3.22]). Figure 4*a* refers to $\chi_r - \chi_{r,s} = h\nu_0 = 8$ ev and Figure 4*b* to $\chi_r - \chi_{r,s} = 1$ ev, and Q/N_eS is the parameter of the curves. The points giving the T, N_e values for $\bar{\tau} = 0.05$ in the solar atmosphere[6] (according to Böhm 1954*a*) and the O9 V star 10 Lac (according to Traving 1957) have been marked, indicating the range in the diagrams which the higher layers of the atmospheres of main-sequence stars occupy. We see that only for $\chi_r - \chi_{r,s} \lesssim 1$ ev are collisional ionizations important. Consequently, it is a good approximation to consider only the radiative ionizations.[7]

[6] For the solar atmosphere we find that, even at a mean optical depth of $\bar{\tau} = 1$, radiative ionizations of Fe from the ground state are more frequent by a factor of about 50 than collisional ionizations.

[7] Actually, the problem is slightly more complicated. Collisional ionization from the high levels of an atom (with say $\chi_r - \chi_{r,s} < 0.2$ ev) is more frequent than radiative ionization from the lower levels. (This is shown by unpublished calculations by Mrs. M. Mädlow.) But the great number of transitions between the highest discrete levels and the continuum leads only to an equipartition of energy between free particles and the electrons in the highest bound states (cf. Giovanelli 1948). There are only very few transitions between these states and the lower levels in which most of the atoms are to be found. In considering the degree of ionization, we compare the number of all electrons in bound states with the number of free electrons. For the calculation of the former we can neglect the contribution of the levels with $\chi_r - \chi_{r,s} < 0.2$ ev. Consequently, the level of ionization is mainly determined by the radiative transitions between the continuum and the lower levels.

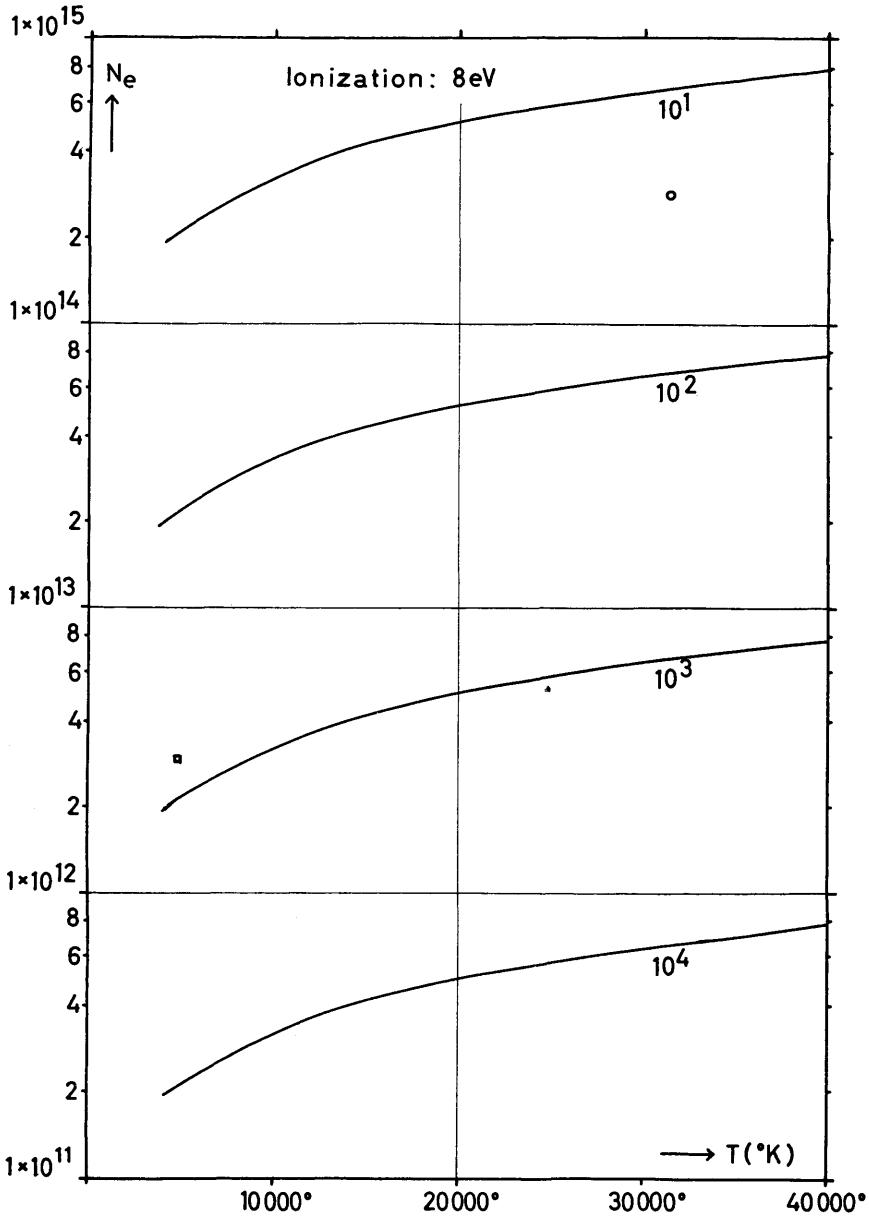


FIG. 4*a*.—The ratio of radiative and collisional ionization (given as parameter of the curves) as a function of the temperature T and the electron density N_e. The diagram refers to the ionization from levels lying 8 ev below the ionization energy. The open circle marks the T and N_e value for an O9 V star at $\tau = 0.05$; the open square shows the values for the sun at the same optical depth.

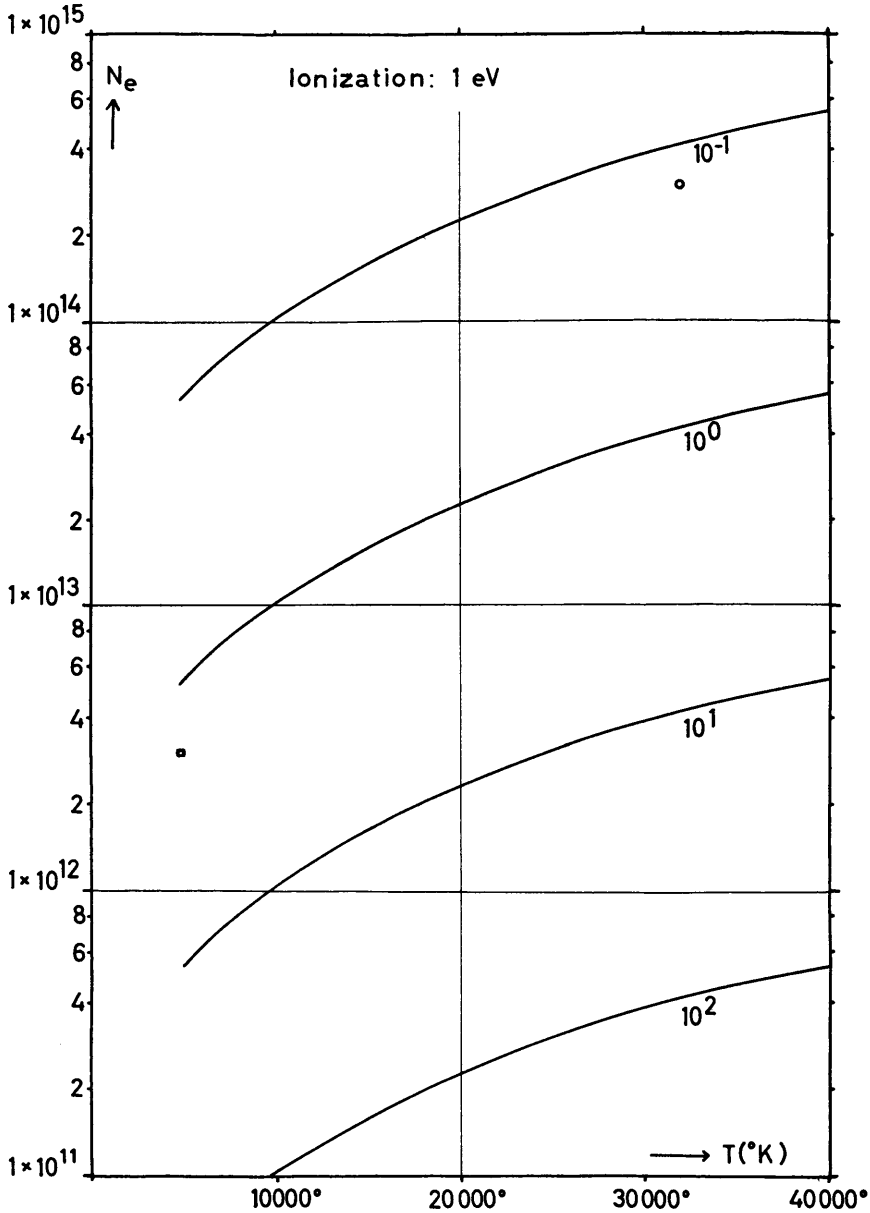


FIG. 4*b*.—The same as Fig. 4*a*, but referring to ionization from levels 1 ev below the ionization limit.

We can now derive a simple formula for the deviation of the degree of ionization from that predicted by the Saha formula. As the electron velocities follow a Maxwellian distribution, the recombination coefficient will be the same as in local thermodynamic equilibrium. Consequently, we get, from the condition for a stationary state,[8]

$$\frac{\left(\frac{N_{r+1}N_e}{N_r}\right)_{NE}}{\left(\frac{N_{r+1}N_e}{N_r}\right)_{E}} = \frac{\int_0^\infty \frac{J_\nu}{h\nu}\,\kappa_{\nu,r}\,d\nu}{\int_0^\infty \frac{B_\nu}{h\nu}\,\kappa_{\nu,r}\,d\nu}, \tag{3.27}$$

where the index NE ("non-equilibrium") now marks the value in an actual stellar atmosphere; E is the value in thermal equilibrium (computed by the Saha equation); and $\kappa_{\nu,r}$ designates the *sum over all continua of the ion considered* (like the Lyman, Balmer, Paschen, etc., continua of H). Now $\kappa_{\nu,r}$ depends on the unknown occupation numbers of all levels. But equation (3.27) can be used to test, for a given stellar atmosphere, how well the assumption of local thermal equilibrium is fulfilled. If we insert a Boltzmann distribution in $\kappa_{\nu,r}$ and take the J_ν calculated for a non-gray atmosphere, a strong deviation of the left-hand side of equation (3.27) from 1 indicates that our picture of the atmosphere is not self-consistent. For the solar atmosphere Böhm (1954*b*) found, for the Fe I–Fe II equilibrium, that at $\bar{\tau} = 0.05$ the left-hand side of equation (3.27) was 1.30 and at $\bar{\tau} = 0.01$ he found 2.88, whereas at $\bar{\tau} = 0.1$ the value was already close to 1. The strong deviation in the high layers is due to the fact that in radiative equilibrium the high absorption coefficient in the Fraunhofer lines causes a steep gradient of T in these layers (Chandrasekhar 1936) and therefore the difference between J_ν and B_ν becomes very large. But this occurs only in non-gray atmospheres, and therefore we cannot learn much about deviations from local thermodynamic equilibrium in actual atmospheres, if we use a gray approximation. It should be added that deviations from equilibrium at about $\bar{\tau} = 0.05$ in stars similar to the sun are important for the interpretation of line profiles. The "center of gravity" for the formation even of the wings of neutral metallic lines lies above $\bar{\tau} = 0.1$. A numerical discussion of equation (3.27) for an O9 V star has been given by Traving (1957).

Deviations from the Boltzmann distribution: At present no simple estimate of the deviations of the occupation numbers of the discrete levels from their equilibrium values can be given, and we may refer to the detailed (and labori-

[8] A formula of this kind was first used by Pannekoek (1927), but his and the other earlier calculations were restricted to ionizations from the ground state. This assumption often leads to considerable error (it would be correct only in a highly diluted radiation field) and has been criticized by Unsöld (1938). The assumption that the number of recombinations is the same as in local thermodynamic equilibrium is strictly valid only if the electron temperature is not changed very much by the deviations from equilibrium (see also Pagel 1955). The present application of equation (3.27)—namely, for testing whether the assumption of local thermodynamic equilibrium is a reasonable approximation—is independent of this difficulty.

ous) methods that will be discussed in the next section. In this section we shall restrict ourselves to a determination of the ratio of radiative to collisional excitations, which is important, as collisional excitations (and collisions of the second kind) tend to establish a Boltzmann distribution (because of the Maxwellian velocity distribution of electrons). As $J_\nu \neq B_\nu$, the Boltzmann distribution will be disturbed by radiative excitations and de-excitations.

The number of radiative excitations per atom in the level i is $B_{ij}B_\nu$, and the number of collisional excitations is $N_e S_{ij}$. We are interested only in the orders of magnitude and have therefore replaced J_ν by B_ν (as in the discussion of the ionization).[9] The temperature and density dependence of the ratio $N_e S_{ij}/B_{ij}B_\nu$ has been discussed by Woolley and Stibbs (1953) under the assumption that the cross-section for the excitation of discrete levels can also be approximated

TABLE 1

RATIO OF COLLISIONAL AND RADIATIVE EXCITATION IN PHOTOSPHERE OF SUN AND OF AN O9 V STAR ($\bar{\tau} = 0.05$)

	λ(A)						
	3000	4000	5000	6000	7000	8000	9000
$N_e S_{ij}/B_{ij}B_\nu$ Sun.....	2.5×10^{-3}	7.4×10^{-3}	1.7×10^{-2}	3.5×10^{-2}	6.1×10^{-2}	9.9×10^{-2}	1.5×10^{-1}
$N_e S_{ij}/B_{ij}B_\nu$ O9 V star.	1.9×10^{-1}	4.4×10^{-1}	8.5×10^{-1}	1.4	2.2	3.1	4.2

by a formula like equation (3.24).[10] From equations (3.23) and (3.24) and the relation between the transition probability B_{ij} and the oscillator strength,

$$f_{ij} = \frac{mc}{4\pi^2 e^2} h\nu B_{ij}, \tag{3.28}$$

we get

$$\frac{N_e S_{ij}}{B_{ij}B_\nu} = 1.2\times10^{15} P_e \left(\frac{5040}{T}\right)^{1/2} \lambda^4 g\left(\frac{h\nu}{kT}\right), \tag{3.29}$$

with

$$g(x) = (e^x - 1) \times E_2(x) \tag{3.30}$$

(see Woolley and Stibbs 1953; these authors have also tabulated $g[x]$). In Table 1 some numerical values of $N_e S_{ij}/B_{ij}B_\nu$ are given as a function of wave length.

[9] In local thermodynamic equilibrium the ratio of collisional to radiative excitation would be related in a simple way to ϵ^*, the energy which is lost from a line by collisions of the second kind,

$$\frac{N_e S_{ij}}{B_{ij}B_\nu} = \frac{\epsilon^*}{1-\epsilon^*}.$$

This follows from the consideration of detailed balancing.

[10] This approximation seems to be better than one would expect. If we take as an example the transition $1 \rightarrow 2$ in the hydrogen atom, we find that the σ computed according to eq. (3.24) differs by less than a factor of 2 from the cross-section given by Massey (1956).

They refer to the physical conditions at $\bar{\tau} = 0.05$ in the solar photosphere (using the model given by Böhm 1954*a*) and in the atmosphere of the O9 V star 10 Lac (model given by Traving 1957).

It follows that collisional excitation can be neglected in the solar photosphere but that it is important in hot stars for transitions in the visual region. But we cannot conclude that the Boltzmann law will be valid in hot stars, because the transitions in the far ultraviolet, which are very important in these stars, will be caused mainly by radiative processes.

The conclusions derived in this section may be summarized as follows: the free electrons in a stellar atmosphere practically follow a Maxwellian distribution. The difference between the electron temperature and the kinetic temperature of the atoms and ions will be small in general. Deviations from equilibrium ionization and excitation will occur because of the large number of radiative processes as compared with collisional processes in most stellar atmospheres. Numerical estimates from equation (3.27) indicate that only for $\bar{\tau} < 0.1$ and only if the atmosphere deviates strongly from a gray one will the difference between J_ν and B_ν be so large that the deviations from local thermodynamic equilibrium are of practical importance. On the sun even the *wings* of a number of important lines originate in layers with $\bar{\tau} < 0.1$; and consequently deviations from local thermodynamic equilibrium have to be considered if we compute the profiles of these lines.

Very recently there has been some controversy about this problem. Pecker (1959) and Thomas especially believe that large deviations from local thermodynamic exist even at $\bar{\tau} \sim 1$. (See the following sections and the *Proceedings* of the 1959 Symposium on Stellar Photospheric Structure at Uccle, Belgium.)

3.13. *General approximations for the source function.*—If $S_\nu = B_\nu$ is not a good approximation, we have to go back to the "microscopic" equations expressing the fact that in a steady state the number of transitions from all other levels into a certain level j is equal to the number of transitions from j to all other levels. Strictly speaking, it is even necessary to take into account that most of the levels are broadened and that the source function in general is not the same for different "substates" or "elements of state" of the level. (This refinement is obviously unnecessary if the process of re-emission is completely non-coherent.) If we call $N_{ij}(\epsilon', \epsilon'')d\epsilon' d\epsilon''$ the number of transitions per second from the substate ϵ' of the level i to the substate ϵ'' of the level j, we can write this condition (cf. Henyey and Grasberger 1955) thus:

$$\sum_{j(\neq i)} \int_{-\infty}^{+\infty} N_{ij}(\epsilon', \epsilon'')\, d\epsilon'' + \int_0^{\infty} N_{i\infty}(\epsilon', \epsilon'')\, d\epsilon'' + \int_{-\infty}^{+\infty} N_{ii}(\epsilon', \epsilon'')\, d\epsilon'' = \sum_{j(\neq i)} \int_{-\infty}^{+\infty} N_{ji}(\epsilon'', \epsilon')\, d\epsilon'' + \int_0^{\infty} N_{\infty i}(\epsilon'', \epsilon')\, d\epsilon'' + \int_{-\infty}^{+\infty} N_{ii}(\epsilon'', \epsilon')\, d\epsilon''. \quad (3.31)$$

The left-hand side corresponds to the number of transitions leaving the substate ϵ'' of the level i and the right-hand side to the number of transitions entering this substate. The first term on each side gives the number of transitions between discrete levels, the second term gives the bound-free or free-bound transitions, and the third term corresponds to the redistribution of atoms over a broadened state (e.g., as caused by collisions). Equations of the form (3.31) written for every substate (of the discrete levels and the continuum) give an extremely complex system of non-linear equations for the occupation numbers $N_i(\epsilon')$. As the N_{ij}'s depend on the radiation field, this system has to be solved simultaneously with the system of transfer equations (2.15), in which, moreover, the continuous absorption has to be included. It is obvious that approximations are necessary.

Milne (1930) has solved the system of equations (2.15) and (3.31) under the following very restrictive assumptions: (1) the atom has two discrete levels only; (2) $\phi_\nu = \psi_\nu$; (3) J_ν can be represented by a mean value for the whole line (see also the critical discussion by Thomas 1957). Milne includes collisional, as well as radiative, processes. He gets a source function of the form

$$S_\nu = \frac{\kappa_\nu + l_\nu}{\kappa_\nu + l_\nu + \sigma_\nu} B_\nu + \frac{\sigma_\nu}{\kappa_\nu + l_\nu + \sigma_\nu} J_\nu , \tag{3.32}$$

a result which can be generalized by making allowance for non-coherent re-emission (Spitzer 1936, 1944; Houtgast 1942; see also the following section). If i_ν is the coefficient of non-conherent scattering, we have

$$S_\nu = \frac{\kappa_\nu + l_\nu}{\kappa_\nu + l_\nu + \sigma_\nu + i_\nu} B_\nu + \frac{\sigma_\nu}{\kappa_\nu + l_\nu + \sigma_\nu + i_\nu} J_\nu + \frac{i_\nu}{\kappa_\nu + l_\nu + \sigma_\nu + i_\nu} \frac{\int i_\nu J_\nu d\nu}{\int i_\nu d\nu} . \tag{3.33}$$

Milne concluded from equation (3.22) that the actual re-emission always lies between local thermodynamic equilibrium and coherent scattering. This result is often quoted in the literature, but one should remember that it has been derived under very special assumptions and that it is certainly not valid in general.

The equation of transfer (2.5*b*) with the source function (3.33) but with $\sigma_\nu = 0$ has been solved by Savedoff (1952) for a Milne-Eddington model by transforming it into an integral equation and using a kind of Neumann expansion for the solution. Similar calculations for the general case (κ_ν, l_ν, and i_ν arbitrary functions of x_ν) have been carried out by de Jager (1952). Different ways of approach have been used by Labs (1951*a*, 1954), Münch (1949), and Suemoto (1949). Labs and Suemoto use a step function for the absorption coefficient as a function of ν. Both authors use Eddington's approximation for J_ν (see, e.g., Unsöld 1955). Suemoto applies an iterative procedure starting from the case of coherent scattering, whereas Labs derives a straightforward solution within the frame of Eddington's approximation. Münch uses the Wick-Chandrasekhar method of discrete ordinates (see Chandrasekhar

1950), without introducing an approximation for the wave-length dependence of the absorption coefficient. Exact solutions for simplified cases have been obtained by Sobolev (1949) and Busbridge (1953, 1955) and Stibbs (1953) by essentially the so-called "principle of invariance" (see Ambarzumian 1943; Chandrasekhar 1950). The general result of all these calculations is that—unless l_ν is exactly zero—the wings of the line show a profile very similar to the case of local thermodynamic equilibrium; considerable deviation occurs only in the core of the line. This result can also be derived from the fact that we have $\phi_\nu = \psi_\nu$ in equation (2.15) for local thermal equilibrium, as well as for completely non-coherent scattering. Both cases differ only with respect to the occupation numbers N_i. Differences in the observed line profile should consequently occur only in those parts of the line that are not optically thin (see also Warwick 1955; Thomas 1957).

TABLE 2

$l_\nu/\sigma_\nu + i_\nu$ FOR $T_{\text{rad}} = 5600°$

Element	Line or Multiplet		Element	Line or Multiplet	
H	Hα	1.3	Ca I	4^1S–4^1P^o	0.05
	Hβ	4.0	Ca II	4^2S–4^2P^o	.001
	Hγ	8.4		3^2D–4^2P^o	.001
	Ly-α	0.01			
Na	3^2P^o–3^2D	0.01	Fe I	d^5D–z^5D^o	.15
	3^3P^o–3^3D	0.04		a^5F–y^5F^o	0.6
Mg	3^3P^o–4^3S	0.02			
	3^3P^o–5^3S	0.3			

If we restrict ourselves to the approximation (3.33) for the source function, we have to know the ratio $\sigma_\nu + i_\nu/l_\nu$ for the different lines. (The determination of i_ν/σ_ν will be considered in § 4.) Unsöld (1938, 1955) has suggested that the following approximation be used for a line $i \to j$, if the conditions are not too far from local thermodynamic equilibrium:

$$\frac{i_\nu + \sigma_\nu}{l_\nu} = \frac{A_{ji}}{\sum\limits_{\substack{k<j \\ (\neq i)}} A_{jk} + \sum\limits_{l>j} B_{jl} I_\nu}. \tag{3.34}$$

The assumption is that all transitions that do not correspond to a scattering process finally correspond to a re-emission $l_\nu B_\nu$. Estimates of $l_\nu/i_\nu + \sigma_\nu$ for some lines as derived by Unsöld (1938, 1955), Labs (1951*b*), and de Jager (1952)[11] are given in Table 2.

A rather different approach to the solution of equation (3.31) has been made by Rosseland (1926). He considered a three-level atom and neglected collisional excitations, as well as the detailed structure of the levels.

[11] De Jager's Table 55 contains some misprints.

Usually one identifies the highest level with the continuum. (It is not possible to find three discrete states of an atom between which all transitions are permitted. At least one of the transitions violates the selection rules for the quantum number l.) If the radiation field corresponds to a Planck function multiplied by a dilution factor W (< 1), "uncompensated cycles" occur, i.e., cycles $1 \rightarrow 3 \rightarrow 2 \rightarrow 1$ occur more often than the reverse ones, $1 \rightarrow 2 \rightarrow 3 \rightarrow 1$. In other words, the assumption of detailed balancing is no longer valid. Now define the excitation temperature, T_{exc}, by the relation

$$\frac{N_j}{N_i} = \frac{g_j}{g_i} \exp\left(\frac{\chi_{ij}}{kT_{\text{exc}}}\right). \tag{3.35}$$

It follows from Rosseland's analysis that T_{exc} is lower for $j = 2$, with respect to $i = 1$, than for $j = 3$. Both are lower than the radiation temperature. Rosseland's investigations have been extended by a great number of authors to atoms with many states and have found important applications in the theory of gaseous nebulae (corresponding to the limiting case $W \rightarrow 0$). In this case the (emission) line formation is due mainly to recombination and subsequent cascade jumps to the ground level (see especially the work of Menzel and his collaborators 1937–1945; Wurm 1951; Aller 1956). In general, the conclusions of Rosseland are confirmed qualitatively, especially the low population of low-excitation levels with respect to the ground state. In most of these treatments the radiation field has been considered as known, and consequently one could avoid investigating the coupling between the equation of transfer (2.15) and the condition of a stationary state (3.31). This coupling has been considered by Ambarzumian (1931), Chandrasekhar (1935), and in a more complete way by Henyey (1938). As these papers have been written mainly with respect to applications to gaseous nebulae, we shall not discuss them in detail.

An interesting attempt to allow for the deviations of S_ν from B_ν in atmospheres in which the opacity is due to H^- has been made recently by Plaskett (1955). He assumes that the radiation field can be described by a temperature T_r and that T_r is equal to the ionization temperature of hydrogen, T_i, and of the metals, T_i^*, as well as to the kinetic temperature, T_k. Furthermore he supposes that the excitation of the metal atoms can be described by an excitation temperature, T_e^*. In other words, Plaskett tries to reduce the whole problem to the determination of two temperatures at every point of the atmosphere, namely, $T_r = T_i = T_i^* = T_k$ and T_e^*. These assumptions are rather restrictive and there may be some doubt whether such a treatment can give complete insight into the physics of the processes occurring. But it may prove useful as an additional test (in the same sense as eq. [3.27] has been used) whether the assumption $S_\nu = B_\nu$ is a reasonable approximation or not.

We shall now consider approximations for the solution of equations (2.15) and (3.31), which give a more realistic determination of S_ν in normal stellar atmospheres.

In two papers Henyey (1946; Henyey and Grasberger 1955) has tried to develop a theory of first-order deviations from local thermodynamic equilibrium. At present, this seems to be the most satisfactory attempt to solve the problem. Henyey introduces only very few *ad hoc* assumptions. In accordance with our results in the preceding section, Henyey assumes that the electrons have a Maxwellian velocity distribution and that collisional excitations and ionizations can be neglected. Collisions are taken into account insofar as they redistribute the atoms in the element of state ϵ over the whole level j. The deviations from the Boltzmann distribution, from the Saha formula, and from a black-body radiation field are written in the following form:

$$\frac{N_k(\epsilon)}{N_k^{(0)}(\epsilon)} = 1 + \xi_k(\epsilon) \tag{3.36}$$

$$\frac{N_i N_e}{N_i^{(0)} N_e^{(0)}} = 1 + \xi_\infty, \tag{3.37}$$

$$J_\nu = B_\nu(1 + \eta_\nu), \tag{3.38}$$

where N_k is the actual occupation number and N_i is the concentration of ions. The index zero designates the corresponding equilibrium values of these quantities. If we introduce equations (3.36), (3.37), and (3.38) into equation (3.31) and, in accordance with our basic assumption (i.e., neglecting of second-order terms), neglect the products of η_ν with the ξ's, we get a linear system for the ξ_k, ξ_∞, and η_ν, in which the coefficients depend only on the equilibrium values $N_\kappa^{(0)}$, $N_i^{(0)}$, and B_ν. Let us call the re-emission totally non-coherent if there is no correlation between the substate ϵ' of the level k, which the atom reached by the preceding quantum jump, and the substate ϵ'', from which it leaves the level k. In this case, which is a good approximation for lines broadened by collisions, we have

$$\frac{N_k(\epsilon)}{N_k^{(0)}(\epsilon)} = \frac{N_k}{N_k^{(0)}}, \tag{3.39}$$

where N_k is the total occupation number of the level k. Equation (3.39) simplifies the treatment of equation (3.31) considerably. Henyey shows that the coefficients occurring in the linearized form of equation (3.31) reduce essentially to quantities p_{mn}, which have the following physical meaning: p_{mn} is the probability that under conditions of local thermal equilibrium an atom in the level m, if it makes a transition, will choose the level n. The p_{mn}'s depend on the transition probabilities and the radiation field in local thermal equilibrium, i.e., on the temperature. They can be computed once and for all. This has been done by Grasberger (1957) for a pure hydrogen atmosphere. Because of their simple physical meaning, these numbers are very instructive also in other connections (e.g., for the calculation of $l_\nu/\sigma_\nu + i_\nu = (1 - p_{nm})/p_{nm}$ in Unsöld's approximation), and we reproduce part of Grasberger's results in Table 3.

Henyey has shown that the ξ_k and consequently the source functions S_ν and the absorption coefficient in any line and the continuum can be written as a function of η_ν integrated over all frequencies and the quantities q_{ik}, which also depend only on the *equilibrium values* of the occupation numbers, ionization, etc. The q_{ik}'s can be computed from the p_{ik}'s by solving the linear system of equations

$$\sum_k q_{ik} p_{kl} = q_{il} - p_{il}. \tag{3.40}$$

The q_{ik}'s (which have no simple physical meaning; they somehow express the coupling between all possible transitions) have also been derived by Grasberger (1957). This author has further calculated the deviations of the residual intensities of Hα, Hβ, and Pα from the values that these quantities would have under the assumption of local thermodynamic equilibrium for atmospheres in the range $7000° \leq T \leq 11{,}500°$. In Table 4 we give the relative deviation of the flux in the line center from its value for local thermodynamic equilibrium $[F_\nu - F_\nu^{(0)}]/F_\nu^{(0)}$ as calculated by Grasberger for an atmosphere with the sur-

TABLE 3

RELATIVE PROBABILITIES p_{mn} OF TRANSITION $m \rightarrow n$ FOR HYDROGEN ACCORDING TO W. GRASBERGER (1957)

$T = 7000°$

m	n						
	1	2	3	4	5	6	7
1.....	.....	0.9855	0.0115	0.00158	0.00048	0.00021	0.00011
2.....	0.9886	.....	.00955	.00105	.00030	.00012	.00006
3.....	.4929	.4084	.....	.07109	.01359	.00497	.00241
4.....	.2873	.1921	.3041	.....	.1430	.03287	.01326
5.....	.1740	.1078	.1163	.2855	.....	.1973	.0486
6.....	.1113	.0661	.0620	.0958	.2882	.....	0.2296
7.....	0.0752	0.0438	0.0383	0.0494	0.0908	0.2933	.....

$T = 11{,}500°$

m	n						
	1	2	3	4	5	6	7
1.....	.....	0.9427	0.03725	0.00784	0.00291	0.00141	0.00080
2.....	0.9525	.....	.03518	.00564	.00191	.00088	.00049
3.....	.4164	.3878	.....	.1263	.02769	.01089	.00553
4.....	.2145	.1530	.3106	.....	.1954	.04779	.02005
5.....	.1206	.07853	.1034	.2965	.....	.2361	.06065
6.....	.07387	.04577	.05117	.09117	.2970	.....	0.2603
7.....	0.04858	0.02946	0.03028	0.04455	0.08877	0.3029	.....

face temperature T_0 and a linear distribution of T^4. For comparison, we give $F_\nu - F_\nu^{(0)}/F_\nu^{(0)}$ as one gets it from Unsöld's rough approximation for the same atmosphere. This comparison is instructive, as it gives an estimate of how large an error is introduced by Unsöld's assumption that all re-emission processes other than scattering can be approximated by $l_\nu B_\nu$. The agreement is surprisingly good for Hα, but relatively poor for Hβ and Pα for the following reason. The populations of the terms $n = 2$ and $n = 3$ are mainly controlled by the radiation field in Hα itself and in the Lyman lines. (The latter is already isotropic at those depths in which Hα is formed.) On the other hand, the ratio of the occupation numbers of $n = 4$ and $n = 3$ is strongly influenced by the radiation field in Hα, Hβ, and Pα. Consequently, deviations from local thermodynamic equilibrium, which cannot be described by scattering, should have been expected for Hβ and Pα.

TABLE 4

RELATIVE DEVIATION OF FLUX AT LINE CENTER FROM ITS VALUE FOR LOCAL THERMODYNAMIC EQUILIBRIUM $F_\nu - F_\nu^{(0)}/F_\nu^{(0)}$

T_0	Hα		Hβ		Pα	
	Grasberger	Unsöld's Approx.	Grasberger	Unsöld's Approx.	Grasberger	Unsöld's Approx.
7000°.....	−0.0977	−0.122	−0.1137	−0.049	−0.1467	−0.085
11,500°.....	−0.1165	−0.114	−0.1169	−0.039	−0.1967	−0.085

From a consideration of Grasberger's results it seems that the effects of deviations from local thermodynamic equilibrium in the line center are not very great (smaller than 20 per cent). In the line wings Grasberger finds only differences of the order of 1 per cent. But these results may be misleading if we apply them to actual stellar atmospheres. The reason is that Grasberger uses a linear approximation for the distribution of T^4, for which, of course, the differences $(J_\nu - B_\nu)$ are small; moreover, he neglects deviations of the ionization from the value given by the Saha equation. It was shown in the preceding section that the differences between J_ν and B_ν are great only in a non-gray atmosphere. In the case of the solar atmosphere, a preliminary estimate using equation (3.27) shows a considerable influence of the deviations of the ionization from the Saha equation even on the wings of Fe lines (Böhm 1954*b*). It seems promising to use the p_{ik} and q_{ik} calculated by Grasberger for an investigation of deviations from local thermal equilibrium, starting from more realistic assumptions.

The limitation of Henyey's method lies in the fact that—as we have seen in the preceding section from a discussion of equation (3.27)—even in normal stellar atmospheres, the assumption that the deviations are small quantities

of the first order may often not be fulfilled. Nevertheless, at present there is no method available which seems to be practicable and more promising. Only if we restrict our considerations to resonance lines need the problem not be linearized. (Cf. Thomas 1957.)

As our general knowledge about deviations from local thermal equilibrium is very restricted, it may be useful to discuss briefly also some papers referring to special models of the solar chromosphere. (We should remember that the cores of the very strong Fraunhofer lines are formed in the chromosphere; see, e.g., Böhm-Vitense 1955.)

Calculations of this kind have been carried out by Thomas (1948, 1949), Giovanelli (1948, 1949), Matsushima (1952), Athay and Thomas (1956), and others. In the earlier publications these authors assumed that T_e was considerably greater than the radiation temperature ($T_e = 35{,}000°$, $T_{\rm rad} = 6000°$). (This assumption contradicts some optical as well as radio astronomical observations, see, e.g., Wurm 1948; Unsöld 1952, 1955; van de Hulst 1953). In a more recent paper Athay and Thomas (1956) have also considered the possibility that, at least in a part of the chromosphere, T_e is of the order of 10,000°, but still $T_e > T_{\rm rad}$. In all these investigations it has been assumed that T_e and the radiation field are already known (e.g., from observation). For the sake of simplicity, it is assumed that the radiation field has the form $W \times B_\nu$, with $W < 1$ but constant. The assumption that T_e is considerably greater than $T_{\rm rad}$ is possible only if there is no pure radiative equilibrium. (It is usually assumed that hydrodynamic transfer of energy plays a role in the solar chromosphere.) If T_e is considerably higher than $T_{\rm rad}$, collisional excitation and ionization cannot be neglected. Matsushima especially has paid attention to a satisfactory treatment of the collision terms.[12] One finds that, because of the preponderance of collisional excitation, the lower levels are overpopulated. The overpopulation is stronger the lower the level lies in the energy-level diagram. A consequence is that the excitation temperature, $T_{\rm exc}$, for transitions between low levels is considerably lower than T_e. It is customary to write the population of the levels analogous to a combination of the Boltzmann and Saha equations (2.18) and (2.19):

$$N_n = b_n N_p N_e n^2 h^3 (2\pi m k T_e)^{-3/2} \exp\left(\frac{\chi_r - \chi_{r,n}}{kT_e}\right). \qquad (3.41)$$

For thermodynamic equilibrium, obviously $b_n = 1$. In the calculations for the chromosphere one finds, e.g., $b_2 \sim 10^4$, whereas for $n > 7$, b_n is often of the order of 1. Athay and Thomas (1956) find, for $T_e = 10^4$ and $N_e = 10^{11}$, an excitation temperature for Lyman-α of 5050°.

Recently Pecker (1957 and 1959) has tried to determine the deviations from local thermodynamic equilibrium in the solar *photosphere* from empirical data.

[12] The relevant cross-sections for hydrogen seem to be known within a factor of 2 (see, e.g., Massey 1956*a*, *b*; Bransden and McKee 1956).

He compares the distribution of the electron temperature, as derived from older observations of the continuous spectrum, with the distribution of excitation temperatures for some Ti I lines. The optical depths are computed by assuming $T_e = T_{exc}$. The deviations from local thermodynamic equilibrium found in this way are unexpectedly large (they include, however, the effect of temperature inhomogeneities; see next paragraph). For some theoretical arguments in this connection see also Jefferies and Thomas (1958).

3.2. Atmospheres Which Are Not in Radiative Equilibrium

It is well known that, in stellar atmospheres of spectral types later than about F0, thermal convection plays an important role. From the solar photosphere we know that such a convection zone causes considerable temperature and density inhomogeneities even above the unstable zone (see especially Böhm-Vitense 1953). It has become obvious (Böhm 1954*b*; de Jager 1954; Voigt 1956; Schröter 1957) that the temperature inhomogeneities especially strongly influence the line profiles. As far as the solar atmosphere is concerned, this effect has found a direct observational confirmation (McMath, Mohler, Pierce, and Goldberg 1956).

At present, one uses the following procedure to include the effect of temperature inhomogeneities in the calculation of line profiles. One constructs a model atmosphere consisting of cooler and hotter columns of gas, each of which is nearly in radiative equilibrium. One assumes that the pressure is the same in all columns for a given geometrical depth. The line profile due to every column can be found by integration of equations (3.1), (3.2), or (3.6). In this calculation we can allow for the Doppler shift, which is caused by the macroscopic hydrodynamic motion in a given column (Voigt 1956; Schröter 1957) and its microturbulence (Voigt). The observed line profile then corresponds to a mean taken over all the individual profiles. Usually one restricts one's self to two or three different types of columns. If the mean temperature distribution is known from theory, one can then try to adjust the temperature inhomogeneities by trial and error in such a way that one gets a good fit with the observations for a great number of lines. This method is certainly not very satisfactory, as it is too schematic. Real progress in this part of the theory of line formation will be possible only after the development of a hydrodynamic theory of stellar atmospheres with thermal convection.

§ 4. THE LINE ABSORPTION COEFFICIENT

4.1. The Harmonic Oscillator and the Theory of Radiation Damping

In the classical theory of electrons, the vibration of a linear, harmonic oscillator in the changing electric field, E_x, of a light-wave is described by

$$\ddot{x} + \omega_0^2 x + \gamma \dot{x} = \frac{e}{m} E_x . \tag{4.1}$$

The dots indicate, as usual, the differentiation with respect to time; ω_0 is 2π times the eigen-frequency of the oscillator; and γ is the damping constant. If we put $x = x_0 e^{i\omega t}$, we get, from equation (4.1),

$$(-\omega^2 + \omega_0^2 + i\omega\gamma)\, x = \frac{e}{m} E_x . \tag{4.2}$$

In the electromagnetic theory of light, one uses the complex index of refraction,

$$\tilde{n} = n\,(1 - ik^*)\,, \tag{4.3}$$

where n is the ordinary refractive index. The imaginary part of n corresponds to an absorption of the light-wave; k^* is related to the absorption coefficient per centimeter k[13] by

$$k = \frac{2\omega n k^*}{c} = \frac{4\pi n k^*}{\lambda} . \tag{4.4}$$

Furthermore, there exists a well-known relation between the complex refractive index and the polarizability $\alpha = (ex)/E$,

$$\tilde{n}^2 - 1 = 4\pi \tilde{N} \alpha\,, \tag{4.5}$$

where $\tilde{N}$ is the number of oscillators per cubic centimeter. From equations (4.2) and (4.5) we get

$$\tilde{n}^2 - 1 = \frac{4\pi \tilde{N} e^2}{m} \frac{1}{\omega_0^2 - \omega^2 + i\gamma\omega} . \tag{4.6}$$

In the neighborhood of the eigen-frequency ("spectral line"), i.e., for $|\omega - \omega_0| \ll \omega_0$ and for $k \ll 1$ and $n \sim 1$ (conditions which are fulfilled in a not too dense gas) we get, from the imaginary part of equation (4.6) and from equation (4.4),

$$k = \frac{\pi e^2 \tilde{N}}{m c} \frac{\gamma}{(\Delta\omega)^2 + (\gamma/2)^2} . \tag{4.7}$$

Equation (4.7) is called a "damping profile." It is symmetrical with respect to $\omega = \omega_0$, and its total half-width is equal to the damping constant γ. At great distances from the line center, the absorption coefficient varies like $\Delta\omega^{-2}$ or (on a wave-length scale) proportional to $\Delta\lambda^{-2}$.

In a highly diluted gas the damping constant γ is mainly due to the radiation damping of the vibrating oscillator. At higher densities the disturbances of the oscillation due to collisions with neighboring particles are often of greater importance.

According to Hertz's theory, the radiative energy loss of an oscillator per time unit is

$$-\frac{dW}{dt} = \frac{2}{3} \frac{e^2}{m} \frac{\omega_0^2}{c^3} W\,, \tag{4.8}$$

[13] This symbol is different from that used in the preceding sections, in order to show that we are not concerned with the mode of re-emission here.

where W is the total energy of the oscillator. By integration of equation (4.8) we get

$$W = W_0 \exp(-\gamma_{cl} t), \qquad \text{with} \qquad \gamma_{cl} = \frac{1}{\tau_{cl}} = \frac{2}{3}\frac{e^2\omega_0^2}{mc^3}, \tag{4.9}$$

where τ is the decay time of the oscillator. On a wave-length scale, λ (instead of the angular frequency scale, ω), we get the natural line width

$$\Delta\lambda_N = \frac{2\pi c}{\omega_0^2}\gamma_{cl} = \frac{4\pi e^2}{3mc^3} = 1.18 \times 10^{-4}\,\text{A}, \tag{4.10}$$

which is a constant for all lines, in the classical theory.

So far, we have used only classical physics. If we wish to proceed to a quantum-mechanical description, we must replace $\tilde{N}$, the number of absorbing oscillators per cubic centimeter, by N, the number of absorbing atoms per cubic centimeter, times the oscillator strength, f. Furthermore, γ_{cl} has to be replaced by the corresponding quantum-mechanical quantity. This can be done in the following way. The decay time of the classical oscillator corresponds to the mean lifetime of an excited state in quantum theory. Consequently, it seems natural to introduce a damping constant for every state (instead of a damping constant for every line, as in the classical theory). The mean lifetime τ_m of the state m is obviously reciprocal to the sum of all transition probabilities for leaving this state:

$$\frac{1}{\tau_m} = \gamma_m = \sum_n A_{mn} + \sum_{m>n} B_{mn} I_\nu + \sum_{m<k} B_{mk} I_\nu . \tag{4.11}$$

(The relation between τ_m and the width of the level γ_m can be considered as a consequence of Heisenberg's uncertainty principle, $\Delta E \Delta t \sim \hbar$). The second and third terms on the right-hand side of equation (4.11), corresponding to the stimulated emissions and the absorptions, can be neglected if the intensity I_ν is not too great. How is the damping constant γ_{mn} of the line $m \rightarrow n$ related to the damping constants of the lower and upper states as given by equation (4.11)? From the quantum theory of radiation one finds

$$\gamma_{mn} = \gamma_m + \gamma_n \tag{4.12}$$

(Weisskopf and Wigner 1930; see also Heitler 1954). Equation (4.12) is essentially a consequence of the simple product rule of the probability calculus (cf. Unsöld 1955). Let $P_m(E)dE$ be the probability that an atom in the state m is found in the energy range between E and $E + dE$, and call $P_n(E')dE'$ the corresponding probability for the state n. The probability of a transition from $E \ldots E + dE$ to $E' \ldots E' + dE'$ is $P_m(E)dE\ P_n(E')dE'$, and consequently the probability distribution for the emission or absorption of a photon of the angular frequency ω is (with $\hbar = h/2\pi$)

$$J(\omega) = \hbar \int P_m(E)\, P_n(E - \hbar\omega)\, dE . \tag{4.13}$$

If P_m and P_n are damping profiles with half-widths γ_m and γ_n, we find from equation (4.13) that $J(\omega)$ is also a damping profile with the half-width $(\gamma_m + \gamma_n)$.

Before entering into the complex question of line broadening due to interactions with other particles, we shall consider in the next section the relatively simple problem of line broadening due to the Doppler effect caused by the thermal and turbulent velocities of the radiating particles.

4.2. Doppler Broadening and the Voigt Profile

If the velocities of the radiating particles follow a Maxwellian distribution, the velocity component ξ in the direction of the line of sight has this distribution:

$$\frac{dN}{N} = \frac{1}{\pi^{1/2}}\left[\exp\left(-\frac{\xi^2}{\xi_0^2}\right)\right]\frac{d\xi}{\xi_0}, \qquad \text{with} \qquad \xi_0^2 = \frac{2RT}{\mu}. \tag{4.14}$$

It is customary to assume that the velocity distribution due to the turbulence in the stellar atmosphere is also of the form (4.14). Actually, our knowledge of astronomical turbulence is very restricted, and such an assumption cannot be justified at present from hydrodynamical considerations, but it is probably a reasonable approximation. If we take into account the thermal and the turbulent velocities, ξ_t, we get a velocity distribution of the form (4.14), but with

$$\xi_0^2 = \frac{2RT}{\mu} + \xi_t^2. \tag{4.15}$$

According to Doppler's principle, the radial velocity ξ and the corresponding frequency or wave-length shift $\Delta\omega$ or $\Delta\lambda$ are related by

$$\frac{\Delta\omega}{\omega} = \frac{\Delta\lambda}{\lambda} = \frac{\xi}{c}. \tag{4.16}$$

We define the so-called "Doppler width," $\Delta\omega_D$ or $\Delta\lambda_D$, as follows:

$$\frac{\Delta\omega_D}{\omega} = \frac{\Delta\lambda_D}{\lambda} = \frac{\xi_0}{c}. \tag{4.17}$$

If we integrate equation (4.7) over the whole line profile, we get

$$\int k_\omega d\omega = \frac{2\pi^2 e^2}{mc}\tilde{N} \qquad \text{or} \qquad \int k_\lambda d\lambda = \frac{\pi e^2 \lambda_0^2}{mc^2}\tilde{N}, \tag{4.18}$$

an expression independent of γ. These integrals must remain unchanged if the line is broadened by the Doppler effect, and consequently we get, for the absorption coefficient of a line that is broadened exclusively by the Doppler effect,

$$k_\omega = \frac{2\pi^{3/2}e^2}{mc}\frac{\tilde{N}}{\Delta\omega_D}\exp\left(-\frac{\Delta\omega^2}{\Delta\omega_D^2}\right), \text{ or } k_\lambda = \frac{\pi^{1/2}e^2}{mc^2}\frac{\lambda_0^2\tilde{N}}{\Delta\lambda_D}\exp\left(-\frac{\Delta\lambda^2}{\Delta\lambda_D^2}\right). \tag{4.19}$$

The total half-width of such a line is obviously $2\pi\lambda_D\sqrt{\ln 2}$. Under astrophysical conditions the Doppler width is always much greater than the line width due

to radiation damping. In the solar photosphere ($T \sim 5800°$) we find, e.g., for Hβ, $\Delta\lambda_D = 0.159$ A, and, for an Fe line near 3900 A, $\Delta\lambda_D = 0.017$ A. This means that in the core of the line the Doppler effect is always more important than the damping. As the influence of the Doppler effect decreases as $\exp[-(\Delta\lambda/\Delta\lambda_D)^2]$ for increasing $\Delta\lambda$, while the damping profile decreases only as $\Delta\lambda^{-2}$, the damping profile will always become important beyond a certain $\Delta\lambda$. Roughly speaking, we may say that the line can be separated into a Doppler core, in which the intensity decreases very rapidly with increasing $\Delta\lambda$, and relatively extended wings, which can be described essentially by a $\Delta\lambda^{-2}$ law. This also follows from a thorough discussion of the line profile, if the combined effects of the Doppler and radiation or collision broadening are taken into ac-

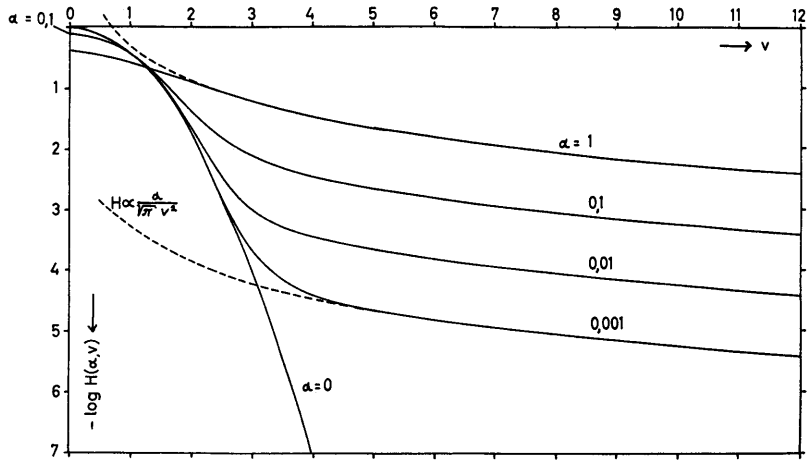


FIG. 5.—The function $H(a, v)$ for different values of a

count. The exact line profile is given by the convolution ("folding") integral over the Gaussian and damping functions:

$$\frac{2\pi^{3/2}e^2}{mc}\frac{\tilde{N}}{\Delta\omega_D}\frac{a}{\pi}\int_{-\infty}^{+\infty}\frac{e^{-v^2}dy}{a^2+(v-y)^2}=\frac{2\pi^{3/2}e^2}{mc}\frac{\tilde{N}}{\Delta\omega_D}H(a,v)=k(a,v), \quad (4.20)$$

with $v = (\omega - \omega_0)/\Delta\omega_D$ and $a = \gamma/2\Delta\omega_D$. The function $H(a, v)$ is 1, if $v = 0$ (line center) and $a \ll 1$. If we multiply $H(a, v)$ by $(\pi^{1/2}\Delta\omega_D)^{-1}$, we get the so-called Voigt function, $V(a, v)$. This function is normalized in such a way that the integral from $-\infty$ to $+\infty$ over V gives 1. The functions $H(a, v)$ and $V(a, v)$ have been tabulated and discussed by several authors (cf. van de Hulst and Reesinck 1947; Harris 1948; Elste 1953). In Figure 5 we reproduce a number of curves $H(a, v)$ in a logarithmic scale (see Unsöld 1955). This figure exhibits the fact that in the line wings the function $H(a, v)$ practically coincides with a pure damping profile, i.e.,

$$H(a, v) \sim \frac{a}{\pi^{1/2}v^2} \quad (4.21)$$

is a good approximation. For $a \ll 1$, the core of the line is very similar to a pure Doppler profile. So one can get a reasonable approximation for a Voigt profile by fitting together a pure Doppler profile and pure damping profile and just adding them in the transition range (Pannekoek 1930).

So far, we have considered only the broadening of lines due to the velocities of the radiating atoms. A different problem is the following: How will an originally sharp line be broadened, if the light is scattered by moving electrons or atoms before it finally leaves the stellar atmosphere? If the scattering is due to free electrons, the probability that a photon will be scattered in a direction inclined at an angle θ to the direction of incidence is (in the reference frame of the electron)

$$\sigma(\theta) = \frac{8\pi}{3}\left(\frac{e^2}{mc^2}\right)^2 \times \tfrac{3}{4}(1+\cos^2\theta)\,. \tag{4.22}$$

If we assume that the electrons have a Maxwellian velocity distribution, we get from a geometrical analysis of the scattering process at a moving electron the probability $\sigma(\theta, \omega_1, \omega_2)$ that a photon is scattered by an angle θ and that its frequency is shifted from ω_1 to ω_2 during this process:

$$\sigma(\theta, \omega_1, \omega_2) = \frac{8\pi}{3}\left(\frac{e^2}{mc^2}\right)\frac{3}{4}\frac{(1+\cos^2\theta)}{(1-\cos\theta)^{1/2}}\frac{1}{\Delta\omega_D} \times \exp\left[-\frac{(\omega_2-\omega_1)^2}{\Delta\omega_D{}^2(1-\cos\theta)}\right], \tag{4.23}$$

(Dirac 1925; Münch 1948; Chandrasekhar 1950). The source function in an atmosphere in which only electron scattering according to equation (4.23) occurs is, consequently,

$$S_\nu = N_e \int\int \sigma(\theta, \nu, \nu')\, I_{\nu'} d\nu' \frac{d\omega^*}{4\pi}, \tag{4.24}$$

with $d\omega^*$ = element of the solid angle. According to equation (4.23), an incident sharp line has a width of

$$\Delta\omega_D\,(1-\cos\theta)^{1/2} \tag{4.25}$$

after the scattering process. This means that the line is extremely narrow for pure forward scattering ($\cos\theta = 1$) and very diffuse for pure backward scattering. Because of equation (4.24), we can never observe one of these "pure" cases in a spherically symmetric atmosphere. In consequence of the small mass of the electrons, $\Delta\omega_D$ is relatively great; hence the lines broadened by this mechanism usually look rather diffuse. For 30,000°, $\lambda = 5000$ A, and $\theta = \pi/2$, we find $\Delta\lambda = 22$ A.

The corresponding problem for the scattering by moving atoms is more complicated because of the fact that the scattering probability for an atom at rest now depends on the frequency. Equation (4.22) has to be replaced by

$$\sigma(\theta, \omega) = \frac{\pi e^2}{mc} N f \gamma \frac{\frac{3}{4}(1+\cos^2\theta)}{(\omega-\omega_0)^2 + (\gamma/2)^2}. \tag{4.26}$$

Putting $\pi - \theta = 2\phi$, $v_1 = (\omega_1 - \omega_0)/\Delta\omega_1$ and $v_2 = (\omega_2 - \omega_0)/\Delta\omega$, one finds

$$\sigma(\phi, \omega_1, \omega_2) = \frac{2\pi e^2}{mc} \frac{Nf}{\Delta\omega_D} \tfrac{3}{4}(1+\cos^2 2\phi)\, e^{-[(v_2-v_1)/2\cos\phi]^2} \frac{1}{\sin 2\phi} \times \frac{a}{\pi \sin\phi} \int_{-\infty}^{+\infty} \frac{\exp(-y^2)\,dy}{\{[(v_2+v_1)/2\sin\phi] - y\}^2 + (a/\sin\phi)^2}. \tag{4.27}$$

Equation (4.27) has been derived by Henyey (1940) (see also Unsöld 1955). Note the similarity between the integral in equation (4.27) and the function $H(a, v)$ discussed above.

4.3. Pressure Broadening of Spectral Lines

4.31. *Derivation of different approximations from the general theory.*—The problem of pressure broadening has been approached from two apparently quite different starting points.

a) We have seen in the preceding section that the finite duration of the radiating process leads to a finite width of the line. Now the interruption of the radiation process by a collision must certainly have the same effect. This is a consequence of the general properties of Fourier integrals. The line width in angular frequency units is of the order of $1/t$, where t is the duration of the radiation process. But even if the radiated wave is not completely interrupted and if every collision causes only a phase shift of the wave, we must get an additional broadening of the line. This is obvious in the case that the phases before and after the collision are uncorrelated. (Actually, phase-shift collisions are much more important for the line-broadening problem than are collisions of the second kind.) The method based on these ideas is called the *collision* or *phase-shift* approximation.

b) The field due to the neighboring particles (e.g., the microscopic electric field of charged particles in a plasma) causes a splitting and a shift of the energy levels of the perturbed atom (e.g., by the Stark effect). The amount of the splitting and the shift depends, of course, on the local field strength. One can calculate the probability distribution of the field strengths and consequently of the corresponding splittings of the upper and lower levels of the line. The most successful approach of this kind is the well-known Holtsmark theory. Such a theory is called *statistical* or *static*, as it neglects the velocities of the perturbing particles.

Conditions *a* and *b* are limiting cases of a more general treatment. The intensity distribution of the dipole radiation from a time-dependent charge distribution is given in classical physics by the Fourier integral,

$$I(\omega) = \lim_{t_0\to\infty} \frac{2\omega^4}{3\pi c^3} \frac{1}{t_0} \left| \int_0^{t_0} \mu(t)\, e^{i\omega t} dt \right|^2, \tag{4.28}$$

where $\mu(t)$ is the dipole moment. The quantum-mechanical generalization of equation (4.28) has been given by Weisskopf (1933*a*, *b*), Anderson (1949), Bloom and Margenau (1953), and others:

$$I(\omega) = \frac{2\omega^4}{3\pi c^3} \text{Trace}\left[\varrho \int_{-\infty}^{+\infty} \mathfrak{y}(t)\, e^{-i\omega t} dt \int_{-\infty}^{+\infty} \mathfrak{y}(t)\, e^{i\omega t'} dt'\right]. \quad (4.29)$$

In this expression ϱ and $\mathfrak{y}$ are matrices and ϱ is the so-called density matrix. The diagonal elements ρ_{mm} of this matrix give the probability that an arbitrarily chosen atom is in the state m. The elements of the density matrix can often be approximated by the usual Boltzmann factors. According to equation (4.29), we have to take the trace of the matrix product in the brackets, i.e., the sum over all diagonal elements. (Taking the trace of a matrix is a quantum-mechanical analogue of taking an average.) In order to find the matrix elements of dipole moment,

$$\mu_{mn} = \int \psi_m^*(t)\, \mu \psi_n(t)\, dV\,, \quad (4.30)$$

the time-dependent Schrödinger equation, which allows for the varying position of the perturbing particles, has to be solved (μ = the operator of the dipole moment = er, ψ = the eigen-functions of the problem, dV = volume element).

This general formulation is too complex to be used as a starting point for practical calculations. Often the following approximations can be made:

1. It is assumed that the perturbing particle can be *localized exactly* in every point of its path and that the distance between perturber and radiator is given by

$$r(t) = (\rho^2 + v^2 t^2)^{1/2}\,, \quad (4.31)$$

i.e., that the path of the perturbing particle is a straight line (ρ is obviously the shortest distance between perturber and radiator, the so-called impact parameter). This assumption is called the *classical path approximation.* Though it cannot be fulfilled exactly because of Heisenberg's uncertainty principle, it is often a good approximation. The usual argument is that the angular momentum of the perturber with reference to the radiator is much larger than $\hbar$ and that therefore the perturber can be localized almost exactly. If we assume $T = 10{,}000°$; $N = 10^{15}$, corresponding roughly to the photospheric conditions in an A0 star, we find, for the angular momentum of a proton passing an atom at the mean distance between two particles, $r_0 = (4/3\pi)^{-1/3} N^{-1/3}$: $mr_0 v \sim 2.0 \times 10^4\, \hbar$ and, for an electron, $mr_0 v \sim 3.3 \times 10^2 \hbar$. (We would have numerically almost the same result if we had used ρ_0, the so-called Weisskopf radius for linear Stark effect—see below—instead of r_0.) The estimate indicates that the classical path approximation is valid for protons under astrophysical conditions. A more detailed investigation shows that its application to electrons may be problematic. This question has been discussed in detail by Margenau and Kivel (1955) and Margenau and Landwehr (1956). Their thorough quantum-mechanical discussion leads to an inequality between λ, the mean de Broglie wave length of the perturber, d, the Debye length, and the Weisskopf radius ρ_0:

$$(d\lambda)^{1/2} \ll \rho_0\,,$$

which must be fulfilled for the classical path approximation to be valid. For the special case of the broadening of Hα by first-order Stark effect, Margenau and Landwehr give the upper limits of the temperature, below which the classical path approximation is valid (quoted in Table 5). This confirms the result of the crude estimate made above, namely, that the classical path approximation is valid under astrophysical conditions if the line broadening is due to heavy particles. For the broadening by electrons, the applicability of this approximation is questionable.

2. It is assumed that the collisions are adiabatic, i.e., that no collision-induced (radiationless) transitions occur between the different Stark effect states (into which the original energy level is split in the field of the perturbing particle). Under which conditions do we have such an adiabatic collision? The duration of the collision is of the order of ρ/v. According to Heisenberg's un-

TABLE 5

TEMPERATURE LIMITS FOR VALIDITY OF CLASSICAL PATH APPROXIMATION
(First-Order Stark Effect of Hα) According to Margenau and Landwehr (1956)

N (cm^{-3})	T (° K)		N (cm^{-3})	T (° K)	
	Protons	Electrons		Protons	Electrons
10^{12}	5.2×10^{5}	6.7	10^{16}	5.2×10^{7}	6.7×10^{2}
10^{14}	5.2×10^{6}	6.7×10^{1}	10^{18}	5.2×10^{8}	6.7×10^{3}

certainty principle, a quantum-mechanical description then requires that the energy be uncertain by an amount of

$$\Delta E \sim \frac{\hbar}{\rho/v} = \frac{\hbar v}{\rho}. \tag{4.32}$$

According to the general principles of quantum mechanics (cf. Schiff 1949), a considerable number of induced transitions will occur if ΔE is comparable to, or greater than, the energy difference between two Stark effect states (classically speaking, between two orientations of the atom in the field of the perturber). If the classical path approximation is valid, the frequency shift due to the field of the perturber may be written as follows:

$$\Delta\omega = \frac{2\pi C}{r^n}, \tag{4.33}$$

where C is the so-called constant of interaction; $n = 2$ for linear Stark effect, $n = 4$ for quadratic Stark effect, and $n = 6$ for van der Waals interaction. From equation (4.33) it follows that the energy difference between two orientations is of the order of

$$\Delta E^* \sim \hbar \frac{2\pi C}{\rho^n}. \tag{4.34}$$

Our condition for the non-occurrence of induced transitions, i.e., for adiabacy, is $\Delta E \ll \Delta E^*$. Using equations (4.32) and (4.34), this inequality can be written

$$\rho \ll \left(\frac{2\pi C}{v}\right)^{1/(n-1)} \sim \rho_0 , \tag{4.35}$$

where ρ_0 is the so-called Weisskopf radius (see below). So we may say that collisions within the Weisskopf radius are adiabatic.

In most of the calculations of pressure broadening the assumptions (1) validity of the classical path approximation and (2) adiabacy have been made. They are implicit in the classical form of the phase-shift theories of Weisskopf *et al.* (1933) as well as in the static approximations. If these assumptions are made, the time-dependent (quantum-mechanical) equation of motion for the matrix of the electric moment $\mathfrak{y}$ (H is the time-dependent Hamilton matrix),

$$i\hbar\dot{\mathfrak{y}} = (H\mathfrak{y} - \mathfrak{y}H) , \tag{4.36}$$

which is essentially equivalent to the time-dependent Schrödinger equation mentioned above, can be integrated explicitly (Foley 1946; Anderson 1949).

By using the result of this integration, equation (4.29) can be written

$$I_{mn}(\omega) = \frac{2\omega^4}{3\pi c^3}\left[\exp\left(-\frac{\chi_m}{kT}\right)\right]\left|\mu_{mn}\int_{-\infty}^{+\infty}\exp\{i[\eta(t) - (\omega-\omega_0)t]\}\,dt\right|^2 , \tag{4.37}$$

where μ_{mn} is the dipole moment of the unperturbed atom and ω_0 is the unperturbed frequency of the line $m \rightarrow n$. The integral on the right-hand side of equation (4.37) is the Fourier integral over the function

$$\exp\{i[\omega_0 t + \eta(t)]\} , \tag{4.38}$$

which can be interpreted in the following way. The phase of the unperturbed wave (with frequency ω_0) is shifted during the collision i by an amount of η_i, and $\eta(t)$ is the integral over all these phase shifts up to time t. Equation (4.38) gives the time dependence of the phase of the radiated wave, if phase disturbances by collisions play a role. It is the starting point of the classical theory of phase-shift collisions (cf. Weisskopf 1932; Lindholm 1942; Unsöld 1943), in which it is assumed that $\eta(t)$ has the form of a step function. Equation (4.38) has been derived originally from more heuristic considerations. Holstein (1950) has shown that the static theories also follow as a limiting case from equation (4.37), provided that we restrict ourselves to the case of *one* perturbing particle (see also Sobelman 1954, 1957). Holstein uses the following procedure: If $(\omega - \omega_0)$ is large, the integrand in equation (4.37) oscillates rapidly, except at those times t_k at which $d\eta/dt \sim (\omega - \omega_0)$. At these times the integrand remains almost constant. Therefore, the main contributions to the integral (4.37) come from the time intervals around the t_k. Consequently, the in-

tegral in equation (4.37) can be written as the sum of the contributions from the time intervals around the t_k:

$$\sum_k \int_{\Delta t_k} \exp\{i[\eta(t) - (\omega - \omega_0)(t - t_k) - (\omega - \omega_0) t_k]\} dt. \quad (4.39)$$

Now $\eta(t)$ can be expanded into a Taylor series at $t = t_k$, and $d\eta/dt$ is equal to the frequency shift $\omega - \omega_0 = \Delta\omega$ in the moment of a collision. Using this identity and neglecting terms of the third and higher order, we get

$$I(\omega)\, d\omega = \frac{1}{T} \sum_k \left[\frac{d(\Delta\omega)}{dt}\right]^{-1}_{t_k} d\omega. \quad (4.40)$$

Here $\Sigma[d(\Delta\omega)/dt]^{-1} d\omega$ is the time during which $\omega_0 + \Delta\omega$ lies in the interval ω, $\omega + d\omega$. Therefore, we can consider equation (4.40) as a general expression for a static theory, since it depends only on the probability of the occurrence of a certain $\Delta\omega$. Now we shall derive a criterion for the validity of equation (4.40). The derivation of equation (4.40) requires that

$$\frac{1}{6} \frac{d^3\eta}{dt^3} (t - t_k)^3 \ll 1. \quad (4.41)$$

For the integration of equation (4.39), only those intervals are important for which

$$\frac{1}{2} \frac{d^2\eta}{dt^2} (t - t_k)^2 \leq 1. \quad (4.42)$$

The reason is that the linear terms in equation (4.39) cancel, and consequently the integrand will oscillate rapidly if the left-hand side of inequality (4.42) gets larger than 1. From relations (4.41) and (4.42) and replacing $(d\eta/dt)$ by $\Delta\omega$, we get

$$\left[\frac{d^2(\Delta\omega)}{dt^2}\right]\left[\frac{d(\Delta\omega)}{dt}\right]^{-3/2} \ll 1. \quad (4.43)$$

Now assume that only one perturbing particle has to be taken into account and that the classical path approximation and consequently equation (4.31) are valid. So we get, from equation (4.33),

$$\Delta\omega = \frac{2\pi C}{[\rho^2 + v^2 (t - t_k)^2]^{n/2}}. \quad (4.44)$$

It follows that

$$\frac{d(\Delta\omega)}{dt} \sim \frac{(2\pi C)\, v}{\rho^{n+1}}; \qquad \frac{d^2(\Delta\omega)}{dt^2} \sim \frac{(2\pi C)\, v^2}{\rho^{n+2}}, \quad (4.45)$$

as far as the order of magnitude is concerned. (We have set $t - t_k \sim \rho/v$.) From relations (4.43) and (4.45) it follows that

$$\frac{v^{1/2} \rho^{1/2(n-1)}}{(2\pi C)^{1/2}} \ll 1; \qquad \frac{2\pi C}{v \rho^{n-1}} \gg 1. \quad (4.46)$$

The points t_k occur (by definition) only if the maximal frequency shift during an encounter $(2\pi C)/\rho^n$ is larger than, or equal to, $(\omega - \omega_0)$, i.e.,

$$\frac{2\pi C}{\rho^n} \geq \Delta\omega\,; \qquad \text{or} \qquad \rho \leq \left(\frac{2\pi C}{\Delta\omega}\right)^{1/n}, \tag{4.47}$$

Inserting formula (4.47) in formula (4.46), we have

$$\Delta\omega \gg \frac{v^{n/(n-1)}}{(2\pi C)^{1/(n-1)}}, \tag{4.48}$$

which is usually called the "Holstein inequality." (It was stated earlier by other authors; cf. Unsöld 1943.) Relation (4.48) must be fulfilled if a static approach (like the Holtsmark theory) is applicable. It shows that the static theory must be always valid in the far wings of the line beyond a certain critical $\Delta\omega$. This $\Delta\omega$ just corresponds to the frequency shift caused by a perturber at a distance of the Weisskopf radius, as can be seen from a comparison with equation (4.35). Spitzer (1939, 1940) has shown that the other limiting approximation—the phase-shift theory—can be applied if

$$\Delta\omega \ll \frac{v^{n/(n-1)}}{(2\pi C)^{1/(n-1)}} \tag{4.49}$$

(see also Burkhardt 1940). So we may say that in a pressure-broadened line there will be an inner part which follows essentially the phase-shift theory and an outer part in which the static theory is applicable. In the transition region, equation (4.37) has to be used without approximations. In practice, such a detailed solution of equation (4.37) is not very helpful. If we want to have a really better theory, we have to take into account deviations from adiabacy. In Table 6 we reproduce as an illustrative example the limits $\Delta\lambda_c = (\lambda^2/2\pi c)\Delta\omega_c$

TABLE 6

LIMITS $\Delta\lambda_c$ (IN ANGSTROM UNITS) BETWEEN RANGES OF VALIDITY OF PHASE-SHIFT AND STATIC THEORY

(From Unsöld 1943)

	T			
	25,000°	10,000°	5000°	3000°
$H\alpha$ electrons	580	230	110	70
$H\alpha$ protons	0.63	0.25	0.12	0.08
$H\beta$ electrons	120	48	24	14
$H\beta$ protons	0.13	0.05	0.03	0.02
$H\gamma$ electrons	48	19	9	6
$H\gamma$ protons	0.05	0.02	0.01	0.006
$H\delta$ electrons	32	13	6	4
$H\delta$ protons	0.03	0.01	0.007	0.004

which separate the range of validity of static and phase-shift theories for the broadening of the Balmer lines by linear Stark effect. Here $\Delta\omega_c$ is essentially given by the right-hand side of equation (4.48) or (4.49), it contains an additional numerical constant $[\pi^{1/2}\Gamma(\frac{1}{2})/\Gamma(1)]^{-2} = \pi^{-2}$. This factor occurs in Spitzer's (1940) and Unsöld's (1943) papers (see below), but it does not appear in Holstein's analysis (1950). The table shows that for $H\alpha - H\delta$ the broadening by ions can be described by the static theory, whereas the broadening by electrons follows the phase-shift theory.

In the next two sections we shall consider briefly the phase-shift and the static theories based on the assumption of adiabacy and the classical path approximation. In §§ 4.34 and 4.35 some recent approaches of astrophysical interest will be discussed, in which these assumptions have been partly dropped and different kinds of perturbing particles have been taken into account simultaneously.

4.32. *The phase-shift theory.*—In this approximation $\eta(t)$ is considered as a step function. The "height of a step" corresponding to a collision with the relative velocity v and an impact parameter ρ_i is given by

$$\eta_i = \int_{-\infty}^{+\infty} \Delta\omega_i dt = 2\pi C \int \frac{dt}{(\rho_i^2 + v^2 t^2)^{n/2}} = \frac{2\pi C}{v\rho^{n-1}} \frac{\pi^{1/2}\Gamma[(n-1)/2]}{\Gamma(n/2)}, \quad (4.50)$$

(see eq. [4.44]). The impact parameter ρ_0 for which $\eta = 1$ is called the "Weisskopf radius." It differs only by the numerical factor $\{\pi^{1/2}\Gamma[(n-1)/2]/\Gamma(n/2)\}^{1/(n-1)}$ from the critical radius in equation (4.35).

In a phase-shift theory, $\eta(t)$ has to be composed of the different η_i's according to the relative probability of collisions with an impact parameter ρ_i. This can be done in the following way (cf. Margenau and Landwehr 1956; Sobelman 1957): The right-hand side of equation (4.37) can be written (we drop the constants and the Boltzmann factor, which are unimportant in this connection) as follows:

$$\left| \int_{-\infty}^{+\infty} \exp\{i[\eta(t) - (\omega - \omega_0)t]\} dt \right|^2 = \int_{-\infty}^{+\infty} \int_{-\infty}^{+\infty} \exp\{i[\eta(t) - \eta(t') + (\omega_0 - \omega)(t - t')]\} dt dt'. \quad (4.51a)$$

Putting $t' = t + s$, we get

$$\left| \int_{-\infty}^{+\infty} \exp\{i[\eta(t) - (\omega - \omega_0)t]\} dt \right|^2 = \int_{-\infty}^{+\infty} \{\exp[i(\omega_0 - \omega)s]\} \phi(s) ds, \quad (4.51b)$$

with

$$\phi(s) = \int_{-\infty}^{+\infty} \exp\{i[\eta(t) - \eta(t+s)]\} dt;$$

$\phi(s)$ is the so-called correlation function. If $\eta(t)$ and $\eta(t+s)$ are strongly correlated, i.e., if η has a "long memory," $\phi(s)$ decreases only slowly with increasing s. The reverse is true if the correlation is small. (The integrand oscillates strongly in this case for $s \neq 0$.) Now define

$$\eta(t+s) - \eta(t) = \eta(t, s) . \tag{4.52}$$

Then we take the difference

$$e^{-i\eta(t,\, s+ds)} - e^{-i\eta(t,s)} = e^{-i\eta(t,\, s)} (e^{-i\eta'} - 1) , \tag{4.53}$$

where η' means the additional phase shift during the time ds. If we take the mean over t of equation (4.53), we get, according to the definition of ϕ in equation (4.51),

$$\phi(s+ds) - \phi(s) = d\phi(s) = \langle e^{-i\eta(t,\, s)} (e^{-i\eta'} - 1) \rangle_{\mathrm{Av}} , \tag{4.54}$$

where "Av" means that the time average has to be taken of the expression in angular brackets. Now, according to our basic assumption, the phase always jumps abruptly; so η' is independent of the phase at the time $t+s$. Consequently, the mean over both factors on the right-hand side of equation (4.54) can be taken separately. We have, by definition of ϕ,

$$\langle e^{-i\eta(t,\, s)} \rangle_{\mathrm{Av}} = \phi(s) . \tag{4.55}$$

When taking the mean over the second factor, we replace the time average by the average over all impact parameters. During the time ds there are $2\pi\rho d\rho N v ds$ perturbers with impact parameters in the range ρ, $\rho + d\rho$. Consequently,

$$\langle e^{-i\eta} - 1 \rangle = 2\pi N v ds \int_0^\infty [e^{-i\eta(\rho)} - 1] \rho d\rho = -N v ds (\sigma_r + i\sigma_i) , \tag{4.56}$$

with

$$\sigma_r = 2\pi \int_0^\infty [1 - \cos\eta(\rho)] \rho d\rho \quad \text{and} \quad \sigma_i = 2\pi \int_0^\infty \sin\eta(\rho) \rho d\rho . \tag{4.57}$$

Now we can integrate equation (4.54),

$$\phi(s) = \exp[-N v (\sigma_r + i\sigma_i) s] . \tag{4.58}$$

Inserting ϕ into equation (4.51*b*), we get

$$I(\omega) \propto \frac{1}{\pi} \frac{\gamma/2}{(\omega - \omega_0 - \beta)^2 + (\gamma/2)^2} , \tag{4.59}$$

with $\gamma/2 = N v \sigma_r$ and $\beta = N v \sigma_i$.

We get a damping profile, whose center is shifted by the amount β. The same result was derived by Lindholm (1941), using a mathematically different method.

In astrophysics this theory has found important applications in the case of van der Waals broadening due to neutral hydrogen atoms ($n = 6$), for electron broadening by quadratic Stark effect ($n = 4$), and sometimes in the case of

collision broadening by electrons ($n = 2$). For the latter case, such calculations are of problematic value because of the importance of non-adiabatic effects (but see Meyerott and Margenau 1955). For $n = 4$ and $n = 6$ the adiabatic approximation is satisfactory (Spitzer 1940; Lindholm 1942). In general, the adiabatic approximation is reasonable for perturbations which shift all the line components in the same direction.

In the case of van der Waals broadening, we find from equations (4.57) and (4.50), $\gamma_6/\beta_6 = 2.80$. From equation (4.57) it also follows that

$$\gamma_6 = 17.0 C^{2/5} v^{3/5} N \,. \tag{4.60}$$

For a hydrogen-like atom the interaction constant C is (cf. Unsöld 1955)

$$C = 64.4 \times 10^{-35} \frac{n^{*2}}{2Z^2} [5n^{*2} + 1 - 3l(l+1)] \,, \tag{4.61}$$

where n^* = effective quantum number and l = azimuthal quantum number. For an estimate of C we may neglect the term $[1 - 3l(l+1)]$ and get the simple expression

$$C = 1.61 \times 10^{-33} \left(\frac{13.5}{\chi_r - \chi_{r,s}} \right)^2 \tag{4.62}$$

if we measure the χ's in ev. Unsöld and Weidemann (1955) have compared the experimentally determined γ_6 of Na, K, Rb, Cs, Ag, and Hg lines (broadened by rare-gas atoms) with the results of equations (4.60) and (4.61). They find satisfactory agreement. Recent experiments by Kusch (1958) indicated that the actual van der Waals broadening of Fe I lines is usually greater than that predicted by equations (4.60) and (4.61), by factors between 2 and 5.

In the case of quadratic Stark effect one finds, from equation (4.57),

$$\gamma_4 = 38.8 C^{2/3} v^{1/3} N \quad \text{and} \quad \beta_4 = 34.4 C^{2/3} v^{1/3} N \,. \tag{4.60a}$$

For linear Stark effect we get, from the same formula by cutting off the integral at the Debye radius d (the integral from zero to infinity diverges in this case),

$$\gamma_2 = 8\pi^5 \frac{C^2 N}{v} \left[0.923 - \ln\left(\frac{2\pi^2 C}{vd}\right) + \frac{1}{6}\left(\frac{\pi^2 C}{vd}\right) - \ldots \right]. \tag{4.60b}$$

4.33. *The static theory of line broadening.*—In the static case, $I(\omega)d\omega$ is proportional to the probability of a configuration of perturbers which causes a frequency shift in the range $\Delta\omega$, $\Delta\omega + d(\Delta\omega)$ (see eq. [4.40]).

The problem has a simple solution if only one perturbing particle has to be considered (far wings of the line). The probability that the nearest perturber lies in the distance range r, $r + dr$ is the product of the probability that one particle lies in the range r, $r + dr$ times the probability $W^*(r)$ that there is *no* perturber within the sphere with the radius r. If $w^*(r, dr)$ is the probability that *no* particle is in the range r, $r + dr$, we have, according to the product rule for probabilities,

$$W^*(r, dr) = W^*(r)\, w^*(r, dr) \tag{4.63}$$

and w^* is 1 less the probability that one particle is in the shell r, $r + dr$. If forces between the particles can be neglected, the latter is equal $4\pi N r^2 dr$. We obtain

$$w^*(r + dr) = 1 - 4\pi r^2 N dr , \tag{4.64}$$

and, from equation (4.63),

$$W^*(r) + \frac{dW^*}{dr} dr = W^*(r)(1 - 4\pi r^2 N dr) . \tag{4.65}$$

Integrating, we get

$$W^*(r) = \exp\left(-\frac{4\pi}{3} r^3 N\right). \tag{4.66}$$

Consequently, the probability that the nearest perturber lies in the range $r, r + dr$ is

$$W(r)\, dr = 4\pi r^2 N dr \exp\left(-\frac{4\pi}{3} r^3 N\right) = e^{-(r/r_0)^3} d\left(\frac{r}{r_0}\right), \tag{4.67}$$

where r_0 is the mean distance between two perturbers, defined by $(4\pi/3) r_0^3 N = 1$. Using equation (4.33), we get

$$\begin{aligned} I(\omega)\, d\omega &= \left\{\exp\left[-\left(\frac{\Delta\omega_0}{\Delta\omega}\right)^{3/n}\right]\right\} d\left(\frac{\Delta\omega_0}{\Delta\omega}\right) \\ &= \frac{3}{n}\left(\frac{\Delta\omega_0}{\Delta\omega}\right)^{3/n+1} \left\{\exp\left[-\left(\frac{\Delta\omega_0}{\Delta\omega}\right)^{3/n}\right]\right\} \frac{d\omega}{\Delta\omega_0}. \end{aligned} \tag{4.68}$$

It follows from this equation that

$$\begin{aligned} &I(\omega) \propto \Delta\omega^{-5/2} \text{ for linear} \\ \text{and} \qquad &\\ &I(\omega) \propto \Delta\omega^{-7/4} \text{ for quadratic Stark effect} \end{aligned} \tag{4.69}$$

if $\Delta\omega$ is sufficiently great.

If we wish to consider the co-operative effects of many perturbing particles, we have (in the case of the Stark effect), first, to superpose the field vectors due to the different perturbers (Holtsmark 1919, 1924; Verwey 1936; the quantum-mechanical explanation of this procedure has been given by Margenau and Meyerott 1955). The probability W that the resulting field strength has components X_0, Y_0, and Z_0 in the range X_0, $X_0 + dX_0$; Y_0, $Y_0 + dY_0$; Z_0, $Z_0 + dZ_0$ is

$$W(X_0, Y_0, Z_0)\, dX_0 dY_0 dZ_0 = \frac{1}{V^N} \int \ldots \int \prod_k dx_k dy_k dz_k . \tag{4.70}$$

The integration in equation (4.70) has to be extended only over those elements of volume that contribute to resulting field vectors in the range considered, according to

$$X_0 = \Sigma X_k ; \qquad Y_0 = \Sigma Y_k ; \qquad Z_0 = \Sigma Z_k . \tag{4.71}$$

This can be accomplished by multiplying the right side by

$$\delta(X - X_0)\, \delta(Y - Y_0)\, \delta(Z - Z_0)$$

and extending the integration over the whole space. The δ-functions are zero if $X \neq X_0$, etc.; for $X = X_0$, they go to infinity in the sense that the integral over the δ-function is dX_0. As an analytical description we can use

$$\delta(X - X_0) = \frac{dX_0}{2\pi}\int_{-\infty}^{+\infty} d\xi \exp\{i\xi[\Sigma X_k(x_k, y_k, z_k) - X_0]\}. \quad (4.72)$$

The right-hand side has just the required property (cf. Schiff 1949, p. 51). The most satisfactory procedure using δ-functions to evaluate equation (4.70) is Markoff's method (cf. Chandrasekhar 1943; for an application of this method to the line broadening by linear Stark effect see also Margenau 1951). A different method has been suggested by Ecker (1957*a*).

Let us consider the case of linear Stark effect. We call the "length" of the field vector $F = (X_0^2 + Y_0^2 + Z_0^2)$. Now introduce a "normal" field strength,

$$F_0 = 2.61\, eN^{2/3}, \quad (4.73)$$

and set $\beta = F/F_0$, where F_0 is approximately equal to the field strength caused by a perturber at the mean distance r_0 defined above. The evaluation of equation (4.70) then leads to

$$W(\beta) = \frac{2}{\pi\beta}\int_0^{\infty} v \sin v\, e^{-(v/\beta)^{3/2}} dv. \quad (4.74)$$

The asymptotic behavior of $W(\beta)$ is given by the series expansions,

$$W(\beta) = \frac{4\beta^2}{3\pi}(1 - 0.463\beta^2 + 0.1227\beta^4 \mp \ldots) \quad \text{for} \quad \beta \to 0, \quad (4.75)$$

$$W(\beta) = \frac{15}{8}\left(\frac{2}{\pi}\right)^{1/2}\beta^{-5/2}\left(1 + \frac{5.107}{\beta^{3/2}} + \frac{14.43}{\beta^3} + \ldots\right) \text{ for } \beta \to \infty. \quad (4.76)$$

According to the basic assumption of the static theory, $W(\beta)$ is connected in a simple manner with $I(\omega)$. We have

$$\Delta\omega = \frac{2\pi C}{r^2} = \frac{2\pi CF}{e} = \frac{2\pi CF_0}{e}\beta = \Delta\omega_0\beta. \quad (4.77)$$

So we get, in analogy with equation (4.68),

$$I(\omega)\, d\omega = W\left(\frac{\Delta\omega}{\Delta\omega_0}\right)\frac{d\omega}{\Delta\omega_0}, \quad (4.78)$$

where the integral over $I(\omega)$ is normalized to unity. Every Stark effect component (except the central component) is widened according to equation (4.78). The intensity distribution of the whole line is found by a superposition of the contributions of the different Stark effect components according to

$$S(a) = \sum_k I_k W\left(\frac{a}{c_k}\right)\frac{1}{c_k} \quad \text{with} \quad a = \frac{\Delta\lambda}{F}, \quad (4.79)$$

where c_k is the shift of the Stark effect component for $F = 1$ and I_k is the relative intensity of the component k.[14] Pannekoek (1938) and others have suggested an approximate treatment of equation (4.79). The separation of the outermost components is

$$\Delta\lambda^* = 0.0192\lambda^2 [n(n-1) + 2] F \qquad (4.80)$$

(cf. Unsöld 1955). The Stark effect splitting is then approximated by a range of width $\Delta\lambda^*$ with constant intensity. This method is especially useful for the calculation of the higher Balmer lines, for which the Stark effect splitting has not yet been calculated in detail. (Very recently Underhill and Waddell [1959] have computed tables of Stark broadening functions up to $n = 18$.)

Numerical computations of $W(\beta)$ have been made by Holtsmark, Verwey (1936), Schmaljohann (1936), and Chandrasekhar (1943). In Table 7 we re-

TABLE 7

THE HOLTSMARK DISTRIBUTION FUNCTION $W(\beta)$

β	$W(\beta)$	β	$W(\beta)$	β	$W(\beta)$
0	0	3.0	0.176	6.0	0.0242
0.2	.0167	3.2	.150	6.2	.0219
0.4	.0631	3.4	.128	6.4	.0199
0.6	.1296	3.6	.111*	6.6	.0181
0.8	.2033	3.8	.098*	6.8	.0166
1.0	.2713	4.0	.086	7.0	.0153
1.2	.3240	4.2	.075	7.5	.0125
1.4	.3562	4.4	.065	8.0	.0104
1.6	.3673	4.6	.0573	8.5	.0087
1.8	.3600	4.8	.0494	9.0	.0075
2.0	.3392	5.0	.0431	10.0	.0056
2.2	.3095	5.2	.0379	15.0	.00188
2.4	.2749	5.4	.0336	20.0	.00089
2.6	.238	5.6	.0299	25.0	.00050
2.8	0.206	5.8	0.0268	30.0	0.00031

* Determined by quadratic interpolation from the values given by Schmaljohann (1936).

produce $W(\beta)$, using the results of these authors. The expression $S(\alpha)$ has been calculated by Schmaljohann for Hα, Hβ, Hγ, and Hδ according to equation (4.79). The results are given in Figure 6. (An error in the original calculation for Hβ, as found by Jürgens, has been corrected.)

The intensity distribution for lines broadened by quadratic Stark effect is

$$I(\omega)\, d\omega = \frac{W(\beta)}{2\beta} \frac{d\omega}{\Delta\omega_0}, \qquad (4.81)$$

with the same W as discussed above.

Recently it has been shown in detail that we are justified in neglecting the

[14] In this calculation we have to give the σ-components double weight relative to the π-components, as the radiation into all directions must be taken into account in the same way (see Schmaljohann 1936; Unsöld 1955).

influence of the electrostatic interaction on the distribution of the perturbing particles under the conditions which occur in stellar atmospheres (Edmonds 1956; Ecker 1957*a*, *b*). This result refers to linear as well as quadratic Stark effect. This can be seen qualitatively as follows: Take, e.g., $T = 10^{4}°$, $N_e = 10^{15}$. Then the Debye shielding distance $r_0 = 2.2 \times 10^{-5}$ cm is greater than the mean distance between the particles and greater than the Weisskopf radius.

4.34. *Non-adiabatic effects in phase-shift theories.*—In a static theory the assumption of adiabacy is justified because it refers to perturbing particles lying within the Weisskopf sphere (see eqs. [4.35] and [4.48]). No argument of

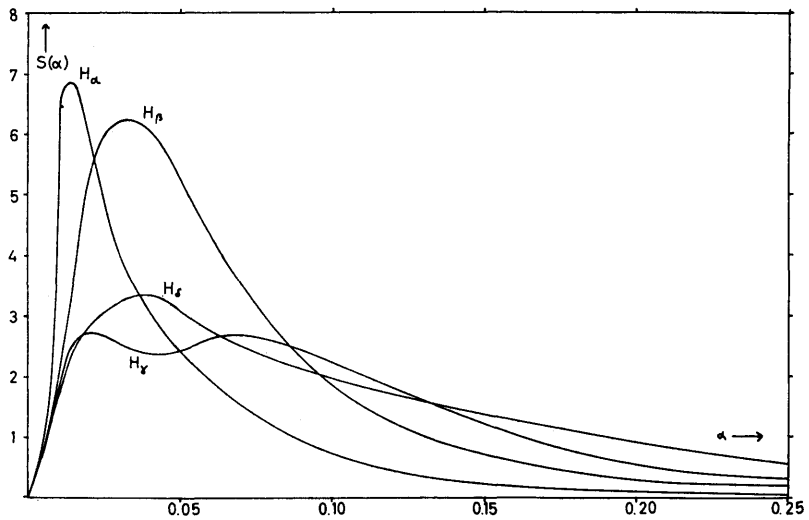


FIG. 6.—$S(\alpha)$ for the first four Balmer lines

this kind is available in the case of phase-shift theories, though the adiabatic approximation may be reasonable under certain conditions (e.g., in the case of van der Waals broadening, see § 3.2).

Spitzer (1940) has shown that, besides the transitions between the different Stark effect states (called non-adiabatic effects in § 3.1), the so-called rotation effect must be considered. Since the radiating atom is observed in a stationary co-ordinate system, the radiator (which is oriented toward the perturber during the collision in the adiabatic case) is turned by 180° during the collision. This should cause a phase shift of π for every collision. Spitzer demonstrated that often the effects of non-adiabacy and the rotation effect cancel each other to a certain extent, so that the adiabatic theory gives reasonable results. In a quantum-mechanical picture, non-adiabatic effects can be described as follows: In the basic equation of motion (4.36) the Hamilton matrix H can be written as

$$\boldsymbol{H} = \boldsymbol{H}_0 + \boldsymbol{H}_1 ,$$

where $\boldsymbol{H}_0$ is the matrix of the unperturbed atom and $\boldsymbol{H}_1$ is the time-dependent perturbation matrix (due to the moving perturbing particles). (In the line-broadening problem we always have $\boldsymbol{H}_0 \gg \boldsymbol{H}_1$.) In the adiabatic case there are no transitions between different eigen-states, i.e., all non-diagonal elements in $\boldsymbol{H}_1$ are zero. In the non-adiabatic case the matrix elements outside the diagonal are different from zero if they correspond to possible induced transitions between different Stark effect states. This shows that the investigation of non-adiabatic effects will be comparatively simple only for lines with simple Stark effect splitting. Therefore, the numerical calculations of this kind have usually been restricted to Ly-α. Very recently the wings of Hα, Hβ, Hγ, Hδ, have been calculated allowing for non-adiabatic effects (Griem, Kolb, and Shen 1959; see next section).

Spitzer (1939) has investigated in detail non-adiabatic effects in the broadening of Ly-α by ions (linear Stark effect). These become important only in the line core. The wings can be described by the static Holtsmark theory (in accordance with the general ideas discussed in § 3.1).

Recently the theory of electron impact broadening of hydrogen lines has received special attention. In this case it is necessary to abandon even the classical path approximation and to develop a completely quantum-mechanical theory (a significant theory of this kind was given by Kivel, Bloom, and Margenau 1955; Landwehr 1956). Meyerott and Margenau found that the numerical results derived from this theory do not differ greatly from the results of the classical phase-shift theory (see eq. [4.60*b*]). Kolb (1957) has used the classical path approximation but paid attention to non-adiabatic effects. Kolb assumes that that the non-diagonal elements of $\boldsymbol{H}_1$ are small and of the first order compared to the non-diagonal elements. An essential point in Kolb's theory is that he tries to consider broadening by electrons and by ions simultaneously. Therefore, we shall consider it in the next section.

4.35. *Hydrogen lines broadened simultaneously by ions and electrons.*—It follows from Table 6 that under astrophysical conditions the broadening of the strongest Balmer lines by the slowly moving ions follows the static theory, whereas the broadening by the fast-moving electrons can be described by a phase-shift theory. Numerical estimates show that under astrophysical conditions the contribution of the electrons can often be neglected (Spitzer 1939; Unsöld 1943, 1955; Kivel, Bloom, and Margenau 1955; Margenau and Landwehr 1956), because the half-width γ of the line due to collision broadening by electrons is much smaller than the half-width Γ due to the Holtsmark broadening by ions. At a temperature of 12,000°, both half-widths are equal to Hα, if $N_e \sim 5 \times 10^{18}$ cm^{-3}, and for Hδ if $N_e \sim 4 \times 10^{16}$ cm^{-3}. We have seen in the preceding sections that the intensity in the line wings varies as $\Delta\lambda^{-2}$ for collision broadening and as $\Delta\lambda^{-5/2}$ for the statistical broadening due to linear Stark effect. Therefore, the broadening by electrons can be important in the outer wings of a line even if $\Gamma > \gamma$, i.e., at lower densities. The available estimates in-

dicate that, e.g., for Hβ at $\Delta\lambda \sim 20$ A, the electrons cannot be neglected if $N_e > 10^{15}$ (where we have again assumed $T = 12{,}000°$).

A preliminary theory of simultaneous line broadening by both ions and electrons can be based on the following concept. During an impact of an electron, the hydrogen level is split up because of the static ion field, which remains practically unchanged during the electron impact. This leads to a line profile which is given by the convolution ("folding") integral over the Holtsmark profile for the *ions* and the phase-shift profile for the *electrons* (Griem 1954; Ecker 1957*b*). Griem assumed that the phase-shift profile for the electrons is essentially given by equations (4.59) and (4.60*b*). This seems reasonable in the light of the investigation of Meyerott and Margenau (1955), who showed that the numerical results of the electron-broadening theory of Kivel, Bloom, and Margenau (1955) do not differ very much from the classical adiabatic theory.

The same problem has been discussed in detail by Kolb (1957). His procedure is similar to Griem's in several respects. The main difference between both investigations is that Kolb tries to allow approximately for non-adiabatic effects during electron collisions. He assumes that the non-diagonal elements of the perturbation matrix $\boldsymbol{H}_1$ cannot be neglected (in contrast with the adiabatic theory) but that they are small and of the first order ("weak-collision theory"). The theory is given in detail for Ly-α. The non-adiabatic effects in the Balmer lines are estimated by using the results for Ly-α. As one would expect, the line profiles computed by Kolb are slightly narrower than those calculated by Griem, who neglected adiabatic effects. In Figure 7 we compare the profiles of Hβ computed according to Griem's (1954) and Kolb's theory with the usual Holtsmark profile. The curves, which refer to $T = 11{,}500°$, $N_e = 10^{16}$, give an impression of the magnitude of the electron broadening that may be expected in addition to the usual Holtsmark broadening by ions.

A refined theory, including the effect of simultaneous perturbations by ions and electrons and taking into account non-adiabatic effects, has been developed by Griem, Kolb, and Shen (cf. their paper 1959). They give numerical results for Ly-α, Ly-β, Hα, Hβ, Hγ, and Hδ.

The conclusions of Griem and Kolb are compatible with the experimental results of the Kiel group using water-stabilized arcs (Griem 1954; Bogen 1957) and of the Michigan group using the shock-tube technique (Turner 1956).

§ 5. COHERENT AND NON-COHERENT RE-EMISSION

5.1. General Remarks

If deviations of the source function from B_ν are taken into account, we have to know whether an electron, after entering the sublevel ϵ' of the level j, remains in ϵ' before it leaves j or whether it first jumps to some other ϵ'' of the same level (see § 3), before the re-emission takes place. In the simple case of line scattering, this problem is reduced to the question whether the absorbed quantum is re-emitted in the same frequency (coherent scattering) or not (non-

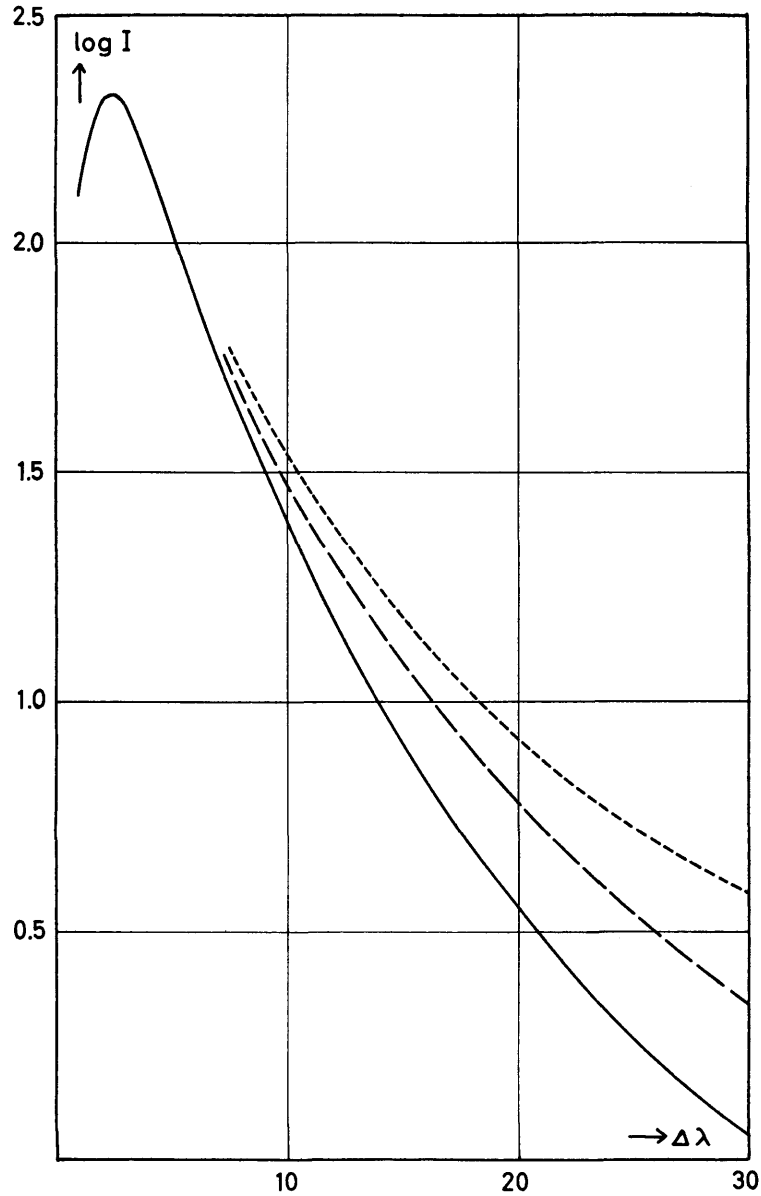


FIG. 7.—Comparison of the profiles of Hβ at T = 11,500°; $N_e = 10^{16}$ derived from —— the Holtsmark theory; — — Kolb's theory (1957); - - - - Griem's theory (1954).

coherent scattering). We call the re-emission completely non-coherent ("complete redistribution") if there is no correlation between the sublevel ϵ', first entered by the electron, and the sublevel ϵ'', from which the electron leaves the level j. For completely non-coherent scattering the re-emission is proportional to the scattering coefficient for every ν (see eq. [3.33]).

In the following sections we shall discuss the relative importance of coherent and non-coherent scattering for different broadening mechanisms.

5.2. Radiation Damping

The quantum theory of radiation shows that we can get completely coherent scattering only if the lower level of the line is infinitely narrow. In other words, coherent scattering may be expected only for resonance lines formed in a relatively weak radiation field (because the lifetime of the ground level should not be shortened too much by stimulated absorptions).

The general case, in which both levels are broadened, has been treated by Weisskopf and Wigner (1930), Weisskopf (1933*b*), Spitzer (1936), and Woolley (1938). The exact expression for $p(\omega, \omega')$—the probability that the absorption at an angular frequency ω will be followed by an emission at a frequency ω' in the same line—is derived essentially in the following way: The probability for an absorption from the substate $E_j + \hbar\Delta\omega$ of the level j to the substate $E_k + \hbar(\Delta\omega + \omega - \omega_0)$ of the level k is $P_j(\Delta\omega)P_k(\Delta\omega + \omega - \omega_0)d(\Delta\omega)$ (E_j and E_k are the energies of the level center, ω_0 is the angular frequency of the line center, P_j is the "damping profile" as used in eq. [4.13]). The probability that this absorption will occur and be followed by an emission within ω', $\omega' + d\omega'$ is

$$P_j(\Delta\omega)\, P_k(\Delta\omega + \omega - \omega_0)\, P_j(\Delta\omega + \omega - \omega')\, d(\Delta\omega)\,. \qquad (5.1)$$

In order to find the probability that an absorption in the range ω, $\omega + d\omega$ (but between arbitrary substates of j and k) is followed by an emission within ω', $\omega' + d\omega'$, we have to integrate over $\Delta\omega$. In other words, $p(\omega, \omega')$ is given by a "folding integral" over three "damping functions" of the form (4.7). The resulting expression is very complex (see Henyey 1946; Woolley and Stibbs 1953) The ratio of coherent and non-coherent scattering is not constant within a line Only in the far wings are the conditions relatively simple (Woolley 1938; Unsöld 1955). Consider a frequency ω for which $\omega - \omega_0 \gg \gamma$. Because of the form of the P_j's in expression (5.1) (damping functions with a strong maximum at the level center), the absorption at ω will be due mainly to transitions (1) starting from the center of the lower level and ending at $\hbar(\omega - \omega_0)$ below the center of the upper level or (2) starting at $\hbar(\omega - \omega_0)$ above the center of the lower level and ending at the center of the upper level (see Fig. 8). Because both downward transitions end close to the center of the lower level j, transition 1 will be followed by coherent and 2 by non-coherent re-emission. The number of transitions of type 1 will be proportional to the damping constant γ_k of

the upper level, the number of transitions 2 will be proportional to γ_j. So we have, for the ratio of coherent (σ_ν) and non-coherent scattering (i_ν),

$$\frac{\sigma_\nu}{i_\nu} = \frac{\gamma_k}{\gamma_j}, \qquad \text{for the far-line wings.} \tag{5.2}$$

For a rigorous proof cf. Woolley (1938). Equation (5.2) contains as a special case the scattering in the wings of the resonance lines discussed above.

5.3. Pressure Broadening

The problem is relatively simple in the case of statistical broadening. Take, e.g., $N = 10^{15}$ and $T = 10{,}000°$; the mean distance between particles is $r_0 \sim 10^{-5}$ cm, the mean relative velocity between protons and hydrogen atoms is of the order of 2×10^6 cm/sec, and the duration of a collision $t_0 = r_0/v$ is 5×10^{-12}

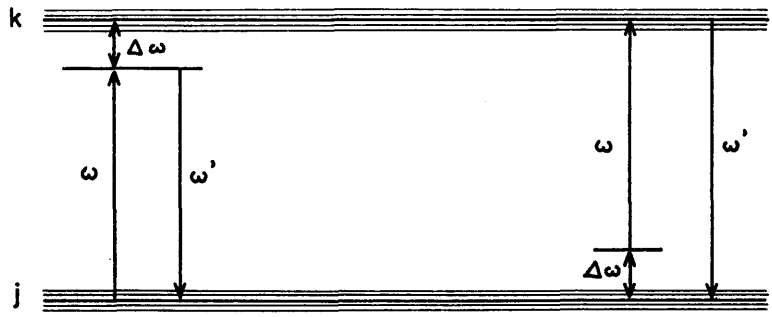


Fig. 8.—Coherent and non-coherent scattering for levels broadened by radiation damping

sec. On the other hand, the mean lifetime of an excited state is of the order of 10^{-8} sec for the strongest transitions. Consequently, there can be no correlation between the distribution of perturbing particles at the time of absorption and the time of re-emission. The re-emission is completely non-coherent.

The problem of re-emission in the case of phase-shift broadening has been discussed by Zanstra (1941), Spitzer (1944), and Edmonds (1955).

Restricting ourselves to a qualitative and classical description, we may argue as follows: The duration of the whole scattering process is of the order $t_0 \sim 1/\gamma_n$, where γ_n is the radiation damping constant. The oscillator will radiate at the unperturbed frequency only for the time between two collisions $t_1 \sim 1/\gamma_c$, where γ_c is the collision damping constant. Assuming that the phase of the light-wave after the first collision will be completely uncorrelated with the unperturbed phase, we get

$$\frac{\sigma_\nu}{i_\nu} = \frac{\gamma_n}{\gamma_c}. \tag{5.3}$$

In most cases of astrophysical interest we have $\gamma_c \gg \gamma_n$. Then the scattering is almost completely non-coherent. A more rigorous description, also based on

classical considerations, has been given by Zanstra (1941). A complete quantum-mechanical theory would be very difficult (see the interesting remarks made by Spitzer [1944] and Edmonds [1955]).

We may conclude that the scattering will be almost completely non-coherent if any kind of pressure broadening is the dominant mechanism.

5.4. Doppler Effect

In this case the relation between the frequencies of the absorbed and re-emitted light-quantum is given by equation (4.27). We restrict ourselves to the Doppler core of the line, as the damping case has already been treated in the preceding sections. The integral on the right-hand side of equation (4.27), including the factor $(a/\pi \sin \phi)$ then reduces to

$$\exp\left[-\left(\frac{v_2+v_1}{2\sin\phi}\right)^2\right], \tag{5.4}$$

as we can conclude directly from the analogy between this integrand and the function $H(a, v)$. (We should remember that v_1 is $[\omega - \omega_0]/\Delta\omega_D$ and v is $[\omega' - \omega_0]/\Delta\omega_D$ in our present notation.) Furthermore, v_2 and v_1 occur in the exponential before the integral of equation (4.27); since $p(\omega, \omega')$ for a fixed scattering angle 2ϕ is essentially

$$p(\omega, \omega') \propto \sigma(\omega, \omega', \phi) \propto \exp\left[-\left(\frac{v_2-v_1}{2\cos\phi}\right)^2 - \left(\frac{v_2+v_1}{2\sin\phi}\right)^2\right]. \tag{5.5}$$

Using the trigonometric relations $2\cos\theta = \sin 2\theta/\sin\theta$ and $2\sin\theta = \sin 2\theta/\cos\theta$, we get

$$p(\omega, \omega') \propto \exp\left[-\left(\frac{v_2+v_1\cos 2\phi}{\sin 2\phi}\right)^2 - v_1^2\right]. \tag{5.6}$$

For $2\phi = \pi$ (forward scattering), $\cos 2\phi = -1$, and $\sin 2\phi = 0$, the exponent goes to infinity, and $p(\omega, \omega')$ to zero, unless $v_2 = v_1$; i.e., the scattering is completely coherent. For backward scattering we find, correspondingly, $v_2 = -v_1$. For $2\phi = \pi/2$, we have $p(\omega, \omega') \propto \exp(-v_2^2)$ for a fixed v_1, i.e., the scattering is completely non-coherent. Now introduce a co-ordinate system with its zero point in the scattering particle and the z-axis directed toward the observer. If an equal number of photons are originally moving along the x-, y-, and z-axis, one-third of the scattering processes are coherent, two-thirds are non-coherent.

5.5. Coherent Scattering and Polarization

At the limb of a star, the light which is due to *coherent* scattering is partly polarized (cf. Zanstra 1941; Chandrasekhar 1950; Voigt 1951). For completely non-coherent scattering, as produced by pressure broadening, no polarization is to be expected. Therefore, the observation of polarization in Fraunhofer lines gives a possibility of checking the ratio σ_ν/i_ν. But we must keep in mind that the non-coherent scattering due to the *Doppler effect* gives polarization in essentially the same way as coherent scattering.

The polarization effect can be observed so far only in the solar spectrum. Its interpretation is difficult because the polarization depends strongly on local magnetic fields (Thiessen 1952; Jäger 1957). Nevertheless, it remains true that polarization occurs only if the scattering is coherent. The observations of Jäger (1954, 1957) indicate that coherent scattering plays an important role in the core of the Ca I resonance line λ 4227 in the solar spectrum.

§ 6. THEORETICAL AND EXPERIMENTAL DETERMINATION OF OSCILLATOR STRENGTH AND TRANSITION PROBABILITIES

6.1. Wave Functions and Atomic Structure

In quantum mechanics the stationary state of an electron is described by the Schrödinger equation,

$$\nabla^2\psi + 2\,(E - U)\,\psi = 0\,, \tag{6.1}$$

and the relevant boundary conditions, where ∇^2 is the Laplace operator, E is the energy of the state, U is the potential energy, and ψ is the wave function. In equation (6.1) we have used atomic units—unit of mass = m_0 (rest mass of the electron); unit of charge = e (charge of the electron); and unit of length = a_0 (first Bohr radius). If U is a central field, $U = U(r)$ (as, for example, in the problem of the hydrogen atom), equation (6.1) is separable in polar co-ordinates. It can be separated into the equation for the surface spherical harmonics $Y(\theta, \phi, l, m)$ (cf. Sommerfeld 1948) (where θ and ϕ are the polar angles, l and m are the number of nodes in each co-ordinate), and an equation depending on r only:

$$\frac{d^2R\,(r)}{d\,r^2} + \left[2\,U\,(r) - \frac{l\,(l+1)}{r^2} - 2E\right]R\,(r) = 0\,. \tag{6.2}$$

The term $l(l+1)/r^2$ in equation (6.2) is obviously analogous to the centrifugal potential energy $M^2/2mr^2$ (M = angular momentum) in classical mechanics. We can conclude that $l\hbar$ is the angular momentum of the electron; $m\hbar$ can be shown to be the component of the angular momentum in the direction of a fixed axis (cf. Schiff 1949). The number of nodes of $R(r)$, which depends, according to equation (6.2), on the energy eigenvalue E, is called n. The complete eigenfunction of equation (6.1) is

$$\psi = Y\,(\theta, \varphi, l, m)\,R\,(r, n, l)\,. \tag{6.3}$$

Finally, the spin should be included. If the interaction between the spin and the orbital motion is small, this can be accomplished formally by multiplying equation (6.3) by the spin function, which has two stationary values only. So we may write the complete wave function $\phi = \psi X(s)$ thus:

$$\phi\,(r, \theta, \varphi, n, l, m, s) = Y\,(\theta, \varphi, l, m)\,R\,(r, n, l)\,X\,(s)\,, \tag{6.4}$$

where n, l, m, and s are called the principal, azimuthal, magnetic, and spin quantum numbers. All four specify the "state" of the electron. For a given n and l, there are $2(2+1)$ different wave functions or atomic states, namely, $2+1$ different Y's (according to the known properties of spherical surface harmonics) and two different X's (i.e., different orientations of the spin). Wave functions with $l = 0, 1, 2, 3, 4, \ldots$, are specified by the letters s, p, d, f, g, . . . ; n is given as a number in front of this letter. So (2p) means an atomic state with $n = 2$ and $l = 1$. It is useful to introduce the quantum number j for the total angular momentum. The latter is found by a vector addition of l and s. The spin-orbit interaction energy is usually small compared with the electrostatic energy in equation (6.1). Therefore, the energies of the states with equal n and l, but different j's differ only slightly.

Equation (6.1) can be generalized for an i-particle system (atom with i electrons) to the $3i$-dimensional Schrödinger equation,

$$\sum_i \nabla^2\psi + 2\,(E - U)\,\psi = 0\,, \tag{6.5}$$

where U now includes the potential energy of every electron in the field of the nucleus, as well as the interaction energy between the electrons. The spectroscopic classification of atomic states and most methods for the approximate calculation of wave functions are based on the following approximation of equation (6.5). We assume that every electron moves in a static field due to the nucleus and the other electrons but independent of the *position* of the other electrons, i.e.,

$$U = \Sigma\, U\,(r_i)\,, \tag{6.6}$$

where r is the radius vector. Inserting equation (6.6) into (6.5), we can separate (6.5) into i equations of the form (6.1). The solution of equation (6.5) simplifies to a product of i one-particle wave functions. Including the spin functions, this may be written

$$\Phi = \phi_\alpha\,(r_1)\;\phi_\beta\,(r_2)\;\ldots\;\phi_\pi\,(r_i)\,, \tag{6.7}$$

where $\alpha, \beta, \ldots$, are an abbreviation for all four quantum numbers introduced above. If we interchange 2 electrons in equation (6.7), Φ remains unchanged. Now, according to Pauli's principle, there can be no two electrons for which all four quantum numbers are the same. This requirement is fulfilled if we introduce the following wave function instead of equation (6.7):

$$\Phi = \begin{vmatrix} \phi_\alpha\,(r_1) & \phi_\alpha\,(r_2) & \ldots & \\ \phi_\beta\,(r_1) & \phi_\beta\,(r_2) & \ldots & \\ \cdot & & \cdot & \\ \cdot & & & \cdot \\ \cdot & & & \phi_\pi\,(r_i) \end{vmatrix}. \tag{6.8}$$

By using this Φ, we satisfy the Pauli principle, because the determinant is zero if two wave functions are identical. We have assumed that the ϕ_a's are of the "central-field type," i.e., that all wave functions have the form (6.4). So every electron can be specified by four quantum numbers, as in the one-particle problem. A group of q-wave functions with the same n and l is written $(nl)^q$. Take the ground state of carbon as an example. Using the above designation, the distribution of the electrons over the different quantum numbers may be written $(1s)^2\ (2s)^2\ (2p^2)$. Such a symbol is said to specify the *configuration* of the atomic system.

Because of the interaction energy between the different electrons, the energy of the atom is not the same for all states that correspond to the same configuration. If we neglect the spin for a moment, we find that the interaction energy depends on the relative orientation of the different wave functions. In terms of the "vector model" we say that, in order to find the number of terms with different energies, we have to count how many possibilities exist to add (vectorially) the orbit angular momenta $l\hbar$ of the individual electrons. The quantum number of the resulting total angular momentum is called L.

If the spin-orbit interaction is small compared with the interaction energy of the different electrons, we can proceed as follows: Find the total orbital angular momentum $L\hbar$ by vector addition of the individual $l\hbar$ and compute separately the total spin angular momentum $S\hbar$ by vector addition of the individual $s\hbar$. The total angular momentum $J\hbar$ is found, finally, by a vector addition of $L\hbar$ and $S\hbar$. This case (spin-orbit interaction small compared with orbit-orbit interaction) is called LS coupling or Russell-Saunders coupling. It occurs in light atoms and for low-excitation states.

Because of the smallness of the spin-orbit interaction, the different possibilities of the vector addition of L and S possess only slightly different energies. The *atomic term* (L and S are fixed) splits up into *levels* (L, S, and J fixed). An *atomic state* is defined by L, S, J, and M, where M is the projection of J in a given direction. The atomic states of a given level have different energies only if the spherical symmetry is disturbed by an external field. The number of possibilities of the vector addition of L and S, namely, $(2S + 1)$ is called the *multiplicity* of the term. It is often useful to introduce a "polyad" as a set of terms of the same multiplicity, derived from the same parent term by the addition of one electron (cf. Condon and Shortley 1935).

In the classification of terms and levels, the following symbols are used. Terms with $L = 0, 1, 2, 3, 4, \ldots$, are called S, P, D, F, G, . . . , terms, in analogy with the one-particle designation. The multiplicity is indicated by an index in the following way: ^{1}S is a singlet S, ^{3}P a triplet P term, etc. Individual levels are indicated by adding the value of J as a lower index: $^3P_1$ is the level with $J = 1$ of the triplet P term.

For LS coupling the so-called Landé interval rule holds, i.e., the energy difference between two levels of the same term is proportional to the greater of the

two J-values occurring. Consider, for example, the three levels of a ^3P term: $^3P_0$, $^3P_1$, $^3P_2$. According to Landé's rule, the ratio of the two energy intervals is 1:2. The Landé interval rule gives a simple possibility of testing whether the assumption of LS coupling is valid.

Another limiting case of coupling occurs in heavy atoms, especially for highly excited states: $j-j$ coupling. In this case the interaction energy between the different electrons is small compared to the spin-orbit interaction energy of each electron. The total angular momentum is found in the following way: The spin of every electron is quantized with respect to its own angular momentum, i.e., we must add vectorially s_i and l_i of the ith electron to get its j_i. If we add the j_i's of the different electrons in all possible ways, we get all levels.

6.2. Transitions

It is convenient to introduce the following definitions: (1) A transition between two states is called a *line* (Zeeman) *component.* (2) A transition between two levels gives a *line.* (3) The set of possible transitions between two terms is a *multiplet.* (4) The totality of transitions between two polyads is a *supermultiplet,* and (5) between two configurations it is a *transition array.*

The intensity of a line (due to a dipole transition) is in analogy with the classical expression,

$$I_{\alpha\beta} = \frac{\omega^4}{3c^3} P_{\alpha\beta}^2 , \tag{6.9}$$

where $P_{\alpha\beta}$ is the quantum-mechanical dipole moment of the transition $\alpha \rightarrow \beta$ (a Greek letter specifies—as above—all four quantum numbers):

$$P_{\alpha\beta} = 2\int \tilde{\phi}\, P \phi_\beta d\, V = 2\, e \int \phi_\alpha \mathbf{r} \phi_\beta d\, V = 2\, e S^{1/2} , \tag{6.10}$$

where $P = e\mathbf{r}$ is the "operator" of the dipole moment and dV is the volume element. Equation (6.10) also defines the line strength, S. From equations (4.7) and (6.10) we get, for the oscillator strength,

$$f_{\alpha\beta} = \frac{8\pi^2 m\nu}{3he^2} P_{\alpha\beta}^2 . \tag{6.11}$$

For the corresponding spontaneous transition probability, we have

$$A_{\alpha\beta} = \frac{64\pi^4\nu^3}{3hc^3} P_{\alpha\beta}^2 . \tag{6.12}$$

If the wave functions ϕ_α are of the central-field type (see above), the integral (6.10) can be split up into a factor depending only on the radial-wave functions $R_\alpha(r)/r$,

$$\int_0^\infty R_\alpha R_\beta r\, d\, r , \tag{6.13}$$

and an integral over two surface spherical harmonics used in equation (6.4). From the properties of these functions it follows that equation (6.10) is zero,

unless $\Delta l = \pm 1$ and $\Delta M = 0$ or ± 1 for the transition $\alpha \rightarrow \beta$. These are the "selection rules" for l and m. For two-electron jumps we have $\Delta l_1 = \pm 1$ and $\Delta l_2 = 0$ or ± 2 for the l-selection rule.

For LS coupling the following additional selection rules can be derived (cf. Condon and Shortley 1935):

$$L = \pm 1 , \tag{6.14a}$$

$$S = 0 , \tag{6.14b}$$

$$J = 0, \pm 1 \qquad \text{(but } 0 \rightarrow 0 \text{ excluded)} . \tag{6.14c}$$

All wave functions are either even or odd with respect to changes of sign of all space co-ordinates, and we may say that they have even or odd parity. It follows from equation (6.10) that the electric dipole moment $P_{\alpha\beta}$ is zero, if ψ_α and ψ_β have the same parity. This is the Laporte selection rule. Transitions between levels of the same parity are forbidden for electric dipole radiation.[15] The symbol o is attached to the designation of an odd term, if the parity is stated explicitly, e.g., $^3P^o$. The parity can be derived from the *arithmetic* sum of the l's. If the sum is even, the parity is even; if the sum is odd, the parity is odd.

6.3. The Theoretical Determination of Oscillator Strengths

The approximation (6.6) naturally leads to the following expression for the line strength S defined in equation (6.10):

$$S = \mathfrak{S}(\mathfrak{M})\, \mathfrak{S}(\mathfrak{L})\, \sigma^2 , \tag{6.15}$$

where σ^2 depends only on the transition array and $\mathfrak{S}(\mathfrak{M})$ and $\mathfrak{S}(\mathfrak{L})$ are the relative intensities of the multiplet in the transition array and of the line in the multiplet. $\mathfrak{S}(\mathfrak{M})$ and $\mathfrak{S}(\mathfrak{L})$ are independent of the radial wave functions R_α introduced above, and they can therefore be calculated without the knowledge of the R_α's (e.g., from a Fourier analysis of the precessing electron orbits using the correspondence principle).

For the calculation of $\mathfrak{S}(\mathfrak{L})$, the Burger-Dorgelo sum rule is often useful: The sum of the strengths of all lines of a multiplet ending on, or starting from, a common level is proportional to the statistical weight of this level.

From this rule alone one can calculate the relative intensities of the lines in doublets or in other multiplets, if they are combinations with S terms.

Tables of $\mathfrak{S}(\mathfrak{L})$ (based on formulae derived by Sommerfeld, Hönl, Russell, Kronig, and Dirac) have been given by White and Eliason (1933) and by Russell (1936) (see also Allen 1955).

Numerical calculations of $\mathfrak{S}(\mathfrak{M})$ have been carried out by Goldberg (1935,

[15] Note that for electric quadrupole and magnetic dipole radiation—e.g., for the forbidden lines occurring in nebulae and stellar envelopes—the opposite is true. Transitions between terms of the same parity are permitted, and those between terms of different parity are forbidden.

1936). His calculations also include the complicated case in which configurations with equivalent electrons (i.e., electrons with the same n and l) occur.

These computations refer to LS coupling only. Pure j-j coupling can be handled in a relatively simple manner too (see Condon and Shortley 1935), but it occurs rather seldom. The complex case of intermediate coupling has been considered by Condon and Shortley. Following this treatment, Gottschalk (1948) has computed the relative intensities for the $3d^74s$–$3d^74p$ transitions of Fe I.

The essential and most difficult problem is the determination of σ^2, which depends only on the radial wave functions R_α. Before discussing this question, we wish to mention the useful Kuhn-Thomas Reiche f-sum rule, which states, for an arbitrary system with z electrons,

$$\sum_\beta f_{\alpha\beta} = z\,. \tag{6.16}$$

The sum has to be taken over the transitions to all states β. This rule follows from the first principles of quantum mechanics and is valid for every quantum-mechanical system (cf. Bethe 1933). In applications, one often uses this rule in a more specialized form. Only the electron making a radiative transition and those having the same n and l as the jumping electron ("equivalent electrons") are considered (cf. Unsöld 1955). In this case also the transitions to the lower occupied levels which are forbidden by the Pauli principle have to be counted.

We now consider the calculation of σ^2, which gives the absolute values of the oscillator strengths; σ^2 is proportional to the integral (6.13):

$$\sigma^2 = (4l^2 - 1)^{-1} \left(\int R_\alpha R_\beta r\, dr\right)^2, \tag{6.17}$$

where l is the greater of the two azimuthal quantum numbers involved in the transition (cf. Bethe 1933). The numerical methods for the evaluation of R_α are essentially based on the separable-wave-function approximation described above. The prototype of these methods is Hartree's self-consistent field approximation (for a review of this approach cf. Hartree 1956). Each electron is assumed to obey a "one-particle" Schrödinger equation (6.1), as in the separable-wave-function approximation. Furthermore, the central-field approximation (6.4) is assumed to be valid. Consequently, one gets an equation of the form (6.2) for every electron. One supposes that the potential energy occurring in this equation is due partly to the field of the nucleus and partly to all other electrons, i.e.,

$$U_i(r) = -\frac{Ze^2}{r} + e^2 \sum_{j \neq i}^{Z} \frac{\psi_j(r')}{(r - r')}\, dV'. \tag{6.18}$$

Every ψ_i in this equation is a product of a surface spherical harmonic (as introduced above) and a radial wave function R_i, which itself must be a solution of an equation of the form (6.2). Introducing equation (6.18) into equation (6.2)

and writing down an equation of this form for every electron obviously lead to a system of Z simultaneous integrodifferential equations, which can be solved by an iterative procedure. In this method the wave function of the whole atom is (obviously) assumed to be of the form (6.7), which is not compatible with Pauli's principle. It can be shown (cf. Hartree 1956) that Hartree's method is equivalent to making the integral

$$\int \Phi H \Phi d\, V \tag{6.19}$$

an extremum, where

$$H = -\frac{1}{2}\sum_i \nabla_i^2 - U$$

is the so-called Hamilton operator occurring in the many-particle Schrödinger equation (6.5) and Φ is assumed to be of the form (6.7) and dV is the $3n$-dimensional volume element. Making (6.19) an extremum would be identical only with solving the Schrödinger equation (6.1), if no restrictions were imposed on the form of Φ. A better approximation than Hartree's original one is Fock's method (1930), in which Φ in (6.19) is assumed to have the form of the determinant (6.8). Fock showed that, with this assumption, the variation principle is also equivalent to a system of integrodifferential equations. But this system is considerably more complicated than Hartree's equations. The physical meaning of Fock's procedure is that the quantum-mechanical exchange energy is taken into account.

Hartree's or Fock's method has been applied to find wave functions and oscillator strengths for a number of the lighter atoms and ions. We can refer only to the extended reference lists and tables of oscillator strength published by Allen (1955), Biermann (1950), Hartree (1948, 1956), and Unsöld (1955).

Several authors have tried to improve the Hartree-Fock method, in order to achieve a higher accuracy in the f-value calculations. The Hartree-Fock method is based on the assumption that an atomic state can be represented by a single configuration. Of course, this is only an approximation, as the interelectronic distances, which are inherent in the problem, do not appear at all in this treatment. The situation can be improved by either introducing the interelectronic distance explicitly into the problem (cf. Trefftz, Schlüter, Dettmar, and Jörgens 1957) or by superposing a number of wave functions belonging to different configurations ("configuration mixing"; cf. Hartree, Hartree, and Swirles 1939; Trefftz 1949).

Another effect which is included in some modern calculations is the polarization of the core electrons (the electrons in the closed shells) by the "valency" electron (see Bates 1947; Biermann and Trefftz 1949, 1952). For a thorough discussion of the calculation of atomic wave functions we refer to Hartree's monograph.

Calculations based on the Hartree-Fock method or the extensions just discussed are laborious, even for comparatively simple atoms, and therefore the

demand of the astrophysicist that a great number of oscillator strengths for many different atoms should be computed has not yet been met. But if only modest accuracy is necessary (as often is the case in astrophysics), the f-values of not too complex atoms can be calculated in a simple manner following the method of Bates and Damgaard (1949). These authors recognized that usually the main contribution to the integral (6.17) comes from regions in which the potential energy U has already reached its asymptotic form (for large r). This means that U can be described as a Coulomb potential (C/r). For this potential the general solution of (6.2) is known (a confluent hypergeometric function). As these solutions are valid only for large r, the boundary condition for $r = 0$ is not fulfilled in general. In other words, the energy parameter E cannot be determined as usual from the boundary value problem but has to be taken from empirical data. The effective quantum number $n^* = (C/E^{1/2})$, which immediately follows from the observed term value, has to be used. Bates and Damgaard have calculated extensive tables of σ^2 as a function of n^* and l, which are extremely useful.

The Bates-Damgaard method is rather accurate either if there is only one electron in an outer shell (alkali atoms) or if both levels involved in the transition are moderately or highly excited. But even if these conditions are not fulfilled, the method often gives fair results. In fact, the oscillator strengths calculated by the Bates-Damgaard method are of the same accuracy as those based on Hartree functions in several cases. Traving (private communication) found for Ti I that in all cases in which an application of the method is at all possible (i.e., transitions of one electron only, no intercombination) the results were correct within a factor of 3. Allen and Asaad (1955, 1957) come to different conclusions for reasons which are not yet completely understood.

6.4. The Experimental Determination of Oscillator Strengths

According to § 4.1, k (the absorption coefficient per cm) and n (the real refractive index) are both proportional to the number of absorbing atoms N per cm^3 times the oscillator strength f. So we may use the measurement of either k or n in the wave-length range of a spectral line to determine the oscillator strengths, provided that we know N, the number of absorbing or emitting atoms.

For the determination of n, one usually uses a Jamin interferometer. The interference fringes are projected onto a slit of a spectrograph in such a way that the directions of dispersion of the interferometer and the spectrograph are perpendicular to each other. Near a spectral line, one gets the typical "hook-form" of the interference fringes, from which the wave-length dependence of n can be derived. This method, which had been developed by Roschdestwensky, Ladenburg, and others, has been recently applied by Penkin and his collaborators to measure a great number of relative oscillator strengths of low-excitation lines of titanium, manganese, chromium, and scandium (Ostrofskij, Partschefskij, and Penkin 1956; Ostrofskij and Penkin 1957*a*, *b*).

Another method for the determination of oscillator strengths is to derive the "total absorption," $\int k_\lambda d\lambda$, of a line by measuring either the absorption or the emission of an *optically thin layer*. According to equation (4.18), the total absorption is $\pi e^2 \lambda_0^2 Nf/mc^2$. Consequently, f can be derived if N is known, and N can be determined in a reliable way if an absorption tube or a light-source (for the measurement of the emission) meeting the following requirements can be constructed. The geometrical temperature and density distribution should be simple (if possible, the same temperature and density should prevail everywhere in the source). The physical conditions should remain constant for a sufficiently long time. Temperature and density should be measurable with sufficient accuracy.

It is, of course, considerably simpler to meet these requirements when measuring low-excitation lines (for which one needs only comparatively low temperatures) than in an investigation of high-excitation lines or lines of ionized elements.

Most of the f-value determinations for low-excitation lines have been made by using an electrical furnace—the so-called King furnace—for heating an absorption tube or an emission source. Relative f-values can be determined by this method with fair accuraty because only the knowledge of the temperature is necessary, which can be measured with a pyrometer or sometimes even with a thermocouple. We mention only the classical absorption measurements of Fe I and Ti I lines made by R. B. and A. S. King (1935, 1938) and the emission measurements of Fe I lines performed by Carter (1940).

The absolute calibration of these f-values is more uncertain. A sample of the material (e.g., iron) is brought into the furnace in an evacuated quartz tube. In order to determine the number of absorbing atoms, we must know rather accurately the vapor pressure of the material as a function of temperature. R. B. King and Stockbarger (1940) and R. B. King (1942) have measured absolute oscillator strengths for Fe I, Cu I, and Cd I by this method.

The knowledge of vapor pressure as a function of temperature is unnecessary in the ingenious atomic-beam method developed by Kopfermann and Wessel (1951). They use an atomic beam as absorbing medium, which immediately condenses on a thin plate connected with a sensitive balance. So N follows directly from the increase in mass per second on the plate. Kopfermann and Wessel found absolute values of the oscillator strengths for the Fe I resonance lines λ 3720 and λ 3737, which were greater by a factor of 3.3 than those derived earlier by R. B. King. The f-value for λ 3720 derived by Kopfermann and Wessel has been confirmed by Ziock (1957) by a completely different method. He directly measured the lifetime of the upper level of λ 3720. The recent work of R. B. King (1957) and Bell, Davis, King, and Routly (1958) yielded f-values smaller by about 30 per cent than those derived by Kopfermann and Wessel.

Many lines of astrophysical importance are high-excitation lines. In order

to measure the oscillator strengths of these transitions, high-temperature light-sources are needed (high-excitation lines can, of course, be observed conveniently only in emission). Higher temperatures than in the King furnace are achieved in free-burning arcs. But these have the disadvantage that they are not stationary because of hydrodynamical convection currents; moreover, the temperatures reached are not so high as are often needed. These difficulties have been overcome by the construction of *water-stabilized* arcs (Maecker 1951, 1953) and of *copper-stabilized* arcs (Maecker 1956; Richter 1958). The water-stabilized or whirling-water arc is based on the following principle. The arc burns in a

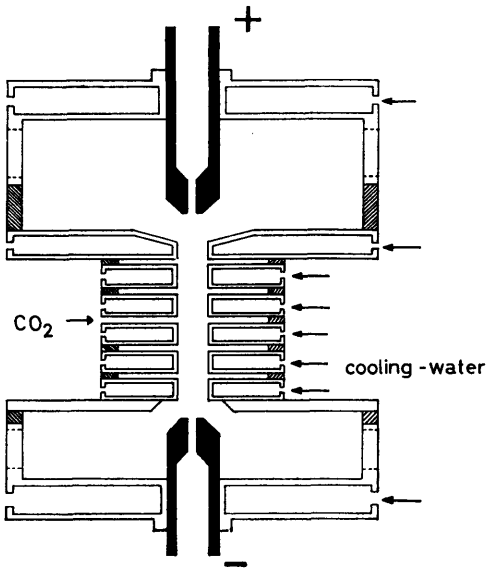


FIG. 9.—Apparatus for a copper-stabilized arc, as used by Richter (1958) for the measurement of C I oscillator strengths. CO_2 is blown continuously into the arc. The known oscillator strengths of O I are used for the derivation of f-values of C I. See the text for further details.

cylindrical tube. A high-velocity stream of water continuously flows tangentially into the tube, where it whirls along the walls of the cylinder (and around the burning arc) because of the centrifugal forces. The water supply and the outflow are adjusted in such a way that the greatest part of the tube is filled with water and only a narrow cylindrical channel in the center of the tube is left for the burning arc. This channel is relatively stable. The arc is strongly constricted by the whirling water, and consequently the temperature is raised. ($T \sim 50{,}000°$ has been reached!) Usually the arc contains mainly oxygen and hydrogen from the vaporized water of the whirl, but it is also possible to blow gases into the arc. Therefore, it can be used for the measurement of f-values of high-excitation lines. It has been found recently that the water-stabilized arc still shows small fluctuations of its location with time, which possibly might influence the ac-

curacy of the *f*-value measurements to a certain extent. This cannot occur in the copper-stabilized arc, in which the stabilization is due to solid copper walls. A cross-section of the apparatus is shown in Figure 9 according to Richter (unpublished). The channel for the burning arc is provided by the circular holes (perpendicular to plane of the drawing) in a number of copper plates, which are separated by rings of insulating material. The copper plates are cooled by a stream of water. Because of the high heat conductivity of copper, the heat from the edge of the arc is carried off rapidly. The separation of the copper plates by insulating material is necessary in order to avoid electric conduction along the walls.

These arcs have been used extensively by Lochte-Holtgreven and his collaborators for measuring a great number of *f*-values for different elements. The following method of determining the number of absorbing atoms is used. In the whirling-water arc the ratio of the number of hydrogen and oxygen atoms is known, namely, 2:1. Consequently, we can derive the number of oxygen atoms by using the known *f*-values of hydrogen. Moreover, T and N_e can be determined from the hydrogen lines. Thus the oscillator strengths of oxygen can be derived (Jürgens 1954). The procedure can be continued by blowing gases with a known ratio of oxygen and some other element into the arc. Motschmann (1955) determined *f*-values of N I by blowing air into the arc. Richter (1958) used CO_2, blown into a copper-stabilized arc, for measuring *f*-values of C I lines in the ranges 4700 A $< \lambda <$ 5800 A and 8000 A $< \lambda <$ 17,000 A. Oscillator strengths for N II and O II have been determined by Mastrup and Wiese (1958), using a slightly different method. Measurements of C II, Si I, and Si II have been finished or are now in progress.

The author is indebted to Professor A. Unsöld for reading the manuscript and offering stimulating criticism and many helpful suggestions. Furthermore, I am obliged to Dr. J. Richter, of the Institute of Experimental Physics of Kiel University, for a clarifying discussion about the experimental determination of oscillator strengths.

REFERENCES

ALLEN, C. W. 1955 *Astrophysical Quantities* (London: Athlone Press).

ALLEN, C. W., and ASAAD, A. S. 1955 *M.N.*, **115**, 571.

1957 *Ibid.*, **117**, 36.

ALLER, L. H. 1953 *Astrophysics*, Vol. **1**, *The Atmospheres of the Sun and Stars* (New York: Ronald Press Co.).

1956 *Gaseous Nebulae* (London: Chapman & Hall, Ltd.).

AMBARZUMIAN, V. A. 1931 *M.N.*, **93**, 50.

1943 *C.R. Acad. Sci. USSR*, **38**, 229.

ANDERSON, P. W. 1949 *Phys. Rev.*, **76**, 647.

ATHAY, R. G., and THOMAS, R. N.	1956	*Ap. J.*, **124**, 586.
BARBIER, D.	1944	*Ann. d'ap.*, **7**, 115.
BATES, D. R.	1947	*Proc. R. Soc. London, A*, **188**, 350.
BATES, D. R., BUCKINGHAM, R. A., MASSEY, H. S. W., and UNWIN, J. J.	1939	*Proc. R. Soc. London, A*, **170**, 322.
BATES, D. R., and DAMGAARD, A.	1949	*Phil. Trans. (London)*, **242**, 101.
BELL, G. D., DAVIS, M. H., KING, R. B., and ROUTLY, P. M.	1958	*Ap. J.*, **127**, 775.
BETHE, H.	1933	*Hdb. d. Phys.*, **24, 1**, 434 (Berlin: Springer-Verlag).
BHATNAGAR, P. L., KROOK, M., MENZEL, D. H., and THOMAS, R. N.	1955	In *Vistas in Astronomy*, ed. A. BEER, **1**, 296.
BIERMANN, L.	1950	In LANDOLT-BÖRNSTEIN, *Zahlenwerte und Funktionen aus Physik, Chemie, Astronomie, Geophysik und Technik* (Berlin, Göttingen, Heidelberg: Springer-Verlag), **1**, 260.
BIERMANN, L., and TREFFTZ, E.	1949	*Zs. f. Ap.*, **26**, 213.
BLOOM, S., and MARGENAU, H.	1953	*Phys. Rev.*, **90**, 791.
BÖHM, K. H.	1954*a*	*Zs. f. Ap.*, **34**, 182.
	1954*b*	*Ibid.*, **35**, 179.
BÖHM-VITENSE, E.	1953	*Zs. f. Ap.*, **32**, 135.
	1955	*Ibid.*, **36**, 145.
BOGEN, P.	1957	*Zs. f. Phys.*, **149**, 62.
BRANSDEN, B. H., and MCKEE, J. S.	1956	*Proc. Phys. Soc. London, A*, **69**, 422.
BROUT, R.	1957	*Phys. Rev.*, **107**, 664.
BRUGGENCATE, P. TEN, LÜST-KULKA, R., and VOIGT, H. H.	1955	*Veröff. U.-Sternw. Göttingen*, No. 110.
BURKHARDT, G.	1940	*Zs. f. Phys.*, **115**, 592.
BUSBRIDGE, I. W.	1953	*M.N.*, **113**, 52.
	1955	*Ibid.*, **115**, 661.
CARTER, W. W.	1940	*Phys. Rev.*, **76**, 962.
CAYREL, R.	1957	"Observations et étude théorique du spectre de ζ Per," thesis, Paris.
CHANDRASEKHAR, S.	1935	*Zs. f. Ap.*, **9**, 266.
	1936	*M.N.*, **96**, 771.
	1943	*Rev. Mod. Phys.*, **15**, 1.
	1950	*Radiative Transfer* (Oxford: Clarendon Press).

CONDON, E. U., and SHORTLEY, G. H.	1935	*The Theory of Atomic Spectra* (Cambridge: Cambridge University Press).
DIRAC, P. A. M.	1925	*M.N.*, **85**, 825.
ECKER, G.	1957*a*	*Zs. f. Phys.*, **148**, 593.
	1957*b*	*Ibid.*, **149**, 254.
EDMONDS, F. N.	1955	*Ap. J.*, **121**, 418.
	1956	*Ibid.*, **123**, 95.
ELSTE, G.	1953	*Zs. f. Ap.*, **33**, 39.
FOCK, V.	1930	*Zs. f. Phys.*, **61**, 126.
FOLEY, H. M.	1946	*Phys. Rev.*, **69**, 616.
GIOVANELLI, R. G.	1948	*Australian J. Sci. Res.*, **1**, 275, 289, 305, 360.
	1949	*M.N.*, **109**, 298.
GOLDBERG, L.	1935	*Ap. J.*, **82**, 1.
	1936	*Ibid.*, **84**, 11.
GOTTSCHALK, W. M.	1948	*Ap. J.*, **108**, 326.
GRASBERGER, W.	1957	*Ap. J.*, **125**, 750.
GRIEM, H.	1954	*Zs. f. Phys.*, **137**, 280.
GRIEM, H. R., KOLB, A. C., and SHEN, K. Y.	1959	*Phys. Rev.*, **116**, 4.
HARRIS, D. L., III	1948	*Ap. J.*, **108**, 112.
HARTREE, D. R.	1948	*Repts. Prog. Phys.*, **11**, 113.
	1956	*The Calculation of Atomic Structures* (New York: John Wiley & Sons).
HARTREE, D. R., HARTREE, W., and SWIRLES, B.	1939	*Phil. Trans.* (London), **238**, 229.
HEISER, A. M.	1957	*Ap. J.*, **125**, 470.
HEITLER, W.	1954	*The Quantum Theory of Radiation* (3d ed.; Oxford: Clarendon Press).
HENYEY, L. G.	1938	*Ap. J.*, **88**, 133.
	1940	*Proc. Nat. Acad. Sci.* (Washington), **26**, 50.
	1946	*Ap. J.*, **103**, 332.
HENYEY, L. G., and GRASBERGER, W.	1955	*Ap. J.*, **122**, 498.
HOLSTEIN, T.	1950	*Phys. Rev.*, **79**, 744.
HOLTSMARK, J.	1919	*Ann. Phys.*, **58**, 577; *Phys. Zs.*, **20**, 162.
	1924	*Phys. Zs.*, **25**, 73.
HOUTGAST, J.	1942	Dissertation, Utrecht.
HULST, H. C. VAN DE	1953	"The Chromosphere and the Corona," in *The Sun*, ed. G. P. KUIPER (Chicago: University of Chicago Press).
HULST, H. C. VAN DE, and REESINCK, J. J. M.	1947	*Ap. J.*, **106**, 121.
JÄGER, F. W.	1954	*Zs. f. Ap.*, **34**, 237.
	1957	*Ibid.*, **43**, 98.

JAGER, C. DE	1952	*Rech. Astr. Obs. Utrecht*, Vol. **13**, Part I.
	1954	*Nature*, **173**, 680.
JEFFERIES, J. T., and THOMAS, R. N.	1958	*Ap. J.*, **127**, 667.
JÜRGENS, G.	1954	*Zs. f. Phys.*, **138**, 613.
KING, R. B.	1942	*Ap. J.*, **95**, 78.
	1957	*A.J.*, **62**, 20.
KING, R. B., and KING, A. S.	1935	*Ap. J.*, **82**, 377.
	1938	*Ibid.*, **87**, 24.
KING, R. B., and STOCKBARGER, D. C.	1940	*Ap. J.*, **91**, 488.
KIVEL, B., BLOOM, S., and MARGENAU, H.	1955	*Phys. Rev.*, **98**, 495.
KOLB, A.	1957	Thesis, University of Michigan.
KOPFERMANN, H., and WESSEL, G.	1951	*Zs. f. Phys.*, **130**, 100.
KUSCH, H. J.	1958	*Zs. f. Ap.*, **45**, 1.
LABS, D.	1951*a*	*Zs. f. Ap.*, **28**, 150.
	1951*b*	*Ibid.*, **29**, 199.
	1954	*Ibid.*, **34**, 173.
LANDWEHR, G.	1956	Thesis, Yale University.
LINDHOLM, E.	1941	*Ark. f. mat., astr. o. fys.*, Vol. **28B**, No. 3.
	1942	"Über die Verbreiterung und Verschiebung von Spektrallinien," dissertation, University of Uppsala.
MCMATH, R. R., MOHLER, O. C., PIERCE, A. K., and GOLDBERG, L.	1956	*Ap. J.*, **124**, 1.
MAECKER, H.	1951	*Zs. f. Phys.*, **129**, 108.
	1953	*Ibid.*, **136**, 119.
	1956	*Zs. f. Naturforsch.*, **11a**, 457.
MARGENAU, H.	1951	*Phys. Rev.*, **82**, 156.
MARGENAU, H., and KIVEL, B.	1955	*Phys. Rev.*, **98**, 1822.
MARGENAU, H., and LANDWEHR, G. W.	1956	"The Structure of Spectral Lines from Plasmas" (Yale University, mimeograph).
MARGENAU, H., and MEYEROTT, R.	1955	*Ap. J.*, **121**, 194.
MASSEY, H. S. W.	1956*a*	"Theory of Atomic Collisions," in *Hdb. d. Phys.*, Vol. **36**, ed. S. FLÜGGE (Berlin, Göttingen, Heidelberg: Springer-Verlag).
	1956*b*	"Excitation and Ionization of Atoms by Electron Impact," *ibid.*
MASSEY, H. S. W., and BURHOP, E. H. S.	1952	*Electronic and Ionic Impact Phenomena* (Oxford: Clarendon Press).

MASSEY, H. S. W., and MOISEIWITSCH, B. L.	1951	*Proc. R. Soc. London, A*, **205**, 483.
MASTRUP, F., and WIESE, W.	1958	*Zs. f. Ap.*, **44**, 259.
MATSUSHIMA, S.	1952	*Ap. J.*, **115**, 544.
MENZEL, D. H.	1937	*Ap. J.*, **85**, 330.
MENZEL, D. H., *et al.*	1937–1945	"Physical Processes in Gaseous Nebulae," papers in *Ap. J.*, Vols. **85–102**.
MEYEROTT, R. E., and MARGENAU, H.	1955	*Phys. Rev.*, **99**, 1851.
MILNE, E. A.	1930	"Thermodynamics of the Stars," in *Hdb. d. Ap.*, Vol. **3** (Berlin: Springer-Verlag).
MOTSCHMANN, H.	1955	*Zs. f. Phys.*, **143**, 77.
MÜNCH, G.	1948	*Ap. J.*, **108**, 116.
	1949	*Ibid.*, **109**, 275.
OSTROFSKIJ, J. U., PARTSCHEFSKIJ, G. F., and PENKIN, N. P.	1956	*Optik. i Spektrosk.* (Moscow), **1**, 821.
OSTROFSKIJ, J. U., and PENKIN, N. P.	1957*a*	*Optik. i Spektrosk.* (Moscow), **3**, 193.
	1957*b*	*Ibid.*, p. 391.
PAGEL, B. E. J.	1955	*M.N.*, **115**, 493, esp. p. 518.
	1959	In *The Empirical Determination of Stellar Photospheric Structure*, ed. C. DE JAGER and L. NEVÉN (Brussels: Comm. de l'Observatoire Royal de Belgique), **157**, 32.
PANNEKOEK, A.	1927	*B.A.N.*, **4**, 7.
	1930	*M.N.*, **91**, 139.
	1938	*Ibid.*, **98**, 694.
PECKER, J. C.	1957	*C.R.*, **245**, 639.
	1959	*Ann. d'ap.*, **22**, 499.
PLASKETT, H. H.	1955	*M.N.*, **115**, 256.
PRIESTER, W.	1953	*Zs. f. Ap.*, **32**, 200.
RICHTER, J.	1958	*Zs. f. Phys.*, **151**, 114.
ROSSELAND, S.	1926	*Ap. J.*, **63**, 218.
RUSSELL, H. N.	1936	*Ap. J.*, **83**, 129.
SAVEDOFF, M.	1952	*Ap. J.*, **115**, 509.
SCHIFF, L. I.	1949	*Quantum Mechanics* (New York: McGraw-Hill Book Co.).
SCHMALJOHANN, P.	1936	"Staatsexamensarbeit Kiel," unpublished; cf. A. UNSÖLD, 1955.
SCHRÖTER, E. H.	1957	*Zs. f. Ap.*, **41**, 141.
SEATON, M. J.	1953	*Proc. R. Soc. London, A*, **218**, 400.
SOBELMAN, I. I.	1954	*Doklady Akad. Nauk SSSR*, **98**, 43.
	1957	*Fortschr. d. Phys.*, **5**, 175.
SOBOLEV, V.	1949	*Russian Astr. J.*, **26**, 129.

SOMMERFELD, A.	1948	*Partielle Differentialgleichungen der Physik* (Leipzig: Akademische Verlagsgesellschaft).
SPITZER, L.	1936	*M.N.*, **96**, 794.
	1939	*Phys. Rev.*, **55**, 699, and **56**, 39.
	1940	*Ibid.*, **58**, 348.
	1944	*Ap. J.*, **99**, 1.
	1956	*Physics of Fully Ionized Gases* (New York: Interscience Publishers).
STIBBS, D. W. N.	1953	*M.N.*, **113**, 493.
SUEMOTO, Z.	1949	*Pub. Astr. Soc. Japan*, **1**, 78.
SWAN, P.	1955	*Proc. Phys. Soc. London, A.*, **68**, 1157.
THIESSEN, G.	1952	*Zs. f. Ap.*, **30**, 307.
THOMAS, R. N.	1948	*Ap. J.*, **108**, 142.
	1949	*Ibid.*, **109**, 480 and 500.
	1957	*Ibid.*, **125**, 260.
THOMSON, J. J.	1912	*Phil. Mag.*, **23**, 449.
TRAVING, G.	1957	*Zs. f. Ap.*, **41**, 215.
TREFFTZ, E.	1949	*Zs. f. Ap.*, **26**, 240.
TREFFTZ, E., and BIERMANN, L.	1952	*Zs. f. Ap.*, **30**, 275.
TREFFTZ, E., SCHLÜTER, A., DETTMAR, K. H., and JÖRGENS, H.	1957	*Zs. f. Ap.*, **44**, 1.
TURNER, E. B.	1956	Thesis, University of Michigan.
UNDERHILL, A. B., and WADDELL, J. H.	1959	*Nat. Bureau Standards Circ.*, No. 603.
UNSÖLD, A.	1932	*Zs. f. Ap.*, **4**, 339.
	1938	*Physik der Sternatmosphären* (Berlin: Springer-Verlag).
	1943	*Vierteljahrschr. d. Astr. Gesellsch.*, **78**, 213.
	1948	*Ann. d. Phys.*, **3**, 124.
	1952	*Zs. f. Naturforsch.*, **7a**, 121.
	1955	*Physik der Sternatmosphären* (2d ed.; Berlin, Göttingen, Heidelberg: Springer-Verlag).
UNSÖLD, A., and WEIDEMANN, V.	1955	In *Vistas in Astronomy*, ed. A. BEER (London: Pergamon Press), Vol. **1**.
VERWEY, S.	1936	"The Stark Effect of Hydrogen in Stellar Spectra," dissertation, Amsterdam.
VOIGT, H. H.	1951	*Zs. f. Ap.*, **28**, 176.
	1956	*Ibid.*, **40**, 157.
WARWICK, J. W.	1955	*Ap. J.*, **121**, 190.
WEISSKOPF, V.	1932	*Zs. f. Phys.*, **75**, 287.
	1933*a*	*Phys. Zs.*, **34**, 1.
	1933*b*	*Zs. f. Phys.*, **85**, 451.
WEISSKOPF, V., and WIGNER, E.	1930	*Zs. f. Phys.*, **63**, 54, and **65**, 18.

WESSEL, G.	1951	*Zs. f. Phys.*, **126**, 440.
WHITE, H. E., and ELIASON, A. Y.	1933	*Phys. Rev.*, **44**, 753.
WILDT, R.	1956	*Ap. J.*, **123**, 107.
WOOLLEY, R. v. d. R.	1938	*M.N.*, **98**, 624.
WOOLLEY, R. v. d. R., and STIBBS, D. W. N.	1953	*The Outer Layers of a Star* (Oxford: Clarendon Press).
WURM, K.	1948	*Zs. f. Ap.*, **25**, 109.
	1951	*Die planetarischen Nebel* (Berlin: Akademie-Verlag).
ZANSTRA, H.	1941	*M.N.*, **101**, 273.
ZIOCK, K.	1957	*Zs. f. Phys.*, **147**, 99.

CHAPTER 4

Quantitative Analysis of Normal Stellar Spectra

LAWRENCE H. ALLER
University of Michigan

§ 1. BRIEF HISTORICAL SUMMARY

A CENTURY has elapsed since the discovery of the principles of spectrum analysis by Bunsen and Kirchhoff opened the way for the qualitative analysis of the sun and stars. The early work was carried out by a direct comparison of the laboratory source with the solar or stellar spectrum; later, when accurate wave-length measurements became practicable, close coincidences in wave lengths were employed. Although it was quickly demonstrated that every element prominent in the Fraunhofer spectrum of the sun was abundant on the earth, the converse was not true. For example, no atomic lines of the halogens are found in the solar spectrum, nor do we observe the lines of argon, one of the most prominent gases in the earth's atmosphere. Although every abundant element found on the earth is found in the sun or stars, not all these elements are detected in all stars. For example, the metals are much more prominent in the solar spectrum than are the permanent gases. On the other hand, the spectrum of a B0 star such as ϕ Orionis shows prominent lines of the permanent gases but no lines of iron, calcium, vanadium, or chromium.

We now recognize that the differences between the spectra of most stars (excluding certain supergiants and other well-evolved objects) come from differences in the temperatures and pressures in their atmospheres. The spectrochemical analyses of stars cannot be disengaged from a determination of the physical conditions existing in their atmospheres. With each improvement in our understanding of the structure of the solar and stellar atmospheres has come the possibility of better information on their quantitative chemical composition.

Before the formulation of the Saha ionization theory, little progress could be made in understanding the physics of stellar atmospheres. Once the stellar tem-

perature scale was roughly established and the ionization potentials and spectroscopic term structures of the atoms were determined, the ionization theory could be used to obtain the electron pressures and to improve the temperature scale itself.

The early work by Saha, by Milne and Fowler, by Menzel, and by Miss Payne established the general run of the temperature scale and showed that the pressures existing in stellar atmospheres were very low compared with that of the atmosphere. Meanwhile, the quantitative problem of the passage of light through a stellar atmosphere and of the formation of spectral lines had been considered by a number of investigators—Schuster, K. Schwarzschild, E. A. Milne, A. S. Eddington, J. Q. Stewart, and A. Unsöld. The combination of the theories of ionization and dissociation and the Boltzmann equation, on the one hand, with the theories of spectral line formation, on the other, made possible the theoretical developments of the last quarter-century. As the quality of the observational material improved, so has the sophistication of the theoretical treatment, and fairly elaborate calculations are now commonplace.

The earliest attempts at a semiquantitative analysis of stellar spectra involved eye-estimates of intensity on an arbitrary scale. That is, to each spectral line appearing upon a solar or stellar spectrogram, the observer assigned a number which depended on the depth, blackness, or width of the line. Such eye-estimates, although subjective and therefore differing from one observer to another, could sometimes be calibrated in terms of physically meaningful quantities. The greatest set of such homogeneous data was the Rowland Atlas and table of the solar spectrum. The wave length of each solar line was measured with high accuracy, and to each of these lines an eye-estimate of intensity was assigned.

In 1928, Russell, Adams, and Moore showed that the Rowland intensity of a line could be calibrated in terms of the number of atoms acting to produce it. They selected lines of multiplets wherein the relative line strengths were known and then constructed the empirical relation between the relative numbers of atoms and the Rowland intensity. This relationship varied from one part of the spectrum to another; further, the functional dependence of the intensity on the number of active atoms was not a linear one. One of the most striking results of the calibration was the demonstration of the huge differences in the numbers of atoms responsible for the Fraunhofer lines. Thus about a million times more atoms acted to produce the Hα line than acted to produce a line of Rowland intensity -3.

Adams and Russell (1928) took advantage of the calibration of the Rowland intensity scale to investigate stellar spectra observed with the coudé spectrograph of the 100-inch reflector. By photographing the solar spectrum with the same instrument, they could express all their intensity estimates on the Rowland scale. The weakest stellar lines were about Rowland intensity 1 and, in going from these to the strongest stellar lines such as the H and K lines in later

spectral types or to the Balmer lines in A stars, the number of atoms must increase by a factor of 10,000 or more. Adams and Russell analyzed their data on the assumption that atoms at different levels are equally effective in producing a line and that local thermodynamic equilibrium obtains.

Their work indicated that in the atmospheres of late-type giant and supergiant stars the numbers of atoms in excited levels, particularly those of high energy, greatly exceeded the predictions of theory. This effect, commonly called the "Russell-Adams phenomenon," is particularly marked in the hydrogen lines. Russell and Adams theorized that the behavior of the lines of ionized iron, titanium, etc., in red giant stars suggested that they were produced largely in extended chromospheres, a view which now appears substantiated by the data from eclipsing binaries and studies of such stars as α Herculis (Deutsch 1956). They also found that the amount of material above each unit area of the photosphere of a supergiant star such as Betelgeuse, Antares, or γ Cygni was of the order of a hundred times as great as that above a similar area of the solar photosphere. For Arcturus or α Persei the amount was about ten times as great, whereas in Sirius it is smaller. They suggested that in Sirius the metallic vapors were diluted by some other constituent, presumably hydrogen.

As compared with the spectra of many other stars, the solar spectrum has relatively weak and narrow lines. In giant and supergiant stars, not only is the amount of material in the visible atmosphere greater, but the lines are broadened by large-scale mass motions popularly called "turbulence."

One additional application of the Rowland calibration must be mentioned—Russell's (1929) classical paper on the composition of the solar atmosphere, which established the order of magnitude of the cosmic abundances of the various elements. Although the details have been improved, the general run of Russell's results has been retained. Russell (1933) subsequently undertook an elaborate investigation of the theoretical intensities of the Fraunhofer lines, making use of an approximate method due to Milne of deriving a mean optical depth which could be regarded as the depth above which all the spectrum was formed. The effect of the variability in the continuous absorption coefficient with wave length is included, in that the amount of material above the photosphere varies with wave length. Elaborate tables of ionization and excitation were included in this work.

Eye-estimates, besides being subjective and notoriously inaccurate, suffer from the disadvantage that they do not correspond with any theoretically predictable quantity. Hence attention was devoted to the measurement of the profiles of absorption lines (e.g., von Klüber 1927) and to the theoretical interpretation of the shapes of these lines (Unsöld 1928). In addition to the profiles, we may also measure the total amount of energy subtracted from the line, expressed in equivalent angstroms of the neighboring continuous spectrum. Thus, for example, Minnaert (1927) found the equivalent width of the Hα line to be 4.2 A. It is possible to calibrate the Rowland scale in terms of these equiva-

lent widths, as was done, for example, by Mulders, by Menzel, Goldberg, and Cook (1940), and by Unsöld (1938). A more interesting relationship is the connection between the equivalent width and the number of active atoms, i.e., the curve of growth introduced by Minnaert and Slob (1931) and developed and applied by hosts of workers. The curve of growth enables the astrophysicist to handle quickly large quantities of observational data and to deduce such parameters as mean temperatures and pressures, turbulent velocities, and chemical compositions. Against these advantages must be set a number of disadvantages that we shall describe later. As a means for quick reconnaissance of a stellar atmosphere, the curve of growth remains a favorite tool.

The curve of growth, as well as the more primitive techniques that preceded it, is based on the approximation that the formation of a spectral line can be calculated as though it were formed in an atmosphere of some fixed temperature and density. This assumption is not a bad one as long as we are comparing lines of atoms or ions in the same stage of excitation and ionization, e.g., lines of Fe II, V II, Ti II, etc., in the sun. It is less satisfactory when we wish to compare lines of very different excitation and ionization potential, e.g., the resonance lines of neutral potassium with the infrared lines of neutral carbon whose excitation potentials are of the order of 8 ev.

The fact that different depths in a stellar atmosphere may contribute in very different ways to lines of different excitation potential was clearly recognized by Pannekoek, who attempted to take into account the effects of stratification in a stellar atmosphere by numerically integrating the equations of transfer. Pannekoek (1935) computed the "half-width" of lines, i.e., the point at which the residual intensity $r = 0.5$. Hence his theoretically predicted quantities could not be converted readily into measurable quantities. Since the calculations were carried out before the negative hydrogen ion was recognized as the principal source of continuous absorption in the cooler stars, marked discrepancies between theory and observations occurred in the behavior of the lines at lower temperatures and particularly for the lines falling below the Balmer limit (Aller and Stoddard 1938); also the theory tended to predict lines that were too strong in giants and supergiants.

Strömgren's (1940) classical paper on the composition of the solar atmosphere effectively introduced the model-atmosphere technique. Since then, analyses of stellar spectra have increasingly relied on approaches based on this point of view. One determines the structure of a model atmosphere or family of model atmospheres and calculates the observable parameters of a spectrum. These are then compared with the observations, to secure estimates of surface gravity, effective temperature, and chemical composition. Methods based on model atmospheres are sometimes referred to as "fine analyses," as distinct from the "rough analysis" or curve-of-growth technique. Both have their advantages, and the use of the fine-analysis technique is justified only when the quality of the observational material merits it. A preliminary survey by the curve-of-

growth method is required in order to establish some average value of the temperature and density encountered in the stellar atmosphere. In such objects as late-type supergiants, where no sound theoretical basis exists for the calculation of model atmospheres, the curve-of-growth approach is the only one available except for the isolated instances of a few eclipsing binaries in which the structure of the atmosphere can be observed more directly (Wilson and Abt 1954).

§ 2. METHOD OF FINE ANALYSIS

2.1. The Mechanism of Line Formation

The theory of the calculation of line profiles in the spectrum of the sun or star involves several distinct steps. We must know the structure (or model) of the atmosphere, i.e., the dependence of temperature, density, and the coefficient of continuous absorption on the depth. Next, we must know the mechanism of the energy exchange. Are the lines formed by a process of absorption (or thermal equilibrium) in which the emission is controlled entirely by the local temperature in accordance with Kirchhoff's law—or are the lines formed by the mechanism of scattering? In the latter event, a quantum that is absorbed by the atom is re-emitted forthwith, and hence the amount of energy in a spectral line emerging from a given volume element will depend on the amount of energy within the same spectral line that impinges on the volume element. The local temperature does not enter the scene directly, but only insofar as it may influence the local state of ionization and excitation in accordance with the Boltzmann formula and the Saha equation.

Scattering may be of two types, coherent or non-coherent. In coherent scattering, the light is re-emitted with exactly the same frequency. In non-coherent scattering, energy absorbed at one part of the line profile may be re-emitted at another part of the line profile. Under these circumstances the transfer of radiation is enormously complicated. The Doppler effect introduces some non-coherency (Henyey 1940), while radiation scattered by atoms whose line profiles are determined by pressure effects will be entirely non-coherent. Qualitatively, non-coherent scattering tends to remove energy from the wings of the line and to reintroduce it nearer to the center, with the result that the profile of the line is appreciably altered. Since the original suggestion by Eddington (1929), contributions have been made by a great number of investigators, including Spitzer (1936), Houtgast (1942), Woolley (1938), Münch (1949), Zanstra (1941, 1946), Labs (1951, 1954), Miyamoto (1953, 1954*a*), Suemoto (1949), Savedoff (1952), Woolley and Stibbs (1953), and Stibbs (1953), Miss Busbridge (1953), Inaba (1955), Ueno (1955), and Edmonds (1955).

In the far wings of a line, non-coherent scattering can be treated formally as a combination of absorption and extinction, with the result that it is difficult to make a definitive test of the hypothesis of scattering versus the hypothesis of absorption. Unsöld (1955) suggested that one might interpret the observations by Houtgast and others on the assumption that the lines are formed ac-

cording to the mechanism of pure absorption with a solar model atmosphere that has a very sharp temperature drop near the boundary. Careful studies of the blanketing effect, particularly by K. H. Böhm (1954), show that the effect of the Fraunhofer lines is to alter the temperature distribution from that of a black body in such a way as to cause a sharp temperature drop near the surface. The limb-darkening measurements in the sun lead to temperature distributions that are meaningful only between optical depths 0.1 and 1.0 (cf., e.g., Chalonge and Kourganoff 1946; Pierce and Aller 1951; and Pierce and Waddell 1960). They tell nothing about the temperature distribution in the outermost layers, where the blanketing effect of the Fraunhofer lines has its largest effect. Böhm's work suggests that, after due allowance is made for plausible deviations from thermodynamic equilibrium in the outermost layers and possible temperature fluctuations in the photosphere, the center-to-limb variations of lines may be fairly well explained. In particular, the small central intensities of strong lines near the limb of the sun could be understood equally well in terms of the mechanism of scattering (with a little admixture of absorption) or in terms of the absorption mechanism with a low temperature in the outermost layer and inner chromosphere.

On the other hand, there are some strong theoretical reasons for favoring the mechanism of scattering for resonance lines. For example, Plaskett (1955*b*) calculated that at an optical depth of about 0.5 in the solar photosphere, where the electron pressure was 18 dynes/cm^2, a sodium atom which is excited to the 4^2P terms by the absorption of a quantum of "D-line" radiation had a chance of about 0.46 per cent of being de-excited by a collision with a neutral hydrogen atom, while the chance of losing energy in a superelastic collision with an electron is even smaller. Other calculations have indicated that the chance of the atom's becoming ionized from the 4^2P term is about 1 per cent, so that the probability that the atom will reradiate the same D-line quantum as it absorbed is around 98 per cent. In spite of repeated scattering events, each of which is characterized by a small chance that the atom will not re-emit the D line, Plaskett concludes that the mechanism of absorption, favored by Unsöld, is unlikely to prevail in such a resonance line.

The observational picture is less convincing. Sobolev (1954) concluded that the theory of line formation by non-coherent scattering is in better agreement with the observations than is the theory of coherent scattering. The best tests for the theory are, of course, the center-limb profile changes of strong resonance lines such as the K line of ionized calcium and D lines of sodium and the magnesium "b" lines. Münch (1949) and Savedoff (1952) discussed the K line, making simplified assumptions about the variation of the ratio of the line to the continuous absorption coefficient. A detailed numerical calculation in which the model of the solar atmosphere was taken into account indicated that the hypothesis of non-coherent scattering gave a better representation than did the hypothesis of coherent scattering (Aller 1953). Although the assumed model

had a somewhat higher boundary temperature than we now accept, a good representation was obtained in the wings, where the influence of the error in the model was small.

On the basis of calculations with an approximate theory and Münch's model of the solar atmosphere (1946), Harris (1949) concluded that non-coherent scattering would have to be invoked to explain the center-limb variations in the D-line profiles. On the other hand, Hitotuyanagi and Inaba (1954), who used the empirical model of the solar atmosphere by Pierce and Aller (1952), concluded that the coherent-scattering theory would be adequate if one made small adjustments to the temperature and pressure. Priester (1953) found that his measurements of the profiles of the D lines could be accounted for with the theory of pure absorption.

For the magnesium "b" lines, Miyamoto (1954*b*) decided that the center-limb variations did not lead to a conclusive choice between coherent and non-coherent scattering. From measurements of the polarization at the core of the λ 4227 resonance line of calcium from the center of the sun's disk to the limb, Jäger (1957) concluded that the center of the line was formed by coherent scattering. On the assumption that the statistical broadening by ions and electrons produced non-coherent scattering, de Jager (1952) tried to represent the center-limb variations of the Balmer lines. It is unlikely, however, that the Balmer lines are formed by the mechanism of scattering, since the absorption of a Balmer line is more likely to be followed by the emission of a Lyman quantum than by the re-emission of the same Balmer quantum.

Calculations of theoretical profiles have been carried out for pure absorption, coherent scattering, and non-coherent scattering. The simplest situation is presented by pure absorption, and we shall discuss it *in extenso* in § 2.3. Non-coherent scattering presents formidable difficulties to the calculation of line profiles—cf., e.g., Miyamoto (1953, 1954*a*, *c*), Woolley and Stibbs (1953), Sobolev (1949, 1951, 1954), and Ueno (1955). More attention needs to be devoted to the physical situation in which the ratio of line to continuous absorption coefficient changes with depth, and numerical methods have to be applied.

Straightforward methods exist for the calculation of line profiles on the hypothesis of coherent scattering, cf., e.g., Aller (1953, chap. 8). Among these methods the most often used are the following:

a) *The "mean-value method" due to Strömgren* (1937).—Precise solutions of the equation of transfer (Chandrasekhar 1950) with optical depth may be obtained for the situation in which the ratio of the line to the continuous absorption coefficient, $\eta = l/\kappa$, is constant. One replaces the quantities depending on η by appropriate mean values.

b) *Direct numerical integration of the equations of transfer.*—This is Pannekoek's method, which may be adaptable to electronic computing machines.

c) *Strömgren's iteration procedure.*—In this method the equation of transfer

with its appropriate boundary conditions is replaced by the equivalent integral equation, which in turn is solved by a simple iteration procedure. The method works well as long as the scattering coefficient is not large compared with the absorption coefficient, but it becomes inefficient for strong lines formed primarily by scattering.

d) *Method of weighting functions.*—It is possible to define weighting functions for scattering as well as for absorption (cf. § 2.3) and to apply the Pecker theory (1951) to lines of moderate strength.

Special mention must be made of the method proposed by Plaskett (1955*b*), who makes no a priori commitment to the mechanism of line formation but proceeds from what might be called the "mechanistic" point of view. He derives the values of the source function and the ratio of the line to the continuous absorption coefficient in terms of kinetic, excitation, and ionization temperatures with the aid of transition probabilities for radiative excitation and ionization. These quantities depend on the depth in such a way that a numerical method of integration may be followed. Only a single constant has to be evaluated by means of an iterative procedure. Plaskett's method is particularly useful for resonance lines, but it can be applied in principle to higher levels. In practice, it would appear to involve lengthy numerical calculations and would require somewhat more accurate knowledge of fundamental atomic parameters, transition probabilities for the lines, and continua than we possess at present. It should be applied to suitable lines in the solar spectrum.

To summarize, scattering is probably the most likely mechanism for the resonance lines, and it seems certain that the wings of strong resonance lines would be formed by non-coherent, rather than by coherent, scattering. Nevertheless, some success has been attained in explaining the behavior of resonance lines by the mechanism of absorption. The problem of line formation is far from solved. For subordinate lines, scattering is probably much less important than absorption, and therefore lines arising from excited levels several volts above the ground level can be handled according to the mechanism of absorption.

In hotter stars we observe only subordinate lines; hence the choice in favor of the absorption mechanism is clear-cut. The source of the continuous absorption and extinction is mostly atomic hydrogen or helium and electron scattering, for which the coefficients are accurately known. Since we deal with transitions between the higher, hydrogen-like levels, mostly of light atoms, for which the wave functions are better known than for resonance transitions, theoretical atomic parameters such as f-values should be more accurate. From the theoretical point of view the atmospheres of main-sequence stars earlier than A0 are simpler than those of the cooler stars because there should be no hydrogen-ionization convection zone. If we use weak lines (often there is no other choice), inaccuracies due to damping constants, etc., can be avoided. We shall first discuss the atmospheres of hot stars and then those of stars like the sun.

2.2. Selection of Model Atmospheres

Before the problem of the formation of an absorption line can be considered, we have to obtain a suitable model atmosphere that will give the gas pressure, the electron pressure, the temperature, and the continuous absorption coefficient as functions of the optical depth at some wave length. Some workers prefer to use a mean absorption coefficient and hence an optical depth defined in terms of this mean absorption coefficient. Thus optical depths defined in terms of the Chandrasekhar mean, the Planck mean, and the Rosseland mean have all been used, although the latter has been generally favored. Actually, it is not necessary to employ a mean absorption coefficient at all, provided that one can find the temperature distribution as a function of the optical depth at some one frequency. For the sun, it is possible to obtain empirical temperature distributions throughout the layers between optical depths 0.1 and 1.0 by making use of the limb-darkening data. At shallower optical depths than 0.1 and in layers below 1.0 it is necessary to extend the model by theoretical considerations.

The big initial difficulty is the establishment of the temperature distribution, and theories of model atmospheres tend to give a weak determination of this relationship precisely in those layers which are most important for the formation of spectral lines. In the earlier work it was generally assumed that one could compute the Rosseland mean absorption coefficient of the material and then suppose that the dependence of the temperature on the optical depth defined in terms of this mean was exactly the same as the temperature dependence on the optical depth for a gray body. That is,

$$T^4(\tau) = \sqrt{(3)}\, T_0^4 [\tau + q(\tau)], \qquad (1)$$

where $q(\tau)$ has been computed by various workers. Mustel (1943, 1944) demonstrated that this procedure was not valid when the stellar material exhibited pronounced departures from grayness, as in an early-type star. Since then, increasingly elaborate attempts have been made to compute model atmospheres for various types of stars. Most of them have assumed radiative equilibrium, in which case the flux must be constant with optical depth. This boundary condition is difficult to impose and is rather insensitive to small changes in the temperature distribution, as was demonstrated, for example, in the calculations of Miss McDonald (1953). Unfortunately, however, small changes in the temperature can lead to large changes in the Boltzmann factor for certain lines. Thus, as has been pointed out by Traving (1955) and by Jugaku (1957), the intensities of He II lines in late O and early B-type stars are extremely sensitive to the temperature.

If the stellar atmosphere is in radiative equilibrium and the flux is constant with depth, we may compute quantities that can be compared with observations of the stellar continuum. These include color temperatures in regions above and below the Balmer limit (or the spectrophotometric gradients) and the

amount of the Balmer discontinuity. We then compare the theoretical predictions with the observed values of these quantities for the stars under investigation. Thanks to work of Barbier, Chalonge, and collaborators (1935, 1939, 1941), spectrophotometric gradients longward and shortward of the Balmer limit, ϕ_1 and ϕ_2, and the amount of the Balmer discontinuity, D, have been measured for stars of all spectral classes. Furthermore, by methods we shall describe shortly, the equivalent widths or profiles of certain temperature- (or surface gravity) sensitive lines may be computed and compared with the observations. If a network of model atmospheres has been computed as a function of surface gravity and temperature, we may be able to interpolate a model corresponding to the star of interest. In the hottest stars of the main sequence, the ratio of λ 4686 (He II) to λ 4471 (He I) provides a sensitive criterion. From B1 to B5 we may use the ratios of the lines of Si II, Si III, and Si IV to establish the temperature. Throughout the entire range from early O to A, the profiles of the hydrogen lines are more sensitive to the surface gravity than they are to the temperature. In still later spectral classes there are other line ratios, molecular bands, etc., that can be utilized. For stars of spectral classes in the neighborhood of late F and G we can make differential comparisons with the sun itself. In yet later spectral classes the problems of blanketing effect, possible unknown sources of continuous absorption, and the difficulty of constructing meaningful model atmospheres complicate the problem. The necessary conditions for a model atmosphere, then, are that it must reproduce the spectrophotometric gradients, the Balmer discontinuity, and intensity ratios of temperature-sensitive lines as well as the profiles of surface gravity-sensitive lines, e.g., the Balmer lines in hotter stars.

In actual practice, the predictions for the continuous spectra based on the model atmospheres in B-type stars have not been too successful, but exact comparisons are difficult because of the influence of space reddening. Greater success is attained near spectral class A, where Bless (1958), using a photoelectric scanner, finds that the models of Osawa (1956) give a satisfactory representation of the continuous spectrum and the Balmer discontinuity. He finds that, using these models, it is possible to deduce the effective temperature and the surface gravity from the spectrophotometric measurements alone. This work is being extended to a consideration of the hydrogen lines as well.

Further checks on the models should be provided by the limb-darkening data. Unfortunately, in light-curves of eclipsing binaries it is very difficult to separate limb-darkening effects from those arising from other causes. It is necessary to assume a form for the law of limb darkening and determine the coefficients from observations. Whereas limb-darkening data can perhaps distinguish between model atmospheres that differ grossly from one another, they cannot provide accurate data on the temperature distribution, as is possible for the sun. Nevertheless, eclipsing binary data should provide some checks on model atmospheres.

Eclipsing binary data supply important information on such critical criteria as surface gravity and ultimately brightness temperatures. More spectrophotometric and line-profile and intensity studies should be made on eclipsing binaries for which good data on stellar masses and radii are available.

2.3. Calculation of Theoretical Line Intensities

In this section we shall emphasize the calculation of profiles and equivalent widths according to the mechanism of pure absorption, although we shall point out the modifications needed in the theory if the scattering mechanism is assumed.

The element of optical depth in the continuum is

$$d\tau_\lambda = (\kappa_\lambda + \sigma)\,\rho dh = \kappa_{\lambda\ \mathrm{eff}}\rho dh\,, \tag{2}$$

while the element of optical depth in the line is written as

$$dt_\nu = (\kappa_\nu + \kappa_{\lambda\ \mathrm{eff}})\,\rho dh = \left(1 + \frac{\kappa_\nu}{\kappa_{\lambda\ \mathrm{eff}}}\right) d\tau_\lambda \equiv d\tau_\lambda + d\tau_\nu\,. \tag{3}$$

Here κ_ν is the line absorption coefficient, which depends sharply on frequency; κ_λ is the coefficient of continuous thermal absorption; and σ is the coefficient of electron scattering. In cooler stars such as the sun, σ may be neglected, but it assumes considerable importance for hotter stars, particularly supergiant O and B stars. We shall use the subscript λ throughout to denote quantities connected with the continuum; the subscript ν will be used for quantities connected with lines.

Since the model atmosphere is presumably described in terms of the optical depth, τ_0, at some wave length λ_0, we refer the optical depth in the continuum at any wave length λ to the optical depth at λ_0 by

$$d\tau = \frac{\kappa}{\kappa^0_{\mathrm{eff}}}\, d\tau_0\,, \tag{4}$$

and we will drop the subscript λ henceforth as a matter of convenience.

First, let us consider the simplified case in which the continuum is formed according to the mechanism of pure absorption (as is true for most stars) and write down the equation for the specific intensity of an emergent ray which makes an angle θ with the outward normal. Thus, assuming local thermodynamic equilibrium,

$$I(0, \mu) = \int_0^\infty B(\xi)\, e^{-\xi/\mu} \frac{d\xi}{\mu}, \tag{5}$$

where, in accord with the usual notation,

$$\mu = \cos\theta \tag{6}$$

and also

$$d\xi = d\tau \qquad \text{for the continuum}\,, \tag{7a}$$

$$d\xi = dt_\nu = d\tau_\nu + d\tau \qquad \text{for a point in the line}\,. \tag{7b}$$

Let us denote by I_μ the intensity of the emergent ray in the continuum, and by $I_{\mu,\nu}$ the same quantity for the line. At a point $\Delta\lambda$ from the line center, the absorption is given by

$$r_\mu(\Delta\lambda) = \frac{I_\mu - I_{\mu,\nu}}{I_\mu}. \tag{8}$$

Making use of equations (2), (3), (4), and (5), we find, for the numerator of equation (8),

$$I_\mu - I_{\mu,\nu} = I_\mu - \int_0^\infty B[T(\tau)]\, e^{-(\tau_\nu+\tau)/\mu}\left(1+\frac{\kappa_\nu}{\kappa}\right)\frac{d\tau}{\mu} \tag{9}$$

$$= I_\mu - \int_0^\infty e^{-\tau_\nu/\mu} B(\tau)\, e^{-\tau/\mu}\frac{d\tau}{\mu} - \int_0^\infty \frac{\kappa_\nu}{\kappa}\, e^{-\tau_\nu/\mu} B(\tau)\, e^{-\tau/\mu}\frac{d\tau}{\mu}. \tag{10}$$

Let us define

$$\int_{\tau_\lambda}^\infty B(\zeta)\, e^{-\zeta/\mu}\frac{d\zeta}{\mu} = \Phi_\mu^*(\tau_\lambda). \tag{11}$$

By differentiation,

$$-B(\tau)\, e^{-\tau/\mu}\frac{d\tau}{\mu} = d\Phi_\mu^*.$$

Furthermore,

$$\Phi_\mu^*(\tau=0) = I(0,\mu). \tag{12}$$

Now integrate the second term on the right-hand side of equation (10) to obtain

$$\begin{aligned}\int_0^\infty e^{-\tau_\nu/\mu} d\Phi_\mu^*(\tau_\lambda) &= [e^{-\tau_\nu/\mu}\Phi_\mu^*]_0^\infty + \int_0^\infty e^{-\tau_\nu/\mu}\Phi_\mu^*(\tau)\frac{d\tau_\nu}{\mu} \\ &= -I(0,\mu) + \int_0^\infty \frac{\kappa_\nu}{\kappa}\, e^{-\tau_\nu/\mu}\Phi_\mu^*(\tau)\frac{d\tau}{\mu},\end{aligned} \tag{13}$$

where we have noted that $d\tau_\nu = \kappa_\nu/\kappa d\tau$. Put equation (13) in equation (10) to obtain

$$I_\mu - I_{\mu,\nu} = \int_0^\infty \frac{\kappa_\nu}{\kappa}\, e^{-\tau_\nu/\mu}\Phi_\mu^*\frac{d\tau}{\mu} - \int_0^\infty \frac{\kappa_\nu}{\kappa}\, e^{-\tau_\nu/\mu} B(\tau)\, e^{-\tau/\mu}\frac{d\tau}{\mu}. \tag{14}$$

The absorption in the line is now expressible as

$$r_\mu(\Delta\lambda) = \int_0^\infty \frac{\kappa_\nu}{\kappa}\, e^{-\tau_\nu/\mu}\, g_\lambda^\mu(\tau_\lambda)\frac{d\tau_\lambda}{\mu}, \tag{15}$$

where the weight function, g_λ^μ, is given by

$$g_\lambda^\mu(\tau_\lambda) = \frac{\int_{\tau_\lambda}^\infty B(\tau)\, e^{-\tau/\mu}\frac{d\tau}{\mu} - B(\tau)\, e^{-\tau/\mu}}{\int_0^\infty B(\tau)\, e^{-\tau/\mu}\frac{d\tau}{\mu}} \tag{16}$$

for pure absorption. An analogous expression may be obtained for the case of coherent scattering. The concept of weighting function was first introduced by

Unsöld (1932) and has since been developed by Minnaert (1936, 1948), by Pecker (1949, 1951), and by Barbier and many others.

Using relations (5) and (7*a*) and recalling that the denominator is $I_\mu(\tau_\lambda = 0) = I_{\mu,\,\mathrm{cont}}$ is the emergent intensity in the continuum, we find that

$$I_{\mu,\,\mathrm{cont}}\, g_\lambda^\mu(\tau_\lambda) = \int_{\tau_\lambda}^{\infty} \frac{dB_\lambda(\zeta)}{d\zeta} \exp\left(-\frac{\zeta}{\mu}\right) d\zeta\,. \tag{17}$$

In a more general case the Planck function must be replaced by the source function. Retaining our assumption that the lines are formed according to the mechanism of pure absorption, the source function for the continuum will be given by the integral relation

$$S_\lambda(\tau_\lambda) = \frac{\kappa_\lambda}{\kappa_\lambda + \sigma} B_\lambda(\tau_\lambda) + \frac{\sigma}{\kappa_\lambda + \sigma} \frac{1}{2} \int_0^\infty S_\lambda(\zeta_\lambda) E_1(|\tau_\lambda - \zeta_\lambda|)\, d\zeta_\lambda\,, \tag{18}$$

while that for the lines will be

$$\begin{aligned} S_\nu(\tau_\nu) = {} & \frac{\kappa_\lambda + \kappa_\nu}{\kappa_\lambda + \kappa_\nu + \sigma} B_\nu(\tau_\nu) \\ & + \frac{\sigma}{\kappa_\lambda + \kappa_\nu + \sigma} \frac{1}{2} \int_0^\infty S_\nu(\zeta_\nu) E_1(|\tau_\nu - \zeta_\nu|)\, d\zeta_\nu\,. \end{aligned} \tag{19}$$

In most instances, S_ν will lie very close to B_ν, but in early-type stars, especially supergiants, electron scattering can make an appreciable contribution to the coefficient of continuous extinction. Therefore, in the upper part of an atmosphere where electron scattering plays a considerable role, the source function will deviate from a pure Planck function. In analyses of the type proposed by Pecker, one must assume the same kind of source function for both lines and continuum. If electron scattering is important, the source function in the continuum will approach that in the lines only in the far wings. Throughout the part of the line that makes the major contribution to the equivalent width, the source function in the line will be Planckian, whereas that in the continuum will be Planckian only in deeper layers. Jugaku (1957) showed that it makes little practical difference whether one uses the continuum source function throughout or the Planckian function throughout in calculations of line intensities in main-sequence B stars. In most work it is more convenient, as well as theoretically sounder, to use a Planckian type of source function.

Now equation (15) gives us the absorption in the line at a point $(\lambda - \lambda_0)$ from the line center, for a ray emerging at an angle θ with respect to the outward normal. Notice that the weighting function is independent of the type of atom or excitation potential and depends only on the wave length and model atmosphere. Hence it can be computed once and for all for a given problem (cf., e.g., Pecker 1949). The line absorption coefficient enters in the exponential term and in the coefficient κ_ν/κ. This quantity varies steeply across the line and also with depth in the atmosphere. It will differ from one line to another and has to be evaluated numerically for each problem.

Although equation (15) is suitable for solar problems, in which one can make observations across the disk, for stellar problems we need the radiation integrated over the entire disk of the star. The equivalent width is obtained by integrating over the line and then over the entire disk of the star; thus

$$\frac{W_\lambda}{\lambda}=\frac{1}{\lambda}\int_{-\infty}^{+\infty}\frac{F_{\text{cont}}-F_\nu}{F_{\text{cont}}}\,d\,(\Delta\lambda)$$
$$=\frac{1}{\lambda}\int_{-\infty}^{+\infty}\int_0^{+1}\frac{I_{\mu,\,\text{cont}}-I_{\mu,\,\nu}}{I_{\mu,\,\text{cont}}}\,\frac{I_{\mu,\,\text{cont}}}{F_{\text{cont}}/2}\,\mu d\mu d\,(\Delta\lambda)\,, \tag{20}$$

since

$$\pi F_\lambda=2\pi\int_0^{+1}I_{\text{cont}}\,(0,\,\mu)\,\mu d\mu\,,$$
$$\pi F_\nu=2\pi\int_0^{+1}I_{\text{line}}\,(0,\,\mu)\,\mu d\mu\,. \tag{21}$$

We compute the equivalent width in two steps. First, for a fixed μ, integrate over the relevant wave lengths. Thus

$$W_{\mu,\,\lambda}=\int_{-\infty}^{+\infty}\frac{I_{\mu,\,\text{cont}}-I_{\mu,\,\nu}}{I_{\mu,\,\text{cont}}}\,d\,(\Delta\lambda)\,, \tag{22}$$

an expression of interest in connection with the center-limb variations of solar lines of weak or moderate strength. Finally, from equation (20) we get

$$\frac{W_\lambda}{\lambda}=\int_0^1\frac{W_{\mu,\,\lambda}}{\lambda}\,\frac{I_{\mu,\,\text{cont}}}{F_{\text{cont}}/2}\,\mu d\mu\,, \tag{23}$$

where $I_{\mu,\,\text{cont}}$ is given by equation (17).

Consider, first, the evaluation of $W_{\mu,\,\lambda}$ (cf. eq. [22]). From $r_\mu(\Delta\lambda)$ (cf. eqs. [8], [15]) we calculate $\int r_\mu(\Delta\lambda)d\lambda$. The integration therefore involves two integrations, one over optical depth and the other over wave length.

Actually, the optical depth, τ, itself is not the most convenient variable of integration, since in practice one has to change the interval very frequently in proceeding from the layers that make the greatest contribution to the stronger lines to those that make the most important contributions to the continuum. Furthermore, the relation between optical depth and geometrical distance in the atmosphere is far from a linear one. Geometrical heights become important when we consider stars with extended envelopes or chromospheres. Elste (1955) suggested that, instead of using τ itself, we introduce a new variable,

$$x=\log_{10}\,\tau_\lambda\,. \tag{24}$$

Thus

$$\tau_\lambda=10^x \qquad \text{and} \qquad d\tau_\lambda=\frac{10^x}{\text{Mod}}\,dx\,,$$

where Mod = 0.4343. Then equation (15) becomes

$$r_\mu(\Delta\lambda)=\int_{-\infty}^{+\infty}\frac{1}{\mu}\,\frac{\kappa_\nu}{\kappa_{\lambda\,\text{eff}}}\,\frac{10^x}{\text{Mod}}\,\exp\left(-\int_{-\infty}^{x}\frac{1}{\mu}\,\frac{\kappa_\nu}{\kappa_{\lambda\,\text{eff}}}\,\frac{10^y}{\text{Mod}}\,dy\right)g_\lambda^\mu(x)\,dx\,, \tag{25}$$

since

$$\tau_\nu = \int_0^h \kappa_\nu \rho d h = \int^{\tau_\lambda} \frac{\kappa_\nu}{\kappa_{\lambda\ \mathrm{eff}}} d\tau_\lambda = \int_{-\infty}^{x} \frac{\kappa_\nu}{\kappa_{\lambda\ \mathrm{eff}}} \frac{10^y}{\mathrm{Mod}} dy. \qquad (26)$$

Now $\kappa_{\lambda\ \mathrm{eff}}$ is known as a function of optical depth in the atmosphere, whereas the line absorption coefficient, κ_ν, is given by

$$\kappa_\nu = n_{r,\,s} a_0 H = n_{r,\,s} \frac{\pi\epsilon^2}{mc} f_{r,\,s} \frac{c}{\nu_0 \sqrt{\pi}\ \sqrt{V^2}} (1 - e^{-hc/\lambda kT}) H, \qquad (27)$$

where $n_{r,\,s}$ is the number of atoms in the level s in the rth stage of ionization. It may be written in the form

$$n_{r,\,s} = \left(\frac{n_{r,\,s}}{\Sigma n_r}\right) \frac{N_E}{N_H} \frac{1}{m_H \mu_0}, \qquad (28)$$

where the summation is carried out over all stages of excitation and ionization for the atoms of a given element; N_E/N_H is the ratio of the number of atoms of the element E to the number of hydrogen atoms; and μ_0 is the mean molecular weight with respect to hydrogen of un-ionized material of the same composition as the star, viz.,

$$\mu_0 = \frac{\Sigma \mu_i N_i}{N_H}. \qquad (29)$$

The symbols π, ϵ, m, and c have their usual meanings, while $f_{r,\,s}$ is the Ladenburg oscillator strength. V is the most probable velocity of the atoms; it includes the contributions of both their gas kinetic motion and "microscopic" turbulence, i.e., large-scale motions of the gas in which the optical thickness of the moving volume elements is smaller than the mean-free path of a light-quantum. Thus

$$V = \sqrt{(\xi_{\mathrm{th}}^2 + \xi_{\mathrm{turb}}^2)}. \qquad (30)$$

Here ξ_{th} is the most probable thermal velocity, and ξ_{turb} is the most probable velocity of the microturbulence. It is assumed that the turbulent elements have a random distribution of velocities. We shall express both ξ_{th} and ξ_{turb} in kilometers per second. Then

$$\xi_{\mathrm{th}}^2 = \frac{2RT}{\mu_{el}} = \frac{83.83}{\mu_{el}} \frac{1}{\theta}, \qquad (31)$$

where μ_{el} is the atomic weight of the atom in question (on the usual scale) and $\theta = 5040/T$.

The factor $[1 - \exp(-h\nu/kT)]$ allows for the stimulated emissions or "negative absorptions." This factor has already been included in the coefficient of continuous absorption. The function H allows for the type of line broadening; for example, it goes as $N_\epsilon(\Delta\lambda)^{-5/2}$ for the Holtsmark type of broadening. Here we shall be concerned primarily with lines that are subject to Doppler broadening plus radiation and collision damping. Under these circumstances we express $H(\Delta\lambda)$ as $H(v, a)$, where a and v are the usual parameters:

$$a = \frac{\Gamma}{4\pi\Delta\nu_0}, \qquad v = \frac{\Delta\lambda}{\Delta\lambda_D}. \tag{32}$$

Here Γ is the total damping constant, i.e.,

$$\Gamma = \Gamma_{\text{coll}} + \Gamma_{\text{rad}}, \tag{33}$$

and

$$\Delta\nu_0 = \frac{\nu_0}{c}\sqrt{V^2}, \tag{34}$$

while $H(v, a)$ is given by the integral

$$H(v, a) = \frac{a}{\pi}\int_{-\infty}^{+\infty} \frac{\exp(-y^2)}{a^2 + (v-y)^2}\, dy. \tag{35}$$

This function can be tabulated as a function of a and v (e.g., Hjerting 1938) or expanded in a series of the form

$$H_0(v) + aH_1(v) + a^2H_2(v) + \ldots \tag{36}$$

(cf. Harris 1948). For small values of v, it approaches a Gaussian form and for large values of v the damping wing form, i.e., $\sim v^{-2}$.

Following the notation of Elste (1955) and Aller, Elste, and Jugaku (1957), let us write

$$\frac{\kappa_\nu}{\kappa_{\lambda\ \text{eff}}}\frac{10^x}{\text{Mod}} = \frac{M^*Z(x)\,H(v, a)}{\sqrt{V^2}}\left[1 - \exp\left(-\frac{hc}{\lambda kT}\right)\right]. \tag{37}$$

Here M^* is a constant for each spectral line, $H(v, a)$ depends on the distance from the line center, and $Z(x)$ (which contains the Boltzmann and Saha factors) depends steeply on the depth. Now

$$M^* = \frac{N_i}{N_H}\, gf_{r,\,s}\lambda\,[A]\,\frac{10^{-8}}{\text{Mod}}\,\frac{\epsilon^2\sqrt{\pi}}{mc}\,\frac{1}{m_H\mu_0}\,10^{\theta_0\Delta\chi}. \tag{38}$$

Here

$$\theta_0 = \frac{5040}{T_0} \tag{39}$$

corresponds to some convenient temperature T_0 (for example, the mean ionization temperature obtained from the curve-of-growth analysis or the temperature corresponding to an optical depth between 0.1 and 0.5). It is to be emphasized that T_0 *is not* the boundary temperature of the model.

The quantity $\Delta\chi$ is defined from the following considerations: Let a given element be present in three important stages of ionization, $r-1$, r, and $r+1$ (e.g., Si II, Si III, and Si IV in a B2 star). Let s denote the lower level of the transition under consideration. Then

$$\begin{aligned} \Delta\chi &\equiv (\chi_{r-1} - \chi_{r-1,\,s}) && \text{for} \quad (r-1, s) \\ &\equiv -\chi_{r,\,s} && \text{for} \quad r, s \\ &\equiv -(\chi_{r+1,\,s} + \chi_r) && \text{for} \quad r+1, s\,. \end{aligned} \tag{40}$$

In equation (38) the wave length is expressed in angstrom units, g is the statistical weight of the level (r, s), and $f_{r,s}$ is the oscillator strength for the transition.[1] The quantity $gf\lambda$ varies from one line to the next, but the other factors remain constant for all lines arising from all terms with the same value of $\Delta\chi$. Slight variations in $\Delta\chi$ from one level (or even one term in a given configuration) to another can easily be taken into account in the analysis. The expression for $Z(x)$ is

$$Z(x) = \frac{1}{\kappa_{\lambda\,\mathrm{eff}}} \frac{n_{r,s}}{\Sigma n_r} \frac{10^{x-\theta_0\Delta\chi}}{g_{r,s}}. \tag{41}$$

Elste introduced the factor $10^{\theta_0\Delta\chi}$ into the expressions for M^* and Z in order to normalize Z within each ionization stage, to facilitate the use of electronic computing machines, and for making differential corrections of the model atmosphere.

Note that the factor $n_{r,s}/\Sigma n_r$ varies strongly with depth in the star and that it differs from one level to another. For a given model atmosphere we calculate its dependence on depth with the aid of the equations of Saha and Boltzmann. Let u_r denote the partition function for the rth stage of ionization. Then

$$\frac{n_{r,s}}{\Sigma n_r} = \left(\frac{n_{r,s}}{n_r/u_r}\right) \frac{1}{u_r\,(\ldots n_{r-1}/n_r + 1 + n_{r+1}/n_r + \ldots)}. \tag{42}$$

If r denotes the middle one of the three stages of ionization observed (or the most important stage if only two are observed), let us define

$$U_r \equiv u_r \frac{n_{r-1}}{n_r} + u_r + u_r \frac{n_{r+1}}{n_r}. \tag{43}$$

The Saha ionization equation,

$$\log \frac{n_{r+1}}{n_r} P_e = -\frac{5040}{T}\chi_r + \tfrac{5}{2}\log T - 0.48 + \log \frac{2u_{r+1}}{u_r}, \tag{44}$$

is written as

$$\log u_r \frac{n_{r+1}}{n_r} = \log u_{r+1} - \chi_r\theta + (9.080 - \tfrac{5}{2}\log\theta - \log P_e) \tag{45}$$

and

$$\log u_r \frac{n_{r-1}}{n_r} = \log u_{r-1} + \chi_{r-1}\theta - (9.080 - \tfrac{5}{2}\log\theta - \log P_e). \tag{46}$$

Then $Z(x)$ can be written for the three ionization stages $r-1$, r, and $r+1$ in the following form:

$$\log Z = x - \log \kappa_{\lambda\,\mathrm{eff}} - \log U_r + (\chi_{r-1} - \chi_{r-1,s}) \times (\theta - \theta_0) - (9.080 - \tfrac{5}{2}\log\theta - \log P_e) \quad \text{for } r-1, s, \tag{47}$$

$$\log Z = x - \log \kappa_{\lambda\,\mathrm{eff}} - \log U_r - \chi_{r,s}(\theta - \theta_0) \quad \text{for } r, s, \tag{48}$$

[1] In a longer, but more explicit, notation we often write $f(\alpha'J'; \alpha J)$, where $\alpha'J'$ denotes the lower level and αJ the upper level.

$$\log Z = x - \log \kappa_{\lambda\ \mathrm{eff}} - \log U_r$$
$$- (\chi_{r+1,\,s} + \chi_r)(\theta - \theta_0) + (9.080 - \tfrac{5}{2}\log\theta - \log P_e) \quad \text{for } r+1, s\,. \tag{49}$$

Our expression (25) for the line depth in the intensity can be written as

$$r_\mu(\Delta\lambda) = \int_{-\infty}^{+\infty} \frac{M^*}{\mu}\frac{Z^*}{\sqrt{V^2}} \times H(v, a) \exp\Big[-\int_{-\infty}^{x} \frac{M^*}{\mu}\frac{Z^*}{V} H(v, a)\, dy\Big] g_\lambda^\mu(x)\, dx\,, \tag{50}$$

where Z^* denotes $Z(x)$ multiplied by the negative absorption factor $[1 - \exp(-hc/\lambda kT)]$. We now make use of equations (8) and (22) to compute $W_{\mu,\lambda}/\lambda$. Note further that

$$d(\Delta\lambda) = \Delta\lambda_D\, dv = \frac{\lambda}{c}\sqrt{(V^2)}\, dv\,.$$

Furthermore, since $H(v, a)/\sqrt{V^2}$ varies only slowly with depth, we can take it out from under the integral sign in the exponent without serious error. In an atmosphere in which the turbulence varied steeply with depth, this approximation might have to be examined carefully. Thus we obtain for $W_{\mu,\lambda}/\lambda$, whose logarithm is the ordinate of the curve of growth,

$$\frac{W_{\mu,\lambda}}{\lambda} = \int_{-\infty}^{+\infty} \frac{M^*}{c\mu} Z^*(x) \int_{-\infty}^{+\infty} H(v, a) \times \exp\Big[-\frac{H(v, a)}{\sqrt{V^2}}\int_{-\infty}^{x} \frac{M^*}{\mu} Z^*(y)\, dy\Big] dv\, g_\lambda^\mu(x)\, dx\,. \tag{51}$$

Let us define

$$\frac{Y}{\mu} = \frac{M^*}{\mu\sqrt{V^2}}\int_{-\infty}^{x} Z(y)(1 - e^{-hc/\lambda kT})\, dy = \frac{M^*}{\mu\sqrt{V^2}}\int_{-\infty}^{x} Z^*(y)\, dy\,. \tag{52}$$

Elste introduced the normalized saturation function,

$$\Psi\Big(\frac{Y}{\mu}, a\Big) = \frac{2}{\sqrt{\pi}}\int_0^\infty H(v, a) \exp\Big[-H(v, a)\frac{Y}{\mu}\Big] dv\,, \tag{53}$$

which approaches 1 as $Y \to 0$. The Pecker (1951) saturation function differs from this expression by the coefficient $2/\sqrt{\pi}$. Hence equation (51) becomes

$$\frac{W_{\mu,\lambda}}{\lambda} = \int_{-\infty}^{+\infty} \frac{M}{\mu} Z(x)\, \Psi\Big(\frac{Y}{\mu}, a\Big)\, g_\lambda^\mu(x)(1 - 10^{-\chi_\lambda\theta})\, dx\,, \tag{54}$$

where we have defined

$$M = \frac{M^*\sqrt{\pi}}{c} = \frac{N_i}{N_H}\, g f_{r,\,s}\lambda\,[A]\, 10^{\theta_0\Delta\chi}\, \frac{\pi e^2}{mc^2}\, \frac{10^{-8}}{\mathrm{Mod}}\, \frac{1}{m_H\mu_0}\,, \tag{55}$$

or

$$\log M = \log\frac{N_i}{N_H} + \log\, g f_{r,\,s}\lambda\,[A]\, k + \theta_0\Delta\chi\,, \tag{56}$$

where

$$k = \frac{\pi e^2}{m c^2} \frac{10^{-8}}{\text{Mod}} \frac{1}{m_H \mu_0}. \tag{57}$$

Also

$$\log Y = \log M + \log \frac{c}{\sqrt{\pi}} + \tfrac{1}{2} \log \frac{\mu_i}{83.83} + \log \sqrt{\theta} \int_{-\infty}^{x} Z(x)\,(1 - 10^{-\theta_\lambda x})\, dx \tag{58}$$

if turbulence can be neglected. Otherwise V has to be used in place of ξ_{th} (cf. eq. [31]). Equation (54) permits the calculation of the center-limb variations of the equivalent widths of lines observed on the disk of the sun, once one has the weighting functions for a selected model. These equations have been applied for the calculation of the theoretical curves of growth used in the application of the Pecker theory to the analysis of the solar spectrum (Goldberg, Müller, and Aller 1960).

Now, using equations (17), (23), and (54), we proceed to calculate the equivalent widths as observed from the total disk of the star,

$$\frac{W_\lambda}{\lambda} = \frac{1}{F_{\text{cont}}/2} \int_0^1 \mu d\mu \int_{-\infty}^{+\infty} dx \frac{MZ}{\mu} \Psi\left(\frac{Y}{\mu}, a\right)(1 - 10^{-x^\theta}) \times \int_{r_\lambda}^{\infty} \frac{dS_\lambda(\zeta_\lambda)}{d\zeta_\lambda} \exp\left(-\frac{\zeta_\lambda}{\mu}\right) d\zeta_\lambda. \tag{59}$$

Now change the order of integration, integrating successively over μ, ζ_λ, and finally x, viz.,

$$\frac{W_\lambda}{\lambda} = \frac{2}{F_{\text{cont}}} \int_{-\infty}^{+\infty} dx MZ(x)\,(1 - 10^{-x_\lambda^\theta}) \times \int_{r_\lambda}^{\infty} d\zeta_\lambda \frac{dS_\lambda(\zeta_\lambda)}{d\zeta_\lambda} \int_0^1 d\mu \Psi\left(\frac{Y}{\mu}, a\right) \exp\left(-\frac{\zeta_\lambda}{\mu}\right). \tag{60}$$

The integration over the disk of the star involves the function $\Psi(Y/\mu, a)$.[2] We note that, over small regions in Y/μ, Ψ can be approximated by a formula of the type

$$\log \Psi = -m \log \frac{Y}{\mu} + \text{const.}, \qquad 0 \leq m \leq 1.25. \tag{61}$$

That is,

$$m = -\frac{d \log \Psi(Y/\mu, a)_{\mu=1}}{d \log (Y/\mu)_{\mu=1}} \tag{62}$$

and

$$\Psi\left(\frac{Y}{\mu}, a\right) \cong \Psi(Y, a)_{\mu=1} \mu^m. \tag{63}$$

With this approximation we then carry out the integration over the disk, to obtain

$$\int_0^1 \mu^m \exp\left(-\frac{\zeta_\lambda}{\mu}\right) d\mu = E_{m+2}(\zeta_\lambda). \tag{64}$$

[2] An alternate procedure has been proposed by H. van Regemorter.

The value of m will change with the depth in the star and will depend on the value of Y in a fashion known for any given model.

The exponential integral functions have been computed not only for integral values of m but also for $m = \frac{1}{2}, \frac{3}{2}, \ldots$ (Pecker 1953). For very weak lines, $m = 0$, and the corresponding weight function for the flux is simply

$$G_\lambda^0(\tau_\lambda) = \frac{2}{F_{\text{cont}}} \int_{\tau_\lambda}^{\infty} \frac{dS_\lambda(\zeta_\lambda)}{d\zeta_\lambda} E_2(\zeta_\lambda)\, d\zeta_\lambda, \tag{65}$$

while, for medium-strong lines, we have to calculate

$$G_\lambda^m(\tau_\lambda) = \frac{2}{F_{\text{cont}}} \int_{\tau_\lambda}^{\infty} \frac{dS_\lambda(\zeta_\lambda)}{d\zeta_\lambda} E_{m+2}(\zeta_\lambda)\, d\zeta_\lambda, \tag{66}$$

where m is a known function of Y which can be computed for any model atmosphere. The ratio by which the weight function $G_\lambda^0(\tau_\lambda)$ has to be multiplied in order to handle the gradient of the saturation function is called the "saturation weight" with respect to μ, W_S; hence

$$W_S = \frac{G_\lambda^m(\tau_\lambda)}{G_\lambda^0(\tau_\lambda)}. \tag{67}$$

The actual calculation of the weight function is conveniently carried out on a logarithmic scale as follows: It is assumed that the source function is linear for each step of $\log \tau_\lambda$. Then from equation (66) we find

$$G_\lambda^m(\log \tau_\lambda) = \frac{2}{F_\lambda(0)} \sum_{\log \tau_\lambda = 1}^{\log \tau_\lambda} \frac{\Delta S_\lambda(\log \tau_\lambda)}{\Delta \log \tau_\lambda} \times \int_{\log \tau_\lambda}^{\log \tau_\lambda + \Delta \log \tau_\lambda} E_{m+2}(\log \zeta_\lambda)\, d \log \zeta_\lambda \tag{68}$$

by summing upward from the deeper layers toward the surface. The weight functions and the saturation weights have to be computed for the optical-depth scale for the particular wave length under consideration. Then $G_\lambda^m(\log \tau_\lambda)$ has to be expressed in terms of $G_\lambda^m(\log \tau_{\lambda_0})$ by transforming to the $x = \log \tau_{\lambda_0}$ scale by using the relation

$$\tau_\lambda = \int_0^{\tau_{\lambda_0}} \frac{\kappa_{\lambda\ \text{eff}}}{\kappa_{\lambda_0\ \text{eff}}}\, d\zeta_{\lambda_0}. \tag{69}$$

We are now prepared to write down the basic equations for the curve of growth in the Pecker theory. Consider, first, the straight-line relation that would exist if no saturation effects were present. We set $\Psi(Y, a) = 1$ and $G_\lambda^m(x) = G_\lambda^0(x)$. Then we obtain, by integrating equation (54) over the disk of the star, using equation (17),

$$\frac{W_\lambda}{\lambda} = \int_{-\infty}^{+\infty} MZ(x)\, G_\lambda^0(x)\, (1 - 10^{-\kappa_\lambda \theta})\, dx = ML_\lambda^*. \tag{70}$$

We write the stimulated emission factor as

$$(1 - e^{-hc/\lambda kT}) = (1 - 10^{-\chi_\lambda \theta}) \qquad \text{with} \qquad \chi_\lambda = \frac{12395}{\lambda\,[A]}. \tag{71}$$

Very weak lines should fall on the straight-line asymptote to the curve of growth given by equations (70). Hence it is natural to choose as the abscissa for the curve of growth the quantity

$$\log C = \log g_r, {}_s f_r, {}_s \lambda k + \Delta\chi\,\theta_0 + \log L_\lambda^* . \tag{72}$$

We compute the integral L_λ^* for several values of the wave length over the observable range of the spectrum and for the necessary values of $\Delta\chi_{r,s}$. Then, for a given model atmosphere, an empirical curve of growth will consist of a plot of $\log W_\lambda/\lambda$ against $\log C$. Further, the straight line defined by equation (70) may be written with the aid of equation (56) in the form

$$\log \frac{W_\lambda}{\lambda} = \log C + \log \frac{N_i}{N_H}. \tag{73}$$

Hence, as soon as we can find the position of the theoretical curve of growth with respect to the 45° line, we can fit the empirical plot of $\log W_\lambda/\lambda$ versus $\log C$ against this theoretical curve to establish the abundance.

Making use of equations (59), (60), (63), (65), (66), and the definition (67), we obtain:

$$\frac{W_\lambda}{\lambda} = \int_{-\infty}^{+\infty} MZ\,(x)\,\Psi\,(Y,\,a)\,\frac{G_\lambda^m\,(x)}{G_\lambda^0\,(x)}\,G_\lambda^0\,(x)\,(1 - 10^{-\chi_\lambda\theta})\,dx = M\mathfrak{R}_\lambda^* \tag{74}$$

as the expression for the theoretical curve. The integrand is called the "contribution function." Let us now define

$$\begin{aligned}\Delta &= \log\left(\frac{W_\lambda}{\lambda}\right)_{\text{unsaturated}} - \log\left(\frac{W_\lambda}{\lambda}\right)_{\text{saturated}} \\ &= \log L_\lambda^* - \log \mathfrak{R}_\lambda^* ,\end{aligned} \tag{75}$$

which is the vertical distance of a point on the actual curve of growth from a point on the 45° line defined by equation (70).

2.4. Application of the Model-Atmosphere Procedure

The detailed procedure for computing a theoretical curve of growth is described elsewhere (Aller, Elste, and Jugaku 1957), and we merely summarize the essential steps here. First, one selects the model atmosphere he plans to use. With P_e, P_g, and T and $(\kappa_{\lambda_0} + \sigma)$ given as functions of τ_0, he computes τ_λ with the aid of equation (69) and the weighting functions $G_\lambda^0(x)$ for the range of wave lengths covering the observed spectral region (cf. eq. [68]).[3] Next one computes

$$G_\lambda^*\,(x) = G_\lambda^0\,(x)\,(1 - 10^{-\theta\chi_\lambda}) . \tag{76}$$

[3] The weighting functions are not very sensitive to the model either in the hot stars or in the sun, but the Boltzmann and Saha factors are sensitive to the model.

Then, for the element of interest, he computes U_r (eq. [43]), and $\log Z(x, \Delta\chi)$ for the energy levels of interest. For this step we must have appropriate tables of partition functions for the elements of interest. Next, one computes $L_\lambda^*(\Delta\chi)$ for each level $\chi_{r,s}$ and for a range of wave length sufficient to cover the lines of interest. With the aid of equation (72) one can then obtain the abscissae for the empirical curve of growth. The empirical plot enables one to guess the range of Δ, the amount of the displacement of a segment of the empirical curve below the 45° line. One then estimates a range of values of M, by noting that (cf. eq. [75])

$$\log\left(\frac{W_\lambda}{\lambda}\right)_{\text{saturated}} + \Delta = \log\left(\frac{W_\lambda}{\lambda}\right)_{\text{unsaturated}} = \log ML_\lambda^*, \qquad (77)$$

since $\log ML_\lambda^*$ defines the 45° line. For a given value of M and wave length in the spectrum, we compute $Y(x)$ with the aid of equation (58). With $Y(x)$ and a as arguments, one then finds $\Psi(Y, a)$ as defined by equation (53) and the corresponding saturation weights as given by equation (67). Then, using the integrand $L_\lambda^*(\Delta\chi)$ and the factors $\Psi W_s G_\lambda^0$, we compute the integrand of equation (74), which is the contribution function. If we are interested in the equivalent width as measured at a particular point on the disk, as in discussions of solar-line intensities, we can use equation (54) or its equivalent. Examples of calculations of contribution functions for lines of C, Ni, and Fe at different points on the solar disk are given, for example, by Elste (1955). For each different point of the solar disk one obtains a distinct curve of growth.

Furthermore, different curves of growth are obtained for different wave lengths and excitation potentials. As an illustration let us consider the curves of growth obtained by the Pecker theory for lines of C II and C III in a specific model atmosphere, in this instance Miss Underhill's Model II (1957). The parameters of this model are:

Composition — pure hydrogen, $\log g = 4.20$,

Boundary temperature, $T_0 = 16{,}800°$ K,

Effective temperature, $T_{\text{eff}} = 27{,}870°$ K.

Figure 1 shows the contribution functions for C II at λ 6600 with $\Delta\chi =$ 6.31 ev and for C III at λ 4650 with an excitation potential of 29.39 ev. The contribution function is of interest, in that it shows which layers of a stellar atmosphere contribute to particular lines. See, for example, the discussion by ten Bruggencate, Lüst-Kukla, and Voigt (1955) involving solar applications. Each curve in Figure 1 is characterized by the parameter $\log (W_\lambda/\lambda)_{\text{unsaturated}}$ as defined by equation (73). The larger the value of this quantity, the greater the number of atoms. Curves are exhibited for $\log (W_\lambda/\lambda)_{\text{unsaturated}} = -5.0$ and -4.0, corresponding to a tenfold difference in the number of atoms. The weaker C II lines are formed over a range in optical depth from 0.001 to 1.0, with a maximum near $\tau = 0.09$. If the number of C II atoms is increased by a factor of 10, the maximum is shifted to $\tau = 0.02$ as a consequence of the in-

fluence of the saturation function, $\Psi(Y, a)$. Notice that the C III lines are formed at much deeper layers than are the C II lines. The weaker lines originate, on the average, at optical depths of the order of 0.9. The stronger lines are formed, on the average, at $\tau \sim 0.5$ as a consequence of the influence of the saturation function. The integrals of the contribution functions over x give the theoretical log (W_λ/λ) as a function of the number of atoms acting to produce the lines.

Elste (1955) has published similar curves for the sun, e.g., for the lines of C I and Ni I at the center ($\mu = 1.0$) and near the limb (0.1). As would be expected, they show that the effective level of the origin of the lines is in much shallower layers near the limb than near the center of the disk.

Figure 2 gives the theoretical curve of growth for C II and C III. Notice that the C II curve for λ 3800 lies above the curve for λ 6600. The transparency of the atmosphere is greater near λ 3800 than it is near λ 6600. In the λ 6600 spectral region a greater contribution to the continuous spectrum arises in the same layers as those producing the C II lines than is true for the λ 3800 region. Similar considerations hold for the C III lines. Notice that for the smaller numbers of atoms the curve falls well below the 45° line. Referring to Figure 1, we note that the contribution function is shifted to such deep layers for the weaker lines that a substantial contribution to the continuum must occur above the line-forming region. Figure 2 exhibits the fact, previously noted in connection with the silicon lines in hotter stars (Elste, Aller, and Jugaku 1956), that for atoms in different stages of ionization it is necessary to use different curves of growth.

Before proceeding to the applications of the Pecker theory, we must discuss the implications of some of the approximations involved. The quantity a, defined by equation (32), must be taken as a constant throughout the atmosphere. We can estimate a by evaluating $\bar{x}$, the mean optical depth at which the line is formed, on the assumption of no saturation and then computing a for this point. We define this near optical depth, $\bar{x}$, by the expression

$$\int_{-\infty}^{\bar{x}} Z(x)\, G_\lambda^*(x)\, dx = \frac{1}{2}\int_{-\infty}^{+\infty} Z(x)\, G_\lambda^*(x)\, dx\,. \tag{78}$$

It corresponds to Traving's (1955, 1957) "Schwere Punkt." For this value of $\bar{x}$ we calculate a for the spectral line in question. In the second approximation we must take into account the saturation weights and obtain an improved value of a.

For weak or moderately strong lines the equivalent width does not depend critically on the value of a, and the assumption of a mean value for the atmosphere is sufficiently accurate. The Pecker theory would be less satisfactory for strong lines whose wings were determined by collisional damping which increased rapidly with depth in the star.

Nevertheless, it is of interest to carry out calculations by the Pecker theory

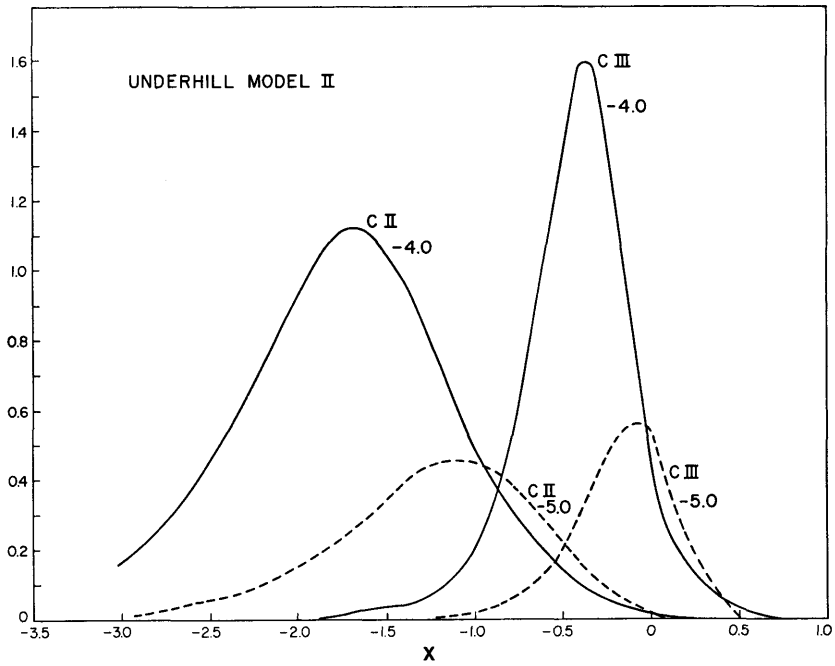


FIG. 1.—The contribution function for C II and C III in Underhill's Model II. Notice how lines of C III are formed in much deeper layers than are those of C II. Compare Fig. 4.

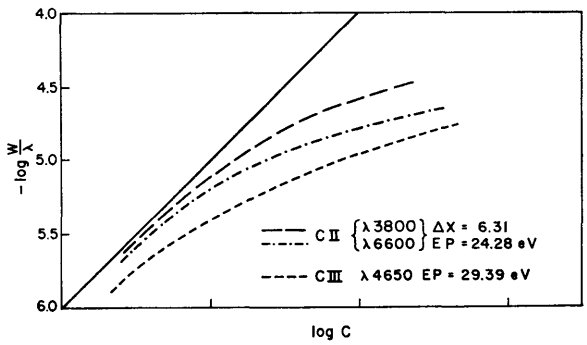


FIG. 2.—Theoretical curves of growth for C II and C III in Underhill's Model II. The two uppermost curves are for C II lines arising from a level at excitation potential = 24.3 ev, at λ 3800 and λ 6600 A, respectively. The lowest curve, C III, applies to a level at 29.4 ev, λ 4600, log $a = -2.0$.

and compare them with the results obtained by direct numerical integration. In Table 1 we compare the results obtained by direct numerical integration, by Miss Underhill, for three lines of Si II, Si III, and Si IV for her model atmospheres II and IV, with the predictions of the Pecker theory. For the lines of Si II and Si IV the agreement is satisfactory, but for the strong Si III lines the precise method predicts larger equivalent widths than does the Pecker theory. Hence, for very strong lines whose intensities are largely influenced by the damping constants, the Pecker theory may not be entirely adequate. In the analyses that we shall describe, the Pecker theory is applied for the most part to weaker lines ($W_\lambda < 100$ mA), which do not fall on the damping part of the curve of growth. If a line is so strong as to be affected by damping, the uncertainties in the collisional damping constants are often so large as to more than mask the theoretical approximations.

TABLE 1

COMPARISON OF EQUIVALENT WIDTHS CALCULATED BY PECKER THEORY WITH THOSE OBTAINED BY PRECISE CALCULATION

Ion	Wave Length	$\bar{x}$(U II)	Underhill Model II W_λ (mA)		Underhill Model IV W_λ (mA)	
			Pecker Theory	Precise Calculation	Pecker Theory	Precise Calculation
Si II	λ 4130	−1.1	80	85	59	58
Si III	λ 4552	−0.5	115	131	100	124
Si IV	λ 4089	+0.3	54	48	76	76

Miss Underhill determined the spectral types of her model atmospheres by calculating the intensity ratios of the aforementioned Si II, Si III, and Si IV lines and comparing them with the observations. If the theoretical Si III/Si IV ratio was fitted to the observations, the predicted intensities of the Si II lines would be too great, while if the Si II/Si III ratio was adjusted, the Si IV lines would not agree. Miss Underhill concluded that the proper procedure was to fit the Si II/Si IV line ratio. Then the observed Si III lines would be too strong. She attributed this discordance to the formation of the lines in possible chromospheric layers rather than to errors in the damping constants. The calculation of the corresponding contribution functions (Aller and Jugaku 1959*a*) to some degree substantiates Miss Underhill's conclusion. A substantial fraction of the integrand of equation (74) must be provided by layers above $x = -3$, and the atmosphere is not defined in this region. Of course, we cannot be sure that B stars have chromospheres comparable with that of the sun. The most frequently invoked mechanisms for the production of the solar chromosphere involve the unstable hydrogen-ionization zone that lies below the visible layers. A chromospheric explanation is not necessarily the whole story.

To state the problem in another way, the model atmospheres do not represent all the observations and therefore must be subject to some error. Similar difficulties are found with the McDonald-Milligan model and do not depend on the details of the model. We have assumed a static non-rotating star. If the star is rotating but is observed pole-on, zones of different latitude will have different effective temperatures, and hence the spectrum will be a composite one corresponding in detail to no unique static atmosphere structure. This question has been discussed by Struve (1945) and by Huang and Struve (1956), but it needs further investigations from the point of view of model atmospheres.

Figure 3 illustrates the curve of growth for the silicon lines in 22 Orionis. The theoretical curves are interpolated between two model atmospheres—

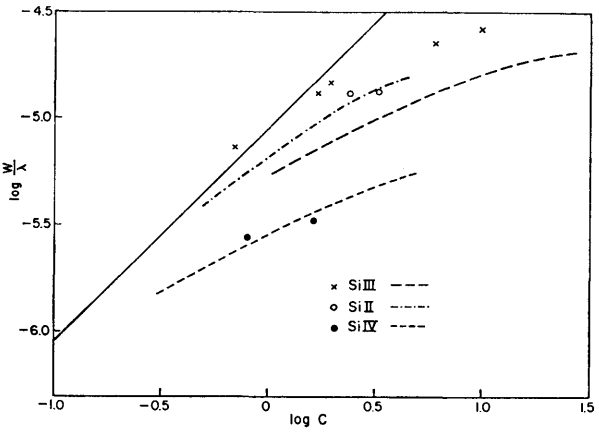


FIG. 3.—Curves of growth for silicon in 22 Orionis. The uppermost curve is for Si II; the lowest curve is Si IV. The observed lines of Si II (*circles*) and Si IV (*dots*) are fitted to the theoretical curves for Si II and Si IV. Notice that the Si III points (*crosses*) then fall far above the theoretical Si III curve, which is in the middle.

Underhill II ($\theta_{\text{eff}} = 0.181$) and the McDonald-Milligan model ($\theta_e = 0.252$)—by the method described on page 185. We have fitted the Si II and Si IV lines with a silicon abundance ratio $N(\text{Si})/N(\text{H}) = 0.85 \times 10^{-5}$. Notice that the Si III lines lie above their theoretical curve of growth but that the observed curve would fit the theoretical curve if shifted to the right by $\Delta \log C \cong 0.4$. We could fit the Si III and Si IV lines to the theoretical curve of growth by choosing a model with a lower temperature ($\theta_{\text{eff}} = 0.252$), but then the observed intensities of the Si II lines would greatly exceed the predicted values. If we fit the Si II and Si III lines, the predicted Si IV line intensities would greatly exceed their observed values. Evidently, a chromospheric origin cannot entirely remove the Si III discrepancy. We are left with a variety of alternatives: (1) A rapidly rotating star may have different effective temperatures at different parts of its surface. (2) Systematic errors in the f-values may exist, since, if the f-values for Si II and Si IV were each too large by about a factor of 3, the

discrepancy could be removed. (3) Errors in the equivalent widths occur; e.g., Miss Underhill suggests that the Si IV lines may have wings that would be lost in the background of the Hδ line. (4) Deviations from local thermodynamic equilibrium may be important. A considerable difficulty is encountered in the calculation of the magnitude of these deviations, since they depend on interlocking between widely separated spectral regions. Furthermore, accurate collision cross-sections, recapture coefficients, and other atomic parameters are required (cf. K. H. Böhm's discussion in chap. 3). Deviations from thermodynamic equilibrium are more pronounced higher in the atmosphere. Stronger lines formed principally in the uppermost layers (cf. Fig. 4) are more likely to

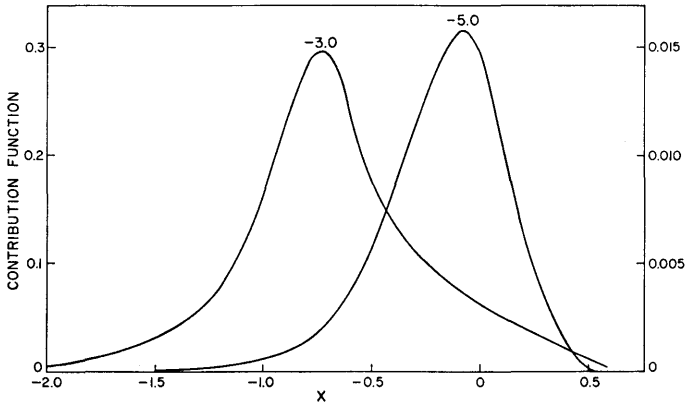


FIG. 4.—Contribution function for C III in Underhill's Model II. The abscissa is $x = \log \tau_0$; the ordinate is the contribution function,

$$Z(x)(1 - 10^{-\theta x_\lambda})\Psi(Y, a)\frac{G_\lambda^n}{G_\lambda^0}G_\lambda .$$

The scale on the left applies to the curve for $\log W/\lambda = -5.0$ or $\log M = -4.74$. The scale on the right applies to $\log W/\lambda = -3.0$ or $\log M = -2.74$. Notice that the weak line is formed primarily in optical depths between 0.4 and 1.5, whereas the strong line is formed mostly between $\tau = 0.07$ and $\tau = 0.5$.

be so affected. (5) The models themselves may be in error in the uppermost layers where strong lines are formed, because we have neglected their influence on the structure of the atmosphere itself, i.e., the "blanketing effect." In the region of the Lyman lines the continuous absorption is small, so these lines should attain a considerable breadth and appreciably affect the outflow of radiation in this general region and hence the temperature distribution in the uppermost layers.

For the time being, we shall follow the procedure of fitting the Si II and Si IV lines rather than use either the Si II/Si III or the Si III/Si IV ratio. If the error is due to inaccuracies in f-value, it seems more plausible that the errors occur in all three ions rather than that two are correct and the other is subject to a very

large error. A discriminant might be provided by measurements of the continuous spectrum and of the Balmer discontinuity. That is, one might use the continuous spectrum to decide between the models, as Bless (1958) has done for the A stars. Here the influence of the composition, particularly the H/He ratio, enters and affects the stellar continuum.

Model-atmosphere techniques may be applied to the analysis of actual stellar spectra in a variety of ways. In the sun the temperature distribution in the deeper layers $0.1 < \tau < 1.0$ is known from limb-darkening measurements. Strömgren (1940) assumed that the lines he studied in the solar spectrum were formed by the mechanism of scattering, and he calculated the profiles and total intensities of a number of lines for which estimates of f-values and damping constants were available. A similar procedure was applied to the B2.5 V star γ Pegasi (Aller 1949) with essentially the same model atmosphere as that used later by Miss McDonald (1953). This model atmosphere represented the Si III and Si IV lines but not the Si II lines. Later Nevén and de Jager (1954) employed an empirical model atmosphere intended to represent the profiles of the H lines. It did not reproduce the intensities of the ionized helium lines in the early-type stars for which it was intended.

Traving (1955) calculated a model atmosphere for use in the analysis of the spectrum of τ Scorpii. He assumed that the line profiles could all be represented by the empirical Minnaert (1935) formula,

$$\frac{1}{R} = \frac{1}{X_\nu} + \frac{1}{R_c}, \tag{79}$$

where R_c is the depth of the line at its center and R is the depth at the point ν in the profile. Here X_ν is the effective optical depth in the line, which is given by

$$X_\nu = \tilde{X}_0 H(v, a), \tag{80}$$

where $H(v, a)$ is the function tabulated by Harris (1948) and is defined by equation (35). The equivalent width is given by

$$W_\lambda = \int R d\lambda = \int \frac{d\lambda}{1/X_\nu + 1/R_c}. \tag{81}$$

The relation between W_λ and $\tilde{X}_0$ is nothing other than the Unsöld curve of growth (cf. § 2.3), where the ordinate is $\log (1/R_c)(W_\lambda/2\Delta\lambda_D)$ and the abscissa is $\log \tilde{X}_0/R_c$, where

$$\tilde{X}_0 = \frac{N_i}{\Sigma N_i} \frac{\pi e^2}{m c^2} \lambda^2 f \frac{1}{\sqrt{(\pi)}\,\Delta\lambda_D} \int_0^\infty \frac{N_{i,r,s}}{\Sigma N_{i,r}} \frac{G_\lambda(\tau_\lambda)}{\kappa_\lambda \mu_0 m_H} d\tau_\lambda. \tag{82}$$

Here N_i is the number of atoms of the element i per gram of stellar material; $N_{i,r,s}/\Sigma N_{i,r}$ is the fraction of all atoms of the given element that are capable of absorbing the line in question; κ_λ is the continuous absorption coefficient computed per gram of stellar material; μ_0 is the mean molecular weight of the unionized material; m_H is the mass of a hydrogen atom; and τ_λ is the optical

depth in the continuum at λ. The abscissa of the curve of growth is somewhat similar to the log C employed in the Pecker theory, but the method differs, in that a single curve of growth—namely, that of Unsöld—is used throughout.

From the curves of growth for different ions of the same element, e.g., C II and C III, O II and O III, Si III and Si IV, Traving derived a differential correction to the initially assumed model, namely, a lowering of the surface gravity. He applied a similar analysis (Traving 1957) to the O9 star 10 Lacertae, which had previously been analyzed by the curve-of-growth method (Aller 1946).

Aller, Elste, and Jugaku (1957) employed new observational data to analyze the spectrum of τ Scorpii by the Pecker theory. They used the temperature distribution of Traving's model atmosphere but chose a surface gravity of 2×10^4 dynes/cm^2 on the basis of the profiles of the hydrogen lines as interpreted by the Kolb theory (1956) (cf. § 4). The derived abundances differed from those obtained by Traving, partly because of the different theoretical treatment and partly because of the different observational material used in the two studies. Traving (1958) suggested that, by choosing different values of R_c for different ions, one could still use the Unsöld curve of growth, thus retaining the same type of formula for all profiles. This assumption is not made in the Pecker theory and is not supported by the precise line profiles calculated by Miss Underhill.

Probably the most precise calculation of the theoretical spectrum of a star was that carried out by Cayrel (1957) on the supergiant ζ Persei, Bl I*b*. He did not use the Pecker theory but computed the profiles and equivalent widths of the lines individually. He assumed a turbulent velocity of about 10 km/sec, computed a number of model atmospheres for surface gravities and temperatures in the neighborhood of the values appropriate to ζ Persei, and used the silicon lines to establish the temperature and the ratio of the depths in the Balmer line wings to the Balmer discontinuity to get the surface gravity. Since he took into account only the broadening due to ions, this method gives a surface gravity that is systematically too high. His model did give a good representation of the energy distribution in the continuum but yielded a Balmer discontinuity that was too large.

It is of interest that Cayrel found discordances between the abundances derived from the various silicon lines of the same magnitude as those obtained from the Underhill models. Thus he obtained the values for the ratio $N_{\text{element}}/N_{\text{total}}$ given in the accompanying table. The silicon lines would appear to present the same difficulties in all B-star atmosphere models.

	Si II		Si III		Si IV
λ 4128.....	0.23×10^{-4}	λ 4552....	1.0×10^{-4}	λ 4116....	1.2×10^{-4}
λ 4130.....	0.22×10^{-4}	λ 4567....	0.85×10^{-4}		
		λ 4575....	0.68×10^{-4}		

Hunger (1955) applied the same type of analysis to Vega as Traving used on τ Scorpii. From a curve-of-growth study he found $T_e = 9200° \pm 500°$ and selected log $g = 4.3$. He then computed four models with log $g = 4.3$ and effective temperatures $T_{\text{eff}} = 8160°$, 8660°, 9000°, and 9500°. He computed the Balmer line profiles by the Holtsmark theory, the spectrophotometric gradients, and the Balmer and Paschen discontinuities and compared these with the observations. Finally, he adopted $T_{\text{eff}} = 9500° \pm 300°$, log $g = 4.4 \pm 0.2$, and determined the abundances of the various elements. The surface gravity in Hunger's model seems to be too large. In view also of the appreciable differences between the curves of growth of neutral and ionized elements found in the more precise theories, some corrections to the numerical values for the abundances may be required.

Osawa (1956) at the Yerkes Observatory calculated a series of model atmospheres for A3–A9 stars with surface gravities of 0.32, 1.0, and 3.2×10^4 dynes/cm^2 and effective temperatures of 8900° and 7560° K. His calculations were more precise than those of previous workers, in that he took into account the continuous absorption by atomic hydrogen, the negative hydrogen ion, and the H_2^+ ion. Osawa did not calculate the detailed line spectrum but gave only the profiles of the H lines according to the Kolb theory. Bless (1958) finds an excellent agreement between the observations and the predicted continuous spectra and Balmer discontinuities. These models should prove very useful for studies of the absorption-line spectrum. Observational data for numerous main-sequence A stars are available or may be easily obtained. It is of interest that the assumption of pure radiative equilibrium in the atmospheres of these stars leads to predictions that are in good agreement with the observations of the continuous spectra. We might have anticipated that convective transport of energy would occur, since the hydrogen-ionization zone lies in the atmospheres, but convection does not appear to alter these temperature distributions.

When families of model atmospheres have been computed, as, for example, by Osawa and by Underhill, it is possible that none of them will represent the atmosphere of any particular star. Under these circumstances, one may interpolate between the different models. That is, we compute the theoretical curves of growth for each ion of interest according to the Pecker theory or by the method of direct numerical integration and also the values of log C. From a comparison of the predictions made from each model atmosphere we guess the best value of the effective temperature and surface gravity. Some features of the spectrum are sensitive to temperature, e.g., the intensities of lines of a given element in successive stages of ionization, e.g., C II/C III, O II/O III, etc. Other features, such as the profiles of the hydrogen lines in certain temperature ranges, are more sensitive to surface gravity.

Let us suppose we have two models—call them a and b—of the right surface gravity and that the effective temperature of the star in question, T_e, lies between them. $T_b < T_e < T_a$. Letting $\theta_e = 5040/T_e$, $\theta_a = 5040/T_a$, and $\theta_b =$

$5040/T_b$, we interpolate the abscissae in the curve of growth by the following expression:

$$\log C = \frac{(\theta_e - \theta_a) \log C_b + (\theta_b - \theta_e) \log C_a}{\theta_b - \theta_a}. \tag{83}$$

This method has been employed by Aller and Jugaku (1959*a*) and by Aller, Boury, and Jugaku in their analyses of B stars between B0 and B3. When only one model atmosphere is available, as was true for the investigation of τ Scorpii, it was necessary to use the method of differential correction (cf. Traving 1955 and Aller, Elste, and Jugaku 1957). The differential correction formulae, however, involve a number of assumptions, e.g., that the integral of the contribution function can be replaced through the atmosphere by the value of the integrand at some representative point and that the influence of the change in the weighting function can be neglected. Jugaku (1957) finds that, although the values derived by the formulae for the differential corrections can show qualitatively what occurs if the model is corrected for a small change in the temperature and electron pressure, it does not give the right amount of the correction quantitatively.

There are a number of limitations in the fine-analysis procedure that must be mentioned:

1. The fine-analysis method should be applied only after a simple curve-of-growth type of discussion has been completed (rough analysis). The amount of labor involved, even with simple graphical methods, is so great that it can be carried out only for a limited number of ions in a limited number of atmospheres.

2. In view of the labor involved, the method is worthwhile only if excellent observational material is available. It is not worthwhile, except for special problems, e.g., the hydrogen and helium lines, with low-dispersion material.

3. The assumed temperature distribution in the model atmosphere for any star except the sun is based on a number of assumptions:

a) Radiative equilibrium is usually assumed, although, if a good theory of convective transport of energy is available, there is no reason why it could not be applied.

b) Plane-parallel stratified layers are usually postulated. This assumption might break down in stars in which convection plays an important role, e.g., late-type stars and supergiants.

c) The influence of stellar rotation is generally neglected.

d) The influence of the chromosphere is likewise omitted; in fact, there is no theoretical basis for the calculation of chromospheres in early-type stars.

4. We have no checks on the data such as are provided by center-limb variations of the line and continuous spectrum of the sun.

5. Turbulence is difficult to take into account. By "turbulence" we mean the large-scale motion of masses of material. If the dimensions of the turbulent elements exceed appreciably the thickness of the atmosphere (i.e., the mean-free path of a light-quantum in the continuum is smaller than the diameter of

an eddy), we are concerned with macroturbulence. This type of turbulence will affect the profiles of the lines, very likely in such a way as to make it indistinguishable from the effects of an axial rotation of the star. Macroturbulence does not affect the equivalent widths of the lines. It simply widens them out and makes them shallower. On the other hand, if the mean-free path of a light-quantum is large compared with the size of the eddy, the equivalent width, as well as the line profile, will be affected. Both this microturbulence and the macroturbulence may occur in a stellar atmosphere. Furthermore, the sizes of the turbulent eddies may depend on the depth in the star, leading to a very complex situation. It is difficult to assess the role of turbulence in the sun and extremely hard to introduce it in a meaningful way in calculations of other stellar atmospheres (see Struve and Huang, in this volume, chap. 8).

6. In order to fit the model atmospheres to a particular star, we depend on certain physical parameters, such as *f*-values, damping constants, and the theory of line broadening. For example, in fitting the surface gravity, we are dependent on the theory of broadening of the hydrogen lines—a problem which fortunately appears to have been worked out in a satisfactory way.

7. Finally, there are possible deviations from thermodynamic equilibrium to be considered, particularly among the stronger lines. These effects are extremely difficult to handle by theoretical means.

2.5. Results Obtained for the Cooler Stars and the Sun

In the preceding section we emphasized the stars hotter than early A. Similar calculations can be carried out for stars of later spectral classes. In these stars, however, the hydrogen-ionization zone appears, at higher temperatures, in the visible layers and, at lower temperatures, just below the photosphere. Different authors have taken into account the role of this zone in different ways. Saito (1954, 1956) calculated models for an effective temperature of 10,700° K and tabulated the radiative and adiabatic gradients as functions of the mean optical depth and the geometrical depth. Saito assumed a H/He ratio of 17/3 and $\log g = 3.8$ and 4.2. On the other hand, Ueno and Matsushima (1950) computed a pure hydrogen model for the same effective temperature but for a slightly different temperature distribution. Saito's temperature distribution for his radiative models appears not to have satisfied the conditions of constancy of flux. Osawa's previously mentioned models referred to a spectral class of about A3 and were obtained for pure hydrogen, while Hunger's calculations were carried out for effective temperatures 8660° and 9500°. Przybylski (1953) calculated models of both the radiative type and the adiabatic type for $\log g = 4.5$ and $\theta_0 = 0.6$, 0.7, 0.8, 0.9, and 1.0 and for $\log g = 3.5$ and $\theta_0 = 0.6$, 0.8, and 1.0. Here $\theta_0 = 5040/T_0$, where T_0 is the boundary temperature. He used the Planck mean and the gray-body temperature distribution. Hack (1956*b*) carried out similar calculations for A stars and found considerable difference between convective and radiative models. She assumed that convection would set in as soon

as the radiative gradient exceeded the adiabatic gradient. Both Przybylski and Hack appear to have overestimated the effects of convection.

The theoretical treatment of convection in the atmospheres of A and cooler stars is extremely difficult. The problem has been examined in some detail by Spiegel (1958), but precise numerical calculations of the relative role of radiation and convection have not yet been carried out. It must be noted that Bless (1958) confirms the continuous energy distributions computed on the basis of pure radiative equilibrium by Osawa. Bless used a photoelectric scanner and was able to secure observations of high accuracy. Przybylski (1954) calculated the theoretical colors and equivalent widths of the K line of calcium for his models and compared them with the observations. He also reached the conclusion that the stellar atmospheres are probably not far from radiative equilibrium. Quoting Spiegel, "we must conclude that either convection is not extensive in A star atmospheres or that if it is, the effect on the structure of the stars is too deep optically to be detected." Convection might be stabilized by other factors, such as rotation (equatorial velocities of the order of 100–200 km/sec are common), or in some stars by magnetic fields. At the present time it would seem appropriate to assume, as a working hypothesis, that the atmospheres are in radiative equilibrium in the layers where the observable features of the spectrum are formed.

Probably the most ambitious project for the calculation of theoretical line intensities, hydrogen-line profiles, and features of the continuous spectra was that carried out by de Jager and Nevén (1957). They adopted surface gravities ranging from 10 to 100,000 dynes, and temperatures ($\tau = 0.0$)—i.e., limb temperatures—of 4000°, 4500°, 5000°, 6000°, 7000°, 8000°, 10,000°, 14,000°, 18,000°, and 25,000°. They computed the weighting functions for five wave lengths, the flux at nine points in the continuous spectrum, the spectrophotometric gradients, the Balmer discontinuities, and also the profiles of Hγ and Hδ and two lines of ionized helium. They also predicted the equivalent widths of seventy-eight lines of helium, carbon, nitrogen, oxygen, magnesium, silicon, calcium, and strontium, although the important elements of the iron group were omitted. They also give the mean optical depths of formation of these lines in the atmosphere.

Unfortunately, no effort was made to insure constancy of flux for the models in radiative equilibrium. They simply adopted a gray-body temperature distribution with a mean absorption coefficient defined by the Rosseland mean, an approximation that has been shown to be unsatisfactory for the hotter stars (e.g., Pecker 1951). Their predicted Balmer discontinuities for the A stars differ from those of Osawa and Hunger and also from the observations, and Bless concludes that their model atmospheres are of little use for the interpretation of the accurate spectrophotometric measurements now possible. The hydrogen-line profiles also disagree with the observations, probably mostly because the temperature distributions are at fault.

Martini and Masani (1957) have calculated model atmospheres for effective temperatures of 9700° K, and log g = 1.3, 3.5, 4.5; 5920° K with log g = 4.5; and 5300° K with log g = 4.5. For the cooler stars they have given models in both radiative and convective equilibrium. Canavaggia and Pecker (1952, 1953) have given models for giant stars with temperature between 5300° and 7750° and log g = 1.3–2.8.

Summarizing, a number of good model atmospheres have been computed in the neighborhood of spectral class A (e.g., Hunger, Osawa), but for stars of spectral class F, such as the dwarf Procyon, no such calculations are presently available. The giants and supergiants pose problems of a very different type, which we discuss in Section 4. For the sun, very detailed studies may be carried out which may serve as a guide for the analysis of similar stars.

Numerous models of the solar atmosphere have been computed, both empirical models based solely on observed data and theoretical models. An excellent summary of the earlier work has been given by Minnaert (1953). We concentrate our attention here on models that have been suggested for the study of the absorption-line spectrum.

From studies of the limb darkening and the energy distribution at the center of the solar disk, one can deduce the temperature distribution in the layers between $\tau = 0.10$ and $\tau = 1.0$ with reasonable accuracy (cf., e.g., Aller 1953, chap. 7). The continuous spectrum gives little information on the layers shallower than $\tau = 0.10$ or on the layers deeper than $\tau = 1.0$. For the deeper layers one may assume a radiative equilibrium temperature distribution or attempt to take the structure of the convection zone into account (e.g., Vitense 1953; Unno 1957; Spiegel 1958). These deeper layers have little influence, however, on the spectral-line intensities. The shallower layers, $\tau < 0.1$, on the other hand, do have a profound influence on the Fraunhofer spectrum.

Among recent models of the solar atmosphere we mention particularly that of E. Vitense Böhm (1954), who used Barbier's (1946) photographic limb-darkening measurements to establish the temperature distribution in the intermediate range of optical depth. She then used the center-limb variations of the stronger Fraunhofer lines (H, Fe) as measured by Houtgast (1942) and de Jager (1948) to get the temperature distribution in the outermost layers. She found the boundary temperature of the sun to be 3800° K. The best purely theoretical model of the upper photosphere is that by K. H. Böhm (1954*a*). He assumed that local thermodynamic equilibrium held right up to the surface and applied the Λ iteration technique of Unsöld (1955) and Strömgren to allow for the blanketing effect in the superficial layers. The strongest absorption lines affect the layers shallower than $\tau = 0.01$, while those of moderate strength affect the strata between 0.01 and 0.1. The boundary temperature of 3400° K corresponds to the central intensities of strong Fraunhofer lines interpreted according to the mechanism of absorption. The temperature corresponding to the ionization equilibrium in these outermost layers is certainly higher, and one

is tempted to conclude that the Kirchhoff law may fail in these strata. Neckel (1958) used the partial eclipse of June 30, 1954, to get the limb darkening in the sun for sin $\theta > 0.98$ at λ 4674 and hence the temperature distribution in the outermost layers. The model he found agreed with that by ten Bruggencate, Gollnow, and Jäger (1950) for $\tau_0 > 0.05$. At $\tau = 0.05$ he found a sharp temperature drop that led to a boundary temperature of 3500°–3600° K. From the central intensities of Fraunhofer lines of known relative *gf*-values Neckel then estimated the temperature distribution in the upper atmosphere and found a temperature fall in the outer layers that led to a temperature of 3600° K at $\log \tau = -5$. This point lies in the chromosphere, of course.

Michard (1953) obtained the temperature distribution from the limb darkening in the continuum and corrected it in the outer layers to get the excitation temperature of Fe I and Ti I. He obtained a boundary temperature of 4270° K.

TABLE 2

MODEL SOLAR ATMOSPHERE

(Compilation by G. Elste)

τ	log P_e	Temperature (° K)	τ	log P_e	Temperature (° K)
0.001	−0.78	4508	0.2	1.082	5373
.002	− .57	4520	0.3	1.231	5588
.003	− .45	4532	0.4	1.335	5747
.004	− .36	4549	0.5	1.444	5908
.005	− .288	4565	0.7	1.623	6146
.007	− .169	4590	1.0	1.837	6437
.010	− .047	4624	1.3	1.972	6684
.020	+ .197	4706	1.6	2.18	6895
.030	+ .352	4768	2.0	2.36	7119
.040	+ .464	4823	2.5	2.54	7390
.050	+ .554	4879	3.0	2.70	7556
.070	+ .685	4966	4.0	2.96	7863
0.100	+0.826	5091	5.0	3.13	8038

The solar model used in the Michigan abundance work was adapted by Elste in the following way. For the layers $0.1 < \tau < 1.0$ he used the (Pierce and Aller 1952) solar model with a metal abundance of 4×10^{-4} and a H/He ratio of 1/5. He adjusted the deeper layers to allow for the onset of convection and adopted a boundary temperature of 4500° K as corresponding more closely to the state of ionization and excitation. With this model he calculated a number of theoretical curves of growth by the Pecker theory and assumption of pure absorption. Table 2 gives temperatures and pressures on this model.

Although these models have some success in explaining the general behavior of lines in the solar spectrum, it appears to be impossible to represent the center-limb variations of the different Fraunhofer lines with a plane-parallel stratified solar atmosphere everywhere in local thermodynamic equilibrium (cf., e.g., Böhm 1954*b*; Elste 1955; Bretz 1956; Schröter 1957). It appears that the models

have to be modified to take into account the influence of large-scale mass motions (popularly known as "turbulence"), the temperature fluctuations connected with granulation, and, finally, the deviations from local thermodynamic equilibrium. Insofar as strong Fraunhofer lines are used to construct or modify existing models, the question of line-broadening mechanisms and non-coherent scattering comes in. For example, de Jager (1952) used the Balmer lines; but, since their cores arise in the chromosphere and a quantitative theory of hydrogen-line broadening is not available, the validity of this procedure is open to question. Hitotuyanagi and Inaba (1954) used the Na "D" lines and coherent scattering and attempted to derive temperature and pressure corrections, but the mechanisms of line formations and broadening are not quantitatively known.

By using weaker lines, some of the difficulties may be avoided. The weaker lines often arise from higher levels, and hence the mechanism of absorption may be assumed. The temperature distribution may play an important role through the Boltzmann factor, and, if there are "granular" and "intergranular" regions of different temperatures, the effects may not compensate. Furthermore, for these weaker lines the Doppler broadening becomes very important. The turbulence is anisotropic (Allen 1949), and the ratio of the tangential velocity to the radial component is about 1.6 (Waddell 1956; Suemoto 1957). For accurately determined profiles of weak lines, Goldberg (1958*a*) has devised a very simple and accurate method for obtaining the Doppler broadening parameter. In agreement with the results of Waddell and of Rogerson (1957), he finds that the turbulent velocity appears to be constant with depth. The motions deduced from the irregularities in the Fraunhofer lines observed under conditions of good seeing (Richardson and Schwarzschild 1950; McMath *et al.* 1956) refer to large-scale or macroturbulence, whereas the microturbulence that occurs in the equivalent width of the line is about five times greater.

Among the attempts to correct the solar model atmosphere by using the data of the weak lines, we mention those by Pagel (1955) and by Mitchell (1958). Pagel studied the center-limb behavior of infrared Fe I lines and compared the observations with the theoretical predictions based on the models of Pierce and Aller, de Jager, and Michard (1953). His final model agreed closely with that of Michard for layers deeper than about $\tau = 0.06$. In the outer regions he found a steeper temperature gradient and actually a temperature inversion. Mitchell adopted a new metal abundance ratio, $\log A = 4.28$ (A = H/metals), and concluded that his observations of the center-limb variations of weak lines could be best explained by lowering the electron pressure by about 50 per cent in the line-forming region.

Temperature inhomogeneities have led to various "two- or three-stream models" in which it is assumed that the photosphere consists of alternate ascending hot and descending cool columns, with perhaps a third column at rest. By introducing columns differing in temperature by 500° K, Böhm found that

an improved agreement between theory and observations for the center-limb variations of lines could be obtained. The discrepancies could not be removed entirely. Voigt (1956) used Böhm's three-stream model to explain the observations of the center-limb behavior of the infrared oxygen triplet λλ 7772, 7774, 7775, while Schröter (1957) found that the center-limb variations of weak lines and the profiles of several strong lines could be accounted for in a satisfactory manner by a two-stream model and the hypothesis of pure absorption.

Deviations from thermodynamic equilibrium exist in the outermost layers of the photosphere. Böhm (1954*b*) found that in the outermost layers the energy density of the radiation in the lines corresponded to the local temperature but that in the continuum it did not. The ionization was affected by an amount that depended on the element involved, the equivalent ionization temperature being always higher than the local temperature. Elste (1955) found that the ionization temperature exceeded the local temperature, and similar conclusions were reached by Miss Bretz (1956) from a study of the equivalent widths of 150 weak to moderately strong lines of titanium, vanadium, and chromium. Pecker and his associates (see especially the conference report, *Empirical Determination of Stellar Photospheric Structure*, ed. de Jager and Nevén, 1959) compared the central intensities of lines of the same multiplet, whose relative *f*-values were known, in an effort to find deviations from local thermodynamic equilibrium empirically. The large deviations which they find for some elements, e.g., titanium, are not confirmed by other studies (Goldberg, Müller, and Aller 1960) which use equivalent widths rather than central intensities. Uncertainties in the model atmosphere, in the *f*-values, in the relative roles of scattering and absorption, and in the central intensities themselves make it very difficult to assess the results obtained. Deviations from thermodynamic equilibrium certainly exist, but it seems unlikely that for the weaker lines they are as large as Pecker and his associates have claimed. For a concise account of the problems of the Fraunhofer spectrum see the article by Goldberg (1958*b*).

Summarizing, we note that the study of the center-limb variations of the continuous spectrum of the sun and of both the weak and the strong Fraunhofer lines leads to a number of conclusions concerning the solar atmosphere. The homogeneous atmosphere consisting of stratified plane-parallel layers is only a rough approximation, which has to be modified whenever high-precision applications are made. The modifications consist in replacing the homogeneous atmosphere by one in which streams of different temperatures ascend and descend, by the introduction of anisotropic turbulence, and by deviations from local thermodynamic equilibrium. These last-mentioned corrections differ from one element and probably from one energy level to the next. In addition to the difficulties posed by the atmospheric model, there are those associated with the mechanism of line formation, particularly with regard to the resonance lines. Also the damping constants and line-broadening coefficients are not well enough known for the stronger transitions. Solar model atmospheres might be

improved by using the center-limb variations of weak to moderately strong lines arising from higher levels, so that the mechanism of "absorption" could be assumed with some confidence.

Naturally, the hope is that from a study of the sun we may gain enough insight into the mechanics and physics of a dwarf-star atmosphere to make meaningful approximations to other stars. It is probable that G and K dwarfs have atmospheres that can be handled by techniques developed for the solar atmosphere. The M dwarfs probably present a host of other problems—similar to those we confront when we try to analyze the rocket ultraviolet spectrum of the sun. In the visible and photographic regions of an M dwarf the "continuum" is provided mostly by the overlapping wings of strong lines and densely packed molecular lines. Here one may have to proceed by a synthetic process, computing a family of model atmospheres and predicting the line spectrum and the continuous energy distribution by numerical integration. Such a problem need not be prohibitively time-consuming with the aid of modern electronic computational techniques.

Few theoretical model atmospheres have been attempted for late-type stars. As an example we may mention the work of Koelbloed (1953), who constructed atmospheric models partly analytically and partly by numerical integration for dwarf K1 and K5 stars and for a giant K2 star. He assumed a black-body type of temperature distribution (cf. eq. [1]) and compared results obtained by both the Rosseland and the Chandrasekhar mean absorption coefficient. He found no substantial differences between the model atmospheres thus obtained. The opacity was supposed to be produced by H^- ions only. The upper limit of the convection zone was found to be higher ($\bar{\tau} = 1.2$) for the K5 dwarf than for the K1 or the giant ($\bar{\tau} \sim 2$). Koelbloed calculated weighting functions and also contribution functions for the iron lines for weak lines in his model atmospheres. The lines used in his study were hardly "weak" in the sense of the theory of line formation. The analysis should be repeated with better data, atmospheric models, and an improved theory of line formation. We discuss Koelbloed's results after treating the curve of growth.

§ 3. THE CURVE OF GROWTH

The application of the fine-analysis procedures involving the model-atmosphere techniques and elaborate line-intensity calculations is hardly justified unless high-quality, high-dispersion data are available and good preliminary estimates of the surface gravity and effective temperature are known. The curve of growth, proposed originally by Minnaert and Slob (1931), provides a quick method for an analysis of a stellar spectrum.

For example, in the Milne-Eddington approximation, the ordinate is the quantity $\log (W/\lambda)(c/v)$, while $\log \eta_0$ is the abscissa. Here $\eta_0 = l_0/\bar{\kappa}$ is the ratio of the absorption coefficient at the center of the line to the continuous absorption coefficient. The theoretical curve consists of the precise relationship

between these two quantities; the empirical curve is a plot of log W/λ versus log η_0/N, where N is the number of atoms capable of absorbing the lines in question. N is, a priori, unknown, and the displacement of the empirical curve of growth vertically and horizontally to fit the theoretical curve establishes N and (c/v). The curve-of-growth analysis involves the following approximations:

1. The lines are all formed according to a specific mechanism, e.g., scattering or absorption or some mixture of the two.

2. We can specify a unique temperature and electron pressure which will completely describe the state of excitation and ionization for all elements in the atmosphere.

3. All lines have profiles given by a specific formula, and all lines of the same total intensity (equivalent width) have exactly the same profile.

4. The damping constant occurs as a free parameter, which may be adjusted for the atmosphere under question.

5. The stratification is specified. That is, the ratio of line to continuous absorption is constant (as in the Milne-Eddington approximation), or all the lines are formed in a layer overlying a photosphere which radiates a continuous spectrum (Schuster-Schwarzschild approximation).

There are often additional approximations in the practical working-out of the curve of growth. For example, it is frequently assumed that the Planck function can be developed as a linear function of the optical depth at the point in question, viz.,

$$B = B_0 + B_1 \tau_\nu \,. \tag{84}$$

This assumption is not essential, and some writers have examined the influence of the inclusion of other terms, e.g.,

$$B = B_0 + B_1 \tau_\nu + C e^{-a\tau_\nu} \,. \tag{85}$$

Hunger (1956) concluded that, with his formulation of the curve of growth for pure absorption, this exponential term has only a negligible effect. For scattering, there is likewise only a small effect. Hence, even if B is not a linear function of τ, one can use Hunger's formulation of the curve computed for a linear Planck function.

3.1. The Schuster-Schwarzschild Approximation

In the Schuster-Schwarzschild approximation, one supposes that the photosphere radiates a pure continuous spectrum and that the dark-line spectrum is produced in an overlying layer that absorbs (or scatters) only at the monochromatic frequencies.

Let us consider, first, Menzel's (1936) formulation of the curve of growth. Let $N_{r,s}$ denote the number of "active" atoms above the photosphere in the level (r, s) and let a_ν denote the atomic coefficient of line absorption. We postulate pure scattering. Menzel adopts as the formula for the residual intensity in the line the simple expression

$$r(\nu) = \frac{1}{1 + N_{r,s} a_\nu} \,. \tag{86}$$

The corresponding expression for the equivalent width, W_ν, expressed in frequency units, is

$$W_\nu = \int_0^\infty [1 - r(\nu)]\, d\nu = \int_0^\infty \frac{N_{r,s} a_\nu}{1 + N_{r,s} a_\nu}\, d\nu . \tag{87}$$

For lines broadened by the Doppler effect plus radiation and collision damping, $a_\nu = a_0 H(v, a)$ (cf. eqs. [27] and [35]). Menzel adopted a simpler expression, writing (Menzel 1931)

$$a_\nu = \frac{\pi e^2}{m c} f \left\{ \frac{1}{\sqrt{\pi}} \frac{c}{v\nu_0} \exp\left[- (\nu - \nu_0)^2 c^2 / \nu_0^2 v_0^2 \right] \right\}, \quad \text{or} \quad \frac{\pi e^2}{m c} f \left[\frac{\Gamma}{4\pi^2} \frac{1}{(\nu - \nu_0)^2} \right], \tag{88}$$

where v_0 is the most probable velocity of the atoms, ν_0 is the frequency at the line center, and Γ (cf. eq. [33]) is the damping constant. The first term is applied near the line center and for weak lines; the second term is applied only in the wings of strong lines. With this approximation for $H(v, a)$ (eq. [35]), Menzel then proceeds to the calculation of the curve of growth. Defining

$$X_0 = N_{r,s} \frac{\pi e^2}{m c} f \frac{1}{\sqrt{\pi}} \frac{c}{v_0 \nu_0}, \tag{89}$$

the optical depth at the center of the line, we find for small values of X_0, after noting that $W_\nu/\nu = W_\lambda/\lambda$,

$$\frac{W}{\lambda} = \sqrt{\pi} \frac{v_0}{c} X_0 \left(1 - \frac{X_0}{\sqrt{2}} + \frac{X_0^2}{\sqrt{3}} \cdots \right) \sim \sqrt{\pi} \frac{v_0}{c} X_0 , \tag{90}$$

when $X_0 << 1$.

When $\ln X_0 >> 1$, he finds the following asymptotic expansion:

$$\frac{W}{\lambda} = 2 \frac{v_0}{c} \sqrt{\ln X_0} \left[1 - \frac{\pi^2}{24} \frac{1}{(\ln X_0)^2} - \frac{7\pi^4}{384} \frac{1}{(\ln X_0)^4} \cdots \right], \tag{91}$$

while for very large values of X_0, when the line develops pronounced damping wings,

$$\frac{W}{\lambda} = \frac{\pi^{1/4}}{2} \left(\frac{v_0}{c} \right)^{1/2} \left(X_0 \frac{\Gamma}{\nu_0} \right)^{1/2} . \tag{92}$$

For intermediate ranges of X_0, Menzel used a semiempirical formula derived by J. G. Baker (1936). If we can assume that Γ/ν_0 is constant for the group of lines under consideration, then

$$\frac{W}{\lambda} = F(X_0) . \tag{93}$$

In order to represent the empirical curve of growth for iron obtained by Allen (1934), Menzel had to choose $\Gamma/\nu_0 = 1.52 \times 10^{-6}$, corresponding to a damping constant ten times the classical value.

Unsöld (1938) proposed a curve of growth very similar to that of Menzel except that, instead of using equation (86) for the residual intensity, he used Minnaert's empirical expression (eq. [79]) for the depth in the line. If $N_{r,s}H$ is the number of atoms above the photosphere, X_ν may be written as $N_{r,s}Ha_\nu$, where a_ν is the atomic-line absorption coefficient. As ordinate in the curve of growth, Unsöld employs $(1/R_c)(W_\lambda/2\Delta\lambda_D)$; as abscissa, $(1/R_c)(N_{r,s}Hf/\Delta\omega_D)$, where

$$\begin{aligned} \Delta\omega_D &= \frac{2\pi}{\lambda}\sqrt{\frac{2kT}{M}}, \qquad \text{circular-frequency units}, \\ \Delta\lambda_D &= \frac{\lambda}{c}\sqrt{\frac{2kT}{M}}, \qquad \text{wave-length units (cm)}. \end{aligned} \tag{94}$$

The Unsöld curve of growth can also be used in connection with model-atmosphere calculations (cf., e.g., Traving 1955). He then used, in place of $N_{r,s}Hf/R_c\Delta\omega_D$ as the abscissa, the quantity $\bar{X}_0/R_c$, where $\bar{X}_0$ is defined by equation (82), which reduces to

$$\bar{X}_0 = 3.75\times 10^{22}\frac{N_i}{\Sigma N_i}\frac{f}{\Delta\omega_D}\int_0^\infty \frac{N_{i,r,s}}{\Sigma N_{i,r}}\frac{G_\lambda(\tau_\lambda)}{\kappa_\lambda}\,d\tau_\lambda. \tag{95}$$

If we put in mean values of the quantities under the integral sign, there results

$$\bar{X}_0 = 9.40\times 10^{-2}\frac{N_{r,s}H}{\Delta\omega_D}f. \tag{96}$$

Hunger calculated curves of growth for true absorption for both the Milne-Eddington and the Schuster-Schwarzschild approximation, all based on the Minnaert formula (eq. [79]).

Wrubel (1954) has calculated exact curves of growth for the Schuster-Schwarzschild model for the integrated flux, based on Chandrasekhar's (1950) exact solution of the equation. If the law of darkening of the underlying photosphere (which radiates a pure continuous spectrum) is given as

$$I(0,\mu) = a + b\mu \tag{97}$$

and the optical depth at any point in the line is τ_1, then the residual intensity at that point in the line is

$$r = \frac{{}^4 + Ky}{\frac{4}{3} + \tau_1 + 2y}, \tag{98}$$

and

$$K = \frac{4}{3a/b + 2}, \qquad y = \frac{\alpha_2 + \beta_2}{\alpha_1 + \beta_1} - \frac{2}{3}, \tag{99}$$

where α and β are moments of Chandrasekhar's X- and Y-functions and y may be calculated in terms of τ_1. Then the equivalent width is computed from

$$\frac{W}{\lambda}\frac{c}{v} = \int_{-\infty}^{+\infty}(1-r)\,du, \tag{100}$$

where r is the residual intensity in the line (= 0 at the center of a perfectly black line) and

$$u = \frac{(\nu - \nu_0)}{\Delta\nu_0}$$

where $\Delta\nu_0 = (\nu/c)v$ (cf. eq. [34]). Here v (which is identical with the V of eq. [30]) denotes the most probable velocity of the atoms; it may include turbulent as well as gas kinetic contributions. Wrubel calculated curves for six values of the damping constant from $\log a = -3.0$ to $\log a = -1.0$ (cf. eq. [32]) in intervals of 0.4 and for $a/b = \frac{1}{4}, \frac{1}{2}, 1$, and 2. As abscissa, one employs τ_0, the optical depth at the center of the line. It is possible to interpolate between values of $\log a$ or between different values of a/b for a fixed τ_0 and reduce the calculations to a single curve of growth.

Pecker and van Regemorter (1955) have discussed the curve of growth for the Schuster-Schwarzschild model. Their curve agrees with that of Menzel only for very weak and for very strong lines, but the departures are not large. Furthermore, his curves corresponded to taking the weighting function at the surface, $G(0)$, equal to 1, but actually $G < 1$. The correct Schuster-Schwarzschild model curve of growth can be found from that of Menzel by a small deformation and by the translation in the abscissa by $\log G(0)$ for the curves for the total flux. Similarly, the Unsöld curve of growth does not coincide with the curve computed from the Schuster-Schwarzschild model with weighting functions. The curves may be brought into satisfactory coincidence by a shift in the abscissa by setting $\log R_c/\mu = \log g(0, \mu)$ for a curve of growth computed for $\cos\theta = \mu$.

3.2. Curves of Growth for the Milne-Eddington Model

In the Milne-Eddington model it is supposed that $\eta = l_\nu/\kappa_\lambda$ is constant with optical depth. That is, instead of the continuous spectrum being formed in one layer and the line spectrum in another, both the line and the continuous spectra are formed in the same layers.

Strömgren (1940) computed a convenient curve of growth based on the Milne-Eddington model. Wrubel (1949, 1950) used Chandrasekhar's exact solutions of the equations of transfer for the Milne-Eddington approximation to compute precise curves of growth. The expression for the residual intensity in the total flux is

$$r(\lambda) = \frac{L^{3/2}}{\frac{1}{3} + B_0/2B_1}\left(a_2 + \frac{B_0 a_1}{B_1 L} + \frac{1-L}{2\sqrt{L}}\, a_1^2\right), \tag{101}$$

where B_0 and B_1 are the coefficients in equation (84), for pure scattering

$$L = \frac{1}{1+\eta}, \tag{102}$$

and a_1 and a_2 are the first and second moments of Chandrasekhar's (1947) $H(\mu)$ function. Similarly, the expression for the residual intensity in the line at a point μ on the solar disk is

$$r(\lambda, \mu) = \frac{L^{3/2}}{\mu + B_0/B_1}\left(\mu + \frac{B_0}{LB_1} + \frac{1-L}{2\sqrt{L}}\, a_1\right) H(\mu). \qquad (103)$$

Wrubel computed curves for the flux for values of the damping ranging from $\log a = -3.0$ to $\log a = -1.0$ and for values of $B_0/B_1 = \frac{1}{3}, \frac{2}{3}, \frac{4}{3}$, and $\frac{10}{3}$. He computed curves of growth for $\mu = 1$ (center of solar disk), for the same values of B_0/B_1, and for $B_0/B_1 = \frac{1}{3}, \frac{2}{3}, \frac{11}{9}$, and $\frac{7}{3}$, in order to facilitate interpolation.

Curves of growth for pure absorption with profiles given by the Minnaert formulae have been published by Hunger. His curve of growth is almost exactly the same as that given by Unsöld (1938). Rough curves of growth based on the Milne-Eddington approximation for pure absorption (Aller 1956) have been replaced by exact curves computed by Wrubel, which we shall now describe.

Suppose that a spectral line is formed partly according to the mechanism of absorption and partly according to that of scattering. If the total line absorption coefficient is l_λ, let the fraction ϵl_λ be due to pure thermal processes that obey Kirchhoff's law, and let the fraction $(1-\epsilon)l_\lambda$ be due to pure scattering. Let us now redefine

$$L = \frac{1+\epsilon\eta}{1+\eta}. \qquad (104)$$

For pure absorption, $\epsilon = 1$, $L = 1$, and equations (101) and (103), which are valid for the Milne-Eddington model, now become

$$\begin{aligned} r(\lambda) &= \frac{1}{\frac{1}{3} + B_0/2B_1}\left(a_2 + \frac{B_0}{B_1}\, a_1\right), \\ r(\lambda, \mu) &= \frac{1}{\mu + B_0/B_1}\left(\mu + \frac{B_0}{B_1}\right) H(\mu). \end{aligned} \qquad (105)$$

Hence it is possible to compute curves of growth not only for $\epsilon = 1.0$ but also for any intermediate choice. One has to make the assumption that ϵ as well as η remains constant with depth in the atmosphere. Wrubel has computed curves for $\epsilon = 0.2, 0.4, 0.8$, and 1.0. We reproduce here, Figure 5, the curve for $B_0/B_1 = \frac{2}{3}$, and tabulate his results for $B_0/B_1 = \frac{2}{3}$ and $\frac{10}{3}$ and two values of the damping $\log a = -3$ and $\log a = -1$ (see Table 3). These curves should be used for curve-of-growth analyses for pure absorption and the Milne-Eddington approximation.

One cumbersome feature of the analysis with the aid of the Wrubel curves of growth is that the shapes and zero points in the abscissa scale depend on the wave length as the ratio B_0/B_1 varies. Hence it is necessary to apply corrections, $\Delta \log \eta_0$, to the abscissae to transform all the calculation to a single curve of growth. These corrections depend on the intensity, $\log (W/\lambda)(c/v)$, as well as on B_0/B_1. If all the lines fall in a given wave-length range, it is simpler to interpolate the whole curve of growth.

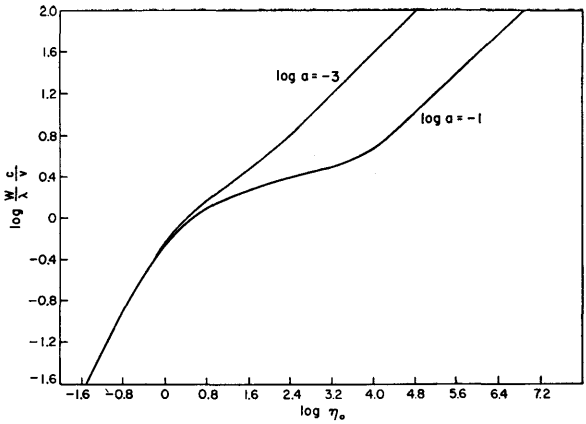


FIG. 5.—Wrubel's curve of growth for pure absorption $B_0/B_1 = \frac{2}{3}$. We plot log (W/λ) (c/v) against log η_0 for damping/Doppler ratios given by log $a = -3$ and log $a = -1$. (Note: the curves are mislabeled, the upper curve corresponding to log $a = -1$, the lower to log $a = -3$).

TABLE 3

CURVES OF GROWTH FOR PURE ABSORPTION ($\epsilon = 1.0$)
(Table Gives log W/b)

LOG η_0	$B_0/B_1=\frac{2}{3}$		$B_0/B_1=\frac{1.0}{3}$	
	log $a=-3$	log $a=-1$	log $a=-3$	log $a=-1$
−1.6	−1.660	−1.659	−2.137	−2.136
−1.2	−1.271	−1.269	−1.748	−1.746
−0.8	−0.898	−0.892	−1.375	−1.369
−0.4	−0.556	−0.543	−1.034	−1.020
0	−0.270	−0.244	−0.748	−0.721
+0.4	−0.055	−0.008	−0.533	−0.485
+0.8	+0.094	+0.171	−0.383	−0.306
+1.2	+0.196	+0.319	−0.281	−0.158
+1.6	+0.270	+0.463	−0.207	−0.014
+2.0	+0.327	+0.620	−0.150	+0.142
+2.4	+0.376	+0.794	−0.101	+0.317
+2.8	+0.424	+0.981	−0.053	+0.504
+3.2	+0.480	+1.176	+0.002	+0.698
+3.6	+0.556	+1.373	+0.078	+0.896
+4.0	+0.665	+1.572	+0.187	+1.095
+4.4	+0.811	+1.772	+0.334	+1.295
+4.8	+0.986	+1.972	+0.509	+1.495
+5.2	+1.176	+2.172	+0.699	+1.695
+5.6	+1.372	+2.372	+0.895	+1.895
+6.0	+1.570	+2.572	+1.093	+2.095

3.3. Comparison of Curves of Growth

All curves of growth have the same qualitative shape, an initial 45° rise where W_λ is proportional to Nf; a flat portion of varying length; and, finally, a damping-region rise, where $W_\lambda \sim \sqrt{Nf\Gamma}$. They differ from one another in details, depending on (*a*) the mechanism, absorption or scattering; (*b*) the model, usually Milne-Eddington or Schuster-Schwarzschild; and (*c*) the mathematical approximations made in the basic formulae.

Since different writers generally use different combinations of factors *a*, *b*, and *c*, meaningful comparisons are difficult. The general shape of the curve is fixed more by the absorption coefficient than by the model. Comparing the curves derived from the Schuster-Schwarzschild and Milne-Eddington approximation for pure scattering in the flux, Wrubel notes a number of differences. The effect of limb darkening is smaller in the Schuster-Schwarzschild model than in the Milne-Eddington model. In the latter model, line scattering and continuous absorption occur in the same layers, and hence a greater limb darkening affects the lines more than it would in the Schuster-Schwarzschild model. Furthermore, toward the limb, radiation leaving the photosphere at a large angle to the normal passes through more material in the reversing layer, and hence a stronger line is produced. Also the curves for different values of the limb darkening are shifted in opposite directions in the two models.

In comparing absorption and scattering for the same model (e.g., Milne-Eddington), it is found that the curves for the pure absorption mechanism change much more abruptly with B_0/B_1 than for the scattering mechanism. If a line is formed by the mechanism of pure scattering, its central intensity will always be zero, whereas the central intensity of a line formed according to the mechanism of pure absorption will always be fixed by the ratio B_0/B_1. A large B_0 and slow gradient of B_1 will yield a shallow line, regardless of the number of atoms acting to produce it.

Huang concluded from arguments based on averages of physical quantities evaluated through the atmospheres that Menzel's and Unsöld's curves of growth were among the best that have been proposed. We have seen how Unsöld's curve, originally applied to a Schuster-Schwarzschild model, can be used for absorption or for models taking into account stratification. Thus, for absorption, Hunger (1956) wrote

$$\frac{R}{R_c} = \left[1 + \frac{1}{CH(v, a)}\right]^{-1}, \tag{106}$$

where $C = \tilde{X}_0/R_c$. Barbara Bell (1951) modified Menzel's procedure by writing, in place of equation (86),

$$1 - r = \frac{R_c N a_\nu \kappa_0/\kappa_\lambda}{1 + N a_\nu \kappa_0/\kappa_\lambda}. \tag{107}$$

Here R_c is the central depth, which is computed on the assumption that the residual intensity at the center of the line is

$$r_c = \frac{B_\nu(T_0)}{B_\nu(T_b)}, \tag{108}$$

where she chose $T_0 = 4000°$ K as the boundary temperature of the sun. The factor κ_0/κ_λ allows for the variation in the optical depth of the photosphere with the wave length. For stars like the sun, $R \sim 1$.

Münch (1958) has criticized the use of the Minnaert formula (which was derived for the sun) in the analysis of hot stars. In the Milne-Eddington approximation he shows that the line depth is given simply by

$$R = R_c \frac{\overline{\eta}}{1+\overline{\eta}}, \tag{109}$$

as compared with the Minnaert-Unsöld expression,

$$R = R_c \frac{\overline{\eta}}{R_c+\overline{\eta}}, \tag{110}$$

where $\overline{\eta}$ is the mean value of η with respect to optical depth. When $R_c \sim 1$, the two formulae agree, but in hot stars, where R_c may be much smaller than 1, Münch concludes that the Unsöld approximation predicts line intensities that are systematically in error.

3.4. Construction of the Curve of Growth

Many examples of the actual construction of curves of growth based on various of the aforementioned approximations are to be found in the literature. A few examples of stellar applications are Greenstein (1942, 1948, 1949); Wright (1944, 1946, 1948, 1950); Koelbloed (1953); Unsöld (1941); Voigt (1952); Melnikov (1950, 1954); Miczaika *et al.* (1956), Huang and Struve (1956), and Helfer, Wallerstein, and Greenstein (1959). The curve of growth is also described in a number of handbooks and textbooks; cf., e.g., Barbier (1958), Hynek (1951, chap. 2) for Menzel's curve of growth, Unsöld (1955), Ambarzumian *et al.* (1958), and Aller (1953) (for Wrubel's curve of growth with an example worked out in detail).

We turn now to the practical problems that must be faced in the calculation of the curve of growth. The abscissa is usually something like X_0 defined by equation (89) for the Schuster-Schwarzschild model, or

$$\log \eta_0 = \log \frac{N a_0}{\kappa_\lambda} \tag{111}$$

in the Milne-Eddington model, which may be written in the form

$$\log \frac{N_{r,s}}{\kappa_\lambda} \frac{\pi e^2}{m c} \frac{c}{v\nu\sqrt{\pi}} f. \tag{112}$$

Furthermore, in order to use the curve of growth, we should know the damping constant Γ. Usually Γ is determined empirically.

Our observational data consist of measurements of the equivalent width, W_λ, for a number of lines for which estimates of f-values are available. Transition probabilities are obtained from one or another of the following sources: (1) theoretical f-values obtained by precise calculations in a few of the lighter atoms or by some kind of a "hydrogenic" approximation for transitions involving higher terms; (2) experimental f-values obtained from measurements made with, e.g., anomalous-dispersion methods, electric furnace, whirling-water arc, luminous shock tube, and electric-arc intensities; (3) empirical f-values obtained from solar or stellar curves of growth.

Most of these methods, particularly (3), give relative f-values, although some theoretical calculations can yield absolute f-values. The experimental methods can sometimes be calibrated to yield absolute f-values, although the best method appears to be the atomic-beam method introduced by Kopferman and Wessel (1951) and developed further by R. B. King and his collaborators (1954). Extensive discussions, compilations, and bibliographies of f-values have been published by various investigators. We shall not try to summarize the literature here but shall cite references and review articles where detailed data are listed (Landolt-Börnstein 1950; Unsöld 1955; Condon 1958; and Minnaert 1958). The determination of empirical strengths from solar and stellar data will be described below.

In order to combine into a single curve of growth all the lines of a given element in a given stage of ionization, we must make use of transitions that arise from different lower levels. The number of atoms in the level $N_{r,s}$ is related to the total number in the rth ionization stage by the Boltzmann formula,

$$N_{r,s} = N_r \frac{g_{r,s}}{u_r(T)} e^{-\chi_{r,s}/kT}. \tag{113}$$

Hence equation (89) may be written in the form

$$X_0 = N_r \frac{\sqrt{(\pi)}\,\epsilon^2}{mc} \lambda g_{r,s} f \frac{10^{-\theta\chi_{r,s}}}{v_0 u_r(T)}, \tag{114}$$

or

$$\log X_0 = \log N_r + \log g_{r,s} f\lambda - \theta\chi_{r,s} - \log v_0 u_r(T) + \log \frac{\sqrt{\pi}\,\epsilon^2}{mc}. \tag{115}$$

For a given element in a particular stage of ionization, everything on the right-hand side of the equation is constant except the second and third terms, so we may write

$$\log X_0 = \log C_{r,T} + \log gf\lambda - \theta\chi_{r,s}. \tag{116}$$

For each line $\log gf\lambda$ is known, so that we may form an empirical plot of $\log gf\lambda$ against $\log W/\lambda$ for each multiplet. The amount of the shift necessary to fit these empirical plots to the theoretical curve of growth will be

$$\log X_0 - \log gf\lambda = \log C_{r,T} - \theta\chi_{r,s} = \log Y, \tag{117}$$

and will depend on the excitation potential of the level and the value of θ. Each multiplet will give a distinct value of the shift $\log Y$, and a plot of $\log Y$ against $\chi_{r,s}$ will give, as the slope, the value of θ and, as the intercept, the value of $\log C_{r,T}$. If the absolute values of the f's are known, if the temperature is known sufficiently well to permit the calculation of $u_r(T)$, and if v_0 can be computed from the temperature (or the turbulent velocity found by methods to be described presently), we can find the absolute abundance N_r—the number of atoms above the photosphere in that particular stage of ionization. The slope θ gives us $5040/T_{\text{excit}}$, where T_{excit} is the so-called excitation temperature. This temperature is not necessarily the actual excitation temperature in the stellar atmosphere and, indeed, usually differs substantially from the ionization temperature or the effective temperature of the star. The T_{excit} may also differ from one element to another.

Once T_{excit} has been determined, all the data for a particular stage of ionization may be combined into a single curve of growth. The weaker lines often show a large scatter, and the stronger lines may not be sufficiently numerous to define the square-root portion of the curve of growth very accurately. The flat portion of the curve of growth is usually well defined. The vertical shift required to fit the theoretical curve of growth gives v, the most probable velocity of the atoms. If microturbulence is present, the required velocity will be

$$v = \sqrt{\left[\left(\frac{2kT}{M}\right) + \xi_{\text{tur}}^2\right]} \tag{118}$$

(cf. eq. [30]). In many giant and supergiant stars the turbulent velocity can be large (cf. § 3.6).

If the Milne-Eddington curve of growth is used in place of the Menzel curve, we replace the number of atoms above the photosphere by $N_{r,s}/\kappa_\lambda$, where $N_{r,s}$ now denotes the number of atoms per gram of material and κ_λ is the coefficient of continuous absorption per gram of material. Since $\kappa_\lambda = \kappa_\lambda(P_e, T)$ while P_e and T are not yet known, we can, in practice, replace κ_λ by $\kappa_{\lambda_0}(\kappa_\lambda/\kappa_{\lambda_0})$, where the ratio $(\kappa_\lambda/\kappa_{\lambda_0})$ usually depends on the electron pressure and on the temperature less steeply than does κ_λ itself. Thus

$$\log \eta_0 = \log N_r + \log gf\lambda \left(\frac{\kappa_{\lambda_0}}{\kappa_\lambda}\right) - \theta\chi_{r,s} - \log \kappa_{\lambda_0} v_0 u_r(T) + \log \frac{\sqrt{(\pi)}\, e^2}{mc}. \tag{119}$$

The analysis may be carried out in exactly the same fashion as before.

One of the frequent uses of the curve of growth is the comparison of the atmosphere of a particular star with that of the sun. This technique works well for comparing stars that do not differ greatly in temperature from the sun. For each line observed in the sun and in the star in question the following relation holds:

$$\log \frac{N_r^*}{N_r^\odot} = \log \frac{\eta_0^*}{\eta_0^\odot} + \chi_{r,s}(\theta^* - \theta^\odot) + \log \frac{\kappa_\lambda^*}{\kappa_\lambda^\odot} \frac{v_0^*}{v_0^\odot} \frac{u_r(T^*)}{u_r(T^\odot)}. \quad (120)$$

Notice that the f-values (which are often poorly known) cancel out and that one is left with ratios of other quantities, such as coefficients of continuous absorption, partition functions, and velocities. This technique, therefore, has some of the advantages of a "null" method and has been used particularly for comparing with the sun stars suspected of having abnormal compositions (cf., e.g., Greenstein 1948), although it may also be used for getting differences in T and P_e for a star's atmosphere (Hynek 1951, p. 63). In a more general form, the method consists of choosing a "normal" star of nearly the same spectrum and luminosity class as the object to be examined and then comparing with it the object of interest. We assume that we know the temperature, electron pressure, and composition of the "standard" star and proceed to derive the corresponding quantities for the "unknown" for both neutral and ionized atoms. One is also guided by the data of the continuous spectra, gradients, and Balmer discontinuities. In a more refined treatment, the line profiles as well are included in the analys is (cf., e.g., Chamberlain and Aller 1951; G. and M. Burbidge 1956, 1957). In comparing stars of different compositions, particularly of different H/metal ratios, we note the effects on $\kappa_\lambda(T, P_e)$, mean electron pressures, etc.

3.5. Applications of the Curve of Growth to Specific Stars

Studies of hotter stars by the curve-of-growth, Unsöld's (1941) method, have been carried out, for example, by Miczaika (1948), Voigt (1952), and Aller (1946, 1949) and by curves of growth based on the Milne-Eddington approximation by Aller (1949) and Hynek (1951, chap. 2). A comparison of results obtained for the supergiant ϵ Canis Majoris by different curves of growth has been given (Aller 1956), but the problem will have to be rediscussed, using better observational material and the more accurate Wrubel curves of growth for pure absorption. These studies are now in progress. Curves of growth for stars of spectral class A have been discussed by many observers. Vega has been discussed both by curve-of-growth and by model-atmosphere methods (Hunger 1955). Sirius and γ Geminorum were discussed by Aller (1942), while α Cygni has been studied by Buscombe (1951) and by Huang and Struve (1956). Stars in spectral classes F, G, and K have been investigated by many observers, particularly Greenstein, Fofanova (1950), and K. O. Wright.

As an example, one may mention K. O. Wright's curve of growth obtained for the neutral iron and titanium lines in the sun (see *Ap. J.*, **99**, 253, Fig. 2, 1944). He used equivalent widths measured by Allen and also values obtained from the Utrecht photometric atlas. The abscissae $\log X_f$ were based on King's laboratory gf-values, where

$$\log X_f = \log gf\lambda - \theta\chi_i. \quad (121)$$

Wright's empirical curve differs slightly from that of Menzel. In order to fit it, he had to adopt excitation temperatures of 4550° K for Ti I lines and 4900° K for Fe I. More recent curves of growth (e.g., Bell 1951) have allowed for the variation of the coefficient of continuous absorption with wave length.

With the aid of empirical curves of growth established originally from lines of known relative f-values, many workers have attempted to derive empirical line strengths by reading off log η_0's or log X's from the value of log W/λ. For example, Greenstein (1948) showed that if one selected a particular F star and established for it a good curve of growth, he could then use this curve to obtain empirical log η_0's that enabled him to construct curves of growth that had relatively little scatter for other F stars. Menzel and his co-workers at Harvard and later Wright (1944) and Barbara Bell (1951) used this method to determine empirical log X's for lines of many elements. Miss Bell asserted that different elements or even different excitation levels of the same element (e.g., Fe I) had different curves of growth. This result would be expected on the basis of a fine analysis, but it is doubtful whether the purely empirical approach is the best method for handling this problem.

Empirical line strengths derived from solar or stellar curves of growth possess certain advantages. They allow, albeit crudely, for blends and stratification effects and are doubtless useful for comparing stars of nearly the same spectral classes, e.g., the sun with a G5 V star. They are of dubious value if we try to use them for stars of very different temperature. The large scatter in some of the published curves of growth for A stars, for example, may arise from the use of solar log X_f's. The contribution functions, blends, etc., are quite different in the two kinds of stars. Generally speaking, it is better to use laboratory gf-values than empirical line strengths derived from stellar curves of growth. Effort should be concentrated on the improvement in the fundamental physical data on f-values and damping constants.

As one example of the application of the curve-of-growth technique to a giant star, we give some results obtained at Michigan from an analysis by Wright's (1950) methods of his (unpublished) observations of the K2 III giant γ^1 Andromedae (see accompanying table). An ionization temperature of 4230° K

Ion	T_{exeit} (° K)	Turbulent Velocity (km/sec)		Ion	T_{exeit} (° K)	Turbulent Velocity (km/sec)	
Fe I.....	2940	3.26	All lines	Ti I.....	3578	3.6	$3d^34s$ configuration
V I.....	3550	2.8	All lines	Ti I.....	2560	5.1	$3d^24s^2$ configuration

was assumed. For comparison, we include a summary of the results obtained by Wright from his analyses of the curves of growth for α Bootis, K2 IIIp,

and γ Draconis, K5 III (Table 4). Notice that for V I and Ti I different turbulent velocities are found for different configurations, illustrating one of the difficulties in the curve-of-growth analysis. The damping constants do not differ greatly from the classical values, except for the high-excitation Fe I lines, a result in harmony with theoretical expectations.

Different ions may show different curves of growth in supergiant stars. This phenomenon, suggested for α Cygni (Aller 1942*b*), seemed established convincingly by K. O. Wright's (1946) studies of α Persei, where the neutral iron followed a curve of growth somewhat different from that found from ionized atoms.

3.6. Effects of Turbulence on the Curve of Growth and on Line Profiles

Many years ago Struve noticed that in certain stars, such as 17 Leporis or ϵ Aurigae, the flat part of the curve of growth was very much higher than in

TABLE 4

ATMOSPHERIC PARAMETERS DERIVED FROM CURVES OF GROWTH FOR ARCTURUS AND γ DRACONIS*

Atom	Configuration	Arcturus			γ Draconis		
		v (km/sec)	Γ/γ	T_{excit} (° K)	v (km/sec)	Γ/γ	T_{excit} (° K)
Ti I	$3d^24s^2$	3.3	1.6	2475	6.0	1.6	2725
	$3d^34s$	4.4	1.5	3300	5.4	1.5	3125
V I	$3d^34s^2$	3.8	3.2	3550	5.8	2.6	3375
	$3d^44s$	2.8	3.2	3550	3.1	1.6	4125
Fe I	$3d^74s$	2.7	1.3	3500	3.4	3.6	3175
	$3d^64s^2$	.....	.....	.....	.....	.....	.....
	$3d^64s4p$	2.7	6.3	3900	3.4	10.0	4275

* K. O. Wright, *Pub. Dom. Ap. Obs. Victoria*, **8**, 315, 1950.

normal main-sequence stars. Interpreted as gas kinetic motions of the radiating atoms, the temperatures derived corresponded to fantastic values of hundreds of thousands or millions of degrees. The observations could be explained by postulating mass motions in the radiating gases, called "turbulence" by more or less common consent.

These large-scale mass motions appear to be common in the atmospheres of giants and supergiants (cf. Wright's 1957 report and chapters 8 and 9 of this volume). Here we shall be concerned with turbulence from the point of view of the curve of growth. The hydrodynamic implications of this phenomenon in connection with the interpretation of giant and supergiant atmospheres are also treated.

From a careful study of the curves of growth of individual elements in late-

type giant and supergiant stars, Wright and van Dien (1949, 1955) concluded that turbulent velocities derived from curves of growth for giant stars are different for ionized and for neutral atoms. In Fe I the turbulent velocities are different for lines of different excitation potentials. In ϵ Aurigae turbulent velocities found from the curve of growth ranged from about 20 km/sec for $\chi_i = 0.5$ ev to 2 km/sec for $\chi_i = 4.0$ ev!

The curve-of-growth results are based on an integration over a large range in optical depth, and it is of interest that Wright's results are substantiated by independent investigations based on line profiles (Huang and Struve 1952) and in the atmosphere of the eclipsing star ζ Aurigae (Wilson 1948; Wilson and Abt 1954).

It is important to realize that turbulence affects not only the equivalent widths but also the line profiles, and in different ways. Huang and Struve (1952) proposed a method utilizing both the equivalent widths, W_λ, and the half-widths, D_λ, of absorption lines to get turbulent velocities of both large and small eddies. One kind of Doppler width is obtained from an analysis of the equivalent widths, viz.,

$$(\Delta\lambda_D)_1 = \xi_1 \frac{\lambda}{c},$$

where ξ_1 is the turbulent velocity obtained from the curve of growth, i.e., the thermal motion plus the motion of the small eddies (diameter $\ll$ thickness of line-forming region).

On the other hand, the line profiles yield a half-Doppler width,

$$(\Delta\lambda_D)_2 = \xi_2 \frac{\lambda}{c},$$

where ξ_2 is the turbulent velocity implied by the line profiles, i.e., it includes the thermal motion plus the contributions from both kinds of eddies.

They developed a theoretical line-width correlation-curve between $W_\lambda/\Delta\lambda_D$ and $D_\lambda/\Delta\lambda_D$. Then, from the observations, log W_λ/λ is plotted against log D_λ/λ, and the shifts required to fit the empirical to the theoretical curves give log $(2\xi_1/c)$ and log $(2\xi_2/c)$, respectively. Applying this method to δ Canis Majoris, they found that the large eddies seem to have a velocity of about 6 km/sec, whereas the small eddies had velocities that depended on the excitation potential of the line in question. Huang and Struve used a Minnaert type of formula. With a curve of growth based on the Pecker type of theory, van Regemorter (1955) obtained a theoretical correlation-curve that was sufficiently different to produce profound changes in the numerical values of the macroturbulence and microturbulence that were obtained.

Huang and Struve (1955) subsequently developed another type of analysis of turbulence in which they considered the correlation between the central depth of the line and the equivalent width. The plot of central depth versus equivalent width gives a curve whose slope is well defined for $W_\lambda = 0$, but broadening by

convection or rotation gives theoretical curves so closely resembling one another that they cannot be distinguished. Deviations from thermodynamic equilibrium could further complicate the picture.

Since turbulent eddies of different sizes appear to exist in stellar atmospheres, particularly late-type giants and supergiants, the curve-of-growth analysis by itself would appear to be inadequate. Most urgently needed are accurately measured profiles of lines of different intensities and excitation potentials. Engaging results on the possible relative roles of micro- and macroturbulence have been obtained by Gathier (1955) with material of relatively low dispersion. Higher-dispersion material might decide some of the questions raised in this study (cf. § 4). An application of the method proposed by Goldberg (1958*a*) for the empirical analysis of line profiles should prove fruitful if observations of sufficient resolution can be attained.

Eclipsing binaries such as 31 Cygni (McKellar *et al.* 1952; Underhill 1952*b*) or ζ Aurigae (Beer 1933, 1940; Wellman 1936; Fracastoro 1949; Wilson 1948; Groth 1955, 1957) offer some of the most promising means for studying the atmospheres of supergiant stars and evaluating the role of turbulence. Wilson and Abt (1954) found that they could explain the observations of ζ Aurigae only by assuming discrete clouds of absorbing material, while the variable complex structure of the K line in 31 Cygni (McKellar *et al.* 1952, 1958) gives evidence for the existence of these absorbing clouds and filaments. In late-type giants there is probably no clear demarcation between chromosphere and photosphere.

3.7. Specific Advantages and Disadvantages of Curve of Growth

The great advantage of the curve of growth is that it provides a rapid means for the analysis of a stellar spectrum to yield such quantities as the mean electron pressure, average excitation temperature, ionization temperature, etc. These quantities are indispensable preludes to further analyses by more refined methods. The curve of growth is useful for making comparisons with normal stars of abundances in stars suspected of having abnormal compositions.

In certain types of objects, such as cool giants and supergiants, model-atmosphere techniques often cannot be used, as we cannot yet calculate the structures of atmospheres which are dominated by large-scale hydrodynamic turbulent motion. Eventually, with the aid of advances in aerodynamics and careful studies of certain eclipsing systems, we may be able to construct appropriate models. For such stars we cannot yet go far beyond certain of the limitations of curve-of-growth techniques.

One shortcoming of the curve of growth is that it makes no use of much important data—namely, the profiles of the lines. Particularly in studies involving turbulence and large-scale motion it is desirable to use line-profile data, as the studies of Huang and Struve have shown. Furthermore, even when there is no turbulence, line-profile studies sometimes enable the observer to make judicious

estimates concerning the effects of line overlaps and blends, as illustrated, for example, in the study of the λ 4227 and K lines in the K0 V dwarf ε Eridani (Liller and Lewis 1952). By concentrating on lines whose profiles are sensitive to density effects, e.g., the H lines and certain strong resonance lines of abundant elements, as well as on the measurement of the equivalent widths of lines over a large range in excitation potential, we can obtain much more information than can be gotten from a curve of growth alone.

The accurate measurement of equivalent widths is necessary to a curve-of-growth analysis as well as to fine-analysis procedures. Aside from the photometric difficulties, there are two intrinsic sources of trouble that beset any line-intensity measurements, particularly those of weak lines: (*a*) the location of the continuum and (*b*) the influence of blends. Both these difficulties become enhanced in cool stars, particularly in blue and violet spectrum regions.

3.8. Comparison of Curve-of-Growth and Model-Atmosphere Results

It is of considerable interest to compare results obtained from the analysis of the same data by the curve-of-growth and by the model-atmosphere technique. A number of such comparisons have been made by the Kiel group (Hunger 1955; Traving 1955, 1957) for τ Scorpii, 10 Lacertae, and Vega, with the conclusion that, for the hottest stars at least, the two methods give closely comparable results for abundances. Since the same theoretical curve of growth was used in each case, although the effects of stratification were taken into account in the abscissa with the aid of the model atmosphere, some of the intrinsic differences are minimized. In the analysis of the sun, large abundance differences are found between the two methods when we consider elements represented by lines of widely differing excitation and ionization potentials, e.g., K I and O I, which cannot be represented on the same curve of growth.

Stratification may tend to falsify ionization temperatures derived by curve-of-growth analyses. For example, in his study of dwarf and giant K stars by both curve-of-growth and model-atmosphere methods, Koelbloed (1953) noted that the observable Fe II lines, $\chi_i \sim 2.8$ ev, were formed in much deeper layers than in the sun. When the ionization is derived from the Fe II and Fe I lines, we are comparing neutral lines formed in shallow layers with ionic lines formed in deep layers. Hence a degree of ionization that is systematically too high is obtained. Koelbloed concluded that seemingly more reliable ionization temperatures could be found when weak resonance lines from both neutral and ionized atoms could be compared, but the problem has to be re-examined with a more detailed theory of line formation and more precise models.

Stratification may affect the excitation temperature and turbulent velocities derived from the curve of growth in a complicated way. Thus the excitation temperature would appear to have a meaning only if weak lines are used; otherwise the excitation "temperature" depends on the intensity in a complicated way and may not even correspond to any temperature existing in the atmosphere.

The excitation temperature appears to fall with increasing line intensity. Van Regemorter (1955) explained qualitatively a result by King and Wright (1947) that they had attributed to microturbulence. Vanadium ($\theta_{\text{excit}} = 0.94$) has mostly weak lines, titanium ($\theta_{\text{excit}} = 1.06$) has both moderate and weak lines, and chromium ($\theta_{\text{excit}} = 1.33$) has strong, moderate, and weak lines.

Conclusions drawn from curve-of-growth studies concerning the dependence of turbulence on excitation potential and height may have to be re-examined with the aid of line-profile studies and model-atmosphere calculations.

§4. ABSOLUTE-MAGNITUDE EFFECTS

Luminosity effects in stellar spectra were first explored by qualitative methods. Eye-estimates of line-intensity ratios or sometimes of the background continuum were correlated with absolute magnitudes. Among the most extensive early studies were those of Adams and Kohlschütter and of Adams and Joy, culminating in the catalogue of 4179 stars by Adams, Joy, Humason, and Brayton (1935). The Yerkes or Morgan-Keenan (1943) system of spectral classification is based on empirical criteria which differ for different parts of the spectral sequence. The system is tied to specific stars for which the excitation or effective temperature or bolometric absolute magnitude is not necessarily known. In practice, one observes both standard and program stars with his own spectrographic equipment and then finds the particular criteria which can be employed at the available dispersion. Although the Morgan-Keenan system is invaluable for practical work, from the theoretical point of view it suffers from the fact that it is not defined in terms of quantitatively measured parameters.

Theoretical calculations of stellar structure and evolution lead to models with specified masses, radii, and effective temperatures. Model stellar atmospheres may then be computed for a given surface chemical composition, surface gravity, and temperature. On the basis of these models, it is possible to compute certain observable parameters, such as spectrophotometric gradients, Balmer discontinuities, and the profiles of certain hydrogen lines, at least for spectral classes earlier than F and G. For the later spectral classes, only a few parameters may be computed reliably by theory, and no detailed theoretical studies have yet been made.

Many years ago Lindblad (1922) attempted to apply spectrophotometric methods to determination of intrinsic stellar luminosities. He used the relative intensity of spectral regions on either side of λ 3907 and the relative intensities of the CN bands and the adjacent spectral region. Since then, he and his coworkers have devoted much attention to this problem, with the result that it is now possible to get the absolute magnitudes of stars that are too faint to classify by the usual methods. Much of the Swedish effort has been devoted to the later spectral classes, and the criteria employed are purely "empirical" in the sense that they cannot be predicted quantitatively from the mass and radius of the star.

More immediately tractable from the theoretical point of view are the classification criteria measured by Chalonge and his various co-workers (1952, 1956) and by Strömgren (1955). In both these systems, one uses as the basis of classification the hydrogen lines or the continuous background that depends on hydrogen.

Chalonge *et al.* use three parameters: (1) the magnitude of the Balmer discontinuity, D; (2) the wave length, λ_1, at which the logarithm of the intensity of the smoothed continuum drawn over the confluent Balmer lines falls to a value $D/2$ below the continuum on the longward side of the Balmer discontinuity; and (3) the absolute gradient, ϕ_B, in the blue region λλ 3800–4600 A. The first two criteria are not affected by space reddening, but the gradient is steepened thereby. Hence it is necessary to use unreddened stars to secure a suitable calibration. The measurement of these three parameters defines a three-dimensional surface that permits, without ambiguity, the assignment of all stars classified on the Morgan-Keenan system. Since the MK system uses discrete steps and the D, λ_1, ϕ_B system uses continuously varying quantities, the former occupies distinct areas on the $D\lambda\phi$ surface. For many purposes, it suffices to use λ_1 and D only. These define the properties of the star more precisely than does the MK system, even though they are measured on plates of lower dispersion.

The U, B, V three-color photometry system of Johnson and Morgan (1953) may also be used to estimate luminosity effects. The $U - B$ color index is essentially a measurement of the Balmer jump, although it can be affected by space reddening. Spectral-energy scans, such as those obtained by Code and by Bless, provide a refinement of this technique, in that they permit one to make use of additional parameters and to assess the effects of the lines.

One of the most powerful methods of two-dimensional spectral classification is that of photoelectric narrow-band photometry developed by B. Strömgren. The method as applied to early-type stars is based upon the following considerations: In the B-type stars, for example, where the effects of stellar evolution occur most rapidly, the Balmer discontinuity is a good index of the surface temperature, whereas studies by Lindblad, Anger, Öhman, Petrie, and others have shown that the total intensities of $H\beta$, $H\gamma$, and $H\delta$ are good indices of the surface gravity. Strömgren used six filters, which enabled him to compare the energy subtracted by the $H\beta$ line with that in spectral regions on either side and also the amount of the Balmer jump. Thus he was able to measure two indices, l, which gave the strength of $H\beta$, and c, which gave the Balmer discontinuity. When a plot of c versus l is made, the main-sequence and supergiant stars are clearly separated. Furthermore, the accuracy of the technique is sufficiently great that stars of different ages on the main sequence may be separated from one another. As a star evolves, its radius and luminosity change. Hence the surface gravity and temperature change, and the observable parameters, such as the Balmer discontinuity, the gradients, and the hydrogen-line inten-

sities, all vary in a way that can be calculated by the method of model atmospheres. With his observed parameters, c and l, and with the aid of the aforementioned theoretical considerations, Strömgren was able to determine the ages of clusters or even individual stars. Narrow-band photometry and age determinations may also be carried out for stars of spectral classes A and F. Strömgren found, however, that all F stars with the same position on the c, l diagrams were not identical. In fact, there was conclusive evidence that in one group the ultraviolet portion of the spectrum was too bright, indicating a lower metal/hydrogen ratio than in the sun. Thus the spectrophotometric techniques may be used to investigate not only luminosity differences but certain chemical composition differences as well.

In the later spectral classes G, K, and M, the details of the line and continuous spectra cannot yet be computed sufficiently accurately from theoretical considerations. For example, the cyanogen bands form a very important criterion for luminosity effects (and sometimes also for separating stars of different population types). No fully satisfactory quantitative theory for their behavior has yet been worked out. Another example is provided by the λ 4227 line of neutral calcium. This line attains an enormous strength in dwarf M stars, and Lindblad has suggested that quasi-molecules, perhaps unstable CaH molecules, are formed. Again the theory of line broadening has not been worked out. The problem of overlapping lines is so severe that it may be necessary to proceed by synthesizing the spectrum, i.e., by adopting a set of chemical abundances, choosing a range of effective temperatures and surface gravities, and calculating the line plus continuous spectrum over the necessary wave-length range. Some programs of this nature have been planned, but results have not yet been obtained. One obstacle is the lack of suitable model atmospheres for late-type supergiants and giants. Eventually, this difficulty may be overcome when more is understood about the structure of stellar envelopes such as that of VV Cephei.

A most interesting correlation between the width of the emission component of the H and K lines of ionized calcium and absolute magnitude was established by Wilson and Bappu (1957). They find the relation between M_v and log W (where W is the corrected emission line width) to be linear over a range of 15 magnitudes. There is no dependence on emission line intensity or spectral type, and the calibration appears to be valid for stars as bright as $M_v = -6$ (Wilson 1959).

§ 5. HYDROGEN LINES AS CRITERIA FOR DETERMINATION OF SURFACE GRAVITY

In spectral classes earlier than the sun's, the hydrogen lines provide a very useful criterion for absolute magnitudes. The width of a Balmer line, expressed as $\Delta\lambda$ at half-maximum depth, steadily increases with decreasing stellar luminosity or, more particularly, with increasing surface gravity, whereas the dependence on temperature is relatively slight (e.g., Lindblad and Schalén

1929; Miss Williams 1929; Miss Anger 1930; Elvey and Struve 1930; Öhman 1930; E. G. Williams 1932; Petrie 1952). The luminosity-spectrum criteria used by Chalonge and by Strömgren make explicit use of this dependence. The higher the surface gravity, the greater the equivalent width of $H\beta$ and also the longer the wave length λ_1. As the electron pressure in the atmosphere increases, the higher members of the Balmer series coalesce, and the wave length λ_1 falls farther to the red.

Petrie showed that the equivalent width of $H\gamma$ was closely correlated with the luminosity of the B star, but it is hoped that measurements of the hydrogen-line profiles will help us to assess not only the stellar luminosities but also the models of the atmospheres. Among the recent investigations of the profiles of the hydrogen lines in B stars, we may mention especially those by Miss Underhill (1948) and by Miss McDonald (1953) at the Dominion Astrophysical Observatory. With the introduction of photoelectric techniques, the accuracy of line-profile measurements should be greatly increased.

Theoretical hydrogen-line profiles based on the Holtsmark statistical broadening theory and rough model atmospheres were computed by Verweij (1936). Although these calculations agreed qualitatively with the observations, in that they predicted stronger lines for higher surface gravities, the observed cores were shallower and narrower than the theoretical ones, and the shapes of the observed profiles differed from the theoretical ones. The discrepancies do not arise entirely from the failure of the Holtsmark theory; they are probably due mostly to the model atmospheres. Miss McDonald found that, although she could represent the wings of the hydrogen-line profiles, she could not represent the line near the center, probably as a consequence of the failure of the model near the boundary and the breakdown of the line-broadening theory in this region as well. Traving (1955, 1957) used the Holtsmark theory in connection with his model-atmosphere calculations to compute the profiles of $H\gamma$ and $H\delta$ in the spectra of τ Scorpii and 10 Lacertae. One consequence of these calculations was that the surface gravities required to represent the observed line profiles were larger than those computed from the masses and radii of the star as determined from the data of eclipsing binaries.

The Holtsmark line-broadening theory customarily employed in the calculation of hydrogen-line profiles neglects the influence of the electrons and assumes that the perturbing ions are at rest and are randomly distributed. Miss Underhill (1952*a*) concluded that the Holtsmark theory would not give a sufficiently wide profile, but the astrophysical data by themselves are not adequate to discriminate between competing physical theories. The structures of the model atmospheres are not well enough known.

On the theoretical side, Odgers (1952) has argued that the broadening influence of the electrons is not negligible and that the great width of the $H\gamma$ line in A stars arises from their contributions. He and, more recently, Hoffman and Theimer (1958) have suggested that the Holtsmark probability distribution

overestimates the effects of large fields. Experiments by Griem with the whirling-water arc in the laboratory of Lochte-Holtgreven in Kiel and by Turner and Doherty with the luminous shock tube in Laporte's laboratory at the University of Michigan have demonstrated that the Holtsmark theory predicts a profile that is too narrow. On the other hand, the profiles predicted by the Kolb theory showed a good agreement with the Michigan shock-tube results. Kolb and his associates are carrying out further experiments at the Naval Research Laboratory which should throw more light on this problem.

We shall not review here the theory of the broadening of the hydrogen lines. For a summarizing account of developments to mid-1958 see Aller and Jugaku (1959*b*). The hydrogenic-line-broadening problem is complicated by the fact that each energy level comprises a number of closely coincident states. As a consequence of this degeneracy of the hydrogenic energy levels, the atom is subject to the first-order Stark effect. The application of a macroscopic (or interatomic) electric field removes this degeneracy, and each line is broken up into a number of Stark components, whose separation depends on the strength of the field and whose intensities may be computed by well-known quantum-mechanical formulae. Under the influence of the randomly distributed ions, the emission of each component is "washed out," according to the Holtsmark probability distribution. The sum of these individual blurred-out intensity profiles gives the shape of the final absorption coefficient. The disturbing influence of the electrons contributes further broadening. While the ions broaden the line according to the Holtsmark distribution, the electrons broaden the line according to the discrete-encounter theory. Since the shape of the widened line profile is different for the two types of line broadening, we cannot allow for the electronic contribution simply by multiplying the ionic absorption coefficient by some constant factor.

In his theoretical treatment of the problem, Kolb showed that electron broadening is comparable with ion broadening at all densities and cannot be neglected in theoretical calculations of the hydrogen-line profiles. In the adiabatic approximation, it is assumed not only that an incoming perturber fails to induce an optical transition between two levels of principal quantum numbers n and n' but that it also fails to induce a transition between two energy states belonging to the same energy level. One might suppose that if such transitions do occur, they will have little influence on the line profile, but Kolb's detailed calculations for the Lyman-α line show that these collisionally induced reshufflings do made a difference. The absorption coefficient that results when these transitions are taken into account differs appreciably from that found for the situation in which they do not occur.

Kolb originally developed the theory for the line wings; later in collaboration with Griem he developed it in a form that holds for the cores as well.

An electric field, E, will cause a given Stark component to suffer a displacement,

$$\Delta\lambda = \frac{3h}{8\pi^2 m_\epsilon c}\lambda^2 X_k E, \tag{122}$$

where

$$X_k = [n(n_2 - n_1) - n'(n_2' - n_1')]. \tag{123}$$

Each Stark component X_k is defined with the aid of three quantum numbers, n_1, n_2, and m, corresponding to the upper level n, and three quantum numbers n_1', n_2', and m', corresponding to the lower level n'. Here $0 \leq n_1 \leq n-1$, $0 \leq n_2 \leq n-1$, and $|m| = n - 1 - n_1 - n_2$. The strength of each component may be expressed in terms of its f-value (cf., e.g., Underhill 1951). Let f_D denote the sum of the strengths of the displaced components. Some Balmer lines such as Hα and Hγ have central, undisplaced components which are broadened only by the Doppler effect and radiation damping. Let us define

$$s_k = \frac{f_k}{\Sigma f_k} \tag{124}$$

as the relative strength of the kth component.

We shall give here the asymptotic form of the absorption coefficient for the far wings of the line (cf., e.g., Aller and Jugaku 1958, eq. [50]):

$$\begin{aligned} \alpha(\Delta\lambda) &= 3.54 \times 10^{-15}\lambda^5 f_D F_0^{3/2} \sum \frac{s_k X_k^{3/2}}{(\Delta\lambda)^{5/2}}\left[1 + \frac{\alpha_\epsilon}{\alpha_H}(\Delta\lambda, N_\epsilon, T)\right] \\ &= \frac{CF_0^{3/2}}{(\Delta\lambda)^{5/2}}\left[1 + \frac{\alpha_\epsilon}{\alpha_H}(\Delta\lambda, N_\epsilon, T)\right], \end{aligned} \tag{125}$$

where F_0 is the mean value of the field produced by the neighboring ions:

$$F_0 = 2.603\epsilon N_i^{2/3}. \tag{126}$$

The factor C is the normal Holtsmark coefficient which has been computed for various Balmer lines. The values for Hα–Hδ have been published in a number of astrophysical texts (see Aller 1953; Unsöld 1955), while Traving has calculated these coefficients for the higher Balmer series members. The term in the brackets in equation (125) represents the correction to the Holtsmark theory required by the electronic contribution. The ratio of the electronic to the ionic contribution may be written in the following form:

$$\frac{\alpha_\epsilon}{\alpha_H}(\Delta\lambda, N_\epsilon, T) = R(N_\epsilon, T)(\Delta\lambda)^{1/2}. \tag{127}$$

Since the electronic contribution falls off as $(\Delta\lambda)^{-2}$, rather than as $(\Delta\lambda)^{-5/2}$, it dominates at large distances from the line center.

Table 5 gives the coefficient $R[A^{-1/2}]$ as calculated by Kolb, Griem, and Shen (1959) for a range of temperature and density of astrophysical interest (a more complete table with improved values is given in their paper).

The electronic contribution is relatively larger at lower densities, where it

increases steadily from one line in the Balmer series to the next. The correction, R, increases from Hβ toward the higher series numbers at such densities as are likely to be encountered in the photospheres of main-sequence stars. This behavior is to be attributed to an increase in the number of non-adiabatic matrix elements with principal quantum number. Except at the highest densities, R decreases as the temperature increases, and we might expect that in late A or F stars the electronic contribution would dominate. At densities appropriate for atmospheres of white dwarfs, the electronic contribution is relatively decreased. Kolb, Griem, and Shen emphasize that their table describes only the wing distribution, where only the nearest-neighbor interactions are important. The shielding effects are small when this limit is applicable. In their general theory and detailed numerical applications, they have taken into account both shield-

TABLE 5

CORRECTION FACTOR FOR ELECTRONIC CONTRIBUTION TO LINE BROADENING
$R(N, T)$ [$A^{-1/2}$]

LOG N	T (° K)											
	Hα			Hβ			Hγ			Hδ		
	10^4	2×10^4	4×10^4	10^4	2×10^4	4×10^4	10^4	2×10^4	4×10^4	10^4	2×10^4	4×10^4
10.....	1.05	0.79	0.59	1.05	0.80	0.60	1.37	1.04	0.78	1.66	1.27	0.96
12.....	0.82	.63	.48	0.81	.62	.48	1.03	0.80	.62	1.24	0.96	.75
14.....	0.59	.46	.36	0.56	.45	.35	0.70	0.56	.45	0.81	0.67	.53
15.....	0.47	.38	.30	0.45	.35	.28	0.53	0.44	.35	0.60	0.52	.43
16.....	0.35	.30	.25	0.33	.26	.22	0.37	0.31	.26	0.39	0.37	0.32
17.....	0.24	.22	.19	0.21	.17	.15	0.21	0.19	.17	.....	.....	.....
18.....	0.12	0.14	0.13	0.09	0.09	0.08	.....	.....	.....	.....	.....	.....

ing effects and ion-ion correlations. The effects predicted by Hoffman and Theimer (1958) and independently by Ecker (1957) are therefore explicitly included.

Very near the core ($\Delta\lambda < 1$ A in hotter stars) the Holtsmark theory is no longer applicable, but Kolb and Griem (1958) have developed a theory that is valid in this region. The mathematical expressions, although accurate, are extremely involved, and no attempt has yet been made to apply them to stellar atmospheres. In the cores the line-broadening problem is overshadowed by theoretical difficulties connected with the structure of the stellar atmosphere.

Finally, the residual intensity at a point $\Delta\lambda$ in the hydrogen-line profile is given by

$$r_\lambda = \frac{\int_0^\infty S_\nu(\tau_\nu) E_2(\tau_\nu)\, d\tau_\nu}{\int_0^\infty S_\lambda(\tau_\lambda) E_2(\tau_\lambda)\, d\tau_\lambda}, \tag{128}$$

where $S_\lambda(\tau_\lambda)$ is the source function in the continuum at optical depth τ_λ and $S_\nu(\tau_\nu)$ is the source function in the line at optical depth τ_ν in the line. That is,

$$\tau_\nu = \int_0^{\tau_\lambda} \frac{\kappa_\nu + \kappa_\lambda + \sigma}{\kappa_\lambda + \sigma} \, d\tau_\lambda , \tag{129}$$

where κ_ν, the coefficient of line absorption, is given by

$$\kappa_\nu = N_{0,2} a_\nu (1 - e^{-h\nu/kT}) . \tag{130}$$

Here $N_{0,2}$ is the number of hydrogen atoms in the second level per gram of stellar material, while the last factor allows for the negative absorptions.

The theory of hydrogen-line broadening developed by Kolb in his thesis (1956) takes the electronic contributions into account for Balmer lines in an

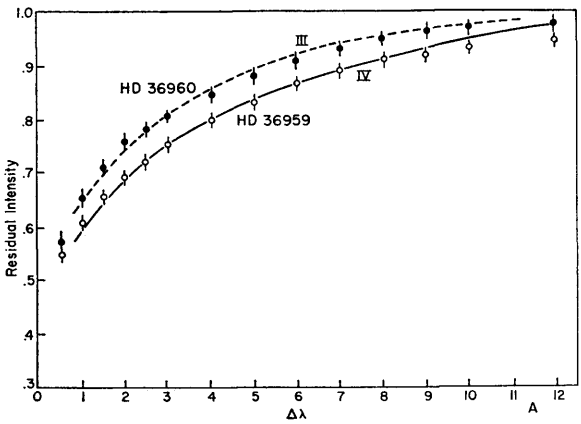


FIG. 6.—Profiles of Hγ in HD 36959 and HD 36960. The theoretical profiles computed for Underhill's Models III and IV are fitted to the observed points. The spectral classes for both stars are B1.5 V.

approximate way. It was applied to the calculation of line profiles in hot stars by Elste, Aller, and Jugaku (1956), by Osawa (1956), and by van Regemorter (1958).

In Figure 6 we compare the observed Hγ line profiles for the two components of the B1.5 V binary, HD 36959 and HD 36960, with predictions based on Kolb's (1956) theory and Miss Underhill's model atmospheres III and IV (boundary temperatures, 18,800° K and surface gravities, $\log g = 3.80$ and 4.20, respectively). These observed profiles are based on means of several plates secured with the 100-inch coudé spectrograph at the Mount Wilson Observatory. Approximate uncertainties are indicated by arrows. The discrepancies between theory and observation are less than the observational errors; furthermore, the profiles are obtained with surface gravities consistent with those of eclipsing binary stars of similar spectral class. More recently, Aller and Jugaku (1959*b*) have applied Kolb's and Griem's more accurate theory of Balmer line absorp-

tion coefficients to calculate precise Hγ profiles for model atmospheres of early-type stars. The line profiles are about 2 per cent deeper than the values previously obtained with Kolb's (1956) theory. The differences are least near the center of the line. Slightly smaller surface gravities are obtained by fitting the theoretical to the observed profiles.

§ 6. ABUNDANCES OF ELEMENTS IN NORMAL STARS

The determination of the abundances of the elements in the stars has occupied the attention of astrophysicists for some time. Early work (e.g., Payne 1925) demonstrated that most stars had very nearly the same composition as the sun. Differences in stellar spectra were attributed exclusively to the vagaries of excitation and ionization mechanisms. In the late 1940's one distinguished astrophysicist remarked that he did not think a single composition difference existed between the stars. Since then, composition differences have been established with certainty at least in some late-type stars. The character of these differences can be understood in terms of nuclear processes occurring in the hot, dense core of cool supergiant stars and have provided the observational background for the new field of nuclear astrophysics. Nevertheless, in any practical instance, one should examine all possibilities of explaining spectral abnormalities by excitation mechanisms before resorting to differences in chemical composition.

Of great interest also is the composition of "normal" matter, i.e., the average sample of our part of the universe. Here we are concerned with the composition of the sun, which reflects the primordial chemical makeup of the solar system, and also that of very young stars, which have been formed only recently from the interstellar medium. If, as recent theories of element building indicate, elements are continually being built in stars and dispersed throughout the interstellar medium when the stars expire, there should be a gradual enrichment of the heavy elements. Thus young stars which are formed recently out of the interstellar medium should have a greater amount of carbon, nitrogen, oxygen, magnesium, sulfur, etc., per gram of stellar material than has the sun.

The accurate establishment of abundance differences between stars is extremely difficult. In previous sections of this chapter, we have mentioned the factors that introduce uncertainties in the abundance determinations. These are as follows: (1) the limitations in the model atmosphere, particularly the temperature distributions and effects of rotation in the hotter stars, and the temperature inhomogeneities in the sun; (2) deviations from thermodynamic equilibrium, which differ from level to level in a manner that cannot be handled quantitatively; and (3) inaccuracies in the experimental f-values and damping constants. This last-mentioned difficulty is particularly serious for many of the elements whose lines are observed in the sun. In some elements, notably the rare earths, the spectroscopic terms are not known, so that the partition functions cannot be computed.

We concern ourselves here with the results for normal stars only; stars of abnormal composition are treated elsewhere in this volume. Summarizing reports on the earlier work have been given by de Jager (1953), by Minnaert (1957), and by the present writer (Aller 1958). Valuable reconnaissance work has been done by curve-of-growth methods (cf. § 3 and references therein), and, for stars with intrinsically fuzzy lines, spectrograms of moderate dispersion can be employed (cf., e.g., Hack 1954, 1956*a*). Definitive results which require for most elements the measurement of intrinsically faint lines can be obtained for both the sun and the stars only with high-dispersion plates. Further, although the curve-of-growth technique provides us with a good initial estimate of the composition, the model-atmosphere method, although laborious, is to be preferred. Only when precise calculations are carried out with the aid of model atmospheres can discrepancies between theory and observation be used to secure an improvement in the theoretical analysis.

Table 6 summarizes the results obtained for the B stars by model-atmosphere methods. We set log $N = 12.00$ for hydrogen, so that we have to deal only rarely with negative logarithms. For ζ Persei, Cayrel employed a model atmosphere and a precise calculation of the line intensities. The analyses for 10 Lacertae, 55 Cygni, and τ Scorpii (Traving) were done with the Unsöld curve of growth. The analyses for γ Pegasi, 22 Orionis, 114 Tauri, and τ Scorpii (Aller, Elste, and Jugaku) were carried out by the Pecker theory. The discrepancies

TABLE 6

ABUNDANCES OF ELEMENTS IN B STARS*
(log N)

ELEMENT	γ PEG AJ	ζ PER C	τ SCORPII		10 LAC T	55 CYG A	22 ORI ABJ	114 TAU ABJ
			T	AEJ				
H	12.00	12.00	12.00	12.00	12.00	12.00	12.00	12.00
He	11.17	11.31	11.23	.....	11.23	11.18	.....	.....
C	8.58	8.26	8.37	7.70	8.37	8.41	8.34	8.10
N	8.01	8.31	8.57	8.26	8.37	8.63	7.79	7.83
O	8.63	9.03	9.12	8.63	8.77	8.98	8.60	8.52
F	6.5:	.....	.....	.....	.....	.....	.....	.....
Ne	8.73	8.61	8.72	8.86	8.72	.....	.....	.....
Mg	7.95	7.76	7.73	8.30:	8.22	.....	8.06	7.64
Al	5.76	6.78	6.58	6.40	7.07	.....	5.74	5.63
Si	7.03	7.96	7.95	7.63	7.75	7.46	7.03	6.93
P	5.50	.....	.....	.....	.....	.....	5.45	.....
S	7.80	7.48	.....	.....	.....	.....	7.40	7.25
Cl	6.21	.....	.....	.....	.....	.....	.....	.....
A	6.90	.....	.....	.....	.....	.....	.....	.....

* The letters in columns indicate the following sources:
T = G. Traving, 1955, *Zs. f. Ap.*, **36**, 1, 1955; *ibid.*, **41**, 215, 1957.
C = R. Cayrel, thesis, Paris, 1957.
A = L. H. Aller, *Ap. J.*, **123**, 117, 1956.
AEJ = Aller, Elste, and Jugaku, *Ap. J. Suppl.*, **3**, 1, 1957 (No. 25).
AJ = Aller and Jugaku, *Ap. J., Suppl.*, **4**, 109, 1959.
ABJ = Aller, Boury, and Jugaku, unpublished.

between the results found for τ Scorpii are due partly to differences in the method of analysis and partly to different sources of material. The Michigan group found a high abundance of magnesium because they regarded the λ 4481 line as completely blended. The analysis for 55 Cygni was carried out with the aid of an approximate model atmosphere.

Turning to the individual elements, we note that the abundance of carbon appears to be somewhat higher in γ Pegasi as compared with the other stars. The determination for τ Scorpii was insecure, as it was not possible to obtain a satisfactory fit for both C II and C III with the given model atmospheres. Both nitrogen and oxygen show a number of fluctuations from star to star, although the Pecker analysis tends to give a smaller O/H ratio than do some of the other studies. The abundances of argon, chlorine, phosphorus, and especially fluorine are based on only a few lines and are therefore rather insecurely established. Fairly good agreement between the different stars is found for magnesium, whereas excellent agreement is obtained for neon, even though the neon abundance is found from the lines of Ne II in ζ Persei, 10 Lacertae, and τ Scorpii and from the lines of Ne I in γ Pegasi. For aluminum and silicon the Pecker theory seems to give abundances that are systematically lower than those found by other methods, at least for the cooler stars. Part of this discordance may be attributed to the model or to deviations from thermodynamic equilibrium; if one fits the Si III and Si IV lines (and ignores the Si II lines), the silicon abundance is enhanced, but the predicted Si II line intensities then far exceed observed line intensities. The high abundance of sulfur in the early-type stars is also of considerable interest.

One of the most exasperating aspects of the abundance problem has been the determination of the H/He ratio in the hotter stars. Earlier work by Unsöld and others who used Unsöld's methods gave a H/He ratio of about 5. Later, Miss Underhill and also Nevén and de Jager obtained considerably smaller abundances of helium, while Traving, who used model atmospheres and the Unsöld curve of growth, got results more nearly in agreement with those of Unsöld. Jugaku's (1957) calculations based on the Pecker theory and various model atmospheres showed the extreme dependence of the derived H/He ratio on the line-broadening parameters for helium. With the presently available, unsatisfactory line-broadening data, the most plausible estimate for the H/He ratio seemed to be near 7, in fair accord with the ratio obtained by Traving and with the result by Mathis (1957) for the Orion Nebula. Accurate laboratory data on line-broadening absorption coefficients are urgently needed.

Vega (spectral class A0 V) has been analyzed with the aid of a model atmosphere based on radiative equilibrium and Unsöld's curve of growth (Hunger 1955). The surface gravity adopted in this study appears to be too high, but this factor probably does not greatly influence the final relative abundances. Analyses for other stars are in progress at various observatories, but no results have yet been reported.

The most detailed studies are, of course, those that have been carried out for the sun. Table 7 gives the results obtained in the Michigan survey by Goldberg, Müller, and Aller (1960). This investigation was based on Pecker's theory of line formation and the model atmosphere compiled by Elste. For the most part, the abundances are gotten from observational data obtainable in the literature. For a few elements, new observational material has been obtained at the McMath-Hulbert Observatory.

In this investigation, weak or moderately strong lines were used throughout.

TABLE 7

ABUNDANCES OF ELEMENTS IN THE SUN

(Derived from Model-Atmosphere and Pecker Theory)

Element	log N	Remarks	Element	log N	Remarks
H	12.00		Ni	5.91	8,3
Li	0.96	1,2	Cu	5.04	1,9
Be	2.36	1	Zn	4.40	4,1
C	8.72	5	Ga	2.36	3,5,1
N	7.98	5	Ge	3.29	5,1
O	8.96	5	Rb	2.48	1,2,5
Na	6.30	2	Sr	2.60	1,3
Mg	7.40	3,5	Y	2.25	6,1
Al	6.20	2,5	Zr	2.23	6,1
Si	7.50	3,5	Nb(Cb)	1.95	6,1
P	5.34	5	Mo	1.90	5,1
S	7.30	5	Ru	1.43	6,1
K	4.70	2	Rh	0.78	6,1
Ca	6.15	2,8	Pd	1.21	6,1
Sc	2.82	7,5	Ag	0.14	3,1
Ti	4.68	8,7	Cd	1.46	1
V	3.70	7,8	In	1.16	5,1
Cr	5.36	8,3	Sn	1.54	3,1
Mn	4.90	3	Sb	1.94	5,1
Fe	6.57	8,9	Ba	2.10	5,1
Co	4.64	3,8	Yb	1.53	5,1
			Pb	1.33	3,1

NOTES TO TABLE 7

1. This element is being reinvestigated observationally and theoretically, taking into account the structure of the solar atmosphere and the effects of blends.

2. The f-values for these alkali or alkaline earth metals were found by quantum mechanics and checked experimentally, viz., Li (Trumpy, Veselov), Na (Prokofiew, Righini, Stephenson), Al (Biermann and Lübeck), Mg (Kirsten and Ornstein), K (Biermann and Lübeck, Villars, Stephenson), and Ca (Treffetz, Prokofiew, Olsen).

3. The f-values are taken from Allen and Asaad or from Allen.

4. The f-values are from Schuttevaer and Smit.

5. The f-values were calculated by tables of D. R. Bates and A. Damgaard.

6. The f-sum rule was used with $f_T = 1.0$ for the transition array, and LS coupling is assumed.

7. The f-sum rule was used, but $f_T = 0.5$ was assumed for the transition array.

8. Relative f-values by R. B. King and associates.

9 Absolute f-values by Kopferman and Wessel and by Bell, Davis, King, and Routly.

For many elements, no choice of line intensity is available, since even the strongest lines of a rare element are weak, if they are observable at all! Good reasons for choosing weak rather than strong lines for abundance determinations were given some time ago by Minnaert. In order to interpret the profile or total intensity of a strong line, it is necessary to know not only the f-values for the line but also the collisional damping constant. These quantities are difficult to ascertain, either experimentally or theoretically. The chief collisional broadening agent in the solar atmosphere is neutral hydrogen, but the interactions of this atom with radiating metallic atoms are troublesome to handle theoretically. It is, of course, possible to study the broadening of spectral lines in atmospheres of inert gases such as helium or argon, but the extrapolation of the experimental data so obtained to an atmosphere of atomic hydrogen is difficult.

A second difficulty with strong lines is that their centers are formed at high levels in the solar atmosphere—actually in the chromosphere, where deviations from the thermodynamic equilibrium are going to be pronounced. Although these central regions of a line may not contribute much to the equivalent width, they can be troublesome to any theoretical treatment.

Weak lines have the disadvantage that they are subject to large experimental errors or are often affected by blends with other lines. Blends are important not only in the sun but also in hot stars, where we might have anticipated that the number of such blends would be very small.

The first column of Table 7 gives the element, the second column log N (on the scale log $N = 12.00$ for hydrogen), and the third column the type of data used for the f-values. Detailed references are found in the previously cited article by Goldberg *et al.*

Transition probabilities for the resonance lines of the alkalis and alkaline earths may be obtained relatively easily, either experimentally or theoretically, but the transition probabilities for the higher transitions are more difficult to handle. For a number of metals, fairly reliable absolute transition probabilities have been measured, but the situation is far from satisfactory (see the discussion by Böhm, chap. 3).

Relative f-values for a number of atoms of the iron group have been measured by King and his associates with the electric furnace. For a few metals, absolute f-values have been measured by the atomic-beam technique, using a modification of the technique introduced by Kopfermann and Wessel. This procedure seems to be the most reliable, but unfortunately there are a number of technical difficulties. Allen obtained f-values for a number of metals of astrophysical interest by a different technique. He examined the spectra of arcs struck between copper rods alloyed with small quantities of other metals. Then, by comparing the intensities of lines of unknown f-values with lines of known f-values, he was able to deduce the transition probabilities for many metals, such as lead, silver, etc. The technique assumes (without much experimental proof) that the relative proportions of the atoms in the metallic vapor is the

same as in the rod itself. Another experimental technique which offers much promise for the future is the luminous shock tube. Vapors of metallic compounds can be introduced to produce the line spectra of neutral metal atoms, e.g., chromium carbonyl to get the arc spectrum of Cr. Unfortunately, these procedures have not yet been fully developed.

For many elements no f-value data of any kind are available, and various approximations have been employed. For transitions between high-level lines of light atoms, the Bates and Damgaard (hydrogenic) tables seem to give results that are fairly reliable. For the more complex elements, the sum rules have been employed in connection with the hypothesis of LS coupling. Here again, a very rough approximation is employed which will be supplanted when accurate experimental data are available.

In addition to these problems arising from the f-values, other uncertainties pertain to the solar atmosphere itself and the mechanisms of line formation. The interpretation of the data is based on a definite model of the atmosphere and the assumption that the lines are formed according to the mechanism of local thermodynamic equilibrium. The solar model determines the distribution of radiating atoms with depth and hence the precise relation between the equivalent width of the line and the product Nf. Part of the difference between the results obtained by Claas (1951) and those by Goldberg, Müller, and Aller is to be attributed to the different atmospheric models assumed, part of it to the different observational data.

The mechanism of line formation by pure absorption has been assumed in this analysis, but if deviations from local thermodynamic equilibrium occur, the mechanism of scattering may be important, and the population of the levels may deviate from the Boltzmann values by an amount varying from one level to another. As noted above, Pecker and his associates claim that there are large deviations from thermodynamic equilibrium, but these results have not been confirmed by others. Any empirical determination of deviations from local thermodynamic equilibrium suffers from uncertainties in the solar model and in the f-values, as well as difficulties of a theoretical nature.

Although stratification effects (i.e., those depending on the structure of the atmosphere) are taken into account in the work of Claas, Weidemann (1955), and of Goldberg, Müller, and Aller, the precise effects of blending, which are important for certain strategic lines of critical elements, will have to be handled on an individual basis. Observationally, such a program entails the measurement of the equivalent width of the line and its neighbors at various points on the disk of the sun. With the aid of such data, one may allow for the effects of stratification upon the blending and employ an improved theoretical treatment. Elements indicated by 1 in the remarks column of Table 7 are at present under study in this way at the University of Michigan.

It is clear that such a program must be supplemented by the experimental determination of f-values and also damping constants for the relevant lines of

the strategic elements. Until reliable *f*-values and damping constants are obtained, the abundance problem cannot be solved. With the limited effort which has so far been brought to bear on these experimental studies, progress must necessarily be painfully slow.

Mention must be made of the solar abundance work of Mugglestone and his associates (1958, 1960), who have concentrated on elements such C, N, and O, whose lines are formed predominantly in the deeper layers of the solar atmosphere. They have used a method similar to Pecker's weighting function method and have pointed out influences of uncertainties in solar models in deeper layers and of a possible importance of the quadratic Stark effect.

Theories of element building and related problems require the measurement of relative abundances of elements in the stars. Most convincing arguments for element building in stars are, in fact, provided by stars of unusual composition, which are discussed only briefly in this volume. Certain abundance ratios are of particular interest, e.g., lead to gold and to other nearby elements, lead to iron, metals to hydrogen, and helium to hydrogen. We generally assume that the composition of the surface layers of the sun have been unchanged since the formation of the solar system. Recent work (Aller and Chapman 1960) indicates that thermal diffusion may have played a role in altering the amounts of heavy elements in the photospheric layers of the sun over the last four billion years.

The editor wishes to express his thanks to Dr. Jun Jugaku for assistance in checking this chapter during Dr. Aller's visit to Australia.

REFERENCES

Adams, W. S., Joy, A. H., Humason, M. L., and Brayton, A. M.	1935	*Ap. J.*, **81**, 187.
Adams, W. S., and Russell, H. N.	1928	*Ap. J.*, **68**, 9.
Allen, C. W.	1934	*Mem. Commonwealth Solar Observatory Canberra*, Vol. **5**, Part 1.
	1949	*M.N.*, **109**, 343.
Aller, L. H.	1942*a*	*Ap. J.*, **96**, 321.
	1942*b*	*Ibid.*, **95**, 73.
	1946	*Ibid.*, **104**, 347.
	1949	*Ibid.*, **109**, 244.
	1953	*Atmospheres of the Sun and Stars* (New York: Ronald Press Co.), chap. 8.
	1956	*Ap. J.*, **123**, 117.
	1958	*Hdb. d. Phys.*, **51**, 324.
Aller, L. H., and Chapman, S.	1960	*Ap. J.*, **132**, 461.
Aller, L. H., Elste, G., and Jugaku, J.	1957	*Ap. J. Suppl.*, **3**, 1.

ALLER, L. H., and JUGAKU, J.	1958	*Ap. J.*, **128**, 616 (Paper VI).
	1959*a*	*Ap. J. Suppl.*, **4**, 109.
	1959*b*	*Ap. J.*, **130**, 469.
ALLER, L. H., and STODDARD, L. G.	1938	*Ap. J.*, **87**, 53.
AMBARZUMIAN, V. A.	1958	*Theoretical Astrophysics* (London: Pergamon Press).
ANGER, C. J.	1930	*Harvard Obs. Circ.*, No. 352.
BAKER, J. G.	1936	*Ap. J.*, **84**, 474.
BARBIER, D.	1946	*Ann. d'ap.*, **9**, 173.
	1958	*Hdb. d. Phys.*, Vol. **50**, ed. FLÜGGE (Heidelberg: Springer).
BARBIER, D., and CHALONGE, D.	1939	*Ann. d'ap.*, **2**, 254.
	1941	*Ibid.*, **4**, 30.
BARBIER, D., CHALONGE, D., and VASSY, E.	1935	*J. phys. et rad.*, **6**, 137.
BEER, A.	1933	*M.N.*, **95**, 24.
	1940	*Ibid.*, **100**, 693.
BELL, B.	1951	*Special Report 35*, Harvard Observatory.
BLESS, R.	1958	Thesis, University of Michigan.
BÖHM, E. VITENSE	1954	*Zs. f. Ap.*, **34**, 209.
BÖHM, K. H.	1954*a*	*Zs. f. Ap.*, **34**, 182.
	1954*b*	*Ibid.*, **35**, 179.
BRETZ, M.	1956	*Zs. f. Ap.*, **38**, 259.
BRUGGENCATE, P. TEN, GOLLNOW, H., and JÄGER, F. W.	1950	*Zs. f. Ap.*, **27**, 223.
BRUGGENCATE, P. TEN, LÜST-KUKLA, R., and VOIGT, H. H.	1955	*Nachr. Wiss. Göttingen*, No. 3.
BURBIDGE, E. M., and BURBIDGE, G. R.	1956	*Ap. J.*, **124**, 116, 130, 655.
	1957	*Ibid.*, **126**, 357.
BUSBRIDGE, IDA	1953	*M.N.*, **113**, 52.
BUSBRIDGE, IDA, and STIBBS, D. W. N.	1954	*M.N.*, **114**, 2.
BUSCOMBE, W.	1951	*Ap. J.*, **114**, 73.
CANAVAGGIA, R., AND PECKER, J. C.	1952	*Ann. d'ap.*, **15**, 260.
	1953	*Ibid.*, **16**, 47.
CAYREL, R.	1957	Thesis, Paris.
CHALONGE, D.	1956	*Vistas in Astronomy*, ed. A. BEER (London: Pergamon Press), **2**, 1328.
CHALONGE, D., and DIVAN, L.	1952	*Ann. d'ap.*, **15**, 201.

CHALONGE, D., and KOURGANOFF, V.	1946	*Ann. d'ap.*, **9**, 69.
CHAMBERLAIN, J. W., and ALLER, L. H.	1951	*Ap. J.*, **114**, 52.
CHANDRASEKHAR, S.	1947	*Ap. J.*, **106**, 151.
	1950	*Radiative Transfer* (Oxford: Oxford University Press).
CLAAS, W. J.	1951	*Rech. Ast. Obs. Utrecht*, Vol. **12**, Part I.
CONDON, E. U.	1958	*Handbook of Physics* (New York: McGraw-Hill Book Co., Inc.), Part 3, chap. 7.
DEUTSCH, A.	1956	*Ap. J.*, **123**, 210.
ECKER, G.	1957	*Zf. f. Phys.*, **148**, 593.
EDDINGTON, A. S.	1929	*M.N.*, **89**, 620.
EDMONDS, F.	1955	*Ap. J.*, **121**, 418.
ELSTE, G.	1955	*Zs. f. Ap.*, **37**, 184.
ELSTE, G., ALLER, L. H., and JUGAKU, J.	1956	*Pub. A.S.P.*, **68**, 23.
ELVEY, C. T., and STRUVE, O.	1930	*Ap. J.*, **72**, 277.
FOFANOVA, T. M.	1950	*Izvest. Glavnoi. Astr. Obs.*, No. 114, p. 68.
FRACASTORO, M. G.	1949	*M.N.*, **109**, 586.
GATHIER, P. J.	1955	*Utrecht Res.*, Vol. **13**, Part 2.
GOLDBERG, L.	1958*a*	*Ap. J.*, **127**, 308.
	1958*b*	*Hdb. d. Phys.*, Vol. **52**.
GOLDBERG, L., MÜLLER, E., and ALLER, L. H.	1960	*Ap. J. Suppl.*, Vol. **5**, No. 45.
GREENSTEIN, J. L.	1942	*Ap. J.*, **95**, 161.
	1948	*Ibid.*, **107**, 151.
	1949	*Ibid.*, **109**, 121.
GRIEM, H., KOLB, A. C., and SHEN, K. Y.	1959	*Phys. Rev.*, **116**, 4.
GROTH, H. G.	1955	*Zs. f. Ap.*, **37**, 261.
	1957	*Ibid.*, **43**, 185.
HACK, M.	1954	*Mem. Soc. astr. ital.*, **25**, 17, 481.
	1956*a*	*Ibid.*, **27**, 201, 249, 469, 547.
	1956*b*	*B.A.N.*, **13**, No. 4.
HARRIS, D.	1948	*Ap. J.*, **108**, 112.
	1949	*Ibid.*, **109**, 53.
HELFER, H. L., WALLERSTEIN, G., and GREENSTEIN, J. L.	1959	*Ap. J.*, **129**, 700.
HENYEY, L. G.	1940	*Proc. Nat. Acad. Sci.*, **26**, 50.
HITOTUYANAGI, Z., and INABA, H.	1954	*Sci. Repts. Tohoku U.*, Ser. I, Vol. **38**, No. 3.
HJERTING, F.	1938	*Ap. J.*, **88**, 508.

HOFFMAN, H., and THEIMER, O.	1958	*Ap. J.*, **127**, 477.
HOUTGAST, J.	1942	Thesis, Utrecht.
HUANG, S. S., and STRUVE, O.	1952	*Ap. J.*, **116**, 410.
	1955	*Ibid.*, **121**, 84.
	1956	*Ibid.*, **123**, 231.
HUNGER, K.	1955	*Zs. f. Ap.*, **36**, 42.
	1956	*Ibid.*, **39**, 36.
HYNEK, A.	1951	*Astrophysics* (New York: McGraw-Hill Book Co., Inc.).
INABA, H.	1955	*Sci. Repts. Tohoku U.*, **39**, 60.
JÄGER, F. W.	1957	*Zs. f. Ap.*, **43**, 98.
JAGER, C. DE	1948	*Proc. Acad. Wetensch. Amsterdam*, **51**, 731.
	1952	*Utrecht Obs. Res.*, **13**, 731. Part I, chap. 8.
	1953	*Fundamental Principles of Stellar Classification: Conference on Stellar Atmospheres, Institut d'Astrophysique* (Paris: Paris Observatory), p. 141.
JAGER, C. DE, and NEVÉN, L.	1957	*Utrecht Obs. Res.*, Vol. **13**, No. 4.
	1959	Comm. Royal Obs., Belgium, No. 157.
JOHNSON, H., and MORGAN, W. W.	1953	*Ap. J.*, **117**, 313.
JUGAKU, J.	1957	Thesis, University of Michigan.
KING, R. B.	1954	*Proc. Indiana Conference on Stellar Atmospheres*, ed. M. WRUBEL, p. 41.
KING, R. B., and WRIGHT, K. O.	1947	*Ap. J.*, **106**, 224.
KLÜBER, H. VON.	1927	*Zs. f. Phys.*, **45**, 610.
KOELBLOED, D.	1953	*Pub. Astr. Inst. U. Amsterdam*, No. 10.
KOLB, A. C.	1956	Thesis, University of Michigan.
KOLB, A. C., and GRIEM, H.	1958	*Phys. Rev.*, **111**, 514.
KOLB, A. C., GRIEM, H., and SHEN, K. Y.	1959	*Phys. Rev.*, **116**, 4.
KOPFERMANN, H., and WESSEL, G.	1951	*Zs. f. Phys.*, **130**, 100.
LABS, D.	1951	*Zs. f. Ap.*, **28**, 150.
	1954	*Ibid.*, **34**, 173.
LANDOLT-BÖRNSTEIN	1950	*Zahlenwerte u. Funktionen aus Physik, Chemie, Astronomie, Geophysik u. Technik* (Berlin: Julius Springer), **1**, Part I, 260.
LILLER, W., and LEWIS, E. M.	1952	*Ap. J.*, **116**, 428.
LINDBLAD, B.	1922	*Ap. J.*, **55**, 85.
LINDBLAD, B., and SCHALÉN, C.	1929	*Medd. Astr. Obs. Uppsala*, No. 17.

McDONALD, J. K. 1953 *Pub. Dom. Ap. Obs. Victoria*, **9**, 269.
McKELLAR, A., ALLER, L. H., and RICHARDSON, E. H. 1958 *Pub. Dom. Ap. Obs. Victoria*, Vol. **11**, No. 2.
McKELLAR, A., ODGERS, G. J., ALLER, L. H., and McLAUGHLIN, D. B. 1952 *Nature*, **169**, 990.
McMATH, R. R., MOHLER, O. C., PIERCE, A. K., and GOLDBERG, L. 1956 *Ap. J.*, **124**, 1.
MARTINI, A., and MASANI, A. 1957 *Milano-Merate Obs. Contr.*, No. 119.
MATHIS, J. 1957 *Ap. J.*, **125**, 328.
MELNIKOV, O. 1950; 1954 References quoted on p. 626 of Ambarzumian's (1958) *Theoretical Astrophysics*.
MENZEL, D. H. 1931 *Pub. Lick Obs.*, **17**, 230.
1936 *Ap. J.*, **84**, 462.
MENZEL, D. H., GOLDBERG, L., and COOK, E. M. 1940 *Ap. J.*, **91**, 320.
MICHARD, R. 1953 *Ann. d'ap.*, **16**, 217.
MICZAIKA, G. R. 1948 *Zs. f. Naturforsch.*, **3**, 241.
MICZAIKA, G. R., FRANKLIN, F. A., DEUTSCH, A. J., and GREENSTEIN, J. L. 1956 *Ap. J.*, **124**, 134.
MINNAERT, M. 1927 *Zs. f. Phys.* **45**, 610.
1935 *Zs. f. Ap.*, **10**, 40.
1936 *Ibid.*, **12**, 313.
1948 *B.A.N.*, **10**, 339.
1953 Chapter in *The Sun*, ed. G. P. KUIPER (Chicago: University of Chicago Press).
1957 *M.N.*, **117**, 315.
1958 *Draft Repts. Internat. Astr. Union* (Moscow), p. 124.
MINNAERT, M., and SLOB, C. 1931 *Proc. Amsterdam Acad.*, **34**, Part 1, 542.
MITCHELL, W. 1959 *Ap. J.*, **129**, 369.
MIYAMOTO, S. 1953 *Zs. f. Ap.*, **31**, 282.
1954*a* *Ibid.*, **35**, 145.
1954*b* *Pub. Astr. Soc. Japan*, **5**, 142.
1954*c* *Ibid.*, **6**, 140, 150.
MORGAN, W. W., KEENAN, P. C., and KELLMAN, E. 1943 *Atlas of Stellar Spectra* (Chicago: University of Chicago Press).

MÜNCH, G.	1946	*Ap. J.*, **104**, 87.
	1949	*Ibid.*, **109**, 275.
	1958	*Ibid.*, **127**, 642.
MUGGLESTONE, D.	1958	*M.N.*, **118**, 432.
	1960	*Ibid.*, **120**, 193.
MUSTEL, E. R.	1943; 1944	See AMBARZUMIAN (1958) for a survey of this method.
NECKEL, H.	1958	*Zs. f. Ap.*, **44**, 153.
NEVÉN, L., and JAGER, C. DE	1954	*B.A.N.*, **12**, 103.
ODGERS, G.	1952	*Ap. J.*, **116**, 444.
ÖHMAN, Y.	1930	*Medd. Astr. Obs. Uppsala*, No. 47.
OSAWA, K.	1956	*Ap. J.*, **123**, 513.
PAGEL, B. E. J.	1955	*M.N.*, **115**, 493.
PANNEKOEK, A.	1935	*Publ. Astr. Institute Amsterdam*, No. 4.
PECKER, C.	1957	*Ann. d'ap.*, **20**, 196.
PECKER, J. C.	1949	*B.A.N.*, **11**, 43.
	1951	*Ann. d'ap.*, **14**, 383.
	1953	*Contr. Inst. d'ap., Ser. A*, No. 132.
	1957	*C.R.*, **245**, 499.
PECKER, J. C., and REGEMORTER, H. VAN	1955	*Contr. Inst. d'ap.*, No. 196.
PETRIE, R.	1952	*Pub. Dom. Ap. Obs. Victoria*, Vol. **9**, No. 8.
PIERCE, K., and ALLER, L. H.	1951	*Ap. J.*, **114**, 145.
	1952	*Ibid.*, **116**, 176.
PIERCE, K., and WADDELL, J.	1960	*Ap. J.* (in press).
PLASKETT, H.	1955*a*	*Vistas in Astronomy*, ed. A. BEER (London: Pergamon Press), **1**, 637.
	1955*b*	*M.N.*, **115**, 256.
PRIESTER, W.	1953	*Zs. f. Ap.*, **32**, 200.
PRZYBYLSKI, A.	1953	*M.N.*, **113**, 683.
	1954	*Ibid.*, **114**, 406.
REGEMORTER, H. VAN	1955	*Contr. Inst. d'ap.*, No. 197.
	1958	Thesis, Paris Inst. d'Astrophysique.
RICHARDSON, R. S., and SCHWARZSCHILD, M.	1950	*Ap. J.*, **111**, 351.
ROGERSON, J.	1957	*Ap. J.*, **125**, 275.
RUSSELL, H. N.	1929	*Ap. J.*, **70**, 11.
	1933	*Ibid.*, **78**, 239.
RUSSELL, H. N., ADAMS, W. S., and MOORE, C. E.	1928	*Ap. J.*, **68**, 1.
SAITO, S.	1954	*Contr. Kyoto Inst. Ap.*, No. 48.
	1956	*Ibid.*, No. 69.

SAVEDOFF, M. P.	1952	*Ap. J.*, **115**, 509.
SCHRÖTER, E. H.	1957	*Zs. f. Ap.* **41**, 141.
SOBOLEV, V. V.	1949	*Russian Astr. J.*, **26**, 129.
	1951	*Ibid.*, **28**, 355.
	1954	*Ibid.*, **31**, 231.
SPIEGEL, E.	1958	Thesis, University of Michigan.
SPITZER, L.	1936	*M.N.*, **96**, 794.
STIBBS, D. W. N.	1953	*M.N.*, **113**, 493.
STRÖMGREN, B.	1937	*Ap. J.*, **86**, 1.
	1940	*Pub. Copenhagen Obs.*, Vol. **127**.
	1955	*Third Berkeley Symposium on Mathematical Statistics*, **3**, 49.
STRUVE, O.	1945	*Pop. Astr.*, **53**, 271.
SUEMOTO, Z.	1949	*Pub. Astr. Soc. Japan*, **1**, 78.
	1957	*M.N.*, **117**, 2.
TRAVING, G.	1955	*Zs. f. Ap.*, **36**, 1.
	1957	*Ibid.*, **41**, 215.
	1958	*Ibid.*, **44**, 142.
UENO, S.	1955	*Contr. Inst. Ap. Kyoto*, No. 58.
UENO, S., and MATSUSHIMA, S.	1950	*Pub. Astr. Soc. Japan*, **2**, 32.
UNDERHILL, A. B.	1948	*Ap. J.*, **107**, 337.
	1951	*Pub. Dom. Ap. Obs. Victoria*, **8**, 385.
	1952*a*	*Ap. J.*, **116**, 446.
	1952*b*	*Contr. Dom. Ap. Obs. Victoria*, No. 37.
	1957	*Pub. Dom. Ap. Obs. Victoria*, **10**, 357.
UNNO, W.	1957	*Ap. J.*, **126**, 259.
UNSÖLD, A.	1928	*Zs. f. Phys.*, **46**, 765.
	1932	*Zs. f. Ap.*, **4**, 339.
	1938	*Physik der Sternatmosphären* (Berlin: Springer).
	1941	*Zs. f. Ap.*, **21**, 1, 22.
	1955	*Physik der Sternatmosphären* (2d ed.; Berlin: Springer).
VERWEIJ, S.	1936	*Pub. Astr. Inst. Amsterdam*, No. 5.
VITENSE, E.	1953	*Zs. f. Ap.*, **32**, 135.
VOIGT, H. H.	1952	*Zs. f. Ap.*, **31**, 48.
	1956	*Ibid.*, **40**, 157.
WADDELL, J.	1956	Thesis, University of Michigan.
WEIDEMANN, V.	1955	*Zs. f. Ap.*, **36**, 101.
WELLMAN, P.	1936	*Zs. f. Ap.*, **12**, 140.
	1939	*Veröff. Babelsberg*, **12**, 4.
WILLIAMS, E. G.	1932	*Ann. Solar Phys. Obs. Cambridge*, **2**, II.
WILLIAMS, E. T. R.	1929	*Harvard Obs. Circ.*, No. 348.
WILSON, O. C.	1948	*Ap. J.*, **107**, 126.
	1959	*Ibid.*, **130**, 499.
WILSON, O. C., and ABT, H. A.	1954	*Ap. J. Suppl.*, **1**, 1.

WILSON, O. C., and BAPPU, M. K. V.	1957	*Ap. J.*, **125**, 661.
WOOLLEY, R. v. d. R.	1938	*M.N.*, **98**, 624.
WOOLLEY, R. v. d. R., and STIBBS, D.	1953	*Outer Layers of a Star* (Oxford: At the University Press).
WRIGHT, K. O.	1944	*Ap. J.*, **99**, 249.
	1946	*J.R.A.S. Canada*, **40**, 183.
	1947	*Ibid.*, **41**, 49.
	1948	*Pub. Dom. Ap. Obs. Victoria*, **8**, 1.
	1950	*Ibid.*, p. 281.
	1954	*Indiana University Conference on Stellar Atmospheres*, ed. M. WRUBEL, p. 128.
	1955*a*	*Trans. Internat. Astr. Union*, **9**, 739.
	1955*b*	*J.R.A.S. Canada*, **49**, 221.
WRIGHT, K. O., and DIEN, E. VAN.	1949	*J.R.A.S. Canada*, **43**, 15.
WRUBEL, M.	1949	*Ap. J.*, **109**, 66.
	1950	*Ibid.*, **111**, 157.
	1954	*Ibid.*, **119**, 51.
ZANSTRA, H.	1941	*M.N.*, **101**, 250, 273.
	1946	*Ibid.*, **106**, 225.

CHAPTER 5

Interpretation of Normal Stellar Spectra

LAWRENCE H. ALLER
University of Michigan Observatory

In this chapter we shall consider the interpretation of "normal" stellar spectra from the most elementary point of view. That is, we shall exclude variable stars of practically all types, stars of abnormal composition (except those of spectral classes R, N, and S), metallic-line and peculiar A stars, subdwarfs, and white dwarfs. Some of these objects are treated elsewhere in this volume.

§ 1. THE ISOTHERMAL APPROXIMATION

At the outset, let us introduce the approximation that the entire stellar-line spectrum is produced at an "average" point in the atmosphere, i.e., that a unique temperature and pressure can be assigned to each star that will permit the calculation of observable characteristics of the stellar-line spectrum. Clearly, such an assumption will be valid only for lines of comparable total excitation, e.g., lines of Ti II and Fe II in the spectrum of α Cygni. The approximation will be less satisfactory if we wish to compare lines of neutral oxygen and potassium in the sun or ionized and neutral metals in K stars.

Nevertheless, in a first reconnaissance the isothermal-isobaric approximation is justified. The main differences between the spectra of stars of different Draper classes arise from differences in ionization and excitation. The hydrogen lines are strong in spectral class A because the temperature is high enough to produce a substantial excitation of atoms to the second level, but yet not high enough for ionization to deplete seriously the number of neutral hydrogen atoms. The effect of stratification in the atmosphere is of relatively secondary importance. Differences in mean electron pressure in going from one atmosphere to another will be taken into account. The classical early work on the interpretation of the spectral sequences by Saha, by Milne and Fowler, by Payne (1925),

and by Menzel (1924) employed the ionization and excitation formulae and the isothermal approximation. They did not, however, take into account the variability of the continuous absorptivity of the stellar atmosphere.

We shall proceed in the following way: The excitation of a given atomic level is determined by the temperature, the ionization by both the temperature, T, and the electron pressure, P_e. Hence (T, P_e) will determine the number of atoms per gram of the element involved capable of absorbing the spectral line in question. For a star of given effective temperature the electron pressure in the atmosphere will depend on the surface gravity and the ratio of gas pressure to electron pressure. What we are really interested in is the number of atoms capable of absorbing the line in question in the observable layers of the stellar atmosphere. In addition to the temperature and electron pressure, this quantity will depend on the abundance of the element in question and the continuous absorption coefficient at the given wave length.

Therefore, we shall have to establish the following functional relationships: first, the value of

$$P_g = P_g (P_e, T) . \tag{1}$$

This function will depend on the assumed abundances, particularly the ratio of the metals to hydrogen. Also, we want

$$\kappa_\lambda (P_e, T) = \kappa_\lambda [P_g (P_e, T), T] , \tag{2}$$

the coefficient of continuous absorption at some convenient frequency in the observable part of the spectrum. This relation is necessary to establish the connection between surface gravity, P_e, and T, viz.,

$$P_e = P_e (g, T) , \tag{3}$$

and the mass of material above the photosphere,

$$\mathfrak{m} = \frac{\text{Const.}}{\kappa_\lambda (P_e, T)} . \tag{4}$$

Relations (3) and (4) are derived from the equation of hydrostatic equilibrium,

$$\frac{dP}{d\tau_\lambda} = \frac{g}{\kappa_\lambda (P_e, T)} , \tag{5}$$

whose solution within the framework of the present approximation is

$$P = \frac{g \tau_0}{\kappa_\lambda (\bar{P}_e, \bar{T})} , \tag{6}$$

where $\bar{P}_e$ and $\bar{T}$ denote some sort of average over the stellar atmosphere or the values of these quantities corresponding to the optical depth τ_0. Our task in this chapter will be to utilize these relationships to predict the gross features of stellar spectra.

§ 2. THE RELATION BETWEEN GAS AND ELECTRON PRESSURE

Russell (1932) was the first to calculate extensive tables of the relation between gas and electron pressure as a function of temperature. He noted that, at low temperatures, almost all the electrons come from the metals. Hydrogen is so abundant that, as soon as it starts to become substantially ionized, it supplies the great majority of electrons. Russell assumed hydrogen to be sixty times as abundant as all metals together. In calculating the ionization, however, he assumed that the temperature of the radiation field differed from the gas kinetic temperature. Pannekoek (1935) likewise used a modified ionization formula, but he assumed a ratio of hydrogen to metals of 1000. Unsöld (1934) and later Strömgren (1940) also computed the $P_g(P_e, T)$ relation.

Improved abundance ratios based on the analyses of τ Scorpii by Unsöld (1941) and of the sun by Menzel and Goldberg (1943) were utilized by the present writer to compute $P_g(P_e, T)$ (Aller 1942). Rosa (1948) carried out calculations with a very similar composition. Both Strömgren and Rosa used an H/metal ratio of 5000.

TABLE 1

ADOPTED ABUNDANCES OF THE ELEMENTS

(log A = 4.13)

Element	Abundance	Element	Abundance
H.....	1,000,000	Mg.....	19
He.....	140,000	Al.....	1.6
C.....	250	Si.....	40
N.....	410	K.....	0.09
O.....	1300	Ca.....	2.4
Ne.....	2000	Fe.....	5.8
Na.....	2	Ni.....	0.6

The present calculation of the $P_g(P_e, T)$ relationship is based on the abundances derived by Goldberg, Müller, and Aller (1958) and from data for the B stars. The hydrogen/metal ratio is $A = 1.35 \times 10^4$. The hydrogen/helium ratio (which has not been established in a satisfactory way for the sun) is taken from the work of Mathis (1957) on the Orion Nebula and from that of Jugaku (1957) on the B stars.

Table 1 gives the adopted abundances of the elements important in establishing the $P_g(P_e, T)$ relation. All metals other than those specifically listed are assumed to contribute 2 atoms per million hydrogen atoms, and a mean ionization potential of 7.6 ev is assumed for them. Carbon, nitrogen, oxygen, neon, and argon do not contribute electrons until hydrogen starts to become ionized, at which point hydrogen dominates the picture because of its overwhelming abundance. They do contribute to the mean molecular weight, μ_0, of the un-ionized material, which is 1.43 for this composition ($\mu_0 = 1.38$ if they are neglected).

TABLE 2A

RELATION BETWEEN GAS PRESSURE AND ELECTRON PRESSURE AS FUNCTION OF TEMPERATURE ($\theta = 5040/T$) FOR LOG $A = 4.13$
(The Composition Is That Given in Table 1)
(log P_g)

LOG P_e	θ																	
	0.20	0.30	0.40	0.50	0.60	0.70	0.75	0.80	0.85	0.90	0.95	1.0	1.1	1.2	1.4	1.6	1.8	2.0
−2.0	−1.9:	−1.70	−1.69	−1.69	−1.68	−1.65	−1.60	−1.55	−1.40	−0.50	+0.08	+0.80	+1.91	+2.22	+2.65	+3.34	+3.65	+4.16
−1.5	−1.32	−1.19	−1.18	−1.18	−1.18	−1.16	−1.00	−0.85	−0.38	+0.42	+1.07	+1.80	+2.55	+2.81	+3.42	+3.92	+4.31	+5.02
−1.0	−0.76	−0.70	−0.69	−0.68	−0.67	−0.62	−0.46	−0.02	+0.62	+1.34	+2.04	+2.67	+3.18	+3.39	+4.13	+4.55	+5.10	+5.94
−0.5	−0.23	−0.20	−0.19	−0.18	−0.17	−0.07	+0.29	+0.92	+1.64	+2.33	+2.97	+3.42	+3.78	+4.06	+4.75	+5.21	+6.0	+6.85
0	+0.28	+0.30	+0.32	+0.32	+0.36	+0.64	+1.16	+1.91	+2.63	+3.30	+3.83	+4.14	+4.41	+4.77	+5.41	+6.00	+6.95	.....
+0.5	+0.79	+0.80	+0.82	+0.84	+0.89	+1.50	+2.11	+2.91	+3.59	+4.16	+4.58	+4.83	+5.09	+5.48	+6.10	+6.84	.....	.....
+1.0	+1.29	+1.30	+1.32	+1.35	+1.46	+2.41	+3.13	+3.91	+4.51	+5.01	+5.24	+5.49	+5.83	+6.22	+6.85	.....	.....	.....
+1.5	+1.80	+1.81	+1.82	+1.87	+2.14	+3.36	+4.14	+4.84	+5.34	+5.72	+5.93	+6.24	+6.56	+6.95	.....	.....	.....	.....
+2.0	+2.30	+2.31	+2.34	+2.39	+2.96	+4.37	+5.08	+5.76	+6.14	+6.42	+6.63	+7.04	.....	.....	.....	.....	.....	.....
+2.5	+2.80	+2.81	+2.84	+2.94	+3.89	+5.38	+6.00	+6.62	+6.91	.....	.....	.....	.....	.....	.....	.....	.....	.....
+3.0	+3.30	+3.31	+3.34	+3.62	+4.86	+6.31	+6.89	.....	.....	.....	.....	.....	.....	.....	.....	.....	.....	.....
+3.5	+3.82	+3.83	+3.86	+4.42	+5.86	.....	.....	.....	.....	.....	.....	.....	.....	.....	.....	.....	.....	.....
+4.0	+4.32	+4.34	+4.43	+5.35	+6.86	.....	.....	.....	.....	.....	.....	.....	.....	.....	.....	.....	.....	.....

TABLE 2B

RELATION BETWEEN GAS PRESSURE AND ELECTRON PRESSURE AS FUNCTION OF TEMPERATURE ($\theta = 5040/T$) FOR LOG $A = 5.63$ ($\log P_g$)

LOG P_e	θ													
	0.50	0.60	0.70	0.80	0.85	0.90	0.95	1.0	1.1	1.2	1.4	1.6	1.8	2.0
−3.0	.....	.....	.....	.....	.....	.....	.....	.....	.....	+2.05	+2.77	+3.44	+3.87	+4.23
−2.5	.....	.....	.....	.....	.....	.....	.....	.....	+1.30	+2.70	+3.44	+4.06	+4.49	+4.92
−2.0	.....	.....	.....	.....	.....	−0.67	+0.06	+0.70	+2.27	+3.36	+4.12	+4.70	+5.11	+5.62
−1.5	.....	.....	.....	.....	−0.37	+0.31	+1.08	+1.81	+3.21	+4.03	+4.81	+5.35	+5.83	+6.39
−1.0	−0.70	−0.69	−0.64	−0.08	+0.62	+1.33	+2.08	+2.87	+4.09	+4.72	+5.52	+6.02	+6.59	+7.30
−0.5	−0.20	−0.17	0.00	+0.90	+1.60	+2.34	+3.09	+3.87	+4.92	+5.44	+6.22	+6.75	+7.40	.....
0	+0.30	+0.36	+0.71	+1.85	+2.60	+3.33	+4.10	+4.81	+5.73	+6.18	+6.91	+7.49	.....	.....
+0.5	+0.80	+0.90	+1.53	+2.79	+3.59	+4.34	+5.10	+5.72	+6.51	+6.94	+7.62	.....	.....	.....
+1.0	+1.31	+1.50	+2.47	+3.71	+4.59	+5.31	+6.04	+6.60	+7.28	+7.71	.....	.....	.....	.....
+1.5	+1.84	+2.16	+3.35	+4.69	+5.59	+6.30	+6.97	+7.45	.....	.....	.....	.....	.....	.....
+2.0	+2.37	+2.91	+4.29	+5.75	+6.57	+7.25	.....	.....	.....	.....	.....	.....	.....	.....
+2.5	+2.97	+3.83	+5.25	+6.72	.....	.....	.....	.....	.....	.....	.....	.....	.....	.....
+3.0	+3.65	+4.88	+6.25	.....	.....	.....	.....	.....	.....	.....	.....	.....	.....	.....

The computational procedure is to adopt a pair of values (P_e, T) and compute the corresponding P_g values (see, e.g., Aller 1942, 1953; Rosa 1948; Unsöld 1955). In the present calculations we treat the metals individually rather than in groups, as was the custom in some of the earlier calculations of this type. Table 2A gives the results. As a consequence of the high abundance of hydrogen and in accordance with the earlier calculations, the electron pressure is approximately half the gas pressure at the higher temperatures. At the very highest temperatures and lowest pressures, the ionization of helium becomes important. Proceeding toward lower temperatures, the functional relationship becomes relatively complex because the metals supply the electrons. The details of the curves in this region depend on the relative abundances assumed for the different metals. While we now believe that these relative abundances are fairly well established, improvements in the absolute f-value determinations may lead to a few changes.

It is also of interest to carry out calculations for stars in which the hydrogen/metal ratio is substantially greater. The $P_g(P_e, T)$ relationship has been computed for the situation in which the abundance of H is taken as 31,600,000, that of helium is 4,200,000, and the other elements in Table 1 are left unchanged, i.e., log $A = 5.63$. Because of its overwhelming predominance, hydrogen continues to supply most of the electrons even at relatively low temperatures, and the metallic contribution to the supply of electrons dominates only at temperatures lower than that of the sun (see Table 2B).

§ 3. THE COEFFICIENT OF CONTINUOUS ABSORPTION

Before we can derive the relationship between the mean electron pressure, temperature, and surface gravity, we must know the coefficient of continuous absorption as a function of wave length, temperature, pressure, and composition. In the present discussion we shall fix attention on a particular wave length in the middle of the photographic region of the spectrum, λ 4235. Most spectroscopic studies usually cover much of the range from about λ 3700 to λ 4800. For other wave lengths in the observable region similar studies could be undertaken.

First of all, let us consider primarily stars of spectral class earlier than M2, i.e., temperatures above 3200° K or values of $\theta = 5040/T$ less than 1.6. We enumerate the following sources of continuous absorption (or extinction) in these stellar atmospheres: (1) hydrogen absorption (*a*) atomic hydrogen ($\theta < 0.9$), (*b*) negative hydrogen ion ($\theta \geq 0.4$), (*c*) ionized molecular hydrogen (H_2^+)($0.4 < \theta < .9$); (2) helium absorption ($\theta < 0.3$); (3) metallic absorption ($\theta > 1.0$); (4) electron scattering ($\theta < 0.3$, low P_e); and (5) Rayleigh scattering ($\theta > 1.0$, low P_e). The first three of these factors involve conventional thermal absorption, and the stellar material is usually regarded as obeying Kirchhoff's law. Electron and Rayleigh scattering cannot be regarded as absorption processes because the local temperature is not involved.

Various workers have calculated extensive tables of the continuous absorption coefficient. The early computations by Unsöld, Russell, and Pannekoek were carried out before the importance of the negative hydrogen ion was recognized. Among recent calculations of tables of the stellar absorption coefficient, we mention especially those by Vitense (1951*a*) and by Strömgren. Miss Vitense's calculations embrace l the range from $\theta = 0.05$ to $\theta = 1.3$, whereas Strömgren has tabulated log $\bar{\kappa}$ and log $\kappa_\lambda/\bar{\kappa}$ for the range log $P_e = 0.0$–4.0 and $\theta = 0.30$–1.10. Here $\bar{\kappa}$ is the Rosseland mean absorption coefficient.

Since Wildt (1939) demonstrated the role of the negative hydrogen ion, it has been recognized that the principal sources of the continuous absorption in stellar atmospheres are the bound-free and free-free transitions in atomic hydrogen and the photodissociation of the negative hydrogen ion or the interaction of electrons with neutral hydrogen atoms. Chandrasekhar and Breen (1946) computed the continuous absorption coefficient for both the bound-free and the free-free transitions of the negative hydrogen ion. Their bound-free absorption coefficients are substantiated by the more recent work of Geltman (1956), but Ohmura (1960) finds that the free-free absorption coefficient should be decreased. Since the dissociation energy is only 0.7 ev, continuous absorption in the visual region of the solar spectrum is produced mostly by the photodetachment of the extra electron.

Tables of the continuous absorption coefficient of atomic hydrogen and helium have been computed by Saito, Ueno, and Jugaku (1954). To these absorbers must be added other sources of opacity which cannot be neglected in the most accurate work. Miss Vitense considered the contributions of electron scattering, Rayleigh scattering by neutral hydrogen atoms, and continuous absorption by metals. For the metals she assumed hydrogen-like absorption coefficients, although the experimental data and the discussions by Bates (1946) indicate that, for most metals, the absorption coefficients are not hydrogen-like.

The most recent work suggests that continuous absorption by metals is probably so small compared to that by hydrogen that it can be neglected. On the other hand, the model-atmosphere calculations by Osawa (1956) indicate that H_2^+ absorption can become important.

Wildt (1947) had suggested that a significant contribution to the opacity of stellar atmospheres can arise from the bound-free absorption by H_2^+ ions, viz.,

$$H_2^+ (1s\sigma) + h\nu \rightarrow (H + H^+)(2p\sigma),$$

and from the free-free absorption by colliding H atoms and H^+ ions,

$$(H + H^+)(1s\sigma) + h\nu \rightarrow (H + H^+)(2p\sigma).$$

Bates (1951, 1952) has calculated the absorption coefficient for an atmosphere containing H, H^+, and H_2^+ by using accurate quantum-mechanical dipole moments but treating the nuclei as classical particles.

Our present calculations of the coefficient of continuous absorption for the

TABLE 3

RELATION BETWEEN ABSORPTION COEFFICIENT (λ4235 A), GAS PRESSURE, AND TEMPERATURE

($\log A = 4.13$)

$\log \kappa_\lambda(P_g, \theta)$

log P_g	θ															
	0.20	0.24	0.30	0.40	0.50	0.60	0.70	0.80	0.90	1.0	1.1	1.2	1.4	1.6	1.8	2.0
1.0	−0.56	−0.54	−0.52	−0.48	−0.48	−0.44	−1.00	−1.70	.....	.....	.....	.....	.....	.....	.....	.....
2.0	−0.36	−0.33	−0.33	−0.09	+0.11	−0.21	−1.00	−1.72	−2.24	−2.68	.....	.....	.....	.....	.....	.....
2.5	−0.13	−0.08	−0.04	+0.29	+0.44	−0.08	−0.90	−1.57	−2.06	−2.55	−2.67	−2.72	.....	.....	.....	.....
3.0	+0.23	+0.28	+0.36	+0.74	+0.74	+0.06	−0.74	−1.36	−1.87	−2.31	−2.40	−2.44	−2.55	−2.62	−2.74	.....
3.5	+0.67	+0.71	+0.81	+1.20	+0.98	+0.22	−0.53	−1.15	−1.66	−2.00	−2.07	−2.13	−2.28	−2.37	−2.45	.....
4.0	+1.14	+1.19	+1.27	+1.61	+1.18	+0.38	−0.32	−0.92	−1.39	−1.66	−1.72	−1.80	−1.95	−2.01	−2.05	−2.14
4.5	+1.65	+1.70	+1.76	+1.97	+1.37	+0.55	−0.08	−0.67	−1.09	−1.29	−1.34	−1.46	−1.61	−1.67	−1.73	−1.88
5.0	.....	.....	.....	.....	+1.49	+0.70	+0.15	−0.40	−0.77	−0.93	−0.99	−1.11	−1.24	−1.32	−1.43	−1.61
5.5	.....	.....	.....	.....	.....	+0.90:	+0.40	−0.13	−0.43	−0.59	−0.63	−0.76	−0.88	−0.95	−1.14	−1.35
6.0	.....	.....	.....	.....	.....	+1.14:	+0.64	+0.17	−0.09	−0.26	−0.29	−0.40	−0.53	−0.63	−0.86	−1.08
6.5	.....	.....	.....	.....	.....	.....	+0.90:	+0.45	+0.27	+0.06	+0.03	−0.06	−0.20	−0.32	−0.58	−0.80
7.0	.....	.....	.....	.....	.....	.....	.....	+0.75	+0.60	+0.38	+0.33	+0.28	+0.14	−0.00	−0.30	−0.54

purposes of obtaining mean electron pressures and masses above photospheres are carried out for λ 4235. From $\theta = 0.3$ to $\theta = 1.0$ we used Strömgren's tables, to which we added the contributions of Rayleigh scattering (Vitense 1951*a*) computed per neutral, ground-state hydrogen atom, according to the following numerical expression used by Koelbloed (1953):

$$\log \sigma_R = -26.844 + 4 \log \frac{4650\ \mathrm{A}}{\lambda}. \tag{7}$$

For the range $1.0 < \theta < 2.0$ we employed the negative hydrogen-ion absorption coefficient given by Chandrasekhar and Breen. Thus

$$\kappa_\lambda(\mathrm{H}^-) = a_\lambda(\mathrm{H}^-) P_e (1 - x) N_\mathrm{H}, \tag{8}$$

where $a_\lambda(\mathrm{H}^-)$ is tabulated by Chandrasekhar and Breen, $(1 - x)$ is the fracrion of hydrogen that is neutral at the assigned P_e and T, while N_H is the number of hydrogen atoms per gram of stellar material. Then we added the contribution of Rayleigh scattering.

For $\theta < 0.3$ we combined the coefficients of absorption of hydrogen and helium with electron scattering. Thus

$$\kappa_\lambda(\mathrm{H}) = a_\lambda(\mathrm{H})(1 - e^{-h\nu/kT})(1 - x_\mathrm{H}) N_\mathrm{H}, \tag{9}$$

$$\kappa_\lambda(\mathrm{He}) = a_\lambda(\mathrm{He})(1 - e^{-h\nu/kT})(1 - x_\mathrm{He}) N_\mathrm{He}, \tag{10}$$

where $a_\lambda(\mathrm{H})$ and $a_\lambda(\mathrm{He})$ are taken from the Kyoto tables (Saito, Ueno, and Jugaku 1954). The second factor allows for the negative absorptions, $(1 - x)$ is the fraction of atoms that are neutral, and N_He is the number of helium atoms per gram of stellar material. The total coefficient of extinction, then, is

$$\kappa_\mathrm{eff} = \kappa_\lambda(\mathrm{He}) + \kappa_\lambda(\mathrm{H}) + \sigma, \tag{11}$$

where σ here denotes the coefficient of electron scattering.

The following procedure was then adopted: For selected values of θ and for log P_e ranging from -2 to $+4$, we compute log $\kappa_\lambda(P_e, T)$. Then, using the data of Table 2, we may obtain $\kappa_\lambda(P_g, T)$. Table 3 gives the results. The lower limit to the coefficient of continuous extinction at high temperatures and low atmospheric pressures is provided by electron scattering and at low temperatures by the Rayleigh scattering. At the higher temperatures the relation between θ and κ_ν is complex. For a fixed pressure, κ_ν at first increases as the temperature rises but finally decreases again as hydrogen and helium become predominantly ionized.

§ 4. MEAN ELECTRON PRESSURE AND MASS ABOVE PHOTOSPHERE

In his original discussion of the problem, Milne supposed that we could take $\tau = 0.5$ as the representative optical depth for the formation of spectral lines. Later, Strömgren (1940) showed that $\tau = 0.25$ is a better choice for lines of neutral elements such as sodium. In the present application we have adopted

TABLE 4

MASS ABOVE PHOTOSPHERE ($\tau_0 = 0.4$) AS FUNCTION OF GRAVITY AND TEMPERATURE
($\log A = 4.13$)
$\log m$

LOG g	θ																
	0.20	0.25	0.30	0.35	0.40	0.50	0.60	0.70	0.80	0.90	1.0	1.1	1.2	1.4	1.6	1.8	2.0
0.....	+0.15	+0.15	+0.15	+0.15	+0.15	+0.08	+0.15	+0.62	+1.38	+1.86	+2.24	+2.35	+2.37	+2.40	+2.46	+2.52	+2.57
1.....	+0.08	+0.08	+0.08	+0.08	+0.06	+0.05	+0.02	+0.58	+1.24	+1.80	+2.00	+2.05	+2.09	+2.10	+2.16	+2.21	+2.25
2.....	−0.02	−0.03	−0.05	−0.12	−0.20	−0.30	−0.21	+0.52	+1.00	+1.34	+1.58	+1.60	+1.66	+1.74	+1.80	+1.80	+1.97
3.....	−0.32	−0.35	−0.42	−0.52	−0.61	−0.70	−0.39	+0.24	+0.68	+0.98	+1.17	+1.19	+1.23	+1.35	+1.38	+1.40	+1.48
4.....	−0.72	−0.78	−0.87	−0.98	−1.08	−1.10	−0.55	−0.05	+0.30	+0.62	+0.72	+0.76	+0.81	+0.91	+0.96	+1.02	+1.12
5.....	−1.20	−1.27	−1.36	−1.48	−1.56	−1.40	−0.77	−0.34	0.00	+0.22	+0.32	+0.37	+0.43	+0.50	+0.55	+0.64	+0.78

TABLE 5

MEAN ELECTRON PRESSURE AS FUNCTION OF SURFACE GRAVITY AND TEMPERATURE

($\log A = 4.13$)

$\log P_e(\theta, g)$

LOG g	θ																
	0.20	0.25	0.30	0.35	0.40	0.50	0.60	0.70	0.80	0.90	1.0	1.1	1.2	1.4	1.6	1.8	2.0
0....	−0.10	−0.10	−0.10	−0.10	−0.10	−0.10	−0.12	−0.01	−0.24	−0.76	−1.23	−1.78	−1.95	−2.24	−2.53	−2.84	−3.17
1....	+0.84	+0.85	+0.85	+0.85	+0.85	+0.85	+0.65	+0.55	+0.16	−0.37	−0.83	−1.19	−1.32	−1.66	−2.00	−2.34	−2.65
2....	+1.69	+1.68	+1.66	+1.59	+1.48	+1.41	+1.27	+1.04	+0.55	+0.01	−0.41	−0.64	−0.81	−1.20	−1.57	−1.88	−2.20
3....	+2.38	+2.36	+2.28	+2.18	+2.06	+1.90	+1.82	+1.43	+0.89	+0.33	+0.01	−0.17	−0.37	−0.79	−1.10	−1.45	−1.85
4....	+2.97	+2.90	+2.82	+2.70	+2.59	+2.43	+2.31	+1.78	+1.23	+0.75	+0.45	+0.26	+0.07	−0.38	−0.68	−1.02	−1.45
5....	+3.51	+2.44	+3.31	+3.19	+3.10	+3.03:	+2.70	+2.15	+1.59	+1.14	+0.90	+0.66	+0.45	+0.08	−0.26	−0.70	−1.08

$\tau_0 = 0.40$ as the representative optical depth for lines at λ 4235. Hence, from equation (6), the following relationship between P_g, $\kappa_\lambda(P_e, T)$, and g holds, viz.,

$$\log P_g = \log g - \log \kappa_\lambda - 0.40 . \tag{12}$$

Miss Vitense (1951*b*) has used a more sophisticated formula due to Unsöld, but it seems scarcely necessary to introduce such refinements for this preliminary type of calculation.

We assume different values of log g and read off pairs of values of P_g and $\kappa_\lambda(P_g, T)$ for each θ from data of Table 3. Then for each (P_g, θ, g) combination, we find, from Tables 2 and 3, $P_e(g, \theta)$ and $m = \tau_0/\kappa_\lambda(P_g, \theta)$, the mass above the photosphere. Table 4 gives the "mass above the photosphere" for $\tau_0 = 0.4$, while Table 5 gives $P_e(g, \theta, \tau_0 = 0.4)$. The rapid decrease of atmospheric transparency with increasing temperature is strikingly displayed. Table 6

TABLE 6

MEAN GAS PRESSURE AS FUNCTION OF SURFACE GRAVITY AND TEMPERATURE
log $P_g(\theta, g)$

LOG g	θ													
	0.5	0.6	0.7	0.8	0.9	1.0	1.1	1.2	1.3	1.4	1.5	1.6	1.8	2.0
0...	0.20	0.20	0.56	1.40	1.86	2.23	2.34	2.39	2.40	2.42	2.46	2.50	2.60	2.63
1...	1.02	1.06	1.60	2.23	2.64	2.93	3.02	3.00	3.04	3.09	3.11	3.12	3.14	3.19
2...	1.71	1.82	2.47	2.98	3.32	3.56	3.60	3.67	3.73	3.77	3.80	3.82	3.83	3.86
3...	2.30	2.64	3.24	3.68	3.98	4.16	4.20	4.24	4.27	4.30	4.34	4.37	4.40	4.49
4...	2.90	3.47	3.93	4.34	4.61	4.74	4.80	4.82	4.85	4.88	4.93	4.98	5.06	5.17
5...	3.65	4.20	4.62	5.00	5.22	5.30	5.34	5.40	5.45	5.48	5.51	5.54	5.65	5.79

gives the mean gas pressure as a function of surface gravity and temperature. This quantity is needed for the calculation of molecular equilibria and pressure-broadening effects.

In order to exhibit such quantities as the change in the number of atoms capable of absorbing certain observable spectral lines, we must make some allowance for the change in surface gravity with temperature along the main sequence, in the giant branch, and in supergiants. For a preliminary reconnaissance we use an empirical formula for main-sequence stars obtained some years ago by Russell (1933) from the data of eclipsing binaries, viz.,

$$\log g = 3.79 + 0.64\theta . \tag{13}$$

No unique relationship between surface gravity and temperature exists for the giant stars. Stars falling in a rather broad domain of luminosity and spectral class may represent either relatively young, massive stars, recently evolved away from the main sequence, or very ancient stars, similar to those found in M67, with masses only slightly greater than that of the sun. Nevertheless, for

purposes of a qualitative discussion, we take the following rough relation, based on data compiled by Allen (1955):

$$\log g = 5.45 - 2.70\theta\,. \qquad (14a)$$

The supergiant stars exhibit a large range in luminosity and presumably also in mass. Hence the relation between g and θ must have an even more statistical nature. From the data of Allen we obtain the following rough interpolation formula:

$$\log g = 3.42 - 2.06\theta\,, \qquad (14b)$$

which differs somewhat from the correlations suggested by other investigators (cf., e.g., Payne 1930; Ambarzumian *et al.* 1958, p. 255). We must expect that for any given value of θ there is a considerable range in log g.

TABLE 7

GAS PRESSURE, ELECTRON PRESSURE, AND MASS ABOVE PHOTOSPHERE FOR DWARFS, GIANTS, AND SUPERGIANTS
(log A = 4.13)

θ	MAIN SEQUENCE			GIANTS			SUPERGIANTS		
	log P_g	log P_e	log m	log P_g	log P_e	log m	log P_g	log P_e	log m
0.2	+3.24	+2.92	−0.70	.....	.....	.....	.....	.....	.....
0.25	+3.18	+2.87	−0.76	.....	.....	.....	.....	.....	.....
0.3	+3.12	+2.80	−0.85	.....	.....	.....	.....	.....	.....
0.35	+3.04	+2.70	−0.96	.....	.....	.....	.....	.....	.....
0.4	+2.95	+2.62	−0.99	.....	.....	.....	.....	.....	.....
0.5	+2.95	+2.50	−1.00	.....	.....	.....	+1.92	+1.57	−0.45
0.6	+3.54	+2.36	−0.61	.....	.....	.....	+1.98	+1.40	−0.20
0.7	+4.10	+1.89	−0.12	.....	.....	.....	+2.46	+1.19	+0.48
0.8	+4.68	+1.37	+0.26	+3.90	+1.12	+0.52	+2.95	+0.55	+1.00
0.9	+4.86	+0.89	+0.48	+4.00	+0.41	+0.95	+3.14	0.00	+1.40
1.0	+4.96	+0.64	+0.55	+4.00	−0.19	+1.25	+3.15	−0.70	+1.78
1.1	+5.04	+0.45	+0.56	+3.95	−0.41	+1.43	+3.17	−1.00	+1.90
1.2	+5.16	+0.28	+0.59	+3.80	−0.70	+1.57	+3.10	−1.22	+1.96
1.3	+5.26	+0.07	+0.60	+3.66	−1.01	+1.70	+2.93	−1.58	+2.08
1.4	+5.32	−0.09	+0.60	+3.50	−1.35	+1.82	+2.78	−1.90	+2.22
1.5	+5.35	−0.21	+0.60	+3.30	−1.73	+1.96	+2.64	−2.22	+2.32
1.6	+5.41	−0.31	+0.60	+3.12	−2.11	+2.08	+2.52	−2.52	+2.40
1.8	+5.60	−0.73	+0.67	+2.87	−2.60	+2.28	+2.32	−3.01	+2.58
2.0	+5.84	−1.04	+0.75	+2.52	−3.10	+2.45	+2.00	−3.44	+2.70

Accordingly, the values given in Table 7 for the gas and electron pressures and the mass above the photosphere, m, for giant and supergiant stars are to be regarded as very rough. The "best" choices of $\bar{P}_g$ and $\bar{P}_e$ will vary along the spectrum and, as previously emphasized, with the type of ion as well.

§ 5. VARIATION IN NUMBER OF ABSORBING ATOMS WITH TEMPERATURE FOR DWARFS, GIANTS, AND SUPERGIANTS

We shall now calculate the variation in the numbers of atoms capable of absorbing certain observable lines as a function of temperature for main-

sequence, giant, and dwarf stars. First (cf. Table 7), log P_e and log m are interpolated from the data of Tables 4 and 5 for the three groups of stars. Then for each line or multiplet of astrophysical interest we compute the following quantity:

$$\log \frac{N_{r,s}}{N_T} \mathrm{m},$$

where $N_{r,s}/N_T$ denotes the ratio of the number of atoms in the sth term of the rth stage of ionization to the total number of atoms of that element. This ratio is, of course, computed from the Saha and Boltzmann equations. Since m is the total mass of material above the photosphere, we still have to multiply by the number of atoms of the particular element per gram of stellar material to obtain the actual number of atoms involved. Thus for each element we can give the relative numbers of active atoms as a function of temperature.

In order to apply the Saha equation, we must know the partition functions for the atoms and ions involved. Convenient tables have been given for several elements by a number of workers, e.g., Koelbloed (1953) and particularly Claas (1951) for elements at the lower temperatures. Additional calculations have been carried out at Michigan. Partition functions for ions at high temperatures have been calculated by de Jager and Nevén (1957*a*), by Aller, Elste, and Jugaku (1957), and by Boury and Jugaku (unpublished). Table 8A gives the results for the partition functions for a number of metals of astrophysical interest; in most instances our more recently computed values are in good agreement with those of Claas, whose approximations for the convergence of the partition function we have adopted.

For any atom or ion, the partition function depends on the density as well as on the temperature, the density dependence being more marked at the higher temperatures. In Table 8A we have allowed for this effect in a general way. At the pressures encountered in normal stellar atmospheres the values of the partition function should not differ much from the numbers tabulated. For the atoms and ions in Table 8B, $u(T)$ may be taken as roughly constant for temperatures less than 10,000° K.[1]

We illustrate here the results for hydrogen, a permanent gas, and for calcium and iron as typical metals. Iron is represented in three stages of ionization as Fe I, Fe II, Fe III. The lines considered are as shown in Table 9. The effects of both thermal excitation and ionization can be examined for this element. Table 10 gives the relative numbers of atoms capable of absorbing λ 4045 and λ 5563 Fe I, λ 4924 Fe II, and λ 4419 Fe III as a function of $\theta = 5040/T$ for main-sequence stars, giants, and supergiants. The Fe I (a^3F) atoms have a maximum at $T = 4200°$ K in the main sequence and near 3300° K in the supergiants. At lower temperatures the Boltzmann factor works against them. The atoms acting to produce the Fe II λ 4924 line have a maximum near 6300° K in the main sequence and 5300° K in the supergiants, whereas the

[1] Adopted from Claas's table.

TABLE 8A

VALUES OF PARTITION FUNCTION FOR LOWER TEMPERATURES

log $u(T)$

ELEMENT	T(° K)				ELEMENT	T(° K)			
	3600	5700	8000	10,000		3600	5700	8000	10,000
Li I	0.30	0.38	0.47	0.56	Ge I	0.88	0.94	0.99	1.02
Be I	0.00	0.02	0.06	0.15	Ge II	0.58	0.64	0.68	0.70
Be II	0.30	0.30	0.31	0.32	Rb I	0.34	0.38	0.92	.....
Na I	0.30	0.38	0.50	0.63	Sr I	0.02	0.15	0.46	0.72
Mg I	0.00	0.02	0.08	0.17	Sr II	0.31	0.36	0.45	0.54
Al I	0.76	0.77	0.79	0.82	Y I	1.04	1.15	1.34	1.40
Si I	0.95	0.98	1.02	1.05	Y II	1.17	1.24	1.33	1.41
Si II	0.75	0.76	0.76	0.77	Y III	.....	.....	1.02	1.03
P I	0.60	0.65	0.76	.....	Zr I	1.37	1.61	1.83	1.99
P II	0.90	0.92	0.95	.....	Zr II	1.62	1.71	1.83	1.95
K I	0.54	0.61	0.89	1.19	Zr III	.....	.....	1.40	1.44
Ca I	0.01	0.12	0.42	0.67	Nb I	1.60	1.78	1.96	2.11
Ca II	0.31	0.36	0.45	0.55	Nb II	1.52	1.72	1.89	1.99
Sc I	1.04	1.14	1.32	1.48	Mo I	0.87	1.03	1.28	1.53
Sc II	1.32	1.38	1.47	1.52	Mo II	0.73:	0.91	1.18	1.40
Ti I	1.36	1.53	1.73	1.91	Ru I	1.41	1.58	1.75	1.90
Ti II	1.68	1.75	1.86	1.93	Ru II	1.29	1.42	1.55	1.67
V I	1.58	1.73	1.88	2.03	Pd I	0.29	0.59	0.79	0.92
V II	1.55	1.69	1.76	1.84	Pd II	0.84	0.88	0.93	0.97
Cr I	0.92	1.08	1.27	1.41	Ag I	0.30	0.30	0.33	0.36
Cr II	0.79	0.91	1.07	1.24	Ag II	0.00	0.00	0.01	0.02
Mn I	0.78	0.85	0.97:	1.12	Cd I	0.00	0.00	0.02	0.05
Mn II	0.86	0.92	0.98:	1.03	In I	0.56	0.63	0.70	0.76
Fe I	1.38	1.49	1.65	1.78	In II	0.42	0.61	0.71	0.77
Fe II	1.57	1.67	1.75	1.83	Sn I	0.61	0.77	0.86	0.92
Fe III	.....	.....	1.41	1.46	Sn II	0.44	0.53	0.59	0.62
Co I	1.39	1.54	1.67	1.78	Sb I	0.63	0.71	0.80	0.87
Co II	1.34	1.49	1.60	1.67	Sb II	0.39	0.58	0.70	0.78
Co III	.....	.....	1.41	1.45	Ba I	0.18	0.55	0.91	1.15
Ni I	1.45	1.51	1.57	1.62	Ba II	0.51	0.67	0.78	0.85
Ni II	0.95	1.08	1.22	.....	La I	1.28:	1.34	1.50	.....
Ni III	.....	.....	1.26	1.28	La II	1.45	1.52	1.62	.....
Cu I	0.31	0.40	0.51	0.61	Pb I	0.08	0.26	0.42	0.55
Cu II	0.00	0.02	0.11	0.24	Pb II	0.30	0.33	0.37	0.40
Ga I	0.78	0.78	0.79	0.81					

TABLE 8B

ADDITIONAL PARTITION FUNCTIONS FOR ATOMS AND IONS

H	2.0	1.0	S	8.6	4.3
He	1.0	2.0	Cl	5.7	8.3
B	6.0	1.0	A	1.0	5.4
C	9.5	6.0	Br	4.8	.....
N	4.2	8.9	Kr	1.0	4.6
O	9.0	4.0	Ag	2.0	1.0
F	5.9	8.7	Cd	1.0	2.0
Ne	1.0	5.7	Hg	1.0	2.0

Fe III a^5P atoms reach a maximum on the main sequence at a temperature of about 18,000° K.

Table 11 shows the results for the resonance lines of neutral and ionized calcium. The number of Ca I atoms decreases monotonically with the rising temperature, whereas the Ca II ions show a flat maximum near 4200° K in the main sequence. The effect of the increased transparency and lower electron pressure of the giant and supergiant atmospheres is to cause the number of Ca II ions to increase right up to the temperature of 3100° K.

Similar results are found for resonance lines of other metals, e.g., Ti I, Na I (D lines), and Ba II. The numbers of absorbing atoms decrease monotonically with increasing temperature for sodium and neutral titanium. Ba II has a maximum at a low temperature in the main sequence but continues to increase to the lowest temperatures tabulated for supergiants. The fall in temperature is

TABLE 9

DATA FOR TRANSITIONS IN IRON

Ion	Line	Term	χ (ev)	Ion	Line	Term	χ (ev)
Fe I.....	λ 4045	a^3F	1.60	Fe II.....	λ 4924	a^6S	2.88
	λ 5565	y^3F^o	4.59	Fe III....	λ 4419	a^5P	8.22

TABLE 10

POPULATION OF IRON LEVELS

θ	Fe III	Fe II			Fe I					
	λ 4419	λ 4924			λ 4045			λ 5563		
	Main Sequence	Main Sequence	Giant	Super-giant	Main Sequence	Giant	Super-giant	Main Sequence	Giant	Super-giant
0.2.....	−4.98	.....	.....	.....	.....	.....	.....	.....	.....	.....
0.25.....	−3.80	.....	.....	.....	.....	.....	.....	.....	.....	.....
0.30.....	−3.79	.....	.....	.....	.....	.....	.....	.....	.....	.....
0.35.....	−4.24	−4.79	.....	.....	.....	.....	.....	.....	.....	.....
0.4.....	−4.66	−4.12	.....	.....	.....	.....	.....	.....	.....	.....
0.5.....	−6.51	−3.46	.....	.....	.....	.....	.....	.....	.....	.....
0.6.....	−8.21	−3.30	.....	.....	.....	.....	.....	.....	.....	.....
0.7.....	.....	−3.06	.....	−2.46	−3.79	.....	−3.89	−5.89	.....	−5.99
0.8.....	.....	−2.95	−2.68	−2.20	−2.92	−2.91	−3.00	−5.31	−5.30	−5.39
0.9.....	.....	−3.00	−2.52	−2.06	−2.42	−2.40	−2.36	−5.11	−5.09	−5.05
1.0.....	.....	−3.27	−2.50	−1.95	−1.89	−1.83	−1.91	−4.88	−4.82	−4.90
1.1.....	.....	−3.77	−2.66	−2.13	−1.58	−1.32	−1.37	−4.87	−4.61	−4.66
1.2.....	.....	−4.54	−2.92	−2.39	−1.48	−0.84	−0.84	−5.07	−4.43	−4.43
1.3.....	.....	−5.60	−3.28	−2.68	−1.55	−0.60	−0.48	−5.44	−4.49	−4.37
1.4.....	.....	−6.56	−3.93	−3.11	−1.69	−0.52	−0.23	−5.87	−4.70	−4.41
1.5.....	.....	.....	−4.55	−3.72	−1.84	−0.50	−0.17	−6.32	−4.98	−4.65
1.6.....	.....	.....	−5.17	−4.34	−2.00	−0.53	−0.22	−6.78	−5.31	−5.00

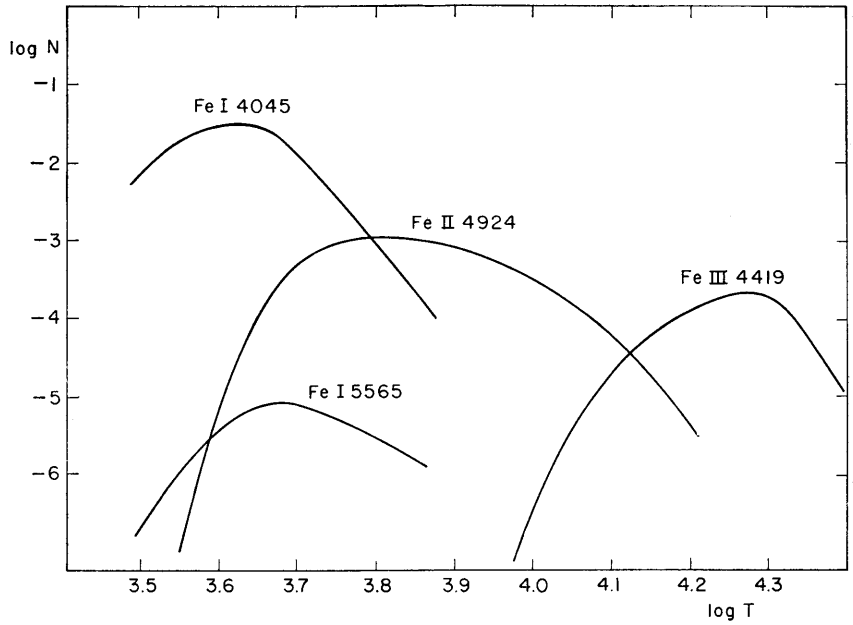


FIG. 1.—The relative numbers of iron atoms above the photosphere for main-sequence stars. The behavior of log N for two typical lines of Fe I and for a line of Fe II and of Fe III is plotted against log T.

TABLE 11

POPULATIONS OF CALCIUM LEVELS

θ	λ 4227			λ 3933		
	Main Sequence	Giant	Super-giant	Main Sequence	Giant	Super-giant
0.4	.....	.....	.....	−3.40	.....	.....
0.5	−6.70	.....	.....	−2.15	.....	.....
0.6	−4.71	.....	−6.97	−0.91	.....	−1.12
0.7	−3.89	.....	−5.06	−0.28	.....	+0.22
0.8	−3.21	−3.22	−3.33	+0.16	+0.41	+0.86
0.9	−2.72	−2.72	−2.70	+0.43	+0.90	+1.34
1.0	−2.09	−2.22	−2.20	+0.51	+1.21	+1.78
1.1	−1.51	−1.58	−1.70	+0.55	+1.42	+1.90
1.2	−0.98	−0.97	−1.20	+0.58	+1.57	+1.96
1.3	−0.53	−0.47	−0.68	+0.57	+1.70	+2.08
1.4	−0.06	0.00	−0.15	+0.49	+1.81	+2.22
1.5	+0.30	+0.44	+0.32	+0.30	+1.95	+2.32
1.6	+0.50	+0.84	+0.77	+0.10	+2.05	+2.39

more than compensated for by a decline in electron pressure. Magnesium shows an interesting behavior. The 3^2D term of Mg II has a relatively high population over a considerable range in temperature.

Calculations for permanent gases show that the maxima for the various ions fall at high temperatures as is to be expected. Indeed, these maxima have traditionally been employed to establish the ionization temperature scale for the hotter stars. Perhaps the most significant calculations are those pertaining to the hydrogen lines. The population of the $n = 2$ level shows a broad maximum around 10,000° K and falls off sharply in the direction of decreasing tem-

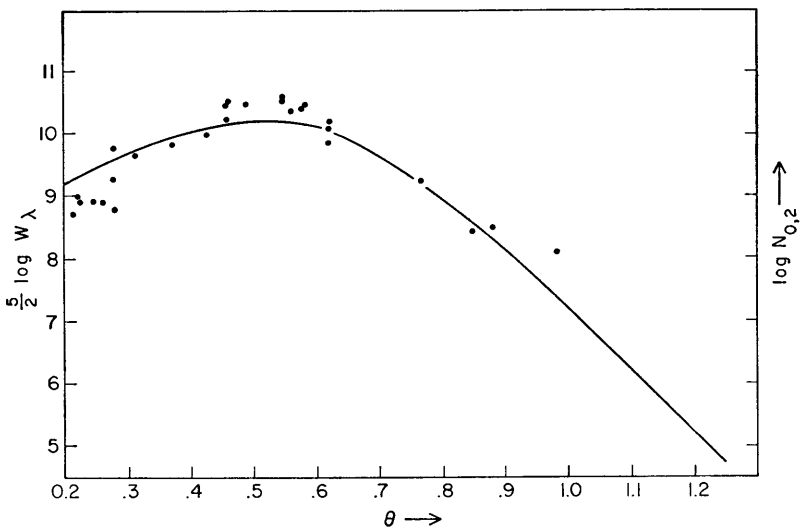


FIG. 2.—The predicted variation with temperature of the population of the second quantum level of hydrogen and the observed strengths of Hγ (equivalent widths in mA).

perature. The hydrogen lines are broadened by the interatomic Stark effect. Very roughly, the equivalent width is related to the product Nf by the following relation:

$$W_\lambda \sim (Nf)^{2/5} . \qquad (15)$$

Figure 2 (prepared by Paul Mutschlecner) gives the predicted number of atoms as a function of θ. The observed equivalent widths of Hγ as measured by Günther (1933) are plotted on the same diagram, as $\frac{5}{2}$ log W(mA). The observed points define a curve of the same shape as the theoretical curve. (We would not expect a quantitative agreement since the relation between W and Nf is not exact.) Some of the discrepancy is accounted for by the assumption that the line is formed at a uniform temperature and density. The line-broadening coefficient is strongly dependent on the ionic density; the wings of the lines are formed in deep layers, the core is formed in the highest layers of the atmosphere, probably in the chromosphere of the star itself.

§ 6. COMPARISONS BETWEEN THEORY AND OBSERVATION, ABSOLUTE-MAGNITUDE EFFECTS

The equivalent width of a spectral line depends on a number of factors, only one of which is the number of atoms in a level capable of absorbing it. The gross qualitative features of the spectral sequence, insofar as they depend on temperature, are well explained by the ionization theory, as was demonstrated long ago by Saha, by Milne and Fowler, by Payne (1925), and by Menzel (1924). Our calculations represent a refinement over the earlier work, in that they allow for the variation in the atmospheric opacity as a function of temperature and take into account the partition functions of the various atoms and ions.

The predicted maxima of the hydrogen lines near spectral class A0 ($\theta = 0.5$), the N III and O III lines in late O ($\theta = 0.15$), the N II and O II lines near B1 or B2, and the Mg II lines in the late B's are in accord with observations. The Fe III lines appear in early B stars in accordance with the predictions of theory and fade out rapidly with decreasing temperature.

Comparisons between stars of the same spectral class but of different luminosity classes do not show a good agreement with our elementary picture. In the cooler stars the theory predicts a great increase in atmospheric transparency (number of atoms above the photosphere) for the giants and supergiants, as compared with the main-sequence stars. Hence most spectral lines would be intensified in the latter group of stars, as compared with the former if the same relation between numbers of atoms and equivalent widths held.

For example, in late K or early M types, the number of atoms capable of absorbing the λ 4227 line of neutral calcium would appear from our computations actually to be greater in the supergiants or giants, as compared with the dwarfs. Yet this line is a reliable index of absolute magnitude, in the sense that it is very much stronger in the dwarfs than in giants or supergiants. Another example in point is provided by the Hγ and Hδ lines in the A stars. The number of "active atoms" is very nearly the same for both main-sequence stars and supergiants. Nevertheless, these hydrogen lines are much stronger in the dwarfs than in the supergiants. The effects are not small; the equivalent width of Hγ in a star of absolute magnitude +1.5 is about five times as great as in a star of absolute magnitude −5 and of the same spectral class.

The behavior of both the λ 4227 line of Ca I and Hγ and Hδ may be understood in terms of density broadening (sometimes called "pressure broadening"). The hydrogen lines are broadened by the first-order Stark effect due to the microscopic fields produced by ions (mostly hydrogen ions) and (to a lesser extent) the effects of electrons. The broadening effect of the ions may be calculated by the Holtsmark theory, that of the electrons by the phase-shift theory (Kolb and Griem 1958). The dependence of the absorption coefficient in the

line wings on the density and temperature is known but is somewhat complicated. Roughly, the absorption coefficient in the wing falls off as

$$a_\nu = \text{Const. } N_e (\Delta\lambda)^{-s}, \tag{16}$$

where $s = \frac{5}{2}$ for the Holtsmark theory and somewhat smaller for the theory that takes into account electronic, as well as ionic, effects.

Thus, although the number of active atoms above the photosphere remains the same in going from main-sequence stars to supergiants for stars with temperatures of 10,000° K or above, the line-broadening coefficient in the wing decreases as the electron density decreases. Hence the much greater strength of the lines in the dwarf stars can be explained, at least qualitatively. In yet hotter stars, those of class O, the absolute-magnitude effects are much reduced, a phenomenon that can be understood with the aid of a more sophisticated theory. In G and K stars the hydrogen lines in giants and supergiants appear abnormally strong (the Russell-Adams phenomenon). Part of this behavior may be attributed to chromospheric effects, since it is well established that supergiant stars like VV Cephei, ζ Aurigae, and 31 Cygni have extended atmospheres. In such envelopes it is scarcely to be expected that the isothermal assumption would be a good approximation.

The λ 4227 Ca I line is broadened by collisions between the radiating atoms and perturbing particles, mostly hydrogen atoms or molecules. The interaction between neutral atoms is of the van der Waals type (which depends on the inverse sixth power of the distance between the particles). A radiating atom may also be perturbed by ions or electrons, i.e., charged particles; the disturbance depends on the square of the microscopic electric field (i.e., on the inverse fourth power of the distance between the radiating particle and the perturbing charges). This quadratic Stark effect is important at higher densities for all atoms other than those of hydrogen and helium. The helium lines show both first-order and quadratic Stark effects in a very complicated manner.

For the quadratic Stark effect and for the van der Waals type of interaction, the shape of the line-broadening coefficient is the same as for natural damping, except that the radiative damping constant, Γ_{rad}, is now replaced by $\Gamma_{\text{rad}} + \Gamma_{\text{coll}}$. Since the absorption coefficient in the wing of a strong line is proportional to $Nf\Gamma$, where N is the number of atoms capable of absorbing the line (i.e., the quantity computed in § 4), the larger the value of Γ, the stronger the line. Curve-of-growth studies (cf. chap. 4) show that in late-type giant and supergiant stars the damping constant for the strong lines is nearly Γ_{rad}, whereas in dwarf stars the collisional damping constant may be ten or even fifty times as great as the radiative damping constant. Thus, among the cool stars, certain of the very strongest lines, such as λ 5889 and λ 5896 of Na I may tend to be strengthened in the dwarf stars.

Lines of intermediate intensity which do not show broad damping wings, but bell-shaped profiles, are often noticeably stronger in giants and supergiants

than in dwarfs of the same spectral class, even though the number of active atoms above the photosphere may be the same. Except for rather strong lines, the shape or profile is controlled by the Doppler broadening. In dwarf stars this Doppler broadening is mostly due to the gas kinetic motions of the radiating atoms themselves. Broadening due to large-scale motions, commonly referred to as "turbulence," is usually relatively unimportant. In the giant and supergiant stars, on the other hand, large-scale mass motions of the radiating gases with velocities of the order of 20–30 km/sec are common. Hence the Doppler-determined part of the absorption coefficient is much broader, and the lines may attain a much greater strength than they do for comparable numbers of active atoms among the dwarf stars.[2]

Absolute-magnitude effects are, of necessity, established empirically. A few of them are readily explained by theoretical considerations. Others involve line-ratio effects that would require detailed studies with the aid of model atmospheres and elaborate theories of spectral-line formation. Yet others involve the behavior of blends and molecular bands that show a pronounced sensitivity to luminosity but will not be explained theoretically until the detailed intensity distributions in entire spectral regions can be handled with the aid of model-atmosphere theories.

Among the most frequently used criteria in G and K stars is the strength of the cyanogen bands, which are intensified in giant and supergiant stars as compared with dwarfs. This empirically established result is also in accordance with theory, although a detailed quantitative interpretation will require model atmospheres or at least a careful study of curve-of-growth effects.

§ 7. THE ROLE OF MOLECULES IN STELLAR SPECTRA

Up to this point we have limited our discussion to stars hotter than 3200° K (corresponding to spectral class M2 on Kuiper's scale [1938]). At lower temperatures, the blocking of outgoing radiation in the visible and photographic region is primarily due to molecular bands. Hence calculations of continuous absorption coefficients on the basis of the agents responsible in a star like the sun, e.g., the negative hydrogen ion, may be inadequate.

In the normally observed regions of stars of spectral classes M, R, N, and S the blocking of radiation is done by well-recognized bands of TiO, carbon and its compounds, and ZrO, etc. Most of the stellar radiation in the cool stars falls in the spectral region λλ 9000–25000 A. In this region the principal source of opacity is probably still the negative hydrogen ion, although blocking by rotation-vibration bands of polyatomic molecules, e.g., HOH in the coolest stars, may become an important factor. See, for example, the discussion by Swings (1958). Although the temperature and pressure distribution in the atmosphere (i.e., the structure of the atmosphere) is more intimately influenced by the

[2] See, for example, the discussion in the author's *Atmospheres of the Sun and Stars* (New York: Ronald Press Co., 1953), pp. 304 ff., esp. Fig. 16, p. 307.

sources of opacity in the 1μ–2μ region, what we actually observe is a region far on the short-wave-length side of the energy maximum. In the M stars the overlapping bands of TiO depress the continuum far below its predicted position in the ordinary visual region of the spectrum. The cool carbon stars have a continuous absorption coefficient so strong that their spectra are difficult to observe below about λ 4000. Since the source of this continuum has not been positively identified, we cannot make any theoretical predictions concerning the structure of the atmosphere or the number of atoms above the photosphere. The existence of such a continuous absorption is demonstrated by comparing the strong λ 10900 (0, 0) band of the red CN system in the spectra of the late N-type stars with the weak λ 3883 band of the violet CN system in these same stars (McKellar 1954). Both these bands originate from the normal state of the CN molecule and must have approximately equal transition probabilities and therefore comparable intrinsic intensities. In the long-period variable Y CVn, for example, the λ 3883 band is virtually absent, whereas the red bands exhibit outstanding strength.

In passing from K to M stars the atomic lines show a relatively small intensity change compared with the huge variation in the molecular bands. The "true" continuum (produced by continuous absorption) is probably never seen (as is true for the solar spectrum below λ 3500 A); the effective depth of the photosphere is rendered much smaller by an amount that varies drastically from one wave-length region to another.

In view of these considerations, we have not extended our calculations of the numbers of atoms, mass above the photosphere, or electron pressures beyond $\theta = 2.0$. In fact, in the usually observed spectral regions it is likely that our calculations give results that are systematically too large for all these quantities beyond $\theta = 1.4$, because of the onset of the pronounced blending effects of densely packed atomic lines and molecular bands. When we observe late-type stars in ordinary spectral regions (or the sun in the rocket ultraviolet), we see only the cores of the strongest lines. The effective "level of the photosphere" is substantially raised, and each spectral region must be treated separately. Furthermore, some of the atoms of titanium, zirconium, etc., are tied up in molecules, so that the number available for absorbing atomic spectral lines is diminished.

The dissociation equilibrium of the compounds likely to be found in the atmospheres of cool stars was treated *in extenso* by Russell (1934). He showed that in stars like the sun, where oxygen was more abundant than carbon, the latter element tended to be tied down in CO, while titanium formed TiO upon combination with oxygen. The most abundant oxygen compound in the cooler stars was water, however. The general qualitative behavior of the spectra of stars of Draper classes G, K, and M could be explained. Russell also investigated the situation exhibited by the carbon stars, i.e., stars in which carbon was more abundant than oxygen. Here it is the oxygen that is all consumed to form CO,

while C_2, CN, and CH dominate the atmospheres. The simple model proposed by Russell qualitatively explained the broad features of spectral classes R and N. By carrying out separate calculations for giants and dwarfs, Russell was also able to explain some of the absolute-magnitude differences found in molecular bands, e.g., why stars with much stronger TiO bands exist among giant M stars than are ever found among dwarf stars.

One of the big difficulties in analyses of this type is that fundamental physical constants, particularly the dissociation potentials of certain astrophysically important compounds, e.g., C_2, are not known. Nevertheless, so much progress has been made since Russell's work that substantially improved calculations of the dissociation equilibrium can be made. Among recent calculations we may mention those of de Jager and Nevén (1957*b*), who used dissociation equilibrium constants, K_{AB}, defined by

$$\frac{P_A P_B}{P_{AB}} = K_{AB}$$

for C_2, N_2, O_2, CH, CN, CO, NH, NO, and OH, computed by Pecker and Peuchot, to calculate the concentrations of these compounds (and also H_2O) over a range in temperatures, pressures, and compositions expected to obtain in stellar atmospheres. They used six values of the gas pressure, log P(H) = 1, 2, 3, 4, 5, and 6; six values of the temperature, θ = 0.8, 1.0, 1.2, 1.4, 1.7, and 2.0; and also six different choices of the abundance of C, N, and O with respect to H. These choices of abundance simulated both ordinary oxygen-rich stars and carbon stars. On the basis of these calculations de Jager and Nevén were able to draw a number of interesting conclusions. Using Hunaerts' (1947) data for the sun, they were able to conclude that the dissociation of C_2 must be 6.7 ev rather than 4.3 ev. Furthermore, they concluded that the O abundance was probably of the order of 10^{-3} that of hydrogen or even less. This result is in good accord with that found from the atomic lines by the curve-of-growth method.

One important factor to be considered in connection with the formation of molecular bands in stellar atmospheres is that, at least in stars of spectral classes G and K, the molecular lines are formed in shallower layers than are the atomic lines. That is, if we wish to use the isothermal approximation, we should select lower values of $\bar{T}$ and $\bar{P}_g$ for molecular lines and bands than for atomic lines. In the sun, de Jager and Nevén find that molecular bands of CN, OH, etc., are formed in strata where the temperature is 4300 $\pm$ 100° K, i.e., in the uppermost layers of the photosphere. A similar conclusion had been reached by Newkirk (1957) in his discussion of the CO bands in the solar atmosphere. Similarly, they use Keenan's data on the spectral classes where the CN bands attain their maximum strength to estimate the temperatures of the layers at which these bands are predominantly formed. They assume that the lines are formed at an optical depth of τ_0 = 0.2 (de Jager and Nevén 1957*b*) and at log P = 3.2, 4.0, and 5.0 for dwarfs, giants, and supergiants, respectively. The

fourth column of Table 12 gives their derived temperatures. For comparison they also give (second column) the effective temperatures for these same stars. These latter values are obtained from colors, bolometric measurements, studies of the line spectrum, etc. Corroborative results are obtained from the CN bands.

Much of the interest in molecular bands in cool stars arises from the fact that substantial differences in chemical composition are found in these objects. Since stars of peculiar or unusual composition are to be treated elsewhere in this series, we shall make here only a few very general remarks. The difference between the G, K, and M stars, on the one hand, and the R and N stars, on the other, can be explained by a "normal" composition (i.e., oxygen more abundant than carbon) for the former and a carbon-rich composition for the latter. The S stars show the bands of ZrO and a general enhancement of the abundances of the elements in the second long period. Stars of intermediate composition, enhanced in both the zirconium group and carbon, are observed by Merrill (1955).

TABLE 12

TEMPERATURES IN LINE-FORMING STRATA FOR CN BANDS

Spectral Class for CN Band Maximum	Effective Temperature (Kuiper 1938)	log P (Assumed)	Temperature ($\tau_0=0.2$) (° K)
G6 I.....	3920	3.2	3660
G9 III.....	4325	4.0	3900
K1 V.....	4810	5.0	4200

Quantitative discussions of the data are difficult because of complexities of late-type stellar spectra, on the one hand, and absence of certain essential physical data, on the other. The work of Bouigue (1957), for example, illustrates some of the intricacies of the problem. He studied the equilibrium of TiO, ZrO, CN, and C_2 as a function of the abundance of carbon, using the same surface gravities and pressures as Russell had employed for the oxygen-rich red giants. From a study of the dissociation equilibrium he found evidence for two groups of stars with very different abundances of zirconium, but that the relative amounts of ZrO and TiO were very sensitive to the abundance of carbon. In their discussion of the dissociation equilibrium, de Jager and Nevén had found that in cool stars the strength of TiO and ZrO was very sensitive to small variations in the oxygen abundance. These calculations illustrate that care must be taken in the interpretation of data for late-type stars.

With the aid of the data in Table 7, calculations of the dissociative equilibria may be carried out for main-sequence stars, giants, and supergiants in a manner closely analogous to that employed by Russell. At the lower temperatures, the amount of material above the photosphere (and the gas pressures as well) is

certainly too high, but at the moment we cannot make any accurate correction for the general absorption produced by molecular and atomic lines.

Consider, first, the results obtained for stars of normal composition. In dwarfs, molecular hydrogen is the most abundant atmospheric constituent below 3000° K; it is the most abundant molecule in giants and supergiants as well, although it does not become as abundant as atomic H in the larger stars. The next most abundant molecule, below about 4700° K, is CO, which uses up most of the carbon in all oxygen-rich stars. In the dwarfs, H_2O is the next most abundant molecule below 3300° K; OH reaches a maximum log $N \sim 21.0$ near 3600° K and levels off. CH, CN, and C_2 reach maxima of log $N \sim 19.4$, 18.5, and 17.5 near 4200° K and decline thereafter, while N_2 rises rapidly in abundance from 6000° to 3800° K and then increases more slowly as T declines. The bands of TiO and ZrO never attain the great strength exhibited in the giant stars.

In the supergiants we find that CO and OH rise steadily as T declines. At the lowest temperature, the H_2O abundance approaches log $N = 22.0$, but at $T =$ 3600° K, the concentration is about six hundred times lower than in dwarfs at the same temperature. Nitrogen, N_2, rises rapidly as the temperature falls to 3600° K and then increases more slowly thereafter; NH has a flat maximum between 3400° and 3900° K. The CN, CH, and C_2 molecules show maxima near 3500° K.

TABLE 13

LOG N/N(H)

	Designation	C	N	O
Oxygen-rich.....	(O)	−3.6	−3 9	−3.1
Oxygen=carbon....	(C=O)	−3.1	−3.9	−3.1
Carbon-rich.....	(C)	−2.8	−3.9	−3.1

Giant and supergiant stars of certain typical ratios of carbon to oxygen and with different heavy-metal contents are listed in Table 13. Table 14 gives the concentrations of the various compounds for giant stars of the (C=O) composition. In all groups, atomic hydrogen is the most abundant atmospheric constituent; for all temperatures below 4200° K, H_2 is the next most abundant component of the atmosphere. Carbon monoxide is the prevailing compound below 5000° K in the oxygen stars and below 5600° K in the (C) stars. In the (O) stars it takes up nearly all the carbon, in the (C) stars it takes virtually all of the oxygen and in the (C=O) stars it depletes both carbon and oxygen. At the lowest temperatures in the giant (O) stars, OH is comparable in abundance with CO. In the (C=O) stars, at its maximum near 3400° K, it is a hundred times less abundant than CO, whereas in the (C) stars at the lowest temperatures it is 10^{-5} as abundant as CO! The maximum concentration of H_2O in the (C) stars is about five hundred times smaller than the maximum value it attains in the

(O) stars, while in the (C = O) stars it is about ten to fifty times smaller. The N_2 concentration is much less affected. In the carbon stars the concentrations of the carbon compounds are naturally enhanced and the oxygen compounds are suppressed. The extreme sensitivity of the number of TiO molecules to the C/O ratio, indicated in the work of Bouigue, de Jager and Nevén, and Russell, is well substantiated by our calculations. For example, between 3400° and 2500° K, the number of TiO molecules is between one hundred and one thousand times smaller in the giant (C) stars than in the giant (O) stars, even though the carbon abundance is enhanced by a factor of only six in going from the (O) stars to the (C) stars.

Examination of the molecular equilibria suggests that the spectroscopic data on late-type stars may be utilized to obtain accurate information on the C/O ratios in these objects. Discussions of the Ti/Zr ratio, for example, must be handled with care, since the relative TiO and ZrO concentrations, as well as their absolute values, depend critically on the physical state of the atmosphere and its chemical composition. All calculations that have been carried out so far are of the qualitative variety; necessarily they neglect the stratification in the atmosphere and the marked influence of the temperature gradient on the equilibria of the compounds. Model atmospheres for late-type stars necessarily will be difficult to construct.

TABLE 14

CONCENTRATION OF MOLECULES IN GIANT STARS
$\log A = 4.15$; $N(\mathrm{C}) = N(\mathrm{O})$
($\log N$)

MOLECULE	θ					
	0.8	1.0	1.2	1.4	1.7	2.0
H	24.05	24.82	25.14	25.38	25.71	25.80
H_2	19.33	21.02	22.10	23.13	24.33	25.17
CH	16.47	17.96	18.80	19.21	19.04	18.65
NH	15.65	17.14	17.98	18.42	18.27	17.80
OH	17.04	18.72	19.75	20.46	20.35	19.74
C	20.95	21.72	22.00	21.86	21.11	20.27
C_2	15.07	17.20	18.64	19.29	19.00	18.66
CN	15.26	17.60	19.26	20.12	20.20	20.11
CO	16.16	18.86	20.89	22.11	22.63	22.86
N	20.15	20.92	21.19	21.02	20.20	19.19
N_2	15.08	17.81	19.85	21.02	21.54	21.76
NO	14.41	16.49	17.88	18.44	17.98	17.12
O	20.95	21.72	22.00	21.86	21.05	19.93
O_2	13.14	14.89	15.97	16.25	15.34	13.94
H_2O	12.60	15.25	17.09	18.50	19.48	19.72
Ti	13.75	14.88	16.22	17.29	18.32	18.66
Ti^+	16.75	17.62	17.83	18.03	17.84	16.66
TiO	7.65	10.14	12.67	14.55	16.04	16.62
Zr	14.00	15.11	16.47	17.52	18.34	18.66
Zr^+	16.75	17.62	17.82	17.97	17.59	16.27
ZrO	8.44	11.11	13.82	15.86	17.41	18.24

REFERENCES

ALLEN, C. W.	1955	*Astrophysical Quantities* (London: Athlone Press).
ALLER, L. H.	1942	*Ap. J.*, **96**, 321.
	1953	*Atmospheres of the Sun and Stars* (New York: Ronald Press Co.).
ALLER, L. H., ELSTE, G., and JUGAKU, J.	1957	*Ap. J. Suppl.*, **3**, 1.
AMBARZUMIAN, V. A. (ed.)	1958	*Theoretical Astrophysics* (London: Pergamon Press).
BATES, D. R.	1946	*M.N.*, **106**, 432.
	1951	*Ibid.*, **111**, 303.
	1952	*Ibid.*, **112**, 40.
BOUIGUE, R.	1957	*Liège Mém.*, **18**, 346.
CHANDRASEKHAR, S., and BREEN, F. H.	1946	*Ap. J.*, **104**, 444.
CLAAS, W.	1951	*Rech. Obs. Utrecht*, Vol. **12**, Part 1.
GELTMAN, S.	1956	*Phys. Rev.*, **104**, 346.
GOLDBERG, L., MÜLLER, E., and ALLER, L.	1958	Quoted in *Hdb. d. Phys.*, Vol. **51** (Berlin: J. Springer).
GÜNTHER, S.	1933	*Zs. f. Ap.*, **7**, 106.
HUNAERTS, J.	1947	*Ann. d'ap.*, **10**, 237.
JAGER, C., DE, and NEVÉN, L.	1957*a*	*Rech. Obs. Utrecht*, Vol. **13**, No. 4.
	1957*b*	*Liège Mém.*, **18**, 357.
JUGAKU, J.	1957	Thesis, University of Michigan.
KEENAN, P. C., and MORGAN, W. W.	1951	*Astrophysics: A Topical Symposium*, ed. J. A. HYNEK (New York: McGraw-Hill Book Co., Inc.), p. 20.
KOELBLOED, D.	1953	*Pub. Astr. Inst. Amsterdam*, No. 10.
KOLB, A. C., and GRIEM, H.	1958	*Phys. Rev.*, **111**, 514.
KUIPER, G. P.	1938	*Ap. J.*, **88**, 429.
MCKELLAR, A.	1954	*Pub. A.S.P.*, **66**, 320.
MATHIS, J. S.	1957	*Ap. J.*, **125**, 328.
MENZEL, D. H.	1924	*Harvard Circ.*, No. 258.
MENZEL, D., and GOLDBERG, L.	1943	Quoted on p. 114 of *Atoms, Stars, and Nebulae* by L. GOLDBERG and L. H. ALLER (Cambridge: Harvard University Press).
MERRILL, P. W.	1955	*Pub. A.S.P.*, **67**, 199.
MOORE, CHARLOTTE	1950	*Bur. Standards Circ.*, No. 467.
NEWKIRK, G.	1957	*Ap. J.*, **125**, 571.
OHMURA, T., and OHMURA, H.	1960	*Ap. J.*, **131**, 8.

OSAWA, K.	1956	*Ap. J.*, **123**, 513.
PANNEKOEK, A.	1935	*Pub. Astr. Inst. Amsterdam*, No. 4 and Addendum.
PAYNE, C. H.	1925	*Stellar Atmospheres* ("Harvard Observatory Monographs," No. 1).
	1930	*Stars of High Luminosity* ("Harvard Observatory Monographs"), p. 113.
PECKER, J. C., and PEUCHOT, M.	1957	*Liège Mém.*, **18**, 352.
ROSA, A.	1948	*Zs. f. Ap.*, **25**, 1.
RUSSELL, H. N.	1932	*Ap. J.*, **75**, 337.
	1933	*Ibid.*, **78**, 239.
	1934	*Ibid.*, **79**, 317.
SAITO, S., UENO, S., and JUGAKU, J.	1954	*Kyoto Ap. Contr.*, No. 43.
STRÖMGREN, B.	1940	*Festschrift für Elis Strömgren* (Copenhagen: Munksgaard).
SWINGS, P.	1958	*Hdb. d. Phys.*, **50**, 125.
UNSÖLD, A.	1934	*Zs. f. Ap.*, **8**, 225.
	1941	*Ibid.*, **21**, 22.
	1955	*Physik der Sternatmosphären* (Berlin: J. Springer).
VITENSE, E.	1951*a*	*Zs. f. Ap.*, **28**, 81.
	1951*b*	*Ibid.*, **29**, 73.
WILDT, R.	1939	*Ap. J.*, **89**, 295; **90**, 611.
	1947	*Relations entre les phénomènes solaires et géophysiques* (Paris: Centre National de la Recherche Scientifique), p. 7.

CHAPTER 6

Non-thermal Phenomena in Stellar Atmospheres

L. BIERMANN AND R. LÜST
Max-Planck-Institut für Physik und Astrophysik, München

§ 1. INTRODUCTION

THE importance of non-thermal phenomena in stars seems to have been recognized only in recent years. In advance of the discussion of specific problems, some general considerations seem appropriate, in order to indicate the types of non-thermal emissions to be considered and the relative orders of magnitude of the energies involved.

From our *sun* four types of non-thermal emissions are known (Kuiper 1953; Unsöld 1955*a*): (1) excess electromagnetic radiation, above the level indicated by the temperature of the photospheric layers, (*a*) in the Lyman and X-ray range and (*b*) in radio frequencies, observable below the ionosphere from about 15 or 20 Mc/s to about 50,000 Mc/s; (2) corpuscular emissions, usually (*a*) in the form of streams of ionized matter but occasionally (*b*) of relativistic particles with energies in the 0.1–10 Bev range. These emissions result from processes in the interior, which collectively may be termed the "activity" of the sun and which, in their statistical behavior, underlie the cycle of 11 or 22 years; at times they may rise to extraordinary levels during flares or to more moderate, but still remarkable, levels over extended periods of time in longer-lived "active" regions of the surface. Estimates of the output of energy, in ergs per square centimeter per second, at the solar surface are given in Table 1 (the output of thermal energy being 6×10^{10} ergs/cm^2 sec) (for references see § 2). The radio values refer to the frequency range below 30,000 Mc/s; the values under 2*b* only to certain apparently rare events.

For the *stars* in general, considerations of their mass loss which have been made in connection with the problem of the mass balance of the interstellar medium indicate the amount of component 2*a*. These have been summarized elsewhere (Biermann 1955), but it may be mentioned here that a conservative

estimate for the current mass loss of all ordinary stars in the Galaxy seems to be a total of between 0.1 and $1M\odot$ per year, which, at approximately 10^{15}–10^{16} ergs/gm, leads to 10^{40}–10^{42} ergs/sec. For comparison, the thermal radiation of all stars in the Galaxy corresponds to about 10^{44} ergs/sec. Finally, some information about the integrated amount of mass loss since the formation of the Galaxy may be derived from the present number of white dwarfs. From their density in the sun's neighborhood their total number in the whole galactic system may be very uncertainly estimated to be $\approx 10^{10}$. According to current ideas on stellar evolution, these must originally have had a mass of $> 1.5\ M\odot$, the excess mass of at least $1\ M\odot$ having been lost at some stage after the star was on the main sequence. The average mass loss would hence seem to have been larger in the early stages of evolution of our Galaxy, but this would be true also for the thermal radiation.

TABLE 1

MAGNITUDE OF THE NON-THERMAL SOLAR ENERGIES

Type	Radiation		Corpuscles	
	1*a*	1*b*	2*a*	2*b*
Average in absence of special activity (depending on phase in cycle)	10^5–10^6	10^{-1}	10^5–10^6	.....
Longer-lived active regions	$\gtrsim 10^6$	10^0–10^1	10^6–10^7	.....
Flares	10^8–10^{10}	10^2–10^3	10^7–10^9	10^7–10^8

The most strongly pronounced non-thermal character may be ascribed to cosmic radiation, which consists mainly of atomic nuclei with energies of $\gtrsim 0.1$ Bev/nucleon, ranging up to some 10^9 Bev (which should be compared with $kT \approx 1$ ev in stellar atmospheres and H II regions in interstellar space). It will be seen below that on certain occasions (and on certain stars perhaps even continuously) the cosmic radiation represents a non-negligible fraction of the thermal output to which it is, or should be, related.

Hence it appears that it must be regarded as a fairly normal feature of stellar structure that amounts of the order of 0.01–1 per cent of the thermal energy is transformed into some sort of non-thermal emission, by which we now mean every type of electromagnetic or corpuscular radiation connected with the deviations from thermal equilibrium in the surface layers of the stars.

It seems appropriate to distinguish the following three main problems: (1) the mechanism of the particular non-thermal emission at the place of its origin (e.g., chromosphere or corona); (2) the form in which the energy maintaining the emission in question has been brought from lower to higher layers; and (3) the mechanism by which the energy which will ultimately appear in non-thermal form has been deviated from the main flux of thermal energy.

It is obvious that this list opens more questions than can be answered now. In the sun and similar stars the answer to question 2, with respect to the stationary or slowly varying features, appears to be that the energy feeding most of the non-thermal emissions is transmitted by generalized acoustic or hydromagnetic waves, which (problem 3) draw their energy from the turbulence of the hydrogen convection zone. These answers seem to be valid (but probably not exhaustive) for fairly large classes of stars, as will be discussed in later sections. The answer to problem 1 will differ from case to case (e.g., microscopic, or collective, for the electromagnetic radiations) and in some instances seems still very uncertain. For more violent phenomena, as, for example, solar or stellar flares, no satisfactory explanation appears yet to have been given.

In § 2 observational facts bearing on the questions enumerated above will be collected and discussed for the sun, for the stars in general, and for double stars, magnetic stars, and flare stars in particular. Section 3 contains discussions of the theoretical aspects of the theory of the hydrogen convection zone and the creation of acoustic or hydromagnetic progressive waves (problems 3 and 2) and of the mechanism of the various non-thermal emissions (problem 1). With respect to the solar flares, the reader is referred to a discussion by Cowling (1953) because the position does not appear to have been materially changed since that article was written.

§ 2. OBSERVATIONS

The solar corpuscular radiation, on account of its fairly low penetrating power and the absence of any photospheric features indicating localized high velocities, must be accelerated mainly in the coronal regions. Similarly, the non-thermal electromagnetic radiations originate in the corona (for example, the radiation in the X-ray range and the radio-frequencies below 1000 Mc/s) or in the chromosphere (for example, Lyman range and radio-frequencies above 1000 Mc/s).

The considerations in § 3 will be based on the hypothesis that for large classes of stars the energy supply which maintains the typical features of the physical state of these outer layers of the atmosphere is related, not to the flux of thermal energy, but to the flux of a field of acoustic or magnetohydrodynamic (and partly also gravitational) progressive waves generated mainly in the uppermost layers of the hydrogen convection zone. In this picture the non-thermal emissions are ultimately related to the turbulence of the hydrogen convection zone, the properties of which hence seem fundamental for understanding the origin of these emissions. This connection is less marked for features associated with special high-intensity activity. It seems certain, however, that the "activity" below the photosphere and the local magnetic fields both play an important role for the longer-lived active regions and the flares.

2.1. Turbulence in the Solar Photosphere

For interpretation of the observations it seems essential to make a distinction between turbulence in the strict sense of fluid dynamics, which is a state of motion maintained by some sort of large-scale instability, the energy of which is transmitted to successively small-scale elements, to be ultimately dissipated into heat by small-scale motions, and the quite different state of motion resulting from the superposition of progressive waves, which are generated by the turbulence of other layers and in which the relative role of dissipation may be different. The visible layers of the photosphere, of optical depth less than unity, are probably turbulent in the strict sense; the state of motion of the lower chromosphere is not, according to the hypothesis referred to above. This distinction seems useful, even though the picture of sonic or supersonic turbulence is not so well understood as that of subsonic turbulence and although the influence of exterior large-scale magnetic fields or of local fields resulting from the turbulence itself cannot yet be predicted theoretically.

We now turn to the observations of the photospheric turbulence (de Jager 1955). The visible elements of granulation are now known with certainty (Schwarzschild 1959) to have diameters of between $\frac{1}{3}''$ and $2''$ (250–1500 km). Their lifetime has probably been given correctly by the older observations (ten Bruggencate and Grotrian 1936) as approximately 3 minutes, and their relative contrast (Thiessen 1955) as approximately 35 per cent. The velocity may be found from the curve of growth, from the line contours, or from direct measurements of the Doppler displacements (Voigt 1956). According to the analysis of Thiessen, they all agree in pointing to values around ± 1.7–1.9 km/sec, if account is taken of the scattering of light in the telescope. These different methods of observation now seem to lead to consistent results. The turbulence of the upper photospheric layers is subsonic, its Mach number being 0.2–0.25. An important unsolved question is the possible variation of the photospheric turbulence with the general cycle of solar activity (Miller 1956).

2.2. Motions in the Solar Chromosphere and Corona

The state of motion of the chromosphere may be inferred from the development of visible features, of which the spicules have received particular attention in recent years, from measurements of spectral-line contours and from the density gradients. These observations show that in the lowest layers, near the limb, the non-thermal "turbulent" component of the velocity is smaller than, or equal to, the velocity of sound (5 km/sec for $c_p/c_v = 1$) but that it rises to approximately 15 km/sec at the level of 4000 km (middle chromosphere) and to still higher values at higher levels. The higher chromosphere appears to consist of spicules with diameters of approximately 2000 km, which reach heights of 5000–10,000 km with velocities up to 30 km/sec; their direction appears to be guided by the local magnetic fields or the polar magnetic field at high lati-

tudes ($>45°$). The quiescent prominences appear to be maintained by magnetic fields (Menzel 1951; Cowling 1957; Kippenhahn and Schlüter 1957). The active prominences and, in particular, the flares occur mainly in the neighborhood of active complex sunspot groups. While it seems certain that the strong local magnetic fields and the subphotospheric "activity" are essential conditions for their appearance, the nature of the instability itself does not yet seem to have been understood. The energy output of a big flare is of the order of 10^{30} ergs/sec at maximum, or at least 10^{32}–10^{33} ergs when integrated over time; if the effective area is taken as 3×10^{19}–10^{20} cm^2, according to data by Ellison (1955) and Unsöld (1955*b*), the corresponding flux value would be 10^{10} ergs/cm^2 sec.

The direct observational evidence regarding the state of motion of the corona is still scanty. The line contours point to tangential velocities of only 30–50 km/sec, as compared with a velocity of sound of 120 km/sec (or more, depending on the local magnetic field which also makes it anisotropic). The observed rather stationary features of the corona are probably maintained by magnetic fields. Direct knowledge of the state of motion indicating the mechanism maintaining the energy balance is still lacking. The relative intensities of the coronal emission lines of various stages of ionization observable in some elements also indicate that, at times, considerable differences in temperature exist along the line of sight. Long streamers in the outer corona seem to be connected with corpuscular radiation.

2.3. Non-thermal Emissions of the Sun

We now turn to the several non-thermal emissions of the sun. According to arguments summarized elsewhere by Biermann (1957), the most reliable estimate of the average intensity of the solar corpuscular radiation that can be made at present (uncertain by ± 0.5 in the exponent) appears to be around 10^9 ions/cm^2 sec at 1 a.u., having an above-average intensity in the ecliptic and a below-average value at high latitudes. The total potential and kinetic energy per ion is approximately 10^{-8} erg (the values for great magnetic storms being up to four times as large). Locally, the intensities at 1 a.u. may be as high as 10^{13} ions/cm^2 sec (Unsöld and Chapman 1949). The average intensity corresponds to a flow of $\lessapprox 10^{14}$ ions/cm^2 sec at the solar surface, or a mean velocity outward equal to $\lessapprox 10$ km/sec at the coronal level at an electron density of 10^8 ions/cm^3. The geomagnetic observations and those of comets with type I tails (Biermann 1951) indicate that there is almost always some corpuscular radiation present and that therefore the average energy output 10^5–10^6 ergs/cm^2 sec (about 10^{-6} of the total heat radiation) appears to be well established. It is difficult to estimate the orders of magnitudes attained in events of bigger scale. The complete disruption of the corona (which has about 10^{-5} gm/cm^2) over a certain area would require an energy of $\gtrsim 2 \times 10^{10}$ ergs/cm^2 and even more if parts of the chromosphere are also involved, as is sometimes observed. Since the time scale of such events is of the order of 10^3 sec,

the amounts of energy involved in the transient events appear to range up to 10 per cent of the thermal radiation.

The emission of ultraviolet light takes place mainly in the Lyman region (from the chromosphere) and in the X-ray region (from the corona). The rocket measurements of the Lyman-α intensity (Byram *et al.* 1956) indicate values of from 10^{-1} to 10^{+1} ergs/cm^2 sec at 1 a.u., depending considerably on the general level of solar activity, and to still higher values during flares. The normal values correspond to some 10^3–10^5 ergs/cm^2 sec at the sun's surface. The X-ray intensity may be found from the observed values of the temperature and density of the corona; it has also been directly observed, and both methods agree in leading to values of several times 10^3 ergs/cm^2 (Elwert 1956). The total energy emitted in radio frequencies by the corona and chromosphere under undisturbed conditions amounts to 10^{-4} and 10^{-1} erg/cm^2 sec, respectively.

The most violent deviations from thermal conditions occur during solar flares. The spectroscopic optical evidence points to maximum values of the integrated energy output of around 10^{33} ergs, most of which should be delivered in the form of ultraviolet light and of mechanical energy (for example, partial disruption of the chromosphere and corona and corpuscular emission). The amounts going into "cosmic" radiation are on some occasions by no means small. In the event of February 23, 1956, this latter must have been of the order of 10^{31} ergs (Meyer, Parker, and Simpson 1956). Less significant periods of production of relativistic charged particles seem to occur more often, possibly at a rate of 10 per year, if the interpretation of the type IV radio bursts as due to synchrotron radiation of relativistic electrons is correct. The integral energies involved may be of the order of 2×10^{27}, possibly up to 10^{28} ergs (de Jager 1959). The radio-frequency emission, in contrast, amounted to only 10^{25} ergs.

2.4. Turbulence in Stellar Atmospheres

Two methods are used in observing turbulent motions in stellar atmospheres. In the first method the curves of growth are used; in the second the line profiles are analyzed. The use of curves of growth for deriving turbulent velocities has the advantage that much more observational material is available, since good line profiles are difficult to obtain. On the other hand, the study of line profiles will give more detailed results. In addition to the differing experimental feasibility of these methods, there is also a fundamental difference in the scale of the turbulence observed. Any large-scale turbulence in a stellar atmosphere will not change the equivalent width of a line but, as in stellar rotation, only the line shape. Therefore, the curves of growth will not be affected and will not be useful for measuring large-scale motion. Small-scale turbulence will influence the equivalent width as well as the line profile and therefore will be detected by both methods. Large-scale turbulence, often called "macroturbulence," will be observed if the optical thickness of the large eddies is greater than unity. The large eddies will then contribute to the macroturbulence and the smaller

ones only to the microturbulence. If the optical thickness of the large eddies is smaller than unity, only microturbulence will be observed, and the turbulent velocities are superposed directly on the thermal velocities. If one assumes that the diameter of the largest eddies is about equal to one scale height, it follows that their optical thickness in stars of the main sequence with spectral types B–K and also in supergiants is always near unity at a wave length of 5000 A (Unsöld 1955*c*). Therefore, one should observe only microturbulence.

We shall briefly discuss the observational results according to Wright (1955). If v_0 is the observed line-of-sight component of the velocity determined by the curve of growth or by the line profile, the turbulent velocity, v_T, is defined by the following relation:

$$v_0^2 = v_T^2 + \frac{2RT}{\mu}, \tag{1}$$

where T is the temperature, R is the gas constant, and μ is the atomic weight of the atom being studied. Not many measurements are as yet available using line profiles. The turbulent velocities obtained by this method are in most cases somewhat larger than those measured by the curves of growth. From the theory of turbulence this is understandable because the velocities of larger eddies should exceed those of smaller ones. According to the considerations above, it is clear that the curve of growth gives the microturbulent velocity, while the line profile is a combination of the macro- and microturbulence, and therefore the former method should give smaller velocities.

For most stars the turbulent velocities observed by both methods are still in such a range that one should not properly speak of macroturbulence. This is in agreement with the statement above that for most stars the optical thickness of the largest eddies is only near unity but not much larger. A general relation between turbulent velocity and luminosity seems to hold in the sense that turbulent velocities are usually greater in stars of high luminosity than in stars of low luminosity. Whether early-type dwarfs in general have turbulent atmospheres does not seem to be established beyond doubt (Elste 1958). Furthermore, it looks as if turbulence is greater in the atmospheres of early-type supergiant stars than in those of later types. In most cases the Mach number is smaller than 1. The velocities range from zero to 10 or 20 km/sec. In addition, metallic-line stars and stars with large magnetic fields show larger turbulent velocities than do normal stars of the same luminosity. Finally, it should be mentioned that the largest turbulent velocity observed has a value of 67 km/sec, determined by Struve and Elvey (1934) from the curve of growth for 17 Leporis. While 17 Leporis is a main-sequence star of type A0, its spectrum is variable and shows shell characteristics at times.

The foregoing results refer to absorption lines mainly of photospheric origin. Wilson and Bappu (1957*a*) have studied the H and K emission lines of Ca II in late-type G, K, and M stars. They found that the line width varies as the one-sixth power of the luminosity over a range of 15 mag. If one interprets the

observed line widths as turbulent velocities, then the velocities increase from 20 km/sec for a star with the absolute magnitude +9 to about 200 km/sec for a star with the absolute magnitude −6. These high velocities should be connected with the state of the chromospheres, while the lower velocities above refer to the photospheres. But the interpretation of the line width as turbulent velocities produced in optically thin layers is not beyond doubt. Goldberg (1957) has pointed out that the assumption of optically thick emitting layers reduces considerably the turbulence required to yield the observed line widths. On this assumption, Wilson (1957*b*) finds a range of 6.6–33 km/sec for the same interval of luminosities.

2.5. Motions in Double Stars and Eclipsing Binaries

The observations of double stars and eclipsing binaries indicate that some of these stars show violent activity on a very large scale. In these stars it is sometimes possible, during an eclipse, to observe the motion in different layers of a stellar atmosphere. Furthermore, close double stars are usually surrounded by extended gaseous envelopes. The observed state of motions in these envelopes may not have a very close relation to turbulence, but in some cases it indicates a considerable loss of mass from these stars. The activity and mass loss should be related to the turbulence of the deeper layers of these stars, which may be enhanced by the nearness of the companion and should therefore also be of non-thermal origin.

For some eclipsing binaries the conditions for observing the motions in a stellar atmosphere and the chromospheric structure are especially favorable, for instance, in such systems as ζ Aurigae, VV Cephei, and 31 and 32 Cygni. ζ Aurigae has been known longer and investigated more completely than the others. Wellmann (1939) found for the eclipses of 1934 and 1937 a turbulent velocity of 22 km/sec for the K-type component, by using curves of growth, and a comparable value is derived from the observed density gradient (see also Groth 1957). The results obtained by Christie and Wilson (1935) and by Wilson and co-workers (1948, 1954) for the 1939–1940 eclipse indicated an increase in the microturbulence, derived from curves of growth, with height in the atmosphere of the cool star from 6.5 km/sec at 8×10^5 km to 13.0 km/sec at 20.6×10^5 km. However, the observations during the 1948 eclipse showed that this result was somewhat uncertain, although they confirmed a difference in turbulent velocity between lines of neutral and ionized atoms. Turbulent velocities also in the range of 5–20 km/sec are observed for 31 Cygni in the chromospheric lines by Wright (1952), who used curves of growth, and by McKellar *et al.* (1952), who studied the profile of the Ca II K line. According to Unsöld and Struve (1949), these large turbulent velocities and their observed variations suggest prominence activity on a very large scale.

Some evidence of such activity also exists for some other spectroscopic binaries (Struve 1950). For instance, in the case of HD 47129, both components of

which belong to spectral type O, the secondary shows a radial velocity which is about 100 km/sec smaller than the velocity of the system as measured by the brighter component. Here the prominence activity should be associated primarily with the advancing hemisphere of the fainter component. A very good example of strong prominence activity is UX Monocerotis. This is a two-component system with an A5 and a G2 star. The observations show that the Ca II atoms are ejected, on the average, with a velocity of 250 km/sec from the surface of the G-type star. The velocity of escape for this object is not really known, but it should be considerably smaller than the value of 618 km/sec for the sun, because the radius of the star is probably large and the mass of the order of the mass of the sun.

It seems difficult to make an estimate of the loss of mass in close binary systems. But the observed activity and also the observed changes in the periods indicate that the loss of mass might be quite considerable. For instance, the period of β Lyrae, which is nearly 13 days, increases about 9.4 seconds per year, according to Kopal. Huang has estimated that this change in period requires a loss of mass of 3×10^{22} gm/sec (1 $M\odot$ each 2000 years) if the mass of the principal component is fifty times that of the sun (Struve 1955).

2.6. Active Magnetic Stars

Active magnetic stars are of interest in the present connection in two ways: first, because of the partly irregular nature of the variation of the magnetic field in times of the order of 1 or several days and the connected radial motions and, second, because of the irregular overabundances of some heavy elements, e.g., rare earths, observed on some of these stars. Fowler, Burbidge, and Burbidge (1955) and Burbidge and Burbidge (1955) have ascribed these anomalous abundances to nuclear processes on the surface, resulting from the acceleration of a sufficient number of ions to energies of the order of from a few Mev to about 100 Mev. If, as seems likely, the hydrogen convection zone on these stars is only shallow and if, furthermore, no circulations are operative, then the slowness of diffusion limits these changes of the nuclear composition to depths of, at most, 10^5 gm/cm^2 (corresponding to 10^9 dynes/cm^2). Estimates of the efficiency of this process by Biermann (1956) reveal that acceleration of the ions would require 1 per cent (if not 10 per cent) of the thermal energy output in order to produce the observed amount of nuclear transformations. This appears to be a high, but still a possible, percentage on the basis of the evidence from other stars; the observational basis for this picture still should be strengthened. Since on the sun the observed properties of the sunspots and their cycle of activity seem to be closely connected with the comparatively large thickness of the solar hydrogen convection zone, no direct analogue to the sunspots should be expected on such stars (see § 3.1). The irregular part of the variations in the magnetic field should have a cause connected with their internal constitution, since the time scale of these variations is orders of magnitude longer than that which can be associated with the photospheric turbulence.

2.7. Flare Stars

We have seen that on the sun the flares are extreme examples of non-thermal phenomena. Similar events seem to take place on some stars on a still larger scale. These stars are called "flare stars" and are M-type dwarfs (dM, often dMe), which show very rapid and non-periodic changes in brightness. In times of the order of minutes, the luminosity of these stars increases, in some cases by up to 1 mag. (in the photographic range up to 4 mag.), and then decreases somewhat more slowly. They are not rare objects but are hard to detect because of their low luminosity. By 1955, nine or ten flare stars had been found in the vicinity of the sun, within a radius of 10 parsecs (Haro 1957). Hence the kind of "activity" observed on the sun may not be a rare phenomenon but might occur on late-type stars quite normally. This is not surprising, because the hydrogen convection zone should be of major importance for the cool stars of the main sequence (see § 3.1). At first sight, it seems difficult to understand the large observed increases in the photographic brightness of such stars. But, as Unsöld has pointed out, the Planck function for the photographic range depends very critically on the temperature for those stars because of their low surface temperatures ($T = 2900°$). Therefore, it is possible to explain the observed increases in brightness by a flare which has about the same energy flux as a solar flare but a somewhat larger relative size.

§ 3. THEORETICAL INTERPRETATIONS

3.1. The Hydrogen Convection Zone

The hydrogen convection zone in and below stellar photospheres is characterized by thermal instability. The heat flux from below maintains the average temperature gradient at a level above the adiabatic gradient, thereby causing a stationary turbulent state with random velocities, which for the sun and later-type stars are of the order of 1 or several km/sec near the surface. In contrast, the velocity of large-scale circulations seems to be small, at least in the case of slowly rotating stars; for the sun the displacement of the sunspot belts seems to indicate a meridional velocity of about 1 m/sec in the surface layers in question.

The instability of the photospheric and the subphotospheric layers is due to the higher value of the specific heats in the region where the hydrogen is partially ionized and, in stars of middle and late spectral type, also to the effect of the increase in the opacity toward the interior. If the contribution of the turbulence to the transport of heat is relatively small—and therefore also its influence on the density distribution—only a shallow zone results, as was found first by Unsöld (1931). The turbulent transport of heat is given (apart from a numerical coefficient of order unity) by the expression

$$H_K = \left(\frac{c_p \mu}{R}\right) p_g v \frac{\Delta T}{T} \text{ ergs/cm}^2 \text{ sec}, \qquad (2)$$

where c_p is the specific heat at constant pressure, including radiation; μ is the molecular weight; R is the gas constant; p_g is the gas pressure; and ΔT is the average temperature excess of the elements of turbulence referred to their surroundings. The turbulent velocity, v, is determined by a relation expressing the energy balance (g acceleration of gravity, l mixing length):

$$v^2 \approx \tfrac{1}{2} gl \frac{\Delta T}{T}. \tag{3}$$

The larger the relative contribution of H_K and the smaller $\Delta T/T$, the further the temperature gradient is reduced toward its adiabatic value. If the structure of the convection zone is nearly adiabatic, its depth is considerably larger, as was recognized by Biermann (1938); in main-sequence stars of type F to M it may well occupy a considerable part of the radius or the whole interior, especially for the later types (Osterbrock 1953; Vitense 1953; Limber 1958). This is due to the fairly large value of the photospheric pressure, 10^4–10^5 dynes/cm^2, for those stars and the low value of the energy flux.

Combination of the two last equations yields

$$v^3 \approx \tfrac{1}{2} \left(\frac{R}{\mu c_p}\right) \frac{gl}{p_g} H_K. \tag{4}$$

From this the resulting velocity is found to be only a fraction of the velocity of sound in the sun and similar stars. The scale height at the level of origin of the elements, or a small multiple, b, of it, should be expected to provide a first estimate for the diameter of the elements and for the mixing length, l; this leads to

$$gl = b \frac{RT}{\mu} = b \frac{c_v}{c_p} v_s^2. \tag{5}$$

Solar observations give $\Delta T/T \gtrapprox 0.06$, and the expected velocity of approximately 1 km/sec ($b/\mu = 1.9$ would lead to 1.7 km/sec). The observed average diameter of the visible surface structures—the granules—is around 700 km, and, although the scale height is only 100–150 km in the photosphere (dependent on the assumed chemical composition), it increases rapidly inward according to recent computations, being 400–500 km at a depth of 600–800 km below the photosphere. Hence the average surface diameter can be understood on the assumption that both the diameter, which increases further during the outward motion, and the mixing length are roughly equal to $\frac{3}{2}$ scale heights at the depth of origin of the elements.

In main-sequence stars earlier than type F it is essential to take explicit account of the relation between the temperature gradient and the radiative flux, H_R ($=H_{\text{total}} - H_K$) and also of the radiative equalization of horizontal temperature differences. When this is done, it appears that the influence of convection on the structure of the subphotospheric layers is small. The best numerical estimate that can be made at present leads to the conclusion that A

and earlier-type stars have indeed only shallow convection zones with turbulent velocities which are smaller than the velocity of sound by several powers of 10 (Böhm-Vitense 1958). However, Kippenhahn (1959) has shown that in such stars instability due to high speed of meridional circulations might lead to turbulence. In contrast, the existence of turbulence in the atmospheres of early-type dwarfs is not certain (see § 2.4). In giants and especially in supergiants of middle or late spectral type, the difference in surface conditions from those in the sun does not result in large differences in the turbulent velocities in the zone itself, according to unpublished results of Kippenhahn and Temesváry. In the photospheric layers of stars of late spectral type, somewhat larger velocities would be expected as a consequence of the outward decrease in the density. Hence, for these stars, theory and observation seem to be in reasonable agreement. The white and yellow dwarfs, far below the main sequence, owing to their large photospheric density, should have smaller values of v, but quite extended convective zones.

3.2. Acoustic Waves

From the general laws of thermodynamics it must be concluded that the high temperature of the chromosphere and the corona is maintained by a supply of non-thermal energy. The supply of this energy is here assumed to be provided by the hydrogen convection zone in the form of progressive pressure waves, which must also have gravitational components. These waves originate, as will be discussed below, at the upper boundary of the hydrogen convection zone, and their amplitude increases outward because of the decreasing density. The dissipation of their energy remains small, disregarding a small transition region in the photosphere (Schirmer 1950) until the material velocities become comparable to the sound velocity, that is, as soon as the shock-wave condition is approached (Schatzman 1949). The energy dissipation will be mainly confined to the upper chromosphere and corona only if the initial amplitudes are small enough. The observed low temperature of the lower chromosphere shows that this must be the case. The initial velocity amplitude of the wave is proportional to the square root of the energy which is transferred into acoustic waves from the turbulence of the hydrogen convection zone. In the earlier investigations of Biermann (1946, 1948) and Schwarzschild (1948) the amount of this energy was assumed to be very high; if so, the waves should dissipate their main energy in the lower chromosphere. This argument was perhaps the strongest objection against the theory. Biermann had assumed that practically all turbulent energy would be emitted as sound if the frequency of the corresponding turbulent motion corresponded with that of a possible sound wave. Thus the only limit to the energy emitted was the condition that the frequency be higher than a certain critical value, the eigen-frequency of an atmosphere in a gravitational field, with lower frequencies leading to other types of wave motion. However, this critical

frequency turns out[1] to be approximately the minimum frequency present in the solar turbulence, as determined by the observed 3-minute lifetime of the granules, and thus the energy transferred to sound waves was expected to be of the order of the total turbulent energy.

It is now clear that the radiated acoustic energy is, in fact, much smaller and that almost all the turbulent energy is dissipated in heat. The usual theory of turbulence applies only to an incompressible fluid or a fluid which is not compressed much by the turbulent motion. In this case the velocity field is divergence-free and will not give rise to traveling waves. The acoustic waves arise from the curl-free part of the velocity field that is associated with compressibility. The conversion of turbulent energy into noise has been quantitatively treated by Lighthill (1952), Proudman (1952), and Parker (1953). It follows from their work that the fraction of the turbulent energy which escapes dissipation by conversion into sound energy is comparatively small because the turbulent regions which are becoming sources of sound will radiate only like a quadrupole in the case of isotropic turbulence. The rate of production of sound depends in a very sensitive way on the ratio of the turbulent velocity, v, to the velocity of sound, v_s, i.e., on the Mach number $M = v/v_s$. In the case of isotropic turbulence the ratio of the noise production to the dissipated energy is proportional to M^5, and the energy flux, E_s, which is generated per square centimeter per second by the turbulent motion, is given by

$$E_s \approx 19\,\rho\,\langle v^2\rangle^{3/2} M^5 \text{ erg/cm}^2 \text{ sec}\,, \tag{6}$$

where $\langle v^2\rangle$ is the mean square turbulent velocity of the largest elements of turbulence. Owing to the influence of the gravitational field, the turbulence cannot be isotropic in the scale of the largest elements of turbulence. If an element of turbulence moves in an outward direction, it will expand and will generate noise probably more like a monopole. The exponent of the Mach number should not therefore be as high as 5. But in any case the energy going into noise depends on a high power of the turbulent velocity, probably between 6 and 8. Also the numerical coefficient, 19 in equation (6), is uncertain and may be only of order unity for the case of non-isotropic turbulence.

Using the above formula with $\rho = 10^{-6.3}$ gm/cm^3 for the density of the lower photosphere, with 1.7 km/sec for the turbulent velocity, and with 8 km/sec for the velocity of sound, one gets, for the energy flux, $E_s \approx 10^6$ ergs/cm^2 sec; E_s is the energy flux going into acoustic waves and therefore is equal to

$$E_s = \tfrac{1}{2}\,\rho\,(\Delta v)^2\, v_s\,, \tag{7}$$

where Δv is the amplitude of the material velocity. For instance, in the photosphere at an optical depth of 0.06 ($\rho = 10^{-7}$ gm/cm^3 and $v_s = 6.7$ km/sec) one

[1] The corresponding critical period is $\tau_c = 4\pi H/v_s$, where v_s is the sound velocity and H is the scale height. In the uppermost region of the hydrogen convective zone, v_s is about 7 km/sec, the scale height of the order of 350 km, which gives a value of approximately 3–4 minutes for the critical period.

finds $\Delta v/v_s \approx 10^{-2}$. From this equation it follows that, as long as no dissipation occurs, the amplitude Δv increases in inverse proportion to the square root of the density. If one also takes into account that the velocity of sound will increase somewhat in the outward direction, the waves will become shock waves and therefore start to dissipate their energy if the particle density is smaller than 10^{11} particles/cm^3. This is the region between the lower and the upper chromosphere, about 5000 km in height. Part of the energy will go further outward and also heat the corona.

As far as the balance of energy is concerned, the radiation losses in the transition region between the chromosphere and the corona is important. The amount radiated from this layer has been estimated by de Jager (1959) to be $10^{5.4}$ ergs/cm^2 sec. The exact value of the energy flux E_s is, of course, not well known, but if one compares the value given here with the values for the radiative emission of the chromosphere and the corona, including the transition region, and also the loss of the corona due to ordinary conduction (for which de Jager [1959] finds the amount of $10^{5.6}$ ergs/cm^2 sec) plus the corpuscular emission under normal conditions, the agreement is perhaps reasonable. It was mentioned that this acoustic energy depends in a very sensitive way on the turbulent velocity of the hydrogen convection zone, and therefore the chromospheric and coronal activity should depend in the same way on the turbulent velocity. The observed variations in the extent of these layers with phase in the cycle of solar activity may reflect just this critical dependence, since relatively small variations in the turbulence would be sufficient for their explanation.

Thomas (1948, 1950) has also discussed the problem of the heating of the chromosphere. He proposed a theory according to which the chromosphere should be heated by mass motions starting from the photosphere, and he interprets the observed spicules—one of the important features of the chromosphere (see § 3.3)—as supersonic jets, in which gas at an assumed initial velocity of 90 km/sec is pushed into the chromosphere. According to his theories, the spicules should be cool compared to the surrounding medium, and the latter should be heated by the escape of fast particles from the side of the jet. Athay *et al.* (1956*a*, *b*, 1957) give some observational evidence for this cool spicule model from the 1952 eclipse data.

3.3. Hydromagnetic Waves

The presence of magnetic fields gives rise to the appearance of a new class of phenomena, those of hydromagnetics. Whether or not magnetic fields are of importance will depend on the ratio of the magnetic pressure $(1/8\pi)B^2$ to the gas pressure p, where B is the magnetic-field intensity. Outside spots, this ratio is small in the photosphere but has a value around unity in the transition region between the chromosphere and the corona, if we assume a field strength of 1 gauss for the large-scale magnetic field of the sun. Therefore, in such regions the influence of the magnetic field must be taken into account. In the presence

of magnetic fields new types of waves are possible—for example, the so-called Alfvén waves, which are transverse waves with a velocity of propagation $v_A^2 = \frac{1}{4}\pi B^2/\rho$. The magnetic field leads to a coupling between the longitudinal sound waves, which may propagate in any direction, and the transverse Alfvén waves, which propagate only along the magnetic lines of force. In general, there exist three different modes of hydromagnetic waves (Herlofson 1950; van de Hulst 1951). The velocity of propagation of the different modes is anisotropic in general and depends on the direction of propagation with respect to the magnetic field.

Kulsrud (1955) has studied the effect of magnetic fields on the generation of noise by isotropic turbulence, extending the treatment by Proudman and Lighthill. As stated before, the noise will be generated mainly near the upper boundary of the hydrogen convection zone. In this region the magnetic pressure is small compared with the gas pressure. Kulsrud's investigations lead to the conclusion that, in this case, only the modified sound mode of the hydromagnetic waves is generated, and no energy is transferred into the Alfvén and modified Alfvén waves. The magnetic field in the outer part will then cause this energy flux to flow along the magnetic lines of force and not at right angles to them. The fact that the chromosphere spicules are tilted in the same manner as the coronal rays above them may be an observational indication of this behavior. Furthermore, it is found that the amount of energy going into noise increases somewhat with the ratio of the magnetic pressure to the gas pressure and therefore will be large in regions with larger than average values of the magnetic field, in particular in sunspots.

The energy flux of a modified sound mode of a hydromagnetic wave depends on both the velocity amplitude and the amplitude of the variation in the magnetic-field strength. If their contributions are about equal, the velocity amplitude connected with a given energy flux is, to a first approximation, $1/\sqrt{2}$ of that of a pure pressure wave with the same energy flux, in the absence of the magnetic field. It may be inferred that in the transition region between the chromosphere and the corona, outside spots, the energy flux connected with the velocity amplitude is larger, by a considerable factor, than that obtained from the picture of a pure pressure wave and that this factor should still increase with height in the corona. Alternatively, it may be concluded that the velocity amplitudes to be expected from the energy flux which is needed to maintain stationary conditions in the corona requires smaller velocity amplitudes than in the earlier picture. It will be remembered that the turbulent velocities observed in the corona are somewhat small compared to those expected in the theory of pure pressure waves.

3.4. Ambipolar Diffusion

The presence of magnetic fields may lead to additional energy losses of the progressive waves. The ordinary Joule heat losses are unimportant because of

the low electric resistance of the layers in question, but ambipolar diffusion, or relative diffusion of the non-ionized component and of the plasma component, is in a sense coupled with the magnetic field and may under certain circumstances lead to significant amounts of energy dissipation. The velocity of ambipolar diffusion, v_d, the relative velocity of the plasma and the non-ionized component, and the resulting energy dissipation may be found from a consideration of the momentum balance (Schlüter and Biermann 1950; Cowling 1956; Piddington 1956; Biermann and Schlüter 1958). When applied to the present problem, it leads to the conclusion that v_d is a very small fraction of the thermal velocity up to the top of the solar chromosphere, certainly so in regions with $B \lesssim 10$ gauss and probably also around or above sunspots, although here v_d may become $\gtrsim 10^{-3} v_s$. Hence the plasma and the non-ionized component are effectively coupled to each other by friction. The energy losses may become appreciable outside shock fronts only in the top layers of the chromosphere and only for the higher-frequency components of the acoustic noise in the range around $\frac{1}{20}$ sec^{-1}. Since in this region the dissipation takes place mainly in shock fronts, it follows that ambipolar diffusion does not affect the character of the progressive waves before they develop shocks; it is found that the energy dissipation in the shock fronts is somewhat increased but not altered in its order of magnitude. Therefore, the hydromagnetic character of the waves should be of importance only in the upper layers of the chromosphere, except in the neighborhood of spots, where general hydromagnetic waves may develop at low levels.

3.5. Emission of Corpuscular Radiation

We want to discuss here two different theories which may explain the existence of the normal corpuscular radiation. The first one may be characterized as evaporation guided by magnetic fields. If, as some eclipse photographs suggest, the lines of force of the magnetic field in the outer regions of the sun extend far into that part of interplanetary space in which the matter rotates with the sun, then the pressure waves traveling outward should be guided by the magnetic-field lines into these regions rather than refracted back toward the surface by the density gradient. Although these waves will dissipate most of their energy in the transition region between the chromosphere and the corona, some will continue outward and heat the outer layers to higher temperatures. Ultimately a point will be reached where some ions have velocities that exceed that of escape. Since the root-mean-square velocity of protons is 200 km/sec for $T = 10^6\,^\circ$ K and since their velocity of escape from r solar radii is $1/\sqrt{2}\ (616/\sqrt{r})$ km/sec (the coefficient $1/\sqrt{2}$ resulting from the electrostatic field), a temperature of $10^6\,^\circ$ K at 5 solar radii will easily suffice. Collisions will not hinder escape under these circumstances because the effective collisional cross-section for particles with only twice the thermal velocity is of the order of 10^{-18} cm^2, and even the total mass of the corona corresponds to only some 10^{18} ions/cm^2. The only question is whether ions whose velocities are properly directed along the

magnetic lines of force can escape completely or whether the lines of force return to the sun too soon. The tendency of the ionized material to be linked to lines of force that connect it with the sun is the main difficulty in every theory of the solar corpuscular radiation.

A second theory—the so-called "melon-seed" mechanism of Schlüter (1957)—circumvents this difficulty by assuming that macroscopic elements become effectively non-magnetized by heating and subsequent expansion. The material then behaves like a diamagnetic body; the Maxwellian tensions of the adjacent magnetized regions produce an accelerating force that will eject material heated to a few million degrees by leading to a motion of the elements between the lines of force. In this theory, too, the energy of the particle clouds comes ultimately from the mechanism which heats the corona.

3.6. Emission of Radio-Frequency Radiation

In relating the emission of radio-frequency radiation from the sun to the non-thermal phenomena, we should distinguish two different classes of mechanisms. The first—microscopic emission—refers to incoherent radiation from individual charged particles, while the second—macroscopic emission—refers to coherent radiation from groups of charged particles, e.g., plasma oscillations (Schlüter 1952). The source for microscopic emission is thermal radiation by free-free transitions of electrons in the Coulomb fields of ions. The radio-frequency radiation of the quiet sun can be explained in this way. In the meter-wave region the radiation originates in the corona; in the centimeter and millimeter region the principal radiation comes from the chromosphere. Hence this thermal part of the radio-frequency radiation has its energy source in the non-thermal processes discussed above. The slowly varying component is also of thermal origin and is probably emitted from coronal condensations (Waldmeier and Müller 1950).

The other components are also probably maintained by the same supply of mechanical energy. The enhanced radiation and the outbursts must be of non-thermal origin and are likely to be some kind of macroscopic emission. We shall not discuss this question here in detail. There exist different possibilities for such macroscopic emission by plasma oscillations. Whether such oscillations are able to emit radiation will depend either on the presence of magnetic fields (Lüst 1955*a*) or on the influence of inhomogeneities (Field 1956), since no energy is emitted by an ideal plasma oscillation in a homogeneous medium devoid of magnetic fields. The plasma oscillations themselves may be generated by the pressure waves, which finally lead to shock waves (Bohm and Gross 1949, 1950; Sen 1952, 1956; Lüst 1955*b*, *c*).

Another mechanism which may also contribute to the macroscopic emission is synchrotron radiation produced by jets of electrons spiraling up out of sunspots around the magnetic lines of force (Kruse *et al.* 1956). To explain the observed intensities, the electrons must have velocities of the order of 6×10^3

km/sec, which would correspond only to about 3×10^6° K. In the particular case of type IV radio bursts, which last for several hours, electrons of roughly 3 Mev seem to be responsible for the radiation in the 100 Mc/s range (Boirdot 1958). Their integral energy is of the order of 10^{27}–10^{28} ergs. Such events have been observed about ten times in one year of observation. These jets of fast electrons may also give rise to Cerenkov radiation in regions where the refractive index is favorable, and this kind of radiation may also contribute (Marshall 1956).

We have seen that on cool stars of the main sequence the activity could be much greater than on the sun (see § 2.7), and this does not seem to be surprising in view of the large depth of their convective layers (see § 3.1). According to Unsöld (1949), these cool dwarf stars may be very strong radio sources because of their higher activity and might contribute part of the general galactic radio-frequency emission that is concentrated toward the galactic plane.

3.7. Emission of Cosmic Radiation

There are two types of mechanism for the acceleration of charged particles to high energies. In the first, all particles in a given region are accelerated by an electric force induced by changing magnetic fields (e.g., those of active sunspots). In the second, the statistical increase of the kinetic energy of those particles which initially possess an above-average energy is assumed to be operative. In both types of theory, close investigation shows that rather stringent conditions must be fulfilled; since the subject of cosmic radiation will be discussed elsewhere in this series, it will not be followed further in the present section. It may only be mentioned that the production of "cosmic radiation" during intense solar flares can probably be understood only on the basis of a theory of the type first described, because the observed time scale of the events does not appear to allow the second mechanism to become operative, even if the other circumstances were favorable.

3.8. Chromosphere and Corona in Other Stars

The properties of the chromospheres and coronas of other stars depend mainly on two conditions—the supply of acoustic energy and the gravitational potential, which limits the possible temperature of the outer atmosphere. The gravitational potential varies only as $M^{1/3}$ (approximately) along the main sequence; the Mach number of the turbulence according to the observations is, at most, about unity for A and B stars but possibly $\ll 1$. Whether, on the basis of theoretical arguments, larger or smaller amounts of non-thermal radiations would be expected from such stars, in proportion to their luminosity, cannot be said at present.

The gravitational potential of giants and particularly of supergiants is very much smaller than that of main-sequence stars. This has the consequence that the upper limits to the temperature of their outer atmospheres are lower by 10 or 30, respectively. No corona of the type we observe around the sun is possible,

therefore, around such stars; but, since the supply of acoustic energy is ample, extended turbulent atmospheres of the type observed, for example, around ζ Aurigae should be common.

The flux of acoustic energy had been found to be of the order of

$$E_s \approx \tfrac{1}{2} \rho \, (\Delta v)^2 v_s \, . \tag{8}$$

In stars with nearly sonic turbulent velocities, $\rho(\Delta v)^2$ should be more nearly of the order of the gas pressure, p_g, in contrast to conditions in the sun and similar stars. In early-type main-sequence stars ($g = 10^4$, $T = 10^4$–2×10^4), p_g is near 10^3 dynes/cm^2, as it is in late-type supergiants ($g = 10^1$ cm/sec^2), but in normal giants the photospheric pressure should be nearer to 10^4 dynes/cm^2. For type K and later stars the hydrogen convection zone is below the surface, and the pressure to be used in equation (8) should therefore be somewhat larger. It follows that in the majority of these stars values of E_s roughly of the order of 10^7–10^9 ergs/cm^2 sec might be expected, that is to say, values representing up to 10 per cent of the thermal flux and exceeding the probable solar value by 10 to 1000. If most of this energy is used to maintain corpuscular emission, the resulting mass loss for high-luminosity stars would possibly be comparable to, if not larger than, the amount of hydrogen burned to helium by thermonuclear processes, since the ratio of E_s to the radiative flux H_R would be comparable to, or even larger than, the ratio of the potential energy ($\approx 10^{15}$ ergs/gm) to the energy gained in conversion of H to He ($10^{18.8}$ ergs/gm).

The authors are greatly indebted to L. Davis, Jr., R. Kippenhahn, A. Schlüter, and S. Temesváry for a number of discussions and to L. Davis in particular for his assistance in the final drafting of the manuscript. The literature referred to is, in general, that published prior to 1958, omitting therefore some of the new data obtained by satellites.

REFERENCES

ATHAY, R. G., and MENZEL, D. H. 1956*a* *Ap. J.*, **123**, 285.

ATHAY, R. G., and THOMAS, R. N. 1956 *Ap. J.*, **123**, 300.
1957 *Ibid.*, **125**, 788, 804.

BIERMANN, L. 1938 *A.N.*, **264**, 395.
1946 *Naturwiss.*, **33**, 118.
1948 *Zs. f. Ap.*, **25**, 161.
1951 *Ibid.*, **29**, 274.
1955 *Gas Dynamics of Cosmic Clouds*, ed. J. M. BURGERS and H. C. VAN DE HULST (Amsterdam: North Holland Publishing Co.), chap. 39.
1956 *Zs. f. Ap.*, **41**, 46.
1957 *Observatory*, **77**, 109.

BIERMANN, L., and SCHLÜTER, A.	1958	*Rev. Mod. Phys.*, **30**, 975.
BÖHM-VITENSE, E.	1958	*Zs. f. Ap.*, **46**, 108.
BOHM, R., and GROSS, E. P.	1949	*Phys. Rev.*, **75**, 1851, 1864.
	1950	*Ibid.*, **79**, 992.
BOIRDOT, L.	1958	Thesis, Paris.
BRUGGENCATE, P. TEN, and GROTRIAN, W.	1936	*Zs. f. Ap.*, **12**, 323.
BURBIDGE, G. R., and BURBIDGE, E. M.	1955	*Ap. J. Suppl.*, **1**, 431.
BYRAM, E. T., CHUBB, T. A., FREIDMAN, H., and KUPPERIAN, J. E., JR.	1956	*Ap. J.*, **124**, 480.
CHRISTIE, W. H., and WILSON, O. C.	1935	*Ap. J.*, **81**, 426.
COWLING, T. G.	1953	*The Sun*, ed. G. P. KUIPER (Chicago: University of Chicago Press), chap. 8.
	1956	*M.N.*, **116**, 114.
	1957	*Magnetohydrodynamics* (New York: Interscience Publishers), p. 24.
ELLISON, M. A.	1955	*Trans. I.A.U.*, **9**, 651.
ELSTE, G.	1958	Personal communication.
ELWERT, G.	1956	*Zs. f. Ap.*, **41**, 67.
FIELD, G.	1956	*Ap. J.* **124**, 555.
FOWLER, W. A., BURBIDGE, G. R., and BURBIDGE, E. M.	1955	*Ap. J. Suppl.*, **2**, 167.
GOLDBERG, L.	1957	*Ap. J.*, **126**, 318.
GROTH, H. G.	1957	*Zs. f. Ap.*, **43**, 185.
HARO, G.	1957	*Non-stable Stars*, ed. G. HERBIG (Cambridge: Cambridge University Press), p. 26.
HERLOFSON, N.	1950	*Nature*, **165**, 1020.
HULST, H. C. VAN DE	1951	*Problems of Cosmical Aerodynamics*, ed. J. M. BURGERS and H. C. VAN DE HULST (Dayton: Central Air Documents Office), p. 45.
JAGER, C. DE	1955	*Trans. I.A.U.*, **9**, 727.
	1959	*Nuovo cimento Suppl.*, **13**, Ser. X, 284, 291.
KIPPENHAHN, R., and SCHLÜTER, A.	1957	*Zs. f. Ap.*, **43**, 36.
KIPPENHAHN, R., and TEMESVÁRY, S.	1958	Unpublished.
KRUSE, U. E., MARSHALL, L., and PLATT, J. R.	1956	*Ap. J.*, **124**, 601.
KUIPER, G. P. (ed.)	1953	*The Sun* (Chicago: University of Chicago Press), chaps. 5–7.

KULSRUD, R. M.	1955	*Ap. J.*, **121**, 461.
LIGHTHILL, M. J.	1952	*Proc. R. Soc. London, A*, **211**, 564.
LIMBER, N. N.	1958	*Ap. J.*, **127**, 363, 387.
LÜST, R.	1955*a*	*Zs. f. Ap.*, **37**, 67.
	1955*b*	*Zs. f. Naturforsch.*, **10a**, 125.
	1955*c*	*Abh. d. Deutsch. Akad. Wiss. Jahrb.*, p. 119.
MCKELLAR, A., ODGERS, G. J., ALLER, L. H., and MCLAUGHLIN, D. B.	1952	*Nature*, **169**, 990.
MARSHALL, L.	1956	*Ap. J.*, **124**, 469.
MENZEL, D. H.	1951	See COWLING 1957.
MEYER, P., PARKER, E., and SIMPSON, J. A.	1956	*Phys. Rev.*, **104**, 768.
MILLER, W. A.	1956	*A.J.*, **61**, 187.
OSTERBROCK, D.	1953	*Ap. J.*, **118**, 529.
PARKER, E.	1953	*Phys. Rev.*, **90**, 240.
PIDDINGTON, H.	1956	*M.N.*, **116**, 314.
PROUDMAN, I.	1952	*Proc. R. Soc. London, A*, **214**, 119.
SCHATZMAN, E.	1949	*C.R.*, **228**, 738; *Ann. d'ap.*, **12**, 203.
SCHIRMER, H.	1950	*Zs. f. Ap.*, **27**, 132.
SCHLÜTER, A.	1952	*Ann. Phys.*, **10**, 418.
	1957	*Radio Astronomy*, ed. H. C. VAN DE HULST (I.A.U. Symposium, No. 4 [Cambridge: Cambridge University Press]), p. 356.
SCHLÜTER, A., and BIERMANN, L.	1950	*Zs. f. Naturforsch.*, **5a**, 237.
SCHWARZSCHILD, M.	1948	*Ap. J.*, **107**, 1.
	1959	*Ibid.*, **130**, 345.
SEN, H. K.	1952	*Phys. Rev.*, **88**, 820.
	1956	*Ibid.*, **102**, 5.
STRUVE, O.	1950	*Stellar Evolution* (Princeton: Princeton University Press), p. 228.
	1955	*Sky and Telescope*, **15**, 65.
STRUVE, O., and ELVEY, C. T.	1934	*Ap. J.*, **79**, 409.
THIESSEN, G.	1955	*Zs. f. Ap.*, **35**, 237.
THOMAS, R. N.	1948	*Ap. J.*, **108**, 130.
	1950	*Ibid.*, **112**, 343.
UNSÖLD, A.	1931	*Zs. f. Ap.*, **1**, 138; *Ibid.*, **2**, 209.
	1949	*Nature*, **163**, 489; *Zs. f. Ap.*, **26**, 176.
	1955*a*	*Physik der Sternatmosphären* (Berlin: Springer), chaps. 20, 21.
	1955*b*	*Trans. I.A.U.*, **9**, 667.
	1955*c*	*Physik der Sternatmosphären* (Berlin: Springer), p. 462.
UNSÖLD, A., and CHAPMAN, S.	1949	*Observatory*, **69**, 219.

UNSÖLD, A., and STRUVE, O.	1949	*Ap. J.*, **110**, 455.
VITENSE, E.	1953	*Zs. f. Ap.*, **32**, 135.
VOIGT, H. H.	1956	*Zs. f. Ap.*, **40**, 157.
WALDMEIER, M., and MÜLLER, H.	1950	*Zs. f. Ap.*, **27**, 58.
WELLMAN, P.	1939	*Veröff. U. Sternw. Berlin-Babelsberg*, **12**, 4.
WILSON, O. C.	1948	*Ap. J.*, **107**, 126.
	1957	*Ibid.*, **126**, 525.
WILSON, O. C., and ABT, H. A.	1954	*Ap. J. Suppl.*, **1**, 1.
WILSON, O. C., and VAINU BAPPU, M. K.	1957	*Ap. J.*, **125**, 661.
WRIGHT, K. O.	1952	*Pub. Dom. Ap. Obs. Victoria*, **9**, 189.
	1955	*Trans. I.A.U.*, **9**, 739.

CHAPTER 7

Stellar Magnetic Fields

H. W. BABCOCK
Mount Wilson and Palomar Observatories
Carnegie Institution of Washington, California Institute of Technology

§ 1. INTRODUCTION

THE search for stars with observable magnetic fields was undertaken in 1946 on two basic premises. One was that polarization is a quality of stellar radiation formerly neglected, yet capable of conveying highly significant information. The other was that stars in rapid rotation might very probably possess magnetic fields far stronger than that of the slowly rotating sun.

Direct detection and measurement of stellar magnetic fields could be based only on the Zeeman effect, which is quantitative and fundamental. The specific, but diverse, Zeeman patterns of spectral lines, with predictable polarization of the components, could provide incontrovertible evidence of the existence of stellar magnetic fields and could be expected ultimately to yield quantitative measures of field intensity and direction. The association of magnetization with stellar rotation could be based on the assumption that, notwithstanding certain theoretical difficulties, a regenerative process might be found whereby internal fluid circulation could amplify an initial weak field to produce a strong general field. Alternatively, the possibility of a fundamental physical relationship between angular momentum and magnetic moment of massive rotating bodies was briefly entertained (Blackett 1947, 1952; Babcock 1947). At present, the possibility must be highly regarded that stellar magnetic fields, however much modified, are primeval, having condensed from the interstellar medium along with the gaseous material that formed the stars.

Almost the first tests for the presence of magnetic fields in sharp-line A-type stars, made with the 100-inch telescope of the Mount Wilson Observatory, gave positive results (Babcock 1947*a*, *b*). The data that have since been accumulated show that stellar fields are not uncommon and that both the strength and the variations of some of them are quite remarkable. There is support for the view that a majority of all stars possess magnetic fields of significant intensity.

The diversity of magnetic phenomena revealed by spectroscopic observation is considerable, and it is desirable that these phenomena be effectively interpreted and integrated into our knowledge of the physics of the stars. Development of the subject has required that observation and description of stellar magnetic fields be actively pursued. At the same time, the theory of the behavior of an ionized gas, or plasma, in a magnetic field has been advanced rapidly. But, at present, a large gap exists between the rather general theory, on the one hand, and the observations of magnetic stars, on the other. It is the purpose of this chapter to collate and discuss the observations, in order to provide a broader basis for the development of satisfactory physical models and the application of theory.

Methods of measuring the intensity and polarity of stellar magnetic fields by means of the Zeeman effect have been discussed in my article in Volume 2, chapter 12, of this series. Because the Zeeman broadening of spectral lines in a magnetic field is usually (but not invariably) small compared with other possible sources of broadening, magnetic fields can be measured in only a limited number of stars with sharp spectral lines, whose spectra can be photographed with a dispersion of 2 to 10 A/mm. Another important condition is that the magnetic field should be coherent, with one outstanding polarity, so that when observations are made with an analyzer for rotatory polarization, actual displacements in the position of the lines due to the longitudinal Zeeman effect can be measured.

Up to the present, magnetic fields have been observed in nearly one hundred stars, mostly brighter than the eighth magnitude. Effective intensity ranges up to a maximum of the order of 34 kilogauss in the A star HD 215441. The precision of measurement depends strongly on line sharpness; in a few stars with ultra-sharp lines, where the probable error of measurement may be as low as ± 25 gauss, the presence of fields as weak as about 200 gauss can be established. To judge from the evidence for magnetic fields in the sun and in diffuse interstellar material, as well as in the stars themselves, it is becoming more and more likely that magnetic fields of significant intensity are associated with all plasmas on a cosmic scale and that most stars, if they do not possess coherent fields, have local fields of mixed polarity related to small-scale turbulence. In part, this likelihood derives from the argument that some approach to equipartition is to be expected between the magnetic energy and the kinetic energy of turbulence. In stars showing coherent fields, the predominant configuration is probably that of a dipole, and on general grounds it is likely that such a field is related to the organizing influence of axial rotation in the fluid. Mestel (1956) has shown that only slowly rotating stars will preserve an initial obliquity of the magnetic and rotation axes. It has been found that strong coherent magnetic fields occur in the great majority of the stars of type A that have sufficiently sharp lines to be tested, and it has long been known that, as a group, the stars of type B, A, and early F are in rapid rotation. There is good support for

the inference that all the rapidly rotating A stars have strong fields but that these are observable only in the small percentage of such stars that happen to be observed at small axial obliquity, i.e., nearly pole-on. The fact that B-type stars, also in rapid rotation, provide little evidence for strong fields may be attributed provisionally to the lack of significant convection zones, on the grounds that rotation and convection are mutually necessary if stellar magnetic fields are to be accounted for by regenerative dynamo processes of the kind proposed by Elsasser (1956) and by Parker (1955).

All stellar magnetic fields adequately observed are found to be variable, and the majority vary irregularly, showing that magnetohydrodynamic fluctuations occur. Because, in the highly conductive plasma that constitutes a star, the magnetic lines of force can be visualized as imbedded in the material and moving with it, the magnetic field can be regarded as a tag or tracer by the observation of which fluid motions in the star can be inferred. Magnetic observations, in combination with other spectroscopic data, can in some degree provide information on turbulence and on circulation patterns at and near the stellar surface.

It is as yet unknown to what extent stellar magnetic fields influence internal mixing and to what degree they may affect the internal constitution and evolution of stars. But in the problem of "external evolution"—the disposition and control of gaseous material in the outer layers and in the circumstellar region—there can be no doubt that the governing effect of a strong magnetic field is of prime importance. Such a field can transfer angular momentum from a rotating star to a surrounding cloud of ionized gas. The full significance of such effects for the development of planetary systems and of binary stars remains to be investigated. It seems rather obvious, however, that magnetic coupling offers the most attractive solution to the long-standing problem of the distribution of angular momentum within the solar system.

For many years it has been an attractive hypothesis that stars cooler than type F5 consistently show a low rate of rotation because during their early history as stars—or in the final stages of contraction from the interstellar medium—they lost angular momentum, through magnetic coupling, to surrounding gas clouds. With diminution of angular velocity, any regenerative hydromagnetic process for maintaining a strong field would likewise decay, leaving most late-type stars with slow rotation, weak magnetic fields, and, inferentially, planetary systems.

§2. OBSERVATIONS

Magnetic data on 89 stars showing the Zeeman effect have been compiled in a catalogue (Babcock 1958), which will be frequently referred to. Notes on spectral peculiarities and on line widths are included. For most stars listed, repeated measurements of the effective field, H_e, are given, together with radial velocity. Supplementary tables in the catalogue list 65 stars probably, but not definitely, showing the Zeeman effect, 55 stars having sharp spectral lines that

give no evidence for a magnetic field, and 112 stars tested for various reasons but found to have lines too broad for magnetic measurements.

A condensation of the principal table of the catalogue is given as Table 1 of this chapter. For each star, the position for 1950, spectral type, magnitude, index of line width w, in angstroms, and extreme measured values of H_e in gauss are listed. Column 10 gives the period in days if the magnetic variations are known to be periodic or an indication of irregularity if this has been established. The last column gives an indication of elements showing unusually strong line intensity; italics indicate that the element shows variable lines.

The stellar Zeeman effect is measured in terms of the mutual displacement of line profiles observed through a differential analyzer for right and left rotatory polarization. Each elemental area, da, of the visible disk of the star contributes to the final blended profile in proportion to $WJda$, where W is the local equivalent width of the line and J is the local surface brightness in the direction of observation. The Zeeman displacement is proportional to the component of the magnetic field in the line of sight. These considerations were taken into account when it was shown that a pole-on star, with typical limb darkening, having a regular axisymmetric dipolar field, would produce an observable Zeeman effect corresponding to an "effective" field, H_e. This was shown to be, for an A-type star, about 0.3 times as great as H_p, the field intensity at the pole, and to show the same polarity (Minnaert 1937; Babcock 1947*a;* Schwarzschild 1950; Stibbs 1950).

The data that have since been collected on the magnetic fields of stars and of the sun show that stellar fields are, in general, not simple permanent dipolar fields. All that have been adequately observed are found to vary, and the majority vary irregularly. Small fluctuations in radial velocity suggestive of turbulent atmospheric motions are common. The apparent field of a star carrying a non-axisymmetric magnetic pattern can, of course, be regularly modulated by axial rotation if the inclination is appreciable. But the irregular variations in the effective magnetic field are attributable to intrinsic magnetohydrodynamic fluctuations involving displacements of the material in the photosphere, together with its associated magnetic fields. Variations in H_e can also occur through local changes in surface brightness or equivalent line width.

The line profiles that are observed in the spectra of the sharp-line A stars indicate that, while the dipolar component of the field predominates in many instances, many of the field patterns are probably complex, with considerable fine structure. Because the pattern of the magnetic-field distribution on the surface of a star can generally not be specified, the results are reported in terms of the effective field, H_e, on the simplifying assumption that this is homogeneous.

The broadening of the line profiles in the spectra of most sharp-line magnetic stars is of the same order as the Zeeman displacements of the polarized components in the derived field, H_e. The profiles do not indicate a much larger

TABLE 1

MAGNETIC STARS*

(Short Form)

No. (1)	Star or HD No. (2)	R.A. (3)	Dec. (4)	m_v (5)	Sp. (6)	w (7)	No. Obs. (8)	H_e Extremes (9)	Per. (10)	Remarks (11)
1....	2453	0h25m50s	+32°09′	6.7	A2p	0.14	6/15	− 425 − 710	.....	Like HD 188041
2....	4174	0 41 53	+40 24	7.5	M2e	.....	11/41	−1200 +1100	Irreg.	[Ne III], [O III], *H*
3....	8441	1 21 23	+42 53	6.6	A2p	0.08	13/31	− 750 +400	Irreg.	Sr, Gd; sp. binary
4....	9996	1 35 30	+45 09	6.3	A0	0.1:	2/6	− 990 +135	.....	Sp. binary
5....	43 Cas	1 38 36	+67 47	5.5	A0p	0.7:	1/2	−1200 +	.....	Si, Sr
6....	10783	1 43 04	+ 8 18	6.6	A2p	0.3:	18/53	−1200 +2200	Irreg.	Si, Sr, Cr, (Eu, Gd)
7....	11187	1 48 10	+54 40	7.1	A0p	0.27	7/10	− 70 +1250	.....	Si, λ 4201
8....	HR 710	2 23 37	−15 34	5.8	A4p	0.15	39/50	−1080 − 320	Irreg.	Sr, Eu, Cr; sp. binary
9....	21 Per	2 54 15	+31 44	5.2	A0p	0.6:	13/44	−1270 +1350	Irreg.	Si, Mn, Sr, Eu, λ 4201; variable profiles
10....	19445	3 05 28	+26 09	8.0	F6	.....	1/3	+ 415	.....	High-vel. Subdwarf
11....	20210	3 12 53	+34 30	6.4	A7	0.4	1/4	− 260 +	.....	Ba; sp. binary
12....	9 Tau	3 34 01	+23 03	6.7	A2p	0.15	1/7	+ 140	.....	Si
13....	HR 1105	3 37 48	+63 03	5.3	S	.....	2/9	0: + 450	.....	Heavy elements
14....	25354	3 59 52	+37 55	7.9	A0p	0.2v	4/8	− 380x 0:	.....	*Eu, Cr*, Mn, λ 4201; var. profiles
15....	41 Tau	4 03 32	+27 28	5.3	A0p	0.43	3/8	− 530 + 700	.....	Sr, Si, λ 4201; pec. profiles; sp. binary
16....	68 Tau	4 22 36	+17 49	4.2	A2 V	0.2	1/4	− 400	.....	Metallic-line star
17....	30466	4 46 06	+29 29	7.2	A0p	0.5v	2/8	− ? +2320	.....	Si, λ 4201; var. profiles
18....	32633	5 02 51	+33 51	6.9	B9p	0.4:	24/24	−5870x+2220	Irreg.	Si, Cr; rapid reversal
19....	16 Ori	5 06 34	+ 9 46	5.4	F2	0.3	2/4	− 420 + 375	.....	Metallic-line star
20....	μ Lep	5 10 41	−16 16	3.3	B9p	0.3	5/28	− 170 + 325	.....	Si, Mn, Y
21....	WY Gem	6 08 54	+23 14	7.4	M3p	.....	1/8	− + 540	.....	[Fe II]
22....	42616	6 10 10	+41 43	6.9	A2p	0.4:	4/12	− 840 0:	.....	Sr; K-profile pec. varies
23....	45677	6 25 59	−13 01	7.5	B2e	0.3:	1/7	−1600	.....	H, Fe II, Fe II, S II: in emission; K pec., varies
24....	49976	6 48 18	− 7 59	6.2	A0p	0.4v	1/14	− 810 +	.....	*Sr, Ca;* profiles diverse, vary irregularly
25....	50169	6 49 25	− 1 35	8.9	A4p	0.12	6/11	+ 670 +2120	.....	Sr, (Eu); resembles HD 188041
26....	R Gem	7 04 21	+22 47	6+	Se	.....	2/2	+ 370 + 400	.....	
27....	56495	7 14 33	− 7 26	7.5	A3p	0.4v	2/7	− ? + 570	.....	Sr, *Cr, Mg* I
28....	53 Cam	7 57 27	+60 28	6.0	A2p	½–1v	20/20	−5390x+3750	8.0	*Ti*, Sr, Cr Eu, *Mg* II
29....	15 Cnc	8 10 03	+29 48	5.6	A0p	0.7:	0/9	0: + str	.....	Si; profile of K varies
30....	71866	8 27 52	+40 24	6.7	A0p	0.26	61/65	−1700x+2000	6.80	*Eu, Gd*, Sr
31....	3 Hya	8 33 02	− 7 48	5.6	A2p	0.31	16/22	− 480 + 740	Irreg.	Sr; velocity varies; sp. binary ?
32....	49 Cnc	8 42 02	+10 16	5.6	A0p	0.26	9/26	− 200 +1450	.....	Si, Sr, (*Eu*?)
33....	ν Cnc	8 59 49	+24 39	5.4	B9p	0.5:	2/2	+ 105 + 470	.....	Si, Sr, Cr pec. profiles
34....	κ Cnc	9 05 02	+10 52	5.1	B8p	0.13	8/17	− 640 + 460	.....	Mn, Si; sp. binary (6d4)
35....	30 UMa	10 20 33	+65 49	4.9	A0p	0.08	2/3	− 290 + 340	.....	Si, Sr, (Mn); sp. binary (11d6)
36....	45 Leo	10 25 01	+10 01	5.9	A2p	0.2v	5/14	− + 400	.....	Many profiles peculiar and variable; x
37....	98088	11 14 26	− 6 52	6.0	gFp	0.4:	12/15	−1000 + 800	5.905	*Sr, Ba, Ti*. No x; sp. binary
38....	17 Com A	12 26 25	+26 11	5.4	A0p	0.4:	9/21	−1150 + 360	.....	Sr, Cr, (Eu); profiles vary
39....	17 Com B	12 26 25	+26 11	6.7	A3	.....	0/2	+mod.	.....	Metallic-line star
40....	110066	12 36 51	+36 14	6.3	A4p	0.1:	5/7	− 55 + 300	.....	Sr, Cr, λ 4201 wide
41....	l Cen	12 37 10	−39 43	4.8	B8p	0.2:	1/1	+ 580	.....	Mn, Si
42....	γ Vir	12 39 07	− 1 10	2.9	F0 V	.....	1/3	− 390	.....	Standard F0
43....	111133	12 44 30	+ 6 13	6.4	A4p	0.14	1/2	− 990	.....	Sr, Cr,
44....	α^2 CVn	12 53 42	+38 35	2.9	A0p	0.3v	28/96	−1400x+1600	5.469	*Eu, Cr*, Sr; profiles vary

* Numbered columns have the following meanings:

3 and 4: Position for 1950.

7: Index of line width, *w*.

8: Number of plates measured/number of plates taken.

9: H_e = effective field intensity in gauss; crossover effect indicated by x.

10: Period in days, or irregular. Most not indicated are irregular.

11: Elements showing abnormal line intensity, italic if variable.

TABLE 1—*Continued*

No. (1)	Star or HD No. (2)	R.A. (3)	Dec. (4)	m_v (5)	Sp. (6)	w (7)	No. Obs. (8)	H_e Extremes (9)	Per. (10)	Remarks (11)
45....	115708	13h16m11s	+26°38′	8.3	A2p	0.2:	1/3	+ 740	.....	Sr, Eu
46....	78 Vir	13 31 35	+ 3 55	4.9	A2p	0.2	50/76	−1680x− 140	Irreg.	Sr, Cr, Eu
47....	BD 1913	13 53 50	+45 59	9.7	Ap	0.2:	/1	+ 500:	.....	BD+46°
48....	125248	14 15 52	−18 29	5.7	A0p	0.2v	33/40	−1900x+2100	9.29	*Eu, Cr;* long-*P* sp. binary
49....	126515	14 23 23	+ 1 13	7.0	A2p	0.1+	1/4	− +1310	.....	Cr, Si, Sr; (x); pec. profiles
50....	π Boo A	14 38 22	+16 37	4.9	B8p	0.4	2/12	− 75 + 190	.....	Si, Mn, Y, Sc
51....	μ Lib A	14 46 34	−13 56	5.4	A0p	0.3:	7/13	−1300 − 200	.....	Sr, Cr
52....	133029	14 58 56	+47 28	6.2	A0p	0.4	50/74	+1150 +3270	Irreg.	Si, Cr, λ 4201
53....	134793	15 09 05	+ 8 43	8.2	A3p	.3+v	4/11	− 530 + 450	.....	*Eu, Sr,* Cr; widths vary
54....	135297	15 11 48	+ 0 33	8.0	A0p	0.3:	1/3	−1110 +	.....	Sr, Cr
55....	β Cr B	15 25 46	+29 17	3.7	F0p	0.15	61/89	− 960 +1020	Irreg.	Sr, Eu; sp. binary
56....	33 Lib	15 26 45	−17 16	7.2	F0p	0.15	1/2	+1120	.....	Sr, Eu
57....	ι Cr B	15 59 26	+29 59	4.9	A0p	0.07	6/10	− 340 + 75	.....	Mn, Si, Sr, Zr, Y
58....	ω Oph	16 29 10	−21 21	4.6	A7p	0.6	0/19	− +	.....	Sr, Cr; pec. profiles
59....	45 Her	16 45 19	+ 5 20	5.3	A0p	.4+v	0/6	−	.....	*Eu,* Sr, Si; profiles vary
60....	52 Her	16 47 46	+46 04	4.9	A4p	0.4	2/19	+ 840 +1430	.....	Sr, (Eu)
61....	153286	16 54 41	+47 26	6.9	F	.....	2/3	− 500	.....	Sr, metallic-line star
62....	153882	16 59 16	+15 01	6.2	A4p	0.4:	32/38	−1200x+1440	6.01	(*Sr,* Cr, Mn); profiles vary
63....	165474	18 03 25	+12 00	7.4	A7p	0.15	1/3	+ 900	.....	Eu, Sr
64....	171586	18 33 08	+ 4 54	6.7	A2p	0.8:	1/4	− 740	.....	Sr, Cr
65....	173650	18 43 28	+21 55	6.4	A0p	0.2+	20/43	− 540 + 700	Irreg.	*Sr, Eu,* Si, Mn, Cr, Gd, λ 4201; pec. variable profiles
66....	10 Aql	18 56 29	+13 50	5.9	A4p	0.1:	5/10	− 315 + 440	.....	Sr, Eu, Mn
67....	21 Aql	19 11 11	+ 2 12	5.2	B8	0.4	4/6	− 590 + 170	.....	Si
68....	RR Lyr	19 23 52	+42 41	7–8	F	.....	18/47	−1580 +1170	?	
69....	51 Sgr	19 33 00	−24 50	5.7	F	.....	1/3	− 230	.....	Sr, Eu; metallic-line star; sp. binary
70....	184905	19 33 09	+43 50	6.6	A0p	1:v	0/26	−	.....	*Si, Eu, Ca;* profiles vary
71....	187474	19 48 27	−40 01	5.4	A0p	0.1+	5/5	−1870 − 200	?	Eu, Si, Ti, Fe, (Mn, Al); sp. binary
72....	188041	19 50 42	− 3 15	5.6	A5p	0.11	75/84	− 230 +1470	226	*Gd, Eu, Sr;* secular changes; variable amplitude
73....	190073	20 00 31	+ 5 36	7.9	Aep	0.2+	1/12	+ 120	.....	*Ca*
74....	191742	20 08 04	+42 24	7.8	A7p	0.12	2/5	− 510 − 175	.....	Sr, (Si, Eu)
75....	192678	20 12 18	+53 30	7.1	A4p	0.2:	0/1	+2000:	.....	Cr
76....	192913	20 14 23	+27 37	6.7	A0p	0.2:	4/10	− 670 + 380	.....	Si, λ 4201
77....	73 Dra	20 32 11	+74 47	5.2	A2p	0.13	9/14	− 700 + 200:	Irreg.	*Ti, Eu, Sr;* sp. periodic?
78....	γ Equ	21 07 55	+ 9 56	4.8	A7p	0.09	21/31	+ 180 + 880	Irreg.	Eu, Mg, Sr (Si)
79....	θ^1 Mic	21 17 34	−41 01	4.9	A2p	0.6−	1/3	− 650	.....	*Eu, Sr,* Cr; diverse profiles
80....	AG Peg	21 48 37	+12 23	7.6	B+M	.....	14/30	−1000 + 500	.....	
81....	VV Cep	21 55 14	+63 23	5–6	M+B	.....	5/17	− 360 + 850	.....	Sp. binary
82....	215038	22 38 18	+75 24	8.0	A0p	0.8:	0/2	−3000:	.....	Si, λ 4201
83....	216533	22 50 36	+58 33	7.9	A2p	0.15	5/6	− 650 0	.....	*Sr,* Cr, Eu, (Si)
84....	κ Psc	23 24 22	+ 5 58	4.9	A2p	0.8v	0/17	− +	.....	*Sr, Ca, Eu,* Cr
85....	β Scl	23 30 18	−38 06	4.5	B9p	0.3:	1/3	+ 660	.....	Mn, Si; Y has neg. polarity
86....	ι Phe	23 32 23	−42 54	4.8	A2p	0.4:	0/2	+	.....	Sr, Cr; pec. profiles
87....	108 Aqr	23 48 46	−19 11	5.3	A0p	0.8:	0/12	− +	.....	*Sr, Ca, Eu,* Si, λ 4201; pec.
88....	224801	23 58 10	+44 58	6.2	A0p	0.8:	2/22	− +2300	.....	*Eu,* Si, Sr, λ 4201
89....	4778	0 47 30	+44 44	6.1	A0p	½-1	0/4	− +	.....	*Eu, Mg,* Sr, Cr

degree of broadening, such as might result if there were averaging of very strong and very weak distributed fields. This, together with the tendency of the line profiles to be sharp-edged, indicates that the effective field has approximately uniform intensity over the extended photospheric area in which the lines are produced. In measuring a stellar field of 2 kilogauss, for example, we are not measuring the mean of a field-free photosphere averaged with an area of 2 per cent of the disk that carries, say, a concentrated field of 10^5 gauss. Thus the

fields that are observed are inferred to be essentially photospheric, and there is no direct evidence from the observations either for or against the occurrence of small, localized dark spots, similar to sunspots, but with superstrong fields. Particularly among the later subdivisions of type A, the line intensity and the considerable depth of the affected line profiles indicate that the magnetic field necessarily affects most, if not all, of the surface. Among the magnetic stars near type A0, however, there are many in which the line intensities are weaker and the profiles are shallower, suggesting that, while the magnetic field may affect the whole stellar surface, the lines may possibly arise in magnetic regions constituting no more than a considerable fraction of the visible surface. The profiles may be diluted by continuous radiation. Such hypothetical limited magnetic regions, with fields of the order of a few kilogauss, may be considered analogous to widely extended magnetic regions or zones on the sun, such as the magnetic polar caps, rather than to sunspots.

Among most of the magnetic stars, lines of the various chemical elements usually agree well in indicating consistently nearly the same field intensity at any given time. This is particularly true in stars with ultra-sharp lines and slowly varying fields, such as are characteristic of the later subdivisions of type A. Examples are 10 Aquilae, γ Equulei, and HD 110066, for which probable errors of only about ± 30 gauss are derived for H_e from measures of numerous lines of several elements. In some other stars with more rapidly varying fields, differences in measured field intensity are found for particular elements as compared with the mean, or differences may be detectable in the field indicated by the ionized, as compared to the neutral, atoms. For example, in HD 125248 near the phase of maximum negative field intensity, lines of chromium show a stronger field than do most other elements. In some of the "silicon stars," e.g., κ Cancri, lines of Si II occasionally yield divergent results. Lines of Sc II and Y II, found in a few stars, are usually discordant. Divergent field intensities, with indications that the field is, in part, of mixed polarity, are particularly evident in such stars as 21 Persei, HD 173650, HD 42616, and HD 56495.

It will be noted that a preponderance of stars in Table 1 are of type A or between the limits B8 and F0. Most of these carry the designation "peculiar," denoting that the K line, λ 3933 of Ca II, is weak and that lines of certain other elements, such as manganese, silicon, strontium, chromium, or the rare earths, are unusually strong. It was found by Deutsch (1947) that a limited number of peculiar A stars for which absolute magnitudes were available are located on, or perhaps slightly above, the main sequence. The preponderance of A stars in Table 1 is partly a matter of observational selection. Sharp-line stars of this type were first tested for magnetic fields on the theory that strong coherent fields should result from rapid axial rotation, and it was known that, as a group, the A stars are in rapid rotation. It was soon found that most A-type stars with truly sharp lines do show observable magnetic fields and that the

strongest fields occur in this group. Because these stars most readily provided significant results and because of the diverse phenomena to be observed among them, they have received most attention. Nevertheless, a considerable number of stars differently situated in the Hertzsprung-Russell diagram have been tested, and several show observable magnetic fields, as indicated in Table 2.

Among the high-luminosity stars that have been observed, fields no stronger than 1 or 2 kilogauss occur, and these seem to fluctuate irregularly. This is what might be expected if a high degree of turbulence prevails, coupled with local fields of mixed polarity. The metallic-line stars as defined by Roman, Morgan, and Eggen (1948) have fields which, when observable at all, are considerably weaker than those of the peculiar A stars, and little is known of their variations. In none of the classical cepheids has the presence of a magnetic field been definitely established, although it is highly significant that RR Lyrae gives evidence of a variable field. No regularity has yet been established in the magnetic variations of this star, but it has been found that the field variations

TABLE 2

NUMBER OF KNOWN MAGNETIC STARS OF VARIOUS TYPES

Sharp-line A stars (B8–F0)	70
Metallic-line stars	7
M-type giants	3
S type (R Gem and HR 1105)	2
Cluster-type variable (RR Lyr)	1

are not simply correlated with the primary variations in luminosity. The presence of a magnetic field in RR Lyrae is of particular interest because of the critical position that this star, as a representative of the cluster-type variables, occupies in the evolutionary sequence and also because it is a pulsating star.

While sampling of stars in various parts of the HR diagram is quite incomplete, sufficient evidence already exists to suggest that stellar magnetic fields of significant intensity are probably ubiquitous, particularly when it is recognized that only strong fields of one outstanding polarity can be detected with present methods.

The remainder of this chapter will be concerned almost entirely with magnetic phenomena of the A-type stars.

§ 3. MAGNETIC CLASSIFICATION

The sharp-line A-type stars of Table 1 may be grouped, according to the characteristics of their magnetic variation, into three classes denoted as α, β, and γ, after the type stars α^2 Canum Venaticorum, β Coronae Borealis, and γ Equulei. Members of these groups are listed in Tables 3, 4, and 5, respectively. Those of the α group, 7 in number, show cyclic or essentially periodic magnetic variations, sometimes with considerable deviations from the mean

TABLE 3

ALPHA VARIABLES

(Arranged in Order of Increasing Period)

Star	Sp.	w	H_e Extremes (Gauss)	P (Days)	$3.6/P$	Remarks
α^2 CVn.....	A0p	0.3v	−1400 x +1600	5.469	0.66	*Cr*, *Eu*, Sr; profiles vary
HD 98088.....	A2p	.4:	−1000 + 800	5.905	.61	*Sr*, *Ba*, *Ti;* No x; sp. binary
HD 153882.....	A4p	.4:	−1200 x +1440	6.01	.60	(*Sr*, *Cr*, *Mn*); profiles vary
HD 71866.....	A0p	.26	−1700 x +2000	6.80	.53	*Eu*, *Gd*, Sr
53 Cam.....	A2p	.25–1v	−5390 x +3750	8.025	.45	*Ti*, *Mg*, Sr, Cr, Eu; profiles vary
HD 125248.....	A0p	.2v	−1900 x +2100	9.295	.39	*Eu*, *Cr*
HD 188041.....	A5p	0.11	− 230 +1470	226	0.01	*Gd*, *Eu*, *Sr;* secular changes; non-uniform amplitude

TABLE 4

BETA VARIABLES (IRREGULAR, REVERSING POLARITY)

(Arranged in Order of Spectral Type)

Star	Sp.	w	H_e Extremes	Remarks
HD 32633.....	B9p	0.3–0.5	−5870 x +2220	Si, Cr, Eu; irregular amplitude, random crossover
21 Per.....	A0p	.6:	−1270 +1350	Si, Mn, Sr, Eu, λ 4201; var. profiles
HD 173650.....	A0p	.2+	− 540 + 700	*Sr*, Si, Mn, Cr, *Eu*, Gd, 4201; pec. var. profiles
HD 8441.....	A2p	.08	− 750 + 400	Sr, Gd; sp. binary
HD 10783.....	A2p	.3:	−1200 +2200	Si, Sr, Cr, (Eu, Gd)
3 Hya.....	A2p	.31	− 480 + 740	Sr; (sp. binary?)
73 Dra.....	A2p	.13	− 700 + 200 est.	*Eu*, *Sr*, *Ti*
β CrB.....	F0p	0.15	− 960 +1020	Sr, Eu; sp. binary

TABLE 5

GAMMA VARIABLES (IRREGULAR AMPLITUDE, CONSTANT POLARITY)

Star	Sp.	w	H_e Extremes	Remarks
HD 133029.....	A0p	0.4	+ 1150 + 3270	Si, Cr, λ4201
HD 215441.....	A0p	.3–1	+12000 +34000	Si, Ti
78 Vir.....	A2p	.2	− 1680 x − 140	Sr, Cr, Eu
HR 710.....	A4p	.15	− 1080 − 320	Sr, Cr, Eu; sp. binary
52 Her.....	A4p	.4	+ 840 + 1430	Sr, (Eu)
γ Equ.....	A7p	0.09	+ 180 + 880	Eu, Mg, Sr (Si)

amplitude or phase. Those of the β group, numbering 8, show magnetic fields with irregular fluctuations, including reversals of polarity. The 6 stars of the γ group always display the same polarity, with irregular magnetic variations. It is probable that nearly all the α variables in Table 1 have been identified, as they are relatively easy to select, partly because they are usually found to be spectrum variables. It is more difficult to prove irregularity for the β and γ variables; hence the probability is high that several more of these remain to be identified.

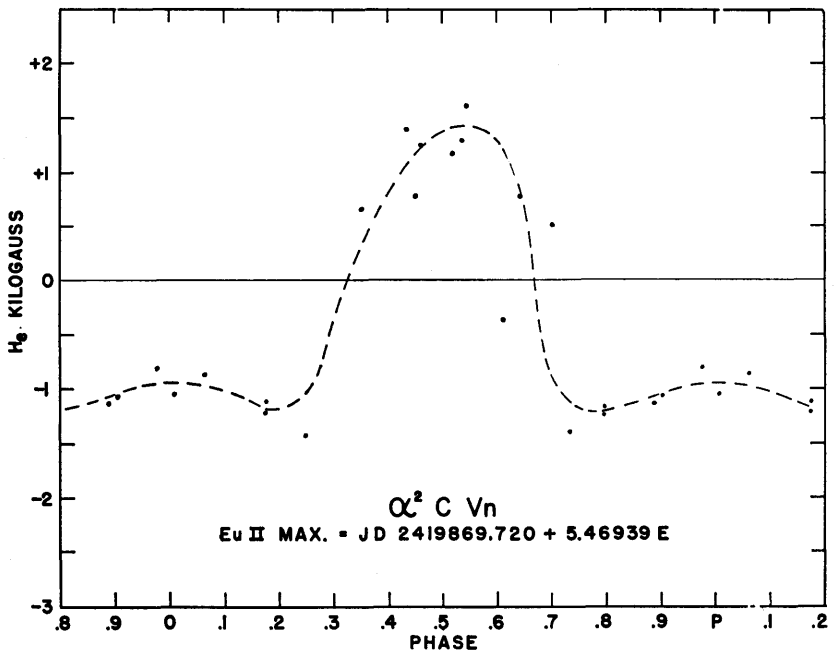


FIG. 1.—Magnetic variations of α^2 CVn (No. 44). Intensity of the Eu II lines varies in antiphase with the intensity of the lines of Cr I and Cr II, which are at maximum when the magnetic field has positive polarity. There occur marked deviations from the mean magnetic curve, particularly near the phase of negative crossover.

The α variables are distinguished not only by periodicity but by large magnetic amplitudes and by variations in line intensity that are synchronous with the magnetic changes; i.e., they are spectrum variables. Two of the α variables are atypical, in that HD 98088 is a short-period spectroscopic binary and HD 188041 has a period far longer than the others; also, neither of these two stars shows the crossover effect. The other, more typical, stars of the group, however, all have magnetic fields of large amplitude that show nearly symmetrical reversals of polarity, and they all show the crossover effect. The ir-

regular variables of groups β and γ have generally lower magnetic amplitudes and usually do not show spectrum variations or the crossover effect.

The term "crossover effect" is applied to the observation that line profiles are definitely sharper in circularly polarized light of one sense than in that of the other (Pl. I). It is generally found in the α variables at those phases when the effective field is changing rapidly from one polarity to the other. The effect is quite pronounced in the spectrum of HD 71866, but, curiously, it has also been observed in a few of the irregular variables, e.g., 78 Virginis, which always

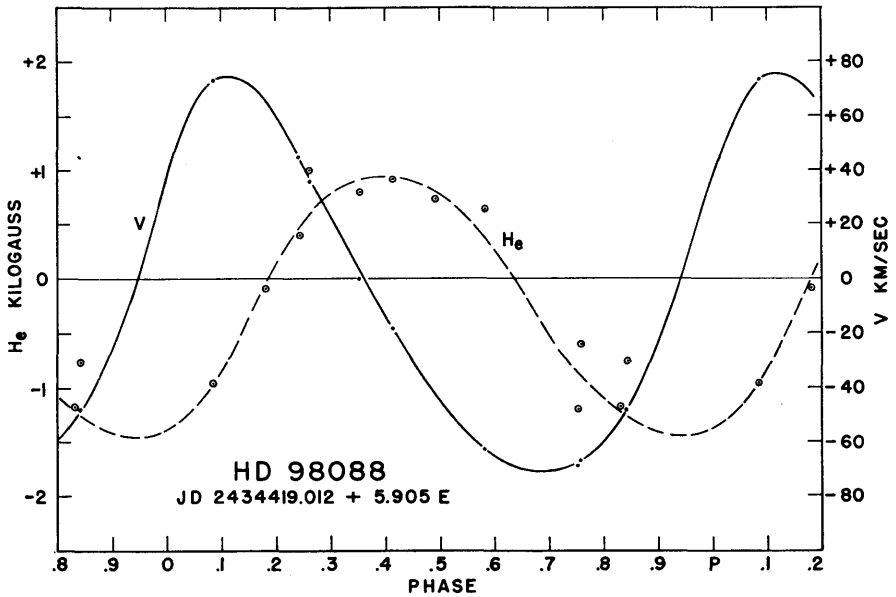


FIG. 2.—Curves of magnetic-field intensity (*dashed line*) and of velocity (*solid line*) for the unique α variable HD 98088 (No. 37). The magnetic variations occur in the period of orbital revolution. The star is also a spectrum variable.

shows the same polarity. In the α variables, the sense of the crossover effect depends upon the direction in which the magnetic field is changing. It is found that the line profiles in right-hand circularly polarized light are consistently sharper when dH_e/dt is positive, and this is known as the positive crossover effect. Most of the metallic lines in the spectrum show the effect but not to the same degree; it is practically certain that variations in the degree to which the crossover effect alters the profiles are related to the specific Zeeman patterns of the lines. Various elements are not always uniformly affected, and it has been noted that in the spectrum of HD 71866 (Babcock 1956) the crossover effect is much more prominent in lines of Fe I than in those of Fe II.

Curves of magnetic variation for the α variables are shown in Figures 1–7,

and sections of their spectra are reproduced in Plate II. It is a common characteristic that, after allowing for errors of observation, deviations from the mean are to be found in amplitude or in phase. Such deviations are perhaps most obvious in α^2 CVn and in HD 188041, which have, respectively, the shortest and longest periods in the group. A second characteristic is that the curves of magnetic variation are not of a simple harmonic type. In general, the magnetic maximum of one polarity is broader than that of the other, and in α^2

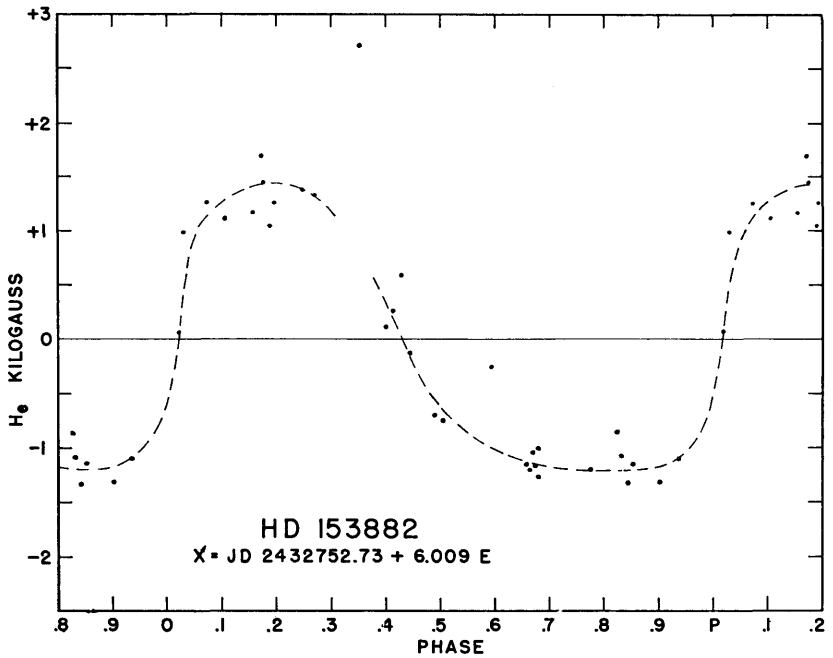


FIG. 3.—Magnetic variation of HD 153882 (No. 62). The probable error of each determination is about ±0.1 kilogauss. Note the anomalous, very strong, field indicated by one plate near phase 0.36. The spectrum shows the crossover effect and certain peculiar profiles, but with little indication of changes in equivalent width.

CVn, HD 71866, and HD 188041 there are indications of a dip or notch in the top of the broader maximum. In HD 125248 and in α^2 CVn the line profiles tend to be considerably narrower at the phase of the broader magnetic maximum, i.e., when the lines of the rare-earth elements, rather than of chromium, are at maximum intensity. In 53 Cam, the systematic variation in line width is most extreme, as is the range of magnetic variation. It may be significant in connection with the interpretation of the observations of the α variables, that in many respects α^2 CVn and HD 125248 are similar, yet in the former the lines of chromium are at maximum intensity when the magnetic polarity is positive,

while the reverse is true in the latter. In each of these stars, chromium varies in antiphase with the rare-earth elements.

The range of magnetic variation for various subdivisions of spectral type is shown in Table 6. It is noteworthy that the strongest fields and the largest variations occur in the range B9–A2. These are the same stars in which the outstanding spectral peculiarities are observed. Among the later A types the magnetic amplitude tends to diminish. The star β CrB is exceptional in having so strong a field for such a late spectral type, and also, according to Eggen (1957), it is unusual in color index. The mean range of variation of the periodic α variables is 4250 gauss. If we exclude HD 98088 and HD 188041, which are not typical members of the group, the mean range is 5100 gauss. The range of the 6 irregular β variables is 1935 gauss in the mean, while that of the 6 irregular non-reversing γ variables is 4620 gauss.

Among the spectral subdivisions B9, A0, and A2 are found the rapid irregular

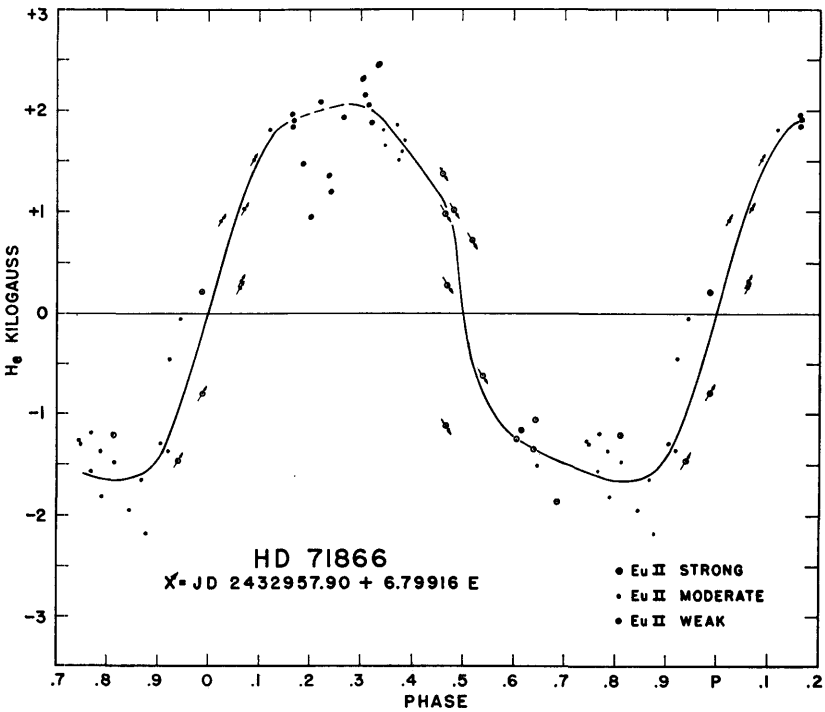


FIG. 4.—Magnetic variation of HD 71866 (No. 30). Near phases 0.0 and 0.5, as indicated by the arrows, the crossover effect is quite prominent in the spectrum of this star. The intensity of the Eu II lines shows a double maximum, being strongest near positive magnetic maximum, moderately strong near negative maximum, and weakest at the crossover phases. There are pronounced deviations from the mean magnetic curve. Radial velocities from various plates are randomly scattered within a range of about 7 km/sec.

variables such as 21 Persei, HD 10783, and HD 133029, as well as the α variables. The typical variables of spectral classes A5, A7, and F0 show notably slower variations. Examples are γ Equulei (A7p), HD 188041 (A5p) with its 226-day period, and β CrB (F0p), which seems to display a pseudo-cycle of length 40–60 days. Except for HD 32633, little is known as yet about the fields of the B8 and B9 stars, in which Mn II is usually the outstanding peculiarity. It is possible that the fields of these stars change quite rapidly.

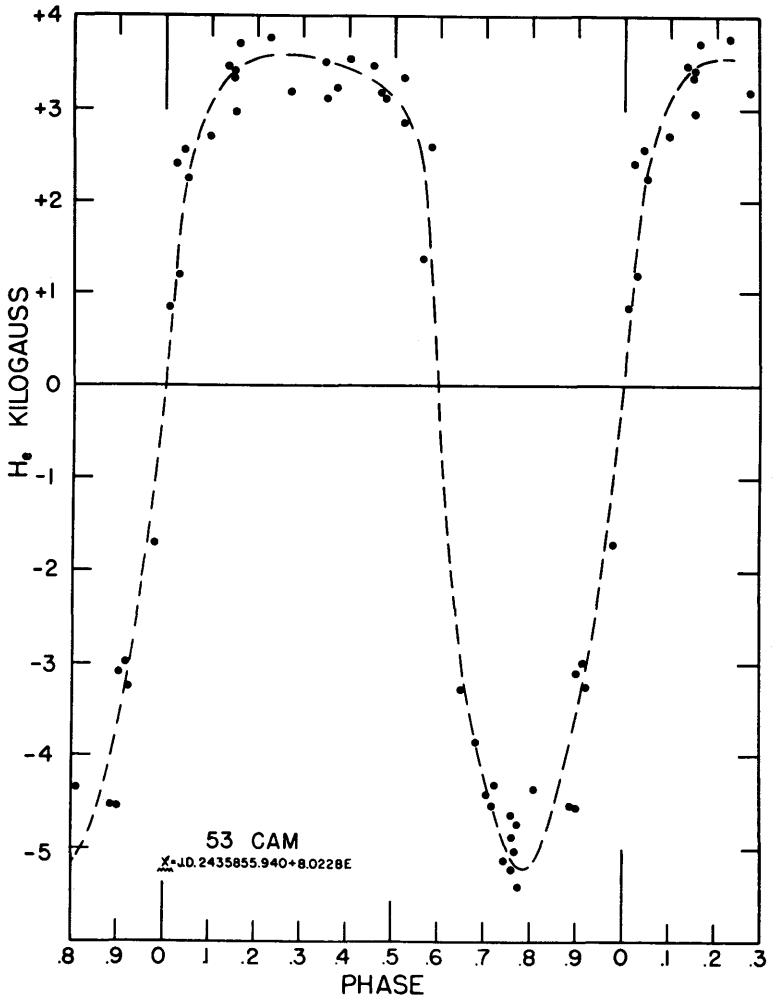


FIG. 5.—The magnetic field of 53 Cam has a larger amplitude than that of any of the other known α variables. Probable errors of individual plates are between 0.1 and 0.2 kilogauss. The lines are much wider, and those of Ti II are stronger, when the field is of negative polarity.

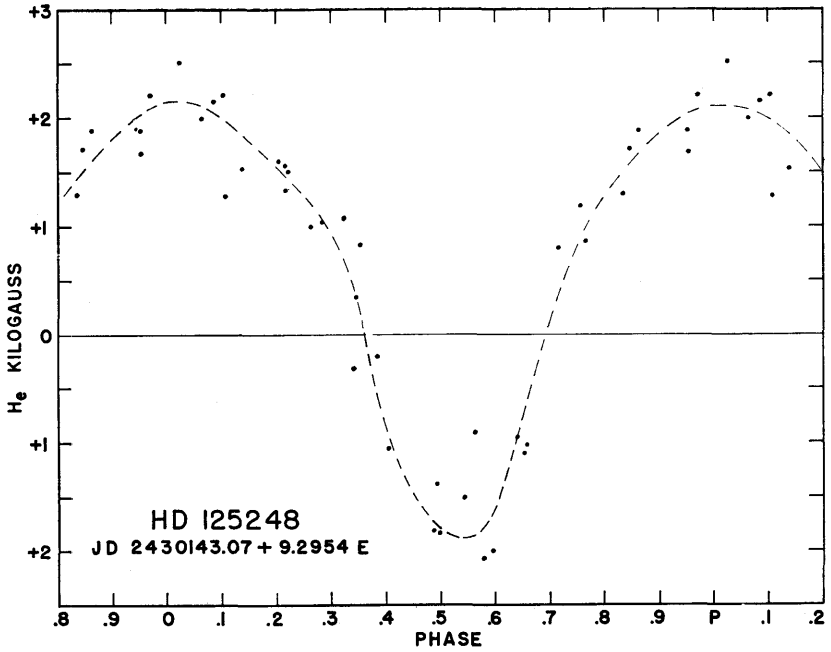


FIG. 6.—Curve of magnetic variation for HD 125248 (No. 48). Zero phase is at maximum positive field intensity, which is also the phase of maximum intensity of the Eu II lines. As in α^2 CVn, the lines of Cr, both neutral and ionized, vary in antiphase with the rare-earth lines, being strongest when the field is of negative polarity. The crossover effect is conspicuous. Field intensity may be systematically weaker subsequent to 1953.

TABLE 6

RANGE OF MAGNETIC VARIATION

Spectral Subdivision	No. of Stars	Mean Range in H_e (Gauss)	Largest Range in H_e (Gauss)	
B8, B9.....	6	1840	8100	HD 32633
A0p.....	22	2700	22000	HD 215441
A2p.....	12	2250	9100	53 Cam
A3p.....	2	775	980	HD 134793
A4p.....	6	1090	2640	HD 153882
A5p.....	1	1700	1700	HD 188041
A7p.....	3	900	1600:	ω Oph
F0p.....	1	1980	1980	β CrB

§ 4. ANOMALOUS LINE INTENSITY

Nearly all the magnetic A stars have the designation "peculiar," indicating that anomalous line intensities have been observed in their spectra. On the other hand, in Table 3 of the catalogue (Babcock 1958), no peculiar A stars are found among the sharp-line stars that do not show the Zeeman effect. There is a close correspondence between the occurrence of the anomalous line intensities and the presence of a strong, perhaps coherent, magnetic field. This correspondence probably comes about through the influence of the field in altering the relative abundances of the elements in the spectroscopically effective regions of the stellar atmosphere, combined with the comparatively minor effect of magnetic intensification through Zeeman broadening of already strong lines.

TABLE 7

ELEMENTS SHOWING LINES OF UNUSUAL STRENGTH

(Number of Stars Characterized by Abnormally Strong Lines of Elements Indicated Is Entered for Each Spectral Subdivision)

Element	B8, B9	A0	A2	A3	A4	A5	A7	F0
Y II	3	.....	.....	.....	.....	.....	.....	.....
Mn II	5	6	.....	.....	2	.....	.....	.....
Si II	8	17	4	.....	.....	.....	(2)	.....
λ4201	.....	8	.....	.....	.....	.....	.....	.....
Sr II	.....	15	14	2	7	1	4	2
Eu II+Gd II	.....	12	9	1	4	1	3	2
Cr I+Cr II	(2)	8	9	2	4	.....	1	.....
No. of stars	8	26	17	2	7	1	4	2

It has been known for some time (Morgan 1935) that, in proceeding from the hotter to the cooler stars in the range B8p to F0p, the accentuated elements, in approximate order of their appearance, are Mn, Si, λ4201 (unidentified), and the group including Sr and Cr with Eu and other rare earths. This is illustrated in Table 7, which has been compiled from the data of Table 1. Among the hotter (B8 and B9) peculiar stars, relatively weak fields with an unknown rate of change characteristically result in abnormally strong Mn II and Si II; in some, Y II is also prominent. The strong and rapidly varying fields of types A0p, A2p, and A3p bring out a variety of abnormally strong elements. Practically the whole array of peculiar elements is found in such stars as 21 Persei and HD 173650. The more slowly varying fields of the cooler subdivisions A5p, A7p, and F0p seem to accentuate only the lines of Sr, Cr, and the rare-earth elements. The most specific peculiarity is λ 4201, which seems to be limited to type A0p.

In some peculiar stars, certain elements other than Ca II are abnormally weak relative to the others. Examples are iron, as shown by the lines of both the neutral and ionized atom in HD 25354, and Mg II in 53 Cam.

In the spectra of the sharp-line A stars that show magnetic fields, the K line of Ca II characteristically has a narrow profile with relatively low total intensity. In some instances the sharp core of the line shows rather broad but very shallow wings, sometimes with widths of several angstroms. To a smaller degree, lines of Sr II show similar profiles, although the total intensity of these lines is often enhanced in the magnetic stars. In a considerable number of the stars with detectable fields, the K line shows even greater anomalies, such as a variable or asymmetric profile, extra components, or temporary disappearance of the core (HD 49967). Such stars are listed in Table 8, which is intended to include those with variable or anomalous K profiles, not those in which variable

TABLE 8

MAGNETIC STARS WITH ANOMALOUS PROFILE OF K LINE

Cat. No.	HD No. or Name	Sp. Type	Remarks on K Line
14	25354	A0p	Strong
15	41 Tau	A0p	Sometimes double
17	30466	A0p	Variable width
18	32633	B9p	Very weak interstellar component
22	42616	A2p	Flat-bottomed profile; longward edge sometimes sharper
24	49976	A0p	Usually sharp; once broad and shallow with no core
29	15 Cnc	A0p	Usually wide and shallow; sometimes profile is square
31	3 Hya	A2p	Variable profile?
35	30 UMa	A0p	Strong
62	153882	A4p	Square
...	168814	(A0p)	Shortward edge rounded; longward edge sharp
65	173650	A0p	Square, sharp-edged
70	184905	A0p	A weak, wide, shallow component plus a sharp, variable component; the wide component is sometimes sharper on the longward side; the sharp component is missing on two plates
82	215038	A0p	Very sharp

equivalent width has been reported. The asymmetric K profile, sharper on the longward side, as observed in a few of the stars of Table 8, suggests the ejection of ionized clouds or streams such as the sun produces on a relatively insignificant scale.

The "metallic-line" stars, as distinguished from the peculiar A stars (Roman, Morgan, and Eggen 1948), show notably greater equivalent widths of lines of the metals and particularly of Ca II; anomalous relative intensities within the group are not outstanding. The distinctly greater color index of these stars is well shown in Eggen's (1957) results. The presence of magnetic fields in several of the metallic-line stars is either observed or suspected (Table 9) ("T2" is Table 2 in Babcock 1958).

The spectral anomalies thus far referred to are readily visible upon compari-

son of spectrograms. Beyond the descriptive phase are measurements of equivalent width such as have been made by G. R. and E. M. Burbidge (1955*b*). Using a curve-of-growth method, they have compared line intensities and have derived abundance ratios for 23 elements in comparing α^2 CVn with the normal A0 IV star γ Geminorum and in comparing HD 133029 with α^2 CVn. Such measurements support the original suggestion of Morgan (1935) that the anomalous line intensities result from abnormal abundances of the elements in the spectroscopically effective parts of the atmospheres of the peculiar A stars. A survey of the spectra of the stars of Table 1 emphasizes the individual deviations that occur in the spectral peculiarities of the magnetic stars. Diversity in detail is the rule, and it is seldom that two or more such stars can be found with spectra that are essentially identical. The unpredictable variations in line profiles and in total intensities observed in many of the magnetic stars (e.g., 21 Persei, HD 25354, 41 Tauri, HD 49976, HD 56495, 45 Leonis, 45 Herculis, HD 173650, and HD 4778) emphasize the difficulties of quantitative investigations in this field.

TABLE 9

METALLIC-LINE STARS, PROBABLY WITH MAGNETIC FIELDS

No.	Star	No.	Star	No.	Star
16.....	68 Tau	T2.....	15 UMa	61.....	HD 153286
T2.....	HD 16956	39.....	17 Com B	19.....	16 Ori
T2.....	HD 50168	69.....	51 Sag		
27.....	HD 56495	T2.....	γ Cap		

§ 5. SPECTRUM VARIABLES

The known magnetic A stars are "peculiar" stars, and, among the peculiar stars, those that have periodically varying magnetic fields are found to be spectrum variables, in the sense that lines of certain elements, including some, but not all, of those showing marked intensity anomalies, display variations in intensity. In typical spectrum variables, such as α^2 CVn and most other members of the α group (Table 3), these variations are synchronous with the magnetic variations. In contrast, the typical irregular magnetic variables of the β and γ groups (Tables 4 and 5) are not spectrum variables. It is evident that there exists a close relationship between the spectral peculiarities (abundance anomalies) and the magnetic field. It further appears that spectrum variability in a star results from a higher degree of organization in the magnetic pattern of its outer layers, that occurs in periodic magnetic variables but not in irregular magnetic fluctuators.

The spectrum variables of type A were discussed by Deutsch (1947), who compiled a catalogue of 20 such stars with descriptions of their variations. A subsequent paper on spectrum variables (Deutsch 1956) includes references to

more recent observations, while the catalogue of magnetic stars (Babcock 1958) contains a number of notes on spectrum variations in certain objects.

Intensity variations of the largest amplitude are found for the elements Sr II (HD 49976, HD 134793) and Eu II (HD 125248). Marked variations in the chromium lines are much less common but are outstanding in α^2 CVn and in HD 125248, where they vary in antiphase with the rare-earth elements. Lines of Si II and the unidentified λ 4201, although frequently of abnormal strength in A0p stars, show only limited intensity variations in a few of the short-period variables (Table 11) and to an even lesser degree in α^2 CVn and a few others. Iron and manganese lines are rarely found to show appreciable intensity variations. Ti II has seldom been observed to vary except in 53 Cam and 73 Dra, where the changes are marked. While Ca II is abnormally weak in nearly all the peculiar stars and profile variations of the K line have been noted, as in

TABLE 10

IRREGULAR (δ) SPECTRUM VARIABLES

Cat. No.	Star	H_e Extremes (Gauss)		Remarks
14.....	HD 25354	−380	0:	*Eu*, *Cr*, Mn, λ 4201; Fe weak; variable profiles
24.....	HD 49976	−810	+	*Sr*, *Ca;* profiles diverse and variable
27.....	HD 56495	− ?	+ 570	*Cr*, *Mg* I, Sr
53.....	HD 134793	−530	+ 450	*Bu*, *Sr*, Cr; line widths vary
65.....	HD 173650	−540	+ 700	*Sr*, *Eu*, Si, Mn, Cr, Gd, λ 4201; peculiar variable profiles
87.....	108 Aqr		+	*Sr*, *Ca*, λ 4123
88.....	HD 224801		+2300	*Eu*, Si, Sr, λ 4201

Table 8, periodic intensity variations are apparently quite rare. Mg II is nearly invariant in most stars of the group, but λ 4481 undergoes periodic changes of intensity in 53 Cam, while Mg I varies in HD 56495. Periodic variations in line intensity are usually attended by systematic variations in profile width and in many cases, but not invariably, by small systematic fluctuations in differential radial velocity.

Until recently, it was believed that all spectrum variables of type A were periodic, like those of the α group. It now appears, however, that there are several magnetic stars showing irregular spectrum variations, or variations that are not simply correlated with the magnetic changes. These, which have been denoted as the "δ group," are listed in Table 10. Assignments to this group should be regarded as somewhat tentative, for some of these stars have not been studied so thoroughly as have the members of the α, β, and γ classes of magnetic stars. With the exception of HD 224801, the irregular spectrum variables have one common characteristic: the range of magnetic-field variation is limited to about 1 kilogauss, or much less than the range of the α variables.

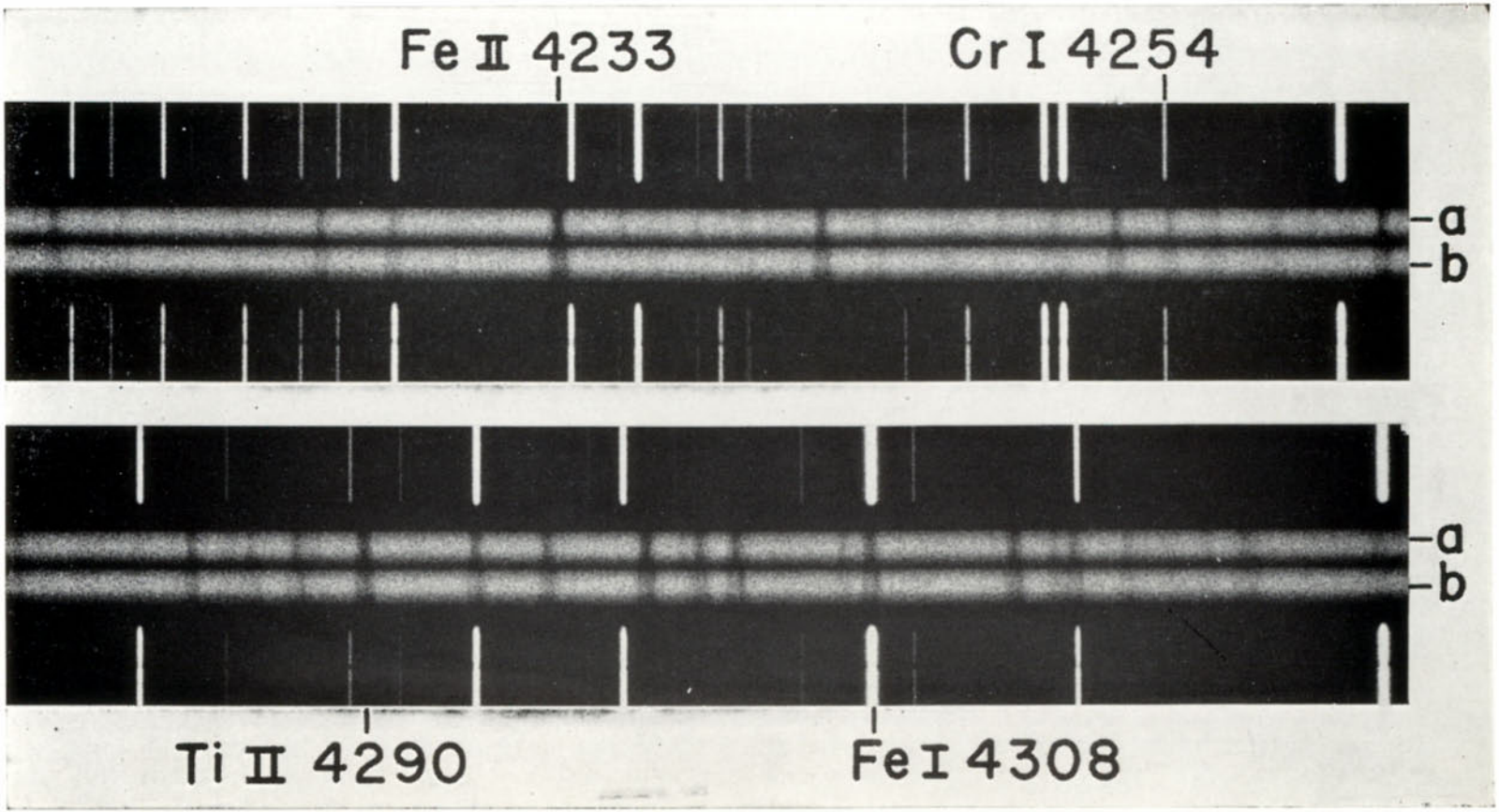


PLATE I.—Crossover effect on the lines in the spectrum of HD 32633. The profiles are sharper in spectrum *a* (left-hand rotatory polarization). In spectrum *b*, analyzed for rotatory polarization of the opposite sign, the lines are broadened or doubled.

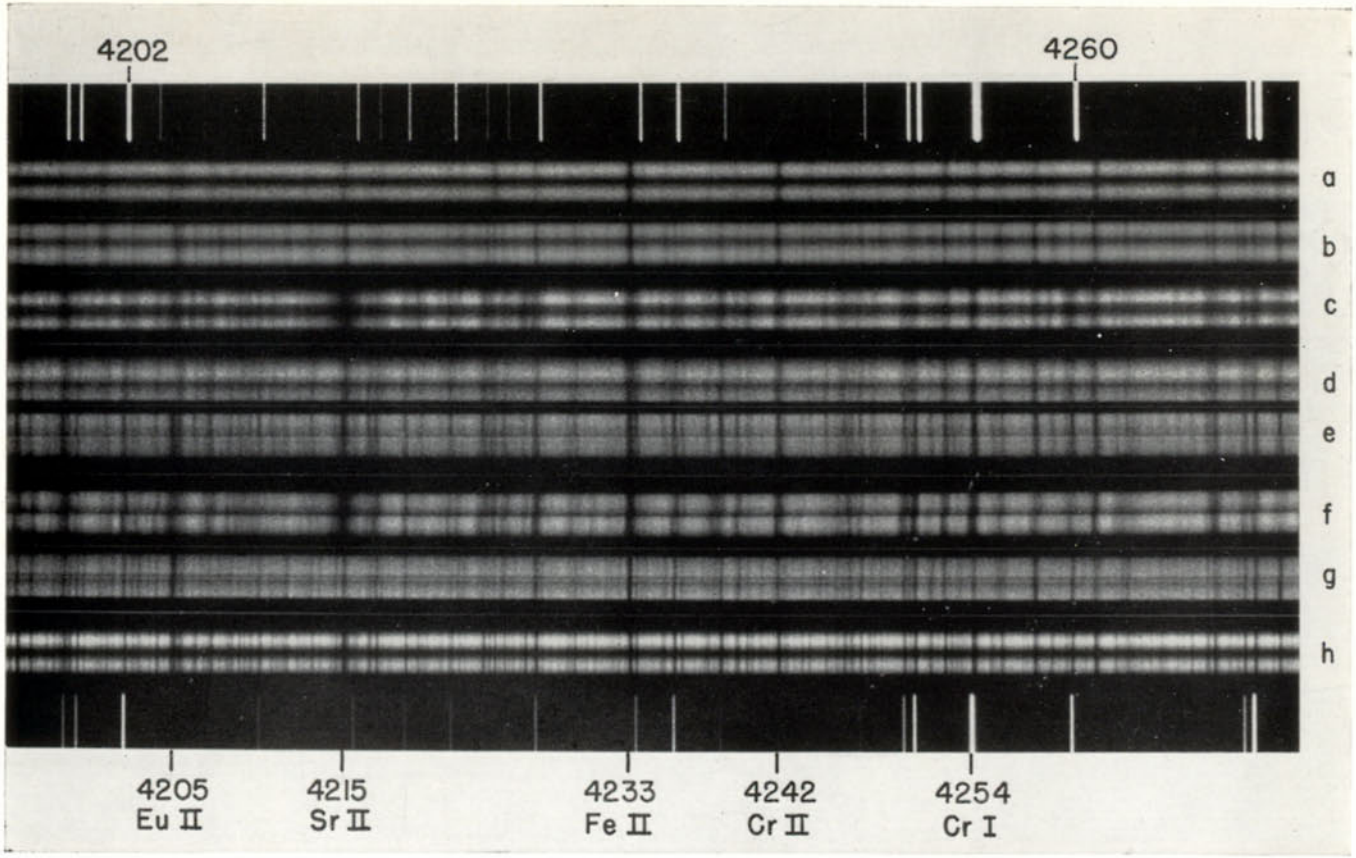


PLATE II.—Spectrograms, made with the double analyzer for rotatory polarization, of eight magnetic variables. *a*, HD 32633 (B9p, $w = 0.4$, irregular); *b*, α^2 CVn (A0p, $w = 0.3v$, $P = 5.5$ days); *c*, HD 98088 (A2p, $w = 0.4$:, $P = 5.9$ days, spectroscopic binary); *d*, HD 153882 (A4p, $w = 0.4$:, $P = 6.0$ days); *e*, HD 71866 (A0p, $w = 0.26$, $P = 6.8$ days); *f*, 53 Cam (A2p, $w = 0.25$–$1v$, $P = 8.0$ days); *g*, HD 125248 (A0p, $w = 0.2v$, $P = 9.3$ days); *h*, HD 188041 (A5p, $w = 0.11$, $P = 226$ days). Zeeman displacements are most readily seen in *f* (53 Cam), while the crossover effect is seen in *e* (HD 71866).

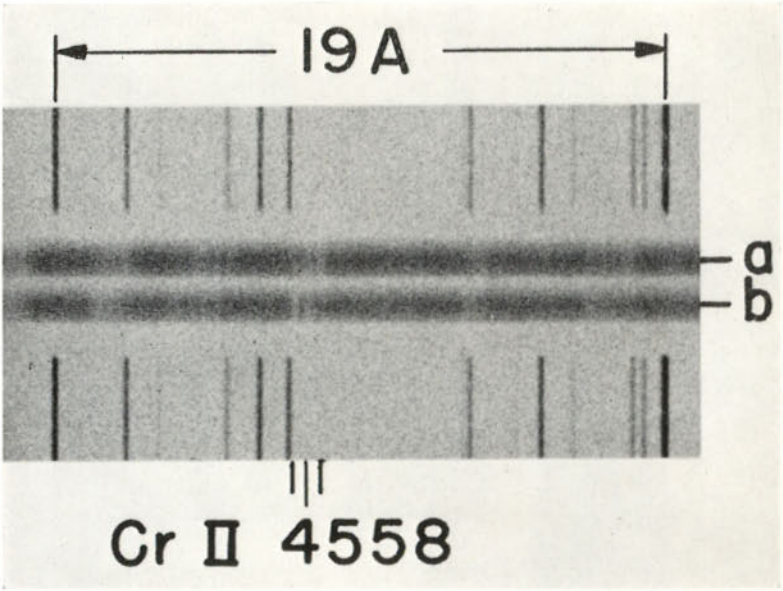


PLATE III.—Resolution of the Zeeman pattern of the line λ 4558.659 of Cr II in the spectrum of the star HD 215441. A magnetic-field intensity of 34,000 gauss is derived from the measured separation (0.81 A) of the displaced (σ) components. The analyzer has rejected all left-hand circularly polarized light from spectrum *a* and all right-hand circularly polarized light from spectrum *b*. The fact that the central groups of π components are seen shows that the field is not purely longitudinal. The Zeeman pattern of the line is (**0.05**, 0.14, 0.24, 0.33) **1.00**, 1.10, 1.19, 1.29, 1.38, 1.48, 1.57, 1.67, and the z value is 1.17. Obviously, the Zeeman effect is the predominant source of line broadening in this spectrum.

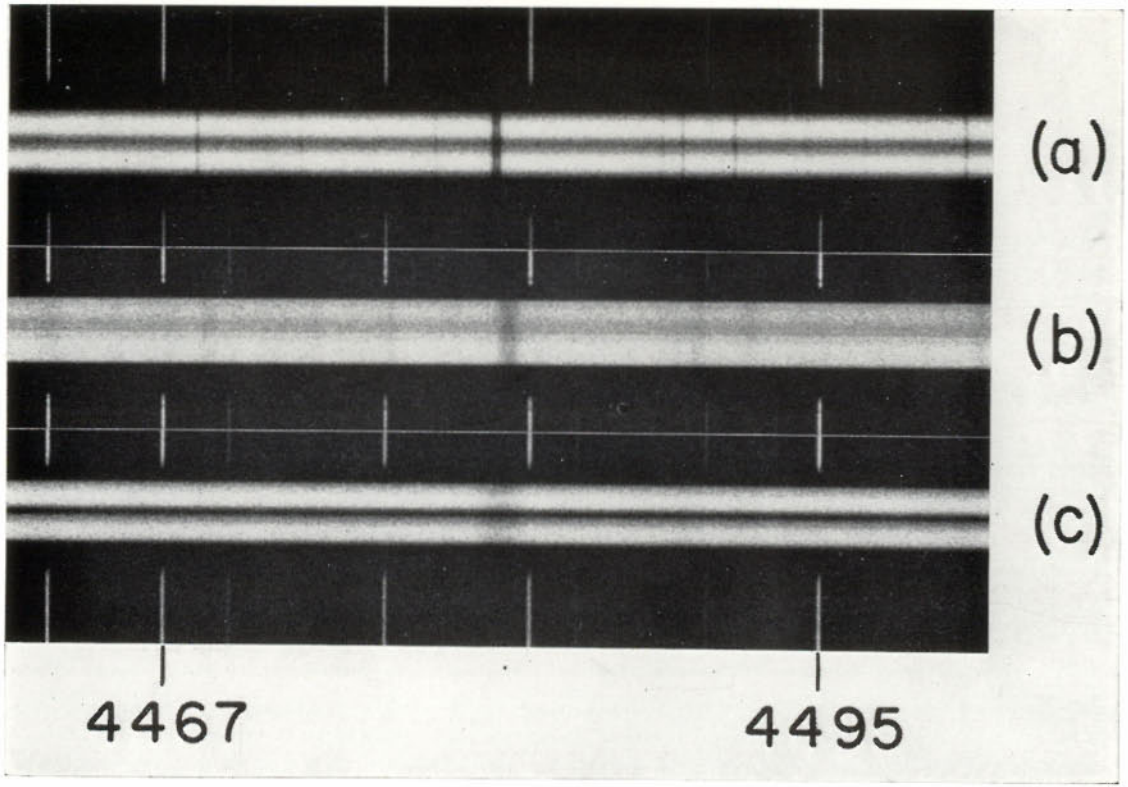


PLATE IV.—Rotational broadening of the doublet of Mg II at λ 4481 in (*a*) ι CrB, (*b*) ε UMa, and (*c*) HD 140728. Approximate line widths are, respectively, 0.07, 0.8, and 2 A.

The elements listed in Table 10 are of anomalous intensity; italics indicate variability.

Because of the association of peculiar spectra with magnetic fields, it is reasonable to infer that the peculiar A stars and spectrum variables with lines too wide to permit measurement of the Zeeman effect likewise possess magnetic fields. About 84 such stars are listed in the catalogue (33 in Table 2, for which Zeeman effect is doubtfully observed, and 51 in Table 4, for which the lines are definitely too broad). Of the broader-line peculiar stars, those with spectrum variations of known period are listed in Table 11, which has been adapted from Deutsch's paper of 1956. Small variations in luminosity and color have been measured for several of these stars by Provin (1953).

TABLE 11

BROAD-LINE SPECTRUM VARIABLES

Star	HD No.	Sp.	Period	Variable Elements	Index of Line Widths (w)
HR 5313	124224	A0p	0.52	Si	.....
56 Ari	19832	A0p	0.73	Si ? λ4201	.....
21 Com	108945	A2p	1.03	Sr	1:
χ Ser	140160	A0p	1.60	Sr, Cr	1.4
ι Cas	15089	A5p	1.74	Sr, Cr	1.3:
.....	107612	A2p	2:	Sr, Cr	0.8:
HR 1732	34452	A0p	2.7	Sr, λ4201	1.2
γ Ari (S)	11503	A0p	(2.607)	Cr, Eu, Si	1.2
ε UMa	112185	A0p	5.09	Cr, Ca	0.8

The spectrum variables of Table 11 have short periods and, with the exception of ι Cas, are of type A0p or A2p. The values of the index of line width, w, as listed, are only provisional; in some cases, it is apparent that diverse line widths occur in the same spectrum.

In Table 1 there are listed several magnetic variables having comparatively broad lines, with widths in the range 0.4–1 A. These stars have been grouped in Table 12, where those known to be spectrum variables are marked with asterisks. Notwithstanding the breadth of the lines, efforts have been made to estimate the upper limit of the magnetic-field intensity of the stars of Tables 11 and 12. Indications are that the fields of these stars are probably no stronger than the fields of the α variables, and it is unlikely that any of them equals the 5-kilogauss field of 53 Cam. For several of these stars, there is evidence that the line profiles have diverse and variable widths.

It has been shown that anomalous line intensities occur in the spectra of both the periodic and the irregular magnetic variables and that these variables are indistinguishable on the basis of isolated spectrograms. If the anomalous line intensities result from abnormal relative abundances of the elements in the spectroscopically effective outer layers of the stars, one is led to suppose

that in the irregular magnetic variables the surface has a sensibly uniform, though abnormal, composition that has been mixed through irregular hydromagnetic turbulence. In the periodic magnetic variables, on the other hand, the surface layers of the star are presumed to be more highly organized into distinct zones or regions, each with its identifiable peculiarities. The magnetic field associated with the respective surface regions may be supposed to preserve their identity, though at the same time allowing relative motion or even cyclic submergence and emergence of volumes of material associated with the magnetic field. Presumably the processes responsible for the abundance anomalies have been going on over long intervals of time, but only a very small fraction of the mass of the star need have been affected.

A secondary and probably minor cause of anomalous line intensity is "magnetic intensification" (Babcock 1949). Lines showing a multiplicity of components in the Zeeman pattern can, if the pattern is wide and if the number of effec-

TABLE 12

MAGNETIC STARS HAVING LINE WIDTHS BETWEEN 0.4 AND 1 ANGSTROM

No.	Star	Sp.	w	No.	Star	Sp.	w
5.....	43 Cas	A0p	0.7	82.....	HD 215038	A0p	0.8:
29.....	15 Cnc	A0p	0.7:	84.....	κ Psc*	A2p	.8v
58.....	ω Oph	A7p	0.6	87.....	108 Aqr*	A0p	.8:
64.....	HD 171586	A2p	0.8:	88.....	HD 224801*	A0p	.8:
59.....	45 Her*	A0p	0.6±	89.....	HD 4778*	A0p	0.5–1
70.....	HD 184905*	A0p	1:				

tive atoms is sufficient to place the line on the otherwise flat, or saturated, portion of the curve of growth, be intensified in a strong field by a factor that approaches as an upper limit $n/2$, where n is the number of components in the pattern. Such intensification should be particularly effective for such lines as λ 4205 Eu II ($^9S_4$–$^9P_3$), which has the theoretical pattern (**0.00,** 0.25, 0.50, 0.75) **1.25,** 1.50, 1.75, 2.00, 2.25, 2.50, 2.75. It has not been possible to show, however, that magnetic intensification is capable by itself of accounting for the relative intensities of peculiar lines of the various elements as encountered in the magnetic stars. G. M. and E. R. Burbidge (1955*a*) suggested that the apparent unimportance of magnetic intensification in α^2 CVn and in HD 133029 is probably due to its masking by local turbulent velocities.

If the anomalous abundances in the atmospheres of the magnetic A stars are the result of surface nuclear reactions, as argued by Burbidge, Burbidge, Fowler, and Hoyle (1957), it is required that these reactions result from highly energetic collisions of ions accelerated in rapidly varying magnetic fields. The significant fact here in regard to models of the α variables is that the abundance anomalies point to rapid intrinsic changes in the atmospheric magnetic fields of the α variables, as well as in the β and γ variables. This supports the argument for

a pole-on model of the α variables involving hydromagnetic fluctuations rather than simple oblique rotation of a magnetically rigid star carrying an oblique magnetic field. Hence one is led to suspect that the principal difference between the periodic α variables and the irregular magnetic variables is that the atmospheric motions in the former have become co-ordinated in a large-scale magnetohydrodynamic cycle which dominates the surface layers. The force of this argument is diminished by the fact that the observed stellar magnetic-field intensities and rates of change are insufficient energetically, and the proponents of the theory of surface nuclear reactions on magnetic stars are forced to invoke the action of superstrong magnetic "star spots" that undergo large changes in only a few seconds. For activity of this kind, there is no direct observational evidence, at least among the A stars.

At the present time it can hardly be regarded as proved that the abundance anomalies in the magnetic stars result from surface nuclear reactions. This

TABLE 13

SPECTROSCOPIC BINARIES WITH OBSERVED MAGNETIC FIELDS

No.	Star	Period	No.	Star	Period
3.....	HD 8441*	Weeks?	35.....	30 UMa	11^d6
4.....	HD 9996*	?	37.....	HD 98088	5^d905
8.....	HR 710*	$2^d997814$	46.....	HD 125248*	1618^d
15.....	41 Tau*	.....	55.....	β CrB	10.496 yr.
32.....	3 Hya*	Months?	71.....	HD 187474*	Years?
34.....	κ Cnc	6^d39316			

theory seems not to account for the great overabundance of europium that is so characteristic of many of the magnetic stars, and there are other discrepancies. It would seem that other theories, leading to progressive sorting or segregation of chemical elements in the atmospheres of magnetic stars, deserve critical investigation.

§ 6. SPECTROSCOPIC BINARIES

Fourteen spectroscopic binaries occur among the known magnetic stars, as listed in Table 13. Those that are believed to be newly identified as binaries are marked with asterisks.

The fact that some binaries with periods of a few days have strong observable magnetic fields is noteworthy in itself, for, under such conditions, the effect of magnetic forces on ionized material in the vicinity of the binary system cannot fail to be of importance. Consideration of these forces and processes is therefore essential in discussions of corpuscular streaming and of the evolution of such systems. It is hardly surprising that several of the binaries listed show magnetic variations that are apparently quite unrelated to the orbital motion. It is also noteworthy that, with the exception of HD 98088 and HD 125248,

none of the periodic magnetic variables (Table 3) displays any evidence of binary motion. For the latter, Deutsch (1957) has found evidence for a 1618-day period in the velocity, but this seems quite independent of the 9-day magnetic cycle.

HD 98088 is an exceptional star, which differs from the other α variables in that the crossover effect is not observed in its spectrum and it is a spectroscopic binary (Abt 1953), with a period of revolution equal to the period of magnetic variation. The magnetic and line-intensity variations can be represented formally by a model viewed at large obliquity which rotates on its axis in the same period as that of the orbital revolution and maintains one face toward the companion star. This does not exclude the possibility that the star undergoes a magnetohydrodynamic oscillation in resonance with the tidal effects of its elliptical orbit ($e = 0.176$).

Of the seventy sharp-line A stars in Table 1, eleven, or 16 per cent, are spectroscopic binaries. This may be compared with an independent study of one hundred and twenty-four peculiar A-type stars by M. Jaschek and C. Jaschek (1958). They found that twenty-one systems, or 17 per cent, are spectroscopic binaries. In contrast, they found that in "normal" A stars with $v \sin i$ no greater than 75 km/sec and in luminosity classes between II and V the percentage of binary systems was 43. The Jascheks also concluded that the percentage of visual binaries among the peculiar A stars is normal.

§ 7. COMMENTS ON CERTAIN MAGNETIC STARS

A few stars exhibiting magnetic phenomena of particular interest have been selected for discussion in this section. Numbers refer to Table 1.

HD 133029 (No. 52).—(52 Herculis and HD 215038 are probably similar.) One of the strongest stellar fields is found in this γ variable. Results based on 74 plates distributed over 8 years show that the variations are irregular, between the limits +1150 and +3270 gauss. Values near the mean are more common than near the extremes. Some of the changes in H_e are quite rapid. There are pronounced anomalies in line intensity, and these have been measured by Burbidge and Burbidge (1955*b*), but no spectrum variations have been reported. The line width, w, is about 0.4 A. It is assumed that the dominant component of the stellar field is dipolar and that the star must have rotated many times on its axis during the years covered by the observations. The most satisfactory model for this star seems to be a rapid rotator, observed nearly pole-on, in which the magnetic field is essentially symmetric with the rotational axis. Magnetohydrodynamic fluctuations at the surface are presumed to account for the irregular variations in H_e and, in part, for Doppler broadening of the lines. It has not seemed possible to devise a model for this star in which the magnetic axis is appreciably inclined to the rotational axis.

HD 188041 (No. 72) (Fig. 7).—Because the lines are sharp and numerous, measurements of H_e can be made with good precision. Rather large random

deviations are superposed on a regular cycle. The magnetic maxima are non-uniform in amplitude, but the minima recur at regular intervals of 226 days. It is improbable that the period of axial rotation could be so long. There is evidence for an abrupt change in H_e near mid-period. It is considered that the magnetic variations are best attributed to some intrinsic magnetohydrodynamic process. If this is correct, it proves that a magnetohydrodynamic cycle can result in spectrum variations, for changes in intensity of the Gd II and Eu II lines in the 226-day period are established.

RR Lyrae (No. 68).—Observations suggest that a strong, variable magnetic field can occur in a pulsating star. It is hardly necessary to add that the cluster-

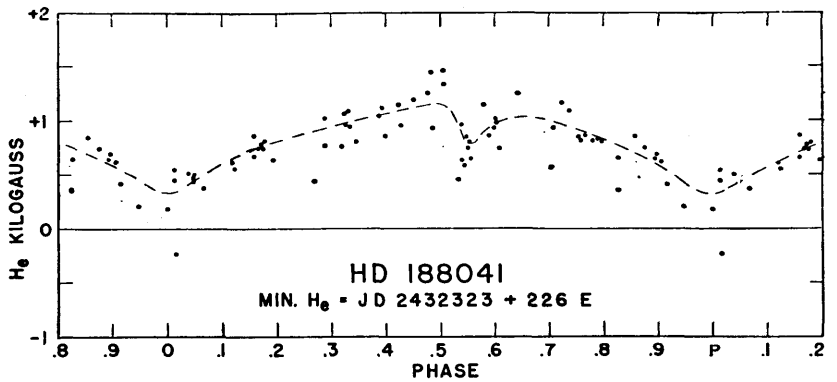


FIG. 7.—Magnetic variation of the 226-day variable HD 188041 (No. 72). Because the lines are ultra-sharp and numerous, the probable errors are only about ±0.04 kilogauss, and the large, apparently random, dispersion of the individual observations is physically real. There are strong indications of an abrupt discontinuity in the magnetic variation between phases 0.5 and 0.6. All plates but one show positive magnetic polarity, but there is no doubt about the unique reversal. Intensity of lines of Sr II and the rare earths varies in the same period as the magnetic field.

type variables like RR Lyr are far removed in the HR diagram and in evolutionary status from the main-sequence A stars.

HD 187474 (No. 71).—Six plates covering a 1-year interval in 1957–1958 indicated that this star might be unique in showing a constant magnetic field. The mean value was −1860 gauss. Later, however, the field slowly decreased, reaching about zero in July, 1959. The lines are of diverse widths, between 0.1 and 0.4 A, those of Eu II being the broadest. All elements are in good agreement in yielding nearly the same value of H_e, with the exception of the Cr lines on one plate. If the magnetic field is essentially dipolar, the inclination of the dipole axis to the line of sight cannot be large, because the Zeeman effect is principally longitudinal and the changes are so slow. It is considered most probable that the rotational axis has only a small inclination and that the field is essentially axisymmetric. By June, 1960, the field had reversed, reaching

+2880 gauss. Exceptionally large changes in line intensity also occurred. The star may be an α variable with a period of about six years.

HD 71866 (*No. 36*).—This star is a typical α variable, with a period of 6.8 days and nearly symmetric magnetic reversals between the approximate extremes −1700 and +2000 gauss. It is also a spectrum variable. If one attempts to represent the star as a rigid oblique rotator with a rotational period of 6.8 days, then, assuming that the obliquity of the axis of rotation to the line of sight is 90° and that the stellar radius is 2.3 $R\odot$, the equatorial velocity is found to be 18 km/sec. This leads to expected Doppler rotational broadening of 0.53 A at λ 4300. Other effects contributing to line broadening can scarcely be neglected. However, several measurements of the over-all widths of typical metallic lines of moderate intensity yield the mean value $w = 0.26$ A. Thus it appears practically impossible that the obliquity, i, of the axis can be greater than 30°. On the other hand, unless i is large, it is extremely difficult, if not impossible, to represent the nearly symmetric and complete magnetic reversals by a rigid oblique rotator model. Observations near positive and negative magnetic maximum show a longitudinal Zeeman effect that is essentially "pure" as regards polarity; there is no trace of contamination of the profiles by components showing the opposite polarity. Further, it has been shown for this star that the crossover effect is not compatible with the rigid rotator model for the following reasons: (*a*) the mean matching velocity required to yield maximum visibility of the effect, on the assumption that it arises from the differential motion of two areas of opposite polarity, is only 3.5 km/sec, yet for this model $v_e = 18$ km/sec; (*b*) the crossover effect is uniquely conspicuous for particular lines of Fe I, but far less so for lines of Fe II. The random fluctuations of velocity in HD 71866, with a range of about 8 km/sec, are perhaps best attributed to magnetohydrodynamic disturbances at the surface.

53 Camelopardalis (*No. 28*).—This star is unique among the α variables in the strength of its field and the amplitude of the variation, which occurs in an 8-day period. The longitudinal Zeeman effect at maximum appears to be uncontaminated by transverse or reversed fields. The rate of change, dH_e/dt, is quite high near the crossover phases. The crossover effect in the line profiles is prominent, but not so extreme as in the spectrum of HD 71866. On the oblique rotator model, the line widths in 53 Cam should be about 0.45 A, but the observed range of w is about 0.15–1 A, so that a simple model does not suffice.

HD 32633 (*No. 18*).—The reversing magnetic field fluctuates rapidly. Extremes of −5800 and +2200 gauss have been measured. At one time thought to have a period of about 4 days, the variations now seem to be irregular and the star must be classed as a β variable. The crossover effect is unusually prominent (Pl. II) but seems quite erratic, like the variations in magnetic amplitude. One suspects that this star, like other β variables, is closely related to the α variables. The lack of line-intensity variations may be attributed to atmospheric mixing that results from the randomness of magnetic activity.

HD 215441.—This eighth-magnitude A0p star has the strongest magnetic field yet discovered. Spectrograms at 4.5 A/mm (Pl. III) show distinct resolution of the σ and π groups of components of the Zeeman patterns of several lines. Such a degree of magnetic resolution has been found in no other star. Direct measurement of the separation of the σ groups, unblended by the π components, yields an effective field of the order of 34 kilogauss. The field is strong and the magnetic polarity is positive on all 18 plates. No regularity is evident either in the moderate magnetic variations or in the rather minor changes of line intensity. Therefore, the star is to be classed as a γ variable. Jarzebowski (1960), however, has reported variations in light that are typical of the α variables. He finds variations of 0.14 mag. occurring in a period of 9.5 days.

§ 8. LINE WIDTH AND OBLIQUITY OF ROTATING A-TYPE STARS

The visibility of metallic lines in the spectra of main-sequence A stars depends very strongly on the degree of rotational broadening, i.e., on $v_e \sin i$. This becomes particularly evident if one arranges a number of A-type spectrograms in a sequence of line width from ultra-sharp ($w = 0.10$ A) to normal ($w = 4$ A). The examples chosen for Plate IV show rotational broadening of the strong doublet of Mg II at λ 4481. (The components are separated by 0.198 A.) The three stars are ι CrB, ϵ UMa, and HD 140728, which have line widths of approximately 0.07, 0.8, and 2 A, respectively. The numerous weak metallic lines seen in ultra-sharp-line spectra are largely obliterated with increasing $v_e \sin i$ as the profiles become shallow and broad. Indeed, in the typical A-type spectrum viewed at large obliquity, one sees, in addition to the hydrogen lines, only the K line, Mg II λ 4481, and perhaps with difficulty a few others. (There is also a marked increase in the mean equivalent width of the metallic lines in passing from type B8 through the various subdivisions of type A to F0.) Typically, the line widths in the photographic region are in the vicinity of 4 A, indicating that $v_e \sin i$ is about 150 km/sec. If randomness of orientation prevails for the axes of the rapid rotators that make up the great majority of the A stars, then a small proportion of these must be observable nearly pole-on and must show sharp lines. If the brighter, pole-on, rapid rotators are not included in Table 1, we may ask where they are.

Whereas in the past it has sometimes been stated that the peculiar A stars are slow rotators, the alternative is examined in the following paragraphs. Here it is contended that most of the sharp-line A stars are rapid rotators seen pole-on; that these are the stars in which magnetic fields can be observed; that the strong fields and spectral "peculiarities" are closely related to the rapid rotation; that the visibility of the peculiarities, as well as of the metallic-line spectrum in general, decreases with increasing obliquity; and that the relatively numerous broad-line A stars probably also possess magnetic fields and "peculiar" spectra that are unobservable only because the obliquity happens to be large. An addi-

tional hypothesis—that the equivalent widths of the metallic lines vary with latitude, being strongest near the poles, where the axisymmetric magnetic field is also strongest—helps to account for the low visibility of these lines when they are very wide.

Before considering the statistics of line width, it may be noted that there is no known evidence that the "peculiar" A stars are distributed differently from the "normal" A stars in the galaxy or in clusters. It has also been shown by Provin (1953) that, when plotted in a $U-B$, $B-V$ color diagram, the peculiar stars lie on a sequence defined by normal dwarf stars.

Rotational velocities for the B8–A2 stars have been published by Miss Westgate (1934), by Huang (1953), and by Slettebak (1954). For 87 normal main-sequence stars, Slettebak found $\bar{v}_e = 177$ km/sec, and for 16 peculiar stars, $\bar{v}_e = 52$ km/sec. For the present purpose we group these together, obtaining a weighted mean of 158 km/sec. Correspondingly, $\langle v_e \sin i \rangle = 124$ km/sec. In theory, the distribution function can be obtained according to the methods of Chandrasekhar and Münch (1950) or Böhm (1952). However, a comparison of the observational data obtained with a dispersion of about 30 A/mm with the newer measures of line width on high-dispersion, high-resolution spectrograms (4.5 A/mm) shows that considerable revisions are required for the stars with sharper lines. There are fewer stars with very small line broadening than indicated by the low-dispersion observations. The data are inadequate to define an accurate distribution function, but, for various values of v_e, the fraction of the group having rotational broadening less than a specified value can be found. On the assumption of random orientation of axes, the fraction of stars with obliquity less than i_0 is $F = 1 - \cos i_0$. An upper limit of 0.48 A is arbitrarily set for the line width of the stars of interest.

If all A stars were like the average, with $v = 158$ km/sec, and if $i = 90°$, the line width w would be 4.5 A in the vicinity of λ 4200. For the limit $w = 0.48$ A, the corresponding i is 6°.1 and $\cos i_0 = 0.994$. Therefore, 0.6 per cent, or about 12 stars of the approximately 2000 stars brighter than magnitude 6.0 in the range of types B8–F0, would have rotational broadening less than our limit of 0.48 A. Because of the distribution of velocities, the observed group with $w < 0.48$ A will include all slow rotators with $v < 16.8$ km/sec, as well as a decreasing fraction of those in more rapid rotation (see Fig. 8). For different values of v_e, the fraction, F, of stars having $w < 0.48$ A is given in Table 14.

Evidently the number of sharp-line extremely rapid rotators ($v_e > 200$ km/sec) will be quite small, but we may expect to find a few dozen A stars brighter than the sixth magnitude with lines sharper than 0.48 A that are rotating with $v_e > 75$ km/sec and a comparable number with slower rotation.

Inspection of lines on plates of 4.5-A/mm dispersion shows that many of the sharp-line stars display profiles that are somewhat diverse and variable in width. It is evident that, for lines sharper than about 0.4 A, rotational broadening falls to a level that is comparable with Zeeman broadening and

that the profiles are affected by the specific Zeeman patterns, as well as by peculiar atmospheric motions in some cases. Therefore, precise measurements of line width have not been attempted. An "index of line width," w, has been measured or estimated for most of the stars of Table 1, but this is simply a provisional value of the apparent line width in the vicinity of λ 4300.

The extended search for sharp-line A stars that has resulted in the bulk of entries in Table 1 is believed to be reasonably complete, although not exhaustive, down to a limit between the sixth and seventh magnitudes; a few eighth-magnitude stars are included. Some of the relevant data have been arranged in Table 15, in which the A-type stars (B8–F0) of Table 1 have been listed according to line width from $w = 0.07$ to $w = 0.48$. These groups

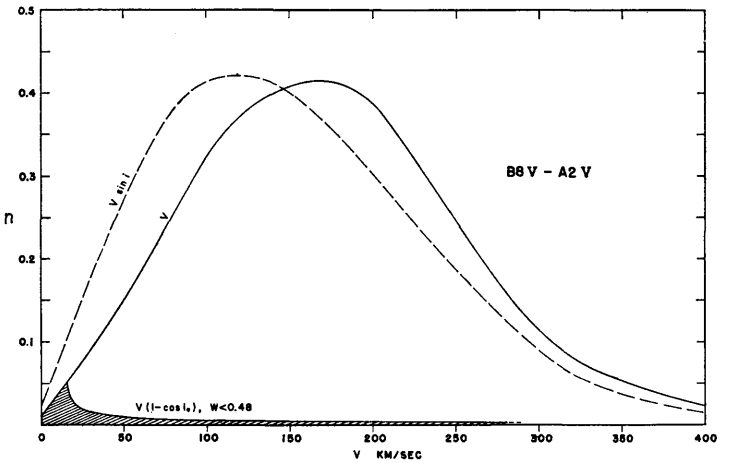


FIG. 8.—Curves showing distribution of equatorial velocity, v, and $v \sin i$, among the stars of types B8 V–A2 V. The curves have been adapted from the results of Slettebak (1954), but n has been arbitrarily diminished for $v < 50$ km/sec in accord with results from plates of high dispersion. The area under the lowest curve represents stars with $w < 0.48$.

TABLE 14*

STATISTICS OF LINE WIDTH

v_e (km/sec)	F	P (days)	v_e (km/sec)	F	P (days)
16.8.....	1.000	6.4	100.....	0.014	1.1
20.....	0.461	5.4	125.....	.009	0.86
25.....	0.262	4.3	150.....	.007	0.72
30.....	0.173	3.6	200.....	0.003	0.54
50.....	0.059	2.2	250.....	.....	0.43
75.....	0.026	1.4			

* On the assumption that spin axes are oriented at random, F represents the fraction of A stars showing rotational broadening less than 0.48 A for various values of v_e. The corresponding rotational period in days is also listed.

TABLE 15

SHARP-LINE STARS FROM TABLE 1

(List Limited to A-Type Stars, "Metallic-Line" Stars Being Excluded)

w	BRIGHTER THAN $6^{m}.0$		FAINTER THAN $6^{m}.0$	
	No.	Name	No.	Name
0.07–0.12 . . .	35	30 UMa	3	8441
	40	110066	4	9996
	57	ι CrB	25	50169
	66	10 Aql	74	191742
	72	188041	.....	.....
	77	γ Equ	.....	.....
.13– .17 . . .	8	HR 710	1	2453
	34	κ Cnc	12	9 Tau
	43	111133	49	126515
	55	β CrB	56	33 Lib
	71	187474	63	165474
	76	73 Dra	81	216533
.18– .22 . . .	36	45 Leo	14	25354
	41	l Cen	45	115708
	46	78 Vir	65	173650
	48	125248 (v)	73	190073
			75	192913
.23– .27 . . .	32	49 Cnc	6	10783
			7	11187
			30	71866
.28– .37 . . .	20	μ Lep	28	53 Cam (v)
	31	3 Hya	54	135297
	44	α^2 CVn	53	134793 (v)
	51	μ Lib A	.....	.....
	83	β Scl	.....	.....
38– .47 . . .	15	41 Tau	18	32633
	37	98088	22	42616
	38	17 Com A	24	49976
	50	π Boo A	27	56495
	59	45 Her	52	133029
	60	52 Her	67	21 Aql
	62	153882	.....	.....
	84	ι Phe	.....	.....
0.48+	5	ω Cas	17	30466
	9	21 Per	64	171586
	29	15 Cnc	70	184905
	33	ν Cnc	66	224801
	58	ω Oph	.....	.....
	78	θ^1 Mic	.....	.....
	82	κ Psc	.....	.....
	85	108 Aqr	.....	.....

have been further divided to separate the stars, 30 in number, that are brighter than magnitude 6.0.

The magnetic stars of Table 15 constitute the majority of bright, sharp-line A stars. A few others can be added by scanning Tables 2 and 3 of the catalogue. From the former (magnetic field possibly present), excluding "metallic-line" objects as well as high-luminosity stars of classes I, II, and III, we have ϵ Arietis (A4p composite), θ Leonis (A2 V), υ Herculis (B9p), and ρ Herculis (B9p). Similarly, from Table 3 of the catalogue (sharp-line stars without observable magnetic field), we select the 8 stars in the present Table 16.

To summarize, the group of sharp-line A-type stars brighter than magnitude 6.0 is constituted of 33 with the designation "peculiar," all but 3 of which show the Zeeman effect, plus 10 apparently normal main-sequence stars showing no evidence of a magnetic field. Thus the number of sharp-line A stars found after a diligent search and the proportion of "peculiar" and "normal" sharp-line

TABLE 16

SHARP-LINE A-TYPE STARS SHOWING NO MAGNETIC FIELD

Star	Sp.	m_v	π	M	$M-M_0$
γ Gem	A0 IV	+1.9	0.047	+0.2	−0.7
α CMa	A0 V	−1.6	.375	+1.2	+0.3
21 Lyn	A1 V	+4.4	.020	+1.0	−0.3
95 Leo	A4	+5.5	.013	+1.1	−1.0
HD 186568	B9	+5.9	.....	.....	.....
ν Cap	B9 IV	+4.8	.018	+1.1	+0.8 ($w = 0.4$:)
o Peg	A1 V	+4.8	.017	+0.9	−0.4
σ Aqr	A0 IV	+4.9	0.014	+0.6	−0.3 ($w = 0.3$:)

spectra are statistically in good accord with the predictions of the foregoing paragraphs and with Figure 8. These findings support the view that most of the A stars with sharp-line spectra showing magnetic fields are rapid rotators observed pole-on, while the 10 stars of Table 16 are presumed to be inherently slow rotators, located under the toe of the curve of Figure 8.

Not only the line widths but the total intensities must be functions of latitude on a rapidly rotating star. Considering that the magnetic field, as well as the temperature and surface gravity, varies between the equator and the poles of rotation, it is a reasonable inference from observation that certain of the spectra peculiarities found in the A stars arise preferentially near the poles and that not only the depths of the profiles but also the equivalent widths of the peculiar lines become suppressed with increasing obliquity. Line intensities at large i will be diminished by dilution of the profiles by the continuum of the low latitudes and also by limb darkening. With moderate obliquity, there is also the possibility of accounting for diverse line widths if various lines arise in different latitudes.

The oblateness resulting from rapid rotation gives the star a greater effective

area for small i, and the relatively greater surface gravity near the poles will result in a higher effective temperature and greater surface brightness. Variations in ionization as a function of latitude will accentuate the dependence of the spectrum on obliquity. These considerations were discussed by Baldwin (1944) with particular reference to the rapidly rotating B stars. If an ordinary rapid rotator could be observed as the obliquity diminished toward zero, the star would become slightly brighter and bluer, while the line spectrum would take on characteristics of higher temperature and pressure. The lines would become sharper, and any anomalies originating in high astrographic latitudes would be enhanced. A strong axisymmetric magnetic field, through its influence on energy transport in the presence of turbulence and through selective intensification of lines, would further complicate the obliquity effect. While quantitative predictions are impossible at present, it may be pointed out that Deutsch (1947) concluded that the peculiar A stars lie, on the average, more than half a magnitude above the main sequence when absolute magnitude is plotted against spectral type in the HR diagram.

If, because they are seen pole-on, the peculiar A stars lie slightly above the main sequence, the few slow rotators of type A should have spectra virtually independent of obliquity, and they should lie on the main sequence. The number of such stars in Table 16 is only 8. Absolute magnitudes are listed in the table for 7 of these stars for which trigonometric parallaxes are available. Also listed is the difference, $M-M_0$, between the absolute magnitude of the star and the absolute magnitude, M_0, of a main-sequence star of corresponding spectral type. The values of M_0 have been taken from the work of Trumpler (1930). The mean $M - M_0$ is -0.2. Therefore, the evidence indicates that the few stars supposed to be slow rotators lie on or close to the main sequence, along with the numerous oblique rapid rotators, while the pole-on rapid rotators tend to lie on the upper fringes of the main sequence.

The relationship between obliquity and line profiles in rapid rotators may be illustrated by an example. Let us assume that the strongest magnetic fields, as well as the greatest degree of enhancement of peculiar lines, are to be found in the most rapid rotators. We are then justified in assuming that v_e is well above the average, say 280 km/sec (Fig. 8). Let us further assume that the spectrum is normal in a wide equatorial belt in latitudes below $\pm 45°$ but that the "polar caps," between $\pm 45°$ and the poles, produce a spectrum with strong peculiar lines. In the spectrum of the polar caps (without rotation), let a line such as Eu II λ 4205 have a width $w = 0.4$ A, an equivalent width $W = 0.4$ A, and a central depth $d = 1$. Then, in integrated light for $i = 0°$, $w = 0.4$ A, $W = 0.2$ A, and $d = 0.5$. Such a line would be typical of the stronger peculiar lines in A-type spectra. But, when viewed at $i = 90°$, the line would be broadened by rotation to a width, w, of about 5 A; its equivalent width would be multiplied by a factor 0.36 by dilution, reducing it to $W = 0.072$ A; and its central depth, d, would be diminished to about 0.02. Limb darkening, neglected here, would

further diminish the equivalent width and depth of profile. Thus such a line would probably go undetected.

We have seen that there is good supporting evidence for the hypothesis that the ordinary, typical, broad-line A stars are rapid rotators with strong magnetic fields and that, if they could be observed pole-on, they would show "peculiar" spectra. But before this hypothesis can be fully accepted, new data on the statistics of line width for stars of moderate or intermediate obliquity will be required. If the foregoing considerations are in error and if we return to the alternative hypothesis that the magnetic stars are to be regarded as slow rotators observed at large obliquity, it is plausible to attribute their slow rotation to a loss of angular momentum through the agency of the magnetic field. Angular momentum can be transferred through the external field to a circumstellar gas cloud (Lüst and Schlüter 1956). But in the low proportion of spectroscopic binaries observed among the A stars of Table 1 (11 out of 70 stars) there is little evidence that such a transfer has occurred.

§ 9. THE PERIODIC (α) MAGNETIC VARIABLES

The typical α variables (Table 3) constitute perhaps the most interesting group of magnetic stars; yet the development of a physical model that will represent them satisfactorily is a problem that is far from solution. The outstanding members of the group, with their respective periods, are 53 Cam (8.025 days), HD 125248 (9.295 days), HD 71866 (6.80 days), and α^2 CVn (5.469 days). They show large-amplitude reversing fields with some approach to symmetry, but generally the magnetic maxima of opposite polarity are of unequal width, and the spectrum lines are systematically broader at the phase of the sharper magnetic maximum. There is a peculiar grouping of their periods in the vicinity of 1 week, which suggests that some physical process of basic significance is operating. A number of interrelated phenomena are involved: variations in the Zeeman effect, in profiles and in equivalent widths, in the crossover effect, in differential velocities, and in luminosity. For details, and for references to original observations, the reader is referred to Table 1 of the Catalog of Magnetic Stars (Babcock 1958).

There is every indication that the α variables are very closely related to the irregular β and γ magnetic variables. On the basis of single spectrograms, members of these groups are indistinguishable. The difference seems to lie in the fact of periodicity and in the greater degree of spectrum variability usually found in the α variables.

In this section the approach to two basically different models will be considered in the light of available data. The two models are (1) the magnetic oscillator, based on a vastly amplified and accelerated magnetohydrodynamic cycle similar in kind to the 22-year magnetic cycle of the sun, and (2) the oblique rotator, an essentially rigid star carrying an appropriate pattern of magnetic areas distributed over its surface, which rotates about an axis oblique to the

line of sight, resulting in a periodically changing effective field. The oblique rotator has the appeal of simplicity, while the oscillator model has the advantage of similarity to physical phenomena, complicated though they may be, that are observed on the sun.

9.1. The Magnetic Oscillator or Solar-Cycle Model

There is no reason to believe that the sun is unique in undergoing a magnetic cycle. It is a typical main-sequence star, with a diameter half that of an average A-type star and a rotational period forty times as long. Differential rotation gives the sun a period of about 25 days near the equator and 34 days near the poles. The 22-year magnetic cycle, affecting surface activity and the sun's outer atmosphere, reflects the subsurface fluid circulation of material with its associated magnetic fields according to some magnetohydrodynamic process that must be closely connected with axial rotation. A solar model having a torsional oscillation as a basic feature of the magnetic cycle has been suggested both by observation (Richardson and Schwarzschild 1953) and by theory (Walén 1949). In stars possessing convective zones and rotating ten to a hundred times as rapidly as the sun, it is only to be expected that a greatly enhanced magnetohydrodynamic cycle of the same general kind will operate. But an extrapolation to stars having magnetic fields three or four orders of magnitude stronger than the general field of the sun cannot be secure. Therefore, the following considerations, based on the sun, are intended only to show that magnetohydrodynamic oscillations may plausibly account for the observations of the α variables, without implying a close similarity to the solar magnetic cycle.

The sun possesses a poloidal or "general" magnetic field, limited to high latitudes (Babcock and Babcock 1955). This poloidal field has been found to show significant systematic variations in intensity and polarity that are almost certainly related to the progress of the main 22-year magnetic cycle (H. D. Babcock 1959). If the sun could be viewed along the direction of its axis, the contributions to the effective magnetic field in integrated light would be partly from the polar regions and partly from the toroidal fields of the lower latitudes. The transitory activity in the low latitudes is now believed to arise through the action of subsurface toroidal fields encircling the sun, of opposite polarity in the northern and southern solar hemispheres. Portions of these toroidal fields are occasionally brought to the surface, permitting the lines of force to arch into the solar atmosphere and corona; they control the formation of surface magnetic regions, faculae, spots, flares, and prominences.

It has been pointed out by Grotrian and Künzel (1950) and by Kienle (1950) that the integrated light of the low-latitude zone of the sun, in either hemisphere, would yield, in the mean, a symmetrically reversing effective magnetic field. This follows from the facts that div $\boldsymbol{H} = 0$, so that we must expect conservation of magnetic flux in the surface bipolar regions, and that sunspots

(from which the optical contributions to the Zeeman effect are suppressed through darkening) are larger, more frequent, and of longer duration in the "preceding," as contrasted with the "following," parts of bipolar magnetic regions. Hence, in integrated light, the polarity that predominates in the lower latitudes is the polarity characteristic of the "following" parts of these regions, and this polarity is reversed every 11 years.

There occur in the sun systematic migratory motions in latitude of the toroidal fields; the peculiar meridional motions of the individual surface features, such as prominences and spots, are more rapid. Magnetic regions associated with the toroidal activity actually push into high northern and southern heliographic latitudes—even as far as the poles—at certain phases of the solar cycle, as evidenced by the solar magnetograms and by the variation in latitude of the stable prominences (see Fig. 9, adapted from Anathakrishnan 1952) that mark the boundaries of such magnetic regions, especially on the poleward side (Babcock and Babcock 1955).

The integrated effect, as viewed along the axis of the model, would then be a combination of the "polar" and the "toroidal" contributions, each of which varies systematically with the progress of the main magnetic cycle. Each is subject to appreciable short-term fluctuations, and if the obliquity is not precisely zero, there may be intermittent modulation in the period of the axial rotation, owing to the fact that the distribution of magnetic activity in longitude is not uniform. Such effects on an amplified scale in a star having a surface field of a few kilogauss could go far toward accounting for the phenomena observed in the α variables.

To develop this model a little further, two distinct regimes can be identified by the poloidal and the toroidal fields. The highly conductive material associated with the respective regimes is effectively prevented, by its fields, from intermixing. Over long periods of time, the abundance ratio of the elements becomes altered, either through nuclear reactions or through segregation by differential mobility. Different relative abundances may be expected for the two magnetic regimes, because of the difference in the degree and kind of magnetic activity at the stellar surface for the poloidal and toroidal fields. For example, more flare activity may be expected in the toroidal regime. In this way one can see the basis for the grouping of elements that alternate periodically in the spectra of the α variables and for their differential velocity-curves. Extensive transitory clouds of optically thick prominences arising out of the toroidal regime, in an atmosphere in which the magnetic pressure is high, could be effective in producing a variable component of the absorption spectrum, and, if such prominences were sufficiently dense in low latitudes, they could account for the emission wings sometimes observed or suspected on absorption lines in certain magnetic stars, including α^2 CVn. The meridional component of motion, varying with phase, could produce the differential velocities which, when

integrated, lead to displacements of the order of a stellar radius. The randomness of detailed magnetic activity within a magnetic cycle plausibly accounts for the observed deviations in magnetic amplitude and phase and for the fluctuations in velocity. Finally, a resonance in the primary oscillation, depending upon the magnetohydrodynamic properties of the star, is invoked to explain the concentration of the periods of the large-amplitude magnetic variables in the range 4–9 days.

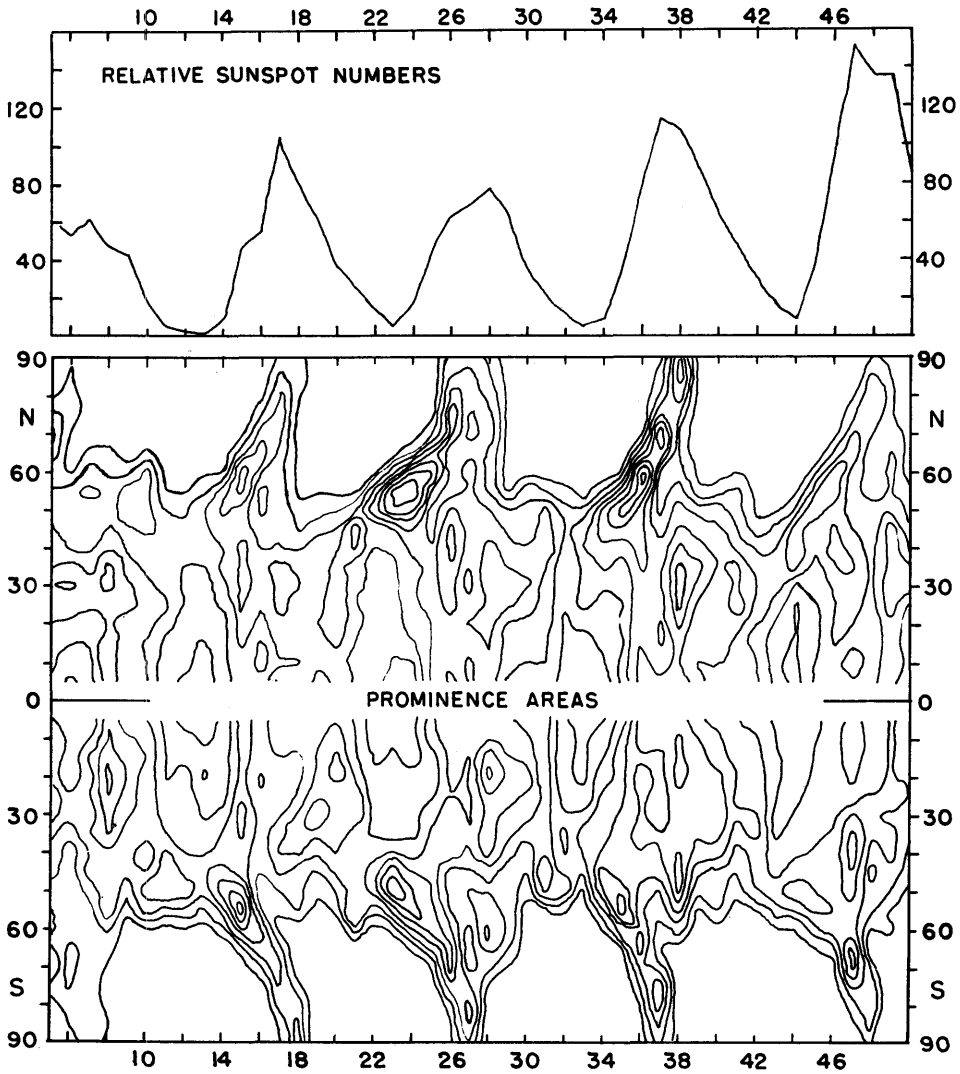


FIG. 9.—Cyclic shifting of magnetic areas on the sun as reflected by prominence areas, plotted as a function of latitude, for the years 1906–1950. (Adapted from Anathakrishnan 1952.)

9.2. The Oblique Rotator

Initially, the oblique rotator model was envisioned in terms of a rigid sphere with a magnetic dipole field inclined to the axis of rotation, which in turn was inclined to the line of sight. Expressions for the harmonic variations of the effective field were given by Stibbs (1950). As this model was inadequate, although promising in some respects, more elaborate *ad hoc* oblique rotator models were developed, principally by Deutsch (1956, 1958).

In proposing the oblique rotator model, one must grant at the outset that differential rotation does not occur as in the sun; otherwise, the asymmetric pattern of magnetic areas would rapidly be destroyed by shearing. Possibly the strong field provides the internal rigidity to eliminate differential rotation, but it is difficult to maintain this view in the light of evidence for the β and γ (irregular) magnetic variables and the irregular (δ) spectrum variables, which must be closely related to the α variables. In any event, complete rigidity cannot be admitted, since some of the α variables show random deviations in amplitude or phase. Thus, on the rotator model, some degree of shifting and activity of the surface areas must be presumed to occur.

The strongest support for the oblique rotator hypothesis comes from the finding by Deutsch (1956) that the periods and line widths of many of the spectrum variables correspond fairly well with the inverse period–line-width relationship. For an A0 star having a radius of 2.3 $R\odot$, the equatorial velocity of rotation, v_e, is about $125/P$ km/sec, where P is the period in days. Accordingly, at a wave length of λ 4300 A, the Doppler broadening by rotation is represented by $w_r = 3.6 (\sin i)/P$ angstroms.

But for the α variables the agreement has not been so good as to be really convincing, as shown when, in Table 3, w is compared with $3.6/P$. Discrepancies occur in the sense that the observed line widths are generally too narrow, yet the α variables are sharp-line stars in which sources of line broadening other than rotation are important. This difficulty is emphasized by comparing the line widths of the α variables with those of such γ variables as HD 215441, HD 133029, 52 Herculis, and 78 Virginis, which also have w in the range 0.1–1.0 A, yet which are, in all probability, nearly pole-on and therefore show little rotational broadening. Further difficulties arise in accounting for the irregular spectrum variables of Table 10.

In an attempt to verify the oblique rotator hypothesis and to map the magnetic fields and abundance anomalies of the stellar atmosphere of HD 125248, Deutsch (1958) elaborated the model by developing the magnetic potential and the local equivalent widths in spherical harmonics. The Laplace coefficients of these expansions were related to the Fourier coefficients of the observed curves. The solution yielded a model with an axial obliquity of 30° and with various skewed, asymmetric distributions of the magnetic field and of the equivalent widths for the three groups of elements typified by europium, chromium, and

iron. The comparison of the prediction of the model with the observations appears reasonably satisfactory with regard to the mean magnetic field, equivalent widths, and velocities. But there is little or no indication that the model is capable of accounting for the crossover effect at the phases when $H_e = 0$ or for the purity of the observed polarity in the Zeeman patterns at the phases of maximum field intensity. Further, the model for HD 125248 does not yield entirely acceptable values for the line widths. The contours of magnetic-field intensity required by the model show values ranging from 8 to 20 kilogauss, with a mean of about 12 kilogauss in the vicinity of the locus of the subsolar point. In a field of 12 kilogauss, the Zeeman broadening for typical lines ($z = 1.4$) amounts to about 0.3 A. If the widening due to rotation ($P = 9.3$ days, $i = 30°$), which by itself yields $w_r = 0.2$ A, is taken into account and if some allowance is made for intrinsic line width, the predicted widths are roughly 0.5 A, which is about twice the observed value.

A further difficulty with the model is that, as Deutsch points out, the distribution of equivalent widths is distinctly asymmetric about the equator, so that all three abundance maxima occur in the unobserved zone of the star. His calculations have shown that if this configuration were observed under an equally probable inclination of 150°, instead of 30°, all three groups of lines would be about four times stronger when averaged over the cycle. The amplitudes of the curves giving H_e and v as functions of phase would be comparable with the values actually observed, but the variation in equivalent width would be less than one-third as great. No magnetic star is known to correspond to these conditions.

It is significant that no periodic magnetic variable (with the single exception of the 226-day variable HD 188041) shows a field that varies harmonically without reversal of magnetic polarity. Indeed, all the typical α variables approach a fair degree of symmetry about the axis ($H = 0$) in their reversals. Yet, supposing for the moment that all the α variables of Table 3 plus the broad-line spectrum variables of Table 11 are oblique rotators, it is to be expected that at least 1 of the 16, with a period of less than 10 days, should have a moderately small axial inclination such that the effective magnetic field would show limited harmonic variations always of the same polarity. This evidence favors the view that when magnetic variables show periodicity, it is the result of some intrinsic physical process resulting necessarily in reversals of polarity and favoring periods of the order of 1 week.

Some other types of evidence, none really conclusive, bear on the problem of the interpretation of the α variables. Two promising approaches for future investigation lie in the analysis of the crossover effect and in the observation of more of the A stars with lines slightly wider than 0.5 A. For reasons already brought out, such stars have been specifically excluded from the observing program for magnetic fields, but additional results on line profiles and their variations would be valuable. It is a weakness of the axisymmetric oscillator

theory that none of the known α variables has lines that are too broad to be accounted for on the oblique rotator model, but it may also be counted a weakness of the oblique rotator theory that only two of the known broad-line spectrum variables (Table 11) have periods as short as that of the mean period of rotation of the A stars.

REFERENCES

ABT, H. A.	1953	*Pub. A.S.P.*, **65**, 274.
ANATHAKRISHNAN, R.	1952	*Nature*, **170**, 156.
BABCOCK, H. D.	1959	*Ap. J.*, **130**, 364.
BABCOCK, H. W.	1947*a*	*Ap. J.*, **105**, 105.
	1947*b*	*Pub. A.S.P.*, **59**, 112.
	1949	*Ap. J.*, **110**, 126.
	1951	*Ibid.*, **114**, 1.
	1956	*Ibid.*, **124**, 489.
	1958	*Ap. J. Suppl.*, Vol. **3**, No. 30.
BABCOCK, H. W., and BABCOCK, H. D.	1955	*Ap. J.*, **121**, 349.
BALDWIN, R. B.	1944	*Pop. Astr.*, **52**, 134.
BLACKETT, P. M. S.	1947	*Nature*, **159**, 658
	1952	*Phil. Trans. R. Soc. London*, A, **245**, 309.
BÖHM, K.-H.	1952	*Zs. f. Ap.*, **30**, 117.
BURBIDGE, E. M., BURBIDGE, G. R., FOWLER, W. A., and HOYLE, F.	1957	*Rev. Mod. Phys.*, **29**, 547.
BURBIDGE, G. R., and BURBIDGE, E. M.	1955*a*	*Ap. J. Suppl.*, Vol. **1**, No. 11.
	1955*b*	*Ap. J.*, **122**, 396.
CHANDRASEKHAR, S., and MÜNCH, G.	1950	*Ap. J.*, **111**, 142.
DEUTSCH, A. J.	1947	*Ap. J.*, **105**, 283.
	1956	*Pub. A.S.P.*, **68**, 92.
	1957	*Yearbook, Carnegie Inst. Washington*, **56**, 49.
	1958	*Symposium Vol.*, No. 6, *Internat. Astr. Union*, p. 209.
EGGEN, O. J.	1957	*A.J.*, **62**, 45.
ELSASSER. W. M.	1956	*Rev. Mod. Phys.*, **28**, 135.
GROTRIAN, W., and KÜNZEL, H.,	1950	*Zs. f. Ap.*, **28**, 28.
HUANG, S. S.	1953	*Ap. J.*, **118**, 285.
JARZEBOWSKI, T.	1960	*Acta Astronomica* (in press).
JASCHEK, C., and JASCHEK, M.	1958	*Zs. f. Ap.*, **45**, 35.
KIENLE, H.	1950	*Naturwiss.*, **37**, 137.
LÜST, R., and SCHLÜTER, A.	1956	*Zs. f. Ap.*, **38**, 190.

MESTEL, L.	1956	*M.N.*, **116**, 324.
MINNAERT, M.	1937	*Observatory*, **60**, 292.
MORGAN, W. W.	1935	*Pub. Yerkes Obs.*, Vol. **7**, Part 3.
PARKER, E.	1955	*Ap. J.*, **122**, 293.
PROVIN, S.	1953	*Ap. J.*, **118**, 489.
RICHARDSON, R. S., and SCHWARZSCHILD, M.	1953	*Convegno Volta, Accademia Nazionale dei Lincei*, **11**, 228.
ROMAN, N. G., MORGAN, W. W., and EGGEN, O. J.	1948	*Ap. J.*, **107**, 107.
SCHWARZSCHILD, M.	1950	*Ap. J.*, **112**, 222.
SLETTEBAK, A.	1954	*Ap. J.*, **119**, 146.
STIBBS, D. W. N.	1950	*M.N.*, **110**, 395.
STRUVE, O., and HUANG, S. S.	1952	*Ap. J.*, **116**, 410.
TRUMPLER, R.	1930	*Lick Obs. Bull.*, **14**, 157.
WALÉN, C.	1949	*On the Vibratory Rotation of the Sun* (Stockholm: Henrik Lindstahl's Bokhandel).
WESTGATE, C.	1934	*Ap. J.*, **79**, 357.

CHAPTER 8

Stellar Rotation and Atmospheric Turbulence

SU-SHU HUANG* AND OTTO STRUVE†
Berkeley Astronomical Department, University of California

§ 1. INTRODUCTION

THE absorption and emission lines in stellar spectra are broadened by several different mechanisms. Table 1 (Struve 1931*b*) lists most of them. In addition to these "stellar" mechanisms, other effects of broadening are caused by instrumental imperfections (e.g., Unsöld 1955) and the length of the photographic exposure (Huang and Struve 1955*b*). Both the latter types of broadening behave

TABLE 1

THE BROADENING MECHANISMS OF STELLAR SPECTRAL LINES

Physical Causes	Geometrical Causes	Physical Causes	Geometrical Causes
Stark effect	Convection	Collisional damping	Rotation
Zeeman effect	Contraction	Thermal motion	Surface wave, etc.
Compton effect	Expansion		
Radiation damping	Pulsation	Microturbulence, etc.	.....

like that caused by a geometrical mechanism (§ 5). The task of disentangling from the observed profiles of the lines those mechanisms that are particularly relevant is often a difficult one. Detailed discussions of various broadening mechanisms may be found in such standard texts as those of Aller (1953) and Unsöld (1955). However, the Stark effect is important only in the hydrogen and helium lines, the Zeeman effect has thus far been found in only a relatively small number of magnetic stars (chap. 7), and the Compton effect is negligibly small

* Now at Astrophysics Branch, Goddard Space Flight Center, National Aeronautics and Space Administration, Washington 25, D.C.

† Now at National Radio Astronomy Observatory, Green Bank, W.Va.

except in a few peculiar stars (Münch 1950; Struve 1957). The effect of damping can be easily discerned by its characteristic behavior in the wings of the lines. Therefore, various types of Doppler motion remain as the main mechanism of line broadening in stellar spectra. That the motions of the absorbing medium are often responsible for the line broadening can be inferred from the fact that the broadening is proportional to the wave length of the spectral line. In our discussion we shall, therefore, assume that only Doppler motions (including all items in Table 1 listed as geometrical causes, but only thermal and microturbulent motions under physical causes) are responsible for broadening. Discussions on other aspects of broadening mechanisms appear elsewhere in this volume.

§ 2. ROTATION OF STARS

2.1. Evidence of Stellar Rotation

Although the idea that the axial rotation of stars can be determined from the widths of their spectral lines had been suggested by Abney (1877), it was actually not observed until thirty years later, when Schlesinger (1909, 1913) found a small distortion of the radial velocity-curve during the ingress to and egress from eclipse of the principal components of δ Librae and of λ Tauri. He correctly interpreted this distortion as a consequence of axial rotation. Later Adams and Joy (1919) estimated the equatorial rotational velocity of W Ursae Majoris from the widths of the absorption lines of the two component stars. A direct determination of the rotational velocities of μ^1 Scorpii and V Puppis from the line widths was then made by Miss Maury (1920). Immediately afterward, Hellerich (1922) measured the line widths of a number of stars. The use of high-dispersion spectrographs in stellar astronomy clearly revealed diffuse lines in many early-type stars. The subscript "n" was introduced in the spectral classification to denote broad-lined stars (Adams and Joy 1922). However, convincing evidence of the rotation of stars was first given by the systematic studies of the radial velocities during eclipse of β Lyrae by Rossiter (1924) and of β Persei by McLaughlin (1924). Their investigations showed a gradual increase in the distortion of the velocity-curve at the beginning of the eclipse and the reverse phenomenon at the end, which is in full agreement with the prediction based upon the geometrical circumstances of the eclipse of a rotating component. Later investigations have shown that the rotational distortion of the velocity-curve is a common phenomenon in eclipsing binaries; it is sometimes known as the "Rossiter effect." The sense of the rotation of a component star is invariably the same as that of the orbital motion (Struve 1950).

The hypothesis that the diffuseness of the spectral lines in many early-type stars is due to rotation is further supported by the study of (1) the synchronization of rotation and orbital motion in many close binaries and (2) the analysis of line profiles. Shajn and Struve (1929) found that broad lines are always associated with binary stars of short period. Later studies by Swings (1936) and Mathèwe (1937) confirmed this result. Since it is reasonable, on dynamical

grounds, to expect synchronization of rotation and orbital revolution in close binaries, the component stars in such binaries must be rotating rapidly. Therefore, we are safe in attributing the great widths of the spectral lines in close binaries to rotational broadening. The diffuse lines observed in many single stars resemble in all respects those in close binaries, and we can conclude that they are also produced by rotation.

The most significant results on stellar rotation are derived from a study of the profiles of stellar absorption lines. Such a study was initiated by Shajn and Struve (1929) and carried out at the Yerkes Observatory (Elvey 1929, 1930; Struve 1930). An interesting early investigation was concerned with the change in profile of a line in the spectrum of β Persei (Algol) during eclipse (Struve and Elvey 1931). Together with McLaughlin's discussion of the radial-velocity distortion during eclipse, this study proved beyond any doubt that the principal component of Algol does indeed rotate with an equatorial velocity of about 60 km/sec. For a more detailed discussion on the rotation of close binary stars, we refer the reader to other compilations (Struve 1950; Struve and Huang 1958; also § 3.3).

2.2. Methods of Measuring the Rotation of a Star

A theoretical study of the rotational profiles of a line was made by Shapley and Nicholson (1919) and more extensively by Carroll (1928, 1933). The latter not only derived the integral equation governing the rotational broadening but also suggested several methods for determining the rotational velocity of a star from the profiles of its spectral lines. His methods have been applied to several actual cases by Carroll and Ingram (1933) and by Colacevich (1937, 1939, 1942). We shall later discuss one of these methods. The most intuitive derivation of a rotationally broadened profile is by means of the geometrical considerations used by Shajn and Struve (1929), and this method has been adopted by most of the later investigators.

In the study of stellar rotation we frequently use, as the unit of wave length, the rotational width, $\Delta\lambda_R$, defined as

$$\Delta\lambda_R = \lambda \frac{V_R \sin i}{c}, \tag{2.1}$$

where V_R represents the equatorial rotational velocity of the star, i is the inclination of its equator to the celestial plane, and c is the velocity of light. Our aim is to determine $V_R \sin i$ (or, equivalently, $\Delta\lambda_R$) from the observed profile of a line. Since we cannot separate V_R and $\sin i$, it is convenient to call $V_R \sin i$ the "observed rotational velocity of a star."

If we express the wave length in units of $\Delta\lambda_R$, we find that the relation between the line profile in depth (fractional absorption), $R(x)$, observed in integrated light, and $R'(x - y)$, which would be seen in each individual element on the stellar disk, is given by

$$R(x) = \int_{-1}^{1} R'(x - y)\, B(y)\, dy, \tag{2.2}$$

where y in $R'(x-y)$ denotes the over-all shift of the line as the result of rotation and therefore varies from element to element, while the function R' itself is assumed to be the same for all surface elements on the stellar disk (§ 5.3). The rotational broadening function, $B(y)$, is given by (Unsöld 1955)

$$B(y) = \frac{3}{3+2\beta}\left[\frac{2}{\pi}(1-y^2)^{1/2} + \frac{\beta}{2}(1-y^2)\right], \tag{2.3}$$

where β denotes the coefficient of limb darkening of the continuous radiation over the stellar disk (chaps. 1, 2). Since the maximum shift in wave length due to rotation is $\Delta\lambda_R$ at the equator, we have $|y| \leq 1$.

The rotational broadening function, $B(y)$, can be visualized as the line profile that would be observed in a rotating star if the line profile produced by each element on the disk of the star is extremely narrow. Therefore, when the rotational broadening is large compared with the natural width of $R'(\lambda)$, the spreading-out of the resulting profile has a spectroheliographic effect, i.e., it distinguishes between differences of surface brightness of different strips on the apparent disk of the star having different projected velocities of rotation (Struve 1948*c*). Accordingly, if the distribution of light over the stellar disk is not uniform, the profile will show an asymmetry (McCarthy 1935; Struve 1937). For the same reason, Öhman (1946) suggested the possibility of tracing polarization effects in the rotational profiles of early-type stars.

Since $B(y)$ is a normalized function, i.e.,

$$\int_{-1}^{1} B(y)\, dy = 1, \tag{2.4}$$

the equivalent width of the resultant profile, $R(x)$, is equal to that of the profile $R'(x-y)$, which would be observed in any individual element on the disk. In § 5.3 we shall see that rotational broadening is only a special case of geometrical Doppler broadening. A more detailed discussion of the derivation of and the approximation used in equation (2.2) will be given there.

In equation (2.2) we encounter one unknown function, $R'(\lambda/\Delta\lambda_R)$, and one unknown parameter, $\Delta\lambda_R$. In general, the latter is much greater than the width of the original profile $R'(\lambda/\Delta\lambda_R)$. Therefore, the exact form of R' does not seriously affect the observed profile R, which suggests that we may approximate $R'(\lambda/\Delta\lambda_R)$ by the profile of a particular line observed in a sharp-line star that is of the same spectral class and luminosity type as the rotating star we are considering. We then determine the remaining parameter, $\Delta\lambda_R$, in equation (2.2) from the observed profile $R(x)$ of that particular line. Since rotation occurs, with a few exceptions, only in early-type stars, the lines Mg II 4481 A and He I 4471 A are frequently chosen. In practice, we assume a series of values for $V_R \sin i$, compute from equations (2.2) and (2.3) the broadened profiles, and plot them in angstrom units on transparent paper. By comparing directly the observed profile with the series of computed profiles, we can determine

$V_R \sin i$ by simple interpolation. This method has been used successfully by many investigators.

Instead of deriving $R'(\lambda/\Delta\lambda_R)$ from some non-rotating star, we can assume that it is represented by a Gaussian function which is defined by only one adjustable parameter (say, the dispersion of the profile) when the equivalent width is given (Ogrodnikoff 1933; Krat 1935, 1938, 1940). Huang and Struve (1953) have recently developed a graphical method that permits both the dispersion of the original profile R' and the rotational width $\Delta\lambda_R$ to be determined simultaneously. This method has been applied to the profiles of lines observed in ρ Leonis. The result of this investigation will be discussed in § 5.4.

A simpler way of determining the rotational velocity of a star is the direct measurement of the line width in the spectrogram. This method has the advantage of greater efficiency, in that it takes only a few minutes to determine the rotational velocity of a star with a fair degree of accuracy. The difficulty with this method is that, even when using the same instrument and the same dispersion, the line width measured directly on the spectrograms taken of a star varies with the photographic density of the plates. However, because of the behavior of the broadening function (eq. [2.3]), this difficulty is not so serious as it appears to be (Huang 1953). Consequently, we can derive the observed rotational velocity directly from the measured width with the aid of a calibration-curve. This method has been used extensively for the study of a great number of stars.

A theoretically ideal method should, of course, determine from equations (2.2) and (2.3) both $\Delta\lambda_R$ and $R'(\lambda)$. Such a method has been proposed by Carroll (1933), making use of the well-known theorem of inversion of the integral equation (2.2) by a Fourier transform (Levi-Civita 1895; Schwarzschild 1910). The scale factor $\Delta\lambda_R$ is determined by the zeros of the Fourier transform of the observed profile. Mathematically, this is the most elegant method for determining the rotation of a star. It has been applied by Carroll and Ingram (1933) to the line profile observed in β Persei (Struve and Elvey 1931) with seemingly satisfactory results. However, Krat (1935, 1938, 1940) has pointed out that, because of observational errors, which are usually large with the present photographic techniques, the Fourier transform of the observed profile may not have any zeros. Moreover, when zeros do exist, they may not be identical with those which correspond to the profile $R(x)$. Indeed, Krat could not find any zero in the Fourier transform of the observed profile obtained on a spectrogram of α Aquilae. A further discussion of the difficulty involved in the inversion of the integral equation (2.2) can be found in a recent paper by Huang (1955).

We have thus far neglected several factors that may influence the observed profile. First of all, the rotational broadening function given by equation (2.3) does not include the effect of gravity darkening (§ 2.5). Also a star may rotate differentially (Slettebak 1949). Even if the rotational periods of a star at its equator and near its poles are in the same ratio as for the sun (Abetti 1955), the

deviation of the broadening function from equation (2.3) is quite appreciable (Huang, unpublished). Finally, the observed rotational profiles are further complicated by the presence of turbulence in stellar atmospheres (§ 5), by the variation of ionization with latitude (Swings and Chandrasekhar 1936), etc.

2.3. Stellar Rotation along the Spectral Sequence

As soon as the study of stellar rotation became a subject of serious research, it was recognized that rapid rotation of single stars occurs almost only in spectral types O, B, A, and early F, although it is quite common to find rapidly rotating stars of later types in close binary systems (Shajn and Struve 1929; Elvey 1930; Struve 1930; Struve and Elvey 1931; Shajn 1933). The Be stars rotate most rapidly, and rotational velocities of 500–600 km/sec have been observed (Slettebak 1949). The highest rotational velocity observed in the B and A stars is probably of the order of 400–500 km/sec. The highest rotational velocity of the F stars is around 200–300 km/sec. It was believed that stars later than F5 did not show appreciable rotation. Only recently Merrill (1948) discovered a star of type G whose absorption lines give $V_R \sin i = 75$ km/sec if their broadening is due to axial rotation. Later, a number of giant stars of late F and early G types were found to have appreciable rotations, with a maximum rotational velocity of the order of 100 km/sec (§ 3.2) (Greenstein 1953; Herbig and Spalding 1955; Slettebak 1955; Struve and Franklin 1955). As a rule, the rotations of supergiant stars are small (§ 5.4).

Table 2 summarizes the investigations of stellar rotations. Those containing fewer than ten stars are not included. The first and second columns indicate the spectral range and the number of stars studied; the third and fourth give the dispersion of the spectrogram and the spectral lines that were used. Under the heading "Method" we denote by *a* microphotometric measurements, by *b* direct measurements on the spectrograms, and by *c* visual estimates. An asterisk following the spectral range in the first column indicates that the spectral classification of the stars is based on the MK or the MKK systems (Keenan and Morgan 1951).

Because of differences in the calibration of the rotational velocities, as well as in the manner of sampling, it is difficult to combine all the results into a single statistical study. From the histograms obtained by the various investigators we have shown in Figure 1 four smoothed distribution functions $\phi(V_R \sin i)$ for the Be and main-sequence stars of spectral types B, A, and early F. The smoothed curves are shown merely to indicate the general trend of the change in the distribution with spectral type. Because of observational indeterminateness, even the general behavior of these functions is uncertain near zero rotational velocity.

If we plot the average value of $V_R \sin i$ against spectral type, we obtain the well-known result that the rotation of main-sequence stars drops quite sud-

denly at about F5. Generally the giant stars of early types (B and A) rotate more slowly than the dwarf stars of the same types (Slettebak 1954), while for the later types (F and G) the average rotational velocity of the giants is greater than that of the dwarf stars. The latter fact was pointed out independently in 1953 by Slettebak (1955) and by Herbig and Spalding (1955). For the peculiar A and the metallic-line stars, Slettebak (1954) found rotational velocities on the average smaller than for others of the same spectral type.

TABLE 2

SYSTEMATIC INVESTIGATIONS OF ROTATION OF STARS

Sp. Range	No. of Stars	Dispersion	Lines Used	Method	Reference
O–A.....	46 (O–B), 37 (A), (all sp. binaries)	10 A/mm at λ4500	He I 4471 Mg II 4481	*a*	Shajn and Struve (1929)
O–B.....	28	10 A/mm at λ4500	He lines	*a*	Elvey (1929)
O–F.....	59	10 A/mm λ4500	Mg II 4481	*a*	Elvey (1930)
F–K.....	31	10 A/mm at λ4500	.....	*c*	Struve and Elvey (1931)
Be.....	59	.....	.....	*c*	Struve (1931*a*)
B.....	275	30 A/mm at λ4500	He I 4471, Mg II 4481	*b*	Westgate (1933)
A.....	413	30 A/mm at λ4500	Mg II 4481	*b*	Westgate (1933)
F.....	112	30 A/mm at λ4500	Sr II 4215	*b*	Westgate (1934)
B–K.....	71 (in Pleiades)	55 A/mm at Hγ	.....	*c*	Smith and Struve (1944)
B–G.....	75 (in Pleiades)	30–51 A/mm at Hγ	Mg II 4481	*a*	van Dien (1948)
O–B*.....	21(O), 52(B), 50(Be)	40 A/mm at λ4026	He I 4026	*a*	Slettebak (1949)
A.....	12 (spectrum variables)	10 A/mm	Mg II 4481	*a*	Deutsch (1952*b*)
O–G.....	620(O–B), 598(A), 313(F), 10(G)	10–26 A/mm at λ4475	He I 4471, Mg II 4481, and other lines	*b*	Huang (1953)
B–A*.....	179	32 A/mm at λ4481	Mg II 4481	*a*	Slettebak (1954)
A–G*.....	34 (mainly giants)	3–20 A/mm	Fe I 4476.0, Fe II and Ti II 4549.6	*a*	Oke and Greenstein (1954)
F–K*.....	656	11 A/mm	Fe I 4472, Fe I 4476	*a*	Herbig and Spalding (1955)
A–G*.....	215	32 A/mm at λ4481	Mg II 4481, Fe I 4072	*a*	Slettebak (1955)
B*.....	185	32 A/mm at λ4471	He I 4471	*a*	Slettebak and Howard (1955)
A–K*.....	51 (visual binaries)	3–10 A/mm	Several lines	*c*	Struve and Franklin (1955)
O–B*.....	153	10–28 A/mm	Several lines	*a* and *c*	Slettebak (1956)

When we have obtained the distribution function of the observed rotational velocities, i.e., $\phi(V_R \sin i)$, a question arises as to what is the distribution function of the true equatorial velocities, say, $f(V_R)$. This question is related to another, namely, that of the orientations of the axes of the stars. A clue to the latter question is provided by the Be stars, which are usually regarded as in a state of rotational instability (Struve 1931*a;* also § 2.5); hence they represent a sample of rapidly rotating stars. Slettebak's (1949) study of the distribution of their rotation velocities (Fig. 1) indicates that their axes are oriented at random in space; another supporting fact is discussed in § 3.3.

If we assume a random orientation of the axes in space, the distribution

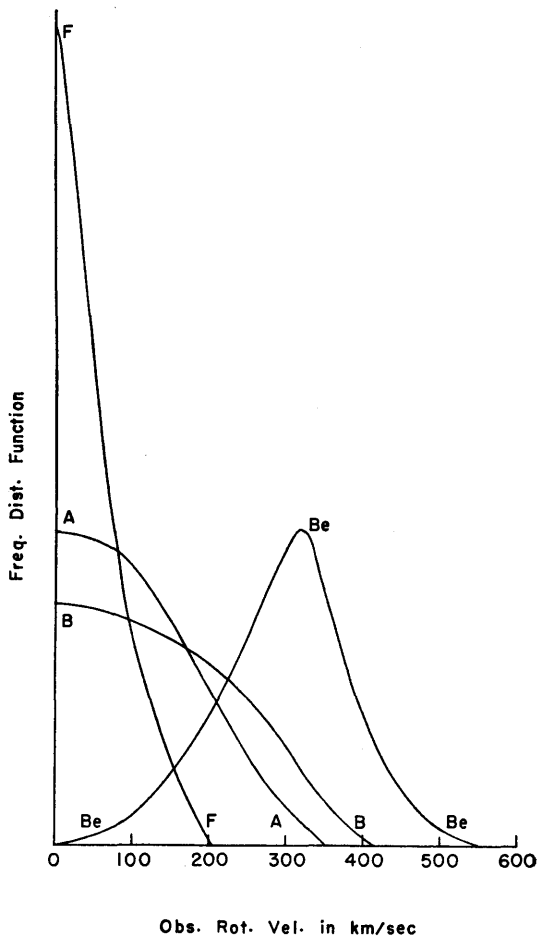


FIG. 1.—The frequency distributions of observed rotational velocities ($V_R \sin i$). The four curves represent, respectively, the normalized distribution functions for the Be stars, and the main-sequence B, A, and early F (F0–F5) stars.

function $\phi(y)$ of $y = V_R \sin i$ is related to that of $f(x)$ (with $x = V_R$) by the following integral equation (Kuiper 1935):

$$\phi(y) = y\int_y^\infty \frac{f(x)\,dx}{x(x^2 - y^2)^{1/2}}, \tag{2.5}$$

which can be easily transformed into Abel's integral equation, for which the formal solution is well known. From equation (2.5) it can be shown (Chandrasekhar and Münch 1950) that a simple relation exists between the nth moment of $\phi(y)$ and that of $f(x)$. For $n = 1$ and 2, we have

$$\langle V_R \rangle = \frac{4}{\pi}\langle V_R \sin i \rangle, \qquad \langle V_R^2 \rangle = \tfrac{3}{2}\langle (V_R \sin i)^2 \rangle. \tag{2.6}$$

Therefore, from the mean value of the observed rotational velocity, $V_R \sin i$, of a large group of stars we can directly compute the mean value of the rotational velocity, V_R. The formal solution requires differentiation—a process that cannot be performed reliably in the present case because of the uncertainty in the empirically determined function $\phi(y)$—and it therefore has little practical value. Instead, we assume a certain form for $f(x)$ and determine the adjustable parameters in $f(x)$ to fit the observed function $\phi(y)$ (van Dien 1948; Brown 1950; Chandrasekhar and Münch 1950; Böhm 1952). Since the distribution function $\phi(V_R \sin i)$ itself is somewhat uncertain, $f(V_R)$ thus derived is uncertain to at least the same extent.

From a purely theoretical point of view we might have expected that the rotations, like the space motions, would be given by an ellipsoidal distribution (Huang 1953). As an approximation we may expect a Maxwellian distribution. In reality, except for the Pleiades (van Dien 1948), this prediction does not agree with the observations. This fact may prove to be an important clue to an understanding of stellar rotation in general.

2.4. Other Statistical Results concerning Stellar Rotation

Struve (1945) concluded from the results obtained by Westgate (1933, 1934) that no correlation existed between the observed rotational velocity of a star and its location in the galactic co-ordinate system. This conclusion was confirmed by later investigations (Slettebak 1949; Huang and Struve 1954). It suggests that the rotational axes of the stars are not predominantly perpendicular to the galactic plane. The implication of this result is far-reaching; it rules out, in the study of star formation, any condensation theory which requires the conservation of the local angular momentum associated with the systematic galactic rotation of the prestellar medium (Edgeworth 1946). If the rotating axes are not parallel to the axis of galactic rotation, it is highly probable, though not certain, that the axes are oriented in space at random. The evidence in this case is indirect and consequently weak because it relies not only upon the observational data but also upon arguments concerning different mechanisms for the origin of the angular momenta of rotating stars (§ 3.3).

Another interesting result by Struve (1945) is the large fluctuations of the average rotational velocities of stars in different regions in the sky. There seems to be some tendency toward the clustering of rapidly rotating stars in one region and of slowly rotating stars in another region. Thus rapidly rotating stars are more frequent in the Pleiades than in the Hyades or in the Galaxy at large. In the Pleiades the fastest rotations seem to occur near the center of the cluster (Smith and Struve 1944). Recently Roberts (1957) found in a study of galactic clusters that there is a general tendency for the more massive members to be concentrated near the center of the cluster. The two results seem to indicate that more massive stars rotate faster—a result consistent with other evidence (Fig. 1).

Thus far, the rotations of stars have been fairly well investigated in only three clusters: the Pleiades (Smith and Struve 1944; Struve 1945; van Dien 1948), the Hyades (Struve 1945), and the Scorpio-Centaurus cluster (Huang and Struve 1954). It appears that the distribution of the observed rotational velocities in the latter does not deviate appreciably from that derived from B stars in general (Fig. 1). On the other hand, the distribution in the Pleiades derived by van Dien shows an unmistakable maximum at about 75 km/sec.

One of the many problems of stellar rotation which have cosmogonical significance concerns the relation between the rotations and the relative space motions of the stars in a cluster or in an association. A study by Huang and Struve (1954) of the Scorpio-Centaurus cluster seems to show some correlation between these two kinds of motion. The implication of such a correlation is discussed in § 3.3.

2.5. Effects of Rotation on the Stars

Three effects upon the surface conditions of a star attract our attention—change in the shape of the star, formation of a rotating gaseous ring as a result of rotational instability at the equator, and change in surface brightness as a consequence of the change in effective gravity. Before discussing these effects, we define a dimensionless parameter,

$$\phi = \frac{\omega^2}{2\pi G\langle \rho \rangle}, \tag{2.7}$$

where ω is the angular velocity, which is assumed to be uniform throughout the star, $\langle \rho \rangle$ is its mean density, and G is the gravitational constant. For a spherical star, ϕ is two-thirds the ratio of centrifugal force to gravity at the equator and therefore provides a measure of the effect of rotation upon the star itself.

The equilibrium configuration of a rotating star is a problem that has not yet been satisfactorily solved. Only two limiting cases have been explored: one under the assumption of incompressibility and homogeneity (liquid masses) and the other under the assumption of an infinite central concentration (Roche model). The problem of rotating liquid masses under self-gravitation has been extensively investigated by several mathematicians since the early nineteenth

century. References to these studies can be found in a recent review by Lyttleton (1953), and an excellent account of the essential results has been given by Jeans (1928). It is under the assumption of liquid masses that Jeans proposed his theory of fission of rotating stars as a mechanism for the formation of binary stars. However, Eddington's (1926) pioneering study of stellar structure clearly showed that the assumption of liquid stars is untenable. On the other hand, the Roche model of infinite central condensation may represent a fair approximation to the outer layers of a rotating star. Mathematically, the Roche model is much simpler because the whole mass, M, is centered at a point, and, therefore, the gravitational potential at any point r from the central mass is GM/r. If we choose a co-ordinate system centered in the mass point and such that the z-axis is in the direction of the axis of rotation, we define a scalar field,

$$\Omega \equiv \frac{GM}{r} + \tfrac{1}{2}\omega^2 (x^2 + y^2) , \tag{2.8}$$

which may be regarded as an effective potential field in the rotating star. It can be shown (Jeans 1928) that the boundary surface of a star rotating freely in space is given by one of the equipotential surfaces defined by

$$\Omega = \text{Constant} = k . \tag{2.9}$$

These surfaces, being axially symmetric as can be seen from equation (2.8), can be divided into two classes: (1) closed around the central mass and (2) open and far away from it. The two classes are separated by the critical potential surface (closed) which passes through all points in the equatorial plane at which the centrifugal and gravitational forces balance each other. We shall denote this critical surface by Ω_c and the corresponding constant in equation (2.9) by k_c and introduce a new variable,

$$\varpi = (x^2 + y^2)^{1/2} ,$$

which is obviously the distance of any point from the rotating z-axis. When the centrifugal force balances the gravity in the equatorial plane, we have

$$\frac{GM}{\varpi_0^2} = \omega^2 \varpi_0 , \tag{2.10}$$

where ϖ_0 denotes the equilibrium points and is known for given M and ω. Setting $x^2 + y^2 = \varpi_0^2$ and $z = 0$ in equation (2.8), we obtain, with the aid of equation (2.10),

$$k_c = \tfrac{3}{2} (GM\omega)^{2/3} = \tfrac{3}{2} (\omega \varpi_0)^2 . \tag{2.11}$$

Therefore

$$\Omega = k_c , \tag{2.12}$$

or, explicitly,

$$\frac{1}{r} + \frac{1}{2}\frac{\varpi^2}{\varpi_0^3} = \frac{3}{2}\frac{1}{\varpi_0} , \tag{2.13}$$

defines the critical potential surface (Jeans 1928).

Any closed equipotential surface given by equation (2.9) can be the boundary of a stable rotating star. For given M and ω the critical equipotential surface, Ω_c, gives the largest dimension that a rotationally stable star can assume. In this limiting case we have (Jeans 1928)

$$\phi = \frac{\omega^2}{2\pi G\langle \rho \rangle} = 0.36075 = \phi_c, \tag{2.14}$$

where ϕ_c is the highest value of ϕ that a rotationally stable star can have. In other words, for a given value of $\langle \rho \rangle$ there exists a critical value of the angular velocity ω_c beyond which the star will become unstable at its surface. The critical value ω_c can be derived from either equation (2.10) or equation (2.14). They give the same result only when the star follows exactly the Roche model.

Now consider a numerical example (Slettebak 1949). A normal B3 star of mass $8.0\odot$ and a mean radius of $4R_\odot$ has a mean density of 0.18 gm/cm^3. The critical angular velocity ω_c is 1.65×10^{-4} rad/sec from equation (2.14). From equation (2.10) we derive $\varpi_0 = 4.88\,R_\odot$, giving an equatorial rotational velocity of 560 km/sec, which is close to the largest rotational velocity of 500–600 km/sec actually observed in Be stars.

When $\omega > \omega_c$, the centrifugal force overcomes the gravitational attraction, and ejection of matter at the equator occurs. In fact, prominence activity (§ 5.4) will help to produce surface ejection long before the critical value ω_c is reached. Since the ejected matter possesses high angular momentum, it will form a gaseous ring in the equatorial plane and revolve around the star, which is actually the case in a Be star, according to Struve (1931*a*).

The emission lines in Be stars appear either as single bright lines, centrally superposed over normal absorption lines, or as double bright lines, symmetrically placed on both sides of the normal wave length. The widths of the single lines, as well as the distances between the components of the double lines, are not the same for all stars. For example, the widths of Hβ range from about 1 to more than 10 A. No emission lines are known in B stars that are as narrow as the bright lines in the spectra of diffuse gaseous nebulae. The widths of the emission lines show a pronounced proportionality to wave length, suggesting Doppler effect (Curtiss 1923). Also a definite correlation exists between the broadening of the absorption lines and the widths, or separations, of the emission lines. Moreover, the emission lines frequently change in intensity, and two distinct types of this variation are discerned: in some stars the total amount of energy in the emission lines changes and sometimes vanishes completely (Pleione and κ Draconis); in others the relative intensities of the two bright components vary periodically (π Aquarii), the total energy remaining approximately constant. The periods are usually long, often several years (Struve 1931*a*). In many cases the periods have not yet been established, and it is likely that these phenomena are not strictly periodic but that there exists for each star a characteristic *mean* interval between identical appearances of the emis-

sion lines. These phenomena can be understood if we assume a gaseous envelope or a ring around the Be star. The emission lines come from the gaseous ring that is revolving around the star in its equatorial plane. When the rotating axis makes a small angle with the line of sight, both its absorption and its emission lines will be relatively narrow. When the rotating axis is nearly perpendicular to the line of sight, the observed rotational velocity will be large. At the same time, even if the distribution of mass in the ring is uniform everywhere, the emission line will become double as a result of geometrical projection (Struve 1931*a*). Collisions among the gaseous particles will bring the ring eventually to a circular form. Actually, variation in the intensities of the emission lines indicates that the gaseous ring associated with a Be star is not stable. It loses its mass continuously to outer space. On the other hand, it is replenished by matter ejected from the stellar surface. The ejection, like prominence action observed on the solar surface but on a much larger scale, is probably intermittent. This explains the formation and disappearance of the gaseous ring at irregular intervals.

The effect of rotation on the surface luminosity has been investigated by Milne (1923) and von Zeipel (1924). The latter has shown that the brightness, H, of a surface element of a rotating star is directly proportional to the effective gravity, g, i.e.,

$$H \propto g \,, \tag{2.15}$$

which is sometimes inappropriately known as the "law of gravity darkening" (§ 2.2). We refer the reader to Eddington's (1926) treatise for the derivation of this relation. Since the surface brightness is proportional to the fourth power of the effective temperature, T, we have, from equation (2.15),

$$T \propto g^{1/4} \,. \tag{2.16}$$

For a rapidly rotating star the effective gravity increases greatly from the equator to the poles because of the variation in centrifugal force with latitude, and corresponding variation will occur in surface brightness. Based on equation (2.16), Slettebak (1949) has given some numerical examples of the effective temperatures T of a star of 8.0⊙ and 4.0 $R_\odot$ at different latitudes for several values of the equatorial rotational velocity. Table 3, adapted from Slettebak's results, gives a general idea of the differences in temperature over the surface of a rotating star. In the table ω_c is the critical angular velocity derived from equation (2.14). We infer from the table that the difference in temperature between the poles and the equator is quite appreciable and might be observable in extreme cases. Struve (1945) has called attention to the possibility that Maia (20 Tauri) may be such a case. It is the only star of type B in the Pleiades that has fairly sharp lines, which, moreover, show some composite nature, indicating a wide range of temperature. Huang and Struve (1956) found that the ionization temperature from the helium lines is 13,500°–14,500° K, while that from the iron lines is about 10,000° K. It is quite possible that this star is in rapid

rotation but is seen pole-on. The metallic and the helium lines come from the equatorial area and the polar region, respectively. This interpretation would also explain the general weakness of both the metallic and the helium lines.

Maia is, of course, not the only example of a pole-on star. If we assume random distribution of the axes of rotation, we might expect that a few rapidly rotating stars, including the Be stars, would be seen pole-on. However, no Be star has been found to have very sharp lines like those of γ Pegasi. This may be due to the small probability of finding a star whose inclination $i < 1°$. On the other hand, it is also possible that rotational instability on the surface of a star creates turbulent motions in its reversing layer, as well as in its shell. In the latter case turbulent motion would broaden the spectral lines of pole-on stars (§ 5.1).

TABLE 3

VARIATION IN EFFECTIVE TEMPERATURE ON SURFACE OF A ROTATING STAR

LATITUDE	ANG. VEL.....	T(° K)				
		ω_c	$7\omega_c/8$	$3\omega_c/4$	$\omega_c/2$	$\omega_c/4$
	EQ. ROT. VEL. IN KM/SEC.....	560	432	362	234	115
1°.....		8190	16,390	17,320	18,370	18,670
10°.....		14,470	16,770	17,520	18,370	18,800
30°.....		19,080	18,605	18,570	18,580	18,800
80°.....		23,750	22,020	20,970	19,600	19,010
90°.....		23,850	22,110	21,070	19,690	19,010

Rotation also affects the structure of a star, in that it induces circulating currents (Eddington 1929) which tend to mix the chemical composition in the stellar interior, causing the star to evolve along a different path from that of a star without mixing (e.g., Strömgren 1952). The time scale of mixing in a rotating star, which proves to be very long, has recently been discussed by Sweet (1950*b*) and Opik (1951). A discussion of their results will be found in studies of the structure of stellar interiors.

An interesting problem concerns the magnetic fields of massive rotating bodies. Blackett (1947) and Babcock (1947) renewed the old hypothesis of a direct proportionality between the magnetic moment and the angular momentum of a massive body. We do not definitely know the orientation of the rotating axis of any star other than the sun. Consequently, we have only statistical information regarding the angular momenta of the stars. An observational verification of this relation would require a large sample of stars. Moreover, Babcock's (1953) recent determination of the general magnetic field on the solar surface by means of his magnetograph does not strengthen our belief in such a general law of nature. Therefore, we may disregard this relation for the present; if it should later be verified, its impact would be far-reaching.

A more realistic connection between the magnetic field and the rotation of

a star can be found in the case of the spectrum variables. Babcock (1949) advanced the hypothesis that the period of magnetic and spectral variations of a spectrum variable is merely the period of its rotation, although its magnetic axis may be more or less highly inclined to its rotational axis. More recently Deutsch (1952*a*, *b*, 1955, 1956) has actually found an inverse relation between period and line width in the spectrum variables of type A.

It has been shown (e.g., Cowling 1957) that only the dynamo theory can produce and maintain the magnetic field in a star. This theory provides a mechanism resembling a self-exciting dynamo which maintains its magnetic field by electric currents generated by itself. Since the dynamo action of generating stellar magnetic fields requires the simultaneous presence of convection and rotation, it agrees, as Elsasser (1956) has pointed out, with the observed fact that most magnetic stars belong to spectral types A and F because only these stars both rotate and possess convective zones in their outer layers. For further information on magnetic stars the reader should consult chapter 7 of this volume.

The reverse effect—that of the magnetic field upon rotation—was investigated by Ferraro (1937), who found that a star can possess a steady magnetic field only if (1) the field is symmetric about the axis of rotation and (2) each magnetic line of force lies wholly within a surface symmetric about the axis and rotates with a uniform angular velocity. This is the so-called "law of isorotation of the magnetic field" and should be satisfied by any theory that requires a steady magnetic field in the stars. Consequently, the magnetic field in a spectrum variable must be either steady and symmetric with respect to its axis of rotation or changing continuously.

§ 3. SIGNIFICANCE OF ROTATION IN THE STUDY OF STELLAR EVOLUTION AND STAR FORMATION

3.1. Braking Mechanisms of Stellar Rotation

Not all the early-type stars rotate rapidly. Therefore, we shall first investigate whether there exists any effective mechanism that can brake the rotation of a star in a time scale which is short as compared to the life-span of the star in the thermonuclear stage. We shall consider three such mechanisms: (1) viscosity (including turbulent eddy viscosity), (2) radiation, and (3) electromagnetic interaction.

1. We consider, first, braking of the rotation of a star by both molecular and eddy viscosity of the medium surrounding it. It can be shown (Lamb 1932) that a medium that is stationary at infinity exerts upon the rotating star a net moment of force N equal to

$$N = 8\pi\mu R^3\omega \,, \tag{3.1}$$

where μ is the coefficient of viscosity (molecular or turbulent). Therefore, the time scale of viscous braking can be obtained by dividing the total angular momentum of the star $MR^2k^2\omega$ by N, that is,

$$t_v \sim \frac{Mk^2}{8\pi\mu R}, \tag{3.2}$$

where k is the radius of gyration as a fraction of the geometrical radius R of the star. If we substitute the coefficient of molecular viscosity, $\mu = 10^{-4}$, and $k^2 = 10^{-1}$ (Motz 1952), the time scale for braking in a main-sequence B5 star will be 5×10^{17} years. Therefore, viscous braking would not produce any appreciable effect in a time interval of 10^8 years.

Equation (3.1) and, consequently, equation (3.2) involve a serious limitation because of the neglect of the second-order terms in the hydrodynamic equation of motion and of the effect of gravitational attraction of the star. A rigorous formula for the retarding couple N exerted on the rotating star is therefore difficult to derive and is not now available. However, it is reasonable to expect that N will increase with μ and R in any case. Therefore, an increase in μ and/or R will enhance the retarding couple and diminish the time scale of braking.

Von Weizsäcker (1947, 1948) has pointed out that if a gaseous envelope is formed around a rotating star, the star will lose its angular momentum because of the drag of the envelope. Treating the motion of gas in the envelope as a two-dimensional problem in the gravitational field of the central star instead of as a hydrodynamic problem, ter Haar (1949) derived the following formula for the retarding couple:

$$N = f\mu\,(GM)^{1/2}R^{3/2}, \tag{3.3}$$

where f is a numerical factor of the order of unity. In such a case the efficiency of braking depends not only on the magnitude of N but also on the lifetime of the gaseous envelope before its dissipation. According to ter Haar, braking by the gaseous envelope can decelerate the rotation of the star at most by a fraction of 10^{-4} during the lifetime of the envelope. He also concludes that the presence of turbulence in this case will decrease the net effect of braking because the increase in viscosity by turbulent eddies is more than offset by the rapid dissipation of the gaseous envelope by turbulence. For a more detailed discussion we refer the reader to the papers by von Weizsäcker (1948) and Lüst (1952).

2. Jeans (1926) first pointed out the braking effect of radiation and likened the passage of radiation through stellar material to a radial flow of fluid through a sponge. On the average, the stream of radiation will move along the direction of the temperature gradient in the frame of the rotating star. Therefore, the radiation shares the rotation of the stellar material through which it passes, just like the fluid in a rotating sponge. For an amount mc^2 of radiative energy which flows out, there is a corresponding mass m threading its way through the star. Therefore, if ω had a uniform value throughout the star, the angular momentum $m\varpi^2\omega$ of the radiation about the axis of rotation would increase, at the expense of the angular momentum of the stellar material, as the square of its distance ϖ from the axis. In other words, the passage of radiation through a rotating star produces a braking effect on the rotation.

As was previously shown, the total angular momentum of a star is $MR^2k^2\omega$. The rate of loss of angular momentum through the emergent radiation is $(L/c^2)R^2\omega$, where L is the luminosity of the star. The time scale t_R of radiation braking is given by the ratio of these two quantities, that is,

$$t_R \sim \frac{Mk^2c^2}{L}, \tag{3.4}$$

which is of the order of 10^{10} years for a B5 star.

Jeans's idea of transport of the angular momentum by radiation has been applied by Alter (1934) to several problems associated with the solar atmosphere. It appears, however, that the time scale of the transport phenomenon has not been sufficiently emphasized in this interesting investigation.

3. Alfvén (1942) has suggested the braking effect of the stellar magnetic field in an ionized medium. Suppose that a star rotates with constant angular velocity around the axis of magnetization. If, at the beginning, the ionized medium does not partake in the rotational motion of the star, induced electric currents will set in. The effect upon the currents of the magnetic field is to speed up the rotation of the gaseous medium and, at the same time, to slow down the rotation of the star. The retarding torque exerted on the star depends upon the magnitude of the currents, which have a certain upper limit because they set up additional magnetic fields and thereby disturb the original magnetic field that produces the e.m.f. of the induced currents. Eventually, the ionized gas in the neighborhood of the star will rotate with the same angular velocity as the star itself. There remains the question of what is the extent of the gaseous medium that will finally rotate with the star. According to Alfvén, this will be determined by the centrifugal force of the charged particles. This force must be much smaller than the electromagnetic force, in order not to disturb the motion of the charged particles.

Magnetic braking is an efficient means for the transfer of the angular momentum of a star to its surrounding medium. However, it is limited by the total mass in the medium that will take part in the rotation of the star. Usually the total mass is too small to absorb an appreciable fraction of the stellar angular momentum. Two suggestions have been made to increase the amount of mass that could absorb the angular momentum. Ter Haar (1949) suggested that a magnetic star moving in space transfers its angular momentum through electromagnetic interaction to the many clouds which it encounters, the latter being ionized by the stellar radiation (Strömgren 1939). He also suggested that the volume of the medium that will be affected by the stellar magnetic field is determined by electric polarization in the medium. The magnetic field pulls the protons and electrons in opposite directions, thus creating an electric field due to the separation of positive and negative charges. The electric field tends to cancel the effect of the stellar magnetic field. On the other hand, Lüst and Schlüter (1955) considered a stationary star in a turbulent medium. The stellar magnetic

field transports the angular momentum from the star outward to a certain radius R_c at which the transfer mechanism is taken over by the turbulent mixing with the outside medium. Therefore, the flow of angular momentum is determined by the efficiency of turbulent transport and becomes a problem of viscous braking. We have shown in mechanism 1 that the viscous braking increases with the coefficient of viscosity and the radius of the star. While the existence of turbulence in a medium increases the effective viscosity (eddy viscosity), the effect of the stellar magnetic field virtually increases the radius of the star because the ionized medium rotates rigidly within the sphere of radius R_c. It is apparent that the value of R_c should be determined by the strengths of the magnetic field and the turbulence. When turbulent motion becomes the dominant factor in a region of the medium, the magnetic lines of force will be twisted by turbulence, creating sharp turns of large curvatures. Since the ionized gases can pass through points of large curvature, the magnetic lines of force can no longer control the motion of their surrounding medium (Sweet 1950*a*, 1957).

At present, the magnetic fields of relatively few stars have been investigated (chap. 7), and consequently we cannot now decide whether magnetic braking is of any importance. In the late-type main-sequence stars, rotation is always small, but only a few (Babcock 1958) have large magnetic fields. It would be difficult, therefore, to suppose that the original rotations of the late-type stars have been reduced to the observed values by the magnetic fields (§ 3.2).

Aside from the three braking mechanisms discussed above, it should be added that the rotational angular momentum of a star may be dissipated through the loss of mass from the surface. It is quite certain that a considerable amount of mass must be ejected by a rapidly rotating star with an accompanying loss of its angular momentum (§ 2.5). Even for a moderately rotating star, for which no hydrodynamic flow from the surface to outer space takes place, the loss of its mass and of its angular momentum could be accomplished by the corpuscular radiation which it emits. Indeed, Fessenkov (1949) and Massevich (1949) have formulated a theory of the evolution of stars down the main sequence as a result of such a loss of mass which explains satisfactorily the decrease in rotational velocity as stars evolve from early spectral types toward later types. However, the suggested evolution is not in complete accord with our current understanding of stellar evolution as derived from studies of stars in globular and galactic clusters.

3.2. Rotation of Stars along the Evolutionary Sequences

After the discovery by Slettebak and by Herbig and Spalding that the giant stars of late F and early G types rotate much faster than the dwarf stars of the same spectral types, Oke and Greenstein (1954) and Slettebak (1955) independently proposed an interpretation of this phenomenon. It was suggested that when a main-sequence star which has exhausted the hydrogen in its core evolves toward the upper right in the HR diagram, its envelope expands (San-

dage and Schwarzschild 1952; Hoyle and Schwarzschild 1955), and the rotational velocity of the surface layers of the star, consequently, decreases as a result of conservation of angular momentum. The actual change in the rotational velocity during evolution depends upon two factors—the change in stellar structure and the rate of transfer of angular momentum between different layers as compared with the rate of expansion of the envelope. A discussion of the first factor would be out of place in this chapter. Regarding the second factor, Oke and Greenstein have considered two extreme cases: (1) the star rotates at all times as a rigid body, and (2) each thin shell in the star preserves its own angular momentum. In this way they computed, by assuming an initial value for $V_R \sin i$, two curves which relate $V_R \sin i$ with R/R_0 at any time according to the two extreme cases, R_0 being the radius of the star when it is still on the main sequence. The curves provide a semiquantitative explanation for the rotation of some giant stars of spectral types from late F to early K.

Sandage (1955) went one step further by studying the distribution function of rotational velocities of these giant stars. Using the evolutionary tracks computed previously (Sandage and Schwarzschild 1952), he derived from the present value of $V_R \sin i$ of a giant star the value of the same quantity that the star should have had when it was still on the main sequence. Thus he was able to reconstitute the velocity distribution that would have been observed before the evolution of the stars away from the main sequence had started. These distributions are then compared with those of the rotational velocities of present main-sequence stars. It appears that the reconstituted distributions derived from the assumption of case 1 of Oke and Greenstein agree fairly well with the present distribution of rotational velocities of the dwarf A–F stars, although neither assumption 1 nor assumption 2 gives a primeval rotational distribution which agrees with the presently observed distribution of the B stars. Sandage concluded that the stars rotate more nearly as rigid bodies than as bodies consisting of independent shells. On the other hand, in a recent study of the line profiles of a random sample of ten A- and F-type giants, Abt (1957*b*) derived a mean $V_R \sin i$ of 26 km/sec. According to him, this mean value will agree with that predicted on the basis of the Sandage-Schwarzschild tracks of B stars only if these giant stars do not rotate as rigid bodies. While it is very difficult to judge these two conflicting results without repeating their detailed analysis, we are inclined to accept Abt's conclusion because of our own conviction that rigid rotation, especially in the surface layers of a star, is difficult to maintain. Indeed, the surface layers of the sun are rotating differentially with respect to both depth and latitude (e.g., Abetti 1955).

It is obvious that the decrease in rotational velocity during evolutionary expansion, as proposed by Oke and Greenstein and by Slettebak, should hold true for binary stars as well as for single ones. Indeed, Kopal (1956) found an example of the former case in β Lyrae of which the primary component—a B8 supergiant star—has a rotational velocity of about 40 km/sec (Mitchell 1954).

The small rotational velocity observed in β Lyrae agrees with the well-known fact that all supergiant stars have small rotations (§ 5.4). What makes this star more interesting than other supergiants is the fact that its rotation is not synchronized with its orbital revolution (Struve 1952*b*). Consequently, one can deduce that the decrease in the rotation of β Lyrae is perhaps only a recent event, in agreement with the idea of decrease in stellar rotation due to evolution.

No systematic investigation has been carried out for the rotation of stars below the main sequence. A few subdwarfs and high-velocity stars, the line widths of which have been examined, all show very small rotation (Greenstein and Cuffey 1954; Greenstein 1956). An extensive study of the rotations of these stars is desirable and may help us to understand certain aspects of the problem of stellar evolution.

As regards the rotations of white dwarfs, our knowledge is extremely meager. Their spectral lines are complicated by pressure broadening. Microphotometric studies of their spectra have been undertaken by several authors (Kuiper 1941; Greenstein 1956, 1958; Lynds 1957), but no discussion of their rotations has been given. Theoretically, one may argue that if the angular momentum of a star is conserved during its evolution, white dwarf stars should all rotate very rapidly because of their small radii. However, before becoming a white dwarf, a star first evolves into a giant or supergiant, at which time it may lose a large fraction of its angular momentum as well as mass.

Another interesting result of the relationship between rotation and evolution concerns the newly formed stars. Since the T Tauri–like stars are believed to be very young (Ambarzumian 1949, 1952), it is interesting to note that some of them show line broadening too large for their spectral types of G (Herbig 1952). Herbig interpreted the broadening as due to rotation and considered it as evidence that the stars were still in the stage of gravitational contraction, as we shall see later.

A significant result in this respect has recently been obtained by Walker (1956) through a photometric and spectroscopic study of the cluster NGC 2264. This cluster possesses a normal main sequence extending from O7 to A0 and is therefore young. At the same time, stars of spectral types later than A0 fall above the main sequence. The shape of the color-magnitude diagram below A0 suggests that the fainter stars are still in the process of contracting gravitationally and have not yet reached the main sequence. Indeed, the observed diagram agrees qualitatively with the evolutionary tracks computed by Henyey, LeLevier, and Levée (1955) for newly formed stars in gravitational contraction. Walker further called attention to the fact that broadening of the spectral lines of a star becomes noticeable at about F8 and increases with advancing spectral type. He also attributed the broadening to rotation and suggested that these stars had not yet had time to dissipate the original angular momentum of the material from which they were formed.

According to Henyey, LeLevier, and Levée (1955), a newly formed star

reaches the main sequence through the giant stages. For example, a contracting G-type star that now lies about 1.5 mag. above the main sequence will eventually become a main-sequence star of early F type. This, according to Herbig (1957), explains the rotational velocities observed in the T Tauri-like stars. They will become early F main-sequence stars and could have appreciable rotational velocities, in agreement with the results obtained in § 2.3. A difficulty arises from the fact that some T Tauri–like stars are believed to be dwarfs instead of giants. However, Herbig's explanation accounts very well for Walker's result, since the late-type stars in the cluster NGC 2264 are all above the main sequence. It is apparent that the same kind of analysis that has been performed by Sandage and by Abt for stars that have passed the main-sequence stage can be used for examining the rotation of those stars that are evolving toward the main sequence. No such analysis, however, is available at present. According to these views, a star has the largest rotational velocity when it is on the main sequence.

Another interpretation of the change in rotation during the evolution of T Tauri–like stars has been implied in a recent suggestion of the formation of planetary systems from these stars (Struve and Huang 1958). During the contracting stage, a greater part of the stellar angular momentum could be transferred through some of the mechanisms discussed in § 3.1 or other possibilities to the surrounding medium, which, like the solar nebula envisaged by von Weizsäcker (1944), Kuiper (1951), and others, in their theory of formation of the solar system, has a much greater density than ordinary interstellar clouds.

3.3. Origin of the Rotational Angular Momentum

There are two processes by which a star may acquire its angular momentum (e.g., Huang and Struve 1954). First, when a cloud, which shares in the galactic rotation, condenses into a star, the local angular momentum is absorbed by the condensing star. Second, a star may acquire its angular momentum through collisions which take place either in its early stellar stage or, more likely, in the prestellar stages. For example, as a result of turbulence, the local angular momentum in a medium can be different from zero, although the net angular momentum of the medium as a whole may vanish. Also, when two clouds collide, local angular momentum is created in the boundary layers. This latter possibility has been discussed in a recent theory of star formation (Huang 1957*c*). It is obvious that both processes are working in the actual shaping of a star. However, in the following, we shall discuss these two processes individually in a hypothetical manner, so that we can see the difference in their bearings on observational results. The difference thus derived will eventually lead us to the understanding of the dominant process which determines the final angular momentum of a star.

According to the first hypothesis, stars thus formed should have rotational axes predominantly perpendicular to the galactic plane. In other words, the

observed rotational velocities of stars would be correlated with their galactic latitudes because the angle of inclination of the rotating plane would then become identical with the galactic latitude of the star. No such correlation has been found (§ 2.4). Moreover, the distribution of observed rotational velocities of Be stars also favors the assumption of random orientation of the rotational axes in space (§ 2.3). Therefore, the first hypothesis seems to contradict the observational results.

While the second hypothesis is consistent with the random orientation of rotating axes, there are other difficulties. A simple calculation shows that the localization of the angular momentum of galactic rotation predicts a very high value of angular momentum per unit mass for stars formed out of any extended cloud. Indeed, the excess angular momentum has always been one of the serious difficulties (e.g., Edgeworth 1946) of the condensation theory of star formation (Jeans 1928). In order to assume the second hypothesis, we should first find a mechanism that does not require the localization of galactic angular momentum. While mechanisms for transporting local angular momentum have recently been suggested (Edgeworth 1946; Oort 1955; Huang 1957*a*), no quantitative analysis is now available.

The second hypothesis also predicts some observational results. (1) Rapidly rotating stars should be found close together. In a prestellar medium where turbulent transport of momentum and vorticity (§ 4.2) is efficient, we would expect a certain kind of homogeneity of the kinematic behavior among different regions of the medium. Therefore, when the local angular momentum is large in one region, it is likely to be large in other regions of the same medium. While this has not been definitely established by observations, the clustering of stars of large rotational velocity in some regions and of stars of small velocity in others (§ 2.4) is consistent with the prediction. (2) There should exist a correlation between the rotation and space motion of the stars in a physical group (e.g., an association or a cluster). When the linear motions of different parts of a medium are large, energy will be transferred through collisions from the translational motion to the circulatory motion of these parts. We may regard this process as a tendency toward equipartition of energy between translational motion and rotation. In § 2.4 we have already seen that such a correlation appears to exist in the Scorpio-Centaurus cluster. From these considerations, Huang and Struve (1954) concluded that the angular momentum associated with the rotation of a star is derived from the collisions of clouds or of turbulent eddies in the prestellar medium. This conclusion has recently been used to account for the angular momentum not only of rotating stars but also of planetary systems and binary stars (Huang 1957*c*). In any case, whatever theory of star formation one may consider, it is imperative, we believe, that the rotations of stars and the orbital revolutions of binaries should be considered together (Struve 1950). In this respect, it would be especially interesting to know the rotation of the component stars of widely separated binary components in which the transfer of angular momentum between the orbital motion and the

axial rotation is small. Toward this end, pioneering investigations have been carried out by Hynek (1937) and Struve and Franklin (1955). However, because the inclinations of both the orbital plane and the equatorial plane cannot be determined directly, we are unable with the available data to answer the question about the relative orientations of these two fundamental planes.

§ 4. TURBULENCE AS UNDERSTOOD IN AERODYNAMICS

4.1. The Reynolds Number

When sea waves hit the shore, the water develops a mode of motion that is distinctly different from that of the quiet flow in a stream. Man must have recognized the difference between these two modes of motion long before written history. However, the first scientific paper on this difference was published in 1883 when O. Reynolds presented the results of his now classical experiments on flow in long straight pipes. He introduced dye into the liquid in the pipe through a small auxilary tube and thereby was able to observe the flow patterns in the pipe. In this way he demonstrated the nature of the two modes of motion: (1) laminar motion, which is characterized by a smooth thread of dye in the liquid, and (2) turbulent motion, which is characterized by the rapid breakup of the filament of dye, so that the dye spreads quickly over the entire cross-section of the pipe. Let v be the average velocity of the fluid, r be the radius of the pipe, and ν be the kinematic viscosity of the fluid. Reynolds found by dimensional analysis that the transition from laminar to turbulent flow occurs when the dimensionless quantity, now known as the "Reynolds number,"

$$R = \frac{v r}{\nu}, \tag{4.1}$$

reaches a certain critical value which is about 1000 from his experiments. However, if one takes great pains in obtaining a smooth entry of the liquid and insulates the apparatus from all external disturbances, laminar flow can be observed even when r reaches a value as high as 20,000 (e.g., Prandtl 1952). On the other hand, no matter how great the initial disturbances, turbulence cannot persist in a long pipe if $R < 1000$.

Since the Reynolds number is derived from dimensional analysis, we should be able to define this number in any flow in which one can find a characteristic velocity v of mass motion, like the mean velocity of flow in a pipe, and a characteristic length l which measures the linear dimensions of the system, like the radius of the pipe. As the kinematic viscosity ν is related to the dynamical viscosity μ by the relation

$$\nu = \frac{\mu}{\rho}, \tag{4.2}$$

where ρ is the density of fluid, we can define very generally the Reynolds number as

$$R = \frac{\rho v l}{\mu} \tag{4.3}$$

for any flow in which the density is uniform. As an example, in convective motion in shallow layers the thickness of the fluid can be regarded as the characteristic length l. In the case of stellar atmospheres, where the onset of turbulence depends on the influence of gravitational force (Richardson 1920; also, e.g., Sutton 1955), we may still use the Reynolds number as a criterion for the transition from laminar to turbulent flow within a layer of the order of thickness equal to the scale height—i.e., the height within which the density decreases by a factor of e. In the upper part of the solar convective zone the scale height is of the order of 100 km and increases downward. Thus Minnaert (1953) derived $R > 10^{11}$ in the solar atmosphere, which insures the development of turbulence by the convecting currents or by other stirring agencies. Historically, it was Rosseland (1928) who first pointed out the importance of turbulent motions in stars in general and suggested in particular the solar granulation as a manifestation of turbulence and the eruptive prominences as an example of the transition of laminar to turbulent motion.

4.2. Theories of Turbulence

We may intuitively regard turbulence as a kind of random motion of swarms of molecules like thermal agitation. Such a swarm of molecules is known as an "eddy" in turbulent motion. Thus an eddy is a mass of fluid capable of retaining some measure of individuality and able to move as a separate entity in the surrounding medium. It lives, so to speak, only a short interval of time and then loses its identity by mixing with the surrounding medium. Therefore, a turbulent field can be visualized as the continuous formation and destruction of eddies of different sizes.

Prandtl (e.g., 1952) argued that the random motions of eddies in a turbulent fluid produce eddy viscosity, just as the random motions of molecules in a gas produce molecular viscosity. However, instead of the collision processes of molecules which transfer the momentum, he introduced the concept of turbulent mixing of eddies. When an eddy is formed at a certain place, it possesses, apart from its random motion, the mean momentum of the region in which it is located. The momentum is conserved as it moves a certain distance, which Prandtl called "the mixing length." After having traveled a distance of the mixing length, the eddy mixes with the surrounding medium and thereby transfers its momentum to the medium. Therefore, the mixing length corresponds to, and has the same function as, the free path in the kinetic theory of gases. Since the momentum is assumed to be conserved along the path, the theory bears the name of "momentum transport." On the other hand, G. I. Taylor, in his vorticity transport theory, maintained that vorticity, instead of momentum, was conserved along the path of an eddy. Both transport theories have been mathematically formulated and have met with some success in their applications. However, it is obvious that the concept of the mixing length oversimplifies the picture of turbulence. For a more detailed description of the theories of mixing

in turbulent fluids we refer the reader to a standard book on this subject (Goldstein 1938).

If we regard the turbulent motion as a realization of all the possible motions of which a system is capable, the fundamental problem of turbulence becomes a statistical one of specifying the probability with which the various types of motion may occur. For this purpose, we make a harmonic analysis of the instantaneous velocity field $\boldsymbol{v}(\boldsymbol{r}, t)$ in the form

$$\boldsymbol{v}(\boldsymbol{r}, t) = \Sigma_{\boldsymbol{k}} \boldsymbol{v}_{\boldsymbol{k}}(t)\, e^{i\boldsymbol{k}\cdot\boldsymbol{r}}, \tag{4.4}$$

and study the average energy stored in the various wave lengths. The magnitude of the vector $\boldsymbol{k}$, i.e., k, is the wave number which is related to the wave length λ by $k = 2\pi/\lambda$. In equation (4.4) we treat the velocity field at any instant as a superposition of periodic variations with all possible wave lengths. The direction of the vector $\boldsymbol{k}$ denotes the direction of propagation of the component wave associated with $\boldsymbol{k}$. Therefore, $\boldsymbol{k}$ is sometimes known as the propagation vector. For turbulence in an incompressible fluid, it can be shown that $\boldsymbol{v}_{\boldsymbol{k}}$ must be perpendicular to $\boldsymbol{k}$, i.e., the instantaneous velocity distribution can be represented by the superposition of transverse waves alone. The component with a wave length λ may be regarded as an eddy of size λ. We can then define the spectrum of turbulence $F(k)$ by equating $\rho F(k)dk$ to the energy per unit volume stored in eddies with wave numbers between k and $k + dk$. The name "spectrum" is derived from its optical counterpart of the distribution of energy of radiation with respect to λ (or k). We should, however, emphasize that the analogy is more formal than physical. For, in equilibrium, the distribution of energy in the continuous spectrum of radiation follows Planck's law for the entire range of wave lengths, while no such general law exists for the turbulent spectrum. However, in the steady state in which turbulent energy is dissipated by molecular viscosity at the same rate as it is supplied by the external agency, we may expect the turbulent spectrum to approach a general law in the region of large k (i.e., small λ), on the ground that the small eddies will not be influenced by the stirring mechanism. Indeed, this equilibrium spectrum is given by

$$F(k) \propto k^{-5/3}, \tag{4.5}$$

which was first derived by A. N. Kolmogoroff in 1941 and independently obtained by L. Onsager in 1945 and C. F. von Weizsäcker in 1948. Therefore, expression (4.5) is frequently referred to as the "Kolmogoroff spectrum."

If we define the mean velocity v_k of all eddies with wave numbers exceeding a certain value of k (i.e., with wave lengths less than a certain value of λ) by

$$v_k^2 = \int_k^\infty F(k)\, dk, \tag{4.6}$$

we obtain in the Kolmogoroff region of the turbulent spectrum the relation

$$v_k \propto k^{-1/3} \propto \lambda^{1/3}. \tag{4.7}$$

Expressions (4.5) and (4.7) are equivalent, but in astronomical literature the Kolmogoroff spectrum is usually expressed in the form of equation (4.7).

The Kolmogoroff spectrum is derived for homogeneous isotropic turbulence in incompressible fluids under the assumption that it depends only on the rate of dissipation per unit mass and the kinematic viscosity. Whether such an equilibrium spectrum exists in stellar atmospheres is open to question at present. Even if it exists, it may not be observed spectroscopically, as we shall see in the next section.

A brief survey of the statistical theory of turbulence in connection with its various astrophysical applications has been given by Chandrasekhar (1949). A more extensive treatment of the turbulent theories of astrophysical problems has been published by Wasiutyński (1946). The success of the statistical theory of turbulence in hydrodynamics has led some investigators to overemphasize its importance in astrophysics. This tendency may be useful in the study of turbulence in interstellar clouds. But in stellar atmospheres the statistical theory of turbulence has not yet proved to be of great value. The convective motion has a preferential direction, and, moreover, transport of energy in the convective zone is most likely affected by large eddies. Consequently, most theoretical investigators of the problem of energy transport in the convective zone have based their work on the idea of mixing length.

4.3. Thermal Instability and Convection

In this subsection, we shall digress from the topic of turbulence and discuss a kind of motion that is not turbulence but is closely related to it, namely, the convective motion arising from thermal instability. It differs from turbulence by its regular pattern. Convection may be one of the agencies that create turbulence in stellar atmospheres. Moreover, what we know spectroscopically as turbulence (§ 5) may turn out to be simply a result of convective motion. Since the convective velocity field can be expressed by the same equation (4.4) that defines a turbulent velocity field, we frequently use the term "eddies" for denoting convective current elements.

Most convective motions, such as those in our own atmosphere, arise from thermal instability. When a liquid is heated from below, the portion at the bottom becomes hotter, and consequently lighter, than that on the top. As a result, the liquid at the bottom rises and that on the top sinks, thus creating a convective flow. This phenomenon can be easily seen by heating a glass of water on a hot plate.

Extensive experimental studies of this phenomenon were first carried out in 1901–1902 by H. Bénard, who found that if the vertical temperature gradient at the bottom exceeded a certain critical value, cellular circulation of a definite structure was developed in the liquid. The circulation structure consists of a number of vertical cells of hexagonal cross-sections with nearly equal size filling completely the space of the liquid, like a honeycomb. These cells are now fre-

quently called "Bénard cells." The current flows upward in the center of each cell and downward along its walls. This kind of cellular convection has frequently been observed in nature (e.g., Wasiutyński 1946; Chandrasekhar 1952).

Lord Rayleigh found in 1916 from theoretical considerations that the instability of a layer of liquid heated from below depends on a non-dimensional number R_y (now known as the "Rayleigh number"),

$$R_y = \frac{g\alpha\,|\,\beta\,|}{\kappa\nu}\, d^4, \tag{4.8}$$

just as the onset of turbulence depends on the Reynolds number. In equation (4.8) g denotes the gravity; α, κ, and ν denote the coefficients of thermal expansion, thermometric conductivity, and kinematic viscosity, respectively; d denotes the depth of the layer of liquid; and β is the adverse temperature gradient that is maintained in the layer. The exact value of R_y at which convection sets in depends also on the conditions (i.e., free or rigid) of the boundary surfaces. Experiments show that the critical value of R_y is about 1750 when the liquid is confined between two rigid conducting boundaries, in agreement with the theoretical calculations (e.g., Chandrasekhar 1952). The criterion given by equation (4.8) can be applied to compressible fluids, provided that β is then understood as the excess of the actual temperature gradient over the adiabatic gradient.

Plaskett (1936) suggested that the solar granules may be identified with the Bénard cells formed in the solar convective zone. For a detailed discussion of this theory and other applications of the Bénard cells in the convective layer, we refer the reader to Wasiutyński's (1946) comprehensive treatment.

More recently, Chandrasekhar has studied the effects on thermal convection of (1) rotation, (2) magnetic field, and (3) both rotation and magnetic field. His theoretical predictions have been verified experimentally by Y. Nakagawa and others at the Enrico Fermi Institute of the University of Chicago. For a brief review of these results we refer the reader to an article by Chandrasekhar (1957) in which one can also find references to the original papers.

4.4. Near-sonic and Supersonic Turbulence

Let us again consider steady flow in a pipe. If the velocity of flow is v and the velocity of sound in the medium is a, then

$$M = \frac{v}{a} \tag{4.9}$$

is known as the "Mach number" of the flow. Flow for which $M < 1$ is called "subsonic"; that for which $M > 1$, "supersonic." The two kinds of flow have greatly different behavior. For example, in a one-dimensional flow with a velocity v at infinity, the pressure disturbance created at a fixed obstacle in the

stream propagates in all directions if $v < a$, but is confined to a cone behind the obstacle when $v > a$. The semiangle of the cone, α, is given by

$$\sin \alpha = \frac{a}{v} \qquad (v > a) \qquad (4.10)$$

and is known as the "Mach angle." Since only relative motion between the obstacle and the mass of fluid is relevant here, the same results hold in the case of the passing of a body (e.g., a bullet or a supersonic jet plane) through a mass of fluid at rest—a phenomenon studied in a now classical experiment by E. Mach and his associates in 1887–1889.

The problem of supersonic flow is closely related to that of compressibility. This can be demonstrated by a simple example of steady adiabatic flow of an ideal gas in a tube of smoothly varying cross-section. It can be easily shown (e.g., Liepmann and Roshko 1957) that, in such a flow,

$$\frac{d\rho}{\rho} = -M^2 \frac{dv}{v} \qquad (4.11)$$

and

$$\frac{dv}{v} = -\frac{1}{1-M^2} \frac{dA}{A}, \qquad (4.12)$$

where A denotes the cross-section area of the tube and is a function of the coordinate along the axis of the tube. Equation (4.11) indicates the dependence of compressibility on the Mach number. At low M, the density changes are very small compared with the velocity changes, and incompressibility will be a good approximation for the flow. However, compressibility becomes important when M is of the order of, or greater than, unity. Because of the compressibility of the gas, the velocity in supersonic flow increases when the motion is from the narrow part to the wide part of the tube, as can be seen from equation (4.12).

Likewise, when the velocity fluctuations in a turbulent medium become equal to, or greater than, the local velocity of sound, the effect of the compressibility of the gas should be taken into account. Also, the turbulent pressure becomes important (Batchelor 1955). It can be shown that, for a turbulent velocity field in a compressible gas, the Fourier components $\boldsymbol{v}_{\boldsymbol{k}}$ in equation (4.4) are not necessarily perpendicular to the propagation vector $\boldsymbol{k}$. Therefore, the resolution of the instantaneous velocity field will require longitudinal waves in addition to the transverse waves used for an incompressible fluid. The former waves are sometimes called the "noise component" of the turbulence because they tend to propagate as sound waves. However, this does not mean that turbulence is an effective acoustic source. The difficulty in studying supersonic turbulence is that the longitudinal and transverse waves continuously interact with each other so that we cannot separate them (Batchelor 1952; Moyal 1952).

The amplitudes of the transverse waves for Mach numbers comparable with, or greater than, unity must be very large. When the amplitude of a wave is

large, its form becomes distorted as it propagates, because of the effect of the non-linear terms in the equations of motion. It can be shown that the region of high condensation tends to overtake that of low condensation, thereby creating a steep gradient of density and finally forming a shock wave. Lighthill (1953, 1955) visualized turbulence as a velocity field consisting of eddy motions of all sizes, together with shock waves of all shapes rushing about in all directions. According to him, a part of the energy in shock waves is fed back into the shearing turbulence because interactions between shock waves create additional vorticity.

4.5 Turbulent Motion in a Conducting Medium under the Action of a Magnetic Field

Turbulent motion in a conducting medium will amplify any small magnetic field that may be present in the medium, although the asymptotic level of the magnetic field (measured, say, by the magnetic energy density as compared with the turbulent energy density) that will finally be reached is still a question. Let us investigate qualitatively this situation without going into mathematical details. Consider a tube of magnetic lines of force to which ionized particles are glued (e.g., Alfvén 1950). The ionized particles are participating in the turbulent motion. Therefore, the turbulent motion of the ionized particles twists the tube of lines of force and stretches it. An increase in the length of the tube would reduce its cross-section as a result of conservation of mass in the tube and would thereby raise the number of magnetic lines of force per unit cross-section of the tube. In other words, the magnetic field is strengthened. In this way, turbulent energy is converted into magnetic energy. However, the tension along each magnetic line of force has a tendency to straighten it out. Therefore, a steady state will eventually be reached when the inertial force of twisting becomes comparable with the magnetic force of straightening. Thus we have an approximate equipartition of energy between the turbulent velocity field and the magnetic field. Since the magnetic field can be resolved into Fourier components in the same way as the turbulent velocity field, the above intuitive reasoning would suggest that there is an approximate equipartition between magnetic and turbulent energy in all wave lengths. Actually, this intuitive conclusion remains somewhat controversial. Some investigators have concluded that, instead of equipartition of energy in all wave lengths, the energies of the magnetic field and of the turbulent motion are approximately equal only for small wave-length components. For large wave-length components the magnetic energy may be far less than the turbulent energy. No consensus has been reached regarding this point.

Twisting of magnetic lines of force by turbulence in a conducting medium not only increases the magnetic energy but also helps its dissipation into heat because turbulence reduces the effective electric conductivity of the medium (Sweet 1950*a;* see also Spitzer 1957). The net change in magnetic energy would

be the difference between these two effects. It can be shown that the increase in the rate of dissipation is greater than that of the building-up of the magnetic field. As a result, the turbulent motion reduces the time of decay of the magnetic field. For a more detailed discussion of turbulence in magnetic fields we refer the reader to review articles by Cowling (1953, 1957) and Elsasser (1955).

§ 5. TURBULENCE AS UNDERSTOOD IN STELLAR SPECTROSCOPY

5.1. The Two Kinds of Doppler Broadening of Stellar Spectral Lines

The only means, at present, by which we can derive some information concerning the gaseous motion in stellar atmospheres is through the study of the Doppler broadening of spectral lines. Stellar spectroscopists have designated the kinematic behavior of stellar atmospheres which broadens the spectral lines as "turbulence," when the observed lines cannot be satisfactorily interpreted on the basis of either rotation or thermal motion. We shall follow this usage of the term "turbulence," although the agency, apart from rotation and thermal motion, that is responsible for the Doppler broadening of lines in stellar spectra is *not necessarily* turbulence as understood in aerodynamics (e.g., Biermann 1955; Thomas 1955). Instead, it includes all kinds of motion that are conceivable in stellar atmospheres. The ultimate purpose of this type of research is to identify the character of the motion by means of spectroscopic observations. In order to do so, we must first analyze the relationship between the Doppler broadening of spectral lines, on the one hand, and the gaseous motion in stellar atmospheres, on the other.

Let us choose a rectangular co-ordinate system centered in the star such that the z-axis is in the direction of the line of sight. Imagine, now, that we observe only a surface element—say the ith element—on the photosphere of the star. Absorption lines are formed in the column parallel to the z-axis and above the surface element. A spectral line thus formed will depend upon the distribution function $f_i(\zeta - \langle\zeta_i\rangle_z)$ of the velocity components, ζ, in the z-direction of the absorbing atoms in the column. Here $\langle\zeta_i\rangle_z$ denotes the mean line-of-sight velocity of the atoms in the ith column. Indeed, the effective atomic-line absorption coefficient in the column should be given by averaging the atomic-line absorption coefficient over $f_i(\zeta - \langle\zeta_i\rangle_z)$. In this way we obtain, for the column above each surface element of the photosphere, an effective atomic-line absorption coefficient. We define the broadening of a spectral line caused by such a distribution of velocity components as "physical Doppler broadening." It is evident that physical Doppler broadening should, in principle at least, determine the function $f_i(\zeta - \langle\zeta_i\rangle_z)$ within the ith column and vice versa, if we could observe the ith element alone. Spectroscopically, the form of the function f_i determines the broadening, and $\langle\zeta_i\rangle_z$ determines the over-all shift of the line. Obviously, thermal broadening is the prototype of physical Doppler broadening. When the dispersion of the z-components of velocity in the column increases, the equivalent widths, w_i, of the spectral lines formed in the column

also increase. This is the characteristic property of physical Doppler broadening. Since the effective atomic absorption coefficient for a spectral line in different columns over the same star may not be the same, physical Doppler broadening varies, in general, from point to point over the stellar disk.

In a star we observe only the integrated light over the disk. If the average value $\langle \zeta_i \rangle_z$ varies from column to column, the spectral line observed in the integrated light is further broadened by this kind of differential motion. Since the broadening thus effected is simply a result of combining radiation from different parts of the stellar disk, we shall designate it as "geometrical Doppler broadening." In principle, it should determine the distribution function $\phi(\langle \zeta \rangle_z)$ of $\langle \zeta_i \rangle_z$ of various columns over the surface of a star or vice versa. Obviously, rigid rotation of a star is a good example of geometrical Doppler broadening. For a star without geometrical broadening, $\langle \zeta_i \rangle_z$ is the same for all columns of the atmosphere and represents the radial velocity of the star. Otherwise, the radial velocity should be a weighted mean of $\langle \zeta_i \rangle_z$ over the disk—say $\langle \zeta_i \rangle_{xyz}$.

Let w_i be the equivalent width that would be observed in the radiation coming from the ith element alone. If l_i is the relative intensity of continuous radiation from the ith element, the equivalent width, W, observed in the integrated light over the entire disk will be

$$W = \frac{\Sigma l_i w_i}{\Sigma l_i}, \tag{5.1}$$

the summations being over all n elements. Here we see that the observed equivalent width of a line in stellar spectra is a kind of weighted mean of all w_i's, the latter depending only upon physical Doppler broadening at various points on the stellar disk.

The dispersion of $f_i(\zeta - \langle \zeta_i \rangle_z)$ in each column of a stellar atmosphere is usually known as the "turbulent velocity of small eddies" (including thermal motion) or the velocity of microturbulence. The dispersion of $\phi(\langle \zeta \rangle_z)$ over the stellar disk is usually known as the "turbulent velocity of large eddies," "velocity of macroturbulence," or simply "mass motion." In the sense of the mixing-length theory of turbulence, the thickness of the reversing layer can be taken as a measure for distinguishing large and small eddies in stellar spectroscopy. A criterion can be established for dividing large and small eddies by using the Fourier representation of a velocity field (Wrubel 1950). It should again be emphasized that sometimes the velocities of eddies derived from observation have nothing to do with turbulence. For example, if the angular velocity of a rotating star has a vertical gradient in its atmosphere, it would give rise to a turbulent velocity of small eddies. The same is true for differential radial expansion or contraction. Similarly, a longitudinal wave propagating in the direction which has a non-vanishing z-component produces physical Doppler broadening. On the other hand, transverse waves propagating along the stellar

surface will increase the turbulent velocity of large eddies. The only rigorous way to denote the nature of physical Doppler broadening is by $f_i(\zeta - \langle\zeta_i\rangle_z)$ and to denote the nature of geometrical Doppler broadening is by $\phi(\langle\zeta\rangle_z)$. If we should assign only one value of the velocity for denoting the general behavior of these Doppler broadenings, the best choice would be the standard deviations of the functions $f_i(\zeta - \langle\zeta_i\rangle_z)$ and $\phi(\langle\zeta\rangle_z)$ with respect to their mean values $\langle\zeta_i\rangle_z$ and $\langle\zeta_i\rangle_{xyz}$, respectively. For physical reasons we do not follow this rule in practice. For example, we use the equatorial rotational velocity ($V_R \sin i$) to denote the extent of broadening by rotation. Also, in the case of thermal broadening we have traditionally used the random (i.e., the most probable) velocity.

If the form of the function f_i depends upon the subscript i, it would be difficult, if not impossible, to derive any information regarding this function from the spectra obtained in integrated light. Only in an eclipsing binary do we have a chance of observing the stellar disk differentially, and a better understanding of the motion of gases may then become possible (chaps. 11, 12). However, because of the difference in the force field, the results obtained in eclipsing binaries cannot be applied to single stars without careful examination.

5.2. Physical Doppler Broadening

Whatever are the nature and the stirring mechanism of "turbulence" in stellar atmospheres, the turbulent velocity field must not be isotropic, as a result of the existence of a preferential direction along the radius of the star. This is especially true for large eddies, which are created and consequently determined by the external stirring agency, such as the fluctuation of radiation pressure (e.g., Chandrasekhar 1934), convection (e.g., Vitense 1953), differential rotation, etc. For small eddies, however, we might expect the turbulent fluctuations to be isotropic (§ 4.2). This is fortunate because the isotropy of small eddies means that the form of the distribution function f_i may be assumed to be independent of the location on the stellar disk (i.e., independent of the subscript i). However, we must always remember that the invariance of the form of the function f_i over the entire disk is an assumption based only on heuristic reasoning. As a matter of fact, even for pure thermal motion, the form of the function f_i varies slightly from point to point on the stellar disk, owing to the temperature gradient in the atmosphere. Since we see deeper into the atmosphere at the center of the disk than at the limb, the distribution of ζ will correspond to a higher temperature at the center than at the limb. Therefore, the assumption that one and the same function f exists at all points breaks down seriously if the gradient of the turbulent velocities in depth is much greater than that of the thermal velocities, even when the turbulence is locally isotropic. With these limitations in mind, in the following discussion we shall assume the invariance of the function f over the disk and thereby simplify the problem of Doppler broadening to one of determining two functions, i.e., f and ϕ, from the spectral

lines, the former from the physical Doppler broadening, the latter from the geometrical Doppler broadening.

It is evident that the observed profile of a line is determined by the combined effect of the functions $f(\zeta - \langle\zeta_i\rangle_z)$ and $\phi(\langle\zeta\rangle_z)$ and that we have no a priori means of separating their individual effects. On the other hand, the equivalent width of a line is completely determined by the function f alone. Therefore, a study of equivalent widths of lines in a spectrum—for example, by the curve of growth (chaps. 3–5) or by the curve of line-width correlation (Huang and Struve 1952, 1955*a*; Regemorter 1955)—can yield information regarding the function f. It is true that the form of the curve of growth or of the curve of line-width correlation depends on the behavior of the function f (e.g., Jentzsch and Unsöld 1948; Huang 1950), but the dependence is so insensitive that we are unable to determine the function f from the observed curves, which are usually subject to large uncertainties caused by the scatter of observed points. Consequently, we must assume a definite form for the function, with only one adjustable parameter (of the dimension of a velocity), and determine this parameter from the observed results. Usually, we assume a Maxwellian distribution of space velocities, which is equivalent to a Gaussian form for f, and use the most probable velocity ζ_p as the parameter for defining the function f. This velocity, ζ_p, is sometimes known as the "curve-of-growth velocity" and is responsible for the physical Doppler broadening. To assume f to be a Gaussian function has some theoretical justification because turbulence in the small-wave-length region can be regarded as a completely random process (§ 4.2).

If distributions of both thermal velocities and small eddy velocities are independently Maxwellian, we have

$$\zeta_p^2 = \zeta_{th}^2 + \zeta_s^2 , \tag{5.2}$$

where ζ_{th} and ζ_s represent the velocities of thermal motion and of turbulent motion of small eddies. The random velocity, ζ_{th}, corresponding to thermal motion is, of course, given by

$$\zeta_{th} = \left(\frac{2kT}{m}\right)^{1/2} . \tag{5.3}$$

Turbulent motions of small eddies in stellar atmospheres were first discovered by Struve (1932). From the curves of growth of several supergiant and shell stars he derived values of ζ_p which are too large to be due to thermal motion alone, and therefore he interpreted these large values as turbulent velocities. Hence the name "turbulence" was originally introduced into stellar spectroscopy for the sole purpose of giving a name to the excess value of ζ_p over the random velocity of thermal motion. A systematic study of turbulence in stellar atmospheres by the curve-of-growth method was later undertaken by Struve and Elvey (1934). Since then the determination of turbulent velocities of small eddies ζ_s has become one of the standard procedures in the analysis of stellar spectra. Among the many investigators of the turbulent velocity by the curve of

growth, we mention only a few: Abt on W Virginis (1954) and on U Monocerotis (1955); Aller on α Cygni (1942) and on ϵ Canis Majoris (1956); E. M. and G. R. Burbidge (1956) on five stars of population II; G. R. and E. M. Burbidge on α^2 Canum Venaticorum (1955) and on HD 151199 (1956); Buscombe (1951) on α Cygni and γ Geminorum; Dijke (1946) on α Bootis; Goldberg (1939) on several early supergiant stars; Greenstein on α Carinae (1942) and on some F giants (1948); Greenstein and Hiltner (1949) on α Canis Minoris and α Persei; Hack (1957) on ϵ Aurigae; van Hoof and Deurinck (1951) on η Aquilae; Huang and Struve (1956) on Maia; Koelbloed (1953) on some giant and dwarf K-type stars; Melnikov (1950) on η Aquilae; Miczaika, Franklin, Deutsch, and Greenstein (1956) on some metallic-line stars; Pannekoek and van Albada (1946) on π Cephei; Sahade and Cesco (1946) on γ Cygni; Schwarzschild, Schwarzschild, and Adams (1948) on η Aquilae; Steel on α Persei (1945*a*) and δ Canis Majoris (1945*b*); Struve and Elvey (1934) on α Persei, ϵ Aurigae, and 17 Leporis; Unsöld (1941) on τ Scorpii; Voigt (1952) on 55 Cygni; Walraven (1948) on δ Cephei; Wehlau on δ Equulei (1955) and γ Leonis A and B (1956); Wilson (1948) on ζ Aurigae; Wilson and Abt (1954) on ζ Aurigae; Wright on α Persei (1946), on α Carinae and δ Canis Majoris (1947), on γ Cygni, α Persei, and α Canis Minoris (1948), on α Bootis (1950), and on 31 Cygni (1955); and Wright and van Dien (1949) on ϵ Aurigae. Some of the results of these investigations have been collected in a recent review by Wright (1955). The only other way of determining ζ_p is by the curve of line-width correlation, which was used by Aller (1956) for ϵ Canis Majoris, Huang and Struve (1952) for δ Canis Majoris, Kilby (1953) for ϵ Aurigae, and Wehlau (1956) for γ Leonis A and B.

We can now safely conclude that the turbulent velocities of small eddies in stellar atmospheres are large in most stars with extended atmospheres, such as giant, supergiant, shell stars, etc., but relatively small or even undetectable in dwarf stars (Struve and Elvey 1934). We suggest two heuristic reasons for this phenomenon. First, the geometrical thickness of the reversing layer of a supergiant is several orders of magnitude greater than that of a dwarf star (e.g., Unsöld 1955). Hence eddies of certain sizes that would behave in dwarf atmospheres like large eddies will act like small eddies in supergiant atmospheres. Second, with small surface gravity and high radiation pressure, the atmosphere of a supergiant star is more liable to become unstable than that of a dwarf star. In this respect, supergiant atmospheres may resemble the solar chromosphere on a much larger scale. Indeed, several investigators have suggested that the solar chromosphere is supported by turbulent motion (e.g., van de Hulst 1953). On the other hand, no correlation has been found between microturbulent velocity and spectral type for the supergiants, or for stars of any other luminosity class. However, we should not rule out the possibility that such a correlation may actually exist (§ 5.4) because, at present, errors in determining the microturbulent velocity are large and the sample of data is too small.

In passing, we should mention that the *c*-characteristic of stellar spectra (e.g., Payne 1930) used frequently in the earlier literature is related to the fact that

the broadening of the lines is predominantly due to physical causes rather than to geometrical causes. In Plates I and II we have shown some spectra illustrating stars of varying kinds of Doppler broadening.

Another interesting phenomenon regarding the turbulent velocity of small eddies has recently been discovered by Wright (1946, 1947). He found that in some giant stars (α Persei, γ Cygni) the turbulent velocity derived from the curve of growth is greater for ionized than for neutral atoms and, in the case of Fe I, decreases progressively for lines of increasing excitation potentials. Later investigators have confirmed his results in other stars, namely, ϵ Aurigae (Wright and van Dien 1949), ζ Aurigae (Wilson 1948; Wilson and Abt 1954), and δ Canis Majoris (Huang and Struve 1952). This phenomenon can obviously be attributed to the increase in turbulent velocity with height in the atmospheres because ionized atoms and low-excitation states are favored in the upper layers, whereas neutral atoms and high-excitation states are in the lower layers (Unsöld and Struve 1949; Huang 1951, 1952). Such a stratification of turbulent velocity in stellar atmospheres agrees with what has been found in the solar atmosphere (Unsöld 1929; Menzel 1931; Böhm-Vitense 1955). It is also reasonable from consideration of the equation of continuity because the density decreases with height. Indeed, recent calculations by Henyey (unpublished) and by Whitney and Stone (1957) on the propagation of longitudinal waves in stellar atmospheres shows that the amplitudes of the waves and the velocities of particles increase outward. It is interesting to note that the longitudinal waves themselves, which act like microturbulence in producing line broadening (§ 5.1), could have produced the observed phenomenon of velocity stratification.

Stratification of microturbulent velocities in stellar atmospheres would make for strong dependence of the distribution function $f(\zeta - \langle\zeta_i\rangle_z)$ on the optical depth and consequently on the line strengths. As a result, the theoretical curve of growth changes its shape, especially in its transition portion (Huang 1954). This effect becomes important when the gradient of microturbulent velocity is large.

At this point we should mention that in some giants and supergiants (especially classical cepheids) like α Bootis (Adams 1911; St. John and Adams 1924), δ Cephei (Adams and Shapley 1916), o Ceti (Adams 1941), S Sagittae (Aldrich 1932), W Sagittarii (Curtiss 1926), η Aquilae (Lee 1932; Rufus 1932*a*), ζ Geminorum (Rufus 1932*b*), RT Aurigae (Petrie 1932), α Cygni and β Orionis (Sanford 1947; Shajn and Shajn 1949), and ϵ Aurigae (Struve and Elvey 1930), the radial velocities differ for lines of different elements or of different ionization stages. More recently, Abt (1957*a*) found the same phenomenon in eight A–F I*a* supergiant stars selected at random. This type of difference in radial velocity has also been found in several β Canis Majoris stars, namely, β Canis Majoris (van Hoof and Struve 1953), 16 Lacertae (van Hoof, de Ridder, and Struve 1954), BW Vulpeculae (McNamara, Struve, and Bertiau 1955), σ Scorpii (Struve, McNamara, and Zebergs 1955), 12 Lacertae (Struve and Zebergs 1955), and has been known in the current literature as the "van Hoof effect" (e.g., Struve

1955*b*). These phenomena can be understood on the assumption either of compression waves associated with stellar pulsation or of convective currents. Recently van Hoof (1957) emphasized the latter view and was able to explain several observational facts.

5.3. Geometrical Doppler Broadening

When $\langle \zeta_i \rangle_z$ is not constant over the entire disk of a star, we have the case of geometrical Doppler broadening. Its presence in stellar atmospheres greatly complicates the computation of the profile of a line. In the theory of stellar atmospheres one computes the profile of a line by assuming an invariant form for the effective atomic absorption coefficient in the atmosphere and integrates the intensity over the entire disk for one wave length at a time. In this way, the variation of the emergent radiation with angle (i.e., the angle which the line of sight makes with the normal to the stellar surface) is fully taken care of according to any theory of radiative transfer. It is no longer possible to do so when $\langle \zeta_i \rangle_z$ varies with i, because there are relative shifts of the lines formed at different parts on the disk. In order to reduce the problem of geometrical Doppler broadening to a manageable form, we have to make the simplifying assumption that, apart from a multiplying factor depending on the depth, the lines formed in different parts of a stellar disk have the same profile. Of course, each line shifts as a whole in the wave-length scale by

$$\Delta\lambda_i = \lambda \frac{\langle \zeta_i \rangle_z}{c} \tag{5.4}$$

from its normal position. Denoting by $r_i(\lambda)$ the profile (in depth) of a line that would be observed in the ith element of the stellar disk, we have assumed that

$$r_i(\lambda) = l_i R'(\lambda - \Delta\lambda_i), \tag{5.5}$$

where l_i, being independent of λ, may vary with i according to the law of darkening of the continuous radiation and the form of the function R' is independent of i, although its argument is a function of i (through $\Delta\lambda_i$). The assumption introduced by equation (5.5) certainly cannot be the result of an elaborate theory of radiative transfer. However, only under this simplifying condition are we able to study the problem of geometrical Doppler broadening.

Combining all n elements of the disk, we obtain the profile of the line $R(\lambda)$ that would be observed in the integrated light:

$$R(\lambda) = \frac{\Sigma l_i R'(\lambda - \Delta\lambda_i)}{\Sigma l_i}. \tag{5.6}$$

We now express l_i in terms of $\Delta\lambda_i$ from the geometrical nature of the assumed mass motion, make n approach infinity, and finally obtain the well-known formula for geometrical Doppler broadening,

$$R(\lambda) = \int_{-\infty}^{\infty} B(\Delta\lambda) R'(\lambda - \Delta\lambda)\, d(\Delta\lambda), \tag{5.7}$$

where $B(\Delta\lambda)$ is called the "broadening function" and includes the rotational broadening function given in equation (2.2) as a special case. It is obvious that both $B(\Delta\lambda)$ and $\phi(\langle\zeta\rangle_z)$ characterize the mass motion in stellar atmospheres. However, $B(\Delta\lambda)$ depends on the law of darkening of continuous radiation, as well as on the nature of mass motion, while $\phi(\langle\zeta\rangle_z)$ depends on the nature of mass motion alone.

Equation (5.7) opens two ways for investigating mass motion in the atmosphere of a star. (1) We can derive, from the observed profile $R(\lambda)$, the broadening function $B(\Delta\lambda)$ by assuming a form for $R'(\lambda)$ which may be obtained from the spectra of stars of the same spectral type and luminosity class as the one we are considering with no geometrical broadening. From the form of the broadening function, we might then be able to infer the nature of mass motion that is responsible for the geometrical Doppler broadening. Because of the high accuracy demanded of $R(\lambda)$ and of the difficulty in obtaining a good $R'(\lambda)$, this method has not been used. (2) We can assume the general nature of the mass motion and derive from the observed profile $R(\lambda)$ the true profile $R'(\lambda)$, as well as the scale of the mass motion. The best example of this inductive method can be found in Carroll's study of rotational broadening (§ 2.2). The assumed mass motion is now the rigid rotation of a star, and its scale of motion is $V_R \sin i$. That this method is not satisfactory has already been pointed out. Consequently, the determination of an exact function from the spectroscopic data does not seem promising without a drastic improvement in observational technique.

Although we cannot solve the problem of geometrical Doppler broadening in a general way, we can still tackle some simpler cases. When the spectra are characterized by deep lines, we know that the spectral lines are only slightly broadened by mass motion. In such cases we can assign a single characteristic velocity for defining the mass motion, just as we have assigned a single value for defining the microturbulent motion. The easiest way to derive two characteristic velocities representing motions of large and small eddies is through the use of the curve of line-width correlation (Huang and Struve 1952). On the other hand, if all lines (except the hydrogen lines) in the spectra are shallow, the observed profile represents rather closely the broadening function itself. Since the broadening functions corresponding to various kinds of conceivable mass motion in stellar atmospheres can be computed (e.g., Huang and Struve 1953), we can compare the computed $B(\Delta\lambda)$'s with the observed profile $R(\lambda)$ and then infer the nature of the mass motion. It was found that the broadening functions for two completely different kinds of mass motion can be so alike that both would agree with the same observed profiles, especially in view of the uncertainty involved in smoothing the microphotometric tracings. For example, convection, with a finite upper limit to the velocities of the convective currents, and rotation give similar broadening functions. In spite of this uncertainty, we believe that much information regarding mass motion in stellar atmospheres will be obtained in the future from this extreme case of geometrical broadening.

For intermediate cases, where the widths of both $B(\Delta\lambda)$ and $R'(\lambda)$ are comparable, the study of Doppler broadening becomes very difficult, and not much progress has been made. We have emphasized the relation between equivalent width and central depth of a line (Huang and Struve 1955*a*). But from this type of study we derive simply a characteristic velocity of the observed profile as a whole. The velocity thus derived is therefore similar in nature to the direct measurement of the linear width of a line.

The existence of macroturbulent velocities in stellar atmospheres was suggested when Struve (1946) and Schwarzschild, Schwarzschild, and Adams (1948) noticed that the velocity derived from the line widths is much greater than that from the curve of growth. Most papers that are concerned with the study of broadening by mass motion simply determine a velocity ζ_l corresponding to the observed line profile as a whole from the linear width (Struve 1946; van de Hulst and Reesinck 1947; Schwarzschild, Schwarzschild, and Adams 1948; Underhill 1948; Unsöld and Struve 1949; Wright and van Dien 1949; Buscombe 1951; van Hoof and Deurinck 1951; Voigt 1952; Oke 1954; van Wijk 1957) or from the curve of line-width correlation (Huang and Struve 1952; Kilby 1953; Aller 1956; Wehlau 1956), or from the relation between the depths and equivalent widths (Huang and Struve 1955*a*, *b*; Wehlau 1956; Wehlau and Wehlau 1956). If the broadening function can be expressed in terms of the Gaussian function, we can define a random velocity ζ_g corresponding to the broadening function and regard it as representing the random velocity of large eddies. The subscript g is used to denote the fact that the velocity is responsible for geometrical broadening. In this case we can regard ζ_l as the resultant random velocity of both large and small eddies and write

$$\zeta_l^2 = \zeta_g^2 + \zeta_p^2 . \tag{5.8}$$

One should use equation (5.8) with caution, because it has a meaning only when the broadening function is Gaussian. In general, it is very difficult to single out one characteristic velocity ζ_l to represent the results of both physical and geometrical broadening. Aside from rotation, geometrical Doppler broadening can be affected by several other kinds of mass motion, such as pulsation, expansion, convection, ejection, surface waves, etc. Broadening caused by these processes would usually make the observed line unsymmetrical (Shapley and Nicholson 1919; Carroll 1928; Wilson 1935; Spitzer 1939; Underhill 1947; van Hoof and Deurinck 1951) or even split it into two or more components. Indeed, the splitting of spectral lines is frequently observed in intrinsic variable stars (Struve 1948*a*; Kraft 1956), as well as in peculiar stars (e.g., Struve 1951*a*; Bidelman and McKellar 1957). In some cases the splitting of lines is associated with the discontinuity of the velocity-curve (Sanford 1949, 1952; Struve 1954, 1955*a*). This phenomenon is most probably the result of gaseous motions in the atmospheres of the variables (Struve 1955*a*; Huang 1957*b*) and provides an important clue for the understanding of the nature of these stars.

In some cases the study of the emission lines could yield more information

about the nature of mass motion than the study of the absorption lines (Gerasimovič 1933, 1935; Beals 1940, 1941; Beals and Rottenberg 1952; Rottenberg 1952; Aller 1954; Wilson 1954, 1957; Goldberg 1957; Payne-Gaposchkin 1957; Wilson and Bappu 1957; Weaver, unpublished). A better understanding of the kinematic behavior of gases in an extended atmosphere may be obtained from the study of atmospheric eclipses (e.g., Wilson and Abt 1954; McKellar, Wright, and Francis 1957). However, lack of space does not permit us to discuss these problems here, and we refer the reader to chapters 10, 11, and 12 in this volume.

5.4. General Conclusions concerning the Doppler Motion in Stellar Atmospheres

While we have no doubt about the rotation of early-type main-sequence stars, the question of the line broadening in supergiant stars is far from settled (Struve 1952*a*). In the first place, the profile of the lines in a supergiant does not completely agree with the rotational hypothesis. For example, consider the case of ρ Leonis, which has been studied microphotometrically in great detail (Huang and Struve 1953). It is a supergiant of class B1 *Ib* (Morgan and Roman 1950), and its absorption lines are broad and shallow, showing clearly the presence of geometrical broadening. If we assume that the observed profile $R(\lambda)$ can be expressed in terms of a Gaussian profile $R'(\lambda)$ broadened by the rotational broadening function (eq. [2.2]), we find that the observed profiles of weak and medium-strong lines correspond to a rotational velocity of 60 km/sec and a half-half-width of $R'(\lambda)$ of 30 km/sec. Strong lines (not including those of H and He) indicate even smaller rotational velocities and larger half-half-widths for $R'(\lambda)$. From these results we have concluded that rotation accounts, at most, for a part of the geometrical Doppler broadening. Actually, rotation may contribute only an insignificant part.

Since we cannot distinguish unambiguously, from the study of the profiles in a single star, between broadening by rotation and that by other types of mass motion, we have to resort to a statistical study to settle this point (Huang and Struve 1954). We plotted the widths of a particular line measured directly on the spectrograms of early B-type stars against the absolute visual magnitudes of the stars and found a sharp distinction between the distributions of line widths for stars brighter, and for stars fainter, than $M_v = -4^m.5$. For the less luminous stars, the line widths are distributed at random from zero to an upper limit (corresponding to more than 400 km/sec). For the brighter stars, the measured widths are concentrated in a narrow horizontal strip with an average value corresponding to a velocity of 80 km/sec. Although the velocities measured from line widths of highly luminous stars are small compared with those found in the dwarf stars, none has zero velocity. A similar phenomenon has been found also in the B6–A2 stars. In this case the discontinuity in the distribution of the observed points occurs at $M_v = -3^m.5$, and the velocities measured from the line widths of the highly luminous stars never deviate more than by 10 km/sec from their average value of 50 km/sec. Therefore, the distribution of

the line widths of the dwarf stars clearly shows the rotational nature of the broadening. Their upper limit corresponds to the equatorial rotational velocity of a star on the verge of instability. The frequent occurrence of sharp lines must be caused in part by the orientation of the rotational axes nearly in the direction of the observer. On the other hand, the frequency distribution of the line widths of supergiant stars suggests mass motions with spherical symmetry, at least in a statistical sense, like a field of prominences over the stellar surface. It cannot be due to rotation. A similar statistical study by Slettebak (1956) of some O5–B5 stars confirms the conclusion that large-scale atmospheric motions play an important role in the highly luminous stars.

When the velocities of Doppler motions in supergiant atmospheres are plotted against their spectral types (O9–F8), there is a distinct trend toward smaller values along the spectral sequence (Huang and Struve 1954). Moreover, the velocities in supergiants of luminosity class I*a* are systematically higher than those in luminosity class I*b* of the same spectral type according to the MK system (Keenan and Morgan 1951). In other words, the higher the temperature or the lower the pressure, the greater is the line broadening. This result was also confirmed by Slettebak (1956) in the O5–B5 stars. Since it is difficult to suppose that there is a correlation between stellar rotation and surface temperature or pressure, we again conclude that the observed line widths in supergiant stars are not due to rotation. The fact that supergiant stars have small rotations is consistent with current ideas of stellar evolution (§ 3.2).

We summarize these results by saying that turbulent motions in stellar atmospheres are favored in regions of low density in hot stars and that radiation pressure is probably important in creating turbulence. The problem of inducing motions of particles by radiation has been investigated by several persons (Chandrasekhar 1934; Gerasimovič 1934; Greenstein 1937, 1951).

The nature of the mass motions in supergiants probably resembles prominence activity (Struve 1948*b*, 1951*b* and *c*). This view is shared by Bhatnagar, Krook, Menzel, and Thomas (1955) and others. In this sense, the motions observed in stellar atmospheres may be related to the ejection phenomenon (e.g., Merrill 1956). They are also consistent with the irregular variations in radial velocity of the supergiant stars (Paddock 1935; Poveda 1951; Struve 1951*a;* Abt 1957*a*), as well as with the large-scale motions sometimes observed in the atmosphere of 31 Cygni (McKellar, Odgers, Aller, and McLaughlin 1952), of υ Sagittarii (Bidelman 1949), etc. This view is further strengthened by the ejection phenomenon observed in many close binaries (Struve 1941, 1948*b*, 1949, 1950; Struve and Huang 1957). Other peculiarities observed in stellar spectra (e.g., Swings and Struve 1940; Struve 1951*d*) may also be understood in the light of gaseous streams in and around the stars.[1]

[1] The authors wish to note that the major portion of this study of stellar rotation and turbulence was completed in 1958. Consequently, few citations of the literature beyond 1957 are included.

REFERENCES

ABETTI, G.	1955	*The Sun*, trans. J. B. SIDGWICK (London: Faber & Faber).
ABNEY, W. DE W.	1877	*M.N.*, **37**, 278.
ABT, H. A.	1954	*Ap. J. Suppl.*, **1**, 63.
	1955	*Ap. J.*, **122**, 72.
	1957*a*	*Ibid.*, **126**, 138.
	1957*b*	*Ibid.*, p. 503.
ADAMS, W. S.	1911	*Ap. J.*, **33**, 64.
	1941	*Ibid.*, **93**, 11.
ADAMS, W. S., and JOY, A. H.	1919	*Ap. J.*, **49**, 186.
	1922	*Communication to National Academy of Science*, **2**, 141.
ADAMS, W. S., and SHAPLEY, H.	1916	*Proc. Nat. Acad. Sci. Washington*, **2**, 139.
ALDRICH, J. A.	1932	*Pub. Obs. U. Michigan*, **4**, 75.
ALFVÉN, H.	1942	*Ark. f. mat. astr. o. fys.*, Vol. **28A**, No. 6.
	1950	*Cosmical Electrodynamics* (Oxford: Clarendon Press).
ALLER, L. H.	1942	*Ap. J.*, **95**, 73.
	1953	*Astrophysics* (New York: Ronald Press Co.), Vol. **1**.
	1954	*Ibid.*, Vol. **2**.
	1956	*Ap. J.*, **123**, 117.
ALTER, D.	1934	*Ap. J.*, **79**, 498.
AMBARZUMIAN, V. A.	1949	*A.J., U.S.S.R.*, **26**, 3.
	1952	*I.A.U. Trans.*, **8**, 665.
BABCOCK, H. W.	1947	*Pub. A.S.P.*, **59**, 112.
	1949	*Ap. J.*, **110**, 126.
	1953	*Ibid.*, **118**, 387.
	1958	*Ap. J. Suppl.*, **3**, 141.
BATCHELOR, G. K.	1952	*Repts. Prog. Phys.*, **15**, 101.
	1955	*Vistas in Astronomy*, ed. A. BEER (London: Pergamon Press), **1**, 290.
BEALS, C. S.	1940	*J.R.A.S. Canada*, **34**, 169.
	1941	*Observatory*, **64**, 42.
BEALS, C. S., and ROTTENBERG, J. A.	1952	*J.R.A.S. Canada*, **46**, 133.
BHATNAGAR, P. L., KROOK, M., MENZEL, D. H., and THOMAS, R. N.	1955	*Vistas in Astronomy*, ed. A. BEER (London: Pergamon Press), **1**, 296.
BIDELMAN, W. P.	1949	*Ap. J.*, **109**, 544.
BIDELMAN, W. P., and MCKELLAR, A.	1957	*Pub. A.S.P.*, **69**, 31.

BIERMANN, L.	1955	*I.A.U. Trans.*, **9**, 750.
BLACKETT, P. M. S.	1947	*Nature* (London), **159**, 658.
BÖHM, K.-H.	1952	*Zs. f. Ap.*, **30**, 117.
BÖHM-VITENSE, E.	1955	*Zs. f. Ap.*, **36**, 145.
BROWN, A.	1950	*Ap. J.*, **111**, 366.
BURBIDGE, E. M., and BURBIDGE, G. R.	1956	*Ap. J.*, **124**, 116.
BURBIDGE, G. R., and BURBIDGE, E. M.	1955	*Ap. J. Suppl.*, **1**, 431.
	1956	*Ap. J.*, **124**, 130.
BUSCOMBE, W.	1951	*Ap. J.*, **114**, 73.
CARROLL, J. A.	1928	*M.N.*, **88**, 548.
	1933	*Ibid.*, **93**, 478, 680.
CARROLL, J. A., and INGRAM, L. J.	1933	*M.N.*, **93**, 508.
CHANDRASEKHAR, S.	1934	*M.N.*, **94**, 14, 726.
	1949	*Ap. J.*, **110**, 329.
	1952	*Pub. A.S.P.*, **64**, 98.
	1957	*Daedalus*, **86**, 323.
CHANDRASEKHAR, S., and MÜNCH, G.	1950	*Ap. J.*, **111**, 142.
COLACEVICH, A.	1937	*Mem. Astr. Soc. Italy*, **10**, 163.
	1939	*Rend. R. Accad. Lincei* (6), **29**, 585.
	1942	*Ibid.* (7), **3**, 83.
COWLING, T. G.	1953	*The Sun*, ed. G. P. KUIPER (Chicago: University of Chicago Press), chap. 8.
	1957	*Magnetohydrodynamics* (New York: Interscience Publishers, Inc.).
CURTISS, R. H.	1923	*Pub. Obs. U. Michigan*, **3**, 1.
	1926	*Pub. A.S.P.*, **38**, 148.
DEUTSCH, A. J.	1952*a*	*Ap. J.*, **116**, 536.
	1952*b*	*I.A.U. Trans.*, **8**, 801.
	1955	*Pub. A.S.P.*, **67**, 342.
	1956	*Vistas in Astronomy*, ed. A. BEER (London: Pergamon Press), **2**, 1421.
DIEN, E. VAN	1948	*J.R.A.S. Canada*, **42**, 249.
DIJKE, S. E. A. VAN	1946	*Ap. J.*, **104**, 27.
EDDINGTON, A. S.	1926	*The Internal Constitution of the Stars* (Cambridge: Cambridge University Press).
	1929	*M.N.*, **90**, 54.
EDGEWORTH, K. E.	1946	*M.N.*, **106**, 470, 476, 484.
ELSASSER, W. M.	1955	*Am. J. Phys.*, **23**, 590.
	1956	*Ibid.*, **24**, 85.
ELVEY, C. T.	1929	*Ap. J.*, **70**, 141.
	1930	*Ibid.*, **71**, 221.
FERRARO, V. C. A.	1937	*M.N.*, **97**, 458.
FESSENKOV, V. G.	1949	*A.J., U.S.S.R.*, **26**, 67.

GERASIMOVIČ, B. P.	1933	*Zs. f. Ap.*, **7**, 335.
	1934	*M.N.*, **94**, 737.
	1935	*Zs. f. Ap.*, **10**, 154.
GOLDBERG, L.	1939	*Ap. J.*, **89**, 623.
	1957	*Ibid.*, **126**, 318.
GOLDSTEIN, S. (ed.)	1938	*Modern Developments in Fluid Dynamics* (Oxford: Clarendon Press), Vol. **1**, chaps. 5, 7; Vol. **2**, chap. 15.
GREENSTEIN, J. L.	1937	*Harvard Circ.*, No. 422.
	1942	*Ap. J.*, **95**, 161.
	1948	*Ibid.*, **107**, 151.
	1951	*Astrophysics*, ed. J. A. HYNEK (New York: McGraw-Hill Book Co.), chap. 13.
	1953	*Ap. J.*, **117**, 269.
	1956	*Third Berkeley Symposium on Mathematical Statistics and Probability*, ed. J. NEYMAN (Berkeley: University of California Press), p. 11.
	1958	*Encyclopedia of Physics*, ed. S. FLÜGGE (Berlin: Springer-Verlag), **50**, 161.
GREENSTEIN, J. L., and CUFFEY, J.	1954	*Pub. A.S.P.*, **66**, 187.
GREENSTEIN, J. L., and HILTNER, W. A.	1949	*Ap. J.*, **109**, 265.
HAAR, D. TER	1949	*Ap. J.*, **110**, 321.
HACK, M.	1957	*Pub. A.S.P.*, **69**, 389.
HELLERICH, J.	1922	*A.N.*, **216**, 277.
HENYEY, L. G., LELEVIER, R., and LEVÉE, R. D.	1955	*Pub. A.S.P.*, **67**, 154.
HERBIG, G. H.	1952	*J.R.A.S. Canada*, **46**, 222.
	1957	*Ap. J.*, **125**, 612.
HERBIG, G. H., and SPALDING, J. F., JR.	1955	*Ap. J.*, **121**, 118.
HOOF, A. VAN	1957	*Pub. A.S.P.*, **69**, 308.
HOOF, A. VAN, and DEURINCK, R.	1951	*Ap. J.*, **115**, 166.
HOOF, A. VAN, RIDDER, M. DE, and STRUVE, O.	1954	*Ap. J.*, **120**, 179.
HOOF, A. VAN, and STRUVE, O.	1953	*Pub. A.S.P.*, **65**, 158.
HOYLE, F., and SCHWARZSCHILD, M.	1955	*Ap. J. Suppl.*, **2**, 1.
HUANG, S.-S.	1950	*Ap. J.*, **112**, 399.
	1951	*Ibid.*, **114**, 287.
	1952	*Ibid.*, **115**, 529.
	1953	*Ibid.*, **118**, 285.
	1954	*Proc. N.S.F. Conference on Stellar Atmospheres* (Bloomington: Indiana University Press), p. 137.

HUANG, S.-S.	1955	*Ann. d'ap.*, **18**, 42.
	1957*a*	*A.J.*, **62**, 19.
	1957*b*	*Pub. A.S.P.*, **69**, 65.
	1957*c*	*Ibid.*, p. 427.
HUANG, S.-S., and STRUVE, O.	1952	*Ap. J.*, **116**, 410.
	1953	*Ibid.*, **118**, 463.
	1954	*Ann. d'ap.*, **17**, 85.
	1955*a*	*Ap. J.*, **121**, 84.
	1955*b*	*Ibid.*, **122**, 103.
	1956	*Ibid.*, **123**, 231.
HULST, H. C. VAN DE	1953	*The Sun*, ed. G. P. KUIPER (Chicago: University of Chicago Press), chap. 5.
HULST, H. C. VAN DE, and REESINCK, J. J. M.	1947	*Ap. J.*, **106**, 121.
HYNEK, J. A.	1937	*Pub. A.A.S.*, **9**, 7.
JEANS, J. H.	1926	*M.N.*, **86**, 328, 444.
	1928	*Astronomy and Cosmogony* (Cambridge: Cambridge University Press).
JENTZSCH, C., and UNSÖLD, A.	1948	*Zs. f. Phys.*, **125**, 370.
JOHN, C. E. ST., and ADAMS, W. S.	1924	*Ap. J.*, **60**, 43.
KEENAN, P. C., and MORGAN, W. W.	1951	*Astrophysics*, ed. J. A. HYNEK (New York: McGraw-Hill Book Co.), chap. 1.
KILBY, R. F.	1953	Thesis, Berkeley Astronomical Department.
KOELBLOED, D.	1953	*Pub. Astr. Inst. Amsterdam*, No. 10.
KOPAL, Z.	1956	*Ann. d'ap.*, **19**, 298.
KRAFT, R. P.	1956	*Pub. A.S.P.*, **68**, 137.
KRAT, W.	1935	*A.N.*, **256**, 101.
	1938	*A.J., U.S.S.R.*, **15**, 437.
	1940	*Poulkovo Circ.*, No. 30, p. 5.
KUIPER, G. P.	1935	*Pub. A.S.P.*, **47**, 15, 121.
	1941	*Colloque International d'Astrophysique: Les Novae et les naines blanches*, **3**, 3.
	1951	*Astrophysics*, ed. J. A. HYNEK (New York: McGraw-Hill Book Co.), chap. 8.
LAMB, H.	1932	*Hydrodynamics* (Cambridge: Cambridge University Press, reprinted New York: Dover Publications, 1945).
LEE, D. W.	1932	*Pub. Obs. U. Michigan*, **4**, 109.
LEVI-CIVITA, T.	1895	*Torino Atti*, **31**, 25.
LIEPMANN, H. W., and ROSHKO, A.	1957	*Elements of Gas Dynamics* (New York: John Wiley & Sons, Inc.), chap. 2.

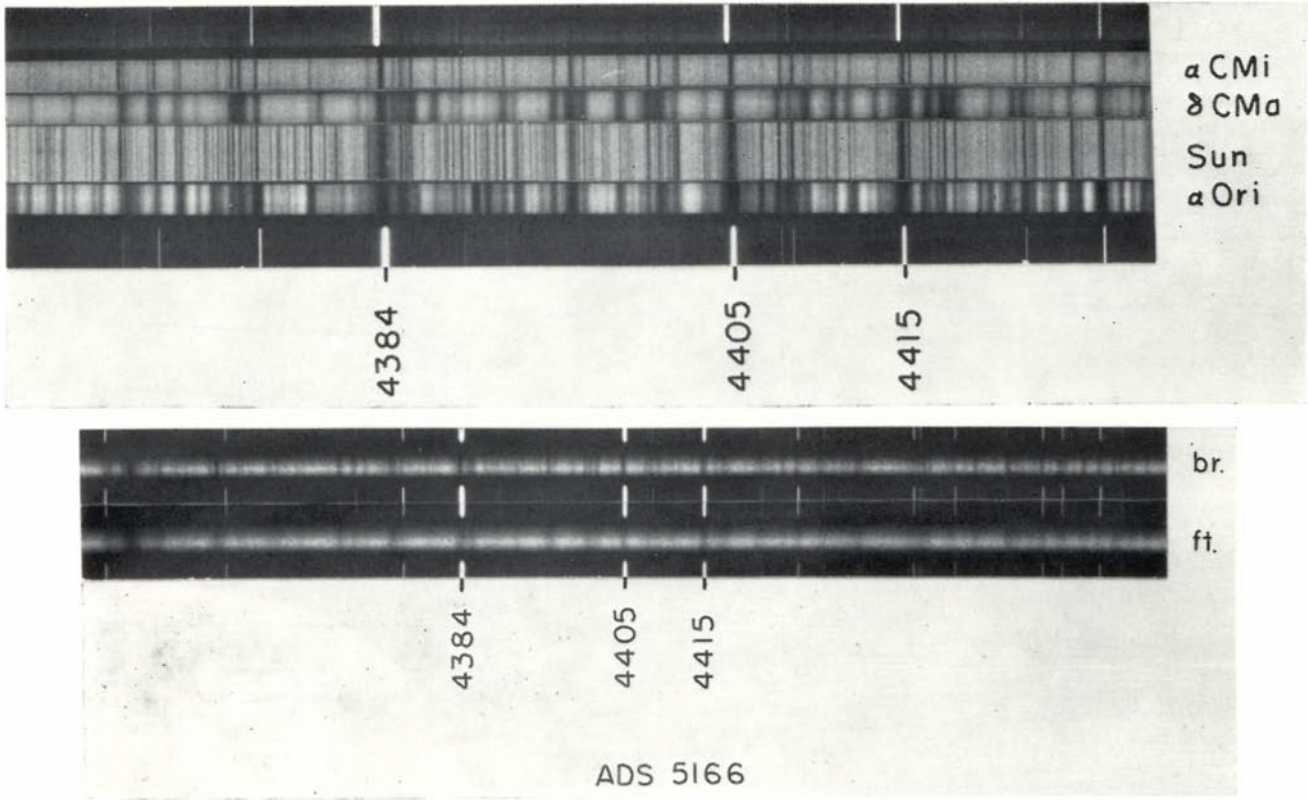


PLATE I.—The effect of physical broadening on the appearance of spectral lines. The spectra of both α Canis Minoris (Procyon) and the sun are typical of dwarf stars. The line widths in these spectra are due mainly to the thermal motion of absorbing atoms. On the other hand, δ Canis Majoris and α Orionis (Betelgeuse) can be regarded as representatives of supergiant stars. Their spectral lines are noticeably broadened by turbulence in their atmospheres.

PLATE II.—The effect of geometrical broadening on the appearance of spectra lines. Here are the spectra of two components of a visual binary star, ADS 5166 (20 Geminorum). The lines of the faint component of the binary are broadened by rotation and are characterized by their shallowness.

LIGHTHILL, M. J.	1953	*Proc. Cambridge Phil. Soc.*, **49**, 531.
	1955	*Gas Dynamics of Cosmic Clouds: A Symposium* (Amsterdam: North Holland Publishing Co.), chap. 22.
LÜST, R.	1952	*Zs. f. Naturforsch.*, **7a**, 87.
LÜST, R., and SCHLÜTER, A.	1955	*Zs. f. Ap.*, **38**, 190.
LYNDS, B. T.	1957	*Ap. J.*, **125**, 719.
LYTTLETON, R. A.	1953	*The Stability of Rotating Liquid Masses* (Cambridge: Cambridge University Press).
MCCARTHY, E. L.	1935	*Ap. J.*, **82**, 261.
MCKELLAR, A., ODGERS, G. J., ALLER, L. H., and MCLAUGHLIN, D. B.	1952	*Nature* (London), **169**, 990.
MCKELLAR, A., WRIGHT, K. O., and FRANCIS, J. D.	1957	*Pub. A.S.P.*, **69**, 442.
MCLAUGHLIN, D. B.	1924	*Ap. J.*, **60**, 22.
MCNAMARA, D. H., STRUVE, O., and BERTIAU, F. C., S.J.	1955	*Ap. J.*,, **121**, 326.
MASSEVICH, A. G.	1949	*A.J., U.S.S.R.*, **26**, 207.
MATHÈWE, L.	1937	*Contr. Inst. Ap., U. Liége*, Vol. **9**, No. 210.
MAURY, A. C.	1920	*Harvard Ann.*, **84**, 157.
MELNIKOV, O. A.	1950	*Pub. Poulkovo Obs.*, Vol. **64**, Part 2.
MENZEL, D. H.	1931	*Pub. Lick Obs.*, Vol. **17**, Part 1.
MERRILL, P. W.	1948	*Pub. A.S.P.*, **60**, 382.
	1956	*Vistas in Astronomy*, ed. A. BEER (London: Pergamon Press), **2**, 1375.
MICZAIKA, G. R., FRANKLIN, F. A., DEUTSCH, A. J., and GREENSTEIN, J. L.	1956	*Ap. J.*, **124**, 134.
MILNE, E. A.	1923	*M.N.*, **83**, 118.
MINNAERT, M.	1953	*The Sun*, ed. G. P. KUIPER (Chicago: University of Chicago Press), chap. 3.
MITCHELL, R. I.	1954	*Ap. J.*, **120**, 274.
MORGAN, W. W., and ROMAN, N. G.	1950	*Ap. J.*, **112**, 362.
MOTZ, L.	1952	*Ap. J.*, **115**, 562.
MOYAL, J. E.	1952	*Proc. Cambridge Phil. Soc.*, **48**, 329.
MÜNCH, G.	1950	*Ap. J.*, **112**, 266.
ÖHMAN, Y.	1946	*Ap. J.*, **104**, 460.
ÖPIK, E. J.	1951	*M.N.*, **111**, 278.
OGRODNIKOFF, K.	1933	*A.J., U.S.S.R.*, **10**, 135.
OKE, J. B.	1954	*Ap. J.*, **120**, 22.

OKE, J. B., and GREENSTEIN, J. L.	1954	*Ap. J.*, **120**, 384.
OORT, J. H.	1955	*Gas Dynamics of Cosmic Clouds: A Symposium* (Amsterdam: North Holland Publishing Co.), p.246.
PADDOCK, G. F.	1935	*Lick Obs. Bull.*, **17**, 99.
PANNEKOEK, A., and ALBADA, G. B. VAN	1946	*Pub. Astr. Inst. Amsterdam*, No. 6, Part 2.
PAYNE, C. H.	1930	*The Stars of High Luminosity* ("Harvard Obs. Monographs," No. 3 [New York: McGraw-Hill Book Co.]).
PAYNE-GAPOSCHKIN, C.	1957	*The Galactic Novae* (Amsterdam: North Holland Publishing Co.), chap. 3.
PETRIE, R. M.	1932	*Pub. Obs. U. Michigan*, **5**, 9.
PLASKETT, H. H.	1936	*M.N.*, **96**, 402.
POVEDA, A.	1951	*Pub. A.S.P.*, **63**, 254.
PRANDTL, L.	1952	*Essentials of Fluid Dynamics* (Glasgow: Blackie & Son, Ltd.), chap. 3.
REGEMORTER, H. VAN	1955	*Contr. Inst. Ap. Paris*, Ser. A, No. 197.
RICHARDSON, L. F.	1920	*Proc. Roy. Soc. London, A*, **97**, 354.
ROBERTS, M. S.	1957	Thesis, Berkeley Astronomical Department.
ROSSELAND, S.	1928	*M.N.*, **89**, 49.
ROSSITER, R. A.	1924	*Ap. J.*, 60, 15.
ROTTENBERG, J. A.	1952	*M.N.*, **112**, 125.
RUFUS, W. C.	1932*a*	*Pub. Obs. U. Michigan*, **4**, 101.
	1932*b*	*Ibid.*, p. 151.
SAHADE, J., and CESCO, C. U.	1946	*Ap. J.*, **104**, 133.
SANDAGE, A. R.	1955	*Ap. J.*, **122**, 263.
SANDAGE, A. R., and SCHWARZSCHILD, M.	1952	*Ap. J.*, **116**, 463.
SANFORD, R. F.	1947	*Ap. J.*, **105**, 222.
	1949	*Ibid.*, **109**, 208.
	1952	*Ibid.*, **116**, 331.
SCHLESINGER, F.	1909	*Pub. Allegheny Obs.*, **1**, 123.
	1913	*Ibid.*, **3**, 23.
SCHWARZSCHILD, K.	1910	*A.N.*, **185**, 81.
SCHWARZSCHILD, M., SCHWARZSCHILD, B., and ADAMS, W.S.	1948	*Ap. J.*, **108**, 207.
SHAJN, G.	1933	*Zs. f. Ap.*, **6**, 176.
SHAJN, G. A., and SHAJN, P. F.	1949	*Comm. Crimean Ap. Obs.*, **4**, 49.
SHAJN, G., and STRUVE, O.	1929	*M.N.*, **89**, 222.
SHAPLEY, H., and NICHOLSON, S. B.	1919	*Comm. Nat. Acad. Sci. Mt. Wilson Obs.*, **2**, 65.

SLETTEBAK, A.	1949	*Ap. J.*, **110**, 498.
	1954	*Ibid.*, **119**, 146.
	1955	*Ibid.*, **121**, 653.
	1956	*Ibid.*, **124**, 173.
SLETTEBAK, A., and HOWARD, R. F.	1955	*Ap. J.*, **121**, 102.
SMITH, B., and STRUVE, O.	1944	*Ap. J.*, **100**, 360.
SPITZER, L., JR.	1939	*Ap. J.*, **90**, 494.
	1957	*Ibid.*, **125**, 525.
STEEL, H. R.	1945*a*	*Ap. J.*, **102**, 43.
	1945*b*	*Ibid.*, p. 429.
STRÖMGREN, B.	1939	*Ap. J.*, **89**, 526.
	1952	*A.J.*, **57**, 65.
STRUVE, O.	1930	*Ap. J.*, **72**, 1.
	1931*a*	*Ibid.*, **73**, 94.
	1931*b*	*Observatory*, **54**, 80.
	1932	*Proc. Nat. Acad. Sci.*, **18**, 585.
	1937	*Ap. J.*, **86**, 198.
	1941	*Ibid.*, **93**, 104.
	1945	*Pop. Astr.*, **53**, 201, 259.
	1946	*Ap. J.*, **104**, 138.
	1948*a*	*A.J.*, **54**, 50.
	1948*b*	*Ap. J.*, **107**, 327.
	1948*c*	*Ibid.*, **108**, 154.
	1949	*M.N.*, **109**, 487.
	1950	*Stellar Evolution* (Princeton: Princeton University Press).
	1951*a*	*Pub. A.S.P.*, **63**, 82.
	1951*b*	*Ibid.*, p. 138.
	1951*c*	*A.J.*, **56**, 114.
	1951*d*	*Astrophysics*, ed. J. A. HYNEK (New York: McGraw-Hill Book Co.), chap. 3.
	1952*a*	*Pub. A.S.P.*, **64**, 117.
	1952*b*	*Ibid.*, p. 180.
	1954	*Ibid.*, **66**, 329.
	1955*a*	*Ibid.*, **67**, 135.
	1955*b*	*Ibid.*, p. 173.
	1957	*Non-stable Stars*, ed. G. H. HERBIG (Cambridge: Cambridge University Press), p. 93.
STRUVE, O., and ELVEY, C. T.	1930	*Ap. J.*, **71**, 136.
	1931	*M.N.*, **91**, 663.
	1934	*Ap. J.*, **79**, 409.
STRUVE, O., and FRANKLIN, K. L.	1955	*Ap. J.*, **121**, 337.

STRUVE, O., and HUANG, S.-S.	1957	*Occasional Notes R. Astr. Soc.*, **3**, 161.
	1958	*Encyclopedia of Physics*, ed. S. FLÜGGE (Berlin: Springer-Verlag), **50**, 243.
STRUVE, O., MCNAMARA, D. H., and ZEBERGS, V.	1955	*Ap. J.*, **122**, 122.
STRUVE, O., and ZEBERGS, V.	1955	*Ap. J.*, **122**, 134.
SUTTON, O. G.	1955	*Atmospheric Turbulence* (New York: John Wiley & Sons), chap. 6.
SWEET, P. A.	1950*a*	*M.N.*, **110**, 69.
	1950*b*	*Ibid.*, p. 548.
	1957	Private discussions.
SWINGS, P.	1936	*Zs. f. Ap.*, **12**, 40.
SWINGS, P., and CHANDRASEKHAR, S.	1936	*M.N.*, **96**, 883.
SWINGS, P., and STRUVE, O.	1940	*Ap. J.*, **91**, 546.
THOMAS, R. N.	1955	*I.A.U. Trans.*, **9**, 755.
UNDERHILL, A. B.	1947	*Ap. J.*, **106**, 128.
	1948	*Ibid.*, **107**, 349.
UNSÖLD, A.	1929	*Ap. J.*, **69**, 209.
	1941	*Zs. f. Ap.*, **21**, 22.
	1955	*Physik der Sternatmosphären* (2d ed.; Berlin: Springer-Verlag).
UNSÖLD, A., and STRUVE, O.	1949	*Ap. J.*, **110**, 455.
VITENSE, E.	1953	*Zs. f. Ap.*, **32**, 135.
VOIGT, H.-H.	1952	*Zs. f. Ap.*, **31**, 48.
WALKER, M. F.	1956	*Ap. J. Suppl.*, **2**, 365.
WALRAVEN, T.	1948	*Pub. Astr. Inst. Amsterdam*, No. 8.
WASIUTYŃSKI, J.	1946	*Astrophysica Norvegica*, **4**.
WEAVER, H. F.		"A Physical Model of Nova Aquilae 1918," unpublished.
WEHLAU, A. W., and WEHLAU, W. H.	1956	*Pub. A.S.P.*, **68**, 358.
WEHLAU, W. H.	1955	*Ap. J.*, **121**, 77.
	1956	*Ibid.*, **123**, 34.
WEIZSÄCKER, C. F. VON	1944	*Zs. f. Ap.*, **22**, 319.
	1947	*Ibid.*, **24**, 181.
	1948	*Zs. f. Naturforsch.*, **3a**, 524.
WESTGATE, C.	1933	*Ap. J.*, **77**, 141; **78**, 46.
	1934	*Ibid.*, **79**, 357.
WHITNEY, C., and STONE, P.	1957	*A.J.*, **62**, 149.
WIJK, U. VAN	1957	*A.J.*, **62**, 148.

WILSON, O. C.	1935	*Ap. J.*, **82**, 233.
	1948	*Ibid.*, **107**, 126.
	1954	*Proc. N.S.F. Conference on Stellar Atmospheres* (Bloomington: Indiana University Press), p. 147.
	1957	*Ap. J.*, **126**, 525.
WILSON, O. C., and ABT, H. A.	1954	*Ap. J. Suppl.*, **1**, 1.
WILSON, O. C., and BAPPU, M. K. V.	1957	*Ap. J.*, **125**, 661.
WRIGHT, K. O.	1946	*J.R.A.S. Canada*, **40**, 183.
	1947	*Ibid.*, **41**, 49.
	1948	*Pub. Dom. Ap. Obs. Victoria*, **8**, 1.
	1950	*Ibid.*, p. 281.
	1955	*I.A.U. Trans.*, **9**, 739.
WRIGHT, K. O., and DIEN, E. VAN	1949	*J.R.A.S. Canada*, **43**, 15.
WRUBEL, M. H.	1950	*Ap. J.*, **112**, 424.
ZEIPEL, H. VON	1924	*M.N.*, **84**, 665.

CHAPTER 9

The Spectra of Supergiants and Cepheids of Population I

ROBERT P. KRAFT*
Goethe Link Observatory, Indiana University

§ 1. INTRODUCTION

In the eighty years that have elapsed since August Ritter (1879) suggested pulsation as the basic cause of cepheid variability, no completely satisfactory explanation of this complex phenomenon has been found. During the early years of this century, which were characterized by a more rapid growth of techniques in stellar spectroscopy than in the other astronomical fields, a body of observational evidence, consisting largely of radial velocities, was assembled which tended to support the pulsation picture in its broad outlines. Eddington's (1930) elegant treatment of the problem of adiabatic pulsation, in particular, spelled the doom of the older binary hypothesis, though annoying difficulties, such as the phase lag between light and displacement, remained. Eddington himself (1941, 1942) dealt with this problem by showing that a modification of the boundary conditions near the surface of the star (the introduction of a region of convective energy transport) might give the observed phase relation between light and displacement. Schwarzschild (1935, 1938), however, suggested that standing waves in the interior might become running waves near the surface, and he showed that the flux must, of necessity, be in phase with the velocity and not with the displacement.

With the possible exception of Eddington's treatment of 1941–1942, it has generally been supposed that the origin of the "pulsations" is to be found in some variation of the flux near the central regions of the star. One imagines that the collapse of the star triggers, deep in the interior, thermonuclear reactions which are highly temperature-sensitive. The increased energy output

* Now at the Mount Wilson and Palomar Observatories.

then gives birth to the new cycle, etc. Such a picture seemed reasonable until recent developments in our understanding of the interior structure of red giants led to difficulties with the damping time for the pulsations (Cox 1956). As long as it was supposed that the cepheids were polytropes of some index, the damping time for the pulsations was of the order of thousands of years (Eddington 1930). The red giant models of cepheids which seem to be required by modern theories of evolution suggest damping times of only a few days. Some progress has been made in predicting the period-luminosity relation from the assumption of a $\pi/2$ phase lag between light and displacement and from the physical properties of the He II convection zone (Cox and Whitney 1958; Cox 1959; Zhevakin 1959).

Apart from these theoretical considerations, progress in our understanding of the cepheid phenomenon has developed recently with the recognition that certain cepheids belong to galactic clusters (Irwin 1955; van den Bergh 1957; Kraft 1957*d;* Kholopov 1958). These studies enable one to assign rough ages to the cepheids and to suggest that the cepheid phenomenon is a transitory disturbance in the life of a supergiant as it evolves across the top of the HR diagram. It is possible that these evolutionary considerations, together with theoretical work on the outer envelopes of supergiants, will give a solution to the basic problem of why a non-variable star becomes a cepheid.

In view of the foregoing considerations, it would seem profitable to compare the spectroscopic properties of cepheids, on the one hand, and the "non-variable" supergiants, on the other. It has often proved to be the case that studies of variable stars give insight into the properties of non-variable stars. For example, the enormous size of supergiant stars was confirmed by the time for travel of a sound wave (essentially the period of a cepheid) through a distance the order of the radius. Two important spectroscopic features of non-variable supergiants are (1) the H and K emission lines (Wilson and Bappu 1957) and (2) the increase in the width of the absorption lines with increasing luminosity (Herbig and Spalding 1955). As we shall see, both these features exist in the spectra of the cepheids. However, the phenomena are "steady" in the former and time-dependent in the latter. It is possible that this time dependence may permit an interpretation of the effect in the non-variable stars.

At the same time, the cepheids are recognized tools of galactic research, and it is important that their gross spectroscopic properties—i.e., spectral types and luminosities—be understood in terms of a sequence of spectral types and luminosities among the non-variable stars. For example, the spectra of the classical cepheids are known to be peculiar at maximum light (Struve 1944), and the peculiarity is the more pronounced, the longer the period. On the other hand, there is some photometric evidence (Gascoigne and Eggen 1957) that the cepheids have nearly the same colors at maximum, independent of period. This result is somewhat puzzling. Taken at face value, it implies that the peculiarities of the spectrum cannot have much to do with the excitation temperature

or degree of ionization of the cepheid atmosphere. Thus it is important that spectrograms of the highest possible dispersion of representative cepheids of different period be compared with normal non-variable stars.

There is, finally, the observational evidence concerning the pulsation theory itself. This problem can perhaps be stated in another way. Recent studies of cepheids in clusters, of the envelopes of supergiants, and of the slight variability of non-cepheid supergiants (Abt 1957*a*) leave little doubt that the idea of pulsation is basically correct, even though the central regions of the star may not be directly involved. What is accessible to observation is the way in which the pulsation manifests itself in the outer layers of the star. One may ask, for example: Is the spectroscopic behavior of the outer layers consistent with the idea of a running wave, as suggested by Schwarzschild? Or are the observations more nearly compatible with Pannekoek's (1946) suggestion that shells are ejected at maximum light?

In the present chapter I do not propose to offer definitive solutions to these problems or to those in the preceding paragraphs. Indeed, more questions may be raised than answered. However, it is possible to find from spectroscopic observations some sign posts that may guide us in placing the cepheids in proper perspective with respect to their non-variable neighbors in the HR diagram.

§ 2. THE CEPHEID SPECTRUM AS A GALACTIC RESEARCH TOOL; CRITIQUE OF THE ANALYSIS OF CEPHEID SPECTRA AT LOW DISPERSION

In a fundamental paper Struve (1944) has described the cyclical variation of the spectra of seven classical cepheids with periods between 5 and 17 days. Moderately low dispersion (76 A/mm at Hγ) was employed, typical of that used for spectral classification, and the types were those of the MKK system. The results, which were later confirmed and extended by Code (1947), were essentially as follows:

1. At minimum light the spectra of cepheids are nearly normal and, as a function of period, show a systematic increase in luminosity from class II to class I*a*. Most cepheids, i.e., those with periods between 4 and 25 days, belong to luminosity class I*b*.

2. With increasing period, the spectra at minimum light are of later type.

3. The spectral types at maximum light are nearly the same, ranging from F5 to F8, with increasing period.

4. The spectra at maximum light (or, perhaps, a short interval before maximum) are, however, not normal. The types are based primarily on the appearance of the G band and the ratios of intensities of Fe I and Fe II lines. The hydrogen lines are much too strong, the Ti II lines are conspicuously enhanced, and the Fe II lines are slightly strengthened in comparison with MKK standards in the range F5 I*b*–F8 I*b*. These peculiarities are almost absent in the cepheids

of short period (~5 days) but become increasingly conspicuous with increasing period.

The results were summarized in the well-known diagram by Code (1947) (Fig. 1), and the spectra were reproduced in a paper by Struve (1945).

Code emphasized the importance of these results for problems in galactic research. If the spectra of all cepheids were essentially the same at maximum light, then the measurement of the colors of (presumably) unreddened nearby cepheids would permit the assignment of normal colors to all cepheids. Consequently, the measured color of any cepheid would immediately give an estimate of its color excess, and this, together with its luminosity estimated from the period-luminosity law, would give the distance.

The main drawback to this approach would seem to be the uncertain relation between the "peculiarities" and the period. The peculiarities themselves

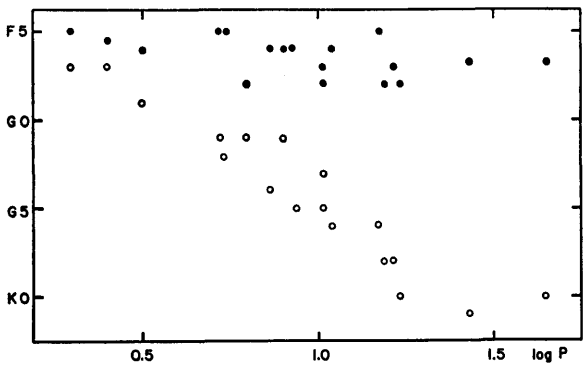


FIG. 1.—The spectral types of cepheids at maximum and minimum light as a function of period (courtesy A. D. Code). Filled circles correspond to maximum, open circles to minimum light.

might indicate a significant change in the color, and Struve emphasized that it was probably safer to use the spectra at minimum light rather than at maximum. It may well have been these peculiarities that led Eggen (1951) to attach little significance to the fact that "the constancy of spectral type at maximum, suggested by Code, is not matched by the colors." Eggen found an increase ΔC_p of about 0.4 mag. from $P = 4$ days to $P = 16$ days. Recent investigations (Stibbs 1956; Gascoigne and Eggen 1957; Kron and Svolopoulos 1959) make it appear quite certain, however, that Eggen originally underestimated the reddening of the longer-period cepheids, and the near-constancy of color with period at maximum light is fairly well established.

Nevertheless, we are left with unexplained spectral peculiarities that demand an astrophysical explanation. Struve suggested that these effects might be taken as observational evidence in support of Pannekoek's (1946) hypothesis that cepheids perform a relaxation oscillation, i.e., that they are a mild form

of the nova phenomenon. At minimum light the cepheid is to be thought of as normal; at maximum light it develops an extended atmosphere and perhaps ejects a shell. The hypothesis was regarded as particularly attractive, since it afforded a means of dissipating the pulsation energy by actual ejection of material. Evidence in support of this proposal was found in the fact that shell spectra usually have strong hydrogen lines and high-luminosity characteristics, such as the enhancement of the lines of ionized metals, e.g., Ti II.

Recent work on the spectra of cepheids with high dispersion (~10 A/mm) gives, in my opinion, a reasonable, though rather unexpected, explanation of

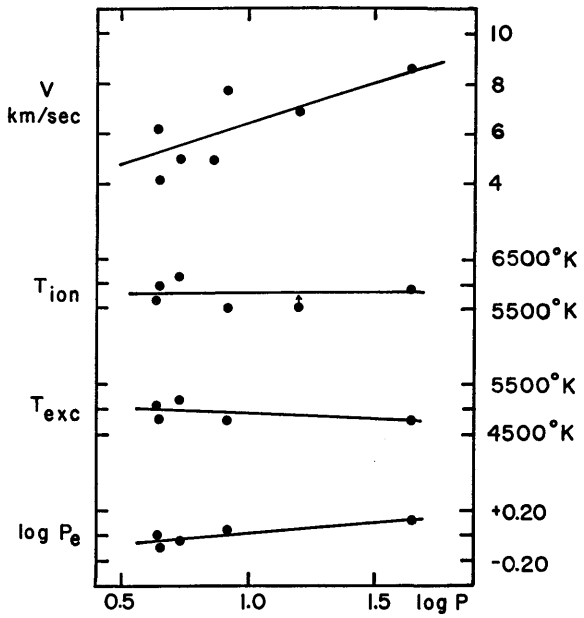


FIG. 2.—T_{exc}, T_{ion}, and log P_e at maximum light as a function of period, P, in cepheids; mean value of turbulent velocity as a function of P.

these spectral anomalies and shows why they bear no direct relationship to the colors. The results also offer no direct support for Pannekoek's suggestion.

First, if the intrinsic colors and spectral types of cepheids at maximum light were constant and independent of period, as Gascoigne and Eggen (1957) and Code (1947) suggest, one might expect the ionization temperatures, excitation temperatures, and electron pressures also to be independent of period. In Figure 2 these quantities (at maximum light) are plotted as a function of period for the six classical cepheids, T Vul and S Sge (Lüst-Kulka 1954), FF Aql (Hack 1955), δ Cep (Walraven 1948), X Cyg (Abt, unpublished), and SV Vul (Kraft, Camp, Fernie, Fujita, and Hughes 1959). The T_{ion} for X Cyg was actually determined at phase 0P18 and is therefore only a lower bound to the

T_{ion} at maximum light. Moreover, the temperature determinations of Schwarzschild, Schwarzschild, and Adams (1948) for η Aql were omitted because the zero points of the ionization and excitation temperatures were not determined directly from the spectra of the cepheid and are therefore inconsistent with the other determinations. (The results for T_{ion} and P_e are actually in excellent agreement with the other stars.) While the number of stars involved is admittedly small, the location of the 16- and 45-day cepheids in Figure 2 are altogether consistent with the constancy at maximum light of spectral type and color.

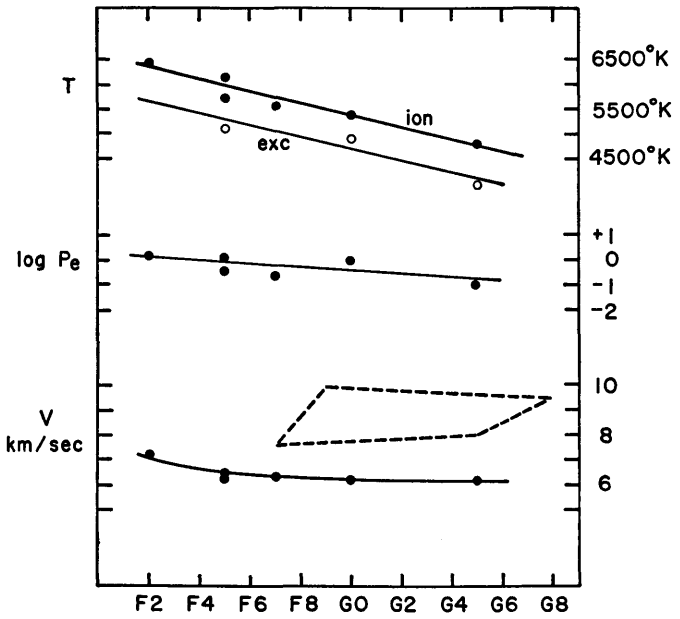


FIG. 3.—T_{exc}, T_{ion}, and log P_e for non-variable supergiants as a function of spectral type. The dashed line represents the variation of V in SV Vul at four phases. Reading counterclockwise and starting in the lower left-hand corner, we have maximum light, maximum radius, minimum light, and minimum radius, respectively.

An additional test may be made of the absolute assignment of the spectral types of cepheids at maximum light. One may inquire, for example, how it is possible to assign unambiguously spectral types of F5–F8, if the great strength of the hydrogen lines suggests an earlier type. It is well to remember that the original Draper classes for cepheids near maximum light were earlier than F5, in general, because the Harvard workers were impressed (on objective-prism plates) by the great strength of these lines. In Figure 3 are plotted T_{ion}, T_{exc}, and log P_e for a number of non-variable stars of luminosity class I*b* as a function of spectral type on the MK system. The method of analysis is by curves of growth and in all cases follows the treatment by Greenstein (1948). The data

were obtained from the following sources: α Per (Greenstein 1948); ν Aql, 35 Cyg, and HR 690 (Abt 1958); and β Aqr and 9 Peg (Kraft *et al.* 1959). Since log P_e shows almost no variation with spectral type in this range, the T_{ion}- and T_{exc}-curves were entered with the values of these quantities for the five cepheids T Vul, FF Aql, δ Cep, S Sge, and SV Vul, the data being taken from Figure 2. In this way the temperatures of the normal supergiants were used to calibrate the spectral types of the cepheids at maximum light. The results are shown in Table 1, in which the determination from T_{ion} has been given twice the weight of that from T_{exc}. In no case is the spectral type of a cepheid earlier than F4, and satisfactory agreement is found with the spectral types given by Code (1947) for three of these stars. It must be admitted, however, that the agreement in the case of SV Vul may be a little fortuitous, since the star is of class I*ab* rather than I*b*.[1]

TABLE 1

SPECTRAL TYPES OF CEPHEIDS AT MAXIMUM LIGHT

Star	T_{ion}	T_{exc}	Weighted Mean	Code (1947)
T Vul	F7.5	F7	F7.5	.....
FF Aql	F5	F8.5	F6	.....
δ Cep	F4	F6	F5	F5
S Sge	F9	F9	F9	F6
SV Vul	F6	F8.5	F7	F7

These results are therefore in complete agreement with Code's and suggest that the peculiarities in the spectrum at, or before, maximum light cannot be sought in an ionization or excitation effect, unless there is some unusual stratification effect in the cepheids, not shared by the normal supergiants, which might not be detected by conventional curve-of-growth analysis. High-dispersion studies of long-period cepheids show, however, that these peculiarities probably arise from mass motions of an unusual sort in the cepheid atmospheres. In X Cyg (P = 16.4 days), the writer (1956) discovered doubling of many of the low-excitation lines of Ti II (the same lines described as "enhanced" by Struve) and of the zero-volt lines of Fe I shortward of K (these could not have been well exposed on Struve's spectrograms) at phase 0$^{\text{p}}$.82. This doubling persists as a bona fide splitting or widening, at least to phase 0$^{\text{p}}$.85 (Kraft 1957*a*), after which it is conspicuously wide (incipient doubling?) until after maximum light. The profiles of Hβ (Abt, unpublished) do not remind one of hydrogen lines in shell spectra: they are wide and steep-sided but relatively shallow, hav-

[1] Dr. Helmut Abt (private communication) informs me that some unpublished excitation temperatures determined by him for four non-variable F stars indicate that my T_{exc} curve in Fig. 3 may be too high by 100° at F5. This will have the effect of making the spectral types of cepheids in Table 2 determined from T_{exc} at most 0.1 spectral class earlier.

ing central intensities of about 20 per cent. They suggest that there are either two or more unresolved components or possibly a single wide line filled in by emission. Very similar effects have been found by Sanford (1956) in T Mon (P = 27.0 days) and SV Vul (P = 45.1 days). No genuine splitting of the Ti II and low-excitation Fe I lines was found, but an intercomparison of the spectra of these stars with those of X Cyg convinces the writer that the same effect of widening (incipient doubling?) is present in all three stars in varying degree. Sanford finds that the lines of Ti II are particularly wide from phase 0^{p}87 to 0^{p}01 in T Mon and from phase 0^{p}89 to 0^{p}00 in SV Vul; in the former star, Hβ, Hγ, and Hδ are particularly wide from phase 0^{p}93 to 0^{p}18; in the latter from phase 0^{p}89 to 0^{p}22. No splitting of Hα has been found in these two stars, but very few spectrograms were obtained in the red by Sanford and, judged by the results in X Cyg, not at the most likely phases for uncovering the effect. It may also be mentioned that Hα splitting was found by the author (1957*a*) in TT Aql (P = 13.8 days) and WZ Sgr (P = 21.8 days) at phases similar to those found for doubling in X Cyg.

We can perhaps summarize these observations in the following way: Among the best-studied cepheids of long period ($P > 10$ days), during an interval on the rising branch of the light-curve, lines of Ti II and hydrogen and, to a lesser extent, Sr II and Fe II become conspicuously widened, and their equivalent widths are increased. This widening is probably not an ionization or excitation effect because (1) in the metallic lines it is not symmetrical with respect to the time of bluest color (maximum light) and (2) it becomes a genuinely resolved doubling of Ti II in at least one of the stars and a genuine doubling of Hα in three of them. At the same time, all the lines in the spectrum become somewhat wider, though their equivalent widths are not conspicuously increased (see § 4). The widening moves closer to the time of maximum light with increasing period. Moreover, the profiles of the hydrogen lines do not suggest the development of a shell spectrum, since the detailed behavior of the doubling consists of the development of *longward*-displaced cores and therefore must be associated with collapsing, rather than expanding, material.

Another argument against the development of a shell spectrum at maximum light, at least among the metallic lines, is found by comparing the mean deviation from the curve-of-growth of Fe I lines arising from non-metastable with those arising from metastable levels. A test of this sort can be carried out from the spectrograms studied by Kraft *et al.* (1959) for phase 0^{p}99 in SV Vul, which, since it is virtually the longest-period cepheid known, provides a particularly good test. Let $\log X_f'''$ be the line strength that an Fe I line ought to have for a given measured value of $\log W/\lambda$ (i.e., the value taken from the curve of growth), and $\log X_f''$ be the actual value. Define

$$S = \log X_f''' - \log X_f'' .$$

Let the average value of S be determined for lines arising from both metastable and non-metastable levels. The mean difference in the values of S for ten non-metastable and twenty-six metastable lines was -0.15 ± 0.06 (p.e.) in SV Vul, in the sense non-metastable *minus* metastable. This is to be compared with the value -0.11 ± 0.06 (p.e.) found by Greenstein (1949) for five F stars of different luminosity classes. I conclude, therefore, that there is no evidence in favor of the development of a shell spectrum at maximum light in SV Vul in excess of that present in typical non-variable F-type stars. A similar test of the spectrum of X Cyg (Kraft 1955) near maximum radius, phase $0^{p}45$ (defined by integration of the radial velocity-curve), rather than near maximum light yielded a difference of -0.16; again this is not significantly different from that of the normal F-type stars.

We summarize this section as follows: The physical parameters of the cepheid atmospheres at maximum light, viz., T_{exc}, T_{ion}, and log P_e are very similar to those of normal F5 I*b* to F7 I*b* stars, no matter what the period may be. Thus the color of cepheids at maximum light ought to be nearly constant as a function of period. The spectroscopic anomalies that become more pronounced with increasing period, viz., the enhancement of Ti II and hydrogen, probably result from mass motions in the atmosphere and are not related to excitation or ionization effects. These mass motions require spectrograms of high dispersion for their detection and might therefore be mistaken for a temperature or pressure effect on spectrograms taken for spectral classification purposes. There is no evidence in favor of the hypothesis that cepheids develop expanding or stationary shells at maximum light (see Appendix I).

§ 3. HIGH-DISPERSION STUDIES: ROTATION AND TURBULENCE IN SUPERGIANTS AND CEPHEIDS

The existence of small-scale turbulence as revealed by curve-of-growth studies is a well-known and well-established feature of supergiant stars of late spectral type and need not be commented on extensively here. These microturbulent velocities for a number of F-type (Greenstein 1948; Abt 1958) and G-type stars of class I*b* (Kraft *et al.* 1959) are plotted as a function of spectral type in Figure 3. The microturbulent velocities of cepheids are not constant throughout the cycle; the largest variation known at present is that for SV Vul (Kraft *et al.* 1959), about 30 per cent. These variations make it difficult to assign a definite value of V to each cepheid; except for δ Cep (Walraven 1948) and η Aql (Van Hoof and Deurinck 1952), we do not have a complete record of the variation throughout the cycle. Consequently, in the plot of V versus log P of Figure 2, I have simply taken a mean for each star of those determinations which are available. Ideally, we would want a time average over the cycle. Nevertheless, it is possible to draw some fairly definite conclusions from Figure 2. First, the mean value of V for the six cepheids of class I*b* (SV Vul is of class I*ab*) is 5.9 km/sec, a value in quite good agreement with the mean V for the six

non-variable F and G stars of class I*b*, viz., 6.5 km/sec. Second, the microturbulent velocities for cepheids increase with increasing period, i.e., with increasing luminosity. This is in agreement with the results obtained for individual stars of luminosity class I*a*. For example, in δ CMa (F8 I*a*), Huang and Struve (1952) found a mean microturbulent velocity of about 10 km/sec (actually, V increased with decreasing excitation potential from 3.9 to 15.0 km/sec), and in ϵ Aur (F0 I*a*) Wright and Miss Van Dien (1949) found a mean velocity of about 10 km/sec as well. (Actually, it increased in the same sense from 2 to about 20 km/sec.) It is true that Wright (1947) found a similar, though much less pronounced, variation of V with excitation potential in α Per; however, it is the average value of V which concerns us here.

Numerous studies have indicated that these microturbulent velocities derived from curves of growth are insufficient to explain the shapes and widths of the lines. Various forms of large-scale mass motion have to be invoked, usually large-scale turbulence or rotation. Huang and Struve (1952), for example, found that a macroturbulent velocity of about 6.5 km/sec was needed, in addition to the microturbulence mentioned in the preceding paragraph, to explain the line profiles in δ CMa. Wright and Miss Van Dien (1949) suggested macroturbulent velocities of more than 30 km/sec for all lines of ϵ Aur. Schwarzschild *et al.* (1948) proposed that large-scale masses of gas, moving with velocities of 12 km/sec, could not only explain the line profiles of the cepheid η Aql but remove the (then existing) discrepancy between the spectroscopic and dynamical gravities. On the other hand, various investigators (Schwarzschild *et al.* 1948; Huang and Struve 1953; Huang 1957; Abt 1958) have pointed out that certain types of large-scale motions (rising and falling eddies) produce line profiles that are virtually indistinguishable from rotation. In view of the fact that modern evolutionary theories suggest that the progenitors of the present late-type supergiants are main-sequence B stars, which are known to have rapid rotations, some residual rotation might be expected in these supergiants. It would seem that the most likely way of clarifying the situation for a particular line in a given star would be as follows: (1) calculate from the curve-of-growth parameters the line profile to be expected; (2) broaden this profile by some suitable function corresponding to rotation, large-scale radial motions, etc.; (3) test, by means of some evolutionary track, the consistency of the derived rotational velocity with the rotational velocity of the main-sequence progenitor.

Investigations of this type have been carried out by Abt (1957*b*) for stars of luminosity class II, using the evolutionary tracks computed by Sandage and Schwarzschild (1952). Two kinds of assumptions were made: (1) the star conserves its angular momentum in shells as it evolves (case B); (2) free transfer of angular momentum occurs (rigid-body rotation) (case A). In the first case, the change in rotational velocity is inversely proportional to change in the radius; in the second, the change in rotational velocity is more complicated but has been calculated by Oke and Greenstein (1954) for the Sandage-Schwarz-

schild models. In general, for ratios of final to initial radius greater than 5, the rigid-body rotation results in velocities about twice as large as that for differential rotation for a given initial value of $v \sin i$. Abt finds that the stars of class II originated from the main sequence at about B7.5. According to Slettebak and Howard (1955), the mean value of $v \sin i$ for main-sequence stars of types B5–B7 is 203 km/sec; for B8–A2 stars, the mean value is 152 km/sec (Slettebak 1954). From the excellent agreement between the observed and rotationally broadened line profiles of λ 4508 of Fe II for these bright giants, Abt predicts that these stars had mean projected rotational velocities on the main sequence of 76 ± 15 km/sec for case A and 162 ± 31 km/sec for case B. The latter is in excellent agreement with the observed value. This suggests that the line profiles of bright giants can be explained completely by microturbulence from the curve of growth and rotation, the present rotational velocities having been derived by evolution from the main sequence with angular momentum conserved in shells.

A similar investigation by Abt (1958) of the I*b* stars has led to somewhat less conclusive results. It is found that large-scale radial motions with a Gaussian velocity distribution and a dispersion of 13 km/sec will give as good a fit to the observed line profiles of α Per as rotation with $v \sin i = 20$ km/sec. However, a mean rotational velocity for twelve class I*b* stars (range A0–F8) of 17 km/sec would require their main-sequence progenitors to have projected rotational velocities of 177 km/sec in case B and 77 km/sec in case A. The former value is in excellent agreement with the 157 km/sec given by Slettebak and Howard (1955) for main-sequence stars at B2.5. Consequently, while the existence of large-scale turbulence in I*b* A–early F stars cannot be ruled out altogether, it appears to be unnecessary to invoke its presence in light of current evolutionary considerations.

Among the stars of still higher luminosity, however, the situation is quite confused. Interpreting formally the line breadths of supergiants as due to rotation, Herbig and Spalding (1955) found that the mean projected rotational velocity of F0–G5 stars of class I*b* was "$\leq$20 km/sec," whereas the mean value for six I*a* supergiants was 28 km/sec. Abt (1957*b*) has plotted the half-half-widths of λ 4508 of Fe II as a function of M_v for a group of thirty-eight bright giant and supergiant stars of types A and F. From class I*b* to I*a* ($M_v = -4.5$ to -8.5) the half-half-width increases from about 0.25 to 0.45 A. This diagram is reproduced in Figure 4, together with the half-half-widths of λ 4508 in β Aqr (G0 I*b*) and 9 Peg (G5 I*b*), as well as the mean half-half-width in the cepheid SV Vul (Kraft *et al.* 1959). Line widths of λ 4508 based on intensity tracings have not been given in the literature for other cepheids; however, Kraft *et al.* (1959) concluded from visual inspection of this line on 10 A/mm-dispersion Mount Wilson plates of various cepheids that the width was constant, or perhaps increased slightly with increasing luminosity.

Thus among both variable and non-variable stars there is an increase in line

width with increasing luminosity. We ask, therefore, Is the width of the lines in supergiants brighter than I*b* also consistent with the rotational velocities that would be expected as a result of evolution from the main sequence? In an attempt to find some reasonable answer to this question, I have plotted in Figure 5 a portion of the HR diagram fainter than $M_{bol} = -6$. Evolutionary tracks are drawn with an initial 1-mag. rise from the zero-age (Johnson and Hiltner 1956) main sequence, following Sandage (1958). The treatment differs slightly from that of Sandage, in that the mass-luminosity law (Kuiper 1938) is applied to the standard (Johnson and Morgan 1953) rather than zero-age main sequence, in order to allow for the evolved mixture of main-sequence stars implied in Kuiper's work. The horizontal tracks are meant to be largely schematic, but, according to Sandage, they imply a mass-luminosity law for cepheids which predicts well the observed period-luminosity (Arp 1957) and period-color (Sandage

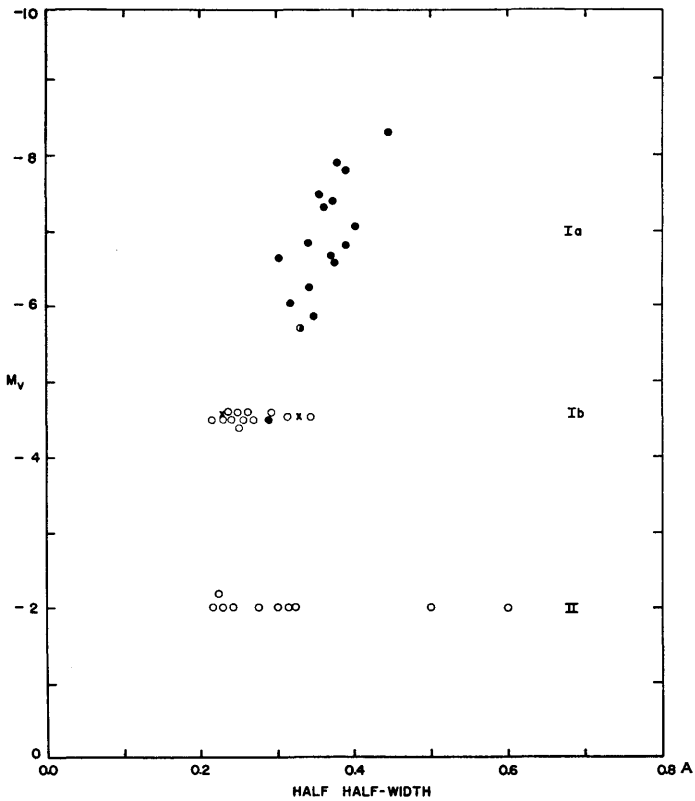


FIG. 4.—The half-half-width of λ 4508 (Fe II) in a group of supergiants (courtesy H. A. Abt). Filled circles represent stars of classes A and F whose luminosities are determined by measurements of the equivalent width of Hγ or by membership in associations; open circles represent A and F stars whose luminosities are assigned by MK types. The crosses represent β Aqr (G0 I*b*) and 9 Peg (G5 I*b*), and the half-filled circle, the cepheid SV Vul.

1958) relations when the equation $P\sqrt{\rho/\rho\odot}$ = Const. is taken as fundamental. As a check, we note that the position of α Per requires a B2.5 star for its progenitor, the location on the diagram having been found by fitting Harris' (1956) normal colors and magnitudes for the α Per association to the zero-age main sequence. Using the Sandage-Schwarzschild (1952) tracks, Abt (1957*a*) predicts main-sequence progenitors for I*b* stars (α Per included) at B2.5. It may be noted, too, that Tayler's (1954) theoretical track for a star of mass 9.9 $\odot$ agrees well with our assumed track for a star of mass 10 $\odot$. Altogether, the greatest uncertainty exists among the tracks for stars more massive than 10 $\odot$. We have not attempted to extend the diagram above $M_{bol} = -6$, since neither the main-sequence nor the rotational velocities thereon are well enough known or, indeed, the bolometric corrections. Thus we cannot expect to derive a convincing answer to our question for stars brighter than class I*ab*.

In Figure 5, I have also plotted lines of constant rotational velocity on the

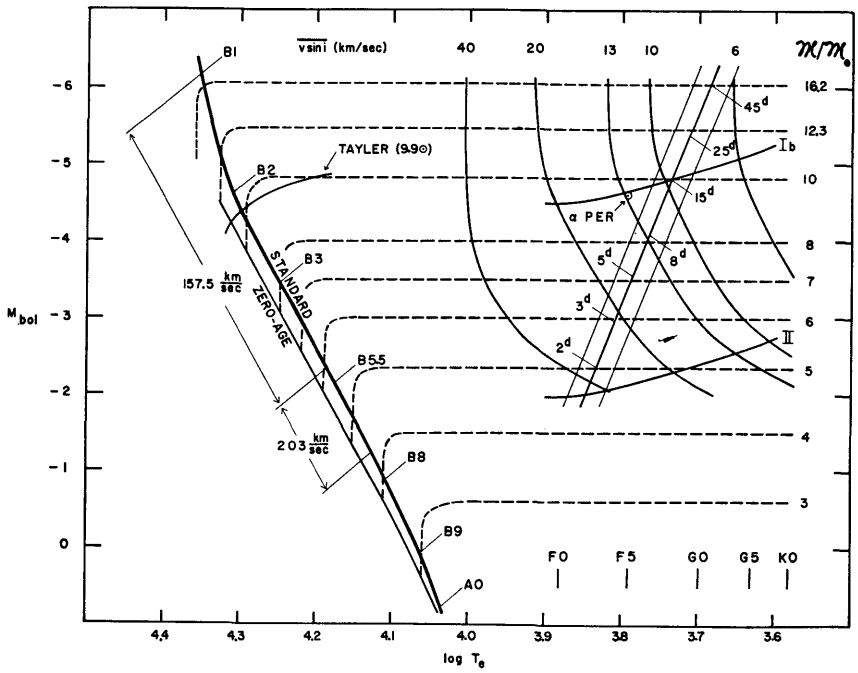


FIG. 5.—Evolutionary tracks in the HR diagram (after Sandage 1958). The position of the cepheids is that given by Sandage. The masses are assigned to the tracks according to the $\mathfrak{M}-L$ law on the standard main sequence, after Kuiper (1938). Rotational velocities on the main sequence are those of Slettebak and his associates. The lines of constant rotational velocity ($v \sin i$) assume that the angular momentum is conserved in shells. The spectral types later than F0 are assigned by the Keenan and Morgan (1951) calibration of T_e; these are slightly inconsistent with the Sandage relation of $(B-V)$ versus log T_e. Thus the spectral types assigned to the cepheids are 0.3–0.4 spectral class too early. For consistency, the Keenan-Morgan types should be moved left in the diagram about 0.3–0.4 of a spectral class.

assumption that, as evolution proceeds, the angular momentum is conserved in shells. The main-sequence projected rotational velocities from B2 to B7 are those given by Slettebak and Howard (1955). In agreement with Abt, it is found that stars between A0 and F8 of class I*b* should have projected rotational velocities between 40 and 10 km/sec. For the cepheid η Aql (P = 7.2 days), we predict $v \sin i$ = 14 km/sec. According to Schwarzschild *et al.* (1948), the line profiles of η Aql are consistent with a microturbulence of 4 km/sec and a projected rotational velocity of 15 km/sec; this may be considered in excellent agreement with our prediction. With the more luminous cepheid SV Vul (P = 45 days) (class I*ab*), however, the situation is less satisfactory. An analysis of λ 4508, almost identical with that of Abt (1958) for the I*b* stars, leads to a mean projected velocity of 24 km/sec (Fig. 6) (Kraft *et al.* 1959). This is to be compared with a predicted value of 7 km/sec. That the discrepancy is probably not due to differences in the method of analysis is shown by the fact that Kraft *et al.* derive a projected rotational velocity of 19.5 km/sec for α Per in comparison with Abt's 20 km/sec. The only other star of class I*ab* for which I find a rota-

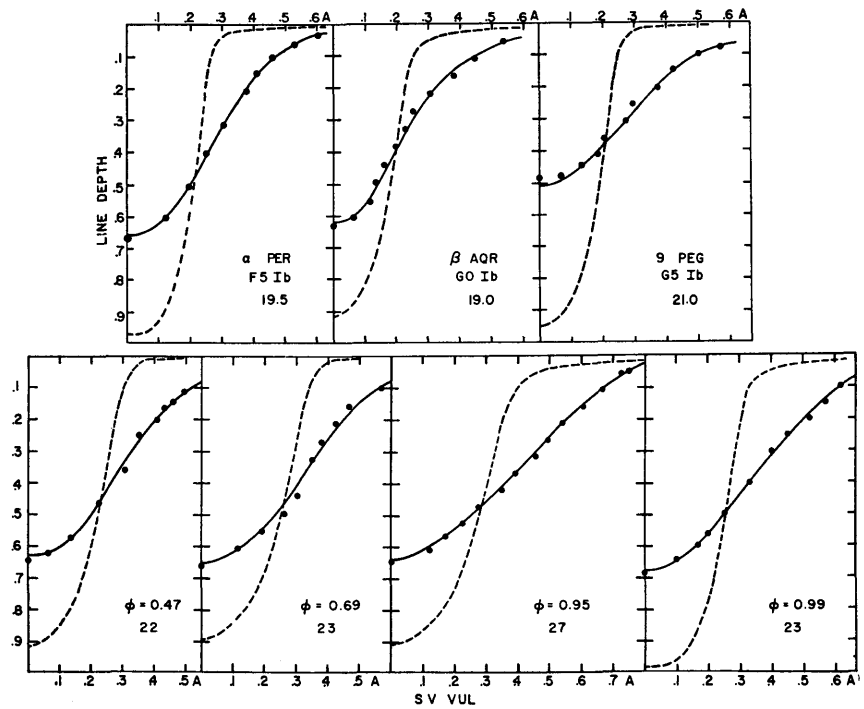


FIG. 6.—Profiles of λ 4508 (Fe II) in α Per, β Aqr, 9 Peg, and at bottom at four phases of SV Vul. The dashed lines represent profiles computed from the parameters of Table 2 by means of the IBM 650 program of M. H. Wrubel. η is taken constant, $\epsilon = 0$ and $B^{(0)}/B^{(1)} = \frac{2}{3}$. These are broadened by rotation, using Unsöld's (1938) graphical method. The projected rotational velocities are given on the diagram in km/sec.

tional velocity measured is o^1 CMa; Herbig and Spalding (1955) find $v \sin i \leq$ 20 km/sec. From Figure 5 we predict $v \sin i = 6$ km/sec for this star. Putting the case another way, if we suppose that the projected rotational velocity of SV Vul is, in fact, 24 km/sec, its main-sequence progenitor would have had $v \sin i = 540$ km/sec. The assumption of rigid-body rotation would be expected to reduce this by a factor of 2; nevertheless, it is difficult to understand how the stars of class *Ib* can differ sufficiently in internal structure from those of *Iab* that the former permit no radial transfer of angular momentum, whereas the latter transfer it freely!

There are, of course, several ways out of the difficulty, since we are discussing, at most, two stars of class *Iab* when we should have several times that many for a reasonable statistical discussion. Perhaps SV Vul and o^1 CMa were originally Be stars; on the other hand, they may have originated on the main sequence at a luminosity so high that the change in radius is considerably smaller than that we have assumed in drawing the tracks of Figure 5. For example, if SV Vul started as an O5 star with a rotational velocity of 215 km/sec, it would now have the observed value of $v \sin i$ for case B. The rotational velocity of 9 Sgr (O5), for example, is given by Slettebak (1949) as 210 km/sec. In that case, however, we would have to accept a mass of more than 40 $\odot$ (Kuiper 1938). The spectroscopic gravity of SV Vul (Kraft *et al.* 1959) at maximum radius (when the accelerations and velocities are a minimum) is 6.0 cm/sec^2; the dynamical gravity for a mass of 40 $\odot$ would be 40 cm/sec^2; a mass of 16 $\odot$ (Fig. 5) would produce more satisfactory agreement.

On the other hand, there is some observational evidence that we are dealing with a spectral-type as well as a luminosity effect, at least among *Ib* and *Iab* stars. In Figure 6 I have plotted the line profiles obtained for λ 4508 in β Aqr (G0 *Ib*) and 9 Peg (G5 *Ib*). These stars are both later than any of the *Ib* stars considered by Abt, as is SV Vul. It is found that projected rotational velocities of 19 and 21 km/sec, respectively, fit the profiles of these two non-variable stars very well. We predict from Figure 5 that $v \sin i = 10$ and 8 km/sec, respectively, if we assign M_v from the Wilson-Bappu (1957) effect. Thus we must conclude either that after the curve $v \sin i = 10$ km/sec (approximately) is crossed, stars of class *Ib* again take up rigid-body rotation or that large-scale turbulence begins to contribute appreciably to the "rotational" broadening. Again the number of stars involved is too small to make a convincing argument. Nevertheless, the profiles of SV Vul and o^1 CMa would fit in well with this hypothesis, without requiring any change in our assumed evolutionary tracks.

Against the argument that increases in macroturbulent motions accompany advancing spectral type among *Ib* and *Iab* stars is the fact that the microturbulent velocities of β Aqr and 9 Peg are not larger than those of the F-type *Ib* stars. On the other hand, the K-type supergiant components of the eclipsing systems ζ Aur (K4 II) (Wilson and Abt 1954) and 31 Cyg (cK5) (McKellar, Odgers, Aller, and McLaughlin 1952) have chromospheric regions in which

large-scale mass motions (prominence-like activity) take place. This says nothing, of course, about the existence of such motions in stars of classes II, I*b*, or I*ab* among the A and F types; unfortunately, no apparently bright stars of these types are known to be members of eclipsing binary systems similar to ζ Aur.

Turning to the stars of class I*a*, we find many cases of mass motions on a large scale. In such stars as ρ Cas (F8 I*ap*) (Bidelman and McKellar 1957), 89 Her (F2 I*a*) (Böhm-Vitense 1956), and RW Cep (G8 I*a*) (Merrill and Wilson 1956) certain spectral lines split into components, and there is evidence in favor of an expanding shell. It must not be supposed that these stars are all alike in manifesting the phenomenon; for example, in 89 Her, shortward-displaced components of hydrogen and the D lines appear; in ρ Cas, only low-excitation strong lines develop these shortward-displaced absorption cores, and hydrogen not at all; in RW Cep, three spectral components appear: very wide, stationary absorption lines, emission components in most lines, and strong, shortward-displaced absorption cores in the resonance lines of Ca I, Cr I, Mn I, and Sr II. The I*ab* star α Ori also belongs in this group; the assignment of luminosity classes in accordance with M_v rather than M_{bol} is rather misleading among the very late-type stars. Adams (1956) found evidence for a slowly expanding shell in the sharp components of the resonance lines of Mn I, Cr I, Sr II, Ca I, and certain Fe I lines.

The relationship of these mass motions to the phenomenon of macroturbulence or "large-scale" turbulence is not, however, completely clear. There is little question that the underlying absorption lines in RW Cep are wide: Merrill and Wilson estimate half-half-widths of 40 km/sec. On the other hand, according to McKellar and Bidelman, Herbig and Spalding (1955) found that "the widths of weak lines in the spectrum of ρ Cas in November, 1953, when many of the strong lines were double, were no greater, and may have been slightly less, than those of δ CMa." The strong lines that split in ρ Cas, however, are just the lines whose equivalent widths in δ CMa are so conspicuously enhanced when compared with α Per (cf. Struve 1946). The lines of δ CMa, it may be added, have never been observed as double. If macroturbulence is responsible for the line profiles in both δ CMa and ρ Cas, it would seem to have decidedly different properties as a function of height in these atmospheres. However, even if one could prove beyond doubt that macroturbulence was present in ρ Cas and was responsible for the broadening of lines, we would still have no assurance that it was also responsible for the double lines and/or the ejection of a shell.

What is known about the spectrum of δ CMa (or, perhaps more appropriate ly, what is not known), together with some speculations derived from Figure 5, may be instructive in this connection. Struve (1946) showed that the strong lines of δ CMa could not be explained by the microturbulence of Miss Steel's (1945) curve of growth. He suggested a (micro)turbulent velocity of 30 km/sec for the strong lines and Miss Steel's value of 5 km/sec for the weak lines. On

the other hand, Unsöld and Struve (1949) found that they could explain the profiles of *all* lines with a projected velocity of 30 km/sec (recall $v \sin i = 20$ km/sec for α Per). This would be in agreement with Struve's (1946) statement that the strengths and profiles of weak lines in δ CMa are not much different from those in α Per. Nevertheless, Unsöld and Struve thought it more likely that the explanation of all profiles lay in macroturbulent motions with a characteristic velocity of 22 km/sec, though the appearance of the profiles did not permit a clear-cut decision between these alternatives. Finally, in a reinvestigation of this star, Huang and Struve (1952) found that a combination of both large-scale and small-scale turbulence was necessary to explain the properties of the spectrum. The last-named investigation used the method of half-widths versus equivalent widths, which enables large-scale and small-scale motions to be separated. This comes about essentially because the reversing layer is thicker for a weak line than for a strong one, and therefore a strong line is broadened less by velocities of small elements of gas than is a weak line. (The details of this procedure are discussed in chap. 8.) It was found that the profiles could be explained by microturbulent velocities which increased with decreasing excitation potential (from 3.9 km/sec at $\chi = 3.4$ volts to 15.0 km/sec at $\chi = 0.5$ volts) and a macroturbulent velocity showing no systematic variation with excitation potential and having a mean value of 6.6 km/sec.

What is one to make of these essentially contradictory results? It seems rather obvious that the observed profiles do not permit a distinction between them; in other words, the representation is not unique. Because of this, the author wishes to advance another proposal. As I have already mentioned, not much confidence can be felt in the assignment of an evolutionary track higher than $M_{\text{bol}} = -6$ (if, indeed, that high) in Figure 5. Nevertheless, if we draw a horizontal track corresponding to $M_{\text{bol}} = -7$, we can predict the rotational velocity to be expected for δ CMa. With a B0 V star as a progenitor of this star, we predict $v \sin i = 6$ km/sec, if the mean main-sequence value is the same as that for B1 stars. Thus it is quite possible that the line profiles of δ CMa can be explained completely by microturbulence that is a function of excitation potential plus a constant rotational component, without the need for invoking macroturbulent motions at all. I do not wish to emphasize this point unduly. It is an observed fact that, among certain late-type supergiant eclipsing systems, large-scale gas motions take place in extended atmospheres. But we should remind ourselves that systems like these among the A and F supergiants are not well known (ϵ Aur is a poor example, since we cannot be sure that the gas streams do not come from the "invisible" star, which may fill the inner Lagrangian surface), and we should not uncritically embrace large-scale turbulence without first investigating rotation.

As an example of the way in which new observational data may eliminate the necessity for invoking macroturbulence, consider the analysis of η Aql by Schwarzschild *et al.* (1948). We have already mentioned that the line profiles

of this star near maximum radius are consistent with a microturbulence of 4 km/sec and a projected rotation of 15 km/sec, which is in very good agreement with the prediction obtained from Figure 5. With the mass and radius taken from Figure 5 and the latter adjusted to a value appropriate to the mid-descending branch of the light-curve, we find a dynamical gravity of 35 cm/sec^2. Following the Schwarzschild treatment, we can write, for the spectroscopic gravity,

$$g_{sp} = \frac{X}{\tau} \frac{P_k}{P_g} \frac{P_g}{P_e} P_e \frac{\kappa}{2}, \tag{1}$$

where P_k is the kinetic pressure resulting from turbulence, X is the hydrogen abundance by weight, and the other symbols have their usual meanings. For turbulence of characteristic velocity 4 km/sec, $P_k \sim P_g$, and with $X = 0.35$ and $\tau = 0.3$, we find $g_{sp} = 8$ cm/sec^2, again for a κ appropriate to the mid-descending branch of the light-curve. On the other hand, Schwarzschild *et al.* find that the line profiles are fitted as well by large-scale turbulence with a characteristic velocity of 12 km/sec and no rotation. In that case, $P_k \sim 4P_g$ ($\mu = 1.7$), and $g_{sp} = 32$ cm/sec^2. It does not seem that the discrepancy between g and g_{sp} in the first determination is sufficiently larger than the second to permit an unambiguous decision. This is more striking if we take $X = 0.75$ (solar value). (Schwarzschild's method of obtaining the hydrogen abundance is very sensitive to the assumed T_{ion}. If T_{ion} were decreased by only 200° K, the hydrogen-to-metal ratio would increase by 50 per cent.) Then $\mu = 1.2$, and we obtain

$$g_{sp} = 17 \text{ cm/sec}^2 \quad \text{(rotation plus microturbulence)},$$

or

$$g_{sp} = 24 \text{ cm/sec}^2 \quad \text{(macroturbulence)}.$$

Schwarzschild's choice of macroturbulence was, of course, a result of the old distance scale, which gave for g the dynamical value of 132 cm/sec^2, and thus, with the value $X = 0.35$, the g_{sp} from rotation and microturbulence appeared to give much too large a discrepancy.

We can summarize this section as follows: The line profiles of A and early F stars of classes II and I*b* can be explained by a combination of microturbulence (obtained from curves of growth) and rotation, in which the values of $v \sin i$ are those that would be expected if angular momentum were conserved in shells as stars evolved from the main sequence across the top of the HR diagram. The profiles of the cepheids with $P < 10$ days are probably also consistent with this hypothesis. There is some evidence that, after a star passes approximately the $v \sin i = 10$ km/sec curve in Figure 5, large-scale turbulence becomes relatively more important than rotation in broadening the lines. G- and K-type stars of class I*ab* and cepheids with $P > 10$ days may behave similarly, but the data are too scarce to make a firm statement.

Some recent considerations by Schatzman (1960) are of interest in this connection. The HR diagram may be divided into two regions according to the

presence or absence of an extended convective envelope in stars. Schatzman suggests that the boundary between these regions crosses the main sequence at F2 and extends upward and somewhat in the direction of later spectral types. This division line lies close to the cepheid instability strip; one is encouraged to think that cepheids are stars having envelopes on the border line between radiative and convective equilibrium. Though the connection between photospheric macroturbulence and the existence of a subphotospheric convection zone is not clear, we might tentatively suppose that when the latter is well developed, the former is also. Such a view would fit in well with our conclusion that, as a star evolves to the right in the HR diagram, the line profiles at first are due primarily to rotation but that, after the star crosses the cepheid gap, the line profiles are mostly a result of macroturbulence.

The situation among the stars of class I*a* in the range A–K is, however, highly confused. Line doubling occurs in many of these stars, but it is not certain that large-scale turbulence necessarily underlies the phenomenon. In at least one star δ CMa, it seems possible that the line profiles can be explained as a combination of a rotation consistent with a possible evolutionary track and microturbulence with velocities that are a function of excitation potential.

§ 4. VARIATION OF ATMOSPHERIC PARAMETERS OF CEPHEIDS THROUGH CYCLE; TESTS OF RUNNING-WAVE HYPOTHESIS; DERIVATION OF MEAN RADIUS

So far, we have advanced the picture that cepheids represent a transient stage in the life of a supergiant and have emphasized the fact that the spectra do not greatly differ from non-variable nearby supergiants in the HR diagram. However, in order to test any theory regarding the nature of the variability, we need to discuss the derivation of temperatures, pressures, and opacities throughout the cycle.

In general, these quantities can be found at present only through rather crude procedures. Ideally, we should like to have model atmospheres, i.e., to predict the spectrum from some assumed chemical composition, effective temperature, and surface gravity. The method has numerous difficulties, however: (1) the calibration of T_e versus spectral type for late-type supergiants is in a rather uncertain state; and (2) the gravity is difficult to estimate because it is influenced by pressure terms resulting from turbulence and the acceleration terms of the pulsation itself. An additional difficulty has developed recently in the fact that the period-luminosity law is not a narrow relation (Arp 1957), so that we cannot know directly the luminosity for a cepheid of a given period unless we also know the color (Sandage 1958). And then, of course, the masses remain rather uncertain.

Thus we fall back on curve-of-growth analyses. The criticisms that have been leveled at the curve of growth are well known (cf., for example, Unsöld and Struve 1949), but, in addition to the stratification effects that might be expected

in stars as bright as cepheids, there are possibly unique complications. For example, the different layers of the cepheid atmosphere may move slightly out of phase (the "level effect"). If the velocity differences are sufficiently large, line broadening will result that might be mistaken for rotation or macroturbulence. (The cepheid spectra are so crowded with lines that distortion of the profile may go undetected.)

Only two cepheids have had a complete cyclical analysis, δ Cep (Walraven 1948) and η Aql (Schwarzschild *et al.* 1948). Since the results of the two studies are similar, we shall discuss here only the latter paper, which is somewhat more extensive. Schwarzschild *et al.* determined T_{ion}, P_e, $\bar{\kappa}$, and ρ from twenty high-dispersion spectrograms well distributed over the cycle. Actually, curves of growth themselves were not used, but rather "pseudo-curves," which related line depth rather than equivalent width to log X_f. It was found that T, P_e, and $\bar{\kappa}$ were in phase with the light-variation; P_e decreased by a factor of about 10 and $\bar{\kappa}$ by a factor of 4 from maximum to minimum light. The variation of ρ was more difficult to obtain. In a study of the dynamics of pulsation, what one wants is the variation of ρ at a given mass of gas. From the spectra, one obtains ρ at the local level of formation of the spectral lines which may not coincide with a given mass element as the cycle progresses. In order to obtain the required variation, Schwarzschild *et al.* assume that hydrostatic equilibrium underlies the pulsation and therefore that the optical depth at a given mass element and a given time will be proportional to the instantaneous absorption coefficient at the element multiplied by the average density (taken over the cycle) at the element. If it is then supposed that the Fe lines used are characterized by a fixed optical depth (in the continuum), then, by this argument, the absorption coefficient at the level of formation of these lines varies inversely as the average density (over the cycle) of the mass element at that place. This is equal to the density determined from the spectrograms. Thus the ratio of the actual density at the level of formation of the Fe lines to its average density varies directly as the spectroscopic density times the spectroscopic absorption coefficient. Since the time average density of a given mass element is constant, the instantaneous density ρ_m of the element is proportional to $\rho\bar{\kappa}$. It is found, in this way, that ρ_m varies by a factor of 4 and is nearly in phase (it actually leads by 0.1 period) with the velocity. The running-wave theory (Schwarzschild 1936, 1938) requires that these be in phase.

In order to put the argument for progressive waves on a firmer footing, Schwarzschild *et al.* suggest the use of the Rankine-Hugoniot equation for the isothermal case as a fair approximation for continuous waves of appreciable amplitude, viz.,

$$\left(\frac{\partial r}{\partial t}\right)_2 - \left(\frac{\partial r}{\partial t}\right)_1 = \frac{\xi_0}{\sqrt{2}} \frac{\rho_2 - \rho_1}{\sqrt{\rho_1 \rho_2}}, \tag{2}$$

where the left-hand side represents the amplitude of the velocity variation, equal to 24/17 ΔV; ρ_2 and ρ_1 are the maximum and minimum densities, respec-

tively; and ξ_0 is the total random motion of the stellar material. With $\rho_2/\rho_1 = 4$ and a velocity amplitude of 60 km/sec, the equation can be satisfied if $\xi_0 = 60$ km/sec. This is substantially larger than the 14 km/sec from the line profiles and pure thermal motions if macroturbulence is assumed as the broadening agent; if we have only rotation and small-scale turbulence, the discrepancy becomes even larger—a factor of 10. Schwarzschild *et al.* then propose that the way out of the difficulty is to assume that the atmosphere has two layers, one characterized by a macroturbulence plus thermal motions of 14 km/sec, surmounted by a second having $\xi_0 = 85$ km/sec. The solution of the wave equation in this composite atmosphere shows that "if the level represented by the

TABLE 2

LINE PROFILE AND CURVE-OF-GROWTH PARAMETERS FOR α PER, β AQR, 9 PEG, AND SV VUL

	Star						
	α Per*	β Aqr	9 Peg	SV Vul	SV Vul	SV Vul	SV Vul
Sp.	F5 I*b*	G0 I*b*	G5 I*b*	G5 I*ab*	G8 I*ab*	G0 I*ab*	F7 I*ab*
Phase (P)	.....	.....	.....	0.47	0.69	0.95	0.99
log κ (λ 4300)	−1.64	−1.55	−2.39	−2.18	−3.28	−1.42	−1.48
T_{exc} (° K)	5150	4900±300	4000±400	4600±300	4000±300	5200±300	4900±200
T_{eff}	6200	5000	4290	4290	4000	5000	5300
T_{ion}	6140	5370	4810	4950	4630	5820	5900
log P_e	+0.1	−0.07	−1.05	−0.81	−1.99	+0.37	+0.12
log P_g	+2.3	+3.10	+2.35	+2.45	+1.35	+3.35	+2.65
log ρ	−9.4	−8.55	−9.28	−9.19	−10.26	−8.37	−9.06
log a	−2.7	−1.86	−2.59	−2.60	−3.96	−1.83	−2.42
v sin i (km/sec)	19.5	19	21	22	23	27	23
v sin i (predicted) (Fig. 5)	13	7	5	7	7	7	7
V (km/sec)	6.3	6.2	6.2	8.0	9.4	9.9	7.6

* Data, except for v sin i, taken from Greenstein (1948).

observed lines falls in this photospheric layer not far below the base of the corona (upper layer), the observed line profiles will correspond closely to the turbulence of the photosphere, whereas the observed pulsation will be determined closely by the pulsation of the corona."

Because of the difficulties encountered in η Aql (particularly the fact that the density variation is close to the limit of detection and also the uncertainty about rotation versus macroturbulence), we have attempted a study of a more favorable case, viz., SV Vul (Kraft *et al.* 1959). In Table 2 are listed the parameters derived from curve-of-growth analysis at phases corresponding approximately to maximum radius, minimum light, minimum radius, and maximum light, the radius variation being defined by the integration of the radial velocity-curve. Then T, P_e, $\bar{\kappa}$, and the spectroscopic ρ are in phase with the light and nearly in phase with the velocity. As mentioned in § 3, we are quite certain that the

line profiles corresponding to $v \sin i = 24$ km/sec are mostly a result of macroturbulence. If we subtract out 7 km/sec as probably being due to rotation, we are left with radial macroturbulent motions having a characteristic velocity of 12 km/sec. (According to Abt 1958 and Unsöld and Struve 1949, such motions usually correspond to about two-thirds of the $v \sin i$ formally fitted to the line profiles.) The velocity amplitude of SV Vul is about 80 km/sec when limb darkening and foreshortening are allowed for. The ratio of densities at minimum and maximum velocity (approximately maximum and minimum light, respectively), following the motion, are very difficult to estimate. We probably cannot apply arguments similar to those of Schwarzschild *et al.* because the spectroscopic change in density is very large, a factor of 80! If we use simply this spectroscopic change and substitute the values in equation (2), we derive $\xi_0 = 13$ km/sec, a value in very good agreement with the "observed" value. Actually, however, this may be only fortuitous. If we suppose that, following the motion, we must take at each point in the cycle $\rho_m \propto \rho\bar{\kappa}$, then the variation of the density is a factor of about 600, and equation (2) gives $\xi_0 = 5$ km/sec. This may perhaps be regarded as reasonable agreement with 12 km/sec; nevertheless, it seems advisable to regard this test of the running-wave hypothesis with suspicion until the motion of the material can be found.

It is of interest to find the change in the extent, z, of the atmosphere at maximum and minimum light. Let R_* equal the radius of the star. Taking $\tau \sim 1$ as the depth of the atmosphere and the values of $\bar{\kappa}$ and ρ from the spectroscopic analysis (Table 2), we find $z_{\max} \sim 2 \times 10^{10}$ cm $= 0.002\ R_*$, but $z_{\min} \sim 2 \times 10^{13}$ cm $\sim R_*$. This is probably to be taken only as an indication that the atmosphere is considerably more extended at minimum light than at maximum, since we would not expect the densities and opacities to remain constant with depth in the atmosphere and equal to the values at the level of formation of the Fe I lines. Very similar results have been obtained by Abt (unpublished) in the case of X Cyg. At minimum light, he finds $\log \bar{\kappa} = -3.1$ and $\log \rho = -10.0$; thus $z \sim 10^{13}$ cm $\sim R_*$.

Another kind of test of the running-wave hypothesis is found in the "level effect." If a running wave should pass through the atmosphere, it might be expected that the higher layers of the atmosphere would lag behind and have a slightly greater velocity amplitude than the lower layers. Radial-velocity studies of the effect have tended to give somewhat contradictory results. In relatively high-dispersion studies ($\sim$10 A/mm) of RT Aur ($P = 3.7$ days) (Petrie 1932), η Aql (Jacobsen 1950), and δ Cep (Jacobsen 1949), lines were grouped according to height in the solar chromosphere as given by Mitchell (1913). In RT Aur a compression of the atmospheric layers was found at phases preceding and during light-maximum, as would be expected on the running-wave hypothesis; however, the effect was generally less than 5 km/sec. Rather similar effects were found when the lines were grouped according to excitation potential and in groups according to ionization. Jacobsen's studies show similar

small differences between layers, but the results are not in mutual agreement as far as a test of the running-wave idea is concerned. In δ Cep, atmospheric compression occurs at phases on the rising branch of the light-curve; in η Aql, however, these phases are associated with rarefaction. In the latter star, Schwarzschild *et al.* (1948) found no difference between the velocity-curves of Fe I and those of Fe II from plates of dispersion 2.8 A/mm. From a study made of the same spectrograms, however, Grandjean (1956) found evidence of differential velocities near maximum and minimum light when the lines were grouped according to solar chromospheric height, excitation potential, and residual central intensity. The results were based on the velocities of about six hundred unblended lines. At maximum, it was found that high-level lines are collapsing with respect to low-level lines, that strong lines are collapsing with respect to weak lines, and that low-excitation lines are collapsing with respect to those of high excitation; exactly opposite effects were found at minimum. The differences never exceeded 2.5 km/sec, however.

In order to find out whether this is consistent with the concept of a running wave, Grandjean calculated from model atmospheres (which represent the Balmer jump according to the measurements of Miss Canavaggia [1949]) the depth of formation of lines of different excitation potential. We have already pointed out some of the difficulties in principle with model atmospheres; however, we might expect a discussion of this sort to give us some idea of the *relative* depths of line formation. In order to avoid the highest levels of the atmosphere, a point in the line profile about 3 Doppler widths from the center was chosen as the representative point. The optical depths in the continuum of the level of line formation as a function of excitation potential were found to be as shown in the accompanying table. Thus, since the low-excitation lines are formed at $\bar{\tau}$'s

Pure Abs.	Pure Scat.	Av.	Lines
Phase 0.013 (max. light):			
$\bar{\tau}$ 0.07	0.05	0.06	Fe I, $0.0 \leqq \chi \leqq 0.5$ ev
$\bar{\tau}$ .20	.15	.17	Fe I, $4.0 \leqq \chi \leqq 4.5$
$\bar{\tau}$ 0.07	0.05	0.06	Fe II, $2.5 \leqq \chi \leqq 3.0$
Phase 0.556 (min. light):			
$\bar{\tau}$ 0.012	0.008	0.01	Fe I, $0.0 \leqq \chi \leqq 0.5$
$\bar{\tau}$ .41	.32	.36	Fe I, $4.0 \leqq \chi \leqq 4.5$
$\bar{\tau}$ 0.08	0.04	0.06	Fe II, $2.5 \leqq \chi \leqq 3.0$

smaller than the high-excitation lines, it is quite clear that the atmosphere is undergoing a compression at maximum light and a rarefaction at minimum.

More striking effects among these short-period cepheids are found from studies of the core of the K line of Ca II of ζ Gem (Adams and Joy 1939), δ Cep, and η Aql (Jacobsen 1956). The radial velocities are shown in Figure 7. The amplitude of the K-line curve is, in all cases, greater than that of the photo-

spheric velocity-curve, but only in ζ Gem and η Aql does there appear to be definite evidence of a phase lag. Complications are introduced into the results by the presence of stationary interstellar (or circumstellar) absorption cores. While these are often well separated from the stellar lines, during some portions of the cycle the velocities are affected by blending. Only very high dispersion can be used if the lines are to be disentangled, but, owing to the fact that reaching the center of K requires five to ten times the normal exposure, this is a problem exclusively for large telescopes.

Among the longer-period cepheids, the level effect is more complicated than an explanation in terms of a simple phase lag of the higher levels would seem to permit. The writer (1954) pointed out that in X Cyg (P = 16.4 days), on the rising branch of the light-curve, the radial velocities of certain strong lines showed positive displacements of the order of 5–10 km/sec; we have already

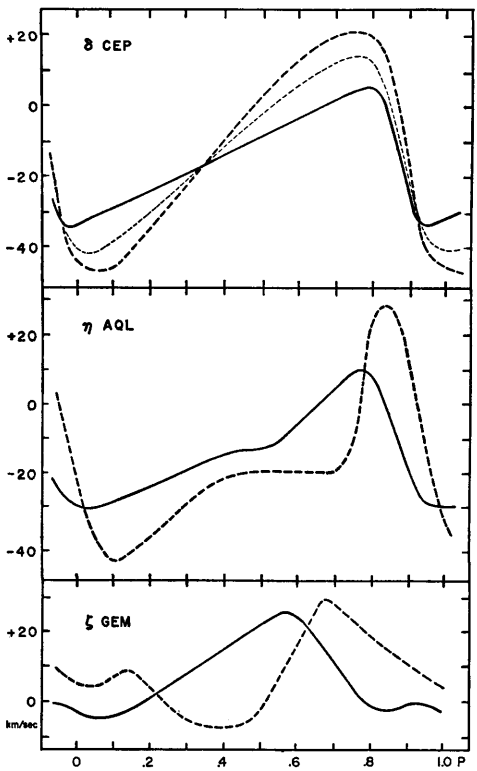


FIG. 7.—Level effect of the K-line absorption core in 3 cepheids (courtesy T. S. Jacobsen and A. H. Joy). The observed velocities are not shown. The dashed line represents the radial velocities of K in δ Cep and η Aql (Jacobsen 1956) and in ζ Gem (Adams and Joy 1939); the solid curve represents the photospheric velocity-curve. According to Jacobsen, the solid curve in η Aql should have been drawn a little lower in the region between 0.2 and 0.7 P. The heavy and light dashed curves in δ Cep represent two possible interpretations of the observed points.

noted (§ 2) the widening and positive displacement of certain lines of Ti II, hydrogen, and Sr II in the cepheids T Mon (P = 27.0 days) and SV Vul (P = 45.1 days) discovered by Sanford (1956). We recall here also the doubling of certain zero-volt lines of Fe I, Hα, and low-excitation lines of Ti II discovered by the writer in X Cyg (1956). I believe that these effects are manifestations of the same phenomenon in various degrees of development. But the manner of development of the doubling of Hα in X Cyg is not a clear-cut example of a "phase lag." Consider the spectrum just prior to minimum light. At this phase Hα appears single and is falling with a velocity of only about 5 km/sec (see Fig. 8). Almost precisely at minimum light, a feeble longward-displaced addi-

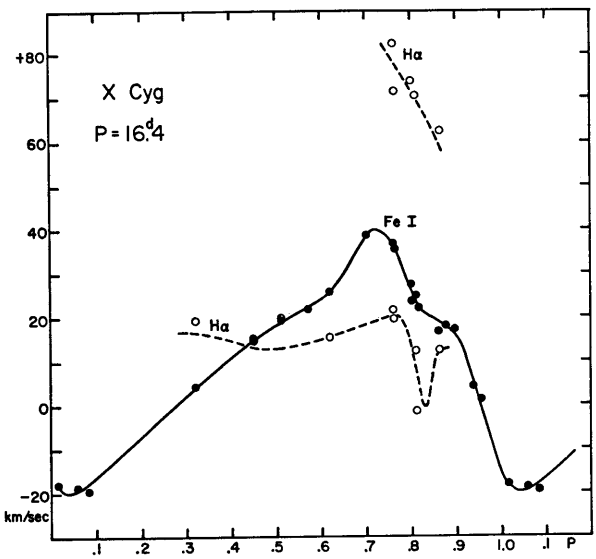


FIG. 8.—Radial velocities of Fe I and Hα in X Cygni. Before 0.75 P, the longward-displaced Hα core is absent. No plates of the Hα region have been obtained prior to phase 0.30 P or later than 0.90 P.

tional absorption core appears. This core does not develop out of any longward wing of the normal Hα component. It maintains a constant velocity displacement of about 50 km/sec from the moment it first appears and for about 0^p1 thereafter. During this time it gradually increases in strength, until it becomes as strong as the shortward component. After this, it merges with the shortward component; too few Hα plates exist after phase 0^p87 to determine the subsequent behavior. The behavior of Hα in TT Aql (P = 13.8 days) is almost identical with that in X Cyg. The nature of the doubling in Fe I (λ 3923) of X Cyg is less well understood because the development of the phenomenon requires only a few hours and evidently can take place at different phases in different cycles. A plate taken by Struve with the Mount Wilson 100-inch coudé spectrograph

in 1954 shows the splitting at phase 0^p815; plates taken by the author with the same equipment in 1956 show no sign of the effect as late as phase 0^p809. On the next night, at phase 0^p874, λ 3923 was clearly resolved into two components. In both cases the splitting consisted of a "normal" component, i.e., one whose velocity agrees with that of single lines, and a "satellite" displaced longward about 30–40 km/sec. The author has tried repeatedly to "catch" the moment of onset of the doubling to see whether it is similar to the development of the doubling in Hα, but without success. If it should prove to be similar to Hα, how is one to explain it? One would have supposed some such model as this: at minimum light, the atmosphere is falling. Gradually, owing to encounter with the upward-moving wave, it is slowed and stopped (minimum radius). But the lower layers are stopped first, while the upper layers still fall. If the line is formed over a sufficient extent of the atmosphere, it will presumably first broaden and, if the velocity gradient becomes discontinuous (development of a shock?), possibly split. But the behavior of Hα does not conform to this pattern at all; it remains to be seen whether or not this is true of Fe I.

Four other points may be mentioned. First, the satellite lines do not give the impression of arising from a shell. They are nearly as wide as the primary lines and no deeper than would be expected for their widths if they were formed in the normal photospheric regions. Second, the shortward components have the same velocities as the single lines; the velocity-curve is completely continuous. Third, the behavior of the splitting in X Cyg is not at all like that of W Vir (Sanford 1952; Abt 1954) beyond the superficial resemblance that many of the lines which split in the former also split in the latter. Fourth, the *development* of the doubling of Hα is extraordinarily similar to that in 89 Her (F2 Iα)(Böhm-Vitense 1956), but the satellite is displaced longward in the cepheids and shortward in this star.

Having discussed these complications in the interpretation of the radial velocities, we turn to the continuous Fe I radial velocities themselves. One of the uses to which these velocities are frequently put is the derivation of the radii of cepheids. However, in typical analyses—e.g., the Wesselink (1946) method —certain assumptions are made which ignore the change in continuous opacity through the cycle. It is supposed that (1) at points of equal color on the ascending and descending branches of the light-curve, the difference in light results solely from a difference in surface area; (2) the observed velocity-curve follows the motion of a particle throughout the pulsation; and (3) if R_{abs} is the radius at the mean level of formation of the lines and R_{phot} is the photospheric radius, R_{abs}/R_{phot} is constant with phase. With these assumptions, the integral of the velocity-curve can be used to scale (in km) the relative radius change determined from the light- and color-curves for the proper choice of the integration constant (the mean radius).

Whitney (1955*a*, *b*) has discussed the validity of these assumptions and checked them by an absolute photometric analysis in the case of δ Cep and

η Aql. In this method he attempts to predict the fluxes of the six-color photometry of Stebbins (1945) for δ Cep and of Stebbins, Kron, and Smith (1952) for η Aql from model atmospheres computed for the cepheid range by Miss Canavaggia and Pecker (1952). With appropriate blanketing corrections and allowance for interstellar reddening in the case of η Aql, it is found possible to match four of the six fluxes with proper choices of T_e and g. However, it turns out that the fluxes are very insensitive to g for a given value of T_e. Consequently, the values of T_e can be found essentially independent of g, the luminosity at any phase estimated from the light-curve and period-luminosity law, and the variation of R obtained independent of the radial velocities. In the first paper it was found that the radius obtained in this way was 10–20 per cent smaller than the results of the Wesselink analysis and had a phase lag of about $0^{p}1$ for both stars. However, in the second paper, he was able to get a very satisfactory agreement between the two analyses in the case of δ Cep with a more satisfactory evaluation of the blanketing at minimum light.

If the latter result is, in fact, true, it is very important. It means that we can probably trust the Wesselink method of analysis (at least among the cepheids of short period) to obtain radii, and it also gives us an independent method of estimating the effective temperatures. On the other hand, the following difficulties have arisen: (1) the period-luminosity law is not a narrow relation, and (2) δ Cep is undoubtedly slightly reddened—about 0.11 mag. on Eggen's color system (Gascoigne and Eggen 1957). A way of circumventing these complications would consist of observing the variation of U Sgr in six colors, which is known to be a member of an open cluster (Irwin 1955). The normal magnitudes and colors are known at present on the U, B, V system (Kraft 1957*c*). The theoretical calculations could then be put on a firm observational footing.

Whitney's derived effective temperatures are considerably higher than the values that would be assigned from Keenan and Morgan's (1951) calibration of the spectral types. For example, at maximum light in η Aql, Whitney assigns $T_e = 6470°$ K; for Code's spectral type, Keenan and Morgan give $T_e = 5800°$ K; at minimum, the values are $T_e = 5160°$ and $4450°$ K, respectively. As I pointed out in § 3, there is nothing unusual about the ionization and excitation temperatures of the cepheids when compared with non-variable stars of like spectral type. It is difficult to see how the effective temperatures could be much different. In Table 2 we also see that the values of T_e in all stars later than α Per are consistently lower than T_{ion}, which would not, in general, be expected. It is, of course, possible that our method of analysis by curves of growth is systematically in error, owing to some stratification effect; possibly the G supergiants and cepheids have some ultraviolet excess of radiation which leads to $T_{\text{ion}} > T_e$. However, it is possible that the effective temperatures assigned to G stars of class I*b* may need some revision upward. Keenan and Morgan (1951) point out that their effective temperatures for late-type supergiants are based in part on photoelectric color measurements; it is now known that probably

even the nearest supergiants are appreciably reddened, 0.12 mag. in $(B - V)$ in the case of α Per, for example (Harris 1956). If the rate of change of color with spectral class were the same among F supergiants as among F dwarfs, a change of 0.12 mag. $(B - V)$ would correspond to an increase of 400° K in T_e. Thus it would be helpful to calibrate T_e for late-type supergiants directly from the luminosities and radii of eclipsing variables, but, unfortunately, there are no bright G I*b* stars that are known to be members of eclipsing binary systems (see Appendix II).

§ 5. THE Ca II EMISSION

A recent study of the Ca II emission in G, K, and M stars by Wilson and Bappu (1957) is of the greatest interest both for astrophysics and for galactic-structure problems. It is found that over a range of almost 16 mag. a close correlation exists between the width of the Ca II emission and the absolute visual magnitude. The sun is found to fit the relation, and it therefore seems likely that if an explanation for the phenomenon can be found in the sun, a similar process must be at work in the stars. Among the supergiants, the emission is wide and, expressed as a velocity, increases from about 100 km/sec at $M_v = -2$ to 200 km/sec at $M_v = -6.8$. The calibration is useful in obtaining more refined estimates of absolute magnitudes of these stars than is given by the assignment of the MK luminosities; the method is limited by the fact that five to ten times the normal exposure is required to reach the center of K. However, for highly luminous stars the emission is so wide that dispersions in the 20–50-A/mm range might profitably be used.

Aside from the widths themselves, the emission lines have interesting radial-velocity properties. It is found that many stars, especially those of higher luminosity, have an absorption component (or components) superimposed on the emission; we shall employ the usual notation of K2 for the emission and K3 for the non-interstellar absorption. On the average, it turns out that K2 shows a small (~ -1 to -2 km/sec) outward motion and K3 a similar small inward motion when measured with respect to the nearby photospheric lines of Fe I. However, among the M stars of luminosity greater than +1.5, a large majority have K3 shortward-displaced, a phenomenon probably resulting from secular mass loss in the manner of α Her (Deutsch 1956).

The Wilson-Bappu results are particularly remarkable because they imply that the width of K is determined solely by the absolute visual magnitude and not at all by the photospheric temperature or surface gravity. One might ask, for example, what combination of circumstances allows the stars to "know" that they must correlate the width of K with those wave lengths of light to which our eyes are sensitive. Naturally, if one tries to correlate the width of K with M_{bol}, there is a spread among the luminous stars depending on spectral type. While the Wilson-Bappu results have been well calibrated by means of trigonometric parallaxes, absolute magnitudes of stars in the Hyades, certain

visual binaries, and the K star in ζ Aur, it must be admitted that, brighter than $M_v = -2.5$, the correlation depends on the Yerkes luminosities, which in turn are based primarily on statistical studies of radial velocities.

Nevertheless, it seems doubtful that the luminosities of the bright stars could be in error sufficiently to vitiate the Wilson-Bappu correlation. Thus we are confronted with two complex astrophysical problems: (1) What physical processes determine the K-line width? and (2) How are these processes controlled by the luminosity, and the luminosity alone? Goldberg (1957) has pointed out that photographs made with the McMath-Hulbert vacuum spectrograph leave little doubt that the origin of the feature lies in the chromosphere rather than in the photosphere of the sun. Thus we must find some means of pumping energy into the upper level of the K-line transition of Ca II atoms lying in the chromospheres of these stars. Wilson and Bappu suggest a picture in which matter flows out (perhaps in the form of jets or streamers) as a result of motions in the hydrogen convection zone. The flow is transformed into turbulence in some region responsible for the Ca II emission; the characteristic velocity of the turbulence is then related to the velocity of the original flow, which in turn is a function only of the luminosity. Line emission takes place probably by electron collisional excitation, as electrons cross the boundaries between fast-moving elements of gas. Such a picture seems to derive some support from the correlation found in the sun by Goldberg and Muller (1957) between shortward-displaced emission structures in Hα (which are of chromospheric origin) and shortward-displaced absorption structures in a nearby Fe I line of only moderate intensity.

In a more quantitative answer to the first question of the preceding paragraph, Wilson and Bappu suggest that the emission arises in an isothermal optically thin layer in which the lines are broadened by turbulence. In that case, equality of the measured half-widths of H and K would be expected, and this is confirmed by observation. In order to reproduce the observed half-widths, it is necessary to have a Doppler width of about 18 km/sec in the sun and about 100 km/sec in a supergiant of $M_v = -6$. This was criticized by Goldberg (1957) on the grounds that the velocities required seemed to be higher by a factor of 3 or 4 than those expected in the solar chromosphere or in the chromospheres of supergiants, if one judges the latter by the results obtained from studies of the eclipses of ζ Aur, etc. He suggests that we should rather consider an optically thick isothermal layer, in which the lines are broadened by pure Doppler motions; the gas pressures are too low to expect much contribution from collision damping. Following Goldberg, let us write the equation for the intensity of an emission profile produced in an isothermal gas layer thus:

$$I(\lambda - \lambda_0) = B\left[1 - e^{-\tau(\lambda-\lambda_0)}\right], \tag{3}$$

where B is the Planck function appropriate to the excitation temperature and $\tau(\lambda - \lambda_0)$ is the optical depth at a distance $\lambda - \lambda_0$ from the line center. If the

gas is optically thin at the line center, the relation between the half-half-width and the Doppler width is

$$\Delta\lambda = 0.833\Delta\lambda_D \ . \tag{4}$$

On the other hand, if the layer is optically thick and Doppler-widened,

$$\Delta\lambda = 1.52\Delta\lambda_D \left[\log (1.44\ N\alpha_0)\right]^{1/2} . \tag{5}$$

Goldberg then shows that, for the chromospheric Ca II abundance given by Cillié and Menzel (1935), equation (5) leads to a half-half-width about three times the Doppler width, and the latter corresponds to velocities of about 6 km/sec. Furthermore, for reasonable assumptions about the abundance of Ca II in supergiant chromospheres, he finds a Doppler width of only about 20 km/sec. Note also that equation (5) is very insensitive to a change of a factor of 2 in α_0; thus the near-equality of the width of the H and K emission in the sun and stars is readily understandable (see Appendix III).

We turn now to the Ca II emission in the spectra of the classical cepheid variables. The phenomenon has been studied by Herbig (1952) in S Sge, by Jacobsen (1956) in δ Cep, η Aql, and S Sge, and by the writer (1957*b*) in a number of other cepheids. The questions are: What relationship, if any, exists between the emission in the variables and the emission in the non-variables? Are the origin and production of the emission in the cepheids better understood than they are in non-variables? In answer to the first question, there are five points to consider. (1) In cepheids, the emission is transitory; it appears shortly after minimum light and lasts for a longer fraction of the period with increasing period. In no case, however, does it last longer than about 0.4 of the period. (2) No emission is found in cepheids with periods under 4 days. This may reflect nothing more than the fact that such stars do not become later than G0; Ca II emission is rarely observed in non-variable F-type stars. (3) The shape of the emission profile is usually unlike that of non-variable stars. It is broad and hazy on the shortward side and sharp on the longward. However, at phases when the emission appears, the K3 core is usually displaced greatly longward (see Fig. 8), and the shape of the resulting profile may reflect only a differential radial-velocity effect. (4) In the spectra of only two cepheids is there a component of K2 longward of the K3 core (or cores). The total emission feature in X Cyg is found to be displaced shortward of the nearby Fe I lines by 15 km/sec; in ζ Gem the displacement is about zero. However, the probable error of making such a measurement is large (± 10 km/sec), owing to the hazy boundaries of the feature. (5) The peak intensity of H often exceeds that of K.

A comparison of cepheids and non-variables with regard to points 3 and 5 is made in Figure 9. If V is the intensity of the violet emission component and R is the intensity of the red, V/R is plotted as a function of spectral type for stars of classes *Ib* and II. The spectral types are those given by Bidelman (1954), and the intensity ratios are the eye-estimates of Joy and Wilson (1949). In

cepheids other than those indicated, the ratio of V/R is still larger. The second part of Figure 9 consists of eye-estimates by the writer of the peak intensities of the H and K emissions on spectrograms of G and K stars of classes II and I*b* from the collection taken by Wilson and Bappu. These are plotted as a function of the strength of the K3 absorption core as estimated by Joy and Wilson (1949). The estimates are difficult to make and should be supplanted with real intensity measurements; however, it appears that the peak intensity of H tends to be stronger relative to K whenever the K3 core is strong. This agrees with the suggestion by Herbig (1952) that the inversion of the normal intensities of H and

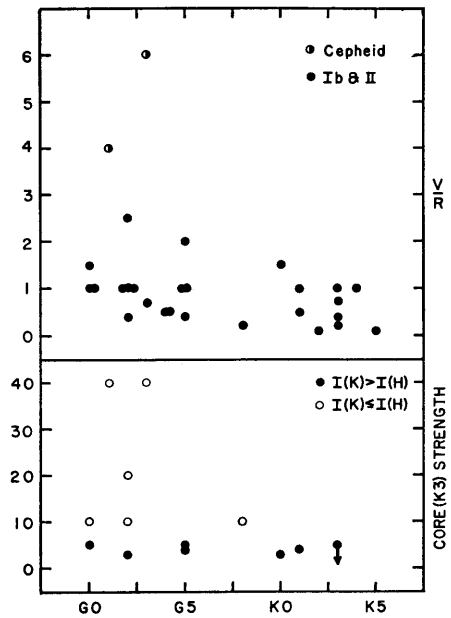


FIG. 9.—V/R and $I(\mathrm{H})/I(\mathrm{K})$ in cepheids and stars of luminosity classes II and I*b*

K comes about, in both cepheids and long-period variables, as a result of self-absorption by overlying cooler vapors. A similar result seems to apply to the non-variable stars; however, in general, K3 tends to be less strong in these stars than in the cepheids.

Another kind of comparison that can be made between the cepheids and non-variable stars is the correlation of K2 with M_v. The method can be applied only to X Cyg and ζ Gem, for the reasons already cited. Eleven G and K supergiants of classes I*b* and II, selected from the Wilson-Bappu collection, were measured for K2 width by the author; a correlation-curve was then drawn up. The author's measurements of K2 width in X Cyg and ζ Gem were then transferred to the Wilson system. The period-luminosity law (Arp 1957) gives $M_v = -4.5$ for X Cyg and $M_v = -4.0$ for ζ Gem; the measured line widths of

213 and 175 km/sec lead to $M_v = -7.3$ and $M_v = -5.9$, respectively. Thus the K-emission method applied to the cepheids gives results about 2 mag. too bright.

The picture that emerges from the preceding discussion is this: Properties 3–5 are not exactly like those of normal supergiants, but, when allowance is made for radial-velocity effects, the H and K emission phenomena seem to exaggerate the properties of these phenomena in the non-variable stars. This certainly does not prove that the emission arises from some common activity in the two kinds of stars; against this view is property 1, for which there seems

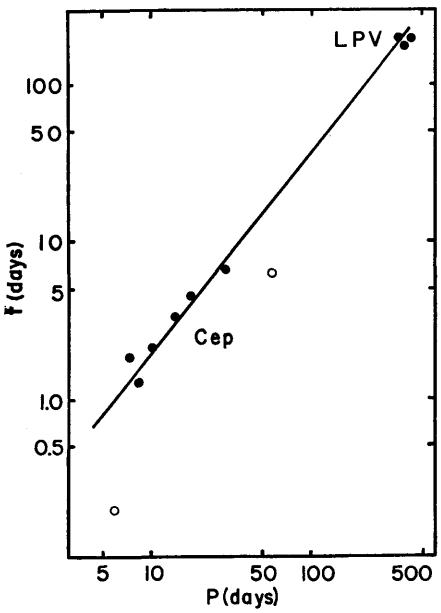


FIG. 10.—Ca II emission time scale in cepheids and long-period variables as a function of P. Open circles denote points of low weight.

to be no explanation. However, there is a related property of the emission which can be studied only in the variable stars, viz., its time scale. The writer (1957*b*) found a correlation between the length of time that Ca II emission is present in the spectra of cepheids and the period. This correlation (Fig. 10) was found, on extrapolation, also to fit the long-period variables of period 300–400 days. It was suggested that a common activity was responsible for the emission in the two kinds of stars. On the basis of reasonable assumptions, it appeared possible that the time scale could be interpreted as the time for the decay of homogeneous turbulence in the upper regions of the hydrogen convection zone. The emission was to be thought of as arising from recombination in the rising element of gas that were out of ionization equilibrium with their surroundings (cf. McKellar and Odgers 1952).

This result was criticized by Whitney (1958), who showed that departures from ionization equilibrium were too small to give the observed emission intensity. Under the most favorable assumptions, he could account for only half the observed emission intensity in η Aql, and this without taking into account the powerful overlying opacity at K. Another argument against the recombination hypothesis not mentioned by Whitney is the fact that no hydrogen emission is observed. With the cross-section for capture of electrons on the $^2P^o$ level of Ca II given by Green (1949), it is easy to show (because of the near-equality of ionization potentials of Ca II and hydrogen and the overwhelming abundance of the latter) that the number of captures per cubic centimeter per second on upper levels of the Balmer lines greatly exceeds (factor $\sim 10^4$) the number of captures on the upper level of K. Of course, many more of the former will result in absorptions to higher levels; nevertheless, it is difficult to see why no strong hydrogen emission is observed. A possible way out of these difficulties might be to retain the basic argument about the convection zone but to use its mechanical energy properties in the manner suggested by Wilson and Bappu. In this way, particle collisions could be made responsible for the bright lines of Ca II; this would relieve the difficulties about the hydrogen emission, since the Balmer levels are too high to be excited by low-energy collisions.

Some observational evidence exists in the spectrum of SV Vul, suggesting that these speculations may, in fact, be true. If the Ca II emission is excited by an increased activity of the convection zone, we should perhaps find an increase in photospheric turbulence at the same time. From Table 2 and Figure 6 we see that microturbulence from the curve of growth increases at phases on the ascending branch of the light-curve when the Ca II emission is present. Furthermore, we have already suggested that the line profile of λ 4508 probably results from macroturbulence; the line is obviously wider at phase 0^p95 than at the other phases; again this is just the time of peak Ca II emission intensity. The energy per unit volume bound up in these turbulent motions is about twenty times larger at phase 0^p95 than at phase 0^p47 when the emission is absent, because both the turbulent velocity and the atmospheric density are larger at the former phase. Results very similar to these are found from the atmospheric parameters of X Cyg (Abt, unpublished; Kraft, unpublished) and to a lesser extent those of η Aql (Schwarzschild *et al.* 1948; Van Hoof and Deurinck 1952). Against this argument is the possibility that the representation of the line profile is not unique. Recall that these phases are also associated with increased "level effect." At present, we cannot be sure that λ 4508 is not widened by differential motions of this sort that tend to simulate a true increase in turbulence. Even so, if the turbulence were constant with phase, the energy per unit volume would still be larger at phase 0^p95 than at other phases because of the increase in the density.

If, as these observations may indicate, the Ca II emission is excited at the same time that atmospheric turbulence is increased, we are still confronted

with complications if we try to invoke a common mechanism for the production of these lines in both the cepheids and the non-variables. For example, at phase 0P47 in SV Vul, there is no Ca II emission; yet the atmospheric parameters (V and ρ) are almost identical (cf. Table 2) with those of 9 Peg, a star which has no trouble producing bright H and K! If the latter arise in the chromosphere and if we invoke a common region of origin in the two kinds of stars, we then have to admit that the cepheid chromosphere must be different from that of 9 Peg; for example, perhaps essentially all the Ca is Ca III in the chromosphere of the cepheid at this phase. But then it is difficult to maintain the position that the time scale for emission is governed only by the decay time for turbulence; rather it would seem that it must depend largely on the state of excitation and ionization of the chromosphere at any moment. Thus we probably cannot have it both ways. Either we must admit that the cepheids and non-variables produce their emission lines by a different mechanism or in a different part of the atmosphere, or we must find some other explanation for the emission time scale in the variables.

For what it is worth in this connection, it is possible to show quite easily that the Ca II emission in the long-period variable R Leo arises in an optically thick region. The writer (1957*b*) has observed the bright lines of the infrared triplet at phase 60 days after maximum light. Let us suppose that the K emission, which is also present at that phase, is produced in an optically thin region. Then, because of the smaller transition probability, the infrared triplet line λ 8662 is certainly produced in a thin region. The line shows little or no self-absorption; consequently, we measure its half-half-width directly, and from equation (4) we have $\Delta\lambda_D = 17$ km/sec. This must be the Doppler width of K as well, from the thin-atmosphere assumption. But the measured Doppler width of K at this phase is at least 40 km/sec. Thus we must conclude that the assumption that K is produced in a thin region is wrong.

Because of the mutilation of the K emission in long-period variables, it is not possible to state whether R Leo fits on the Wilson-Bappu relation. At phase +60 days, $M_v \sim +0.5$ (Safronov 1955) and the relation predicts a half-width of 65 km/sec; we measure 65 km/sec. We expect the latter value to be smaller than the former because of the mutilation; however, it is not possible to find the factor of diminution directly from observation. As with the cepheids, the true width of the K emission is probably larger than would be predicted by the Wilson-Bappu effect.

§ 6. CEPHEIDS AND STELLAR EVOLUTION: CONCLUDING REMARKS

The foregoing discussion leads us to the conclusion that, so far as the photosphere is concerned, the classical cepheids have spectra that, in detail, are virtually identical with those of the non-variable supergiants at all phases of the variation. The properties of the emission lines, however, are puzzling and may or may not arise from an activity common to the two kinds of stars. Another

kind of connection between the cepheids and nearby stars in the HR diagram is the suggestion by Abt (1957*a*) that all stars in the brighter regions of the HR diagram are, in fact, variable. Radial-velocity variations are found in virtually all stars of class I, and, while these are often quite small and only quasi-regular, there seems to be a $P\sqrt{(\rho/\rho\odot)} = Q$ relation. The change in the line shapes and wave lengths indicates that pulsation is a likely cause of the variability rather than some fluctuation of turbulence. The values of Q found by Abt turn out to agree within a factor of about 2 with those of the classical cepheids (see Fig. 11).

These results might mean, for example, that the cepheid phenomenon is a resonance effect such as one has in the classical problem of the forced oscillations of a dissipative system. As the star evolves across the HR diagram, it tries to pulsate, but resonance conditions set in only in a fixed narrow region. One observable quantity about cepheids, viz., the secular period changes, may tell us something about this rate of evolution. According to Sandage (1958), a star crossing the region of cepheid instability will change its color by 0.2 mag.

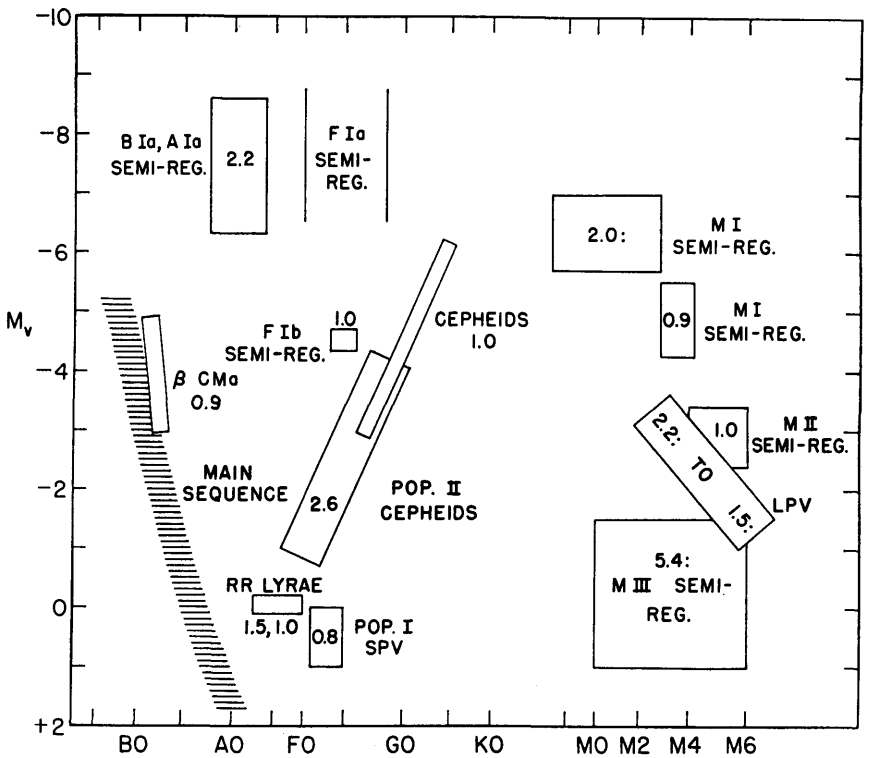


FIG. 11.—The upper part of the HR diagram, showing classes of variable stars (courtesy H. A. Abt). The numbers near the class names are the ratio of Q for the class to that of the classical cepheids. Recent results by J. D. Fernie (1959) on the mass of the LPV X Oph indicate that Q_{LPV} should be considerably reduced.

$(B - V)$ and its period by about a factor of 2. From a variety of sources, mostly the *Variable Star Catalogue* (Kukarkin and Parenago 1948) and its *Supplements*, I have found, for twenty cepheids having secular terms, the time it takes to change the period by a factor of 2 if the rate of change is constant and equal to that observed at present. This time (log T in years) is plotted as a function of log P in Figure 12. It is seen that a reasonably good correlation exists and that there are two points of interest: (1) log T decreases with increase in log P, and (2) both positive and negative period changes fit the correlation. The question is whether these can be interpreted as resulting from evolution.

For a star of mass 4 ⊙, I have calculated from the Sandage-Schwarzschild (1952) models the time it takes to move 0.2 mag. in $(B - V)$ at the position of the cepheids. This turns out to be about twenty times shorter than the time

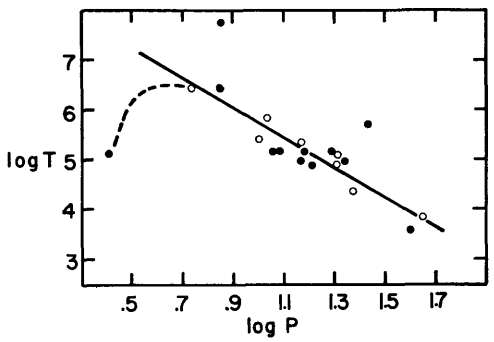


FIG. 12.—Log T in years versus log P for 20 classical cepheids. Open circles are stars with decreasing periods; filled, increasing. The dashed curve represents a possible alternative interpretation of the data among the short-period stars.

predicted from the period changes for a cepheid having the Sandage-Schwarzschild luminosity for the above mass. If we take a mass twice as large for this luminosity (as indicated by Fig. 5), the time is still too short by a factor of 10. Thus the evolutionary models considered would give a time considerably less than that indicated by the period changes! If one were to maintain the hypothesis that these period changes are evolutionary in character, the result would at least be more comforting than the other way about. Nevertheless, one would have to explain the negative period changes as well as the positive ones, and the former would have to be associated with stars moving to the left in the HR diagram. About this, stellar evolution at present has little or nothing to say.

I am indebted to Dr. Marshal H. Wrubel for permitting me to use his IBM 650 program for the computation of line profiles and also for instruction in the use of the machine. Thanks are due Dr. O. C. Wilson for permitting me to study some coudé spectrograms of supergiants taken by him. Grateful acknowl-

edgment is made also of the assistance of Mr. D. C. Camp and Mr. W. T. Hughes with the line drawings.

The following appendices were added March 22, 1960, in order to bring the chapter more nearly up to date.

APPENDIX I

The Colors of Cepheids at Maximum Light

Kron (1958) has investigated the intrinsic colors of nearby supergiants that had been classified on the MK System by Bidelman. Color indices $(V - B)$ and $(R - I)$ were measured for 139 stars. From the observed colors of supergiants of the same spectral type but at different distances (i.e., absorptions), reddening "trajectories" in the $(V - B)$ versus $(R - I)$ diagram were found, and an envelope drawn corresponding presumably to unreddened stars.

For any phase of a classical cepheid, $(V - B)$ and $(R - I)$ were measured and the reddening obtained by moving the observed point along the trajectory (Kron and Svolopoulos 1959). The intrinsic colors of cepheids at maximum light were found to vary from about $(B - V) = 0.35$ at $P = 3$ days to about $(B - V) = 0.55$ at $P = 20$ days, on the Johnson-Morgan system.

In another investigation, Kraft (1960*a*, *b*) calibrated the strength of the G band in cepheids and supergiants as a function of MK spectral type, using narrow band-pass interference filters. It was shown that the G band is relatively insensitive to the kinematic disturbances described in §§ 2 and 4. A relation between intrinsic $(B - V)$ and MK spectral type was set up by using the intrinsic colors of cepheids in galactic clusters for calibration. At 3 days, the intrinsic color at maximum light averaged $(B - V) = 0.40$; at 20 days, $(B - V) = 0.48$, results similar to those of Kron and Svolopoulos (1959). The conclusion that the kinematic disturbance of cepheid atmospheres at maximum light has little or no effect on the ionization, excitation, or color seems borne out by these investigations.

APPENDIX II

The Applicability of Wesselink's Method to Classical Cepheids

Abt (1959) suggests that Wesselink's method can be used to predict an accurate radius if the total stellar expansion is of the order of 50 or more atmospheric scale heights. Thus changes in the opacity and in the relative position of line-forming and photospheric regions are unimportant because the scale height is presumably a rough measure of the optical thickness of the atmosphere. Expansions of this order are found in all classical cepheids, but not necessarily in all types of intrinsic variables.

Oke (private communication) is studying the spectrum of η Aql with photoelectric scanning equipment. It should be possible to predict the shape of the spectrum over a wide wave-length interval from model atmospheres and to obtain log T_e at any phase. The reddening of η Aql is known from the accurate colors of Kron and Svolopoulos (1959) and Kraft (1960*a*, *b*). If the relationship between MK types and intrinsic $(B - V)$ color is taken from the latter's work, log T_e can be calibrated in terms of spectral type and intrinsic color at any phase. Improvement in the bolometric corrections may also be possible.

Absolute magnitudes of field cepheids can be found by fitting a grid of period lines (Sandage 1958) in the HR diagram to the cepheids in galactic clusters; the latter have

accurately known intrinsic colors and absolute magnitudes. With M_v, M_{bol}, $\log T_e$, and intrinsic $(B - V)$ determined at any phase of η Aql, an adequate test of Wesselink's method can be carried out.

APPENDIX III

The Wilson-Bappu Effect

Since early 1958, several partial explanations of the Wilson-Bappu effect have been advanced (Hoyle and Wilson 1958; Schatzman 1958; Kraft 1959). The most successful of these is probably that by Hoyle and Wilson, who show that the characteristic velocity of flow in the subphotospheric convection zone depends on L_v in the same way as the width of the K2 line. This velocity actually varies with L_{bol} and temperature in such a way that a dependence on L_v alone is simulated. The theory requires, however, that the flow velocity in the convection zone be equal to the chromospheric velocity associated with the width of K2. How the one velocity can be transformed into the other remains physically unexplained, but Hoyle and Wilson suggest that the necessary energy is transported out of the convection zone by hydromagnetic waves that are dissipated in the chromosphere.

Schatzman (1958) suggests that acoustical waves generated in the photosphere become shock waves as they pass into the chromosphere. He shows that, if the mechanical flux is proportional to the luminous flux in any of these stars, if the coefficient of proportionality is independent of spectral type and luminosity, and, further, if the K2 line is produced at optical depth ~ 0.01, the dependence of the characteristic velocity of the material on L is the same as that given by the Wilson-Bappu correlation.

Kraft (1959) proceeds from observation to show that the turbulent velocities in the photospheres of late-type stars are proportional to the K2 widths. From model atmospheres the correct dependence of K2 width on L_v is derived, provided that the ratio of photospheric turbulent flux to radiative flux is a constant, independent of luminosity and spectral type.

None of these papers shows in detail how the K2 emission itself is generated. However, the discovery of localized solar magnetic fields around Ca^+ plages (H. W. and H. D. Babcock 1955, 1958; Howard 1959) has led to a proposal (Leighton 1959) that Ca^+ ions, bound by the fields, are excited in collision with neutral H and He atoms as a result of the motions responsible for granulation.

Observations of K2 in the M-type supergiants of h and χ Per (Wilson 1959) strengthen the correlation considerably among the stars of high luminosity.

REFERENCES

Abt, H. A.	1954	*Ap. J. Suppl.*, Vol. **1**, No. 3.
	1957*a*	*Ap. J.*, **126**, 138.
	1957*b*	*Ibid.*, p. 503.
	1958	*Ibid.*, **127**, 658.
	1959	*Ibid.*, **130**, 824.
Adams, W. S.	1956	*Ap. J.*, **123**, 189.
Adams, W. S., and Joy, A. H.	1939	*Pub. A.A.S.*, **9**, 254.
Arp, H. C.	1957	Symposium paper, 99th meeting, A.A.S.
Babcock, H. W., and Babcock, H. D.	1955	*Ap. J.*, **121**, 349.

BABCOCK, H. W., and BABCOCK, H. D.	1958	*I.A.U. Symposium*, No. 6 (Cambridge: Cambridge University Press).
BERGH, S. VAN DEN	1957	*Ap. J.*, **126**, 323.
BIDELMAN, W. P.	1954	*Ap. J. Suppl.*, Vol. **1**, No. 7.
BIDELMAN, W. P., and MCKELLAR, A.	1957	*Pub. A.S.P.*, **69**, 31.
BÖHM-VITENSE, E.	1956	*Pub. A.S.P.*, **68**, 57.
CANAVAGGIA, R.	1949	*Ann. d'ap.*, **12**, 21.
CANAVAGGIA, R., and PECKER, J.-C.	1952	*Contr. Inst. Ap. Paris*, Ser. A, No. 109.
CILLIÉ, G., and MENZEL, D. H.	1935	*Harvard Circ.*, No. 410.
CODE, A. D.	1947	*Ap. J.*, **106**, 309.
COX, J. P.	1956	*Ap. J.*, **122**, 286.
	1959	*Ibid.*, **130**, 296.
COX, J. P., and WHITNEY, C.	1958	*Ap. J.*, **127**, 561.
DEUTSCH, A. J.	1956	*Ap. J.*, **123**, 210.
EDDINGTON, SIR A. S.	1930	*The Internal Constitution of the Stars* (Cambridge: Cambridge University Press).
	1941	*M.N.*, **101**, 182.
	1942	*Ibid.*, **102**, 154.
EGGEN, O. J.	1951	*Ap. J.*, **113**, 367.
FERNIE, J. D.	1959	*Ap. J.*, **130**, 611.
GASCOIGNE, S. C. B., and EGGEN, O. J.	1957	*M.N.*, **117**, 430.
GOLDBERG, L.	1957	*Ap. J.*, **126**, 318.
GOLDBERG, L., and MULLER, E. A.	1957	*A.J.*, **62**, 92.
GRANDJEAN, J.	1956	*Mém. Acad. R. Belg.*, Vol. **29**, No. 7.
GREEN, L. C.	1949	*Ap. J.*, **109**, 289.
GREENSTEIN, J. L.	1948	*Ap. J.*, **107**, 151.
	1949	*Ibid.*, **109**, 121.
HACK, M.	1955	*Contr. Os. Astr. Milano Merate*, Nuova Ser., No. 70.
HARRIS, D. L.	1956	*Ap. J.*, **123**, 371.
HERBIG, G. H.	1952	*Ap. J.*, **116**, 369.
HERBIG, G. H., and SPALDING, J. F.	1955	*Ap. J.*, **121**, 118.
HOWARD, R.	1959	*Ap. J.*, **130**, 193.
HOYLE, F., and WILSON, O. C.	1958	*Ap. J.*, **128**, 604.
HUANG, SU-SHU	1957	*Pub. A.S.P.*, **69**, 65.
HUANG, SU-SHU, and STRUVE, O.	1952	*Ap. J.*, **116**, 410.
	1953	*Ibid.*, **118**, 463.
IRWIN, J. B.	1955	*M.N. Astr. Soc. South Africa*, **14**, 38.

JACOBSEN, T. S.	1949	*J.R.A.S. Canada*, **43**, 142.
	1950	*Ibid.*, **44**, 104.
	1956	*Pub. Dom. Ap. Obs. Victoria*, **10**, 145.
JOHNSON, H. L., and HILTNER, W. A.	1956	*Ap. J.*, **123**, 267.
JOHNSON, H. L., and MORGAN, W. W.	1953	*Ap. J.*, **117**, 313.
JOY, A. H., and WILSON, R. E.	1949	*Ap. J.*, **109**, 231.
KEENAN, P. C., and MORGAN, W. W.	1951	In *Astrophysics*, ed. J. A. HYNEK (New York: McGraw-Hill Book Co., Inc.), pp. 21–23.
KHOLOPOV, P. N.	1958	*Peremennye Zvezdy*, **11**, 325.
KRAFT, R. P.	1954	*Pub. A.S.P.*, **66**, 136.
	1955	Dissertation, University of California.
	1956	*Pub. A.S.P.*, **68**, 137.
	1957*a*	*A.J.*, **62**, 93.
	1957*b*	*Ap. J.*, **125**, 336.
	1957*c*	Symposium paper, 99th meeting, A.A.S.
	1957*d*	*Ap. J.*, **126**, 225.
	1959	*Ann. d'ap.*, **22**, 164.
	1960*a*	*Ap. J.*, **131**, 330.
	1960*b*	*Ibid.*, **132**, 404.
KRAFT, R. P., CAMP, D. C., FERNIE, J. D., FUJITA, C., and HUGHES, W. T.	1959	*Ap. J.*, **129**, 50.
KRON, G.	1958	*Pub. A.S.P.*, **70**, 561.
KRON, G., and SVOLOPOULOS, S.	1959	*Pub. A.S.P.*, **71**, 126.
KUIPER, G. P.	1938	*Ap. J.*, **88**, 472.
KUKARKIN, B., and PARENAGO, P.	1948	*General Catalogue of Variable Stars* (Moscow: Academiia Nauk, U.S.S.R.).
LEIGHTON, R. B.	1959	*Ap. J.*, **130**, 366.
LÜST-KULKA, R.	1954	*Zs. f. Ap.*, **33**, 211.
MCKELLAR, A., and ODGERS, G. J.	1952	*Pub. A.S.P.*, **64**, 222.
MCKELLAR, A., ODGERS, G. J., ALLER, L. H., and MCLAUGHLIN, D. B.	1952	*Contr. Dom. Ap. Obs. Victoria*, No. 24.
MERRILL, P. W., and WILSON, O. C.	1956	*Ap. J.*, **123**, 392.
MITCHELL, S. A.	1913	*Ap. J.*, **38**, 407.
OKE, J. B., and GREENSTEIN, J. L.	1954	*Ap. J.*, **120**, 384.
PANNEKOEK, A.	1946	*Physica*, **12**, 761.
PETRIE, R. M.	1932	*Pub. Obs. U. Michigan*, **5**, 27.

RITTER, AUGUST	1879	*Wiedemanns Ann.*, **8**, 172.
SAFRONOV, V. S.	1955	*Peremennye Zvezdy*, **10**, 236.
SANDAGE, A. R.	1958	*Ap. J.*, **128**, 150.
SANDAGE, A. R., and SCHWARZSCHILD, M.	1952	*Ap.J.*, **116**, 463.
SANFORD, R. F.	1952	*Ap. J.*, **116**, 331.
	1956	*Ibid.*, **123**, 201.
SCHATZMAN, E.	1958	*Mém. in-8° Soc. R. Sci. Liège*, 4th ser., **20**, 370.
	1960	*Mount Wilson and Palomar Observatories: Special Technical Rept.*, No. 3.
SCHWARZSCHILD, M.	1935	*Zs. f. Ap.*, **11**, 152.
	1938	*Harvard Circ.* Nos. 429, 431.
SCHWARZSCHILD, M., SCHWARZSCHILD, B., and ADAMS, W. S.	1948	*Ap. J.*, **108**, 207.
SLETTEBAK, A.	1949	*Ap. J.*, **110**, 498.
	1954	*Ibid.*, **119**, 146.
SLETTEBAK, A., and HOWARD, R. F.	1955	*Ap. J.*, **121**, 102.
STEBBINS, J.	1945	*Ap. J.*, **101**, 47.
STEBBINS, J., KRON, G. E., and SMITH, J. L.	1952	*Ap. J.*, **115**, 292.
STEEL, H.	1945	*Ap. J.*, **102**, 429.
STIBBS, D. W. N.	1956	*M.N.*, **116**, 453.
STRUVE, O.	1944	*Observatory*, **65**, 257.
	1945	*Ap. J.*, **102**, 232.
	1946	*Ibid.*, **104**, 138.
TAYLER, R. J.	1954	*Ap. J.*, **120**, 332.
UNSÖLD, A.	1938	*Physik der Sternatmosphären* (1st ed.; Berlin: Julius Springer), pp. 318–319.
UNSÖLD, A., and STRUVE, O.	1949	*Ap. J.*, **110**, 455.
VAN HOOF, A., and DEURINCK, R.	1952	*Ap. J.*, **115**, 166.
WALRAVEN, T.	1948	*Pub. Astr. Inst. Amsterdam U.*, No. 8.
WESSELINK, A. J.	1946	*B.A.N.*, **10**, 91.
WHITNEY, C.	1955*a*	*Ap. J.*, **121**, 682.
	1955*b*	*Ibid.*, **122**, 385.
	1958	*Mém. in-8° Soc. R. Sci. Liège*, 4th ser., **20**, 298.
WILSON, O. C.	1959	*Ap. J.*, **130**, 499.
WILSON, O. C., and ABT, H. A.	1954	*Ap. J. Suppl.*, Vol. **1**, No. 1.
WILSON, O. C., and BAPPU, M. K. V.	1957	*Ap. J.*, **125**, 661.
WRIGHT, K. O.	1947	*J.R.A.S. Canada*, **41**, 49.
WRIGHT, K. O., and VAN DIEN, E.	1949	*J.R.A.S. Canada*, **43**, 15.
ZHEVAKIN, S. A.	1959	*Astr. J. U.S.S.R.*, **36**, 996.

CHAPTER 10

Early-Type Stars with Extended Atmospheres

ANNE B. UNDERHILL
Dominion Astrophysical Observatory

§ 1. INTRODUCTION

MANY of the stars of type B and earlier appear to be surrounded by extensive envelopes of gas at low pressure in addition to the usual atmospheric layers. The envelope is recognized by the presence of emission lines in the stellar spectrum and, if there is much material in the envelope, by the occurrence of relatively sharp and deep absorption lines corresponding to a lower degree of excitation than that of the underlying stellar spectrum. The schematic model shown in Figure 1 will serve to explain most of the observations. Surface A represents the outer limit of observable material, surface B represents the outer layer of the star proper—that is, the region where the cores of the stellar absorption lines are formed—and surface C represents the deepest layer to which one can observe at a wave length in the continuous spectrum, that is, surface C represents the photosphere of the star. The region between surfaces C and B represents the stellar atmosphere. The extended envelope occupies the region between surfaces B and A. These surfaces have been drawn as though they were spherical. This may not be so; in fact, an important part of the problem is to establish the shapes and sizes of these surfaces and the physical state and distribution of the material between them. For example, the extended atmospheres around rapidly rotating stars are probably confined largely to the equatorial plane. From the observed stellar spectra we should like to deduce the chemical composition, the temperature, density, and state of motion of the envelope, as well as the total radiation field.

It is a gross simplification to state that surfaces A, B, and C exist and to define separate regions, such as the reversing layer and the envelope; but the observations which can be made are so limited in scope that a more detailed model is hardly warranted. It should be noted that surfaces A, B, and C will occur at

different geometrical depths when one observes in different parts of the spectrum, for they are essentially defined by the optical depth, which is a product of the geometrical depth and the monochromatic opacity. A model like Figure 1 underlies all the discussion of this chapter.

The parts of the envelope or extended atmosphere that are not projected against the stellar disk will contribute emission features to the spectrum. If the emission is strong enough to fill in any underlying line absorption, a definite emission line will be seen in the spectrum. If the emission is weak, it may scarcely distort the underlying stellar absorption feature. The part of the envelope projected on the disk of the star will act more or less like an absorption tube and will produce additional absorption lines in the stellar spectrum. If the gases in the envelope have motions in the line of sight different from that of the star as

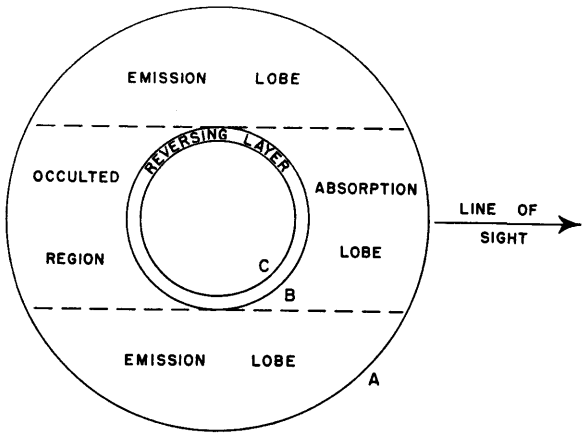


FIG. 1.—A schematic model of an early-type star with an extended atmosphere

a whole, the spectral features originating in the envelope will be displaced and broadened according to the Doppler principle. For an emission line to occur, it is necessary that the material in the envelope be transparent at wave lengths of the continuous spectrum in the neighborhood of the emission line, but relatively opaque in the line wave lengths.

The early-type stars with extended atmospheres fall into four groups: the Be stars; the B- and O-type supergiants, including stars like P Cygni; the Of stars; and the Wolf-Rayet stars. All these objects have some spectral peculiarities in common, which is natural, since the laws of physics are universal and gas and radiation under the same conditions must always produce the same observable effects; however, the underlying stars in each group are different. The Be stars may be subdivided into two groups. These are Be stars, which are stars with a B-type spectrum plus emission at the hydrogen lines, and shell stars. The latter are stars with a Be spectrum and additional sharp absorption lines, chiefly from the once-ionized metals, as well as prominent hydrogen absorption

cores, which have been observed to extend to H41 of the Balmer series. The spectra of a number of stars have been observed to change from purely absorption B-type to Be or from Be to B with a shell and vice versa within 15–20 years (Merrill and Burwell 1933, 1943, 1949). Whether the classification is B, Be, or B with a shell depends on the amount of material in the line of sight through the envelope at the moment of observation. When the envelope contains enough material to form absorption lines, it is called a "shell." No specific geometric form is connoted by this term.

Spectra illustrating the observable effects of the extended atmospheres around some early-type stars are shown in Plate I. The linear dispersion on the spectrograms is 46 A/mm at Hα, 14 A/mm at Hβ, and 11 A/mm at Hγ. The first strip, *A*, gives the spectrum of the normal sharp-lined B3 main-sequence star ι Her. Strip *B* is the spectrum of the B3e star 48 Per. The strong, relatively sharp emission at Hα and the double emissions at Hβ and Hγ are typical of many Be spectra. This star is rotating with a velocity of the order of 230 km/sec (Slettebak 1949), and consequently the B-type absorption lines are diffuse, with dish-shaped profiles. The spectra in this illustration were obtained in 1953. Strip *C* is the spectrum of the shell star ζ Tau. The spectral type of the underlying star is about B2, and the star is rotating with a velocity of the order of 350 km/sec (Underhill 1951). A few shell absorption lines are visible near Hγ. The great width of the emission at Hα is a characteristic difference between B-type shell stars and Be stars (Underhill 1953). The spectrograms used for this illustration were obtained at different epochs, and, since the spectrum of ζ Tau changes fairly rapidly, the structure of the hydrogen emission is not the same on each plate. The dates of the exposures are (U.T.) Hα: February 28.114, 1953; Hβ: March 10.142, 1953; Hγ: January 28.189, 1957. Strip *D* gives the spectrum of the B3 supergiant 55 Cyg. Here there is a weak P Cygni-type emission at Hα, and the C II absorption lines at λ 6578, λ 6582 are very strong. No emission is apparent at Hβ and Hγ. Strip *E* gives the spectrum of the typical main-sequence O9 V star 10 Lac. The lines are all in absorption, and members of the $4 - n$ series of He II blend with the Balmer lines of hydrogen. Strip *F* gives the spectrum of the O7f star, 9 Sge. The He II lines are comparable in strength to the hydrogen absorption lines. There is a moderately strong emission feature at Hα, and the complex profile at Hβ gives some evidence of emission. The underlying absorption-line profiles are shallow and diffuse. Strip *G* shows the spectrum of the WC7 star, HD 192103, in the region of Hα, Hβ, and Hγ; strip *H* gives the spectrum of the WN6 star, HD 192163. The linear dispersions of the spectrograms used for these stars at Hγ and Hβ are 30 and 46 A/mm, respectively. The dispersion at Hα is the same as for the other stars.

§ 2. THE Be STARS

The spectrum of most Be stars is that of a rapidly rotating B star with superposed double hydrogen lines in emission. The emission is strongest at Hα and

decreases toward the head of the series. The over-all intensity of the emission varies greatly from star to star, emission occurring only at the early members of the Balmer series for most stars. In a few stars such as HD 32343, 11 Cam, the Balmer series extends in emission to about H22, even though the underlying absorption series breaks off near H15. In principle, the decrement in intensity should yield important data on the physical conditions in the shell, but it is difficult to make a meaningful analysis because of the problem of self-absorption in the higher series members. Lesser practical difficulties are raised by the necessity of evaluating the sensitivity changes in the recording unit between the wave length of Hα and the wave lengths of the higher series members and because the emission must be observed on top of the usually ill-defined stellar B-type spectrum.

Following and expanding earlier work by others, E. M. and G. R. Burbidge (1951, 1953*a*, *b*) have made detailed attempts to interpret the emission intensities in a few Be stars. They have shown that the hydrogen emission spectrum may be interpreted as a recombination spectrum modified somewhat by self-absorption in the higher series members and by electron scattering. These authors (1956) give a method of estimating the size of the emitting region from the measured line intensities, and they find that, on the average, the radius of this region is 10 stellar radii and the electron density, N_e, is of the order of $10^{13}/\text{cm}^3$, which corresponds to an electron pressure of the order of 30 dynes/cm^2. Further studies of Be stars are currently in progress at many observatories, in the hope of elucidating the physical picture by means of quantitative measures.

The emission lines appear to be single in a few Be stars which have quite sharp stellar absorption lines. It has frequently been suggested that these stars are rotating rapidly, like the more common Be stars which have rotationally broadened lines, but that in the sharp-lined cases the axis of rotation is nearly parallel to the line of sight. These stars are consequently referred to as "pole-on" stars. No conclusive proof has yet been given that the stars with apparently single emission lines are truly "pole-on," but this seems likely from statistical studies of the rotational velocities of B and Be stars (Slettebak 1949, 1955). The use of high dispersion frequently resolves into two components emission lines that appear to be single at moderate dispersion.

Profiles of the hydrogen lines in a typical Be star and in a shell star are given in Figure 2. The spectra of the Be star, 48 Per, were obtained in 1953; those of the shell star, 48 Lib, in 1950 and 1956. Each profile is the mean from two spectrograms except for Hα and Hβ of 48 Per and of 48 Lib 1956, which are from one plate. The dispersions on the plates are 46, 14, 11, and 8 A/mm, respectively, at Hα, Hβ, Hγ, and Hδ. The plotted points give a somewhat smoothed representation of the intensity tracings, for the points were read at intervals of 0.1 inch on the original tracings, which were magnified 200$\times$ in the direction of the dispersion. Since it is probable that line-of-sight motions are the dominant

broadening agent of the emission-line profiles, the abscissa is plotted in kilometers per second. The ordinates express the intensity in terms of the continuum equal to 100. The vertical scale of the Hα profiles is more compressed than that of the other lines. It is apparent that the emission lines are double in 48 Per, although Slettebak (1949) calls this star "pole-on." The resolution of the present spectrograms at Hα is insufficient to show the doubling, but the Hα profile is asymmetrical in a manner suggesting a doubling, as at Hβ. The self-reversals in the shell star, 48 Lib, are much stronger than those in 48 Per, the cores approaching zero residual intensity at the center. The change in appearance of the Hα emission in 48 Lib in 6 years is conspicuous, and the wings of Hα are much broader than those in 48 Per. Because of the Balmer decrement, the wide wings cannot be traced unequivocally at Hβ and higher series members. A detailed study of the Hα emission of 48 Lib shows that the wings of the emission (region where the intensity <200) do not change from year to year even when striking changes occur in the central regions of the line.

Work by R. H. Curtiss and others at the University of Michigan showed long ago that the over-all width of the hydrogen emission lines in Be stars, when expressed in velocity units, was approximately constant. This fact strongly suggests that the width is due to line-of-sight motions. Struve (1942, 1945) has summarized many observations of early-type objects with extended atmos-

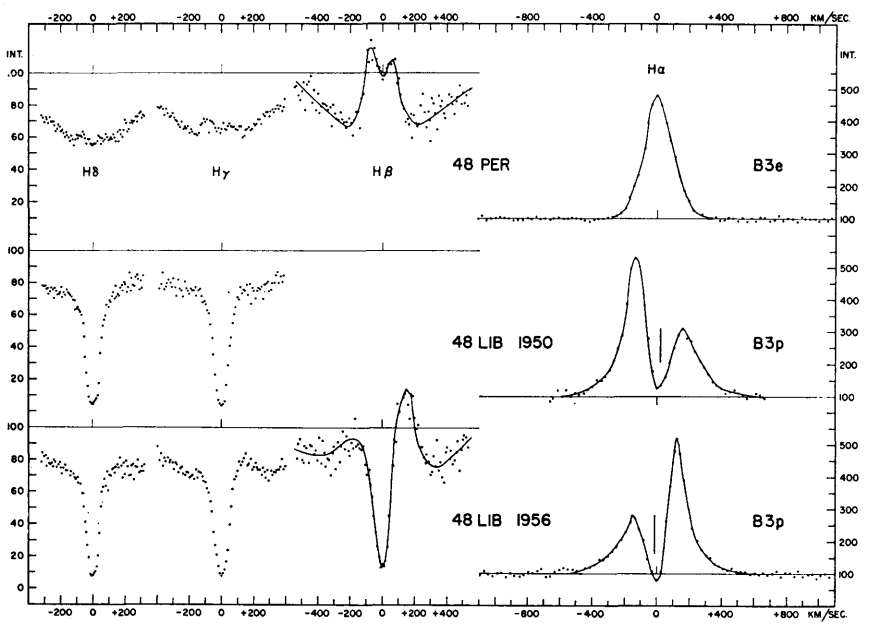


FIG. 2.—Profiles of Hα, Hβ, Hγ, and Hδ in the Be star 48 Per and in the shell star 48 Lib. The vertical scale for the Hα profiles is more compressed than that for the other profiles. The intensity of the continuum is taken as 100.

pheres and has demonstrated that the emission widths, of the order of 400 km/sec over-all, might be interpreted to mean that the emission lines come from an extended atmosphere rotating with the star in such a way as to conserve angular momentum. From a comparison of the estimated speed of rotation of the star, obtained from the width of stellar absorption lines, and the apparent speed of rotation of the emitting gas, it may be deduced that the main body of gas lies 2 or 3 stellar radii from the star. Rottenberg (1952) has given some examples of how line-of-sight motions combined with scattering in an emitting ring may produce various emission-line profiles of the type observed in early-type stars with extended envelopes. Slettebak (1949, 1955) has investigated the rotational speeds of B and Be stars, and he finds that the Be stars, on the average, rotate a little faster than the B stars, which do not show emission lines. This would imply that emission lines are most likely to be observed in the spectra of rotating B stars with their axes of rotation most nearly perpendicular to the line of sight. In such a system it is likely that the extended atmosphere is concentrated to the equatorial plane as a result of the rotation.

When Be stars lose their hydrogen emission lines, their spectra are indistinguishable at low dispersion from the spectra of ordinary rapidly rotating B stars. Consequently, there appears to be little fundamental difference between B stars and Be stars. Statistical studies by Wilson (1941) have shown that the mean absolute magnitude of B stars and of Be stars of the same spectral subdivision is the same, and investigations under way at the Dominion Astrophysical Observatory, using the strength of the Hγ line in absorption as an indicator of absolute magnitude (Petrie 1952), confirm this conclusion. A study of the radial velocities and absolute magnitudes of the Be stars by Smith (1947) also points to this conclusion.

The occurrence of hydrogen emission lines in B-type spectra is quite common. About 15 per cent of the stars in several comprehensive catalogues of B- and O-type stars (Plaskett and Pearce 1931; Morgan, Code, and Whitford 1955; Hiltner 1956) are listed as Be stars. These spectral classifications were carried out with low-dispersion spectra covering the blue part of the spectrum; the use of high-dispersion spectra and red-sensitive plates would probably reveal more stars with weak emission lines. Merrill and Burwell (1933, 1943, 1949, 1950) have given lists of A- and B-type stars with emission lines. They give a full bibliography for these stars, as well as notes about the changes that have been observed in the spectra of many stars. From this material it is apparent that most of the changes are not periodic in character and that the time scale of the events causing the changes in spectrum may be of the order of 5–10 years. A few of the Be stars are known to vary in magnitude as their spectrum changes, but the variations are small (≤ 0.2 mag.) in most cases. Thorough documentation of the light and color changes of a number of Be stars, together with a record of the spectral changes, would aid in determining the physical origin of the Be phenomenon, but few data of this type exist at present. According to Ed-

wards (1956), most Be stars are reddened intrinsically. This reddening indicates an apparent color temperature lower than the ionization temperature given by their line spectra. However, Dokutchaeva (1955) finds that Be and B stars have similar energy distributions.

Table 1 contains a list of Be stars brighter than 4.6 mag. compiled from the catalogues of Merrill and Burwell. The MK spectral type is given if it could be found in the literature; otherwise the type given by Merrill and Burwell is listed. The letter "e" has been suppressed. All these stars have shown hydrogen emission at some time, although some do not now. The letter "n" indicates broad shallow lines (rapid rotation), and the letter "p" indicates that the spectrum is peculiar in some respects. The star *o* And is not in the Merrill and Burwell catalogues, but Hα has faint emission wings on a plate obtained at

TABLE 1

BRIGHT B-TYPE STARS WITH HYDROGEN EMISSION LINES

HD	Name	α(1900)	δ(1900)	Mag.	Sp.	HD	Name	α(1900)	δ(1900)	Mag.	Sp.
2905.....	κ Cas	00^{h}27^m.3	62°23′	4.2	B1 Iα	50013....	κ CMa	06^{h}46^m.1	−32°23′	3.8	B2n
5394.....	γ Cas	00 50.7	60 11	2.2	B0 IV*	58715....	β CMi	07 21.7	08 29	3.1	B8n
6811.....	ϕ And	01 03.7	46 42	4.3	B8*	91465....	p Car	10 28.5	−61 11	3.6	B5n
10516.....	ϕ Per	01 37.4	50 11	4.2	B0n*	102776....	j Cen	11 44.8	−63 14	4.5	B5n
22192.....	ψ Per	03 29.4	47 51	4.3	B5n*	105435....	δ Cen	12 03.2	−50 10	2.9	B3n
23302.....	17 Tau	03 39.0	23 48	3.8	B6 III	109387....	κ Dra	12 29.2	70 20	3.9	B5
23480.....	23 Tau	03 40.4	23 39	4.2	B6 IV	120324....	μ Cen	13 43.6	−41 59	3.3	B3
23630.....	25 Tau	03 41.5	23 48	3.0	B7 III	127972, 3..	η Cen	14 29.2	−41 43	2.6	B3n*
25940.....	48 Per	04 01.4	47 27	4.0	B3 V	138749....	θ CBr	15 28.9	31 42	4.2	B5n
30614.....	α Cam	04 44.1	66 10	4.4	O9.5 Iα	158427....	α Ara	17 24.1	−49 48	3.0	B3n
34085.....	β Ori	05 09.7	−08 19	0.3	B8 Iα	166937....	μ Sgr	18 07.8	−21 05	4.0	B8 Iαp
37128.....	ϵ Ori	05 31.1	−01 16	1.8	B0 Iα	173948....	λ Pav	18 43.0	−62 18	4.4	B2 III*
37202.....	ζ Tau	05 31.7	21 05	3.0	B2 V*	174638, 9..	β Lyr	18 46.4	33 15	4 v	B9p†
37490.....	ω Ori	05 33.9	04 04	4.5	B3 III	198183....	λ Cyg	20 43.5	36 07	4.5	B5 V
37742.....	ζ Ori	05 35.7	−02 00	2.0	O9.5 Ib	202904....	υ Cyg	21 13.8	34 29	4.4	B2 V
37795.....	α Col	05 36.0	−34 08	2.8	B8n	214748....	ϵ PsA	22 35.1	−27 34	4.2	B8
45542.....	ν Gem	06 23.0	20 17	4.1	B7 IV	217675, 6..	*o* And	22 57.3	41 47	3.6	B6.5*

* Shell star.

† Peculiar spectroscopic binary.

the Dominion Astrophysical Observatory on July 7, 1953, and Slettebak (1952) has also observed this feature. Some of the stronger Fe II lines (e.g., $\lambda\lambda$ 5169, 5018, 4923, 4583, 4549, 4233) show emission wings at times in some of the spectra, but [Fe II] lines in emission do not occur in normal Be spectra. The N III lines, $\lambda\lambda$ 4634–4641, and the C III line, λ 5696, occur weakly in emission in the spectra of the O9.5 I*a* stars α Cam and ζ Ori; in addition, there is emission at Hα. One of the most characteristic features of the Be stars is that the emission lines change in intensity from time to time. For instance, Lockyer (1930) observed hydrogen emission lines in the spectrum of θ CBr between 1922 and 1930, but no emission lines are present now or were present before about 1920. The emission lines also change in appearance, the relative intensity of the violet component to the red component varying. Such changes are called V/R changes, and McLaughlin (1957) has followed these changes in several Be stars for many years. These changes are not strictly periodic in character, and they are accompanied by a shift in velocity of the absorption core, the core being dis-

placed to the violet when the red side is strong and to the red when the violet side is strong. Stars that have at one time shown rapid V/R changes may for periods of 10–20 years remain quiescent, with the emission components about equal in strength and the absorption core yielding a constant velocity.

In addition to being generally distributed among the B-type stars (Minkowski 1951), Be stars occur in clusters (the Pleiades) as components of spectroscopic binaries (ζ Tau) and of eclipsing binaries (V367 Cyg), and as the early-type component of a K + B composite (HD 50820). Thus it would appear that the instability which produces the Be phenomenon is a property of the star itself and that it is not fundamentally affected by the position of the star in space relative to any other stars. The resulting spectroscopic phenomena may, of course, be modified by the atmosphere of a neighboring star if the star is close enough.

§ 3. SHELL SPECTRA

Shell spectra differ from Be spectra in that an absorption-line spectrum resembling that of α Cyg is present in addition to the B-type absorption spectrum and the hydrogen emission lines. The chief physical difference between shell stars and Be stars is that for shell stars there is much more material in the envelope than in the case of Be stars. Consequently, the absorption lobe (Fig. 1) acts like an absorption tube and produces deep, relatively sharp absorption lines. The apparent spectral type of the shell spectrum, insofar as a spectral type can be assigned, is always later than that of the underlying star; it usually corresponds to that of an early A-type supergiant, the lines of the ionized metals, Fe II, Cr II, Ti II, etc., being strong, while the lines of the neutral metals are weak. Shell absorption spectra have been observed for stars from spectral type A5 III (14 Com) to O7 (9 Sge; Underhill, 1958). Hiltner (1947) and Slettebak (1951) have shown that the O I line, λ 8446, and the Paschen lines are in emission in some shell stars and in some Be stars.

A rough estimate of the temperature and pressure in shells may be obtained from curve-of-growth studies of the equivalent widths of the shell lines. These results, though crude, confirm the impression that the temperatures and pressures in the shells around the B-type stars are similar to those in supergiant atmospheres. Struve and Wurm (1938) pointed out a significant difference between the spectra of supergiants and shells. In shell spectra, lines arising from metastable levels are relatively strong in comparison with lines from normal levels. This effect arises because the gas in a shell is not in a state of thermodynamic equilibrium, and the radiation field is diluted. Struve and Wurm have developed the consequences of this fact quantitatively, so that one can, from the apparent intensities of lines from normal and metastable levels, obtain an estimate of the physical conditions in the shells. Wellman (1956) has discussed these ideas more fully. Of the lines from metallic atoms and ions most commonly observed in the blue part of the spectrum, only Mg II λ 4481 and Si II λ 4128

and λ 4130 arise from normal levels. Because of the dilution effect, these three lines in shell spectra are abnormally weak (as referred to supergiant spectra) in comparison with the strength of the lines from the ionized metals. This is a criterion for recognizing a shell spectrum. If the spectral type of the underlying star is near B0, lines of He I may appear in the shell spectrum. The lines arising from metastable levels, λλ 5015, 3965, 3889, and 3188, are then much stronger and deeper than the other shell helium lines.

The main body of the gases comprising the shell can be considered to form an equatorial extension of the rapidly rotating star. This extension is believed to rotate so as to conserve angular momentum. Detailed observations of several stars give strong evidence that the material in the shell is often not stationary or in uniform motion but that various parts of the shell are moving with different velocities. This is indicated by the unsymmetrical profiles of some lines, notably Fe II and H; these lines even become double occasionally in some stars. Merrill and Sanford (1944) have observed that the radial velocity from the higher members of the Balmer series may be quite different from that of the earlier members, such as Hγ and Hδ, in a shell that is active. This effect they have called the "Balmer progression," and it is another indication that the different parts of the shell may be in relative motion. The hydrogen emission may also affect the measured radial velocity of the hydrogen absorption cores of the first few members of the series.

The changing spectra of a few shell stars have been observed in considerable detail, and more long-continued observations would be useful. Most work has been done on the bright shell stars γ Cas, φ Per, Pleione, ζ Tau, 17 Lep, β^1 Mon, 14 Com, 48 Lib, and HD 33232. The initial observations were made chiefly by Merrill, McLaughlin, and Struve; less extensive series of observations have been obtained by many others. Merrill and Burwell (1949) give a brief list of stars with shell spectra.

Although the spectral changes occurring in shell spectra differ in detail with each star, a review of the changes observed for 48 Lib (Merrill and Sanford 1944; Merrill 1953; Underhill 1954, 1957*a*) will indicate the general pattern of events that occurs. The radial velocity of 48 Lib was approximately constant at −5 km/sec, a value appropriate for membership in the Scorpio-Centaurus stream, until 1935, when the shell lines were observed to be displaced to the violet by some 70 km/sec. Since then, the velocity of the shell has oscillated with a period of about 10 years from large negative velocities to a positive velocity of about 25 km/sec. The velocity displacements of the hydrogen lines and of the various metallic lines are not always the same at any epoch, those lines which it seems reasonable to believe are formed in the denser layers near the star usually showing greater negative velocities than the high-level lines. The differences are greatest when the velocities are most negative. For instance, in 1956 at the recent velocity minimum, the velocity from Hγ, Hδ, and Hε was −48 km/sec; that from the Fe II lines was −74 km/sec; and that from the

Ti II lines was −80 km/sec. At this stage the high members of the Balmer series (H22–H30 or so) have large negative velocities more in accord with the velocities from Ti II than with the Hγ velocities, and the Fe II lines, like the hydrogen lines, are asymmetric, the red side being sharper than the violet side.

Since 1950 the intensity of the shell lines has changed considerably. The equivalent widths increased by about 25 per cent in 1951, when the shell appeared to be condensed and the radial velocity of the shell appeared to be directed toward the star. Since then, as the outward velocity of the material in the shell increased, the equivalent widths have decreased irregularly until in 1956 they reached about 40 per cent of their 1950 value. The Si II and Mg II lines, which are sensitive to the dilution effect, have weakened more rapidly than the Fe II and Ti II lines. During this time the shape and peak intensity of the hydrogen emission have changed from being slightly stronger on the violet side to being very strong on the red side and weak on the violet side. Weak emission wings have appeared at the strongest Fe II lines. The V/R changes of the hydrogen lines are similar to those observed by McLaughlin (1957) for other shell stars.

Merrill and Sanford (1944) showed that the absorption core moved across a stationary emission feature and that this would explain the observed V/R changes of the hydrogen lines. Measurements made at the Dominion Astrophysical Observatory on intensity tracings of spectrograms of Hα obtained between 1950 and 1957 confirm this result. In 48 Lib the hydrogen emission is stationary at the velocity of the star.

Since the interpretation of the V/R changes depends greatly upon whether one concludes that the emission line moves with the sharp shell absorption cores or maintains that the emission is stationary, moving only with the star as a whole, and that the absorption core moves across the emission, it is perhaps worthwhile to discuss the observational problem briefly. The apparent line-of-sight velocity of the absorption core may be readily derived by standard methods of measuring radial velocity; for, although the cores are asymmetrical in many shell stars (the violet side usually being less steep than the red side), the asymmetry is generally not sufficient to disturb one seriously from bisecting the core with the reticule of the measuring machine. The problem arises in determining the center of the emission feature. Reference to Figure 2 shows that generally the absorption core obscures the central region of the emission line. Therefore, to find the center of the emission, one must adopt an indirect method. The usual procedure is to locate the edges of the emission and, assuming that the feature is symmetrical, to find the mid-point. The difficulty is to locate precisely such an elusive feature as the *edge* of the emission. It is advantageous to work with Hα, for this is the strongest emission line, and the wings of the emission feature are therefore well defined, the underlying stellar feature being weak. In fact, in most shell stars and Be stars the stellar absorption Hα is completely filled in, and the emission appears to rise directly from the continuum.

Intensity tracings of the Hα emission in 48 Lib reveal that the emission profile is symmetrical at intensity levels less than twice the intensity of the continuous spectrum and that the shape of this part of the profile does not change as the velocity of the absorption core changes, and large V/R variations occur. By measuring on the tracings, it was found that the core moved relative to the wings of the profile and that the amount of this motion is about equal to the directly measured motion of the core relative to the stellar velocity, believed to be that of the Scorpio-Centaurus stream. The profiles of Figure 2 illustrate this point. Here the wings of the Hα emission are lined up. A line representing the reticule of the measuring machine was drawn in the absorption core. This was placed so as to bisect the core at an intensity level of about 200 in the confining emission wings. If the depth at which the bisection is made is raised, the reticule will move toward the emission peak of least intensity in each case. At the measuring machine the core appears as a uniform, well-defined, deep absorption feature that can be bisected with ease. The asymmetry that appears on the intensity tracings is not apparent to the eye. Therefore, one will tend to place the reticule in a position as sketched rather than through the deepest point of the line profile. It is clear that there is a displacement of some 40 km/sec between the line bisecting the core in 1950 and that bisecting the core in 1956. The positions of the apparent edges of the emissions were measured on all plates by standard radial-velocity methods; it was found that it is difficult to define the same point in the profile visually each time and that one tends to measure always at a certain distance from the core. The result is, of course, that the emission line appears to move with the absorption core. This result is an illusion, however, and measures made on the weaker emissions at Hβ, Hγ, and Hδ may be even more illusory. It is extremely doubtful that any such direct measurements truly evaluate the position of the center of the emission, at least on plates of moderate (40–50 A/mm) dispersion.

The great width of the Hα emission in shell stars and the fact that this emission moves with the star as a whole are properties in common with the emission lines in Of stars and Wolf-Rayet stars (see below). This signifies that the emitting regions in all these objects are somewhat similar, a conclusion that has been emphasized by Struve (1942) and by Beals (1940).

The changes observed in the shell spectrum of 48 Lib may be explained by postulating a shell consisting of a dense region, probably largely contained in an equatorial extension near the star, and an extensive low-density region extending to large distances from the star. The metallic absorption lines originate mainly in the first region; only the strongest lines (that is, the early members of the Balmer series and the strongest Fe II lines) are formed in absorption chiefly in the second region. This region contributes the emission features. From 1950 to about 1952, the inner shell appeared to contract, but by 1953 an outward motion of the inner shell became dominant, and the velocity of ejection increased until about 1956. At present, the inner layers of the shell have the most rapid

outward velocity; the outer layers are decelerated, probably by gravity. Since 1951 the shell has been dissipating, so that less material is visible in the line of sight in 1956 than earlier. The inner part of the shell may rotate, but the ejection velocity dominates the line profiles, in contrast with the case of ζ Tau and Pleione, where the rotational broadening of the shell lines is readily observable. Different material is observed each year, for the outward velocities are large enough to move the material a long way from the star in a year.

The phenomenon causing shell eruptions is not known, but the triggering action is most likely caused by irregularities in the radiation field from the star. The ejection of the shell is probably not caused primarily by the rapid rotation of the stars, for Be and shell stars, when they lose their envelopes, still rotate as before and it is difficult to think of the Be process changing the angular momentum of a star. Shell stars do not shed much material; a generous estimate of the amount of material in a shell at any moment is 10^{-9} solar mass.

The amount of material in a shell may be estimated in the following way: Suppose that the shell is confined to an annular disk of outer radius 10 R_* and thickness 0.1 R_*. Then, if the shell is attached to the star, the volume of the shell is 9.9 π R_*^3. If we further assume that the radius of an average Be star is 5 $R\odot$ and that the average density in the shell is 2×10^{-11} gm/cm^3 (a value which would correspond, for an atmosphere of pure hydrogen, to an electron density of the order of 10^{13}/cm^3 at a temperature of the order of 12,000°), the mass in the shell is about 10^{-8} $M\odot$. If the outer radius of the shell is only 3 stellar radii, the mass in the shell may be of the order of 10^{-9} $M\odot$. This is a generous estimate, for we have assumed that N_e is 10^{13}/cm^3 throughout the shell, whereas comparison with the solar chromosphere would suggest that the density in the shell might be considerably less at large distances from the star.

The gases in many shells appear to be in motion, and it seems probable that these gases eventually escape from the star; for at a radius of 5 $R\odot$ the escape velocity from a main-sequence star is close to 300 km/sec. At greater distances the escape velocity will decrease as $R^{-1/2}$. The ejection of shells is a means by which early-type stars may shed mass. The rate at which this loss may occur is difficult to assess. Presuming a loss of 100 shells (10^{-7} $M\odot$) per year, it will take a Be star 10^7 years to reduce its mass by 1 solar mass. This period is comparable to the "age" often postulated for B-type stars. Since the average early B-type star has a mass of the order of 10 $M\odot$, the mass loss per year from B-type stars due to the ejection of shells would have to be considerably greater than the present estimate if the Be instability is to be the means whereby B-type stars lose sufficient mass to evolve into subdwarfs or white dwarfs in a comparatively short time.

§ 4. THE B-TYPE SUPERGIANTS AND P CYGNI STARS

In this section the stars with spectra of luminosity class I*a*, spectral types between B8 and O9, and the stars like P Cygni will be discussed. In the blue

spectral region the spectral lines of supergiants are usually in absorption, and they have the steep-sided, blunt profiles associated with the concept of macroturbulence. In these stars Hα is in emission, the profile being of the P Cygni type; that is, it consists of a sharp emission peak with a violet-displaced absorption component. Similar emission appears sometimes at He I λ 5876 and at Hβ and occasionally at He I λ 6678. In the late O-type supergiants, weak emission lines appear at C III λ 5696 and at N III $\lambda\lambda$ 4634–4641; also He II λ 4686 is at least partially filled in by emission. These lines do not show the P Cygni characteristics strongly, and they will be discussed further in the section on Of stars. They are composed of a moderately sharp peak superimposed on a broad emission, which rises only a few per cent above the continuous spectrum. Wilson (1956) has observed similar broad, weak emission features at Hα and at Hβ in the spectrum of the B1 supergiant HD 190603.

Beals (1950) has made a comprehensive survey of stellar spectra containing P Cygni-type emission lines, and he includes a number of B-type supergiants among the heterogeneous group of objects that he observes. We prefer to use the designation "P Cygni star" only for very luminous stars closely resembling P Cygni (see below). A few bright B-type supergiants are listed in Table 1, and more are contained in the catalogues of Merrill and Burwell (1933, 1943, 1949), in the extensive lists of O and B stars by Morgan, Code, and Whitford (1955) and by Hiltner (1956).

In terms of the model sketched in Figure 1, P Cygni profiles (Beals line types I–IV) can be explained by an expanding envelope of moderate density. The displaced absorption component is formed by the absorption lobe, and the emission feature comes from the emission lobes. The envelope is probably symmetrical about the star, for there is no preferential plane such as that defined in the case of Be stars by the plane perpendicular to the axis of rotation.

In the B- and late O-type supergiants the hydrogen emission is quite weak, and it seems probable that the emitting envelope is not very extensive. Since no observations have been obtained showing the absorption and emission pattern reversed, it seems unlikely that the outer atmosphere of a supergiant ever contracts, although irregular changes in velocity do occur, indicating that the velocity of expansion is variable (Abt 1957). No early-type supergiant has yet been proved to be a member of a spectroscopic binary, although approximately one-third of the normal O and B stars that have been observed in detail for radial velocity have turned out to be spectroscopic binaries. Most early-type supergiants vary in light irregularly by a small amount.

It is very difficult to establish accurately the absolute magnitudes of the early-type supergiants. They are too distant for trigonometric methods to be useful; one must rely on indirect methods, such as membership in clusters and associations and the intensity of the interstellar lines. These methods are not very precise as they have been applied so far. Membership in a cluster should be proved by factors other than apparent propinquity, and the depth

of an association is an unknown but vital quantity. The Hγ method (Petrie 1952) breaks down for the most luminous stars because the equivalent width of Hγ becomes small and the calibration-curves are insensitive in this region. Also the measured result may be falsified by unresolved weak emission. The visual absolute magnitudes of the early-type supergiants of class I*a* would appear to run from about −6.5 to brighter than −7. There is weak evidence that one or two B0 supergiants—for instance, HD 194279 (Underhill 1955) and stars like β Ori and 6 Cas (Abt 1957)—may be as bright as −8 mag. These luminosities are comparable to those assigned to P Cygni and similar stars and to the luminosities of the extreme F-type supergiants in the Andromeda Nebula (Hubble and Sandage 1953).

As soon as stellar spectra were studied in detail, it was noted that the spectrum of P Cygni was unusual, being that of a B1 star plus many emission lines of a characteristic shape—sharp emission accompanied by a violet-displaced absorption core. This star has become a type star, and relatively sharp emission lines which are accompanied by violet-displaced absorption cores are called "P Cygni lines." It is different from other stars discussed in this chapter, in that it has changed magnitude in a nova-like manner. It is probably more closely related to the so-called, but poorly named, slow novae RR Tel, RR Pic, η Car, etc., than to normal B-type stars. The star S Dor is called a P Cygni star (Wesselink 1956), but it would appear to resemble more closely the Hubble and Sandage (1953) F-type supergiants in spectral type. Good replicas of P Cygni are HD 94910 (AG Car), HD 37836, and HD 269858.

Beals long ago pointed out that the typical emission-absorption pattern of P Cygni lines could be explained by an expanding atmosphere. The P Cygni stars are related to the Be stars, Of stars, Wolf-Rayet stars and novae by this feature, for all have extended envelopes which expand at times. However, the spectroscopic phenomena of an expanding envelope, striking as they may be, are not a fundamental reason for classing all these types of stars together. The spectroscopic details are the normal result of a stream of high-temperature radiation passing through a moving, low-density gas. The fundamental relationships between the various stars with extended atmospheres are to be sought in the way these stars release energy and in the amount and quality of energy released at any one time. The point of view of this chapter is that B, Be, and shell stars are related and that the Of and Wolf-Rayet stars probably are their counterparts at higher surface temperatures. The early-type supergiants are another basic group. It is interesting to speculate whether or not they are related to objects like η Car and P Cyg. Gratton (1955) and the La Plata astronomers have commented on a possible connection, noting that S Dor and η Car are probably members of O associations. However, Thackeray (1957) states that there is evidence that η Car is a slow "supernova" which attained an absolute magnitude between −13 and −14 in 1841.

There are a few stars with a dominant early-type spectrum and a very extensive atmosphere producing irregularly variable emission lines and displaced sharp absorption lines that are not easily put into any of the classes discussed here. At present, each requires a separate description. Examples are HD 108, which may be a shell star with an O-type star as the underlying star, and XX Oph, which Merrill and Burwell call a "shell star." The symbiotic stars, such as Z And, which show an M-type spectrum and characteristics of a very high-excitation spectral type are discussed in the literature. Further details are given by Merrill (1957).

§ 5. THE Of STARS

The designation Of is given to stars which have a spectrum containing absorption lines of type O and, in addition, emission lines at He II λ 4686 and at N III λλ 4634, 4640, and 4641. The hydrogen lines visible on blue-sensitive plates are not in emission in most Of stars. However, there is usually weak emission at Hα and at the line C III λ 5696. The lines N V λ 4603 and λ 4619, N IV λ 4057, Si IV λ 4088 and λ 4116, and He I λ 5876 have been observed in emission in a few Of stars of very early type; there is some evidence for an unidentified emission line at λ 4485 in the spectrum of 9 Sge and other late-type Of stars. A detailed study of high-dispersion plates might reveal more weak emission lines.

About 13 per cent of the O stars in the catalogues by Morgan, Code, and Whitford (1955) and by Hiltner (1956) are listed as Of. In these catalogues the "f" designation is given only to stars of type O8 and earlier. Apparently, no emission at the N III λ 4640 multiplet or at He II λ 4686 was detected at type O8.5 and later on the low-dispersion spectra of these studies. However, detailed quantitative measurements on moderate- and high-dispersion spectra (Wilson 1955; Underhill 1957*b*) indicate that some emission at the N III λ 4640 multiplet occurs in practically all O-type stars. Therefore, it would appear that the pure absorption-line O stars and the Of stars do not form separate groups, but that there is a continuous gradation in the strength of the N III λ 4640 emission.

Although the Of designation does not define a sharp group of objects, it is probably worth retaining because it does isolate the O-type stars with the strongest emission lines in their spectra and thus presumably those with the most extensive atmospheres. The last conclusion arises if one assumes a model such as that sketched in Figure 1 to account for the emission lines. The absorption lines in most O-type spectra are shallow and diffuse, but not enough detailed information is available to permit one to infer that the extended atmosphere is preferentially confined to an equatorial plane (as for many Be stars) because of the rapid rotation of the star. Large-scale, chaotic motion of the outer atmosphere, possibly in a field of large prominences, is another model consistent with the few available observations. Moreover, it is reasonable to ex-

pect that electron scattering will broaden all line profiles in the stars of earliest spectral type.

Intensity tracings of the region λλ 4600–4730 in the spectra of some Of stars, some O stars, and some late O-type supergiants are shown in Figure 3. The relatively sharp emission features on which the Of classification is based are readily visible in the first three strips. The faint, extended emission wings discovered by Wilson (1955) can also be traced in most of these stars. The C III λ 4650 absorption lines are very strong in the late O-type supergiants HD 188209 and α Cam and decrease in intensity in the stars of earlier spectral type. There is weak emission at N III λλ 4634–41 in the spectrum of α Cam, and the line He II λ 4686 is almost completely filled in with emission.

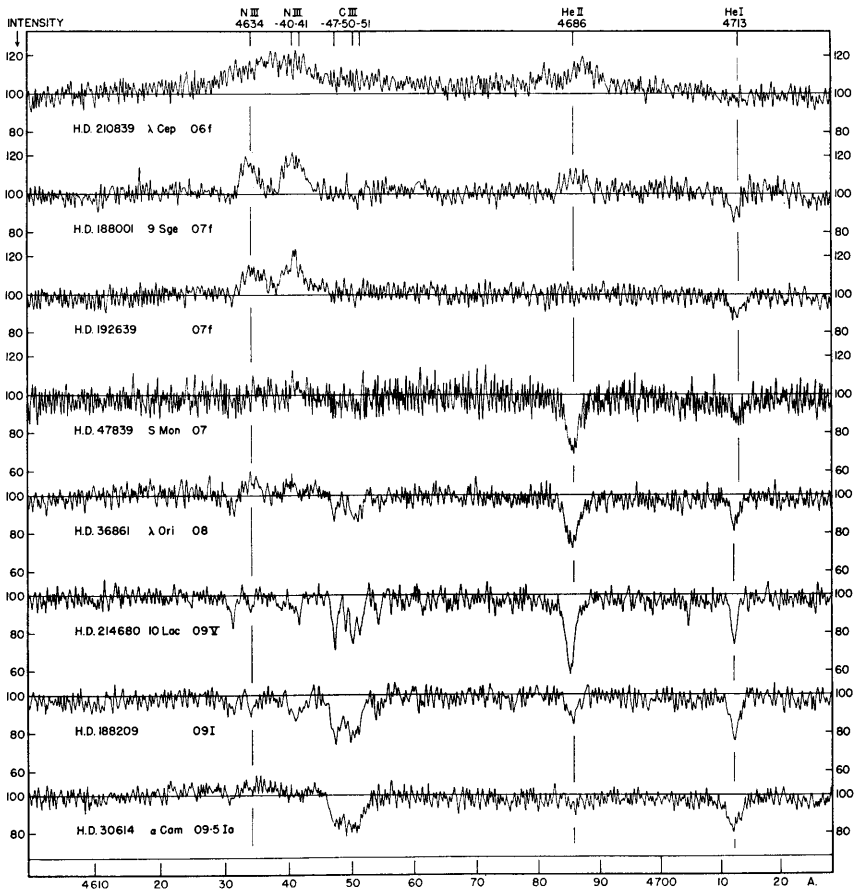


FIG. 3.—Intensity tracings of some O-type spectra in the region λλ 4600–4730. The continuum has been drawn as high as possible in this illustration. Arguments could be given to lower the continuum by 3 or 4 per cent, but not to lift it farther. The linear dispersion on the plates is 15.5 A/mm at λ 4680.

It is not clear at present whether the Of stars are significantly more luminous than the pure absorption O stars of the same spectral subdivision. Roman (1951) from a study of some stars in Cygnus suspected that the Of stars might be more luminous than the O stars, but Underhill (1955) was not able to substantiate this claim. The extended atmosphere in which the emission features originate is not necessarily a criterion of high luminosity. This point is illustrated by the Be shell stars, which are main-sequence objects, even though they have extended atmospheres and have spectra with many features in common with spectra of A-type supergiants. The f characteristics alone will not distinguish between a shell star and a supergiant.

The emission at the hydrogen lines is probably a pure recombination spectrum. At the He II lines, it may also be a recombination spectrum, except for the rather strong emission at He II λ 4686, which is considerably stronger than the emission at any other observable He II line. Bowen (1935) has suggested a cycle involving Lyman-α of hydrogen, which would account for the strong emission at He II λ 4686. The other emission lines appearing in Of spectra probably are excited by selective processes. Swings (1948) has summarized the relevant information regarding many of these lines. Here we shall mention only the exciting mechanisms for the N III λλ 4634–4641 multiplet and for the C III λ 5696 line, since these lines are the selectively excited emission lines most frequently observed in Of spectra. The N III lines are probably excited by the cycle proposed by Bowen (1935) to account for the occurrence of these lines in the spectra of gaseous nebulae. This cycle involves a wave-length coincidence between He II λ 303 and an O III line and another coincidence between O III λ 374 and an N III line. The result is that the N III lines, λλ 4634–4641, will be excited in emission whenever a strong flux of He II λ 303 passes through a high-temperature gas at low density. The C III line, λ 5696, is probably excited by preferential ionization from the 3^2D level of C II by He II λ 303 quanta (Underhill 1957*c*). This process, which is the same as ejection from the K and L shells known from γ-ray work, selectively creates C^{++} ions in the 3^1D level, which is the upper level of λ 5696. The 3^1D level cannot be reached from the ground level of the C^{++} ion by the absorption of one quantum of radiation because such a transition is forbidden by parity selection rules.

It has been suggested from time to time that the emitting shells around O stars are variable. Consideration of the well-established variations in many Be spectra makes this suggestion plausible, but it is a difficult observational problem to establish firmly such variations. It is extraordinarily difficult to define the level of the continuous spectrum in an O-type spectrum because of the shallow, diffuse character of the many possible absorption lines. The apparent strength of weak emission features depends greatly upon the assigned level of the continuum. One of the outstanding problems in the study of O-type spectra is the careful delineation of the continuum and the measurement of the extended shallow absorption features and of the faint extended emission

features that exist. The intensity tracings of Figure 3 give an example of the problem posed. Here the continuum has been drawn as high as possible, in order not to exaggerate the faint emission wings at N III λλ 4634–4641; nevertheless, these emission wings are seen to be real, though their height above the continuum may be less than 5 per cent.

No evidence of dilution is found in the He I absorption spectrum of Of stars. Thus it seems clear that the extended atmosphere which produces the emission lines and which may produce shell absorption lines does not extend far from the stellar surface. No forbidden emission lines have been observed in Of spectra.

§ 6. THE WOLF-RAYET STARS

The Wolf-Rayet stars are few in number, about 150 being listed in the *Henry Draper Catalogue* and its *Extensions*, but their spectra are conspicuous, consisting primarily of broad emission bands. In some stars there are violet-displaced absorption components, chiefly accompanying He I lines, and occasionally central absorptions are observed. Beals (1930) lists all Wolf-Rayet stars observable from the Dominion Astrophysical Observatory, as well as some southern objects. Henry Smith (1955) has observed the southern Wolf-Rayet stars, and he lists all but two of the known Wolf-Rayet stars brighter than the eleventh magnitude and south of the equator. All Wolf-Rayet stars brighter than 9.5 mag. are given in Table 2.

TABLE 2

WOLF-RAYET STARS BRIGHTER THAN MAGNITUDE 9.5

HD	α(1900)	δ(1900)	Mag.	Sp.	HD	α(1900)	δ(1900)	Mag.	Sp.
50896.....	6^h50^m0	−23°48′	6.6	WN5	156385....	17^h12^m1	−45°32′	7.2	WC7
66811*....	8 00.1	−39 43	2.3	WN7+O5	164270....	17 55.2	−32 43	8.8	WC8
68273*....	8 06.5	−47 03	2.2	WC7+O7	165763....	18 02.5	−21 16	7.8	WC6
76536.....	8 51.6	−47 13	9.0	WC6	168206*†..	18 13.5	−11 40	8.9	WC7+O
86161.....	9 51.6	−57 15	8.5	WN8	190918*...	20 02.2	35 31	7.0	WN5+B0
92740.....	10 37.4	−59 09	6.5	WN7	191765....	20 06.5	35 53	7.8	WN6
92809†....	10 37.8	−58 15	9.0	WC6	192103....	20 08.1	35 54	7.9	WC7
93131.....	10 40.1	−59 36	6.7	WN7	192163....	20 08.4	38 03	7.4	WN6
93162*....	10 40.3	−59 12	8.4	WN7+O7	192641....	20 10.8	36 21	7.9	WC7
96548†....	11 02.3	−64 58	7.8	WN8	193077....	20 13.3	37 07	8.0	WN6
97152*....	11 05.8	−60 26	8.1	WC6+B0	228766*...	20 13.8	37 00	9.1	WN7
113904*....	13 01.7	−64 46	5.6	WC6+O	193576*†..	20 15.8	38 25	8.0	WN6+B1
115473.....	13 12.2	−57 37	9.3	WC6	193793....	20 17.1	43 32	6.8	WC6
136488.....	15 15.8	−62 19	9.4	WC8	193928*...	20 17.8	36 36	9.4	WN6
143414.....	15 55.0	−62 24	9.5	WN6	211853*...	22 15.0	55 37	8.9	WN6+B
151932.....	16 45.3	−41 41	6.6	WN7	214419*†..	22 32.9	56 23	8.9	WN6+O
152270*....	16 47.3	−41 40	6.7	WC7+O8	219460*...	23 10.8	59 55	9.0	WN5+B0
156327*....	17 11.8	−34 18	9.4	WC7+B0					

* Spectroscopic binary.
† Light-variable.

Comprehensive lists of observed lines with identifications are given by Beals (1930), Payne (1933), Swings (1942), H. Smith (1955), Edlén (1956), and Underhill (1959). Some observations in the near infrared have been made by Swings and Jose (1950), by Smith, and by Andrillat (1955). These investigations show that the Wolf-Rayet spectra apparently fall into two classes: the WC stars,

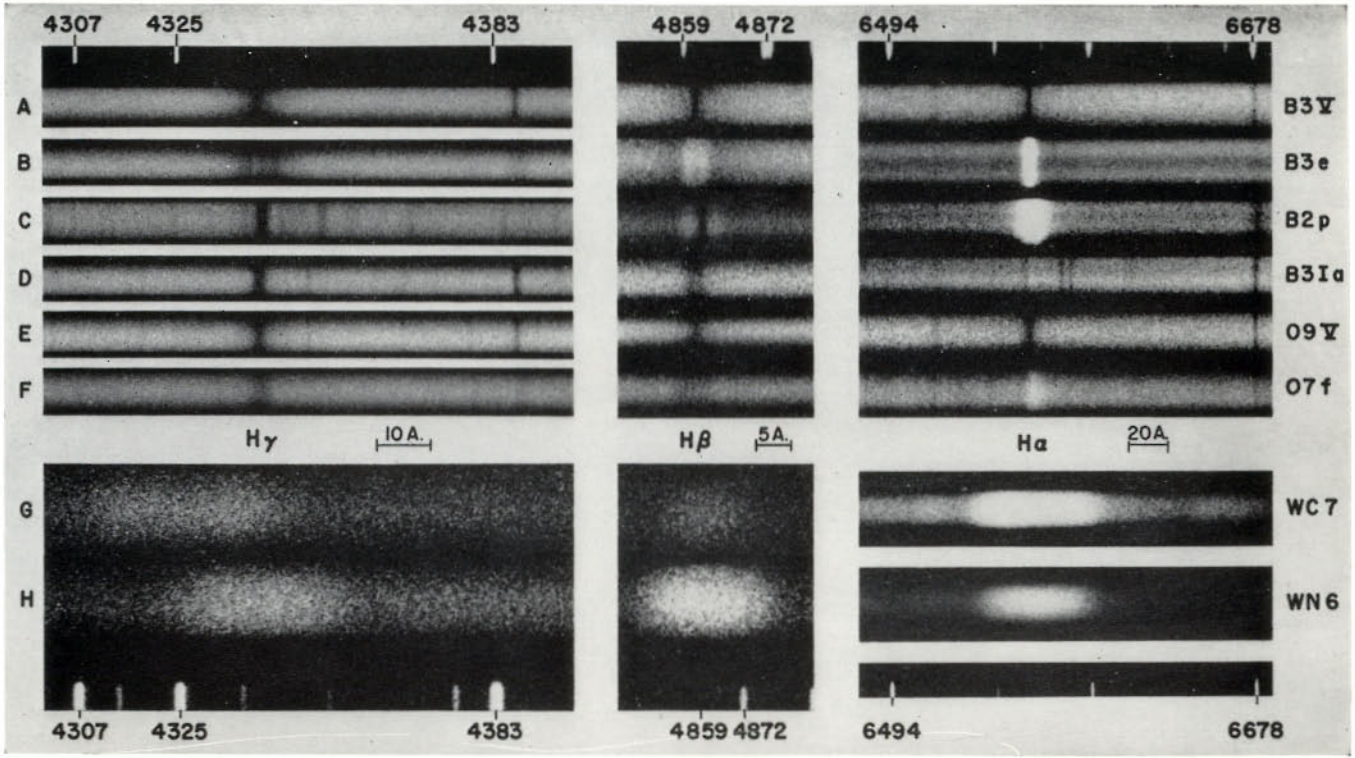


PLATE I.—Spectra of Hα, Hβ, and Hγ in early-type stars with extended atmospheres: (*a*) HD 160762, ι Her, B3 V; (*b*) HD 25950, 48 Per, B3e; (*c*) HD 37202, ζ Tau, B2p; (*d*) HD 198478, 55 Cyg, B3 Ia; (*e*) HD 214680, 10 Lac, O9 V; (*f*) HD 188001, 9 Sge, O7f; (*g*) HD 192103, WC7; (*h*) HD 192163, WN6.

in which emission lines of C II–C IV and O II–O VI are prominent in addition to lines of H, He I, and He II, and the WN stars, in which emission lines of N II–N V dominate to the nearly complete exclusion of lines from the carbon and oxygen ions. The present system of classification for Wolf-Rayet stars (Beals 1938) recognizes this apparent dichotomy, the stars being designated WC if the carbon lines dominate and WN if the nitrogen lines dominate. Classification ratios in the near infrared in step with the Beals system have been established by Andrillat. Spectral types WC8–WC6 and WN8–WN5 are recognized. This classification system attempted to assign similar numbers (e.g., WC6 and WN6) to stars of the different sequences which have atmospheres of about the same general level of ionization, but subsequent investigations have indicated that the WC and WN sequences are not strictly parallel. At present, these sequences cannot be simply interpreted in terms of a single temperature in the manner that has been so successful for the stars of other spectral types.

Although the majority of Wolf-Rayet spectra are dominated exclusively by emission lines either from carbon and oxygen ions or from nitrogen ions, a few objects have been observed in which the carbon and oxygen lines appear with comparable intensity to the nitrogen lines. Examples are HD 62910, HD 104994, and HD 143414, which are described by Smith (1955). Both Swings (1942) and Aller (1943) showed independently that the strong C IV lines, λλ 5801–5812, are present in WN stars, but lines from the oxygen ions and other carbon lines are not usually observed with any appreciable strength. The nuclei of some planetary nebulae have Wolf-Rayet spectra, and, though the nucleus may be classified WC, the nebula will usually radiate emission lines from nitrogen, oxygen, and carbon ions. No forbidden lines are observed in Wolf-Rayet spectra.

Short regions at Hα, Hβ, and Hγ in a WC7 and in a WN6 spectrum are shown in Plate I. These broad profiles are typical of all Wolf-Rayet emission lines. The lines at the wave lengths of Hα, Hβ, and Hγ are blends of H and He II. A strong C III line, λ 4326, blends with Hγ in the WC7 star, causing an apparent elongation of the spectral feature to the violet; another blend with the C IV line, λ 6592, more clearly visible on less densely exposed plates, occurs at Hα.

Because the apparent division into WC and WN sequences is so striking in the usually observed spectral range, it has been suggested that in the Wolf-Rayet stars a real case of anomalous abundances is observed. The WN stars are postulated to contain little or no carbon and oxygen in their atmospheres, while the WC stars are postulated to contain little or no nitrogen. Since the abundances of certain carbon and nitrogen isotopes are intimately connected with the cycle proposed by Bethe to account for the energy generation of stars, the observation of a true abundance anomaly in carbon and nitrogen would be of great significance. However, the intensity of any spectral line depends not only on the abundance of the carrier atom but also on the conditions of excitation. A thorough examination of the methods of excitation of emission-line

spectra in Wolf-Rayet atmospheres should be made before it is concluded that a true abundance anomaly exists. Such an examination requires quantitative measurements of significant spectral features and a basic physical understanding of the excitation and ionization processes acting in Wolf-Rayet atmospheres. At present, both the observations, because of the faintness of the stars, and the theory, because of the incompletely understood situation, are rudimentary. Therefore, the suggestion that a real abundance anomaly exists should be treated with reserve. References to a number of the theoretical papers dealing with Wolf-Rayet atmospheres are given elsewhere (Underhill 1957).

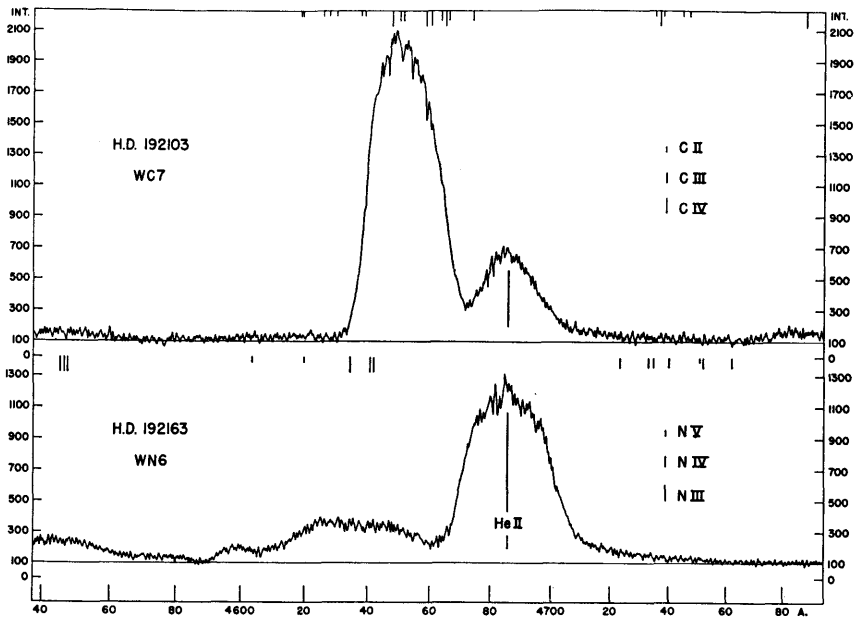


FIG. 4.—Intensity tracings of some Wolf-Rayet spectra in the region λλ 4540–4800. The linear dispersion on the plates is 30 A/mm at λ 4680.

A crude theoretical estimate of the far ultraviolet spectrum of Wolf-Rayet stars (Underhill 1957*b*) indicates that departures from a black-body intensity distribution of the radiation from the underlying star may serve to explain the division into WC and WN sequences.

The most difficult observational result to accept is that no evidence of N III and N IV is found in WC spectra. In particular, it seems most peculiar that no traces are found of the N III λλ 4634–4641 multiplet, which is intrinsically strong and which appears in emission in Of stars and in gaseous nebulae. In order that this problem may be examined, sections of intensity tracings of the spectrum of HD 192103, WC7, and of HD 192163, WN6, are presented in Figure 4. The linear dispersion on the plates is 40 A/mm at λ 4680. The posi-

tions of all C II, C III, C IV, N III, N IV, and N V lines in this spectral region are marked. Some of these lines are intrinsically strong and certainly present, while others are intrinsically weak and may not be present. Attention should be directed to the faint, extensive emission feature shortward of the prominent line λ 4650 in the WC spectrum and to the longward wing of He II λ 4686 in both spectra. The faint emission shortward of the λ 4650 emission has not been noted previously in the literature; no comment has been made on the He II wing. Another significant point is that the N III and N V feature at λ 4640 in the WN spectrum is approximately one-third as intense as the He II λ 4686. Considering this and the fact that the shortward edge of the λ 4650 emission is steeper than the longward edge (which possibly is caused by displaced absorption in the C III lines, which are strongly in absorption in late O-type supergiants), can one unequivocally say that there is no N III emission in WC stars? The longward wing of He II λ 4686 may be interpreted as partly due to N IV or as a true part of the He II line. A decision on these points would be aided by observations of the shape of the profile of He II λ 3203 and by detailed observation of the line profiles in the region near Hδ, where another group of strong N III lines occurs. The fact that most of the emission bands in Wolf-Rayet spectra are blends of lines from several different ionic spectra makes the problem of analysis and interpretation very difficult (see Underhill 1959).

Attempts have been made by Beals (1934, 1940) to estimate the ionization temperatures in Wolf-Rayet atmospheres, using Zanstra's theory for nebular spectra. The resulting temperatures are high, from 60,000° to 110,000°, and their real meaning is obscure because many lines of reasoning, particularly concerning the observations of Wolf-Rayet spectroscopic binaries, indicate that conditions in Wolf-Rayet atmospheres are not those postulated in the theory. The color temperatures of Wolf-Rayet stars estimated from spectrophotometric measures are low, being of the order of 13,000° in the blue spectral region (Vorontsov-Velyaminov 1945; Andrillat 1955); interstellar absorption corrections are uncertain.

The absolute magnitudes of Wolf-Rayet stars are somewhat uncertain, for it is very difficult to find criteria of distance. Most reliance has to be placed on the strength of interstellar features. If the resulting absolute magnitudes are to be compared with the visual absolute magnitudes of O and B stars which give a measure of the brightness of the continuous spectrum in the visual spectral range, the apparent magnitudes of the Wolf-Rayet stars must be corrected for the brightness of the emission bands. It may readily amount to between 0.5 and 1.0 mag. When appropriate corrections are made for the strength of the emission bands and for the interstellar extinction, the average visual absolute magnitude of a Wolf-Rayet star is probably about -2 to -4. Andrillat gives some evidence that WC stars are brighter than WN stars by about 0.7 mag.

The following physical processes have been suggested to explain the charac-

teristic shape of the emission lines in Wolf-Rayet spectra: (1) Beals (1930), arguing from the similarity to nova spectra, has proposed an ejection mechanism; (2) Münch (1950) has emphasized the broadening effects of electron scattering; (3) Thomas (1949) has drawn attention to turbulent motion and to the contribution that such motion can make to the problem of atmospheric support; (4) Johnson (1954), arguing from solar-flare phenomena, has suggested that the broadening effects of discharges in crossed magnetic fields may be relevant. The first three phenomena almost certainly play a role; the fourth probably does not (see recent work by Underhill [1959]). Sobolev (1947), following up the work of Kosirev and Chandrasekhar, has developed the theory of expanding atmospheres in some detail with special reference to Wolf-Rayet stars.

About half the stars in Table 2 are known to be spectroscopic binaries. Those north of the equator have been observed for radial velocity chiefly by Hiltner and by O. C. Wilson (1948). The southern stars have not all been observed for radial velocity, and some are called "spectroscopic binaries" on the basis that Smith (1955) observed composite spectra. Two of the southern Wolf-Rayet stars in Table 2 have been announced to be light-variables by S. Gaposchkin (1942, 1959).

Spectroscopic and photometric observations of the eclipsing binaries have given some clues to the physical conditions in and extent of Wolf-Rayet atmospheres. The most complete set of observations are available for HD 193576 (V444 Cyg), and a detailed discussion of the observational results is given by Münch (1950). These investigations indicate that the model of Figure 1 will suffice for Wolf-Rayet stars if an extensive atmosphere of electrons is added outside the extended atmosphere in which the emission lines originate. Münch's analysis shows that electron scattering and large turbulent velocities are probably important in producing the observed shapes of the emission lines. Irregular variations in the line profiles of the Wolf-Rayet components of spectroscopic binaries have been observed from time to time. These are likely to be due to selective excitation effects, such as those causing the appearance of emission lines in Of stars, and they illustrate the dynamic character of Wolf-Rayet atmospheres. Further investigation of these in HD 193576 is made by Sahade (1957). Münch's analysis of the spectrum of HD 193576 indicates that the observed features can be interpreted in terms of an envelope with radially decelerated motions. There is some indication that the degree of ionization increases outward. It is very difficult to obtain a secure estimate of the radius of the emitting region of a Wolf-Rayet star and of the electron density in this atmosphere. Reasonable values may be 10–15 solar radii and N_e of the order of 10^{12}–10^{13}/cm^3.

Hiltner (1951) and O. C. Wilson (1941) noted that the γ-velocity obtained from the measurement of the emission lines (usually only He II λ 4686) of the Wolf-Rayet component is often about 100 km/sec longward of that derived from the absorption lines of the companion star. Münch (1950) has given evi-

dence to show that this effect is probably a result of self-absorption and blending in the profiles and is of no fundamental significance. It is a severe problem in the study of Wolf-Rayet spectroscopic binaries to establish standard wave lengths which will yield the motion of the star on an absolute scale. Keeping (1947) has shown how the study of microphotometer tracings can assist the solution of this problem. Hiltner (1950) has observed the light-curve of the eclipsing binary CQ Cep in λ 4686 and found unusual variations; this line is stronger at the conjunctions than at the elongations.

REFERENCES

Abt, H. A.	1957	*Ap. J.*, **126**, 138.
Aller, L. H.	1943	*Ap. J.*, **97**, 135.
Andrillat, Y.	1955	Thesis, Université de Lyon.
Beals, C. S.	1930	*Pub. Dom. Ap. Obs. Victoria*, **4**, 288.
	1934	*Ibid.*, **6**, 95.
	1938	*Trans. I.A.U.*, **6**, 248.
	1940	*J.R.A.S. Canada*, **34**, 169.
	1950	*Pub. Dom. Ap. Obs. Victoria*, **9**, 1.
Bowen, I. S.	1935	*Ap. J.*, **81**, 1.
Burbidge, E. M., and Burbidge, G. R.	1951	*Ap. J.*, **113**, 84.
	1953*a*	*Ibid.*, **117**, 407.
	1953*b*	*Ibid.*, **118**, 252.
	1956	*Vistas in Astronomy*, ed. A. Beer (London and New York: Pergamon Press), **2**, 1446.
Dokutchaeva, O. D.	1955	*Trans. I.A.U.*, **9**, 392.
Edlén, B.	1956	*Vistas in Astronomy*, ed. A. Beer (London and New York: Pergamon Press), **2**, 373.
Edwards, D. L.	1956	*Vistas in Astronomy*, ed. A. Beer (London and New York: Pergamon Press), **2**, 1470.
Gaposchkin, S.	1942	*Pub. Am. Astr. Soc.*, **10**, 250.
	1959	*A.J.*, **64**, 127.
Gratton, L.	1955	*Non-stable Stars* (Symposium No. 3 of I.A.U.), ed. G. H. Herbig (Cambridge: Cambridge University Press), p. 87.
Hiltner, W. A.	1947	*Ap. J.*, **105**, 212.
	1950	*Ibid.*, **112**, 477.
	1951	*Ibid.*, **113**, 317.
	1956	*Ap. J. Suppl.*, **2**, 389.
Hubble, E., and Sandage, A.	1953	*Ap. J.*, **118**, 353.
Johnson, M.	1954	*Observatory*, **74**, 124.
Keeping, E. S.	1947	*Pub. Dom. Ap. Obs. Victoria*, **7**, 349.
Lockyer, W. J. S.	1930	*M.N.*, **91**, 187.
McLaughlin, D. B.	1957	*Proc. Liège Symposium on Emission Line Stars*, p. 231 (Mém. Soc. Roy. Liège, 4th ser., Vol. **20**).

MERRILL, P. W.	1953	*Ap. J.*, **117**, 7.
	1957	*Proc. Liège Symposium on Emission Line Stars*, p. 436 (Mém. Soc. Roy. Liège, 4th ser., Vol. **20**).
MERRILL, P. W., and BURWELL, C. G.	1933	*Ap. J.*, **78**, 87.
	1943	*Ibid.*, **98**, 153.
	1949	*Ibid.*, **110**, 387.
	1950	*Ibid.*, **112**, 72.
MERRILL, P. W., and SANFORD, R. F.	1944	*Ap. J.*, **100**, 1.
MINKOWSKI, R.	1951	*Pub. U. Michigan Obs.*, **10**, 25.
MORGAN, W. W., CODE, A. D., and WHITFORD, A. E.	1955	*Ap. J. Suppl.*, **2**, 41.
MÜNCH, G.	1950	*Ap. J.*, **112**, 266.
PAYNE, C. H.	1933	*Zs. f. Ap.*, **7**, 1.
PETRIE, R. M.	1952	*Pub. Dom. Ap. Obs. Victoria*, **9**, 251.
PLASKETT, J. S., and PEARCE, J. A.	1931	*Pub. Dom. Ap. Obs. Victoria*, **5**, 1.
ROMAN, N. G.	1951	*Ap. J.*, **114**, 492.
ROTTENBERG, J. A.	1952	*M.N.*, **112**, 125.
SAHADE, J.	1957	*Proc. Liège Symposium on Emission Line Stars*, p. 46 (Mém. Soc. Roy. Liège, 4th ser., Vol. **20**).
SLETTEBAK, A.	1949	*Ap. J.*, **110**, 498.
	1951	*Ibid.*, **113**, 436.
	1952	*Ibid.*, **115**, 573.
	1955	*Ibid.*, **121**, 653.
SLETTEBAK, A., and HOWARD, R. F.	1955	*Ap. J.*, **121**, 102.
SMITH, B.	1947	*Ap. J.*, **105**, 489.
SMITH, H. J.	1955	Thesis, Harvard University.
SOBOLEV, V. V.	1947	*Moving Stellar Envelopes* (Leningrad: Leningrad State University).
STRUVE, O.	1942	*Ap. J.*, **95**, 134.
	1945	*Pop. Astr.*, **53**, 201, 259.
STRUVE, O., and WURM, K.	1938	*Ap. J.*, **88**, 84.
SWINGS, P.	1942	*Ap. J.*, **95**, 112.
	1948	*Ann. d'ap.*, **11**, 228.
SWINGS, P., and JOSE, P. D.	1950	*Ap. J.*, **111**, 513.
THACKERAY, A. D.	1957	*M.N.*, **117**, 296.
THOMAS, R. N.	1949	*Ap. J.*, **109**, 500.

UNDERHILL, A. B.	1951	*Pub. Dom. Ap. Obs. Victoria*, **9**, 139.
	1953	*M.N.*, **113**, 477; *Contr. Dom. Ap. Obs.*, No. 32.
	1954	*Pub. Dom. Ap. Obs. Victoria*, **9**, 363.
	1955	*Ibid.*, **10**, 169.
	1957*a*	*Pub. A.S.P.*, **69**, 401.
	1957*b*	*Proc. Liège Symposium on Emission Line Stars*, p. 17 (Mém. Soc. Roy. Liège, 4th ser., Vol. **20**).
	1957*c*	*Ap. J.*, **126**, 28.
	1958	*Pub. Dom. Ap. Obs. Victoria*, **11**, 143.
	1959	*Ibid.*, p. 209.
VORONTSOV-VELYAMINOV, B.	1945	*A.J., U.S.S.R.*, **22**, 2.
WELLMAN, P.	1955	*Vistas in Astronomy*, ed. A. BEER (London and New York: Pergamon Press), **1**, 303.
WESSELINK, A. J.	1956	*M.N.*, **116**, 3.
WILSON, O. C.	1941	*Ap. J.*, **91**, 379.
	1948	*Ibid.*, **109**, 76.
WILSON, R.	1955	*Observatory*, **75**, 222.
	1956	*Pub. R. Obs. Edinburgh*, **2**, 16.
WILSON, R. E.	1941	*Ap. J.*, **94**, 12.

CHAPTER 11

Eclipses by Extended Atmospheres

O. C. WILSON
Mount Wilson and Palomar Observatories
Carnegie Institution of Washington, California Institute of Technology

§ 1. INTRODUCTION

It is difficult, for obvious reasons, to obtain information about the outer atmospheric layers of stars. The sun is near enough for its surface to be studied in considerable detail, and a good deal is known about the phenomena which take place there. Also, since the sun is a normal star, one presumes that stars in general are probably equipped with chromospheres, coronas, prominences, etc. But to carry the matter further than this is not at all easy, since we must, in general, deal with radiation that originates at all parts of the stellar surface and through a range of depths. In this integrated radiation, virtually the entire continuum and probably nearly all (except the central cores) of the line absorption originate in the lower, denser, atmospheric zones, known formerly as the "photosphere" and the "reversing layer." The tenuous outer regions make an unknown, though probably small, contribution to the integrated spectrum. Only in the supergiants does it appear likely that the contribution of the outer layers to the absorption lines may be significant (see, e.g., Adams 1956). Apart from these objects, it appears that the only spectral features in the stars of later type (G–K–M) which can be assigned with reasonable certainty to chromospheric origin are the centrally reversed emission components in the H and K lines of Ca II.

There is, however, a small group of highly specialized objects which permit the investigation in some detail of the chromospheric zones of a few giant stars of late spectral type. These are eclipsing binary systems, one member of which is a late-type giant and the other an early-type star of much smaller radius. In a favorable case the diameter of the smaller, bluer star will be only a few per cent of that of its larger companion, but the large difference in surface temperature causes the continuous radiation of the two to be equal somewhere in the photographic region. Outside the eclipse, the radiation of the blue star will predominate at shorter wave lengths, while the reverse is true at longer wave

lengths. Before and after totality the small star passes behind the various atmospheric layers of the large one, and the atoms and ions in the chromosphere of the late-type giant produce absorption lines in the continuum of the companion. Measures of displacement and intensity of these chromospheric absorption lines at different heights then yield valuable information as to the physical state of the chromospheric material.

§ 2. AVAILABLE BINARY SYSTEMS

As would be expected from general considerations, binary systems fulfilling the conditions mentioned above are not very numerous. In fact, there are only four which, up to the present, have been investigated in more or less detail. These are ζ Aurigae, 31 Cygni, 32 Cygni, and VV Cephei. In addition, ϵ Aurigae might be considered to display atmospheric eclipses of a sort, but this system is so different in characteristics from the other four and presents so many uncertainties in interpretation that it will not be discussed in detail. According to the most recent discussion (Struve 1956), ϵ Aurigae is probably a pair of stars, both surrounded by huge nebular envelopes filling completely their respective loops of the critical zero-velocity surfaces. Matter is supposed to stream outward from these envelopes through the inner Lagrangian point. Finally, the entire system is pictured as being imbedded in an enormous expanding nebulosity of low density.

Every 27.1 years an eclipse occurs; the depth is 0.8 mag., and the total duration is 714 days, of which the length of the total phase amounts to 300 days. The most recent eclipse began on June 5, 1955 (Struve 1956), and presumably ended in May, 1957. Spectroscopic coverage of this eclipse seems to have been fairly complete, but it is evident that some time must elapse before the collected material on either spectra or photometry will be available. The spectroscopic phenomena are complex, and their interpretation cannot yet be regarded as final. It therefore seems more advantageous in this chapter to devote most of the available space to the other four stars mentioned above, in which the spectroscopic phenomena evidently arise in stellar atmospheres of a much more "normal" kind than in ϵ Aurigae.

§ 3. COMPARISON OF ζ AURIGAE, 31 CYGNI, 32 CYGNI, AND VV CEPHEI

Table 1 contains data on the first three of these systems as compiled by McKellar and Petrie (1958) and is based partly upon their own work (31 Cygni) and partly upon the work of a number of other investigators. It represents, in their judgment, the best information currently available, but many of the entries will undoubtedly undergo modification in the course of time. Pending further improvement, however, Table 1 will serve as a good guide for the main features of the three systems included.

A simple comparison of the eclipse phenomena of the four stars has been made

by McLaughlin (1952*a*) on the basis of careful eye-estimates of intensities of chromospheric lines during the atmospheric eclipses. When the relative time scales are adjusted according to the ratios VV Cep: 32 Cyg: 31 Cyg: ζ Aur = 60:5. 0:3. 0:1, plots of the chromospheric line intensities against time for the four stars agree reasonably in shape and clearly demonstrate the general similarity of the eclipse phenomena.

In the following sections the four stars will be discussed individually. It should be mentioned that, because of space limitations and the extensive literature on these objects, no attempt is made to cover the literature completely or

TABLE 1

DATA ON THREE BINARIES HAVING ATMOSPHERIC ECLIPSES

	31 Cygni	ζ Aurigae	32 Cygni
Combined visual magnitude	4.0	3.9	4.2
Depth of eclipse in visual region	0.1 mag.	0.2 mag.	0.2 mag.
Depth of eclipse in photographic region	0.4 mag.	0.7 mag.	.....
Depth of eclipse in ultraviolet region	1.6 mag.	2.2 mag.	.....
Nature of eclipse	Nearly central	Nearly central	Not central
Spectral type of primary	K3 or K4 I*b*	K3 or K4 I*b*	K5 I
Spectral type of secondary	B3–B5 V	B8	B3 V
Wave length at which primary and secondary are equally bright	~3900 A	~4300 A	~3940 A
Period of revolution	~3780 days	972.16 days	~1148 days
Length of total eclipse of B star	61 days	38 days	~13 days
Length of partial eclipse of B star	~1.7 days	1.5 days	~4 days
Length before or after totality of atmospheric eclipse as detected spectroscopically	~70 days	10–40 days (variable)	~70 days
Mass ratio, m_p/m_s	~2.0	~1.8	~2.8
Minimum mass of primary star	18⊙	14⊙	21⊙
Projected semimajor axis of orbit of primary ($a_1 \sin i$)	720×10^6 km	294×10^6 km	250×10^6 km
Estimated inclination of orbital plane	$89°5<i<90°$	$88°<i<90°$	~72°
Minimum diameter of primary	~170⊙	~190⊙	~350⊙
Minimum diameter of secondary	~5⊙	~7⊙	~4⊙

to adhere to a historical presentation. The aim is rather to summarize what is now known and can be deduced about these systems, and the emphasis will necessarily be on the more recent and more complete observations in all cases.

§ 4. DETAILED STUDIES OF ECLIPSE PHENOMENA

4.1. ζ AURIGAE

Since ζ Aurigae has been known longer as an eclipsing system and has been subjected to considerably more observation and analysis than the others, it is appropriate to begin with it.

ζ Aurigae had been listed as a star with a composite spectrum in the *Henry Draper Catalogue*. Toward the long-wave-length end of the photographic region the spectrum was given as type K0; progressively toward shorter wave

lengths the K-type spectrum was more and more washed out until, shortward of the K line, only traces of it remained and the principal features were the Balmer lines of a spectrum rather uncertainly estimated at about B1.

Following scattered spectroscopic observations by various observers, which had already established variations in the radial velocity of the K-type star, Harper (1924) published an orbit for the object. On one of his spectrograms, taken not far from conjunction and with the K-type star on the side toward the sun, Harper noted that the B-type spectrum was no longer present. This fact led Bottlinger (1926) to predict that ζ Aurigae was an eclipsing star. At the eclipse of January–February, 1932, photometric and spectroscopic observations by Guthnick and Schneller (1932) fully confirmed this prediction and were, indeed, adequate to yield data on dimensions of the stars not greatly different from those accepted at present. Guthnick and Schneller observed and correctly interpreted the nature of the K line of Ca II produced in the spectrum of the B star by the atmospheric layers of the K star for about a month following the end of totality.

Since 1932 many observations have been made at successive eclipses. These have led to improved knowledge of the elements of the orbit, of the characteristics of the two stars, and of the physical state of the outer chromospheric layers of the K-type star. Since the methods used in investigating these stars are essentially the same for all of them, they will be described rather fully for ζ Aurigae and can then be referred to more briefly for the other objects.

4.11. *Spectroscopic orbit.*—Harper's orbit (1924) depended entirely on Victoria observations. Hopmann and Schaub (1936) have determined revised elements by using all available radial velocities. The period which they adopt, 972.15 days, due to Miss Swope (1935), is very close to that found by Wood (1951), who gives for the times of primary minimum JD $2432553.666 + 972^{d}162E$.

4.12. *Mass ratio.*—This important datum is exceedingly difficult to determine accurately for systems such as ζ Aurigae, because traces of the underlying K-type spectrum show through in the Balmer lines of the early-type star and render accurate measures of the latter impossible. Christie and Wilson (1935) from measures of four spectrograms heavily exposed to bring out the higher members of the Balmer series derived a value $m_K/m_B = 1.85$. Hopmann and Schaub (1936) from Babelsberg spectrograms found the ratio 2.25 and recalculated from the data of Christie and Wilson to get a revised value of 2.04 and a finally adopted mean mass ratio $m_K/m_B = 2.15$.

The writer has no great confidence in these results but, for want of better material, has generally used a ratio 2.0 in calculations involving this quantity. At present the mass ratio of ζ Aurigae is being investigated by D. M. Popper, but no new results are as yet available.

4.13. *Dimensions, temperatures, luminosities, masses.*—The dimensions of the stars may be computed from the spectroscopic orbital elements, the duration of

total and partial phases of the eclipse, and the mass ratio, provided that the orbital inclination to the line of sight is known or can be safely assumed. Wellmann (1951) has carefully estimated the spectral types and luminosity classes of the two stars and finds them to be K4 II and B7 V. The spectral type of the B-type star follows from an estimate of the intensity of the He I lines λ 3819.6 in its spectrum, and the luminosity from the fact that H14 is the last Balmer line to be seen with certainty. From the orbital elements of Hopmann and Schaub (1936)—duration of totality, 38.4 days, and duration of partial eclipse, 1.3 days—Wellmann finds

$$R_K = 143 \times 10^6 \text{ km} = 205.3 \odot ,$$
$$R_B = 4.8 \times 10^6 \text{ km} = 6.9 \odot .$$

These values are for an assumed inclination $i = 90°$; hence R_K and R_B as given are lower and upper limits, respectively.

According to Keenan and Morgan (1951), the temperatures and absolute visual magnitudes of K4 II and B7 V stars are, respectively, 3480°, −2.3, and 13,500°, −0.8. An independent determination of M_v for the K-type component is −2.1, from the width of the central reversal in the K line of Ca II (Wilson and Bappu 1957). Also a well-determined datum of observation from the eclipse amplitudes at various wave lengths (Guthnick, Schneller, and Hachenberg 1935) is the difference in apparent visual (and therefore in absolute) magnitudes:

$$M_B - M_K = 2.0 \text{ mag.}$$

Now, if following Wellman (1951), one attempts to use the equation

$$M_v = -0.09 - 5 \log \frac{R}{R_\odot} + \frac{29{,}150}{T}, \qquad (1)$$

the foregoing figures do not lead to entirely consistent results, and there is no certainty as to where to place the blame. A reasonable adjustment of the various data which does no violence to any of the observations yields the following:

$$R_K = 205.3 \odot , \qquad M_v(K) = -2^m.5 ;$$
$$R_B = 3.5 \odot , \qquad M_v(B) = -0^m.6 ;$$
$$T_K = 3200° , \qquad M_K = 22.0 \odot ;$$
$$T_B = 13{,}500° , \qquad M_B = 10.2 \odot ;$$
$$i = 90° .$$

Almost certainly the major weakness in these calculations lies in the mass ratio. Until a more reliable observational determination of this quantity is available, there seems little point in attempting further refinements of the foregoing quantities. On the other hand, the moderately good consistency attained would seem to indicate that the adopted mass ratio cannot be seriously in error.

4.14. *Light-curves.*—One serious difficulty in the photometric study of the eclipses of ζ Aurigae is that the duration of partial phase is too long to be covered by any single observer. Hence it has been necessary to combine measures by a number of individuals, sometimes made under adverse conditions and therefore of varying degrees of reliability; the judgment of the analyst necessarily affects the conclusions. For instance, in the past there have been disagreements between analysts who have had access to the same observational data as to whether a bodily eclipse, as by a geometrical straight edge, gives as good a representation of the measures as does one involving an opacity increasing with depth.

Figure 1, taken from the paper of Roach and Wood (1952), shows that a simple geometrical eclipse cannot account for the observations because the

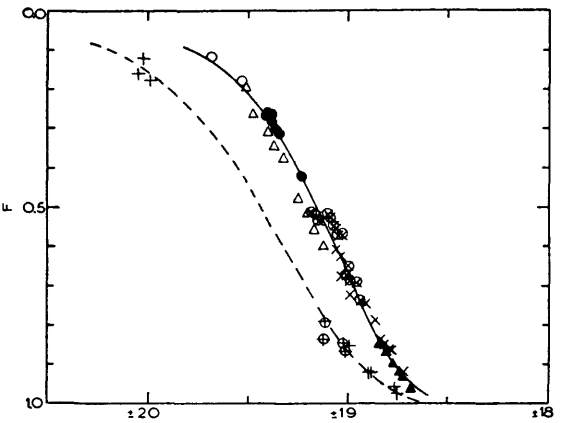


FIG. 1.—ζ Aurigae. Fraction of eclipse versus phase in days. Left-hand curve for $\lambda \sim$ 3800 A; right hand for $\lambda \sim$ 4500 A. For further details see original paper (Roach and Wood 1952).

fraction of eclipse at a given phase is greater in the ultraviolet ($\lambda \sim 3800$ A) than in the blue ($\lambda \sim 4500$ A). Roach and Wood proceed further and show that the observed intensities of the chromospheric lines are such that the total extinction of light of the B star by the cumulative effect of the chromospheric absorption lines is substantially equal to the observed fraction of eclipse. This simple mechanism accounts for the deeper and earlier eclipse at the shorter wave lengths mentioned above and also for the approximate equality of the atmospheric logarithmic gradient found from the photometric data with that deduced in entirely independent fashion from the chromospheric-line intensities.

Finally, it should be noted that many observers have found variations in brightness of ζ Aurigae during totality. Hopmann and Schaub (1936) reproduce some curves showing that the amplitude of these fluctuations decreases toward shorter wave lengths. Presumably, therefore, they are to be attributed to the K-type star. It may be significant in this connection that Roach and Wood

(1952) give photometric evidence that the diameter of the K star was about 1 per cent larger at the time of the 1939–1940 eclipse than during that of 1947–1948.

4.15. *Observations of chromospheric absorption lines.*—It is convenient to divide these observations into two types—(1) measures of line displacement, i.e., of radial velocity, and (2) measures of line strength or equivalent width—and to begin with the first.

1. A number of the earlier observers noticed that the chromospheric lines, especially the H and K lines of Ca II, were displaced toward the red with respect

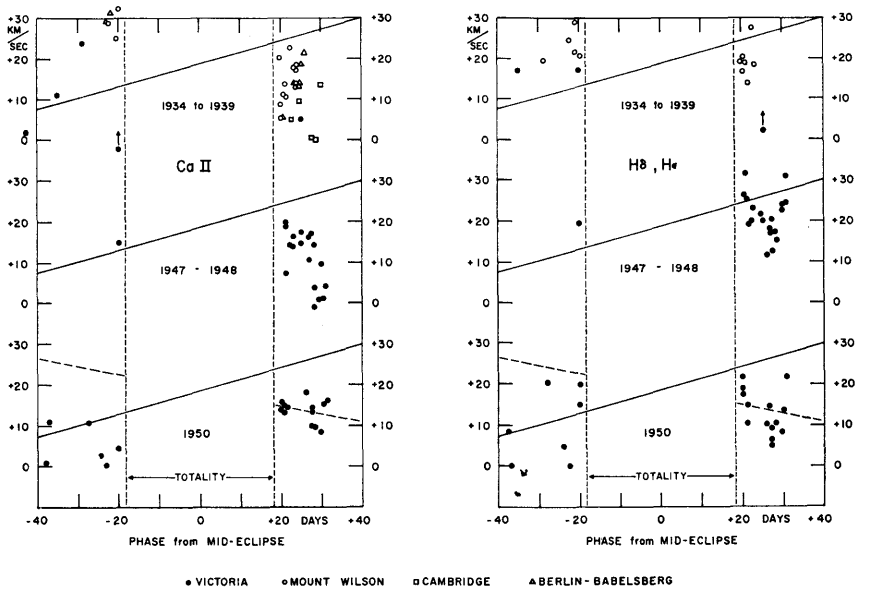


FIG. 2.—Radial velocities from the chromospheric lines of ionized calcium and of hydrogen in ζ Aurigae at various eclipses. Solid diagonal lines are radial velocity-curve of K-type star (McKellar and Petrie 1952).

to the orbital velocity at ingress and toward the violet at egress. A rotation of the star in the same direction as its orbital motion would account for the signs of these displacements, and, indeed, this is the way in which they were usually interpreted. Typical velocity measures of this kind may be found, for instance, in the paper by Christie and Wilson (1935).

More recently it has become evident that rotation alone cannot account for the observed displacements. This is well illustrated by McKellar and Petrie (1952) from whom Figure 2 is taken. A rotational effect should be symmetrical, i.e., equal and opposite at ingress and egress, and the radial velocities of the chromospheric lines should fall upon a straight line intersecting the orbital velocity-curve at a point corresponding to mid-eclipse and inclined to it at an

angle depending on the speed of rotation. Broken lines of this type have been drawn in the lower sections of Figure 2, and it is obvious that the rotational explanation must be abandoned.

Another study of the chromospheric radial velocities made with somewhat higher dispersion than that used at Victoria is contained in a paper by Wilson and Abt (1954), and the results are shown in Figures 3 and 4. As in Figure 2,

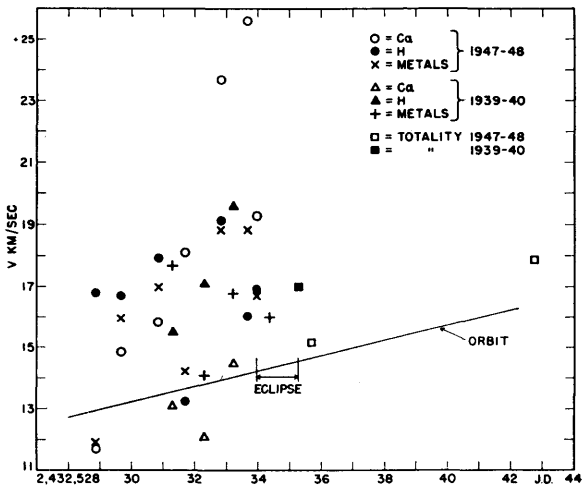


FIG. 3.—Mount Wilson radial velocities of chromospheric lines of ζ Aurigae near ingress. JD numbers (also for Fig. 4) are for 1947–1948 eclipse (Wilson and Abt 1954).

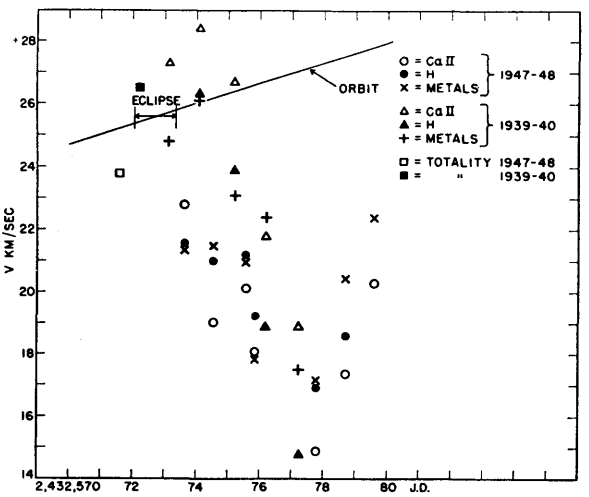


FIG. 4.—Mount Wilson radial velocities of chromospheric lines of ζ Aurigae near egress (Wilson and Abt 1954).

one sees that the deviations from the orbital velocity are larger following egress than prior to ingress, contrary to the predictions of simple rotation. Indeed, the tendency, at least after egress, is for the velocity deviations to rise to a maximum and then diminish again, as can also be seen in some of the Victoria measures of Figure 2. Wilson and Abt looked for differences in velocity between groups of weak and strong metal lines and between groups of lines of neutral atoms and of ions but found none. All the metal lines (apart from Ca II) have therefore been lumped together in Figures 3 and 4. For the most part, the velocities from the metals and from hydrogen agree fairly well, with the largest deviations being shown by Ca II. These deviations occur in the lower levels, where the Ca II lines are strong and of almost rectangular shape. This fact suggests that the Ca II lines are really composite, made up of a number of overlapping components distributed in some manner about the mean wave length. If these individual components are themselves strong, saturated lines, the accidental addition of such a component near one edge of the composite line can introduce an appreciable shift of the mean, whereas the effect on much weaker lines of a similar off-center component would be much less.

The foregoing supposition is supported by the fact that McKellar and Petrie (1952) measured faint displaced Ca II components on plates of January 30, 1948, and September 22, 1950. The measured deviations of these satellites from the main line ranged from -109 to $+92$ km/sec.

Conclusions to be drawn from these radial-velocity measures are as follows: (1) if there is any rotation effect, it is much smaller than was formerly believed to be the case and is largely obscured by internal chromospheric motions; (2) there appears to be a kind of chromospheric equatorial current which is not, however, constant either in time or with respect to location on the K star or in height; (3) the changes in measured velocity, especially in Ca II, from night to night are large enough to suggest that the chromosphere contains sizable concentrations of matter moving with different velocities.

2. The intensities of the chromospheric lines yield very important information on the chemical composition and physical state of the chromospheric material. But in this kind of work there are pitfalls to be avoided, and one finds that, while different observers arrive at qualitatively similar results, there are considerable differences in some of the derived parameters and in the conclusions drawn from them.

Consider, first, the spectrum of ζ Aurigae at a phase where the light of the B-type star is shining through the chromosphere of its companion. In the spectrum of the B star the only absorption lines which have been identified are those of the Balmer series of hydrogen and λ 3819.6 He I. Hence, much of the B-star spectrum is a continuum quite suitable for a study of the chromospheric absorption lines produced in it by the intervening chromospheric material of the K star. However, at each wave length where a chromospheric line is found, the same line will exist also in the underlying K-type spectrum, and what is

actually observed is a blend of the K-star spectrum, the B-star spectrum, and the virtually coincident absorption lines in both. The first problem, then, is how to unscramble these blended spectra so as to deduce the values of the chromospheric absorption alone.

Consider the pure K-type spectrum, and let $r_K = I_K/I_{CK}$ be the light-ratio at some point within an absorption line. Similarly, at the same wave length in the line produced by the chromosphere, one has $r_B = I_B/I_{CB}$. The light-ratio in the blended, composite line which is directly observed is evidently

$$r_{BK} = \frac{I_K + I_B}{I_{CK} + I_{CB}}. \tag{2}$$

If the ratio of the two continuous spectra is denoted by $a = I_{CB}/I_{CK}$, one finds

$$r_{BK} = \frac{r_K + a r_B}{1 + a}. \tag{3}$$

The equivalent width of an absorption line is, by definition, $W = \int\int dr d\lambda$, which is usually written after one integration as $W = \int(1 - r)d\lambda$. Hence, if we differentiate equation (3), multiply through by $d\lambda$, and rearrange the terms, we find

$$\int\int d r_B d\lambda = \frac{1 + a}{a}\int\int d r_{BK} d\lambda - \frac{1}{a}\int\int d r_K d\lambda, \tag{4}$$

or

$$W_B = W_{BK} + \frac{1}{a}(W_{BK} - W_K). \tag{5}$$

In equation (5), W_B is the desired equivalent width of a line produced in the continuum of the B star by the atoms in the K-star chromosphere; W_{BK} is the equivalent width measured in the composite spectrum; and W_K is the equivalent width of the line in the pure K-type spectrum, which can be measured on plates taken during the total eclipse. Equation (5) is still valid completely outside eclipse, when $W_B = 0$, and in this case gives

$$a = \frac{W_K}{W_{BK}} - 1. \tag{6}$$

Equation (6) thus provides a means of determining the ratio of the two continuous spectra as a function of wave length by means of spectrograms taken outside eclipse and during totality. The foregoing equations, or simple modifications of them, have been used in most spectrophotometric investigations of ζ Aurigae–type stars since 1935.

The extent to which equation (5) is used in practice depends on circumstances. For lines like H and K of Ca II and 4227 Ca I, in the lower chromospheric levels, the equation must be used to separate the chromospheric component. On the other hand, at Mount Wilson most of the work on the other metallic lines has been to the violet of λ 3900, where a is of the order of 3–5 and where

the dispersion is large enough that the background in the individual K-type lines can be drawn in and allowed for, at least approximately. Under these circumstances it can be shown that equation (5) may be replaced by

$$W_B = W_{BK} + \frac{1}{a'} W_{BK}, \tag{7}$$

where

$$a' = \frac{a}{r_K}, \tag{8}$$

r_K being the depth of the line in the K-type spectrum. If a and r_K are such that a' is likely to be of the order of 10 or more, it is probably sufficient to neglect the correction term in equation (7) altogether. In a K-type spectrum it is, in any event, exceedingly difficult to determine quantities like r_K or W_K with any accuracy in the crowded violet region, and it is a matter of judgment in a particular case whether equation (5), equation (7), or the foregoing short-cut method is to be preferred.

During the partial phases of the eclipse it is to be understood that the light-ratio a in equations (5)–(8) should be modified appropriately according to the observed light-curve. Recently Miss Underhill (1957) has proposed a procedure which should be capable of determining both a and the chromospheric absorption components from spectrographic observations alone.

After equivalent widths of a sufficient number of chromospheric absorption lines have been measured, preferably at a number of heights above the limb of the K star, curves of growth must be constructed in order to derive information on the physical state of the chromospheric material. This involves rather standard procedures, and the individual papers should be consulted for details (Wellmann 1939; Wilson 1948; Wilson and Abt 1954; Groth 1957).

By fitting the observed line intensities to theoretical curves of growth, the turbulence in the chromospheric matter is immediately determined, and the numbers of atoms or ions responsible for given lines can be read off the curves for the various paths at different heights above the limb of the K star. Comparison of the numbers of particles for different heights leads to knowledge of the density gradient in the chromosphere. Also, if the relative numbers of atoms of a given species in more than one energy state can be determined, the corresponding excitation temperature can be computed. Finally, comparison of the numbers of ionized and neutral particles of the same kind yields the ionization as a function of height.

Unfortunately, this program cannot be carried out with complete satisfaction, for reasons beyond the control of the observers. For instance, at a height of 14×10^6 km above the limb, Table 2 shows the numbers of lines of various metals in the neutral and ionized states that have been measured and identified in the region 3070–3970 A (Wilson 1957). For Na, Mg, Al, Ca, Mn, and Yb the results are those to be expected from the nature of their spectra, but Sc, Ti, V, Cr, and Y have strong lines of both neutral and singly ionized stages within

the measured wave-length region. Ni II has no outstanding lines in this region, and the available Fe II lines do not arise from the ground state, nor are they very intense in the laboratory. The conclusion is that both Ni and Fe must be fairly heavily ionized and that the metals with ionization potentials about 1 volt less are virtually completely ionized. However, Table 2 shows that only for Fe are there enough lines of both stages for a reasonable study of the ionization as a function of height, and, unfortunately, the *f*-values of the Fe II lines are unknown. Apart from Fe, only Ca II and Ca I are available for this purpose, and, as will be shown, the results from Ca and from Fe are in complete disagreement. These facts introduce a serious restriction into the study of the physical state of the ζ Aurigae chromosphere.

Table 3 gives a summary of some of the circumstances pertaining to and the results of the major spectrophotometric investigations of ζ Aurigae. Wellmann

TABLE 2

NUMBERS OF OBSERVED LINES IN ζ AURIGAE
($H = 14.3 \times 10^6$ km)

Element	I	II	I.P. (ev)	Element	I	II	I.P. (ev)
Na.....	1	0	5.12	Cr.....	4	36	6.74
Mg.....	4	0	7.61	Mn.....	0	9	7.40
Al.....	2	0	5.96	Fe.....	62	28	7.86
Ca.....	0	2	6.09	Ni.....	9	2	7.61
Sc.....	0	18	6.7	Y.....	0	6	6.5
Ti.....	0	114	6.81	Zr.....	0	9	6.92
V.....	0	22	6.71	Yb.....	0	1	6.23

(1939) and Groth (1957) derive excitation temperatures at only one chromospheric level. The Mount Wilson observers measured T_{exc} (chiefly from multiplets of Fe I) at several heights and found that this quantity increased with distance from the limb. As far as the rather scattered measures can be interpreted, the increase of T_{exc} with height seems to be approximately linear. Wellmann and Groth agree in finding a turbulent velocity nearly twice that derived by Wilson and by Wilson and Abt—a difference which is uncomfortably large. Since no two of the observers covered an eclipse in common, it is possible that part of this discrepancy could be attributed to real variations in $\Delta\lambda_D$, but it is unlikely that the whole amount can be so explained. The larger dispersion and more favorable location (farther to the violet) of the Mount Wilson observations should perhaps entitle them to greater weight, but it would be very valuable to have an independent investigation by an additional observer with access to suitable equipment.

A comparison of the numbers of atoms in the line of sight at various heights is shown in Figures 5, 6, and 7 for Ca I, Ca II, and excited hydrogen. There is some scatter in all the data, but it is fairly small in the Mount Wilson results,

TABLE 3

OBSERVATIONS AND RESULTS OF ECLIPSE PHENOMENA, ζ AURIGAE

Author	Eclipse	Dispersion* and Region	Range of Height (km)	Gradients, α, for Metals (cm^{-1})			Excitation Temperature		Turbulent Velocity	
				Neut.	Ions	Ht. (km)	Deg.	Ht. (km)	km/sec	Ht. (km)
Wellmann (1939)....	1934 Ingr. Egr.	Pr. 34 A/mm Hγ λλ 3856–4383	$1–55\times10^6$	2.7×10^{-12}	3.2×10^{-12}	Mean	4300	4×10^6	22	4×10^6
Wilson (1948).....	1939–1940 Ingr. Egr.	Gr. 10 A/mm λλ 3100–3900	$1–29\times10^6$	4.4×10^{-12}	4.0×10^{-12}	10×10^6	3780 4450 5660	1×10^6 7×10^6 14×10^6	7 9 12	1×10^6 7×10^6 15×10^6
Wilson and Abt (1954).....	1947–1948 Egr.	Gr. 10 A/mm λλ 3100–3900	$12–54\times10^6$	.....	1.1×10^{-12}	40×10^6	4630 4675	12×10^6 18×10^6	8 (neut.) 11 (ion) 8 (neut.) 11 (ion) 12 to ≥13 (ion)	12×10^6 ..... 18×10^6 ..... 26 to 48×10^6
Wilson and Abt (1954).....	1947–1948 Ingr.	Gr. 10 A/mm λλ 3100–3900	$9–46\times10^6$	3.7×10^{-12}	2.8×10^{-12} 0.8×10^{-12}	10×10^6	4325 4500	9×10^6 12×10^6	8 (neut.) 10 (ion)	9×10^6 .....
						40×10^6	4315 5015	18×10^6 24×10^6	(8 neut.) 10 (ion) 7 (neut.) 10 (ion) 8 (neut.) 13 (ion) 11 to ≥13 (ion)	12×10^6 ..... 18×10^6 ..... 24×10^6 ..... 26 to 46×10^6
Groth (1957).....	1950 Ingr. Egr.	Pr. 42 A/mm Hγ λλ 3813–4417	$1–85\times10^6$	15×10^{-12} 1.4×10^{-12}	6×10^{-12} 1.3×10^{-12}	$<4\times10^6$ $>4\times10^6$	4100	5×10^6	23	5×10^6 .....
Groth (1957).....	1953 Ingr.	Pr. 42 A/mm Hγ λλ 3813–4417	$2–77\times10^6$	.....	.....	.....	3900	5×10^6	20	5×10^6

* "Pr" = prism; "Gr" = grating.

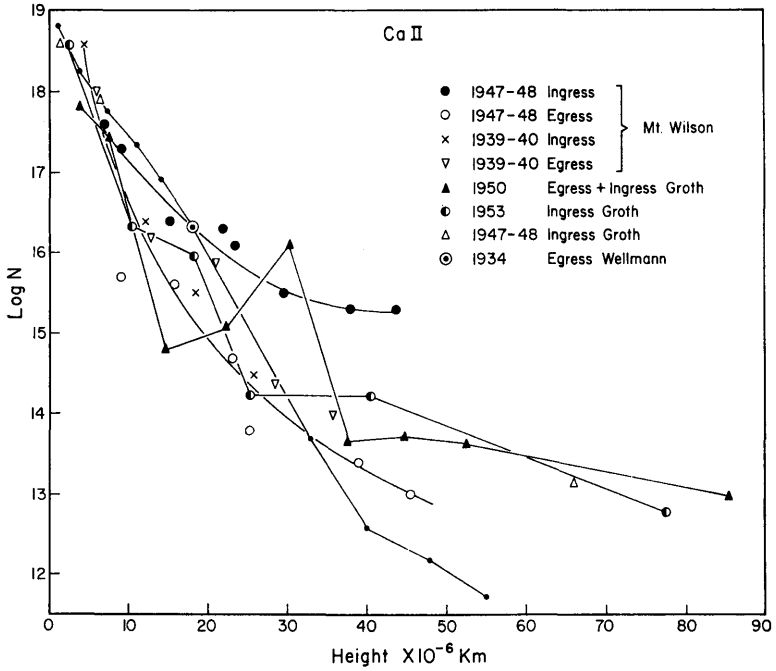


FIG. 5.—ζ Aurigae. Log N versus height for Ca II. Symbols have same meaning in Figs. 6 and 7

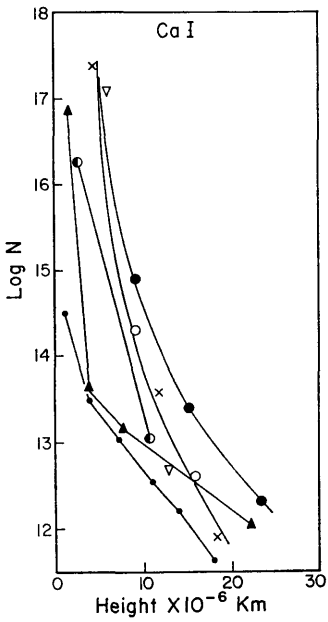


FIG. 6.—ζ Aurigae. Log N versus height for Ca I

and smooth curves have been drawn through the points. Note that one of the atmospheric transits observed at Mount Wilson deviates systematically from the other three, a result which has been found also by Welsh (1949). Groth's measures, although showing considerable irregularities, parallel the Mount Wilson values quite satisfactorily, whereas those of Wellmann are systematically different from those both of Groth and of Mount Wilson. Similar results are found for the other metal lines, both neutral and ionized, which agree closely with each other and are not much different from those of Ca II. It is noteworthy that all observers agree reasonably well in showing that Ca I decreases in strength with height much more rapidly than does Ca II and that the excited hydrogen falls off much more slowly than anything else.

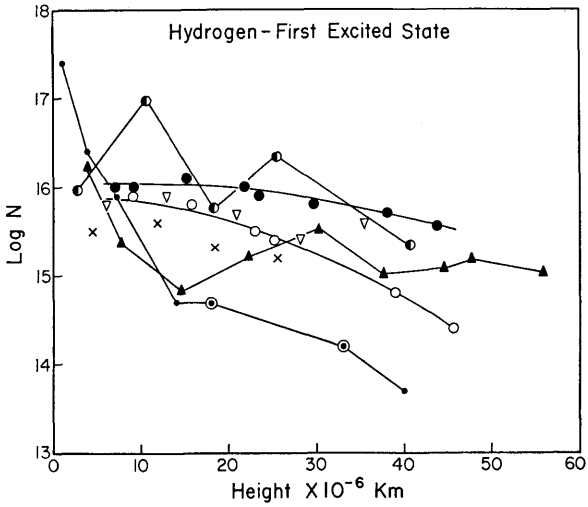


FIG. 7.—ζ Aurigae. Log N versus height for hydrogen (first excited state)

The general agreement in gradient between the neutral and ionized particles indicates no large variation of ionization with height, and this is borne out by the measures of Fe I and Fe II lines. From the latter, the Mount Wilson observers found no change of ionization with height. The much steeper gradient of Ca I than Ca II, however, indicates that the ionization of Ca increases rapidly with height in the chromosphere.

4.16. *Interpretation.*—Let us summarize briefly the results of observations to this point: (1) Radial velocities indicate discontinuous mass motion (McKellar and Petrie 1953; Wilson and Abt 1954). (2) Excitation temperatures are higher than the boundary temperature of the K star (Wellmann 1939; Wilson and Abt 1954; Groth 1957) and increase with height above the photosphere (Wilson and Abt 1954). (3) Turbulence from curves of growth has been given the following values: $V_T \sim 22$ km/sec (Wellman 1939; Groth 1957); $V_T \sim 8$

km/sec for neutral atoms; $V_T \sim 13$ km/sec for ions (Wilson and Abt 1954). (4) Atmospheric gradients are approximately equal for neutral atoms and ions (all authors). Exceptions: Considerably steeper for Ca I; somewhat steeper for Ca II; less steep for H (all authors).

Although the facts deduced from the observations by the various investigators agree fairly well, with the exception of the magnitude of the turbulence derived from the curves of growth, there are wide divergences in the interpretation. These have to do chiefly with the question of the source of the excitation and ionization of the chromospheric matter. This is, of course, a very important point, since one wishes to know whether the observations reveal the intrinsic state of the K-star chromosphere or whether the radiation of the companion plays a major role.

Wilson and Abt (1954) adopt the viewpoint that the radiative flux from the B star is likely to be the chief source of chromospheric excitation, and they explore the consequences of this assumption. The first step is to suppose that the chromospheric material is smoothly distributed according to a simple barometric law,

$$n = n_0 e^{-\alpha \Delta h} , \tag{9}$$

and to deduce corresponding central densities on a specified ray. For this purpose, the ray passing at a height[1] 5.6×10^6 km above the K-star limb was chosen as being typical of the lower chromosphere. In order to derive actual numbers of particles along the ray, only Ca is available because the numbers for Ca I and Ca II are known from observation and, even so, it is necessary to assume, at the start, that none of the Ca is doubly ionized. Next, on the assumption that the solar abundance ratios of hydrogen to calcium and of hydrogen to iron apply also to ζ Aurigae, the expected numbers of H and Fe along the ray are computed. By comparison of the expected numbers along the ray with the observed numbers of second-state hydrogen atoms and of Fe I, two things follow at once: (1) the excitation temperature for H must be about 6800°, i.e., nearly twice the measured T_{exc} for Fe I on this ray, and (2) the ionization of iron must be rather high: $N(\text{Fe II})/N(\text{Fe I}) \sim 500$. This last result is at least consistent with the observed fact that the Ti II lines are somewhat stronger than those of Fe I, even though Ti is completely ionized (no Ti I observed), and that Ti is probably only about one one-hundredth as abundant as Fe.

The Mount Wilson observers next investigate the ionization of hydrogen along the ray according to the methods developed by B. Strömgren (Kuiper, Struve, and Strömgren 1937) and show that practically all the hydrogen must be neutral and hence that the electrons must originate from the ionization of the metals. From these circumstances it follows that, with a smooth density

[1] This height is on the scale as used by Groth, i.e., the height of the center of the B star above the limb. In their original work Wilson and Abt counted heights from second and third contacts.

distribution, the B star would ionize the metals much more heavily than is observed to be the case.

By such rather indirect methods, dictated by the nature of the observational material, Wilson and Abt are led to the conclusion that a smooth density distribution is impossible and that the chromospheric matter of the K star must occur as condensations of sufficiently high density to prevent excessive ionization by the radiation of the B star. The most obvious consequence of this model is that the metal ionization should not vary with height, and, indeed, this is observed to be the case over a height range in which the total amount of matter in the line of sight diminishes by a factor of 100. The condensations turn out to be rather dense and small, with the number of hydrogen atoms per $cm^3 \sim 10^{13.8}$ and a thickness $\sim 10^2$–10^3 km.

Since the foregoing results were based on the assumption that there was no Ca III along the ray under consideration, this point must be investigated. Wilson and Abt show that, with the condensations as specified, second ionization of the metals other than Ca is negligible at all heights. For Ca, second ionization is largely suppressed by the proximity of the very strong Lyman-β absorption line of H to the principal Ca II absorption edge at 11.82 volts in the lower levels, but is not thus suppressed in the outer chromospheric regions. In this manner the rather steep gradient of Ca II compared to the other metals can be accounted for. No quantitative explanation for the apparent rise in excitation temperature with height is available, nor is it possible to account for the rapid decline (according to the Mount Wilson observations) in the ionization of Ca in the lower chromospheric levels. To summarize: the discussion of Wilson and Abt, which attributes the ionization in the K-star chromosphere to the radiation of the companion, is fairly successful in accounting for the spectroscopic observations. According to this point of view, the observations of this system can tell us little, if anything, about the intrinsic excitation level in the chromosphere of the K-type component.

Wellmann (1939) and Groth (1957) believe, on the contrary, that the role played by the B star in this connection is minor and that a kind of superexcitation is responsible for the excitation and ionization in the K star's chromosphere. Groth's analysis of the situation, based chiefly on his own observations of the 1950 eclipse, leads to the following conclusions: (1) The excitation temperature of hydrogen must exceed that of the metals, which is 4100°. (2) For a smooth distribution of matter, the ionization of Ca cannot be accounted for by $T = 4100°$. The density would have to be $\sim 10^3$ greater than that given by the smooth distribution. (3) Using Strömgren's analysis, the hydrogen along the ray in question ($h = 8 \times 10^{11}$ cm) is found to be mostly neutral when the ionizing effects of the B star are considered. (4) Similarly, the B star would ionize the metals too heavily with a smooth distribution, and concentrations of matter would be necessary to keep it down.

To this point, Groth's conclusions agree with those of Wilson and Abt. He

next considers the ionization of the metals by the B star and comes to the following conclusions: (5) If the reaction Ca II → Ca III is suppressed, the metallic ionization does not agree with the observed value. The discrepancy comes out of Groth's analysis in the form of a predicted ratio of Fe/Ca which differs by a factor of the order of 10 from the solar value. (6) By considering the strength of Lyman-β, Groth concludes that the ionization of Ca II to Ca III is indeed largely suppressed, in agreement with Wilson and Abt. (7) And, finally, neither the excitation of hydrogen to the second state nor the metallic ionization can be explained by the B-star radiation alone, even with concentrations of matter. Groth suggests that the source of the superexcitation lies in the ultraviolet radiation from the transition zone between the chromosphere and the corona where turbulent energy is dissipated.

In considering all the foregoing results, it seems that the idea of the metal ionization being due to the radiation of the B star gives close enough agreement with the observations to remain a distinct possibility. The excitation of hydrogen is more difficult; as Groth shows, Lyman-α absorption will quickly remove the radiation from the B star and prevent much direct population of the second state. However, conditions in such a chromosphere appear to be nearly ideal for the trapping of Lyman-α quanta, since the densities are many orders of magnitude larger than in the nebular case, and most of the hydrogen is neutral. Whether enough such quanta can be held in the chromosphere to produce an appreciable overpopulation of the second state is a question that seems not yet to have been investigated.

TABLE 4

ELECTRON AND NEUTRAL HYDROGEN DENSITIES ACCORDING TO GROTH

H (cm)	log N_e	log N_H
4×10^{11}	10.20	11.70
8×10^{11}	9.85	11.17
20×10^{11}	10.43	10.48

One feature of Groth's analysis is disturbing. In order to evaluate the superexcitation function, he assumes that all the electrons come from hydrogen: $N_e = N_{H^+}$. Then, for the heights given in Table 4, he deduces the densities of electrons and the total hydrogen densities as shown. Thus at $h = 20 \times 10^{11}$ cm the hydrogen is already virtually completely ionized; yet the Balmer lines are observed far beyond this point, being nearly as persistent as those of Ca II.

A third attempt to explain the ionization in the ζ Aurigae K-type chromosphere has been made by Kawabata (1957). He is concerned especially with the observed lack of height dependence of the metal ionization, apart possibly from the Ca II/Ca I ratio, and draws upon conditions in the solar corona for an anal-

ogy. Kawabata's basic hypothesis is that the electron temperature is high and that ionization by electron collision is more important than ionization by radiative processes. With these circumstances, especially if ionization by the B-star radiation can be neglected entirely, he finds that the metal ionization is indeed nearly independent of height. In order to attain this result, Kawabata must assume electron temperatures in the range 12,000°–14,000° and an electron density of 3×10^{10} cm^{-3} in the lower chromosphere.

To conclude the discussion of ζ Aurigae, one may perhaps make the following statement about the structure of the chromosphere of the K-type component: The observational data by the various investigators are in fair agreement except for some minor discrepancies concerning some of the gradients and a rather major one as to the amount of turbulence. There is a diversity of opinion, however, concerning the smaller-scale structure and the source of the observed excitation and ionization. Wilson and Abt (1954) get fairly satisfactory results by assuming the radiation of the B star to be chiefly responsible, but they are left with the difficulty of accounting for the excitation of hydrogen and are required to assume that the chromosphere consists largely of discrete and rather dense condensations whose nature is unexplained. Wellmann (1939) and Groth (1957), by introducing superexcitation, can account for the hydrogen excitation, but they also require condensations; otherwise, as Groth shows, in agreement with Wilson and Abt, the B star will produce more ionization in a smoothly distributed chromosphere than is observed. Actually, the case for superexcitation is not entirely convincing. If it does exist, its effects (apart possibly from those on hydrogen excitation) would appear to be so nearly the same order as those due to the B-star radiation that a disentangling of the two might be extremely difficult. Finally, Kawabata's viewpoint requires the explanation of the high electron temperature, and, in addition, there is no good reason why the radiation from the B star should not be completely effective in contributing to the ionization. In view of the foregoing, it is evident that a definitive description of the chromosphere of the K-type component of ζ Aurigae is not yet possible. None of the models is completely satisfactory.

4.2. 31 Cygni

Like ζ Aurigae, 31 Cygni has long been known to show a composite spectrum and to be a spectroscopic binary. A preliminary orbit by Christie (1936) was followed by a more accurate one by Miss Vinter-Hansen (1944) based on many three-prism, Lick Observatory spectrograms. Since the announcement by McLaughlin (1950) that Ann Arbor spectrograms of 1941 showed a chromospheric K line and hence that at least atmospheric eclipses occurred, many observations have been made. We now give a summary of the results available up to the present time.

4.21. *Spectroscopic orbit.*—The orbital elements given by Miss Vinter-Hansen

(1944) have not been superseded, but it is clear that they do not yield the correct times of eclipse. McLaughlin (1952*b*) and Larsson-Leander (1953) called attention to the fact that the 1951 eclipse came 78 days earlier than predicted by the spectroscopic elements. By consideration of all available information, McKellar and Petrie (1958) estimate the true period as 3781 ± 8 days, compared to Miss Vinter-Hansen's value of 3803 days, and give the predicted times for the next eclipse shown in the accompanying table. The star should thus be

	JD
First occurrence of chromospheric K line....	2437565 = September 22, 1961
First contact.....	632 = November 28, 1961
Second contact.....	635 = December 1, 1961
Mid-eclipse.....	666 = January 1, 1962

favorably placed for observation during ingress, and the observed times, compared with those of the 1951 eclipse, will remove the remaining uncertainty in the period.

4.22. *Mass ratio.*—Miss Vinter-Hansen derived the value $m_K/m_B = 1.7$ from a relatively few spectrograms. McKellar and Petrie (1958) made a series of careful velocity measurements of tracings of high-dispersion Victoria plates and found $m_K/m_B = 2.0$. Similarly, Wright (1958) made differential measures of six grating spectrograms, with the result $m_K/m_B = 1.7$; McKellar and Petrie, combining both values, regard $m_K/m_B = 1.9$ as the best ratio currently available.

4.23. *Dimensions, temperatures, luminosities, masses.*—The spectral types for the components of 31 Cygni given in the *Henry Draper Catalogue* are K0 and B8, but these have now been replaced by more modern estimates. Wright and Lee (1956) used a spectrophotometric process to separate the spectra of the two stars and were able to measure some of the hydrogen and helium lines in the spectrum of the B star. Intensities of these lines in comparison with the values in other early-type spectra led Wright to these results: spectral type of B star and absolute visual magnitude B4 and −2.0, respectively. These indicate that the early-type component of 31 Cygni is probably close to the main sequence.

For the primary star, McKellar and Petrie (1958) conclude that its spectrum is very similar to that of the primary of ζ Aurigae. By comparison with standard spectra, they adopt K4 I*b* as the best estimate of the spectral type, and, according to the Yerkes calibration, this would imply, for the luminosity, $M_v = -4.5$.

However, McKellar and Petrie consider that the best-determined observational quantities are the duration of totality, the magnitude difference, and the spectroscopic absolute magnitude of the B star. These may be combined with the orbital elements and various assumptions concerning the mass ratio and the surface temperature of the K star (i.e., the spectral type). As a compromise

solution that fits the current data, they give the main physical properties of the system shown in the accompanying table. The other numerical data involved in

	Primary	Secondary
Spectral type	K3 Ib	B3 V
Absolute magnitude (M_v)	−4.0	−2.0
Mass (assumed mass ratio 2:1)	18⊙	9⊙
Radius	174⊙	4.7⊙

this solution are given in a table as follows:

Duration of totality	61.2 ± 0.5 days
Duration of partial eclipse	1.7 ± 0.5 days
Inclination or orbit	$89°.5 < i < 90°$

As is usual in such situations, better observational material may effect appreciable changes in some or all of these quantities which should therefore be regarded as provisional.

4.24. *Light-curves.*—Photometric studies of the eclipses of 31 Cygni are still very inadequate. Only enough has been accomplished to yield the approximate duration of partial phase quoted above and to show that, as with ζ Aurigae, the fractional part of eclipse is a function of wave length. At a given time the eclipse is more pronounced, the bluer the light being observed, and hence the eclipse is not a geometrical one but involves an extinction varying with wave length. For details of the existing photometric observations, the paper of McKellar and Petrie (1958) should be consulted, since some of them are not available elsewhere.

4.25. *Observations of chromospheric lines.*—1. Radial velocities of chromospheric lines in the spectrum of 31 Cygni at the 1950 eclipse have been measured by McLaughlin (1952*c*) and on higher-dispersion spectrograms by McKellar and Petrie (1958). The two sets of measures agree reasonably well and are illustrated by the Victoria results shown in Figure 8. Unlike the ζ Aurigae chromospheric velocities (see Figs. 2, 3, and 4), those for 31 Cygni seem to deviate from the orbital velocity in the negative sense at both ingress and egress, and the deviations are somewhat smaller. Otherwise they show similar night-to-night variations. In any event, they cannot be ascribed to rotation of the K star, as is shown by the dashed line in the upper part of Figure 8, which is the minimum rotational effect, assuming equal rotational and orbital periods and the same directions of motion. No theory for these deviations and fluctuations of radial velocity is available other than that they probably indicate a combination of random and systematic motions of gaseous masses in the chromosphere.

The existence of rapidly moving condensations in the chromosphere of 31 Cygni has been demonstrated in spectacular fashion by the discovery of displaced satellite components of the Ca II K line on Victoria spectrograms of

4.6-A/mm dispersion. These were found during the 1950 eclipse (McKellar, Odgers, Aller, and McLaughlin 1952) and were especially prominent during egress. The components show appreciable variation over times of 1 or 2 days and indicate rather large motions, the maximum measured displacement from the main line amounting to 130 km/sec. Since the relative motion of the B star is about 2.5 solar diameters per day, the conclusion must be that the chromosphere contains large, rapidly moving clouds or condensations.

2. Studies of chromospheric-line intensities in this object are as yet not very extensive. Miss Underhill (1954) applies a photometric technique to spectrograms and deduces that there is appreciable light-loss as much as 3 days prior

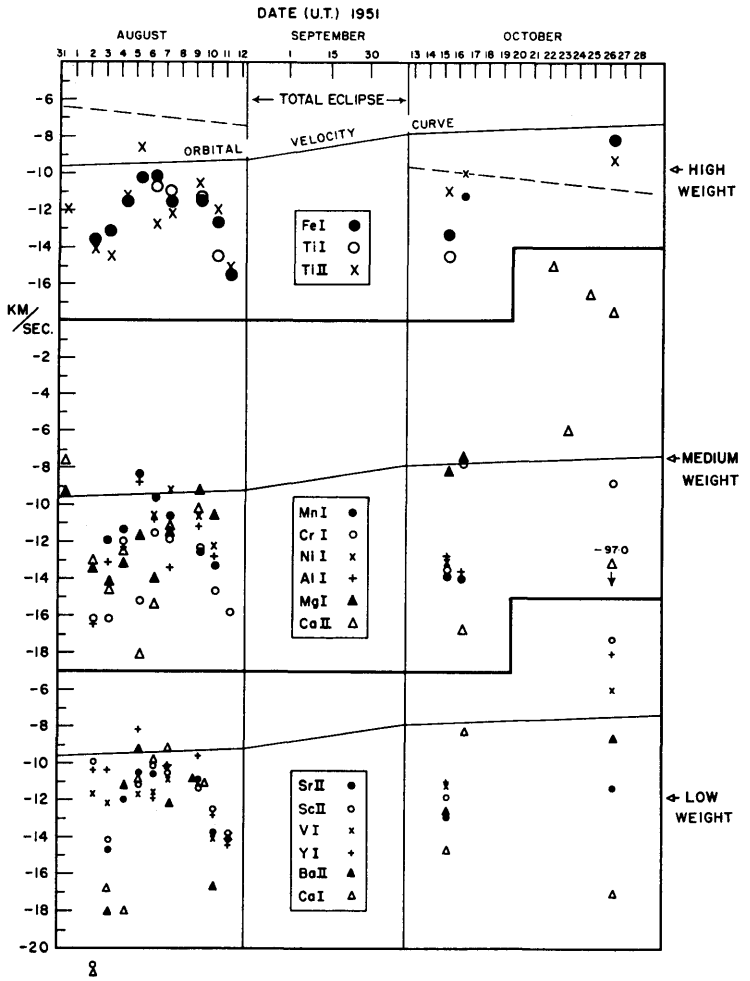


FIG. 8.—31 Cygni. Chromospheric radial velocities (McKellar and Petrie 1958)

to the onset of geometrical eclipse. The same method determines the light-ratio of the two stars, α, as 2.3 at a wave length about 3925 A. By application of equation (6) to the lines 3920, 3922, 3927, 3930, and 3944, the result is $\alpha = 1.9$. Miss Underhill is inclined to attribute the difference to instrumental broadening which, in principle, should not make any difference, and prefers the larger value. Finally, from the widths of the Fe lines, an upper limit to the turbulent velocity of 20 km/sec is derived.

Wright and Lee (1956) have made a similar study over the wave-length range λλ 4600–3800 and derive values of α in the usual manner. Their value of α at λ 3930 is about 0.8, in complete disagreement with the result of Miss Underhill who worked only in the limited region, λλ 4100–3700. This difference illustrates well the difficulties encountered in such work and is probably to be ascribed to different choices of the location of the continuous background of the K-type star. Suitable photometric measures at future eclipses can determine the true light-ratio of the stars as a function of wave length.

Wright (1955, 1956) states that unpublished curves of growth yield turbulent chromospheric velocities in the range 8–15 km/sec, which may increase with height, and that excitation temperatures also show an increase with height from 2500° at ±2-day to 4500° at ±10-day phase. If these results are borne out by further investigation, the parallelism with Wilson and Abt's (1954) data on ζ Aurigae is quite pronounced.

Larsson-Leander (1953, 1957) has made two studies of the 1951 eclipse. The first, based on rather low-dispersion spectrograms taken at the Stockholm Observatory, has been largely superseded, as far as chromospheric analysis is concerned, by the second. For the latter, spectrograms of 12-A/mm dispersion at K_2, obtained by the observers at the University of Michigan, have been used. The wave-length range covered is approximately λλ 3750–4100. Equation (7) was used in the reduction, justified by the fact that α, as determined by equation (6), was fairly large—$\alpha = 2.5$ at λ 3900. This is in good agreement with Miss Underhill, but note the discrepancy with Wright's value discussed above. In any event, the parameters deduced by Larsson-Leander are quite similar to those found for ζ Aurigae. He finds, for the mean turbulent velocity, 16.6 km/sec and, for the excitation temperature, 3900°, but for neither of these is there evidence of a variation with height.

The densities and gradients derived by Larsson-Leander are also very similar to those of ζ Aurigae. There is little difference between the mean gradients for neutral and ionized particles except that the Ca II gradient is steeper and the hydrogen gradient less steep than the others in the lower chromospheric levels. In the higher levels all the gradients are much alike. Unfortunately, λ 4227 Ca I could not be measured by Larsson-Leander, and it is not known, therefore, whether the Ca I gradient is even steeper than that of Ca II, as was found by Wilson and Abt (1954) for ζ Aurigae. On the whole, however, the general chromospheric structure appears to be very similar for these two objects.

Larsson-Leander's analysis of his results for 31 Cygni also parallels closely that of Wilson and Abt for ζ Aurigae, and it is therefore not too surprising that he arrives at very similar conclusions. Indeed, the only difference of moment is that the chromospheric condensations, which he must postulate for 31 Cygni, are less dense and larger in size, by about one order of magnitude, than those deduced for ζ Aurigae. It appears from the analysis that this difference is a consequence of the smaller dilution factor of the B star in 31 Cygni.

A series of spectrograms of 31 Cygni taken during ingress 1951 at Victoria is shown in Plate I. These will serve to illustrate the general nature of the chromospheric eclipse phenomena in all such systems.

4.3. 32 Cygni

Although this system will be seen to be quite similar to the two discussed previously, there is less information available on it. The spectrum had long been recognized as composite (types K0 and A3 in the *Henry Draper Catalogue*), and a spectrographic orbit had been obtained at Ottawa (Cannon 1918); not until 1949 was the eclipsing nature of the system recognized (McLaughlin 1949*a*, *b*). Following his discovery of the eclipses, McLaughlin (1950) published eye-estimates of the intensities of the chromospheric lines for the eclipse of November, 1949, which showed the phenomena to be similar to those in ζ Aurigae and gave preliminary values of the constants of the system.

The spectrographic orbit has been completely revised on the basis of a long series of Victoria spectrograms and remeasures of many of the earlier Ottawa plates (Wright 1952). The period, 1140.8 days, was derived by Wright on the assumption that the width of the chromospheric K line varied symmetrically on the two sides of the eclipse in 1949. From this assumption, which, on the basis of the evidence from ζ Aurigae, may not be fully unjustified, Wright estimated the time of mid-eclipse. Comparison with early Harvard observations showing eclipse phenomena in 1890 and 1896 then gave the period.

Wellmann (1957), using a somewhat similar procedure based on several series of spectrograms covering the 1949 and 1952–1953 eclipses, deduces a period of about 1149 days and a duration of totality of 12.5 ± 0.6 days. The latter agrees well with Wright's (1952) estimate of 13 days for the length of totality.

The only velocity measures of the chromospheric lines are those of Wright (1952) on the K line of Ca II during the 1949 egress. They do not show the systematic increase with height above the limb to be anticipated if stellar rotation is responsible and are probably similar in nature to the velocities discussed above for 31 Cygni and ζ Aurigae.

Both Wright and Wellmann have measured the intensities of the chromospheric K line and give plots of equivalent width against phase in days. Wellmann finds excellent agreement between egress 1949 and ingress and egress 1952–1953, and Wright's measures of egress 1949 do not differ greatly from

Wellmann's plot. The general result is that the K-line intensity falls off very rapidly for about 4 days after third contact, after which there is a slow, steady decline for about 60 days to the termination of the observations.

Both Wright and Wellmann derive the relative intensities of the continua of the two stars by means of equation (6), with results which are in fair agreement. The two stars are of equal brightness in the vicinity of the K line, according to both observers. In Wright's work it was necessary to use the spectrum of γ Draconis to derive the equivalent widths in the pure K spectrum, for lack of suitable plates of 32 Cygni taken during totality, and this has doubtless introduced some measure of uncertainty. However, by means of the photometric processes in use at Victoria, Wright was able to separate the spectrum of the early-type star from the composite spectrum. From the equivalent widths of the

TABLE 5

PARAMETERS OF THE SYSTEM, 32 CYGNI

	Wright		Wellmann	
	Primary	Secondary	Primary	Secondary
Spectral type	K5	B8	K6 I	B3 V
Eff. temp. (° K)	3150	12,600	.....	.....
Abs. mag. (M_v)	−2.7	0.0	−6	−1.7
Radius	195⊙	2.5⊙	353⊙	3.9⊙
Mass	21⊙	7.6⊙	22.7⊙	8.1⊙
r_K/r_B	.....		90	
a_1+a_2	0.95×10^9 km		1.01×10^9 km	
Inclination of orbit	82°		72°.5	

hydrogen lines in the early-type spectrum, and from the presence of He I lines, Wright concludes that the type is probably about B8 and the absolute magnitude 0.0, with an uncertainty of about ½ mag. Wright then calculates the absolute visual magnitude of the K star from the equality of the two spectra at λ 3900, the ratio of the Planck functions for the assumed temperatures of 3150° and 12,600° at the wave lengths 3900 and 5480 A, and the adopted absolute magnitude of the B star. The stellar radii are computed from the usual formula relating R, T, and M_v.

Wellmann (1957), partly from the relative photometric gradients of the two stars and partly from the equivalent widths of the hydrogen lines in the B spectrum (his values are about half of Wright's), concludes that B3 V is the most probable spectral type for the B star. This result enables him to estimate the ratio of the radii of the two stars and thus to proceed to a calculation of some of the other parameters of the system. The results of Wright and of Wellmann are given in Table 5. It is clear that the detailed agreement is poor, partly because of differences in the numerical data used and partly because of the choice of the items which have been regarded as the more fundamental in the course

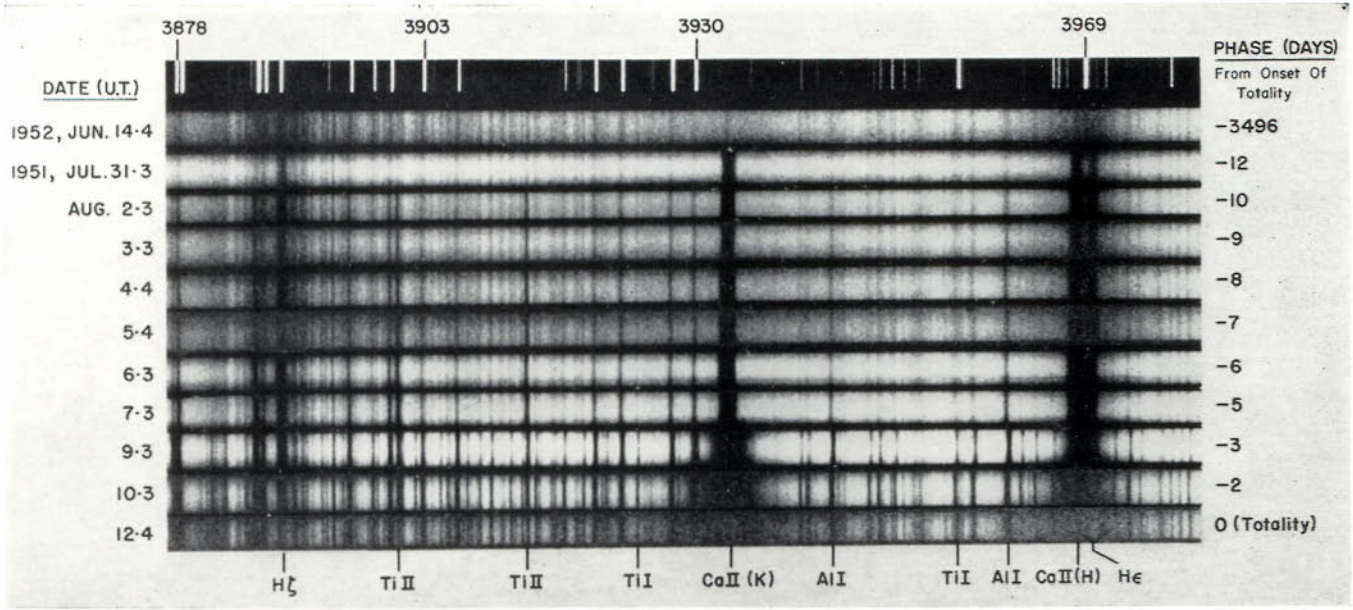


PLATE I.—Spectra of 31 Cygni (from McKellar and Petrie 1958)

of the calculations. The general similarity between ζ Aurigae and 31 Cygni is, however, obvious. Indeed, perhaps the major difference between these two systems and 32 Cygni is that total eclipse barely occurs at all in the latter star, owing to the relatively high inclination, whereas the transits are probably close to central for the first two.

4.4. VV Cephei

For this system, also, our knowledge is still in a rather elementary stage because the recognition of VV Cephei as an eclipsing star dates only from 1936 (McLaughlin 1936) and because of the long period—over 20 years—between eclipses. Indeed, the eclipse phenomena have been observed only twice, and since the total phase of the second one ended (December, 1957) only a few months before this chapter was written, definitive results are naturally not yet available.

Christie (1933) combined Lick and Mount Wilson radial velocities which, while insufficient for an accurate orbit computation, sufficed to indicate a period of the order of 20 years and a mass function of 6⊙ and left no doubt that the object was unusual. Following McLaughlin's (1936) suggestion that the system exhibited eclipses, Gaposchkin (1937) examined nearly three thousand plates from the Harvard collection and produced a light-curve covering the period October, 1890, to March, 1937. This curve shows three minima with depths of about 0.8 mag. and separated, on the average, by 7430 days or 20.4 years. The length of totality was 450 days and of eclipse 490 days. Gaposchkin also computed a spectroscopic orbit, confirming Christie's mass function and allowing him to estimate the dimensions of the stars. This was done by assuming temperatures of the M and B stars to be 2500° and 11,000°, respectively, and led to an orbital inclination of 72° and radii $R_M = 2400\odot$ and $R_B = 240\odot$.

A similar investigation by Goedicke (1939) led to results of the same order. For somewhat different assumed temperatures than Gaposchkin's, Goedicke finds $i = 70°$, $R_M = 3000\odot$, $R_B = 22\odot$, $m_M = 57\odot$, and $m_B = 40\odot$. In the limiting case of $i = 90°$, the radius of the M star is still very large, $R_M = 1220\odot$, and the masses are $m_M = 47\odot$ and $m_B = 38\odot$. The masses are computed with an assumed mass ratio of 0.7. It is necessary to proceed in this manner because the Be spectrum of the companion is complicated by the presence of both emission and absorption components to a degree that renders the measurement of its radial velocity very difficult, if not impossible. Reproductions of spectrograms which illustrate the reversed P Cygni character of the hydrogen lines in VV Cephei have been published by Christie (1938).

Goedicke (1939) also determined a by means of equation (6) and measured the equivalent widths of a number of chromospheric absorption lines, but did not attempt a detailed analysis of the results. From his measures it appears that the gradients of the neutral atoms are considerably steeper, especially in the lower chromospheric levels, than those for the ions. In addition, Goedicke points out that, as the Be star emerged from eclipse in 1937, the hydrogen emission

reappeared first at Hβ, followed by Hγ and Hδ at intervals of about a month, and that the radial velocities of the hydrogen emission lines remained sensibly constant over one-quarter of the period of revolution, during which time the velocity of the M star changed by 24 km/sec.

In a later paper Goedicke (1942) considers the radial velocities during some 500 days after emergence from totality. The lines shortward of λ 4000 are largely chromospheric in origin, and those to the red of λ 4200 originate mostly in the reversing layer and the portion of the chromosphere overlying the M-star disk. Goedicke finds that the radial velocities of the first group, formed in the continuum of the B star by rays passing tangentially through the M-star chromosphere, closely follow the orbital velocity of the M star itself. The second group, however, deviates in a non-constant fashion from the orbital velocity. Goedicke concludes that there is no evidence of rotation of the M star from the chromospheric lines but that the M star probably undergoes pulsations of some sort.

McLaughlin (1951) discusses the spectrum of VV Cephei in some detail. According to him, the uneclipsed spectrum is composed of the following components: (1) a supergiant M-type absorption spectrum, (2) a strong violet continuum, (3) wide hydrogen emissions split by shell absorption components, and (4) narrow bright lines of Fe II and [Fe II]. Components 2 and 3 disappeared during the 1936–1937 eclipse and are therefore attributed to the Be star, but component 4 remained the same during eclipse as outside eclipse and therefore probably originates in a nebular envelope surrounding the system. The hydrogen emission is normally unsymmetrical about the absorption component, with the shortward emission usually the stronger. However, the V/R ratio of the emission is variable. Strong absorption satellites displaced by 100–200 km/sec appear sometimes in the higher Balmer lines and in H and K and have also been seen in the Fe II and Ti II lines. Other transient spectroscopic phenomena are also discussed by McLaughlin.

The foregoing work—all done at moderate dispersion—shows that the M-type star of VV Cephei is of enormous size and that both components are probably massive, but it is also evident that no very precise numbers can be given. Both stars appear to be contributors to types of activity which give rise to the various variable spectral features, quite apart from those phenomena associated with the atmospheric eclipses. In view of these facts, it is not surprising that high-dispersion spectrograms reveal still further complications. One of these (Babcock 1958) is that VV Cephei shows evidence of a magnetic field varying from +850 to −360 gauss. It would obviously be of interest to know whether variations in the magnetic field are correlated in any way with the other variable spectroscopic features.

VV Cephei, according to Gaposchkin's (1937) results, was expected to enter totality in late August, 1956. High-dispersion (3.6-A/mm) observations were begun at Victoria in March, 1956, and will doubtless be extended through the egress side of the chromospheric eclipse as far as is warranted by the results. Two

brief papers have appeared thus far, which described some of the principal spectroscopic phenomena observed during ingress. Wright and McKellar (1956) began observing in March, 1956, and their account of the observations extends through May, 1956. A second paper (McKellar, Wright, and Francis 1957) carries the description to June, 1957. The principal results, from the standpoint of the atmospheric eclipse, are as follows:

The chromospheric spectrum was well developed at the time the observations were begun. All the chromospheric absorptions appeared with two components, the separation for most being about 29 or 30 km/sec, except for the Ti II lines λλ 3685, 3759, and 3761, in which it was about 50 km/sec. As time progressed, the components drew closer together, except for the Ti II group mentioned above. Moreover, through June and July, the ionized lines had largely faded out, the neutral lines were strong, and little further change took place. McKellar, Wright, and Francis conclude that totality occurred between July 21 and July 28, 1956, i.e., about 1 month earlier than predicted. Since emergence from totality did not occur until early December, 1957, it is evident that the recent eclipse was longer in duration by about 40 days than those investigated by Gaposchkin. It is quite likely that the duration of totality (i.e., the diameter of the M star) is variable, although a variation of 10 per cent seems somewhat excessive.

During totality the Ti II lines lost their redward component which had evidently been a normal chromospheric line, but the shortward component persisted unchanged into totality and gave velocities of about −20 km/sec with respect to the orbital motion. Since a similar absorption component of the K line of Ca II was also visible on properly exposed plates, the Victoria observers interpret these results as evidence for a circumstellar envelope having an expansion velocity of 20 km/sec.

The explanation of the duplicity of the chromospheric lines is not entirely satisfactory. Since most of them become single before totality, McKellar, Wright, and Francis feel that the doubling was probably due to real velocity differences between large masses of chromospheric material in the line of sight. However, in the case of the Ti II lines, real emission components developed at the position of the peak between the two absorption lines. This is not the same as the line structure found by Merrill and Wilson (1956) in the spectrum of the supergiant M star, RW Cephei. In the λ 3900 region of the latter object, it is clear that the apparent doubling of the lines is caused by the superposition of emission components near the centers of the broadened absorption lines.

§ 5. CONCLUDING REMARKS

In the course of preparing this chapter the writer has become more impressed by what we do not know, or at best know only approximately, about the topics covered than by those things which can be considered as sound, accurate knowledge. Indeed, one might say with considerable truth that the surface has barely

been scratched. The binaries discussed here offer unequaled opportunities to learn not only about the chromospheric structures and excitations of giant and supergiant stars but about the dimensions, masses, and temperatures of the stars themselves. One may hope that all the various methods of approaching these quantities will ultimately converge into a self-consistent set of numbers in which we can have confidence. Particularly for ζ Aurigae, 31 Cygni, and 32 Cygni it would appear reasonable to entertain such hopes, but VV Cephei, because of its spectral peculiarities which are extraneous to the phenomena of the chromospheric eclipses themselves, may be a more difficult subject.

REFERENCES

Adams, W. S.	1956	*Ap. J.*, **123**, 189.
Babcock, H. W.	1958	*Ap. J. Suppl.*, **3**, 141.
Bottlinger, K. F.	1926	*A.N.*, **226**, 239.
Cannon, J. B.	1918	*Pub. Dom. Obs. Ottawa*, **4**, 151.
Christie, W. H.	1933	*Pub. A.S.P.*, **45**, 258.
	1936	*Ap. J.*, **83**, 433.
	1938	*Pub. A.S.P.*, **50**, 52.
Christie, W. H., and Wilson, O. C.	1935	*Ap. J.*, **81**, 426.
Gaposchkin, S.	1937	*Harvard Circ.*, No. 421.
Goedicke, V.	1939	*Pub. Obs. U. Michigan*, **8**, 1.
	1942	*Ap. J.*, **95**, 319.
Groth, H. G.	1957	*Zs. f. Ap.*, **43**, 185.
Guthnick, P., and Schneller, H.	1932	*Sitzber. Preuss. Akad. Wiss.*, Vol. **57.**
Guthnick, P., Schneller, H., and Hachenberg, O.	1935	*Sitzber. Akad. Berlin*, No. 1.
Harper, W. E.	1924	*Pub. Dom. Ap. Obs. Victoria*, **3**, 151.
Hopmann, J., and Schaub, W.	1936	*Veröff. Leipzig*, No. 6.
Kawabata, S.	1957	*Contr. Kwasan Obs. U. Kyoto*, **9**, 72.
Keenan, P. C., and Morgan, W. W.	1951	*Astrophysics*, ed. J. A. Hynek (New York: McGraw-Hill Book Co.), chap. 1.
Kuiper, G., Struve, O., and Strömgren, B.	1937	*Ap. J.*, **86**, 570.
Larsson-Leander, G.	1953	*Stockholm Obs. Ann.*, Vol. **17**, No. 5.
	1957	*Ibid.*, Vol. **19**, No. 8.
McKellar, A., Odgers, G. J., Aller, L. H., and McLaughlin, D. B.	1952	*Nature*, **169**, 990.
McKellar, A., and Petrie, R. M.	1952	*M.N.*, **112**, 641.
	1958	*Pub. Dom. Ap. Obs. Victoria*, **11**, 1.

McKellar, A., Wright, K. O., and Francis, J. D. 1957 *Pub. A.S.P.*, **69**, 442.
McLaughlin, D. B. 1936 *Harvard Ann. Card*, No. 397.
1949*a* *Ibid.*, No. 1043.
1949*b* *Ibid.*, No. 1044.
1950 *Pub. A.S.P.*, **62**, 13.
1951 *Ap. J.*, **114**, 47.
1952*a* *Pub. A.S.P.*, **64**, 173.
1952*b* *Ibid.*, p. 109.
1952*c* *Ap. J.*, **116**, 546.
Merrill, P. W., and Wilson, O. C. 1956 *Ap. J.*, **123**, 392.
Roach, F. E., and Wood, F. B. 1952 *Ann. d'ap.*, **15**, 21.
Struve, O. 1956 *Pub. A.S.P.*, **68**, 27.
Swope, H. 1935 *Harvard Circ.*, No. 399.
Underhill, A. B. 1954 *M.N.*, **114**, 558.
1957 *Ap. J.*, **125**, 118.
Vinter-Hansen, J. M. 1944 *Ap. J.*, **100**, 8.
Wellmann, P. 1939 *Veröff. Sternw. Berlin-Babelsberg*, Vol. **12**, Part IV.
1951 *A.N.*, **279**, 257.
1957 *Ap. J.*, **126**, 30.
Welsh, H. L. 1949 *J.R.A.S. Canada*, **43**, 217.
Wilson, O. C. 1948 *Ap. J.*, **107**, 126.
1957 *J.R.A.S. Canada*, **51**, 70.
Wilson, O. C., and Abt, H. A. 1954 *Ap. J. Suppl.*, **1**, 1.
Wilson, O. C., and Bappu, M. K. V. 1957 *Ap. J.*, **125**, 661.
Wood, F. B. 1951 *Ap. J.*, **114**, 505.
Wright, K. O. 1952 *Pub. Dom. Ap. Obs. Victoria*, Vol. **9**, No. 5.
1955 *Trans. I.A.U.*, **9**, 739.
1956 *A.J.*, **61**, 194.
1958 Quoted by McKellar and Petrie (1958).
Wright, K. O., and Lee, E. K. 1956 *Pub. A.S.P.*, **68**, 17.
Wright, K. O., and McKellar, A. 1956 *Pub. A.S.P.*, **68**, 405.

CHAPTER 12

Composite and Combination Spectra

JORGE SAHADE*
Berkeley Astronomical Department, University of California

§1. INTRODUCTION

In 1889, E. C. Pickering, at the Harvard Observatory, announced that the star ζ^1 Ursae Majoris (Mizar) is a double system. The two components are so close together that they cannot be resolved with a telescope, and the discovery of the binary nature of this star was possible only with the use of a spectrograph. It happens that the components of Mizar are of about the same spectral type (A2) and of comparable brightness; furthermore, the plane of the orbit is not perpendicular to the line of sight. Therefore, when the spectrum of Mizar is photographed outside conjunctions, we obtain, because of the relative radial velocities of the two components, an A2 spectrum displaying double lines, one set of lines originating in each of the two stars. Spectra resulting from the superposition of the two sets of lines, each ascribable to a definite spectral class, were called "composite" by Pickering (1891), and this designation was also used by Miss Cannon in the *Henry Draper Catalogue*. The same term could more appropriately be used in general to designate spectra showing features which cannot all be traced to a single source.

If we do so, we can distinguish two main types of composite spectra. The first group consists of the unresolvable physical and optical binary systems. In the second group we have (*a*) close binary systems which display peculiar features arising from the interaction between the two stars of the system and/or peculiar features as yet unexplained and (*b*) objects which display the superposition of spectral features normally arising under widely different excitation conditions.

The latter subgroup includes the stars with so-called combination spectra, which combine spectral features of low-temperature stars with emission features requiring high-excitation conditions. Objects which show "combination spectra"

* Now at Observatorio Astronómico, La Plata, Argentina.

are often called "symbiotic stars"; both designations were first used by P. W. Merrill.

We shall devote this chapter to the discussion of the spectra of close binary systems and to the spectra of symbiotic stars.

§ 2. CLOSE BINARY SYSTEMS

2.1. Superposition of Normal Spectra

Most investigations of close binary systems carried out thus far have been limited to the photographic spectral region; only very recently have these studies been extended into the visual and near infrared wave lengths. The great majority of the close binaries known to display composite spectra are systems formed by two stars of about the same photographic brightness and, therefore, of nearly the same spectral type. A large number of systems, however, are formed by two stars of very different luminosities, and, in these cases, only the spectrum of the brighter component has been photographed except when the system is also an eclipsing variable and the geometry of the principal eclipse is favorable.

As is well known, the analysis of the radial velocities of the two components yields the orbital elements of the system and also the masses of the stars. When only one spectrum is observed, the individual masses cannot be derived, but only the mass function,

$$f(\mathfrak{M}) = \frac{\mathfrak{M}_2^3 \sin^3 i}{(\mathfrak{M}_1 + \mathfrak{M}_2)^2} = 1.0346 \times 10^{-7} P K_1^3 (1 - e^2)^{3/2}, \qquad (1)$$

where $\mathfrak{M}_1$ and $\mathfrak{M}_2$ are the masses of the brighter and fainter stars, P is the orbital period, K_1 is the velocity amplitude of the brighter star, e is the orbital eccentricity, and i is the inclination of the orbital plane with respect to the line of sight.

The mass function represents the minimum possible value of $\mathfrak{M}_2 \sin^3 i$, i.e., $f(\mathfrak{M})$ equals $\mathfrak{M}_2 \sin^3 i$ when $\mathfrak{M}_1 = 0$. Obviously, the mass function furnishes information about the individual masses, provided that their ratio and the value of i can be estimated from reasonable assumptions or are known from independent data.

If we consider the spectral characteristics of the components of close binary systems, we can distribute them among the following groups: (1) systems with components still gravitationally contracting; (2) systems with both components on the main sequence; (3) systems with one giant or subgiant component; (4) systems with two giant or subgiant components; and (5) systems with components below the main sequence. This classification is suggested by the current ideas on stellar evolution and is related to the evolutionary ages of the different systems.

It has recently been suggested (Sahade 1958*a*) that the Wolf-Rayet stars are

objects in the gravitational contracting stage and that they become Of stars before reaching the main sequence. Accordingly, the Wolf-Rayet binaries which are formed by a Wolf-Rayet star and an O or B companion would be representatives of group 1; V444 Cygni or γ_2 Velorum are the prototypes.

Within the second group we distinguish systems of two components having equal characteristics and systems with dissimilar components. Y Cygni (B0 V+ B0 V) represents the first subgroup, and α Coronae Borealis (A0 V + G6 V) the second.

The third group is represented by U Cephei (B8 V + G8 III).

The fourth group may be divided into two subgroups which are similar to those of the second group; their representatives are AO Cassiopeiae (O9 III + O9 III) and RZ Cancri (K2 III + K4 III).

The fifth and last group might be divided into subgroups according to how far the evolution has proceeded. Representatives, in order of increasing evolutionary age, are β Lyrae, SS Cygni, and perhaps UX Ursae Majoris.

The W Ursae Majoris group of binaries are close systems of late-type components with rather similar spectral characteristics, which seem to belong either to group 3, with one component slightly above the main sequence, or to group 2.

A comprehensive program of two-dimensional spectral classification of close binaries, extending Miss Roman's (1956) work, and studies of the frequency distributions of the different groups (in their relation to spectral types, masses, mass ratios, and separations between the components) discussed in the light of evolutionary ideas would be important for the understanding of the origin and evolution of binary systems. Serious consideration will have to be given to observational selection. In connection with this point, Popper's current work aiming at the determination of reliable masses of close binary systems is of the utmost importance.

C. and M. Jaschek (1957) have recently investigated the frequency distribution of spectroscopic binaries, presumably by considering the spectral and luminosity classes of the brighter components. They reached the conclusion that the percentage of spectroscopic binaries along the main sequence is approximately constant. This result agrees with a result previously derived by Kuiper (1935) with respect to the visual binaries.

2.2. Peculiarities in the Spectrum

Superimposed upon the normal features, the spectra of a number of close binary systems display peculiarities which give us an insight into the structure of the systems and provide us with information which aids in the understanding of their evolution. The spectral peculiarities appear as emission and/or absorption features, and their behavior usually follows definite patterns.

Most of these peculiarities are observed only when the spectroscopic binary is also an eclipsing variable, a fact which suggests that the phenomena involved are mostly confined to regions close to the orbital plane.

Wyse (1934) was the first to call attention to the tendency of eclipsing binaries to display emission of H and in some cases of Ca II. Now we know that, in general, the binaries display essentially the same emission lines as do the single stars, that is, H, He I, He II, etc., in early spectral types; H in intermediate types; and Ca II in late spectral types. We shall first discuss the emissions which arise from gaseous rings.

2.3. Gaseous Rings

The results by Wyse, particularly with reference to RW Tauri, led to a thorough investigation of this system by Joy (1942, 1947) who found that the H emissions reported by Wyse are double and are probably produced by an extended gaseous ring which surrounds the primary component of the system and rotates in the same direction as that of the orbital motion. RW Tauri is an eclipsing system formed by a B9 primary and a giant K0 secondary, the spectrum of which is observed only during primary eclipse.

The existence of a gaseous ring around the B9 primary of RW Tauri is suggested by the fact that the double emission lines—each about 3 A wide and 10 A apart—which flank the edges of the corresponding absorption lines undergo eclipses at the time when, because of its orbital motion, the larger K0 secondary passes in front of the primary star of the system. At second contact, only the red emission is present, that is, the secondary component eclipses that part of the rotating ring which has velocities of approach with respect to the observer. At third contact, only the violet emission is present, and the part of the rotating ring which has velocities of recession with respect to the observer is eclipsed. At mid-eclipse the whole ring is behind the K0 star, and no emission lines are observed. Joy's interpretation was confirmed during an extensive spectrographic survey of eclipsing stars at the McDonald Observatory by Struve and his associates.

Table 1 lists the systems which are known to display gaseous rings. The data in the table show that such rings are observed around the primaries of Algol-type systems with deep principal eclipses and, therefore, with large secondary components. Furthermore, the spectra of these secondaries appear to be those of late-type (G or K) giants or subgiants. On the other hand, while the early-type primaries have in some cases also been classified as giants, these classifications are unreliable because the spectra are usually peculiar and yield velocity-curves which in most cases clearly suggest that they do not represent pure orbital motion. We shall come back to this point later on.

The gaseous rings rotate with velocities of several hundred kilometers per second (in the case of RW Tauri, about 350 km/sec), always in the same direction as that of the orbital motion. It was found empirically (Struve 1946*a*) that the velocities of rotation were related to the period of the binary by the expression

$$V_{\mathrm{em}}^{3} \propto P^{-1} . \qquad (2)$$

The eclipses of the rings tend to be total in systems of relatively short period and annular in systems of longer periods, which suggests that in the latter there is more room available for formation of a ring. As confirmation, we observe that only in systems of relatively long period is the radiation from the rings sufficiently strong to produce observable emission lines throughout the entire orbital cycle. In systems of short period, the radiation from the rings is not strong enough to produce observable emissions outside eclipse; they appear in the spectrum only during eclipse, when the exposure times are lengthened because of the drop in light. It seems clear that the sizes of the rings are comparable to, or larger than, the sizes of the secondary components of the systems.

TABLE 1

SYSTEMS WITH GASEOUS RINGS

Star	Character of Eclipse	Depth of Eclipse (Mag.)	Period (Days)	Spectral Type*	Source
RW Tauri	Total	4.3	2.8	B9+sgK0	Bidelman (1954), Joy (1942), Hiltner and Hardie (1949)
U Sagittae	Total	3.3	3.4	B7 III+K1 III	Roman (1956), McNamara (1951*a*, *b*)
SW Cygni	Total	2.6	4.6	A2+K0	Struve (1946*c*)
W Delphini	Total	2.7	4.8	A0+G5	Struve (1946*c*)
AQ Pegasi	Total	2.7	5.5	A2+G5	Struve (1946*a*)
S Velorum	Total	2.8	5.9	A5 V+K5 III	Sahade (1952*b*)
TT Hydrae	Total	2.5	7.0	A3+G5	Sahade and Cesco (1946)
VW Cygni	Total	2.7	8.4	A3+G5	Struve (1946*a*)
RY Geminorum	Total	2.0	9.3	A2+K2	McKellar (1950)
RS Cephei	Total	1.7	12.4	A5+G	Struve (1946*c*)
DN Orionis	Total	1.4	13.0	A2+gF5	Struve (1946*c*)
RW Persei	Total	2.2	13.2	A5+gG0	Struve (1945)
RX Cassiopeiae	Partial?	0.8	32.3	gA5+gG3	Struve (1944*b*)
SX Cassiopeiae	Shallow total	1.0	36.6	sgA6+gG6	Struve (1944*a*)
RZ Ophiuchi	Shallow total	0.8	262	F3 I*b*+cK5	Bidelman (1954), Hiltner (1946*a*)

* The star which is in front during principal eclipse is listed in the second place; the one in the first place is always associated with the ring.

The variations in character of the emission lines throughout the cycle of the orbital motion in such systems as SX Cassiopeiae and RX Cassiopeiae suggest that the motions within the rings are very complicated. Furthermore, the ring formations seem to be neither permanent nor of uniform density. In RW Tauri (Joy 1947), for instance, the emission lines were variable in intensity throughout the cycle of the orbital motion, and this was regarded as an indication that the material was not uniformly distributed. The observational evidence in RW Tauri (Wyse 1934; Joy 1947) and U Sagittae (McNamara 1951*a*) also suggests that the ring formations are unstable or, rather, that the amount of material in them is different at different times; observations of these two stars failed to

show emission lines in certain years but did in other years. Plate I illustrates the behavior of the double emissions in SX Cassiopeiae.

The problem which immediately arises is: Where does the matter of the rings come from? The gaseous rings are always associated with the small primary components of the systems in Table 1, the secondaries of which are all late-type giant or subgiant stars. Now, consideration of the probable dimensions of the two components led Crawford (1955) to the conclusion that the secondaries very probably filled their lobes of the inner contact surfaces, that is, the zero-velocity surfaces which contain the Lagrangian point L_1 in the restricted three-body problem (Moulton 1914). This situation would set up an instability in the secondary stars, and gases would escape from their atmospheres (Crawford 1955; Kopal 1955); this is actually Kuiper's (1941) ejection mechanism of type A, which arises when one component of a close binary system fills its lobe of the inner contact surface, while the other component is much smaller than its own lobe.

Huang and Struve (1956) were able to show that the motions of the rings were determined primarily by gravitational attraction and that the effect of other forces, if any, must be small. On this assumption they analytically derived the expression

$$V_{\text{em}}^3 \propto P^{-1} , \tag{3}$$

found empirically, and, from the motions of the rings, computed upper and lower limits of the masses of the stars around which the rings revolve.

The emission spectra of the rings are strongest in H, and when the lines of this element are very strong, we also observe double emission lines of other elements, such as Fe II, Ca II, and Mg II. The physical conditions of the rings are such that no forbidden lines have been observed in their spectra. It is probable that their ionization is not very different from that of the atmospheres of the early-type stars responsible for their excitation, but the pressure must be quite low. This is suggested by the fact that the H lines show no Stark broadening.

Struve (1950*a*) has estimated that the integrated light of the rings "within the range of sensitivity of an ordinary photographic plate is of the order of perhaps 10^{-3} of the combined light of the two stars." He also pointed out that, since the sizes of the rings are not very different, as to order of magnitude, from that of the solar corona, they must be about 10^3 times brighter than is the corona relative to the sun. Struve (1951) has further estimated that there are approximately 10^{50} H atoms within the entire ring, which implies a total mass of 10^{26} gm, approximately 10^{-8} of the star's mass, and that the dilution factor is of the order of 10^{-1} or 10^{-2}, as compared with 10^{-2} for a Be star.

2.4. Concentration of Matter at Lagrangian Points

The next question is whether there is any observational evidence in support of the hypothesis that the matter which forms the rings comes from the secondary components through the Lagrangian point, L_1. The answer is affirmative.

There are a few systems which have provided some evidence of the existence of a concentration of matter near L_1 and which suggest that this matter streams toward the following hemisphere of the primary component. This is clearly shown by the eclipsing system, β Persei (Algol) (Struve and Sahade 1957; Sahade 1958*b*), in which the emission lines of H (relatively strong at Hα and extremely weak at Hβ and Hγ) appear only during the elongations. This must mean that, at the conjunctions, the gaseous matter responsible for the emission is eclipsed by either star of the system. At the elongation which follows primary minimum, the emission appears on the red side of the absorption line, and at the other elongation it appears on the violet side of the absorption line. However, the intensity of the emission is very different in the two cases: when it is on the red side of the absorption, it is clearly seen; at the other elongation, it is extremely weak. We have as yet no clue toward the understanding of this behavior. Plate II illustrates the type of emission displayed by β Persei, which has been interpreted as arising from matter concentrated at about L_1 and streaming toward the following hemisphere of the primary component.

There are other systems which give similar evidence, namely, HD 47129 (Struve, Sahade, and Huang 1958), V444 Cygni (Sahade 1958*c*), and UX Monocerotis (Struve 1947). In HD47129 we observe, at Hα, a relatively narrow emission line superimposed upon a broader one. While the latter feature is practically stationary, the former shows a variation in radial velocity that yields a velocity-curve shifted in phase by nearly 180° with respect to the velocity-curve of the primary component of the system, with an amplitude of the order of 300 km/sec.

In the case of the Wolf-Rayet binary, V444 Cygni (Pl. III), a relatively narrow emission was found superimposed upon the broad emission of He II 4686 A characteristic of the Wolf-Rayet spectrum. The narrow emission shifts in position relative to the broad one. The latter partakes of the motion of the Wolf-Rayet component of the system and yields a velocity-curve with an amplitude of some 300 km/sec. On the other hand, the radial velocities from the narrow emission line suggest a velocity-curve with a phase shift slightly larger than 90° with respect to that of the Wolf-Rayet star, but with an amplitude of the order of 700 km/sec.

Both cases have been interpreted as indicating a concentration, in the vicinity of L_1, of gases which, in the case of HD 47129, stream out from the secondary component of the system toward the following hemisphere of the primary star and, in the case of V444 Cygni, stream from the Wolf-Rayet star toward the following hemisphere of the O-type companion.

As for UX Monocerotis, the observations suggest the existence of an emitting mass of gas between the two components of the system; furthermore, Kranjc (1951) has shown that the emitting gaseous mass must be concentrated near L_1. Conceivably, we have a situation similar to that in HD 47129 and V444 Cygni.

The phase shift of the velocity-curves derived from the narrow emissions, at

Hα in HD 47129 and at He II 4686 A in V444 Cygni, must be indicative of the general inclination of the gaseous streams at L_1 with respect to the radius vector joining the two components of the systems. In HD 47129 this inclination seems to be almost 90° in the direction opposite to that of the orbital motion, while in V444 Cygni it is very small. Such different deflections must depend on the velocities of ejection, the space available in the lobe around the star toward which the streams are directed, the radiation pressure, and the extent and density of the gaseous envelope around this star.

In those cases where we observe double emissions arising from gaseous rings, we would expect to find a strengthening and/or a broadening of at least one of the emission components at each elongation. No indication of such an effect is recorded in the literature. Either the effect has passed unnoticed, or the best region to look for it is that of Hα, which was not covered in the early investigations. However, we seem to have an indication of this effect in Struve's observations of SX Cassiopeiae (1944*a*) and RX Cassiopeiae (1944*b*). In the former star the H absorptions, which appear flanked by the two emission components, are suppressed at both elongations; emission from the streaming matter near L_1, filling in the absorption, appears to be an obvious possibility. This phenomenon seems to be unsymmetrical, in the sense that it is more conspicuous at the elongation which precedes principal light-minimum. In RX Cassiopeiae we have a similar phenomenon, but the asymmetry is apparently reversed.

The relative intensities of the emission components seem to be different before and after mid-eclipse (Struve 1944*a*, *b;* Sahade 1952*b*); further investigation is required to understand this behavior.

2.5. Absorption Effects of Gaseous Streams

One would expect that the matter streaming out to form the rings might produce some absorption effects when it is seen projected upon the surface of the star whose spectrum we observe. Such effects have actually been observed.

The first suggestion of absorption effects from the streaming of matter in close binary systems came from the study of the spectrum of the eclipsing system SX Cassiopeiae (Struve 1944*a*). The velocity-curve obtained from the lines of the primary component showed a marked peak in the region of maximum positive velocity (see Fig. 1). The curve did not represent pure orbital motion and gave a value of $e \cos \omega = +0.49$, in contradiction to the value $e \cos \omega \approx 0$ suggested by the light-elements. Struve concluded that the velocity-curve is distorted, at least in part, by the effect of a gaseous stream moving from the secondary component of the system toward the following hemisphere of the primary. The stream is seen projected upon the surface of the primary precisely at those phases at which the velocity-curve shows the marked peak. The velocities of recession of the stream give rise to red-displaced absorptions which blend with the stellar lines, yielding radial velocities much larger than those arising from the orbital motion of the star.

Struve's hypothesis found support in the results from AU Monocerotis (Sahade and Cesco 1945*a*). This star gave different velocity-curves for H and for He I. While the velocity-curve from the lines of He I was a normal sine-curve, the velocity-curve from the lines of H, of larger amplitude, had a peaked maximum (see Fig. 2) similar to the one found in SX Cassiopeiae. The behavior of the velocities of H and He I in the phase interval 0.75 P–1.00 P, counted from principal minimum, was strongly correlated with the appearance of the spectral lines in the same interval. While the He I lines had the same relatively narrow appearance as in the rest of the cycle, the lines of H were much broader, suggesting that they were blended with lines from a receding stream similar to the one postulated in the case of SX Cassiopeiae.

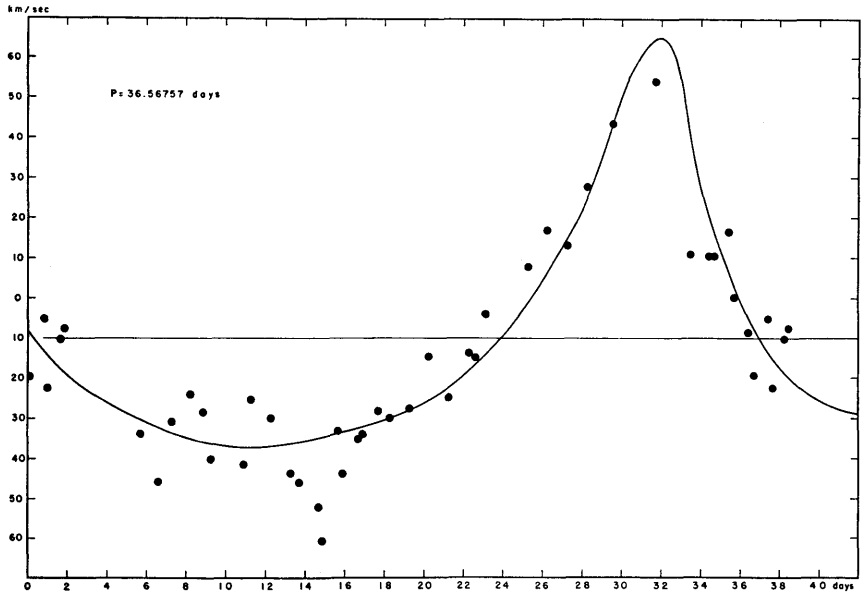


FIG. 1.—The velocity-curve of the eclipsing variable SX Cassiopeiae (Struve 1944*a*)

Peaked maxima in the velocity-curves were later found to be characteristic of many systems with gaseous rings, thus providing a strong piece of evidence in support of the theory of the origin and the dynamics of the gaseous rings.

Incidentally, these peaked maxima in the velocity-curves of close binary systems with gaseous streams are responsible for the so-called Barr (1908) effect, that is, the non-uniform distribution of ω among the spectroscopic binaries. The absorption effects of the gaseous streams immediately after phase 0.75 P produce distorted velocity-curves, which yield values of ω between 0° and 90° and therefore result in a spurious statistical clustering of ω in the first quadrant.

When the two lobes of the inner contact surface are filled with matter (either by the star itself or by an extended atmosphere), we would expect to observe

gases streaming from each lobe toward the other one. Such is indeed the case in β Lyrae (Struve 1957*a*) and ϵ Aurigae (Struve 1956). The situation in these two systems is such that immediately before and after eclipse the two streams produce, respectively, red- and violet-displaced absorption lines, often called "satellite lines" in the case of β Lyrae.

2.6. Absorption Effects of Rings

As one would expect, the rings also produce absorption effects. In a number of systems the absorption spectra of the stars associated with rings show narrow, shell-type lines which have sometimes suggested that the stars may be

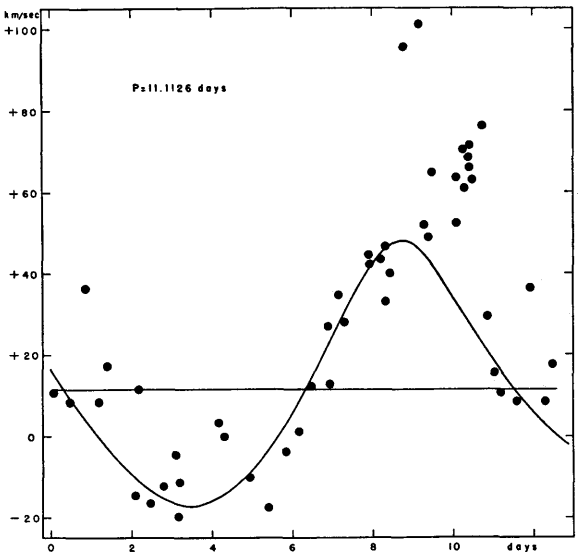


Fig. 2.—The radial velocities from the H lines in AU Monocerotis. The velocity-curve was derived from the lines of He I (Sahade and Cesco 1945*a*).

giants. In some cases—for example, RZ Scuti (Neubauer and Struve 1945; McNamara 1957), V367 Cygni (Sanford 1950; Abt 1954), and W Serpentis (Sahade and Struve 1957)—we observe not only the shell-type absorption lines but also broader lines which originate in the stellar photospheric layers. These three cases are not bona fide binaries with rings, but the results obtained might be of importance in evaluating the information obtained from the systems which do have rings. The results we have in mind are the following: (*a*) the spectral type suggested by the narrow, shell-type lines does not necessarily coincide with the spectral type derived from the stellar lines; and (*b*) the velocity amplitude from the shell lines is smaller than that from the stellar lines: in V367 Cygni,

$$K_* = 51 \text{ km/sec}, \qquad K_{\text{shell}} = 7 \text{ km/sec},$$

and in W Serpentis,

$$K_* \sim 66 \text{ km/sec}, \qquad K_{\text{shell}} \sim 10 \text{ km/sec}.$$

2.7. Mechanism of Mass Loss

We do not know exactly how loss of mass occurs in the vicinity of L_1. One mechanism which comes to mind is that of prominence action. We know that prominence activity in the sun is a very common phenomenon, and we naturally wonder whether hotter stars have prominence activity on a much larger scale than the sun. The observations of such systems as UX Monocerotis (Struve 1947) and S Velorum (Sahade 1952*b*) seem to indicate that prominence activity is indeed at work in them. This is suggested by the large erratic fluctuations in radial velocity and line intensity which take place between consecutive exposures and produce a large scatter from the mean velocity-curve. In the case of S Velorum, whose orbital period is about 6 days, we have from two consecutive plates: at phase 2.795 days (exposure 49 minutes), $+65 \pm 2.3$ (p.e.) km/sec; at phase 2.839 days (exposure 63 minutes), $+28 \pm 1.6$ (p.e.) km/sec, the phases being counted from primary minimum. The same is true for UX Monocerotis, where changes of more than 100 km/sec were found within a 5-hour interval.

A large scatter of the radial velocities is present in nearly all systems with gaseous streams, and it is reasonable to attribute it to rapid fluctuations in a dense network of prominences. Only a few stars have yet been observed in such a manner that rapid fluctuations in the velocities could be detected.

In the case of the spectroscopic binary HD 47129 (Struve, Sahade, and Huang 1958) the observations suggest that the prominence activity of the secondary component is stronger on the hemisphere facing the primary. Appropriate initial velocities and directions of the prominences could result in a loss of mass and could even produce a gaseous stream toward the primary.

According to current ideas of stellar evolution, young stars release energy through the conversion of H into He in their cores. When the hydrogen in the cores is depleted, the stars begin to expand and to brighten. They then leave the main sequence and eventually become giants. In the course of this evolutionary expansion, one component of a binary system may reach a point where it fills its lobe of the inner contact surface. Any further expansion will result in a spilling of matter over the limiting surface and, consequently, in a loss of mass. However, just a spilling of matter over an equipotential surface would not be enough to provide the initial conditions required to set up gaseous streams with the observed velocities—of the order of 200 km/sec in U Sagittae (Struve 1949), 400 km/sec in HD 47129 (Struve, Sahade, and Huang 1958), and 700 km/sec in V444 Cygni (Sahade 1958*c*). It may be that the formation of prominences is favored because of the conical shape of the star at L_1.

To determine the trajectories of the emitted particles under different initial conditions, computations have been undertaken with large electronic calculators (Kopal 1956*a*, 1957; Gould 1957) under the assumption that only gravitational forces are at work and that the particles originate in the stellar compo-

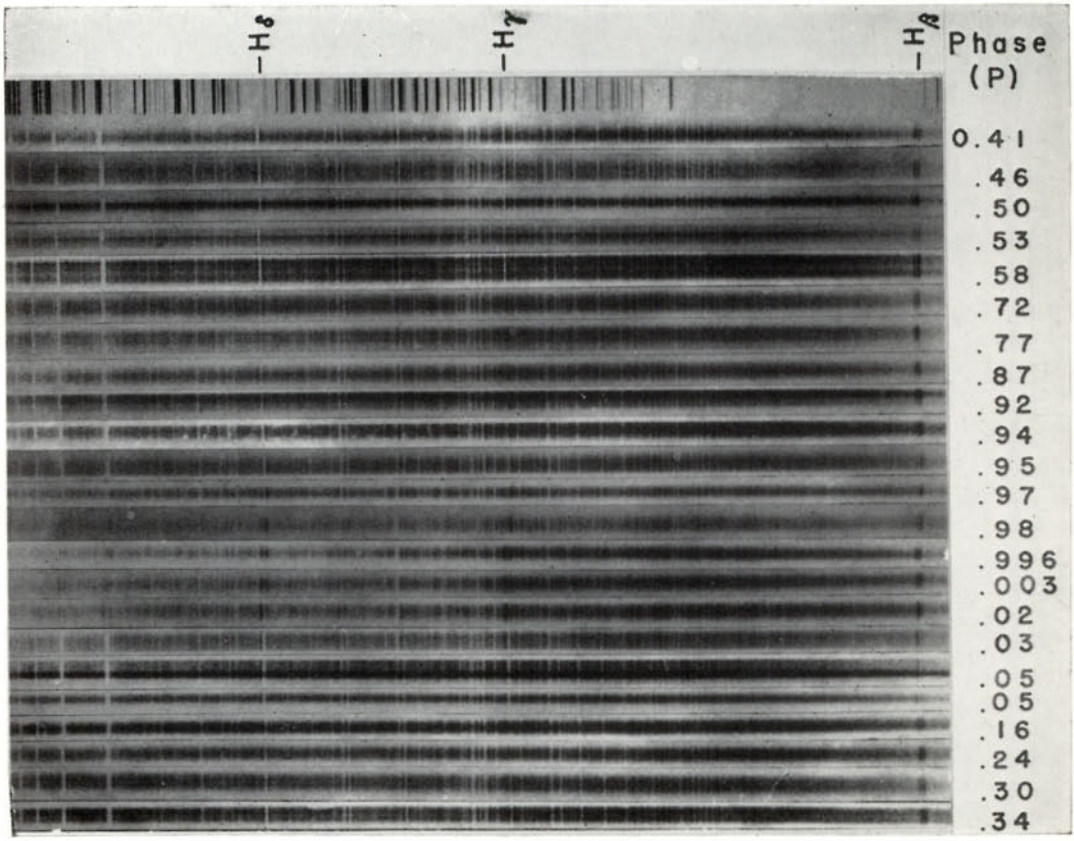


PLATE I.—Behavior of the double emissions in SX Cassiopeiae throughout the cycle of the orbital motion. The phases are counted from primary minimum. (Spectrograms taken at the McDonald Observatory in 1944.)

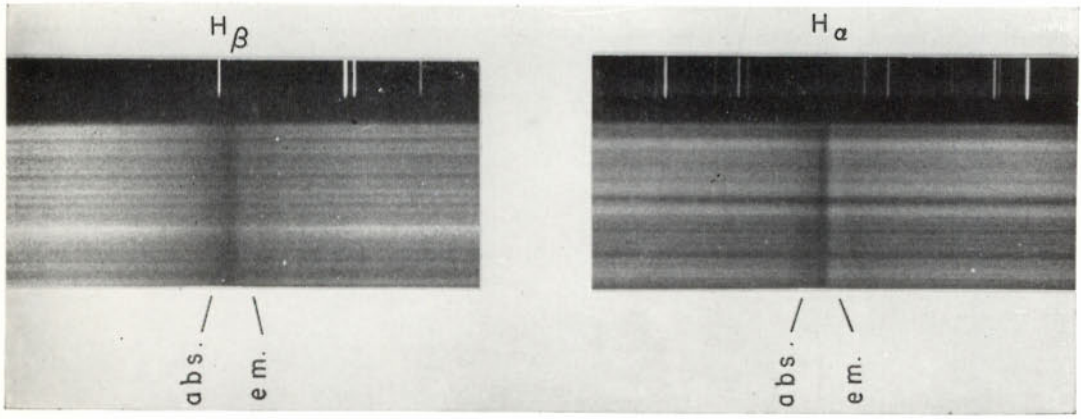


PLATE II.—Emission lines in β Persei at the elongation which follows primary minimum. The feature is weaker at the other elongation and absent at conjunctions. (Spectrograms taken at the Mount Wilson Observatory in 1956.)

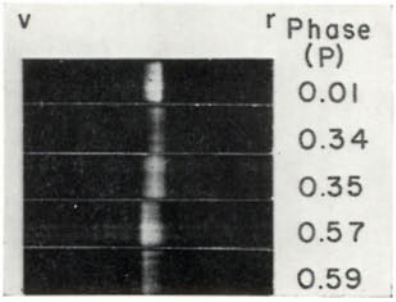


PLATE III.—Structure in the He II 4686 A emission in V444 Cygni. Note the narrow emission superimposed upon the broad one and the relative position with phase. (Spectrograms taken at the McDonald Observatory in 1949.)

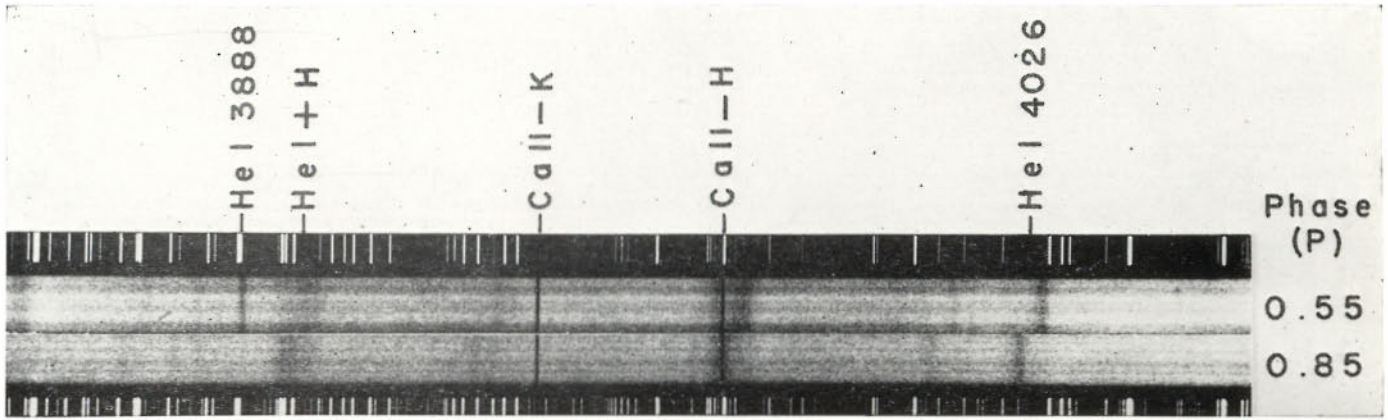


PLATE IV.—He I 3888 A in the expanding shell which surrounds the system of HD 47129. The line is greatly displaced from its normal position and appears only during a part of the cycle: it is present on the top strip and absent on the other one. (Spectrograms taken at the Mount Wilson Observatory in 1957.)

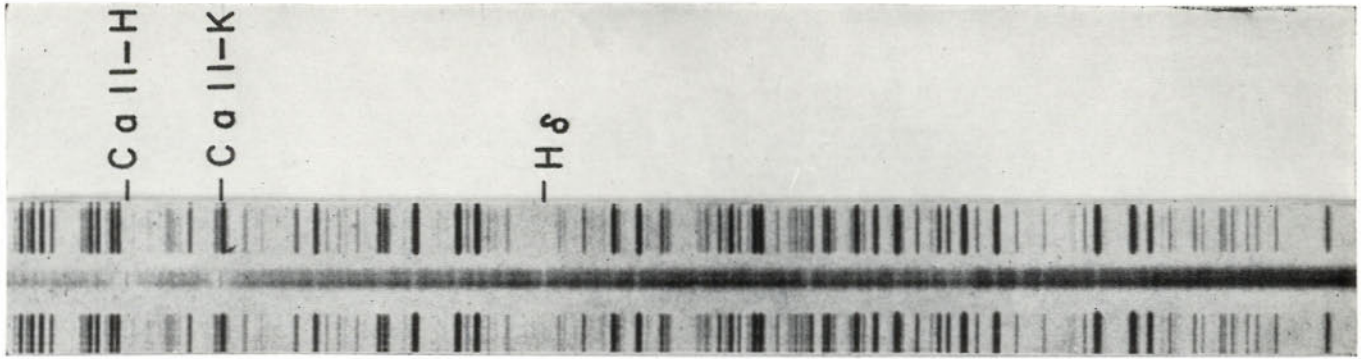


PLATE V.—Ca II emission in the spectrum of SS Bootis at phase 0.081*P*. The spectrum is dG5 + dG8, and the emission is associated with the secondary component (G8). (Spectrogram taken at the McDonald Observatory in 1945.)

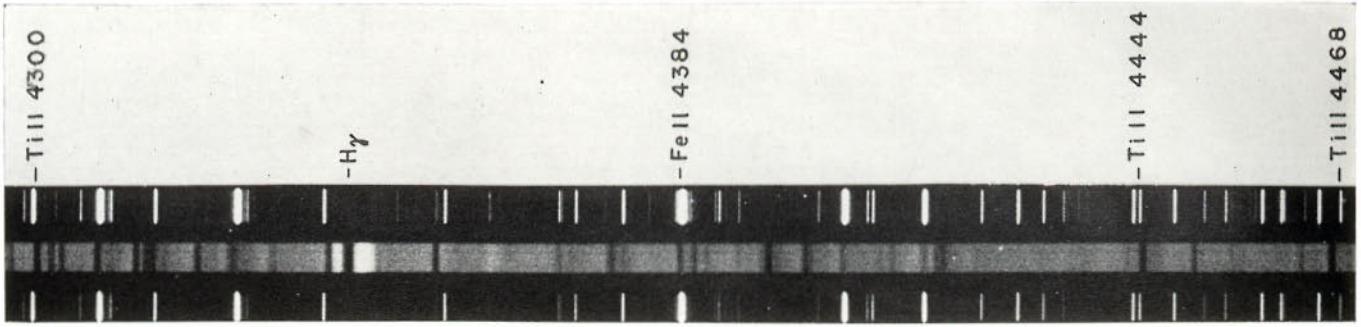


PLATE VI.—The spectrum of the eclipsing variable W Serpentis at phase 0.90*P* counted from primary minimum. Note the broad emission at Hγ. (Spectrogram taken at the Mount Wilson Observatory in 1956.)

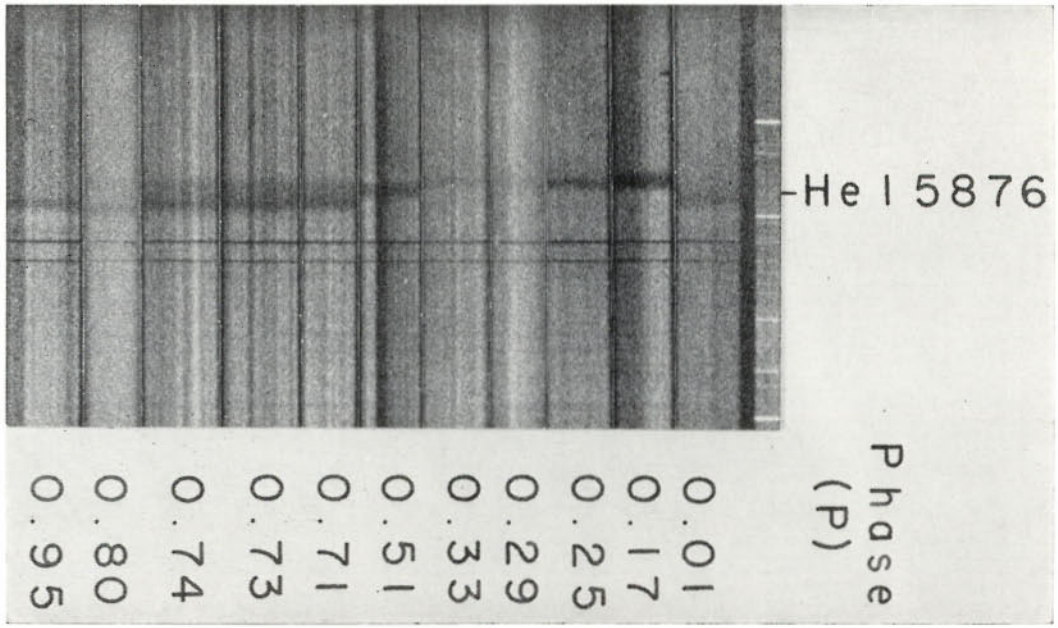


PLATE VII.—The behavior of He I 5876 A in 29 UW Canis Majoris at different phases, counted from primary minimum of light. In the second half of the cycle the line is clearly double in absorption, the weaker, violet component belonging to the secondary star. In the first half of the cycle, however, only the lines of the primary star are clearly visible. (Spectrograms taken at the Mount Wilson Observatory in 1957.)

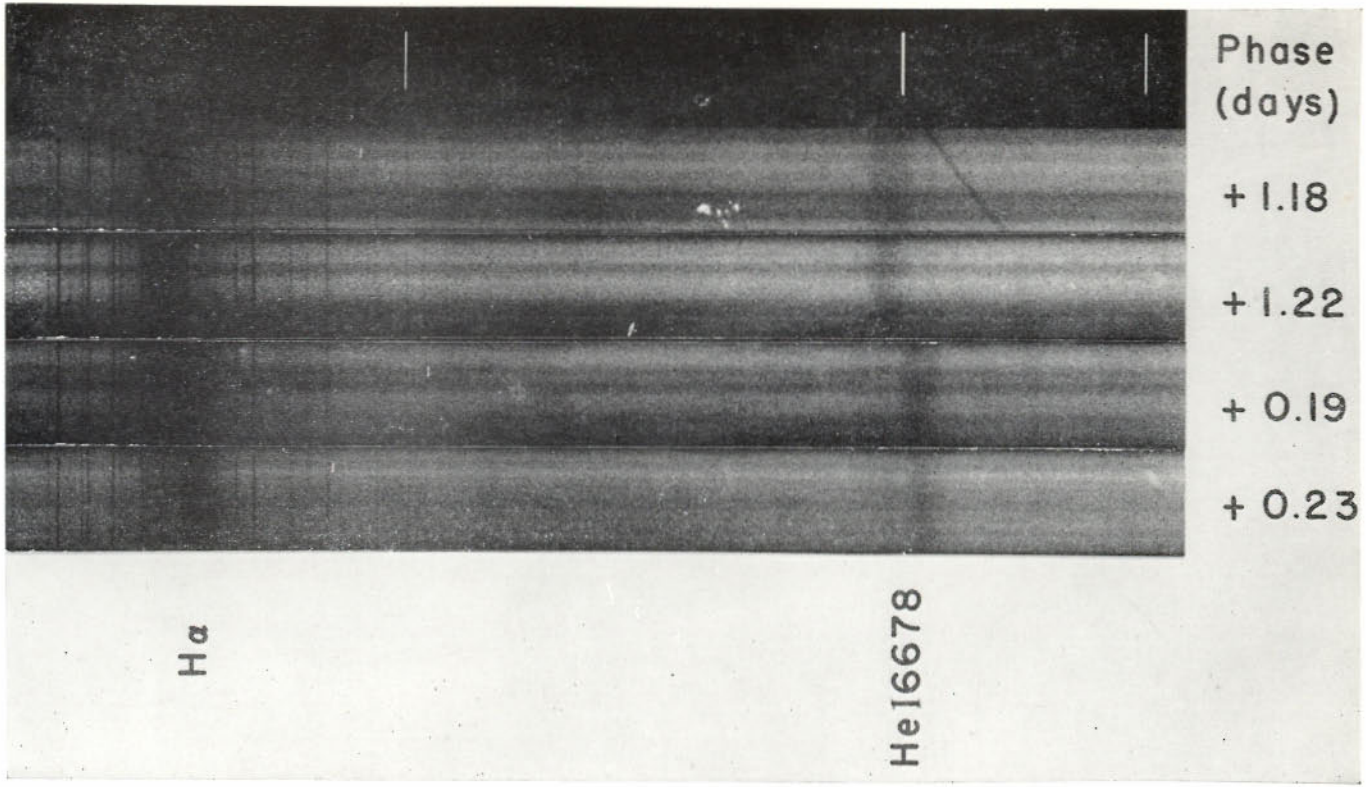


PLATE VIII.—Structure in the broad lines of the primary component of the double-lined spectroscopic binary α Virginis. (Spectrograms taken at the Mount Wilson Observatory in 1957.)

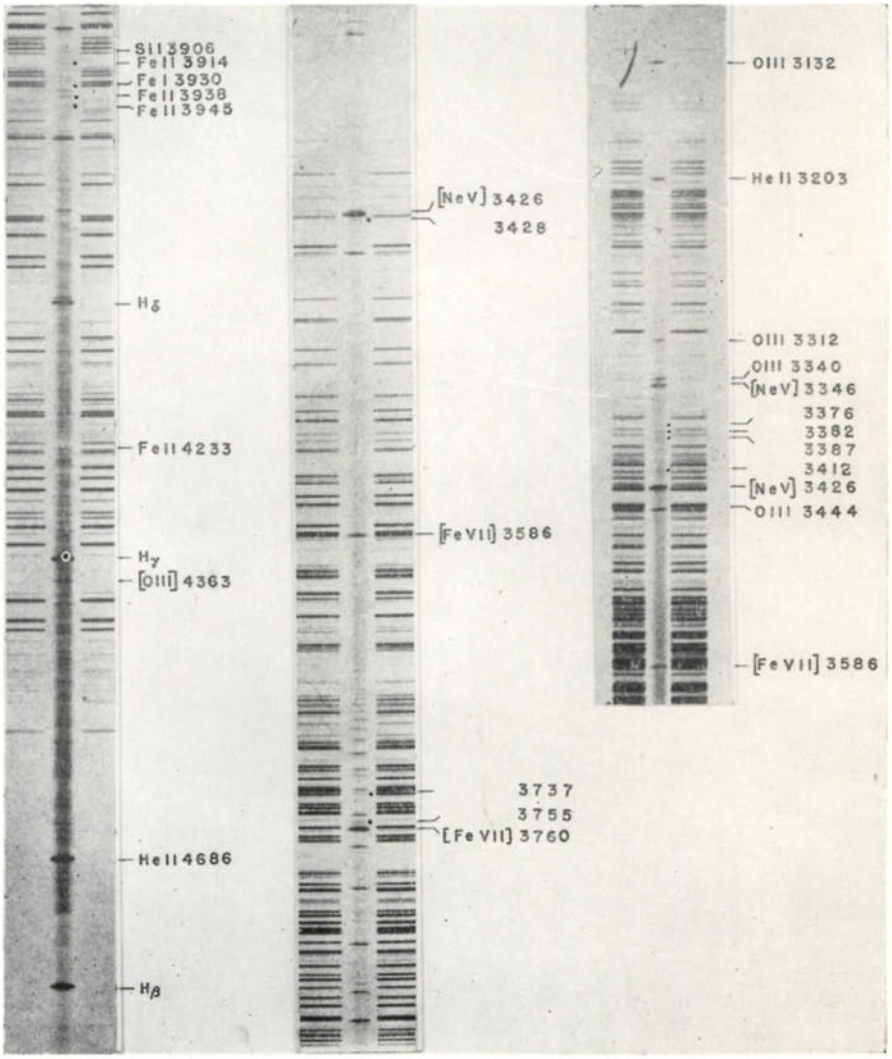


PLATE IX.—The spectrum of the symbiotic star CI Cygni on July 4, 1942. (Spectrogram taken at the McDonald Observatory.)

nent of smaller mass. More recently Mrs. Gould (1959) has considered the case of particles originating in the component of larger mass.

Kopal postulates that the ejection of matter through L_1 takes place because the star of smaller mass fills its lobe of the zero-velocity surface, and, as a result, its angular velocity of rotation differs from that of orbital revolution. The particles which reach L_1 tend to move along the tangent to the equipotential surface, resulting in an ejection of particles into the lobe of the other component. The direction of the particles will depend on whether the angular velocity of rotation is larger or smaller than the orbital velocity. In the first case the direction will be the same as that of the revolution of the system (direct); in the second case the direction will be opposite (retrograde). In both cases the velocity of the particles would be the difference between the velocity of rotation and the velocity of the orbital revolution. If the stars which eject matter fill their lobes of the inner contact surface through expansion, one would expect, because of conservation of angular momentum, the angular velocities of rotation to be smaller than required by synchronization between rotation and orbital revolution. Therefore, if Kopal's mechanism is at work, the streams will start in a direction opposite to that of the orbital motion of the system. This is the direction of motion which is actually observed in the streams, but in many cases the observed velocities seem to be much larger than the differences that one would expect between the rotational and the orbital velocities.

Kopal's results refer to mass ratios $\mathfrak{M}_2/\mathfrak{M}_1$ equal to 1.0, 0.8, 0.6, and 0.4 and, for the retrograde trajectories, could be summarized as follows: (1) particles fall upon the companion star; (2) particles fall back to the parent star after one or more loops around the companion; (3) particles fall back upon the parent star without circling around the companion; (4) particles fall back upon the parent star after circling the whole system; (5) particles escape from the system along a clockwise spiral; in this case the recession of the particles does not continue indefinitely but reaches a limit at a distance of about ten times the radius of the orbit. These results correspond to increasing velocities of ejection, the computations having been performed for the range of v_1/v_0 between 0.5 and 1.6, where v_1 is the velocity of ejection and $v_0 = [G(\mathfrak{M}_1 + \mathfrak{M}_2)/A]^{1/2}$, A being the distance between the two components of the system. Conceivably, appropriate initial conditions would lead to the formation of a gaseous ring. Figure 3 shows one of the diagrams obtained by Kopal.

Mrs. Gould's earlier computations were made for a mass ratio $\mathfrak{M}_2/\mathfrak{M}_1 = 0.2$, under the assumption that ejection takes place as the result of prominence activity at the equator of the star and that the motions of the two stars are synchronized. In this case she finds that, for velocities of ejection smaller than 0.45 (the unit being 264 km/sec), the particles fall back onto the parent star. For a velocity of 0.7 (Fig. 4), there is a strong suggestion that a gaseous ring will be formed. Mrs. Gould's trajectories start in the retrograde direction, in Kopal's nomenclature, that is, in the direction that the observed streams are

moving. For a higher velocity of ejection, namely, 0.9, "there is a slight tendency for particles to slow down temporarily near the third Lagrangian point, providing a series of loops in its vicinity and possibly a predilection for some matter to concentrate there." Some particles are eventually lost to the system. Mrs. Gould's (1959) more recent computations were performed for different mass ratios and initial conditions. She finds that when the ejection starts from the first Lagrangian point, the particles will describe an orbit only if the star which loses mass is less than one-fifth as massive as its companion. On the assumption that the ejections start from a point interior to L_1 but on the line joining the centers of the two stars, Mrs. Gould finds that there will probably be a concentration of matter between the two stars which favors the following hemisphere of the star toward which the ejection takes place and that a ring rotating in the direction of the orbital motion will form around that star. A ring around both components and rotating in the opposite direction will originate in the case of higher initial velocities and mass ratios and there might be some concentration of matter at L_3 "only in the sense that it is in this vicinity that a particle may pause as it changes its direction."

As Struve (1957*b*) has pointed out, it would be important to consider the problem from the hydrodynamical point of view and allow for the effect of radi-

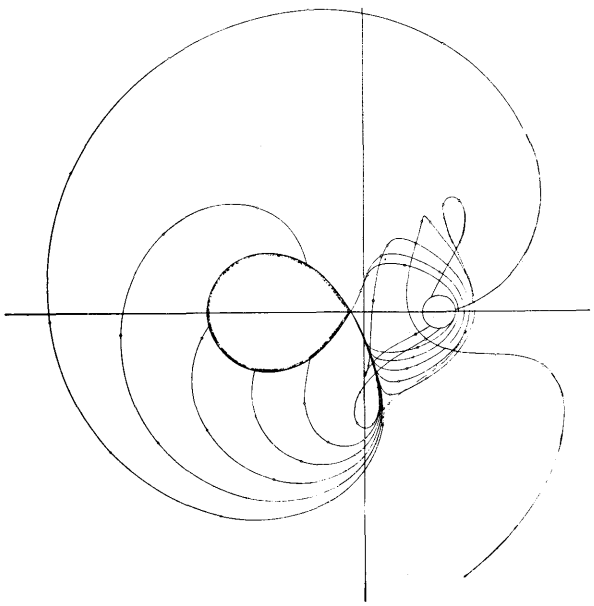


FIG. 3.—Kopal's diagram, showing the trajectories of particles ejected from L_1 with thirteen different values of the initial velocity—ranging from 0.5 to 1.6—in the case of retrograde orbits and a mass ratio equal to 1.0.

ation pressure and perhaps also of magnetic forces. In a gaseous stream which is dense enough to produce observable spectral features, interaction between the particles cannot be neglected. Furthermore, in the case of HD 47129 (Struve, Sahade, and Huang 1958) there is little doubt that radiation pressure is an important factor in determining the direction of motion of the particles.

The question of ring formation came up earlier in Kuiper's (1941) theoretical interpretation of β Lyrae when he considered the ejection mechanism of type A. In Kuiper's own words:

Ejection of type A appears to have the curious result that the large star makes a shell or ring around the small star. It is possible to derive from Jacobi's integral the approximate radius of the ring. If [the velocity of ejection] is not too large, the ejected particles start near their surface of zero-velocity, and the orbit around [the small star] will therefore be eccentric. On account of the perturbations due to [the large star], this orbit will have a rotation of the line of apsides; in addition, the frame is rotating. Orbits of different particles will therefore intersect, and the result of collisions will be that a nearly circular ring will be formed with a radius determined by the available energy.

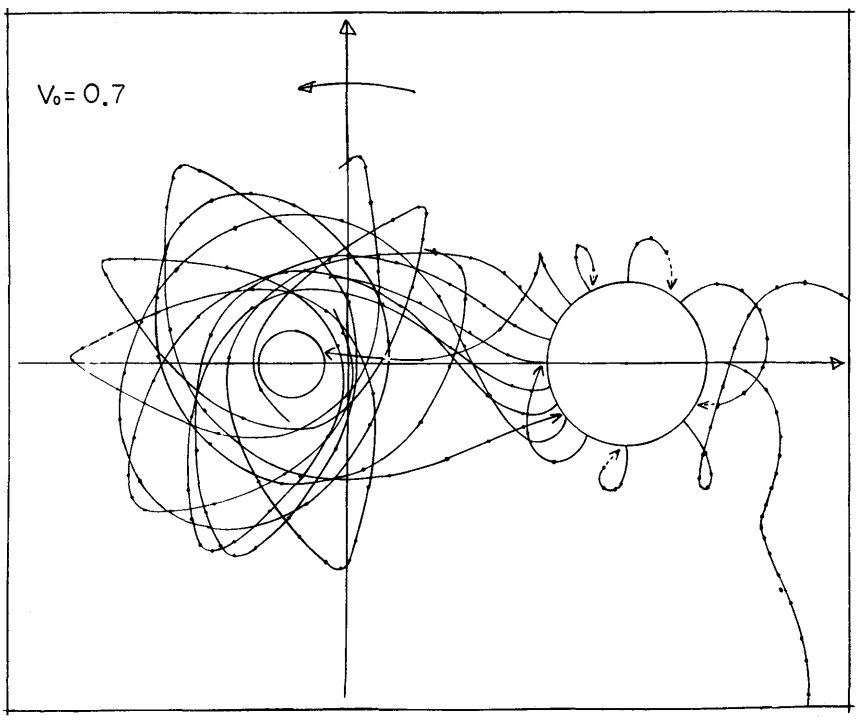


FIG. 4.—Mrs. Gould's diagram, showing the trajectories of particles for a mass ratio of 0.2 and an initial velocity of 0.7, under the assumption that the ejection takes place radially around the equator (like prominences).

The possibility that in some cases the rings have originated because of gravitational instability due to fast rotation (as in Be stars) is apparently ruled out by the fact that among close binaries no stars with very fast rotation appear to be associated with the ring phenomenon.

There are systems, like U Cephei, which show the same kind of distortions of the velocity-curve as does SX Cassiopeiae and yet have no emission lines. It may be that the available space in the lobe of the inner contact surface is not large enough or that the conditions in the ring are such that no lines are observable in the regions investigated.

The question which naturally comes up at this point refers to the fate of the particles in the rings, a problem which has not been discussed in the literature, except for the particular case of the system AE Aquarii (Crawford and Kraft 1956). Undoubtedly, at least two main forces will have to be considered—the gravitational attraction and the radiation pressure. Struve (1942) has discussed their importance in the case of shells around single stars, and the observations of Pleione (Merrill 1952; Struve 1952) and HD 47129, already mentioned, have stressed the role of radiation pressure in early-type stars. The results for Pleione indicate that, as long as the shell is thick, it remains stationary but that, as soon as the shell becomes thin, the radiation pressure blows it away. It then seems reasonable to conclude that, in the gaseous rings we have discussed, radiation pressure is strong enough to prevent the material of the rings from being accreted by the star; the material must eventually escape from the system.

On the other hand, in cases like AE Aquarii we have a different situation. This system is formed by a late-type star which loses mass, presumably through L_1, and a small, less massive, underluminous blue companion. The particles ejected by the late-type component form an emitting envelope around the blue star. Since in this case the gravitational attraction must be much larger than the radiation pressure, at least a part of the matter of the envelope must be accreted by the star, as Crawford and Kraft have concluded (1956).

2.8. Expanding Shells

The possibility that at least a part of the matter which forms the rings escapes from the system is confirmed by the existence of large expanding shells which surround the entire systems in β Lyrae, W Serpentis, HD 47129, the Wolf-Rayet binaries, etc. These shells produce strong absorption lines, which show the effect of dilution of the radiation and yield velocities of approach that do not agree with the orbital motion of the systems. In the case of β Lyrae, HD 47129, and the Wolf-Rayet binaries, these shells display He I lines, those of the triplet series being much stronger than those of the singlet series and He I λ 3888 A being by far the strongest of all. In β Lyrae (Sahade, Huang, Struve, and Zebergs 1959) the velocities are of the order of -170 km/sec, while in HD 47129 (Struve, Sahade, and Huang 1958) they are of the order of -700 km/sec (Pl. IV), and in the Wolf-Rayet binary γ_2 Velorum (Sahade 1955, 1958*c*)

of the order of −1300 km/sec. In the last two stars the shell produces a strong, sharp He I λ 3888 A line greatly displaced from its normal position, which gives a peculiar appearance to the spectra in the photographic region. He I λ 4472 A and λ 5876 A share the same behavior but are much weaker. In HD 47129 the shell also produces a relatively strong and broad emission at $H\alpha$ on the red side of the corresponding absorption feature; in γ_2 Velorum the same is true for He I λ 3888 A.

The distribution of matter in the shells which surround close binary systems seems not to be uniform. In fact, in β Lyrae the variations in the relative intensities of the He I triplet and singlet lines with phase seem to indicate that there is more matter in front of the secondary star at about principal eclipse (Sahade, Huang, Struve, and Zebergs 1959), a fact which may be considered as evidence of escape of matter through the external Lagrangian point which is in front of the secondary component of the system.

The case of HD 47129 is very interesting in this connection. The strong He I lines of the triplet series which originate in the surrounding and expanding shell are present only on that side of the system which corresponds to velocities of recession of the primary star (Struve, Sahade, and Huang 1958); this suggests that the density of the material is higher in that region. Since, as we have mentioned earlier, the gaseous stream from the secondary component of HD 47129 is strongly deflected, presumably by radiation pressure, toward that same side of the system, it would follow that radiation pressure must be important in the dynamics of the expanding shells.

In a few systems the expanding shells display forbidden emission lines. Let us mention W Serpentis (Bauer 1945; Sahade and Struve 1957), which shows the strongest predicted transitions of [Fe II], and T Coronae Borealis (Kraft 1958), which shows [Ne III] and [O III].

Struve (1958*a*) has computed that the expanding shell of β Lyrae contains, at any given moment, about 10^{-9} times the mass of the primary (B8) component.

2.9. Escape of Matter through External Lagrangian Points

There is evidence, in β Lyrae, for instance, that the expanding shell is replenished, at least partly, by material which leaves the system through the external Lagrangian points. We have already mentioned the possibility that matter escapes through the external Lagrangian point in front of the secondary component of the system. A similar escape of matter seems to occur through the external Lagrangian point in front of the primary B8 component. In fact, the radial velocities given by the lines of H and He I (Sahade, Huang, Struve, and Zebergs 1959) at about secondary minimum (when the primary star is in front) are more negative than those given by the lines of other elements which do not display peculiarities. This suggests the existence of an approaching stream in the vicinity of the external Lagrangian point in front of the B8 star. A similar

conclusion was reached in the case of SX Cassiopeiae (Struve 1944*a*) in order to account for the peculiar shape of the velocity-curve in the phase interval corresponding to about secondary light-minimum (Fig. 5).

The escape of material through the external Lagrangian points and the existence of large expanding shells must be common phenomena in close binaries with gaseous streams. The fact that no observational evidence of such shells has been found in bona fide binaries with rings, like RW Tauri, SX Cassiopeiae, etc., may mean either that we should look for such evidence by investigating the region of Hα or that we may have to distinguish between systems which lose mass at a fast rate, like β Lyrae, where the shell produces strong observable features, and systems in which the loss of mass is milder, like SX Cassiopeiae. Abhyankar (1959) has computed, for two values of the mass ratio, about 30 orbits of infinitesimal particles near the external Lagrangian points. His results do not favor the possibility of accumulation of matter around L_2 and L_3, and this essentially agrees with Mrs. Gould's results with regard to L_3.

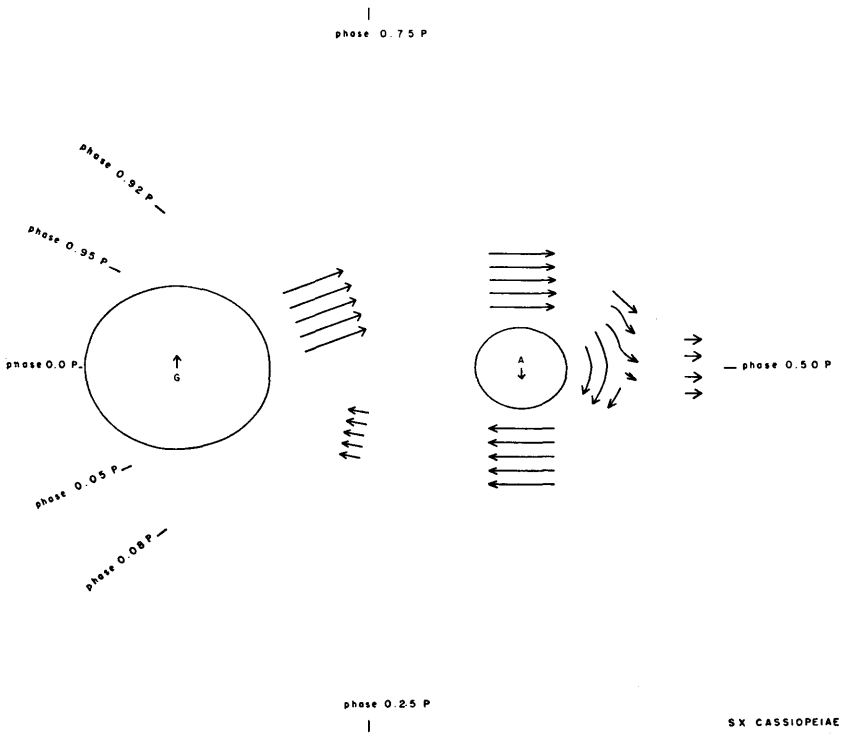


FIG. 5.—The model suggested by the observations of the eclipsing system SX Cassiopeiae (Struve 1944*a*).

2.10. Emission of Ca II

We have discussed the type of emission which appears in binaries with components of early and intermediate spectral types and is interpreted as arising from gaseous rings around one of the stars in each system. As we have seen, these emissions appear as double lines and are strongest in H. When H is very strong, other elements, among them Ca II, also display double emissions.

Another type of emission is present in binary systems of spectral type F5 or later. It is conspicuous in Ca II, and its characteristics are completely different from those originating in rings (Pl. V). The Ca II emission lines in late-type members of close binary systems are usually single, narrow, or slightly broadened, are relatively weak, and are dynamically associated with one of the components of the system. They stand out because they appear superimposed upon the deep and broad stellar absorption lines of Ca II. The emissions we are discussing now resemble those often found in single G-, K-, and M-type stars; however, they are usually stronger in binary systems, suggesting that the binary nature of the object helps in providing the conditions necessary for such emission.

Bidelman (1954) has published a list of 72 spectroscopic binaries with Ca II in emission. Chronologically the first of these systems investigated was WW Draconis, which is formed by two supergiants of types G2 and K0, the emission being associated with the K0 component. Joy (1941) found that the amplitude of the velocity-curve from the emission features of WW Draconis is smaller than the amplitude from the absorption lines, and he concluded that "the secondary star is surrounded with an envelope of calcium gas extended in the direction of the primary by tidal attraction." In most other systems, however, the two amplitudes are practically the same.

Our present understanding of the origin of the Ca II emissions is based principally on the investigations of the eclipsing systems RZ Cancri by Hiltner (1946*b*) and RW Ursae Majoris by Struve (1946*b*). In RZ Cancri the primary component, a giant K2 star, displays the emission; the secondary is also a giant of spectral type K5. Hiltner found that the emissions were absent during a phase interval centered at about the middle of the principal eclipse and extending to points in the light-curve well before the beginning of totality and well after the end of the total phase. His conclusion was that the bright lines were mostly confined to two regions at the extremities of the tidally elongated K2 star. This conclusion was confirmed and extended by the observations of RW Ursae Majoris, a system formed by an F9 primary and a G9 secondary, the emission of Ca II being associated with the latter. Struve's observations of this system showed that the emissions were very strong, appreciably broadened, and perhaps slightly unsymmetrical at both elongations, while they were weaker and narrower at other phases. Furthermore, during the annular phase of sec-

ondary minimum the emissions are absent. Since the loss of light from the secondary in the annular eclipse is of the order of 0.12 mag., the behavior of the emissions of Ca II clearly suggests that the distribution of the emitting matter is not uniform over the stellar disk and that an appreciable amount of emission must come from the outermost tips of the stellar tidal bulges. Therefore, it is reasonable to think that the region responsible for the Ca II emissions in late-type components of close binaries is an extended calcium chromosphere which is tidally elongated along the radius vector joining the two components of the system and extending much farther than the photospheric layers of the star. The broadening of the emissions at the elongations must be due to the effect of the star's rotation. If so, one would expect to observe double lines when the rotational velocities and the dispersion of the spectrograph used were appropriate. In fact, a high-dispersion spectrogram of λ Andromedae (Gratton 1950) has shown that this is indeed the case.

Struve (1946*b*) has suggested that the Ca II emissions are, at least in part, formed by ordinary resonance scattering and that the radiation of the star associated with the emissions provides the mechanism for their production. By estimating the total energy of the K line in terms of the neighboring continuous spectrum and representing the tidal bulges by cylinders which extend above one-quarter of the star's surface, Struve concluded that the number of Ca II atoms in the ground state must be of the order of $10^{14}/cm^2$, as compared with 10^{19}, which contribute to the absorption lines.

It is interesting to note that the binaries of the W Ursae Majoris type also display emission lines of Ca II. The only object of the kind that has been investigated thus far in this connection is W Ursae Majoris itself (Struve 1950*b*; Struve and Horak 1950); the emitting material is associated with the more massive component of this system, and the velocity amplitude from the emissions appears to be much greater than the velocity amplitude from the absorption lines. It is not possible at present to ascertain whether this phenomenon is the same as in systems like WW Draconis or whether both cases require different explanations. It may be that interaction between the two components plays an important role in the W Ursae Majoris stars.

Specific mention should be made of three interesting binary systems, RT Lacertae (Hiltner 1947) and AR Lacertae (Joy and Wilson 1949; Sanford 1951), with two late-type supergiant components, each displaying Ca II emissions, and S Velorum (Sahade 1952*b*). The latter system is formed by a main-sequence A5 primary and a giant K5 secondary; while the early-type component displays the emission characteristics of the rings, the late-type secondary displays emissions of Ca II which arise from its tidally elongated chromosphere.

An interesting behavior of the Ca II emissions is shown by the two M-type components of the system YY Geminorum. Joy and Sanford (1926) found that the emission from the more massive component was about twice as strong as the emission from the secondary when the latter star approached the observer.

On the other hand, the emission from the more massive component was about 20 per cent weaker than the emission from the secondary when the velocities of the latter were of recession. This was tentatively explained as resulting from "the effect of the rapid orbital motion in a resisting medium" which "might be such as to cause the high atmosphere which produces the emission to be dragged behind." The phenomenon was absent in 1948 and 1949 (Struve, Herbig, and Horak 1950).

2.11. Emissions of Another Kind

There are systems which display emission features of a different kind from the ones we have discussed thus far.

1. We know that the Wolf-Rayet stars show broad emissions which are interpreted as arising from matter ejected from these objects. Since a number of them appeared to be spectroscopic binaries, the suspicion arose that all Wolf-Rayet stars were binaries and that their binary character was responsible for their peculiar spectra. However, Sahade (1958*a*) has suggested that the Wolf-Rayet stars may be objects which are still in the contracting stage of their evolution and that the ejection of matter—as seems to be the case in the T Tauri stars (Herbig 1957)—is a mechanism by which the star disposes of excess angular momentum. If this were so, the emission features would not be connected with their binary nature, and there would be no need to suppose that all Wolf-Rayet stars were binary systems.

2. The peculiar eclipsing system β Lyrae displays broad emission features, mainly of H and He I. They suggest a velocity-curve which is opposite in phase with respect to the velocity-curve from the absorption lines of the primary B8 component of the system (Belopolsky 1893; Curtiss 1912). There are reasons to believe that at least part of the matter responsible for the emissions surrounds the secondary component of the system and moves with it (Sahade, Huang, Struve, and Zebergs 1959).

3. The peculiar system W Serpentis also displays broad emission features (Pl. VI), which move with the absorption lines of the primary component (Sahade and Struve 1957) and suggest that the emitting material is ejected by the star and forms an envelope around it.

4. Systems like AE Aquarii (Joy 1954*a*, *b*; Crawford and Kraft 1956), T Coronae Borealis (Kraft 1958), and SS Cygni (Joy 1956) show broad emissions associated with the blue secondary star of each system. As in the case of the secondary component of β Lyrae, we seem to be dealing with stars whose spectra show only broad emission lines.

2.12. Variable Line Intensities

One of the most amazing, and as yet not satisfactorily explained, peculiarities in the absorption lines of close binary systems consists of periodic changes in their intensities. This phenomenon appears in double-lined binaries of about the

same spectral type and was first observed by I. S. Bailey (Pickering 1896) in μ_1 Scorpii. We distinguish three types of variations.

1. One type of variation is that displayed by early-type spectroscopic binaries, like α Virginis, and by all W Ursae Majoris stars. It consists in the tendency of the violet absorption components to be relatively stronger, irrespective of which of the two stars is approaching. This phenomenon is very striking in some stars and apparently varies at different times. In a system like μ_1 Scorpii the variations discovered by Bailey, independently described by Miss Cannon (1901), and confirmed by Miss Maury (1920) were not observed by Struve and Elvey (1942). Something similar has been the case in V Puppis and ζ Centauri, for which the variations announced by Miss Maury (1920, 1922) were not confirmed by Popper (1943).

Aside from the W Ursae Majoris stars, the following binaries show these periodic line-intensity variations: σ Aquilae, 29 UW Canis Majoris, ζ Centauri, 2 Lacertae, V Puppis, β Scorpii, π Scorpii, μ_1 Scorpii, and α Virginis. The phenomenon resembles that shown by the fainter component of AO Cassiopeiae (Struve and Horak 1949) and of HD 47129 (Struve 1948), whose lines are stronger when the velocities are those of approach.

A clue to the explanation of the phenomenon is provided by some recent observations of the eclipsing binary AO Cassiopeiae (Struve and Sahade 1958) which disclosed the presence of a broad emission at Hα. This emission seems to originate in a gaseous envelope surrounding the entire system. It is strongest in the phase interval 0.48 P–0.89 P, counted from primary minimum, and therefore suggests that the density of the envelope is larger in front of the leading hemisphere of the secondary component. This conclusion supports the hypothesis advanced earlier by Struve (1950*a*) as one of the possible causes for the periodic variations in line intensity. Struve had in mind an unsymmetrical common envelope with greater thickness in front of the leading hemisphere of each star of the system. Because the observations of UX Monocerotis (Struve 1947) had suggested that in this system prominence activity was stronger on the advancing side of each star, Struve was led to think that an unsymmetrical envelope might result from prominence activity on a very vast scale.

Huang (1958, 1959) has recently suggested that the components in the systems we are discussing are imbedded in a common envelope much like the solar corona, where high-energy particles are ejected by the brighter component and heat the atmosphere of the secondaries.

It is perhaps in order to point out that, although the phenomenon appears to be identical in stars like α Virginis and in those of the W Ursae Majoris group, it is possible that the underlying physical causes are not exactly the same.

2. Another type of periodic variation in line intensity is displayed by the eclipsing system WX Cephei (Sahade and Cesco 1945*b*). In this binary the lines of the primary component are stronger at the conjunctions, while the lines of

the secondary are stronger at the elongations (Fig. 6). No explanation for the peculiar behavior of WX Cephei has been offered.

3. A third type of variation in the absorption lines of close binary systems is shown by the eclipsing binary AQ Cassiopeiae (Struve 1946*c*). This system has double lines at the first elongation after primary minimum and single lines at the second elongation. The phenomenon reminds us of that found in R Arae (Sahade 1952*a*), where double lines also appear at only one of the elongations. However, in the case of R Arae it was thought that we were not dealing with double stellar lines, one of which became very faint at one quadrature, but rather with the effect of the superposition of a narrow core, perhaps originating

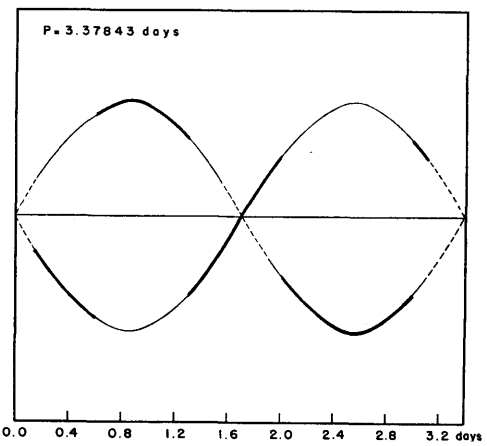


FIG. 6.—Schematic representation of the line intensity variations in the double-lined eclipsing variable WX Cephei (Sahade and Cesco 1945*b*). The velocity curves are drawn heavier in the phase intervals where the spectral lines are stronger. Phases are counted from primary minimum, and the velocity-curve of the primary component of the system is the one which shows velocities of approach immediately after primary minimum.

in an approaching mass of gas, upon the broad stellar line of the primary component of the system.

29 UW Canis Majoris (Struve, Sahade, Zebergs, and Lynds 1958) provides a good example of stellar lines varying drastically in intensity at the elongations; this is especially well shown by the line of He I λ 5876 (Pl. VII). The absence or weakness of the absorption lines of the secondary component of 29 UW CMa when its velocity is positive must be caused by the opacity of the gases that are shed by the primary star of the system and stream toward the following hemisphere of the secondary (Sahade 1959).

The variations in line intensity in close binary systems are not all periodic in character; they may be erratic, as was mentioned in connection with the existence of prominence activity.

2.13. Peculiar Line Structure

An extremely peculiar structure of the absorption lines has been recently found in α Virginis (Struve, Sahade, Huang, and Zebergs 1958). It seems to be present, at all phases, in the broad lines of the primary component of the system and sometimes gives the impression that the line is actually double. The structure does not look the same at different phases or in different cycles. Plate VIII shows the structure at He I 6678 A. The broad lines are from the primary component and the narrow lines from the secondary. At phase +0.19 days, counted from the time of periastron passage, the broad absorptions are clearly double. On the next plate, at phase +0.23 days, the structure is much less striking. The structure of this line may be connected with the fact that the angular velocity of rotation of the star is faster than the orbital velocity or, according to Huang (1959), to the occurrence of stellar flares on the surface of the primary star.

2.14. Discussion

The classification of close binary systems set up at the beginning of this chapter and the spectral peculiarities which we have described pose the question whether different groups do display different peculiarities and whether a scheme of evolution can be inferred from our present knowledge in this field.

It seems clear that the evolution of close binary systems must depend on the initial masses, mass ratios, and separations of the components. Furthermore, systems with massive components must evolve faster than systems with less massive components. If both components are initially equal, one may expect that, along their evolutionary paths, they will reach the same stages at the same time. If the components are initially different, the more massive star will evolve faster than its companion. In close binary systems one would also expect transfer of mass through the inner Lagrangian point to play an important role, but conceivably this effect is not important in wide pairs.

During the gravitationally contracting stage of their lives the stars appear to lose mass in order to dispose of excess angular momentum. This would account for the peculiarities of the Wolf-Rayet spectra. In Wolf-Rayet binaries (Sahade 1958*c*) a gaseous stream seems to pass through the inner Lagrangian point toward the more massive O or B companion, and an expanding envelope develops surrounding the entire system. It seems likely, though this is not as yet certain, that the Of binaries represent a later evolutionary stage of the Wolf-Rayet binaries before they reach the main sequence.

On the main sequence the binaries do not seem to display peculiarities, except when their masses and sizes are such that one or both fill or almost fill the lobes of the inner contact surface. Among systems with both components on the main sequence, we find systems with similar components and systems with dissimilar components. The two components of the former systems would have reached the main sequence at the same time and would probably start evolutionary expansion and therefore leave the main sequence, also at the same time.

The two dissimilar components of the latter systems must have reached the main sequence at different times and will probably leave the main sequence also at different times; the more massive component would be the one which had reached the main sequence first and would also be the one which would leave the main sequence first. The accompanying tabulation lists a few systems with both components on the main sequence.

Star	Spectrum	$\mathfrak{M}_A^*$	$\mathfrak{M}_B^*$	Source
Y Cygni	B0 V+B0 V	17.4⊙	17.6⊙	Roman (1956), Redman (1930)
AR Aurigae	A0 V+A0 V	2.6	2.3	Popper (1957), Harper (1937)
α Coronae Borealis	A0 V+G6 V†	2.5†	0.9†	Kron and Gordon (1953)

* *A* stands for the primary component and *B* for the secondary.
† Derived from the light-curve and the mass-luminosity relation.

Unless some kind of disturbance produces a difference in mass between the two components, the equal components of close binary systems in the expanding stage of their evolution must reach a point where they both fill the lobes of the critical zero-velocity surface at the same time and further expansion will probably result in the formation of a common gaseous envelope. AO Cassiopeiae seems to be a prototype of this kind: the spectral types are O9 III for both components (Morgan, Code, and Whitford 1955), the masses are 29.8⊙ and 27.8⊙, respectively, and there is evidence for a common envelope (Struve and Sahade 1958). Other systems with similar components in the expanding stage of their evolution are given in the accompanying table; but, although

Star	Spectrum	$\mathfrak{M}_A$	$\mathfrak{M}_B$	Source
DI Herculis	B5 III+B5 III	3.7⊙	4.1⊙	Roman (1956), McKellar (1950)
β Aurigae	A2 IV+A2 IV	2.3	2.2	Morgan, Keenan, and Kellman (1943), Smith (1948)

both components of these systems are above the main sequence, not all of them are already filling the lobes of the inner contact surfaces.

As far as we are aware, no case is known with two old and equal components of intermediate or late type above the main sequence. Whether this is due to the lack of accurate spectral classifications of the components of spectroscopic binaries or has an evolutionary significance is not clear at present, although the latter possibility appears to be more probable. Further evolution of the systems would eventually result in two components below the main sequence. The two components of a close binary could fill their lobes of the inner contact surface even when they were on the main sequence, provided that the dimensions were appropriate. The W Ursae Majoris system AB Andromedae, whose components are of spectral types G5 V and G4 V (Kopal 1956*b*), seems to be a good example.

Let us now consider what would happen to systems with dissimilar components after they had reached the main sequence. Since the more massive component evolves faster, this component would leave the main sequence before the other one. Hence, if neither component gains or loses mass appreciably, we should expect to find that the systems we are considering evolve into (*a*) systems with one component above the main sequence, while the other is still on the main sequence; (*b*) systems with the two components above the main sequence, the more massive component being in a more advanced stage of evolution; (*c*) systems with the more massive component below the main sequence, while the less massive component is still on or above the main sequence; (*d*) systems with the two components below the main sequence.

Systems of type *a* deserve a separate discussion and will be dealt with last. A good representative of this group is U Cephei, a system formed by a B8 V primary and a G8 III secondary (Roman 1956). No example of case *b* can be given at present. Perhaps the lifetime of such a configuration is very short. Systems *c* and *d* belong to the fifth group of our classification of close binary systems suggested at the beginning. Under *c* we would include two subgroups, namely: (c_1) Systems in which the star below the main sequence is more massive than the more luminous companion. β Lyrae and perhaps ϵ Aurigae (Sahade 1958*d*) may belong to this configuration. β Lyrae (Sahade 1958*e*; Sahade, Huang, Struve, and Zebergs 1959) has been described as consisting of a B8 II primary, which fills its lobe of the inner contact surface, and an underluminous, more massive secondary, the spectrum of which displays only emission features. (c_2) Systems in which the star below the main sequence is less massive than the more luminous companion. This subgroup includes AE Aquarii, SS Cygni, and T Coronae Borealis.

Under *d* we would include tentatively the system UX Ursae Majoris, whose primary component is a subdwarf B3 (Kuiper; see Struve 1941) or O (Walker and Herbig 1954).

The more massive components of the systems of subgroup c_1 would reach the stage of the secondaries in subgroup c_2 by losing mass at a rate which would depend on how massive they were. β Lyrae, for instance, seems to be losing mass rapidly (Struve and Sahade 1955), and this fact accounts, at least partly, for its peculiar spectrum. Presumably the secondaries of subgroup c_2 have evolved faster than their primaries because they were once the more massive components. In the course of their evolution they must have lost enough mass to have become less massive than their primaries.

Let us now consider the case of old systems with one component above the main sequence, while the companion is on the main sequence. The close binary systems which display gaseous rings around their primaries are in this situation; the secondaries are giants and seem to fill their lobes of the inner contact surfaces, while the primaries are smaller in size and seem to be on the main sequence. One would expect the component above the main sequence to be the

more massive one. Now these secondaries, except in the case of RX Cassiopeiae, are observed only at primary minimum, and therefore we cannot derive their velocity-curves and consequently the mass ratios and/or the individual masses. In the case of RX Cassiopeiae, the velocity-curves from the two components are not compatible and are therefore not suitable for the derivation of the masses. There are, however, two systems—namely, U Cephei and U Sagittae—in which radial velocities of the secondaries measured during principal eclipse allow the determination of the slope of their velocity-curves. These slopes suggest that the secondaries are less massive than their primaries, i.e., the opposite of what we would have expected. One could perhaps argue that the derivation of the masses from the slopes of the velocity-curves at conjunction is not reliable and that, therefore, we have no actual observational information on the masses. There are, however, a number of Algol systems with very deep principal minima which do not display spectral peculiarities and have very small mass functions; XZ Sagittarii (Sahade 1945, 1949) is one well-known case. These systems seem to violate the mass-luminosity relation, suggesting that at least one of the components is off the main sequence. Furthermore, the mass functions strongly suggest that the masses of the primaries are larger, and in a number of cases very much larger, than those of the secondaries. It is possible that these systems have characteristics similar to those with gaseous rings but that their geometry is such that no peculiarities are evident on the spectrograms. The situation, insofar as the mass functions are concerned, seems to be shared by some of the systems with gaseous rings, such as S Velorum.

We should perhaps remember at this stage that in most systems with gaseous rings the spectra which we observe and which yield velocity-curves consistent with that from the primary components display shell-type absorption features which must originate in the material of the rings. Since these shell-type absorption lines are the ones usually measured, some doubt arises, in view of the results for W Serpentis and V367 Cygni discussed in section 2.6, as to whether the mass functions are reliable.

We should also point out that the rings appear to have dimensions comparable with the dimensions of the secondaries, which suggests that both lobes of the inner contact surfaces of these systems are of comparable dimensions, which, in turn, would imply mass ratios close to 1.

Although the mass ratios might be uncertain, there is little doubt that in the systems with gaseous rings the (apparently) main-sequence primaries are smaller and more massive than the giant or subgiant secondaries. This conclusion finds further support in Mrs. Gould's results already mentioned and in Huang's conclusion (1957) that ring formations are a necessary consequence of the fact that the secondaries, which eject matter, are less massive than their primaries.

If we accept the current ideas on stellar evolution, how could these Algol systems, then, be explained? Crawford (1955) postulated that the secondaries were initially the more massive components and that they expanded and reached a

point where they filled the inner zero-velocity surfaces. As they continued to expand, these stars were not able to retain the matter that passed out of the surface. This matter was either collected by the companions or ejected from the system by centrifugal force if violent mechanisms, such as prominences, predominated. Thus the secondaries could become less massive and less luminous than their primaries.

Kopal (1956*a*, 1958), on the other hand, has recently proposed a different explanation. He believes that the primaries have always been the more massive components. Therefore, they must have evolved faster than the secondaries. In the course of their expansion, the lobes of their inner contact surfaces were filled, and mass was lost to the secondaries. The expansion took place rather rapidly, after which the stars collapsed back to their original state as fast as they had expanded. The masses lost to the secondaries must settle very slowly and therefore increase the volumes of the latter, perhaps filling their lobes of the inner contact surfaces. The expansion of the primaries will, in all likelihood, be repeated, and, when this occurs, the masses gained by the secondaries will have settled enough so as to make room for the mass gained from the new ejection from the primaries.

An alternative possibility, for at least some of the Algol systems, is that the primaries, being the more massive components, have evolved faster than the secondaries, have already passed the giant stage, and are now near the main sequence, in their evolution to the left in the HR diagram.

It is not possible at present to find a satisfactory answer to this problem. Reddish (1957) has pointed out that if, in the course of its evolutionary expansion, a component of a close binary system overflows the lobe of the inner contact surface, thereby losing mass, further expansion and therefore further loss of mass will have to occur in order to satisfy the perfect-gas equation and the condition of hydrostatic equilibrium. Since the adjustments could take place in a matter of days or even hours, a fairly violent blowoff might result. Under the assumption that the two components remain synchronized during their evolution and by considering Oke and Schwarzschild's (1952) stellar models, Crawford (1958) has concluded that in binary systems having a total mass of $3.2\odot$ and a separation of $4.7R_\odot$ the process discussed by Reddish will occur only if the more massive star has more than 55 per cent of the total mass. In order to evaluate these possibilities, we have to know more about the relative angular velocities of rotation of the components of binary systems. Moreover, we require better information about the mass ratios in Algol systems. At any rate, the absence of systems with the smaller component on the main sequence and less massive than the larger one seems to suggest that this configuration must be unstable and that Crawford's hypothesis of the genesis of the Algol binaries may not be far from the truth.

We have tried to fit roughly the most common types of close binary systems into an evolutionary scheme as far as the available information permits us to do

so. Some configurations are rather frequent, while others are apparently missing or very rare—for example, systems with more massive, giant or subgiant primaries and less massive, smaller secondaries. It may be that the differences in frequency distribution mean that some configurations are more stable than others. Perhaps loss and transfer of mass are more important in determining the evolution of close binary systems than we are at present prepared to recognize. Huang (1956) has suggested that the evolutionary tracks of close systems must differ markedly from those of single stars precisely because of loss of mass. In this connection we should point out that no pulsating stars have been found to be members of close binary systems, except perhaps UX Monocerotis, where photoelectric observations by Lynds (1955, 1957) suggested that the early-type component might be some kind of intrinsic variable, perhaps related to the RR Lyrae stars.

To visualize the configurations that we may expect among close binary systems, Struve (1957*b*, 1958*b*) has prepared the scheme shown in Figure 7; in this context "wide pairs" mean systems in which the separation of the two components is large compared with their diameters. Configuration *h* would correspond roughly to that of a W Ursae Majoris binary. The large frequency of

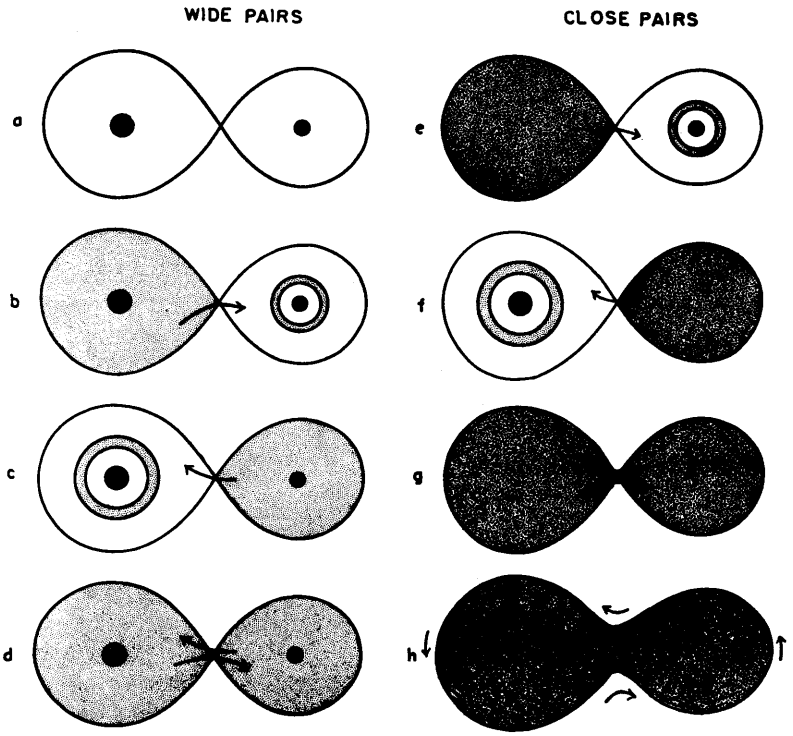


FIG. 7.—Possible configurations in close binary systems (Struve 1957*b*)

these systems, which, according to Huang (1957), are probably born in T-associations, has been known for some time (Shapley 1948) and has induced Mrs. Payne-Gaposchkin (1958) to speculate as to the possible configurations that may result from the evolution of these close systems. She argues that if the components of the W Ursae Majoris stars expand when their cores become depleted of hydrogen, they will eventually become binuclear stars and in their evolution in the HR diagram might show the behavior of a symbiotic variable. Mrs. Gaposchkin suggests that later in their evolution these binuclear stars will again become true binaries and may be similar to systems of the SS Cygni or AE Aquarii type. The question of the evolution of close binaries and a possible interpretation of the W Ursae Majoris systems has been recently discussed in more detail (Sahade 1960).

There are some systems like υ Sagittarii (Greenstein 1940) and AR Monocerotis (Sahade and Cesco 1944), the understanding of which might be important in attaining a comprehensive evolutionary scheme for close binary systems. υ Sagittarii is a hydrogen-poor binary, and AR Monocerotis is a system for which the only velocity-curve observed is that of the secondary component. It is difficult to understand why we do not observe the lines of the brighter star in AR Monocerotis; one possibility is that the primary component of this system is an early-type star with fast rotation whose very broad absorption lines have escaped detection. This possibility finds support in the fact that Sahade and Cesco noticed a strengthening of the continuum and some H lines in the ultraviolet region of some well-exposed spectrograms.

§ 3. SYMBIOTIC STARS

We shall now discuss the peculiar group of objects designated by P. W. Merrill as symbiotic stars (see § 1). These stars display, as we have mentioned, a combination of low-temperature absorption spectrum (commonly of type M) and high-excitation emission lines (Pl. IX).

3.1. Observational Results

The prototype of the group is considered to be Z Andromedae, the first star of the kind investigated in detail. It was noted as peculiar in the *Henry Draper Catalogue* and was studied at Victoria by Plaskett (1928).

Z Andromedae is a variable star whose light-curve is characterized by semi-regular fluctuations. The amplitudes of these fluctuations are usually rather small, but at times they amount to as much as 3 mag. or more, the rises in brightness being steeper than the declines. The level of minimum light has varied by as much as 2.5 mag. in different epochs. The mean cycle is 694 days, while the median cycle is 714 ± 82 (p.e.) days (Payne-Gaposchkin 1946).

The spectral characteristics of the star and their changes during the light-cycle are known, thanks to the efforts of a number of astronomers—Merrill, Swings, Struve, Aller, Mao-Lin, Bloch, and others. References to the literature

prior to 1954 are listed in Bidelman's (1954) *Catalogue and Bibliography of Emission-Line Stars of Types Later than B.*

Let us illustrate the correlation between light and spectrum by describing the changes in the appearance of the spectrum of Z Andromedae from the time of the maximum of light in 1939 through the next maximum in 1941.

At the time of Plaskett's (1928) observations, Z Andromedae showed a late-type spectrum displaying TiO bands (Hogg 1932) and emission lines of H, He I, C II, Mg II, Ti II, and Fe II, characteristic of an early-type star, and of He II, C III, N III, [O III], [Ne III], [Ne V], [Fe III ?], and [S II], characteristic of high-excitation nebulae.

At the light-maximum in 1939 (Swings and Struve 1940; Merrill 1944), the TiO bands, as well as the high-excitation emission lines, had disappeared, the forbidden lines had weakened, and the emissions of H, Fe II, and Ti II had developed violet absorption borders. A strong shell spectrum was present. In 1940 (Swings and Struve 1941*a*), when the brightness was declining, the spectrum of Z Andromedae displayed the nebular features observed by Plaskett, that is, forbidden and permitted emissions usually associated with planetary nebulae—emission lines of N III, C III, and C IV bordered by violet absorptions, and also a P Cygni–type spectrum in H, He I, Fe III, emissions of low-excitation Mg II, Si I, Si II, Ti II, Fe I, and extremely weak [Fe II]. The continuous spectrum in the photographic region was strong and too blue to be associated with the late-type M spectrum, which had reappeared. The shell spectrum had considerably weakened (Merrill 1944).

From August, 1940, to January, 1941 (Swings and Struve 1941*b*), that is, during the time when the star had practically reached minimum, the spectrum of Z Andromedae had a postnova character. There was an increase in the intensity ratio of the nebular to the auroral transitions of [O III], the P Cygni absorptions had disappeared, and a Balmer continuum had appeared in emission.

In 1941 (Swings and Struve 1942*a*) there was a new light-maximum less pronounced than the previous one. During ascending brightness there was an increase in the ratio of the emission lines Fe II/N III, (C III, C IV, O III fluorescence)/[Ne V], He I/[Ne III], Fe II/He I, Fe II/[O III], Si II/continuum, and Mg II/continuum. There was no variation in the structure, but there were a weakening of the early-type emission lines; a general decrease in the intensity of the forbidden lines [O III], [Ne III], [Ne V]; a slight decrease in the intensity ratio of the nebular to the auroral transitions of [O III] from 1940 until about January, 1941; and a very strong Balmer continuum in emission. A new shell had appeared with no appreciable dilution, suggesting that it was still fairly close to the photospheric layers and that its opacity reduced the excitation in the nebula.

It is interesting to add that in January, 1942, 6 months after the minor outburst of 1941 (Swings and Struve 1942*b*), the appearance of the spectrum was

similar to its appearance in August, 1940, about 9 months after the higher maximum of 1939. The evolution toward high excitation continued, and in July and November, 1942 (Swings and Struve 1943), when the star was reaching minimum, lines of [Fe VII] were present.

We summarize the correlation between light and spectrum in Z Andromedae, as follows: (*a*) when the star is faint, an M-type absorption spectrum is prominent; (*b*) when the star brightens, a B-type shell spectrum develops, its continuum dominating the photographic region and covering the M-type spectrum; and (*c*) when the star declines in brightness, the shell spectrum weakens, and emission lines of progressively increasing excitation and forbidden transitions develop.

This general behavior seems to be shared by all the symbiotic stars that have been sufficiently investigated. There are, of course, individual differences. The late-type spectrum may not be quite M, the shell spectrum may suggest a spectral type different from B, and emissions requiring even higher excitation than in Z Andromedae may be present. With reference to this last point, let us mention that lines of [Fe X] which appear in the solar corona have been observed in CI Cygni and AG Pegasi, and lines of [Ca VII] have been observed in RX Puppis.

In short, we seem to be dealing with objects which undergo semiperiodic nova-like outbursts and display the spectral changes of a slow nova superimposed upon the features of a late-type star.

Some spectral lines behave in an unexpected manner. Let us illustrate this with the following cases:

1. In Z Andromedae, Swings and Struve (1943) found strong variations in the relative intensities of triplet and singlet lines of He I, suggesting variations in the relative contributions of the recombination and fluorescence mechanisms.

2. In his study of AX Persei, Gauzit (1955) concluded that lower pressure favors the fluorescence mechanism but that, at the same time, the ionization appears to be weaker.

3. In AG Pegasi (Merrill 1958), [O III] λ 4363 A behaves differently from [O III] λ 4957 and λ 5007 A, as far as both the profiles and the velocities are concerned. While the λ 4363 A line yields a velocity amplitude of about 65 km/sec in a period of 800 days, the other two [O III] lines are nearly stationary. Moreover, the latter lines are wider than the former by about the velocity range.

Since λ 5007 A has a lower transition probability than λ 4363 A, thus requiring a lower density for its efficient production, the phenomenon seems to suggest that different effective layers are responsible for the emission of different lines. The models thought of in this connection are the following (Merrill 1958):

a) The "emitting oxygen atoms are moving outward from a small sphere near the center of the system," λ 4363 A would come "predominantly from the inner zone, while λ 5007 A comes from a toroidal or spherical shell so extended

and so transparent that motions in all directions radial from the center can be observed."

b) A large sphere of gas alternatively expands and contracts about an opaque central star; again λ 4363 A would be produced close to this star, while λ 5007 A would originate much farther out. As Merrill has pointed out, a simple volume pulsation model is unsatisfactory.

c) "There might be running waves in the extended atmosphere with difference in phase between different zones and with a considerable range in radial velocity."

d) The bright lines might originate "in fixed or nearly fixed zones through which the observed atoms move alternatively outward and inward."

TABLE 2

RADIAL-VELOCITY DATA FROM SYMBIOTIC STARS

Star	Period* (Days)		Lag Forbidden – Permitted Lines		Approximate Range in Radial Velocities (km/sec)		
					From Emission		From Absorption
	From Light-Curve	From Radial Velocities	(Days)	(*P*)	Permitted	Forbidden	
Z Andromedae	714	752±	200	0.28	60	30	.....
T Coronae Borealis	.....	227.6	.....	.....	33.5	15	24.0
BF Cygni	754	700–800	120	0.16	30	60	.....
CI Cygni	.....	800–900	200	0.2	25	40	.....
RW Hydrae	370	376?	.....	.....	40	45	(12)
AX Monocerotis	.....	232	.....	.....	.....	.....	104
AG Pegasi	.....	800	120	0.15	40† 10‡	65§ 10‖	Small
AX Persei	600–650	880	160	0.18	23	40	.....

* All these stars are semiregular variables.
† H. ‡ Fe II. § λ 4363. ‖ λ 5007.

e) A continuous gaseous stream discharges "in ever changing direction into a nearly circular outer zone," much like the streams in the eclipsing system of β Lyrae.

In his recent review of the problem of "Symbiosis in Astronomy," Merrill (1958) has collected the available information from the radial velocities of the symbiotic stars. Table 2 is copied from Merrill's paper, except for the data on T Coronae Borealis, which have been taken from the work of Kraft (1958).

Table 2 could be supplemented by pointing out, as Merrill has done, that the velocities from the ionized metals seem to exhibit much smaller fluctuations than those from H, He, N, O, and Ne and that the velocities from the He I singlet and triplet lines may differ appreciably.

The stars known or suspected to have combination spectra have been recently

listed by Bidelman (1954) and by Mrs. Payne-Gaposchkin (1957). The latter has included in her list a few related binaries (among them Bidelman's binaries of the VV Cephei type), from which we would now omit ϵ Aurigae (Hack 1957; Sahade 1958*d*). HD 4174 (Wilson 1950) is not included in either list but seems to belong to this group. We should also add MWC 603 (Tifft and Greenstein 1958), a high-velocity symbiotic star, and perhaps FR Scuti (Bloch and Mao-Lin 1958).

At minimum light, all the stars in Mrs. Payne Gaposchkin's list show features which correspond to those of a giant or supergiant M-type star. Four stars with combination spectra—namely, UV Cephei, WY Geminorum, AG Pegasi, and HD 4174—have been found to have magnetic fields (Babcock 1958).

3.2. Interpretations

Several hypotheses have been advanced to explain the occurrence in combination spectra of features which require widely different excitation conditions. These hypotheses can be separated into two groups. In one we place those which assume that we are dealing with a single star; in the other group we place those which assume that we are dealing with binary systems. A few years ago Johnson (1954, 1956) critically examined these hypotheses. The first type of explanation has been advanced by H. H. Plaskett, Menzel, Sobolev, Aller, Swings, Gauzit, and others.

Plaskett was inclined to believe that the combination spectrum of Z Andromedae was produced by a star with a surface temperature of about 5200°, physically associated with a nebula, a situation which would not occur on the model suggested by Zanstra's (1927) excitation mechanism for gaseous nebulae.

Aller (1954*a*) has mentioned the possibility that the high-excitation emission lines displayed by the combination spectra could be excited by the dissipation of shock waves, much like the solar coronal lines in Schwarzschild's (1948) theory. The idea of a late-type star surrounded by an envelope resembling the solar corona and with Schwarzschild's mechanism at work is shared by Gauzit (1955, 1958), who further suggested that the envelope in a symbiotic star must be a hundred or even a thousand times denser and much more luminous than the solar corona. Moreover, its physical conditions must often vary under the influence of strong prominences.

Other astronomers have thought that the central star is actually very hot. Sobolev (1960), for instance, postulated a hot nucleus with a very large envelope. According to him, when the brightness of the continuous spectrum of the envelope is comparable to the brightness of the continuous spectrum from the star, we must observe a combination of spectral features characteristic of both a hot and a cold source. Menzel (1946) had in mind a more complex picture of a hot star covered only partially, either toward the poles or at the equator, by a cool atmosphere responsible for the M-type spectrum and with

an outer envelope excited by the radiation from the stellar region not covered by the first envelope.

Along the same line of thought, Aller (1957) and Deutsch (1956) suggest the possibility that the symbiotic stars represent the turning point in the evolution of the red giants. At this point the nucleus would begin to contract and become hotter, while the cool atmosphere would gradually dissipate into space. According to this hypothesis, the symbiotic spectra would appear in the transitional stage, when the cool envelope was not yet totally lost. The TiO bands would then be produced in the cool envelope, while the emission features would originate below it.

In a series of papers, Bruce (1955*a*, *b*, 1956, 1957*a*, *b*, 1958) has advanced the hypothesis that electrical discharges in the atmospheres of late-type stars may explain the long-period variables and account for the spectra displayed by the symbiotic stars. In this theory the main difference between a bona fide long-period variable and a symbiotic star would be the extent of their atmospheres. The mechanism proposed seems to require, however, that the star be successively of types M, S, N, and R, as it increases in brightness.

Merrill (1944, 1958) has pointed out that the values of the periods derived for the various symbiotic stars "might possibly correspond to volume pulsations in large spheres of extremely low density" but that "the large ranges of velocities in some objects, however, would seem unfavorable to this hypothesis." As an alternative working hypothesis, Merrill (1958) thinks that "we could consider a mechanism involving rotation of an unsymmetrical body or more probably orbital revolution of two bodies. Unfortunately the observational data are too meager to make the kinematic system obvious."

Hogg (1934) was the first to try to explain the behavior of the symbiotic stars by suggesting that they were binary systems consisting of a "normal, possibly somewhat variable, M giant and a variable, very high-temperature dwarf, of the usual magnitude of about +2, which excites a nebular envelope." Hogg further suggested that the envelope

> is not sufficiently dense or extensive to absorb more than a small part of the ultraviolet radiation of the star and, hence, is fainter than normal planetaries, and does not conform to Zanstra's theory. The nebular shell may arise by ejection of matter in the nova-like outbursts of the star. The addition of two such stellar spectra accounts for the major observed features, such as the presence of titanium oxide in a star of black-body temperature as high as 5200° K, the absence or weakness of the strong absorption lines characteristic of the violet region of an M type spectrum and the general intensity changes of the lines and bands as the star fades. . . . A similar explanation would account for the fact that T Coronae Borealis is the only old nova known to have an M-type spectrum.

The binary hypothesis was later considered by Berman (1932), Merrill (1935, 1940), Payne-Gaposchkin and Gaposchkin (1938), Swings and Struve (1940),

Kuiper (1941), Mrs. Payne-Gaposchkin (1946, 1957), and Aller (1954*a*, *b*). Kuiper thought that ejection mechanism of type A, as described in his interpretation of β Lyrae, was at work in these systems. Figure 8 schematizes the model proposed by Aller (1954*b*) for BF Cygni. The binary hypothesis finds support in the following facts:

1. It provides the simplest explanation (Merrill 1940) for the observed behavior.

2. The light-curves of R Aquarii (Payne-Gaposchkin and Boyd 1946) and of Z Andromedae and AX Persei (Payne-Gaposchkin 1946), analyzed under the

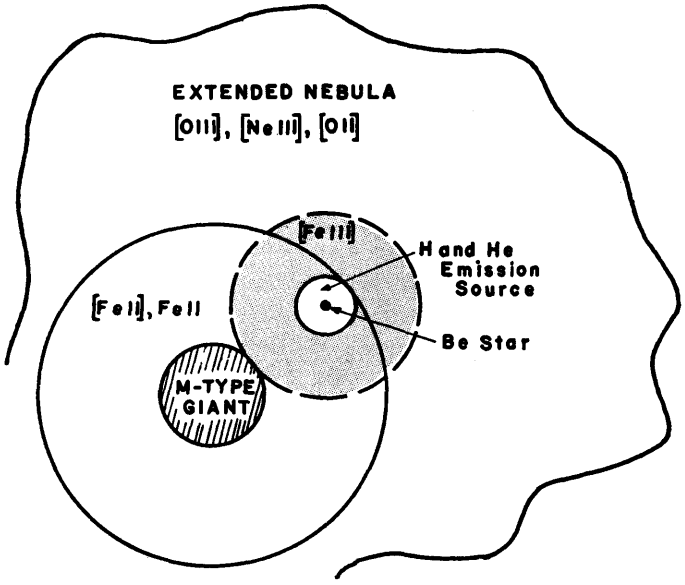


FIG. 8.—Aller's (1954*b*) schematic model for the symbiotic star BF Cygni

assumption that these objects are systems formed by a red and a blue component, show that the behavior of these "components" is strongly correlated with the spectral changes.

3. The current ideas on stellar evolution and the recognition that we can have systems in which the two components have different evolutionary ages suggest that it is possible to have in association a giant late-type star and a hot companion. And this combination seems to "produce a binary system of highly peculiar—we might almost say, of explosive—characteristics" (Struve 1951).

4. The association of a cool late-type star with a hot underluminous companion is displayed by a number of systems, namely, the visual binaries α Scorpii and o Ceti, the long-period eclipsing variable VV Cephei, and the objects, considered by Bidelman as binaries of the VV Cephei type and by Mrs. Payne-Gaposchkin as symbiotic stars, WY Geminorum, W Cephei, Boss 1985, etc.

5. The results of a recent investigation by Kraft (1958), who has shown that the Nova T Coronae Borealis, which displays a spectral behavior similar to that of the symbiotic stars, is a double-lined spectroscopic binary formed by a giant M3 star and an underluminous, blue emission-line companion.

3.3. Discussion

Kraft (1958) has shown that very probably the red component of T Coronae Borealis fills its lobe of the inner contact surface. Kuiper's ejection mechanism of type A, then, results in matter escaping from the M component, which forms an emitting envelope around the blue companion; part of this matter is probably accreted by the latter star. This picture is similar to the one advanced for AE Aquarii (Crawford and Kraft 1956) and possibly is also valid for SS Cygni (Kraft 1958). The apparent similarity between the symbiotic nova and the two U Geminorum stars is further strengthened by the fact that the blue components of the three systems are located below the main sequence in the same general region of the HR diagram (Kraft 1958). Since the U Geminorum stars seem to have composite spectra (Elvey and Babcock 1943; Joy 1954*a*; Kraft 1957), it would follow that the symbiotic and the U Geminorum stars are probably binaries with blue, underluminous secondaries of similar physical characteristics. These systems would belong to our group *e* of close binary systems, as defined at the beginning of this chapter.

Are there further similarities, and in which way are these two groups of variable stars different? The light-characteristics are very similar, in the sense that both groups undergo outbursts which result in sudden increases in light and in slower declines. But in the U Geminorum stars the outbursts are more frequent, the average cycle being of the order of 2 months, as against 2 years in the symbiotic stars. As for the spectral characteristics and behavior, the two groups show differences. While the symbiotic stars are associated with giant late-type primaries, the U Geminorum primaries are late-type dwarfs or subdwarfs. The U Geminorum stars do not display forbidden lines, and their spectra at minimum light show, in general, a continuous spectrum with few or no absorption lines and with emissions of H, He I, Ca II; at maximum light there are no emission lines but only broad and diffuse H absorptions.

Bidelman (1954) and Mrs. Payne-Gaposchkin (1957) have given lists and references of U Geminorum stars. Among them the so-called Z Camelopardalis stars have been included; these have even more frequent outbursts (mean cycle of the order of 2–3 weeks) but slightly smaller amplitudes (about 3.5 mag. as against 4 mag. in the U Geminorum stars). However, these two groups show a continuous distribution, and no dividing line seems to exist between them.

In the case of AE Aquarii, Crawford and Kraft (1956) suggested that the luminosity of the blue component "is mostly the result of the infall of material onto the surface," and they concluded that the sudden increases in light or outbursts exhibited by the system were probably associated with the blue stars

and somehow connected with the transfer of mass from the primary. Crawford and Kraft further suggested that the operating process might be similar to the one advanced by Greenstein (1950) to explain the flares observed in the T Tauri star, BD−6°1253, namely, that the flares result from strong electrical discharges which come about because of the increase in the star's magnetic field caused by the turbulent motion of the accreted ionized material.

If we assume that the novae are binary systems, as Walker's (1954, 1956) discovery of the binary nature of Nova DQ Herculis seems to suggest (Struve 1955), we would have three types of binary systems with one component below the main sequence, i.e., novae, symbiotic stars, and U Geminorum stars, which undergo semiperiodic outbursts; these three types of systems are listed in order of decreasing range in light and increasing frequency of outbursts. Table 3 collects some relevant data for explosive variables.

TABLE 3

DATA ON EXPLOSIVE VARIABLES

Object	Mean Interval between Outbursts (Years)	Mean Range (Mag.)	Visual Absolute Magnitude of Blue Component
Classical novae	?	12.3	.....
Recurrent novae	50	8.6*	+4.5*
Symbiotic stars	3.5	.....	.....
U Geminorum stars	0.2	4.0	+6†
Z Camelopardalis stars	0.05	3.5	.....

* T Coronae Borealis.
† AE Aquarii and SS Cygni (average value).

Mrs. Payne-Gaposchkin (1957) thought that perhaps T Coronae Borealis "represents a transitional stage between the symbiotic stars and the novae proper." Indeed, if all the stars—single or not—reach the white dwarf stage as their ultimate fate and if we could find evidence that in their evolution toward degeneracy the close binary systems with components more massive than the white dwarfs must go through all the configurations listed in Table 3, then we would have to conclude that, as the underluminous components become older and therefore less luminous, the outbursts become more frequent but less violent. Thus the process of getting rid of excess mass would gradually become milder. We do not have enough information to draw a definite picture of the evolution of close binary systems, and it is impossible to say at present whether systems like β Lyrae, for instance, will eventually become a nova, then a symbiotic star, and later a U Geminorum object. A rich field of investigation lies before us.

The investigations of AE Aquarii and T Coronae Borealis suggest that the outbursts of these stars are closely related to the accretion by the blue compo-

nents of matter being lost by the red primaries through the Lagrangian point L_1. This implies that the lobe of the inner contact surfaces around the primaries must be filled. In the case of the symbiotic stars the evidence leaves little doubt that the primaries are red giants, and therefore it is reasonable to expect that they fill the critical lobe. But in the case of the U Geminorum stars the primaries seem to be dwarfs or subdwarfs, and one wonders whether their sizes are large enough to fill their lobes and also whether the outbursts are actually induced by the binary nature of the object or have only an evolutionary origin. However, we must keep in mind that it is possible that the U Geminorum primaries may be old stars which are past the giant stage and are now evolving toward the left of the HR diagram. In this case they are probably surrounded by large envelopes (Deutsch 1956; Aller 1957), as seems to be the case for the secondary component of β Lyrae (Sahade, Huang, Struve, and Zebergs 1959). These large envelopes could conceivably fill the lobe around the star. We must also keep in mind that the wide pair of α Scorpii does not undergo outbursts.

§ 4. CONCLUDING REMARKS

We have tried to review the available information about the spectra of close binary systems and the spectra of the symbiotic stars and to discuss it in the light of the current ideas on stellar evolution. It would appear from this discussion that the designations "composite spectra" and "combination spectra" are to be understood as referring to different evolutionary configurations rather than to two completely different kinds of objects.

The lack of a large enough sample makes it impossible to establish a definite evolutionary sequence of close binaries, step by step, nor are we able to ascertain exactly the importance of mass transfer and/or mass loss in each stage. However, it seems clear that the spectra of close binary systems show peculiarities especially when one or both of the components are off the main sequence, the most bizarre features appearing when one star is still gravitationally contracting or is below the main sequence. Further investigation in the field will certainly lead to a better understanding of the evolutionary trends in stars.

REFERENCES

ABHYANKAR, K. D. 1959 *A.J.*, **64**, 163.

ABT, H. A. 1954 *Pub. A.S.P.*, **66**, 171.

ALLER, L. H. 1954*a* *Nuclear Transformations, Stellar Interiors, and Nebulae* (New York: Ronald Press Co.), p. 180.

1954*b* *Pub. Dom. Ap. Obs. Victoria*, **9**, 321.

1957 *Les Molécules dans les astres* (Cointe-Sclessin: Institut d'Astrophysique), p. 305.

BABCOCK, H. W. 1958 *Ap. J. Suppl.*, **3**, 141.

BARR, J. M. 1908 *J.R.A.S. Canada*, **2**, 70.

BAUER, C. A. 1945 *Ap. J.*, **101**, 208.

BELOPOLSKY, A. 1893 *Mem. Soc. Spett. Ital.*, **22**, 101.

BERMAN, L.	1932	*Pub. A.S.P.*, **44**, 318.
BIDELMAN, W. P.	1954	*Ap. J. Suppl.*, **1**, 175.
BLOCH, M., and MAO-LIN, T.	1958	*Étoiles a raies d'émission* (Cointe-Sclessin: Institut d'Astrophysique), p. 458.
BRUCE, C. E. R.	1955*a*	*Observatory*, **75**, 82.
	1955*b*	*Phil. Mag.*, **46**, 1123.
	1956	*C.R.*, **242**, 2101.
	1957*a*	*Observatory*, **77**, 107.
	1957*b*	*Ibid.*, p. 153.
	1958	*Étoiles a raies d'émission* (Cointe-Sclessin: Institut d'Astrophysique), p. 364.
CANNON, A. J.	1901	*Harvard Ann.*, **28**, 179.
CRAWFORD, J. A.	1955	*Ap. J.*, **121**, 71.
	1958	Private communication.
CRAWFORD, J. A., and KRAFT, R. P.	1956	*Ap. J.*, **123**, 44.
CURTISS, H. R.	1912	*Pub. Allegheny Obs.*, **2**, 73.
DEUTSCH, A. J.	1956	*Pub. A.S.P.*, **68**, 308.
ELVEY, C. T., and BABCOCK, H. W.	1943	*Ap. J.*, **97**, 412.
GAUZIT, J.	1955	*Ann. d'Ap.*, **18**, 354.
	1958	*Étoiles a raies d'émission* (Cointe-Sclessin: Institut d'Astrophysique), p. 474.
GOULD, N. L.	1957	*Pub. A.S.P.*, **69**, 541.
	1959	*A.J.*, **64**, 136.
GRATTON, L.	1950	*Ap. J.*, **111**, 31.
GREENSTEIN, J. L.	1940	*Ap. J.*, **91**, 438.
	1950	*Pub. A.S.P.*, **62**, 156.
HACK, M.	1957	*Pub. A.S.P.*, **69**, 389.
HARPER, W. E.	1937	*Pub. Dom. Ap. Obs. Victoria*, **6**, 311.
HERBIG, G. H.	1957	*Non-stable Stars*, ed. G. H. HERBIG (Cambridge: Cambridge University Press), p. 3.
HILTNER, W. A.	1946*a*	*Ap. J.*, **104**, 396.
	1946*b*	*Pub. A.S.P.*, **58**, 166.
	1947	*Ap. J.*, **106**, 481.
HILTNER, W. A., and HARDIE, R. H.	1949	*Ap. J.*, **110**, 438.
HOGG, F. S.	1932	*Pub. A.S.P.*, **44**, 328.
	1934	*Pub. A.A.S.*, **8**, 14.
HUANG, S.-S.	1956	*A.J.*, **61**, 49.
	1957	*J.R.A.S. Canada*, **51**, 91.
	1958	*Pub. A.S.P.*, **70**, 473.
	1959	*Ann. d'ap.*, **22**, 527.
HUANG, S.-S., and STRUVE, O.	1956	*A.J.*, **61**, 300.
JASCHEK, C. and M.	1957	*Pub. A.S.P.*, **69**, 546.

JOHNSON, M.	1954	*Trans. I.A.U.*, **8**, 839.
	1956	*Vistas in Astronomy*, ed. A. BEER (London: Pergamon Press), **2**, 1407.
JOY, A. H.	1941	*Ap. J.*, **94**, 407.
	1942	*Pub. A.S.P.*, **54**, 35.
	1947	*Ibid.*, **59**, 171.
	1954*a*	*Ibid.*, **66**, 5.
	1954*b*	*Ap. J.*, **120**, 377.
	1956	*Ibid.*, **124**, 317.
JOY, A. H., and SANFORD, R. F.	1926	*Ap. J.*, **64**, 250.
JOY, A. H., and WILSON, R. E.	1949	*Ap. J.*, **109**, 231.
KOPAL, Z.	1955	*Les Particules solides dans les astres* (Cointe-Sclessin: Institut d'Astrophysique), p. 684.
	1956*a*	*Ann. d'ap.*, **19**, 298.
	1956*b*	*Jodrell Bank Ann.*, **1**, 141.
	1957	*Non-stable Stars*, ed. G. H. HERBIG (Cambridge: Cambridge University Press), p. 123.
	1958	*Mem. Soc. Astr. Ital.*, Suppl. No. 2, p. 3.
KRAFT, R. P.	1957	Unpublished.
	1958	*Ap. J.*, **127**, 625.
KRANJC, A.	1951	*Mem. Soc. Astr. Ital.*, **22**, 131.
KRON, G. E., and GORDON, K. C.	1953	*Ap. J.*, **118**, 55.
KUIPER, G. P.	1935	*Pub. A.S.P.*, **47**, 15.
	1941	*Ap. J.*, **93**, 133.
LYNDS, C. R.	1955	Thesis, University of California, Berkeley.
	1957	*Ap. J.*, **126**, 69.
MCKELLAR, A.	1950	*Pub. Dom. Ap. Obs. Victoria*, **8**, 235.
MCNAMARA, D. H.	1951*a*	*Pub. A.S.P.*, **63**, 38.
	1951*b*	*Ap. J.*, **114**, 513.
	1957	Private communication.
MAURY, A. C.	1920	*Harvard Ann.*, **84**, 178.
	1922	*Harvard Circ.*, No. 233.
MENZEL, D. H.	1946	*Physica*, **12**, 768.
MERRILL, P. W.	1935	*Ap. J.*, **81**, 312.
	1940	*Spectra of Long-Period Variable Stars* (Chicago: University of Chicago Press), p. 105.
	1944	*Ap. J.*, **99**, 15.
	1952	*Ibid.*, **115**, 145.
	1958	*Étoiles a raies d'émission* (Cointe-Sclessin: Institut d'Astrophysique), p. 436.
MORGAN, W. W., CODE, A. D., and WHITFORD, A. E.	1955	*Ap. J. Suppl.*, **2**, 41.

MORGAN, W. W., KEENAN, P. C., and KELLMAN, E.	1943	*An Atlas of Stellar Spectra* (Chicago: University of Chicago Press).
MOULTON, F. R.	1914	*Celestial Mechanics* (2d ed.; New York: Macmillan Co.), p. 281.
NEUBAUER, F. J., and STRUVE, O.	1945	*Ap. J.*, **101**, 240.
OKE, J. B., and SCHWARZSCHILD, M.	1952	*Ap. J.*, **116**, 317.
PAYNE-GAPOSCHKIN, C.	1946	*Ap. J.*, **104**, 362.
	1957	*The Galactic Novae* (Amsterdam: North-Holland Publishing Co.).
	1958	*Étoiles a raies d'émission* (Cointe-Sclessin: Institut d'Astrophysique), p. 483.
PAYNE-GAPOSCHKIN, C., and BOYD, C.	1946	*Ap. J.*, **104**, 357.
PAYNE-GAPOSCHKIN, C., and GAPOSCHKIN, S.	1938	*Variable Stars* (Cambridge: Harvard College Observatory), p. 315.
PICKERING, E. C.	1891	*A.N.*, **127**, 155.
	1896	*Harvard Circ.*, No. 11.
PLASKETT, H. H.	1928	*Pub. Dom. Ap. Obs. Victoria*, **4**, 119.
POPPER, D. M.	1943	*Ap. J.*, **97**, 394.
	1957	*J.R.A.S. Canada*, **51**, 51.
REDDISH, V. C.	1957	*Observatory*, **77**, 202.
REDMAN, R. O.	1930	*Pub. Dom. Ap. Obs. Victoria*, **4**, 341.
ROMAN, N. G.	1956	*Ap. J.*, **123**, 246.
SAHADE, J.	1945	*Ap. J.*, **102**, 470.
	1949	*Ibid.*, **109**, 439.
	1952*a*	*Ibid.*, **116**, 27.
	1952*b*	*Ibid.*, p. 35.
	1955	*Pub. A.S.P.*, **67**, 348.
	1958*a*	*Observatory*, **78**, 79.
	1958*b*	*Étoiles a raies d'émission* (Cointe-Sclessin: Institut d'Astrophysique), p. 404.
	1958*c*	*Ibid.*, p. 46.
	1958*d*	*Pub. A.S.P.*, **70**, 316.
	1958*e*	*A.J.*, **63**, 52.
	1959	*Pub. A.S.P.*, **71**, 151.
	1960	*Modèles d'étoiles et évolution stellaire* (Cointe-Sclessin: Institut d'Astrophysique), p. 76.
SAHADE, J., and CESCO, C. U.	1944	*Ap. J.*, **100**, 374.
	1945*a*	*Ibid.*, **101**, 235.
	1945*b*	*Ibid.*, **102**, 128.
	1946	*Ibid.*, **103**, 71.

SAHADE, J., HUANG, S.-S., STRUVE, O., and ZEBERGS, V.	1959	*Trans. Am. Phil. Soc.*, **49**, 1.
SAHADE, J., and STRUVE, O.	1957	*Ap. J.*, **126**, 87; Erratum, 1958, *Ap. J.*, **127**, 512.
SANFORD, R. F.	1950	*Pub. A.S.P.*, **62**, 21.
	1951	*Ap. J.*, **113**, 299.
SCHWARZSCHILD, M.	1948	*Ap. J.*, **107**, 1.
SHAPLEY, H.	1948	*Centennial Symposia* ("Harvard Obs. Monographs," No. 7), p. 249.
SMITH, B.	1948	*Ap. J.*, **108**, 504.
SOBOLEV, V. V.	1960	*Moving Envelopes of Stars*, trans. of S. GAPOSCHKIN (Cambridge: Harvard College Observatory).
STRUVE, O.	1941	*Pub. A.A.S.*, **10**, 206.
	1942	*Ap. J.*, **95**, 134.
	1944*a*	*Ibid.*, **99**, 89.
	1944*b*	*Ibid.*, p. 295.
	1945	*Ibid.*, **102**, 74.
	1946*a*	*Ibid.*, **103**, 76.
	1946*b*	*Ann. d'ap.*, **9**, 1.
	1946*c*	*Ap. J.*, **104**, 253.
	1947	*Ibid.*, **106**, 255.
	1948	*Ibid.*, **107**, 327.
	1949	*M.N.*, **109**, 487.
	1950*a*	*Stellar Evolution* (Princeton: Princeton University Press).
	1950*b*	*Pub. A.S.P.*, **62**, 47.
	1951	*Astrophysics*, ed. J. A. HYNEK (New York: McGraw-Hill Book Co.), p. 85.
	1952	*Sky and Telescope*, **11**, 243.
	1955	*Ibid.*, **14**, 275.
	1956	*Pub. A.S.P.*, **68**, 27.
	1957*a*	*Non-stable Stars*, ed. G. H. HERBIG (Cambridge: Cambridge University Press), p. 93.
	1957*b*	*Sky and Telescope*, **17**, 70.
	1958*a*	*Pub. A.S.P.*, **70**, 5.
	1958*b*	*Étoiles a raies d'émission* (Cointe-Sclessin: Institut d'Astrophysique), p. 377.
STRUVE, O., and ELVEY, C. T.	1942	*Pub. A.S.P.*, **54**, 151.
STRUVE, O., HERBIG, G., and HORAK, H.	1950	*Ap. J.*, **112**, 216.
STRUVE, O., and HORAK, G. H.	1949	*Ap. J.*, **110**, 447.
	1950	*Ibid.*, **112**, 178.

STRUVE, O., and SAHADE, J.	1955	*Science*, **122**, 881.
	1957	*Pub. A.S.P.*, **69**, 41.
	1958	*Ibid.*, **70**, 111.
STRUVE, O., SAHADE, J., and HUANG, S.-S.	1958	*Ap. J.*, **127**, 148.
STRUVE, O., SAHADE, J., HUANG, S.-S., and ZEBERGS, V.	1958	*Ap. J.*, **128**, 310.
STRUVE, O., SAHADE, J., ZEBERGS, V., and LYNDS, B. T.	1958	*Pub. A.S.P.*, **70**, 267.
SWINGS, P., and STRUVE, O.	1940	*Ap. J.*, **91**, 601.
	1941*a*	*Ibid.*, **93**, 356.
	1941*b*	*Ibid.*, **94**, 291.
	1942*a*	*Ibid.*, **95**, 152.
	1942*b*	*Ibid.*, **96**, 254.
	1943	*Ibid.*, **97**, 194.
TIFFT, W. G., and GREENSTEIN, J. L.	1958	*Ap. J.*, **127**, 160; *Étoiles a raies d'émission* (Cointe-Sclessin: Institut d'Astrophysique), p. 449.
WALKER, M. F.	1954	*Pub. A.S.P.*, **66**, 230.
	1956	*Ap. J.*, **123**, 68.
WALKER, M. F., and HERBIG, G. H.	1954	*Ap. J.*, **120**, 278.
WILSON, R. E.	1950	*Pub. A.S.P.*, **62**, 14.
WYSE, A. B.	1934	*Lick Obs. Bull.*, **17**, 37 (No. 464).
ZANSTRA, H.	1927	*Ap. J.*, **65**, 50.

CHAPTER 13

Spectra of Long-Period Variables

PAUL W. MERRILL
Mount Wilson and Palomar Observatories
Carnegie Institution of Washington, California Institute of Technology

§ 1. INTRODUCTION

SPECTRA of long-period variable stars are among the most complex of all stellar spectra. They exhibit a large number of atomic and molecular lines in emission as well as in absorption. Virtually all these lines vary with time. Most of the changes are related to phase in the light-cycle; others have some connection with the maximum magnitude attained in a particular cycle. Occasionally an individual cycle exhibits quite enigmatic spectral peculiarities.

Many, but not all, variations in *absorption* lines and bands can be understood in terms of the changing temperature of the reversing layer, which in turn appears generally to be well correlated with the effective temperature of the photosphere. Some especially interesting non-temperature variations, however, deserve further detailed investigation.

Conspicuous and rapidly changing *emission* lines, some of them requiring high excitation, present intriguing problems. The cyclical behavior of numerous bright lines of various elements has been studied in considerable detail (except near minimum light), and many interesting facts are on record concerning intensities and displacements, mutilation by absorption in the reversing layer, interactions among bright lines (fluorescence), etc.; but the exact nature of the basic exciting mechanism is unknown. It appears probable, however, that many of the bright lines are caused by a disturbance such as a shock or hydromagnetic wave which originates in every cycle somewhere below the photosphere, then moves outward into the observable zones of the star's atmosphere. Displays of bright lines near minimum light are especially curious. This phase of the light-cycle has been neglected in most series of spectroscopic observations because of the faintness of the variables. Nevertheless, fairly rapid progress is now being made in the observation and interpretation of spectra near minimum. One or two recent observations are discussed in this chapter.

Early work on the spectra of long-period variables was summarized, with many references, by Merrill (1940*a*). Since then, spectrograms of higher dispersion than those previously obtained have yielded more accurate and more extensive data on the identifications, displacements, and general behavior of numerous lines both bright and dark. The complex details have been described in published articles and need not be repeated here. A convenient list of references to individual stars was recently given by Bidelman (1954) in his *Catalogue and Bibliography of Emission-Line Stars of Types Later than B*. The present chapter is limited to comments on selected topics.

§ 2. TEMPERATURE

Along the sequence of red giant stars, the proportion of variables increases markedly with decreasing surface temperature until, at the most advanced spectral types observed in the M, S, and N branches, virtually all stars are variable (either Mira type or semiregular). The surface temperatures of advanced Me variables, probably the coolest stars known, are about 2300° K at maximum light. The only known examples of lower stellar temperatures are these variables themselves at their fainter phases. At minimum light the average temperature indicated by the thermocouple measures of Pettit and Nicholson (1933) is about 1800° K (see Table 1).

TABLE 1

SURFACE TEMPERATURES OF ADVANCED Me VARIABLES

(Pettit and Nicholson 1933)

Star	Type	Max. (° K)	Min. (° K)
R Cnc.....	M7e	2310	1700
R Leo.....	M8e	2170	1820
R LMi.....	M8e	2270	1780
R Hya.....	M7e	2330	1900
R Aql.....	M7e	2320	1920
χ Cyg.....	Mpe	2240	1640
Mean.....	.....	2270	1790

At these temperatures the proportion of radiative energy in the infrared is extraordinarily great. The percentages of energy in the ultraviolet, visible, and infrared at various temperatures are shown in Table 2. The march of the energy toward shorter wave lengths with increasing temperature is striking. If the visible light of a long-period variable is equal to that of a B-type star, the ratio of infrared energy can be 500 to 1 in favor of the red variable. In the future the infrared radiations of long-period variables should be increasingly studied both by photography and with various types of photoemissive or photoconductive cells.

The sequence of dwarf red stars, plotted as in the Hertzsprung-Russell diagram, drops rapidly in absolute magnitude with decreasing surface temperature. The coolest known dwarfs are so faint that they must be near the sun before they can be detected in present surveys. Cooler dwarfs presumably would be still fainter but may yet be found as surveys are extended to fainter apparent magnitudes. For giant stars the circumstances are quite different. Here decreasing surface temperature is largely compensated by increasing size, and in the HR diagram, the observed sequence of giant red stars continues toward lower temperatures with little drop in magnitude, to an abrupt end (or sudden drop in frequency) which is brighter by some 12 mag. than the end of the observed dwarf branch. This apparently abrupt termination of the giant branch is probably real and is unlikely to be removed by future observations. It may correspond to an important discontinuity of some kind, possibly the point at which heavy

TABLE 2

PERCENTAGES OF BLACK-BODY RADIATION IN THREE SPECTRAL REGIONS

Temperature (°K)	Ultraviolet $\lambda < 4000$ A	Visible 4000-7600 A	Infrared >7600 A	λ of Maximum (A)
1800.....	0.0	0.7	99.3	16,000
2300.....	0.0	3.4	96.6	12,500
5000.....	6.7	37.8	55.5	5800
10,000.....	48.3	35.7	16.0	2900
20,000.....	85.7	11.3	3.0	1400

veiling occurs in stellar atmospheres. The approach to this discontinuity is marked by an instability which may lead to periodic variation of the Mira type. This does not prove that cooler giants than those now known do not exist. But if they do exist, they are probably fainter in visual light at least by several magnitudes than stars now listed; they might possibly resemble in some respects long-period variables at minimum light. The discovery of stars with surface temperatures decidedly lower than that of a typical Mira-type variable would be of great interest (Merrill 1955).

§ 3. DENSITY

The reversing layers of red giant stars are cool; they are also very tenuous. The stars as a whole are enormous. Toward the low-temperature end of the giant sequence the absolute magnitude drops little, if any, indicating that rapidly decreasing photospheric brightness is compensated for by increasing size. The large diameters of a few extreme stars have been checked by direct measurement with the stellar interferometer. It is improbable that the redder stars, such as long-period variables, are especially massive; hence their mean densities are very low, probably less than 10^{-7} that of the sun. The surface

gravity, of course, is also low, perhaps 10^{-4} that of the sun. The atmospheres, therefore, are extensive and extremely tenuous.

The low density and enormous volume as well as the low surface temperature should be borne in mind in studying the spectra and physical behavior of long-period variables. A volume pulsation could have a period of the order of 1 year; an explosive disturbance originating deep in the body of the star might require months to work its way out to the upper limits of the atmosphere.

Red dwarf stars have cool reversing layers, but their densities appear to be too high to allow variability like that of o Ceti or χ Cygni.

§ 4. VEILING

Why a low temperature at the surface of a star should of itself produce cyclical variability in brightness is not obvious unless at times conditions should allow condensation of solid or liquid particles in the star's outer atmosphere. Among the coolest red variables it is quite possible that veiling by condensed particles does occur during a portion of each cycle and that it is partly responsible for the enormous changes in apparent brightness exhibited by such variables as χ Cygni, R Andromedae, and R Cygni. Variable veiling offers a plausible explanation of large observed changes in brightness (e.g., by a factor of 100), accompanied by only relatively small changes in the details of the continuous and dark-line spectrum.

Perhaps the abrupt drop in absolute magnitude at the low-temperature end of the giant sequence, mentioned in a previous paragraph, marks a point in a physical sequence where much of a would-be star's visible light is shut off from the outer universe by heavy veiling and in part converted to infrared. In any event, the possible veiling of long-period variables and of hypothetical stars with still lower temperatures should have a careful theoretical examination, and there should be an attempt to study their radiometric magnitudes, perhaps in connection with general discussions of the role of interstellar dust in stellar evolution. The problem is difficult because it involves the extremely low vapor pressures of liquids and solids at temperatures considerably below the ordinary boiling and sublimation points. Extrapolation from laboratory data (Kelley 1935) by means of the equation

$$\log p = -\frac{\text{Const.}}{T} + \text{Const.}, \tag{1}$$

where p = pressure, and T = temperature, indicates that at 1600° K the vapor pressure of carbon, for example, is only about 10^{-20} atm.; at higher pressure, carbon and certain other substances might condense.

The problem is difficult for another reason, namely, that the rate of condensation depends not only on temperature and pressure but on the presence of suitable (electrified?) particles to serve as initial nuclei. Similar considerations are involved in the formation of clouds in the earth's atmosphere. Here the pres-

sure is higher than in the atmospheres of red variables, the temperature lower, and the chemical composition entirely different. Nevertheless, physical studies in meteorology might suggest useful procedures in analyzing problems of possible stellar veiling.

A comprehensive study of veiling in stellar atmospheres should give attention to the possibility of heavy absorption throughout long stretches of the spectrum by bands of molecules not yet identified and to any possible long-wavelength re-radiation. Moreover, effects of radiant energy from the photosphere must be taken into account. If veiling occurs, much of this energy would be blocked and thus become available to vaporize the particles or to dissociate the molecules and thus to decrease the opacity. Perhaps this process would be found to be cyclic.

The phenomenon of veiling was considered many years ago by Loreta (1934) and O'Keefe (1939) in connection with the peculiar variable star R Coronae Borealis. Their ideas should have received more attention.

This section on veiling should be concluded with a caution. Veiling is certainly not the sole cause of variability of the Mira type, and it is improbable that it is the primary cause. Observations with the thermocouple indicate considerable changes in photospheric temperature, as do also the changing intensities of spectroscopic absorption lines that are sensitive to temperature. Moreover, the curious behavior of the bright lines points definitely to a very special physical disturbance, such as a shock or hydromagnetic wave (or set of waves) which travels outward, once each cycle, from some level well below the reversing layers. This disturbance might possibly be set off at regular intervals by a volume pulsation of the whole star. Veiling around a star could of itself conceivably come and go in recurring cycles, but in long-period variables it is probably an auxiliary phenomenon operating to increase the light-range in a period determined by other causes.

§ 5. ABSORPTION LINES

5.1. General

The complicated spectroscopic behavior of long-period variables has already received much attention. Large numbers of lines both bright and dark have been accurately tabulated; most of them have been identified, and, for certain lines, changes with phase in the light-cycle have been described in considerable detail. More complete observations are desirable, however, especially at the fainter phases. A close study of the cyclical behavior of the spectral lines, not only of the bizarre emission lines but also of certain peculiar changes among the absorption lines, will doubtless eventually provide valuable clues to the extraordinary physical phenomena which take place in these stars.

Space is lacking for a comprehensive survey of our present knowledge; the interested student should study the original research reports. The complex

question of line displacements has been discussed by Joy (1954) in his study of *o* Ceti. A few selected topics are briefly discussed below.

Typical long-period variables are stars of spectral types M, S, and N, predominantly of the later subdivisions. Near maximum light, the only phase at which most variables have been observed spectroscopically, no gross abnormalities are usually present in the absorption spectra except a few due to superposed bright lines. Closer investigation is desirable, however, because small effects of considerable importance might be revealed. On the rising branch of the light-curve, absorption lines may be studied with little interference by emission lines, but after maximum light the possible effects of emission in weakening or displacing absorption lines must be kept in mind.

5.2. Comparison of M-, S-, and N-Type Variables

The physical and chemical interrelationships of the three types of red stars should be studied more thoroughly; this would involve intercomparing M-, S-, and N-type spectra in greater detail than has yet been done.

TABLE 3

Stars in Order of Increasing Intensity of S-Type Lines

Star	Type	Star	Type
R Leo	M8e	χ Cyg	M6pe
o Cet typical	M6e	19 Psc	N
o Cet (at extremely bright maxima)	M4e	R And, R Cyg	Se

The present consensus is that atmospheres of the three types of stars differ in actual chemical composition. This judgment is based on the fact that two chemical parameters appear necessary for a satisfactory general spectral classification of red stars. One of these parameters is the ratio of oxygen to carbon in the reversing layer, carbon being especially abundant in the N types. The other is the relative abundance of heavy metals of the fifth and sixth periods of the periodic table, including Sr, Y, Zr, Nb, Tc, Ba, and La (Merrill and Greenstein 1956). Lines of these elements are relatively strong in S-type spectra. The chemical composition of a long-period variable of type M is probably similar to that of standard late-type giant stars, which in turn may not differ greatly from that of the dwarf G-type star with which we are best acquainted—our own sun.

The lines characteristic of S-type spectra occur in different intensities in other types. In Table 3, several stars are listed in order of increasing intensity of these S-type lines. One interesting result of recent studies (Sanford 1950*a*; Merrill 1956*a*) is recognition of the fact that the connection between types N and S is probably somewhat closer than was formerly supposed. Stars like R Canis Minoris, which are apparently intermediate between types N and S, will repay intensive investigation.

The atmospheres of M, N, and S stars probably differ in chemical composi-

tion, but we should not assume that the whole interiors of the stars necessarily differ in the same way. This may or may not be true, depending on whether nucleogenesis occurs in the interior as a consequence of thermonuclear reactions, or at the surface in acceleration processes. In either event, it now appears possible that the relative abundance of certain chemical elements in the surface layers of a star, and thus the appearance of the star's spectrum, may be markedly affected by special circumstances that have been of small consequence in the general evolutionary history of the star and may be minor also in the present structure of the body of the star as well as in the total amount of energy developed and radiated. Certain facts tend to favor this rather recent hypothesis (Cameron 1955; Fowler, Burbidge, and Burbidge 1955), which is more flexible than the older concept of three distinct, nearly parallel evolutionary sequences.

The heavy metals constitute only an infinitesimal fraction of a star's total mass. Even if two stars differed by a factor of 100 in the number of zirconium atoms, their over-all chemical composition and physical constitution could still be virtually identical. Thus, in general structure, M- and S-type variables may be much alike, and we can understand why their light-curves and many details of their spectroscopic changes with phase can be so similar. The S types probably have somewhat lower densities. Even the N types may not differ very radically in general structure.

The argument outlined in the preceding paragraph does not preclude the possibility that, under certain circumstances, a relatively slight difference in the chemical composition of two stars might produce considerable difference in behavior, for example, veiling, molecular bands, and details of spectroscopic phenomena.

5.3. Changes with Phase

A line of attack on long-period variables which might lead to new results of considerable physical interest lies in a very detailed scrutiny of the spectral lines with dispersion, 10 A/mm or higher, of (1) changes with phase and (2) peculiarities of individual cycles. Many fairly satisfactory spectrograms of a few bright M-type variables, especially *o* Ceti, have already been accumulated; observations of S-type variables are less complete; and only a beginning has been made on the N types.

Changes in the absorption spectrum of a typical variable during its light-cycle are easily noted; for the most part, they are in line with the changing temperature of the photosphere, which is hottest at maximum light and coolest at minimum. For an advanced Me variable, this range is approximately from 2300° to 1800° K. At maxima brighter than average, the spectral type is earlier than average and the indicated temperature higher. To a first approximation, the chemical composition of the reversing layer appears to remain constant during the changes of brightness, as one might expect.

On the other hand, the well-observed spectrum of *o* Ceti, a long-period variable of type M6e, period 331 days, has revealed certain relatively minor changes

in the absorption lines that are not readily explained by differences in temperature, but seem at first glance to indicate actual variations in chemical composition. For example, near the phase of maximum light the absorption lines appear to resemble those of S-type spectra somewhat more than at the fainter phases (Buscombe and Merrill 1952). This was true to a remarkable degree at the especially bright maxima of October, 1947, and August, 1949, when certain lines of Y and Zr appeared considerably stronger than they regularly do in the spectrum of o Ceti at other times or than they do in typical M-type spectra of non-variable stars. Some of the strengthened lines arise from ground levels of neutral atoms. These lines should normally become relatively weaker rather than stronger as the star brightens and the temperature rises, unless dissociation of oxides or other molecules provides a greater supply of free atoms, a possibility which deserves careful study; increasing ionization, on the other hand, would decrease the number of neutral atoms. These and other non-temperature changes are extremely interesting; they should be studied with great care to derive the correct interpretation. They may eventually help elucidate processes of nuclear reactions occurring in or near the surfaces of stars. Occasionally a particular light-cycle exhibits quite enigmatic spectral peculiarities, such as the extraordinary display of *emission* bands of AlO at the exceptionally low maximum of February, 1924 (Joy 1926; Merrill 1940*b*).

5.4. Displaced Components

The curious fact, now well established in several M- and S-type spectra (references are given by Merrill and Greenstein 1956), that the apparent displacements of absorption lines of neutral metals increase algebraically with excitation potential is probably somehow connected with relative height in the reversing layer; nevertheless, it is in need of detailed interpretation. It may well be a minor manifestation of the bizarre doubling of absorption lines observed in the spectra of several giant and supergiant red stars.

Diagrammatic representations of measurements of double lines in the spectra of several stars are shown in Figure 1. In certain stars not recognized as having double lines, shells expanding with low velocities might be detected through the measured variation of line displacement as a function of excitation potential. In other words, the measured center of a normal line of low-excitation potential might well be displaced slightly shortward by a shell-like component too close to be seen as a separate line. This is suggested by the first sketch in Figure 1. The displaced component may be distinctly separated from the normal line, as in R Andromedae (red and infrared), VV Cephei, and ρ Cassiopeiae; or, if the normal line is wide, as in α Orionis and RW Cephei, the displaced line may lie within it. The observed relative velocity of the displaced component ranges from -10 km/sec, about the smallest for which a line would be seen as distinctly separate, to -37 km/sec for ρ Cassiopeiae. The smaller displacements

are comparable to the relative displacements of emission lines in spectra of long-period variables.

A displaced component of this kind indicates that a gaseous shell above the normal reversing layer contains atoms moving outward with a well-defined velocity. The size of the shell is usually unknown, although approximate limits might be set by studies of effects of dilution. In the double star α Herculis, observations by Deutsch (1956) show the shell to have an outer radius at least two hundred thousand times the radius of the sun. The problems presented by these shells are most intriguing, especially to those who are seeking evidence of a flow of matter from stars into interstellar space.

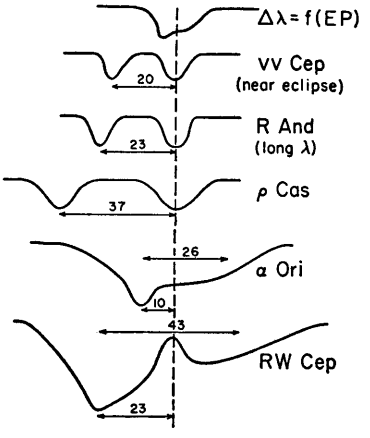


FIG. 1.—Complex absorption lines in spectra of giant and supergiant red stars. Numbers attached to the sketched line profiles indicate displacements in km/sec. References: $\lambda = f(\mathrm{EP})$ (Merrill and Greenstein 1956); VV Cep (Wright and McKellar 1956; McKellar, Wright, and Francis 1957); R And (Merrill and Greenstein 1958); ρ Cas (Bidelman and McKellar 1957); α Ori (Adams 1956); RW Cep (Merrill and Wilson 1956).

An infrared spectrogram of the long-period variable, R Andromedae 001838, type Se, taken by Greenstein with the 200-inch telescope on November 11, 1956, about a month after maximum light, showed many atomic lines to have two narrow absorption components, one in the normal position, the other 23 km/sec (0.6 A) shortward. Another plate taken on January 7, 1958, about a month after the next maximum, is quite similar. The expanding shell indicated by the displaced component (Merrill and Greenstein 1958) offers interesting possibilities for special investigations bearing not only on the flow of matter outward from stars but on the nature of the atmospheres of long-period variables. In the spectra of long-period variables, the shell lines should be observed with high dispersion to find possible changes in line intensity and displacement with phase in the light-cycle. In addition, the apparent chemical composition of the shell, determined from intensities of the absorption lines, should be carefully compared with that of the reversing layer.

5.5. High-Velocity Variables

The existence of a well-defined group of variables with periods between 150 and 300 days and with relatively early M-type spectra has long been recognized (see Fig. 4 and Table 7). Careful comparison of these objects with low-velocity variables might throw light on the far-reaching problems of stellar populations I and II. Such an investigation would require detailed comparisons, preferably of high-dispersion spectra of "normal" variables with those of high-velocity variables of nearly the same types, periods, and amplitudes. The first step would be comparison of spectra of the two groups near maximum light; Keenan has already made observations for this purpose at Mount Wilson. Caution must be used in interpreting the results because the spectra vary with phase and because not all cycles are typical. Eventually, the behavior of the two groups should be intercompared throughout the whole light-cycle. This would be a heavy observational task, but probably worthwhile to fill a serious gap in our knowledge. Moreover, it is possible that the apparently troublesome variations with phase might turn out to be sensitive to relatively slight physical or chemical differences between populations I and II and thus might offer strategic points of attack on certain large problems.

§ 6. EMISSION LINES

6.1. General

Except for a short interval after minimum light, usually about one-third of the period, the nearly normal M- and S-type absorption spectra of long-period variables are decorated by bizarre emission lines which exhibit marked cyclical changes in intensity. The correlation with variability is complete; not a single non-variable star has ever been observed to exhibit a bright-line spectrum like that of a typical Mira-type variable on the declining branch of its light-curve. The anomalous emission lines are obviously called forth, in some manner as yet enigmatic, by physical processes related to light-variation.

Many years ago it was noted that the behavior of the outstanding bright lines in long-period Se variables is much the same as in Me variables of comparable period and light-range. Not only are the stronger lines the same in both types, but the general pattern of behavior during the light-cycle is also the same. Certain differences in relative intensities can be explained by the fact that in Me stars the bright lines are subjected to stronger absorption by TiO bands.

In spectra of N-type variables, bright lines are usually not conspicuous, and relatively little attention has been paid to them. Recent observations, however, have disclosed a few of the stronger Me and Se bright lines in the following N-type variables: U Cygni (Sanford 1950*b;* Bidelman 1952); RS Cygni (McKellar 1952, 1954); and UV Aurigae, the R Aquarii of N-type variables (Sanford 1949).

Thus, in spite of marked surface differences in chemical composition, shown

by the absorption spectra, there are indications that the general structure and the main physical phenomena of variation are much the same in M-, S-, and N-type variables.

6.2. Special Notes

In the ultraviolet spectra of long-period variables, the conspicuous emission lines of Fe II multiplet (1), 3250–3300 A, call for further investigation. The excitation potential of these lines is lower than that of the Fe II emission lines more commonly observed in stellar spectra in the region 4100–4600 A.

The short-lived metallic emission lines of moderate intensity in the spectrum of R Cygni, type Se, near maximum light (Merrill 1952) deserve further investigation. The number of narrow emission lines seen on spectrograms at the 1957 maximum taken by Deutsch with the 200-inch telescope is surprisingly large.

6.3. Hydrogen Lines

The first spectrograms of long-period variables showed surprising deviations in the relative intensities of the bright hydrogen lines from the regular decrease

TABLE 4

Mutilation of Balmer Series of Bright Hydrogen Lines in Spectra of Me Variables

Line	Maximum Absorption	Absorber	Line	Maximum Absorption	Absorber
Hα	Very strong	TiO	Hδ	Slight	In I
Hβ	Complete	TiO	Hε	Complete	Ca II
Hγ	Moderate	TiO	H10–H14	Strong	MI*

*Lines of neutral metals.

(the Balmer decrement) from Hα shortward, observed in the laboratory and in early-type stars. The lines Hβ, Hε, and Hα (observed later) were often far too weak compared to Hγ, Hδ, and Hζ. It was difficult to believe that the abnormal intensities were intrinsic in the light emitted by the glowing hydrogen, for no satisfactory explanation of such behavior was known. On the other hand, emission lines in stellar spectra were supposed to come from the outer portions of an extensive atmosphere, a situation which gave little opportunity for absorption subsequent to emission. Early suggestions by Agnes Clerke and Shane, however, pointed in the right direction, and observations by Merrill (1945) and Joy (1947) later established the fact that absorption by the reversing layer is clearly evident in the profiles of the bright hydrogen lines. Thus it is now certain that the level of hydrogen emission (near maximum light) is in or below the reversing layer. A sketchy summary of the facts is found in Table 4. The maximum mutilation of the series occurs at its first appearance some time before maximum light; the effective absorption then decreases, and the relative intensities of the bright lines approach normal as the phase advances. The same

conclusion may be drawn from the behavior of bright lines of Fe I (Merrill and Burwell 1930; Merrill 1946). The obvious interpretation is that in each cycle the emission (localized in a thin shock wave or in prominence-like streamers) first occurs deep in the star and that its place of origin then rises through the reversing layer.

6.4. Ca II Lines

The behavior of lines of Ca II in spectra of long-period variables is most extraordinary. At times of maximum light the H and K lines at 3933 and 3968 A are dark and wide. They gradually weaken as the light declines. About 40 days after maximum, fairly narrow emission appears within the wide absorption at H; it has an apparent displacement of about −100 km/sec with respect to the absorption-line spectrum. A few days later a bright line appears at K with an even larger negative displacement. As the phase advances, the bright components strengthen, and the negative displacements decrease. Typical be-

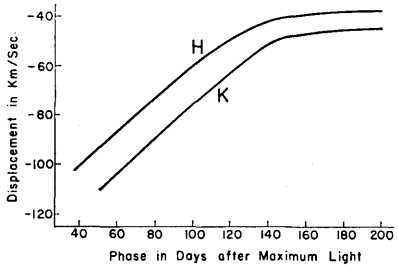


FIG. 2.—Apparent displacements (with respect to the velocity from the dark lines) of bright H and K lines of Ca II in spectra of typical long-period variables.

havior of the displacements is shown in Figure 2. The relative intensities of the bright Ca II lines are abnormal. Instead of being twice as strong as H, as in the laboratory, K is at first much weaker than H and then, as the phase advances, gradually approaches equality.

No plausible hypothesis for the direct emission of the Ca II lines with their observed abnormal intensities and displacements is in sight. The explanation which now appears most probable (Herbig 1952; Kraft 1957) is that these bright lines are emitted in normal relative intensities (K = 2H) and in positions normal for emission lines, that is, with centers yielding a velocity of about −15 km/sec with respect to the general dark-line spectrum, and that they are then subject to very strong absorption by overlying, cooler atoms of Ca II which eat away all the longward portions, leaving only small remnants which yield the measured displacements indicated in Figure 2. While this means that the original emission was extremely intense, no satisfactory alternative hypothesis has yet been proposed. In one important respect the behavior of the Ca II lines resembles that of other emission lines in the spectra of long-period variables,

namely, that they are most greatly mutilated on their first appearance and tend toward normality both in intensity and in position as the phase advances. The explanation probably is that the absorption to which they are subjected decreases as the level of emission rises.

An interesting fact is that in cepheid variables the bright H and K lines of Ca II, while very much weaker than in long-period variables, nevertheless exhibit a general pattern of behavior which qualitatively strongly resembles that in long-period variables (Herbig 1952; Kraft 1957).

An important fact, known for many years, is that the infrared Ca II lines, 8498, 8542, 8662 A, are bright in spectra of long-period variables near time of maximum light when H and K 3933 and 3968 A appear wholly in absorption. The infrared lines are normally stronger in S-type variables than in M types. This is probably because in M types they are weakened by strong TiO bands.

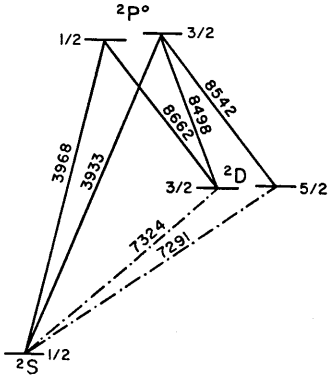


FIG. 3.—Partial Grotrian diagram of Ca II

Fine spectrograms of R Andromedae with dispersion 6.8 A/mm, taken by Greenstein with the 200-inch telescope in 1956 and 1957 shortly after maximum light, show the bright, infrared Ca II lines to be remarkably strong.

The presence of the infrared lines has a bearing on the interpretation of the anomalous behavior of emission H and K. Both groups of lines have the same upper quantum energy levels, $^2P^o_{1/2,\,3/2}$ (Fig. 3); hence they should be emitted in the same relative intensities at all times. Thus bright H and K, if invisible when the infrared lines are prominent, must be subject to strong absorption, presumably by overlying Ca II atoms. This consideration favors Herbig's explanation of the anomalous intensity of H with respect to K and of the shortward displacement of both lines.

In the future, spectroscopic observations of long-period variables in the extreme red, the forbidden ^2S–^2D lines at 7291 and 7324 A (Fig. 3), should be looked for at various phases but especially near minimum light, when forbidden lines of Fe II are known to appear. In Me spectra, identification may be difficult because of the complicated background formed by the absorption bands of TiO.

Up to the present time these [Ca II] lines have been observed only in the spectrum of υ Sagittarii (Merrill 1943).

6.5. Emission Lines of AlH

Attention was called (Merrill 1955) to the disgraceful fact that about forty emission lines, some of them very strong, observed near minimum light in the spectra of χ Cygni and other long-period variables, remained unidentified. The disgrace was soon removed by George Herbig's startling discovery that nearly all these lines belong to the band spectrum of AlH (Herbig 1956). This was quite unexpected because, among the sixty or so lines that strengthened markedly near minimum light, about twenty had been previously identified as forbidden lines of Fe II.

Band lines of AlH actually were first observed in emission in the spectrum of χ Cygni in 1935. They are plainly visible in published illustrations (Merrill

TABLE 5

Rotational Upper Levels of Bright AlH Band Lines in χ Cygni

(Herbig 1956)

Vibrational Levels λ of Band Head	(1, 0) 4066 A	(0, 0) 4241 A	(1, 1) 4353 A
Branch:			
P	6–12	18–22	7–12
Q	6–12	17–21	6–12
R	5–12	16–20	5–11

1936), but the dispersion, 500 A/mm, was so small that individual lines were hopelessly blended. Later, with dispersions of 10 and 18 A/mm, some forty separate lines were measured and tabulated (Merrill 1947, 1953).

A remarkable feature is that the lines near the origins and the heads of the AlH bands do not appear in emission in the spectrum of χ Cygni; the only lines observed are those normally farther out in the band structure. This is not true of the AlH band lines observed in absorption in stellar spectra; their intensities are normal or nearly so. Herbig's statement (1956) is as follows: "A striking feature of the AlH spectrum [in emission] in χ Cygni is the selectivity of excitation, which is the reason that the impression of band structure is lost, and the identification of the emitter was so long delayed."

The upper rotational quantum energy levels of lines observed in emission in χ Cygni are shown in Table 5. The curious selection is probably due to the potential curve of the AlH molecule. This curve shows the potential energy arising from the mutual attraction (or repulsion) of the two atoms, plotted against the distance between the centers of the atoms. From the minimum which corresponds to the normal distance in the unexcited molecule, the curve

rises with increasing distance to a rounded maximum above the horizontal asymptote, which indicates the potential at large distances. The rotational energy levels near this maximum are probably the ones involved in the production of the χ Cygni lines. The effect is called "inverse predissociation," since atoms from the outside penetrate the small potential barrier. Thus the intensities of the band lines in emission are proportional, not to the total number of AlH molecules, but to the rate at which the molecules are being formed. This opens some new and exciting possibilities in the detailed study of the chemistry and chemiluminescence of stellar atmospheres. The stellar AlH lines deserve close study. Similar effects should be looked for in spectra of other molecules. The observational status at the end of the year 1957 of lines of AlH in stellar spectra is indicated in Table 6.

TABLE 6

LINES OF AlH IN STELLAR SPECTRA

STAR	TYPE	ALH LINES
	Absorption	
R And	Se	Numerous and fairly strong
o Cet	M6e	Observable with high dispersion
β Peg	gM2	Observable with high dispersion
Sun	dG2	Doubtful; very weak if present
	Emission (at Minimum Light; See Table 5)	
χ Cyg	Mpe	Very strong
R Cyg*	Se	Very strong
R And	Se	Probably present
o Cet	M6e	Moderate intensity
R Leo	M8e	Moderate intensity
W Hya	M8e	Weak
R Hya	M6e	Not observed
T UMa*	M4e	Not observed

* Bidelman and Stephenson (1957).

6.6. UNIDENTIFIED LINES

A number of other bright lines, as yet unidentified, follow the general behavior of lines of [Fe II] and of AlH in strengthening toward minimum light. A few of the strongest, with approximate relative intensities, are given in the accompanying table. Every effort should be made to identify these lines, especially

λ (A)	Int.	λ (A)	Int.
3735.3	20	4400.6	1
3993.0	2	4455.3	8
4095.5	2	4518.7	2

the outstanding one at 3735.3 A. The wave length of this line agrees within errors of measurement with that of a weak line of Fe I multiplet (388), but the coincidence does not seem significant; other lines in the same multiplet or from the same upper level, e^7P_4, in other multiplets have not been found.

6.7. Absolute Intensities

The intensities of numerous bright lines with respect to the neighboring continuous spectrum can be determined approximately from ordinary slit spectrograms, and the general behavior of the lines with changing phase is fairly well known. A worthwhile task, although not an easy one, would be to determine *absolute* intensities throughout the light-cycle. This might be done (1) directly from slitless spectrograms or (2) indirectly from slit spectrograms by suitable photometric measures which would give absolute intensities of portions of the continuous spectrum near the bright lines. In the second method, changes in the bands will cause uncertainties unless care is taken that both relative and absolute measures refer to the same narrow spectral regions.

Answers to such questions as the following should be obtained: At what phase do the maximum intensities of the hydrogen lines occur? Is the rate of decay exponential? During the postmaximum phase do the intensities of 4202 and 4308 A of Fe I and 4571 A of Mg I and other lines increase absolutely or only in respect to the fading continuum? This question is especially important with respect to lines of [Fe II] toward minimum light. Are their absolute intensities approximately constant throughout the light-cycle, their interval of visibility in the spectrum corresponding to that during which the intensity of the M-type spectrum falls below a certain limit? The present observational material suggests that the [Fe II] lines disappear too soon after minimum light for this hypothesis to be correct, but the answer is not definite.

Rough determinations can be obtained by comparing available slit spectrograms with the light-curves, but more precise photometry is desirable not only for the bright lines, but to ascertain the behavior of the continuous spectrum as modified by absorption lines and bands. The type of measurements made by Payne and Hogg (1927) and by Scott (1945) should be extended and the accuracy improved.

§ 7. PERIOD AND AMPLITUDE OF LIGHT-VARIATION

Certain phases of the general behavior of various groups of long-period variables are shown by plotting light-range against period, as in Figure 4. The data, taken from recent compilations by L. Campbell and M. W. Mayall (Campbell 1955), should be fairly homogeneous. The only strong selectional effect, other than relatively bright apparent magnitude, is probably some discrimination against variables with very small amplitudes. Hence most features shown by the diagram are probably real. Some interesting results are:

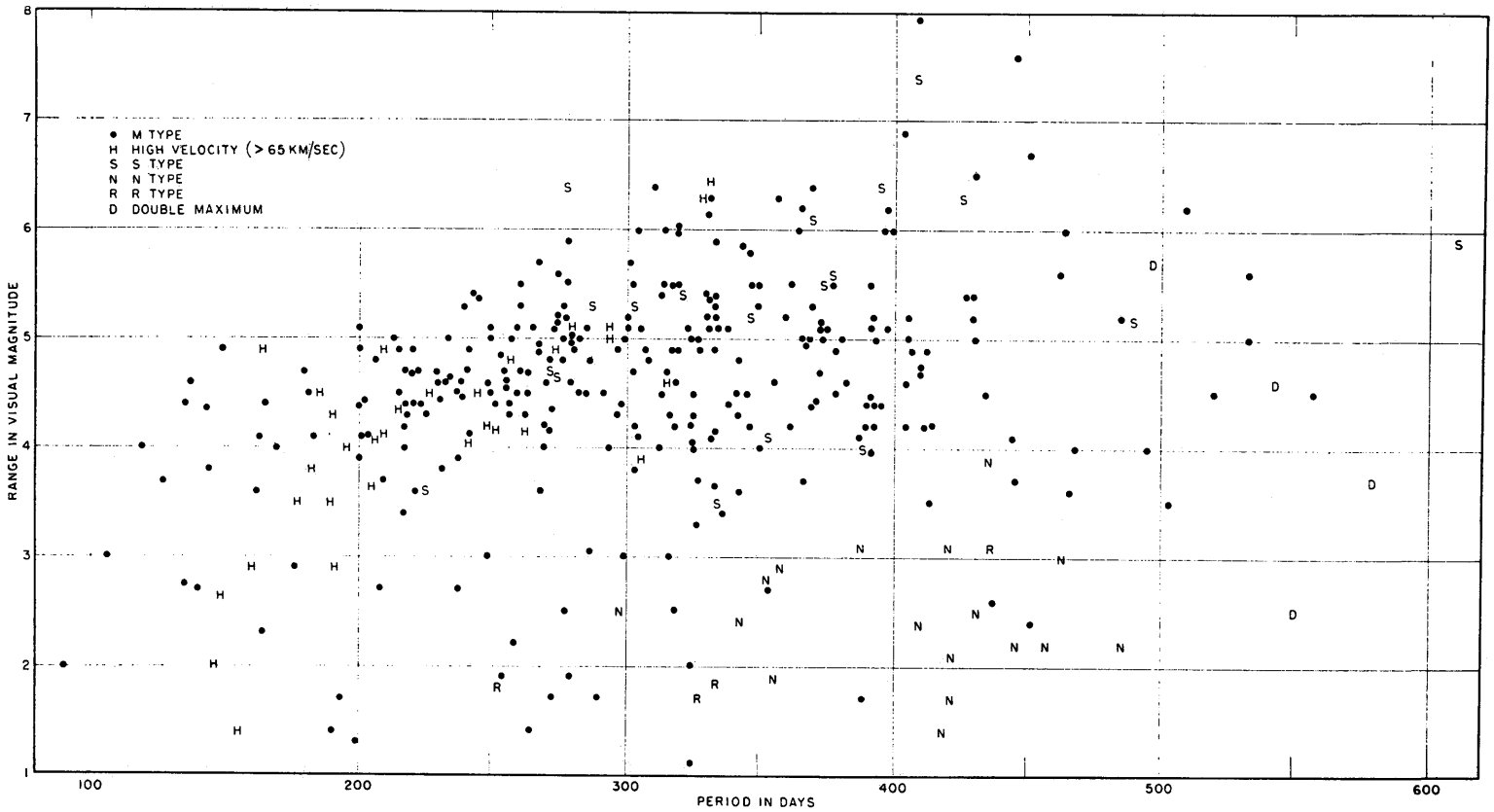


FIG. 4.—Period and light-range of red variables

1. With increasing period, a rather abrupt drop in the number of variables occurs at about 420 days. The actual period-frequency distribution of long-period variables is a complicated matter, and conclusions from selected lists of stars must be drawn with caution. Several angles of this problem have been carefully studied by Hoffleit (1957).

2. Light-ranges exhibit a general increase with increasing period, although there is much scatter among individual stars. The maximum visual range (upper envelope of the points) increases from about 5 mag. at 200 days through 6 mag. at 300 days to 8 mag. at 400 days. The *average* range behaves somewhat differently; it rises from about 4 mag. at 200 days to 5 mag. at 300 days and then remains nearly constant, but for the larger periods the scatter becomes very great. For M- and S-type variables the average range probably continues to rise for periods greater than 300 days.

3. The light-ranges of S-type variables are fully as great as those of the M types and perhaps somewhat greater at the longer periods. Because the TiO bands in M-type spectra are more intense and more extensive than the ZrO bands in S-type spectra, one might have expected the M-type variables to have the larger ranges. Do the S-type variables have a greater range of temperature and/or heavier veiling than the M types? It is interesting that the famous variable χ Cygni, which combines in notable degree the characteristics of M and S types, should have the largest light-range of all known variables.

4. The N-type variables have relatively long periods and notably small ranges. Bands of C_2 and of CN are very strong, but perhaps their differences in intensity between maximum and minimum light are not so great as those of bands in types M and S. Or, perhaps, in N-type variables the range of effective temperature is less than in the other types.

5. Nearly all variables with space velocities exceeding 65 km/sec, indicated in Figure 4 by the symbol *H*, have periods less than 300 days. Between 150 and 250 days the proportion is surprisingly large. These facts have been known for many years; Figure 4 reveals them in a slightly new way. The importance, as well as the difficulty, of comparing in detail the spectra of high-velocity variables, population II, with those of "normal" variables of population I have already been stressed.

§ 8. BRIGHTER VARIABLES OF VARIOUS TYPES

This chapter concludes with lists, in Table 7, of the brighter long-period variables of various types. These stars should be strategic objects for future observation. The data are largely from the compilation by Campbell (1955). To emphasize the importance of the period in intercomparisons of various kinds, the stars in each of four lists are arranged in order of period: M-type, S-type, N-type, and high-velocity variables. A previous listing under different headings may also be of interest (Merrill 1940*c*).

TABLE 7

BRIGHTER LONG-PERIOD VARIABLES OF VARIOUS TYPES
(In Order of Period)

STAR	POSITIONAL DESIGN.	SPEC.	PERIOD (DAYS)	MAX. MAG. (m_v)	MIN. MAG. (m_v)
			M Type		
T Cen	133633	M0e	91	6.0	8.0
R Vir	123307	M4e	145	6.9	11.0
T Aqr	204405	M3e	201	7.8	13.1
RS Lib	151822	M7e	218	7.6	11.7
V Cas	230759	M6e	232	7.9	12.0
U Cet	022813	M3e	236	7.5	12.7
S Hya	084803	M4e	255	7.9	12.7
R Tri	023133	M4e	266	6.3	11.6
RR Sco	165030	M6e	279	6.0	11.7
R Aql	190108	M7e	306	6.2	11.5
R Car	092662	M5e	308	4.6	9.5
R Leo	094211	M8e	313	5.9	10.0
o Cet	021403	M6e	331	3.6	9.2
U Ori	054920	M8e	373	6.5	11.9
R LMi	093934	M8e	373	7.1	12.3
T Cep	210868	M7e	393	6.0	10.3
R Hor	025050	M7e	404	6.0	13.0
R Hya	132422	M7e	407	4.5	9.5
χ Cyg	194632	Mpe	409	5.2	13.3
R Cas	235350	M7e	430	6.5	12.1
T Cas	001755	M8e	445	7.8	12.0
R Nor	152849	M4e	496	7.2	13.0
R Cen	140959	M4e	542	6.0	10.8
			S Type		
S UMa	123961	Se	226	7.9	11.6
V Cnc	081617	Se	272	8.0	12.8
R Gem	070122	Se	370	7.1	13.3
R Lyn	065355	Se	378	7.9	13.7
R And	001838	Se	409	7.0	14.3
R Cyg	193449	Se	426	7.4	13.8
W Aql	191007	Se	489	8.3	13.9
			N Type		
V Oph	162112	N3e	298	7.5	10.1
SS Vir	122001	Npe	356	6.8	8.9
V CrB	154639	N3e	357	7.4	10.4
RS Cyg	200938	N0e	419	7.4	8.9
R Lep	045514	N6e	432	6.8	9.4
U Cyg	201647	Npe	463	7.5	10.7
S Cep	213678	N8e	485	8.5	10.9
			High Velocity		
S Car	100661	K5e	150	5.7	8.5
X Mon	065208	M3e	156	7.6	9.0
RT Cyg	194048	M2e	191	7.4	11.8
S Lib	151520	M2e	192	8.5	11.5
W Lyr	181136	M4e	196	8.0	12.0
R Dra	163266	M7e	245	7.6	12.2
RR Sgr	194929	M5e	332	6.6	13.1

REFERENCES

ADAMS, W. S.	1956	*Ap. J.*, **123**, 189.
BIDELMAN, W. P.	1952	*Pub. A.S.P.*, **64**, 133.
	1954	*Ap. J. Suppl.*, **1**, 175.
BIDELMAN, W. P., and MCKELLAR, A.	1957	*Pub. A.S.P.*, **69**, 31.
BIDELMAN, W. P., and STEPHENSON, C. B.	1957	*Les Molécules dans les astres* (Symposium Liège, July 1956) (Cointe-Sclessin, Belgium), p. 293.
BUSCOMBE, W., and MERRILL, P. W.	1952	*Ap. J.*, **116**, 525.
CAMERON, A. G. W.	1955	*Ap. J.*, **121**, 144.
CAMPBELL, L.	1955	*Studies of Long-Period Variables* (Cambridge, Mass.: American Association of Variable Star Observers).
DEUTSCH, A. J.	1956	*Ap. J.*, **123**, 210.
FOWLER, W. A., BURBIDGE, G. R., and BURBIDGE, E. M.	1955	*Ap. J. Suppl.*, **2**, 167.
HERBIG, G. H.	1952	*Ap. J.*, **116**, 369.
	1956	*Pub. A.S.P.*, **68**, 204.
HOFFLEIT, D.	1957	*A.J.*, **62**, 120.
JOY, A. H.	1926	*Ap. J.*, **63**, 281; see p. 327.
	1947	*Ibid.*, **106**, 288.
	1954	*Ap. J. Suppl.*, **1**, 39.
KELLEY, K. K.	1935	*U.S. Department of Interior, Bureau of Mines Bull.* No. 383.
KRAFT, R. P.	1957	*Ap. J.*, **125**, 336.
LORETA, E.	1934	*A.N.*, **254**, 151.
MCKELLAR, A.	1952	*Trans. I.A.U.*, **8**, 416.
	1954	*M.N.*, **114**, 331.
MCKELLAR, A., WRIGHT, K. O., and FRANCIS, J. D.	1957	*Pub. A.S.P.*, **69**, 442.
MERRILL, P. W.	1936	*Ap. J.*, **83**, 272.
	1940*a*	*Spectra of Long-Period Variable Stars* (Chicago: University of Chicago Press).
	1940*b*	*Ibid.*, p. 58 and Pl. V.
	1940*c*	*Ibid.*, p. 106.
	1943	*Pub. A.S.P.*, **55**, 242.
	1945	*Ibid.*, **57**, 178.
	1946	*Ibid.*, **58**, 304.
	1947	*Ap. J.*, **106**, 274.
	1952	*Ibid.*, **116**, 21.
	1953	*Ibid.*, **118**, 453.

1955 *Pub. A.S.P.*, **67**, 199.
1956*a* *Ibid.*, **68**, 70.
1956*b* *Ibid.*, p. 356.

MERRILL, P. W., and BURWELL, C. G. 1930 *Ap. J.*, **71**, 285.

MERRILL, P. W., and GREENSTEIN, J. L. 1956 *Ap. J. Suppl.*, **2**, 225.
1958 *Pub. A.S.P.*, **70**, 98.

MERRILL, P. W., and WILSON, O. C. 1956 *Ap. J.*, **123**, 392.

O'KEEFE, J. A. 1939 *Ap. J.*, **90**, 294.

PAYNE, C. H., and HOGG, F. S. 1927 *Harvard College Obs. Circ.*, No. 308.

PETTIT, E., and NICHOLSON, S. B. 1933 *Ap. J.*, **78**, 320.

SANFORD, R. F. 1949 *Pub. A.S.P.*, **61**, 261.
1950*a* *Ap. J.*, **111**, 262.
1950*b* *Ibid.*, p. 270.

SCOTT, R. M. 1945 *Ap. J.*, **101**, 71.

WRIGHT, K. O., and MCKELLAR, A. 1956 *Pub. A.S.P.*, **68**, 405.

CHAPTER 14

Physical Properties of the Red Giants

PHILIP C. KEENAN
Perkins Observatory, Delaware, Ohio

OUR understanding of both the internal structure and the atmospheric conditions in the stars that form the giant branch in the Hertzsprung-Russell diagram is still rather primitive. In contrast with most of the stars of the main sequence, for which reasonably good model atmospheres can be constructed, our ignorance of the contributions of the different sources of opacity in the surface layers of the red giants has hindered the application to them of the method of model atmospheres. For this reason we are still sketching the rough outline of a physical picture of their atmospheres by induction from observations of their spectra and colors.

The observations themselves are made difficult by the overlapping of the multitude of lines and bands in late-type spectra. It is discouraging to apply accurate spectrophotometric methods to the measurement of total absorptions of lines and then find that the corrections for blending, etc. (and often also the uncertainties in the estimates of these corrections), are larger than the line absorptions themselves.

Because of these difficulties our most successful line of attack has been the estimation of those integral properties of the stars, particularly *effective temperatures* and *luminosities*, for which relative values can be estimated directly, either from line strengths on small-scale spectrograms or by photometry with selective filters.

§ 1. PROPERTIES DERIVED FROM CLASSIFICATION OF LATE-TYPE SPECTRA

The red giants divide into three spectral groups: (1) the oxygen stars, types K and M; (2) the heavy-metal stars, type S; and (3) the carbon stars, type C (or R and N).

These three main classes are differentiated chemically by the elements giving

rise to the strongest lines and bands in their spectra. The names given to the groups are, of course, not completely descriptive. Thus spectra of both type S and type M have bands of metallic oxides; the difference is that, in type M, stable oxides of metals of the third period (Ti, Sc, V) produce the strongest bands, while in type S the dominant oxides are those of metals of the fifth period (Zr, Y, Ba). Again, the carbon stars resemble the S stars in the relative proportions of heavy and light metals present, but the former contain so much carbon that the bands of carbon compounds (CN, C_2, CH) dominant their spectra, and the metallic oxides are practically not observed. The groups are not actually discrete; there are a number of intermediate stars which make it necessary to define the group boundaries somewhat arbitrarily.

The three groups overlap widely in the ranges of temperature spanned by each and probably also in their ranges of luminosity, although it is only among

TABLE 1

DIRECT DETERMINATIONS OF EFFECTIVE TEMPERATURE

Star	Spectral Type	T_e (° K)	M_v
α Tau.....	K5 III	3890	−0.5 (trig.)
β Peg.....	M2+II–III	3140	−1.4
α Ori.....	M1–M2 I*ab*	3270	−5.5:
α Sco A.....	M1–M2 I*ab*	3270	−5.5:
α Her A.....	M5 I*b*–II*a*	3320	−4:
ο Cet.....	M6e	2210 (Max.)	−1:

the oxygen stars that the dispersion in luminosity has been even reasonably well determined.

1.1. EFFECTIVE TEMPERATURES

Since the effective temperature, T_e, is defined by

$$\sigma T_e^4 = F = \frac{L}{4\pi R^2},$$

the direct determination of temperature involves the measurement of both total radiation (L) and radius (R). For only a few late-type stars has it been possible to combine radiometric measurement of radiation with interferometric measurement of angular diameters (see the discussion of stellar temperatures in chap. 15 of Vol. II of this series). Table 1 gives the fundamental data, taken from Pettit and Nicholson (1928).

Except for these few standards, we must rely on measurements of color for the estimation of the photospheric temperatures of cool stars. The radiometric data of Pettit and Nicholson (1933) for variable stars and the photoelectric colors of Stebbins and Whitford (1945) and of Hall (1941) are the primary sources that have been used to relate temperature to spectral type for the three

groups of red stars in Table 2. The table refers as nearly as possible to giants of luminosity class III for the earlier subdivisions of type M. For stars of types S and C the luminosities may be slightly higher, but this is not certain. For all three groups the data for temperature below about 2500° K are based mostly upon the radiometric measurements on long-period variables. Table 2 is only an approximation, but it should be useful until we have the more extended radiation measurements that are so badly needed.

1.2. Absolute Magnitudes

In the MK system of classification the M-type stars are arranged in a temperature sequence mainly on the basis of the strengths of their bands of TiO (with bands of vanadium oxide useful also beyond M6), with the scale and zero point chosen to bring the types into good agreement with the original Mount Wilson types, as given in the *Mount Wilson Catalogue of Spectroscopic Absolute Magnitudes* (Adams *et al.* 1935). The more sensitive atomic lines can then be

TABLE 2

Temperatures and Types of Red Giants

Group	Effective Temperature (° K)						
	4500	4000	3500	3000	2500	2000	1500
Oxygen sequence II–III	G5	K0–K1	K5	M3	M6	M8	M9–M10
Heavy-metal sequence	.....	.....	.....	S3	S5	S7	S10
Carbon sequence	C0	C2	C4	C5	C6	C7	C9

used to estimate luminosity classes, through types M0–M5. Near M5 the criteria of luminosity become vague because at that temperature the molecular bands are so strong that they begin to coalesce to produce absorption continua extending over hundreds of angstroms, particularly in the yellow and red. The problem is made more difficult by the lack of well-calibrated standards of luminosity among the late M-type giants. A few stars, of which α Herculis is the best known, appear to lie considerably above the main giant branch, but they are too distant to allow direct measurement of their luminosities, and even the assignment of luminosity classes to these few stars remains somewhat arbitrary.

For types K5–M4, however, there are enough apparently bright stars with well-determined types to allow luminosity class III to be calibrated statistically from either trigonometric parallaxes or mean motions. In Table 3 the absolute magnitudes for class III are based on means of trigonometric parallaxes for the groupings K5–M1 and M2–M4, which are to be discussed in Volume III of this series. Among the supergiants, 12 M-type stars with luminosity classes I*ab* to I*b*, which had been established by Bidelman (1947) as members of the double cluster in Perseus, were given the greatest weight in the calibration. These are

all variable stars of small amplitude and, for $\langle M_v \rangle$ values of -4.5 for luminosity class I*b* and -5.3 for class I*ab*, were estimated by Blanco (1955), who adopted a true modulus of 11.8 for h and χ Persei. This modulus is in good agreement with that (11.7) derived more recently by Johnson (1957).

For the other two groups of late-type stars—the S-type stars and the red carbon stars—the effects of abundance differences and overlapping band absorption on line intensities have prevented spectroscopic estimation of their luminosities. It has been necessary to derive mean absolute magnitudes, usually by statistical means, without any preliminary sorting-out into luminosity classes.

Of the known stars of type S, about 45 per cent are long-period variables (Mira type). The others either are not known to vary in brightness or are semi-regular or irregular variables. The amplitudes of the latter variables are quite

TABLE 3

ABSOLUTE MAGNITUDES $\langle M_v \rangle$ OF M-TYPE STARS

TYPE	GIANTS III	BRIGHT GIANTS II	SUPERGIANTS	
			I*b*	I*a*
K5	−0.3	−2.3:	−4.5	−7:
M0	− .4	−2.3:	−4.5	−7:
M1	− .5	−2.3:	−4.5	−7:
M2	− .5	−2.3:	−4.5	−7:
M3	− .5	−2.3:	−4.5	−7:
M4	−0.5	−2.4:	−4.5	?
M5	.....	.....	−4.5	?
M6	.....	.....	−4.5	?
M7	.....	.....	−4.5	?

small for the most part, and their spectra show no striking differences from those of the apparently non-variable S-type stars. It is reasonable, therefore, to group all these together as *small-amplitude variables* for the purpose of deriving their mean absolute magnitudes, which can then be compared with the luminosities of the Mira-type variables of type S. For the latter the small amount of recent data support the estimate of $M_v \approx -1.5$ by Wilson and Merrill (1942). Among the small-amplitude variables, only one, π^1 Gruis, has a dwarf companion. Feast (1953) assigned a type of G0 V to the companion and, from the magnitude difference, estimated that M_v lies between -1.0 and 0 for the S-type primary. There are some indications that there may be a considerable dispersion of luminosities within the group of small-amplitude variables, but the very inadequate statistical data now available scarcely allow us to do more than estimate their mean $\langle M_v \rangle$ at somewhere around -1.5 to -1.0. Thus there is a suggestion that the Mira variables are the slightly more luminous group within type S, but much more data on proper motions and radial velocities of all these stars are needed to carry us beyond the stage of rough guesses.

The luminosities of the red carbon stars have been investigated by Wilson (1939, 1940), Sanford (1944), and van der Vort (1958). Both Wilson and van der Vort compared proper motions and radial velocities in order to derive mean parallaxes, while Sanford based his determinations chiefly upon the galactic rotation terms in the radial velocities of 283 stars, of which most had been measured by him. Since earlier studies had suggested that there probably were systematic differences between the luminosities of the hotter carbon stars (type R) and the cooler ones (type N), all these investigators treated the two groups separately. Table 4, adopted from the one on page 161 of Sanford's paper, gives the results. Van der Vort treated only the R-type stars, for which the addition of new McCormick proper motions brought the number studied to 85, with the high-velocity stars excluded. He further divided the data, obtaining $\langle M_v \rangle = +0.44$ for 43 R0 and R2 stars and -1.10 for 42 R5 and R8 stars.

TABLE 4

MEAN VISUAL ABSOLUTE MAGNITUDES OF CARBON STARS

Method	Author	Type R	Type N
Proper motions and radial velocities...	Wilson	−0.5	−1.9
Proper motions and radial velocities...	Van der Vort	− .3	.....
Galactic rotation (V_r).....	Sanford	− .4	−2.3
Interstellar absorption of D lines.....	Sanford	0.0	−1.8

The figures in the last row of Table 4 refer to the four R-type stars and two N-type stars for which the considerable Doppler shifts produced by their radial motions allowed Sanford to separate the interstellar components of the D lines of sodium from the stellar lines. The tabulated mean absolute magnitudes were derived from Merrill's curve relating total absorption to distance. Since all except one (V Aql) of these six stars belong to the high-velocity group of carbon stars, their luminosities may very well differ systematically from those of the low-velocity carbon stars (which are much more numerous).

Objection may be raised also to the results in the second row of the table, since Sanford used the simple Oort formula for the effect of rotation, with the constant $A = 17.7$ km/sec/kpc. We now know that galactic rotation is a more complicated phenomenon, but, until the situation is far better clarified than at present, there is perhaps not much to be gained by attempting to improve Sanford's solution by tinkering with the constants.

§ 2. ATMOSPHERIC COMPOSITION

Estimates of the chemical composition of the cool stars are as yet only approximate, since we lack curves of growth for the badly blended lines and bands. At present it is most useful to assume that the stars of type M have the same relative abundances of the different atomic species as the hotter stars of the

oxygen sequence (types F–K) belonging to the same population. Then some of the differences in abundances characterizing the *carbon* stars and the *S-type* stars can be inferred from the intensities of their absorption features. For the carbon stars the first numerical estimate of the C/O ratio was made by Russell (1934), who started with C/O $\approx$ 1/30 for the oxygen sequence and showed that the replacement of bands of metallic oxides in the spectrum by bands of carbon compounds (CN and C_2) would result if this abundance ratio were reversed. Actually, Rosenfeld (1933) had made such equilibrium computations a year earlier but had assumed that the abundance of oxygen as compared with carbon was negligible in stellar atmospheres. Thus Russell's work reduced the estimate of the limit of C/O necessary to account for the observed spectra of the carbon stars from ∞ to about 30.

The accuracy of this early work on dissociative equilibrium was limited by uncertainties in the dissociation energies (particularly in D_0 of CO) and by the fact that the relative abundance of hydrogen to heavy elements is now known to be about ten times greater than was assumed then. Another hindrance to the comparison of theory with observation has been the uncertainty in the total gas pressure at the depths at which lines are effectively formed in stars of different luminosities. These and other difficulties prevented much improvement over the work of Russell for the ensuing twenty years. Among those who worked on the problem was Fujita (1939), who made the possibly important suggestion that the abundance of *nitrogen* relative to oxygen and carbon may play a role in producing the characteristics of stars of type S.

Among recent attacks, the computations bearing most directly upon the abundance problem in giants are those of Bouigue (1954, 1957), de Jager and Nevén (1957), and Stanger (1960). Bouigue finds that the relative concentration of C_2 and CN to TiO increases very rapidly as C/O becomes slightly greater than 1. His results suggest that the transition from type M to type C corresponds to a change of C/O from about 0.4 to somewhere between 1.4 and 1.8. De Jager and Nevén do not compute specifically the concentrations of carbon compounds relative to TiO but adopt a ratio of C/O = 10, C/H = 0.01, and C/N = 1 as possibly representative of the composition of carbon stars. More recently Stanger (1960) has been able to extend the predicted concentrations to temperatures as low as 1500° K by including more terms in the set of simultaneous equations.

For the abundances of other elements, particularly the metals, the evidence is even more uncertain. Measurements of total absorptions of some atomic lines have been made in the spectra of the stars listed in Table 5. Because of the heavy blending, with the resulting difficulty in establishing a true continuum in the spectra, these data are quite uncertain. For this reason there is still considerable usefulness in the more extensive lists of line estimates made visually

on spectrograms, such as those of Davis (1947) on β Peg (M2–M3, II–III) and Fujita (1952) on U Cyg (C7, 2 to C9, 2).

The measurements of relative abundances of lithium and vanadium by Bonsack are of particular interest. They establish considerable differences in the amount of lithium present in the atmospheres of several giants, and this implies that there must be differences in the mixing currents that replenish the surface supplies of this easily destroyed element.

Measurements of the integrated intensities of molecular bands will soon provide some of the best determinations of atomic abundances, but very little data have yet been published. Among the parameters needed for such determinations are integrated transition probabilities, of the sort measured in the laboratory for the Swan bands of C_2 by King (1948) and Phillips (1957).

While we must admit that our knowledge of the chemical composition of the cooler stars is yet only qualitative, it may be of some use to those attempting

TABLE 5

MEASUREMENTS OF LINE ABSORPTION

Star	Type	Region	No. of Lines	Observer
α Ori	M1 *Iab*	Blue	59	Spitzer (1939)*
α Her	M5 II:	Blue	47	Spitzer (1939)*
χ Cyg	S	Blue	69	Fujita (1952)
HD 182040	C1, 2	Blue	150	Buscombe (1953)
HD 156074	C1, 2	Blue	150	Buscombe (1953)
HD 16115	C2, 3	Blue	150	Buscombe (1953)
HD 182040	C1, 2	Yellow	75	Buscombe (1955)
HD 156074	C1, 2	Yellow	75	Buscombe (1955)
TX Psc	C6, 2	Yellow	75	Buscombe (1955)
BL Ori	C6, 2	Yellow	75	Buscombe (1955)
UU Aur	C5, 3	Yellow	75	Buscombe (1955)
Y CVn	C5, 4	Yellow	75	Buscombe (1955)
46 giants	G, K, M0	Red	43	Bonsack (1959)

* Spitzer actually measured central intensities and line widths instead of total absorptions.

TABLE 6

POSSIBLE ABUNDANCES IN LATE-TYPE STARS

Types	Abundance Ratios (No. of Atoms)		
	C/O	C/N	Zr/Ti
K–M	0.25	0.5	0.01
C	2	1	.....
S	1	.....	10

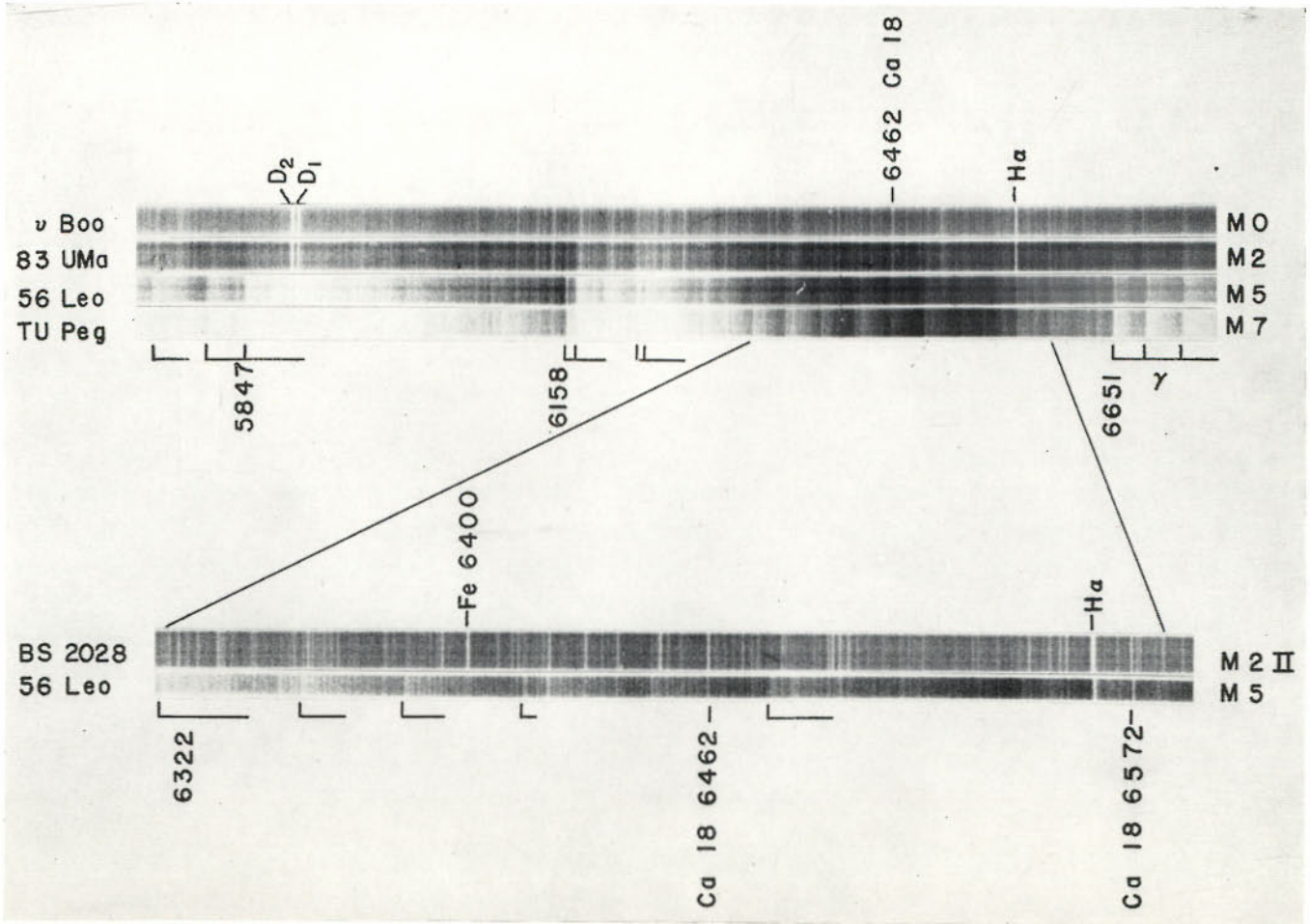


PLATE I.—Opacity from molecular bands in the red. All band heads marked are due to TiO. *Upper set:* region from the D lines to λ 6700. Scale of Perkins negatives = 52 A/mm. *Lower pair:* enlarged section showing suppression of atomic lines by TiO bands at type M5 in "window" near Hα. Scale of Mount Wilson coudé negatives = 20 A/mm.

to make progress in the physical interpretation of their atmospheres to set down in Table 6 a few abundance ratios that seem to be at least consistent with the best-known observations.

The ratio of metals given as Zr/Ti in the fourth column of Table 6 can probably be taken as representing the average ratio of the group of heavy metals (Zr, La, Ba, Y) to the group of lighter metals (Ti, Fe, V, Sc).

The question of the ratio of concentration of different isotopes of certain elements is discussed by McKellar in chapter 16.

§ 3. OPACITIES OF THE ATMOSPHERES

It appears probable that the negative hydrogen ion, which is the dominant source of atmospheric opacity throughout type G and the early subdivisions of type K, becomes less prominent beyond type K3. Direct, but not very precise, evidence of this behavior has been found in the relative strengths of the bands of CN near 4215 and 7850 A. At type K5 the opacities at these two wave lengths seem to be roughly the same (Keenan 1954*b*). From considerations of the equilibrium constants of the most abundant ions and molecules, Wildt (1957) predicted that H^- might remain an *appreciable* source of opacity out to types as late as M2.

As soon as we pass to stars of still lower temperatures ($\approx 3000°$ K), the heavy absorption bands in their spectra make it plain that molecular absorption has become the dominant source of opacity. Even in many regions between the obvious bands, the weakening of atomic lines implies the presence of absorption continua extending over hundreds of angstroms. Plate I illustrates the effect in the visual region of M-type spectra, between the D line and Hα, where titanium oxide is the molecule responsible for most of the absorption. The bands shown are not nearly so strong as those of the lower sequences of the $\alpha(\Delta v = 0$, near 5165 A) and $\gamma(\Delta v = 0$, near 7054 A) systems, but at type M5 the total opacity is enough to make even the strongest lines of neutral atoms appear surprisingly weak. The magnitude and extent of this effect in the visual region are apparently due chiefly to the overlapping here of at least four band systems of TiO, and the separate bands of these systems have not yet been completely disentangled.

Plate I also shows why it is that color indices, or even spectrophotometric gradients measured away from the more conspicuous band heads, have little relation to real color temperatures when the measurements involve such regions of locally high opacity. The influence of TiO in reducing the visual light of M-type stars in comparison with their blue or infrared radiation has long been known, but accurate measurements of the effect, particularly on integrated magnitudes, are difficult to make. Gabovits (1936) used the differences between observed color indices and the computed colors derived from black-body–curves for their effective temperatures as measures of the "TiO color effect." His results for M-type giants are shown in Table 7 in the column headed "ΔC," which is the correction to be added to the observed color indices in the third column,

to give the black-body colors corresponding to their effective temperature. These colors are on Öpik's scale, which used the means of Harvard and Potsdam visual magnitudes. Since the effect of TiO absorption on photographic magnitudes is slight except for types later than M6, the visual magnitudes would be brighter by approximately ΔC if the energy-curves were not distorted by TiO absorption in the λλ 5000–6000 A region.

Dobronravin (1950) carried out spectrophotometry of several M-type stars and gave a table of the reductions in visual and photographic magnitudes corresponding to a change in temperature from 3000° to 2500° K. The corresponding change in types for giants would be from M2 to about M6. Dobronravin's value of −0.46 mag. should then be compared with the difference between the values of C for these temperatures in Table 7, or −0.42 mag. The agreement is good, considering the differences in color systems and the uncertainty in the temperature scale. Dobronravin also computed the deviations from gray-body–curves, obtaining a differential correction of 1.34 mag. for the same temperature range. This corresponds approximately to the difference, 1.37 mag., between the values of ΔC for M2 and M6 in Table 6.

TABLE 7

EFFECT OF TiO BANDS ON COLOR INDICES

Type	ΔC	Observed C	Type	ΔC	Observed C
M0.....	0.28	1.63	M4.....	0.79	1.53
M2.....	0.28	1.72	M6.....	1.65	1.30

Dobronravin attempted also to distinguish variations in the continuous spectrum (against a gray-body–curve) from the local distortions due to recognizable bands and lines. He estimated that the change in color index due to continuous absorption amounts to 1.05 mag. for a drop in temperature of from 3000° to 2500° K, leaving only a change of 0.29 mag. due to the heavier bands and line absorption in the visual region. It is apparent from Plate I that it is very difficult to make such a distinction and locate a true continuum in the yellow and red parts of the spectrum.

These measurements all refer to M-type stars; for types S and C the data are even more scanty. In the spectra of the red carbon stars (particularly those of type N) the remarkable violet depression is so deep that in such stars as RY Dra it is difficult even to record the spectrum below about 4200 A. This was brought out vividly by Shane (1928), when he stated that the spectrum of Y CVn could be recorded with an exposure of 1 second near 4800 A, while an exposure of 5 hours barely reached 3900 A in the violet. More recent estimates of relative exposure times tell the same story but are calibrated in terms of exposures on stars of known color. Shajn and Struve (1947), following Wildt

(1936), compared carbon stars with M-type giants. The former estimated that exposure times at λ 3950 A had to be increased by at least a factor of 30 to record an N-type spectrum at the same density as that of a gM2 star of the same visual magnitude. Shajn and Struve used the weakening of absorption lines in the violet as another means of comparing the opacities of N- and M-type stars. Their method was to assume Eddington's theory of absorption lines, treating the weakened line as though it were one formed in the wing of a strong line. They found that the H and K lines in UU Aur (type N, or C5, 3) were only about one-seventh as strong as in HD 80493 (gM0). This implied that the continuous absorption near λ 3950 A is greater by a factor of 5 in the carbon stars. Now this is much less than the intensity difference corresponding to the exposure times mentioned above. If the carbon star had a lower temperature than the gM0 star, the color difference would have the right sign, but the authors believe that the temperature difference between the two stars is too small to explain the large effect observed. They suggest that differences in the stratification of elements in the two types of stars might account for the discrepancy.

Actual intensity gradients between 4900 and 3900 A were measured for ten carbon stars by McKellar and Richardson (1955). They found that six stars, including the three R-type stars measured, did not show the violet depression but, instead, could be represented well by black-body–curves.[1] U Hya and Y CVn showed the strongest violet depression, which correlated with the strength of the λ 4050 bands of C_3. The depression, however, is also known to correlate with the Merrill-Sanford green bands, identified by Kleman in 1956 as due to SiC_2. (The complicated problem of these band identifications is discussed by McKellar in chap. 16 of this volume.)

McKellar and Richardson used also the weakness of the violet CN bands (λ 3883 A) in comparison with the bands of the red system near λ 11000 A in Y CVn, as evidence that such stars have much greater opacity in the violet than in the λ 11000 A region, but they did not attempt numerical estimates by this method. An earlier comparison of the λ 3883 A bands of CN with the red bands [λ 7873 A (1, 0)] by King and Swings (1945) had shown similar, but smaller, differences. There is no doubt that the blue and violet bands of cyanogen are weakened by the general violet depression in the carbon stars.

Only qualitative estimates of the behavior of the continuum in S-type stars are available. From his small-scale spectrograms Wildt (1936) concluded: "The spectra of five S stars, four non-variables, and one variable near maximum, were found to be very similar in both the ultraviolet and the infrared to M spectra. Judging from these low-dispersion spectra alone, one could not distinguish the two classes."

If we look back over all the published data bearing on the dependence of opacity upon wave length in the spectra of the cool stars, we see that the prob-

[1] These color temperatures were taken into account in the preparation of Table 2 of this chapter.

lems of measurement and of interpretation have been only partially solved. One great need is for more data on absorptions by lines and bands at different wave lengths. Admittedly, the estimation of relative opacities from such data implies particular atmospheric models, but for that very reason the comparison of sufficiently extensive data will begin to give us a picture of the stratification of elements and compounds.

Perhaps the best way to summarize our present knowledge is by such a qualitative compilation as Table 8. Only the strongest sources of molecular absorption are mentioned in the table, but at the lowest temperatures observed ($\approx 1220°$ K) many additional molecules must contribute to the opacity.

Negative ions of atoms and molecules are not mentioned in the table, for none except H^- has been shown conclusively to be important as a source of stellar opacity. Others must exist in relatively cool atmospheres, and the possibility that their opacities might be appreciable has frequently been discussed. Thus the properties of O^- were discussed by Wildt and Chandrasekhar (1944), who suggested that it might contribute to the opacity in the photographic ultraviolet region in late K and M stars. It appears, however, that the electron affinity of O^- is only about 1.5 ev, about half the value assumed at that time, and the concentrations of the ion will be correspondingly reduced. For the same reason, the absorption continuum resulting from detachment of the electron

TABLE 8

CONTINUOUS OPACITY IN COOL STARS

	Type M	Type S	Type C (R and N)
Violet (λλ 3500–4200 A)	Opacity fairly low; departures from blackbody continuum not great	Energy falls off more rapidly than in type M, but this may merely reflect the raising of the green continuum by absence of TiO bands	Deep depression in those with strongest Merrill-Sanford bands; largely molecular, perhaps both C_3 and SiC_2
Visual (λλ 5000–6500 A)	Continuum widely depressed in later types; mostly TiO probably plus other molecular absorbers	Relatively strong continuum, in spite of strong ZrO band heads	Continuum strong between the C_2 and CN bands
Near infrared (λλ 7500–11000 A)	Spectrum very strong in latest types; opacity relatively low between observable bands of TiO and VO	Similar to type M, except that regions of strongest continuum are different, lying between the LaO bands in the coolest stars	Continuum weak in λλ 7500–8500 A region; overlapping CN absorption probably chief source

from O^- should have its longward edge near 8460 A instead of in the violet region. Such great uncertainties in the equilibrium constants of nearly all negative ions vitiate most earlier discussions of their possible influence upon stellar opacities.

The problem has been re-examined by Branscomb and Pagel (1958) with the help of more recent laboratory determinations of the physical constants. They computed the equilibrium concentrations of the ions H^-, O^-, C^-, OH^-, CN^-, and C_2^- for four model atmospheres having compositions of atomic species as assumed by de Jager and Nevén (1957). Their conclusion is that two of the most stable molecular ions—CN^- (EA = 3.1 ev) and C_2^- (EA = 3.2 ev)—may contribute to the ultraviolet continuous absorption of the carbon stars. For oxygen stars they find O^- and O_2^- to be negligible, while OH^- might possibly be detectable in the coolest stars of types M and S. All the estimates remain quite uncertain in the absence of good values for the continuous absorption coefficients for these ions. Very few laboratory observations of their photodetachment spectra have been made, though Branscomb (1957) has observed the OH^- continuum in the far red.

REFERENCES

Adams, W. S., *et al.*	1935	*Ap. J.*, **81**, 187.
Bidelman, W. P.	1947	*Ap. J.*, **105**, 492.
Blanco, V. M.	1955	*Ap. J.*, **122**, 434.
Bonsack, W. K.	1959	*Ap. J.*, **130**, 843.
Bouigue, R.	1954	*Ann. d'ap.*, **17**, 35 (Pub. Obs. Haute-Provence, Vol. **3**, No. 9).
	1957	*Liège Colloquium, Mém.*, No. 386, p. 346.
Branscomb, L. M.	1957	*Adv. Electronics and Electron Phys.*, **9**, 43.
Branscomb, L. M., and Pagel, B. E. J.	1958	*M.N.*, **118**, 258.
Davis, D.	1947	*Ap. J.*, **106**, 28 (*Mt. W. Contr.*, No. 733).
Dobronravin, P. P.	1950	*Izvest. Crimean Ap. Obs.*, **5**, 59.
Feast, M. W.	1953	*M.N.*, **113**, 510.
Fujita, Y.	1939	*Jap. J. Astr. Geophys.*, **17**, 17.
	1952	*Ap. J.*, **116**, 46.
Gabovits, J.	1936	*Pub. Obs. Astr. U. Tartu*, Vol. **28**, No. 5.
Hall, J.	1941	*Ap. J.*, **94**, 71.
Jager, C. de, and Nevén, L.	1957	*Liège Colloquium, Mém.*, No. 386, p. 357.
Johnson, H. L.	1957	*Ap. J.*, **126**, 121.
Keenan, P. C.	1954*a*	*Ap. J.*, **120**, 484.
	1954*b*	*Proc. Indiana Conf. Stellar Atmospheres*, p. 20.
King, A. S., and Swings, P.	1945	*Ap. J.*, **101**, 6.
King, R. B.	1948	*Ap. J.*, **108**, 429.
Kleman, B.	1956	*Ap. J.*, **123**, 162.

McKellar, A., and Richardson, E. H.	1955	*Liège Colloquium, Mém.*, No. 368, p. 256.
Pettit, E., and Nicholson, S. B.	1928	*Ap. J.*, **68**, 279.
	1933	*Ibid.*, **78**, 320.
Phillips, J.	1957	*Ap. J.*, **125**, 153.
Rosenfeld, L.	1933	*M.N.*, **93**, 724.
Russell, H. N.	1934	*Ap. J.*, **79**, 317.
Sanford, R. F.	1944	*Ap. J.*, **99**, 145.
Shajn, G., and Struve, O.	1947	*Ap. J.*, **106**, 86.
Shane, C. D.	1928	*Lick Obs. Bull.*, **13**, 123 (No. 396).
Stanger, P. C.	1960	Thesis, Ohio State University (unpublished).
Stebbins, J., and Whitford, A. E.	1945	*Ap. J.*, **102**, 318.
Vort, G. L. van der	1958	*A.J.* **63**, 477.
Wildt, R.	1936	*Ap. J.*, **84**, 303 (*Mt. W. Contr.*, No. 551).
	1957	*Liège Colloquium, Mém.*, No. 386, p. 319.
Wildt, R., and Chandrasekhar, S.	1944	*Ap. J.*, **100**, 87.
Wilson, R. E.	1939	*Ap. J.*, **90**, 492.
	1940	*Ibid.*, **92**, 188.
Wilson, R. E., and Merrill, P. W.	1942	*Ap. J.*, **95**, 248.

CHAPTER 15

The Loss of Mass from Red Giant Stars

ARMIN J. DEUTSCH
Mount Wilson and Palomar Observatories
Carnegie Institution of Washington, California Institute of Technology

§ 1. INTRODUCTION

A WIDE variety of stars are observed to lose mass to the interstellar medium. The most conspicuous examples are the supernovae, the novae, and the planetary nebulae. Mass loss probably also occurs in the Wolf-Rayet stars and the P Cygni stars; it may take place in some A-type supergiants, Be stars, and shell stars. In a number of close binaries there is evidence that gas streams out of one or both components and that the system loses at least some of this matter. Recent spectroscopic observations have shown that the M giants eject gas into the interstellar medium. Geophysical and astronomical phenomena are known which indicate that even the sun loses some matter. Indirect evidence has also been cited to support the hypothesis that mass loss plays a leading role in the evolution of most massive stars on or near the main sequence.

Theoretical considerations yield an unequivocal prediction that all stars more massive than 1.4 solar masses must fall below this limit when they exhaust their nuclear energy sources. For a secure understanding of the history of massive stars, the evolutionary stage where this mass loss occurs must be isolated and discussed. In a wider context, the exchange of matter between stars and the interstellar medium is a process of fundamental importance for the evolution of the Galaxy as a whole. The details of this process must ultimately govern the luminosity function in different parts of the Galaxy and the other statistical properties of different stellar populations.

With an increase in knowledge about the extreme conditions of temperature and density that prevail in some stellar interiors, it has become widely recognized in recent years that, besides the conversion of hydrogen into helium, a variety of other nuclear transformations can occur in stars (Burbidge and Bur-

bidge 1958). During the lifetime of the galaxy, these reactions may have occurred with sufficient frequency and diversity to generate from pure hydrogen virtually all the nuclei now found in nature. Stellar theories of nucleogenesis always require that some matter be processed successively in different kinds of stars. Exchanges of matter between stars and the interstellar medium are therefore important in determining the nuclear evolution of the galaxy, as well as its macroscopic astronomical evolution.

Mass loss is evidently not an important factor in all evolutionary stages of all stars. For the sun and most other single stars of comparable mass, there appears to be general agreement that theory and observations alike indicate evolution at nearly constant mass, from the time when the star first condenses onto the main sequence at least until it reaches the red giant stage. However, for the stars more than twice as massive as the sun, there is still a controversy over the role of mass loss on or near the main sequence. The observational results for these massive stars are more sparse, and the theory required for their interpretation is not yet worked out in detail. Arguing partly by analogy with the successful theoretical accounts of the evolution at constant mass of solar-type stars, one school of thought holds that massive stars also evolve at constant mass until after they have left the region of the main sequence. Another group cites arguments for believing that mass loss is a dominant factor in the evolution of most massive stars even while they are on the main sequence.

The direct observational evidence for mass loss from some early-type stars near the main sequence has recently been summarized by the Burbidges (1958). These authors have also reviewed the extensive literature relating to mass loss in close binary systems. Fessenkov and Idlis (1959) have recounted the arguments for the hypothesis that mass loss governs the evolution of most early-type stars, and they have given an extensive bibliography. Massevitch (1959) has also reviewed this subject. The principal arguments in support of the hypothesis may be briefly stated as follows:

1. Observation indicates a unique relation between the masses and luminosities of the early-type stars. But theory requires that the luminosity, L, must depend on both the mass, M, and the mean molecular weight, μ. Since μ must change with time as a star converts its hydrogen to helium, the observed mass-luminosity law implies a compensatory change in M.

2. The observed main sequence for early types cannot be explained as the locus of stars having the same initial composition but different masses, regardless of whether each star is chemically homogeneous or not; but it can be exactly explained if the star remains homogeneous and changes M and μ as in argument 1.

3. The law of mass loss which is implied by a dispersionless mass-luminosity law has the simple and physically plausible form

$$\frac{dM}{dt} = -KL, \tag{1}$$

where K is a slowly varying function of μ which very nearly equals 1×10^{-18} gm/erg.

4. With this law, it is possible to understand the general luminosity function as derived from an initial luminosity function such as is observed in OB associations.

5. It is also possible to assign ages to the stars which are compatible with their observed velocity dispersions.

6. If stars evolve with constant mass on and near the upper main sequence, they must then lose mass in the red giant stage at a much more rapid rate than is observed.

7. If a star enters the red giant stage with a large mass, it cannot still occupy this part of the HR diagram after its mass has decreased by a large factor.

In answer to these arguments, one can offer the following:

1. Mass loss is *not* observed to occur in most early-type stars; and if it did occur at a significant rate, one would expect to observe it (Mustel 1959).

2. Mass loss *is* observed to occur in nearly all M giants. As we shall see in the next section, the rate estimated by Deutsch (1956*a*) for α Herculis is nearly sufficient for the evolutionary requirements, if this rate is typical for all M giants. Moreover, this estimate was given as a conservative lower limit; the actual rate may be somewhat greater.

3. The determinations of mass for early-type stars are insufficiently exact to conclude that the mass-luminosity relation is really dispersion-free.

4. Depending mainly on the bolometric correction, which is in some considerable doubt, one *can* reasonably well explain the initial main sequence as the locus of chemically homogeneous stars of the same mean molecular weight.

5. The Trumpler effect in the main sequences of galactic clusters provides evidence that many early-type stars evolve without mixing. Moreover, there are cogent theoretical reasons for believing that massive stars cannot remain chemically homogeneous as they exhaust their hydrogen, any more than can solar-type stars (Mestel 1959).

6. The proposed law of mass loss is physically unexplained; and it does not reflect the circumstance that mass loss should be much more efficient in the late-type giants, where the escape velocity is much lower.

7. Several investigators have shown that one can recover the general luminosity function for $M_v < +6$ from the luminosity functions of open clusters on the hypothesis of evolution at constant mass (Walker 1956, 1957; Jaschek and Jaschek 1957; Sandage 1957; van den Bergh 1957).

It is outside the scope of this contribution to take a position in this controversy. We shall adopt the point of view that, whether or not significant mass loss occurs on the hot side of the Hertzsprung gap, it is observed to occur on the cool side. Since there can be no doubt that at least some stars reach the region of the red giants with masses far above the white dwarf limit (e.g., Capella and ζ Aurigae), for these objects, at least, there is a compelling theoretical requirement for the process which is, in fact, observed in the M giants.

§ 2. OBSERVATIONAL EVIDENCE FOR MASS LOSS FROM LATE-TYPE GIANTS

2.1. Circumstellar Absorption Lines

High-dispersion spectrograms of the M2 I*b* star α Orionis reveal conspicuous doubling of all the strong absorption lines that arise from the lowest term (Pl. I). One component of these double lines is evidently the broad, relatively shallow absorption line that arises in the reversing layer. The other component has a deep, nearly rectangular profile and is usually displaced shortward from the center of the reversing-layer line on which it is superposed.

Adams and MacCormack (1935) discovered these violet-displaced absorption cores in the spectrum of α Orionis and similar but weaker features in α Scorpii (M1 I*b*), α^1 Herculis (M5 II), and the long-period variable o Ceti (M6e). They also noted marked asymmetries in the D lines of β Pegasi (M2 + II–III) and ϵ Pegasi (K2 I*b*), which indicated that these lines are probably similar doublets, although not fully resolved on their plates. The displaced cores were attributed to expanding envelopes of gas about these stars.

In 1956 it was found (Deutsch 1956*a*) that the strongest of the displaced absorption cores in α^1 Herculis can also be seen in the spectrum of its visual companion, α^2 Herculis (Pl. II). This star is a single-line spectroscopic binary of type G0 II–III. The angular distance from the M5 primary is 4.″7, which corresponds to a linear separation of 700 a.u. in projection on the plane of the sky. Since no comparable zero-volt cores are known in any other G-type star, it was concluded that the companion of α^1 Herculis lies well within an expanding envelope of matter ejected from the M star. The anomalous displaced cores in α^1 Herculis were therefore designated as circumstellar lines, and the same designation has subsequently been applied to the similar displaced cores in other M giants and supergiants.

From measures of the radial velocities indicated by the circumstellar lines in α^1 and α^2 Herculis and of the line strengths it was inferred that the M star is losing mass at a rate of at least $3 \times 10^{-8}\ M\odot$/yr. Some of the details of the argument will be reviewed in the next section. To find whether this result can satisfy the evolutionary requirements, let us now tentatively suppose that the same rate of mass loss is typical for all M giants. Becker (1950) has estimated the space density of M giants near the sun as 2.2×10^{-5} pc $^{-3}$. In the direction perpendicular to the galactic plane, the velocities of the M giants have a dispersion of about 18 km/sec (Parenago 1950; Blaauw 1951). With Schmidt's (1956) model of the galaxy, this velocity dispersion yields an effective thickness of about 700 pc for the M-giant distribution near the sun. The total rate of mass ejection from these M giants will then be $4.6 \times 10^{-10}\ M\odot$ pc^{-2} yr^{-1}. But from his study of the luminosity function near the sun, together with the nuclear lifetimes of the stars, Schmidt (1959) has obtained for the present total rate of mass ejection $5.9 \times 10^{-10}\ M\odot$ pc^{-2} yr^{-1}. The close agreement between these

two results suggests that the circumstellar lines in M giants may indicate the primary mass-loss process in stellar evolution.

Since 1956, a systematic search for circumstellar lines has therefore been made in the spectra of M giants—a term which, unless otherwise qualified, will be understood to include the supergiants as well. In only a few very luminous stars can the circumstellar (CS) lines be discerned at 20 A/mm; in most M giants the strongest CS lines can be recognized only at dispersions greater than 10 A/mm. Moreover, the CS lines that are most readily detected lie in the violet part of the spectrum, where these cool stars are relatively faint. Usually they occur well within the wings of strong reversing-layer lines, so that dense spectrograms are necessary for their detection. The program has therefore taxed the capabilities of even the 100- and 200-inch telescopes.

At the time of writing, we have coudé spectrograms of fifty-three M giants, of a kind suitable for the detection of CS lines. These plates show that the strongest CS lines always occur at Ca II H and K, where they are superposed on the broad emission features that are generally present at these wave lengths. Plate III shows the region of H and K in five representative giants. The profiles are evidently complex. In particular, the presence of central absorption reversals in H and K does not necessarily indicate the presence of CS lines; for absorption features which are somewhat similar are usually produced in the chromospheres of late-type giants. The reasons will be given later for drawing this distinction between the chromospheric central absorptions at H and K and the true CS lines. Suffice it to say, for the time being, that the latter can always be distinguished by their very low central intensities, when the dispersion is sufficient to resolve the profiles, and sometimes by their radial velocities as well.

2.2. The Normal Giants

The plates at hand indicate that, at 4.5 A/mm, some CS lines can be recognized in the spectra of all giants of types later than M0 and in no normal giants of earlier types. In giants fainter than $M_v = -2.5$, the strength of the CS lines correlates well with spectral type. Figure 1 illustrates this correlation for the strength of the CS K line; the ordinate W is an estimate of the equivalent width of this feature, expressed in angstrom units. Although no G and K giants are plotted in Figure 1, a number have been observed at 4.5 A/mm, and none of these exhibit CS H and K lines.

At 4.5 A/mm, CS cores can generally be seen in some other strong lines from zero volts whenever the equivalent width, W, of the CS K line exceeds 0.25 A. Figure 2 shows the correlation of W on an arbitrary scale with the intensities of the other CS lines, as estimated at 10 A/mm. The first to appear of these other CS lines are generally Ca I 4227 and Sr II 4078.

Among the M giants fainter than $M_v = -2.5$, the expansion velocity $|\Delta A|$ indicated by the CS H and K lines also correlates well with spectral type, as shown in Figure 3. This implies a similar correlation with the strength of the

CS K line. The relation between these two quantities is depicted in Figure 4. The observed correlations indicate that, as we move toward later spectral type among the red giants with $M_v > -2.5$, we first encounter a CS K line at M0. At this spectral type the line is always weak and is displaced about 0.30 A shortward from the wave length corresponding to the radial velocity of the star. As we then go to later types, the shortward edge of this CS line remains very nearly stationary in this reference frame, while its longward edge moves toward longer wave lengths.

2.3. Two Simple Models

That the strength of the CS K line correlates closely with spectral type among normal giants suggests at once the possibility of a simple excitation effect. Thus we may suppose that all late-type giants possess CS envelopes of comparable density and extent but that only at M0 does the ionization first fall to the level

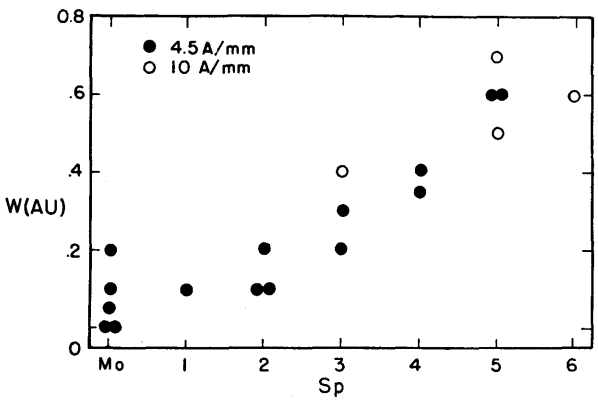


Fig. 1.—The correlation for giants with M_v fainter than -2.5 of the estimated strength, W, of the circumstellar K line, and the spectral type.

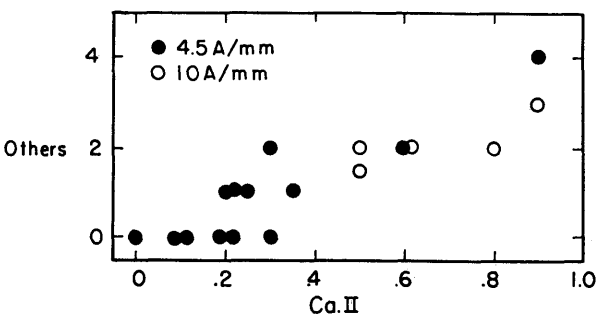


Fig. 2.—The correlation for M-type giants and supergiants of the estimated strength, W, of the circumstellar K line, in angstrom units, and the estimated strength (on an arbitrary scale) of the circumstellar lines arising from atoms and ions other than Ca II.

where Ca II becomes observable. This is an important possibility; for, if it is true, it could in all probability fully account for the whole of Schmidt's estimated total rate of mass ejection. Quantitatively, however, this kind of model presents certain difficulties, which we shall discuss in a later section.

Alternatively, we may try to interpret the observations in terms of the growth of the CS envelope as a star evolves along the giant branch from M0 toward later types. The simplest model of this kind is one in which, beginning at the time when a star reaches type M0, it ejects matter from the photosphere at a constant rate and with an initial velocity equal to the velocity of escape. We neglect the pressure term in the equation of motion and suppose that the ejected gas describes particle trajectories in the gravitational field of the star; if we also suppose that the ionization of the ejected gas remains constant as it expands, we may easily compute the properties of the CS envelope as a function

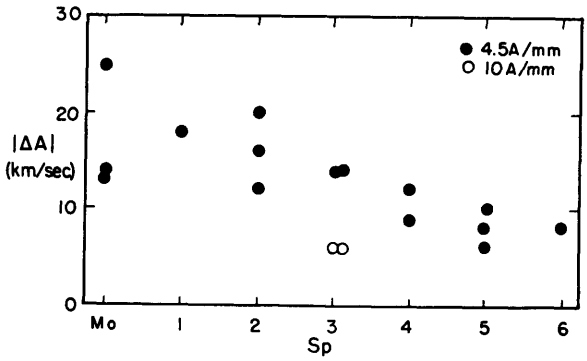


FIG. 3.—The correlation for M-type giants with M_v fainter than -2.5 of the expansion velocity $|\Delta A|$ from the circumstellar K line, and the spectral type.

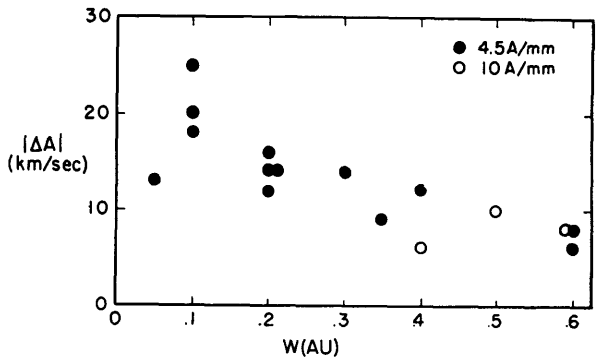


FIG. 4.—The correlation for M-type giants with M_v fainter than -2.5 of the expansion velocity $|\Delta A|$ from the circumstellar K line, and the estimated strength of this line.

of time. In particular, if R_M is the radius of the star and V_M is the velocity of ejection, both assumed to be constant, and if

$$\tau = \frac{2}{3}\frac{R_M}{V_M}, \tag{2}$$

we find that the surface density of Ca II ions along the line of sight to the star may be written, for $t \geq \tau$,

$$N = N_\infty\left[1 - \left(\frac{\tau}{t}\right)^{1/3}\right]. \tag{3}$$

In this expression, N_∞ is the limit which N approaches as $t \to \infty$; it is related to the number density, n_M, of Ca II ions at the surface of the star by the equation

$$N_\infty = 2n_M R_M . \tag{4}$$

Similarly, the mean expansion velocity along the line of sight is

$$V = V_\infty\left[1 + \left(\frac{\tau}{t}\right)^{1/3}\right], \tag{5}$$

with

$$V_\infty = \tfrac{1}{2} V_M . \tag{6}$$

It follows that

$$V = V_\infty\left(2 - \frac{N}{N_\infty}\right), \tag{7}$$

which bears some resemblance to the observed relation between expansion velocity and line strength. However, these equations indicate that both N and V reach 90 per cent of their limiting values when $t = 1000\,\tau$; and, for appropriate values of R_M and V_M, τ is of the order of only 0.1 year. The model therefore implies an evolutionary rate along the giant branch which is inadmissibly fast, and it also implies a frequency function for the M subclasses which is totally different from the observed one. The proposed model is therefore completely unable to represent the observations in a satisfactory way. Possibly a more general model of this kind can still succeed, however, provided that it incorporates the appropriate changes in n_M, R_M, and V_M with spectral type.

2.4. The Supergiants

Table 1 summarizes the existing observations of CS lines in M-type supergiants, which may be taken here as stars with $M_v < -2.0$. The spectral types are compiled; most are by P. C. Keenan. According to more recent determinations, RW Cephei is of type K0 0*b*, and ψ^1 Aurigae of type K5 I*b*. The absolute magnitudes which are not in parentheses have been determined by Wilson and Bappu (1957) from the relation between M_v and the width of the emission line at Ca II K. The Wilson-Bappu method of finding M_v will not work for the most luminous supergiants, for these stars show little or no emission at the K line. Accordingly, the absolute magnitudes for these stars have been assigned on the

basis of Keenan and Morgan's calibration (1951). The same source has also been used for one star in which the emission line at K has not yet been measured. The equivalent width W (K) of the CS K line is an estimate from one or more coudé spectrograms on which the profile is fully resolved. The table also gives an estimate, on an arbitrary scale, of the intensity of the CS lines other than H and K and an indication of the number of these lines that have been detected. This number depends, of course, on the absolute strengths of the CS lines and also on the dispersion that has been used in observing them. For the stars listed, the highest dispersion ranges from 2.9 to 20 A/mm.

TABLE 1

CIRCUMSTELLAR LINES IN M-TYPE SUPERGIANTS

STAR	SPECTRAL TYPE	M_v	CS H AND K		OTHER CS LINES		
			W(K) (A)	ΔA (Km/Sec)	No.	Int.	ΔA (Km/Sec)
RW Cep	M0 I*a*–0	(−8.0)	.....	.....	10	3:	−21
μ Cep	M2 I*a*	(−7.0)	1.2	−14	11	4:	−13
VV Cep	M2+I*a–ab*	(−6.0)	0.25	−19	7	1½	− 8
α Ori	M2 I*b*	−5.7	0.9	− 1	42	4	− 5
ψ^1 Aur	M0 I*ab*	−5.7	0.8:	− 2	6	2	−10
119 Tau	M2 I*b*	−5.1	0.9	− 3	11	3	− 6
α Sco	M1 I*b*	−4.9	0.3:	−18	7	2	−11
HD 20797	M0 II	−3.6	0.5	−16	1	1½	.....
π Aur	M3 II	−3.0	0.5	−18	.....	.....	.....
δ^2 Lyr	M4 II	−2.9	0.6	−11	3	2	−13
U Del	M5 II	(−2.5)	0.7	− 6	11	3	−11
η Gem	M3 II	−2.2	0.6	−26	1	1:	.....
α Her	M5 II	−2.1	0.6	− 6	21	2	−10
g Her	M6 III:	−1.3	0.6	− 8	5	2	−12

As in the normal M giants, the strength W (K) of the CS K line increases with advancing spectral type among the supergiants. In these more luminous stars, however, W (K) also increases rapidly with increasing luminosity; and it is for this reason that these stars have not been represented in Figure 1. The correlation between expansion velocity $|\Delta A|$ and spectral type and that between $|\Delta A|$ and W (K) are also much looser for the supergiants than in Figures 3 and 4. In the supergiants, however, $|\Delta A|$ changes with time; if for each star we could use the value of $|\Delta A|$ averaged over several years, we could probably appreciably diminish the dispersion in the $|\Delta A|$ versus Sp and $|\Delta A|$ versus W (K) relations. The variation of $|\Delta A|$ in a supergiant, incidentally, is due exclusively to changes in the radial velocity of the reversing layer as derived from the subordinate lines in the stellar spectrum. By all indications, the CS lines in an M star always indicate a perfectly constant radial velocity, as we should expect them to do if they are produced in an envelope many times larger than the star itself. The velocity variations in the reversing layers of M stars

have been studied by Sanford (1933), Joy (1942), and McLaughlin (1946), among others. Adams (1945, 1956) has found an irregular variation in α Orionis with a total range of 8 km/sec, and Deutsch discovered (1956*a*) a similar variation in α^1 Herculis with a range of 5 km/sec. The velocity variations show some correlation with the light-variations of these stars, and they may well manifest a kind of activity in the reversing layers that is somehow associated with the mass-ejection process.

Except possibly for the H and K lines, all the CS lines in a stellar spectrum appear to yield the same radial velocity. Recent measures in α Orionis and α^1 Herculis fail to confirm the dependence of velocity upon the strength of the CS line, which was reported by Spitzer (1939) from early coudé spectrograms.

Table 1 shows that even the expansion velocity which is indicated by the CS lines of Ca II is usually nearly the same as that indicated by the CS lines of other elements, where the latter are strong enough for measurement. Some of the velocity differences are probably significant, however, and notably so in the case of α^1 Herculis. From extensive measures of the CS lines in this star and in α^2 Herculis as well, the different expansion velocities are well established as given in Table 1. Probably the difference is caused by the blending of interstellar components of H and K with the corresponding CS lines. However, this explanation will probably not suffice for the velocity difference observed in α Orionis, for the CS lines are so strong in this star that no appreciable effect on their wave lengths can be produced by interstellar components with the expected strengths and wave lengths.

2.5. Line Profiles

The results will probably well repay a careful investigation of differential velocities within the CS spectrum; for, if these exist at all, they afford a measure of the gradients of velocity and ionization within the CS envelope. For the time being, it is convenient to analyze the spectrum of an M giant into two components: a "normal" one due to the reversing layer and an "abnormal" one due to a CS envelope with very low excitation temperature. Actually, the best-observed supergiants show some lines of intermediate character, as was well known to Adams (1941) and Spitzer (1939). Examples are the three strongest Fe I lines in Plate I, $\lambda\lambda$ 4046, 4064, and 4072, with excitation potentials of 1.5 ev. Their profiles are evidently asymmetrical, with the maximum of absorption shifted shortward from the center of the line. The asymmetry indicates that the gas already has a net expansion even near the top of the reversing layer, where these spectroscopic features must be formed.

One might expect the asymmetries present in the profiles of low-excitation subordinate lines in α Orionis to produce an effect on radial-velocity determinations, even when these are made at dispersions too low for the full resolution of the line profiles. A gradient of radial velocity with excitation potential is indeed well established for a number of late-type variable stars. The effect was first

discovered by Adams (1941), and subsequent examples have been discussed by Merrill (1945, 1946*a*, *b*, 1947*a*, *b*), Greenstein (1948), Joy (1954), Merrill and Greenstein (1956), Deutsch and Merrill (1959), and Merrill (1959). The value of $\Delta RV/\Delta EP$ usually lies in the range from +1 to +3 km/sec/ev. Deutsch (1959*a*) has shown that the existence of such a velocity gradient implies the transport of enough momentum through the reversing layer that one can no longer neglect the corresponding term in the momentum equation. This means that the structure of these atmospheres deviates appreciably from that corresponding to hydrostatic equilibrium; it is much more appropriate to consider them as in a stationary state of outflow.

Curiously enough, the best existing high-dispersion measures of (relatively) non-variable M giants fail to show a gradient of radial velocity with excitation potential. The stars that have been investigated are β Pegasi (Davis 1947; Merrill 1960), α^1 Herculis (Merrill 1960), and α Orionis (Deutsch, unpublished).

Apart from the line asymmetries in α Orionis and α^1 Herculis, Spitzer (1939) has found other evidence in the profiles of subordinate lines for marked stratification in the atmospheres of these stars. These profiles approximate damping-curves, but with excessive widths, which vary from line to line. Spitzer attributes these profiles to small-scale turbulence with a velocity spectrum that approximates a dispersion law, with a fictitious damping constant corresponding to a velocity of 8 km/sec for the Fe I lines in α Orionis and of 4 km/sec for these lines in α^1 Herculis. The central intensities show a pronounced increase with excitation potential for lines of the same width. The profiles of H and K most clearly reveal the contributions of atmospheric layers which differ enormously in their properties; in these lines the effects of stratification may be clearly seen even in the normal giants.

2.6. The H and K Lines

Figure 5 shows schematic K-line profiles characteristic of normal late-type giants. Adopting the terminology of the solar spectroscopists, we may designate the damping wings as K_1, the emission line as K_2, and the central absorption reversal as K_3. The reversing layer is evidently responsible for K_1 and the chromosphere for K_2. In giants earlier than type M0, the chromosphere alone is also responsible for K_3; but in the M giants a CS component also appears. This component dominates K_3 in the later subclasses. As stated in an earlier section, the CS component of K_3 may be differentiated from the chromospheric component, when the profile is fully resolved, by a central intensity indistinguishable from zero.

That these attributions are essentially correct is best indicated by observations of M giants in binary systems. From α Herculis itself and from a few comparable visual binaries, we find that K_2 cannot be seen in the space between the stars (see Pl. II) and that only the deep absorption component of K_3 is visible in the spectrum of the companion. In several spectroscopic binaries,

again, we find that only this feature remains stationary, while all other components of the K line display normal orbital Doppler shifts. Moreover, in single M giants, the deep component of K_3 generally yields an expansion velocity between 5 and 25 km/sec, whereas the shallower K_3 line found in spectra earlier than M1 usually yields a differential velocity $|\Delta A| < 4$ km/sec, with a preponderance of velocities indicating slow contraction rather than expansion (Wilson and Bappu 1957).

Considerable diversity exists among the K-line profiles of normal giants, especially in the strength of K_2. However, the profiles do exhibit certain correlations with spectral type, as shown in Figure 5. In particular, as the type grows

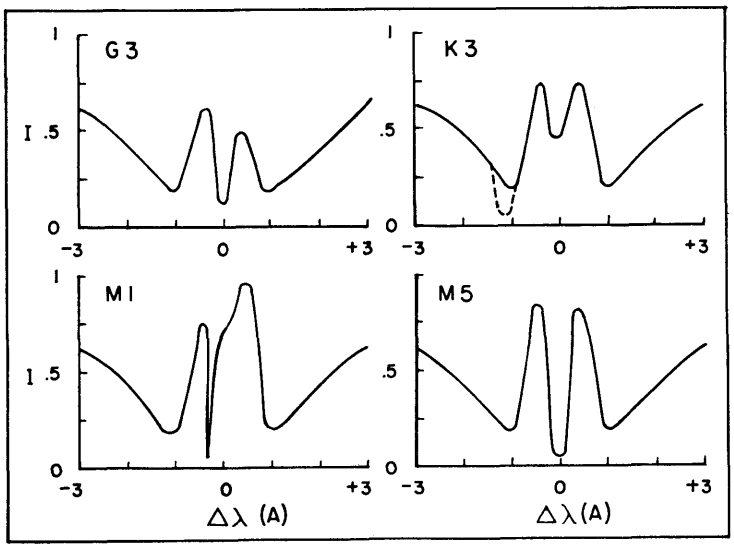


FIG. 5.—Schematic profiles of the K line in the spectra of normal giants

later among normal giants, K_2 tends to strengthen and the chromospheric component of K_3 to become shallower. In the early M giants the latter feature sometimes nearly disappears, leaving a wide, flat-topped emission line interrupted only by the deep and sharp CS core. In some late K and early M giants, there is evidence for a transitory deep absorption component at an expansion velocity of about 75 km/sec, as shown in the K3 profile of Figure 5. Wilson and Bappu (1957) have noted this feature in their published reproduction of the spectrum of γ Aquilae (K3 II). Variable features of this kind may represent the earliest manifestation of mass ejection. Absorption features which are somewhat similar and definitely variable in intensity and wave length have now been observed in several K-type supergiants. While these features evidently cannot be ascribed to envelopes as extensive as those around M-type supergiants, they may reasonably be interpreted as indicators of a mass-loss process in the K-type supergiants.

The most notable regularity in the profiles of H and K in late-type spectra is the remarkable correlation of their widths with M_v (Wilson and Bappu 1957). These authors find that the widths W_0 of H and K are the same in any one star and, over a range of more than 15 mag., are proportional to $L_{\text{vis}}^{1/6}$, where L_{vis} is the visual luminosity of the star. The relation between W_0 and L_{vis} appears to be an exact one and is independent of spectral type. No full theoretical interpretation has yet been given for this observational result, but it appears that the widths of K_2 and H_2 must probably be attributed to Doppler broadening. The velocities required will depend on the optical thickness, τ_0, of the chromosphere in the center of K. If this is small, then the Doppler width of the source function must be nearly equal to the half-width $W_0/2$ of K_2; if τ_0 is large, then the Doppler width may be appreciably smaller than $W_0/2$ (Goldberg 1957). For stars of luminosity class I*a*, where $W_0/2 \simeq 90$ km/sec, the velocities corresponding to these two cases are approximately 110 and 25 km/sec, respectively. Hoyle and Wilson (1958) propose to associate the observed velocities $W_0/2$ directly with an appropriate mean velocity of the convective elements at that level in the photospheric layers where the energy flux is equally shared by convection and radiation. Other theoretical discussions have been given by Kraft (1958), de Jager (1958), and Schatzman (1958).

2.7. Turbulent Velocities

The curves of growth for late-type giants invariably give evidence of small-scale turbulence of the order of 2–5 km/sec, increasing toward higher levels in the reversing layer (Wright 1947; Huang and Struve 1952; Bonsack 1959), and for additional large-scale turbulence in the supergiants which widens the lines without strengthening them. In addition, the spectra of such binary stars as 31 and 32 Cygni, ζ Aurigae, and VV Cephei, during the chromospheric phases of their eclipses, indicate turbulent velocities of the order of 10–20 km/sec in the highest levels of the chromosphere (McKellar 1954). The evidence from these binary stars therefore disposes us to believe that Doppler broadening can indeed account for the observed widths of K_2, provided that one can adopt a model of the chromosphere which is optically thick in H and K.

But, large as these velocities may be relative to thermal motions, they are still appreciably smaller than the velocity of escape at the photosphere. Table 2 gives some representative values for the escape velocity V_∞ and the thermal velocity $V_{\text{Th}} = \sqrt{(3kT/m_H)}$ as computed from the data given by Allen (1955). Evidently the turbulent velocities in the reversing layer and chromosphere, which widen the absorption lines and K_2, are incapable of ejecting matter to infinity. To understand this process, as it occurs in the M giants, we must suppose either that some gas flows through the reversing layer in an unobservable state, at much higher velocities than are measured, or that the gas in the high chromosphere is still subjected to some unknown outward force.

2.8. The Mass-Loss Process

The dynamics of the mass-loss process are evidently still very obscure. Arguing by analogy with the sun, de Jager (1959) attempted to predict the properties of stellar coronas in different parts of the HR diagram, and he then calculated the corresponding rates of mass loss due to evaporation from these hot envelopes. As might have been expected, he found coronas appreciably hotter than that of the sun only among the early-type stars near the top of the main sequence. For these objects, evaporative losses may then be appreciable on their nuclear time scales; but for the late-type giants the process appears to be ineffective. Rubbra and Cowling (1959) considered the possibility of mass loss by the action of radiation pressure, by evaporation, by shock waves, and by electromagnetic acceleration. They conclude that none of these mechanisms is likely to be sufficient, and that, if matter is to move from the photosphere of a star to infinity,

TABLE 2

Thermal Velocities and Escape Velocities in M Giants

	Star			
	⊙	gM0	gM5	cM0
$M/M_{\odot}$	1	4	4	25
$R/R_{\odot}$	1	75	100	630
T (° K)	5800	3400	2800	3000
V_{Th} (km/sec)	13	10	9	9
V_{∞} (km/sec)	620	140	120	125

it is probably necessary to start it off with nearly the velocity of escape. Wilson (1960) has also considered mass loss resulting from radiation pressure; he finds that the force due to radiation pressure in Lyman-α will be sufficient to expel hydrogen at a rate of $1 \times 10^{-8}\ M\odot$/yr, provided that the outward flux of Ly-α at the surface of α^1 Herculis is about two hundred times that at the surface of the sun. As a possible explanation of so high a Ly-α flux, he suggests that the "active areas" where Ly-α originates cover virtually the whole chromosphere of α Herculis and have a temperature some 4000° hotter than the active areas where Ly-α originates in the solar chromosphere. Wilson's hypothesis requires that about 1 per cent of the total luminous flux from α^1 Herculis appear in Ly-α for mass loss at the rate of $1 \times 10^{-8}\ M\odot$/yr.

Hoyle (1956) has pointed out that if the ionization energy of hydrogen atoms could be converted to kinetic energy, it would produce a velocity of 60 km/sec, which is probably very nearly the velocity of escape for many late-type giants and supergiants. He therefore suggests that the atmospheres of these stars are in a sense unstable with respect to escape. He argues that it is plausible to set the rate of momentum transport by mass flow equal to the rate of momentum

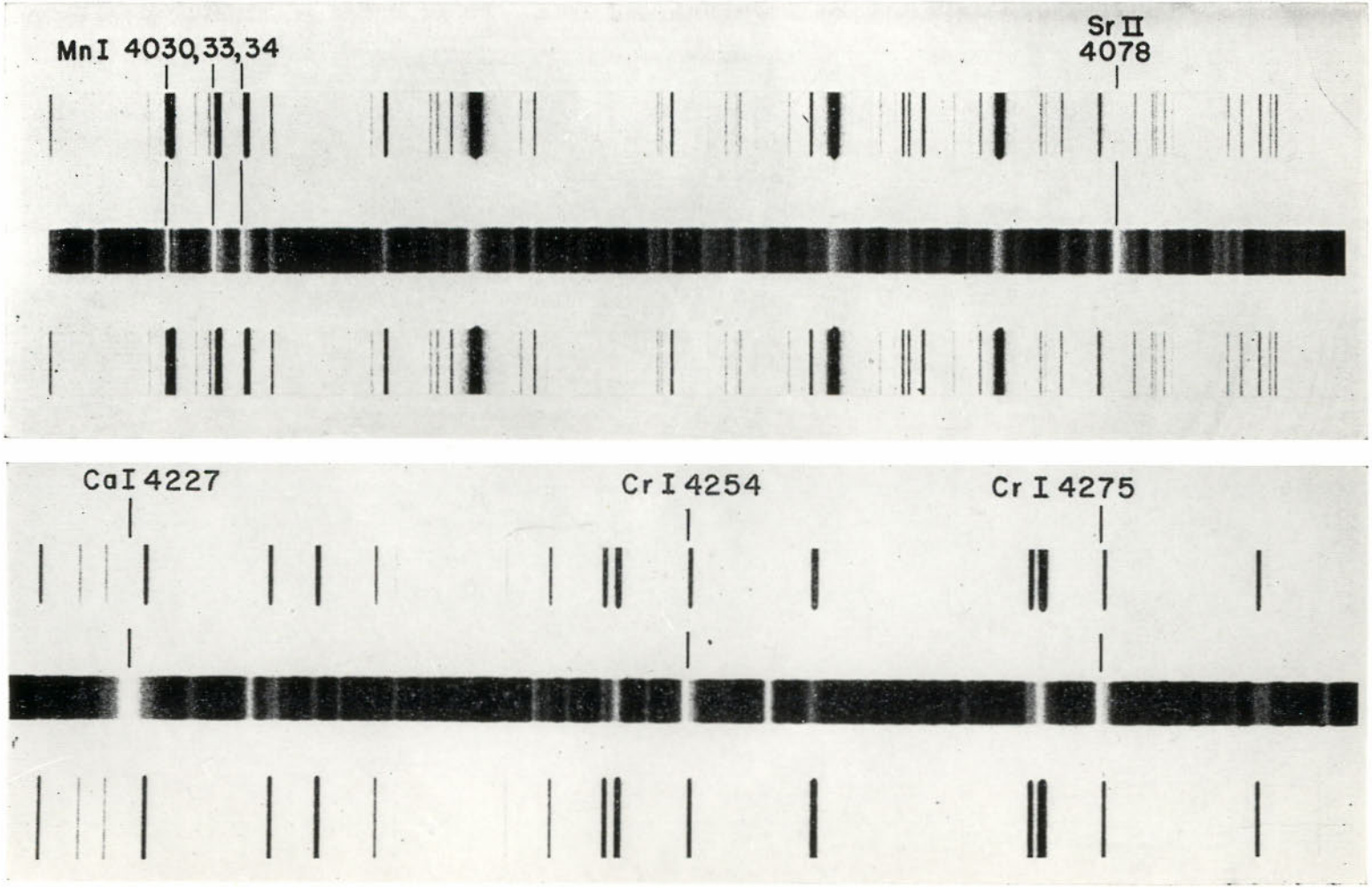


PLATE I.—Two regions in the spectrum of the M-type supergiant α Orionis, showing the doubling of the strong zero-volt absorption lines. Original dispersion, 4.5 A/mm

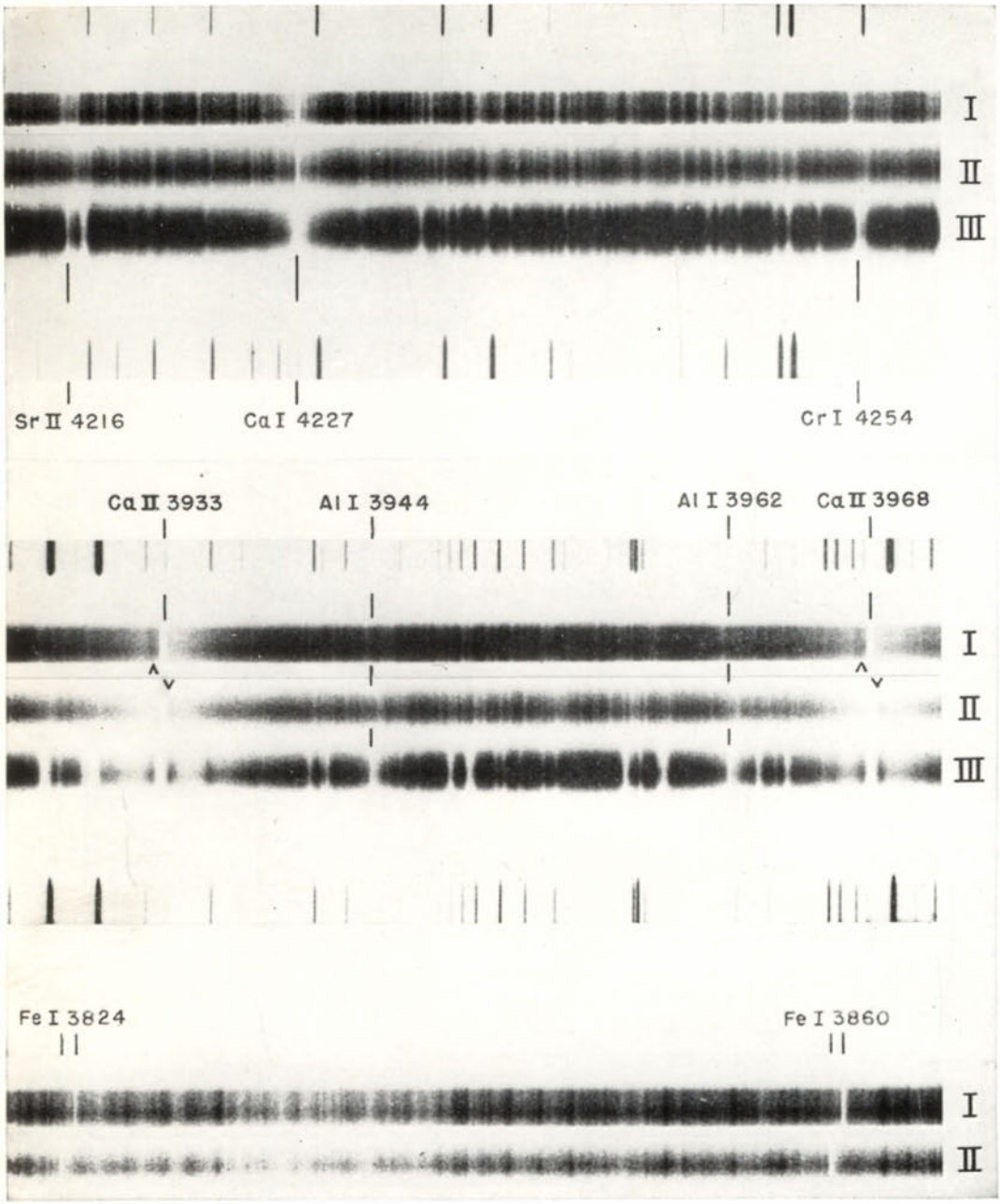


PLATE II.—Coudé spectra of α Herculis. Strips *I* and *II* show α^2 Herculis (the G-type star) at two different phases in its 52-day spectroscopic orbit around an invisible companion. Strips *III* show α^1 Herculis (the M-type star). Strips *II* and *III* are from the same spectrogram, made with both stars on the spectrograph slit. In the lowermost pair, the lines from the reversing layer have been lined up. Original dispersion, 4.5 A/mm.

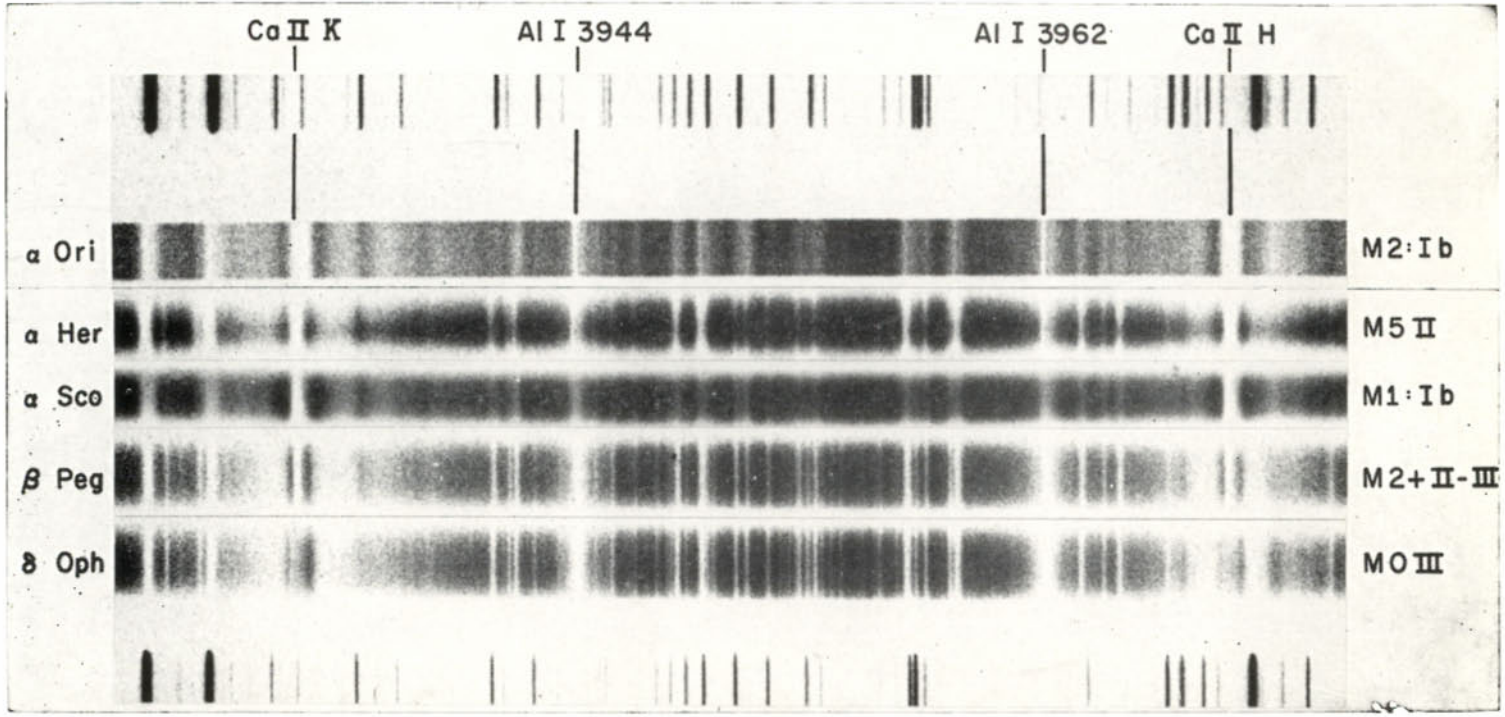


PLATE III.—The region of H and K in the spectra of five representative M-type giants and supergiants. Original dispersion, 4.5 A/mm

transport by radiation, and on this basis he computes a rate of mass loss about one hundred times greater than that found by Deutsch.

The proposals of Hoyle and Wilson can probably be related to each other. As a simple qualitative model, let us suppose that ionized hydrogen emerges from the photosphere of α^1 Herculis with a velocity sufficient to carry it to a relatively small height h above the photosphere. There it recombines and falls back to the photosphere in the neutral state. A small fraction of the ionized hydrogen emerging from the photosphere, say 10^{-4}, possesses enough momentum to rise above h. There it forms an envelope which is optically thick in Ly-α and which expands at a rate of about 10 km/sec. The flux of momentum required to support the expansion is provided by the outward flux of Ly-α produced in the recombination of the hydrogen atoms below h; most of this radiative flux must eventually find its way back to the photosphere. The net outward flux of energy to the envelope results from the longward Doppler shift of the Ly-α, which returns to the star after scattering in the envelope. If the expansion velocity is 10 km/sec, this net energy flux amounts to 10^{-4} of the outward flux of Ly-α from the recombinations at h and is therefore just sufficient to carry the higher gas to infinity.

Another proposal has been put forward by Deutsch (1959*b*), who suggests that the gas is literally "pushed" to very large distances by the upwelling of matter from below. The process is similar to the inverse of the accretion flow studied by Bondi (1952). Deutsch also notes that the observations indicate cold envelopes around the M giants, not hot "coronas." In the sun the temperature decreases in the photosphere, reaches a minimum in the reversing layer, then climbs again through the chromosphere and on into the very hot corona. In the M giants the temperature also falls to a minimum and then rises again in the chromospheric layers that are responsible for K_2. But then, in contrast with the solar case, the temperature falls again to the very low value that characterizes the escaping envelope.

In connection with their work on the S-type long-period variable star R Cygni, Deutsch and Merrill (1959) suggested that this difference in temperature profiles might be understood in terms of the ratio R of the fluxes of kinetic energy and momentum associated with jets of gas in the photospheric layers. Perhaps it is reasonable to suppose that when relatively large quantities of matter are injected into the envelope at low velocities, so that R is relatively small, most of the injected kinetic energy can escape with the matter that flows to infinity. When R is large, however, so that little or no matter escapes, the envelope must become very hot in order to lose the kinetic energy dissipated in the envelope. The processes available are radiation, conduction, and evaporation; and all are likely to occur in a hot corona of relatively low mass.

2.9. Binary Stars and Variable Stars

We have already seen that binary systems involving M giants are especially strategic objects for verifying the true circumstellar nature of the displaced

zero-volt cores and for estimating the dimensions of the envelopes in which they arise. It is now necessary to comment briefly upon a number of systems of this kind.

No visual binaries have yet been found which give such unequivocal evidence of a common envelope as was found in α Herculis. However, there are several other pairs which probably show the same phenomenon. One is η Geminorum (M3 II). The visual companion is of type G0 III or IV; visually, it is nearly 5 mag. fainter than the M star and is separated from it by only 1″. Spectra of the companion can therefore be obtained only on nights of exceptionally good seeing. The best available coudé spectrograms give a strong indication of CS cores in its H and K lines. If the absolute magnitude assigned to the M star by Wilson is correct, the distance between the two stars is about 150 a.u. in projection on the plane of the sky.

The M star is itself a semiregular variable and an eclipsing binary with an orbital period of 2984 days (van Schewick 1949); McLaughlin and van Dijke (1944) have published a spectroscopic orbit. The coudé plates confirm the velocity variation of the M star, and they show that its CS lines at H and K are stationary, or very nearly so. The expansion velocity shown in Table 1 is counted from the systemic velocity given by McLaughlin and van Dijke. Its large value compared with the other stars in Table 1 suggests the very credible inference that mass ejection proceeds more vigorously in the presence of a relatively close companion.

Another visual binary that may have a common envelope is HD 188037. The separation of this pair is only 0″.7; resolution on the slit of the spectrograph has not been attempted. Bidelman classifies the composite spectrum as approximately M5 II + A0. If this classification is correct, the deep absorption line observed at K can probably not be attributed to the interstellar gas, for it is about twice too strong and indicates a discrepant velocity. The line must then arise in a common envelope, with a radius exceeding 500 a.u. However, the coudé spectrograms show that K_2 is absent, and this may be taken as an indication that the M star is of luminosity class I*a*. In this case it lies at the same distance as the OB association I Vulpeculae (Morgan, Whitford, and Code 1953), the center of which is only a degree away, and the K line could be attributed to the interstellar gas alone.

A similar uncertainty exists in the case of α Scorpii. The companion, of type B4 V, lies 3″ from the M star; if the distance is 180 psc (Stone and Struve 1954), the separation is 550 a.u. in projection on the plane of the sky. The B star exhibits two sharp, deep absorption components at K (Deutsch 1959*c*). Both may be interstellar, although the stronger one is then rather discrepant in both strength and velocity.

As compared with other stars of comparable type and luminosity, both HD 188037 and α Scorpii show decidedly weak CS lines. VV Cephei, which is an eclipsing binary with a B-type companion, also shows the same effect; the

CS spectrum is present (McKellar, Wright, and Francis 1957), but much less developed than we might expect. These observations suggest that the radiation from a hot companion may appreciably increase the ionization of an M-star envelope. Supporting evidence for this view comes from observation of other M giants with hot companions, including δ Sagittae (M2 + A), T Coronae Borealis (gM3 + Q), Boss 5481 (M1ep Ib + B), and Boss 1985 (gM3ep). The last three of these stars show emission lines of [Fe II], which indicate that they are immersed in large envelopes of low density. In α Scorpii the envelope is sufficiently large to be resolved against the sky (Struve 1954). In all these stars the CS absorption lines are weak or absent.

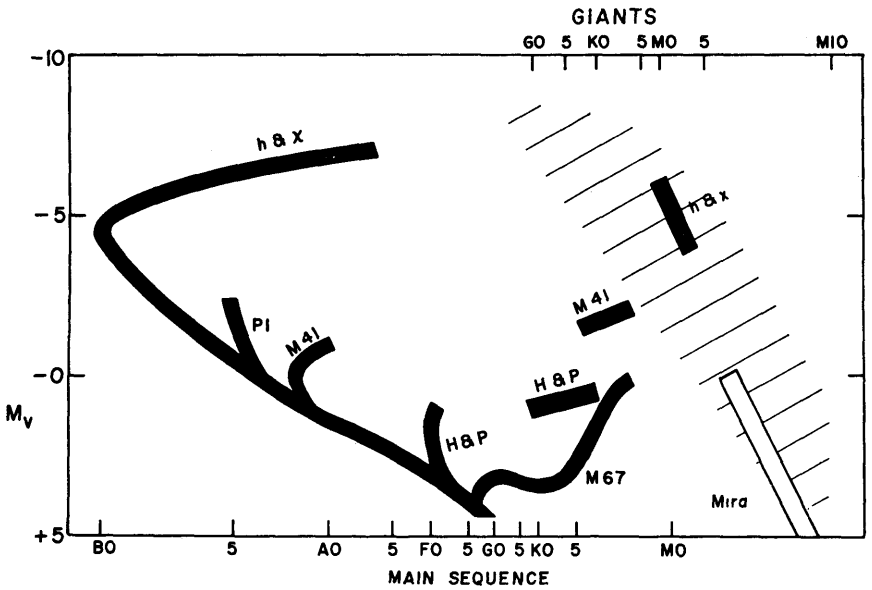


FIG. 6.—Hertzsprung-Russell diagram adopted from Sandage (*Ap. J.*, 125, 436, 1957). Stars within the ruled area show spectroscopic evidence of mass loss.

Mira is another M giant with a hot visual companion, in this case a unique variable star of early type and of absolute magnitude about +8. The spectrum shows variable P Cygni lines of H and variable emission lines of Ca II, He I, and Fe II (Joy 1954). Like the other long-period variables which have been adequately observed, the M star in this system shows a deep absorption core at K, which is probably CS; the B star shows a similar line, but much weaker, in projection against the strong emission line at K. The velocity of the system is large enough that one can confidently rule out an interstellar origin for the Ca II absorption lines in the B star. They evidently arise in a common CS envelope. The projected separation of the pair is only about 50 a.u.; however, the motion is so slow that the orbit must be viewed under a very high inclination,

and the true separation is likely to be at least 500 a.u. Deutsch (1958) has suggested that the B star is actually a white dwarf, which owes its excessive and variable luminosity and its spectroscopic anomalies to the accretion of hydrogen from the CS envelope thrown off by the long-period variable. The unresolved companion of the nebulous long-period variable R Aquarii is likely to be a similar object.

Several other long-period variables with types later than M5 have also been observed for CS absorption lines. Present indications are that they are always present in these objects, including the long-period variables of class S.

Referring to the HR diagram of Figure 6, we may briefly summarize this section, then, with the conclusion that all stars in the ruled area lose mass from cool circumstellar envelopes which can be spectroscopically observed.

§ 3. THE RATE OF MASS EJECTION

The data that have been summarized in § 2 constitute compelling evidence that most M giants are losing mass in a process that can be spectroscopically observed. But in most M giants of luminosity class III, and especially in the early M giants, the observations have now shown that the CS lines are much weaker than in the bright giants and supergiants. Unless most of the calcium is doubly ionized in the envelopes of these more numerous M stars, we must conclude that they lose mass at a much slower rate than does the M5 II star α^1 Herculis. But in the last section we have seen that even if the rate derived from α^1 Herculis could be assigned to all M giants, it would be barely sufficient to satisfy the evolutionary requirements.

We shall shortly discuss the ionization in M-star envelopes. First, however, we shall critically review the determination for the rate of mass loss in α^1 Herculis to establish whether Deutsch's estimate (1956*a*) can be appreciably increased. The determination was made from measures of the equivalent widths of Ca II H and K, and of Ca I 4227 in the CS spectrum of the G-type companion. From these equivalent widths, τ_0 was found in Strömgren's (1948) curve of growth for zero damping and hence the surface density of Ca II and Ca I along the line of sight to the G star. To convert these results into the corresponding numbers of particles for the whole envelope, it was necessary to assume a model for the geometry of the system and for the density gradient in the envelope. Finally, to obtain the rate of mass loss, it was necessary to discuss the ionization in the envelope.

We shall first consider the effects upon the 1956 determination of uncertainties in the geometry of the α Herculis system. The model that was adopted is shown in Figure 7. The visual companion was assumed to lie in the plane of the sky, and the path length from it to the rim of the envelope was taken equal to the projected separation, Δ, of the stars, or 700 a.u. It was also assumed that the gradient of expansion velocity is small, in agreement with the profiles of the CS lines, so that the density follows an inverse-square law.

Let us now take into account the possibility that the G star may lie some distance S in front of the plane of the sky and that the radius of the envelope, R_E, may have any value larger than Δ. If V is the expansion velocity, we may then write, for the rate of ejection R of Ca II ions,

$$R = 16\gamma\Delta V N_G \,. \tag{8}$$

In this expression, N_G is the surface density of Ca II ions along the line of sight to the G star, as derived from the curve of growth, and γ is a factor depending on the geometry, viz.,

$$\gamma = \frac{\pi/4}{\tan^{-1}\Delta/S - \sin^{-1}\Delta/R_E} \,. \tag{9}$$

For the nominal configuration of Figure 7, with $S = 0$ and $R_E/\Delta = \sqrt{2}$, γ then equals unity; for no reasonable values of S and R_E will γ differ appre-

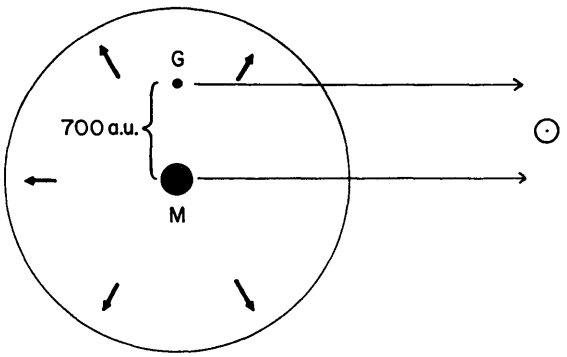


FIG. 7.—The adopted model of α Herculis. The diagram is not to scale; the adopted radii of envelope and M star are in the ratio of 1:370.

ciably from this value. For example, if $S = 0$ and $R_E \to \infty$, then $\gamma = \frac{1}{2}$; if $S \to -\infty$, and $R_E \to \infty$, $\gamma = \frac{1}{4}$. Departures from the nominal geometry assumed in 1956 are therefore unlikely to produce any large error in the rate of Ca II ejection derived from the CS lines in the spectrum of the G star.

The photometry of the CS lines was somewhat crude, and it was seriously complicated at H and K by the complex profiles of the chromospheric lines on which the CS components are superposed. Nevertheless, it is considered unlikely that Deutsch's values for the equivalent widths are in error by more than, say, 20 per cent. A more serious error may have arisen, however, in the determination of the Doppler width, b, of the line absorption coefficient. This is required to give the argument W/b with which one enters the curve of growth. After an approximate correction for the instrumental profile, Deutsch concluded that the contour of λ 4227 was Gaussian, with a central absorption of 90 per cent and a Gaussian parameter $a = 110$ mA. But the spectrograms do not exclude the possibility that this line is really saturated, with a central intensity of very

nearly zero. If this is the case, then the contour cannot be adequately represented by a Gaussian profile, and the Doppler width, b, of the absorption coefficient is appreciably smaller than the measured half-width of the line (Goldberg 1957).

Unfortunately, it happens that in the G-star spectrum the CS H and K lines lie on the flat part of the curve of growth, where the value obtained for N_G depends very sensitively on the entering argument, W/b. If the Doppler width, b, is halved, the curve of growth yields a value of N_G which is 180 times larger than the 1956 result, and the rate of mass loss is increased by the same factor! In fact, the spectrograms do not exclude the possibility that b is as small as 51 mA. This corresponds to the not unreasonable value of $v_0 = 3.8$ km/sec for the Doppler velocity, or to a kinetic temperature of 4×10^4 °K. At Ca I 4227, this Doppler velocity yields a half-width at half-intensity of 86 mA; and if one approximates the contour with a Gaussian profile, he will obtain for the Gaussian parameter $a = 103$ mA, which is near enough to the observed value, $a = 110$ mA.

It is a curious property of the CS H and K lines in the α Herculis visual binary that their equivalent widths differ by a factor of less than 2, as may be recognized by inspection of Plate II. Now, if the G star lies in the plane of the sky, as in the nominal configuration, any admissible density gradient in the envelope will lead to a much higher surface density of Ca II ions in front of the M star than in front of the G star. With the inverse-square density law assumed in 1956, the expected ratio of surface densities in the nominal configuration is $N_M/N_G = 330$. In this case, one can understand the near-equality of the CS K lines only by supposing that in both spectra the K line lies on the flat part of the curve of growth. But this condition on the two K lines will not be satisfied in the nominal configuration by any value of b appreciably different from the 110 mA used in 1956.

However, the ratio of surface densities for an inverse-square density law is given by the relation

$$\frac{N_M}{N_G} = \frac{4\gamma}{\pi} \frac{\Delta}{R_M}, \tag{10}$$

where R_M is the radius of the M star and γ is the factor which describes departures from the nominal configuration. It is therefore possible that N_M/N_G is appreciably less than 330. Its most probable value lies between 160 and a minimum of 80. Moreover, if the expansion velocity is in fact not constant but diminishes slowly outwards, then it can be shown that N_M/N_G is further reduced. For the case where the motion is parabolic, N_M/N_G may assume values approaching 22 as a lower limit. If $b = 51$ mA instead of 103 mA, the curve of growth yields, for the observed ratio N_M/N_G, the value 50 instead of 360.

From this discussion, then, we may conclude that the true value of b for the CS K lines in the α Herculis pair probably lies in the range between 51 and 103 mA. Studies are now under way of the doublet ratio H/K in early M giants to

discover whether the CS lines do, indeed, saturate even at relatively small equivalent widths.

Meanwhile, it is instructive to consider the rates of mass loss in representative M giants of various spectral subclasses corresponding to these two extreme values of the Doppler width. If we suppose that in all M-giant envelopes the ionization is such that nearly all Ca resides in the first state of ionization, we find that the rate of mass loss may be given by the equation

$$\log(-\dot{M}) = -16.28 + \log(b\,\tau_0 R\,V)\,. \qquad (11)$$

In this relation, $-\dot{M}$ is the rate of mass loss per star in units of solar masses per year; b is the Doppler width of the absorption coefficient for the K line, in units of mA; τ_0 is the optical depth at the center of this CS line; R is the stellar

TABLE 3

RATES OF MASS LOSS FOR M GIANTS WITH $M_v > -2.5$

Sp.			M1	M3	M5
$R(R\odot)$			90	125	160
V(km/sec)			18	13	8
W_K(mA)			50	270	550
b(mA)	103	$W_K/2b$	0.24	1.31	2.67
		log τ_0	− 0.4	0.7	2.75
		log N(cm^{-2})	12.0	13.1	15.2
		log $-\dot{M}(M\odot$/yr)	−11.5	−10.4	− 8.4
	51	$W_K/2b$	0.49	2.65	5.40
		log τ_0	− 0.1	2.75	4.1
		log N(cm^{-2})	12.0	14.9	16.2
		log $-\dot{M}(M\odot$/yr)	−11.4	− 8.6	− 7.3

radius, in units of the solar radius; and V is the expansion velocity, in units of km/sec. Invoking the observational results in Figures 1 and 3, we then obtain the rates of mass loss given in Table 3.

For both values of b, Table 3 indicates a sharp increase in $-\dot{M}$ with advancing spectral type. According to Neckel (1958), the space density falls by about 50 per cent in successive subclasses of M giants. Despite their low space density, it is therefore the late M giants (M5–M8) which provide most of the mass ejected per unit volume of space. For these stars Neckel obtains a density near the sun of 5×10^{-7} pc^{-3}. Let us suppose that they are distributed in a layer of 700 pc effective thickness, like the earlier M giants, and that they all lose mass at the rate given for an M5 star in Table 3. For the integrated mass loss from the late M giants we then obtain $1 \times 10^{-12}\,M\odot$ pc^{-2} yr^{-1} if $b = 103$ mA, and $2 \times 10^{-11}\,M\odot$ pc^{-2} yr^{-1} if $b = 51$ mA. Both these rates are significantly smaller than Schmidt's (1959) estimated total rate of mass ejection, viz., $6 \times 10^{-10}\,M\odot$ pc^{-2} yr^{-1}. With the smaller value of b, the M giants still fail to satisfy the evolutionary requirements by a factor of 30.

The very rapid increase in $-\dot{M}$ with advancing type suggests the possibility that the non-Mira M giants with types later than M6 may eject mass at a rate so much greater than do the M5 giants that they, in fact, play the dominant role in mass ejection despite their very low space density. However, the fragmentary observations at hand of very late M giants appear not to support this view.

We now turn to the possibility that we may have seriously underestimated $-\dot{M}$ in the early M giants, because in their envelopes most of the calcium is doubly ionized and hence unobservable. The degree of ionization of Ca I can be shown to be constant throughout the envelope if the following assumptions can be made: that the gas pressure, P, falls as r^{-2}, corresponding to isothermal expansion at constant velocity; that the dilution factor D has its geometrical value; and that the free electrons are provided by single ionization of Na, Al, K, and Ca. These assumptions underlie the 1956 work on α Herculis. However, it is probably more realistic to suppose that the gas is decelerated as it flows outward. Moreover, the effects of physical dilution and of recombinations on excited levels will tend to reduce D below its geometrical value. The ratio P/D is therefore likely to increase outward, and it can then be shown that the ionization falls monotonically toward zero.

The following case of variable ionization has recently been worked out in detail. The flow is taken as parabolic and isothermal, so that $P = P_1\ \rho^{-3/2}$ where ρ is the distance in units of the stellar radius R. The dilution factor is approximated by the expression $D = \rho^{-2}/4$. If double ionization is negligible, it then follows that, in the relevant range of P_1 and T, the surface density of Ca II is

$$N = \frac{2ARP_1}{kT_e}, \tag{12}$$

where A is the abundance of Ca, in Ca nuclei per nucleus. With this relation it is possible to compute the gas pressure P_1 near the star, and then to test a posteriori the assumption that double ionization is everywhere negligible. If we take the ionization temperature T_i and the electron temperature T_e both equal to the effective temperature T_{eff}, we find that this assumption is verified for the late M giants but not for those earlier than M4. When due regard is taken of the unobservable Ca III, the rates of mass loss in the early M giants become more nearly comparable with that in the later types, and all the M giants together lose mass at a rate substantially nearer to Schmidt's estimate.

However, several arguments militate against the conclusion that the M giants can in this way meet the requirements of Schmidt's result. In the first place, we might expect that T_i will be appreciably less than T_{eff} in all M-star envelopes. The accessible ultraviolet continuum of the K giants is known to fall well below the Planck curve, and a large deficiency has recently been demonstrated in the vacuum ultraviolet of the solar spectrum. Moreover, if T_i equals T_{eff}, then

we cannot explain the strength of the neutral CS lines that are observed in the late M giants. On the other hand, if we suppose that T_i equals the boundary temperature, or slightly lower, we can then account for these neutral lines, but at the cost of losing the higher rates of mass loss in the early M giants.

The correlation between radial velocity and spectral type, as observed in the CS lines of the normal M giants, provides another indication that double ionization is negligible in these envelopes. For if the doubly ionized region exists at M1 and contracts toward the star in later types, we should expect the expansion velocities to increase toward the escape velocity as the type grows later—whereas the opposite effect actually occurs.

In the 1956 discussion of α Herculis it was assumed that the ionizing radiation is provided by the invisible companion of the G star, which was taken to be of spectral type A3 V. With due regard for the geometrical dilution, the equation of ionization equilibrium then led to a mean electron density $n_e = 2 \times 10^6$ cm^{-3} along the line of sight to the G star. In the nominal configuration, this is the electron density at a distance from the M star of $r = 620$ a.u. An independent estimate of n_e was also made from the observed surface density N_G (Ca) of all the calcium atoms and ions along the line of sight. This estimate was obtained by supposing that the atomic abundances have their normal (solar) values in the envelope and that the envelope is an H I region in which nearly all the metal atoms are singly ionized. The result of this calculation was the much smaller value $n_e = 0.10$ cm^{-3}. Accordingly, it was necessary to conclude that the gas of the envelope is concentrated in relatively small clouds, which are separated by distances approximately 240 times larger than their diameters.

This awkward result will be somewhat ameliorated if the lower value of b is correct, for this raises the ratio of Ca II to Ca I in the envelope. In addition, recent observations indicate that the third star in the α Herculis system has a spectral type much later than A3 V, and this, too, will relax the difficulty in establishing a reasonable ionization equilibrium. But, after allowance for both these effects, a significant discrepancy still remains. Probably this may be attributed to the severe idealization of the model considered. In fact, each of the three stars in the system probably contributes appreciably to the ionizing radiation along different parts of the two lines of sight through the envelope. With only a minimum of knowledge concerning the true geometry of the system and the aspect in which it is viewed, it seems very difficult to give a definitive discussion of the ionization equilibrium in the envelope.

To summarize this section, we may now draw the following conclusions with respect to the rate of mass loss from α^1 Herculis and from other M giants:

1. The spectrograms of the α Herculis pair admit the possibility that the Doppler widths, b, of the absorption coefficients for Ca II K and for Ca I 4227 are smaller than was assumed in 1956, the correction factor probably being between 0.5 and 1.0.

2. Because the K line lies on the flat part of the curve of growth, this change in b can produce an increase in the surface density of Ca II, along the line of sight to the G star, by a factor as large as 180, and the rate of mass loss increases by the same factor.

3. The ionization temperature was overestimated in the 1956 work. The correction of this error and a simultaneous reduction of b will relax, but not remove, the requirement that the envelope be condensed into relatively small dense clouds.

4. If double ionization of Ca is negligible in all M-star envelopes, as we should expect it to be, then the rates of mass loss are several hundred times less in the early M subclasses than in the late. Despite the greater space density of the early M giants, they then eject less matter in the aggregate than do the later stars, and the net rate of mass loss from all the M giants together fails by a factor between 30 and 200 to satisfy the evolutionary requirements.

5. This deficiency will be removed if unobservable mass loss occurs in the G and K giants at rates comparable with that observed at M1.

REFERENCES

ADAMS, W. S.	1941	*Ap. J.*, **93**, 11.
	1945	*Pub. A.S.P.*, **57**, 95.
	1956	*Ap. J.*, **123**, 189.
ADAMS, W. S., and MACCORMACK, E.	1935	*Ap. J.*, **81**, 119.
ALLEN, C. W.	1955	*Astrophysical Quantities* (London: University of London, Athlone Press).
BERGH, S. VAN DEN	1957	*Ap. J.*, **125**, 445.
BLAAUW, A.	1951	*Sterrekundig Coll. v.d. Nederlandse Astr.-Club*, No. 9, p. 31; see also C. P. GAPOSCHKIN, *Variable Stars and Galactic Structure* (London: Athlone Press, 1954), p. 9.
BONDI, H.	1952	*M.N.*, **112**, 195.
BONSACK, W. K.	1959	*Ap. J.*, **130**, 843.
BURBIDGE, E., and BURBIDGE, G.	1958	*Encyclopedia of Physics*, ed. S. FLÜGGE (Berlin: Springer-Verlag), **51**, 134.
DAVIS, D.	1947	*Ap. J.*, **106**, 28.
DEUTSCH, A. J.	1956*a*	*Ap. J.*, **123**, 210.
	1956*b*	*Pub. A.S.P.*, **68**, 308.
	1958	*A.J.*, **63**, 49.
	1959*a*	*Empirical Determination of Stellar Photospheric Structure*, ed. DE JAGER and NEVEN ("Comm. Obs. Roy. Belgique," No. 157).
	1959*b*	*Ninth International Astrophysical Symposium, Liège*, p. 54.
	1959*c*	*I.A.U. Symp.*, **10**, 109 (Paris).

DEUTSCH, A. J., and MERRILL, P. W.	1959	*Ap. J.*, **129**, 570.
FESSENKOV, V. G., and IDLIS, G. M.	1959	*I.A.U. Symp.*, **10**, 115 (Paris).
GOLDBERG, L.	1957	*Ap. J.*, **126**, 318.
GREENSTEIN, J. L.	1948	*Ap. J.*, **108**, 78.
HOYLE, F.	1956	*Ap. J.*, **124**, 482.
HOYLE, F., and WILSON, O. C.	1958	*Ap. J.*, **128**, 604.
HUANG, S.-S., and STRUVE, O.	1952	*Ap. J.*, **116**, 410.
	1953	*Ibid.*, **118**, 463.
JAGER, C. DE	1958	*Eighth International Astrophysical Symposium, Liège*, p. 172.
	1959	*Ninth International Astrophysical Symposium, Liège*, p. 280.
JASCHFK, C., and JASCHEK, M.	1957	*Pub. A.S.P.*, **69**, 337.
JOY, A. H.	1942	*Ap. J. Suppl.*, **1**, 39.
KEENAN, P. C., and MORGAN, W. W.	1951	*Astrophysics*, ed. J. A. HYNEK (New York: McGraw-Hill Book Co.), p. 12.
KRAFT, R. P.	1958	*Ann. d'ap.*, **22**, 164.
MCKELLAR, A. G.	1954	*Proc. N.S.F. Conference on Stellar Atmospheres*, p. 163.
MCKELLAR, A. G., WRIGHT, K. O., and FRANCIS, J. D.	1957	*Pub. A.S.P.*, **69**, 442.
MCLAUGHLIN, D. B.	1946	*Ap. J.*, **103**, 35.
MCLAUGHLIN, D. B., DIJKE, S. E. A. VAN	1944	*Ap. J.*, **100**, 63.
MASSEVITCH, A. G.	1959	*I.A.U. Symp.*, **10**, 89 (Paris).
MERRILL, P. W.	1945	*Ap. J.*, **102**, 347.
	1946*a*	*Ibid.*, **103**, 6.
	1946*b*	*Ibid.*, p. 275.
	1947*a*	*Ibid.*, **105**, 360.
	1947*b*	*Ibid.*, **106**, 274.
	1960	*Pub. A.S.P.*, **72**, 130.
MERRILL, P. W., and GREENSTEIN, J. L.	1956	*Ap. J. Suppl.*, **2**, 225.
MESTEL, L.	1959	*Ninth International Astrophysical Symposium, Liège*, p. 235.
MORGAN, W. W., WHITFORD, A. E., and CODE, A. D.	1953	*Ap. J.*, **118**, 318.
MUSTEL, E. R.	1959	*I.A.U. Symp.*, **10**, 20 (Paris).
NECKEL, H.	1958	*Ap. J.*, **128**, 510.

PARENAGO, P. P.	1950	*A.J., U.S.S.R.*, **27**, 150.
RUBBRA, F. T., and COWLING, T. G.	1959	*Ninth International Astrophysical Symposium, Liège*, p. 274.
SANDAGE, A. R.	1957	*Ap. J.*, **125**, 422.
SANFORD, R. F.	1933	*Ap. J.*, **77**, 110.
SCHATZMAN, E.	1958	*Eighth International Astrophysical Symposium, Liège*, p. 370.
SCHEWICK, H. VAN	1949	*A.N.*, **279**, 65.
SCHMIDT, M.	1956	*B.A.N.*, **13**, 15.
	1959	*Ap. J.*, **129**, 243.
SPITZER, L., JR.	1939	*Ap. J.*, **90**, 494.
STONE, S. M., and STRUVE, O.	1954	*Pub. A.S.P.*, **66**, 191, 257.
STRÖMGREN, B.	1948	*Ap. J.*, **108**, 242.
STRUVE, O.	1954	*Sixth International Astrophysical Symposium, Liège*, p. 193.
WALKER, M. F.	1956	*Ap. J. Suppl.*, **2**, 365.
	1957	*Ap. J.*, **125**, 636.
WILSON, O. C.	1960	*Ap. J.*, **131**, 75.
WILSON, O. C., and BAPPU, M. K. V.	1957	*Ap. J.*, **125**, 661.
WRIGHT, K. O.	1947	*Pub. Dom. Ap. Obs. Victoria*, Vol. **8**, No. 1.

CHAPTER 16

Isotopes in Stellar Atmospheres

ANDREW McKELLAR

Formerly of the Dominion Astrophysical Observatory, Victoria, B.C. Now deceased

THE study of isotopes in stellar atmospheres may be considered as a step beyond the study of the abundances of the chemical elements in stars. In recent decades our knowledge of the chemical composition of a variety of astronomical bodies and regions (the earth's crust, meteorites, interstellar gas, diffuse nebulae, the solar and stellar atmospheres) has greatly increased. Between the 1920's and the 1940's, the increase in knowledge pointed toward a general similarity of chemical composition for the many and varied cosmic bodies superficially so different and showing such widely different spectra. Since about 1950, it has become possible to study departures from the general "cosmical" abundance pattern for special cases such as the atmospheres of certain stars. Reviews of this subject have been given by Greenstein (1954) and Minnaert (1957). In the further step of obtaining data on abundances of the individual isotopes of elements in extra-terrestrial bodies, the progress has necessarily been more restricted. Isotopes of only a small fraction of the elements in most of the sources can be studied by present means. For meteorites, where actual samples are available, the situation is comparatively favorable, and here no significant differences between meteoritic and terrestrial isotopic ratios have been found for any element. For stellar atmospheres, the study of isotopes dates from 1929, when bands involving the C^{13} isotope were identified by Sanford (1929) in the spectra of the cool carbon stars. Reviews of results on studies of isotopic abundances in stellar sources include those by McKellar (1949*a*) and by Garstang (1955).

In this chapter we shall attempt to outline the present situation regarding the study of isotopic abundances in stellar atmospheres, including that of the

[1] The rapid advances in isotope detection have resulted in a discovery of He^3 in the star 3 Cen A. In addition almost certainly real variations of the abundance ratio Li^6/Li^7 have been detected. A clarification of the confusing situation on the red cyanogen system has occurred so that considerable $C^{13}N^{14}$ has been found in stars which are rich in $C^{12}C^{13}$.—EDITOR, 1964.

TABLE 1

TERRESTRIAL ISOTOPIC ABUNDANCES OF SOME ELEMENTS THAT CAN BE STUDIED IN STELLAR SPECTRA

Element	Atomic Number	Isotope	Relative Terrestrial Abundance (Per Cent)*
Hydrogen	1	H^1	99.985
		H^2 or D	0.015
Helium	2	He^3	10^{-4}–10^{-5}
		He^4	100
Lithium	3	Li^6	7.42
		Li^7	92.58
Carbon	6	C^{12}	98.89
		C^{13}	1.11
Nitrogen	7	N^{14}	99.635
		N^{15}	0.365
Oxygen	8	O^{16}	99.759
		O^{17}	0.037
		O^{18}	0.204
Magnesium	12	Mg^{24}	78.60
		Mg^{25}	10.11
		Mg^{26}	11.29
Silicon	14	Si^{28}	92.18
		Si^{29}	4.71
		Si^{30}	3.12
Scandium	21	Sc^{45}	100
Titanium	22	Ti^{46}	7.99
		Ti^{47}	7.32
		Ti^{48}	73.99
		Ti^{49}	5.46
		Ti^{50}	5.25
Vanadium	23	V^{50}	0.25
		V^{51}	99.75
Yttrium	39	Y^{89}	100
Zirconium	40	Zr^{90}	51.46
		Zr^{91}	11.23
		Zr^{92}	17.11
		Zr^{94}	17.40
		Zr^{96}	2.80
Technetium	43	Tc^{97}	(Radioactive, half-life 2,600,000 years; not yet found naturally occurring on earth)
		Tc^{99}	(Radioactive, half-life 210,000 years; not yet found occurring naturally on earth)
Lanthanum	57	La^{138}	0.089
		La^{139}	99.911

* Abundances obtained from the compilation by Strominger, Hollander, and Seaborg, *Rev. Mod. Phys.*, **30**, 585, 1958.

sun. References may be made, for purposes of comparison, to figures for other celestial sources, but the standards for comparison will be the relative abundances of the isotopes in terrestrial samples. Data on the terrestrial abundances of the elements to be mentioned are listed in Table 1. Unless otherwise stated, when referring to isotopes, we shall include only the stable, naturally occurring varieties and not the usually short-lived products of nuclear reactions.

The estimates of relative abundances of isotopes in stellar atmospheres are generally made, as are those of the relative abundances of elements, from spectrophotometric measurements. For hydrogen, helium, and lithium, isotopic effects are appreciable in atomic spectra; for the heavier elements, recourse must be had to molecular spectra. The actual measurements are often uncertain for several reasons, including blending effects in late-type spectra, smallness of isotopic shift, etc. One feature of the interpretation of the measurements, however, is simpler and more direct than in the intercomparison between two different elements; this is the fact that the comparison is made between essentially identical atomic or molecular transitions. Therefore, such factors as relative transition probability and excitation temperature need not generally be considered.

§ 1. APPLICATIONS IN ATOMIC SPECTRA

As noted above, only the few lightest elements show large enough isotopic shifts in the lines of their atomic spectra to be possibly detected and studied in stellar spectra. For the simple one-electron atoms of the hydrogen and ionized helium isotopes, where the wave numbers of the spectral lines are given by

$$\nu = RZ^2\left(\frac{1}{n_1^2} - \frac{1}{n_2^2}\right),$$

and

$$R_{\mathrm{H}} = 109677.591\ \mathrm{cm}^{-1}, \qquad R_{\mathrm{D}} = 109707.448\ \mathrm{cm}^{-1},$$

$$R_{\mathrm{He}^3} = 109717.405\ \mathrm{cm}^{-1}, \qquad R_{\mathrm{He}^4} = 109722.384\ \mathrm{cm}^{-1},$$

$$R_\infty = 109737.323\ \mathrm{cm}^{-1},$$

the differences in R, the Rydberg constant, with different nuclear mass, give rise to quite large isotopic shifts. For example, in the Balmer series of hydrogen and deuterium, Hα − Dα = 1.78 A, and the shift decreases to 0.99 A at the series limit. Such amounts should be readily detectable with even moderate dispersion and resolving power.

For two- or more electron atoms, the theory of the effect of different nuclear constitutions and masses on the spectral lines becomes more complicated than in the case of the hydrogen-like atom. An early discussion of the subject was given by Hughes and Eckart (1930). A recent one is that by Fred, Tomkins, Brody, and Hamermesh (1951), who treated the cases of He^3 and He^4 and, in addition to a discussion of the theory, gave measured isotopic shifts for 32 lines of He I between λ 3187 A and λ 10830 A.

In the Li I spectrum, measurements in the laboratory on atomic-beam sources by Jackson and Kuhn (1939) and by Meissner, Mundie, and Stelson (1948) have given values of the isotopic shift between Li^6 and Li^7 amounting to 0.16 A for the λ 6708 A resonance doublet.

1.1. Hydrogen and Deuterium

Since the discovery of deuterium in 1932, numerous attempts have been made to detect its presence in celestial sources. None of these attempts has met with certain success, but they have enabled upper limits to the D/H abundance ratio to be estimated.

An early attempt was that of Menzel (1932), who examined lines of the Balmer series in the spectra of the sun and of several stars and nebulae. He concluded that the relative abundance of deuterium to hydrogen in the solar atmosphere was much less than the terrestrial value and found no evidence of deuterium lines in the other spectra. A recent careful study of the Hα absorption line in the normal solar spectrum, using an interferometer with resolving power 1.2×10^5, was carried out by Kinman (1956). He found no detectable trace of a Dα line and, from the estimated equivalent width of the most intense line that could remain undetected, 1.1 mA, concluded that the D/H abundance ratio in the solar atmosphere was $<4 \times 10^{-5}$.

Other studies include those by Severny (1956 and 1957), who has reported results indicating that the normal probable ratio of deuterium to hydrogen for the solar atmosphere is from 3 to 5×10^{-5} but that in disturbed regions the value might rise to 1×10^{-4}. In the latter connection, Goldberg, Mohler, and Müller (1958) have described the structure of the Hα emission line associated with a very bright loop prominence of the great limb flare of February 10, 1956. The emission profile of Hα showed a decided asymmetry that could be explained by a weaker component between 1.5 and 2.0 A to the violet. Of two possible explanations—(1) a separate gas cloud with a high velocity of approach and (2) the presence of an appreciable quantity of deuterium in the region (calculated Δλ between Hα and Dα = 1.78 A)—the authors prefer the latter. On a simple model they calculated that the abundance ratio of D/H would have been from 5 to 18 per cent. There seems some doubt that such a large proportion of deuterium could be produced by the processes suggested for its origin—fast protons, accelerated in the flare, acting upon C, N, O, and Ne atoms to form neutrons and subsequent neutron capture by hydrogen. The possibility that deuterium is formed in appreciable quantities in active regions in the solar chromosphere is an intriguing one, and further observational evidence on the question will be awaited with much interest.

Searches in sharp-lined, early-type stellar spectra for the Balmer lines of deuterium have been made in the last twenty-five years by several investigators, including unpublished work by the present writer. To our knowledge, no trace of a deuterium line has been found, nor has any quantitative limit for the D/H abundance ratio been published for stellar atmospheres.

On spectrograms of galactic nebulae on which the hydrogen emission lines are very strongly exposed, no deuterium components have been seen. From such spectrograms, Greenstein (1953) concludes that the D/H ratio for nebular matter must be less than 10^{-3}. It would be worthwhile to pursue this problem further, to determine whether the limit is below the terrestrial ratio of 1.5×10^{-4}.

There have been several attempts by the methods of radio astronomy to detect the deuterium analogue, at 327 Mc/s, of the 21-cm hydrogen line. Earlier claims to have done so have been largely discounted by the negative results obtained more recently with more sensitive apparatus. A recent attempt reported by Hey and Adgie (1957) gave a negative result that allowed an upper limit of D/H in interstellar hydrogen to be set at 5×10^{-4}.

In summary, deuterium has not been detected with certainty in celestial sources. In these sources, with one exception, it has not yet been possible to set the upper limit of its abundance relative to hydrogen lower than the terrestrial value of 1.5×10^{-4}. For the one exception—the normal solar atmosphere—there is fair evidence that deuterium is relatively less abundant than this value by a factor of 3 or 4. On the other hand, in very active regions of the solar atmosphere it is possible that the production of deuterium takes place at a rapid rate compared with its rate of destruction or mixing with the interior and that there is temporarily a correspondingly high relative abundance of deuterium.

1.2. Helium

Terrestrially, He^4 is the overwhelmingly abundant isotope, and He^3 is found in only minute quantities, with a relative abundance that probably varies for different terrestrial samples of the helium. The source of the data in Table 1 gives the relative abundance of He^3 to He^4 as between 10^{-4} and 10^{-5}, but figures as low as 10^{-7} are found in the literature.

A few years ago Greenstein (1951) made a search for He^3 components of chromospheric lines of helium as observed in the solar spectrum at eclipse and also outside eclipse. The result was negative, and the conclusion was reached that the abundance ratio He^3/He^4 is <0.02, with a probable error of 0.03.

More recently Burbidge and Burbidge (1956) have discussed the possible presence of He^3 in the atmospheres of magnetically variable A-type stars. They suggest that He^3 may be formed in the stellar atmosphere by a three-step process: (1) the production of neutrons by (p, n) reactions on light nuclei, (2) the capture of these neutrons by hydrogen to form deuterium, and (3) the reacceleration of the deuterium in a proton gas, giving, among other reactions, $H(d,\gamma)He^3$. Burbidge and Burbidge made measurements of the wave lengths of the helium absorption lines in the spectrum of the star 21 Aquilae and evaluated the difference between the singlet and triplet lines. They interpreted their results as suggesting that the shift could arise from isotopic effects and that He^3 might exist in the atmosphere of 21 Aquilae in approximately the same abundance as He^4. While the reactions suggested are of much interest, the fact that measurements

were made on the spectrum of only one star—and that one with rather poor helium lines—and that singlet-triplet shifts probably caused by Stark effect are known for many non-magnetic and non-variable B-type stars makes us reluctant to accept Burbidge and Burbidge's conclusion without further evidence.

We conclude, therefore, that there is not yet acceptable evidence of He^3 in stellar sources.

1.3. Lithium

The faintness of the stars which show the λ 6708 line of Li I in their spectrum, the consequent comparatively low resolving power of the spectrographs used, and the diffuseness of the λ 6708 resonance doublet have made it impossible up to the present time to study the isotopic effect in stellar spectra for lithium. It has been possible to study the λ 6708 line in the solar spectrum, and this has been done by Greenstein and Richardson (1951). From a careful study of the profile of the line as found in spectra of the disk and of sunspot penumbra, they were able to conclude that the abundance ratio Li^6/Li^7 is <0.25, which leaves the possibility that it might be the same as the terrestrial value, 0.08.

1.4. Technetium

The presence of technetium lines discovered by Merrill (1952, 1956) in the spectra of certain S-, M-, and N-type stars deserves comment in this chapter, although its detection did not involve the isotope effect in atomic spectra. Technetium, element 43, has not yet been found to occur naturally on earth. Fifteen isotopes of Tc with mass numbers ranging from 92 to 107 have, however, been formed in the laboratory in nuclear reactions. Most of these isotopes have very short half-lives, but one, Tc^{99}, has a half-life of about 210,000 years and another, Tc^{97}, about 2,600,000 years. It was first presumed that the Tc in the stellar atmospheres was Tc^{99}, but recently Cameron (1959*b*) has put forward reasons for believing that it may be Tc^{97}. While long in ordinary terms, the half-lives of these Tc isotopes are short in terms of the accepted value for the lifetime of a star; hence the origin of the Tc in the stellar atmosphere is a question of much interest. More complete discussions of this subject are to be found in articles in the current literature (for example, Anders 1958).

§ 2. APPLICATIONS IN MOLECULAR SPECTRA

Isotopic effects are much more marked in molecular spectra than in atomic spectra. The theory is given in textbooks on molecular spectra—for example, in Herzberg (1950). Since the electronic structures of isotopic molecules are almost identical, electronic effects are very small. The important effects are those of differences in mass upon the vibrational and the rotational energies of the molecules. Quantitatively, the vibrational and rotational isotopic shifts are readily and accurately calculable. Qualitatively, the following brief description will suffice for present purposes.

If μ is the reduced mass of the main molecule, $(1/\mu = 1/m_1 + 1/m_2)$, μ^i that

of the isotopic molecule, and $\rho = \sqrt{(\mu/\mu^i)}$, to a first approximation the vibrational effect is seen as an expansion of the scale of the band system of the lighter molecule compared to that of the heavier, by the factor ρ. The expansion is with respect to the origin of the band system as center. Hence, while the 0,0 band sequence will show little effect, bands involving larger and larger changes in vibrational quanta will show larger and larger effects. For example, in the C_2 Swan system, the 1,0 λ 4737 and the 2,0 λ 4383 sequences show shifts of about 7.5 and 15 A, respectively, between corresponding $C^{12}C^{12}$ and $C^{12}C^{13}$ bands. For band systems of molecules having at least one atom not heavier than those in the first two rows of the periodic table (and this includes all systems of present astrophysical interest) and where isotopes occur, vibrational isotopic shifts of the order of an angstrom or more are expected for some of the bands. Band heads separated by such amounts should be detectable in stellar spectra.

The rotational isotopic effect results in the rotational energies of the main and isotopic molecules being, to a first approximation, different by the factor ρ^2. Thus the rotational structure of the lighter molecule is the more spread out from the band origin by this factor. For a given band, the vibrational and rotational effects are additive. Astrophysically, use of the rotational effect can be made on high-dispersion solar spectrograms and may be further applicable when, in the future, higher resolution can be applied to stellar spectra.

For the study of isotopes in stellar atmospheres by using isotopic effects in molecular spectra, it is clear that we are restricted, first, to those stars cool enough to show bands in their spectra and, second, to those atoms which are constituents of molecules showing bands of appreciable strength in the spectra of these cool stars. The stars are those of type G or later and are principally types M, S, and R–N (or C). The molecules giving bands of appreciable strength include CH, CN, C_2, TiO, LaO, VO, ZrO, YO, ScO, NH, OH, MgH, and SiC_2. Twelve elements are represented in these molecules and are among those listed in Table 1.

The status of the investigation of the elements listed in Table 1, from bands in stellar sources, will be considered in turn, leaving the most fully investigated —carbon—for final discussion.

2.1. Hydrogen

The molecular bands of the diatomic hydrides offer the opportunity of detecting the corresponding deuterides. There are two difficulties. First, only the 0,0 bands of the systems are observed to occur with good strength, and so the vibrational isotopic shift is not large. Second, when recourse is had to the rotational isotopic shifts within the 0,0 band, blending with the many lines occurring in late-type spectra is troublesome. Examination of the λ 4315 CH band in several stellar spectra has failed to show the CD lines. But, as higher spectrographic resolution on stellar spectra becomes available, this subject could be pursued with greater chance of success. To date, then, there are no re-

sults on stellar atmospheres from molecular spectra to supplement the data on deuterium from atomic spectra.

Laboratory spectra of CH_3D and CH_4 were compared with spectra of Uranus and Neptune by Bardwell and Herzberg (1953). They found no evidence of CH_3D bands in the planetary spectra and were able to set an upper limit to the D/H ratio of 1 to 300 in the planetary atmospheres.

2.2. Nitrogen

In stellar atmospheres N^{15} could manifest its presence in the violet or red CN band systems and the λ 3360 NH band. The most favorable band in the violet system would be the 1,0 λ 3590 band, where the $C^{12}N^{15}$ band head would occur about 4 A redward of the main $C^{12}N^{14}$ head. In the red CN system larger shifts occur, up to about 40 A for the 4,0 λ 6192 band. Both the red and the violet CN systems in the spectra of R- and N-type stars have been examined and have shown no evidence of bands involving N^{15} (McKellar 1949*b*). Any results on isotopes (C^{13} or N^{15}) from the red CN bands prior to 1948, when the vibrational analysis of the upper state was corrected by Herzberg and Phillips (1948), must be wholly discounted as being based on incorrectly calculated isotopic shifts. Hence claims to have detected N^{15} (Daudin and Fehrenbach 1948) were erroneous. The λ 3360 NH band has not yet been exploited in a search for N^{15}. There is, up to the present, no evidence of N^{15} in a stellar atmosphere and, in view of its low abundance on earth, no evidence of a difference in isotopic relative abundance between stellar and terrestrial nitrogen.

2.3. Oxygen

Terrestrially O^{17} and O^{18} are very much less abundant than O^{16}. The strong oxide bands in stellar spectra of types M and S (TiO and ZrO) offer good means of detecting the less abundant isotopes of oxygen, but O^{17} and O^{18} would have to be considerably more abundant than their terrestrial relative abundances indicate to be found in stellar spectra. There is as yet no evidence of bands in stellar spectra involving O^{17} or O^{18}.

2.4. Magnesium

The MgH bands that occur in late-type stellar spectra (0,0 band λ 5211; 1,0 band λ 4845) are much weaker than the strong oxide bands in the coolest stars. On the other hand, the terrestrial abundances of Mg^{25} (10 per cent) and Mg^{26} (11 per cent) are comparatively great with respect to Mg^{24}. To our knowledge, no investigation of the MgH bands in stellar spectra for the purpose of studying the isotopes has yet been made; such an investigation should be carried out. The λ 5211 band is the stronger, but, since the vibrational isotopic shifts would be small, the best chances of success might follow from using high resolution and examining the rotational isotopic effect.

2.5. Silicon

A group of bands first found by Merrill (1926) and Sanford (1926) in the blue-green region in the spectra of some cool carbon stars of latest type have recently

been reproduced in the laboratory by Kleman (1956) and shown to arise almost certainly from the molecule SiC_2. In the spectra of a few of the stars (for example, RY Draconis) the bands occur with exceedingly great strength.

The analysis of the bands has been carried out in only a preliminary way, and no work has been reported on the isotope effect. Two types of investigation should be carried out on these SiC_2 bands. First, further work should be done in the laboratory, by means of the isotope effect (if necessary, using samples enriched in C^{13}, as well as determining the shifts for Si^{29} and Si^{30}) to verify the identity of the carrier of the bands and to assist with their analysis. Second, the results of the laboratory investigation should be applied to the stellar spectra. This second stage would require a large telescope and high-resolution spectrograph in view of the faintness of the very red stars in the blue and of the high resolving power required for these bands.

2.6. Scandium

Bands of ScO are known in M-type spectra but are of low intensity. Furthermore, terrestrially, only one isotope, Sc^{45}, is known. Since, in addition, its several laboratory-produced radioactive isotopes are all short-lived, Sc is not of interest to the subject of this chapter.

2.7. Titanium

In the later M-type stars the bands of TiO occur with great strength and therefore provide a good opportunity to investigate the isotopes of titanium. A study of the isotope effect in the blue-green TiO bands in the spectra of eighteen M-type stars has been reported by Herbig (1948). He used spectrograms of high dispersion obtained with the coudé instrument at Mount Wilson and compared them with plates of the TiO bands obtained in the laboratory. He concluded that, for the eighteen stars, in no case was there a significant departure (that is, by as much as a factor of 2) from the terrestrial relative abundances.

2.8. Vanadium

Terrestrially, vanadium consists almost entirely of V^{51}, with a very small proportion, 0.24 per cent, of V^{50}. VO band systems occur with considerable strength in the near and far photographic infrared regions of late M-type spectra. To the best of our knowledge, no work has yet been done on the isotope effect either in the laboratory or in stellar spectra. The work on stellar spectra would require fairly high dispersion in the infrared.

2.9. Yttrium

There are band systems of YO in the yellow-red and in the blue-green regions. The strongest of the red bands occur rather weakly in M- and S-type spectra. Yttrium, like scandium, exhibits terrestrially only one isotope, which is Y^{89}. It shows no long-lived artificial isotopes and so, for present purposes, is likely to be a trivial case, although it is one of the probably overabundant elements in S-type atmospheres.

2.10. Zirconium

Absorption bands of ZrO characterize spectra of type S and become quite intense in the later subtypes. Zirconium has five isotopes, four of which are relatively abundant terrestrially. The isotopic shifts in the band heads are of the same general order as for the TiO bands. There are two disadvantageous facts: first, that the strongest bands in the ZrO systems are the 0,0 bands where the isotopic shifts are small and, second, that the S-type stars are fewer in number than M types and are fainter. Nevertheless, the study of the zirconium isotopes from the ZrO bands in S-type spectra should not be beyond the capabilities of the combination of large telescope and modern coudé spectrograph.

Zirconium is an element of unusual interest in connection with problems of nucleogenesis and of mixing in stars. It is one of the fifth- and sixth-period elements (Zr, Y, Nb, Mo, Ba, rare earths) overabundant with respect to the elements of the fourth period in S-type stars, and it also appears unusually abundant in certain A-type magnetic stars (for example, α^2 CVn) (Greenstein 1954; Cameron 1957*a*). The recent suggestion has been made by Cameron (1959*a*) that, under certain conditions of neutron capture in stellar interiors, the isotope Zr^{96} would be selectively produced.

One of the more recent studies of ZrO bands in the laboratory is that of Afaf (1950), in which references to earlier work can be found. To our knowledge, the only laboratory work done on the isotopic effect in ZrO bands was an unpublished laboratory experiment by R. B. King and P. Routly. Such work should be carried out either before or in conjunction with the investigation, for isotopic abundances, of the ZrO bands in S-type stellar spectra. This is certainly one of the most interesting and promising problems to be investigated in the field of isotopes in stellar atmospheres.

2.11. Lanthanum

Bands of LaO have been found to occur in the spectra of late S-type stars in the photographic infrared region (Keenan 1948). The fact that bands other than the 0,0 band are not strong and that terrestrially La^{139} is overwhelmingly abundant suggests that investigation of the stellar bands for isotopic effects would be very difficult and probably unproductive, even though lanthanum is of interest as an element.

2.12. Carbon

Bands involving the less abundant carbon isotope, C^{13}, were identified in the spectra of the R- and N-type stars soon after the discovery of C^{13} in 1929. Isotopic bands recognized at first were the $C^{12}C^{13}$ and $C^{13}C^{13}$ bands accompanying the main $C^{12}C^{12}$ bands of the Swan system of C_2. Subsequently, a number of $C^{13}N$ bands were found to accompany the $C^{12}N$ bands of the violet CN system in the spectra of stars showing the isotopic C_2 bands.

It was apparent that the isotopic bands of C^{13} appeared with strengths rela-

tive to those of C^{12} considerably in excess of those found in laboratory sources. The interesting questions immediately arose as to whether this indicated that the relative abundance of C^{12} to C^{13} varied from star to star and, if so, how the relative abundances compared to the terrestrial value. Numerous investigators have contributed toward trying to answer these questions, including Sanford (1929, 1932, 1940) Menzel (1930), Wurm (1932), McKellar (1936, 1948, 1949*a*, *b*), Shajn (1942), Herzberg (1946), Daudin and Fehrenbach (1946), Shajn and Gaze (1948, 1950, 1954), Wyller (1957, 1959, 1960), and Climenhaga (1960). The consensus has been that the greater strength of the bands arising from molecules containing C^{13} does indeed indicate that, for the stellar atmospheres concerned, the C^{12}/C^{13} abundance ratio is less than the terrestrial value. The terrestrial relative abundance C^{12}/C^{13} has long been measured as about 90.

Among the N-type stars, values of the C^{12}/C^{13} ratio varying from about 20 to 2 have been quoted. Wyller (1957), using a simplified radiative-transfer treatment as well as the thin-layer hypothesis employed by previous investigators to reduce intensities to relative abundances and also using regions of the 0,2 λ 6191 and 0,1 λ 5635 sequences at some distance from the band heads, found no significant difference for five stars in the numerical results in the two methods of treatment. Among the R-type stars there are at least five which show little evidence of bands involving C^{13} (HD 76396, 112869, 137613, 182040, and 201626), and for these it has been estimated that the C^{12}/C^{13} abundance ratio is at least about 50 and probably 100 (Climenhaga 1960). It could therefore be as great as the terrestrial value or higher. For twelve other R-type stars having spectra showing C_2 bands of the 1,0 sequence (λ 4737) not so strong as obviously to disallow abundance estimates to be made, the C^{12}/C^{13} ratio was measured to be fairly constant, and the former mean value of 3.4/1 has been raised to about 5 by Climenhaga, using a curve of growth for the λ 4737 C_2 band. At least one of the R-type spectra showing no C^{13} bands (e.g., that of HD 112869) exhibits a $C^{12}C^{12}$ band at λ 4737 much stronger than the λ 4737 band in numerous spectra which do clearly show, in addition to the $C^{12}C^{12}$ λ 4737 band, its accompanying $C^{12}C^{13}$ λ 4744 band. This is illustrated in Plate I. Therefore, regardless of saturation effects on strong bands and consequent curve-of-growth effects, which, if more successfully treated in future investigations, will probably alter the numerical results, it does seem at present from the bands near λ 4740 that in the atmospheres of some R-type stars the C^{12}/C^{13} abundance ratio is decidedly greater than in others.

Summarized, the present state of knowledge on the carbon isotopes in the atmospheres of the cool carbon stars is as follows: (1) there is a group of R-type stars for which the C^{12}/C^{13} abundance ratio is about 100 or more; (2) for the remainder of the R-type stars for which measurements can be made with some confidence, those on the 1,0 band of C_2 appear to yield a fairly constant C^{12}/C^{13} ratio of about 5; (3) for the N-type stars, results by various investigators from a wider variety of bands give C^{12}/C^{13} ratios in the range from about 20 to 2, but the latest results of Wyller on C_2 and CN bands in the red and near infra-

red regions indicate an abundance ratio of about 10 or more. Also, for one R-type star, HD 156074, from bands in the red Wyller obtains values as high as 9.

Both Wyller's data and much of Climenhaga's were derived from excellent high-dispersion spectrograms obtained at the Mount Wilson and Palomar Observatories, and so their results should carry considerable weight.

Regarding the discrepancies between results from bands in the blue-green and the red spectral regions, Wyller has suggested that possibly errors involving blends with atomic lines or photometric difficulties in determining the continuous spectrum or serious saturation effects in the strong bands, could have led to the lower values obtained for some stars from the λ 4740 C_2 bands. The differences between the results on the carbon isotopic ratio from the blue and the red bands are indeed disturbing and require further investigation probably most important in the near infrared spectral region. In view of the possible nucleogenetic importance of knowledge of the stellar C^{12}/C^{13} ratio, it is hoped that the further work of Wyller and that to be done at Victoria will bring satisfactory explanations for the present numerical discrepancies. In this connection a possible additional avenue of investigation has recently been opened by the discovery of bands of the Phillips singlet system of C_2 in the spectra of the cool carbon stars (McKellar 1960). These singlet bands have a simple structure and are well resolved on spectrograms of moderately high dispersion. They should therefore be advantageous for study of the C^{13} isotopic abundance problem.

The carbon isotopes have been investigated in other sources. For meteorites,

---

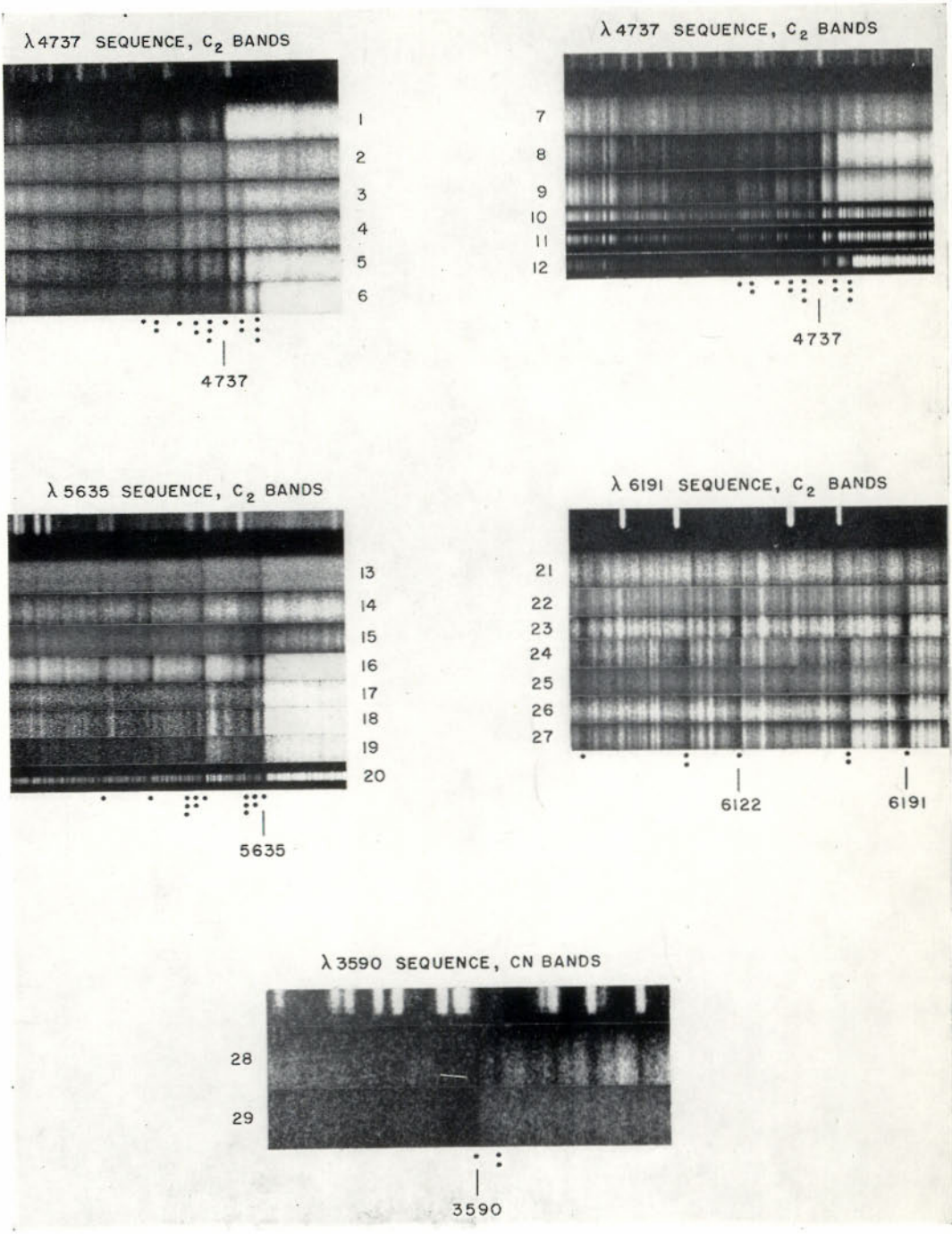
PLATE I.—Isotopic bands in the spectra of cool carbon stars. The plate shows isotopic absorption bands involving C^{12} and C^{13}, in stellar spectra. Reproduction Nos. *10*, *11*, *12*, and *20–27* are from three-prism spectrograms obtained at Victoria. The others are from single-prism spectrograms. In the three sequences of the Swan bands of C_2, positions of $C^{12}C^{12}$ band heads are indicated by a single dot, $C^{12}C^{13}$ by two dots, and $C^{13}C^{13}$ by three dots. In the bottom pair of reproductions showing the λ 3590 sequence of CN violet bands, the single dot indicates the $C^{12}N$ band head, and the double dot, $C^{13}N$.

The numerous reproductions are given to show the ranges found in band intensity. Points of interest include the following: (*a*) In spectrum *1*, the $C^{12}C^{12}$ bands are strong but no bands involving C^{13} are found, whereas in *3* and *4*, the $C^{12}C^{12}$ are not so strong, yet bands involving C^{13} are prominent; (*b*) for WZ Cas, a "lithium" star (spectrum *7*), the C_2 bands are not very intense, yet the $C^{12}C^{13}$ band seems unusually strong compared to the $C^{12}C^{12}$ band; (*c*) from spectra with very strong main and isotopic bands (e.g., strips *6*, *12*, *18*, *19*, etc.) it is not possible to derive reliable isotopic abundances from the intensities of the bands.

The numbered reproductions refer to spectra of the following stars:

1, HD 112869 (R6p);	*2*, HD 182040 (R2);	*3*, HD 5223 (R3);	*4*, HD 223392 (R3);
5, HD 16115 (R3);	*6*, HD 19557 (R5);	*7*, WZ Cas (N1p);	*8*, U Hya (N2);
9, VY UMa (Na);	*10*, 19 Psc (N0);	*11*, DS Peg (N1);	*12*, Y CVn (N3);
13, HD 76396 (R4);	*14*, HD 182040 (R2);	*15*, 19 Psc (N0);	*16*, DS Peg (Nb);
17, RY Dra (N1p);	*18*, Y CVn (N3);	*19*, SU And (Nb);	*20*, VY UMa (Na);
21, WZ Cas (N1p);	*22*, VY UMa (Na);	*23*, U Hya (N2);	*24*, HD 79319 (R6);
25, HD 19557 (R5);	*26*, RY Dra (N4p);	*27*, Y CVn (N3);	*28*, HD 156074 (R0);
29, HD 76396 (R4).			

PLATE I


λ4737 SEQUENCE, C_2 BANDS
1
2
3
4
5
6
4737
λ4737 SEQUENCE, C_2 BANDS
7
8
9
10
11
12
4737
λ5635 SEQUENCE, C_2 BANDS
13
14
15
16
17
18
19
20
5635
λ6191 SEQUENCE, C_2 BANDS
21
22
23
24
25
26
27
6122
6191
λ3590 SEQUENCE, CN BANDS
28
29
3590

a direct spectrophotometric comparison with terrestrial carbon showed no detectable difference (Jenkins and King 1936). For a number of giant stars, types G8–K5, an examination of the λ 3883 CN bands on Mount Wilson spectrograms showed no appreciable enrichment of C^{13} over the terrestrial value (Schopp 1954). The interstellar molecular lines of CH and CH^+ were examined by O. C. Wilson (1948). He was unable to detect absorption where components involving C^{13} would occur and concluded that the C^{12}/C^{13} ratio must be at least 5 in interstellar gas. In the solar spectrum, examination of the rotational structure of the λ 3883 CN band for $C^{13}N$ lines by several investigators has given negative results. In this way the estimated minimum relative abundance of C^{12}/C^{13} was raised from 15 (McKellar 1948) to 35 (Greenstein, Richardson, and Schwarzschild 1950) and, finally, to 10^3 or 10^4 (Righini 1956). There seems no doubt that the C^{12}/C^{13} abundance ratio in the solar atmosphere is at least the terrestrial value and possibly higher. Thus the only places for which there is evidence of enhancement of the C^{13} abundance are the atmospheres of many of the cool carbon stars.

Possible explanations of the existence of different C^{12}/C^{13} abundance ratios in stellar atmospheres involve questions of nuclear reactions in stellar interiors, of stellar evolution, and of mixing between the material of stellar cores and atmospheres. These subjects are being studied currently, and much progress has recently been made. A full discussion is beyond the size and scope of this chapter, but a few of the relevant points are given below. For a more complete description of the present status of the subjects, reference may be made to the recent reviews by Cameron (1957*a*, *b*) and by Burbidge, Burbidge, Fowler, and Hoyle (1957).

The spectrographic measurements of the C^{12}/C^{13} abundance ratio apply to stellar atmospheres. Nuclear reactions that transmute atoms to or from C^{12} and C^{13} in stellar interiors take place in or near the cores. For the composition of the atmosphere to give an indication of that of the star as a whole, there must be a high degree of mixing of the inner and outer material. Convection zones for some stellar models are quite extensive and would provide considerable mixing. This subject is one requiring further study. There is good evidence that supergiant stars are constantly losing material to interstellar space, a process which, if carried on long and extensively enough, would tend to uncover subsurface stellar material.

In a region which has supported the carbon cycle of energy production, the catalytic atoms of carbon, when the cycle has reached equilibrium, should show a C^{12}/C^{13} abundance ratio inversely proportional to the capture cross-sections of these nuclei for protons of the appropriate energy. The latest data on cross-sections indicate a C^{12}/C^{13} ratio of about 4.6, which is fairly close to the figure found for many R-type stars. Hence the abundance ratio of about 5 might indicate carbon that had been through the carbon-nitrogen cycle. The rates at which C^{12} and C^{13} abundances reach their equilibrium value differ; hence a varying ratio would occur en route to equilibrium.

Helium thermonuclear reactions, forming C^{12} but not C^{13}, could occur in cores of stars at very high temperatures and pressures ($T = 100 \times 10^6$ ° K; density 10^5 gm/cm^3). It has been suggested that some stars having an excess of carbon over oxygen (e.g., cool carbon stars) might contain surface material that had previously existed in regions of the above high temperature and density and so contain excess C^{12}. It is not clear how the matter in question could have reached the stellar atmosphere, whether by convection or otherwise without traversing a hydrogen-burning zone; but if the possibility be granted, a high C^{12}/C^{13} abundance ratio, as found for some R-type stars, the sun, etc., could be explained.

It is to be hoped that further work on nuclear astrophysics and on stellar structure will yield results that can more completely and definitely explain the results of improved measurements that will be made on the C^{12}/C^{13} abundance ratio in stellar atmospheres.

§ 3. FUTURE WORK AND PROSPECTS

From the foregoing discussions of individual elements, it would appear that the subjects most urgently requiring further observational study are the following:

a) The Hα emission line produced in highly disturbed areas of the sun should be examined for a Dα component, following the interesting suggestion of Severny (1957) and of Goldberg, Mohler, and Müller (1958).

b) Late B-type stars showing evidence of magnetic phenomena should be sought, so that the He I lines in their spectra can be examined for possible He^3 components.

c) Measurements leading to the C^{12}/C^{13} abundance ratio for cool carbon stars should be made on weaker bands and on bands in the red and photographic infrared regions in the spectra of cool carbon stars, to check on the results available to date.

d) The blue-green bands in the spectra of late N-type stars, attributed to SiC_2, required laboratory work to verify their origin and to analyze the bands; they should also be photographed in stellar spectra with the highest practicable resolving power, for study of the silicon isotopes.

e) The zirconium isotopic abundance ratio in stars is of unusual interest. Hence the ZrO bands in S-type spectra should be studied for this purpose.

It seems unlikely that, in the presently observable regions of stellar spectra, new intense molecular bands will be found and that additional elements can thus be examined for isotopic abundance. In view, however, of recent advances in rocketry, we can look forward with optimism to the possibility of obtaining spectrograms from outside the earth's atmosphere and thus to having available new spectral regions in the ultraviolet and infrared. Here we may expect to find new stellar molecular bands, new molecular interstellar lines, etc., that may help to shed additional light on cosmic isotopic abundances.

REFERENCES

AFAF, M.	1950	*Proc. Phys. Soc. London, A*, **63**, 1156.
ANDERS, E.	1958	*Ap. J.*, **127**, 355.
BARDWELL, J., and HERZBERG, G.	1953	*Ap. J.*, **117**, 462.
BURBIDGE, E. M., and BURBIDGE, G. R.	1956	*Ap. J.*, **124**, 655.
BURBIDGE, E. M., BURBIDGE, G. R., FOWLER, W. A., and HOYLE, F.	1957	*Rev. Mod. Phys.*, **29**, 547.
CAMERON, A. G. W.	1957*a*	*Stellar Evolution, Nuclear Astrophysics and Nucleogenesis* (Atomic Energy of Canada Ltd., Pub. No. 454 [Chalk River, Ontario]).
	1957*b*	*Pub. A.S.P.*, **69**, 201.
	1959*a*	*Ap. J.*, **130**, 429.
	1959*b*	*Ibid.*, p. 452.
CLIMENHAGA, J. L.	1960	*Pub. Dom. Ap. Obs. Victoria*, Vol. **11**, No. 16.
DAUDIN, A., and FEHRENBACH, C.	1946	*C.R.*, **222**, 1083.
	1948	*J. phys. et rad.*, **9**, 163.
FRED, M., TOMKINS, F. S., BRODY, J. K., and HAMERMESH, M.	1951	*Phys. Rev.*, **82**, 406.
GARSTANG, R. H.	1955	*J. British Astr. Soc.*, **65**, 371.
GOLDBERG, L., MOHLER, O. C., and MÜLLER, E. A.	1958	*Ap. J.*, **127**, 302.
GREENSTEIN, J. L.	1951	*Ap. J.*, **113**, 531.
	1954	*Les Processus nucléaires dans les astres* ("Communications to the 5th International Colloquium of Astrophysics, Liège"), p. 307.
GREENSTEIN, J. L., and RICHARDSON, R. S.	1951	*Ap. J.*, **113**, 536.
GREENSTEIN, J. L., RICHARDSON, R. S., and SCHWARZSCHILD, M.	1950	*Pub. A.S.P.*, **62**, 15.
HERBIG, G. H.	1948	*Pub. A.S.P.*, **60**, 378.
HERZBERG, G.	1946	Report of Yerkes and McDonald Obs., *A.J.*, **52**, 149.
	1950	*Spectra of Diatomic Molecules* (2d ed.; New York: D. Van Nostrand Co.).
HERZBERG, G., and PHILLIPS, J. G.	1948	*Ap. J.*, **108**, 163.
HEY, J. S., and ADGIE, R. L.	1957	*Nature*, **179**, 370.
HUGHES, D. S., and ECKART, C.	1930	*Phys. Rev.*, **36**, 694.

JACKSON, D. A., and KUHN, H.	1939	*Proc. R. Soc. London, A*, **173**, 278.
JENKINS, F. A., and KING, A. S.	1936	*Pub. A.S.P.*, **48**, 323.
KEENAN, P. C.	1948	*Ap. J.*, **107**, 420.
KINMAN, T. D.	1956	*M.N.*, **116**, 77.
KLEMAN, B.	1956	*Ap. J.*, **123**, 162.
MCKELLAR, A.	1936	*Pub. A.S.P.*, **48**, 216.
	1948	*Pub. Dom. Ap. Obs. Victoria*, **7**, 395.
	1949*a*	*Pub. A.S.P.*, **61**, 199; *Contr. Dom. Ap. Obs.*, No. 20.
	1949*b*	*Pub. A.S.P.*, **61**, 34.
	1960	*J. R. Astr. Soc. Canada*, **54**, 97; *A.J.*, **65**, 350.
MEISSNER, K. W., MUNDIE, L. G., and STELSON, P. H.	1948	*Phys. Rev.*, **74**, 932.
MENZEL, D. H.	1930	*Pub. A.S.P.*, **42**, 34.
	1932	*Ibid.*, **44**, 41.
MERRILL, P. W.	1926	*Pub. A.S.P.*, **38**, 175.
	1952	*Ap. J.*, **116**, 21.
	1956	*Pub. A.S.P.*, **68**, 70.
MINNAERT, M. G. J.	1957	*M.N.*, **117**, 315.
PHILLIPS, J. G.	1952	*Ap. J.*, **115**, 183.
	1957	*Ibid.*, **125**, 163.
RIGHINI, G.	1956	*Les Molécules dans les astres* ("Communications to the 7th International Colloquium on Astrophysics, Liège"), p. 265.
SANFORD, R. F.	1926	*Pub. A.S.P.*, **38**, 177.
	1929	*Ibid.*, **41**, 271.
	1932	*Ibid.*, **44**, 248.
	1940	*Ibid.*, **52**, 203.
	1950	*Ap. J.*, **111**, 262.
SCHOPP, J. D.	1954	*Ap. J.*, **120**, 305.
SEVERNY, A. B.	1956	*Pub. Crimean Ap. Obs.*, **16**, 12.
	1957	*Russian Astr. J.*, **34**, 328.
SHAJN, G.	1942	*Bull. Abastumani Ap. Obs.*, **6**, 1; *Observatory*, **64**, 255.
SHAJN, G., and GAZE, V.	1948	*Pub. Crimean Ap. Obs.*, **2**, 131.
	1950	*Ibid.*, **5**, 24.
	1954	*Les Processus nucléaires dans les astres* ("Communications to the 5th International Colloquium on Astrophysics, Liège"), p. 397.
WILSON, O. C.	1948	*Pub. A.S.P.*, **60**, 198.
WURM, K.	1932	*Zs. f. Ap.*, **5**, 260.
WYLLER, A. A.	1957	*Ap. J.*, **125**, 177.
	1959	*A.J.*, **64**, 57.
	1960	*Astrophysica Norvegica* (in press).

CHAPTER 17

The Spectra of Novae

DEAN B. McLAUGHLIN
University of Michigan Observatory

§ 1. INTRODUCTION

THE term "nova," a contraction of "nova stella," originally expressed a belief that a star had been newly formed where none previously existed. The term "temporary star" was in use a few decades ago but has since fallen into discard, and "nova" appears to be thoroughly intrenched by usage.

A precise definition of "nova" as the term is used would require many qualifications. It has been applied to such dissimilar objects as GK Persei (1901), T Pyxidis, η Carinae, and P Cygni. It has even been used for Z Andromedae, though practically all students of novae would now call this star "nova-like." A characteristic of all novae is the sudden brightening, by a factor of from several hundred to more than a million, of a previously constant or only moderately variable star. The nova remains near maximum for a few days, occasionally for months, and in rare cases for many years but eventually fades to its former faintness. The changes in brightness are accompanied by spectacular variations in the spectrum.

The term "supernova" is applied to objects demonstrably of much higher luminosity than the more abundant "common novae." In individual cases, available data may not permit distinction between a nova and a supernova. The spectra of supernovae, so far as they are known, differ radically from those of common novae and, when observable, should be a reliable means of identification.

1.1. HISTORICAL

The study of novae, as distinguished from mere notice of their occurrence, can fairly be said to begin with Tycho Brahe's work on the nova of 1572. Prior to that date, only one nova can be considered to be established beyond reasonable doubt. This is the object that appeared near ζ Tauri on July 4, A.D. 1054, and in whose place the Crab Nebula is today a visible remnant. It was undoubtedly a supernova. All other reports of pre-Tychonic novae can be individually

doubted, since early accounts are often vague or incomplete, so that distinctions between novae, comets, and perhaps fireballs, are difficult. However, numerous *probable* novae are recognizable in early chronicles. These have been discussed by Zinner (1920) and by Lundmark (1921) (see also Payne-Gaposchkin 1957, p. 36; Tsê-Tsung 1958). On various grounds Lundmark discarded nine of sixty that he listed. The remaining fifty-one, of which thirty-nine antedate 1572, show a distribution in which we recognize the strong galactic concentration and the clustering in the Sagittarius region that characterize the well-known novae of recent years. A majority of these were probably true novae.

The spectacular nova of 1572, first observed on November 11, is reported to have been as bright as Venus and visible at noon. Decline to the first magnitude required 3 months, and it passed below naked-eye visibility in March, 1574. This is one of three galactic objects that are regarded as supernovae. The next recorded nova appeared as a third-magnitude star in Cygnus in 1600 and remained bright with some fluctuations for many years. After about 1715 it became steady near fifth magnitude and remains so today as P Cygni. Kepler's nova in Ophiuchus in 1604 was another galactic supernova.

A third-magnitude star in Vulpecula, referred to as "Anthelm's nova," was discovered in 1669. It faded to invisibility but had maxima again in 1671 and 1672 before it finally disappeared. It was probably a rare type of slow nova.

For nearly 2 centuries no more bright novae were noted. This curious circumstance is probably due to changes in the emphasis and conditions of astronomical observing. To an increasing extent the eighteenth and much of the nineteenth century saw astronomers engaged in precise position work. Many observers were probably poorly acquainted with the constellations, so that a nova might be seen and yet pass unrecognized. Observation through the narrow shutter of a transit house is ill suited to viewing the constellations or to the recognition of novae. The only probable nova recorded in the eighteenth century was a sixth-magnitude object in Sagitta in 1783. Beginning in 1848, numerous novae have been recognized.

Nova Ophiuchi 1848 (v841 Oph) was followed by T Scorpii in 1860, T Coronae Borealis in 1866, and Q Cygni in 1876, as well as a few poorly observed, but probably real, novae. S Andromedae 1885 was the first extragalactic supernova to be discovered. The first nova to be studied spectroscopically was T CrB. Detailed study of nova spectra had to await the application of photography, and the first star so studied was T Aurigae 1891. It is noteworthy, however, that a visual study of the spectrum of T Aurigae by Campbell (1892) gave enough detailed information to demonstrate the similarity between the star's visual spectrum and that of DQ Herculis 1934.

1.2. Nomenclature

Designations of the earlier novae were not systematic. Some received names of the same form as those of variable stars (T Aur, T Sco, T CrB), while others were known merely by the designation "Nova," followed by the genitive of a

constellation name, as Nova Persei. Distinction between novae when more than one occurred in a constellation was achieved by appending "No. 1," "No. 2," etc., in order of discovery (not date of maximum). This system soon broke down in Sagittarius, and in several cases different authors used different numbers for the same nova. Appending the year of maximum aided in distinguishing novae, as, e.g., Nova Aquilae 1918 (=Nova Aql No. 3). Beginning with RR Pictoris, 1925, all galactic novae have received designations by letter or number[1] like other variable stars, but for many years the older novae retained their former designations. Recently all the old novae have received names in the conventional system of variable-star nomenclature. Thus Nova Persei 1901 has become GK Persei.

§ 2. DISTRIBUTION AND LUMINOSITIES

2.1. Galactic Distribution

The number of known novae in the Galaxy now greatly exceeds one hundred (for complete listing see Payne-Gaposchkin 1957, p. 2). Table 1 gives co-ordinates of the brighter or better-known novae and lists published light-curves and descriptions of spectra.

The novae show a very strong concentration toward the galactic equator and an especially dense clustering in the direction of the galactic nucleus in Sagittarius. These features are so well known as to require little further comment. Of the 135 admitted novae, 67 lie within only 30° of galactic longitude with center at $\lambda = 330°$, while a minimum of frequency occurs around $\lambda = 100°$.

Several novae in relatively high galactic latitude require some comment. A few (T CrB, RR Pic, DQ Her) were among the brightest and closest to the solar system. Their high latitudes, therefore, do not indicate great distances from the galactic plane. Others, however (VY Aqr, W Ari), were faint. If their luminosities were those of typical novae, they must have been far out in the "halo" of the Galaxy. Alternatively, they may have been of unusually low luminosity and at small distances. At least one such "dwarf nova" appears to be well established (WZ Sge). In other individual cases the data do not admit of a unique conclusion.

2.2. Distances and Luminosities

Parallaxes of novae determined trigonometrically and their proper motions, as listed in Jenkins' (1952) catalogue, convey only the information that these objects are so distant that the trigonometric method can give no accurate measure of distance.

The most reliable indirect method depends upon angular rates of expansion of nebulae around novae, combined with velocities of expansion measured spectroscopically. The method is not completely free from objections. In individual cases the assumption of spherically symmetrical expansion may lead to error,

[1] The author uses the nomenclature v for numbered variable stars in place of the more common V; i.e., v841 Oph = V841 Oph.

TABLE 1

SELECTED LIST OF NOVAE: CO-ORDINATES AND LITERATURE

No.	Nova	α1900	δ1900	l	b	Light-Curve	Spectrum
1.....	GK Per	3^h24^m4	+43°34′	118.9	− 9°2	Campbell (1903)	Stratton (1936*a*); McLaughlin (1949*b*)
2.....	XX Tau	5 13.6	+16 37	154.9	−10.2	Beyer (1929)	Schwassmann and Wachmann (1928)
3.....	T Aur	5 25.6	+30 22	144.8	− 0.3	Parenago (1949)	Campbell (1892); McLaughlin (1941*a*)
4.....	RR Pic	6 34.7	−62 33	239.4	−25.2	Campbell (1932)	Jones (1931)
5.....	DM Gem	6 37.8	+30 03	152.8	+13.2	Leavitt (1920)	Cannon (1916); Reese and Curtis (1903)
6.....	DN Gem	6 48.4	+32 16	151.6	+16.2	Campbell (1915)	Stratton (1920); Wright (1926)
7.....	CP Pup	8 08.0	−35 03	220.6	− 0.1	Pettit (1943)	Sanford (1945*a*); Weaver (1944)
8.....	T Pyx	9 00.5	−31 59	225.1	+10.5	Leavitt (1920)	Adams and Joy (1920); Joy (1945)
9.....	CT Ser	15 41.0	+14 41	352.0	+46.1	Lohmann (1949)	Bloch (1950)
10.....	T CrB	15 55.3	+26 12	9.4	+46.8	Pettit (1946)	Herbig and Neubauer (1946); Sanford (1949)
11.....	v841 Oph	16 53.9	−12 44	335.5	+16.3	Parenago (1949)	Humason (1938) (postnova)
12.....	RT Ser	17 34.3	−11 53	341.6	+ 8.6	Payne-Gaposchkin and Gaposchkin (1938, p. 263)	Swings and Struve (1942)
13.....	RS Oph	17 44.8	− 6 41	347.5	+ 8.9	Prager (1940)	Adams and Joy (1933)
14.....	v999 Sgr	17 53.8	−27 33	330.5	− 3.4	Walker (1923)	Wright (1910); Cannon (1916)
15.....	v630 Sgr	18 02.2	−34 21	325.4	− 8.3	Parenago (1949)	Joy *et al.* (1936)
16.....	DQ Her	18 04.7	+45 51	40.3	+25.6	Grouillier (1935)	Stratton (1936*b*); McLaughlin (1954)
17.....	v849 Oph	18 09.5	+11 35	6.8	+12.1	Shapley (1921)	Wright (1920)
18.....	v1017 Sgr	18 25.7	−29 28	332.1	−10.6	McLaughlin (1946)	Humason (1938) (postnova)
19.....	v603 Aql	18 43.8	+ 0 28	0.9	− 0.6	Campbell (1919)	Wyse (1939)
20.....	HR Lyr	18 49.5	+29 06	27.1	+11.3	Harvard, unpublished	Wyse (1940)

TABLE 1—*Continued*

No.	Nova	α1900	δ1900	l	b	Light-Curve	Spectrum
21.....	EL Aql	$18^h50^m.8$	−03°27′	358.1	− 4°.0	Beyer (1929)	Wyse (1940)
22.....	EU Sct	18 50.9	−04 20	357.4	− 4.4	Bertaud (1953)	Wellmann (1951*a*); Heard (1953)
23.....	v1059 Sgr	18 56.2	−13 18	350.0	− 9.7	Walker (1923)	Pickering (1899); Cannon (1916)
24.....	v604 Aql	18 56.8	− 4 35	357.8	− 5.9	Walker (1923)	Cannon (1916)
25.....	v356 Aql	19 12.2	+ 1 33	5.2	− 6.4	Parenago (1949)	McLaughlin (1955)
26.....	v528 Aql	19 14.2	+ 0 27	4.4	− 7.3	Bertaud (1951)	Sanford (1945*b*)
27.....	v606 Aql	19 15.3	− 0 19	4.0	− 7.9	Leavitt (1920)	Cannon (1916)
28.....	v368 Aql	19 21.7	+ 7 24	11.5	− 5.6	Parenago (1949)	Wyse (1936)
29.....	DO Aql	19 26.1	− 6 38	359.5	−13.3	Beyer (1929)	Vorontsov-Velyaminov (1940)
30.....	v465 Cyg	19 49.0	+36 18	39.5	+ 3.7	Beyer (1952)	Bloch (1950)
31.....	v476 Cyg	19 55.9	+53 21	54.8	+11.8	Campbell (1932)	Baldwin (1940)
32.....	RR Tel	19 56.3	−56 00	309.3	−33.4	Mayall (1949)	Payne-Gaposchkin (1957, p. 154)
33.....	WZ Sge	20 03.1	+17 24	25.4	− 9.1	Mayall (1946)	Greenstein (1957)
34.....	v450 Cyg	20 54.8	+35 33	46.9	− 7.2	Ashbrook and Nail (1942)	Sanford (1943)
35.....	Q Cyg	21 37.8	+42 23	57.8	− 8.1	Lockyer (1891)	Lockyer (1891)
36.....	CP Lac	22 12.0	+55 07	69.7	− 1.0	Parenago (1949)	Harper *et al.* (1937); McLaughlin (1947*a*)
37.....	DI Lac	22 31.8	+52 12	70.9	− 5.0	Leavitt (1920)	Cannon (1916)
38.....	DK Lac	22 45.6	+52 46	73.1	− 6.4	Larsson-Leander (1954*a*)	Larsson-Leander (1954*b*)

but it is unlikely that it amounts to a factor of 2 in the parallax. Data on rates of expansion and velocities are given for eight novae in Table 2. Column headings are self-explanatory. Absolute magnitudes at maximum and minimum are given in the last two columns.

The intensities of interstellar calcium lines have been used as rough indicators of distance. When this method was first introduced, it was assumed that the calcium formed a fairly uniform sheet and that the intensities of the lines increased steadily with distance. In view of the known patchiness of the calcium, considerable caution must be exercised in the use of this method. The galactic rotation effect in radial velocities of interstellar calcium lines has also been used as a measure of distance. There is now good reason to believe that the calcium clouds are concentrated in or near the arms of the galactic spiral and are sparse or absent between the arms. The unresolved blend of lines formed in discrete clouds gives a residual velocity averaged over the distances of the clouds, but we can no longer assume, as was done formerly, that the resulting average distance is half the distance of the nova. At best, we have a means of obtaining a rough estimate of distance.

Mean absolute magnitudes depending on the several methods are summarized in Table 3. These are subject to uncertainties in the correction for in-

TABLE 2

DISTANCES AND LUMINOSITIES OF NOVAE FROM NEBULAR EXPANSION

Nova	Year	Expansion Rate ("/yr)	Velocity (km/sec)	Distance (parsecs)	Apparent Magnitudes		Absorption	Corrected Absolute Magnitudes	
					m_{max}	m_{min}		M_{max}	M_{min}
v603 Aql	1918	0".956	1700	376	−1.1	10.8	−0.2	−9.2	+2.7
T Aur	1891	.117	460	830	+4.2	15.4	− .7	−6.2	+5.0
v476 Cyg	1920	.093	700	1590	+2.0	16.1	− .6	−9.6	+4.5
DQ Her	1934	.27	290	230	+1.4	15.1	− .2	−5.6	+8.1
CP Lac	1936	.25	1600	1340	+2.1	15.3	− .8	−9.3	+3.9
GK Per	1901	.54	1200	470	+0.2	13.5	− .3	−8.5	+4.8
RR Pic	1925	.18	410	480	+1.2	13.3	− .2	−7.4	+4.7
CP Pup	1942	0.21	700	700	+0.4	17.5	−0.3	−9.1	+8:

TABLE 3

MEAN ABSOLUTE MAGNITUDES OF NOVAE

Method	M_{max}	No.	M_{min}	No.
Nebular expansion	−8.1	8	+5.2	8
Interstellar-line intensity	−7.6	9	+5.0	7
Galactic rotation	−7.6	6	.....	.....
Trigonometric parallax*	−7.3	9	+4.4	8

* Weighted mean, 0".0020; absorption 0m.3.

terstellar absorption, in addition to the inherent errors of each method. For the brightest and nearest novae, the absorption correction rarely exceeds a few tenths of a magnitude, so that the uncertainty of the absorption is usually less than that arising from other sources. The mean absolute magnitude based on trigonometric parallaxes is probably of greater importance in demonstrating the reliability of the system of parallaxes than in determining independently the absolute magnitudes of novae.

The relation of luminosity to the form of the light-curve will be discussed in a later section.

Detailed treatment of the space distribution of novae is outside the scope of this chapter. In this connection see McLaughlin (1945*b*) and Payne-Gaposchkin (1957, p. 42). The galactic novae form a highly flattened system in the galac-

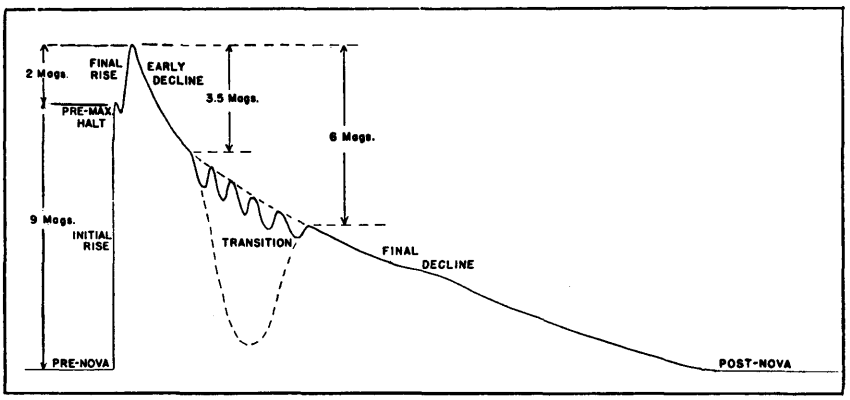


FIG. 1.—Schematic light-curve of a nova. Three types of behavior during the transition are illustrated.

tic plane about the sun, with a large extension for several kiloparsecs toward the nucleus of the Galaxy in Sagittarius. A few of the apparently faintest may lie well within the nucleus, but the majority are probably outside it.

§ 3. LIGHT-VARIATIONS

3.1. NOVA LIGHT-CURVES IN GENERAL

Light-curves of novae show a great variety when plotted to the same extended time scale, since differences between fast and slow novae are then most obvious. When the time scale is drastically compressed, the basic similarity among all nova light-curves becomes evident. Common to all is the rapid rise and much more gradual decline. But, while some drop smoothly from maximum, others have strong oscillations of brightness. We first consider an ideal or schematic light-curve and then note some typical individual stars.

The curve can be divided into the nine segments shown in Figure 1 (McLaughlin 1939). It is not always possible to recognize separately the seg-

ments of the rising branch. Especially in the most rapid novae, these appear to merge into a single very rapid and continuous increase in brightness. But among average and slow novae these stages are often seen well separated.

1. *Prenova stage.*—The star may be constant for many years or may vary irregularly through 1 or 2 mag.

2. *Initial rise.*—Few stars have been observed during this increase, but, for several, the brightening from minimum to only 2 mag. below maximum certainly required no more than 2 or 3 days. Even slow novae brighten with great rapidity.

3. *Premaximum halt.*—About 2 mag. below maximum the brightening may cease for a few hours in a fast nova or several days in a slow one. A fading has been established in several cases.

4. *Final rise.*—The star again brightens, reaching maximum in 1 day for fast novae and several weeks for a few of the very slowest.

5. *Maximum.*—The principal maximum of a fast nova lasts only several hours or a day at most. Even slow novae usually remain at maximum only a few days. Protracted maxima are characteristic of RT Serpentis–type stars.

6. *Early decline.*—The most rapid novae fade rather smoothly through 3 or 4 mag. The slower usually show oscillations of brightness with amplitudes of from a few tenths to 1 or 2 mag.

7. *Transition.*—The greatest differences appear here. The light may fade steadily, or strong oscillations may occur. Finally, a deep minimum of light may occur, with depth of from 1 to several mag., followed by a recovery after several weeks. The transition ends with the completion of the recovery or the cessation of strong fluctuations, usually at 6–7 mag. below maximum, occasionally fainter.

8. *Final decline.*—From the end of the transition all the way to minimum, the light declines fairly steadily and slowly. If there are fluctuations they are much less conspicuous.

9. *Postnova.*—Some stars remain constant after reaching minimum, while others vary irregularly through 1 or 2 mag. for many years.

3.2. Light-Curve Data

Novae are listed in Table 4 by constellation and in chronological order of date of maximum within each constellation. The first column indicates the number of each star as listed in Table 1. The remaining columns contain data concerning the light-curve. Most of the column headings are self-explanatory. The assignment to fast, average, or slow categories depends chiefly upon the rate of decline through 3 mag.

An extended statistical discussion of the characteristics of light-curves is outside the scope of this chapter. For such detail, reference is made to the work of McLaughlin (1939), Bertaud (1948), and Payne-Gaposchkin (1957).

The datum of greatest interest here is the average range. From the maxima and minima in Table 4, with nine additional known ranges, and from the discussions by Bertaud and Payne-Gaposchkin, we get the average values in Table 5. The spread of amplitudes is from 5 to 17, with a maximum of frequency at about 12 mag.

TABLE 4

LIGHT-VARIATIONS OF SELECTED NOVAE

No.	Nova	Year	Min.	Max. Obs.	Max. Extr.	Type	Early Decline	Transition	Initial Rise (Days)	Duration of Decline (Days)			
										2^m	3^m	7^m	All
27.....	v606 Aql	1899	<15.4	6.7	5.5	Fast	Smooth	Dip 1^m0	.....	25	33	320	> 3 years
24.....	v604 Aql	1905	<16.8	8.2	7.6	Fast	Smooth	Smooth	< 9	9	31	230	.....
19.....	v603 Aql	1918	10.8	−1.1	−1.1	V. fast	Smooth	Osc. 0^m8	2	4	8	260	7 years
29.....	DO Aql	1925	<16.5	8.6	8.6	Slow	(Osc.)	.....	.....	300	900	.....	.....
21.....	EL Aql	1927	19.0	6.4	5.5	Fast	Osc.	Osc. 1^m0	< 7	(8)	(22)	.....	.....
25.....	v356 Aql	1936	16.0	7.1	7.0	Slow	Osc. 1^m5	Smooth?	2	145	200	1100	.....
28.....	v368 Aql	1936	<15.0	5.0	5.0	V. fast	Osc. 0^m4	Smooth	2	5	16	220	.....
26.....	v528 Aql	1945	17.5	7.0	6.8	Fast	Smooth	Osc. 0^m4?	< 8	17	31	.....	.....
3.....	T Aur	1891	14.8	4.2	3.8	Slow	Osc!!	Dip 7^m!	< 2	80	.....	1800	15 years
10.....	T CrB	1866	v10.6	2.0	2.0	V. fast	Smooth	Max. 2^m5	.....	3	5	270:	.....
	T CrB	1946	v10.6	3.0	3.0	V. fast rec.	Smooth	Max. 2^m0	.....	5	7	300:	.....
35.....	Q Cyg	1876	v14.8	3.0	3.0	V. fast	Smooth	Smooth	.....	5	10	250	8 years
31.....	v476 Cyg	1920	15.5	2.0	2.0	V. fast	Smooth	Dip 1^m0	≥ 5	7	16	170	> 8 years
34.....	v450 Cyg	1942	<16	7.9	7.4	Slow	Osc!	Dip 5^m	<16	91	100	.....	.....
30.....	v465 Cyg	1948	17.5	9.7	8.0:	Slow?	Osc. 0^m6	Osc. 1^m5	.....	< 40	<160	.....	.....
5.....	DM Gem	1903	16.5	5.0	4.8	V. fast	Smooth	Hump	< 4	6	17	150	.....
6.....	DN Gem	1912	14.7	3.5	3.5	Fast	Osc!!	Osc.	1	16	37	550	.....
16.....	DQ Her	1934	15.0	1.4	1.4	Slow	Osc!!	Dip 7^m	.....	67	100	1000:	.....
37.....	DI Lac	1910	14.4	4.6	4.6	Fast	Smooth	Smooth	< 4	20	37	300	.....
36.....	CP Lac	1936	15.3	2.1	2.1	V. fast	Smooth	Smooth	1	5	10	154	.....
38.....	DK Lac	1950	15.5	5.4	5.0	Fast	Osc.	Osc. 2^m!	2:	19	29	500:	.....

TABLE 4—*Continued*

No.	Nova	Year	Min.	Max. Obs.	Max. Extr.	Type	Early Decline	Transition	Initial Rise (Days)	Duration of Decline (Days)			
										2^m	3^m	7^m	All
20.....	HR Lyr	1919	15.2	6.5	6.5	Slow	Osc. 1^m	Smooth?	< 2	48	92	600	.....
11.....	v841 Oph	1848	v12.6	4.3	4.3	Slow	Osc. 0^m4	Smooth?	.....	50	145	5000:	30 years
13.....	RS Oph	1898	v11.0	.....	.....	.....	.....	.....	.....	.....	.....	.....	.....
	RS Oph	1933	v11.0	4.3	4.3	V. fast rec.	Smooth	Smooth	1.0:	4	9	.....	80 days
17.....	v849 Oph	1919	<15	7.4	7.4	Slow	3 max.	(Osc?)	.....	120	150	.....	.....
1.....	GK Per	1901	v13.5	0.2	0.2	V. fast	Smooth	Osc. 1^m3	1	6	13	300	15 years
4.....	RR Pic	1925	12.7	1.2	1.2	Slow	Osc!!	Dip 0^m6	.....	80	150	1600	.....
7.....	CP Pup	1942	17:	0.4	0.4	V. fast	Smooth	.....	.....	5	7	140	.....
8.....	T Pyx	1920	13.6	6.4	6.4	Slow	Osc.	.....	.....	.....	.....	.....	< 1 year
	T Pyx	1944	13.6	7.0	7.0	S. rec.	Osc.	Smooth?	.....	100	130	.....	200 days
33.....	WZ Sge	1913	15.2	7.2	7.2	Fast	Smooth	Smooth?	.....	14	32	300	.....
	WZ Sge	1946	15.2	7.8	7.8	Fast rec.	Smooth	Steepens	< 2	18	28	.....	.....
23.....	v1059 Sgr	1898	16.5	4.9	4.5	Fast	Smooth	Dip 0^m5?	.....	10	20	340	9 years
14.....	v999 Sgr	1910	16.4	8.1	7.5	Slow	Osc!!	Smooth?	.....	220:	320:	1500:	>> 10 years
18.....	v1017 Sgr	1901	14.0	10.8	10.8	Slow	.....	.....	.....	.....	.....	.....	< 1 year
	v1017 Sgr	1919	14.0	7:	6.5	Slow	Smooth?	Osc.	.....	70	130	400	1.4 years
15.....	v630 Sgr	1936	15.5	4.4	4.4	V. fast	Smooth	Smooth	< 2	4	13	125	.....
22.....	EU Sct	1949	<16	7.4	7.4	Fast	Osc. 0^m3	Steepens	< 3	20	40	70	.....
12.....	RT Ser	1909	<14.5	10.6	10.6	RT	(Osc.)	.....	40:	5y	.....	.....	.....
9.....	CT Ser	1948	<15	8:	4:	Fast?	.....	Osc. 1^m	.....	.....	.....	< 500	.....
2.....	XX Tau	1927	<15.0	6.0	6.0	Fast	Smooth	Dip 2^m5	<14	25	44	320	.....
32.....	RR Tel	1944	v16	6.9	6.9	RT	.....	.....	.....	.....	.....	.....	.....

3.3. Light-Curves of Typical Fast Novae

Figure 2 displays light-curves of the three rapid novae v603 Aql, GK Per, and CP Lac. In CP Lac we see no indication of a premaximum halt. The rise was very rapid and continuous through the last 3 mag. Maximum endured less than a day, and the early decline was smooth. Only a slight undulation appears in the transition. The final decline was steady and uneventful.

GK Per was not sufficiently observed to establish the presence or absence of a premaximum halt. Maximum was brief, and the early decline was continuous

TABLE 5

MAGNITUDE RANGES OF NOVAE

Class	McLaughlin All Known		Bertaud Formula*		Payne-Gaposchkin Select List	
	Range	No.	Range	t_3 (Days)	Range	No.
Very fast....	11.9	8	11.7	12	12.5	6
Fast.....	10.6	10	10.6	30	12.3	4
Slow.....	9.2	13	9.1	100	11.0	4

* $A = -2^m.80 \log t_3 + 14^m.74$ (Bertaud 1948).

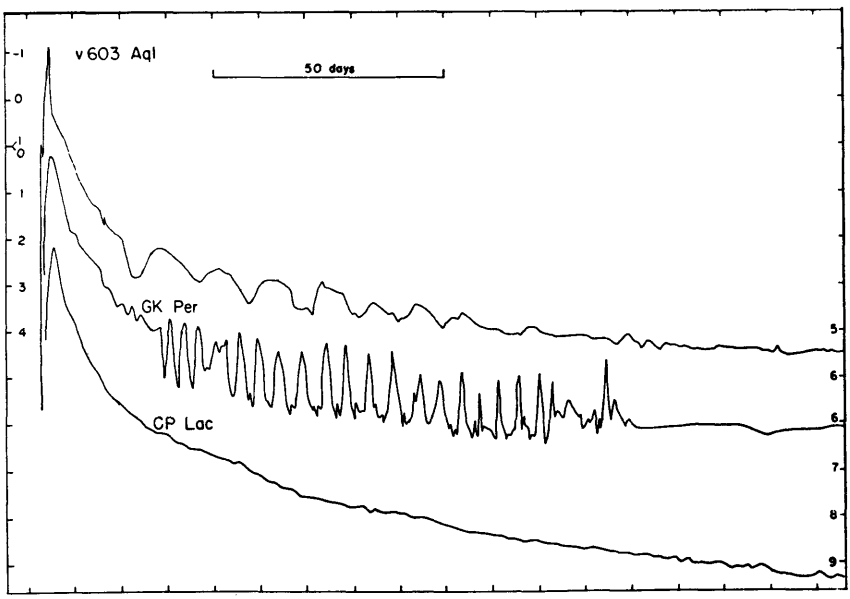


Fig. 2.—Light-curves of fast novae: v603 Aql (Campbell 1919), GK Per (Campbell 1903), and CP Lac (Parenago 1949).

and only slightly undulatory. During the transition there were spectacular oscillations, at first with a rough period of 3 days, later changing to 5 days. The onset of this phase began with a rapid drop below the trend of the early decline; the cessation of the fluctuations came when the star failed to brighten from a minimum. The final decline was without marked irregularities and required 15 years.

The brightening of v603 Aql 1918 from minimum to 2 mag. below maximum occurred within 2 days. The evidence for a premaximum halt appears good but not conclusive. Maximum endured only a few hours, and decline through nearly

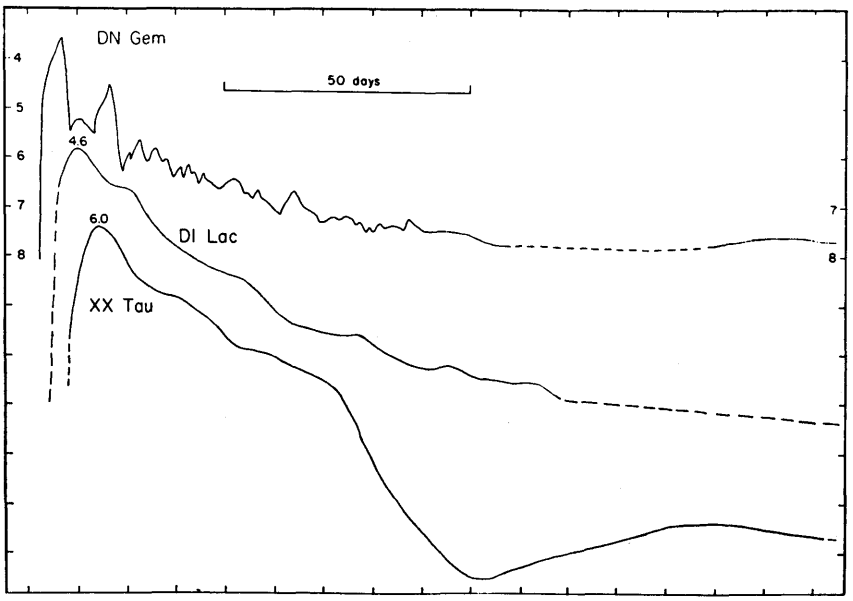


FIG. 3.—Light-curves of DN Gem (Campbell 1915), DI Lac (Leavitt 1920), and XX Tau (Beyer 1929).

a magnitude occurred in about 1 day. The early decline was smooth, the transition similar to that of GK Per, except for the longer period of the oscillations, about 11 days.

3.4. NOVAE OF MODERATE RATE

Among novae near the average rate, a greater variety appears. Three different types are shown in Figure 3. The light-curve of DI Lac 1910 appears smooth throughout; a suitable compression of the time scale would give a curve that could be nearly superimposed on that of CP Lac.

DN Gem shows the characteristic tendency of these novae to fluctuate strongly during the early decline, as well as in the transition stage. Especially noteworthy was the second maximum, 10 days after the first and brightest and 0.9 mag. fainter. The variations during the transition were quite irregular. DK Lac

1950 was similar in many respects, but its transition variations consisted of a number of strong outbursts of brief duration separated by long intervals of relative quiescence.

XX Tau had a smooth early decline, followed by a more rapid fading through 3 mag. and subsequent recovery during the transition. A similar steep drop through a larger range occurred in EU Sct and suggests an affinity with the DQ Her type.

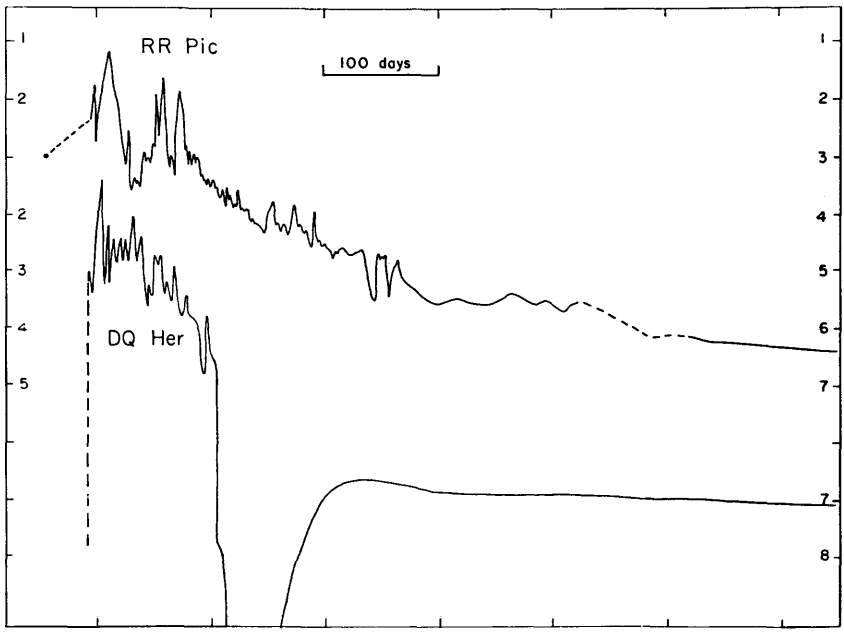


FIG. 4.—Light-curves of slow novae: DQ Her (Grouillier 1935) and RR Pic (Campbell 1932).

3.5. LIGHT-CURVES OF SLOW NOVAE

Two main varieties of slow novae are typified by RR Pic and DQ Her (Fig. 4). In the first there are several maxima of light which may be nearly equal. The transition is passed through with only small fluctuations. In DQ Her the occurrence of secondary maxima was equally well marked, and the oscillations were more irregular during the early decline. The transition set in with a very rapid drop through 7 mag. in a few weeks, followed by a gradual recovery to a brightness 6 mag. below maximum. From there on, the decline was smooth.

3.6. LIGHT-CURVES OF RT SERPENTIS STARS

The RT Serpentis stars, though extremely slow in their changes, cannot be excluded from the nova class. The increase in light is at least several magnitudes and *relatively* rapid, and the decline is gradual. The outstanding feature is the very protracted maximum, 15 years in RT Ser and more than 18 years in FU

Ori, which is still at maximum. Objects such as DO Aql and RR Tel appear to be intermediate between the RT Serpentis type and the majority of the known slow novae.

3.7. Continuing Variations

Several novae after reaching minimum have continued to vary irregularly for many years. We owe most of our knowledge of these continuing variations to W. H. Steavenson, who has followed several of these objects for more than thirty years. Table 6 summarizes the results of his longest series of observations.

Constancy or variation seems to be unrelated to recency of outburst or to any recognized feature of the more spectacular activity. Thus GK Per has varied continually since it reached minimum and shows no sign of subsiding, for its largest changes occurred as recently as 1949. Q Cyg and v841 Oph continue to vary rapidly. On the other hand, novae as recently as 1918 and 1920 have been

TABLE 6

Variability of Old Novae

Nova	Year	Light-Variation	Magnitude
v603 Aql	1918	Constant or slight variation	11.2
T Aur	1891	Constant	14.9
T CrB	1866, 1946	Slow oscillations 1 mag.	10:
Q Cyg	1876	Rapid variations	14.5–15.2
v476 Cyg	1920	Constant	15.4
DM Gem	1903	Constant	16.5
DN Gem	1912	Probably constant	14.7
DI Lac	1910	Constant	14.4
HR Lyr	1919	Constant	15.2
v841 Oph	1848	Rapid variations	12.0–13.1
GK Per	1901	Rapid variations	11.0–14.1

nearly or quite steady ever since reaching minimum. Fast and slow alike are represented in both the constant and the variable group. Nor does the spectrum show any well-defined relationship to constancy or variability. GK Per has the strongest emission lines and the largest light-variations, but v841 Oph, which also varies rapidly, has only a continuous spectrum, so far as known. Among the constant stars, v603 Aql has moderately conspicuous emission lines, while HR Lyr has only a continuous spectrum. However, Greenstein (see chap. 19) has just recently found emission in both v841 Oph and HR Lyr.

Figure 5 shows two typical seasons' observations of GK Per by Steavenson (1923, 1924). No regularity has been found. The typical form of the curve, however, can be described as a rounded maximum lasting several months, with large irregular fluctuations superimposed. In 1948 and 1949 GK Per had unusually bright maxima at about 11.0 mag. (Steavenson 1950).

DQ Her requires special mention. Walker (1956) finds a regularly recurring minimum at intervals of 4 hours, which is interpreted as an eclipse by a com-

panion. In addition, there are remarkable variations with a period of about 1 minute and amplitude of 0.1 mag. (Fig. 6).

Walker (1957) has found that several other old novae have irregular variations, up to a few tenths of a magnitude, with periods of several minutes. Steavenson's visual estimates must represent essentially an averaging of these rapid variations.

3.8. Recurrent Novae

For many years T Pyx was a unique case of repetition of nova outbursts some years apart. It was called "nova-like" by Ludendorff (1928) and was grouped with such different objects as η Car and Z And. The list of fully established recurrent novae is given in Table 7.

In addition to this list, v1017 Sgr (1919) is commonly called a recurrent nova. However, its other known outburst in 1901 was not at all a full-scale nova epi-

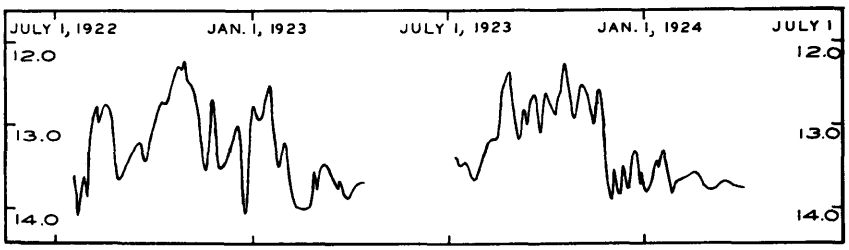


Fig. 5.—Fluctuations of GK Per at minimum, 1922–1924 (Steavenson 1923, 1924)

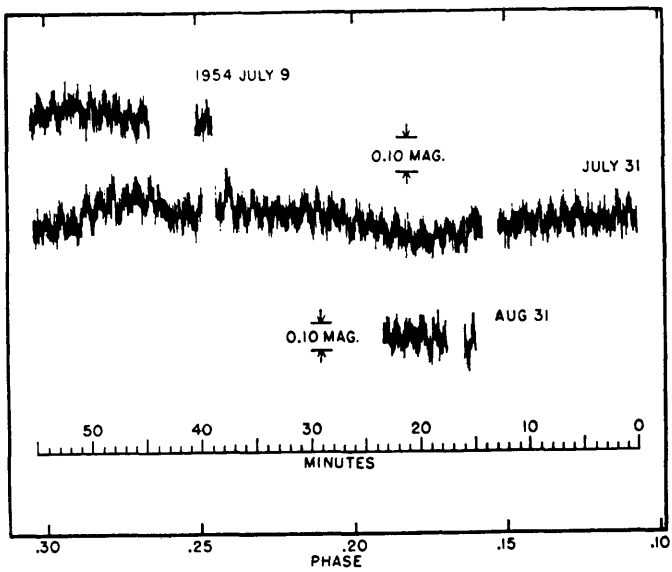


Fig. 6.—Rapid variations of DQ Her, in ultraviolet light, observed 1954, July 9, 31, and August 31. Tracings from Brown recorder sheets (Walker 1956).

sode. The rise was only 3 mag., and the maximum was broad and rounded (McLaughlin 1946). Rather than a true major outburst, it resembled the brightening of T CrB that occurred in 1938, preceding its full-scale outburst in 1946. Another object sometimes noted as a possible recurrent nova was seen in Orion in 1667 and about 1750.

It is not possible to list criteria whereby a recurrent object might be recognized at its first recorded outburst. The fact of observed repetition is the only clearly distinguishing mark. The recognized recurrent novae do, however, show a few distinct points of difference from "typical" novae. The durations of their outbursts are definitely short. While a typical nova is brighter than its minimum for several years, all the recurrent ones have returned to minimum in less than 1 year. The amplitude is less for most recurrent stars, though T CrB had a range of at least 9 mag., well within the dispersion of ranges of novae not known to recur.

TABLE 7

RECURRENT NOVAE

Nova	Max.	Min.	Dates of Max.
T CrB.....	2.0	<10.6	1866, 1946
RS Oph.....	4.3	11.7	1898, 1933, 1958
T Pyx.....	6.4	13.6	1890, 1902, 1920, 1944
WZ Sge.....	7.2	15.2	1913, 1946
U Sco	8.8	<17.6	1863, 1906, 1936

Three recurrent novae faded very rapidly during the first week after maximum (T CrB, RS Oph, U Sco). T Pyx, however, remained for several weeks within about a magnitude of maximum. The light-curve of T CrB (Pettit 1946) at both outbursts had a second low, broad, and rounded maximum a few months after the main brief maximum. No other light-curve is known to have this form.

For T CrB, RS Oph, and WZ Sge the general spectral features differed conspicuously from those of any known typical nova. However, while these peculiarities may be associated only with recurrent objects, their absence certainly does not stamp a nova as non-recurrent, for T Pyx had a spectrum that could not be distinguished from that of a typical nova (see § 4.10).

Both T CrB and RS Oph appear to have been objects of typical nova luminosity at maximum. WZ Sge, however, was pretty surely a "dwarf nova." Unless we are prepared to admit an otherwise unheard-of space motion, its proper motion of 0".08 per year indicates a distance so small that its luminosity must have been several magnitudes fainter than that of typical novae.

Kukarkin and Parenago (1934) pointed out that U Geminorum stars and recurrent novae fit a single relation between amplitude (A) and interval between maxima (P):

$$A = 0.80 + 1.667 \log P \,. \qquad (1)$$

This at least carries a suggestion that all novae may repeat, though such extrapolation may not be correct. If the formula holds for larger amplitudes, then a typical nova with a range of 12 mag. would have a recurrence interval of some 10^4 years.

3.9. Nova-like Variables

The line of demarcation between accepted novae and nova-like stars is difficult to draw. There is no complete agreement as to whether it is legitimate to call η Car and P Cyg novae. The latter star seems to have become stabilized in a nova-like stage and is ejecting matter steadily.

η Car has shown a typical nova amplitude, as well as nova-like changes of spectrum. Its light-curve may be regarded as that of an unusually protracted RT Serpentis–type star. Although its brightest recorded maximum was in 1843 and its steady decline set in about 1857, it was within a few magnitudes of maximum for more than a century before these dates.

Z And may be ruled out of the true nova class on the grounds of too small an amplitude (only 3 mag.). Its long, slow variations following a major maximum are associated with considerable changes of excitation similar to those of novae, and near the brightest maxima its spectrum has the characteristic P Cygni appearance.

Among the nova-like variables we should probably include the companion to R Aquarii, which, for a few years, nearly submerged its long-period class M primary with a P Cygni–like spectrum (Merrill 1935). The companion to *o* Ceti may be considered a suspected member of this group.

3.10. Relation of Luminosity to Rate of Fading

The best-determined absolute magnitudes are brightest for fast and faintest for slow novae (McLaughlin 1945*a*). The trend is shown alike by luminosities derived from nebular expansion, interstellar calcium intensity, galactic rotation effect, and Hubble's (1929) early observations of novae in M31. The relation has recently been rediscussed by Arp (1956) for a new list of novae in M31 and by Kopylov (1952), Schmidt (1957), and Payne-Gaposchkin (1957) for galactic novae. Buscombe and de Vaucouleurs (1955) find that the novae in the Magellanic Clouds fit the relation approximately.

Kopylov applied very large corrections for interstellar absorption, so that he found generally higher luminosities than did the other investigators. Schmidt's discussion shows that these absorption corrections were excessive. Results obtained by Arp, Schmidt, and Payne-Gaposchkin are in rather good agreement. The form of the relation is shown graphically in Figure 7, in which part *A* is based on data from Tables 2 and 4 (plus luminosities determined from interstellar line intensities) and part *B* is from Schmidt. In both parts of the figure, the straight line is represented by

$$M_0 = -11.5 + 2.5 \log t_{3,v} , \qquad (2)$$

where M_0 is the absolute visual magnitude at maximum and $t_{3,v}$ is the duration in days of decline through 3 mag. (visual) from maximum.

3.11. Comparison of Galactic Novae with Those of M31

Arp found that novae in the Andromeda spiral follow closely the same relation between luminosity and rate of fading that fits galactic novae. In general, the light-curves of the Andromeda novae closely resemble those of the galactic objects. Within the accessible parts of the light-curves, practically all types known in our Galaxy are found in M31.

The rapid novae of both systems have the same smooth decline and general form of curve. The slower ones in both galaxies tend to have violent fluctua-

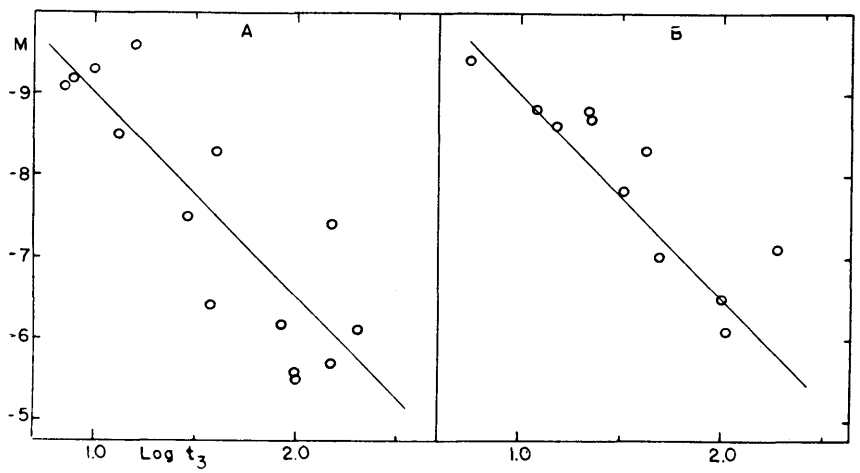


FIG. 7.—Relation between absolute magnitude, M, and log $t_{3,v}$ (duration of decline through 3 mag.). *A*, data from Tables 2 and 4; *B*, data from Schmidt (1957).

tions during the early decline, a characteristic that persists to the longest observed durations in M31. The frequency distribution of different rates, however, is different. The percentage of rapid novae found in M31 is higher than in our Galaxy. This may be purely a discovery effect due to the greater chance of missing a galactic fast nova because of its brief time near maximum. Inspection of Arp's curves gives the impression that the Andromeda novae tend to have somewhat greater incidence of strong fluctuations than those of our Galaxy.

§ 4. SPECTROSCOPIC CHARACTERISTICS AND VARIATIONS

4.1. Outline of Spectral Development

Only one faint record has been obtained of the spectrum of a non-recurrent nova before outburst (§ 4.2). Nothing at all is known of the spectrum during the rapid rise from minimum to about 2 mag. below maximum.

The earliest records of spectra have been obtained near the premaximum halt or equivalent magnitude. All novae observed at this stage have had early-type absorption spectra strongly displaced toward shorter wave lengths. Three were classifiable as peculiar B spectra and others as early class A. Only one, DQ Her, had strong, wide, bright lines. All novae near maximum have had strong, shortward-displaced absorption spectra of class A or F (with certain peculiarities) without conspicuous emission lines. With the first fading from maximum, the spectrum is quickly transformed into the "typical nova" spectrum, a pattern of bright lines widened symmetrically about their normal positions and flanked on their sides of shorter wave length by strong absorption lines. This "principal" absorption spectrum has a greater displacement than its predecessor, the "premaximum" system. The two sets of lines often coexist briefly. Bright lines associated with the principal absorption are those of hydrogen and metals, to which are soon added emissions of [O I] and later [N II].

When the star has faded about 1 mag., a third absorption system appears. It is still more strongly displaced toward shorter wave lengths (about twice the shift of the principal spectrum), and its lines are usually wide and diffuse at first, developing later into several separate components. Hydrogen lines are the most prominent, and lines of Fe II and other ionized metals usually occur. This has been called the "diffuse enhanced" spectrum.

A fourth absorption spectrum having the general composition of that of an early B star emerges as the diffuse enhanced spectrum fades, at about 2 mag. below maximum. This "Orion" spectrum is often subject to large oscillations of position, but its average displacement is comparable with, or a little greater than, that of the diffuse enhanced spectrum. Broad, symmetrically widened emissions accompany both the diffuse enhanced and the Orion absorption lines. The hydrogen emissions are the most conspicuous of the diffuse enhanced system; those of N II and O II are seen in conjunction with the Orion spectra of slow novae, but in the fast novae they are very difficult to recognize because of their extreme width and diffuse character.

During these changes the principal absorption spectrum weakens more or less steadily, but the associated bright lines are seen in better contrast as the continuous spectrum fades. The excitation of the principal emission increases, so that lines of Ca II and Na I, for example, disappear, while those of He I and N III intensify relative to those of hydrogen. When the last absorption lines are gone and the N III emissions near λ 4101 and λ 4640 are prominent, the nebular lines of [O III] make their appearance, soon followed by those of [Ne III]. Thus the spectrum gradually transforms itself into one like that of a gaseous nebula, except for the large Doppler widening of its lines. The transition stage is now past, and during the final decline the bright lines weaken more rapidly than the continuum. Near minimum, when sufficiently exposed, the spectrum shows a strong continuum of great violet extent, indicating a high temperature for the star. Several novae at the end of decline have relatively narrow bright

lines of hydrogen and He II that persist for many years, while others show only the high-temperature continuum. Table 8 summarizes the characteristics of the several systems of absorption and emission lines and their behavior in relationship to the light-variations.

Plate I displays spectra of v603 Aql (1918) in the photographic region and DK Lac (1950) in the visual region.

4.2. The Spectrum before Outburst

The only available record of the spectrum of a nova before outburst is that of v603 Aql 1918. The dispersion was extremely low and the record faint. The energy distribution in the continuum resembled that of an A-type or B-type star (Cannon 1920), and no lines, either bright or dark, could be distinguished (Gaposchkin 1941). While not conclusive, nothing in this observation is incon-

TABLE 8

Absorption and Emission Systems

Absorption System	Emission System	Duration mags. from max.	Part of Light-Curve
Premaximum.....	Premaximum	*	Rise (early decline)
Principal.....	Principal	0.6–4.1	Early decline
Diffuse enhanced.....	Diffuse enhanced	1.2–3.0	Early decline
Orion.....	Orion (hazy bands)	2.1–3.3	Early decline
Nitrogen (Orion).....	"4640" (Orion)	3 –4.5	Transition
.....	Nebular (principal)	4 –11	Trans. to final decline
.....	Postnova stellar	8 to min.	Final decline and postnova

* The premaximum absorption has been observed from about 2 mag. below maximum on the ascending branch of the light-curve, to maximum and down the decline about 1 mag. in several stars. In a few it has continued faintly to about 3 mag. down the decline.

sistent with the suggestion that the spectrum before outburst was essentially the same as that observed many years after the star had returned to minimum.

Among recurrent novae we have two examples of reasonably pure prenova stellar spectra and two others considerably blended with spectra of companion stars. Before their outbursts of 1944 and 1946, T Pyx and WZ Sge, respectively, showed essentially continuous spectra with energy distribution to indicate high temperature and with only faint emission of hydrogen and He II. They were thus practically indistinguishable in appearance from the postnova spectra of several non-recurrent objects (Humason 1938). The spectra of both T CrB and RS Oph at minimum are composite and perhaps not typical. In these the evidence points to a very hot star as the body that produces the nova outburst, while at minimum the spectrum of a companion of late type is prominent. The very strong bright lines of hydrogen, He I, He II, N III, and other atoms requiring moderately high excitation may be due in part to interaction of the two stars, since the spectra resemble those of such "symbiotic" objects as Z And and CI Cyg.

4.3. The Premaximum Spectrum

Seven novae have been observed spectrographically at some time during the final rise. Most of these had moderately diffuse absorption spectra without strong emission lines. DQ Her alone had strong emissions as well. Three stars when first observed had diffuse absorption spectra of class B, displaced toward shorter wave lengths. Three others had A-type spectra and one, RR Pic, class F (see Table 9). Accurate classification is troublesome, owing to peculiarities. Weak, undisplaced, broad emission was visible in some of these spectra at Hα. RR Pic had narrow metallic bright lines which carried the absorption lines on their shortward edges. For most of these spectra the displacements of absorption lines of the different elements were fairly accordant.

TABLE 9

Premaximum Spectra of Novae

Nova	First Observed		Maximum		After Maximum	
	Date	Class	Date	Class	Date	Class
GK Per 1901	Feb. 22	B9p	Feb. 23	A0	Feb. 24	A2:
DN Gem 1912	Mar. 13	A5	Mar. 14	A5?	Mar. 15	cF5
v603 Aql 1918	June 8	A0	June 9	A5	.....	.....
v476 Cyg 1920	Aug. 22	A0	Aug. 23	A2	Aug. 24	A5:
RR Pic 1925	May 31	F2	June 7	gF8	June 12	gF8
DQ Her 1934	Dec. 13	B5p	Dec. 22	cF0	Dec. 24	cF5
CP Lac 1936	June 19	B9p	June 20	gA2	June 21	gA5:

When DQ Her was first observed, it had very strong, wide, and diffuse emission lines of hydrogen, He I, C II, N II, and other elements, bordered on the shortward sides by broad hazy absorption. Displacements of the various lines and widths of the emissions were highly discordant. Thus Stratton (1936*b*) found the absorption velocities given in the accompanying table.

Hζ	−903 km/sec	Hγ	−1023 km/sec	He I:4026	− 750 km/sec
Hε	−929	Hβ	−1179	4472	−1382
Hδ	−746	Hα	−1984	5876	−1409

During the brightening to maximum, the absorption spectrum usually becomes better defined and stronger and always changes to a later class. Each of the B-type spectra quickly changed to class A well before light-maximum was reached. The spectra at maximum range from A0 (GK Per) to F8 (RR Pic). A spectrum of class K has been reported for v1148 Sgr. In general, the spectrum near maximum closely resembles that of a supergiant star such as α Cyg or ε Aur. With the brightening of the star, whatever emission lines are

present are soon submerged by the strengthening continuum, so that at maximum only Hα remains visible in emission.

While resemblances to the absorption spectra of supergiant stars are close, special peculiarities are conspicuous. Thus, in spectra closely resembling those of α Cyg or ε Aur in most features, the Ca II and Na I lines are abnormally strong. The novae that have shown a class B stage have had lines of O II and N II fairly conspicuous, as in class B1 or B2, while the relative strengths of He I and Mg II were those found in class B8 or B9. The spectra thus appear "composite" at most times. Another conspicuous peculiarity is the presence of strong lines of C I and O I (McLaughlin 1936).

The premaximum spectrum usually lasts for a short time after maximum light and disappears when the postmaximum transformation occurs. In six of the seven novae observed before maximum, the displacements of the absorption spectra changed by only small amounts during the observed interval. In DQ Her the displacements diminished markedly during several days. The associated emission lines narrowed, keeping the absorption components on their shortward edges. By the time that light-maximum was reached, the displacements of the various lines had become fairly accordant at −175 km/sec, in contrast with their large scatter a few days earlier.

4.4. The Principal Spectrum

4.41. *The postmaximum transformation.*—The change to the "typical nova spectrum" of bright and dark lines takes place quickly after maximum light. The transformation has been completed in less than 24 hours in fast novae and requires only a few days in such slow novae as RR Pic and DQ Her.

The spectrum at maximum is that of a supergiant A or F star, with shortward displacement of from 60 km/sec (RR Pic) to 1300 km/sec (v603 Aql). The lines are single but may be either diffuse or well defined. During the first drop from maximum, a second set of lines appears with greater shortward displacement and strengthens rapidly until it equals and then surpasses the premaximum spectrum, while the latter weakens. During the stage of near-equality the duplicity of lines gives the spectrum an ill-defined appearance. The newly emerged absorption system is the principal spectrum and is usually very similar in composition to the one it replaces. The double-line stage is so fleeting in the fast novae that it was long overlooked in some. For example, v603 Aql 1918 was recorded clearly in this stage only at the Cape Observatory (Lunt 1919). A few hours later, when spectrograms were taken in North America, only the hydrogen and Ca II lines showed components belonging to the disappearing premaximum spectrum. Most of the lines were those of the newly emerged principal spectrum with velocity about −1500 km/sec.

Simultaneously with the appearance of the principal absorption, bright lines appear throughout the spectrum. The strongest are those of hydrogen and Ca II; next in order are Na I and Fe II. These emissions are symmetrically widened

about their normal positions, and the principal absorption lines lie at their shortward edges. During the early stages of the transformation, the remaining premaximum absorption lines terminate the emissions on their shortward sides.

The principal spectrum shows the same peculiarities as the premaximum, in that the lines of Ca II and Na I appear too strong in comparison with the rest of the spectrum and that strong lines of O I and C I are present. Not all novae show these lines; for example, they were weak or absent in RR Pic. The lines of C I were especially strong in EU Sct in 1949. In DQ Her very strong CN absorption emerged with the principal spectrum and disappeared within a few days.

4.42. *Development of the principal spectrum.*—Changes in the principal spectrum begin immediately after its full emergence. Some strong lines disappear very early, while some others of lesser strength may persist long. Among the first absorptions to fade are Mg II 4481, the lines of O I and C I, and those of Si II. The lines of Fe II and especially Ti II are quite persistent. Those that endure longest are the Balmer series of hydrogen and H and K of Ca II. Mg I 3838, whose lower level is metastable, was one of the most persistent in DQ Her. The long duration of Ti II lines is also due to the metastability of their lower levels. In general, few new absorption lines emerge in the principal spectrum, but near the time of its disappearance, in several novae, fine lines of He I have been observed at λλ 3888, 3965, and 4472. The last lines to fade from view are those of hydrogen, at about 4 mag. below maximum.

In several novae the principal spectrum has developed double and even triple absorption lines. Thus GK Per had triple lines, v603 Aql and DN Gem double lines.

The principal emission undergoes a more striking evolution. The auroral line [O I] 5577 becomes visible soon after maximum, quickly followed by λ 6300 and λ 6364. A little farther on the decline, the "auroral" emission of [N II] 5755 emerges. All these radiations strengthen rather steadily, relative to the remainder of the spectrum, but at 2.6 mag. below maximum the [O I] lines appear to become rapidly stronger (the [O I] flash). At 3.3 mag. down, a similar "flash" occurs for [N II]. Shortly after this, at 3.6 mag. down, He I 5876 brightens rapidly (the helium flash). Actually, almost the entire history of all emission lines is a continuous weakening, but, because the integrated light becomes fainter, the spectra are exposed longer, and the lines that weaken most slowly seem to have strengthened. Only the first emergence of such lines as [O I] and [N II] may involve a real increase in intensity, and, from then on, their apparent strengthening is due merely to increased exposure. The He I lines and also those of N II and O II that appear later surely do strengthen at first, as a result of increasing ionization and excitation.

Meanwhile, the emissions of Ca II, Na I, and Fe II have been steadily weakening, while the hydrogen emission still remains the strongest in the spectrum. Ultimately, lines of N III, He II, [O III], and [Ne III] appear in the principal

emission spectrum. However, these can be discussed more appropriately in connection with the nebular stage. In the slow novae, emissions of [Fe II] appear near the time when the absorption spectrum is about to disappear.

4.5. The Diffuse Enhanced Spectrum

Before the principal spectrum has lost much strength, a new system of lines appears, with shortward displacement roughly twice that of the principal spectrum (−550 to −950 in DQ Her; −2200 in v603 Aql). This "diffuse enhanced" spectrum consists, at first, of wide and hazy lines of hydrogen, Ca II, Mg II, and usually Fe II, Na I, and O I. Slow novae ordinarily have a richer diffuse enhanced spectrum, including lines of Ti II and Cr II. This system reaches maximum strength about 2 mag. below maximum and then declines. In slow novae especially, its lines greatly exceed in strength those of the principal spectrum; in some fast novae it has been conspicuous only at the hydrogen lines. The lifetime may be only a few days in the most rapid novae, but in the slow ones it lasts several weeks. During its decline the lines usually become well defined, even sharp, and develop multiplicity. Apparently, the several components were present at all times, but their overlapping wings produced a single broad blend. The multiple-line stage may include disappearances and reappearances of some of the components, as well as occasional apparent rapid shifts of position. Fluctuations of brightness of these novae are usually accompanied by striking changes in the strength and position of the diffuse enhanced absorption lines. RR Pic and DQ Her showed especially complex behavior.

The stronger lines of this system are accompanied by emission. Like the bands of the principal spectrum, these are widened symmetrically, and the absorption lines lie at their shortward edges. At their greatest strength, these bands at the hydrogen lines may equal the principal bands. The character of the diffuse enhanced spectrum suggests turbulence or a large spread of velocities This is consistent with the relative intensities of strong and weak absorption lines, obvious to inspection, though no determinations have been made of curves of growth.

In the disappearance of this system the line of Mg II is first to fade, and the hydrogen lines disappear at about 3 mag. below maximum.

4.6. The Orion Spectrum

4.61. *Early stage.*—Near the time of maximum strength of the diffuse enhanced system, absorption lines of He I, N II, and O II begin to appear, with displacements usually similar to those of the diffuse enhanced lines but frequently much greater. Hydrogen lines with the same velocities may or may not appear. In v603 Aql the Orion velocity was −2700 km/sec, as against the diffuse enhanced velocity, −2200 km/sec. This Orion absorption spectrum reaches maximum strength close to the date of disappearance of the diffuse enhanced system. Its lines are somewhat diffuse, and, unlike its predecessor, this system does not sharpen with the passage of time, nor does it become conspicuously

multiple in most novae. In only two stars were the Orion absorptions observed other than single. DQ Her had two Orion systems, one of which, with velocity about −1000 km/sec, appeared and disappeared irregularly, while the other, near −450 km/sec, was more nearly constant. In v450 Cyg, a star of the DQ Herculis type, on a single date the Orion system appeared double. The numerous groups of N II and O II lines between λ 4600 and λ 4700 is especially striking when the Orion spectrum is strongest. In the visual region the N II group near λ 5680 is prominent. Strong lines of Ne I appeared in the early Orion spectrum of v528 Aql (1945), but, so far as known, this occurrence in a nova spectrum is unique (McLaughlin 1960*b*).

Hazy and featureless emissions accompany the Orion absorption lines. The most conspicuous is a very broad band centered near λ 4640, which is probably a blend of N II and O II lines when it first appears, but later, as the excitation increases, it gives way to the lines of N III. Still later the vague band in this region is probably due largely to N V. In general, the hazy Orion emissions are more evident in slow novae than in fast ones. In the latter their widths are so great that they show only slight contrast with the continuous spectrum.

The Orion lines undergo large shifts of position that correlate with secondary light-variations (§ 5.4). In CP Lac and v528 Aql, which showed no conspicuous secondary variations, these lines nevertheless oscillated irregularly over a large range.

4.62. *The "4640 stage."*—The numerous N II and O II lines fade gradually, and the pair of N III lines at λ 4097 and λ 4103 emerges along with the broad, hazy emission bands at λ 4640 and λ 4100. With this development the nova has reached the "4640 stage" about 3.5 mag. below maximum. By this time the diffuse enhanced absorption has disappeared, and the principal absorption has been reduced to the hydrogen lines.

The 4640 stage coincides approximately with the transition stage of the light-curve. It marks the change in the spectrum from stellar to nebular type. The fluctuations of light that occur in some novae and the corresponding spectral changes, accompanied by "nitrogen flaring," will be discussed in § 4.11. Here we note one of the striking differences between fast and slow novae. With the exception of CP Pup, every fast nova that has been adequately observed has shown very strong N III absorption at λ 4097 and λ 4103 at some time during the transition. No slow nova has had more than a trace of these lines. RR Pic had them feebly present very briefly; DQ Her failed to show them, though on occasions a broad, hazy emission centered on Hδ indicated the probable presence of the corresponding emissions. DN Gem, which showed some affinity with slow novae, had these lines only sporadically present.

Another distinction between fast and slow novae near this stage is the conspicuous presence of lines of [Fe II] in the principal emission spectra of slow novae and the absence or extreme weakness of these lines in fast novae. This difference may be largely due to contrast, because [Fe II] lines were found in CP Pup (Weaver 1944).

4.7. The Nebular Stage

As the nova continues to fade, the excitation of the principal emission spectrum increases, and its composition changes, as noted previously (§ 4.4). Forbidden lines of O I and N II emerge very early. Lines of He I, N II, N III, and He II appear with the same widths and structural patterns as those of hydrogen. The disappearance of the diffuse Orion band of N III at λ 4640 reveals bands of the principal spectrum due to the same radiation. In a few novae the red coronal line λ 6374 [Fe X] has appeared in greater or lesser strength (McLaughlin 1953*b*). It was very strong in CP Pup, but its strongest known occurrence was in Nova Her 1960. The green line λ 5303 [Fe XIV] has appeared conspicuously in recurrent novae and probably was present in Nova Her 1960.

At about 4 mag. below maximum the emissions of [O III] and [Ne III] first become visible. These strengthen relative to the permitted lines until they dominate the spectrum. Actually, with the probable exception of their first emergence, no real increase in these radiations occurs. Rather, as the nova fades, the exposures are lengthened to record the weakening spectrum, and the more slowly fading forbidden lines are exposed more strongly.

The history of late stages of nova spectra is fragmentary, but the general course of changes is fairly well outlined. The line λ 4363 [O III], among the first to emerge, later fades relative to λ 4959 and λ 5007. After developing to considerable strength, the [O I] lines λ 6300 and λ 6364 weaken relatively, as does the "auroral" line of [N II], λ 5755 (the auroral line λ 5577 [O I] has already weakened earlier). The red pair of [N II] lines flanking Hα at λ 6548 and λ 6584 continues to strengthen relatively. In both DQ Her and v603 Aql these eventually exceeded Hα. Their behavior is not well known in many novae because of blending with Hα on low-dispersion plates.

In the fully developed nebular stage at 7 mag. below maximum, a nova spectrum simulates closely that of a planetary nebula, save for the widths of the lines. However, there are considerable differences from one nova to another that cannot be attributed to incompleteness of the record or to simple differences of excitation. Among the most striking is the strength of the [Ne III] lines (McLaughlin 1944). These were remarkably strong in GK Per and rather weak in v603 Aql. The lines of [O III] were unusually weak in RR Pic. The ejected material continues to show a similar spectrum for many years in those rare cases in which the record has been obtained. Often, however, attention has been concentrated on the star, and no attempt has been made to obtain the spectrum of the feeble surrounding nebulosity. The nebula about GK Per (light-maximum in 1901) still showed a typical nebular spectrum in 1937.

4.8. The Postnova Spectrum

When long exposures are made during the nebular stage, a continuous spectrum can be recorded, at the expense of seriously overexposing the stronger

nebular emissions. Carefully guided spectrograms of novae and their expanding nebular shells show that the emission bands originate mainly in the expanding shell, while the continuum is localized in the central star. As the nebula continues to fade, the continuous spectrum of the star can be recorded with less and less superposed nebular emission, and eventually only the spectrum of the star remains.

The continuous spectra of novae near or at minimum have great extent in the ultraviolet, indicating a star of high temperature (Humason 1938). Greenstein has recently obtained spectra of many old novae. WZ Sge and DI Lac have broad absorption lines, like those in a white dwarf. In some of these, no features of either absorption or emission can be distinguished. Many novae, however, have relatively narrow emission lines of hydrogen, He II, and C III. These are about 12 A wide in v603 Aql and 16 A wide in GK Per (see chap. 19). The postnova emissions of the latter star are the strongest known, with the exception of those in recurrent objects (T CrB, RS Oph).

The development of the postnova stellar emission is best known in v603 Aql (McLaughlin 1953*a*). From 1 to 2 years after maximum, spectra taken with careful guiding to show the structure of the nebular shell recorded a small emission knot in the continuous spectrum of the star at λ 4686 He II. After the nebula had become very faint, this knot remained, and similar knots gradually appeared at the hydrogen lines. These strengthened, while the He II knot weakened somewhat. They were approximately equal in 1942, but in 1957 an observation by Greenstein (personal communication) showed He II appreciably weaker. The postnova emissions are strongest and widest in GK Per, but they have only a fraction of the width of the principal emissions which originated in the expanding nebula.

There are some suggestions that the "postnova" narrow emission at λ 4686 has appeared occasionally and briefly during the transition stage, since a narrow emission maximum that had no counterpart in other emission bands was seen at that position during the fluctuations of light and spectrum that accompanied the transition stages of v603 Aql, DN Gem, and GK Per (McLaughlin 1947*b*).

4.9. Comparison of Fast and Slow Novae

Viewed broadly, fast and slow novae undergo the same spectral changes, and in both classes these are related in the same way to the changes in brightness of the star. When we examine the detailed development, systematic differences appear.

Whether or not it represents inadequacy of the sample, the slow novae at and near maximum appear to have been of later spectral class than fast novae generally. A few fast novae (v603 Aql, v528 Aql) have had principal spectra of class F, but most have been class A0–A5. The slow novae, so far as known, have averaged distinctly later.

The greater observed number and apparently greater strength of emission

lines in the spectra of slow novae are probably illusory and due simply to the narrowness of the emissions and their resultant higher contrast with the continuous spectrum.

Slow novae tend to have a stronger development and proportionally longer duration of the diffuse enhanced spectrum. With this goes greater complexity of behavior, appearance and disappearance of components, and rapid shifts of some lines. In the fast novae the diffuse enhanced absorption emerges quickly, remains for several days, and then fades without large oscillations or complex changes of structure. Fast novae rarely show the extremely heavy and wide absorptions that occur in the diffuse enhanced components of the hydrogen lines of slow novae. In the slow novae the diffuse enhanced spectra tend to show more lines, especially of Fe II and Ti II, while in fast novae we often find only hydrogen, Ca II, and Mg II.

Although the incidence of the Orion spectrum seems equally great in both groups, the strength averages greater in the slow novae. In some of the fast novae the Orion spectrum escaped recognition for many years, because of either its weakness or the brevity of its visibility. On the other hand, slow novae show extreme weakness or absence of the later stage of the Orion spectrum when strong N III absorption lines appear at λ 4097 and λ 4103 in the spectra of fast novae.

The η Car stage, characterized by strong emissions of [Fe II], is conspicuous in slow novae but has been noted in only one fast nova, CP Pup (Weaver 1944). No outstanding differences have been recognized in the nebular stage.

4.10. Spectra of Recurrent Novae

With one exception, observed spectra of recurrent novae have differed considerably from those of typical novae that are not known to repeat. The exception is T Pyx; the observations are fragmentary and refer to two different outbursts. In 1920, shortly after maximum, T Pyx had three strongly displaced absorption systems (Adams and Joy 1920) corresponding to principal, diffuse enhanced, and Orion spectra, with velocities from -1000 to -1900 km/sec. Broad hydrogen emission corresponded in width to the principal emission spectrum. There were no spectrographic observations near maximum in 1944, but when the nova had declined considerably in 1945, several Mount Wilson spectrograms showed a typical nebular stage with great Doppler broadening, as in typical novae (Joy 1945). The only unusual feature was the presence of the coronal lines.

Three other recurrent novae have been observed spectrographically. The record is most extensive for T CrB (Herbig and Neubauer 1946; Sanford 1949). The first observations made at maximum showed strong, broad, and diffuse hydrogen and helium emission with hazy absorption lines on their shortward edges. The excitation was distinctly higher than that of typical nova spectra at maximum. During the decline from maximum the emissions narrowed steadily until they were well defined. Concurrently, the absorption *seemed* to

move inward with the shortward emission edge, so that its displacement decreased. This, however, was illusory. Detailed analysis shows that highly displaced absorptions faded and lines of smaller displacement intensified or were uncovered by the fading hazy emission wings (McLaughlin 1957). A week after maximum, Mount Wilson coudé spectrograms showed six absorption components with displacements ranging from −60 to −360 km/sec. No systems corresponding to diffuse enhanced and Orion spectra could be recognized. However, the fading of the nova was accompanied by a moderate increase in excitation, as He II strengthened relative to He I, and N III emissions became conspicuous. From about 2 mag. below maximum all the way to minimum, the general composition of the emission spectrum remained nearly unchanged. The coronal lines were present throughout this time. After reaching minimum in April, another brightening occurred through about 2 mag. This was accompanied by a strong increase in the continuum and a decrease in excitation (He II disappeared), and all but the strongest emission lines were submerged by the continuum. A stage with strong nebular lines never developed, though narrow [O III] emissions were present at the minimum in April and again for a number of months during and after the decline from the broad second maximum. The coronal line of [Fe X] reappeared at the same time.

The behavior of RS Oph in 1933, though less extensively observed, was somewhat similar. Its absorptions were very weak and vague, except for sharp lines of small displacement near the emission centers. The entire violet half of each hydrogen emission band was apparently depressed by diffuse absorption without discrete components (Wilson and Williams 1934). As the star faded, the emission seemed to narrow (with the fading of its hazy wings), as in T CrB. The coronal lines of [Fe X] and [Fe XIV] were present in great strength as the star approached minimum (Adams and Joy 1933). The 1958 outburst of RS Oph was practically a repetition of the 1933 maximum. A feature not seen clearly in 1933 but conspicuous in 1958 was diffuse hydrogen and helium absorption with velocities ranging from −1800 to −3800 km/sec. Wallerstein (1958) found sharp emission lines of Fe II. The spectrum near minimum was rather similar to that of T CrB. In fact, there are striking resemblances between the spectra of these two recurrent novae and such "symbiotic" variables as Z And, CI Cyg, and AX Per.

WZ Sge differed so greatly from the preceding stars that there is some question whether it should be regarded as a true nova. No observations were obtained until it was near minimum. Then weak and very broad hydrogen emission was seen, with extremely wide central minima resembling absorption (McLaughlin 1953*a*). The appearance was superficially similar to that of a spectrum of class Be. No nebular lines appeared, nor were any high-excitation lines seen. Greenstein (1957) found the spectrum substantially the same in 1956, when the star had been at minimum nearly 10 years. The wide double emission was superimposed on extremely broad absorption lines whose profiles matched approximately those of the hydrogen lines in the white dwarf L 770-3.

4.11. Oscillatory Variations in Magnitude and Spectrum

The most rapid novae pass through the early decline without appreciable fluctuations of light. Their spectral changes during that stage are unidirectional, as outlined in preceding sections. Some novae of intermediate rate and practically all slow novae have large secondary variations of light and concurrent cyclic spectral changes. Good examples of such behavior are DN Gem and v356 Aql.

Correlations between changes of brightness and of spectrum were first generalized by Stratton (1920) in his study of DN Gem: ". . . a maximum corresponds to a spectrum which is normal at an earlier stage of the star's history." Since the trend is toward higher excitation as the star fades, it follows that the excitation is higher at the minima of light than at the maxima.

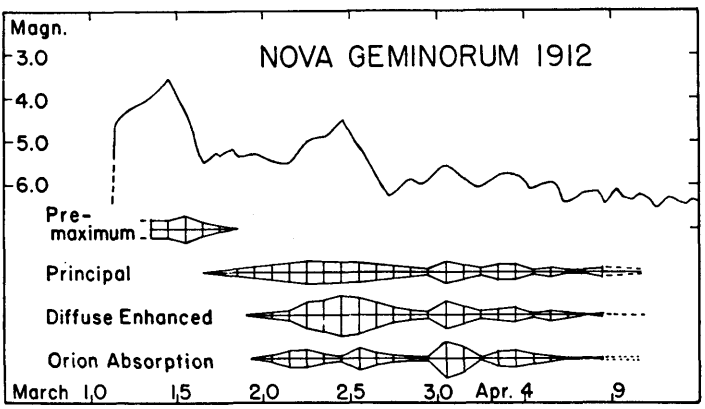


Fig. 8.—Intensity variations of absorption systems of DN Gem. Vertical width of each band indicates intensity.

Variations in intensity of the absorption systems of DN Gem are shown schematically in Figure 8. At the minimum of light following the first maximum, the diffuse enhanced and Orion absorptions both emerged. With the brightening to the second maximum (March 24), the Orion absorption nearly disappeared, while the diffuse enhanced absorption attained its greatest strength at the second light-maximum. In the decline to the next minimum, the diffuse enhanced spectrum faded, and the Orion system at first strengthened but then also faded at the very minimum of light. A small light-maximum on March 30 was accompanied by strengthening of both these spectra.

The emission lines also reflected the variations in light. At the minimum on March 21, He I and Na I emission were about equal. With the brightening, He I disappeared, but Na I remained strong. The reverse change occurred during the following decline.

The changes of v356 Aql were generally similar to those of DN Gem. Figure

9 shows the varying strength of the absorption systems (McLaughlin 1955). During the rise to the maximum of light on October 3, emissions of He I and N II weakened relative to those of Na I and Fe II. RR Pic had equally conspicuous variations of like character. In DQ Her the changes were less obvious but similar. During the month that preceded the sudden drop to the deep minimum, the Orion absorption system fluctuated in strength with the light-variations, being strong at the minima and weaker at the maxima.

The light-variations are chiefly due to changes in the continuous spectrum. At the maxima of light, all the emissions show less contrast with the continuum than at the light-minima.

Correlated variations during the transition stage occur in both fast and slow novae. The most striking changes were those associated with the oscillations of

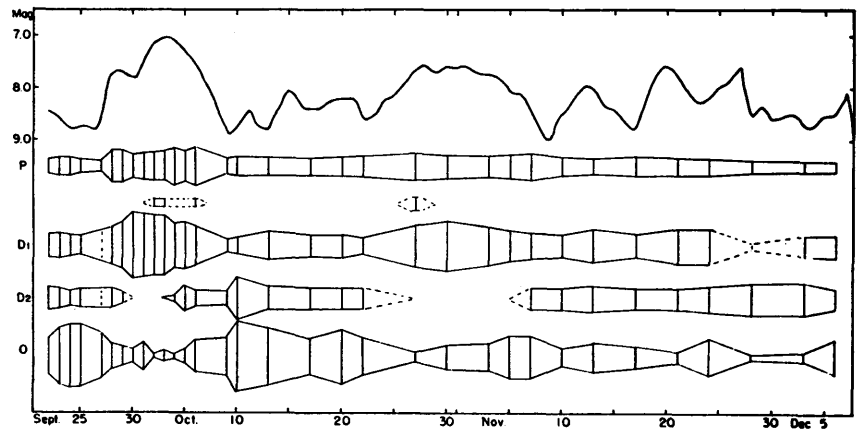


FIG. 9.—Intensity variations of absorption systems of v356 Aql. Vertical width of each band represents intensity of system. Light-curve is shown at top. (*Ap. J.*, **122**, 419, 1955.)

brightness of GK Per and v603 Aql. The phenomenon of "nitrogen flaring" occurs in this stage. Shortly before the onset of the variations, during a smooth decline of light, the broad and hazy emission bands of N III had emerged at λ 4100 and λ 4640. The former band was bordered on its shortward edge by the strongly displaced absorption lines λ 4097 and λ 4103 N III (Pl. II). When the star faded to the first minimum of light, the broad hazy emissions disappeared, and in their places were bands due to N III with the same width and structure as the hydrogen and other lines of the principal emission spectrum. Concurrently, some high-excitation emissions strengthened (e.g., He II). With the rise to the next light-maximum, the broad flaring bands again appeared, and the principal emission bands of N III and He II were extinguished. These changes occurred with every oscillation of light. The N II emission about λ 5680 also took part in the flaring. In the later fluctuations, changes of relative intensity of the nebular [O III] and hydrogen emissions also occurred, the [O III] lines being

relatively stronger at the minima of light. DK Lac showed similar variations (Larsson-Leander 1954*b;* Wellmann 1951*b*). After passing through a "4640 stage" it had developed the nebular spectrum. However, at each of several outbursts (range about 2 mag.), the N III bands flared, and high-excitation emissions in the principal spectrum weakened. The [O III] lines also weakened with each outburst. DN Gem behaved in a similar manner (Wright 1926) but with less violent oscillations. The secondary brightening of T CrB (§ 3.8) was a long-lived maximum of the same type (McLaughlin 1949*a*).

On several occasions during the nitrogen-flaring stages of DN Gem, diffuse apparent absorption was seen in the undisplaced position of λ 4686 He II (Wright 1926). A similar effect is less conclusively established in GK Per (McLaughlin 1949*b*). It is suggested that this is real absorption due to ionized helium ejected from the star with velocity less than that of escape and momentarily silhouetted by underlying emission (McLaughlin 1947*b*).

Conspicuous changes in the relative intensities of He II and hydrogen emission occurred in GK Per at minimum (Humason 1938), but it is not known how these changes were correlated, if at all, with the large variations of brightness.

4.12. Spectra of Supernovae

Detailed treatment of supernovae is outside the scope of this chapter, but a brief summary for comparison with common novae is in order. A more complete discussion has been published recently by Payne-Gaposchkin (1957, chap. 9).

Both light-variations and spectra point to a division of supernovae into two groups called "Type I" and "Type II." Average absolute magnitudes determined from extragalactic objects are near -16 for Type I and -13.6 or brighter for Type II. S And, which appeared in M31, had $M = -17$ and had an anomalous light-curve. The Crab Nebula supernova was Type I and had $M = -16.5$ (Mayall and Oort 1942).

Light-curves of Type I are remarkably similar. After a maximum of several days' duration, the light declines about 3 mag. in 30 days, at which time the rate of fading slackens, and for a year or more the fading rate is 0.0137 mag/day. This represents a half-intensity life of 55 days. The agreement with the fission half-life of californium 254 is suggestive (Baade *et al.* 1956). Type II objects fade a little more than 2 mag. in 90 days, and then the curve abruptly steepens, dropping at the rate of about 1 mag. in 20 days.

Spectra of Type II (Hubble 1941) near maximum are essentially continuous, with great extent in the ultraviolet. During decline, bright bands emerge at the positions of the hydrogen lines, with widths corresponding to velocities of several thousand km/sec. Diffuse absorption borders them on their shortward edges. In the third supernova in NGC 6946, Mayall (1948) measured hydrogen absorption velocities of -5700 km/sec. About 100 days after maximum of the supernova in NGC 4273, Baade (1936) found the strongest emission feature to

be probably λ 4640 N III. Type II supernovae can be described roughly as "gigantic ordinary novae."

Spectra of Type I (Minkowski 1939), even at maximum, consist of very broad and diffuse emission bands, which, if they are Doppler-broadened monochromatic emissions, indicate velocities of several thousand km/sec. In the blue-violet region the strongest band is centered near λ 4640, and weaker bands occur about λ 4300 and λ 4000. During some 10 months these shift steadily toward longer wave lengths, the total displacement accumulating to about 100 A. The red to green region is more complex and does not show the longward shift. Near maximum, prominent emissions are centered about λ 6500 and λ 5900. Between 15 and 70 days after maximum a composite band in the region λλ 5300–5600 strengthens and subsides again with variable structure. This is followed near phase 130 days by the emergence of a strong band near λ 5300. By phase 275 days this is the only remaining strong diffuse emission in the region. Meanwhile, relatively narrow bright lines have emerged at λ 6300 and λ 6364. These are, in all probability, due to [O I] and are the only features in Type I supernova spectra that are identified with any confidence.

Identification of the emissions is rendered extremely difficult by their great breadth and consequent blending. The hydrogen lines are certainly either very weak or absent. The possible conspicuous presence of He I is suggested by the strong persistent band near λ 5876, and the broad radiation about λ 4640 could be the same composite band that appears in common novae before and during the transition stage. Payne-Gaposchkin and Whipple (1940) calculated the intensities of the stronger radiations of helium, carbon, nitrogen, and oxygen, in several stages of ionization, as well as Na I, Ca II, Fe II, and Fe III for temperatures from 15,000° to 100,000° K. By using an expansion velocity of 6000 km/sec, they constructed synthetic spectra that represented fairly well a number of features in the observed spectra (Minkowski 1939). The redward drift of the bands in the blue-violet region appeared to be simply a fortuitous result of the changing composition of the spectrum as the excitation increased. The agreement was improved when the effect of the nebular [O III] emissions was added. On the whole, the result appeared hopeful. The most conspicuous discrepancy was failure to account for the strong band near λ 5300 after phase 130 days.

The supernova which appeared in the irregular galaxy NGC 4214 in 1954 had an unusual spectrum in which two deep minima had the appearance of absorption lines (McLaughlin 1959). When interpreted as λ 4472 and λ 4026 of He I, these gave velocities of about −5000 km/sec. Several weaker absorption-like features gave shifts accordant with these when interpreted as lines of O II, N II, C II, and He I. Three other supernovae of Type I, in NGC 4374 (1957), NGC 3992 (1956), and NGC 5668 (1954), had less conspicuous minima that might be similarly interpreted (McLaughlin 1960*a*). It seems possible that these spectra do contain vague absorption lines of an O — B-type spectrum

with the hydrogen lines very weak or absent, but the observations are inconclusive.

Of the known galactic supernovae, only that of A.D. 1054 has a conspicuous visible remnant, the Crab Nebula. Tycho's star (Hanbury Brown 1952) of 1572 is a radio source, and a faint nebulous wisp is identified (Baade 1943; Minkowski 1943) as a remnant of Kepler's star of 1604. The Crab Nebula is one of the strongest radio sources and is conspicuous in a small telescope. It is composed (Baade 1942*b*; Minkowski 1942) of an amorphous, roughly elliptical mass giving a continuous spectrum and a network of filaments giving nebular emissions—notably [N II] and [O II], which show Doppler ellipses with expansion velocities of 1300 km/sec (Mayall 1937). Recently the continuous light of the amorphous mass has been found to be strongly polarized, showing that it is synchrotron radiation (Oort and Walraven 1956).

§ 5. VELOCITIES OF ABSORPTION SYSTEMS; EMISSION STRUCTURES

The order of magnitude of absorption velocities has been indicated in the descriptions of the absorption systems. We now consider their behavior in greater detail. Fairly complete information is available for the principal, diffuse enhanced, and Orion systems of eleven novae, but data on the premaximum spectrum are still fragmentary. Figure 10 shows the velocity-curves of the absorption systems of CP Lacertae.

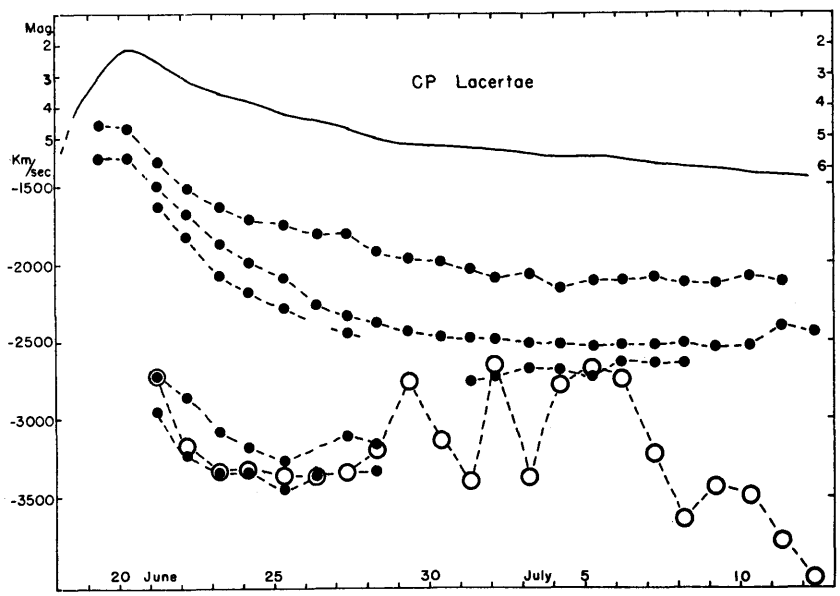


FIG. 10.—Radial velocities of absorption systems of CP Lac. Dots represent premaximum, principal, and diffuse enhanced systems. *Open circles*, Orion system.

5.1. Velocities of Premaximum Absorption

Only in DQ Her do we have observations of conspicuous changes in velocity during the rise to maximum light (Stratton 1936*b*). Table 10 summarizes these variations. The large discordances between different elements (and between different lines of hydrogen) diminished toward maximum, when all lines yielded velocities close to −175 km/sec.

Table 11 lists observed velocities of the premaximum absorption lines for six other novae. In v603 Aql there was a definite, though small, decrease. In others the changes were slight, if real. Perhaps the near-constancy of velocity before maximum in all but two cases is due to failure to obtain observations early enough. This is suggested by the fact that the absorption lines of DQ Her had already settled down to nearly constant velocity 4 days before maximum light.

After maximum, when the premaximum spectrum endures long enough, it tends to move toward the violet (i.e., to increase its shift). DN Gem stands alone in showing decreased displacements.

TABLE 10

Premaximum Absorption Velocities in DQ Herculis

(Km/sec)

Date (Dec.)	Hα	Hβ	Hγ	Hδ	Fe II	Ti II
13.3	−1984	−1179	−1023	−746	.....	.....
13.7	−1082	− 747	− 671	−640	.....	.....
14.3	.....	− 549	− 507	.....	−421	.....
15.3	.....	− 447	− 438	−325	−256	.....
16.1	.....	− 427	− 368	−294	−261	.....
16.8	.....	− 352	− 298	−219	−200	−175
18.0	.....	− 314	− 257	−208	−180	−173
18.8	.....	− 262	− 238	.....	−172	−179
21.8	− 320	− 193	− 169	−177	−166	−172
23.0	.....	− 205	− 169	−180	−178	−173

TABLE 11

Velocities of Premaximum Absorption System

Nova	Before Maximum		Maximum		After Maximum	
	Date	Km/sec	Date	Km/sec	Date	Km/sec
v603 Aql 1918	June 8	−1460	June 9	−1280	June 11	−1450
v476 Cyg 1920	Aug. 22	− 534	Aug. 24	− 507	Aug. 26	− 515
DN Gem 1912	Mar. 13	− 364	Mar. 15*	− 452	Mar. 17	− 360
CP Lac 1936	June 19	−1110	June 20	−1144	July 1	−2114
GK Per 1901	Feb. 22	− 651	Feb. 23	− 713	Feb. 28	−1067
RR Pic 1925	May 25	− 70	June 10†	− 97	June 27	− 110

* One day after maximum: no velocity observations on date of maximum.

† Three days after maximum.

5.2. Velocities of Principal Spectra

Information is fairly complete as regards velocities of the principal spectra. Data on the strongest components of this system are given in Table 12. These show the well-known increases in displacement with passage of time. The ratio of final to initial velocity has a large spread, from less than 1.1 for DN Gem to 1.9 for CP Lac.

Some novae have double, or even triple, lines in the principal absorption system during at least a part of its history. In some cases these components vary in relative strength, and on plates of low dispersion this can lead to the illusion of oscillations of position. When multiplicity does occur, all the components alike seem to be accelerated outward to about the same extent. Thus the velocity-curves of the two components of the principal spectrum of CP Lac were approximately parallel (Figure 10). Table 13 lists the best-established examples of multiple components.

TABLE 12

Velocities of Principal Absorption Spectra

Nova	Early Postmaximum		Mid-early Decline		Late Stage	
	Date	Km/sec	Date	Km/sec	Date	Km/sec
T Aur 1891	.....	.....	Feb. 10	− 399	Mar. 6	− 559
EL Aql 1927	.....	.....	Aug. 16	− 870	.....	.....
v356 Aql 1936	.....	.....	Sept. 22	− 458	Dec. 6	− 504
v368 Aql 1936	.....	.....	Oct. 22	−1087	Oct. 27	−1024
v528 Aql 1945	Aug. 31	−1135	Sept. 5	−1180	Oct. 2	−1250
v603 Aql 1918	June 10	−1380	June 16	−1645	June 25	−1720
v450 Cyg 1942	.....	.....	Sept. 15	− 512	Sept. 22	− 504
v465 Cyg 1948	June 15	− 548	Aug. 24	− 589	.....	.....
v476 Cyg 1920	Aug. 24	− 725	Sept. 1	− 738	Oct. 3	− 820
DN Gem 1912	Mar. 18	− 772	Mar. 24	− 852	Apr. 3	− 830
DQ Her 1934	Dec. 26	− 310	Feb. 7	− 355	Mar. 29	− 394
CP Lac 1936	June 20	−1316	June 27	−2336	July 6	−2527
DK Lac 1950	Jan. 28	− 872	Feb. 5	− 892	Mar. 3	−1170*
HR Lyr 1919	.....	.....	Feb. 5	− 981	Mar. 12	−1021
v849 Oph 1919	.....	.....	Nov. 2	− 310	Nov. 17	− 422
v906 Oph 1952	Aug. 26	− 860	.....	.....	.....	.....
GK Per 1901	Feb. 24	−1308	Mar. 13	−1487	Mar. 18	−1500
RR Pic 1925	June 10	− 298	Aug. 28	− 319	Jan. 5	− 410
CP Pup 1942	Nov. 11	− 890	Nov. 18	−1090*	.....	.....
T Pyx 1920	Apr. 11	−1014	Apr. 30	− 975	.....	.....
v630 Sgr 1936	Oct. 7	−2120	.....	.....	.....	.....
v928 Sgr 1947	.....	.....	May 22	−1032	May 25	−1076
v1275 Sgr 1954	July 7	− 688	July 21	− 729	.....	.....
EU Sct 1949	Aug. 4	− 307	Aug. 14	− 393	Sept. 16	− 352

* Not same component as earlier listing.

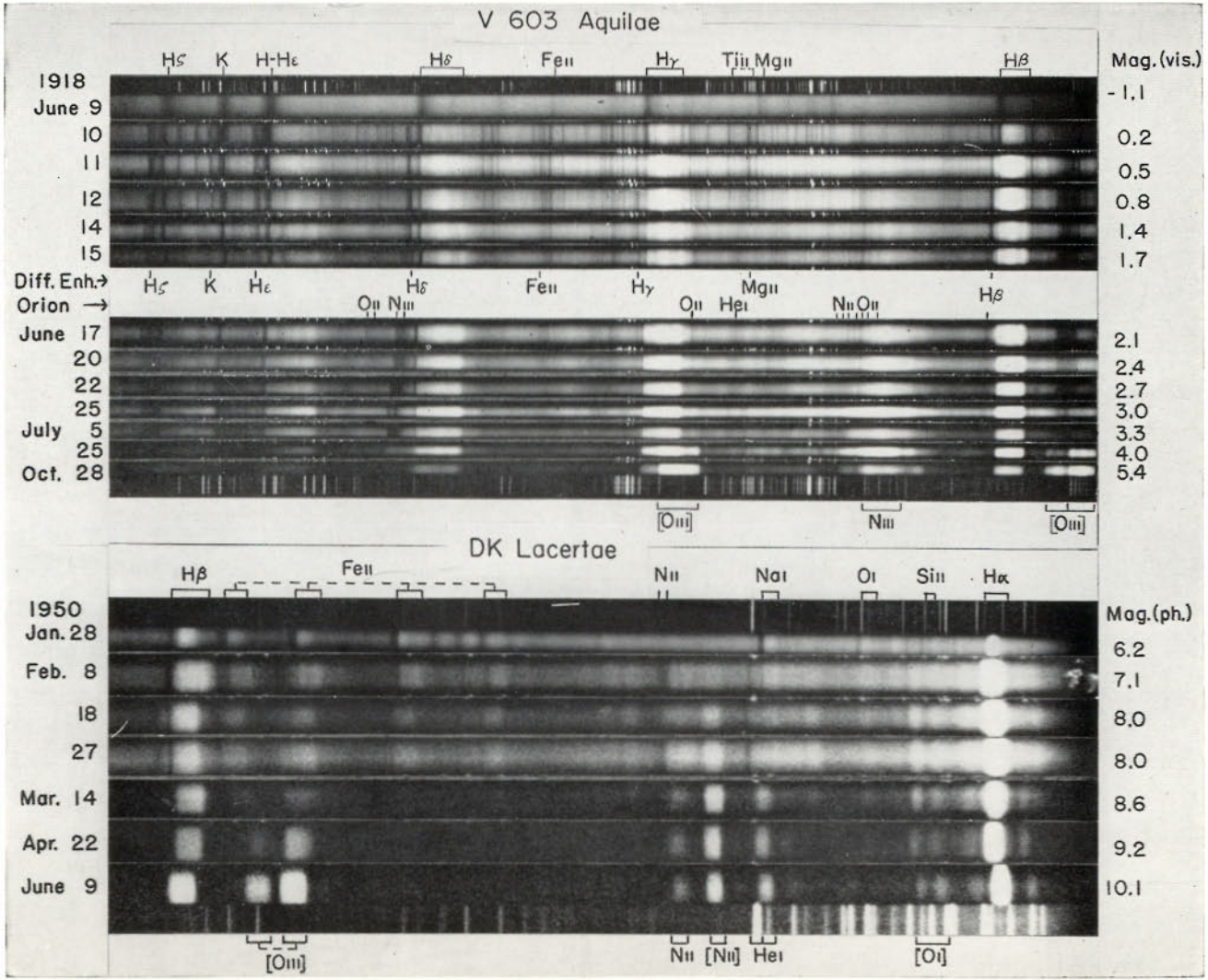


PLATE I.—*Upper two groups:* Spectra of v603 Aql in photographic region, from light-maximum to early nebular stage. *Lower group:* Spectra of DK Lac in the "visual" (red to green) region, from early postmaximum to nebular stage. (University of Michigan Observatory.)

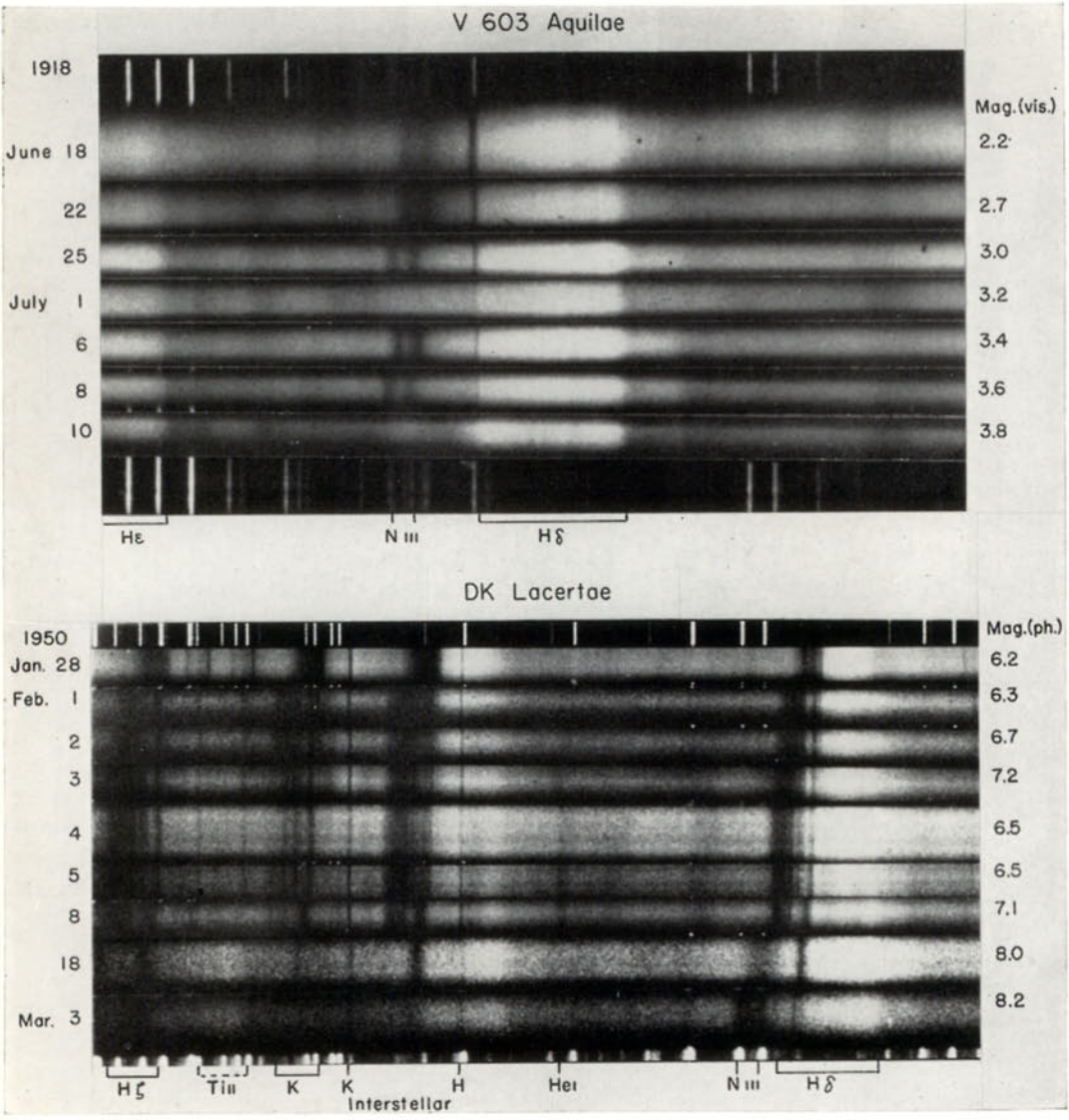


PLATE II.—*Upper:* The Hδ region of the spectrum of v603 Aql, showing variations of N III absorption. *Lower:* Spectra of DK Lac, Hζ to Hδ, showing multiple absorptions. (University of Michigan Observatory.)

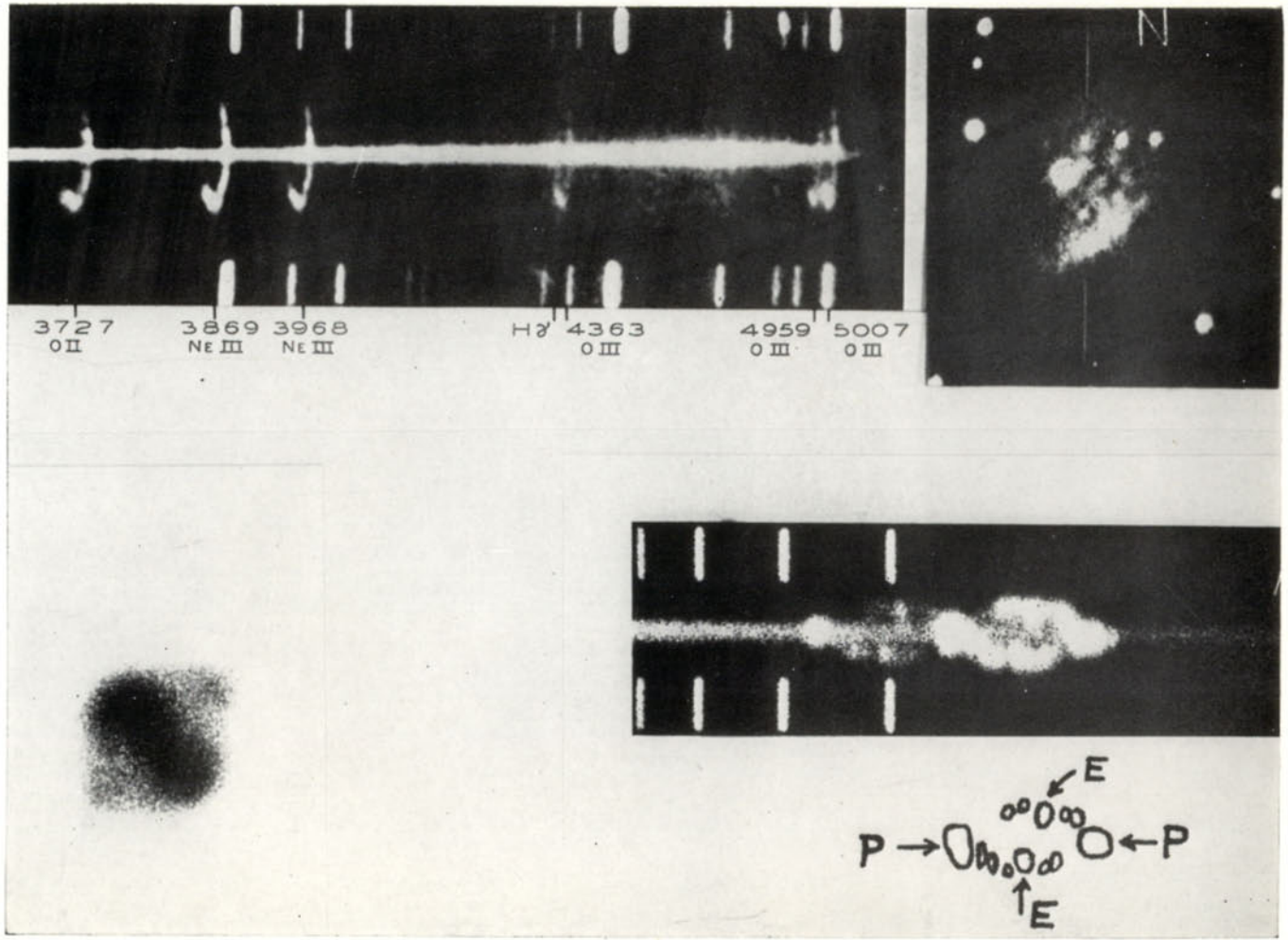


PLATE III.—*Upper:* Direct photograph of the nebula about GK Per (*right*) with spectrum of star and nebula in 1934, showing partial Doppler ellipses. *Lower left:* Nebula about DQ Her photographed in light of the red lines of [N II], July, 1942. *Lower right:* Doppler ellipses of the nebular lines of [O III] in the spectrum of v603 Aql, in July, 1920. (Mount Wilson and Palomar Observatories.)

5.3. Velocities of Diffuse Enhanced Spectra

The phenomena of the diffuse enhanced absorption spectra are somewhat more complex, owing to the usual multiplicity of this system. On plates of low dispersion, variations in the relative intensities of components of the multiple lines may cause apparent, but illusory, shifts of position. Plate II shows the multiple absorption components of DK Lac. During the time covered by these observations, actual shifts of lines were small, yet the center of intensity of the multiple lines underwent a large shift toward shorter wave lengths. Detailed analysis of the spectrum of DQ Her (McLaughlin 1954) also showed that variations in velocity of individual components were small, though definite and persistent trends toward increased velocity for some components and decreased velocity for others were well established. Large and rapid apparent shifts, however, were due to the disappearances of old lines and the emergence of new ones, or to variable blending of poorly resolved components. The velocities of absorption components of DQ Her are shown in Figure 11.

Among fast novae the lifetime of the diffuse enhanced spectrum is short, and multiplicity is less striking. Table 14 lists velocities of components of this system on three dates for several novae. Systematic trends toward greater displacement are seen in most cases.

TABLE 13

MULTIPLE PRINCIPAL ABSORPTION

Nova	Date	Km/sec	Date	Km/sec	Date	Km/sec
v528 Aql 1945.....	Sept. 5	−1180 −1370	Oct. 2	−1250 −1630	.....	.....
v603 Aql 1918.....	June 16	−1590 −1770	July 4	−1660 −1790	.....	.....
v476 Cyg 1920....	Sept. 1	− 738 − 912	Oct. 3	− 820 −1038	.....	.....
DN Gem 1912.....	Mar. 24	− 852 − 986	Apr. 3	− 830 −1014	.....	.....
CP Lac 1936.....	June 27	−2336 −2449	July 6	−2527 −2633	.....	.....
DK Lac 1950.....	Jan. 28	− 872 −1141	Feb. 5	− 892 −1106 −1258	Mar. 3	..... −1170 −1375
GK Per 1901.....	Feb. 28	−1333 −1474 −1614 −2070	Mar. 13	−1487 −1754 −1931	Mar. 18	−1500 −1798 ....
CP Pup 1942.....	Nov. 11	− 890 −1110	Nov. 18	− 886 −1090	.....	.....

5.4. Velocities of Orion Spectra

It is convenient to consider the Orion system in two parts: (1) the majority of lines in the early stages; (2) the N III and N V lines in the later stage. Table 15 lists typical velocities of the early Orion lines. In several novae there was a noticeable increase in displacement with time, but near-constancy appears established in v476 Cyg. In several stars the fluctuations have been so large that systematic trends were masked.

Large oscillations of Orion lines always accompany secondary variations in light. Examples are DN Gem and v356 Aql. In these novae the greatest displacements occurred near minima of light and the least near the maxima, with a tendency to precede the light-maxima. In two well-established cases, CP Lac and v528 Aql, large oscillations of the Orion lines occurred without accompanying conspicuous variations in light.

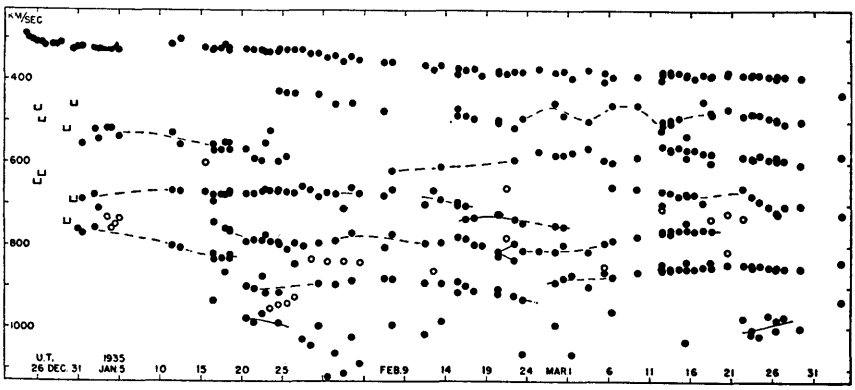


Fig. 11.—Radial velocities of principal and diffuse enhanced absorption components of DQ Her. (*Ap. J.*, 119, 131, 1954.)

In the later stage of the Orion spectrum (N III and N V), the increase in displacement with time continues. In v603 Aql the semiregular secondary variations in light were accompanied by large oscillations of the N III and N V absorption lines (Pl. II). As in the earlier Orion stage, the greatest displacements occurred near the minima and the least near, but a little before, the maxima. Figure 12 is a plot of the velocities measured by Wyse (1939).

5.5. Undisplaced Absorption Lines

In a few novae, in addition to the well-known interstellar lines, an undisplaced system of faint absorption lines has been reported. These included lines of hydrogen and ionized metals and were described as a spectrum of α Cygni type in GK Per (Stratton 1936*a*). In view of what is now known of novae, it does not seem possible to regard these as due to parts of the ejected cloud decelerated to zero velocity. Possible interpretations include (1) circumstellar

TABLE 14

VELOCITIES OF DIFFUSE ENHANCED ABSORPTION

Nova	Date	Km/sec	Date	Km/sec	Date	Km/sec
v356 Aql 1936.....	Sept. 22	−889 −1107	Nov. 10	−1078 −1180	Dec. 6	−1119 −1380
v528 Aql 1945.....	Aug. 31	−2040	Sept. 12	−2215 −2520	.....	.....
v603 Aql 1918.....	June 11	−2210	June 16	−2270	.....	.....
T Aur 1891.....	Feb. 10	−804 −940	Mar. 6	..... −1100	.....	.....
v450 Cyg 1942....	Sept. 15	−1103 −1255 −1510	Sept. 22	−722 −1213 −1502	.....	.....
v465 Cyg 1948....	June 15	−1299	Aug. 24	−1162 −1323	.....	.....
v476 Cyg 1920....	Aug. 26	..... −1181 −1412 −1649	Sept. 1	−1054 −1258 −1417 −1660	Sept. 14	−1086 −1261 −1542 .....
DN Gem 1912.....	Mar. 19	−1540	Mar. 23	−1396 −1490	Apr. 5	−1604 −1807
DQ Her 1934.....	Jan. 11	−527 −667 −800	Jan. 22	−588 −673 −786 −905 −988	Mar. 26	−584 −718 ..... −856 −1004
CP Lac 1936.....	June 21	−2725 −2956	June 25	−3273 −3456	June 28	−3171 −3331
DK Lac 1950.....	Jan. 31	−1414 −1560	Feb. 2	−1438 −1642	Feb. 8	−1509 −1644 −1796
GK Per 1901.....	Feb. 25	−3490	Feb. 28	−3560	Mar. 18	−3737
RR Pic 1925.....	July 31	.... −658 −920	Aug. 28	−468 −612 −723 −1006	.....	.....
CP Pup 1942.....	Nov. 18	−1495 −1822	.....	.....	.....	.....
v630 Sgr 1936.....	Oct. 7	−3381 −3710	.....	.....	.....	.....
v1275 Sgr 1954....	July 11	−1595 −1707	.....	.....	.....	.....
EU Sct 1949.....	Aug. 16	−1150	Sept. 2	−1900	.....	.....

TABLE 15

VELOCITIES OF ORION ABSORPTION SPECTRA

Nova	Date	Km/sec	Date	Km/sec	Date	Km/sec
EL Aql 1927....	Aug. 16	−2070	.....	.....	.....	.....
v356 Aql 1936...	Sept. 22	−1056	Nov. 10	−1117	Dec. 6	−1336
v368 Aql 1936...	Oct. 21	−2226	.....	.....	.....	.....
v528 Aql 1945...	Sept. 6	−2365	Sept. 24	−2745	Oct. 2	−2280
v603 Aql 1918...	June 15	−2730	June 19	−2850	July 2	−4200
T Aur 1891.....	Mar. 6	−1193	.....	.....	.....	.....
v450 Cyg 1942...	Sept. 15	−1335	Sept. 22	−1400 −1575	.....	.....
v465 Cyg 1948...	June 15	−1189	Aug. 24	−1315	.....	.....
v476 Cyg 1920...	Aug. 31	−2480	Sept. 12	−2598	.....	.....
DN Gem 1912..	Mar. 21	−1619	Mar. 23	−1242	Apr. 3	−1840
DQ Her 1934....	Mar. 3	− 474	Mar. 20	− 457 − 630	Mar. 26	− 442 − 980
CP Lac 1936....	June 22	−3184	June 29	−2758	July 10	−3500
DK Lac 1950....	Feb. 4	−1850	Feb. 17	−2140	Feb. 26	−2350
HR Lyr 1919....	Feb. 5	−1809	.....	.....	.....	.....
GK Per 1901....	Mar. 5	−3640	Mar. 12	−3665	Mar. 17	−3686
RR Pic 1925....	Nov. 3	−1157	Dec. 3	−1306	Jan. 8	−1527
T Pyx 1920.....	Apr. 11	−1555	Apr. 30	−1862	.....	.....
v630 Sgr 1936...	Oct. 7	−3657	.....	.....	.....	.....
EU Sct 1949....	Sept. 10	− 574	.....	.....	.....	.....

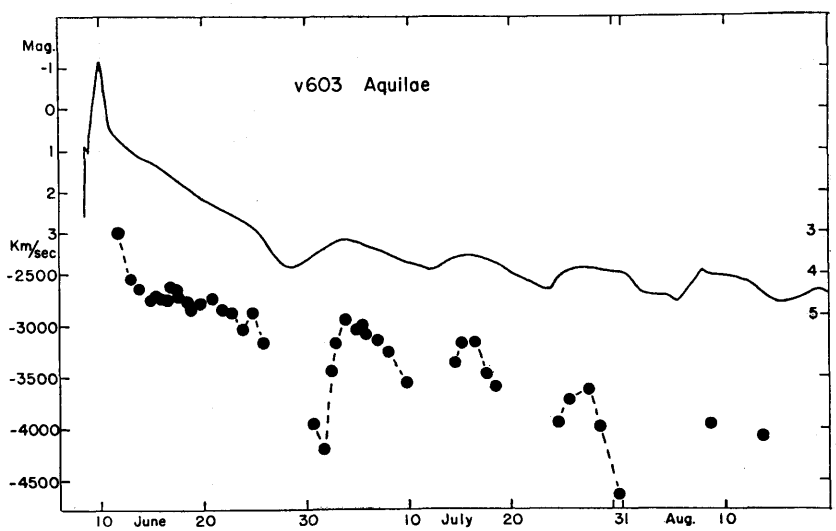


FIG. 12.—Radial velocities of Orion absorption system of v603 Aql, correlated with light-curve.

lines, produced in a nebula near to the star and at rest relative to it and (2) narrow minima of intensity in the emission-band structures.

Mention has already been made of undisplaced He II absorption at λ 4686 in DN Gem and GK Per. In this case deceleration does appear possible because the feature was associated with the waning stages of ejection and with rather narrow He II emission that could represent gases ejected at less than the escape velocity.

5.6. Structure of Emission Bands

An expanding spherical shell of uniform brightness throughout would produce an emission band with sharp outer edges and a flat-topped profile (Beals 1929). Some novae temporarily approximate this condition, but most have unsymmetrical or rounded-topped or saddle-shaped profiles, and some have complicated "castellated" structure. A deep expanding envelope with partial occultation by the star gives profiles that are flat over a large central region and fade off at the edges (Rosseland 1936, p. 294). Accelerated and decelerated envelopes were considered by Chandrasekhar (1934). The accelerated envelope gives profiles with strongly rounded tops, resembling those of the emissions in some novae.

It is exceptional for a nova to have entirely featureless emission bands. Each star very early in its history develops a distinctive pattern of maxima and minima in its principal emission lines, and this pattern persists, in its essential features, as long as the bands are recorded. Emission systems other than the principal are short-lived and usually lack conspicuous structure. The premaximum emission of DQ Her had hazy longward edges and no pronounced internal features. The diffuse enhanced emissions sometimes have well-defined outer edges but appear rather smooth throughout. Orion emissions are, as a rule, extremely hazy and never develop a pattern of maxima and minima.

The principal emission bands at their first emergence after light-maximum appear fairly smooth, but within a few days more or less definite maxima and minima of intensity can be distinguished. Detailed observations over long intervals are limited to a few bright novae. The most complete study is that of v603 Aql by Pearson (1936). Fairly long sequences of observations have been obtained also for GK Per (Stratton 1936*a*; McLaughlin 1949*b*), DN Gem (Stratton 1920; McLaughlin 1948*b*), and CP Pup (Sanford 1947).

The behavior of v603 Aql was typical. On June 10, only a day after maximum light, the bands appeared nearly smooth. A day later, the outer edges of two maxima near the band centers were measurable. By June 14, the stronger intensity maxima showed conspicuous contrast. By July 11, nearly all the minor maxima and minima were measurable. Most of these features endured for at least 2 years with only minor shifts of position, and the maxima could then be identified as knots in the Doppler ellipses on well-guided spectrograms taken with the slit across the nebula.

An almost equally striking pattern developed in the principal bands of GK

Per within a week after maximum light and persisted for many months. The strongest maximum, with velocity about −700 km/sec, was already conspicuous only 2 days after maximum, and several additional features emerged within a few days. Although these weakened during the transition stage, they emerged more strongly than ever, and in practically the same positions, in the nebular stage.

The history of emission structures in other novae, so far as it is known, has been similar. In CP Pup most of the emission maxima that were present in 1943 were still observable in 1947, and three could still be measured in 1956 (Sanford and Greenstein 1957).

All novae that have had strong secondary oscillations of light have shown concurrent variations in contrast in the emission structures. At secondary maxima of light the bands tend to appear smoother, and the pattern of the maxima and minima of intensity becomes most prominent at the minima of light. In spectra that have deep minima in the band centers, the profiles are more nearly flat-topped at the maxima and saddle-shaped at light-minima. With the cessation of secondary variations, the band structures usually remain prominent through the final decline.

Particularly striking variations of emission profiles occurred in v603 Aql during the transition stage (Sayer 1935). A pair of maxima near the band centers stood above the general profile during the light-maxima, while the maxima near the outer edges of the bands were then relatively inconspicuous. During minima of light the maxima at the band edges were much stronger than any other part of the band, and the entire central region, including the central pair of maxima was depressed.

Several novae have developed deep minima of intensity in the band centers (DQ Her, RR Pic, v476 Cyg). In v603 Aql such saddle-shaped profiles which appeared at the minima of light seem to have been associated with ejection of large knots toward and from the earth, but in other cases the maxima in the bands did not all correlate with discrete knots in the nebulosity. Thus DQ Her showed strong maxima at the band edges, and it was at first surmised that each of these belonged to a single component of the apparent "double star." However, this was not the case; each component of the "double" showed both emission maxima (Swings and Struve 1940). The central minima of the bands are certainly not due mainly to line absorption, for they appear as prominently in forbidden as in permitted lines. Scattering (either by electrons or by solid particles) in the limb region of a thick shell has not been ruled out. The tendency of maxima to occur in pairs with roughly equal and opposite velocities, as in v603 Aql (Pearson 1936), is the strongest reason for interpreting the structure in terms of non-uniform ejection, but the apparent discrepancy in DQ Her calls for caution in adopting this as the explanation of all emission structures.

5.7. The Expanding Nebulae

In 1916 a small nebula was detected near GK Per (Barnard 1917). This has now been followed for many years, and it is evidently expanding at such a rate

(0".4 per year) that it must have left the star within a few years of light-maximum (Humason 1935). The early record is more complete for v603 Aql. A nebular disk less than 1" in diameter was detected by Barnard (1919), in October, 1918, about 4 months after maximum. Subsequent visual and photographic measures (Wyse 1939) showed the radius increasing at a uniform rate of about 1".0 per year for some 20 years. The last observation, about 1940, showed no change in the rate of expansion.

DQ Her, about 6 months after maximum, appeared as a double star, but during the next few years the two components grew more diffuse as they separated, and the star itself was detected between them (Kuiper 1941). Their rate of separation and the growth of the radius of the nebula were linear with time. By 1942 the nebula appeared as a rather smooth ellipse in the light of [O III] (Baade 1942*a*). Its major axis lay in the position angle of the "double star." RR Pic showed two nebulous knots moving outward in opposite directions (Jones 1931). For several other novae, isolated observations of nebulae were made many years after maximum (see § 2.2).

Carefully guided spectrograms taken with the slit crossing the star and nebula show each emission line of the nebula as either a complete or a partial Doppler ellipse. This observation has been carried out successfully on v603 Aql, DQ Her, and GK Per. In each case the width of the ellipse along the dispersion corresponded to the velocity of the principal spectrum. In v603 Aql the ellipses consisted of numerous separate knots (see Pl. III), corresponding to discrete parts of the nebulosity, and these apparently formed pairs symmetrically arranged with respect to the star. Pease (1920) found a bright bar crossing the small nebular disk near position angle 40°, and this showed clearly on slitless spectrograms. In 1933, direct photographs showed a small knot of nebulosity emerging from the overexposed star image in position angle 28°. This knot was still visible and completely separated from the star image in 1940. Comparison with the slit spectrograms obtained in different position angles (Wyse 1939) leaves little doubt that this knot was a remnant of the dense condensation that produced the strong knot at the shortward ends of the Doppler ellipses in 1920 (Pl. III) and the strong maximum at the shortward ends of the emission bands beginning only a few days after maximum light.

The Doppler ellipses of GK Per were less knotty but were incomplete (Pl. III). Much material was ejected away from the earth, and the greatest amount moved out laterally as a segment of a spherical shell, parts of which had components of velocity toward the earth. The strong maximum in the principal emission bands with velocity -700 km/sec originated in this brightest part of the nebula south of the star.

In DQ Her the Doppler ellipses of [O III] appeared uniform, in keeping with the smooth appearance of the nebula in those emissions (Humason 1943). The nebula appeared very different in direct photographs taken, respectively, in the green [O III] and the red [N II] lines. The former showed a fairly uniform ellipse a little fainter along its minor axis. In the red photographs there was a very

broad bright bar along the minor axis and relatively weaker condensations near the ends of the major axis (Baade 1942*a*), as shown in Plate III. There is a suggestion of a similar effect in the nebula about v603 Aql. No direct red photographs were obtained, but the intensities of the knots in the Doppler ellipses were very different in [O III] and [N II] (Wyse 1939, Pl. X). Thus, in the [O III] lines, the strongly displaced knots representing material ejected toward and from the earth were strong, and the two central knots from material moving across the line of sight were quite weak. These central maxima were relatively much stronger in the light of [N II]. If the hydrogen emission indicates the distribution of mass in the nebula, then the strongest [O III] knots represent its densest condensations, and the strongest [N II] emission originates in regions of lower density.

The illuminated nebula or "light-echo" about GK Per several months after maximum was apparently unique. Couderc (1939) explained the effect by scattering of light in a plane sheet of nebulosity between the nova and the observer.

5.8. Structure of the Nebula about v603 Aquilae

The fair regularity of the Doppler ellipses of nova nebulae indicates an ellipsoidal (and probably spheroidal) distribution of velocities, but the elliptical cross-section of some nebular shells and the apparent pairing of oppositely moving knots argue against spherical symmetry. Interpretations of the structure of the shell about v603 Aql have been given by Baade and Weaver.

Baade (1950), van de Hulst (1951) studied the spectrograms taken at Lick Observatory with the slit set in different position angles. With the slit in position angle 112°, the Doppler ellipses appear symmetrical about the center line of the star spectrum, and lines joining pairs of knots in the ellipses are perpendicular to the direction of dispersion. With the slit in position angle 22°, maximum asymmetry is seen; the large knot with greatest negative displacement is decidedly off center, and lines joining paired knots are strongly inclined. From these variations Baade inferred a symmetrical system of rings lying in parallel planes (like parallels of latitude) and two very large "polar" knots that were ejected oppositely, one nearly toward the earth and the other away from it. The polar axis made an angle of 16° with the line of sight, and its projection on the sky is in position angle 22°. This falls extremely close to the remaining small bright knot on the direct photographs in 1933 and 1940 at position angle 28° and to the bright bar across the nebula seen by Pease in position angle 40°. There can be little doubt that all these phenomena refer to the same body of gas. In Plate III the numerous knots in the Doppler ellipses are well shown, and in the key diagram the light from the polar knots and from the strong equatorial ring are identified by *P* and *E*, respectively. The model by Weaver (Payne-Gaposchkin 1957, p. 92) is somewhat different, involving cones and jets in place of the rings and polar caps. Mustel (1956*a*) makes use of Weaver's interpretation in connection with his proposal that the material eject-

ed from novae is guided by magnetic fields. In this interpretation, the "polar axis" becomes the axis of the magnetic dipole. He points out that in both v603 Aql and DQ Her the [N II] emission was strongest in the equatorial ring, and he appears to suggest that this represents a chemical separation. However, differences in density, which could arise as a result of the action of the magnetic field, may be the immediate cause of differences in the spectra emitted by different parts of the nebulae.

5.9. Typical Development of Nova Spectra

The spectral development of a nova at any time is closely related to the amount that the light has declined from maximum. For each recognizable stage in any well-observed nova we can evaluate the difference in magnitude, Δm, between maximum and the stage in question and the time interval, Δt, measured from the date of maximum. Table 16, which is abridged from earlier papers (McLaughlin 1942*a*, 1943), contains the results of a study of seven bright novae (GK Per, DN Gem, v603 Aql, v476 Cyg, RR Pic, DQ Her, CP Lac). Spectral stages are named in the first column and are followed by the mean Δm and the "relative Δt," whose unit for any nova is the time required to decline through 3 mag. (visual). For very rapid novae this interval is near 10 days; for typical slow ones it is 100 days or more.

In a general way, the time scale for any nova can be transformed into that of

TABLE 16

SPECTRAL STAGES OF NOVAE

Spectroscopic Stage	Mean Δm	Smoothed Relative Δt
Change from B to A (premaximum absorption)	(1.5)	− 0.1
Maximum light	0.0	0.0
Emergence of principal absorption spectrum	0.6	0.04
Emergence of diffuse enhanced absorption	1.2	0.16
Maximum of diffuse enhanced absorption	2.0	0.42
Emergence of Orion absorption	2.1	0.46
[O I] flash	2.6	0.7
Appearance of N III absorption	2.7	0.8
Maximum of Orion absorption	2.7	0.8
Disappearance of diffuse enhanced absorption	3.0	1.0
Appearance of diffuse "4640" emission	3.0	1.0
[N II] flash	3.3	1.25
Disappearance of Orion absorption	3.3	1.25
Helium flash	3.6	1.5
[O III] first traced	3.7	1.6
Disappearance of principal absorption	4.1	2.2
λ 4959 = λ 4924	4.4	2.7
Disappearance of N III absorption	4.4	2.7
Disappearance of diffuse "4640" emission	4.7	3.5
λ 4363 = Hγ	4.9	4.2
λ 5007 = Hβ	5.4	6.2
λ 4959/Hβ = 2.0	6.7	17

another by means of the ratio of the durations of the 3-mag. decline. However, systematic differences appear, especially in the nebular stage. When the earlier stages of fast and slow novae are brought into coincidence by an appropriate factor, the slow novae are found to reach the late stages too early. Also the slow novae tend to reach many stages of spectral development at a smaller Δm than the average value. Two rather rapid novae, v476 Cyg and CP Pup, both had Δm larger than the average by about 1.0 mag. for most stages with $\Delta m > 3$.

Both the rate of fading and the rate of spectral development are correlated with the velocities of the absorption systems. Slow novae have narrow principal emissions and low absorption velocities and are slow both in their rate of fading and in their progress through the spectral stages. Fast novae have very wide emissions and large absorption displacements and are rapid in both their fading and their spectral changes. None of these relations is perfectly rigorous. Thus v476 Cyg and CP Pup faded more rapidly than would be expected from their line displacements. Their fading of light was also too rapid for their spectral development. However, their velocities and spectral development accorded well with the mean relationship.

Absorption velocity and rate of fading are connected by the following empirical relations which are modified from those published some years ago (McLaughlin 1940):

$$\log_{10} V_1 = 3.70 - 0.5 \log_{10} t_3 = 3.57 - 0.5 \log_{10} t_2 , \qquad (3)$$

$$\log_{10} V_2 = 3.81 - 0.4 \log_{10} t_3 = 3.71 - 0.4 \log_{10} t_2 , \qquad (4)$$

where V_1 and V_2 are the velocities, in km/sec— of the principal and diffuse enhanced absorptions, respectively, and t_2 and t_3 are the durations, in days, of decline through 2 and 3 mag. from maximum. Similar relations were obtained by Bertaud (1945).

Relations between velocities and spectral development have been obtained by expressing the duration of a series of spectral changes in terms of the same developments of CP Lac (McLaughlin 1937*a*). The resulting relations determined from the seven bright novae are

$$\log_{10} V_1 = 3.19 - 0.54 \log_{10} t_s , \qquad (5)$$

$$\log_{10} V_2 = 3.39 - 0.39 \log_{10} t_s , \qquad (6)$$

where the unit of t_s is the duration of the equivalent development of CP Lac. If we make the fit at 3 mag. below maximum and express t in days ($t_3 = 9$ days for CP Lac), the constants become, respectively, 3.71 and 3.76, which are to be compared with 3.70 and 3.81 in the relations between velocity and t_3.

The recurrent novae cannot be fitted to the above relations. Most of the spectral stages listed in Table 16 cannot be identified in these objects, with the possible exception of T Pyx, for which the data are too fragmentary. Again,

except for T Pyx, the recurrent novae did not have identifiable "principal" spectra, and the longest-enduring absorptions of T CrB depart widely from the relations above.

Supernovae are even less tractable. The velocities of hydrogen absorption in Type II are over 5000 km/sec, and similar widths are indicated for Type I emission bands. In the above formulae such velocities would require $t_3 \approx 1$ day! Actually, for Types I and II, t_3 is respectively about 30 and 100 days. We note again that supernovae fail to fit the relation between absolute magnitude and rate of decline for common novae. These discrepancies appear to set the supernovae quite apart.

§ 6. PHYSICAL MEASUREMENTS

The determination of physical conditions in the envelopes of novae requires accurate photometry of the continuous spectrum and of the absorption and emission lines. Only a few bright novae have appeared since astronomical spectrophotometric techniques were developed, and data are therefore scanty. Most of our physical data on novae that appeared before 1930 are based on uncalibrated plates reduced by the use of assumed mean characteristic curves and sensitivity-curves. This method gives useful, but, at best, only approximate, data and is applicable only to intensities of emissions relative to the neighboring continuum or to neighboring emissions. Obviously, no measures can be made of the energy distribution in the continuum for determination of color temperatures because no comparison stars were taken in the earlier series of spectrograms.

6.1. Intensities of Emission Bands

Variations in the relative intensities of emission bands have been described qualitatively in earlier sections. Several spectrophotometric investigations have given quantitative data on these changes. Limitations of space preclude discussion of details, and the reader is referred to the original papers, chief among which are the following:

GK Persei, v603 Aql, v476 Cyg: Payne-Gaposchkin and Gaposchkin (1942), *Harvard Circ.*, No. 445.

RR Pic: Payne-Gaposchkin and Menzel (1938), *Harvard Circ.*, No. 428.

DQ Her: Whipple and Payne-Gaposchkin (1939), *Harvard Circ.*, No. 433.

CP Lac: Popper (1940), *Ap. J.*, **92**, 262.

DK Lac: Larsson-Leander (1954*b*), *Stockholm Ann.*, Vol. **18**, Part 4.

Intensities of emissions relative to the neighboring continuum form the basis for calculation of ionization temperatures (see § 6.3), while relative strengths of emissions of different elements can be used to compute excitation temperatures (§ 6.4). Absolute intensities of emission bands are extremely important but are difficult to obtain accurately, since available light-curves always represent the integrated radiation in the continuum and the emissions cover a considerable range of wave lengths, affected by sensitivity factors that are not

precisely known. However, the intensities in numerous emission bands, expressed in ergs/cm² sec at the earth, have been evaluated in the papers listed above. When the distance of the nova is known or assumed, the total flux from the nova in ergs/sec can be computed. With the adoption of certain physical assumptions, it is then possible to approximate the mass of the ejected material (§ 6.5).

Table 17 lists logarithms of the energy, in ergs/sec, emitted by the novae in Hδ and the nebular [O III] lines. For Hδ, values are given at 3 and 6 mag. below maximum, as well as the largest measured value. For [O III], only the largest measured value is given. Figures for the first five novae are based on the data tabulated by Payne-Gaposchkin and Gaposchkin (1942) but have been recalculated with new distances derived from rates of nebular expansion.

TABLE 17

LOGARITHMS OF ABSOLUTE INTENSITIES IN ERGS/SEC

Nova	Hδ			[O III] Max. Value
	$\Delta m = 3$	$\Delta m = 6$	Max. Value	
GK Per	35.84	34.34	36.45	35.69
v603 Aql	36.65	35.85	36.65	36.99
v476 Cyg	36.57	35.62	36.78	36.03
RR Pic	35.27	34.17	35.85	35.35
DQ Her	32.72	(33.47)*	34.68	35.26
DK Lac	34.07	.....	34.29	34.50

* $\Delta m = 5$.

6.2. Color Temperatures

Measurements of energy distribution in the continuum of a nova spectrum are rendered difficult by superposition of emission bands. There are several relatively clear regions, however, and measurements of color temperature have been obtained for a few novae by comparison with stars of known energy distribution. The data are most extensive for DQ Her. Some selected values by Greaves and Martin (1936) and by Beileke and Hachenberg (1935) are listed in Table 18, along with the magnitude of the star. The data are plotted in Figure 13, *A*, which includes additional measures by Beileke and Hachenberg not listed in Table 18. Figure 13, *B*, is a similar plot of measures by Oehler (1936).

The following general conclusions can be drawn: (1) during the rise to maximum the color temperature fell from about 11,000° to 9000° K and continued to drop for a few days (7800° K on December 27); (2) as the light declined during 3 months after maximum, T_c increased, at first gradually, then more rapidly during March, to about 18,000° K; (3) the secondary fluctuations of light were accompanied by variations in T_c. Maxima of T_c occurred at or near minima of light and vice versa.

Measures by Whipple and Payne-Gaposchkin (1936*a*) are consistent with these conclusions. The trend of T_c was largely obscured by the secondary fluctuations, but T_c was strongly correlated with apparent magnitude as follows: at $m = 2.7$, $T_c = 9000°$; at $m = 3.3$, $T_c = 10{,}000°$; and at $m = 4.1$, $T_c = 11{,}000°$. Measures by Petrie (1935) gave a mean of 10,500° K during January and February. Unpublished values by K. O. Wright ranged from 12,000° to 16,000° K during March.

TABLE 18

COLOR TEMPERATURES OF DQ HERCULIS

Date 1934–1935	T_c (° K)	m_v	Obs.*	Date 1935	T_c (° K)	m_v	Obs.*
Dec. 18.....	11,200	2.72	GM	Feb. 9.....	10,500	2.75	GM
23.....	9100	1.92	GM	19.....	13,321	3.60	BH
27.....	7800	2.44	GM	26.....	10,875	3.29	BH
31.....	10,000	2.75	GM	Mar. 4.....	13,260	3.98	BH
Jan. 13.....	9100	2.87	GM	7.....	10,639	3.71	BH
29.....	13,309	3.51	BH	15.....	16,778	4.60	BH
Feb. 6.....	9835	2.84	BH	Apr. 2.....	17,945	6.72	BH

* GM = Greaves and Martin; BH = Beileke and Hachenberg.

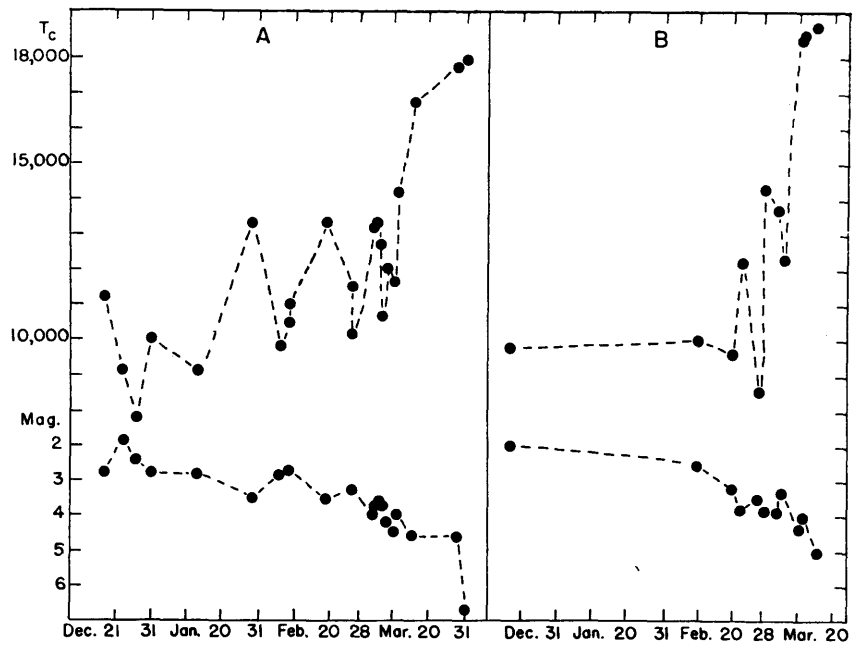


FIG. 13.—Color temperatures of DQ Her, correlated with apparent magnitude. *A*, measures by Greaves and Martin (1936) and Beileke and Hachenberg (1935); *B*, measures by Oehler (1936).

The trend of T_c is very nearly in agreement with values that could be estimated from the composition of the absorption spectra. Thus, between December 18 and 23, the absorption spectrum changed from about A2 to F0, reaching F5 on December 27, when heavy CN absorption was present. During February the diffuse enhanced absorption, approximately class A2, was dominant, and T_c fluctuated about 12,000° K. The large increase in T_c to 18,000° K during March accompanied the strong development of the Orion absorption, approximate spectral class B1.

CP Lac was less extensively observed, but the general conclusion that T_c is inversely correlated with apparent brightness was substantiated. Petrie (1937) obtained the values listed in Table 19, and from data by Cecchini and Gratton and by Behre he obtained values listed in the respective columns. The decline of T_c in the rise to maximum is more conspicuous than would be expected from

TABLE 19

COLOR TEMPERATURES OF CP LACERTAE (° K)

Date 1936	Petrie	Behre	Cecchini and Gratton
June 19	10,250	.....	.....
20	6650	.....	.....
21	7800	8500	.....
22	7700	.....	5400
24	10,500	14,020	8900
25	8400	16,200	.....
28	.....	15,800	.....
July 2	12,500	.....	.....
15	14,000	.....	.....
21	20,500	.....	.....

the observed change of the absorption spectrum from B9 to about A2. Popper (1940) found T_c approximately constant about 14,300° K from July 2 to November 21. Measures by Bloch (1950) on the early postmaximum spectrum of v465 Cyg 1948 gave 5200° K near maximum and 4400° K 2 months later. Possibly space reddening had a strong effect in this and other novae.

Results for the recurrent novae RS Oph and T CrB were probably affected by the presence of late-type companions. In RS Oph, Sayer (1940) found that T_c declined from 7800° K on August 17 to 5500° K on September 10, while the magnitude faded from 6.4 to 8.7. In T CrB, similarly, T_c apparently decreased from 8300° to 6300° K between February 12 and 16 (Bloch *et al.* 1946).

No spectrophotometric measures are available for novae in the late decline or at minimum. The spectra extend far in the ultraviolet, and T_c is undoubtedly high.

6.3. PHOTOIONIZATION TEMPERATURES

Several investigators have calculated ionization temperatures of novae by the method which Zanstra (1931) devised for application to planetary nebulae.

The method, as applied to permitted lines, is based on the assumption that the emissions are due to recombination of atoms photoelectrically ionized from the ground state by absorption of radiation from the ultraviolet stellar continuum (black-body distribution assumed). The sum of all quanta in the Balmer lines is taken as a measure of the number of quanta in the stellar continuum beyond the head of the Lyman series. Comparison with the intensity of the continuum in the neighborhood of the Balmer lines then leads to a calculation of the stellar temperature. The method can be used also with the forbidden lines of [O III]. In this case it is assumed that the O III atoms are excited by collisions with electrons freed from hydrogen and that all the kinetic energy of the electrons is exhausted in the excitation.

For v603 Aql 1918 in the interval August to October (transition and early nebular stage), Beals (1932) found an ionization temperature of 64,500° K from

TABLE 20

TEMPERATURES OF CP LACERTAE (MCKELLAR)

Date	Days after Maximum	Ionization Temperatures (° K)				
		H	N III	He II	N IV	[O III]
July 2.....	11	32,500	63,000	.....	.....	.....
15.....	24	32,500	66,000	.....	.....	.....
28.....	37	34,000	67,500	59,000	74,000	25,000
Aug. 4.....	44	33,500	71,000	64,000	73,000	27,500
24.....	64	39,500	75,000	66,000	76,000	33,500

He II 4686. RS Oph during 3 weeks after maximum (Sayer 1940) yielded temperatures from 31,400° to 42,400° K with no systematic trend. Wilson and Williams (1934) on August 18, 2 days after maximum, found T_i = 35,000° K.

Ionization temperatures of CP Lac determined by McKellar (1937) are listed in Table 20. A tendency to increase with time is indicated, but large systematic differences appear between values based on different elements.

Measures of the hydrogen lines in DK Lac by Larsson-Leander (1953, 1954*b*) gave T_i about 22,000° K on January 25 and 27, just after maximum. On several dates between February 20 and May 13 he obtained values ranging about 30,000° K from hydrogen and 37,000° K from He I. Fluctuations were correlated with the secondary light-variations, with maxima of temperature at the light-minima. On two dates in March, He II gave 61,000° K and the nebular lines 27,000° K. These values and the differences between them were similar to those obtained in other novae.

As a general rule, ionization temperatures run systematically much higher than color temperatures, and values based on He II and N III are approximately double those from hydrogen, while the nebular lines give values somewhat lower than hydrogen.

The correlation of ionization temperatures with secondary light-variations is illustrated best by the results of Vorontsov-Velyaminov (1946) on GK Per. Temperatures at the maxima and minima of light during the transition stage are shown in the accompanying table.

	H	He I	He II	N III
Max.....	31,000° K	32,500° K	52,000° K	55,500° K
Min.....	37,000	42,000	64,000	62,000

6.4. Excitation Tfmperatures

Excitation temperatures have been calculated chiefly from the relative intensities of [O III] and hydrogen lines (Stoy 1933) and from the ratio 4686 He II/Hβ (Ambarzumian 1932). Both methods give temperatures near to, or greater than, those obtained by the original Zanstra method. In DQ Her, Oehler (1936) found from [O III]/H an increase of from 58,500° to 125,000° K between June and September, 1935. During the same interval He II/H gave nearly constant values about 70,000° K. Larsson-Leander later recalculated this as 130,000° K.

In DK Lacertae Larsson-Leander (1954*b*) calculated temperatures as follows:

Date	He II/H	[O III]/H
1950 Mar. 16.....	87,000° K	19,400° K
1951 May 4.....	270,000	75,000

The He II/H ratio for four intermediate dates showed a steady increase in temperature.

No photometric measures have been made in spectra taken during the late decline and postnova stages. Relative intensities of He II and hydrogen lines suggest that the temperature of the star drops appreciably during the last magnitude of the decline and perhaps for several years afterward (McLaughlin 1953*a*). Final postnova temperatures can be only vaguely estimated at 40,000°–50,000° K.

6.5. Electron Temperatures and Densities; Mass of Material Ejected

The electron temperature in the expanding shell can be calculated from the ratio of the [O III] lines λλ 5007 + 4959/4363 by means of the formula

$$\frac{I(N_1+N_2)}{I(4363)} = 0.0775\, e^{33{,}000/T_e}, \qquad (7)$$

in which the coefficient includes new transition probabilities by Garstang (1951). For all novae in which the ratio has been measured, T_e ranges between about 6000° and 10,000° K, with a tendency to decrease as the nova fades, reflecting

the relative gain of strength of the "nebular" lines over the "auroral" transition λ 4363. Results are listed in Table 21. These have been recalculated with Garstang's transition probabilities, from the data by the authors listed in the last column. Payne-Gaposchkin and Gaposchkin (1942) used the [O I] lines in DQ Her in the same way and found that T_e decreased from 6600° to 3500° K during a decline of 3 mag. from maximum. The new transition probabilities change these results very little. In v465 Cyg, Bloch (1950) found $T_e = 5840°$ K near the time of the "[O I] flash," about 2.5 mag. below maximum.

For a spherical nebula of radius A cm whose image in Hδ has surface brightness $I\delta$ (in magnitudes per square minute of arc), the electron density is given by

$$\log N_e = 13.572 - 0.5 \log A - 0.1\, I\delta \qquad (8)$$

(Payne-Gaposchkin and Gaposchkin 1942, adapted from Menzel and Aller 1941). The radius A can be calculated from the velocity of expansion. With an

TABLE 21

ELECTRON TEMPERATURES OF NOVAE

Nova	T_e (° K)	Mag. below Maximum	Photometry by
v603 Aql	6500–6000	5.0–8.0	Payne-Gaposchkin and Gaposchkin (1942)
v476 Cyg	6500–6100	5.7–7.7	*Ibid.*
DQ Her	8200–6700	3.7–5.7	*Ibid.*
GK Per	9200–8200	5.7–6.7	*Ibid.*
RR Pic	9600–6950	4.1–6.1	*Ibid.*
CP Lac	9200	4 –6	Popper (1940)
CT Ser	9700	6:	Bloch (1950)
DK Lac	9700	4 –5	Larsson-Leander (1954*b*)

adopted distance, the angular dimensions are then known, and from the measured radiation in the emission line the surface brightness follows at once. When later direct measures of nebular radius are available, the radius on any earlier date is calculable from the angular rate of expansion, and again the surface brightness can be computed.

Electron densities calculated in this way range from order $10^9/cm^3$ in the early postmaximum stages to $10^6/cm^3$ in the early nebular stage. Values for three comparable stages of v603 Aql and DQ Her (Payne-Gaposchkin and Gaposchkin 1942) are fairly representative and are listed in Table 22.

If it is assumed that $N_e = N_i$, the density of hydrogen ions, the total mass ejected can be calculated. Results are given in the last two columns of Table 22. It is noticeable that the mass increases with time. This does not necessarily measure continuous ejection during the entire period. In the early postmaximum stages, probably outer parts of the shell are relatively inactive as emitters, owing to shielding by inner layers that are opaque to the ionizing frequencies.

Other calculations have been made by Ambarzumian and Kosirev (1933), Sayer (1940), and Whipple and Payne-Gaposchkin (1936*b*), leading to masses of the same order. The total ejected material is 10^{27}–10^{29} and possibly 10^{30} gm in extreme cases. Evidently only a superficial layer of the star, a minute fraction of its total mass, is ejected in the nova explosion.

The total energy emitted in a nova outburst has been calculated as from 2.5×10^{44} to 4×10^{45} ergs (Unsöld 1930; Grotrian 1937*b*; Gaposchkin 1941). The kinetic energy of the expanding nebulae is of the same order.

6.6. Photospheric Dimensions

The well-known approximate formula

$$\log R = \frac{5900}{T_e} - 0.2M_v - 0.02 \qquad (9)$$

can be used to calculate the radii of novae near maximum if we assume effective temperatures based on the class of the absorption spectra. In Table 23 the first

TABLE 22

ELECTRON DENSITIES AND EJECTED MASSES FOR TWO NOVAE

Stage	Electron Density (N_e/cm^3)		Mass Ejected (gm)	
	v603 Aql	DQ Her	v603 Aql	DQ Her
Principal absorption	1.1×10^{9}	1.2×10^{8}	6.3×10^{23}	1.1×10^{24}
"4640" stage	2.8×10^{7}	2.7×10^{6}	1.4×10^{27}	1.4×10^{27}
Early nebular	1.1×10^{6}	7.6×10^{5}	1.7×10^{29}	2.0×10^{28}

TABLE 23

RADII OF PHOTOSPHERES OF NOVAE AT MAXIMUM AND MINIMUM

Nova	Maximum Light				Minimum Light		
	M_v	Spectrum	T_e (° K)	R_{max} ($\odot=1$)	M_v	R_{min} ($\odot=1$) ($T=$ 40,000° K)	R_{min} ($\odot=1$) ($T=$ 10,000° K)
v603 Aql	−9.2	A5	8500	320	2.7	0.33	1.2
v476 Cyg	−9.6	A2	9700	320	4.5	.14	0.52
DN Gem	−7.5	F0:	7500	186	3.7	.21	0.76
DQ Her	−5.6	F0	7500	95	8.1	.03	0.10
CP Lac	−9.3	A2	9700	280	3.9	.19	0.69
GK Per	−8.5	A0	10700	170	4.8	.13	0.46
RR Pic	−7.4	gF8	5800	300	4.7	.13	0.48
CP Pup	−9.1	A5	8500	310	8:	0.03	0.10

five columns contain the names of bright novae, their absolute magnitudes, spectral classes, assumed temperatures, and the resulting radii. With the exception of DN Gem, the absolute magnitudes are based on nebular expansion and are corrected for interstellar absorption. The dimensions, like the luminosities, are those of supergiant stars.

Obviously, the rapid rise of the nova from minimum to maximum requires a rapid expansion of the effective photosphere, for any temperatures within reason that we can assume. Since the spectrum becomes later during the last 2 mag. of the rise, it is clear that the expansion must continue right up to maximum. The decline from maximum and the accompanying increase in excitation and color temperature call for rapidly shrinking dimensions of the effective photosphere. The calculations for DK Lac (Larsson-Leander 1954*b*) are typical. Selected values are given in Table 24. Here the two columns of absolute magnitudes

TABLE 24

PHOTOSPHERIC RADII OF DK LACERTAE
(After Larsson-Leander)

STAGE	DATE 1950	M_{pg}		R ($\odot = 1$)
		Total	Continuum	
Maximum	Jan. 22	−7.5	−7.5	150
Principal abs.	Jan. 28	−6.5	−6.4	90
Orion, minimum	Feb. 20	−4.4	−4.0	5.5
Orion, maximum	Feb. 22	−5.0	−4.7	9.6
Transition, min.	Mar. 16	−3.6	−3.1	2.9
Transition, max.	Mar. 23	−5.0	−4.7	9.8
Early nebular	May 14	−2.9	−2.3	1.7

represent, respectively, the integrated photographic light and the light of the continuous spectrum, obtained by subtracting the energy in the emission bands. During the large fluctuations of brightness in the transition stage, the radius varied by a factor of 2–3. Similar variations were calculated by Vorontsov-Velyaminov (1946) for the transition fluctuations of GK Per. These changes are not true pulsations but are due to variable rate of ejection of material from the star (see § 7.5).

During the later decline and at minimum the approximate formula may become increasingly inaccurate because of high temperature. In this case we apply the bolometric correction appropriate to the assumed temperature, and the radius is then given by

$$\log R = 8.52 - 2 \log T_e - 0.2\, M_{\text{bol}} . \qquad (10)$$

The last three columns of Table 23 contain absolute magnitudes at minimum and the radii computed for assumed $T_e = 40{,}000°$ K (bolometric correction =

-3.7 mag.) and $T_e = 10{,}000°$ K (bolometric correction $= -0.5$ mag.). Two stars, CP Pup and DQ Her, apparently have the radii of white dwarfs when we use $T_e = 40{,}000°$ K, while the others are somewhat larger, but none greater than one-third the sun's radius. If their masses are comparable with those of main-sequence stars having the same bolometric luminosities, their densities must range from fifty to thousands of times that of the sun. Even for 10,000° K the densities are high and the stars are certainly subdwarfs.

Until recently it was usually assumed that the temperatures of postnova stars were 40,000° K or higher. This was based chiefly on the presence of emission lines of He II in the spectra of several of them (Humason 1938). DQ Her, however, has a measured $B - V$ color that indicates a temperature of about 10,000° K (Walker 1956), and the calculated radius is $0.10\odot$. Further, it has a short-period light-variation like that of an eclipsing binary.

6.7. Masses of Novae

For only one nova has an approximate mass been determined. T CrB is a binary composed of a gM3 star and the nova. The velocity variation in a period of 227 days yields minimum masses of $2.9\odot$ for the M star and $2.1\odot$ for the nova (Kraft 1958). If no eclipse occurs, the minimum mass of the nova is $2.6\odot$.

Greenstein and Kraft (1959) found a velocity variation of about 300 km/sec for the nova component of DQ Her, synchronous with the 4-hour photometric period. Lack of a secondary spectrum leaves the mass indeterminate, but if the components are equal, the nova has a mass of $0.27\odot$. Kraft (1959) interprets the nova as a white dwarf with a black-body temperature of 80,000° K, surrounded by a gaseous disk with an electron temperature of 40,000° K and a radius of 2×10^{10} cm (twenty to thirty times the stellar radius). Much of the continuous spectrum is attributed to the disk, and the light minimum is considered to be due to the eclipse of the disk. The companion star may be an M dwarf which fills its lobe of the inner Lagrangian surface.

§ 7. INTERPRETATION OF NOVA PHENOMENA

There is probably complete agreement that the main observable events of a nova outburst are associated with the explosive ejection of a large amount of material radially from the star in all directions, though, as the expanding nebulae attest, there are large deviations from a uniform spherical shell. In a general way this accounts for the shortward-displaced absorption lines of the premaximum spectrum as well as of the principal spectrum after maximum, for the symmetrical widening of the emission lines, and for the expanding nebulae seen for some years after the outburst. Concerning some details and especially as regards the precise meaning of the rise to maximum, there are considerable differences of opinion. In what follows it is possible only to sketch briefly the interpretation of phenomena. For details one must consult the original papers.

7.1. The Rise to Maximum

The hypothesis of continuous ejection seems to have been expressed independently in slightly different forms by several authors (Whipple and Payne-Gaposchkin 1936*b;* Beer 1937; Grotrian 1937*a;* McLaughlin 1937*b*). Following Grotrian's lucid treatment, we suppose that atoms are ejected from the original "stellar surface" of radius r_0 at a rate n_0 per cm^2 per second and with velocity V. Let N be the number of atoms per cm^3 at a distance r from the center of the star (where $r > r_0$). If there is no net acceleration or retardation, the density of the gas will decrease outward according to the formula

$$N = \frac{n_0}{V}\frac{r_0^2}{r^2}. \tag{11}$$

The photosphere is effectively that level in the cloud where the optical depth becomes approximately 1.0. We now make the simplifying assumption that this value of optical depth is associated with a particular density, N_p. Then the photospheric radius will be

$$r_p = r_0\sqrt{\frac{n_0}{vN_p}} = \text{Const.}\sqrt{\frac{n_0}{v}}. \tag{12}$$

Changes of either n_0 or v, or of both, may then cause the photosphere to expand or contract in the expanding cloud, but the material is continually streaming outward and escaping, and none returns to the star. The temperature in the "photospheric layer" and the composition of the radiation that escapes through it determine the continuous spectrum that we observe, and this also determines to a considerable extent the states of excitation of the atoms of the outer gases that form a "chromosphere." The rise to maximum is then due to the ejection of a cloud of gases dense enough to produce the effect of an expanding photosphere. As n_0 increases, r_p also increases. But an increase in r_p may also result from a decrease in v. In the case of DQ Her, both effects were present, for the radial velocity of the absorption spectrum decreased drastically during the first few days.

In the expanding cloud the moving atoms outrun the photosphere, so that the depth of the chromosphere and the number of atoms above the photosphere increase enormously. The spectrum near maximum is therefore similar to that of a supergiant star.

The preceding account of the rise has not been universally accepted. Mustel (1945*a*, *b*, 1956*b*) regards the brightening as due to a rapid expansion of the entire star rather than of a mere ejected cloud. This expansion of the body of the star, according to his view, continues until maximum light, at which time an outer layer is ejected as the principal shell, which later becomes the visible expanding nebula. The body of the star meanwhile gradually contracts again to its prenova state, but continuous ejection of material occurs for a considerable period during this contraction. In order to explain gravitationally the reversal

of such large velocities as we observe, Mustel (1947*c*, 1948*a*) found it necessary to attribute to novae masses hundreds of times that of the sun. More recently he has suggested (Mustel 1956*a*) that magnetic fields may account for the ability of novae to "pull themselves together" after their rapid expansion and that large masses may be unnecessary. In this connection we recall the apparent small mass of DQ Her.

Kopal (1956) interprets the expanding photosphere as a luminous shock front moving through tenuous gas surrounding the star. The hypothesis involves several special assumptions in order to reconcile apparently unfavorable observed features.

7.2. Maximum Light; the Postmaximum Transformation

According to Grotrian's model, we can account for the maximum and the ensuing decrease in brightness by a reduction in photospheric radius that results from a diminution in the rate of ejection, n_0. However, with an extremely deep cloud there would be a time lag, probably of the order of a day, between the change in rate and the visible response in the light-curve. In effect, the decreased rate means that the main ejected cloud becomes a partially detached "shell," but for a short time after its detachment its optical thickness exceeds 1.0, and the photosphere continues to expand with it. Eventually, the optical depth drops below 1.0, the photosphere then recedes to a position inside the "shell," as determined by the new smaller rate n_0, and the brightness declines. The expanding "shell" has now become transparent in the observable spectral region, except for its line frequencies. Strong, widened emission bands then emerge because we see entirely through to the receding side of the shell.

At this stage, acceleration of the inner layers of the shell takes place, and they in turn sweep up the outer parts. Mustel (1944, 1956*b*) has discussed details of this process. He attributes the acceleration mainly to radiation pressure of Lyman-α. During this transformation, double lines can be seen, but at its conclusion the premaximum absorption has disappeared, and the principal spectrum dominates.

7.3. Evolution of the Principal Spectrum

Just after the opacity of the principal shell has cleared away in the observable region, it is still optically very thick to radiation of higher frequency than the head of the Lyman series. All this ionizing radiation will be absorbed in a thin inner layer, and the emission which originates through recombination will come essentially from the *inner surface* of the shell. Differences of density will therefore at first have little observable effect, and the emission bands will be smooth. As the shell expands, excitation can penetrate farther into it, and the structures due to inequalities of density become visible (McLaughlin 1948*a*, 1949*b*, p. 57).

On the near side of the shell, the deep outer layers absorb in their line frequencies the radiation emitted by approaching atoms behind them, so that the

absorption lines cut off the shortward edges of the emissions. The great depth of the outer layers makes possible a nearly black line, in accordance with observation (Williams 1937). Black absorption lines are not explained by the simple Halm (1904) model of a thin expanding shell.

As the principal shell expands, all its lines weaken, for the obvious geometrical reason that the number of atoms in the line of sight from the observer to the photosphere diminishes. However, the lines do not retain the same relative intensities. Such lines as Si II 4128, 4131, Mg II 4481, and those of O I weaken quickly, while those of hydrogen, Fe II, and especially Ti II and Mg I remain strong. The persistence of hydrogen is due primarily to its original great strength, but that of Fe II, Ti II, and Mg I reflects the increasing dilution of the radiation that excites the principal shell. The lines of these elements that persist have lower levels that are metastable. These effects have been discussed at length by Struve (1939). In the late stages of the principal absorption in some novae the He I line 3889, whose lower level is metastable, has been very conspicuous (McLaughlin 1943, p. 156; 1949*b*, p. 27).

7.4. Diffuse Enhanced and Orion Spectra

Both Mustel (1947*a*, *b*) and McLaughlin (1943, p. 192) assign the diffuse enhanced and Orion spectra to the region of continuing postmaximum ejection close around the central star, far inside the principal shell. Effects of superposition of absorption and emission features confirm this arrangement of the sources (McLaughlin 1947*c*). Thus diffuse enhanced emission can be heavily absorbed by a line in the principal spectrum, and principal emission can obliterate an absorption line of the diffuse enhanced or Orion spectrum. Diffuse enhanced and principal lines alike can absorb from an Orion emission background—for example, the broad N III emission about Hδ which is cut by conspicuous Hδ absorption of both systems.

Mustel finds that the ejection of the material that produces the diffuse enhanced spectrum can be accounted for by radiation pressure of Lyman-α, but the Orion cannot. For the latter he requires explosive ejection of knots of material through the photosphere of the enlarged but contracting star. McLaughlin adheres to the Grotrian model, explaining the apparent size of the central star entirely in terms of the rate of ejection.

In the early part of the diffuse enhanced stage the spectrum probably originates in a P Cygni–like cloud surrounding the inner star, but when the lines have developed their striking multiplicity, they surely originate in detached, discrete, outward-moving clouds (not necessarily spherical shells). This material, moving faster than the principal shell, must overtake it and merge with it. This may account in part for the outward acceleration of the principal shell and perhaps also for a part of its excitation (Mustel 1948*b*), which has often been attributed entirely to radiative excitation by the central star. When dates of emergence of components are known, the date of overtaking can be computed

from the measured velocities. In Nova Herculis (McLaughlin 1954) a fair agreement was found between computed dates and the time of rather sudden disappearance of components. Similarly, Larsson-Leander (1954*b*, p. 99) found apparent confirmation of overtaking and engulfment in DK Lac.

The Orion spectrum, responding as it does to all secondary fluctuations of brightness by changes in strength and velocity, must originate close to the star. It represents the continuing ejection of material, and it does not appear to develop into an expanding *detached* cloud or shell.

7.5. The Transition Stage

Many novae pass smoothly through the transition and emerge in the nebular stage. The fading continuum indicates decreased rate of ejection, and the increasing dominance of the nebular type of spectrum reflects the progressive dilution of radiation, while at the same time the ionization increases in response to the higher temperature of the central star.

The strong fluctuations of GK Per, v603 Aql, and other novae are of greater interest. They represent variations in both m_0 and v. Recalling the correlation between the light-curve and the Orion radial velocity, we see that the fluctuations of light are approximately those required by the variations in velocity if Grotrian's formula for the photospheric radius is even roughly correct. Variations in rate could accentuate the changes. During each stage of high-speed ejection, a deeper, hotter photospheric layer is revealed. With decrease in velocity and probably increased rate of ejection, the photosphere expands to a cooler region of the cloud.

The emission bands of the distant principal shell respond to the variations in temperature of the photosphere. During the minima of light, high-excitation lines such as He II and N III appear in the principal shell. These disappear when the star brightens to a maximum, but then the *flaring* bands of N III emerge. These originate in the Orion cloud immediately about the inner star. At the same time, while the flaring of N III lasts, all the emissions of the principal shell show less obvious structural patterns. This is explained by the withdrawal of high-temperature radiation, so that excitation penetrates only partway through the principal shell and inequalities of density are less evident. When the excitation increases again with the decline to a minimum, excitation penetrates through the entire thickness of the principal shell, and the band structures again show prominently (McLaughlin 1949*b*, p. 57). These effects were especially striking in the spectrum of v603 Aql, whose hydrogen emissions showed alternately the "peaked" and "dipped" (saddle-shaped) profiles at maxima and minima, respectively (Sayer 1935; McLaughlin 1956). The "peaked" profile may have been due to the location of the knots responsible for the central "peak" *inside* the main part of the principal shell.

The deep minimum during the transition of stars of the DQ Her type has been variously interpreted. Grotrian (1937*a*) explained it as a result of a sudden

cessation of ejection, followed by a slow establishment of equilibrium between ionization and recombination in the nebula, in response to the high-temperature radiation of the central star. Stratton (1946) suggested absorption due to molecules that formed in material ejected during the Orion stage. Mustel (1950) proposed scattering by free electrons in the principal shell. The present author finds little support for molecular absorption or obscuration by dust as common phenomena of the transition, though some features of the behavior of DQ Her (especially the disappearance of the redward parts of the emission bands) are partially favorable to the hypothesis (McLaughlin 1949*a*). The minimum occurred in a milder form (depth 2.5 mag.) in XX Tau, and even as a broad dip of less than a magnitude in the light-curve of v476 Cyg. The steepening of decline in EU Sct was pretty surely just a variant of the same process, which appears to be very common. On the whole, Grotrian's explanation appears the most satisfactory.

In both the fluctuations of the early decline (e.g., DN Gem) and those of the transition stage, the oscillations of light are accompanied by spectral changes that follow "Stratton's rule": a secondary brightening temporarily returns the nova to a spectral stage already passed on the decline (Stratton 1920, p. 65; 1928, p. 279). In terms of Grotrian's model this simply means that not only the radius but also the temperature of the photosphere are set within limits by the ratio n_0/v. This can be valid, however, only so long as ejection continues. When it ceases, the rule fails, as in the DQ Her type. The rebrightening after the deep minimum is not at all a return to a stage passed in the decline. It is, instead, an advance for the first time into the nebular stage.

7.6. The Nebular Stage

The pure nebular stage of novae is probably better understood than any other. The problems are those of planetary nebulae with the added feature of rapid expansion.

The picturesque phrase "the wrecks of ancient novae" has sometimes been applied to the planetaries. So far as we now know, this can be justified only in the case of the Crab Nebula, whose observable characteristics set it clearly apart. Normal planetaries are more massive by 3 or 4 orders of magnitude than most nova shells, and their expansion velocities cannot be compared with those of the principal shells of any novae except possibly the extremely slow RT Ser type. Minkowski (1948) has concisely summarized the arguments, and no new facts alter the situation. If the existing planetaries had origins that could be likened in any way to the nova process, the phenomena must have differed very greatly from those of the common novae. A possible connection of planetaries with "permanent novae" like P Cyg may be suggested, but at present it is wholly speculative.

One of the interesting regularities in the behavior of novae is the passage into the nebular stage at 6–7 mag. below maximum. Even in the DQ Her type, the

nebular stage first becomes established at about that brightness after the very deep minimum. The reason for this fairly constant difference in magnitude may reside simply in the fact that the total mass ejected by the nova determines both the maximum luminosity and the brightness of the nebula. A constant ratio is therefore to be expected.

The systematic structure of some nova shells raises questions concerning the mechanism of ejection or the forces that act on the material. Most conspicuous is the tendency to eject two large knots in opposite directions. This was directly observed in RR Pic and DQ Her. In v603 Aql the knots were erupted nearly toward and from the earth, but they were plainly indicated in the Doppler ellipses, and the approaching one was later identified directly. GK Per showed the largest known departure from symmetry. Several other novae that did not have visible nebulous disks still displayed saddle-shaped emission profiles that point to a similar pattern of ejections.

In v603 Aql the scheme of two "polar caps" and "equatorial rings" worked out by Baade (van de Hulst 1951) or the alternative picture of conical jets suggested by Weaver may find explanation in the guiding of ions by a magnetic field (Mustel 1956*a*). In a dipole field, knots of ionized gas ejected near the poles can move radially outward from the star along the lines of force without retardation and would appear as the great "polar caps" of Baade's model. Material ejected from middle magnetic latitudes would be deflected toward the equator and give rise to the "equatorial rings." Material that left the star near the magnetic equator would be greatly retarded. Mustel draws parallels between the motion of knots of gas ejected from a nova and solar surges and prominence material moving under the influence of local magnetic fields. He suggests, further, that an "entangled" magnetic field in the expanding star is responsible for the contraction that occurs after maximum, according to his interpretation of the phenomena.

7.7. Origin of Nova Outbursts

Prenova stars appear to differ only minutely from the postnova objects. The mass loss in the explosion is a negligible fraction of the stellar mass, even for DQ Her. Photographic magnitudes before and after the nova episode differ no more than we should expect as a combined effect of observational errors and small real irregular variations. If any drastic change in structure had occurred, such as the collapse suggested by Milne (1931), it is very improbable that it would be accomplished without a large change in photographic magnitude between the pre- and postnova states (McLaughlin 1941*b*).

Recurrent novae emphasize the lack of alteration. The postnova stage of one outburst is the prenova stage of the next. The stars at minimum are small, hot subdwarfs closely similar to the postnova condition of the great novae that have not been recognized as recurrent. The available information appears to justify the conclusion that nova activity is limited to a special class of stars with a narrow range of characteristics. This points strongly toward internal, rather than external, causes.

We can rule out on grounds of extreme improbability the suggestion of collision or tidal encounter of two stars. The frequency of novae in our Galaxy has been estimated as 25 per year (Bailey 1921), and in the Andromeda spiral the observed number is actually of this order (Arp 1956).

The plunge of a star into a dark nebula might satisfy the probability requirements, but hardly the physical ones. The essential similarity of most novae is not at all compatible with the extreme range of conditions that would attend such an event. Further, the sequence of spectral changes contradicts any interpretation involving mere superficial heating and subsequent cooling of a star.

The cause of nova outbursts is not likely to be identified directly by observation. At best, we can only hope to arrive at an idea of the cause by devising hypotheses, calculating their consequences, and comparing the expected results with the observed facts. Biermann's (1939) hypothesis of an unstable layer in which a changeover occurs from radiative to convective equilibrium does not satisfy all the requirements, for it presupposes a low abundance of both hydrogen and helium. There seems to be no considerable deficiency of either of these elements in the observable layers of novae.

For an understanding of the nova outburst we must perhaps look to further development of our knowledge of nuclear processes under stellar conditions and of the theory of stellar interiors. According to a hypothesis developed by Schatzmann (1951), the hydrogen reactions may lead to accumulation of He^3 in excess of a critical concentration. This results in a nuclear explosion in the deep interior, and the shock wave ejects a superficial layer of the star. Such a process appears plausible for the violent rapid novae, but is it reconcilable with the very leisurely progress of the RT Ser stars through stages that closely simulate those of a typical nova?

REFERENCES

Adams, W. S., and Joy, A. H.	1920	*Pop. Astr.*, **28**, 514.
	1933	*Pub. A.S.P.*, **45**, 301.
Ambarzumian, V. A.	1932	*Poulkovo Obs. Circ.*, **4**, 8.
Ambarzumian, V. A., and Kosirev, N.	1933	*Zs. f. Ap.*, **7**, 320.
Arp, H. C.	1956	*A.J.*, **61**, 15.
Ashbrook, J., and Nail, V. M.	1942	*Harvard Bull.*, 916.
Baade, W.	1936	*Pub. A.S.P.*, **48**, 226.
	1942*a*	*Ibid.*, **54**, 244.
	1942*b*	*Ap. J.*, **96**, 188.
	1943	*Ibid.*, **97**, 119.
	1950	*Trans. I.A.U.*, **7**, 303.
Baade, W., Burbidge, G. R., Hoyle, F., Burbidge, E. M., Christy, R. F., and Fowler, W. A.	1956	*Pub. A.S.P.*, **68**, 296.

Bailey, S. I.	1921	*Pop. Astr.*, **29**, 554.
Baldwin, R. B.	1940	*Pub. Michigan Obs.*, **8**, 61.
Barnard, E. E.	1917	*A.J.*, **30**, 86.
	1919	*Ap. J.*, **49**, 199.
Beals, C. S.	1929	*Pub. Dom. Ap. Obs. Victoria*, **4**, 271.
	1932	*M.N.*, **92**, 677.
	1937	*Pub. Dom. Ap. Obs. Victoria*, **6**, 335.
Beer, A.	1936	*M.N.*, **96**, 236.
	1937	*Ibid.*, **97**, 231.
Beileke, F., and Hachenberg, O.	1935	*Zs. f. Ap.*, **10**, 366.
Bertaud, C.	1945	*Ann. Obs. Paris* (Meudon), Vol. **9**, Part 1.
	1948	*Ann. d'ap.*, **11**, 1.
	1951	*J. d. Obs.*, **34**, 38.
	1953	*Ibid.*, **36**, 25.
Beyer, M.	1929	*A.N.*, **235**, 427.
	1952	*Ibid.*, **280**, 276.
Biermann, L.	1939	*Zs. f. Ap.*, **18**, 344.
Bloch, M.	1950	*Ann. d'ap.*, **13**, 390.
Bloch, M., Dufay, J., Fehrenbach, C., and Tcheng, Mao-Lin	1946	*Ann. d'ap.*, **9**, 157.
Buscombe, W., and de Vaucouleurs, G.	1955	*Observatory*, **75**, 170.
Campbell, L.	1903	*Harvard Ann.*, **48**, 39.
	1915	*Ibid.*, **76**, 191.
	1919	*Ibid.*, **81**, 113.
	1932	*Harvard Bull.*, No. 890.
Campbell, W. W.	1892	*Pub. A.S.P.*, **4**, 233.
Cannon, A. J.	1916	*Harvard Ann.*, **76**, 19.
	1920	*Ibid.*, **81**, 179.
Chandrasekhar, S.	1934	*M.N.*, **94**, 444.
Couderc, P.	1939	*Ann. d'ap.*, **2**, 271.
Gaposchkin, S.	1941	*Les Novae et les naines blanches*, **1**, 33 (Paris: Hermann et Cie).
Garstang, R. H.	1951	*M.N.*, **111**, 115.
Greaves, W. M. H., and Martin, E. G.	1936	*M.N.*, **96**, 425.
Greenstein, J. L.	1957	*Ap. J.*, **126**, 23.
Greenstein, J. L., and Kraft, R. P.	1959	*Ap. J.*, **130**, 99.
Grotrian, W.	1937*a*	*Zs. f. Ap.*, **13**, 215.
	1937*b*	*Ibid.*, **14**, 129.
Grouillier, H.	1935	*Lyons Obs. Bull.*, Vol. **1**, No. 16.
Halm J.	1904	*Proc. R. Soc. Edinburgh*, **25**, 513.
Hanbury Brown, R., and Hazard, C.	1952	*Nature*, **170**, 364.

HARPER, W. E., PEARCE, J. A., BEALS, C. S., PETRIE, R. M., and McKELLAR, A.	1937	*Pub. Dom. Ap. Obs. Victoria*, **6**, 317.
HEARD, J. F.	1953	*J.R.A.S. Canada*, **47**, 109.
HERBIG, G. H., and NEUBAUER, F. J.	1946	*Pub. A.S.P.*, **58**, 196.
HUBBLE, E. P.	1929	*Ap. J.*, **69**, 143.
	1941	*Pub. A.S.P.*, **53**, 152.
HULST, H. C. VAN DE	1951	*Problems of Cosmical Aerodynamics* (Dayton, Ohio: Central Air Documents Office), p. 116.
HUMASON, M. L.	1935	*Pub. A.A.S.*, **8**, 115.
	1938	*Ap. J.*, **88**, 228.
	1943	*Pub. A.S.P.*, **55**, 74.
JENKINS, L.	1952	*General Catalog of Trigonometric Stellar Parallaxes* (New Haven, Conn.: Yale University Press).
JONES, H. S.	1931	*Cape Obs. Ann.*, Vol. **10**, Part 9.
JOY, A. H.	1945	*Pub. A.S.P.*, **57**, 171.
JOY, A. H., ADAMS, W. S., and DUNHAM, T.	1936	*Pub. A.S.P.*, **48**, 328.
KOPAL, Z.	1956	*Vistas in Astronomy* (London: Pergamon Press), p. 1491.
KOPYLOV, I. M.	1952	*Crimean Ap. Obs.*, **9**, 116.
KRAFT, R. P.	1958	*Ap. J.*, **127**, 625.
	1959	*Ibid.*, **130**, 110.
KUIPER, G. P.	1941	*Pub. A.S.P.*, **53**, 330.
KUKARKIN, B. V., and PARENAGO, P. P.	1934	*Peremennye zvezdy* (*Veränderliche Sterne*), Gorki, **4**, 251.
LARSSON-LEANDER, G.	1953	*Stockholm Ann.*, Vol. **17**, No. 8.
	1954*a*	*Ibid.*, Vol. **18**, No. 3.
	1954*b*	*Ibid.*, No. 4.
LEAVITT, H. S.	1920	*Harvard Ann.*, **84**, 121.
LOCKYER, J. N.	1891	*Phil. Trans. R. Soc. London, A*, **182**, 414.
LOHMANN, W.	1949	*A.N.*, **277**, 37.
LUDENDORFF, H.	1928	*Hdb. d. Ap.*, **6**, 66.
LUNDMARK, K.	1921	*Pub. A.S.P.*, **33**, 225.
LUNT, J.	1919	*M.N.*, **79**, 416.
McKELLAR, A.	1937	*Pub. Dom. Ap. Obs. Victoria*, **6**, 353.
McLAUGHLIN, D. B.	1936	*Ap. J.*, **84**, 104.
	1937*a*	*Ibid.*, **85**, 362.
	1937*b*	*Pub. Michigan Obs.*, **6**, 107.
	1939	*Pop. Astr.*, **47**, 410, 481, 538.
	1940	*Ap. J.*, **91**, 369.
	1941*a*	*Pub. A.S.P.*, **53**, 102.
	1941*b*	*Pop. Astr.*, **49**, 292.
	1941*c*	*Ap. J.*, **93**, 417.
	1942*a*	*Ibid.*, **95**, 428.

McLAUGHLIN, D. B.	1942*b*	*Pop. Astr.*, **50**, 233.
	1943	*Pub. Michigan Obs.*, **8**, 149.
	1944	*A.J.*, **51**, 20.
	1945*a*	*Pub. A.S.P.*, **57**, 69.
	1945*b*	*A.J.*, **51**, 136.
	1946	*Pub. A.S.P.*, **58**, 46.
	1947*a*	*A.J.*, **52**, 126.
	1947*b*	*Pub. A.S.P.*, **59**, 81.
	1947*c*	*Ibid.*, p. 244.
	1948*a*	*Ibid.*, **60**, 54.
	1948*b*	*A.J.*, **54**, 43.
	1949*a*	*Pub. A.S P.*, **61**, 74.
	1949*b*	*Pub. Michigan Obs.*, **9**, 13.
	1953*a*	*Ap. J.*, **117**, 279.
	1953*b*	*Ibid.*, **118**, 27.
	1954	*Ibid.*, **119**, 124.
	1955	*Ibid.*, **122**, 419.
	1956	*Pub. A.S.P.*, **68**, 444.
	1957	*A.J.*, **62**, 94.
	1959	*Ibid.*, **64**, 130.
	1960*a*	*Ibid.*, **65**, 54.
	1960*b*	*Ap. J.*, **131**, 739.
MAYALL, M. W.	1946	*Harvard Bull.*, No. 918.
	1949	*Ibid.*, No. 919.
MAYALL, N. U.	1937	*Pub. A.S.P.*, **49**, 101.
	1948	*Ibid.*, **60**, 266.
MAYALL, N. U., and OORT, J. H.	1942	*Pub. A.S.P.*, **54**, 95.
MENZEL, D. H., and ALLER, L. H.	1941	*Ap. J.*, **93**, 195.
MERRILL, P. W.	1935	*Ap. J.*, **81**, 312.
MERRILL, P. W., and WILSON, O. C.	1936	*Pub. A.S.P.*, **48**, 230.
MILNE, E. A.	1931	*Observatory*, **54**, 144.
MINKOWSKI, R.	1939	*Ap. J.*, **89**, 156.
	1942	*Ibid.*, **96**, 199.
	1943	*Ibid.*, **97**, 128.
	1948	*Ibid.*, **107**, 106.
MUSTEL, E. R.	1944	*A.J. Soviet Union*, **21**, 276.
	1945*a*	*Ibid.*, **22**, 65.
	1945*b*	*Ibid.*, p. 185.
	1947*a*	*Ibid.*, **24**, 97.
	1947*b*	*Ibid.*, p. 155.
	1947*c*	*Ibid.*, p. 280 (*Astr. News Let.*, No. 37).
	1948*a*	*Ibid.*, **25**, 11 (*Astr. News Let.*, No. 38).
	1948*b*	*Ibid.*, p. 156 (*Astr. News Let.*, No. 39).
	1950	*Sternberg Astr. Inst.*, No. 41 (*Astr. News Let.*, No. 66).

	1956*a*	*A.J. Soviet Union*, **33**, 182.
	1956*b*	*Vistas in Astronomy* (London: Pergamon Press), p. 1486.
OEHLER, H.	1936	*Zs. f. Ap.*, **12**, 281.
OORT, J. H., and WALRAVEN, T.	1956	*B.A.N.*, **12**, 285.
PARENAGO, P. P.	1949	*V.S.*, **7**, 109.
PAYNE-GAPOSCHKIN, C.	1957	*The Galactic Novae* (Amsterdam: North Holland Publishing Co.).
PAYNE-GAPOSCHKIN, C., and GAPOSCHKIN, S.	1938	*Variable Stars* ("Harvard Obs. Monographs," No. 5).
	1942	*Harvard Circ.*, No. 445.
PAYNE-GAPOSCHKIN, C., and MENZEL, D. H.	1938	*Harvard Circ.*, No. 428.
PAYNE-GAPOSCHKIN, C., and WHIPPLE, F. L.	1940	*Proc. N.A.S.*, **26**, 264.
PEARSON, E. S.	1936	*Ann. Solar Phys. Obs. Cambridge*, Vol. **4**, Part 3.
PEASE, F. G.	1920	*Pub. A.S.P.*, **32**, 334.
PETRIE, R. M.	1935	*Ap. J.*, **81**, 482.
	1937	*Pub. Dom. Ap. Obs. Victoria*, **6**, 339.
PETTIT, E.	1943	*Pub. A.S.P.*, **55**, 152.
	1946	*Ibid.*, **58**, 255.
PICKERING, E. C.	1899	*Harvard Ann.*, **56**, 170.
POPPER, D. M.	1940	*Ap. J.*, **92**, 262.
PRAGER, R.	1940	*Harvard Bull.*, No. 912.
REESE, H. M., and CURTIS, H. D.	1903	*Ap. J.*, **18**, 299.
RITCHEY, G. W.	1917	*Pub. A.S.P.*, **29**, 256.
ROSSELAND, S.	1936	*Theoretical Astrophysics* (Oxford: Clarendon Press).
SANFORD, R. F.	1943	*Ap. J.*, **97**, 130.
	1945*a*	*Ibid.*, **102**, 357.
	1945*b*	*Pub. A.S.P.*, **57**, 312.
	1947	*Ibid.*, **59**, 334.
	1949	*Ap. J.*, **109**, 81.
SANFORD, R. F., and GREENSTEIN, J.	1957	*Pub. A.S.P.*, **69**, 75.
SAYER, A. R.	1935	*Harvard Circ.*, No. 406.
	1940	*Harvard Ann.*, **105**, 21.
SCHATZMANN, E.	1951	*Ann. d'ap.*, **14**, 294.
SCHMIDT, T.	1957	*Zs. f. Ap.*, **41**, 182.
SCHWASSMANN, A., and WACHMANN, A. A.	1928	*A.N.*, **232**, 272.
SHAPLEY, H.	1921	*Pub. A.S.P.*, **33**, 190.
STEAVENSON, W. H.	1923	*M.N.*, **83**, 397.
	1924	*Ibid.*, **84**, 538.
	1950	*Ibid.*, **110**, 621.

STOY, R. H.	1933	*M.N.*, **93**, 588.
STRATTON, F. J. M.	1920	*Ann. Solar Phys. Obs. Cambridge*, Vol. **4**, Part 1.
	1928	*Hdb. d. Ap.*, **6**, 251.
	1936*a*	*Ann. Solar Phys. Obs. Cambridge*, Vol. **4**, Part 2.
	1936*b*	*Ibid.*, Part 4.
	1946	*M.N.*, **105**, 275.
STRATTON, F. J. M., and MANNING, W. H.	1939	*Atlas of Nova Herculis* (Cambridge, England: Solar Physics Observatory).
STRUVE, O.	1939	*Proc. Am. Phil. Soc.*, **81**, 225.
SWINGS, P., and STRUVE, O.	1940	*Ap. J.*, **92**, 295.
	1942	*Ibid.*, **96**, 468.
TSÊ-TSUNG, HSI	1958	*Smithsonian Contr. Ap.*, **2**, 109.
UNSÖLD, A.	1930	*Zs. f. Ap.*, **1**, 146.
VORONTSOV-VELYAMINOV, B. A.	1940	*Ap. J.*, **92**, 283.
	1946	*A.J. Soviet Union*, **23**, 286.
	1947	*Ibid.*, **24**, 83.
WALKER, A. D.	1923	*Harvard Ann.*, **84**, 189.
WALKER, M. F.	1956	*Ap. J.*, **123**, 68.
	1957	*I.A.U. Symposium*, No. **3**, p. 46.
WALLERSTEIN, G.	1958	*Pub. A.S.P.*, **70**, 537.
WEAVER, H. F.	1944	*Ap. J.*, **99**, 280.
WELLMANN, P.	1951*a*	*Zs. f. Ap.*, **29**, 101.
	1951*b*	*Ibid.*, p. 112.
WHIPPLE, F. L., and PAYNE-GAPOSCHKIN, C.	1936*a*	*Harvard Circ.*, No. 412.
	1936*b*	*Ibid.*, No. 413.
	1937	*Ibid.*, No. 414.
	1939	*Ibid.*, No. 433.
WILLIAMS, E. G.	1935	*M.N.*, **95**, 573.
	1936	*Ap. J.*, **83**, 305.
	1937	*M.N.*, **97**, 633.
WILSON, O. C.	1936	*Pub. A.S.P.*, **48**, 229.
WILSON, O. C., and WILLIAMS, E. G.	1934	*Ap. J.*, **80**, 344.
WRIGHT, W. H.	1910	*Lick Obs. Bull.*, **6**, 65.
	1920	*Lick Pub.*, Vol. **14**, Part 1.
	1926	*Ibid.*, Part 2.
WYSE, A. B.	1936	*Pub. A.S.P.*, **48**, 302.
	1939	*Lick. Pub.*, Vol. **14**, Part 3.
	1940*a*	*Ibid.*, Part 4.
	1940*b*	*Ibid.*, Part 5.
ZANSTRA, H.	1931	*Pub. Dom. Ap. Obs. Victoria*, **4**, 209.
ZINNER, E.	1920	*Geschichte und Literatur des Lichtwechsels*, **2**, 449.

CHAPTER 18

Spectra of Dwarf Variable Stars

ALFRED H. JOY
Mount Wilson and Palomar Observatories
Carnegie Institution of Washington, California Institute of Technology

Low luminosity among the variable stars was first noted by Shapley (1919) in connection with his studies of the magnitudes and colors of variables in the Orion Nebula. Previously, a remarkable group of about one hundred faint irregular variables near the Orion Trapezium had been discovered, mostly by Wolf (1901, 1903) and by Leavitt (Pickering 1904). Using Kapteyn's parallax of 0".0054 based on the motions of the Orion B-type stars, Shapley pointed out that the fainter stars surrounding the Trapezium must be dwarf stars if they also belonged to the group and were associated with the nebula. At that time, variables were thought to be stars of great intrinsic brightness. The importance of the stars imbedded in nebulosity was considered with reference to ideas then current concerning stellar origin and evolution.

In later studies, using revised luminosities of only those B-type reference stars that were most certainly associated with the nebula and correcting the apparent magnitudes for the estimated effects of interstellar absorption or obscuration, somewhat different values of the distance modulus were derived for the Trapezium cluster by several other astronomers; however, the low luminosity of the faint red variables was quite evident and the existence of variable stars of low luminosity confirmed.

The development of this novel aspect of stellar variability was delayed for many years because the observations were difficult and the chief cause of the light-changes was unfortunately attributed to varying obscuration rather than to possible activities taking place within the stars themselves. The faintness of the stars and the presence of enveloping and nearby nebulosity rendered the estimates of brightness somewhat uncertain by either visual or photographic methods. A range of 2 or more mag. was frequently observed, but the apparent light-changes were found to be most irregular (Shapley 1924).

The spectra of variable stars of late type associated with nebulosity supply unmistakable evidence of low luminosity. In regions of dark clouds the spectra of many dwarf variables have been studied by Joy (1945, 1949), by Struve and Rudkjøbing (1949), by Herbig (1950*b*, 1954*a*), and by Walker (1956). Likewise, the spectra of faint UV Ceti stars and of SS Cygni variables at minimum confirm the dwarf character of unstable bodies of this kind. Upon the absorption-line spectra are usually superposed bright lines originating at higher atmospheric levels.

Under certain conditions, explosive activity may produce an overlying spectrum with a hot violet continuum and strengthened emission lines of hydrogen, but the normal state of all these stars is that of low surface temperature ($<6000°$ K) and relatively high atmospheric density.

§ 1. CLASSIFICATION

Consideration of the various spectroscopic features, together with the light-curves of these variable stars, permits us to suggest preliminary groupings. Until more complete observational data are available, an entirely satisfactory system of classification of the dwarf variable stars with respect to both photometric and spectroscopic criteria seems impossible. The large and sudden light-changes, reaching several magnitudes in some stars, are extremely irregular, while the relationship of the astonishing spectroscopic behavior to the light- and color changes is not yet explained.

With reference to the light-curves alone, three types of variation have been recognized among the dwarfs by variable-star observers—the rapid irregular variables, the UV Ceti flare stars, and the SS Cygni stars. With the aid of spectroscopic observations the scope of these classes can be more rigorously fixed and the first group divided into four subgroups based mostly on spectral type and the peculiarities of their emission spectra. Most of the features can be distinguished even with low dispersion.

A provisional classification system depending largely upon spectroscopic criteria and including nearly all the known dwarf variables for which the necessary data are available can now be proposed.

§ 2. CLASSES OF DWARF VARIABLE STARS

2.1. Group I: Rapid Irregular Variables

a) *B8–G5.*—Bright lines few or absent. Examples, WW Vulpeculae A3e, RY Tauri dG0e.

b) *dGe–dM1e.*—Many bright lines of T Tauri or chromospheric type. Example, T Tauri, dG5e.

c) *dG5e–dM2e.*—Few bright lines: H, Ca II, and He I only. Example, GM Aurigae, dK5e.

d) *dK6e–dM6e.*—Faint bright lines of H seen at times, but bright Ca II weak or absent. Haro's "flash" stars.

2.2. Group II: UV Ceti Flare Stars

dM3e–dM6e.—Emission lines usually strong and narrow. At flare time, bright lines of H wider and stronger, continuum veils the shortward region of the spectrum. Large proper motion.

2.3. Group III: SS Cygni Variables

dG3e–dK0e.—At minimum (normal) phase, bright lines of H, Ca II, and He, 20 A in width; variable velocity. At maximum, veiled by hot continuum.

A descriptive summary of our present knowledge of the low-luminosity stars of these groups and their spectral characteristics follows.

§ 3. GROUP I: RAPID IRREGULAR DWARF VARIABLES

A number of the features of stars associated with interstellar matter are easily observed, even though little is known in detail about the activities. Changes in total light of such stars may take place within a single day or may involve weeks or months. The variations of 1–3 mag. are entirely irregular. In some stars the variations become small at times (Enebo 1907), and the brightness is nearly constant for a considerable period, irrespective of whether the star is near maximum or minimum. Such changes are known to variable-star observers as variations of the RW Aurigae type (Hoffmeister 1949; Herbig 1952, 1954*a*), and the stars are designated in the Kukarkin-Parenago *Catalogue of Variable Stars* as RW, Ori, or XX variables. Apparently, light-curves of this kind are characteristic of dwarf variables associated with dust or emission clouds, although such variations are also found in many which are not involved in observable nebulosity. Their spectral types are scattered from B8 to M6.

The problem of the interaction between stars and dust or gas clouds is at present largely unsolved because of lack of needed physical data. Because they are in early stages on the evolutionary path, these stars may not conform to current ideas of stellar structure, which have been found applicable to more stable bodies, where equilibrium conditions have been more nearly attained. Mass, radius, density, and temperature must play important roles. The effects of the surrounding material on dwarfs may be assumed to be quite unlike those on giants, so that, if both giants and dwarfs are present in the clouds, we may hope, in time, to be able to distinguish between them by their behavior.

Ia. Spectral types B8–G5, with few bright lines.—While the stars of this group show early spectral types and rapid variations in light with an average range of 1.8 mag., little accurate or comprehensive information concerning their spectra or fluctuations in light is available. No characteristic differences between the light-curves of these variables and those of other groups with very different spectra have yet been recognized.

Table 1 contains stars of this subgroup for which spectral types between B8 and G5 are known. The types are mostly from Herbig's list (1954*a*) and from

Mount Wilson spectrograms. The luminosity classes indicated depend upon the source.

The location of these stars suggests that many are associated with the clouds of Taurus, Orion, and Corona Australis. For these, estimates of spectroscopic absolute magnitudes are uncertain because of the presence of nebulosity and probable absorption. Some may be giants or subgiants, but most of them are evidently close to the main sequence. For example, if the modulus, $m - M$, of

TABLE 1

SUBGROUP I*a:* B8–G5 VARIABLES

Star	Magnitude	Range (mag.)	Class	Spectrum	Reference*
BM And	12.7–14.4+	1.7+	RW	F8e	1
AB Aur	7.2– 8.4	1.2	XX	A0e	2
SU Aur	9.0– 9.6	0.6	I?	G2e	1
VX Cas	10.7–13.3	2.6	Ori	dA0	1
BE Cas	13.5–14.4	0.9	RW	F2	1
YZ Cep	12.2–13.5	1.3	XX	dG2	Mt.W.
R CrA	10.0–13.6	3.6	Ori	F5e	3
T CrA	11.7–13.5	1.8	Ori	dF2	3
TY CrA	8.7–12.4	3.7	Ori	dB9	4
V517 Cyg	12.6–13.5	0.9	RW	A5	1
RY Lup	9.9–13.0	3.1	RW	G0 V	1
Z Mic	10.3–13.0	2.7	RW?	F2	1
T Ori	9.5–12.1	2.6	Ori	A3e V	1
RY Ori	10.5–14	3.5:	Ori	dF8	1
UX Ori	8.9–10.6	1.7	Ori	A3e	5
BN Ori	9.3–11.4	2.1	XX	A6	1
CO Ori	10.0–13.0	3.0	RW	G2ep	5
HK Ori	11.4–12.5	1.1	RW	A4ep	6
KS Ori	10.2–11.2	1.0	Ori	A0	7
MR Ori	10.6–11.9	1.3	Ori	A2 V	8
V351 Ori	10.1–11.6	1.5	RW	A2	HD
V380 Ori	9.7–10.3	0.6	RW	dA4e	9
XY Per	8.8–10.1	1.3	XX	A3e	1
AK Sco	8.7– 9.5	0.8	RW	F5 V	1
RR Tau	10.2–14.2	4.0	RW	A2e	10
RY Tau	8.8–11.2	2.4	RW	dG0e	3
UX Tau	10.7–13.4	2.7	RW	dG5e	3
CQ Tau	8.7–10.5	1.8	RW	F2	1
CT Tau	10.4–11.5	1.1	RW	A0 V	11
WW Vul	10.9–12.6	1.7	XX	A3e	1

*The references are as follows:

1. Herbig (1954*a*).
2. Merrill and Burwell (1933).
3. Joy (1945).
4. Gaposchkin (1937).
5. Elvey and Babcock (1943).
6. Joy (1949).
7. Trumpler (1931).
8. Greenstein and Struve (1946).
9. Herbig (1946).
10. Merrill and Burwell (1950).
11. Kukarkin and Parenago, *Catalogue of Variable Stars*.

the Orion stars is 9.0, the median absolute magnitudes lie between +1.0 and +5.0, but, with corrections for the effects of absorption, the resulting luminosities would be brighter. Except for V380 Ori (BD−6°1253) emission is weak or absent but has been observed, mostly at Hα, in fourteen stars of the list. More extended observation will doubtless disclose emission in other stars and provide much needed information concerning their spectral variations.

As Herbig (1954*a*) has remarked, there is little resemblance between the spectra of stars of this subgroup and that of RW Aurigae, although their light-curves may be similar. For this reason it seems incongruous to call these stars "RW Aurigae variables." WW Vulpeculae A3e or RY Tauri G0e are more suitable prototypes for subgroup I*a*.

Ib. Spectral types G5–M2, with many bright lines.—The well-known stars of this group have been recognized for a long time as irregular variables with a range of about 3 mag. The variability of T Tau was discovered by Hind in England in 1852 and that of R Mon and S CrA by Schmidt in Athens in 1861 and 1866, respectively. Their light-changes were discovered visually with the aid of small telescopes while observing the surrounding nebulae. The variation of RW Aur was found in 1906 by Mme Ceraski from Moscow photographs. Because their light-changes show no regularities and because, until recently, it was believed that the variation resulted from obscuration by passing dark clouds rather than from intrinsic variations, these stars have received comparatively little attention from variable-star observers.

The nature of these objects and the importance of their association with nebulosity first became evident from studies of the remarkable Mount Wilson spectra of nine of the typical variables of the group (Joy 1945). Because such stars are faint and because few have had adequate spectroscopic observation, only a small number of additional variables of this type have been identified. Among the faint bright-line stars of the Taurus clouds, Mount Wilson spectrograms (Joy 1949) revealed fourteen new members of the group, five of spectral type Ge, seven dKe, and two dMe. Nearly all these were found by Kholopov (1951) to vary in light. The spectra of these variables show a magnificent array of bright lines, often with varying intensity, of H, Ca II, He, Fe II, Fe I, Ti II, [S II], and other atoms. In 1948, Struve and Rudkjøbing (1949) discovered in the dark clouds of Ophiuchus two stars whose spectra correspond to those of this group. They have yet to be found variable in light. Also, four variables (one Ge, three dKe) of this class were reported by Haro and Herbig (1955) and EX Lup (dKe) by Herbig (1950*c*). Data concerning the thirty-one known variables of the group for which spectral types have been determined are collected in Table 2. The magnitudes are from the Kukarkin and Parenago *General Catalogue of Variable Stars*. Because the spectra vary and the absorption lines are partially filled in with continuous or line emission, the spectral types are only approximate. The emission-line intensities are subject to rapid changes and represent only rough maximum values from low-dispersion Mount Wilson spec-

trograms. Usually the strength of K (Ca II) emission is nearly equal to that of Hγ. The intensity and persistence of the emission of the fluorescent lines λ 4063 and λ 4132 of Fe I (Herbig 1945) and the forbidden [S II] line λ 4068 is remarkable.

A series of eleven spectrograms of UZ Tau (Joy 1942, 1943, 1945) indicates that this star is subject to continual variation both in total light and in spectrum. Fortunately, the variable has a close (distant 3″.7) visual companion of nearly the same type and brightness, which happens to fall upon the slit of the spectrograph with the variable star and serves as a standard by which the brightness of the two stars may be compared with others at different wave lengths. The reason for the different behavior of the two stars which are so close together and so nearly alike in physical structure is a mystery.

Spectra of nine stars of the group, mostly at maximum light, are reproduced

TABLE 2

SUBGROUP I*b*: T TAURI VARIABLES HAVING MANY BRIGHT LINES

STAR	MAGNITUDE	RANGE (mag.)	SPEC.	EMISSION INTENSITY						UV. INTENSITY	REFERENCE*
				Hγ	K Ca II	4233 Fe II	4063 Fe I	4471 He I	4068 [S II]		
RW Aur	9.0–12.0	3.0	dG5e	25	45	6	5	2	2	wk	1
UY Aur	11.6–14.0	2.4	dG5e	40	50	5	3	3	2	m	1
DI Cep	11.9–13.5	1.6	dK3e	25	40	2	1	2	1	.....	2
S CrA	10.8–12.5	1.7	dGe	20	20	5	5	2	2	wk	1
VV CrA	13.0–17	4	—e	(30)	.....	(3)	.....	.....	.....	.....	3
RU Lup	9.3–13.2	3.9	dGe	40	20	12	5	2	2	.....	1
EX Lup	11.4–13.4	2.0	(G)e	20	40	5	1	2	.....	wk	4
R Mon	10 –14	4	Ge	4	5	5	.....	.....	.....	.....	1
NX Mon	14.5–15.8	1.3	dKe	40	40	4	.....	3	1	str	5
OY Mon	14.0–15.2	1.2	dKe	40	20	3	2	2	.....	wk	6
AU Ori	14.5–16.0	1.5	dKe	30	40	3	.....	2	.....	wk	5
BC Ori	15.0–16.1	1.1	dK5e	50	40	.....	2	2	.....	wk	5
HI Ori	13.2–15.5	2.3	dK0e	25	40	2	1	1	1	wk	2
HS Ori	15.2–16	0.9	(G)e	15	40	3	2	2	.....	m	5
IX Ori	13.4–15.1	1.7	(K)e	20	20	3	.....	1	.....	m	5
T Tau	9.5–13.0	3.5	dG5e	30	40	6	2	1	1	wk	1
UZ Tau	11.7–14.9	3.2	dM2e	20	50	16	8	4	3	str	1
XZ Tau	11 –14	3	dGe	40	40	6	4	2	2	m	1
BP Tau	12.3–13.3	1.0	dG5e	35	50	2	1	3	.....	str	2
CI Tau	13.8–14.5	0.7	dGe	50	50	5	4	3	.....	str	2
CW Tau	13.6–16	2	dK5e	20	30	3	1	2	5	m	2
DD Tau	14.5–15.5	1.0	dK6e	50	20	2	.....	4	2	m	2
DE Tau	13.8–14.8	1.0	dM1e	25	50	2	2	1	2	m	2
DF Tau	11.9–13.8	1.9	dM0e	30	20	2	1	3	1	m	2
DG Tau	11.8–14.9	3.1	dGe	20	50	3	10	1	.....	wk	2
DH Tau	14 –15	1	dM0e	40	15	1	.....	4	1	str	2
DL Tau	13.5–14.8	1.3	dGe	30	50	4	4	4	.....	m	2
DN Tau	13.2–14.0	0.8	dK6e	40	15	1	.....	5	2	str	2
DO Tau	13.7–15.5	1.8	dGe	35	50	4	4	2	3	str	2
DQ Tau	14.0–15.0	1	dK0e	25	40	2	1	1	1	wk	2
DR Tau	13.4–14.7	1.3	dK5e	30	40	2	.....	2	.....	wk	2

* The references are as follows:
1. Joy (1945).
2. Joy (1949).
3. Herbig (1954*a*).
4. Herbig (1950*c*).
5. Haro and Herbig (1955).
6. Herbig (1954*c*).

in Plate I. They are arranged in the order of intensity of the emission lines and illustrate the wide differences to be found among the spectra of these stars. The striking spectral differences at two phases of RW Aur and UZ Tau are easily seen in Plate II.

In many stars of the group the relative strength of the ultraviolet continuum at times seems to be greatly enhanced. At such times the Balmer lines are about 4 A wide, have a slow decrement shortward, and the whole photographic spectrum is veiled by continuous emission.

Estimates of the relative intensity of the continuous radiation in the ultraviolet spectra of the stars of subgroup I*b* appear in the eleventh column of Table 2. Definite brightening of this region is apparent in several of the faintest stars, especially in NX Mon, UZ Tau (at certain times), BP Tau, DN Tau, and DO Tau. Their spectra are heavily veiled, and the hydrogen series extends to H15.

The spectra of four of the faint variables in the Taurus cloud—AA Tau (MHα 259-17), M0e; DH Tau (MHα 259-9*n*), M0e; BP Tau (MHα 259-7), K5e; and CI Tau (MHα 259-20), Ge—probably taken at the times of flares, are compared in Plate III with more normal spectra of MHα 259-23, M2.5e; DI Tau (MHα 259-9s), M0.5e; GM Aur (MHα 259-1), K5e; and DG Tau (MHα 259-10), Ge.

Ic. Spectral types G–M2, with bright lines of H, Ca II, and He I, only.—In Group I*c* are thirty-three faint irregular variables of late type whose spectra at the time of observation showed only emission lines of H, He, and Ca II (Table 3). The average magnitude range is less, and the mean spectral type is definitely later, than found in Group I*b*. Three stars are of type G; thirteen of K; nine of M; and eight unspecified.

For twenty-five of the twenty-nine stars in which emission lines of both have been observed, Hγ is equal to, or stronger than, K (Ca II), but the blend of H (Ca II) and Hϵ is unexpectedly strong in a few of the dMe variables in Taurus, as Struve and Rudkjøbing (1949) found for three stars in the Ophiuchus cloud. Strong continuous radiation in the ultraviolet has not been observed in this group, but few observations have been made, and if it was present for only short irregular intervals of time, it may easily have escaped observation.

Id. Haro flash stars, with outbursts of light of less than 100 minutes' duration; spectral type K6–M6, H and Ca II emission weak or absent.—In a survey of the Hαe stars in the Orion nebula, Haro (1953) noted that many of the stars showed variation in the intensity of Hα and the continuous spectrum as well as in light. Considerable changes took place in less than a day in several stars. A search for rapid variables of this kind among the fainter Orion stars by Haro and Morgan (1953), by means of direct photographs with exposures of 10 minutes each, disclosed three stars—Brun Nos. 868 (V378 Ori), 886 (V379 Ori), and 905 (OX Ori)—that showed temporary increases of 0.5–1.0 mag. in light in times ranging from 20 to 60 minutes. These remarkable outbursts in bright-

TABLE 3

SUBGROUP *Ic*: TYPES G–M2 WITH FEW BRIGHT LINES

STAR	MAGNITUDE	RANGE (mag.)	SPECTRUM	EMISSION LINES			REFERENCE*
				Hγ	K Ca II	4471 He I	
V536 Aql.....	12.6–15.2	2.6	dKe	str	m	wk	1
GM Aur.....	13.1–13.9	0.8	dK5e	str	str	wk	2
IP Mon.....	14.2–15.4	1.2	d(K2)e	wk	m	.....	3
LU Mon.....	14.9–16.5	1.6	—e	str	wk	.....	3
MM Mon.....	14.5–15.4	0.9	dGe	m	m	.....	3
NW Mon.....	14.6–15.2	0.6	Me	wk	wk	.....	3
7.1924 Mon.....	17	.....	—e	str	m	wk	3
21.1924 Mon.....	15.5	.....	dK0e	m	wk	.....	3
V853 Oph.....	12.5–14	1.5	dKe	str	m	.....	4
YY Ori.....	13.9–15.7	1.8	dK2e	m	wk	.....	5
YZ Ori.....	15.1–15.8	0.7	Late e	str	wk	m	6
AG Ori.....	14.2–15.6:	>1.4	Cont. e	str	m	.....	6
AM Ori.....	14.1–15.7	1.6	Cont. e	str	m	m	6
AR Ori.....	14.0–15.6	1.6	—e	str	m	.....	6
AZ Ori.....	13.0–15.8:	>2.8	dK3–5e	wk	.....	.....	6
EZ Ori.....	12.3–13.7	1.4	dGe	wk	wk	.....	6
GX Ori.....	14.1–15.2	1.1	dK3e	wk	.....	.....	2
KR Ori.....	13.5–14.9	1.4	K0e:	.....	m	wk	6
LN Ori.....	15.3–16.2	0.9	—e	wk	.....	.....	6
NY Ori.....	13.3–16	>2.7	Cont. e	m	wk	.....	6
V360 Ori.....	13.9–14.7	0.8	dGe	str	str	wk	5
MHα 265-5.....	15.2–16.6	1.4	dM0e	40	25	2	2
MHα 265-9.....	15.2–15.7	0.5	dK4e	5	15	.....	2
SV Sgr.....	13.5–16	>2.5	G5–K2e	wk	wk	.....	7
AA Tau.....	13.1–16.1	3.0	dM0e	40	25	4	2
CX Tau.....	14.5–15.3	0.8	dM1e	40	20	3	2
CY Tau.....	13.4–15.0	1.6	dM2e	20	10	2	2
CZ Tau.....	15.8–17.3	1.5	dM2e	2	20	2	2
DI Tau.....	14 –15	1	dM1e	2	15	2	2
DK Tau.....	12.4–14.9	2.5	dM0e	30	15	.....	2
DM Tau..	14.5–15.2	0.7	dK5e	40	15	3	2
DP Tau.....	13.7–15.4	1.7	dM0e	40	20	.....	2
DS Tau.....	12.1–13.6	1.5	dK4e	50	20	3	2

* The references are as follows:

1. Herbig (1954*a*).
2. Joy (1949).
3. Herbig (1954*c*).
4. Struve and Rudkjøbing (1949).
5. Haro and Herbig (1955).
6. Herbig (1950*b*).
7. Herbig (1957*b*).

ness resemble in some respects those of the flare stars. The photographic absolute magnitudes were estimated to be +8 to +9 or brighter, depending upon the corrections for interstellar absorption—values which are brighter by several magnitudes than those of the flare stars. To distinguish the two groups, Haro suggests the name "flash stars" for the new group.

Later observations by Haro and Terrazas (1954) and by Haro (1954) served to identify nine other stars of the Orion Nebula with variations of this type. Outbursts up to 2 mag. took place in 16–40 minutes, and the brightness returned to normal after a disturbance lasting about 100 minutes. The absolute magnitudes were about the same as those of the three flash stars first discovered.

In 1954, Haro and Chavira (1955) made a thorough search for flash stars in the Taurus region at $\alpha = 4^h29^m$, $\delta = +24°$. They found seven new variables of this class—one with spectral type M0 estimated by Herbig and by Kuiper from slit spectrograms, and six whose spectral types were estimated from Tonantzintla spectra in the red to be from M4 to M6. Feeble Hα emission appeared on a few exposures, and there was evidence of strengthened continuous background on some spectra. For these six stars the flares lasted only from 10

TABLE 4

SUBGROUP I*d:* FLASH STARS

Star	Magnitude	Range (mag.)	Normal Spec.	Time (Min.–Max.) (min.)	Duration of Flash (min.)	Reference*
V378 Ori	17.0–17.5	0.5	.....	20	.....	1
V379 Ori	15.2–16.2	1.0	.....	60	.....	1
OX Ori	15.5–16.1	0.6	.....	30	.....	1
V383 Ori	15.4–16.8	1.4	.....	31	.....	2
V384 Ori	14.0–15.1	1.1	dK6e	29	102	2
V385 Ori	14.1–15.5	1.4	.....	.....	.....	2
V386 Ori	15.9–17.3	1.4	dK6:	17	105	2
V389 Ori	14.2–16.3	2.1	dK6e	39	.....	2
V390 Ori	15.3–17.3	2.0	dK6e	28	104	2
V391 Ori	14.4–15.1	0.7	dK6e	16	90	2
— Ori	17.3	.....	—e	39	.....	3
V393 Ori	15.9–16.8	0.9	dK6e	39	111	3
EY Tau	15.5–16.5	1.0	dM5e	10	28	4
EZ Tau	15.7–17.4	1.7	dM5e	11	29	4
FF Tau	14.4–15.8	1.4	dM0	22	61	4
FG Tau	16.4–17.3	0.9	dM5	.....	10	4
FH Tau	14.8–15.9	1.1	dM5e	.....	21	4
FI Tau	16.3–17.5	1.2	dM5	.....	35	4
FK Tau	17.1–17.8	0.7	dM6e	.....	10	4

* The references are as follows:
1. Haro and Morgan (1953).
2. Haro and Terrazas (1954).
3. Haro (1954).
4. Haro and Chavira (1955).

to 35 minutes. In the duration of their outbursts and their spectral types, the Taurus flash stars bear a close resemblance to the late-type flare stars near the sun, although they lack the strong emission lines of H and Ca II. Data concerning the nineteen Haro flash stars are in Table 4. None are known to be components of close binary systems. Those in Taurus seem to have later types and shorter outbreaks.

Haro and Chavira also discovered for four flare stars and twelve flash stars that a marked correlation exists between the spectral type and the total time when the star was brighter than normal, the disturbance being of shorter duration in the cooler atmospheres.

§ 4. GENERAL CONSIDERATIONS OF VARIABLES IN NEBULOSITY

Among the many Hαe stars which have been found on red-sensitive plates with objective prisms or slitless spectrographs, many new variables will doubt-

TABLE 5

UNCLASSIFIED Hαe STARS IN NEBULOSITY

Number	Region	Reference*	Number	Region	Reference*
4.....	Oph, Sco	1	71.....	Tau, Ori	7
28.....	Oph, Sgr	2	16.....	(IC 348), Per	8
7.....	Tau, Ori	3	68.....	(NGC 2264), Mon	9
1.....	Ori	4	1.....	Ori	10
249.....	Ori	5	20.....	(IC 5070), Cyg	11
98.....	(IC 434), Ori	6	33.....	M8, M20, S188	12

* The references are as follows:
1. Struve and Rudkjøbing (1949).
2. Haro (1949).
3. Joy (1949).
4. Herbig (1950*b*).
5. Haro (1950, 1953).
6. Haro and Morena (1953).
7. Haro, Iriarte, and Chavira (1953).
8. Herbig (1954*b*).
9. Herbig (1954*c*).
10. Haro and Herbig (1955).
11. Herbig (1955).
12. Walker (1957), Herbig (1957*b*).

less be discovered. More than five hundred Hαe stars (Table 5) have been found in regions of dark or bright nebulosity. For most of these, no spectral type or variation of light has yet been determined. A few may be Be stars, but nearly all are probably of late type and belong to Group I*c*. The largest contributions of Hαe observations have been made by Haro at the Tonantzintla Observatory and by Herbig at the Lick Observatory. In many stars the intensity of Hαe varies greatly, and observations over a considerable period of time will be necessary for a complete survey.

Spectral types from B8 to M6 are represented among the variables involved in nebulosity. Many stars showing variation of this type have not yet revealed bright lines, but a majority of them have emission, and doubtless in many

others bright lines will eventually be found. Practically all the stars showing emission also show variation in total light when sufficiently observed. Bright lines originating in the surrounding nebula are sometimes superposed upon the stellar spectrum and cause uncertainty as to the spectrum of the star. The strongest lines originating in the nebula are those of H, He, Fe II, [S II], and [O II].

In general, the bright-line variables are imbedded in dark clouds of the Milky Way near the edges of heavily obscured areas; yet the stars are distinctly concentrated (Joy 1945, 1949; Greenstein 1948; Herbig 1952, 1954*c*) about certain points where the star density is ten to one hundred times as great as in the neighboring fields of stars. From this evident clustering of the bright-line stars, Ambartsumian (1949) was led to conclude that these stars had a definite genetic relationship and perhaps a common origin. He called them "T-associations." In succeeding years twenty-three such aggregations were identified (Kholopov 1955), some of which were believed to be recently formed. Some of the different associations have stars of certain spectral types or features which are characteristic of the particular group and differ from those of other groups. Differences in age may thus be indicated.

Efforts to explain the spectrographic behavior of the variables as the outcome of contact between the cloud particles and dwarf stars moving in from surrounding fields were only partially successful. The appearance of bright lines was attributed to dust or gas particles falling into the star's atmosphere under the influence of gravitation, modified by radiation pressure (Greenstein 1948). Greenstein (1950) also invoked the action of magnetic fields around the stars as a source of heat and energy.

While the idea that the T-associations were composed of extremely young stars was taking root, Herbig (1951) and Haro (1952) independently discovered three nebulous objects in Orion near NGC 1999 whose peculiar spectra seemed to indicate that they were nebulae actually in the process of forming stellar bodies. Four other objects of the same nature were found by Haro. Their spectra have strong nebular bright lines of [O I], [O II], and [S II], together with H and Ca II, but have only weak [O III], [Ne III], [Fe II], [N I], [N II], and Mg I, with a low-temperature continuous spectrum. Two components of one of these objects appeared in 1954 (Herbig 1957*c*), where no object brighter than nineteenth magnitude had shown on plates taken in 1947.

If the Herbig-Haro objects, although not yet stellar, are actually stars in the making, as they appear to be, the observations are of fundamental importance and reveal the direction that evolution is taking in regions of widespread dust clouds. The problem, then, is one of building up new stars from existing material rather than of interpreting the results of encounters of moving stars with the dust clouds. The larger numbers of cluster stars and their concentration in small areas, as well as the similarity between the individual stars, point to a common origin at a time in the not too distant past.

At first, the objects are diffuse and unstable. They could be easily affected by their immediate surroundings. The effects of particle size and magnetic fields (Greenstein 1937, 1948, 1950) would be important in their development, but gravity and radiation pressure would have little effect in small cool masses. It is not unlikely that rotation or turbulence in these bodies might result and would remain to produce widened absorption lines at later epochs in the history of the stars as they contract in their evolutionary course toward the main sequence. Wide lines were noted on high-dispersion spectra by Sanford (1947) in T Tau, by Herbig (1957*a*) for several stars of the group, by Walker (1956) for stars in NGC 2264, and by Bonsack and Greenstein (1960).

Herbig (1952) found that when the absolute magnitudes of the variables of the Taurus and Orion clouds were plotted in a Hertzsprung-Russell diagram, the stars of the lowest luminosity and latest spectral type fell to the right and above the main sequence. In NGC 2264 and NGC 6530 the same result was found by Walker (1956, 1957). The displacement was definite, amounting to 2.5 mag. for dM2e stars. In explanation of this marked discrepancy Walker suggests that these stars, as Salpeter (1953) had inferred from theoretical considerations, had recently been formed and that, in the course of their gravitational contraction from their prestellar form, they had not yet reached their place on the main sequence. This conclusion is an important reason for believing that the stars involved in nebulosity are young stars.

The problem of the interaction between stars and dust clouds is still largely unsolved, but the part played by magnetic fields, first considered by Greenstein (1950), is important. If the gases are ionized and magnetic fields are brought in, sources of energy become available for the production of bright lines in the atmosphere and for the triggering of subatomic reactions which may result in flares or an enhancement of the violet continuum (Greenstein 1957).

§ 5. SPECTRAL PECULIARITIES OF STARS IN NEBULOSITY

The G-type variables at maximum light show the largest number of emission lines. In RU Lup, RW Aur, UZ Tau, and XZ Tau more than one hundred emission lines were measured and identified. The lines of H, Ca II, Fe II, Fe I, Ca I, Ti II, Sr II, and [S II] attain the greatest strength and closely resemble the lines of the chromosphere in the sun. Sanford (1947) found on coudé plates that the emission lines of T Tau had a mean displacement of -5 km/sec as compared with the absorption lines, indicating origin in a rising layer in the star's atmosphere. These bright lines have a width of about 3 A.

The extraordinary intensity of the lines λ 4063.6 A and λ 4132.0 A from the $y^3F_3^o$ upper level of the iron multiplet 43 is unique in the T Tauri stars and furnishes a striking example of fluorescence in stellar atmospheres. Herbig (1945) has explained the effect by the supply of energy from the strong H (Ca II) emission line to the Fe I line λ 3969.3 A, which is also a member of multiplet 43 and has the same upper level, as a means of overpopulating that level. The lines of the multiplet arising from other levels are not greatly affected.

The stars in the heads of variable cometary nebulae deserve special attention because of the connection between their formation and evolutionary processes. The classical examples of such objects are R Mon in NGC 2261, R CrA in NGC 6729, and RY Tau south of Barnard 214. The stars are so closely enveloped in the bright nebulous material at the apex of the fan that they can seldom be seen separately. Their spectroscopic absolute magnitudes seem to be somewhat brighter than other T Tauri stars. Light-variations are complicated by the presence of nebulosity, which reflects and obscures some of the light of the star. Emission lines are few, and the spectral types range from A0 to G0. Whether the nebula is formed by the star from ejected gases and from surrounding nebulosity or whether the star is receiving infalling material from the tail is not known. Continuous activity is definitely present.

The type star T Tauri with its accompanying nebula NGC 1555 (Joy 1945; Herbig 1950*a*, 1953, 1957*c*) resembles the variables in the cometary nebulae in many respects. Its dG5e spectrum and its low luminosity are normal for T Tauri stars, although the light-variations are erratic. T Tauri also has a small envelope of bright nebulosity whose low-excitation spectrum is quite similar to those of the fifteen Herbig-Haro objects now known (Herbig 1951, 1957*c*).

Mount Wilson spectrograms of the T Tauri variables (Joy 1945) show evidence of veiling by continuous emission and excessive intensity of the ultraviolet continuum on certain plates of RW Aur, UY Aur, S CrA, T Tau, UZ Tau, and XZ Tau. A similar effect was noticed in seventeen of the bright-line stars of the Taurus clouds (Joy 1949). The phenomenon occurred in a larger proportion of the Ge and Ke stars than in the M types. One of the most striking examples of strong continuum in stars of this group is DD Tau (MHα 259-6s), which was also observed by Struve and Swings (1948) as star A of the luminous nebula B 10. DD Tau has a companion CZ Tau (distant 30″, dM3e) which is about 1 mag. fainter but lacks the ultraviolet excess radiation. A similar visual pair is composed of DH Tau (MHα 259-9n) and DI Tau (MHα 259-9s), both of type M0 and equal in brightness. Here, again, one showed a strong ultraviolet excess, whereas the other had a normal spectrum. The occurrence of excess ultraviolet energy output in one of the stars but not in the other of these two pairs and also in UZ Tau indicates that the origin of the disturbance is within the stars themselves rather than the result of contact with outlying clouds of dust or gas. This conclusion is also reached by Ambartsumian (1954) in his study of the veiling and excess ultraviolet radiation in flare stars.

Haro and Herbig (1955) investigated this significant outbreak of continuous radiation in stars of the Orion Nebula and NGC 2264 by means of direct photographs and selected filters which separated the yellow, blue, and ultraviolet regions from the remainder of the light of the star. In 16 per cent of the 175 Hαe stars of the Orion Nebula and 19 per cent of the 73 Hαe stars of NGC 2264, strengthened ultraviolet images showed at the time of the observations. The ultraviolet excess was found only in stars with medium to strong bright lines, but it has not always been present at the time of observation in *all* stars with

strong bright lines. Strong Ca II and Balmer lines with a slow decrement shortward usually accompanied the enhanced ultraviolet continuum. Since the light of the star and the intensity of the bright lines and continuum are all variable, simultaneous observations of these quantities are needed to correlate them completely.

Haro and Herbig found that in many of these stars the intensity of the enhanced continuum at different wave lengths did not correspond exclusively to that of a hot source or to that of a late-type star. Shortward of λ 3800 A the distribution of energy in the spectrum was peculiar. Near λ 3750 A the intensity rose and at about λ 3700 A reached a maximum, falling off slowly as far as λ 3500 A.

In search of a cause for this peculiar distribution of intensity, they found that the ultraviolet was too strong to be explained by a hydrogen continuous emission if the emitting layers were optically thin. If, however, the layers are thick, Böhm (1957) concludes that a maximum intensity at a wave length not far from the Balmer limit may result from strong hydrogen emission. Ambartsumian (1954; 1957) believes that the liberation of large amounts of energy, both thermal and non-thermal, in the outer layers of the chromosphere may result from unknown nuclear processes that are initiated by the transfer of unstabilized matter being brought up from the interior of these youthful stars.

Little is known about the length of time that the ultraviolet excess is maintained in the T Tauri stars, but the general impression prevails that the outburst may continue more or less indefinitely for weeks or months. It is not certain how the excess is correlated with the large irregular light-variations of the star, which, in RW Aur at least, are accompanied by changes in temperature and color (Herbig 1948).

§ 6. GROUP II: THE SPECTRA OF UV CETI FLARE STARS

Remarkable sporadic outbursts of total brightness have been observed in a few nearby stars of the lowest intrinsic luminosity and latest spectral type, showing exceptionally strong emission lines. In such flares the intensity of radiation is increased manyfold, especially in the ultraviolet region. At the time of these outbursts the light-curve rises to maximum in a few seconds or minutes of time and declines to normal in less than a half-hour.

At normal brightness the spectra of the twenty stars which have exhibited behavior of this kind are like those of extremely faint M-type dwarfs, which usually have strong, narrow emission lines of H and Ca II. The number of known stars in each subtype are: one M0, one M1, three M3, eight M4, five M5, one M6, and one unknown. Weak He I lines are sometimes seen. At the time of outbursts the bright lines of hydrogen become wider and stronger. The absorption M-type spectrum, especially in the regions shortward of λ 4200 A, may be veiled by a continuous spectrum.

Neither the frequency nor the cause of the flares is known. UV Cet seems to be the most active star both in the intensity and in the number of flares observed. It is the fainter component of a visual double star whose luminosity is among the faintest of the group. More than thirty flares of this star have been observed in the last 28 years. The average increase in brightness is about 2.5 mag. Accurate photoelectric light-curves indicate that a tenfold increase in the total light of the star may take place in only a few seconds of time and that the star declines to normal in 3–6 minutes (Roques 1953). The behavior of the other stars of the group may be somewhat different, but it seems clear that the general features are much the same in all.

The principal data concerning stars for which flares have been suspected or definitely observed are in Table 6. In some stars the outburst was recognized by direct photographic or visual estimates (D, in eighth col.), while for others the observations were photoelectric (Pe), and for some the flare was indicated by

TABLE 6

UV CETI FLARE STARS

Star and Constellation	Catalogue	Normal (Mag.$_v$)	Max. Range (Mag.)	Spec.	M_v	Trig. Par.	Flare Obs.	References*
Gr. 34 B—And...	+43°44 B	11.0	.....	dM4e	+13.1	0".28	Sp	Unpub.
vB. star—Aql...	+4°4048 B	17.9	.....	dM5e	+19.0	.17	Sp	1
YZ CMi...	Ross 882	11.8	1.4	dM4.5e	+12.4	.15	D, Sp	2
DH Car...	— B	12.2	1.8	.....	.....	.....	D	3
Wolf 47—Cas...	20C 70(B)	13.7	.....	dM5e	+13.9	.11	Pe, Sp	4
V645 Cen...	20C 861(C)	13.4	1.0	dM4e	+15.4	.76	Sp, D	5
DO Cep...	20C 1366 B	11.3	1.2	dM4.5e	+13.4	.25	D, Sp	6
UV Cet...	L726-8 B	12.4	5.6	dM5.5e	+16.1	.37	Sp, D, Pe	7
Wolf 1130—Cyg...	20C 1191 AB	11.9	.....	dM3e	+10.8	.06	D, Sp	8
Furj. 54—Cyg...	20C 1250 AB	12.2	.....	dM3e	+11.5	.07	Sp	9
—Dra...	+55°1823	10.1	0.5	dM1.5e	+ 8.5	.05	D	10
GC25394—Dra...	HD 234677	8.6	.....	dM0e	.....	.....	Sp	11
EV Lac..	20C 1382	10.2	2:	dM4.5e	+11.8	.20	D	12
AD Leo...	20C 574 AB	9.4	0.5	dM4e	+10.9	.21	Pe	13
Wolf 359—Leo...	20C 600	13.5	1	dM6e	+16.5	.40	D	14
—Mic...	HD 196982 B	11.1	.....	dM4.5e	+11.4	.11	Sp	15
V371 Ori....	Wachmann AB	11.7	1.9	dM3e	.....	.....	Sp, D	16
EQ Peg...	+19°5116 B	12.8	0.5	dM5.5e	+13.6	.14	Pe, Sp	17
V1216 Sgr....	20C 1108	10.5	0.4	dM4.5e	+13.3	.35	Pe, Sp	18
WX UMa..	20C 606 B	14.8	1.8	dM5.5e	+16.0	0.17	D	19

* The references are as follows:

1. Herbig (1956).
2. Van Maanen (1945); Joy (1957).
3. Hertzsprung (1924).
4. Johnson and Morgan (1953); Bidelman (1954).
5. Thackeray (1950); Shapley (1951).
6. Van de Kamp and Lippincott (1951); Joy (1957).
7. Joy and Humason (1949); Luyten (1949); Roques (1953).
8. Sandig (1951); Joy (1947).
9. Luyten (1925).
10. Petit (1954).
11. Popper (1953).
12. Wagman (1953).
13. Gordon and Kron (1949).
14. Sandig (1951).
15. Luyten (1926); Joy (1957).
16. Wachmann (1939); Hoffleit (1952).
17. Roques (1954); Joy (1957).
18. Kron, Gascoigne and White (1957); Joy (1957).
19. Van Maanen (1940).

characteristic changes in the hydrogen emission lines and continuous background of their spectra (Sp).

The trigonometric parallaxes (seventh col.) of seventeen of these stars indicate that all are within 20 parsecs of the sun, and seven are closer than 5 parsecs. Their visual absolute magnitudes (sixth col.) average +13.1, and they are among the faintest stars known.

Of the twenty flare stars of Table 6, fourteen are known binaries. Two of these (Wolf 1130 and V371 Ori) are spectroscopic binaries, and two (20C 1250 and AD Leo) have visual separations less than 1 second of arc, so that the variable component has not yet been identified. Of the remaining visual pairs, the fainter component is, without exception, the unstable star. Five of these are wide pairs whose separations are so great that little interaction between the components would be expected.

A spectrogram of UV Cet (Pl. IV), which by chance covered the time of a large flare, was obtained with the 100-inch telescope on Mount Wilson on September 25, 1948 (Joy and Humason 1949). On this plate, taken in poor seeing conditions, the combined normal spectrum of the two components of the visual pair was heavily veiled by the strong continuum of the flare. Only a trace of the TiO bands remained visible. The strong continuous spectrum which indicates a temperature of at least 10,000° K is accompanied by widened and strengthened emission lines of hydrogen and weak lines of He I and He II (λ 4686 A). The emission lines of Ca II, which normally are fairly strong, were only slightly strengthened.

This observation was repeated on October 7, 1957, after continuous observation of the star for 4 nights, when the spectrum of another flare was obtained. Although at the 1957 observation the flare was not so bright as in 1948, the general spectrographic behavior was duplicated, and good seeing conditions permitted the exposure to be definitely limited to the light of the fainter component of the pair. These two spectra may be assumed to be typical of the extremely rapid and violent outbursts of this star.

In no other star have the flare characteristics been observed with the outstanding intensity found in UV Cet. The most common effect of a flare on the star's spectrum is to widen and intensify the hydrogen emission lines. The decrement toward shorter wave lengths is slower, and the number of observable lines of the series is increased as in sources of higher temperature. The He I lines are also strengthened. The continuous emission of the flare source, especially in the λλ 4000–4200 A region, becomes strong enough in some stars to veil the M-type absorption lines and cause them to disappear or present a fuzzy look. The four flare stars—V645 Cen observed by Thackeray (1950), +4°4048 B by Herbig (1956), HD 234677 by Popper (1953), and +43°44 B by Joy (unpublished)—exhibited strong Balmer lines on occasions which are believed to have been flares, although in these stars the hydrogen emission lines are normally weak or absent. On account of the short duration of the flares, exposure times cannot usually be limited sufficiently to give pure flare spectra.

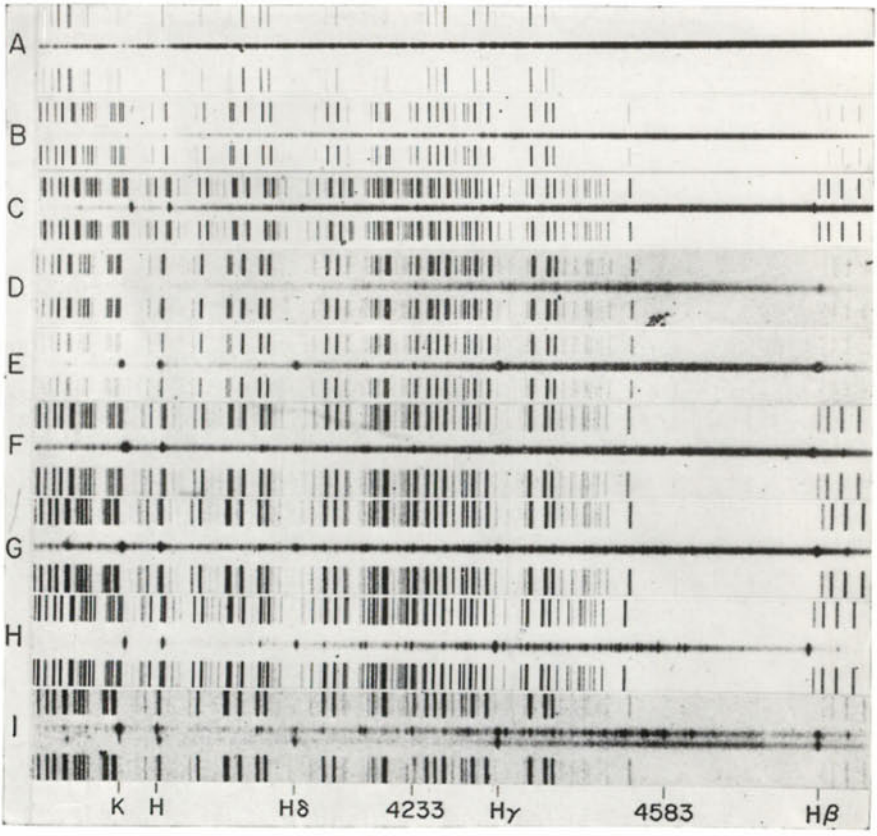


PLATE I.—Spectra of T Tauri variable stars. *A:* UX Tau; *B:* RY Tau; *C:* T Tau; *D:* R Mon; *E:* UY Aur; *F:* RW Aur; *G:* XZ Tau; *H:* RU Lup; *I:* UZ Tau with companion.

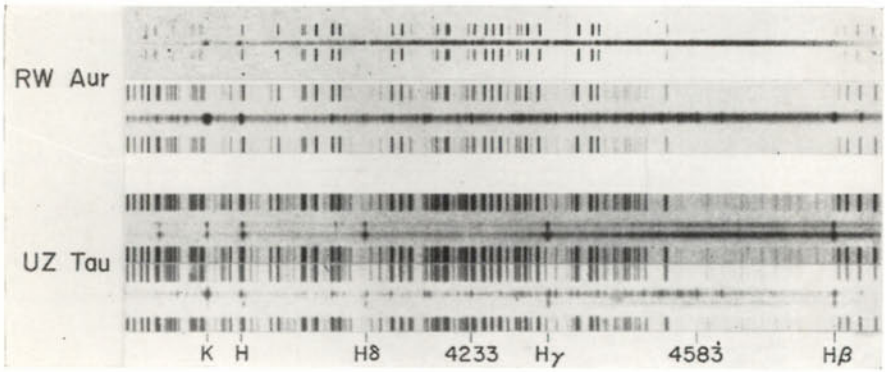


PLATE II.—Changes in the spectra of RW Aur (*above*) and of UZ Tau with companion (*below*).

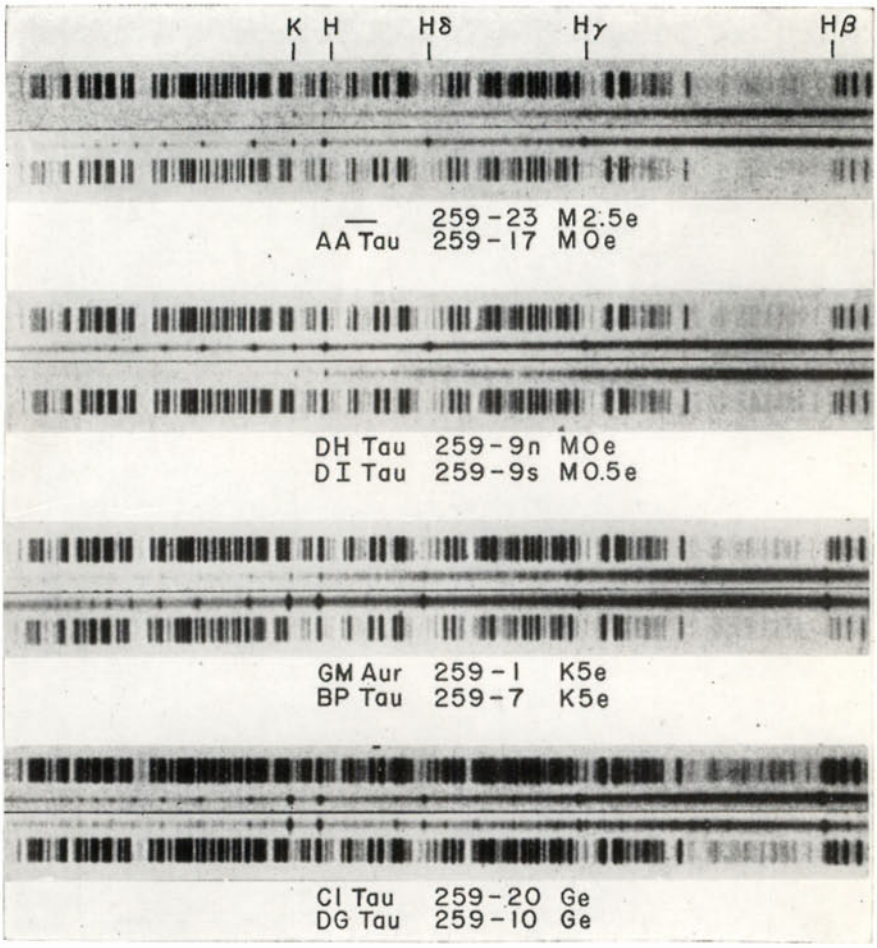


PLATE III.—Comparison of normal with veiled spectra of T Tauri variables of similar spectral types. AA Tau, DH Tau, BP Tau, and CI Tau are veiled and have stronger hydrogen lines.

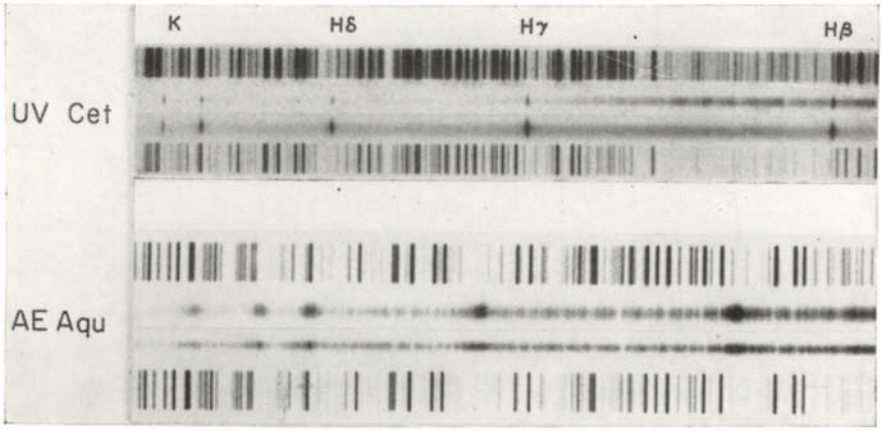


PLATE IV.—Normal and flare spectra of UV Ceti (*above*). Spectra of AE Aquarii (*below*) with absorption lines displaced toward short and toward long wave lengths. Narrow H and K emission lines go with the absorption lines, but wide emission lines have the opposite displacements.

The scarcity of observational material for the study of such stars is indicated by the fact that, for nearly half of them, only a single flare has been observed. For six stars the flares were recognized only by sudden increases in total light and for five stars only by strengthening of the emission lines of hydrogen, especially those lines of shorter wave lengths. Observations (of the same star but at different times) of *both* light and spectral changes which might be attributed to flarelike outbursts are available for nine stars.

From the results of photoelectric observations of a rapid flare of AD Leo, Gordon and Kron (1949) concluded that the outburst could be explained by intense heating of a relatively small area, less than 1 per cent of the star's surface, and involving only a small mass.

On the basis of sudden explosions and heating in a small area, the flares of UV Ceti stars may be accounted for by adjusting the parameters involved, but the underlying causes are unknown. In comparison with flares in disturbed regions of the sun, the times involved are much the same, but spectroscopically the two show considerable differences. The spectra of bright solar flares have narrow emission lines, chiefly of H, Ca II, He I, Na, and Fe II, but the continuous emission is usually too weak to be seen (Richardson and Minkowski 1939; Allen 1940). In general, the total energy output of a strong flare in the sun is less than that of a major flare of UV Ceti, although the brightest of them could increase the total light of a late-type star sufficiently to be observable (Greenstein 1950).

On account of the short-lived association of the T Tauri stars with the clouds of interstellar matter, Greenstein concluded that the location of the flare source must be in a circumstellar fringe or extended chromosphere and that the outburst might be the result of magnetic fields brought in from the interstellar surroundings. The very high abundance of lithium found by Bonsack and Greenstein (1960) and by Bonsack (unpublished) in a total of ten stars closely involved with dust clouds strongly suggests that surface nuclear reactions do occur. This general idea has recently been extended by Ambartsumian (1954, 1957) to account for the rapid action shown by the UV Ceti stars. Since it is obvious that the duration of the outburst is entirely too short to allow heat to flow from the interior of the star, it seems necessary to locate the origin of the flare in the upper atmosphere of the star. As the immediate cause of the outburst, he suggested nuclear reactions of a nature not yet clearly understood. Secondary local thermal effects may result and cause some of the observed changes in the spectrum. If we accept these ideas that nuclear reactions are actuated by eruptions of some kind from below and within the star, it is necessary, as pointed out by Haro (1954), to explain why similar explosive activities are generated in concentrated groups of T Tauri stars involved in interstellar clouds and likewise in UV Ceti and SS Cygni stars, which apparently have no connection with nebulosity. After the original formation of the star, how does the presence of surrounding gas and dust affect the behavior of the star?

§ 7. GROUP III: THE SPECTRA OF SS CYGNI STARS

Stars of the SS Cygni (U Geminorum) class are characterized by frequently repeated outbursts of 2–4 mag. The pattern of the light-curve is fairly definite, and the mean frequency of maxima is different for different stars, varying from 10 to 150 days. The duration of the enhanced light is usually several days. The rise to maximum takes place in about a day, and the peak of the curve is not sharp. The decline in brightness is slower.

Because of the faintness of the stars at minimum phase, which presumably is the normal state of the stars, few accurate photometric observations have been attempted, but evidently, if variation in total light is present, it is small and not easily detected.

In the Kukarkin-Parenago *General Catalogue of Variable Stars* and its eight supplements, only a hundred and two stars are listed as U Gem variables and fifteen as Z Cam stars. Spectrograms indicate that these two classes overlap. No distinguishing criteria for clearly separating the two classes have yet been devised; hence they are here treated as a single group.

Three limited surveys of the spectra of SS Cygni variables have been carried out, together with detailed investigation of five individual stars. Abbreviated results and references for the twenty-three stars observed spectroscopically appear in Table 7.

1. At Mount Wilson, Adams and Joy (1921) and Joy (1940) made observations of U Gem, X Leo, and SU UMa at maximum which showed continuous spectra without lines of any kind. SS Aur and SS Cyg had faint, wide absorption lines of hydrogen and helium, while RU Peg, RX And, Z Cam, and AB Dra had wide emission lines at the same phase. At minimum light, the spectra of SS Cyg and RU Peg showed bright lines, 20 A wide, of H and He, which, relative to the continuous spectrum, were much stronger than at maximum light. In addition, absorption spectra of type about dG5 were noted. Later, more extensive spectroscopic observations at this phase were undertaken for AE Aqr (Joy 1954), SS Cyg (Joy 1956), and RU Peg (unpublished). These three stars were found to be spectroscopic binaries, one component being a dwarf dG5–dK0 star with narrow absorption lines, the other being a hot subdwarf star with bright lines 15–25 A in width but no absorption lines.

2. At the McDonald Observatory in 1939–1941 Elvey and Babcock (1940, 1943) made a general survey of sixteen variables of the SS Cygni class at different phases and gave a comprehensive view of the spectroscopic behavior of stars of this class. The continuous spectrum at maximum light indicated a high-temperature source and bright λ 4686 He II was seen in SS Cyg and U Gem. At minimum, strong, wide bright H lines and a violet emission attributed to the Balmer hydrogen continuum were observed, as well as faint emission lines of Ca II (H and K) and He I. Measurements of the wide emission lines of SS Cyg indicated large variations in velocity. No emission lines appeared in spectra of AY Lyr even at minimum.

3. At Mount Wilson (1955–1956 unpublished), observations of the spectra of several SS Cygni variables were undertaken by Kraft with the chief purpose of finding additional stars with absorption spectra of dG type at minimum, similar to those of AE Aqr, SS Cyg, and RU Peg. He found that the spectra of some of the variables had both absorption and emission lines at minimum, while some had only continuous spectra and some had absorption lines with no bright lines, as Elvey and Babcock (1943) had found.

Detailed spectroscopic observations and studies of five stars of this class have also been made. Some of the most important results obtained follow.

TABLE 7

SS CYGNI VARIABLES

Star	Magnitude	Mean cycle (days)	Spectrum		References*
			At Max.	At Min.	
RX And....	10.3–13.6	14	Cont., br. H	Br. H, Ca II	1
AE Aqr.....	9.7–11.7	.....	.....	dK0e, br. H, Ca II	2
UU Aql.....	11.0–16.8	56	.....	Cont., br. H	3
SS Aur.....	10.5–14.5	54	Cont., br. H	.....	4
Z Cam....	10.2–13.4	23	Cont., abs. H, br. H, He II	Br. H, He, Ca II	1
SY Cnc....	10.9–13.8	50	Abs. H, ft. br. H	Br. H, He I, He II	5
SS Cyg....	8.2–12.1	50	Abs. H, br. He II	dG5e, br. H, He, Ca II	6
EY Cyg....	11.4–15.7	.....	.....	Cont.	7
AB Dra....	12.0–15.8	12	Cont., ft. br. H	.....	8
U Gem....	8.8–13.8	103	Cont., br. H, He II	Cont., br. H	1
AH Her....	10.9–14.7	20	.....	Cont., br. H	7
T Leo.....	15.4	.....	.....	Cont., br. H	9
X Leo.....	12.0–15.1	22	Cont., abs. H	.....	1
AY Lyr.....	12.6–16.0	23	.....	G, abs., no br.	10
CY Lyr.....	13.3–16.8	17	Cont., abs. H	.....	7
CN Ori.....	11.8–14.7	19	Cont., abs. H	.....	11
RU Peg.....	10.0–13.1	70	Cont., br. H, He	dG5e, br. H, He, Ca II	1
TZ Per.....	12.3–15.2	17	Cont.	Br., abs.	10
FO Per.....	13.8–16.2	11	.....	.....	9
UZ Ser.....	12.0–16.6	20	Cont., abs. H	.....	12
SU UMa...	11.1–14.5	16	Cont., br. H	Abs., br. H, He, Ca II	1
SW UMa...	10.8–16.5	450	Cont., br. Hβ, abs.	.....	13
TW Vir.....	11.8–16	25	.....	Br. H, He, Ca II	7

* The references are as follows:
1. Elvey and Babcock (1940, 1943); Joy (1940).
2. Joy (1954).
3. Elvey and Babcock (1940, 1943); Kraft (1956).
4. Elvey and Babcock (1943); Joy (1940).
5. Herbig (1950c); Kraft (1956).
6. Adams and Joy (1921); Elvey and Babcock (1940, 1943); Joy (1940, 1956); Hinderer (1949).
7. Elvey and Babcock (1943).
8. Joy (1940).
9. Kraft (1956).
10. Elvey and Babcock (1943); Kraft (1956).
11. Elvey and Babcock (1940, 1943).
12. Herbig (1944).
13. Wellmann (1952); Kraft (1956).

UZ Ser (*Herbig 1944*).—At maximum similar to SS Cyg; continuous with wide, shallow absorption lines of H and He I.

SY Cnc (*Herbig 1950c*).—At maximum, wide, shallow absorption lines of H and He I. Weak emission cores were seen within the wide absorption at Hβ and Hγ. At fainter magnitudes the Balmer series was strong in emission, and bright He I and He II appeared. Variations in velocity from bright and dark lines have also been measured (not published).

SW UMa (*Wellmann 1952*).—At maximum, wide, shallow H absorption lines, but Hβ showed faint emission.

AE Aqr (*Joy 1954*).—Maximum not observed. At minimum, the emission lines, 20 A wide, of H, He I, and Ca II are superposed upon a dK0 absorption spectrum whose lines are deep and only 1.5–2.0 A in width (Pl. IV). In this K0 spectrum, narrow bright H and Ca II lines sometimes occur. The measured radial velocities indicate two sources moving as components of a spectroscopic binary with a period of 0.70 day, velocity ranges of more than 300 km/sec, and nearly equal masses, about the same as that of the sun. The absolute magnitude of the K0 star is +6.0, and that of the small hot star with wide bright lines is slightly fainter. The bright lines of the hot component vary greatly in width, in intensity, and in their shortward decrement. These variations are accompanied by changes in the intensity of the continuous spectrum, especially in the shortward region. This component is probably a subdwarf with a diameter about 0.08 ⊙ and a temperature near that of an early B-type star. The variations may be due to pseudo-flares in this star. No eclipses have been discovered.

SS Cyg (*Adams and Joy 1921; Joy 1940, 1956; Elvey and Babcock 1940, 1943; Hinderer 1949*).—At maximum, the strong continuum of a hot source veils the broad, shallow absorption lines of H, He I, and Ca II. Emission of He II was reported by some observers at phases near maximum. At minimum, the wide emission lines of H, Ca II, and He I are strong, and a weak dG5 spectrum is measurable. As in AE Aqr, the component with absorption lines and that with wide emission lines compose a spectroscopic binary system whose orbital period is 0.276 day. The velocity ranges are each about 230 km/sec, indicating nearly equal masses somewhat smaller than that of the sun. Since no eclipses have been detected, the inclination of the orbit must be less than 50°, and we may conclude if $R_1 = 0.9$ ⊙ and $R_2 = 0.15$ ⊙, that the distance between the surfaces of the two stars is probably of the same order of magnitude as that between the earth and the moon. Consequently, large disturbing effects of one star upon the other may be expected.

The general problem of the SS Cygni stars is so complicated that little progress has been made toward its solution. The spectrograph has made a distinct contribution in confirming the low luminosity of the stars and revealing the normal spectral types of a few of the brighter members of the group. Velocity measures of four of the stars seem to indicate that they are binaries, composed of a dwarf G-type star and a hot subdwarf companion with wide emission lines

of H, Ca II, and He. The components have about the same masses. The periods of only two have been determined, but they are constant over the interval in which they have been observed.

On the other hand, the photometric observations present no corresponding regularities. Spectroscopically, AE Aqr seems definitely a member of the group, but its unceasing light-variations do not follow the characteristic pattern found in many of the stars of this class. At times, the ultraviolet continuum is considerably enhanced. AE Aqr may be intermediate between the SS Cygni and T Tauri classes in physical behavior.

The differences in the spectra of different stars of the group at minimum can probably be attributed to differences in the relative brightness of the two components and the extent of the envelope of the hot star.

No satisfactory explanation of the nova-like outbursts which occur at semi-regular intervals in the variable stars of this class has been proposed, and their relationship to other groups has yet to be determined.

REFERENCES

ADAMS, W. S., and JOY, A. H.	1921	*Pub. A.A.S.*, **4**, 305.
ALLEN, C. W.	1940	*M.N.*, **100**, 635.
AMBARTSUMIAN, V. A.	1949	*Astr. J. U.S.S.R.*, **26**, 8.
	1954	*Comm. Burakan Obs.*, No. 13.
	1957	*The Non-stable Stars;* A symposium at Burakan (Erevan), pp. 9 and 70.
BIDELMAN, W. P.	1954	*Ap. J. Suppl.*, **1**, 214.
BÖHM, K. H.	1957	*Zs. f. Ap.*, **43**, 245.
BONSACK, W. K., and GREENSTEIN, J. L.	1960	*Ap. J.*, **131**, 83.
ELVEY, C. T., and BABCOCK, H. W.	1940	*Pub. A.A.S.*, **10**, 51.
	1943	*Ap. J.*, **97**, 412.
ENEBO, S.	1907	*A.N.*, **175**, 205.
GAPOSCHKIN, S.	1937	*Harvard Ann.*, **105**, 516.
GORDON, K., and KRON, G. E.	1949	*Pub. A.S.P.*, **61**, 210.
GREENSTEIN, J. L.	1937	*Ap. J.*, **85**, 242.
	1948	*Harvard Mono.*, No. 7, p. 19.
	1950	*Pub. A.S.P.*, **62**, 156.
	1957	*Non-stable Stars*, Symposium at Bjurakan (Erevan), p. 104.
GREENSTEIN, J. L., and STRUVE, O.	1946	*Pub. A.S.P.*, **58**, 366.
HARO, G.	1949	*A.J.*, **54**, 188.
	1950	*Ibid.*, **55**, 72.
	1952	*Ap. J.*, **115**, 572.
	1953	*Ibid.*, **117**, 73.
	1954	*Bol. Obs. Tonantzintla*, No. 11, p. 11.

HARO, G., and CHAVIRA, E.	1955	*Bol. Obs. Tonantzintla*, No. 12, p. 3.
HARO, G., and HERBIG, G. H.	1955	*Bol. Obs. Tonantzintla*, No. 12, p. 33.
HARO, G., IRIARTE, B., and CHAVIRA, E.	1953	*Bol. Obs. Tonantzintla*, No. 8. p. 3.
HARO, G., and MORENA, A.	1953	*Bol. Obs. Tonantzintla*, No. 7, p. 11.
HARO, G., and MORGAN, W. W.	1953	*Ap. J.*, **118**, 16.
HARO, G., and TERRAZAS, L. R.	1954	*Bol. Obs. Tonantzintla*, No. 10, p. 3.
HERBIG, G. H.	1944	*Pub. A.S.P.*, **56**, 230.
	1945	*Ibid.*, **57**, 166.
	1946	*Ibid.*, **58**, 163.
	1948	*Ibid.*, **60**, 256.
	1950*a*	*Ap. J.*, **111**, 11.
	1950*b*	*Ibid.*, p. 15.
	1950*c*	*Pub. A.S.P.*, **62**, 211.
	1951	*Ap. J.*, **113**, 697.
	1952	*J.R.A.S. Canada*, **46**, 222.
	1953	*Leaflet A.S.P.*, No. 293.
	1954*a*	*Trans. I.A.U.*, **8**, 805.
	1954*b*	*Pub. A.S.P.*, **66**, 19.
	1954*c*	*Ap. J.*, **119**, 483.
	1955	*A.J.*, **60**, 283.
	1956	*Pub. A.S.P.*, **68**, 531.
	1957*a*	*Ap. J.*, **125**, 612.
	1957*b*	*Ibid.*, p. 654.
	1957*c*	*Non-stable Stars*, ed. G. H. HERBIG (Cambridge: Cambridge University Press), p. 3.
HERTZSPRUNG, E.	1924	*B.A.N.*, **2**, 87.
HINDERER, F.	1949	*A.N.*, **277**, 193.
HOFFLEIT, D.	1952	*Harvard Bull.*, No. 921, p. 5.
HOFFMEISTER, C.	1949	*A.N.*, **278**, 24.
HUNGER, G. E., and KRON, G. E.	1957	*Pub. A.S.P.*, **69**, 347.
JOHNSON, H. L., and MORGAN, W. W.	1953	*Ap. J.*, **117**, 323.
JOY, A. H.	1940	*Pub. A.S.P.*, **52**, 324.
	1942	*Ibid.*, **54**, 33.
	1943	*Ibid.*, **55**, 38.
	1945	*Ap. J.*, **102**, 168.
	1947	*Ibid.*, **105**, 101.
	1949	*Ibid.*, **110**, 424.
	1954	*Ibid.*, **120**, 377.
	1956	*Ibid.*, **124**, 317.
	1957	*Non-stable Stars*, ed. G. H. HERBIG (Cambridge: Cambridge University Press), p. 31.

JOY, A. H., and HUMASON, M. L.	1949	*Pub. A.S.P.*, **61,** 133.
KHOLOPOV, P. K.	1951	*Variable Stars*, **8,** 83.
	1955	*Trans. 4th Conference on Problems of Cosmogony* (Moscow), p. 375.
KRAFT, R. P.	1956	Unpublished.
KRON, G. E., GASCOIGNE, S. C. B., and WHITE, H. S.	1957	*A.J.*, **62,** 214.
LUYTEN, W. J.	1925	*Harvard Bull.*, No. 830.
	1926	*Ibid.*, No. 835.
	1949	*Ap. J.*, **109,** 532.
MERRILL, P. W., and BURWELL, C. G.	1933	*Ap. J.*, **77,** 103.
	1950	*Ibid.*, **112,** 72.
PETIT, M.	1954	*Ciel et Terre*, **70,** 407.
PICKERING, E. C. (LEAVITT, H.)	1904	*Harvard Circ.*, No. 86.
POPPER, D. M.	1953	*Pub. A.S.P.*, **65,** 278.
RICHARDSON, R. S., and MINKOWSKI, R.	1939	*Ap. J.*, **89,** 347.
ROQUES, P.	1953	*Pub. A.S.P.*, **65,** 19.
	1954	*Ibid.*, **66,** 256.
SALPETER, E. E.	1953	*Les Processus Nucléaires dans les Astres, Liège*, p. 116.
SANDIG, K.	1951	*A.N.*, **280,** 40.
SANFORD, R. F.	1947	*Pub. A.S.P.*, **59,** 134.
SHAPLEY, H.	1919	*Ap. J.*, **49,** 260.
	1924	*Harvard Circ.*, No. 254.
	1951	*Proc. Nat. Acad. Sci.*, **37,** 15.
STRUVE, O., and RUDKJØBING, M.	1949	*Ap. J.*, **109,** 92.
STRUVE, O., and SWINGS, P.	1948	*Pub. A.S.P.*, **60,** 61.
THACKERAY, A. D.	1950	*M.N.*, **110,** 45.
TRUMPLER, R. J.	1931	*Pub. A.S.P.*, **43,** 256.
VAN DE KAMP, P., and LIPPINCOTT, S. L.	1951	*Pub. A.S.P.*, **63,** 141.
VAN MAANEN, A.	1940	*Ap. J.*, **91,** 503.
	1945	*Pub. A.S.P.*, **57,** 216.
WACHMANN, A. A.	1939	*Beob.-Zirk. A.N.*, **21,** 25.
WAGMAN, N. E.	1953	*Harvard Ann. Card*, No. 1225.
WALKER, M. F.	1956	*Ap. J. Suppl.*, **2,** 365.
	1957	*Ap. J.*, **125,** 636.
WELLMANN, P.	1952	*Zs. f. Ap.*, **31,** 123.
WOLF, M.	1901	*A.N.*, **157,** 81.
	1903	*Ibid.*, **163,** 161.

CHAPTER 19

Spectra of Stars below the Main Sequence

JESSE L. GREENSTEIN
Mount Wilson and Palomar Observatories
Carnegie Institution of Washington, California Institute of Technology

§ 1. INTRODUCTION

For a long time the existence of various types of subluminous stars has been known, and some spectroscopic data have been accumulated. In addition to the white dwarfs, a "blue-white sequence" (Vorontsov-Velyaminov 1953) has been known to contain various types of hot stars located at various distances below the main sequence. With increasing knowledge of the color-magnitude diagrams of the globular clusters (Arp 1955) and from spectroscopic investigations it became clear that population II contains (1) blue stars on the horizontal branch, extending downward and to the left toward the very hot subdwarfs; (2) slightly subluminous stars below the main sequence at types O and B; (3) nuclei of planetary nebulae; (4) pre- and postnovae; (5) F, G, and K subdwarfs; (6) dwarf symbiotic stars like SS Cygni; and (7) white dwarfs. In population I much less is known about subluminous stars, and their recognition or classification is much less complete; white dwarfs certainly occur in population I, and some hot subdwarfs may also be found. It is clear that intermediate stages prior to the white dwarf stage must exist; we know remarkably little about evolution in population I after the red giants. Vorontsov-Velyaminov (1953, chaps. v, vi, vii, and ix) gives a general review of data and interpretation of several of the types of stars described here spectroscopically.

The extreme weak-line F and G subdwarfs have been the most extensively studied; thus my discussion will be correspondingly short. The other groups of stars are very little known spectroscopically and deserve further spectroscopic and astrometric attention. Figure 1 shows a schematic HR diagram to provide orientation as to the location of different types of stars under discussion. Our

information on luminosities is extraordinarily slight; the variety and uncertainty of the temperatures found for the hot stars are such that the old novae and hot subdwarfs can be only approximately located. The luminosities of the white dwarfs are better known and will be discussed later.

§ 2. SPECTRA OF OLD NOVAE

The pioneer observations of the spectra of sixteen nova remnants by Humason (1938) showed some weak emission lines on an intrinsically very blue continuous spectrum. His spectra had a scale of 500 A/mm at Hγ and were only

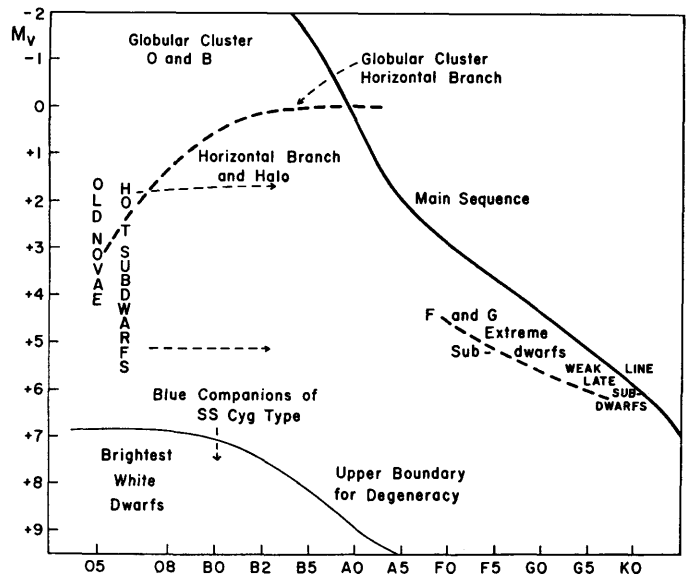


FIG. 1.—Schematic HR diagram showing the location of various types of subluminous stars. Heavy-dashed line represents the blue stars in M13. As the light-dashed arrows show, the hot subdwarfs may occupy considerable intervals in luminosity and spectral type. Stars below the degeneracy boundary will be at least partly degenerate.

slightly widened. Important questions remained unanswered, such as whether the complex emission structure persists after the nova shell has disappeared, whether absorption lines exist, and whether there is postnova activity. If the entire outburst can be viewed as a single event with a short time scale, the density of the ejected shell should decrease as $1/t^3$ and the emission measure as $1/t^5$. Consequently, the old postnova should have the spectrum of a small hot star, possibly with broad absorption lines if the atmosphere is disturbed. If small continued mass loss occurs, emission lines or Be-type absorption phenomena may be expected.

The luminosities of the pre- and postnova are essentially the same. Walker (1957) discovered rapid variations in light and color at minimum, which indi-

cate small instabilities and "hot spots" and suggest that gaseous ejection may continue. Even the oldest, nova (V481) Oph 1848, showed appreciable variation, and Nova Q Cyg 1876 varied by 0.30 mag. in 10 minutes. Whether very old novae vary and whether their spectra show emission lines are unknown. MacRae $+43°1$ shows rapid variations and a typical old-nova spectrum (Greenstein 1954*a*), although not observed as a nova in modern astronomical history. A program of reobservation of old novae with widened spectra at 180 A/mm is being carried out by Greenstein with the nebular spectrograph at Palomar. Table 1 contains a résumé of observations by Humason, Greenstein, McLaughlin (1953), and others on the spectra of novae and nova-like stars. The photoelectric colors and magnitudes by Walker and the spectroscopic appearance establish, for those classical old novae which lack red companions, (1) extreme strength in the ultraviolet except for space reddening; (2) absence of strong absorption lines; (3) absence of Balmer continuous absorption; (4) presence of weak postnova emission, usually of high excitation; (5) no emission lines sufficiently strong to produce appreciable Balmer emission continuum (except possibly DQ Her); and (6) disappearance of the detailed emission-line structure, which seems to be connected with the shell.

The location of the bluest old novae in the $B - V$, $U - B$ diagram is very close to that of the bluest white dwarfs, i.e., nearly where a black-body continuum would lie at very high color temperature. The redder novae lie on or near the space-reddening line. Thus colorimetrically we expect, as is observed, that spectra will not show strong hydrogen lines or continua, either in absorption or in emission. Whether the yellowish colors of many novae are intrinsic or caused by space reddening is not yet clear. No trace of lines of a late-type companion is found even in so red an object as GK Per; thus duplicity cannot be suspected, although it is common among the nova-like symbiotic objects and the U Gem stars.

General reviews of nova light-curves, spectra near maximum, and luminosities are given by McLaughlin, in this volume, and by Payne-Gaposchkin (1957). McLaughlin (1953) discusses the early postmaximum spectra of some of the objects in Table 1 from plates by Humason. Luminosities of old novae can be obtained from the size of the shell and the expansion velocities, as well as by various indirect methods. The absolute magnitudes at minimum are in the range $+2$ to $+6$. The symbiotic and nova-like stars will not be discussed here, in view of the possible effects of duplicity. EM Cyg and V Sge might be related to the U Gem stars, while the composite objects like T CrB or RS Oph provide completely different types of problems from those of the classical novae. While the duplicity of DQ Her suggests that duplicity is important in some classical novae, the interaction occurring at present is between two small, and presumably dense, stars rather than between a small star and an unstable large star, or red giant, as in AE Aqr and T CrB.

In the "classical" old nova we find a blue continuous spectrum with weak superposed emission lines of He II, H and He I. Not too long after the explosion, the shell has dissipated, leaving behind a somewhat unstable hot star. (If, in fact, some old novae are intrinsically red, it is possible that phenomena in an opaque extended envelope are responsible, rather than that there is no hot object in the system.) The star continues to eject gas and to excite a weak small, circumstellar emission region. The velocities of postnovae ejection are generally small, with line widths from 300 to 1000 km/sec (see Table 2). The

TABLE 1*

CHARACTERISTICS OF THE SPECTRA OF OLD NOVAE

Nova	Spectrum and Other Data
V603 Aql 1918.....	H>He II (Hu 1938; Mc 1950; and G 1957); He I, λ 4650 A present; $\Delta\lambda=7$ A; no absorption lines at 18 A/mm
T Aur 1891.....	Weak He II>H (Hu 1933, 1937)
T CrB 1866, 1946.....	Symbiotic, red companion, spec. binary; dwarf blue object is nova; recurrent U?
Q Cyg 1876.....	Em. weak (Hu 1936); sharp and weak (G 1957)
V476 Cyg 1920.....	H=He II (Hu 1936, Mc 1938); H>He II, broad (G 1958)
EM Cyg.....	H>He II, broad (Burbidge); never seen at bright max; U?
DM Gem 1903....	Continuous? (Hu 1933)
DN Gem 1912....	H weak (Hu 1933); He II=H (Mc 1933); He II broad>H (G 1958)
DQ Her 1934.....	He II>H, broad, $\Delta\lambda=20$ A, double em. lines (G 1956); variable in 4^{hr} period (Kraft); ratio of high–low series members changes at quadratures; eclipsing binary; shell still contributes
DI Lac 1910.....	Continuous (Hu 1936); broad absorption lines, like white dwarf, emission H>He II, sharp (G 1959)
HR Lyr 1919.....	Continuous (Hu 1936); weak He II (G 1959)
MacRae +43°1.....	H>He I, variable ratio to continuum; $\Delta\lambda=7$ A (G 1953); never seen at bright maximum
V841 Oph 1848.....	Continuous (Hu 1936); He II>>H, He I weak (G 1956); lines sharp
RS Oph 1898, 1933, 1958....	Symbiotic red star; complex em.; atypical; recurrent
GK Per 1901.....	He II>H, He I, $\Delta\lambda=16$ A (Hu 1937); H>He II, He II=He I; $\Delta\lambda=17$ A (G 1953)
CP Pup 1942.....	He II>>H, He I weak; [O III] persists in shell and shows original ejection velocities still present (G 1956); velocity structure absent in H and He II
T Pyx 1890, 1902, 1920, 1944.....	He II>H, [O III] (Hu 1934); He II>>H, sharp (G 1956, 1958)
V Sge.....	He II>H, V/R variable; $\Delta\lambda=40$ A; shortward-displaced core (Elvey and Babcock); never seen at bright maximum; (U?)
WZ Sge 1913, 1946	Continuous (Hu 1934); white dwarf absorption lines; Be type, H emission (G 1956)
V1017 Sgr 1901, 1919.....	Continuous (Hu 1936)

* G = Greenstein; Hu = Humason; Mc = McLaughlin. Dates given are those of observations of spectra. U? = Object may be related to U Gem stars or other nova-like stars; $\Delta\lambda$ = width of emission lines at half-intensity.

velocities are small compared with those during the nova outburst phase, 1000–5000 km/sec. The velocity of escape may be estimated from

$$v_{esc} = 620 \left(\frac{M}{R}\right)^{1/2} \text{km/sec}. \quad (1)$$

The mass is probably near that of the sun, the radius intermediate between normal stars and white dwarfs, i.e., $M = 1\ \odot$, $R = 0.1\ \odot$. Therefore, $v_{esc} =$ 2000 km/sec, large compared to the observed line widths, except for DQ Her (a double) and WZ Sge (a white dwarf). Since the lines are absolutely weak compared with a Be star, we may conclude that only small amounts of gas are involved in either an extended chromosphere or a field of prominences. Magnetohydrodynamic forces may be required to support this envelope to a distance large compared to R, in which case postnova ejection with such a reduced velocity of escape would result in a continued, but small, loss of mass.

The level of excitation of permitted lines in a planetary nebula or a diffuse nebula near a hot O star resembles that in the old novae. Absence of forbidden lines points to a smaller and denser emitting region, and the absolute intensity of the lines is also small. For example, if the star Nova GK Per (1901) has a visual luminosity at minimum, corrected for absorption, of +4, the observed strength of Hβ corresponds to an emission of 4×10^{31} ergs/sec. The luminosity of Hβ in the planetary nebula NGC 7027 is about 2×10^{34} ergs/sec, or a probable ratio of flux of 500. However, the central star in NGC 7027 is about one hundred times more luminous visually, so that, if we equate the bolometric corrections, the efficiency of conversion of ultraviolet light into Balmer emission is nearly the same in the two circumstellar envelopes. Consider an envelope of volume V, ion and electron densities N_i and N_e, and electron temperature T_e. Then its luminosity in a hydrogen line is

$$L_{nn'} = 3.2 \times 10^{-6} \frac{V N_i N_e}{T_e^{3/2}}\ e^{157000/n^2 T_e} \frac{2hR b_n}{n'^3 n^3}, \quad (2)$$

omitting the Gaunt factors. From analogy with a hot planetary nebula, where $T_e = 2 \times 10^4$, $b_4 = 0.32$, we obtain from the observed strength of Hβ, $N_i N_e V = 10^{57}$. The absence of forbidden emission lines shows that N_e much exceeds its value in planetary nebulae, i.e., requiring rapid collisional de-excitation of the upper levels of O^{++}. Seaton and Osterbrock (1957) give $N_e > 10^6$ or $N_e > 7 \times 10^6$ for IC 4997, which still has [O III] lines. Therefore, we conclude that in the envelope of the nova $N_i = N_e > 10^7/\text{cm}^3$, $V = 10^{43}$, the mass $< 10^{26}$ gm, and the radius $< 10^{14}$ cm, i.e., $< 1000\ R\odot$. These are fairly conservative upper limits because of the complete absence of forbidden lines, so that the postnova envelope is in fact small in size and mass. It is hoped that further spectroscopic observation will permit more quantitative results to be obtained. The rate of mass loss in the long periods between nova explosions may be a significant factor in evolution.

Table 2 gives measured equivalent widths and half-widths of the emission

lines as observed, largely in 1956. The equivalent widths are measured in units of the neighboring stellar continuum and are therefore affected by changes in the brightness of the star. They may prove useful for future studies of the evolution of the intensity and level of excitation in the postnova emission, since most of these objects were near minimum. McLaughlin (1953) suggests that the level of excitation indicated by He II/H varies with time and ultimately drops in the very old novae. The strength of λ 4686 A in Nova Oph 1848, however, clearly shows that not all novae behave similarly. The rapid light-variations

TABLE 2

MEASURED EMISSION-LINE VELOCITY WIDTHS AND EQUIVALENT WIDTHS IN OLD NOVAE

λ	AQL 1918		OPH 1848		PER 1901		PYX 1890–1944		WZ SGE 1913, 1946	
	E.W.	Δλ*	E.W.	Δλ	E.W.	Δλ	E.W.	Δλ	E.W.	Δλ
3889	1.7	6	.....	.....	.....	.....	.....	.....	.....	.....
3970	2.3	7	.....	.....	.....	.....	.....	.....	5:	.....
4026	0.7	7	.....	.....	.....	.....	.....	.....	.....	.....
4101	2.4	7	1.3	9:	8.9	15	.....	.....	7:	30:
4340	3.0	7	1.3	9	10.8	14	3	8:	16	30:
4388	0.3	.....	.....	.....	.....	.....	.....	.....	.....	.....
4472	0.5	7:	.....	.....	3.1	15	2	.....	.....	.....
4645	1.1	8:	.....	.....	.....	.....	.....	.....	.....	.....
4686	1.7	8	3.1	12:	5.9	12	9:	10:	< 2	.....
4861	2.8	7	1.7	11:	.....	.....	14:	.....	35	28
Resolution	0.5 A		5A		1A		5A		5A	

λ	N 408 HER 1936†		N 412 HER 1936†		PUP 1942	
	E.W.	Δλ	E.W.	Δλ	E.W.	Δλ
3727	13.2:	15:	7.6:	.....	.....	.....
3889	5.8:	14:	3.2:	.....	.....	.....
3970	7.6:	18:	3.0:	15	.....	.....
4026	0.8	.....	.....	.....	.....	.....
4101	16.0	19	7.5	17	4.9	.....
4340	14.8	16	9.9	18	6.0	22
4472	2.4	.....	2.3	.....	1.2	.....
4645	17.6	22	10.2	22	3.7	30:
4686	27.3	23	17.8	20	8.2	20
4861	32.0	17	22.1	16	8.8:	18
5007	13.8	24	11.0	17	33:	20‡
Resolution	5 A		5 A		5 A	

* Δλ = Total width at half-central intensity, in angstroms.

† Lines apparently double and variable; higher members of Balmer series disappear on N 412, taken near phase 0.75, and are strong on N 408 near phase 0.25 (July 15, 1956).

‡ Line shows multiple components.

observed by Walker, on the contrary, and the persistence of emission lines both suggest that there is continued postnova activity even after 100 years. Line profiles of Hγ given in Figure 2 show the variety of observed phenomena, although it should be noted that Nova Pup 1942, Nova Her 1936, and WZ Sge are peculiar objects. The two former still have substantial contributions from their expanding shells, and the latter is a white dwarf. Figure 2 and Table 2 show that there are several types of emission lines. In recent novae, furthermore, the nebular lines persist and have some fine structure, with all lines quite broad, 10–20 A wide at half-intensity. Sanford and Greenstein (1957) have traced the similarities with the original structure of the lines of Nova Pup 1942, on plates taken in 1956. After the disappearance of the nebular components, He II, He I, and H remain, with widths of 6–10 A. Weakness of lines in Nova Aql 1918 compared with Nova Per 1901 shows that excitation, line width, and line strength are not uniquely correlated with time since the outburst. There is little doubt that spectra of novae vary erratically with time.

Plate I contains two spectra of Nova Herculis near its two quadratures during one cycle. The spectra were widened so that the spatiovelocity structure of the shell is blurred. Note the over-all change in line intensities (also in Table 2) and

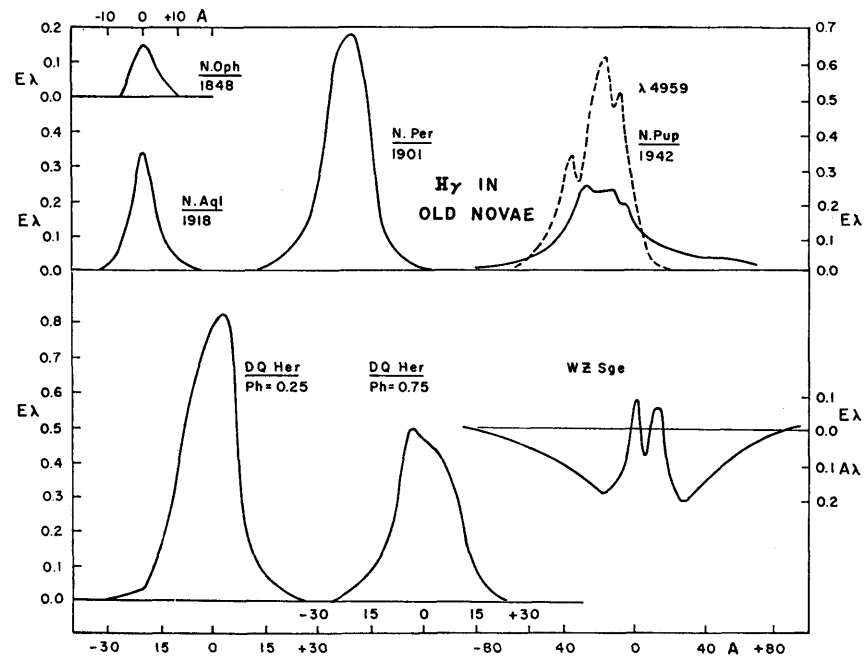


FIG. 2.—Line profiles of Hγ in old novae. $E\lambda$ is emission flux in units of adjacent continuum. Nova Puppis still shows nebular emission in the envelope; λ 4959 has a different profile from Hγ. Nova Herculis has variable line intensity and profiles; WZ Sagittae is a white dwarf.

in particular the apparent weakening of the higher Balmer lines near phase 0.75. This was pointed out first by Kraft; the phenomenon has been studied by Greenstein and Kraft (1959). Note that the emission lines Hζ, Hη, and Hθ, apparently double at phase 0.25, not only weaken but become single at phase 0.75. The effect is much less pronounced at Hβ and Hγ, where presumably the envelope dominates the total hydrogen emission. If the line-intensity changes are aspect or eclipse effects, it is clear that the emission in the higher Balmer lines is produced near the stars and in a relatively small and high-density region. Kraft (1959) has proposed that most of the light of the primary comes from a ring which is eclipsed.

Plate I also contains a spectrum of WZ Sge, a recurrent nova which shows broad Balmer absorption lines characteristic of a white dwarf (Greenstein 1957). The proper motion measured by both van Maanen and Luyten is about 0".08 per year. The broad emission lines partly conceal the strong, broad absorption lines characteristic of a white dwarf. The structure of the emission resembles that in a Be star, except that it is on a ten times greater scale of width. In private correspondence, McLaughlin has suggested a rotating ring. WZ Sge is a recurrent nova, but its subluminous nature and spectrum are not found in another recurrent nova, T Pyx, which shows relatively sharp emission lines and no absorption. The emission lines in WZ Sge, although strong, are measured in units of a star whose brightness is about one hundred times less than other old novae, so the mass of its gaseous envelope will be correspondingly smaller. Nova DI Lac 1910, has recently been found to have broad, shallow hydrogen absorption lines resembling those in a white dwarf. An eventual dying out of the energy for nova outbursts and the postnova emission, before the white dwarf stage, is plausible.

The presence of an emission feature near λ 4645 in Nova Aql, Nova Her, and Nova Pup is of some interest. It is stronger in the two recent novae than in Nova Aql. Its wave length is imprecise because of its breadth. Measured near the continuum, it stretches from λ 4630 to λ 4660 in Nova Pup, from λ 4621 to λ 4665 in Nova Her, and from λ 4638 to λ 4661 in Nova Aql. The contributors to this wide blend could be C III λλ 4647, 4650, 4651, C IV λ 4647, λ 4658, and N III λλ 4634, 4640, 4641. Since the other emission lines have a width Δλ near 8 A, it seems improbable that N III will wholly account for the line. Therefore, a blend of high-excitation C and N lines may exist. The ratio of the blend to λ 4686 of He II resembles that in the emission-line spectra of certain planetary nuclei, to which are ascribed an excitation temperature near 30,000°–35,000° K, and a somewhat higher Zanstra temperature. A visual luminosity of +4 with $T = 35{,}000°$ K gives the stellar radius of 0.2 $R\odot$; such a star would not be degenerate.

The longer-term evolution of the spectrum of an old nova is not clear. The lack of absorption lines (although weak H or He II absorption could be hidden by the overlying emission) distinguishes these stars from all other faint stars

except for some peculiar white dwarfs. The postnova emission process and the instability leading to light-variations could eventually end, and a more usual absorption spectrum appear, but we have no evidence as to its probable nature. I have observed over 70 faint blue stars (not white dwarfs), largely in the galactic halo, and found none with emission lines or purely continuous spectra. Photometric studies could still reveal small, rapid light-variations in stars found colorimetrically in the surveys by Humason and Zwicky (1947), Iriarte and Chavira (1957), Feige (1958), and Luyten (1958).

§ 3. THE SS CYGNI STARS

The SS Cyg objects are defined photometrically by recurrent, small nova-like eruptions, superposed on a minimum which itself has rapid variations in times of the order of 5 minutes; the larger eruptions have a rough periodicity in times from a few weeks to a year. The space velocities are fairly high, and the luminosities at minimum fairly low. Probably, duplicity is an essential feature. It is established for AE Aqr and SS Cyg by Joy (1954, 1956), who determined the orbit of these short-period spectroscopic binaries. They consist of a late-type dwarf or subgiant and a high-temperature emission-line subdwarf, the absorption and most of the emission lines being 180° out of phase. RU Peg is similar (Joy 1954*b*). Elvey and Babcock (1943) have made a survey of the stars and report traces of a late-type continuum or absorption lines in X Leo, AY Lyr, SU UMa, TW Vir, Z Cam, AH Her, and CO Ori. A few objects showed wide, shallow absorption lines of hydrogen, e.g., X Leo, CN Ori, CY Lyr. Superposed is a blue continuous spectrum with broad emission lines of H, He I, Ca II and sometimes He II.

The large-scale variability in light is usually accompanied by a spectroscopic change in which the blue continuum brightens, so that, toward maximum, the emission lines weaken or disappear. However, toward maximum the highest excitation lines are relatively stronger. The half-width of the emission is about $\Delta\lambda = 15$ A in SS Cyg; in Z Cam at maximum $\Delta\lambda = 20$ A, and the emission was superposed on very broad, shallow absorption (Elvey and Babcock 1943). During a quiescent minimum of AE Aqr, Greenstein observed emission lines of H, Ca II, and weak He I with $\Delta\lambda = 15$ A. Such shallow, broad emission can easily be submerged if the stellar continuum brightens by several magnitudes. Since the resolution available at Palomar was high ($\approx$1 A, dispersion 38 A/mm) compared with that used by previous workers, I give the observed emission and absorption profiles in Figure 3. Absorption lines of Ca I, λ 4227 and Fe I, λ 4383, are strong in AE Aqr and reach nearly normal central depth, $A_c \approx 0.6$–0.7 at this dispersion. Therefore, the contribution of the light of the faint blue star is small. The full half-width of the absorption is $\Delta\lambda = 4$ A, about one-quarter that of the emission lines. Since the orbital period is 0.7 day, rapid rotation would produce most of the observed breadth of the emission lines. The reversing layer of the cool component is much more quiescent than is the enve-

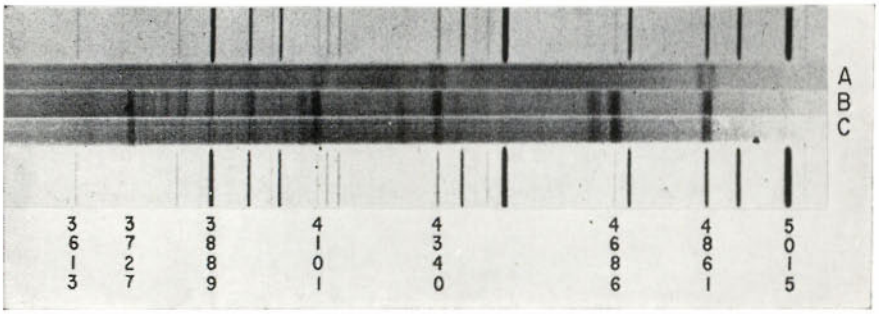


PLATE I.—Spectra of old novae: (*A*) Nova WZ Sge; (*B*) DQ Her, phase 0.25: (*C*) DQ Her phase 0.75. Original 180 A/mm.

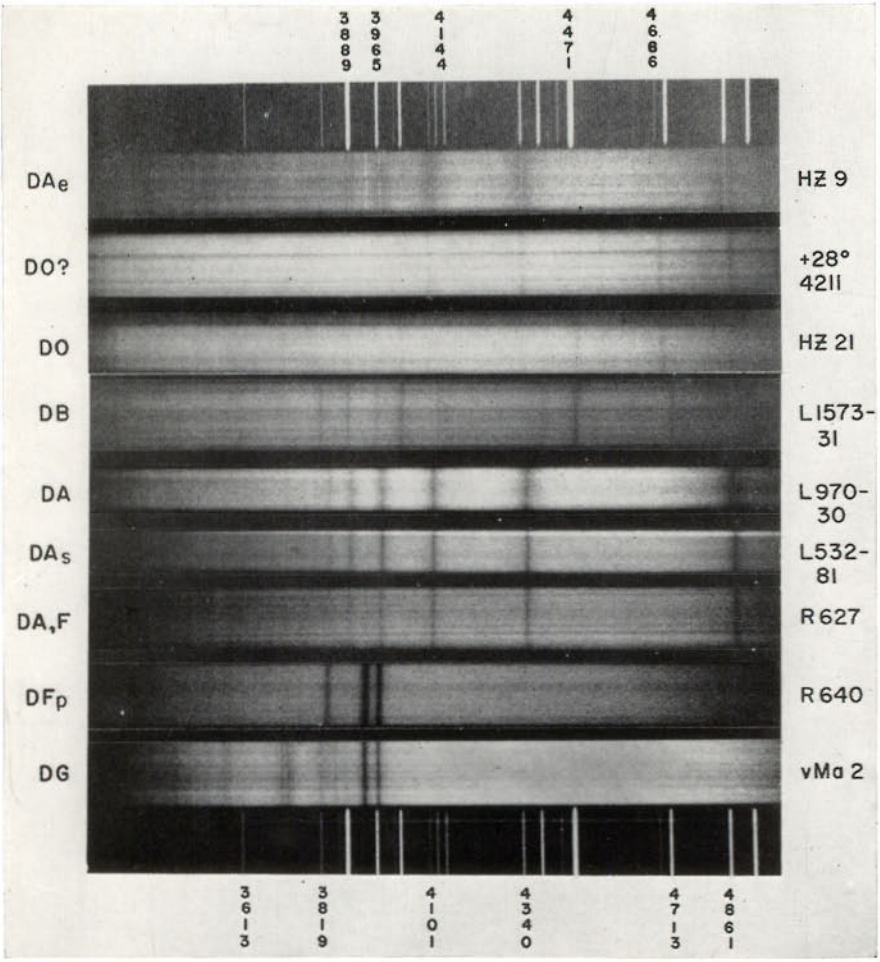


PLATE II.—White dwarf spectra, Palomar 180 A/mm (Greenstein). HZ 9, emission lines; + 28°4211, hot, rather high luminosity; HZ 21 very hot, He II, He I; L1573-31, He I only; R 627 relatively sharp H lines, weak Ca II; R 640, Mg I strong; vMa 2, diffuse Fe I lines in ultraviolet.

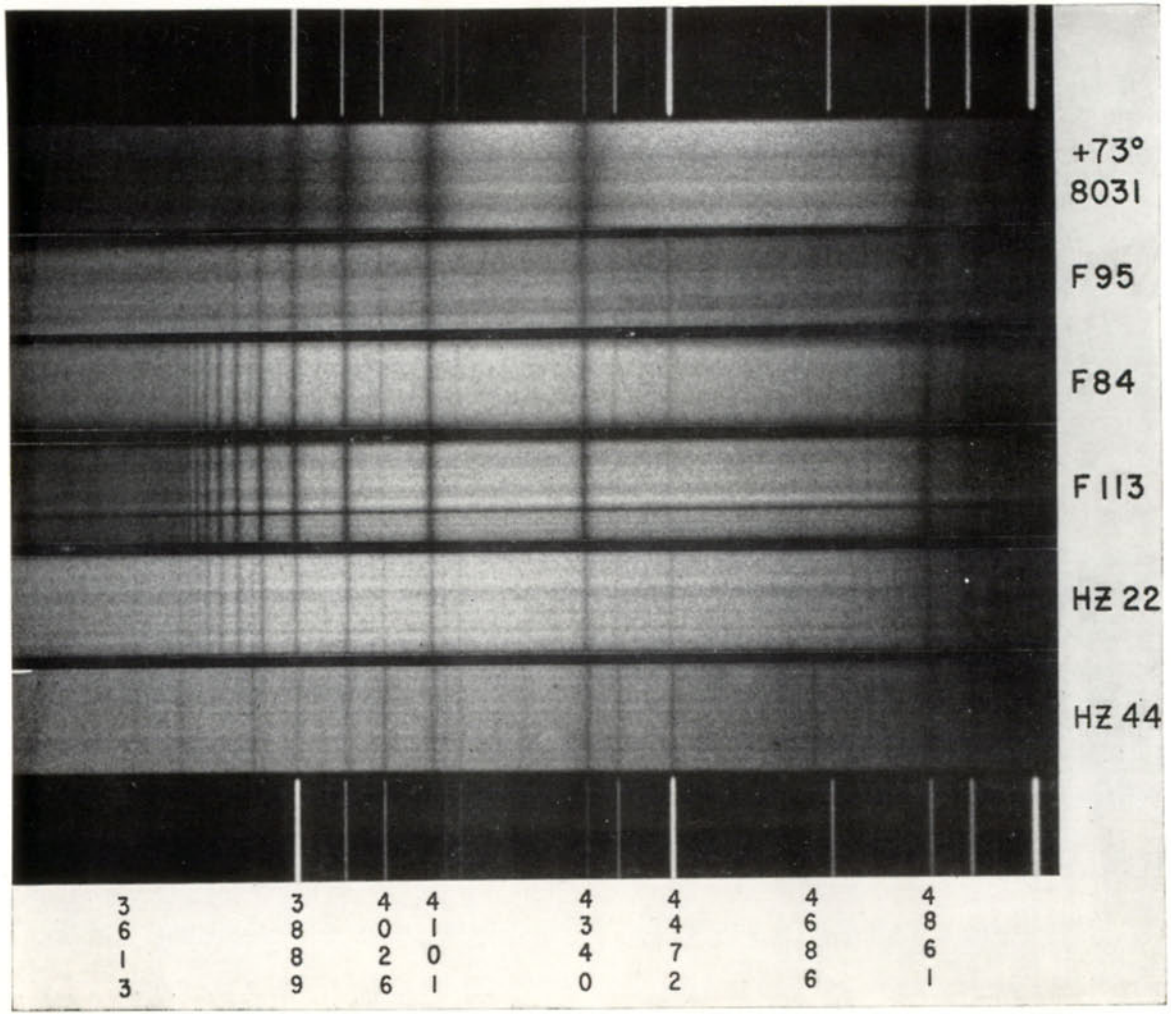


PLATE III.—Peculiar faint blue stars, 180 A/mm. *Top*, white dwarf DA, +73°8031. The star Feige (F)95 is classifiable spectroscopically as sdB; F84 is probably a horizontal-branch star, B3p; F113, horizontal branch B8p. Note the luminosity-sensitive lines λ 4388, and the λ 4121/4144 ratio, in the subluminous stars. HZ 22 is a normal B2 spectroscopic binary of population I. HZ 44 is a very hot, early sdO.

lope, or hot component, which produces the emission lines. The latter is subject to larger forces, gravity and centrifugal, i.e., the hot star is small. In AE Aqr the hot star is relatively faint with equivalent widths of Hγ and Hδ of about 2 A, while in SS Cyg it is bright; the absorption lines are essentially washed out, and the emission lines dominate. In SS Cyg, illustrated in Figure 4, the equivalent width of Hδ varied with phase in the light-variation from 16 to 44 A, of Hγ from 23 to 46 A. In contrast, the strongest absorption, λ 4227 of Ca I had an equivalent width of 1.3 A and a central depth of about 0.23, one-third of the same line in AE Aqr. The differences in absolute magnitude derived for the blue continuous spectrum of the hot star corrected for the cool star can be estimated as $> +2^m$ in AE Aqr and -0^m7 in SS Cyg (at the mean phase of our observations). The strength of the emission lines, in units of the total continuum, is about twenty-five times greater in SS Cyg than in AE Aqr, which is in fair agreement with the deduced strengths of the blue and red components, i.e., the emission-line to blue-continuum ratio is about the same in the two stars. The unknown nature of the light-curve at the time of spectroscopic observation prevents more detailed study. The equivalent widths of the emission lines vary pronouncedly in AE Aqr and may be a combination of intrinsic variations and aspect effects (Joy 1954*a*, 1956). The emission lines of SS Cyg in Fig-

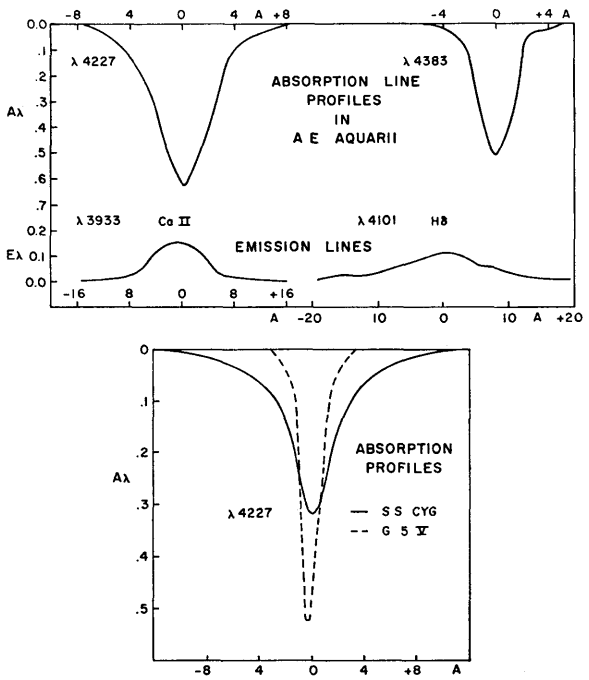


FIG. 3.—Line profiles in AE Aqr, near minimum. The emission lines are broader than the absorption. In SS Cyg the absorption line is filled in by the blue star. Resolution near 1 A.

ure 4 show sharp peaks which move across a broad line; these peaks are connected with the star producing the late-type absorption spectrum and are most conspicuous in Ca II. Thus there also exists a relatively low-excitation envelope with small internal velocities around the redder star. The He I lines are broad and featureless compared with H or Ca II, indicating again a high velocity dispersion around the hot star.

The luminosity of these blue companions can be determined from statistical parallaxes; they lie in the range +4 to +8 from spectroscopic studies (Deutsch 1958; Kraft 1958). Crawford and Kraft (1956) give the type of the K star in AE Aqr as K5 IV–V, with $M_v = +5.5$; in that case my spectrophotometry indi-

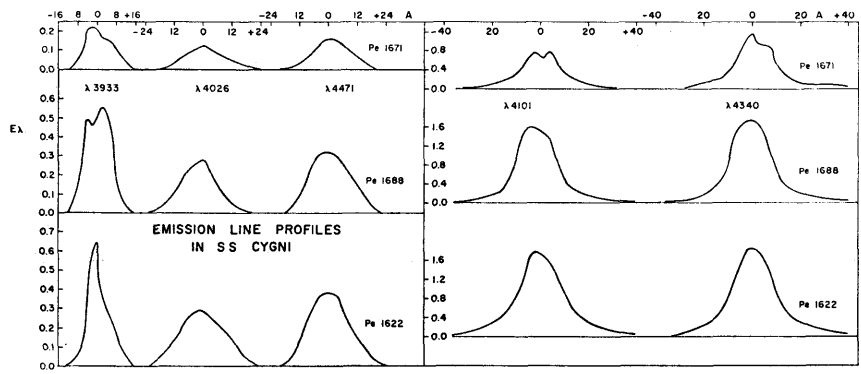


FIG. 4.—Emission-line profiles in SS Cyg at various phases. Pe 1671 was well above minimum. The phases in Joy's orbit are Pe 1671, 0^d086, velocities, absorption −145, emission +117 km/sec; Pe 1688, 0^d236, abs. +79, em. −60 km/sec; Pe 1622, 0^d136, abs. −127, em. +27 km/sec. Note that Pe 1671 shows most clearly doubled emission lines and that Ca II is relatively strong in the cool star. Pe 1688 shows even stronger cool-star Ca II, but no other sharp lines. No trace of duplicity occurs in He I at any phase, showing that the high excitation is confined to near the hotter star.

cates that the blue star has $M_v > +7.5$. The properties of the blue component of SS Cyg are quite uncertain. The red component is too difficult to classify because of the veiling, and the trigonometric parallaxes are discordant. The Yerkes parallax would give a luminosity of +9 for the blue star, the mean *Yale Catalog* parallax +6, and the assumption that the primary is G5 V gives about +4.

However, there is no doubt that a highly subluminous blue companion approaching the white dwarfs is present in at least three and probably in most of the SS Cyg stars, associated with a larger, interacting G dwarf or subgiant. The effect of the binary nature of these systems has been extensively discussed by Crawford and Kraft (1956). Their work suggests that matter ejected through the inner Lagrangian point from the low-density star and falling into the high-density star may provide a significant fraction of the light of the secondary and also a source for the broad emission lines. Since many of these systems are

clearly members of the high-velocity group, these stars are important as representatives of the rare class of population II close binaries.

Another group of faint blue companions exists for the long-period variables (Merrill 1940; Struve 1955) and α Sco. In R Aqr, both the red giant and the faint blue companion are seen to be immersed in nebulosity; in α Sco a small nebulosity surrounds the hot star. The companions of ο Cet and T CrB, studied by Deutsch (1957) and by Kraft (1957), prove to lie in the range +4.5 to +8 at their minima. The suggestion by Crawford and Kraft (1956) that the interaction resulting from duplicity may be a very significant factor in many types of stars has been carried further by Huang (1956), who believes that all old novae are close doubles. My own spectra do not support this suggestion; if the companions are late-type stars, they must be several magnitudes fainter than old novae themselves, i.e., $M > +6$ to $+10$, and would then not fill the Lagrangian surface, unless the separation was extraordinarily small.

§ 4. THE WHITE DWARFS

Extensive reviews of the present stage of observational knowledge (Greenstein 1958) and theoretical interpretation (Schatzman 1958) are available elsewhere. The growth of our knowledge will be largely dependent on technical advances in spectrograph design and availability of large telescopes, because of the faintness of these stars. Only a brief review and new spectrophotometric results will be given here.

White dwarfs occur in both populations; those selected from proper-motion surveys may be of higher-than-average space motion. Combination of trigonometric parallaxes with proper motions yields a tangential velocity dispersion ranging from 30 to 90 km/sec (for the faintest, red, white dwarfs). White dwarfs may exist with a wide variety of ages, chemical compositions, and past evolutionary histories. Their surface composition need not be representative of their interior because of gravitational separation of light and heavy elements. The interior must be largely helium or heavier elements; the non-degenerate, thin surface layer at relatively low densities and temperatures must contain substantially all the hydrogen (Schatzman 1958; Schwarzschild 1958). With the central temperatures expected, about 20 million degrees, any star of radius less than 0.08 $R \odot$ will be largely degenerate, and, if the radius is less than 0.01 $R \odot$ (a typical white dwarf), it will be degenerate,[1] even with $T_c = 10^{9}\,^{\circ}$ K. Thus in the late stage of evolution many of the processes leading to nucleogenesis will occur, and at higher than normal rates, because of degeneracy. Complete exhaustion of hydrogen and of most of the nuclear energy is to be expected; if the star's

[1] Figure 1 shows the degeneracy boundary for hot stars. It is computed by assuming $T_c = 30 \times 10^{6}\,^{\circ}$ K, $M = 0.5 \odot$, Kuiper's temperature scale and bolometric corrections and zero hydrogen content. Our knowledge of the temperature scale of the very hot subdwarfs, old novae, and SS Cyg stars is so poor that we cannot safely assign a spectral type or temperature. The border line between the peculiar hot stars and the white dwarfs is very uncertain.

evolution leads through a stage of high T_c, formation of heavy elements from C to Ca may occur. Only in supernova remnants should we expect the formation of very heavy elements (Fowler and Greenstein 1956; Burbidge *et al.* 1957). Since some of the fainter white dwarfs must be very old, those which have never been at high T_c could show a He excess and a heavy-element deficiency.

A color-magnitude diagram for the spectroscopically best-known white dwarfs is given in Figure 5, together with my spectral types. An illustration of some types of white dwarf spectra recognizable at low dispersion is in Plate II. Greenstein (1958) has given a preliminary classification scheme for the types so far observed; additional types may exist, especially at low temperatures and possibly at high pressures. Normal H-rich stars, He-rich stars, and stars with nearly continuous spectra coexist at the same color. Color is generally correlated with spectral type, although DC stars are found in most color classes. Characteristics of the spectral classes are given in Table 3.

The DA stars showing only hydrogen cover a wide range of color, luminosity, and, obviously, temperature. However, it does not seem profitable to subdivide them by numerical subclass without spectrophotometric measurements. The number of lines visible hardly changes with equivalent width or with sharpness of the cores of the lower series members, H9 usually being the last line visible. Spectrophotometric measures (Lynds 1957; Greenstein 1958)

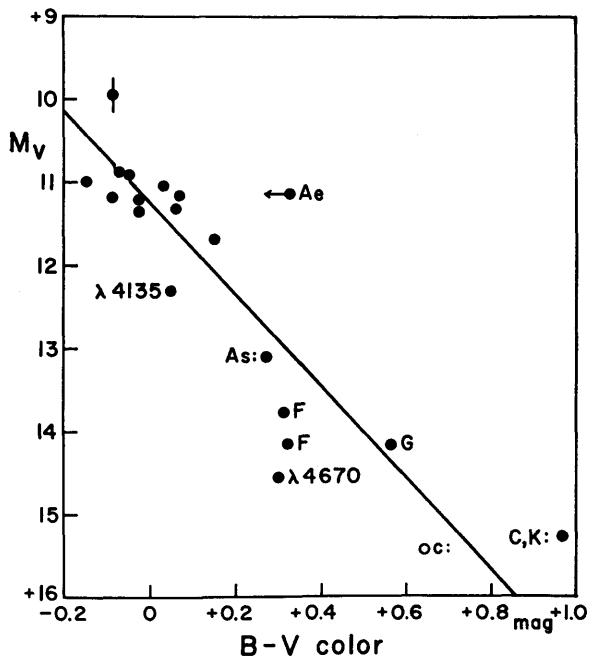


FIG. 5.—Color-magnitude diagram for the white dwarfs with photoelectric colors (Harris), parallax, and spectra by Greenstein. (*Open circle*, Kuiper spectrum.)

show that there is a broad maximum (see Fig. 6) in the equivalent width of Hγ, as a function of color, and that in fact the DA type covers an enormous range of temperature—probably from 22,000° to 9000° K (Greenstein 1958). The absence, over this wide range, of other lines than hydrogen is quite striking and reflects either very high opacity, molecule formation, or differential gravita-

TABLE 3

CHARACTERISTICS OF WHITE DWARF SPECTRAL TYPES

Type*	Description	Example
DC.....	Continuous spectrum, no lines deeper than 10 per cent	W 1516, L 1363
DO.....	He II strong, He I and/or H present	HZ 21
DB.....	He I strong, no H	L 1573-31
DA.....	H present, no He I	40 Eri B
DA, F.....	H sharper and weaker, Ca II weak	R 627
DF.....	Ca II, no H	L 745-46A
DG.....	Ca II, Fe I, no H	vMa 2
λ 4135.....	Broad "Minkowski" bands, unidentified	AC+70°8247
λ 4670.....	Broad bands at λλ 4670, 5140, probably C_2	L 879-14

* In addition, subscripts p = peculiar; wk = weak; e = emission; s = sharp may be added.

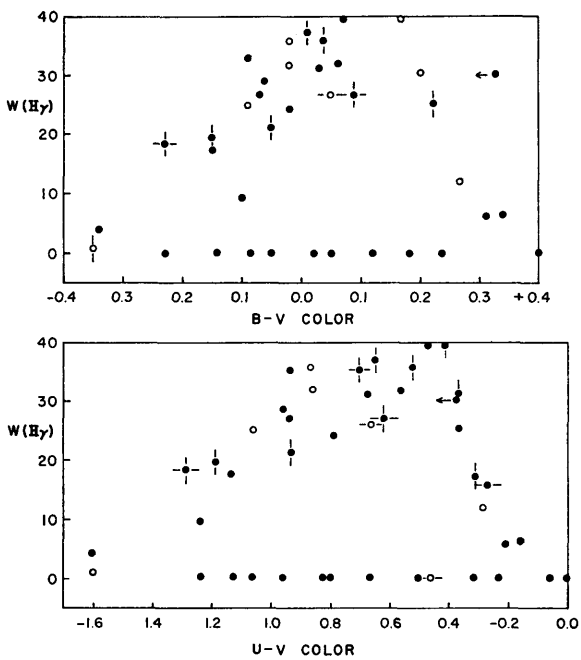


FIG. 6.—Equivalent widths of Hγ as a function of $B-V$ and $U-V$ colors. *Open circles*, other sources; *horizontal lines*, uncertain color; *vertical lines*, uncertain W. Note stars with no hydrogen lines over entire range of color.

tional separation of elements of high atomic weights. It is important to realize that the DA type is a very inhomogeneous one, since it covers a range of 4 mag. visually and probably 6 mag. bolometrically. Figure 6 shows also that the dependence of the strength of Hγ on $U - V$ colors exhibits much less scatter than when $B - V$ colors are used. Two reasons may be advanced: the strength of the hydrogen lines affects the $B - V$ colors by up to 0.25 mag., making strong-line stars appear too red; the $U - V$ color is affected by both temperature and the ratio of the hydrogen continuous absorption coefficient to the total opacity. Since the strength of the Balmer lines also involves these two factors, variations in the opacity source will affect the Balmer jump, $U - V$ color, and Balmer line strength in a similar fashion.

So far, only line profiles in the peculiar white dwarfs have been published (Greenstein and Matthews 1957) and Hγ profiles for DA stars (Greenstein 1958), as well as some low dispersion by Lynds (1957). Table 4 contains data on all the stars that I have so far observed (up to August, 1958) at Palomar, and Tables 5*A*–5*F* contain the details of the line profiles. The spectra were largely of two series: Pe, coudé, 38 A/mm, widened to 0.3 mm on the plate, λλ 4500–3800; N, nebular spectrograph, 180 A/mm, widened to 0.3 or 0.8 mm on the plate, λλ 5000–3400. Some Pd plates, 18 A/mm, were also used. In spite of the lower dispersion, the N series is quite satisfactory because of the width and spectral range. Spectrophotometric calibration was provided by a wedge-slit spectrograph; II*a*-O plates were used with a resolution about 1 A on the Pe series and 4 A on the N series. The major difficulty was the location of the continuum in the DA stars; in these the wings of Hγ and Hδ begin to overlap, and the last line visible was generally Hζ. To provide a systematic, reproducible location of the continuum, straight lines were drawn on intensity-scale microphotometer records connecting the high points of the continuum, midway between the absorption lines. (Note that because of wave-length variations in plate sensitivity and atmospheric and instrumental response-curves, this method cannot eliminate the curvature of the background and thus permits both accidental errors and asymmetries.) Hβ was rarely measured and is badly affected by the drop of plate sensitivity longward; Hϵ, Hζ, and Hη are located on a badly depressed apparent continuum, and only Hγ and Hδ have reasonably well-determined and undistorted continua. In the He I stars there is considerable uncertainty in the continuum from λ 4300 to λ 4500 because of the strong overlapping lines λλ 4388, 4438, 4472. The accuracy attained is far below the third decimal place, which is given only to permit smooth plotting. Tables 5*A*–5*F* give profiles and equivalent widths (derived by planimetry of the profiles). In addition, the total width in angstroms at half-central intensity, 0.5 A_c, is given as w.5; the total width in the wings, at 0.2 A_c, is given as w.2. Profiles were measured at various displacements from the apparent centers of the lines; since the center is poorly defined, differences between line depths A_λ at positive and negative displacements should be interpreted with caution unless many plates are

TABLE 4*

SPECTRA AND COLORS OF WHITE DWARFS

No.	Star†	$B-V$ (mag.)	$U-B$ (mag.)	M'_v	Type	W(Hγ)	Lines Present; Remarks
1....	vMa 2	+0.56	+0.04	14.2	DG	.....	Ca^+, Fe (Mg)
2....	W 1516	+ .12	−0.78	12.8	DC	.....	
3....	L 870-2	+ .34	−0.50	12.1	DAs	6.0	H
4....	W 219	+ .30	−0.52	14.6	λ 4670	.....	λ 4670 band, C_2
5....	HZ 2	− .05	−0.88	9.9:	DA	21.1:	H
6....	40 Eri B	+ .03	−0.70	11.0	DA	31.7	H
7....	HZ 9	+ .33	−0.69	11.1	DAe	30.2:	H; also H, Ca^+, Si emission; composite?
8....	L 879-14	.....	.....	14.0	λ4670	.....	λ 4670 band, C_2
9....	HZ 14	− .15	−1.04	11.0	DA	19.8:	H
10....	L 1244-26	− .15	−0.98	11.5	DA	17.5	H
11....	He 3	− .06	−0.90	11.3	DA	28.8	H
12....	L 745-46A	+ .32:	−0.63:	14.0	DF	.....	Ca^+
13....	L 532-81	.....	.....	12.1	DAs	15.7	H, (Ca^+)
14....	LDS 275AB	.....	.....	12.2	DC	.....	
15....	SA 29-130	+ .07	−0.54	11.2	DA	39.4	H
16....	L 825-14	.....	.....	10.9	DA	17.1:	H
17....	L 970-30	.....	.....	11.3	DA	35.1:	H
18....	L 971-14	.....	.....	13.3	DC:	.....	
19....	R 627	+ .31	−0.52	13.7	DA, F	5.6	H, Ca^+
20....	HZ 21	− .35	−1.25	10.5:	DO	0.8:	He^+, He (H)
21....	HZ 29	− .23	−1.01	8.9:	DBp	.....	He, very diffuse
22....	HZ 43	− .10	−1.14	10.0:	DA	9.1	H shallow, weak
23....	W 485	+ .06	−0.62	11.8	DA	31.9	H
24....	W 489	+ .96	+0.37	15.4	DC, K:	.....	Ca^+ may be weakly present
25....	+70°5824	− .09	−0.84	10.4	DA	35.4	H
26....	R 808	+ .20	−0.56	12.9	DA	30.6:	H
27....	L 770-3	− .23:	−1.06:	10.9	DA	18.7:	H
28....	R 640	+ .18	−0.68	13.2	DFp	.....	Ca^+, Mg
29....	L 1491-27	+ .22	−0.58	12.7	DA	25.3:	H
30....	+70°8247	+ .05	−0.85	12.2	λ 4135	.....	"Minkowski" bands
31....	LDS 678A	+ .02	−0.83	9.8:	DC	.....	
32....	L 1573-31	− .09	−0.97	11.6:	DB	.....	He
33....	Nova WZ Sge	+ .09	−0.71	10.5:	DAep	27.1:	Broad H emission on absorption
34....	W 1346	− .07	−0.87	10.7	DA	27.2	H
35....	L 711-10	.....	.....	10.3	DA	26.3:	H
36....	+73°8031	+ .01	−0.66	11.0	DA	37.3:	H
37....	LDS 749B	− .05	−0.91	11.9	DB	.....	He
38....	+82°3818	− .02	−0.72	12.2	DA	24.4	H
39....	L 1363-3	.....	.....	12.8	DC	.....	
40....	L 930-80	− .14	−0.99	12.7	DB	.....	He
41....	+28°4211	− .34	−1.26	.....	DO?	3.9	He^+, H (He); possibly subdwarf
42....	L 1512-34B	+0.17	−0.58	11.2:	DA	39.6	H

* Colors are largely unpublished by D. L. Harris III. The luminosity is estimated from parallax or proper motion, colon indicating uncertainty. W is the equivalent width of Hγ, with colon indicating only one plate. In "Lines Present" column, parentheses indicate lines very weak.

In addition to the white dwarfs listed above, the following stars have been recently observed by Lynds (1957) to be of type DA: Oxf +25°6725, VR 7, VR 16, L 997-21, R 198. Older classifications are to be found listed in Table 1 of Greenstein (1958), together with co-ordinates, magnitudes, proper motions, etc.

† Abbreviations for finding lists: L = Luyten; LDS = Luyten double stars; R = Ross; SA = Selected area; VR = van Rhijn; W = Wolf; He = Hertzsprung; HZ = Humason-Zwicky.

available. There is some evidence, not yet fully evaluated, that the line profiles are asymmetrical, with the wave length of the mid-point between equal values of A_λ displaced a small amount positive with respect to the wave length of the deepest part of the line. (A combination of pressure and Stark broadening might produce such a shift of the wings with respect to the line core.) Figure 7 shows line profiles from Hα to Hη in 40 Eri B; Figure 8 gives the variety of line profiles shown by Hγ in DA stars with different strengths and depths of lines. The sequence HZ 43 ($U - V = -1^m24$), Wolf 1346 ($U - V = -0^m94$), SA 29-130 ($U - V = -0^m47$), L 870-2 ($U - V = -0^m16$) is one of decreasing temperature. L 870-2 lies beyond the maximum of the Balmer lines and has sharper and

TABLE 5A

Hα AND Hβ PROFILES IN WHITE DWARFS (ABSORPTIONS × 10^3)

A	Line and No. in Table 4														
	6 Hα	5 Hβ	7 Hβ	9 Hβ	13 Hβ	16 Hβ	17 Hβ	19 Hβ	26 Hβ	27 Hβ	29 Hβ	34 Hβ	36 Hβ	41 Hβ	42 Hβ
−110	001	....	....	....	....	....	....	....	....	....	....	....	....	....	....
−100	014	....	025	....	....	....	....	....	....	....	....	....	....	....	....
− 90	030	....	035	....	....	....	....	....	....	....	....	....	....	....	005
− 80	049	....	055	....	....	....	010	....	013	....	....	....	013	....	021
− 70	069	....	076	007	....	....	036	....	038	....	....	030	031	....	043
− 60	091	002	094	022	....	....	062	....	062	....	015	068	053	....	064
− 50	118	041	111	040	011	005	089	....	081	001	049	100	081	....	082
− 40	149	086	132	060	025	018	130	....	105	023	058	124	128	....	102
− 30	183	139	165	088	055	062	233	011	213	062	136	168	194	020	194
− 25	203	178	187	104	084	106	266	019	256	091	212	200	236	028	227
− 20	226	221	216	129	119	168	302	029	310	130	259	239	283	037	265
− 15	255	265	258	182	168	204	341	049	377	183	278	297	335	055	310
− 10	287	317	277	244	226	243	387	107	454	245	368	373	392	097	372
− 5	338	370	200	302	336	293	439	216	540	306	446	462	481	175	455
0	475	445	....	342	479	385	485	414	620	360	500	605	528	276	510
+ 5	336	343	225	295	396	325	420	269	504	287	459	528	476	184	465
+ 10	278	295	255	248	292	259	362	164	422	229	383	466	396	112	400
+ 15	236	239	247	207	213	213	321	097	358	171	300	416	337	073	343
+ 20	206	195	218	162	161	173	286	062	307	110	229	375	290	052	290
+ 25	182	155	189	125	123	111	256	031	267	074	180	342	247	039	250
+ 30	161	121	154	095	093	065	226	004	234	056	144	313	207	026	214
+ 40	126	062	112	054	045	022	130	....	137	020	045	255	142	....	116
+ 50	095	022	077	036	014	007	092	....	106	001	013	183	093	....	082
+ 60	070	001	051	022	....	....	053	....	083	....	....	111	057	....	058
+ 70	048	....	035	007	....	....	023	....	057	....	....	050	028	....	037
+ 80	031	....	024	....	....	....	004	....	028	....	....	....	011	....	020
+ 90	019	....	014	....	....	....	....	....	....	....	....	....	....	....	006
+100	010	....	....	....	....	....	....	....	....	....	....	....	....	....	....
+110	001	....	....	....	....	....	....	....	....	....	....	....	....	....	....
W	27.4	19.3	25.4	15.8	14.7	16.6	32.1	7.3	35.3	12.5	23.2	34.0	29.6	5.2	32.6
w.5	33	37	62	35	22	34	56	13	40	29	40	47	45	15	46
w.2	108	73	132	71	53	73	116	29	99	54	70	100	91	34	104
n	1Pd	2N	1N	1N	1N	1N	1N	2N	1N	1N	1N	1Pd	1N	1Ce	1N
	....	....	....	....	....	....	....	....	....	....	....	....	....	4Pd	....
	....	....	....	....	....	....	....	....	....	....	....	....	....	1N	....

TABLE 5B

$H\gamma$ PROFILES IN WHITE DWARFS (ABSORPTIONS $\times 10^3$)

A	No. in Table 4																								
	3	5	6	7	9	10	11	13	15	16	17	19	20	22	23	25	26	27	29	34	35	36	38	41	42
−110	.....	.....	.....	.....	.....	.....	.....	.....	.....	.....	005	.....	.....	.....	.....	.....	.....	.....	.....	.....	.....	001	.....	.....	.....
−100	.....	.....	.....	.....	.....	.....	006	.....	008	.....	014	.....	.....	.....	.....	.....	015	.....	.....	005	.....	012	.....	.....	005
− 90	.....	.....	.....	.....	.....	.....	015	.....	022	008	021	.....	.....	.....	006	.....	024	.....	.....	013	.....	021	.....	.....	016
− 80	.....	011	012	006	013	.....	025	.....	035	020	032	.....	.....	.....	023	016	035	007	006	020	.....	036	008	.....	029
− 70	.....	025	027	030	026	001	037	.....	051	032	045	.....	.....	008	042	043	048	025	014	037	010	058	028	.....	044
− 60	.....	040	050	063	041	025	055	010	077	044	075	.....	.....	022	072	080	071	035	028	057	029	088	050	.....	067
− 50	.....	062	086	100	057	047	082	025	122	058	122	.....	.....	038	111	127	108	052	053	080	067	128	076	002	115
− 40	001	099	139	153	093	074	124	048	191	080	186	.....	.....	054	161	174	154	086	087	118	125	182	120	007	189
− 30	019	150	214	223	134	117	184	082	280	114	255	005	.....	071	228	228	204	117	127	176	190	254	177	012	257
− 25	028	177	259	261	160	143	224	106	324	139	294	011	.....	079	265	263	235	133	151	212	221	295	205	019	291
− 20	037	212	310	303	196	179	264	135	365	168	334	020	002	090	306	303	271	154	178	250	258	343	235	028	332
− 15	050	255	362	346	245	223	308	173	413	206	379	036	007	101	350	351	316	189	230	295	302	397	276	046	385
− 10	086	307	422	387	300	272	363	236	480	256	436	084	018	115	401	409	389	242	360	350	359	452	327	078	445
− 7.5	122	338	457	405	328	300	397	281	520	281	471	120	025	127	431	445	432	275	420	380	390	482	357	101	482
− 5	185	372	500	423	356	330	435	345	568	310	501	172	032	148	468	481	478	312	469	420	428	521	389	134	519
− 2.5	335	402	547	335	380	388	480	428	626	342	532	265	041	170	512	525	525	356	520	470	477	557	434	175	551
0	471	426	607	297	388	446	539	551	678	365	540	378	045	180	568	575	565	375	550	536	540	567	472	214	560
+ 2.5	290	400	553	420	364	395	480	453	632	329	530	318	037	168	519	544	537	368	521	480	487	538	441	168	542
+ 5	146	365	505	429	327	335	440	362	583	293	500	208	023	152	470	510	481	335	454	433	443	497	397	132	498
+ 7.5	099	332	465	414	286	297	406	304	535	260	467	143	018	136	436	483	438	302	390	393	406	465	365	105	465
+ 10	072	302	427	381	245	265	375	258	497	231	437	107	013	123	410	456	404	273	339	358	373	436	335	085	428
+ 15	045	253	365	325	192	215	322	191	430	183	382	061	007	098	355	408	343	225	270	300	325	382	284	052	372
+ 20	032	213	308	285	166	178	277	139	371	147	331	039	002	080	304	363	294	185	218	254	284	331	242	034	336
+ 25	025	183	260	251	145	146	234	111	320	117	288	022	.....	066	264	322	246	151	181	216	244	283	207	021	310
+ 30	017	156	215	220	125	119	196	089	272	092	250	009	.....	056	226	282	208	123	155	181	206	240	179	014	281
+ 40	001	109	141	163	094	071	132	055	194	055	180	.....	.....	040	159	210	145	082	123	122	138	168	123	008	224
+ 50	.....	072	094	121	068	040	085	028	127	033	117	.....	.....	028	108	149	092	062	095	079	090	115	077	002	167
+ 60	.....	042	062	084	048	021	057	011	085	021	072	.....	.....	019	071	096	046	048	065	050	052	083	050	.....	110
+ 70	.....	023	037	048	030	001	043	.....	057	014	049	.....	.....	008	044	056	020	036	035	030	019	064	030	.....	065
+ 80	.....	010	019	014	014	.....	031	.....	040	008	035	.....	.....	.....	027	025	011	013	011	012	.....	047	009	.....	051
+ 90	.....	.....	005	.....	.....	.....	020	.....	025	004	026	.....	.....	.....	008	.....	008	.....	.....	.....	.....	032	.....	.....	042
+100	.....	.....	001	.....	.....	.....	008	.....	009	.....	015	.....	.....	.....	.....	.....	004	.....	.....	.....	.....	017	.....	.....	035
+110	.....	.....	.....	.....	.....	.....	.....	.....	.....	.....	005	.....	.....	.....	.....	.....	.....	.....	.....	.....	.....	001	.....	.....	021
+120	.....	.....	.....	.....	.....	.....	.....	.....	.....	.....	.....	.....	.....	.....	.....	.....	.....	.....	.....	.....	.....	.....	.....	.....	002
W	6.0	22.7	31.7	30.2	20.7	17.5	28.8	15.7	39.4	17.1	35.1	5.6	0.8	9.1	31.9	35.4	30.6	18.7	25.3	27.2	26.3	37.3	24.4	3.9	39.6
w.5	7	40	41	60	35	28	40	17	46	33	55	10	13	37	45	51	40	35	28	36	40	58	41	14	57
w.2	17	89	86	112	91	71	88	49	96	77	104	23	.....	.....	98	109	95	86	78	85	88	104	91	.....	110
n	2Pe	2N	3Pe	1Pe	2N	4Pe	4Pe	4Pe	3Pe	1N	1N	1Pe	1N	3Pe	3Pe	2Pe	1N	1N	1N	2Pe	1Pe	1N	5Pe	1Ce	1N
	.....	.....	1Pd	.....	.....	.....	.....	1N	.....	.....	.....	2N	.....	.....	.....	.....	.....	.....	.....	2Pd	.....	.....	.....	.....	4Pd	.....
	.....	.....	.....	.....	.....	.....	.....	.....	.....	.....	.....	.....	.....	.....	.....	.....	.....	.....	.....	.....	.....	.....	.....	2Pe	.....
	.....	.....	.....	.....	.....	.....	.....	.....	.....	.....	.....	.....	.....	.....	.....	.....	.....	.....	.....	.....	.....	.....	.....	1N	

TABLE 5C

Hδ PROFILES IN WHITE DWARFS (ABSORPTIONS × 10^3)

A	No. in Table 4																							
	3	5	6	7	9	10	11	13	15	16	17	19	22	23	25	26	27	29	34	35	36	38	41	42
−80	.....	001	.....	.....	.....	.....	006	.....	008	.....	.....	.....	.....	.....	.....	.....	.....	.....	.....	.....	.....	.....	.....	.....
−70	.....	006	002	.....	002	.....	015	.....	019	004	005	.....	.....	009	009	.....	.....	.....	009	012	002	.....	.....	.....
−60	.....	015	017	002	010	002	022	.....	030	010	020	.....	.....	023	020	010	.....	010	023	028	025	007	.....	008
−50	.....	029	040	026	020	015	037	015	044	017	047	.....	011	042	040	031	.....	044	040	051	050	031	.....	028
−40	.....	056	082	085	032	041	063	032	084	038	097	.....	024	079	076	066	010	072	074	089	089	064	.....	089
−30	012	104	154	170	053	082	111	059	170	074	167	008	038	147	149	118	048	108	129	144	153	115	007	162
−25	022	132	201	215	069	104	145	082	231	095	210	019	046	180	200	157	075	130	167	181	204	150	012	201
−20	032	166	262	262	093	132	186	112	290	121	258	031	056	237	256	212	102	154	214	221	257	195	018	242
−15	043	207	328	316	123	167	237	153	355	153	311	050	072	290	321	266	136	224	267	264	315	242	026	287
−10	061	260	397	380	175	216	298	225	431	194	365	082	091	350	383	327	175	343	333	315	378	290	050	342
− 7.5	093	283	440	416	210	245	335	268	478	223	395	111	103	385	414	368	198	391	370	347	414	316	070	384
− 5	149	314	485	450	257	281	374	320	529	253	425	160	114	424	445	423	225	432	410	381	453	348	093	438
− 2.5	236	349	530	424	295	327	416	390	585	290	468	239	126	471	476	489	256	465	455	416	507	387	128	487
0	405	388	576	330	305	374	461	527	654	315	500	328	139	525	491	540	270	495	495	455	522	426	161	510
+ 2.5	245	360	540	454	296	351	410	436	586	273	492	250	130	485	463	527	259	483	445	440	511	393	130	480
+ 5	168	330	496	435	266	306	370	350	536	238	460	171	116	447	431	473	242	438	395	410	483	357	091	447
+ 7.5	116	304	450	406	229	275	333	292	492	213	427	124	101	411	399	425	226	375	353	382	447	325	069	414
+10	087	278	412	378	200	250	302	235	450	188	396	091	088	378	365	380	208	327	320	355	418	296	055	385
+15	063	227	350	316	164	203	251	168	379	148	331	052	068	324	310	300	166	255	263	306	363	250	031	329
+20	045	187	291	262	132	164	208	128	312	117	276	031	053	274	260	243	133	197	218	259	317	212	016	284
+25	031	155	239	218	107	127	172	100	251	090	225	017	040	233	213	201	111	154	181	213	275	182	010	242
+30	018	128	194	180	085	099	140	077	193	069	183	008	030	197	166	166	091	124	146	167	236	150	004	205
+40	.....	086	123	115	054	062	090	044	110	035	118	.....	015	137	093	105	050	081	094	100	171	097	.....	148
+50	.....	051	071	058	032	035	058	018	063	023	066	.....	007	087	057	056	.....	043	058	057	116	050	.....	105
+60	.....	030	045	008	016	010	035	.....	034	014	033	.....	.....	048	035	020	.....	006	035	030	065	015	.....	071
+70	.....	015	024	.....	002	.....	019	.....	022	007	012	.....	.....	017	015	.....	.....	.....	020	012	024	004	.....	040
+80	.....	001	006	.....	.....	.....	010	.....	010	.....	.....	.....	.....	.....	.....	.....	.....	.....	004	.....	.....	.....	.....	015
W	5.3	18.1	26.6	24.2	12.4	14.2	20.3	13.7	28.8	11.9	24.9	5.1	5.3	24.7	23.7	22.1	9.9	20.6	21.5	22.3	28.4	18.7	2.8	27.2
w.5	7	37	36	45	29	30	33	17	36	28	43	10	30	39	43	32	35	30	33	42	47	38	12	42
w.2	19	79	76	82	65	66	73	45	70	64	83	25	.....	82	75	70	68	67	73	81	90	78	.....	89
n	1Pe	2N	3Pe	1Pe	2N	4Pe	4Pe	4Pe	3Pe	1N	1N	1Pe	3Pe	3Pe	2Pe	1N	1N	1N	3Pe	1Pe	1N	5Pe	1Ce	1N
	.....	.....	1Pd	.....	.....	.....	.....	1N	.....	.....	.....	2N	.....	.....	.....	.....	.....	.....	2Pd	.....	.....	.....	5Pd	.....
	.....	.....	.....	.....	.....	.....	.....	.....	.....	.....	.....	.....	.....	.....	.....	.....	.....	.....	.....	.....	.....	.....	2Pe	.....
	.....	.....	.....	.....	.....	.....	.....	.....	.....	.....	.....	.....	.....	.....	.....	.....	.....	.....	.....	.....	.....	.....	1N	.....

TABLE 5*D*

He PROFILES IN WHITE DWARFS (ABSORPTIONS × 10^3)

A	No. in Table 4																							
	3	5	6	7	9	10	11	13	15	16	17	19	22	23	25	26	27	29	34	35	36	38	41	42
−60	.....	.....	.....	.....	.....	.....	005	.....	.....	.....	.....	.....	.....	.....	.....	.....	.....	.....	.....	.....	.....	.....	.....	.....
−50	.....	002	002	011	007	007	016	001	008	002	010	.....	004	002	002	001	.....	.....	.....	013	010	006	.....	.....
−40	.....	014	028	043	026	025	028	023	022	010	034	.....	017	032	036	018	007	008	033	030	022	027	.....	008
−30	002	038	066	078	046	045	045	053	040	029	077	.....	032	060	090	044	021	042	063	050	047	058	.....	041
−25	009	059	098	102	058	059	060	069	066	044	113	008	039	087	131	077	030	068	086	066	078	078	003	069
−20	017	086	148	134	074	073	094	091	113	064	156	023	047	133	176	126	048	101	121	102	132	103	007	106
−15	031	122	213	196	095	110	136	128	176	090	207	044	056	194	228	182	082	140	177	165	205	144	015	153
−10	057	180	288	274	130	155	195	185	270	125	267	082	065	263	286	249	121	206	251	244	282	197	032	217
− 7.5	083	207	333	306	151	184	231	223	335	147	298	114	073	304	321	287	139	250	290	288	318	229	046	261
− 5	109	235	388	333	175	225	275	273	420	172	330	162	085	345	359	333	156	303	331	340	352	270	062	315
− 2.5	192	266	442	243	205	270	325	348	505	197	366	218	102	400	400	392	173	360	370	393	390	317	083	365
0	299	295	483	130	222	296	374	457	589	205	400	250	114	442	426	450	182	410	393	455	420	360	105	383
+ 2.5	137	272	458	266	216	279	335	374	518	193	394	207	105	400	414	439	167	385	368	381	403	335	085	375
+ 5	096	247	416	334	202	239	290	294	447	172	369	151	093	346	383	372	148	345	333	333	366	282	064	347
+ 7.5	077	220	368	325	183	200	245	241	397	150	332	105	083	302	339	315	132	279	295	297	328	245	045	303
+10	064	193	329	294	160	175	210	200	353	132	303	077	075	267	303	274	119	237	252	264	293	209	032	266
+15	042	144	258	238	120	138	155	140	278	099	243	040	060	213	248	208	095	181	186	208	234	156	015	212
+20	023	107	196	190	093	110	112	100	217	072	192	018	050	168	207	153	074	142	135	163	188	125	007	171
+25	012	080	143	149	074	087	082	073	166	049	147	005	042	128	166	108	056	095	099	127	147	101	003	136
+30	002	060	102	115	058	069	059	056	122	034	107	.....	035	093	119	073	038	051	072	098	113	077	.....	110
+40	.....	029	046	055	030	035	031	027	054	013	046	.....	021	036	048	027	013	010	039	052	059	035	.....	066
+50	.....	007	015	013	007	007	015	002	013	002	015	.....	004	006	002	001	.....	.....	018	022	024	006	.....	028
+60	.....	.....	004	.....	.....	.....	008	.....	.....	.....	.....	.....	.....	.....	.....	.....	.....	.....	007	.....	.....	.....	.....	004
W	3.5	10.1	16.2	15.4	8.6	9.5	10.2	11.3	17.8	6.7	15.6	4.2	4.4	14.6	16.8	13.7	5.9	12.1	13.8	14.3	16.0	11.6	1.6	14.2
w.5	6	28	30	37	29	24	23	15	23	27	35	13	30	27	36	25	30	22	28	24	32	24	13	29
w.2	20	55	56	68	66	55	49	42	50	54	63	27	.....	55	65	51	.....	49	54	53	60	57	.....	62
n	1Pe	2N	3Pe	1Pe	2N	4Pe	4Pe	4Pe	3Pe	1N	1N	1Pe	3Pe	3Pe	2Pe	1N	1N	1N	3Pe	1Pe	1N	5Pe	1Ce	1N
	.....	.....	1Pd	.....	.....	.....	.....	1N	.....	.....	.....	2N	.....	.....	.....	.....	.....	.....	2Pd	.....	.....	.....	.....	5Pd	.....
	.....	.....	.....	.....	.....	.....	.....	.....	.....	.....	.....	.....	.....	.....	.....	.....	.....	.....	.....	.....	.....	.....	1Pe	.....
	.....	.....	.....	.....	.....	.....	.....	.....	.....	.....	.....	.....	.....	.....	.....	.....	.....	.....	.....	.....	.....	.....	1N	.....

TABLE 5*E*

Hζ PROFILES IN WHITE DWARFS (ABSORPTIONS × 10^3)

A	No. IN TABLE 4																			
	3	5	6	7	9	10	11	13	16	17	19	23	26	27	29	34	36	38	41	42
−50	.....	.....	.....	.....	.....	.....	.....	.....	.....	.....	.....	.....	.....	.....	.....	.....	.....	035	.....	.....
−40	.....	.....	.....	.....	.....	.....	.....	.....	002	014	.....	.....	.....	.....	.....	.....	006	085	.....	.....
−30	.....	.....	006	002	010	.....	.....	.....	012	045	.....	.....	.....	.....	.....	015	023	138	.....	.....
−20	.....	020	057	024	032	003	030	011	034	099	006	020	044	004	005	055	055	149	.....	015
−15	.....	046	098	059	048	019	047	040	051	135	020	040	086	016	020	088	090	160	015	050
−10	.....	082	156	113	069	047	097	082	074	175	043	090	133	035	078	141	137	171	030	093
− 5	010	127	241	154	096	087	125	149	094	223	081	175	203	064	162	202	207	183	045	152
0	113	150	333	112	114	141	230	286	100	285	138	248	290	085	205	246	248	193	064	220
+ 5	015	136	240	165	103	102	135	199	095	247	090	210	183	052	140	204	228	185	038	196
+10	.....	103	158	093	079	063	091	135	075	183	048	156	102	030	089	140	171	171	020	141
+15	.....	067	098	037	051	026	059	082	053	134	028	102	055	017	061	092	101	158	007	096
+20	.....	034	050	019	035	003	030	033	031	092	011	054	022	005	027	056	058	147	.....	056
+30	.....	.....	004	004	010	.....	.....	.....	008	039	.....	.....	.....	.....	.....	015	023	135	.....	011
+40	.....	.....	.....	.....	.....	.....	.....	.....	001	010	.....	.....	.....	.....	.....	.....	005	084	.....	.....
+50	.....	.....	.....	.....	.....	.....	.....	.....	.....	.....	.....	.....	.....	.....	.....	.....	.....	038	.....	.....
W	0.5	3.8	8.1	4.5	3.5	2.4	4.2	4.9	3.5	8.9	2.3	5.6	5.5	1.5	4.0	6.6	7.4	3.4	1.0	5.5
w.5	5	25	19	23	26	16	13	15	31	28	13	20	16	15	16	23	24	17	16	22
w.2	8	39	37	.....	.....	.....	.....	.....	.....	53	.....	34	33	.....	.....	42	43	.....	.....	.....
n	1Pe	2N	3Pe	1N	2N	4Pe	2Pe	1Pe	1N	1N	1Pe	3Pe	1N	1N	1N	3Pe	1N	5Pe	1Ce	1N
.....	.....	.....	1Pd	.....	.....	.....	.....	1N	.....	.....	2N	.....	.....	.....	.....	2Pd	.....	.....	2Pd	.....
.....	.....	.....	.....	.....	.....	.....	.....	.....	.....	.....	.....	.....	.....	.....	.....	.....	.....	.....	1N	.....

TABLE 5*F*

Hη PROFILES IN WHITE DWARFS (ABSORPTIONS × 10^3)

A	No. in Table 4							
	5	6	11	17	26	34	41	42
−25	.....	.....	.....	017	.....	.....	.....	.....
−20	005	018	.....	045	013	002	.....	013
−15	021	040	003	063	035	024	.....	029
−10	042	083	044	087	061	057	005	048
− 5	069	120	095	131	099	099	027	085
0	107	149	151	175	160	172	050	125
+ 5	080	127	102	142	088	118	022	107
+10	042	081	049	101	047	077	007	062
+15	015	035	008	070	025	042	.....	028
+20	002	016	.....	052	008	009	.....	010
+25	.....	.....	.....	022	.....	.....	.....	.....
W	1.9	3.3	2.2	4.8	2.7	3.0	0.6	2.6
w.5	16	21	14	22	13	15	10	17
w.2	.....	.....	.....	.....	.....	.....	.....	.....
n	2N	1Pe	1Pe	1N	1N	2Pe	1Ce	1N
.....	.....	1Pd	.....	.....	.....	1Pd	1Pd	.....

weaker lines than the hotter stars; at present, no theoretical explanation can be offered except a change in the H abundance, formation of molecules, or a new source of opacity which appears below $U - V = -0.5$ mag. and enormously weakens the lines.

The Balmer decrement is rather flat for the lower series members, as can be seen in Figure 7 for 40 Eri B. Tables 5*A*–5*F* provide reliable data for the decrement for many other stars; the measures for Hβ are the most uncertain, usually

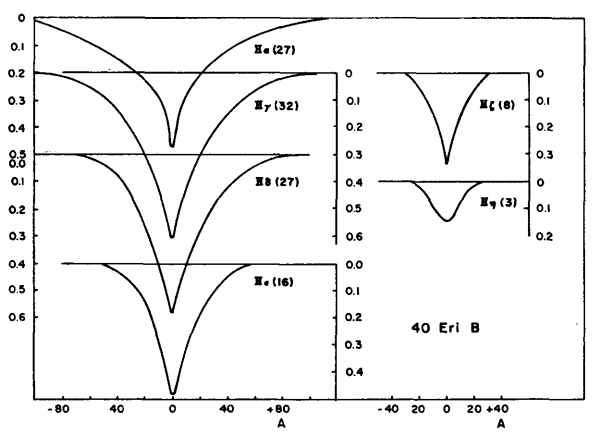


FIG. 7.—Line profiles of Balmer series members in 40 Eri B. Equivalent widths in parentheses. The decrement is rapid because of overlapping beyond Hδ.

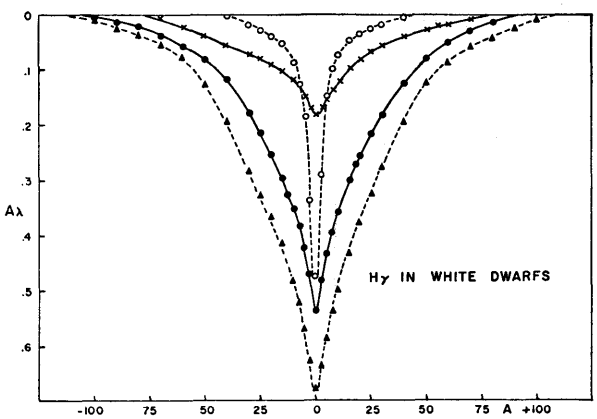


FIG. 8.—Profiles of Hγ in various white dwarfs. *Triangles*, SA 29–130; *dots*, W 1346; *open circles*, L870-2; *crosses*, HZ 43. Note relative sharpness in the cooler star L870-2 as compared with the hot star HZ 43.

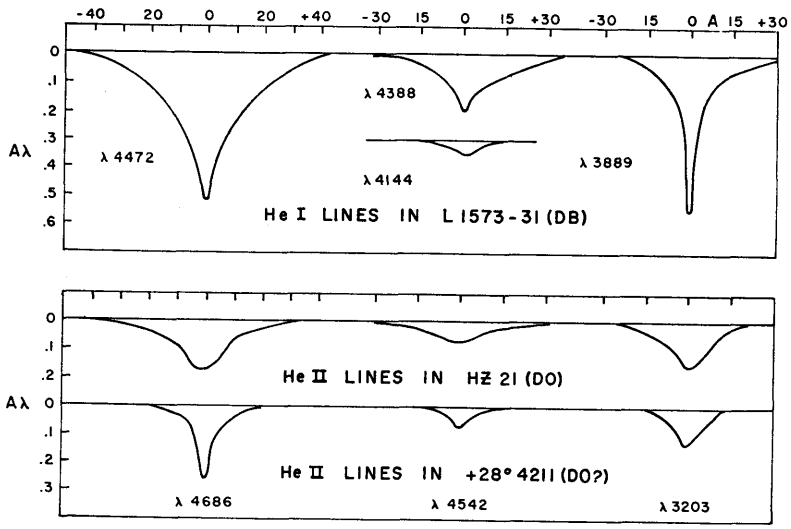


FIG. 9.—Helium lines in the white dwarfs. L1573-31 is DB, HZ 21 is DO, +28°4211 may be intermediate sdO or DO. Note the very great broadening of λ 4144 and the sharp core of λ 3889.

based only on one or two plates of the N series. Beginning at Hγ, the equivalent widths decrease, largely because of overlapping wings; Hζ/Hγ ranges from 0.3 to 0.1, and, by Hη, the lines are only 10 per cent deep; the Balmer discontinuity effectively sets in by upper quantum number $n = 10$.

Intensities and profiles of the He II and He I lines in the DO and DB stars will require very detailed study. The two objects classified as DO are quite different; +28°4211 may not be a white dwarf, but a faint hot subdwarf. Both show λλ 4686, 4542, 3203 of He II, corresponding to very high temperature. HZ 21 has very weak hydrogen lines and very broad He II, e.g., w.5 = 18 A for λ 4542. The temperature may be about 50,000° K and the bolometric correc-

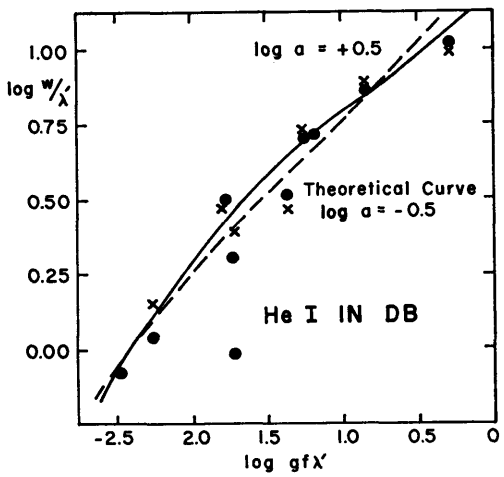


FIG. 10.—Observed line strengths and curve of growth for He I in the DB stars; L1573-31 (*dots*) and L930-80 (*crosses*). The solid line is a theoretical curve of growth for log $a = -0.5$; the dashed line is for log $a = +0.5$, $\lambda' = \lambda/4200$ A.

tion large. The pressure broadening of He I in HZ 21 is less than in the DB star L 1573-31. The latter, as well as L 930-80 and LDS 749B, show very interesting behavior of the He I lines, which are very strong and generally very broad, the widths dependent on the nature of the line. Figure 9 shows some of the varieties of line profile observed; Table 6 contains the tabular data for helium-line profiles so far observed. The equivalent widths and actual half-widths are remarkably poorly correlated, showing that the effective collisional damping varies greatly from line to line, depending on n and on the nature of the spectroscopic term. By inspection, one obtains the impression that a "low-pressure" core is superposed on the broadened wings of λλ 4472, 4026, 3965, 3888 in the DB stars, with λ 3888 in particular being surprisingly sharp. In spite of these differences, a single curve of growth can be plotted for the He I lines in the DB stars, as shown in Figure 10. Here log W/λ is plotted for the average of both L1573-31 and L930-80 (to increase the accuracy) against the theoretical gf-values

TABLE 6

PROFILES OF HELIUM LINES IN WHITE DWARFS (ABSORPTIONS × 10^3)

Line	He I λ 4713			He II λ 4686		He II λ 4542		He I λ 4472					He I λ 4438	He I λ 4388		He I λ 4144
No.	32	37	40	20	41	20	41	20	32	37	40	41	32	32	40	32
Star	L 1573-31	LDS 749B	L 930-80	HZ 21	+28°4211	HZ 21	+28°4211	HZ 21	L 1573-31	LDS 749B	L 930-80	+28°4211	L 1573-31	L 1573-31	L 930-80	L 1573-31
A																
−50								002								
−40				004				008	004		024					
−30				014		005		015	042	005	059			002		
−20	002			034		016		032	125	027	108			025	016	
−15	008		003	046	015	025	005	048	186	046	146	012		036	030	
−10	025	005	020	066	026	036	009	077	259	077	189	024		060	059	007
− 5	084	067	093	112	070	051	020	115	350	138	245	039	043	105	104	021
− 2.5	140	101	174	136	145	066	040	120	425	210	345	044	082	137	149	042
0	168	107	240	144	260	072	058	125	521	301	473	045	111	205	168	049
+ 2.5	152	087	190	133	156	056	045	116	393	247	328	044	098	157	144	042
+ 5	107	035	117	116	086	043	033	108	335	180	252	038	068	131	117	027
+10	045	006	044	075	042	031	014	062	236	083	171	025		094	069	007
+15	018		010	043	017	022	006	040	162	039	126	013		069	036	
+20	004			027	006	016		033	118	020	093			050	019	
+30				009		004		019	057	007	048			016		
+40								008	006		017					
+50																
W	2.3	1.2	2.7	3.7	2.2	1.8	0.7	4.0	10.9	5.0	10.8	1.0	0.9	3.4	3.1	0.9
w.5	11	10	9	19	10	16	6	23	19	11	11	22	10	14	16	10
w.2							14		44	26	42					
Plates	2N	2N	1N	2N	1Ce, 4Pd, 2N	2N	1Ce, 4Pd, 2N	2N	2Pe, 2N	2N	2Pe, 1N	1Pd	1N, 2Pe	2N, 3Pe	1N, 2Pe	2N

Line	He I λ 4121		He I λ 4026				He I λ 3965			He I λ 3889				He I λ 3819		He II λ 3203	
No.	32	40	20	32	37	40	32	37	40	20	32	37	40	32	37	20	41
Star	L 1573-31	L 930-80	HZ 21	L 1573-31	LDS 749B	L 930-80	L 1573-31	LDS 749B	L 930-80	HZ 21	L 1573-31	LDS 749B	L 930-80	L 1573-31	LDS 749B	HZ 21	+28°4211
A																	
−50																	
−40						010											
−30			006	025		040						004		014	005		
−20			017	068	068	090				003	010	019		038	020	013	
−15	003		023	098	014	125	016		010	013	037	034	035	060	030	036	
−10	014		032	135	041	175	036	010	045	022	103	068	095	088	046	052	018
− 5	029	037	052	191	125	245	104	041	120	032	170	145	150	130	068	086	057
− 2.5	068	070	058	242	182	305	163	069	164	038	245	239	235	155	082	115	080
0	118	123	060	398	190	430	315	096	290	044	535	301	525	180	090	157	120
+ 2.5	085	091	058	243	168	235	170	080	180	035	248	240	290	157	088	144	100
+ 5	051	066	050	161	095	145	117	043	155	023	159	150	205	135	075	123	079
+10	018	010	030	090	032	110	054	013	070	012	087	064	110	084	049	054	027
+15	002		020	062	012	080	026		030	004	055	031	080	055	033	020	
+20			014	048	002	060	010			001	043	016	055	039	022	005	
+30			003	023		027					015	005		015	007		
+40						001											
+50																	
W	1.1	1.4	1.8	6.9	2.6	7.2	3.0	1.0	2.8	0.8	4.5	4.3	5.1	4.8	2.5	2.7	1.6
w.5	7	9	21	8	11	10	6	8	9	15	4	10	5	19	21	14	12
w 2					20	35	16				18	22	20				
Plat	2N, 3Pe	1N, 1Pe	2N	2Pe	2N	1N, 1Pe	1N, 3Pe	1N	1N, Pe	2N	N2, 3Pe	2N	1N, 1Pe	2N	1N	1N	2N

(Trefftz *et al.* 1957 and other sources). The theoretical curve of growth for log $a = -0.2$ provides a good fit; the lower part, up to log $W/\lambda' = +0.75$, is fairly well represented by a straight line. Note that the quantity λ' is introduced to reduce all data to λ 4200, i.e.,

$$\log gf\lambda' = \log gf\left(\frac{\lambda}{4200}\right), \tag{3.1}$$

$$\log \frac{W}{\lambda'} = \log W\left(\frac{\lambda}{4200}\right)^{-1}. \tag{3.2}$$

The He I lines increase as the square root of gf up to 5 A equivalent width, requiring an enormous damping constant. This is confirmed by the fact that

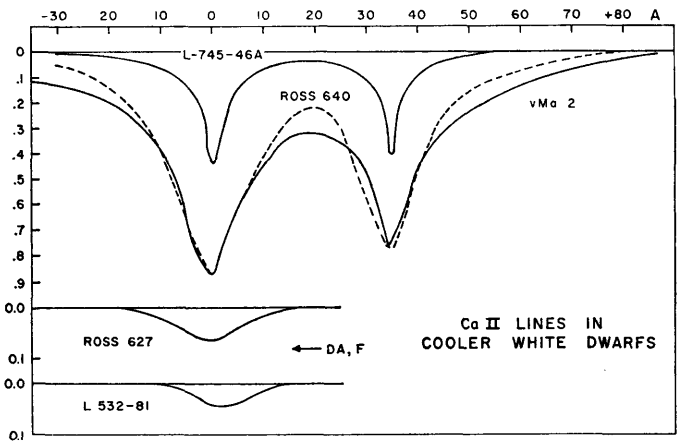


FIG. 11.—Line profiles of Ca II in white dwarfs of the following types: DA, F (R627, L532-81); DF (L745-46 A); DFp (R640); DG (vMa2). The zero point of the wave-length scale is at λ 3933.

the observations fit curves of growth with log a from $+0.5$ to -0.5, i.e., Γ/γ_{cl} from 800 to 8000. The main portion of the line is unsaturated, in spite of great strength. The width of the He I lines indicate that even in the absence of linear Stark effect the collisional broadening is very large. The shock-tube results of Seay (1957) show some of the variety of broadening effects and also the rapid cutoff of the high series numbers of He I. They do not reproduce, however, the sharpness of λ 3889, presumably the result of metastability and the possible existence of a circumstellar envelope.

A few white dwarfs have metallic lines, notably Ca II in the DA, F, and DG stars, and Fe I in vMa 2. The observation and analyses of these has only begun; the stars are faint, and few of the undoubtedly large number of red white dwarfs are yet known. The available results on the strength of the K line indicate an unexpectedly large scatter as a function of color. While the photoelectric colors are few, it is surprising to find strong H and K and no hydrogen in an apparently

white star like Ross 640, DFp, and quite weak K and strong hydrogen in the yellowish star Ross 627, DA, F (Greenstein 1958). In addition, Ross 640 has lines of Ca II as strong as those in vMa 2 but shows strong Mg I and not Fe I; vMa 2 has strong Fe I and very weak Mg I. Table 7 gives the available profiles of Ca II; for such stars as vMa 2, L 745-46A, and R 640 the lines are strong and broad enough to overlap. In consequence, while the profiles are accurate, the equivalent widths are quite uncertain. Figure 11 shows characteristic profiles; L 745-46A has relatively sharp and weak Ca II and no hydrogen; R 640 has less extended wings than vMa 2. The DA, F stars have relatively sharp hydrogen lines and a weak diffuse K line, only marginally visible.

TABLE 7

CA II LINE PROFILES IN WHITE DWARFS

A	vMa 2	L 745-46A	R 640	R 627	L 532-81
−30	0.133	0.001	0.057	.....	.....
−25	.159	.016	.083	.....	.....
−20	.197	.021	.135	.....	.....
−15	.276	.028	.224	0.009	.....
−10	.391	.102	.384	.026	0.004
− 8	.454	.095	.487	.034	.010
− 6	.550	.084	.598	.044	.018
− 4	.745	.143	.710	.056	.025
− 3	.795	.183	.761	.060	.030
− 2	.828	.235	.802	.062	.035
− 1	.859	.365	.846	.065	.041
λ 3933 = 0	.885	.425	.880	.067	.044
+ 1	.845	.412	.840	.065	.045
+ 2	.776	.320	.775	.061	.045
+ 3	.725	.212	.718	.053	.045
+ 4	.668	.174	.671	.046	.043
+ 6	.595	.117	.583	.036	.040
+ 8	.512	.086	.495	.026	.027
+10	.450	.065	.416	.018	0.012
+15	.345	.039	.275	0.004	.....
+20	.322	.050	.218	.....	.....
+25	.360	.050	.305	.....	.....
+30	.488	.108	.555	.....	.....
+32	.595	.160	.690	.....	.....
+33	.670	.201	.738	.....	.....
λ 3968 = +34	.745	.318	.768	.....	.....
+35	.735	.400	.762	.....	.....
+36	.700	.235	.725	.....	.....
+37	.650	.169	.678	.....	.....
+38	.590	.136	.626	.....	.....
+40	.455	.093	.480	.....	.....
+45	.326	.036	.250	.....	.....
+50	.250	.040	.158	.....	.....
+55	.180	0.010	.112	.....	.....
+60	.128	.....	.078	.....	.....
+70	.065	.....	.033	.....	.....
+80	0.025	.....	0.010	.....	.....
Equiv. width K	(25.1)	4.2	19.7	1.1	0.7
Equiv. width H	(20.2)	2.7	16.1	.....	.....
Plates	6Pe, 2N	3Pe, 2N	1Pe, 2N	1Pe, 2N	2Pe, 1N

Spectrophotometry of the white dwarfs is now well under way at Palomar, the foregoing tables and figures representing the data available as of August, 1958. A first theoretical analysis has been given by Greenstein (1958), and an analysis of vMa 2 has been completed by Weidemann (1960). I shall list some of the major unsolved problems suggested by the observation and interpretation of white dwarf spectra.

1. Why is there a complete separation of DA (hydrogen) and DB (helium) spectra? Does this represent a genuine abundance difference?

2. Why do the lines in the DA stars suddenly sharpen and disappear at lower temperatures? No trace of hydrogen is found in stars of color classes f and g, in contrast to main-sequence stars, where hydrogen lines persist to type K. The decline of Balmer line intensity is extraordinarily abrupt near $U - V = -0^m3$. Does this represent molecule formation or a new source of opacity, very sensitive to pressure and temperature?

3. Is the formation of metallic molecules responsible for the weakness of metallic lines in cool DA stars and for the anomalous behavior of Mg, Fe, and Ca observed in the DA and DF stars? Is there gravitational separation, or are the abundances in fact peculiar?

4. What is the origin of the spectra of those stars which, over a wide variety of colors, show an essentially continuous spectrum? Do these require a new continuous opacity source, or do they require such a fantastically high atmospheric pressure that no lines or bands exist?

5. What is the origin of the Minkowski bands (λ 4135, etc.).

6. More generally, will it be possible to derive the abundances of H, He, and the metals in the atmospheres of white dwarfs in view of the uncertainties mentioned above?

§ 5. THE HOT SUBDWARFS

A new and very interesting class of stars has been recognized spectroscopically, largely by Greenstein and by Münch, which fall at the high-temperature edge of the HR diagram and have luminosities greater than the white dwarfs and below the horizontal-branch type of very blue stars. A weak indication that they may evolve into white dwarfs of type DB comes from the general similarity of their helium-line spectrum at low dispersion. Very little has yet been published on these stars. A list of several hundred wave lengths and identifications of the relatively sharp, weak lines is in preparation by Münch and Greenstein. Brief descriptions of HZ 44 (Greenstein 1954*b*) and of $+75°325$ (Gould, Herbig, and Morgan 1957; Elvius and Sinnerstad 1958) have been published. The list in Table 8 contains some of the brighter members with a brief description of their spectra. At low dispersion the characteristic features are strong He II, broadened and often weak H and strong He I (all that is visible in faint stars like HZ 1 and HZ 3). At higher dispersion the spectra of some prove to be very rich, with hundreds of lines from levels of very high excitation in N III, Si IV, Ne II, and

N II. While not all lines are equally sharp, the sharpest seen at 10 A/mm rival those in any O or B star known. The He II, He I, and H show a wide variety of broadening. The presence of the sharp lines distinguishes these hot stars from the white dwarfs, as does the smaller pressure broadening.

The very blue star +75°325 seems to be very hot and has few sharp, weak lines. HZ 1 and HZ 3 can be studied only at 38 A/mm but can be distinguished from white dwarfs by a few characteristic lines of N III and by the fact that white dwarfs do not show H and He in the same spectrum. For this reason, +28°4211 is hard to classify—it may be an extreme subdwarf O (sdO) or a very hot DO. It shows no sharp, weak lines, however, at any dispersion. HZ 21, DO, has much greater line broadening and cannot be confused with an object like +75°325, which it resembles only in having very strong He II. A low-dispersion spectrum of HZ 44, a typical hot subdwarf, is shown in Plate III.

TABLE 8

PRELIMINARY LIST OF HOT SUBDWARFS

Star	α(1950)	δ(1950)	Type	Spectral Characteristics
HZ 3	$3^h50.8$	+10°36	sdB	He I, H strong; N III, Si IV
HZ 1	4 47.3	+17 36	sdO	Very hot; He II, He I>H; N III, Si IV
+75°325	8 04.9	+75 06	sdO	Very hot; He II>H, He I; N IV> N III; Si III; few lines
+25°2534	12 35.0	+25 20	sdOp	H, He I, He II. Ca II weakly present; peculiar
HZ 44	13 21.3	+36 23	sdO	He II<H, 400 lines measured; N III ≈ N II; He I, Ne II, Si IV, Si III
HD 127493	14 29.5	−22 26	sdO	Very hot; He II>H; N III>N II; Si IV, Si III; many lines
+25°4655	21 57.4	+26 12	sdO	Hot; He II>H; N II>N III; Si III, C III; Ne II strong; very many lines

A complete analysis of these stars will involve many new problems. The broadening and line strengths of H and He II in HZ 44 have been studied by Münch (1958) who derives the very high temperature of 35,000° K, log $P_e \approx +4.5$, a helium abundance of $Y = 0.25$, a surface gravity near 10^6, and a radius of 0.27 $R \odot$. Such a star need not be completely degenerate. One interesting observational characteristic is the small rotation; since HZ 44 is at least ten times smaller than a main-sequence star, its rotational velocity should have increased by a factor of 10 during its evolution downward, if the change had occurred without loss of angular momentum. Thus, either the ancestral star was of population II (which has, in general, small rotation), or the evolution was accompanied by loss of mass preferentially carrying away large quantities of angular momentum.

One may expect evolution through the hot subdwarf region toward the white dwarfs, for population II stars. The "horizontal branch" in a globular cluster

like M13 is richly populated and, in fact, inclines downward toward very blue stars with $M_v \approx +2$. It is probable that these branches represent the tops of sparsely populated, nearly vertical sequences (not necessarily coincident). Parts of the general picture advanced by Vorontsov-Velyaminov (1953) are quite relevant here; the dying stars appear to be concentrated at the extreme high-temperature edge of the spectral sequence, and the brightest white dwarfs are also the hottest. The relations between the various types of faint blue stars, hot subdwarfs, old novae, and nuclei of planetary nebulae must still be explained. We do not know the evolutionary tracks in the dying stages of population I, but, since this population contains white dwarfs, it seems probable that at least some of its members traverse the hot subdwarf region. At present we cannot differentiate the two populations among the subdwarf O and B stars. Since large numbers of the faint blue stars were found by surveys at the galactic pole, some are certainly in population II. On the other hand, HZ 1 and HZ 3 are near the galactic plane. The radial velocities are unfortunately not conclusive. The measured velocities have a dispersion of about 30 km/sec, large compared to B stars of population I and like old population I. The proper motions are mostly unknown but seem not to be large.

§ 6. FAINT BLUE STARS

Under faint blue stars I group the large variety of substantially unexplained types of high-temperature spectra below the main sequence. Candidates for this group include the "horizontal-branch stars," which are subluminous if earlier than B8. Greenstein (1956) has given a preliminary description of the results of an investigation of the spectra of the Humason-Zwicky stars, and further unpublished data exist. In particular, new groups of blue stars have been found by Feige (1958) and by Iriarte and Chavira (1957) from colors. Spectra of some brighter stars found by Slettebak (private communication) show the normal A stars to a considerable height above the galactic plane and, in addition, peculiar types of A stars with weak or no lines of Ca II and Mg II. This phenomenon is shown most sharply by my own spectra of the very blue stars found by Feige. A superficial classification at 180 A/mm gives a type for many stars of A0p or B9p, that is, weak or no Ca II and He I and no Mg II. Another impression given by these spectra is that the Balmer lines—the only features—are surprisingly sharp, with about 15 members visible, i.e., somewhat above normal surface gravity. It seems, in fact, probable that these are very weak-line, subluminous B stars, possibly related to the horizontal-branch type objects. The bluer of these have shallow H-line profiles, almost certainly indicating a high temperature. Nevertheless, He I, if it becomes visible, remains very weak. Certainly for the hotter stars a designation of sdB is justified, but the spectra do not show the many weak lines that are seen in the sdO. The excessively large Balmer jump makes it possible that an abnormal atmosphere exists for these stars. Some examples are given in Plate III, which contains several peculiar Feige stars, a white dwarf, and, for contrast, the normal high-latitude popula-

tion I spectroscopic binary, HZ 22. Note the large Balmer jump in Feige 113, type B8p, no Mg II and very weak He I lines. Feige 84 shows stronger He I but still a large Balmer jump and, in the strength of λ 4388, signs of low luminosity. Both these stars have hydrogen lines visible to $n = 15$. The normal star HZ 22 shows weaker H lines, stronger and sharper He I lines, and only a small Balmer jump. The star Feige 95 is clearly hotter and might be best called sdB. The hydrogen lines are more diffuse, the last member visible being $n = 10$, and the He I lines are appreciably pressure-broadened compared with HZ 22. These stars cannot be confused with the sdO star HZ 44, which is much hotter, has broader and weaker H lines (last line H8 or H9), no Balmer jump, and very strong He I lines.

Luyten and Miller (1951) conclude that the mean luminosity of the Humason-Zwicky stars is near 0 mag.; Greenstein (1956) finds about +1. Insufficient knowledge of the spectra, velocities, and proper motions prevents us from ascribing given objects to the horizontal-branch or subdwarf groups. Programs for the measurement of the $B - V$, $U - B$ colors and of the spectra are under way at the Mount Wilson and Palomar Observatories; Luyten has observed the proper motions of the Feige stars. The large numbers of very faint blue stars found near the north galactic pole by Iriarte and Chavira and their photoelectric colors (Iriarte 1958) also indicate that the blue stars of the halo will provide many unusual types of objects. So far, the following types have been recognized among the faint blue stars in the polar caps: white dwarfs; hot subdwarfs of sdO type; intermediate subdwarfs, sdB; possible horizontal-branch dBp and dAp; and "runaway" stars of population I.

The globular clusters contain a few blue stars above the horizontal branch, which are subluminous by about 1 mag. at B2, and more at earlier types. The spectra are unusual in the strength and sharpness of certain He I lines, including λ 4438 and λ 3926 starting from the 2^1P^o level; these lines are usually broad and weak in normal B stars. The lines of N II are also strong, in Barnard 29 in M13 (Münch and Greenstein, unpublished). These phenomena may be connected with abnormally low surface gravity or with an extended envelope. An analysis of two such stars has been completed by G. Traving (unpublished).

Münch has obtained spectra of horizontal-branch stars to the left of the RR Lyr gap in several globular clusters. They are outstanding in the sharpness of the H lines, larger Balmer jump than expected for the colors, and absence of other lines. This description, kindly given in advance of publication, confirms the assignment to the horizontal branch of many of the apparent A-type stars found in the galactic halo.

§ 7. THE NUCLEI OF PLANETARY NEBULAE

In the course of study of the 48-inch Palomar Schmidt plates, a number of new, large, planetary nebulae of very low surface brightness were discovered. The central stars were quite blue and ranged from 11 to 17 mag. Twelve have

been observed so far, spectroscopically, by Greenstein and by Minkowski. Abell deduced luminosities, based on a method due to Shklovski, ranging from $M_v = 0$ to $M_v = +8$. The very low luminosities have been confirmed spectroscopically; if hydrogen lines are present, they are very weak and shallow, with Hζ the last line visible even in the highest-luminosity stars. One star, Abell 36, is almost identical with $+28°4211$, with an $M_v \approx +3$. Others like Abell 7 and 31 have such broad, shallow lines that a luminosity near $M_v = +8$, nearly that of a white dwarf, seems reasonable. However, the most extraordinary feature is the very high temperature indicated for Abell 30 and Abell 78. In these stars and weakly in the central star of NGC 246, lines of O VI are the strongest emission features. Other emission lines include He II, C IV, O V, and a few sharp absorption lines of C IV are also visible. The O VI emission is extremely strong and requires 79-ev excitation in Abell 78; apparently a line at 127-ev excitation is also present in Abell 30. Thus these stars would be among the hottest stars known, perhaps twice as hot as the nuclei of ordinary planetary nebulae.

These faint planetaries and their nuclei, therefore, may represent an evolutionary stage preceding that of the white dwarfs. The high temperatures require a large bolometric correction, so that even the objects of $M_v = +8$ do not lie far below the horizontal-branch stars. The nucleus of Abell 78 must lie far above the horizontal branch, since its $M_v \approx 0$. Such objects must have a very short life-span; the stages preceding them are unknown.

§ 8. THE F AND G SUBDWARFS

That region of the HR diagram of population II apparently to the left and below the main sequence, beginning at equivalent spectral type late A and extending to middle G, has been well investigated recently by Chamberlain and Aller (1951), Roman (1954, 1955), and Greenstein (1954*b*, 1956). Colorimetrically, these stars are recognizable by their ultraviolet excess, pointed out by Roman (1954) and explained by Schwarzschild, Searle, and Howard (1955) as caused by the weakness of the lines, especially in the blue and ultraviolet regions of the spectrum. The characteristic feature of the spectra of these stars is this extreme weakness of metallic lines for the temperature given by the star's color and level of excitation and ionization. There seems to be little doubt that the temperatures of these objects place them among the late F and G stars, while, at first glance and low dispersion, the strength of the metallic lines would have indicated a classification of type A. The hydrogen lines are strong and have relatively sharp and deep cores. Turbulence must be small, from the few data given so far by curves of growth and from the visual appearance of extreme line sharpness. Rotation is small or absent, and spectroscopic binaries are rare or absent. Several visual binaries are found to have two components subdwarfs (e.g., HD 219617, a close double, and the wide pair, HD 134439 and 134440). Greenstein suspects that $-3°2525$ is a spectroscopic binary.

The studies of Chamberlain and Aller (1951) and Burbidge and Burbidge

(1956) showed that the most extreme stars of this class have a hydrogen/metal ratio, A, from three to thirty times that of normal population I stars. Investigation by Aller and Greenstein (1960) of HD 19445 and HD 140283 gives a value of A greater by a factor of 100 than in the sun. Other extensive quantitative studies by Aller and Greenstein and by Unsöld (see Baschek 1959) give not only the change in log A but possible differences between the relative abundances of the various metals. In addition, Greenstein is obtaining spectra at 18 A/mm of 80 F and G subdwarfs for velocity, possible binary nature, and detailed study of line weakness and spectral type. Only one definite subdwarf velocity-variable has been found so far. In view of the current active state of research in this field, it does not now seem profitable to undertake a general review.

The kinematic properties of these stars are those of the most extreme old population II. Miss Roman (1954) finds the mean eccentricity of the galactic orbits to be 0.9, the perigalactic distance 2 kpc. The distribution perpendicular to the galactic plane resembles that of the RR Lyr stars, with a scale height of about 3000 psc. The low metal abundance can be interpreted as reflecting either the metal-poor situation during the earliest stages of star formation or a steep gradient of composition in the z-co-ordinate. Greenstein (1956) found the degree of line weakness, estimated visually, to be well correlated with space motion. The ordinary high-velocity or mild "weak-line" stars show a mean tangential velocity of 57 km/sec, the "subdwarfs" with intermediate line weakness 163 km/sec, and the extremely weak-line "subdwarfs" with 254 km/sec.

It is not established that the majority of these stars are, in fact, subluminous. The situation in the globular clusters is still uncertain. Trigonometric parallaxes are small, and only a dozen are measured; Roman (1954) gives a mean M_v between +4 and +5; Greenstein (1956) finds them to lie about 1.5 mag. below the main sequence. But much depends on the systematic accuracy of the classification. It should be remembered that these objects were originally called "intermediate white dwarfs" of type A and have since been moved to much lower temperatures, corresponding to F or G stars. Figures 3, 4, and 6 in Greenstein (1956) show the present stage of uncertainty. If photoelectric colors alone are used and if corrections are applied for the difference of line blanketing between subdwarfs and main-sequence stars, the subdwarfs are moved about +0.08 in $B - V$ color to the right, where most are less than 1.0 mag. below the main sequence, or on it (Melbourne 1959, 1960).

The outstanding question in the analysis of these subdwarfs is the abundance ratio of hydrogen to the metals. We have no information on masses, and therefore g must be treated as a free parameter. In addition, the temperature is only poorly determined, since there is insufficient range in ionization potential to provide (T, P_e) uniquely. The mean level of ionization as compared with the sun is given, and a fairly wide range of parameters (T, P_e) is then open. The excitation temperature gives a rough indication, and the colors are invaluable especially because of the small line blanketing. In fact, computations of emer-

gent flux combined with the absolute energy distributions observed by Code and by Melbourne (1959, 1960) provide the best values of T. At the (T, P_e) values so far indicated, H^- is the source of opacity, so that the abundances should be determinable. No other suggested source of opacity seems important, although, if one existed, it would weaken the metallic lines and result in a spuriously low metal abundance. It is difficult to see what other opacity sources could exist at temperatures higher than the sun and at similar pressures. No evidence has been found for high abundances of molecules or radicals (and if H/M is large, these should not be expected).

A brief survey of subdwarfs of other spectral types reveals two interesting facts—A-type subdwarfs are rare or absent, and few stars of types late G, K, or M show very weak lines.

Among the very high-velocity stars near the sun, stars which can be classified A are rare or absent. (The halo A stars are probably horizontal-branch stars.) Stars earlier than standard F or G subdwarfs should have very weak neutral metallic lines, relatively stronger lines of ionized metals, and λ 4481 of Mg II. The actual stars found, like λ Boo, studied by Burbidge and Burbidge (1956), are atypical, in that the velocity is only moderately high, rotation is present, but the metal abundance is fairly low. It is probable that the brighter members of the original subdwarf sequence have already evolved (as have stars earlier than F in globular clusters). There should then exist subgiant or giant analogues of the very weak-line subdwarfs, with very weak lines and ultraviolet excesses. None have yet been detected, unless the so-called dwarf RR Lyr stars, like SX Phoenicis, represent this stage. SX Phe has a very short period, a luminosity near +4, and relatively strong ionized lines. Objective-prism or three-color photometry might reveal this group among the fainter stars. Miss Roman's catalogue of high-velocity stars (1955) contains a number of subgiants with ultraviolet excess. Few of these are sufficiently peculiar or sufficiently faint to be descendants of extreme population II subdwarfs.

Less extreme subdwarfs of later type, near G8, like Groombridge 1830, τ Cet, and μ Cas, are only 0.7–1.0 mag. below the main sequence. If the observed colors are corrected for a small line weakening, they move essentially onto the main sequence. The underabundance of the metals in such stars seems to be small, but the extremely metal-poor stars have not yet been recognized later than G8. The M subdwarfs seem not to have extraordinarily weak lines. The explanation of this phenomenon is that the electrons in the hotter stars (F and G) come from hydrogen, in the cooler stars from the metals. The gas pressure in the cooler stars will be very high in the subdwarfs for a given P_e, so that pressure broadening will keep the strong metallic lines strong in spite of possible low abundance. Weak lines will behave differently in F and in M subdwarfs because of this change in the source of the electrons.

Several investigators have suggested that some F and G stars of population I in the Hyades and Praesepe clusters lie 1–2 mag. below the main sequence. The

evidence for membership is still poor, and the stars show no spectroscopic resemblance to the population II extreme subdwarfs. Any peculiarities of these spectra seem to be quite small. A very precise spectrophotometric study would be required to establish the reality of these effects in population I.

REFERENCES

ALLER, L. H., and GREENSTEIN, J. L. 1960 *Ap. J. Suppl.*, No. 46.
ARP, H. C. 1955 *A.J.*, **60**, 317.
BASCHEK, B. 1959 *Zs. f. Ap.*, **48**, 95.
BURBIDGE, E. M., and BURBIDGE, G. R. 1956 *Ap. J.*, **124**, 116.
BURBIDGE, E. M., BURBIDGE, G. R., FOWLER, W. A., and HOYLE, F. 1957 *Rev. Mod. Phys.*, **29**, 547.
CHAMBERLAIN, J. W., and ALLER, L. H. 1951 *Ap. J.*, **114**, 52.
CRAWFORD, J. A., and KRAFT, R. P. 1956 *Ap. J.*, **123**, 44.
DEUTSCH, A. J. 1957 *A.J.*, **62**, 139.
ELVEY, C. T., and BABCOCK, H. W. 1943 *Ap. J.*, **97**, 412.
ELVIUS, T., and SINNERSTAD, U. 1958 *Ark. f. Astr.*, **2**, 189.
FEIGE, J. 1958 *Ap. J.*, **128**, 267.
FOWLER, W. A., and GREENSTEIN, J. L. 1956 *Proc. Nat. Acad. Sci.*, **42**, 173.
GOULD, N. L., HERBIG, G. H., and MORGAN, W. W. 1957 *Pub. A.S.P.*, **69**, 242.
GREENSTEIN, J. L. 1954*a* *Pub. A.S.P.*, **66**, 79.
1954*b* *Ibid.*, p. 126.
1956 *Proc. 3d Berkeley Symposium* (Berkeley: University of California Press), **3**, 11.
1957 *Ap. J.*, **126**, 23
1958 *Hdb. d. Phys.* (Berlin: Springer), **50**, 161.
GREENSTEIN, J. L., and KRAFT, R. P. 1959 *Ap. J.*, **130**, 99.
GREENSTEIN, J. L., and MATTHEWS, M. S. 1957 *Ap. J.*, **126**, 14.
HUANG, S.-S. 1956 *A.J.*, **61**, 49.
HUMASON, M. L. 1938 *Ap. J.*, **88**, 228.
HUMASON, M. L., and ZWICKY, F. 1947 *Ap. J.*, **105**, 85.
IRIARTE, B. 1958 *Ap. J.*, **127**, 507.

IRIARTE, B., and CHAVIRA, E.	1957	*Bull. Obs. Tonantzintla*, No. 16, p. 3.
JOY, A. H.	1954*a*	*Ap. J.*, **120**, 377.
	1954*b*	*Pub. A.S.P.*, **66**, 5.
	1956	*Ap. J.*, **124**, 317.
KRAFT, R. P.	1957	*Ap. J.*, **127**, 625.
	1959	*Ibid.*, **130**, 110.
LUYTEN, W. J.	1958	*Pub. Obs. Univ. Minnesota. A Search for Faint Blue Stars* (series i–xvi).
LUYTEN, W. J., and MILLER, W. C.	1951	*Ap. J.*, **114**, 488.
LYNDS, B. T.	1957	*Ap. J.*, **125**, 719.
MCLAUGHLIN, D. B.	1953	*Ap. J.*, **117**, 279.
MELBOURNE, W. G.	1959	Thesis, California Institute of Technology.
	1960	*Ap. J.*, **132**, 101.
MERRILL, P. W.	1940	*Spectra of Long-Period Stars* (Chicago: University of Chicago Press).
MÜNCH, G.	1958	*Ap. J.*, **127**, 642.
PAYNE-GAPOSCHKIN, C.	1957	*The Galactic Novae* (Amsterdam: North Holland Publishing Co.).
ROMAN, N. G.	1954	*A.J.*, **59**, 307.
	1955	*Ap. J. Suppl.*, **2**, 198.
SANFORD, R. F., and GREENSTEIN, J. L.	1957	*Pub. A.S.P.*, **69**, 75; **69**, 352.
SCHATZMAN, E.	1958	*White Dwarfs* (Amsterdam: North Holland Publishing Co.).
SCHWARZSCHILD, M.	1958	*Structure and Evolution of the Stars* (Princeton: University Press).
SCHWARZSCHILD, M., SEARLE, L., and HOWARD, R.	1955	*Ap. J.*, **122**, 353.
SEATON, M. J., and OSTERBROCK, D. E.	1957	*Ap. J.*, **125**, 66.
SEAY, G. E.	1957	*Visible Radiation from Helium in a Strong Shock Wave* (Los Alamos, LAMS-2125).
STRUVE, O.	1955	*Les Particules solides dans les astres* (Cointe-Schlessin: Inst. d'Ap.), p. 193.
TREFFTZ, E., SCHLÜTER, A., DETTMAR, K. H., and JÖRGENS, K.	1957	*Zs. f. Ap.*, **44**, 1.
VORONTSOV-VELYAMINOV, B. A.	1953	*Gasnebel und neue Sterne*, German translation (Berlin: Verl. Kultur u. Fortschrift).
WALKER, M. F.	1957	*Non-stable Stars*, I.A.U. Symp. **3** (Cambridge: Cambridge University Press), p. 46.
WEIDEMANN, F.	1960	*Ap. J.*, **131**, 638.

Subject Index

Absolute-magnitude effects, 210 f., 250 f., 384
Absorption
  in carbon stars, 253
  Chandrasekhar mean, 17, 164, 193
  continuous
    H, 30 f., 237–40
    H^-, 30 f., 109, 237–40, 252, 709
    H_2^+, 33, 238
    He, 131 f., 237–40
  metals, 32, 237 f.
  negative, 170, 240
  Planck mean, 18, 45, 164
  in red giants, 513, 530, 537 f.
  Rosseland mean, 17, 42, 45, 164, 193, 238
Abundances of the elements
  abundances of molecules or radicals, 709
  anomalous, 268, 299 f., 429, 514, 530, 533, 687, 703
  heavy elements, 2, 535, 571
  helium-rich stars, 688, 704
  hydrogen/metal ratio, 4, 29, 42, 191, 212, 224, 234, 237, 387, 514, 535, 697, 703, 708, 709
  lithium, 536
  normal stars, 158, 218 f., 243, 297, 299, 569
Acoustic wave (sound), 262, 271 f., 278, 371, 407
Activity, 262, 268, 269, 462, 552
Age
  of cepheids, 371
  of clusters, 212
  of stars, 51, 211 f., 422, 545, 663, 687
Ambipolar diffusion, 274
Angular momentum, 284, 329, 337, 339, 342, 379, 416, 477, 488
Atmospheric eclipses, 359
Atmospheric transmission, 51–53
Atomic structure, 139

B and O stars, 411, 425 f.
  emission lines in, 412 f.
  list of, 417
  P Cygni, 412 f., 423, 461
Balmer decrement, 519, 659, 697
Balmer discontinuity (Balmer jump), 29, 57 f., 69–72, 165, 183–88, 210 f., 690, 699, 705, 706
Bénard cell, 307
Binary stars, 268, 284, 323 f., 342, 360, 466–71, 480–84, 662, 668
  Algol systems, 491 f.
  eclipsing, 165, 208, 267, 322, 397, 418, 432 f., 469, 486, f., 558, 679
  spectroscopic, 267, 303 f., 418, 432, 468, 474 f., 485 f., 546, 670 f., 684, 706, 707
  visual, 468, 558, 707
Black body, 6, 51, 61–72, 84, 511
Blanketing effect, 35, 51 f., 66, 75, 161, 182, 189, 708
Blue-white sequence, 676
Bolometer, 55, 61 f.
Boltzmann distribution, 92–93, 113, 172, 202, 245
  collisional versus radiative excitation, 105
  deviations from, 104, 110

C–N cycle, abundances in, 581
Calcium
  absorption, 298, 397, 436, 444, 553, 701
  emission, 266, 397 f., 483, 520, 546 f., 553, 664
Calibration of Rowland intensity, 157
Carbon arc, 66
Carbon stars, 253 f., 531–35, 539, 576, 578, 582
  absolute magnitude of, 534
  carbon isotopes, 578 f.
Center-limb variations of lines, 161–62, 174, 189–93
Cepheids and supergiants of population I
  classical, 289, 370 f.
  in clusters, 372, 396, 406
  curves of growth, 375
  instability strip, 388, 405
  mass motions, 376 f.
  RR Lyrae stars, 289
  radii by Wesselink method, 395, 406
  spectra of, 372 f.
Chromospheres, 113, 180, 186, 398, 403, 547, 555
  condensations in, 452 f.
  data on binaries with, 438
  density gradient and numbers of atoms, 446 f., 458 f.
  dimensions, masses, luminosities, 440
  duplicity of lines, 463
  eclipses by, 436 f.
  light-curves, 441, 456
  magnetic fields, 462
  source of ionization and excitation, 451

Circumstellar lines, 393, 546 f., 679
Cluster-type variables, 289, 305, 708
Clusters, 330, 340, 342, 396, 418, 421, 423, 663 f., 676, 708, 709
Collisional versus radiative ionization, 100 f.
Collisions, elastic and inelastic, 97–100
  broadening, 701
  damping, 699
Color index; *see* also *U*, *B*, *V* magnitudes
  computed and observed, 58
  effective wave lengths, 57
  magnitude diagram, 688
  six-color photometry, 396
  spectrophotometric gradient, 165
  standard, 40, 60, 70
Cometary nebulae, 665
Comets, 264
Contribution function, 176–83
Convection, 555
  currents, 23, 148, 346, 352, 581
  energy transfer by, 24, 185 f.
  equilibrium, 189, 388, 647
  hydrogen convection zone, 22 f., 262, 268–74, 278, 344 f., 398, 407
Copper-stabilized arcs, 148
Corona (stars and sun), 261 f., 390, 436, 471, 496, 498, 556
  condensation in, 276
Corpuscular radiation; *see* Mass loss
Cosmic rays, 261, 265, 277, 572
  Cerenkov, 277
Crab Nebula, 585, 616 f., 645
Critical angular velocity, 332
Crossover effect, 285, 291–96, 304–6, 313, 318
Curve of growth
  empirical, 194, 205
  in giants and supergiants, 205–7, 251
  Pecker theory, 175 f.
  theoretical, 174–79, 194 f.
  in white dwarfs 699
Cyanogen bands, 252, 539, 581, 634

Debye radius, 132
Degeneracy, 687, 704
Detailed balancing, 105, 109
Deuterium, 571 f.
Dilution of radiation, 89, 418 f., 428, 517, 564, 643
Displaced absorption lines, 516
Dissipation, 263, 271, 349, 498
Dissociation equilibrium, 253, 535
Distortion of radio velocity-curves (Rossiter effect), 322, 358, 474
  in chromospheric eclipses, 442 f., 457
Doppler broadening, 117, 170, 191, 195, 252, 350–60, 555
Dwarf variable stars, 653 f.
  classes of, 654
  cometary nebulae, 665
  Herbig-Haro objects, 663, 665
  lithium abundance, 669
  Orion Nebula, 653
  RW Aurigae, 654, 657
  source of energy, 663 f.
  SS Cygni, 654, 670, 676, 684 f.
  stars in nebulosity, 654 f.
  T Tauri stars, 654, 658
  UV Ceti, 654, 666

Eclipse, atmospheric, 359, 436 f.
  by chromospheres, 436
Einstein coefficients; *see f*-Values
Electronic computers for line profiles, 96
Emission, 516, 518 f., 522, 664
  forbidden, 481, 495 f., 521, 607, 610, 613, 617, 658
  of forbidden calcium lines, 521
  in novae, 605 f., 679 f.
  selection rules, 143
Energy distribution of stars, 51 f.
  absolute spectrophotometry, 54 f.
  black-body standards, 64
  U, *B*, *V* magnitudes, 55
Envelope, extended, 169, 267, 333, 411, 416, 423 f., 686, 706
  circumstellar, 680, 701
  cold, 552, 557
  gaseous, 683
Equation of transfer, 5 f., 90 f., 166 f.
Equipotential surface, 331, 489

f-Values (Einstein coefficients), 91 f., 105, 139–49, 170, 202–5, 215, 222–24
  errors in, 181, 192, 218
Faint blue stars, 684, 705
Flare stars, 260, 265, 269, 488, 502, 654, 661, 662, 664–70
Flash stars, 654, 659 f.
Fluorescence, 509, 658, 664
Fraunhofer lines, 38, 104, 157 f., 189–92
Free-free transmission, 276

Gaseous rings, 333, 469–71, 473–80, 490 f.
Gaseous streams, 360, 473 f., 488
Granulation, 24, 191, 263, 270, 344, 347, 407
Gravitational contraction, 340, 666
Gravitational separation of elements, 687 f.
Gravity darkening, 333
Gray body, 68, 164

HR diagram (Hertzsprung-Russell diagram), 2, 51, 289, 312, 338, 372, 382, 387 f., 404, 492, 494, 503, 511, 530, 664, 677, 688, 703
Hartree self-consistent fields, 144

Heisenberg uncertainty principle, 116, 121
High-velocity stars, 340, 518, 534, 684, 687, 708, 709
Holstein inequality, 125
Holtsmark distribution, 131
Hopf solution, 7, 9
Horizontal-branch stars, 676, 705 f.
Hydrogen
  emission lines and continuum, 421, 486, 519, 572, 657, 662, 666 f., 678
  maximum of, 250, 689
Hydrogen-discharge lamp, 66, 71

Instability, 678
  due to rotation, 328, 334, 418
Integral operators, 6, 19
Interstellar absorption 52 f., 373, 590, 601, 653, 656, 657
  lines, 581, 590, 622
  matter, 669
  reddening, 55, 59, 211, 406, 431, 678
Inverse predissociation, 523
Ionization equilibrium (Saha equation), 29, 92–97, 104, 113, 122, 192 f., 402, 431, 564
  deviations from, 100, 104 f.
Isotopic abundances in stars, 569 f.
  from bands, 574 f.
  helium, 573
  hydrogen, 572
  in molecules, 574 f.
  other elements, 574

King furnace, 147 f., 222
Kirchhoff's law, 6, 21 f.

LS and other coupling schemes, 141 f., 223
Lagrangian surface, 386, 437, 471 f., 503, 686
Lead sulfide cell, 55
Limb darkening, 9, 39 f., 161, 189 f., 200, 285, 311, 324
Line absorption
  blanketing, 35, 51, 75, 79 f., 161
  effect on temperature distributions, 104, 161
  in subdwarfs, 79
Line-absorption coefficient, 114 f.
  coherence and non-coherence, 107, 134, 138, 160
Line broadening, 88, 120 f., 133, 134, 136, 195, 207, 212–16, 321 f., 432, 689 f., 701; *see* also Doppler broadening; Stark effect; van der Waals; Zeeman effect
  adiabatic collisions, 122
  Doppler, 117 f., 170, 191, 252, 304, 317 f., 350–60, 555, 603, 612, 617
  Holtsmark distribution, 131, 250
  hydrogen, 214, 217, 250, 701, 704
  Kolb theory, 134, 214
  phase-shift, 125
  pressure, 120, 123, 137, 250, 692, 698 f., 704 f.
  in white dwarfs, 689 f.
Line widths, 309, 325
  curve of line-width correlation, 353 f.
  rotational, 323
Long-period variables, 509 f., 531, 546, 560
  companions, 687
  list of, 527
  Mira-type stars, 510 f.
Luminosity function, 545
Lyman-α, 265, 453

Magnetic fields and magnetic stars, 260 f., 282 f., 334–38, 347–50, 407, 462, 498, 573, 629, 646, 663, 669
  dipole, 143
  intensification, 297, 302
  magnetic oscillator, 314–16
  oblique rotator, 306, 317–19
  poloidal and toroidal, 315
Magnetohydrodynamics (hydromagnetics), 262, 285, 304 f., 513, 680
Mass above the photosphere, 243
Mass loss, 260 f., 273 f., 303, 332, 338, 397, 422, 476 f., 501, 503, 543 f., 549, 563, 632, 638, 677, 680, 704
Mass-luminosity law, 381, 491, 544, 545
Mass ratio, 439, 455, 477, 482, 488, 491, 492
Maxwell velocity distribution, 97–105, 117–19
Mean absorption coefficients, 16
  Chandrasekhar mean, 17
  Planck mean, 18
  Rosseland mean, 17
Metallic-line stars, 266, 289, 298, 326
Metastable lines, 418, 481
Method of discrete ordinates, 9
Milne-Eddington model, 20, 107, 193–204
Milne problem, 8–11
Model atmosphere
  cepheids, 392, 396
  giants, 189
  gray body, 8–11, 25, 37, 44, 68, 79, 97
  high temperatures, 43
  later than A0, 188–93
  lists, 42, 45
  non-gray, 11 f., 25, 43 f., 79, 97, 104, 112
  supergiants, 388, 392
  temperature distribution in, 8, 42, 187
  theory, 1 f.
Molecules, 252–57, 509, 536, 574 f., 697
  formation, 697, 703
  hydrogen, 256
  isotopes, 574 f.

Novae, 496–502, 543, 585 f.
  absorption and emission systems, 603 f.
  dwarf, 587, 600, 682

Novae—*Continued*
eclipse of DQ Her, 682 f.
ejection of material, 640 f.
excitation of old, 681
expanding nebulae near, 587 f., 610 f., 625 f., 638, 646
galactic distribution, 586, 589
light-curves, 591 f., 678
light-echo, 628
luminosities, 590, 678
mass, 640
nitrogen-flaring, 609, 615
nomenclature, 587
nova-like stars, 585, 601
old, 499, 598, 611, 677 f., 683, 687, 705
postnovae, 592, 602, 604, 611, 636, 640, 670 f., 677, 682
recurrent, 599–604, 612 f., 630, 631, 634, 646, 683
relation of luminosity to light-curve, 601, 602
relation of velocity to spectral development, 630
selected list, 588, 589, 594, 595
slow, 424, 586, 597, 598, 608–14, 630
spectral stages, 629
supernova remnants, 586, 618, 688
velocities of, 679 f.
Nuclear reactions, 268, 278, 370, 515, 543–44, 571, 581–82, 666, 687
surface, 302, 515, 572, 666, 669
time scale, 546
Nuclei of planetary nebulae, 676, 683, 706
Numbers of atoms capable of absorbing, 244–49

Opacity; *see* Absorption, continuous
Oscillator strengths; see *f*-Values

Partition functions, tables, 245 f.
Paschen discontinuity, 61, 71, 185
Peculiar A stars, 705
Periodic line-intensity variations; *see* Spectrum variables
Period-luminosity relation, 381, 388, 396, 400
Photoionization and recombination, 26, 34, 97
of H, He, 7, 22
Planetary nebulae, 429, 543, 610, 645, 680, 705–7
Planetary systems, 341
Plasma, 275–76, 283, 284
Polarization, 31, 50, 93, 115, 138, 162, 282, 285, 324, 337
Pole-on stars, 285, 307, 311, 325, 334, 414 f.
Prominences on stars and the sun, 264 f., 315 f., 332 f., 344, 360, 385, 425, 436, 476, 492, 680
Pulsation theory, 370 f., 493, 512
phase-lag, 393
running and standing waves, 370, 389, 391
Pyrometer, 64, 65, 73

Radiation damping, 114–18, 136, 170, 195, 215, 321
Radiation detectors
Golay cells, 53, 55
photomultipliers, 55, 62
phototransistors, 55, 75
thermocouple, 53–63, 73, 510, 513
Radiation pressure, 24, 479, 556, 663
Radiative equilibrium, 3 f., 9, 12–20, 41–46, 68, 93 f., 104, 113, 164, 185–89
Radio-frequency radiation, 260, 262, 265, 276 f.
non-thermal emission, 260–64
synchrotron, 265, 276, 618
Rare-earth stars (peculiar), 288, 293, 297
Rayleigh number, 347
Recombination spectrum, 414, 427, 496
Red giants, 79, 371, 510 f., 516, 530–41, 543–66, 678, 687
envelope models, 548–50
Relation between gas and electron pressure, 234
Relaxation times, atomic collisons, 98 f.
Resonance scattering, 161
Reversing layer (photosphere), 1, 35, 40, 412 f., 436, 509, 520, 552, 557
Reynolds' number, 343
Rotation
braking of, 335–38
broadening of lines, 307–12, 324, 325, 340, 383–87, 414
in clusters, 330, 340
in giants and supergiants, 326, 327, 338–40
pole-on stars, 307, 414 f.
stellar, 186, 265, 282–85, 304, 314–19, 321 f., 380, 411, 416, 442–44, 456, 469, 480, 484, 664, 684, 704, 707, 709
velocity, 326 f.
Rowland *Atlas*, 157
Russell-Adams phenomenon; *see* Superexcitation

Saturation function, 173 f.
Scattering; *see* also Line-absorption coefficient
coherent, 93, 107, 134–39, 160–63, 167
by free electrons, 4, 25, 34, 119, 168, 237–40, 426, 432, 645
non-coherent, 93, 107 f., 134–38, 160–63, 191
Rayleigh, 52, 240
Schrödinger equation, 139
Schuster-Schwarzschild approximation, 194, 196, 201
Self-absorption, 414, 433
Shell stars, 412–28, 480, 517, 543, 646
Shells, 611
expanding, 40 f., 385, 480, 638, 682
spectrum of, 377, 418 f., 475, 677–79

Shock wave, 271 f., 349, 407, 498, 509, 513, 647
Silicon star (peculiar), 288
Sound wave; *see* Acoustic wave
Source function, 5, 18 f., 90 f., 106, 109 f., 168
Spectrophotometry
  absolute, 66 f.
  absolute calibration, 61–66
  analysis of equivalent widths in chromospheric eclipse, 445
  relative, 55 f.
Spectrum of turbulence (Kolmogoroff spectrum), 345
  compressibility, 348
Spectrum variables, 291 f., 299–306, 317 f., 335, 486 f.
Star names; *listed in* Star Index
Stark effect; *see also* Line broadening
  electron and ion broadening, 134, 214
  first order, 93, 120 f., 212 f., 249 f.
  quadratic, 224, 251
Stellar evolution, 261, 340, 403–5, 467, 476, 499, 515, 544–45, 559, 581, 655, 680
  dying stars, 705
  evolutionary tracks, 340, 381 f., 504
  radius, 683, 687
  star formation, 329
Stratification, 159, 355, 396, 553
Subdwarfs, 79, 286, 340, 490, 501, 640, 672, 677, 684, 687, 703 f.
  hot, 480, 490, 499–500, 670, 676, 703 f.
  list, 704
Subgiants, 467, 491, 493, 684, 709
Superexcitation, 158, 452
Supergiants, 206–8, 244 f., 266, 326, 359, 370 f., 436 f., 543, 550 f.
  with atmospheric eclipses, 436 f.
Supernovae, 424, 543, 616 f., 631
Symbiotic stars (combination spectra), 425, 467, 494 f., 604, 613
  objects, 678, 679
Synchrotron radiation, 265, 276, 618

T-associations, 663
Temperature
  boundary, 38–46, 79, 177, 187 f., 450, 509 f.
  color, 51 f., 72, 164, 417, 431, 537–39, 632–34
  effective, 3, 8, 25, 51 f., 68, 165, 177, 185, 187, 333 f., 396, 530 f.
  electron, 99 f., 454, 636, 680, 688
  excitation, 109, 114, 203, 371–76, 398, 446 f., 636, 683, 708
  ionization, 109, 113, 171, 192, 249, 417, 431, 564 f., 635
  kinetic, 21, 99 f., 106
  radiation, 109
Temperature gradient
  adiabatic, 22–26, 269
  gray body, 8, 16–18, 42, 187
  radiative, 22–23
Thermodynamic equilibrium
  deviations from 21, 100 f., 161, 182, 191 f., 218, 418
  local, 3 f., 20 f., 91–96, 104 f., 158, 189 f., 223
Tidal distortion, 483
Tungsten lamp, 70 f.
Turbulence, 117, 158, 173, 186 f., 252, 262 f., 283, 312, 322 f., 379 f., 398 f., 432, 446, 450 f., 555, 608, 664
  in cepheids, 378 f.
  conversion into noise, 272
  in giants and supergiants, 203 f., 252, 266, 378 f.
  macroturbulence, 187 f., 265 f., 321, 358, 384 f., 402, 423, 555
  microturbulence, 170, 187 f., 266, 380 f., 555
  spectrum of, 345
  transport of heat, 269

U, *B*, *V* magnitudes, 55 f., 298, 308, 406, 537, 678, 690, 706
Ultraviolet continuum, 265, 396, 541
  veiling by, 654, 665 f., 684
Unidentified lines, 523

Van der Waals, 127 f.
Variational solution, 11, 18
Veiling, 511 f., 666 f.
Velocity of escape, 268, 275, 422, 549, 556, 680
Viscosity, 335 f., 343
Voigt functions, 117, 171

Weak-line stars (subdwarfs), 676, 707 f.
  ultraviolet excess, 707
Weighting functions, 95, 163, 167 f.
Weisskopf radius, 125
White dwarfs, 261, 340, 502, 560, 611, 613, 640, 677 f., 683, 687 f.
  Balmer lines, 689 f.
  classification, 689
  continuous spectra, 689, 703
  helium lines, 698 f.
  line profiles in, 692 f.
  list of, 691
  spectrophotometry of, 688 f.
  unidentified bands, 689
  velocity dispersion, 687
Wilson-Bappu effect, 397, 403, 407, 555
Wolf-Rayet stars, 412, 421, 424, 428 f., 472, 485, 488
  division into sequences, 429

X-ray radiation, 260, 265

Zanstra theory, 431, 498, 683
Zeeman effect, 283 f., 306, 318, 321
Zero-velocity surfaces, 437, 471, 477, 479, 489

Star Index

Andromedae
- γ^1 205
- λ 484
- R 512 f.
- S 586, 616
- Z 425, 494–500, 585, 599 f.
- AB 489
- RX 670–71
- SU 580

Aquarii
- β 376 f.
- π 332
- σ 311
- 108 287, 300, 302, 310
- R 500, 518, 560, 601, 687
- AE 480 f., 670 f., 678 f.

Aquilae
- γ 554
- η 354, 375 f.
- ν 376
- σ 486
- 10 287–88, 310
- 21 287, 573
- R 510, 527
- V 534
- FF 374–76
- TT 377, 394
- DO 589, 593, 598
- EL 589, 593, 620, 624
- V356 589, 593, 614 f.
- V368 589, 593, 620, 624
- V528 589, 593, 609, 611, 620–24
- V536 660
- V603 (N Aql 1918) 587–98, 604–29, 631–46, 679–83
- V604 589, 593
- V606 589, 593

Arae
- R 487

Arietis
- β 60, 81, 83
- γ 301
- 56 301
- W 587

Aurigae
- α 545
- β 489
- ϵ 206–7, 354–55, 379, 386, 437, 475, 490, 498, 605–6
- ζ 207–8, 251, 267, 278, 354–55, 384–85, 398, 437 f., 545, 555
- π 551
- ψ 550–51
- T 586–93, 598, 620–24, 679
- AR 489
- GM 654, 659–60
- RT 355, 391
- RW 657–66
- SS 670–71
- UU 536, 539
- UV 518
- UY 658, 665

Bootis
- α 158, 205–6, 354–55
- λ 709
- π 287, 310
- σ 58, 81–83

Camelopardalis
- α 417, 426
- 11 414
- 53 286, 290–306, 310, 313
- Z 501, 670–71, 684

Cancri
- κ 286–88, 303, 310
- ν 286, 310
- 15 286, 298, 302, 310
- 49 286, 310
- R 510
- RZ 468, 483
- SY 671–72

Canis Majoris
- α 158, 204, 311
- β 355
- δ 207, 354–55, 379, 385–88
- ϵ 204, 354
- o 384
- 29UW 486–87

Canis Minoris
- α 44, 189, 354
- R 514

Canum Venaticorum
- α^2 286–302, 310–15, 354, 578
- Y 253, 536–39, 580

Capricorni
γ 299
ν 311

Carinae
α 354
η 424, 585, 599, 601, 612
AG 424

Cassiopeiae
β 60
γ 417–19
ι 301
μ 709
ρ 385, 516–17
ω 310
6 424
43 286, 302, 310
AO 468, 486, 489
AQ 487
RX 470, 473, 491
SX 470–74, 480–82
WZ 580

Centauri
ζ 486
I 286, 310
V645 667–68

Cephei
δ 354–55, 374–78, 389 f.
λ 426
μ 551
π 354
U 468, 480, 490–91
W 500
CQ 433
RW 385, 463, 516–17, 550–51
UV 498
VV 212, 251, 267, 287, 437–38, 461–64, 498, 500, 516, 555, 558–59
WX 486–87

Ceti
δ 44
ο 355, 500, 512–16, 523, 527, 531, 546, 559, 601, 687 (Mira)
τ 709
τ 709
UV 667–69

Comae Berenices
β 76–81
14 418–19
17A, B 286, 299, 310
21 301

Coronae Australis
R 656, 665
S 657, 665
T 656

Coronae Borealis
α 468, 489
β 287-96, 303, 310
θ 417
ι 287, 307, 310
R 513
T 481–502, 559, 586–616, 631–40, 678–79, 687

Cygni
α 83, 204–6, 232, 354–55, 418, 605–6
γ 158, 354–55
δ 83
χ 510–14, 522–27, 536
16 58, 83
31 208, 251, 267, 354, 360, 384, 437–38, 454–61, 464, 555
32 267, 437–38, 459–64, 555
35 376
55 83, 219–20, 354, 413
61 83
P 412, 422–24, 461, 585–86, 601
Q 586, 589, 593, 598, 678–79
R 512–14, 519, 523, 527, 557
U 518, 527, 536
X 374–78, 391–402
Y 468–69
BF 497, 500
CI 496–97, 604, 613
EM 678–79
RS 518, 527
SS 468, 485, 490, 494, 501–2, 670–72, 676, 684–86
V367 418, 475, 491
V444 432, 468–76
V450 589, 593, 609, 620–24
V465 589, 593, 620–24, 634, 637
V476 589–93, 598, 605, 619–32, 637–38, 645, 679

Delphini
U 551

Doradus
S 424

Draconis
γ 206, 460
κ 332, 417
73 287, 290, 300, 310
AB 670–71
RY 538, 577, 580
WW 483–84

Equulei
γ 287–90, 295, 310
δ 354

Eridani
ε 209
40B 689–92, 697

Geminorum
- γ 204, 299, 311, 354
- ζ 355, 392–93, 399–400
- η 551, 558
- ρ 83
- R 286, 289, 527
- U 670–71
- DM 588, 593, 598, 629
- DN 588, 593, 596, 598, 607–24, 629, 638–39, 645, 679
- WY 286, 498, 500

Gruis
- π^1 533

Herculis
- α 158, 397, 517, 531–36, 545 f.
- ι 44, 413
- ρ 311
- υ 311
- g 551
- 45 287, 299, 302, 310
- 52 287, 290, 304, 310, 317
- 89 385, 395
- 110 81
- AH 671, 684
- DI 489
- DQ 502, 586 f., 678–83
- Nova 1960 610, 621–23

Hydrae
- 3 286, 290, 298, 303, 310
- R 510, 523, 527
- U 539, 580
- W 523
- RW 497

Lacertae
- 2 486
- 10 22, 44, 46, 58, 75, 83, 101, 184, 209, 213, 219–20, 413, 426
- 12 356
- 16 355
- AR 484
- CP 589–96, 604, 609, 618–24 629–38
- DI 589, 593, 596, 598, 611, 679, 683
- DK 589–604, 616–39, 644
- RT 484

Leonis
- α 354
- γ 354
- θ 311
- ρ 359
- 45 286, 299, 310
- 95 311
- X 670–71, 684
- AD 667 f.

Leonis Minoris
- R 510, 527

Leporis
- μ 286, 310
- 17 206, 266, 354, 419

Librae
- δ 322
- μ 287, 310
- 33 287, 310
- 48 414–21

Lupi
- EX 657–58
- RU 658, 664

Lyncis
- 21 311

Lyrae
- α 45, 58, 60, 70–75, 83, 185, 204, 209, 220
- β 268, 322, 339–40, 417, 468, 475, 480–85, 490, 500–503
- δ^2 551
- AY 670–71, 684
- CY 670–71, 684
- HR 588, 594, 598, 620, 624, 679
- RR 287, 289, 305, 493

Microscopii
- θ^1 287, 310

Monocerotis
- β^1 419
- R 657–58, 665
- S 426
- T 377, 394
- U 354
- AR 494
- AU 474–75
- AX 497
- NX 658–59
- UX 268, 472, 476, 486, 493

Ophiuchi
- ζ 69
- ω 287, 296, 302, 310
- X 404
- RS 588, 594, 600, 604, 611, 613, 634–35, 678–79
- RZ 470
- XX 425
- V841 586, 588, 594, 598, 678–82
- V849 588, 594, 620
- V906 620

Orionis
- α 83, 158, 385, 516–17, 531, 536, 546 f.
- β 60, 83, 355, 417, 424

ϵ 60, 74–75, 83, 417
ζ 417
λ 426
υ 83
φ 156
π^3 58, 81–83
16 286, 299
22 181, 219
U 527, 656
BL 536
CN 671, 684
CO 656, 684
DN 470, 656
FU 597–98
OX 659–61
V371AB 667–68
V378 659–61
V379 659–61
V380 502, 656–57

Pegasi
β 523, 531, 536, 546, 553
γ 44, 183, 219–20, 334
ϵ 546
o 311
9 376 f.
51 58, 81, 83
AG 287, 496–98
DS 580
RU 670–71, 684

Persei
α 158, 206, 354–55, 376 f.
β 322–25, 469, 472, 491–92
ζ 44, 184, 219–20
ϕ 417–19
21 286 f.
48 413 f.
AX 496–500, 613
GK 585 f., 678, 682

Phoenicis
ι 287, 310
SX 709

Pictoris
RR 424, 587 f.

Piscium
κ 287, 302, 310
19 514, 580
TX 536

Puppis
V 322, 486
CP 588 f., 679, 681–83
RX 496

Pyxidis
T 585 f., 679 f.

Sagittae
δ 559
9 413, 418, 425–26
S 355, 374, 376, 399
U 470, 476, 491
V 678–79
WZ 587 f., 679 f., 691

Sagittarii
υ 360, 494, 522
9 384
51 287, 299
U 396
W 355
WZ 377
XZ 491
V630 588, 594, 620 f.
V928 620
V999 588, 594
V1017 588, 594, 599, 600, 679
V1059 589, 594
V1148 605
V1275 620, 623

Scorpii
α 158, 500, 503, 531, 546 f., 687
β 486
μ^1 322, 486
π 486
σ 355
τ 38, 44, 46, 183 f., 209 f., 234, 354
T 586
U 600

Sculptoris
β 287, 310

Scuti
EU 589, 594, 597, 607, 620, 623 f.
FR 498
RZ 475

Serpentis
λ 83
χ 301
W 475, 480–81, 485, 491
CT 588, 594, 637
RT 588, 594, 597
UZ 671–72

Tauri
α 83, 531
ζ 413–22, 585
λ 322
9 286, 310
20 333–34, 354
28 332, 419, 422, 480
41 286, 298–99, 303, 310
68 286, 299
114 219
119 551
T 654 f.
AA 659–60
BP 658–59

Tauri—Continued
CI 658–59
DG 658–59
DH 658–59
DI 659–60, 665
DN 658–59
DO 658–59
RW 469–70, 482
RY 654–57, 665
UZ 658–59, 664–65
XX 588, 594–97, 645
XZ 658, 664–65

Telescopii
RR 424, 589, 594, 598

Trianguli
β 83

Ursa Majoris
ϵ 301, 307
ζ^1 466
η 83
15 299
30 286, 298, 303, 310
T 523
W 322, 468, 484, 493–94
RW 483
SU 670–71, 684
SW 671–72
UX 468, 490
VY 580

Velorum
γ^2 468, 480–81
S 470, 476, 484, 491

Virginis
α 486, 488
γ 286
W 354, 395
TW 671, 684
78 287 f., 310, 317

Vulpeculae
T 374, 376
BW 355
SV 374 f.
WW 654, 656–57

SPECIAL LISTS, BY AUTHORS OR CATALOGUES

Abell
7 707
30 707
31 707
36 707
78 707

Astrographic Catalogue (*AC*)
+70°5824 691
+70°8247 689, 691
+73°8031 691
+82°3818 691

Bonner Durchmusterung (*BD*)
−3°2525 707
−6°1253 502, 656–57
+4°4048B 667–68
+25°2534 704
+25°4655 704
+28°4211 691, 698–700, 704, 707
+43°44B 667–68
+46°1913 287
+75°325 703–4

Boss
1985 559
5481 559

Cincinnati (20*C*)
574AB 667 f.
861C 667–68
1191AB 667–68
1250AB 667–68

Feige (*F*)
84 706
95 706
113 706

Groombridge (*Gr*)
34 667
1830 709

Hertzsprung (*He*)
3 691

Harvard Revised (*HR*)
690 376
710 286, 289, 303, 310
1105 286, 289
1732 301
5313 301

Humason-Zwicky (*HZ*)
1 703–5
2 691
3 703–5
9 691
14 691
21 689, 691, 698–704
22 706
29 691
43 691–92, 698
44 703–6

Luyten (*L*)
532-81 691, 701–2
711-10 691

726-8B 667
745-46A 689, 691, 701–2
770-3 613, 691
825-14 691
870-2 691–92, 698
879-14 689, 691
930-80 691, 699–700
970-30 691
971-14 691
997-21 691
1244-46 691
1363-3 689, 691
1491-27 691
1512-34B 691
1573-31 689, 691, 698–700

Luyten Double Star (*LDS*)
275AB 691
678A 691
726-28B 667
749B 691, 699–700

MacRae
+43°1 678–79

Merrill Hα (*MHα*)
259-1 659
259-7 659
259-9n 659
259-9s 659, 665
259-10 659
259-20 659
259-23 659

Ross
198 691

Selected Area (*SA*)
29-130 691–92, 698

van Maanen (*vMa*)
2 689, 691, 701–3

van Rhijn (*vR*)
7 691
16 691

Wolf (*W*)
219 691
485 691
489 691
1130 667–68
1346 691–92, 698
1516 689, 691

Henry Draper (*HD*)
108 425
1838 527
2453 286, 310
4174 286, 498
4778 287, 299–302
5223 580
5394 417
8441 286, 290, 303, 310
9996 286, 303, 310
10516 417–19
10783 286, 290, 295, 310
11187 286, 310
11503 301
15089 301
16115 536, 580
16956 81, 299
19445 81, 286, 708
19557 580
19832 301
20797 551
21403 527
25354 286 f.
30466 286, 298, 310
30614 417, 426
32633 286 f.
32343 414
33232 419
34452 301
36861 426
36959 217
36960 217
37836 424
42616 286 f.
47129 267, 472 f.
47839 426
49976 286 f.
50168 299
50169 286, 310
50820 418
54920 527, 656
56495 286 f.
62910 429
70122 527
71866 286 f.
76396 580
79319 580
80493 539
81617 527
93934 510, 527
94910 424
98088 286 f.
107612 301
108945 301
109387 332, 417
110066 286, 288, 310
111133 286, 310
112185 301
112869 580
115708 287, 310
124224 301
125248 287 f.
126515 287, 310
127493 704
132422 527
133029 287 f.
133633 527
134439 707
134440 707
134793 287 f.
135297 287, 310
140160 301
140283 81, 708

Henry Draper (*HD*)—Continued
140728 307
143414 428, 429
151199 354
153286 287, 299
153882 287 f.
156074 536, 580
165474 287, 310
168814 298
171586 287, 302, 310
173650 287 f.
174638, 9 268, 322, 339–40, 417, 468, 475, 480–85, 490, 500–3
182040 536, 580
184905 287, 298, 302, 310
186568 311
187474 287, 303, 305, 310
188001 426
188037 558
188041 286 f.
188209 426
190073 287, 310
190603 423
190108 510, 527
191742 287, 310
192103 413, 328, 430
192163 413, 428, 430
192639 426
192913 287, 310
193449 512 f., 557
193576 428, 432
194048 527
194279 424
194632 510 f.
200938 518, 527
201647 518, 527, 536
210839 426
214680 426
215038 287, 298, 302, 304
215441 283, 290, 307, 317
216533 287, 310
219617 707
223392 580
224801 287, 300, 302, 310
234677 667–68
269858 424

SPECIAL TABLES OF CERTAIN TYPES OF STARS NOT COMPLETELY LISTED IN STAR INDEX

Monochromatic magnitudes 83
Magnetic stars 286–87
Bright B stars with hydrogen emission 417
Wolf-Rayet stars brighter than $9^{m}5$ 428
Systems with gaseous rings 470
Bright long-period variables of types M, S, N 527
Selected novae 588–89
Dwarf Variable Stars
Types B8–G5 656
T Tauri stars, with many bright lines 658
Types G–M, with few bright lines 660
Flash stars 661
UV Ceti flare stars 667
SS Cygni stars 671
White dwarfs 691

STARS AND STELLAR SYSTEMS

Compendium of Astronomy and Astrophysics

This series, comprising nine volumes, is intended to present the basic empirical information in each area of astrophysics and stellar astronomy, with an appropriate background of theory, relevant to the current status and development of the science. Extreme specialization has been avoided in order to make the chapters suitable to graduate students and also to the increasing number of scientists in other fields requiring astronomical information.

Separate editors have been appointed for each volume. The volume editors, together with the general editors, form the editorial board which is responsible for the over-all planning of the series.

General Editor . . .

GERARD P. KUIPER, head of the Lunar and Planetary Laboratory, University or Arizona, was formerly director of Yerkes Observatory, University of Chicago.

Associate General Editor . . .

BARBARA M. MIDDLEHURST, Research Associate at the Steward Observatory of the University of Arizona, was formerly lecturer in astronomy, St. Andrews University, Scotland.

PRINTED IN U.S.A.

STARS AND STELLAR SYSTEMS

VOLUME TITLES:

I
TELESCOPES

II
ASTRONOMICAL TECHNIQUES

III
BASIC ASTRONOMICAL DATA

IV
CLUSTERS AND BINARIES

V
GALACTIC STRUCTURE

VI
STELLAR ATMOSPHERES

VII
NEBULAE AND INTERSTELLAR MATTER

VIII
STELLAR STRUCTURE

IX
GALAXIES AND THE UNIVERSE

STELLAR ATMOS-PHERES

Edited by
JESSE L.
GREENSTEIN

STARS
AND
STELLAR
SYSTEMS
VOLUME
VI



CHICAGO